

Rayner Alfred  
Yuto Lim  
Haviluddin Haviluddin  
Chin Kim On *Editors*

# Computational Science and Technology

6th ICCST 2019, Kota Kinabalu,  
Malaysia, 29–30 August 2019

# Lecture Notes in Electrical Engineering

## Volume 603

### Series Editors

Leopoldo Angrisani, Department of Electrical and Information Technologies Engineering, University of Napoli Federico II, Naples, Italy

Marco Arteaga, Departament de Control y Robótica, Universidad Nacional Autónoma de México, Coyoacán, Mexico

Bijaya Ketan Panigrahi, Electrical Engineering, Indian Institute of Technology Delhi, New Delhi, Delhi, India  
Samarjit Chakraborty, Fakultät für Elektrotechnik und Informationstechnik, TU München, Munich, Germany  
Jiming Chen, Zhejiang University, Hangzhou, Zhejiang, China

Shanben Chen, Materials Science and Engineering, Shanghai Jiao Tong University, Shanghai, China

Tan Kay Chen, Department of Electrical and Computer Engineering, National University of Singapore, Singapore, Singapore

Rüdiger Dillmann, Humanoids and Intelligent Systems Lab, Karlsruhe Institute for Technology, Karlsruhe, Baden-Württemberg, Germany

Haibin Duan, Beijing University of Aeronautics and Astronautics, Beijing, China

Gianluigi Ferrari, Università di Parma, Parma, Italy

Manuel Ferre, Centre for Automation and Robotics CAR (UPM-CSIC), Universidad Politécnica de Madrid, Madrid, Spain

Sandra Hirche, Department of Electrical Engineering and Information Science, Technische Universität München, Munich, Germany

Faryar Jabbari, Department of Mechanical and Aerospace Engineering, University of California, Irvine, CA, USA

Limin Jia, State Key Laboratory of Rail Traffic Control and Safety, Beijing Jiaotong University, Beijing, China

Janusz Kacprzyk, Systems Research Institute, Polish Academy of Sciences, Warsaw, Poland

Alaa Khamis, German University in Egypt El Tagamoa El Khames, New Cairo City, Egypt

Torsten Kroeger, Stanford University, Stanford, CA, USA

Qilian Liang, Department of Electrical Engineering, University of Texas at Arlington, Arlington, TX, USA

Ferran Martin, Departament d'Enginyeria Electrònica, Universitat Autònoma de Barcelona, Bellaterra, Barcelona, Spain

Tan Cher Ming, College of Engineering, Nanyang Technological University, Singapore, Singapore

Wolfgang Minker, Institute of Information Technology, University of Ulm, Ulm, Germany

Pradeep Misra, Department of Electrical Engineering, Wright State University, Dayton, OH, USA

Sebastian Möller, Quality and Usability Lab, TU Berlin, Berlin, Germany

Subhas Mukhopadhyay, School of Engineering & Advanced Technology, Massey University, Palmerston North, Manawatu-Wanganui, New Zealand

Cun-Zheng Ning, Electrical Engineering, Arizona State University, Tempe, AZ, USA

Toyoaki Nishida, Graduate School of Informatics, Kyoto University, Kyoto, Japan

Federica Pascucci, Dipartimento di Ingegneria, Università degli Studi "Roma Tre", Rome, Italy

Yong Qin, State Key Laboratory of Rail Traffic Control and Safety, Beijing Jiaotong University, Beijing, China

Gan Woon Seng, School of Electrical & Electronic Engineering, Nanyang Technological University, Singapore, Singapore

Joachim Speidel, Institute of Telecommunications, Universität Stuttgart, Stuttgart, Baden-Württemberg, Germany

Germano Veiga, Campus da FEUP, INESC Porto, Porto, Portugal

Haitao Wu, Academy of Opto-electronics, Chinese Academy of Sciences, Beijing, China

Junjie James Zhang, Charlotte, NC, USA

The book series *Lecture Notes in Electrical Engineering* (LNEE) publishes the latest developments in Electrical Engineering - quickly, informally and in high quality. While original research reported in proceedings and monographs has traditionally formed the core of LNEE, we also encourage authors to submit books devoted to supporting student education and professional training in the various fields and applications areas of electrical engineering. The series cover classical and emerging topics concerning:

- Communication Engineering, Information Theory and Networks
- Electronics Engineering and Microelectronics
- Signal, Image and Speech Processing
- Wireless and Mobile Communication
- Circuits and Systems
- Energy Systems, Power Electronics and Electrical Machines
- Electro-optical Engineering
- Instrumentation Engineering
- Avionics Engineering
- Control Systems
- Internet-of-Things and Cybersecurity
- Biomedical Devices, MEMS and NEMS

For general information about this book series, comments or suggestions, please contact [leontina.dicecco@springer.com](mailto:leontina.dicecco@springer.com).

To submit a proposal or request further information, please contact the Publishing Editor in your country:

#### **China**

Jasmine Dou, Associate Editor ([jasmine.dou@springer.com](mailto:jasmine.dou@springer.com))

#### **India**

Swati Meherishi, Executive Editor ([swati.meherishi@springer.com](mailto:swati.meherishi@springer.com))

Aninda Bose, Senior Editor ([aninda.bose@springer.com](mailto:aninda.bose@springer.com))

#### **Japan**

Takeyuki Yonezawa, Editorial Director ([takeyuki.yonezawa@springer.com](mailto:takeyuki.yonezawa@springer.com))

#### **South Korea**

Smith (Ahram) Chae, Editor ([smith.chae@springer.com](mailto:smith.chae@springer.com))

#### **Southeast Asia**

Ramesh Nath Premnath, Editor ([ramesh.premnath@springer.com](mailto:ramesh.premnath@springer.com))

#### **USA, Canada:**

Michael Luby, Senior Editor ([michael.luby@springer.com](mailto:michael.luby@springer.com))

#### **All other Countries:**

Leontina Di Cecco, Senior Editor ([leontina.dicecco@springer.com](mailto:leontina.dicecco@springer.com))

Christoph Baumann, Executive Editor ([christoph.baumann@springer.com](mailto:christoph.baumann@springer.com))

**\*\* Indexing: The books of this series are submitted to ISI Proceedings, EI-Compendex, SCOPUS, MetaPress, Web of Science and Springerlink \*\***

More information about this series at <http://www.springer.com/series/7818>

Rayner Alfred · Yuto Lim ·  
Haviluddin Haviluddin ·  
Chin Kim On  
Editors

# Computational Science and Technology

6th ICCST 2019, Kota Kinabalu, Malaysia,  
29–30 August 2019



Springer

*Editors*

Rayner Alfred  
Knowledge Technology Research Unit,  
Faculty of Computing and Informatics  
Universiti Malaysia Sabah  
Kota Kinabalu, Sabah, Malaysia

Haviluddin Haviluddin  
Department of Computer Science  
Universitas Mulawarman  
Samarinda, Indonesia

Yuto Lim  
School of Information Science,  
Security and Networks Area  
Japan Advanced Institute of Science  
and Technology  
Nomi, Ishikawa, Japan

Chin Kim On  
Center of Data and Information Management  
Universiti Malaysia Sabah  
Kota Kinabalu, Sabah, Malaysia

ISSN 1876-1100

ISSN 1876-1119 (electronic)

Lecture Notes in Electrical Engineering

ISBN 978-981-15-0057-2

ISBN 978-981-15-0058-9 (eBook)

<https://doi.org/10.1007/978-981-15-0058-9>

© Springer Nature Singapore Pte Ltd. 2020

This work is subject to copyright. All rights are reserved by the Publisher, whether the whole or part of the material is concerned, specifically the rights of translation, reprinting, reuse of illustrations, recitation, broadcasting, reproduction on microfilms or in any other physical way, and transmission or information storage and retrieval, electronic adaptation, computer software, or by similar or dissimilar methodology now known or hereafter developed.

The use of general descriptive names, registered names, trademarks, service marks, etc. in this publication does not imply, even in the absence of a specific statement, that such names are exempt from the relevant protective laws and regulations and therefore free for general use.

The publisher, the authors and the editors are safe to assume that the advice and information in this book are believed to be true and accurate at the date of publication. Neither the publisher nor the authors or the editors give a warranty, expressed or implied, with respect to the material contained herein or for any errors or omissions that may have been made. The publisher remains neutral with regard to jurisdictional claims in published maps and institutional affiliations.

This Springer imprint is published by the registered company Springer Nature Singapore Pte Ltd.  
The registered company address is: 152 Beach Road, #21-01/04 Gateway East, Singapore 189721,  
Singapore

# Preface

Computational Science and Technology is a rapidly growing multi- and interdisciplinary field that uses advanced computing and data analysis to understand and solve complex problems. The absolute size of many challenges in computational science and technology demands the use of supercomputing, parallel processing, sophisticated algorithms and advanced system software and architecture.

With the recent developments in open-standard hardware and software, augmented reality (AR) and virtual reality (VR), automation, humanized big data, machine learning, internet of everything (IoT) and smart home technology, web-scale information technology, mobility and physical-digital integrations, new and efficient solutions are required in Computational Science and Technology in order to fulfilled the demands from these developments.

The conference was organized and hosted by Spatial Explorer and jointly organized with JAIST and Mulawarman Universiti, Indonesia. Building on the previous FIVE conferences that include Regional Conference on Computational Science and Technology (RCSST 2007), the four International Conference on Computational Science and Technology (ICCST2014, ICCST2016, ICCST2017 and ICCST2018), the Sixth International Conference on Computational Science and Technology 2019 (ICCST2019) offers practitioners and researchers from academia and industry the possibility to share computational techniques and solutions in this area, to identify new issues, and to shape future directions for research, as well as to enable industrial users to apply leading-edge large-scale high-performance computational methods.

This volume presents a theory and practice of ongoing research in computational science and technology. The focuses of this volume is on a broad range of methodological approaches and empirical references points including artificial intelligence, cloud computing, communication and data networks, computational intelligence, data mining and data warehousing, evolutionary computing, high-performance computing, information retrieval, knowledge discovery, knowledge management, machine learning, modeling and simulations, parallel and distributed computing, problem-solving environments, semantic technology, soft computing, system-on-chip design and engineering, text mining, visualization and web-based and service computing. The carefully selected contributions to this

volume were initially accepted for oral presentation during the Sixth International Conference on Computational Science and Technology 2019 (ICCST2019) which is an international scientific conference for research in the field of advanced computational science and technology, that was held during 29–30 August 2019, at Hilton Kota Kinabalu, Sabah, Malaysia. The level of contributions corresponds to that of advanced scientific works, although several of them could be addressed also to non-expert readers. The volume brings together 69 chapters.

In concluding, we would also like to express our deep gratitude and appreciation to all the program committee members, panel reviewers, organizing committees and volunteers for your efforts to make this conference a successful event. It is worth emphasizing that much theoretical and empirical work remains to be done. It is encouraging to find that more research on computational science and technology is still required. We sincerely hope the readers will find this book interesting, useful and informative and it will give then a valuable inspiration for original and innovative research.

Kota Kinabalu, Malaysia  
Nomi, Japan  
Samarinda, Indonesia  
Kota Kinabalu, Malaysia

Rayner Alfred  
Yuto Lim  
Haviluddin Haviluddin  
Chin Kim On

# **The Sixth International Conference on Computational Science and Technology 2019 (ISSN: 1876-1100)**

## **Keynote Speakers**

Prof. Dr. Kukjin Chun—Department of Electrical and Computer Engineering, Seoul National University, Seoul, South Korea

Prof. Dr. Rosni Abdullah—School of Computer Sciences, Universiti Sains Malaysia, Pulau Pinang, Malaysia

Dr. Leandro Soares Indrusiak—Reader in Real-Time Systems, Department of Computer Science, The University of York, UK

Dr. Suresh Manandhar—Reader in Natural Language Processing, Department of Computer Science, The University of York, UK

# Contents

<b>Decision Tree with Sensitive Pruning in Network-based Intrusion Detection System .....</b>	1
Yee Jian Chew, Shih Yin Ooi, Kok-Seng Wong and Ying Han Pang	
<b>A Sequential Approach to Network Intrusion Detection .....</b>	11
Nicholas Lee, Shih Yin Ooi and Ying Han Pang	
<b>Implementing Bio-Inspired Algorithm for Pathfinding in Flood Disaster Prevention Game .....</b>	23
T. Brenda Chandrawati, Anak Agung Putri Ratna and Riri Fitri Sari	
<b>Specific Gravity-based of Post-harvest Mangifera indica L. cv. Harumanis for ‘Insidious Fruit Rot’ (IFR) Detection using Image Processing .....</b>	33
N. S. Khalid, S. A. A. Shukor and A. S. Fathinul Syahir	
<b>Reducing Climate Change for Future Transportation: Roles of Computing .....</b>	43
Hairoladenan Kasim, Zul-Azri Ibrahim and Abbas M. Al-Ghaili	
<b>Performance Analysis of the Level Control with Inverse Response by using Particle Swarm Optimization .....</b>	55
I. M. Chew, F. Wong, A. Bono, J. Nandong and K. I. Wong	
<b>3D Keyframe Motion Extraction from Zapin Traditional Dance Videos .....</b>	65
Ikmal Faiq Albakri, Nik Wafiy, Norhaida Mohd Suaib, Mohd Shafry Mohd Rahim and Hongchuan Yu	
<b>3D Motion and Skeleton Construction from Monocular Video .....</b>	75
Nik Mohammad Wafiy Azmi, Ikmal Faiq Albakri, Norhaida Mohd Suaib, Mohd Shafry Mohd Rahim and Hongchuan Yu	

<b>Automated Classification of Tropical Plant Species Data Based on Machine Learning Techniques and Leaf Trait Measurements .....</b>	85
Burhan Rashid Hussein, Owais Ahmed Malik, Wee-Hong Ong and Johan Willem Frederik Slik	
<b>Human Detection and Classification using Passive Forward Scattering Radar System at Different Places .....</b>	95
Noor Hafizah Abdul Aziz, Liyana Nadhirah Phalip and Nurul Huda Abd Rahman	
<b>An Automated Driver's Context Recognition Approach Using Smartphone Embedded Sensors .....</b>	105
Md Ismail Hossen, Michael Goh, Tee Connie, Siong Hoe Lau and Ahsanul Bari	
<b>A Variable Sampling Interval EWMA <math>\bar{X}</math> Chart for the Mean with Auxiliary Information .....</b>	113
Peh Sang Ng, Michael Boon Chong Khoo, Wai Chung Yeong and Sok Li Lim	
<b>Design of Cloud Computing Load Balance System Based on SDN Technology .....</b>	123
Saif Al-Mashhadi, Mohammed Anbar, Rana A. Jalal and Ayman Al-Ani	
<b>Analysis of Expert's Opinion on Requirements Patterns for Software Product Families Framework Using GQM Method .....</b>	135
Badamasi Imam Ya'u, Azlin Nordin and Norsaremah Salleh	
<b>A Multi-Layer Perceptron Model in Analyzing Parametric Classification of Students' Assessment Results in K12 .....</b>	145
Arman Bernard G. Santos, Bryan G. Dadiz, Jerome L. Liwanag, Mari-Pearl M. Valdez, Myen D. C. Dela Cruz and Rhommel S. Avinante	
<b>Redefining the White-Box of k-Nearest Neighbor Support Vector Machine for Better Classification .....</b>	157
Doreen Ying Ying Sim	
<b>Vehicle Classification using Convolutional Neural Network for Electronic Toll Collection .....</b>	169
Zi Jian Wong, Vik Tor Goh, Timothy Tzen Vun Yap and Hu Ng	
<b>Social Media, Software Engineering Collaboration Tools and Software Company's Performance .....</b>	179
Gulshan Nematova, Aamir Amin, Mobashar Rehman and Nazabat Hussain	
<b>The MMUISD Gait Database and Performance Evaluation Compared to Public Inertial Sensor Gait Databases .....</b>	189
Jessica Permatasari, Tee Connie and Ong Thian Song	

<b>Brief of Intrusion Detection Systems in Detecting ICMPv6 Attacks . . . . .</b>	199
Adnan Hasan Bdair, Rosni Abdullah, Selvakumar Manickam and Ahmed K. Al-Ani	
<b>Lake Chini Water Level Prediction Model using Classification Techniques . . . . .</b>	215
Lim Zee Hin and Zalinda Othman	
<b>Development of a Bi-level Web Connected Home Access System using Multi-Deep Learning Neural Networks . . . . .</b>	227
K. Y. Tham, T. W. Cheam, H. L. Wong and M. F. A. Fauzi	
<b>Portrait of Indonesia's Internet Topology at the Autonomous System Level . . . . .</b>	237
Timotius Witono and Setiadi Yazid	
<b>Low Latency Deep Learning Based Parking Occupancy Detection By Exploiting Structural Similarity . . . . .</b>	247
Chin-Kit Ng, Soon-Nyeen Cheong and Yee-Loo Foo	
<b>Sequential Constructive Algorithm incorporate with Fuzzy Logic for Solving Real World Course Timetabling Problem . . . . .</b>	257
Tan Li June, Joe H. Obit, Yu-Beng Leau, Jetol Bolongkikit and Rayner Alfred	
<b>An Investigation of Generality in two-layer Multi-agent Framework towards different domains . . . . .</b>	269
Kuan Yik Junn, Joe Henry Obit, Rayner Alfred, Jetol Bolongkikit and Yu-Beng Leau	
<b><math>\mu^2</math> : A Lightweight Block Cipher . . . . .</b>	281
Wei-Zhu Yeoh, Je Sen Teh and Mohd Ilyas Sobirin Bin Mohd Sazali	
<b>Tweet sentiment analysis using deep learning with nearby locations as features . . . . .</b>	291
Wei Lun Lim, Chiung Ching Ho and Choo-Yee Ting	
<b>Quantifying attractiveness of incomplete-information multi-player game: case study using DouDiZhu . . . . .</b>	301
Yuxian Gao, Wanxiang Li, Mohd Nor Akmal Khalid and Hiroyuki Iida	
<b>An Improvement of Computing Newton's Direction for Finding Unconstrained Minimizer for Large-Scale Problems with an Arrowhead Hessian Matrix . . . . .</b>	311
Khadizah Ghazali, Jumat Sulaiman, Yosza Dasril and Darmesah Gabda	
<b>Semantic Segmentation of Herbarium Specimens Using Deep Learning Techniques . . . . .</b>	321
Burhan Rashid Hussein, Owais Ahmed Malik, Wee-Hong Ong and Johan Willem Frederik Slik	

<b>Development of Variable Acoustic Soundwave for Fire Prevention . . . . .</b>	331
Maila R. Angeles, Jonrey V. Rañada, Dennis C. Lopez, Jose Ross Antonio R. Apilado, Ma. Sharmaine L. Carlos, Francis John P. David, Hanna Joy R. Escario, Andrea Isabel P. Rolloda and Irish Claire L. Villanueva	
<b>Cryptoanalysis of Lightweight and anonymous three-factor authentication and access control protocol for real-time applications in wireless sensor networks . . . . .</b>	341
Jihyeon Ryu, Youngsook Lee and Dongho Won	
<b>Ultimate Confined Compressive Strength of Carbon Fiber-Reinforced Circular and Rectangular Concrete Column . . . . .</b>	351
Jason Ongpeng, Isabel Nicole Lecciones, Jasmine Anne Garduque and Daniel Joshua Buera	
<b>Examining Machine Learning Techniques in Business News Headline Sentiment Analysis . . . . .</b>	363
Seong Liang Ooi Lim, Hooi Mei Lim, Eng Kee Tan and Tien-Ping Tan	
<b>A 2×1 Microstrip Patch Array Rectenna with Harmonic Suppression Capability for Energy Harvesting Application . . . . .</b>	373
Nur ‘Aisyah Amir, Shipun Anuar Hamzah, Khairun Nidzam Ramli, Shaharil Mohd Shah, Mohamad Shamian Zainal, Fauziahanim Che Seman, Nazib Adon, Mohamad Sukri Mustapa, Mazlina Esa and Nik Noordini Nik Abd Malik	
<b>Towards Computer-Generated Cue-Target Mnemonics for E-Learning . . . . .</b>	383
James Mountstephens, Jason Teo Tze Wi and Balvinder Kaur Kler	
<b>Data Integration for Smart Cities: Opportunities and Challenges . . . . .</b>	393
Subashini Raghavan, Boung Yew Lau Simon, Ying Loong Lee, Wei Lun Tan and Keh Kim Kee	
<b>Estimating Material Parameters Using Light Scattering Model and Polarization . . . . .</b>	405
Hadi A. Dahlan, Edwin R. Hancock and William A. P. Smith	
<b>Workplace Document Management System Employing Cloud Computing and Social Technology . . . . .</b>	415
Alfio I. Regla and Praxedis S. Marquez	
<b>The Development of an Integrated Corpus for Malay Language . . . . .</b>	425
Normi Sham Awang Abu Bakar	
<b>Word Embedding for Small and Domain-specific Malay Corpus . . . . .</b>	435
Sabrina Tiun, Nor Fariza Mohd Nor, Azhar Jalaludin and Anis Nadiah Che Abdul Rahman	

<b>Blood Glucose Classification to Identify a Dietary Plan for High-Risk Patients of Coronary Heart Disease Using Imbalanced Data Techniques . . . . .</b>	<b>445</b>
Monirah Alashban and Nirase Fathima Abubacker	
<b>A Review of An Interactive Augmented Reality Customization Clothing System Using Finger Tracking Techniques as Input Device . . . . .</b>	<b>457</b>
Liying Feng, Giap Weng Ng and Liyao Ma	
<b>Classifying Emotion based on Facial Expression Analysis using Gabor Filter: A Basis for Adaptive Effective Teaching Strategy . . . . .</b>	<b>469</b>
Anna Liza A. Ramos, Bryan G. Dadiz and Arman Bernard G. Santos	
<b>A Perspective Towards NCIFA and CIFA in Named-Data Networking Architecture . . . . .</b>	<b>481</b>
Ren-Ting Lee, Yu-Beng Leau, Yong Jin Park and Joe H. Obit	
<b>Augmented Reality for Learning Calculus: A Research Framework of Interactive Learning System . . . . .</b>	<b>491</b>
Md Asifur Rahman, Lew Sook Ling and Ooi Shih Yin	
<b>Development of a Rain Sensing Car Speed Limiter . . . . .</b>	<b>501</b>
Efren Victor N. Tolentino Jr., Joseph D. Retumban, Jonrey V. Rañada, Harvey E. Francisco, Johnry Guillema, Gerald Mel G. Sabino, Jame Rald G. Dizon, Christian Jason B. Gane and Kristian G. Quintana	
<b>Implementation of the 4EGKSOR for Solving One-Dimensional Time-Fractional Parabolic Equations with Grünwald Implicit Difference Scheme . . . . .</b>	<b>511</b>
Fatihah Anas Muhiddin, Jumat Sulaiman and Andang Sunarto	
<b>Particles Aggregation Using Flexural Plate Waves Device . . . . .</b>	<b>521</b>
Wan Nur Hayati Wan Husin, Norazreen Abd Aziz, Muhamad Ramdan Buyong and Siti Salasiah Mokri	
<b>A User Mobility-Aware Fair Channel Assignment Scheme for Wireless Mesh Network . . . . .</b>	<b>531</b>
Bander Ali Saleh Al-rimy, Maznah Kamat, Fuad A. Ghaleb, Mohd. Foad Rohani, Shukor Abd Razak and Mohd Arief Shah	
<b>Tweep: A System Development to Detect Depression in Twitter Posts . . . . .</b>	<b>543</b>
Chempaka Seri Abdul Razak, Muhammad Ameer Zulkarnain, Siti Hafizah Ab Hamid, Nor Badrul Anuar, Mohd Zalisham Jali and Hasni Meon	

<b>Measuring the Application of Anthropomorphic Gamification for Transitional Care; A Goal-Question-Metric Approach .....</b>	553
Nooralisa Mohd Tuah and Gary B. Wills	
<b>An Integration of Image Processing Solutions for Social Media Listening .....</b>	565
Christine Diane L. Ramos, Ivana Koon Yee U. Lim, Yuta C. Inoue, John Andrew Santiago and Nigel Marcus Tan	
<b>On the trade-offs of Proof-of-Work algorithms in blockchains .....</b>	575
Zi Hau Chin, Timothy Tzen Vun Yap and Ian K. T. Tan	
<b>Ideal Combination Feature Selection Model for Classification Problem based on Bio-Inspired Approach .....</b>	585
Mohammad Aizat Basir, Mohamed Saifullah Hussin and Yuhanis Yusof	
<b>Comparison of Ensemble Simple Feedforward Neural Network and Deep Learning Neural Network on Phishing Detection .....</b>	595
Gan Kim Soon, Liew Chean Chiang, Chin Kim On, Nordaliela Mohd Rusli and Tan Soo Fun	
<b>Design and Development of Multimedia and Multi-Marker Detection Techniques in Interactive Augmented Reality Colouring Book .....</b>	605
Angeline Lee Ling Sing, Awang Asri Awang Ibrahim, Ng Giap Weng, Muzaffar Hamzah and Wong Chun Yung	
<b>From A Shared Single Display Application to Shared Virtual Space Learning Application .....</b>	617
Gary Loh Chee Wyai, Cheah Waishiang, Muhammad Asyraf Bin Khairuddin and Chen Chwen Jen	
<b>Towards a Character-based Meta Recommender for Movies .....</b>	627
Alia El Bolock, Ahmed El Kady, Cornelia Herbert and Slim Abdennadher	
<b>A Framework for Automatic Analysis of Essays Based on Idea Mining .....</b>	639
Azreen Azman, Mostafa Alksher, Shyamala Doraisamy, Razali Yaakob and Eissa Alshari	
<b>Advanced Fuzzy Set: An Application to Flat Electroencephalography Image .....</b>	649
Suzelawati Zenian, Tahir Ahmad and Amidora Idris	
<b>Impact Assessment of Large-Scale Solar Photovoltaic integration on Sabah Grid System .....</b>	659
Myjessie Songkin, N. N. Barsoum and Farrah Wong	

<b>i-BeeHOME: An Intelligent Stingless Honey Beehives Monitoring Tool Based On TOPSIS Method By Implementing LoRaWan – A Preliminary Study .....</b>	<b>669</b>
Wan Nor Shuhadah Wan Nik, Zarina Mohamad, Aznida Hayati Zakaria and Abdul Azim Azlan	
<b>Optimizing Parameters Values of Tree-Based Contrast Subspace Miner using Genetic Algorithm .....</b>	<b>677</b>
Florence Sia and Rayner Alfred	
<b>Development of a Self-sufficient Ad Hoc Sensor to Perform Electrical Impedance Tomography Measurements from Within Imaged Space .....</b>	<b>689</b>
Abbas Ibrahim Mbulwa, Ali Chekima, Jamal Ahmad Dargham, Yew Hoe Tung, Renee Chin Ka Yin and Wong Wei Kitt	
<b>Malaysian Road Accident Severity: Variables and Predictive Models .....</b>	<b>699</b>
Choo-Yee Ting, Nicholas Yu-Zhe Tan, Hizal Hanis Hashim, Chiung Ching Ho and Akmalia Shabadin	
<b>Location Analytics for Churn Service Type Prediction .....</b>	<b>709</b>
Nicholas Yu-Zhe Tan, Choo-Yee Ting and Chuing Ching Ho	
<b>Development of Novel Gamified Online ECG Learning Platform (GaMED ECG<sup>TM</sup>) .....</b>	<b>719</b>
May Honey Ohn, Khin Maung Ohn, Shahril Yusof, Urban D'Souza, Zamhar Iswandono and Issa Mchucha	
<b>Author Index .....</b>	<b>731</b>



# Decision Tree with Sensitive Pruning in Network-based Intrusion Detection System

Yee Jian Chew<sup>1</sup>, Shih Yin Ooi<sup>1</sup>, Kok-Seng Wong<sup>2</sup>, and Ying Han Pang<sup>1</sup>

<sup>1</sup> Faculty of Information Science and Technology, Multimedia University, Melaka, Malaysia

<sup>2</sup> Department of Computer Science, Nazarbayev University, Astana, Kazakhstan  
chewyeejian@gmail.com, {yhpang, syooi}@mmu.edu.my  
kokseng.wong@nu.edu.kz

**Abstract.** Machine learning techniques have been extensively adopted in the domain of Network-based Intrusion Detection System (NIDS) especially in the task of network traffics classification. A decision tree model with its kinship terminology is very suitable in this application. The merit of its straightforward and simple “if-else” rules makes the interpretation of network traffics easier. Despite its powerful classification and interpretation capacities, the visibility of its tree rules is introducing a new privacy risk to NIDS where it reveals the network posture of the owner. In this paper, we propose a sensitive pruning-based decision tree to tackle the privacy issues in this domain. The proposed pruning algorithm is modified based on C4.8 decision tree (better known as J48 in Weka package). The proposed model is tested with the 6 percent GureKDDCup NIDS dataset.

**Keywords:** Network-based Intrusion Detection System (NIDS); Decision Tree; Weka J48; Sensitive Pruning; Privacy; GureKDDCup

## 1 Introduction

Trends of coordinated network attacks are rapidly emerging each day with the advancement of technology. To combat the attacks, intrusion detection system (IDS) has been specifically used for flagging the malicious activity and policy violation. Host-based IDS is used to monitor the misuses of an individual user in a single host [1, 4]; while NIDS is used to flag the malicious network traffics [9]. With the proliferation of artificial intelligence, many machine learning techniques are incorporated with NIDS to detect the anomalous traffic patterns automatically.

Decision tree is one of the notable machine learners used in this domain. It was first introduced as ID3 by Quinlan [13], and many variations have been fostered. It is favoured in this domain because the transparency of its decision rules makes the interpretation possible by network administrator. Unlike other works who focus on improving the classification performances, we take a different approach in this work where a pruning method is proposed by considering a privacy preserving mechanism. Each pruning takes place when the splitting attribute disclosing some sensitive values. The sensitive values can be pre-determined by network administrator. In this work, the pro-

posed pruning framework is appended to Weka J48 decision tree [6]. This newly proposed pruned J48 is then tested on the 6 percent version of GureKDDCup IDS dataset [12].

## 2 Related Work

Many machine learning algorithms have been successfully deployed in this domain. In view of the proposed method in this paper is appended on a decision tree, the literature studies will primarily focus on the various modifications done on decision trees despite of all different kinds of machine learning techniques.

Depren et al. [5] proposed a hybrid NIDS by combining self-organising map as the anomaly detection module and J48 decision tree as the misuse detection module. In order to utilise the results of both modules, a decision support system is employed in such a way that if either one of the modules detects the traffic as an attack, the traffic will be automatically classified as an attack. Testing on 10 percent of KDDCup'99 dataset, the work reported with a detection rate (true positive rate) of 99.9%, missed rate (false negative rate) of 0.1% and classification accuracy of 99.84% respectively. In their work, only 6 basic features from each connection are utilised [16].

Bouzida et al. [2] proposed an improved version of C4.5 decision tree by modifying the post pruned rules. Generally, it classifies the training instances which do not match the decision tree rules into the default class (highest frequency class). In the case of NIDS, the highest proportion of a class would probably be the “normal” class. Thus, the training instances which do not conform to the decision tree model will be directly classified into “normal” class. To improve the detection against unknown or first-seen attacks, the authors modified the default class of a decision tree model to be “new” class. Thus, the enhanced decision tree model will assign the training instances which do not fit the rules of a decision tree to the “new” class instead of the highest frequency class (“normal”). With this method, the successful rates of 67.98% in detecting low-frequency attacks for user-to-root (U2R) was attained. Classification accuracy of 92.30% with standard deviation of 0.57% was reported. The authors adopted the entire 10 percent KDDCup'99 [16] without any feature extraction.

Xiang et al. [18] proposed a multiple-level hybrid classifier by leveraging the C4.5 decision tree (supervised) and Bayesian clustering (unsupervised) to detect malicious network traffics. In the first level, C4.5 is used to segregate the traffics into 3 primary classes: denial-of-service (DoS), Probe and “others”. “Others” class consisted all instances from normal, U2R and remote-to-local (R2L) class. To segregate the normal traffics from U2R and R2L in this “others” class, Bayesian clustering is adopted. Subsequently, C4.5 is employed again on top of Bayesian clustering to further separate the U2R attacks from R2L attacks. This multiple-level classification module shown the positive sign in reducing the false negative rate to 3.25% while maintaining an acceptable level of false positive rate of 3.2%. With the combined usage of C4.5 and Bayesian clustering, the overall detection rate obtained were 99.19% (DoS), 99.71% (Probe), 66.67% (U2R), 89.14% (R2L) and 96.8% (normal) when testing on 10 percent KDDCup'99 [16].

Kim et al. [10] proposed a hybrid NIDS with C4.5 decision tree (misuse detection) and support vector machines (SVM) (anomaly detection). Initially, a C4.5 decision tree training model is built based on a full set of training data. Avail with the decision tree rules, all leaves which have the “normal” label are further classified with a 1-class SVM. Then, the non-matching traffics will be flagged as “unknown attack”. This model greatly improved the detection rate for “unknown attack” (by approximately ~10%) comparing to the conventional techniques when tested on NSL-KDD [17] with the condition of false positive rate below 10% under ROC curve.

Rai et al. [14] modified the standard C4.5 split values by considering the average value of all instances in the selected attribute. The proposed splitting algorithm is able to reduce the time taken for building a model because the process for sorting the attribute values are no longer needed. By selecting the 16 attributes with the highest information gain from NSL-KDD [17], the work reported with the best accuracy of 79.5245%.

Cataltepe et al. [3] proposed a semi supervised anomaly NIDS by integrating online clustering, online feature selection and decision tree. Instead of labelling the instances with human efforts, authors adopted Clustream (a type of online clustering) to group the similar instances together and label each of them. Lastly, the classification is based on decision tree. Detection rate (recall) of 98.38% and precision rate of 96.28% were reported when tested on the 10 percent KDDCup’99 [16].

Goeschel et al. [8] proposed a hybrid classifier encompassing SVM, J48 decision tree, and Naïve Bayes classifiers with the aim of reducing false positives in NIDS. The hybrid model works in 3 phases. In phase 1, binary SVM is adopted to classify the network traffics into “attack” or “normal”. If the predicted traffics are classified as “normal”, the traffics or instances will not be further processed by the next two classifiers. Following the similar procedure as phase 1, J48 decision tree is employed in phase 2 while Naïve Bayes is utilised in phase 3. Classification accuracy of 99.62% and false positive rate of 1.57% were attained with this approach.

Though many are working on improving the detection rates for NIDS with decision trees, but none of them are considering the privacy property when adopting the decision tree in NIDS. The issue of privacy related to NIDS, especially IP addresses should not be neglected ever since the IP addresses were perceived as part of personal data under the Court of Justice of the European Union [7]. Thus, we propose a pruning model to integrate into decision tree, where all sensitive information from NIDS will be “pruned” and obscured. In specific, this paper will focus on camouflaging the sensitive IP addresses with the proposed pruning method.

### 3 Proposed Model

#### 3.1 Sensitive Pruning

To obscure the sensitive information from the network traffic, we proposed a modified pruning method in decision tree. This pruning method is modified based on the existing Weka J48 decision tree algorithm, which is a Weka version of C4.8 decision tree algorithm. Predominantly, the proposed sensitive pruning method is conducted based on the

sensitive IP addresses which are determined by the user (i.e. network engineer who is familiar to the organisation network architecture). Whenever an IP address is selected as the splitting attribute, it will be skimmed through for reviewing whether the value collides with the predetermined sensitive IP addresses.

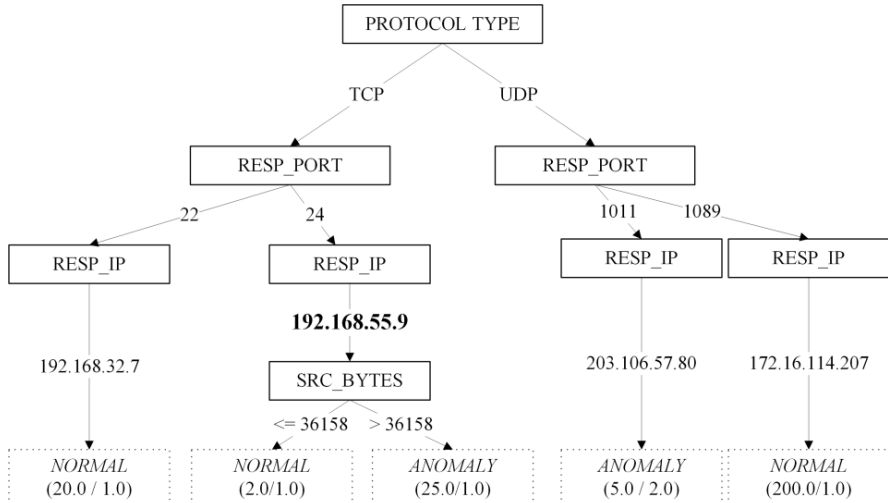


**Fig. 1.** A model of unpruned decision tree

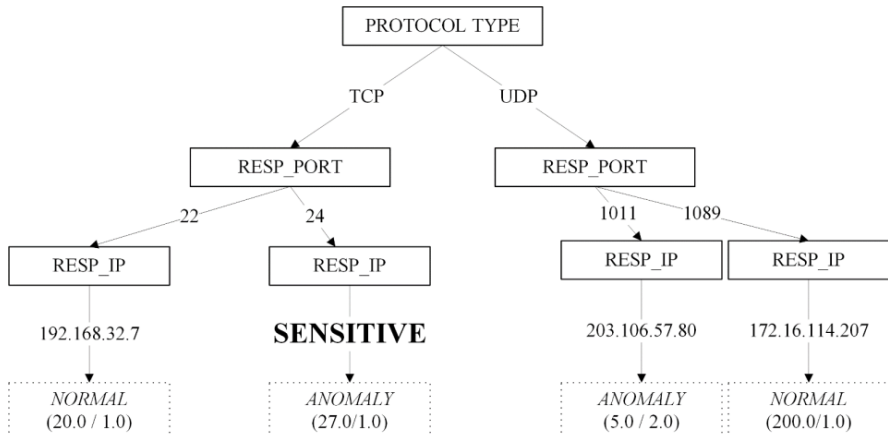


**Fig. 2.** A model of decision tree after Sensitive Pruning

Referring to the example depicted in Figure 1, assume that 192.168.55.9 is pre-set as one of the sensitive IP addresses, this value will be replaced by the word of “SENSITIVE”, thus obscuring its real IP address. Subsequently, all of its child nodes will be pruned into a leaf node as this sensitive branch has been obscured and can no longer be utilised to improve the performance of the model, as depicted in Figure 2. If the sensitive branch is leading to a leaf node, the leaf node is remained as it is without any modification. The sensitive pruning algorithm can be summarised as below:

**Sensitive Pruning Algorithm**

**Input:**  $T_{max}$ , Unpruned Decision Tree;  
Sensitive IP Addresses,  $A_s$

**Output:** Pruned Sensitive Decision Tree

**Procedure:**

1. **for** all node  $t$  in  $T_{max}$ , do
2. Let node  $t_s$  be the child node of  $t$
3. Let Attribute Value  $A$  equals to current split IP Addresses attribute value
4. **if** ( $A == A_s$ ):
5.     Replace  $A$  value with “SENSITIVE”
6.     **if** ( $t_s$  contains any child node):
7.         Replace  $t_s$  with a leaf node
8.     **endif**
9. **endif**
10. **endif**

### 3.2 IP Address Selection and IP Comparison Optimisation

In this proposed pruning algorithm, we supposed the sensitive IP addresses should be determined by the user or network engineer who is familiar to the organisation network architecture itself. Due to the lack of human experts in our case, we take all private IP addresses as the sensitive IP addresses in this paper. It is reasonable to have this assumption because all private IP addresses are part of the organisation, and most of them can reveal a lot of sensitive information [15], including the employees who used the machine, services running on the hosts, activity logs, etc.

**Table 1.** Private IP Addresses Range

Private IP Addresses Range								No. of Hosts
10.	0.	0.	0	~	10.	255.	255.	255
172.	16.	0.	0	~	172.	31.	255.	255
192.	168.	0.	0	~	192.	168.	255.	255

According to Table 1, the total number of private IP addresses approximately reaches 17.8 million. By inputting all of them into the pruning algorithm, the required computation cost and complexity will escalate tremendously to compare each of them during

the iteration of pruning procedure. Therefore, an optimised approach is designed to handle such big amount of private IP addresses. Specifically, each IP address is split into 4 subsets in accordance to the 4 octets available in IPv4. Then, only the first two octets of the IP address will be utilised to determine if it is a private IP address. As a result, instead of comparing 17.8 million IP address, we only have to compare 18 of them. The optimise version for comparing private IP addresses is described as below:

```
Private IP Addresses Comparison Algorithm

Input:           IP , A Single value of IP Address;
Output:          True, If IP Address is Private;
                    False, If IP Address is not Private

Procedure:

1. Split IP into 4 subsets based on dot “.” delimiter.
2. Let IP[1] be the first octet,
   IP[2] be the second octet,
   IP[3] be the third octet and
   IP[4] be the fourth octet.
3. if (IP[1] == 10):
4.   return True
5. elseif (IP[1]==“192” AND IP[2]==“168”):
6.   return True
7. elseif (IP[1]==“192” AND IP[2]==“16~31”:
8.   return True
9. else: return False
```

## 4 Experiment

### 4.1 Experiment Settings

In this paper, it is important to retrieve a pair of IP address because it is one of the required entities for our proposed pruning as described in Section 3. Thus, GureKDDcup [12] is adopted in this study instead of using the classical IDS dataset such as DARPA’98 [11], KDDCup’99 [16] or NSL-KDD [17]. It was generated according to the same process as KDDCup’99 but it additionally includes each pair of IP addresses. As denoted by the creator of GureKDDcup [12], the full dataset of this dataset is too big to be used in learning process. Thus, the reduced sample of 6 percent GureKDDcup (*gureKddcup6percent.arff*) dataset is employed in this paper. All experiments are evaluated in 10 fold cross-validation. To have a fair comparison with other classifiers, no feature extraction process is conducted. Hence, all of the 47 attributes and 28 class labels in the 6 percent GureKDDCup are not normalized or removed. Additionally, unpruned J48 (*J48U*), pruned J48 (*J48P*), unpruned J48 with sensitive pruning (*J48U-SP*), as well as pruned J48 with sensitive pruning (*J48P-SP*) are tested empirically.

## 4.2 GureKDDCup dataset

In Table 2, the name and type of the 47 attributes found in GureKDDCup dataset are tabulated. The metadata are extracted directly from the Attribute-Relation File Format – *gureKDDCup6percent.arff* shared by the dataset creator. As highlighted previously in Section 4.1, all the attributes are not modified or altered to provide a fair judgement between the classifiers.

**Table 2.** Attributes of GureKDDCup Dataset (6 percent)

Attributes	Type	Attributes	Type
connection_number	Num	num_access_files	Num
start_time	Num	num_outbound_cmds	Num
orig_port	Num	is_hot_login	Bin
resp_port	Num	is_guest_login	Bin
orig_ip	Nom	count	Num
resp_ip	Nom	srv_count	Num
duration	Num	serror_rate	Num
protocol_type	Nom	srv_serror_rate	Num
service	Nom	rroror_rate	Num
flag	Nom	srv_rroror_rate	Num
src_bytes	Num	same_srv_rate	Num
dst_bytes	Num	diff_srv_rate	Num
land	Bin	srv_diff_host_rate	Num
wrong_fragment	Num	dst_host_count	Num
urgent	Num	dst_host_srv_count	Num
hot	Num	dst_host_same_srv_rate	Num
num_failed_logins	Num	dst_host_diff_srv_rate	Num
logged_in	Bin	dst_host_same_src_port_rate	Num
num_compromised	Num	dst_host_srv_diff_host_rate	Num
root_shell	Bin	dst_host_serror_rate	Num
su_attempted	Num	dst_host_srv_serror_rate	Num
num_root	Num	dst_host_rroror_rate	Num
num_file_creations	Num	dst_host_srv_error_rate	Num
num_shells	Num		
<b>Num:</b> numeric		<b>Nom:</b> nominal	
		<b>Bin:</b> binary	

## 4.3 Experimental Results

In Table 3, the best classification accuracy is attained by the standard unpruned J48 (*J48U*) and pruned J48 (*J48P*). Although our proposed pruning algorithm (*J48U-SP* and *J48P-SP*) degrades the performance approximately by 0.61%, the loss is considered tolerable as it is able to preserve a certain level of privacy and reduces the complexity of the tree at the same time. Referring to Table 4, the number of final leaves is reduced

by 6355 leaves when adopting the unpruned J48 with sensitive pruning (*J48U-SP*) as compared to the unpruned J48 (*J48U*). In general, a smaller decision tree model with satisfactory performance are preferred in contrast to a larger tree as it is easier to understand and interpret the rules. We also observed the number of prune leaves and nodes does not differ abundantly between *J48P* and *J48P-SP*, the scenario can be justified by the order of pruning operation. For the *J48P-SP*, the default J48 pruning procedure (*J48P*) are performed before the proposed sensitive pruning, and these results depicts that most of the sensitive IP values have already been trim away by the default J48 Pruning (*J48P*) ahead of the proposed sensitive pruning.

**Table 3.** Experimental Results (Classification Accuracy)

Prune Type	Correct Classified Instances	Accuracy (%)	Accuracy Reduction (%)
J48U	178717	99.9480	0.0000
J48P	178710	99.9441	-0.0039
J48U-SP	177626	<b>99.3378</b>	<b>-0.6105</b>
J48P-SP	177612	<b>99.3300</b>	<b>-0.6183</b>

Accuracy Reduced = Accuracy (J48U) – Accuracy (J48P / J48U-SP / J48P-SP) \* 100 (-) Decrease in Accuracy

**Table 4.** Experimental Results (Number of Leaves and Nodes)

Prune Type	Number of Prune Leaves	Number of Prune Nodes	Number of Final Leaves	Number of Final Nodes
J48U	0	0	35805	35876
J48P	357	12393	23448	23483
J48U-SP	<b>6355</b>	<b>6368</b>	29450	29508
J48P-SP	<b>12621</b>	<b>12667</b>	23184	23209

\*Number of prune leaves and prune nodes includes all nodes pruned by sensitive pruning

#### 4.4 Performance Comparison

To corroborate the robustness of the proposed J48 Sensitive Pruning, performance of the proposed algorithm is compared against a set of benchmarks testing as tabulated in Table 5. Due to the lack of prior art, we compare this proposed technique to 8 notable classifiers from Weka package, including SVM (aka SMO in Weka), Naïve Bayes, Adaboost, Bayesian Network, Decision Stump, ZeroR, Random Tree, and Random Forest. All of them are tested and compared on the 6 percent of GureKDDCup dataset with the similar experimental setup as explained in Section 4.1. As can be seen in Table 5, the results obtained are very encouraging. Although *J48U-SP* and *J48P-SP* are

slightly underperforming when compared to the original *J48U* and *J48P*, but the privacy of sensitive rules is conceived. It is also important to note that they are still outperformed Bayesian Network, Adaboost, Decision Stump, ZeroR and Naïve Bayes.

**Table 5.** Benchmark Comparison against other algorithms from Weka Package

Algorithm	Accuracy (%)
SVM (better known as Weka SMO)	99.96
Random Forest	99.96
<b>J48U</b>	99.95
<b>J48P</b>	99.94
Random Tree	99.91
<b>J48U-SP</b>	<b>99.34</b>
<b>J48P-SP</b>	<b>99.33</b>
Bayesian Network	98.80
Adaboost	98.08
Decision Stump	98.08
ZeroR	97.80
NaiveBayes	83.71

## 5 Conclusion and Future Works

In this paper, a sensitive based pruning decision tree is proposed. Through the experimental testing on the 6 percent GureKDDCup dataset, the promising evaluation results spells two advantages: (1) ability to preserve privacy in a fully built decision tree by masking only sensitive values selected, (2) minimal changes on the decision tree structure since the proposed pruning algorithm does not affect the process of attribute selection during tree construction. As the current version of the proposed pruning are not suitable to be applied directly for other domain, further investigation can be conducted on the sensitive pruning to furnish it with flexibility and scalability.

## Acknowledgements

This research work was supported by a Fundamental Research Grant Schemes (FRGS) under the Ministry of Education and Multimedia University, Malaysia (Project ID: MMUE/160029), and Korea Foundation of Advanced Studies (ISEF).

## References

1. Anderson, J.P.: Computer security threat monitoring and surveillance. Tech. Rep. James P Anderson Co Fort Washingt. Pa. 56 (1980).
2. Bouzida, Y., Cuppens, F.: Neural networks vs. decision trees for intrusion detection. Commun. 2006. ICC '06. IEEE Int. Conf. 2394–2400 (2006).
3. Cataltepe, Z. et al.: Online feature selected semi-supervised decision trees for network intrusion detection. Proc. NOMS 2016 - 2016 IEEE/IFIP Netw. Oper. Manag. Symp. AnNet, 1085–1088 (2016).
4. Denning, D.E.: An Intrusion-Detection Model. IEEE Trans. Softw. Eng. SE-13, 2, 222–232 (1987).
5. Depren, O. et al.: An intelligent intrusion detection system (IDS) for anomaly and misuse detection in computer networks. Expert Syst. Appl. 29, 4, 713–722 (2005).
6. Frank, E. et al.: The WEKA Workbench. Morgan Kaufmann, Fourth Ed. 553–571 (2016).
7. Frederik, Z.B.: Behavioral Targeting: A European Legal Perspective. IEEE Secur. Priv. 11, 82–85 (2013).
8. Goeschel, K.: Reducing false positives in intrusion detection systems using data-mining techniques utilizing support vector machines, decision trees, and naive Bayes for off-line analysis. Conf. Proc. - IEEE SOUTHEASTCON. 2016-July, (2016).
9. Heberlein, L.T. et al.: A network security monitor. In: Proceedings. 1990 IEEE Computer Society Symposium on Research in Security and Privacy. pp. 296–304 IEEE (1990).
10. Kim, G. et al.: A novel hybrid intrusion detection method integrating anomaly detection with misuse detection. Expert Syst. Appl. 41, 4 PART 2, 1690–1700 (2014).
11. Lippmann, R.P. et al.: Evaluating intrusion detection systems: the 1998 DARPA off-line intrusion detection evaluation. In: Proceedings DARPA Information Survivability Conference and Exposition. DISCEX'00. pp. 12–26 IEEE Comput. Soc.
12. Perona, I. et al.: Generation of the database gurekddcup. (2016).
13. Quinlan, J.R.: Induction of Decision Trees. Mach. Learn. 1, 1, 81–106 (1986).
14. Rai, K. et al.: Decision Tree Based Algorithm for Intrusion Detection. Int. J. Adv. Netw. Appl. 07, 04, 2828–2834 (2016).
15. Riboni, D. et al.: Obfuscation of sensitive data in network flows. IEEE Conf. Comput. Commun. INFOCOM 2012. 23, 2, 2372–2380 (2015).
16. Stolfo, S.J. et al.: Cost-based modeling for fraud and intrusion detection: results from the JAM project. In: Proceedings DARPA Information Survivability Conference and Exposition. DISCEX'00. pp. 130–144 IEEE Comput. Soc (2000).
17. Tavallaei, M. et al.: A detailed analysis of the KDD CUP 99 data set. IEEE Symp. Comput. Intell. Secur. Def. Appl. CISDA 2009. Cisda, 1–6 (2009).
18. Xiang, C. et al.: Design of multiple-level hybrid classifier for intrusion detection system using Bayesian clustering and decision trees. Pattern Recognit. Lett. 29, 7, 918–924 (2008).



# A Sequential Approach to Network Intrusion Detection

Nicholas Lee, Shih Yin Ooi and Ying Han Pang

Faculty of Information Science & Technology,

Multimedia University, Malacca, Malaysia

lmz.nicholas@gmail.com, {syooi, yhpang}@mmu.edu.my

**Abstract.** In this paper, we combine the sequential modeling capability of Recurrent Neural Network (RNN), and the robustness of Random Forest (RF) in detecting network intrusions. Past events are modelled by RNN, capturing informative and sequential properties for the classifier. With the new output vectors being incorporated into the input features, RF is exacted to consider high-level sequential representation when selecting the best candidate to split. The proposed approach is tested and compared on the UNSW-NB15 data set, demonstrating its competence with encouraging results, and achieving an optimal trade-off between detection and false positive rate.

**Keywords:** Network-based Intrusion Detection System, Machine Learning, Random Forest, Recurrent Neural Network.

## 1 Introduction

An intrusion is any set of actions intended to compromise the confidentiality, integrity, or availability of a resource [1]. Network intrusions are prevalent, increasingly sophisticated, and are adept at hiding from detection [2]. To counteract this ever-evolving threat, Network-based Intrusion Detection System (NIDS) has since become a significant topic of research. IDS generally faces limited tolerance on the number of misclassifications [3]. Being unable to detect traces of intrusion could lead to alarming consequences, while having too much false positives undermines the efforts of investigation, rendering an alarm of IDS inconsequential [4].

In this paper, we present an approach in detecting network intrusions through the use of machine learning techniques. In addition to the connection features extracted from the traffic, our approach also factors in a series of past events to classify an observation. Through a trained RNN: Long Short-Term Memory (LSTM) specifically, high-level features can be retrieved as a representation of the past observations. Since Random Forest (RF) is robust in handling high-dimensional data, the learned representation can be combined to allow improved predictive qualities. Our proposed methodology: RNN-RF has shown its competitive performance on UNSW-NB15 data set, further evident by the comparative results of various existing techniques.

The rest of this paper is organized as follows: Section 2 presents the literature study of recent techniques employed for NIDS. The proposed approach is detailed in Section

3. Section 4 discusses on the particulars of data set, implementation, and the experimental results. Finally, the concluding remarks of the study are provided in Section 5.

## 2 Related Works

In this section, literature study of relevant works and their methodologies are presented. UNSW-NB15 data set is adopted in this study due to it containing modernized network traffic and attacks. Thus, we focus on studies which employed UNSW-NB15 and is by no means exhaustive.

Bamakan et al. [5] proposed Ramp Loss K-Support Vector Classification-Regression (Ramp-KSVCR) under the premise of multi-class classification. Utilizing the proposed methodology, the authors have tackled the issues of imbalanced attacks' distribution, as well as the susceptibility of Support Vector Machine (SVM) to outliers. Improved performance over multi-classification and skewed data set is achieved by adopting K-SVCR as the core of the authors' proposed methodology. Furthermore, the latter issue is solved by implementing Ramp loss function, in which its non-convex property allows for the desired robustness.

Papamartzivanos et al. [6] combined the strengths of both Decision Tree (DT) and Genetic Algorithm (GA) in generating intrusion detection rules. The proposed methodology – Dendron – aims to create linguistically interpretable, yet effective rules when dealing with the detection of attacks and to their corresponding categories. To further increase Dendron's effectiveness over the minority classes, a weighted selection probability function is devised to aid in evolving DT classifiers.

By means of anomaly-based approach, Moustafa et al. [7] introduced Beta Mixture Model (BMM-ADS) to tackle the complexity of intrusion detection. BMM is used to establish normal profile from selected 8 features of legitimate observations. In order to determine the dichotomy of normal and anomaly records, lower-upper Interquartile Range (IQR) baseline is also applied. Any observations outside the baseline are regarded as anomalies, potentially allowing the detection of zero-day attacks.

AL-Hawawreh et al. [8] proposed a model for Internet Industrial Control Systems (IICSs) by employing Deep Autoencoder (DAE) and Deep Feedforward Neural Network (DFFNN). To allow for better convergence properties, initialization parameters are obtained by pre-training DAE on normal traffic instances. Thereafter, pre-trained weights are used in initializing DFFNN before supervised training take place. Emphasis is also given on the importance of IDS components placement in IICS setting.

Yang et al. [9] developed a hybrid technique using Modified Density Peak Clustering Algorithm and Deep Belief Network (MDPCA-DBN). The authors modified DPCA by adopting Gaussian kernel function, this enables the clustering of a more complex and linearly inseparable data set. Each DBN classifier is then independently trained on the now complexity-reduced subset, efficiently extracting abstract features without any heuristic rules.

In view of the recent works, where the trained model makes a prediction independently of previously seen instances, we therefore explore the problem differently by considering the preceding observations. Our approach exploited the modeling

capability of LSTM network in order to extract the representation of previous instances. The acquired output vectors are then additionally incorporated to provide high-level features for the RF classifier.

### 3 Proposed Methodology

#### 3.1 Random Forest

Random Forest (RF) is an ensemble learning technique developed by Breiman [10], incorporating together several novel ideas from previous studies. RF makes a prediction by combining the votes of multiple decision trees. Each decision tree in RF acts as a classifier and contributes to the overall votes. To grow an individual tree:

1. Let  $N$  be the total number of instances from train set, create a bootstrap sample from  $N$  instances.
2.  $m$  sub-features are randomly selected out of  $M$  input features, adhering to the condition where  $m \ll M$ .
3. Best candidate from the selected  $m$  features is chosen to split into daughter nodes.
4. Tree is fully grown, without the need of pruning.

Due to its training procedures, it is more robust to noises and overfitting when compared to its AdaBoost counterpart. Besides, various empirical studies have also shown the performances of RF that rivals some of the popular state-of-the-art methods.

#### 3.2 Recurrent Neural Network

To capture insightful features from a sequence of events, a network specialized in modeling sequential data is required. Hence, a notable architecture of RNN is adopted: Long Short-Term Memory (LSTM). LSTM network is originally proposed by Hochreiter et al. [11] and further improved by Gers et al. [12]. Since then, it has been consistently exploited and found itself useful in many diverse applications.

The forward pass of an LSTM cell is defined as follows:

$$h_t = \tanh(c_t) \odot o_t \quad (1)$$

$$c_t = c_{t-1} \odot f_t + z_t \odot i_t \quad (2)$$

$$z_t = \tanh(W^z x_t + R^z h_{t-1} + b^z) \quad (3)$$

$$f_t = \sigma(W^f x_t + R^f h_{t-1} + b^f) \quad (4)$$

$$i_t = \sigma(W^i x_t + R^i h_{t-1} + b^i) \quad (5)$$

$$o_t = \sigma(W^o x_t + R^o h_{t-1} + b^o) \quad (6)$$

Where  $x_t$  is the input, and  $h_t$  is the output of LSTM cell at time step  $t$ . Input weights, recurrent weights, and biases are denoted by  $W$ ,  $R$ , and  $b$  respectively. The information

flow in an LSTM cell is regulated by forget  $f$ , input  $i$ , and output  $o$  gating units. Essentially, it is the component of state unit  $c$  that allows past information to be transferred over a long distance, and conveniently discard it when necessary.

### 3.3 Proposed RNN-RF

The training phase of the proposed methodology consists of two stages. During the first stage, LSTM is trained with a supervised criterion, learning a good representation for the fully-connected layer. On top of being able to account for the previous traffic events, it also eliminates the need for manual feature engineering. The network is also trained in a many-to-one manner. Having a look-back window of length  $s$ , it seeks to predict the normality of data at current timestep.

The latter part of training phase begins once LSTM has completed its training. Since the network is now able to yield properties that make a classification task easier, new representation of the data can be obtained by taking the output vectors from each layer of the trained model. Finally, the output vectors are concatenated altogether with the original features, serving as the input data for training RF classifier. Original data with  $n$ -dimensional features, will consequently have a representation  $x' \in \mathbb{R}^{n+u \cdot \ell}$ , where  $u$  and  $\ell$  denote the number of LSTM hidden units and layers respectively.

In the testing phase, data are passed through the trained model in the same manner. The newly represented test set is then used by RF classifier to make prediction choices. A summarization of the proposed methodology is illustrated in Fig. 1.

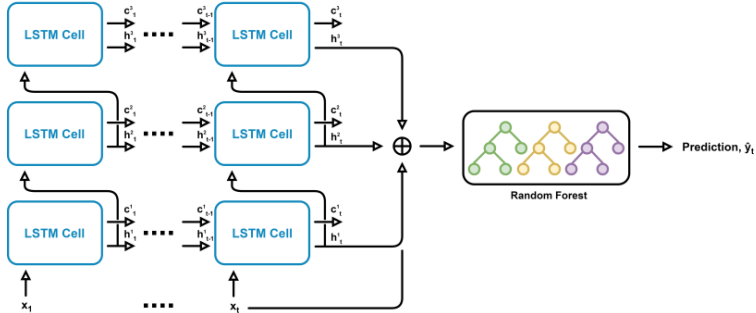


**Fig. 1.** Architectural summary of the proposed methodology

## 4 Experimental Setup

### 4.1 Data set

UNSW-NB15 is created by Moustafa et al. [13-14] in order to improve the complexity of NIDS data set, while addressing some of the major shortcomings found in KDDCup99 [15] and NSL-KDD [16]. Despite NSL-KDD being an improved derivative from KDDCup99 [17], it still carries over few issues found in its preceding counterpart.

Moreover, NSL-KDD does not represent modern low footprint attacks, as is being inherent in KDDCup99 [13,18].

To create UNSW-NB15 data set, the authors deployed IXIA PerfectStorm tool in generating both realistic normal and malicious network traffic. Different techniques were utilized for the extraction of features, capturing a total of 2,540,044 instances in comma-separated values (CSV) format. A partitioned version of the data set is also created by the authors, containing both train and test set, further aiding the evaluation of NIDS.

As hyperparameter optimization and early stopping will be carried out, a validation set is necessary. By observing validation error, it allows for fair selection of best hyperparameter, and hereafter avoiding the pitfall of overfitting to the test set [19]. In this study, validation set is created by extracting 10% of the instances (17,534) from the original train set, while preserving its sequential order to the best extent possible. However, to account for all attack types available, half of 10% had to be split at the leading train set, while the other 5% is extracted at the end.

Table 1 shows the number of instances for each attack types, both before and after the validation split. In this study however, we focus on the detection of attacks, neglecting the concern of correctly classifying an attack type. Thus,  $C_1$  will represent normal class, while  $C_2$  will be the class indicating the presence of attack.

**Table 1.** Total instances of data set

Class	Original Data Set		Split Data Set		
	Train	Test	Train	Validation	Test
Normal	56,000	37,000	47,233	8,767	37,000
Analysis	2,000	677	1,946	54	677
Backdoor	1,746	583	1,705	41	583
DoS	12,264	4,089	11,965	299	4,089
Exploits	33,393	11,132	32,513	880	11,132
Fuzzers	18,184	6,062	17,662	522	6,062
Generic	40,000	18,871	33,356	6,644	18,871
Reconnaissance	10,491	3,496	10,197	294	3,496
Shellcode	1,133	378	1,102	31	378
Worms	130	44	128	2	44
Total	175,341	82,332	157,807	17,534	82,332

The data set contains a total of 42 features, with the exclusion of *id* and ground truths. Features are extracted from varying sources, and are comprised of both categorical and numerical (float, integer or binary) types.

**Data Transformation.** In order to better represent categorical data, 3 features: *protocol*, *service* and *state* are encoded using one-hot encoding scheme. A dimension is created for each new feature value found in the train set. The now extended dimensions

indicate the presence or absence of certain category, represented by binary [0, 1]. Following this scheme, the resulting data sets are extended into 194-dimensional features.

**Data Normalization.** Furthermore, as the range of numerical features differ considerably from one another, features scaling is also applied. Specifically, the general approach: min-max normalization (7) is adopted by scaling feature values linearly into the range of [0, 1].

## 4.2 Evaluation Metrics

Several metrics are used in this study to assess the performance of NIDS model. The metrics hinged on these four predicted conditions:

- $TP_i$  denotes the number of correct predictions on  $i^{th}$  class.
- $TN_i$  denotes the number of correct predictions that are not of  $i^{th}$  class.
- $FP_i$  denotes the instances not belonging to  $i^{th}$  class, but are predicted as one.
- $FN_i$  denotes the instances belonging to  $i^{th}$  class, but are predicted otherwise.

*Accuracy (ACC)* is the prevalent metric used in evaluating NIDS. It shows the proportion of correctly classified instances across all classes ( $|C|$ ), with respect to the total number of instances ( $N$ ).

$$\text{Accuracy (ACC)} = \frac{1}{N} \sum_{i=1}^{|C|} TP_i \quad (7)$$

However, *Accuracy* does not always convey the actual performances. It is especially obvious when the class distributions of the data are exceedingly imbalanced. Hence, *Mean F<sub>1</sub> score* is used alongside to express the balance between *Precision (PPV)* and *Recall (DR)*.

$$\text{Mean } F_1 \text{ score} = \frac{1}{|C|} \sum_{i=1}^{|C|} \frac{2 \cdot PPV_i \cdot DR_i}{PPV_i + DR_i} \quad (8)$$

$$\text{Precision}_i (PPV_i) = \frac{TP_i}{TP_i + FP_i} \quad (9)$$

$$\text{Recall}_i (DR_i) = \frac{TP_i}{TP_i + FN_i} \quad (10)$$

Both *Recall* and *False Positive Rate (FPR)* are metrics often used to present a more detailed interpretation. *Recall* (also known as detection rate) of an attack measures the rate of correctly detected attacks with respect to all the true attack instances. *FPR* in contrast, is the rate at which normal instances are incorrectly classified as an attack.

$$\text{False Positive Rate}_2 (FPR_2) = \frac{FP_2}{TN_2 + FP_2} \quad (11)$$

### 4.3 Results and Discussion

LSTM models are implemented with the aid of TensorFlow 1.12, while the creation of the conventional classifiers: Support Vector Machine (SVM), Naïve Bayes (NB), Decision Tree (C4.5), Adaboost.M1 (with C4.5 as weak learner), and Random Forest (RF), are all carried out using Weka 3.8.

The standard LSTM architecture is trained with Adam optimizer [16], using learning rate of 0.001. To avoid overfitting, early stopping is utilized to decide when to stop the training. With patience level set to 24, training will be halted if no reduction in validation loss is observed after 24 epochs. Except gradient clipping, no other architectural extensions are specifically used throughout this study. Apropos of other hyperparameters, grid search is employed to select the optimal pair, and follows the search space boundary as defined in Table 2.

**Table 2.** Grid search hyperparameters

	C1	C2	C3	C4	C5	C6	C7	C8	C9
Hidden Units	128	128	128	256	256	256	384	384	384
Mini Batch	128	256	512	128	256	512	128	256	512
Network Layer ( $\ell$ )							{1, 2, 3}		
Sequence Length (s)							{4, 8, 16, 32}		

To achieve a fair comparison, the best LSTM model is decided upon by the highest validation *Mean F<sub>1</sub> score*. The best scorer reflects the ability to ascertain most attacks effectively, while keeping false positives to the bare minimum. **Error! Reference source not found.** outlines the validation results of differing hyperparameters. The best validation score is obtained with the setting of 384 hidden units, 128 mini-batch size, 2 layers and a sequence length of 32.

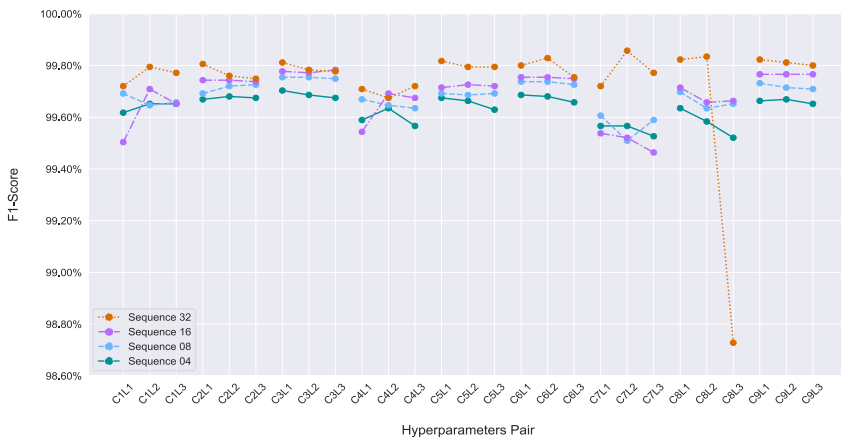


**Fig. 2.** Validation results of trained LSTM

Thereafter, RF classifier is trained on the generated output vectors. The final test results are recorded using the same metric and are shown in Fig. 3. From the figures, varying sequence lengths are distinguished by indifferent markers or line styles. Besides, the connecting lines (extending up to 3 intervals) highlight the changes using the same hyperparameters setting, but with varying number of layers,  $L \in \{1, 2, 3\}$ .

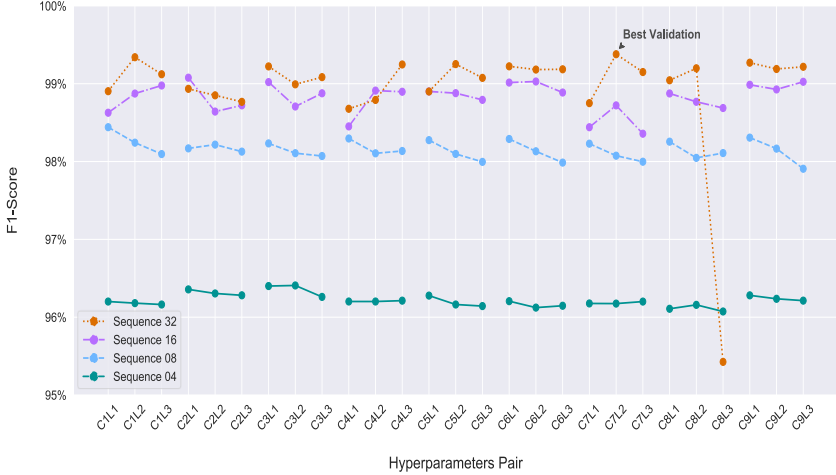


**Fig. 3.** Test results of RNN-RF

From both the validation and test results shown, they consistently display a gain in performance as the sequence length gets longer. Other hyperparameter settings however, do not reflect an apparent causation. In comparison with the test results, validation scores are condensed and do not represent the test set as precisely. This can be seen from the figures wherein the increase in layer size of certain hyperparameters do not reflect the same behavior during the testing phase. In spite of that, the best performing validation setting is able to rank equally as high when evaluated on the test set. Using this hyperparameters setting, the confusion matrix of the final test result is shown in Table 3.

Another notable observation is the performance dip that occurs when using C8L3 with a sequence length of 32. As the parameters and depth of the network increase, the difficulty in learning follows suit. The inability to converge in time has resulted in premature early stopping for the particular setting. This behavior has also suggested the influence of the non-optimal representation, affecting the prediction capability of RF classifier. **Table 1**

**Table 3.** Confusion matrix of the test result

	Prediction: Normal	Prediction: Attack
Label: Normal	36,736	264
Label: Attack	255	45,077

**Comparative study.** To determine the effectiveness of the proposed methodology, the result is compared alongside with other recent aforementioned studies, as well as few of the prevailing classifiers. As each study is conducted on a different subset of train or test set, it might not indicate an entirely comprehensive comparison, albeit using the same data set.

A summarization of the results is reported in Table 4. Our proposed methodology is able to show promising result as compared to other approaches, achieving a high balance between attack detection and false positive rates. Although our methodology did not attain the highest detection rate, approaches which is able to however, comes with a high false positive trade-off.

**Table 4.** Performance comparison of various techniques (%)

Method	Mean F <sub>1</sub>	DR <sub>2</sub>	FPR <sub>2</sub>	ACC
Ramp-KSVCR [5]	98.72	98.68	2.46	93.52 <sup>a</sup>
Dendron [6]	94.14	89.93	2.61	94.49
BMM-ADS [7]	-	92.70	5.90	93.40 <sup>a</sup>
DAE-DFFNN [8]	-	93.00	8.20	92.40 <sup>a</sup>
MDPCA-DBN [9]	89.96	96.22	17.15	90.21
SVM	79.21	<b>99.89*</b>	42.22	80.97
NB	76.66	67.63	12.26	76.67
C4.5	86.67	97.77	25.69	87.23
Adaboost.M1	86.32	97.46	26.06	86.89
RF	86.81	98.51	26.29	87.40
<b>Proposed RNN-RF</b>	<b>99.38*</b>	99.47	<b>0.72*</b>	<b>99.37*</b>

<sup>a</sup>May include the misclassification of attack categories, thus lowering the overall accuracy obtained

## 5 Conclusion

This paper presents a methodology in detecting network intrusions. RF classifier takes on current observation, as well as the bias representation of trained LSTM when making a prediction. Our approach is evaluated on UNSW-NB15 data set, achieving a stable and reasonable performance even on the lowest look-back sequence. The model with the best validation score is chosen for comparison and has demonstrated its efficacy and robustness. One drawback to this approach however, is the difficulty in interpreting classification decisions. Since the structure of deep learning is inherently a “black box”, probing into the inner workings and providing useful semantics will be the future direction of our work.

## Acknowledgement

This research work was supported by a Fundamental Research Grant Schemes (FRGS) under the Ministry of Education and Multimedia University, Malaysia (Project ID: MMUE/160029), and Korea Foundation of Advanced Studies (ISEF).

## References

1. Heady, R., Luger, G., MacCabe, A., Servilla, M.: The architecture of a network level intrusion detection system. Technical Report CS90-20, Department of Computer Science, University of New Mexico. Other Inf. PBD 15 Aug 1990. (1990).
2. F-Secure: The State of Cyber Security 2017. (2017).
3. Sommer, R., Paxson, V.: Outside the Closed World: On Using Machine Learning for Network Intrusion Detection. In: Security and Privacy (SP), 2010 IEEE Symposium on. pp. 305–316. IEEE (2010).
4. Axelsson, S.: The base-rate fallacy and its implications for the difficulty of intrusion detection. In: Proceedings of the 6th ACM conference on Computer and communications security - CCS '99. pp. 1–7. ACM Press, New York, New York, USA (2004).
5. Hosseini Bamakan, S.M., Wang, H., Shi, Y.: Ramp loss K-Support Vector Classification-Regression; a robust and sparse multi-class approach to the intrusion detection problem. Knowledge-Based Syst. 126, 113–126 (2017).
6. Papamartzivanos, D., Gómez Márquez, F., Kambourakis, G.: Dendron: Genetic trees driven rule induction for network intrusion detection systems. Futur. Gener. Comput. Syst. 79, 558–574 (2018).
7. Moustafa, N., Creech, G., Slay, J.: Anomaly detection system using beta mixture models and outlier detection. In: Advances in Intelligent Systems and Computing. pp. 125–135. Springer, Singapore (2018).
8. AL-Hawawreh, M., Moustafa, N., Sitnikova, E.: Identification of malicious activities in industrial internet of things based on deep learning models. J. Inf. Secur. Appl. 41, 1–11 (2018).
9. Yang, Y., Zheng, K., Wu, C., Niu, X., Yang, Y.: Building an Effective Intrusion Detection System Using the Modified Density Peak Clustering Algorithm and Deep Belief Networks. Appl. Sci. 9, 238 (2019).
10. Breiman, L.: Random Forests. Mach. Learn. 45, 5–32 (2001).
11. Hochreiter, S., Schmidhuber, J.: Long Short-Term Memory. Neural Comput. 9, 1735–1780 (1997).
12. Gers, F.A., Schmidhuber, J., Cummins, F.: Learning to forget: Continual Prediction with LSTM. Neural Comput. 12, 2451–2471 (2000).
13. Moustafa, N., Slay, J.: UNSW-NB15: a comprehensive data set for network intrusion detection systems (UNSW-NB15 network data set). 2015 Mil. Commun. Inf. Syst. Conf. 1–6 (2015).
14. Moustafa, N., Slay, J.: The evaluation of Network Anomaly Detection Systems: Statistical analysis of the UNSW-NB15 data set and the comparison with the KDD99 data set. Inf. Secur. J. 25, 18–31 (2016).
15. Hettich, S., Bay, S.D.: KDD Cup 1999 Data, <https://kdd.ics.uci.edu/>.
16. NSL-KDD, <https://www.unb.ca/cic/datasets/nsl.html>.

17. Tavallaei, M., Bagheri, E., Lu, W., Ghorbani, A.A.: A detailed analysis of the KDD CUP 99 data set. In: IEEE Symposium on Computational Intelligence for Security and Defense Applications, CISDA 2009. pp. 1–6. IEEE (2009).
18. McHugh, J.: Testing Intrusion detection systems: a critique of the 1998 and 1999 DARPA intrusion detection system evaluations as performed by Lincoln Laboratory. ACM Trans. Inf. Syst. Secur. 3, 262–294 (2000).
19. Thomas, R.: How (and Why) to Create a Good Validation Set, <https://www.fast.ai/2017/11/13/validation-sets/>.



# Implementing Bio-Inspired Algorithm for Pathfinding in Flood Disaster Prevention Game

T. Brenda Chandrawati, Anak Agung Putri Ratna, Riri Fitri Sari

Electrical Engineering Department, Universitas Indonesia, Jakarta, Indonesia  
{t.brenda, riri}@ui.ac.id, ratna@eng.ui.ac.id

**Abstract.** Flooding is one of the most frequent disasters. There are many risks due to flood incidents. Floods can cause a lot of damage and casualties. Flood prevention measures are needed to reduce the impact of flooding. Throwing the garbage in its place, making tree planting movements and making Bio-pore are some examples that can be done in maintaining the surrounding environment. Our game proposes an alternative tool that can be used to educate and motivate people to take appropriate action in protecting the environment to avoid flooding. This paper discusses the design and implementation of game creation of environmental maintenance. The Flood Disaster Prevention Game developed with Unity. This paper proposes the firefly algorithm as an algorithm in a flood rescue simulation game. The proposed firefly algorithm will be used to pathfinding. The firefly algorithm is simulated with MATLAB R2016a. The simulation result shows the best position that can be reached is (0.00006, -0.00045) with the final value is 12. This position is assumed as the rescue location of flood victims.

**Keywords:** Flood, Disaster Prevention, Pathfinding, Firefly Algorithm.

## 1 Introduction

Responding to the rapid development of information and communication technology, there have been various efforts to exploit the development of information and communication technology as educational tools [1, 2]. One of them uses games as learning media. Games that are used to educate, train and provide information are called educational games [2]. Therefore, the game design process must pay attention to the educational potential of games, domains and computational models used in games.

The purpose of an educational game is to provide an understanding area to make changes in one's behavior. An example is a game for behavior change in preventing flooding in the environment. Flood is not only caused by high rainfall but also people's behavior that tends to dispose of garbage anywhere, such as to the river. They also set up buildings in areas that are supposed to be the water catchment areas, illegal logging in the forested suburbs for settlement and others. In this paper, we present flood prevention methods through games.

We propose the firefly algorithm as an algorithm in the educational game. The firefly algorithm is used to locate the evacuation location. The firefly algorithm simulation

with MatLab is able to show the number of minimal iterations that can be skipped to get the desired position.

The outline of this paper is as follows: section II discusses the educational game, firefly algorithm, and Unity. Then, it also discusses game design and its implementation, simulation of the firefly algorithm in MatLab.

## 2 Related Work

### 2.1 Serious Game

The game is a rule-based system that has different results that give different values, the player tries to get an appropriate result [3]. However, there are also games that are used to support learning activities referred to as educational games. This game interactively teaches about the purpose of the activity, problem-solving, how to interact and adapt [4, 5]. Educational games are part of Serious Game [4-6].

Serious games can also be used for sharing purposes, such as assessment. An assessment is an important part of learning, both self-assessment and peer assessment [7, 8]. Application areas of the serious game are public, health, engineering, education, communication.

### 2.2 Firefly Algorithm

Bio-inspired computing is a field that uses computers to model natural phenomena that have been compiled into an algorithm that aims to increase computer use. One of the bio-inspired algorithms is the firefly algorithm.

The firefly algorithm is an algorithm that is inspired by the collective social behavior of insect colonies ie the flickering behavior and the bioluminescent communication phenomenon of fireflies [9-13]. Based on the flashing characteristics of fireflies, firefly algorithms have specific rules, namely:

1. All fireflies are unisex. It means that fireflies will be attracted to other fireflies regardless of sex.
2. The attractiveness degree of fireflies is proportional to the brightness of other fireflies. Fireworks that have high brightness will attract fireflies that have lower brightness degrees. However, there are no fireflies that have a higher brightness degree than other fireflies: then the fireflies will move randomly. The brightness of the Fireflies is also affected by the distance and the absorption of light by air.
3. The light intensity of fireflies is determined by the purpose function. For maximization problems, the intensity of light is proportional to the value of the objective function.

There are two important variables on the firefly algorithm, i.e. light intensity, and attractiveness. The intensity of their light can be calculated by the formula [13]:

$$I(r) = I_0 e^{-\gamma r^2} \quad (1)$$

Where  $I_0$  is the original light intensity,  $g$  is the light absorption coefficient, and  $r$  is the distance between firefly  $i$  and  $j$ .

While the attractiveness of fireflies will be proportional to the intensity of light seen by adjacent fireflies, then the attraction of the firefly  $\beta$  can be defined by the formula :

$$\beta = \beta_0 e^{-\gamma r^2} \quad (2)$$

where  $\beta_0$  is the attractiveness at  $r = 0$ .

The distance between two fireflies  $i$  and  $j$  can be defined by Cartesian distance :

$$r_{ij} = \|x_i - x_j\| = \sqrt{\sum_{k=1}^d (x_{i,k} - x_{j,k})^2} \quad (3)$$

where  $x_{i,k}$  is the  $k$ th component of the firefly spatial coordinate  $x_i$  firefly. In order to determine the movements of firefly  $i$  that are attracted to firefly  $j$  which is lighter used the formula :

$$x_i = x_i + \beta_0 e^{-\gamma r^2} \beta_{ij} (x_j - x_i) + \alpha \epsilon_i \quad (4)$$

The second part of equation (4) is the part that shows attraction. The third part is randomization,  $\alpha$  is the random parameter and  $\epsilon_i$  is the random number vector of the Gaussian distribution or the uniform distribution.

The Firefly Algorithm is widely used to solve optimization problems and engineering problems, such as Digital Image Processing [14-17], Traveling Salesman Problem [18-20], Routing [21-25], Scheduling [26-29], Clustering [30-32], Antenna Design [33-37]. The firefly algorithm can also be used to minimize the distance that the drill is drilled in the PCB hole drilling process [38].

Path planning is a planning path that will be traversed by robots, starting from the starting point to the destination point. Path planning is the shortest path and is free from obstacles [39, 40]. Liu et al. [41] use Adaptive Firefly Algorithm to plan the path to be taken by the ship. Liu et al. propose some adaptive parameters used to find paths, namely adaptive absorption parameters and adaptive random parameters. These two adaptive parameters aim to increase global search capabilities and accelerate convergence to the optimal global at the end of the search. Liu et al. [42] proposed the Path Planning Modified Firefly Algorithm (PPMFA) to improve the convergence lags of standard firefly algorithms. This PPMFA is used in 3D path planning for the Autonomous Unmanned Vehicles (AUV). Hidalgo-Paniagua et al. [40] solve the problem of planning a robotic multi-objective path using the firefly algorithm (MO-FA) by making an environmental model, coding paths and objectives to be achieved. Environmental modeling is made in 2D space by dividing rows and columns and different colors on the map. The path through which the robot is a set of coordinates,  $(X_1, Y_1)$  is the coordinates of the starting point and  $(X_n, Y_n)$  represents the destination point. The aim to be achieved by MO-FA is path safety, lane length and path smoothness (related to energy consumption). Wang et al. [43] proposed a Modified Firefly Algorithm (MFA) which was used to solve Unmanned Combat Air Vehicle (UCAV) path planning problems. The aim of the proposed MFA is the discovery of safe routes by avoiding threat areas

and minimum fuel costs. Patle and Parhi [44] use the Firefly algorithm to achieve two objectives of mobile robot navigation, namely optimal path generation and avoiding obstacles with co-incentric spherical geometry techniques. The proposed research is the search for the fastest time and with obstacles in each path, to find a relatively safe path and the fastest travel time in the flood disaster rescue simulation.

### **2.3 Tools used to develop the game**

The game engine used to create this Flood Prevention Game is Unity. Unity is one of the free types game engines.

## **3 Flood Disaster Prevention Game**

In the development of our proposed game, two crucial phases are research and development. The first stage of the research is to gain specific knowledge related to game material [45]. The next phase is the development which includes design, implementation and testing activities. Flood Prevention Game is an educational game designed to give people insight into the correct behavior in protecting the environment from floods.

### **3.1 Design of Flood Disaster Prevention Game**

Flood Prevention Game is a 2D game consisting of two stages, game of habit and game of rescue. The first stage has four games. At the first game, players are invited to dispose of garbage in the place that has been provided. At the second game, the player is required to clear the drain. Being at the third and the fourth game, the player will do the simulation by following step by step to complete a particular mission of planting trees and making bio-pore holes. This second stage has two games. The first game will invite players to experience for themselves what to do in case of flooding by doing some technical methods of building sandbags, setting pumps and rescuing property. Moreover, the second game, a rescue simulation for a family. A family consisting of several family members, father, mother, two children, grandma, grandpa, and household assistant.

### **3.2 Implementation Flood Disaster Prevention Game**

Making an exciting game, we need immersion. Immersion is virtual reality or impression that can bring players into the world of games created by adapting real-world conditions into the virtual world.

In this section, the implementation results of the Flood Prevention Game are presented. Flood Prevention Game is a game that has simple rules, namely, grab and drop. At the first and the second game, the player can select one of the garbage (grab) and then throw the selected garbage into the appropriate garbage bins (drop). The third

and the fourth game are simulation games in we have caused which requires advanced algorithms. The screenshot of the game can be seen in Fig. 1.

Game of rescue\_2 is still a draft game, and this is a simulation game. This game tells about the rescue of a family, which consist of father, mother, grandfather, grandmother, two children, and a household assistant. In the event of a flood, the family will be rescued, get out of their house and determine the path to the rescue. In doing the rescue, there are several things to consider are age, disability, health, the ability to swim.

All the family members are in their place; grandmother and grandfather are in their room. Dad is doing office work in his office. The housekeeper was in the kitchen. Mother and children are in their rooms. As when there will be heavy rains, and finally, floods will hit, they will all be evacuated to the evacuation center through a safe route.

### 3.3 Path Optimization Problem in Game of Rescue\_2

In making Game of rescue\_2, a bio-inspired algorithm will be used to find a path for flood victims to reach a safe location. The Firefly algorithm can be adapted in applications in finding the best evacuation center for moving victims [46, 47].

ChePa et al. [46] and Yusof et al. [47] explained their work on creating a decision making an application called the Adaptive Emergency Evacuation Center (AEECM) using firefly algorithm. This algorithm has several factors to be considered when selecting the best evacuation center, i.e. evacuation center size (V1), distance between evacuation centers (V2), nearest river height (V3), and evacuation center distance to a nearby river (V4)). On the other hand, firefly algorithm also takes into account the important parameters in which the algorithm will operate i.e. the light absorption coefficient ( $\gamma$ ), the attractiveness agent ( $\beta$ ), the maximum number of generations, and the number of fireflies.

The firefly algorithm was introduced by Xin-She Yang as one of the Nature-Inspired Metaheuristic Algorithms [48]. Firefly algorithms adapted in Game of Rescue\_2 are used to locate evacuation centers for flood victims.

To see the performance of the firefly algorithm, the specific optimization function is chosen, namely the parabolic function:

$$f(x_1, x_2) = 12 - (x_1^2 + x_2^2)/100 \quad (5)$$

The parameters in the algorithm which will be used for the simulation are  $\gamma$ ,  $\alpha$ , and  $\beta$ . The initial simulation is carried out with the value of  $\gamma$  [0,1], and  $\alpha$  [0,1]. At the parameter value  $\gamma$  is 0.5, the value of  $\alpha$  is 0.2, parameter  $\beta_0$  is 1 is the best result. The number of fireflies is 20. The maximum number of iteration is 100. The final destination point of the firefly is point 0 (0,0).

**Algorithm 1** Psedocode of the Firefly Algorithm (FA)

---

```

1. Objective function  $f(\mathbf{x})$ ,  $\mathbf{x}=(x_1, x_2, \dots, x_d)^T$ 
2. Generate initial population of fireflies  $\mathbf{x}_i(1, 2, \dots, n)$ 
3. Light intensity  $I_i$  at  $\mathbf{x}_i$  is determine by  $f(\mathbf{x}_i)$ 
4. Define light absorption coefficient  $\gamma$ 
5. Define randomization parameter  $\alpha$ 
6. while ( $t < MaxGeneration$ )
7.   for  $i=1 : n$  all  $n$  fireflies
8.     for  $j=1 : n$  all  $n$  fireflies (inner loop)
9.       if ( $I_i < I_j$ ), move firefly  $i$  towards  $j$ ; end if
        Vary attractiveness with distance  $r$  via  $\exp[-\gamma r]$ 
        Evaluate new solutions and update light intensity
10.    end for  $j$ 
11.  end for  $i$ 
12. Rank the fireflies and find the current global best  $g^*$ 
13. end while

```

---

From the predetermined parameters, it shows that the convergent value is achieved in a small number of iterations. The final position of all fireflies is (0.00006, -0.00045) and the distance deviation is 0.045 in the 14th iteration. The speed of convergence and the density of the final position of those fireflies are very important to note because this algorithm will be used to search routes with the fastest travel time for flood victims. Fig. 2 shows that at the 14<sup>th</sup> iteration a convergent value can be reached.

Environmental modeling consisting of several possible paths for flood victims can be seen in Fig. 3. Each pathway has an obstacle. k1, k2, and k3 show some obstacles to describe the condition of the path to be traversed. k1 shows the slippery path, k2 shows the waterlogged path and k3 indicates the level of proximity of the path near the river.

## 4 Conclusion

In this paper, we have discussed a game designed to solve the environmental problems and educate the user to take the right action in treating waste. In the game, we also simulate the condition in which a flood disaster happens, and we have to find an optimal algorithm to find a path from the victim's location to the evacuation location. Disaster Game is an alternative method to induce awareness to the environmental problems, and it changes the behavior of the society in protecting the environment to be free from a disaster such as a flood. The algorithm used is firefly algorithms. The next research, the firefly algorithm will be compared with another optimization algorithm.

## 5 Acknowledgment

This work is supported by a doctoral dissertation research grant from the Ministry of Research, Technology, and Higher Education (Kemristekdikti) under grant no. NKB-1849/UN2.R3.1/HKP.05.00/2019.

## References

1. Ponticorvo, M., et al. Bio-inspired computational algorithms in educational and serious games: some examples. in European Conference on Technology Enhanced Learning. 2016. Springer.
2. Vasudevamurt, V.B. and A. Uskov. Serious game engines: Analysis and applications. in Electro/Information Technology (EIT), 2015 IEEE International Conference on. 2015. IEEE.
3. Juul, J. Half-real: Video games between real rules and fictional worlds. 2011: MIT press.
4. Bubphasuwan, N., et al. Serious game learning for novice practitioners in psychomotor domain. in Student Project Conference (ICT-ISPC), 2016 Fifth ICT International. 2016. IEEE.
5. Toma, I., M. Dascalu, and S. Trausan-Matu. Seeker: A serious game for improving cognitive abilities. in RoEduNet International Conference-Networking in Education and Research (RoEduNet NER), 2015 14th. 2015. IEEE.
6. Furuchi, M., M. Aibara, and K. Yanagisawa. Design and implementation of serious games for training and education. in Control (CONTROL), 2014 UKACC International Conference on. 2014. IEEE.
7. Guenaga, M., et al. A serious game to develop and assess teamwork competency. in Computers in Education (SIIE), 2014 International Symposium on. 2014. IEEE.
8. Rjiba, M. and L.C. Belcadhi. Self-assessment through serious game. in Information & Communication Technology and Accessibility (ICTA), 2015 5th International Conference on. 2015. IEEE.
9. Binitha, S. and S.S. Sathya, A survey of bio inspired optimization algorithms. International Journal of Soft Computing and Engineering, 2012. **2**(2): p. 137-151.
10. Fister Jr, I., et al., A brief review of nature-inspired algorithms for optimization. arXiv preprint arXiv:1307.4186, 2013.
11. Kapur, R. Review of nature inspired algorithms in cloud computing. in International Conference on Computing, Communication & Automation. 2015. IEEE.
12. Kar, A.K., Bio inspired computing—A review of algorithms and scope of applications. Expert Systems with Applications, 2016. **59**: p. 20-32.
13. Qi, X., S. Zhu, and H. Zhang. A hybrid firefly algorithm. in 2017 IEEE 2nd Advanced Information Technology, Electronic and Automation Control Conference (IAEAC). 2017. IEEE.
14. Kanimozh, T. and K. Latha, An integrated approach to region based image retrieval using firefly algorithm and support vector machine. Neurocomputing, 2015. **151**: p. 1099-1111.
15. Mishra, A., et al., Optimized gray-scale image watermarking using DWT-SVD and Firefly Algorithm. Expert Systems with Applications, 2014. **41**(17): p. 7858-7867.
16. Napoli, C., et al. Simplified firefly algorithm for 2d image key-points search. in Computational Intelligence for Human-like Intelligence (CIHLI), 2014 IEEE Symposium on. 2014. IEEE.
17. Rajinikanth, V. and M. Couceiro, RGB histogram based color image segmentation using firefly algorithm. Procedia Computer Science, 2015. **46**: p. 1449-1457.
18. Jati, G.K. Evolutionary discrete firefly algorithm for travelling salesman problem. in International Conference on Adaptive and Intelligent Systems. 2011. Springer.
19. Jati, G.K. and R. Manurung, Discrete firefly algorithm for traveling salesman problem: A new movement scheme, in Swarm Intelligence and Bio-Inspired Computation. 2013, Elsevier. p. 295-312.

20. Kumbharana, S.N. and G.M. Pandey, Solving travelling salesman problem using firefly algorithm. International Journal for Research in science & advanced Technologies, 2013. **2**(2): p. 53-57.
21. Gao, M.-L., et al., Object tracking using firefly algorithm. 2013. **7**(4): p. 227-237.
22. Manshahia, M., A firefly based energy efficient routing in wireless sensor networks. African Journal of Computing and ICT, 2015. **8**(4): p. 27-32.
23. Osaba, E., et al., A discrete firefly algorithm to solve a rich vehicle routing problem modelling a newspaper distribution system with recycling policy. Soft Computing, 2017. **21**(18): p. 5295-5308.
24. Pan, F., et al., Research on the Vehicle Routing Problem with Time Windows Using Firefly Algorithm. JCP, 2013. **8**(9): p. 2256-2261.
25. Xu, M. and G. Liu, A multipopulation firefly algorithm for correlated data routing in underwater wireless sensor networks. International Journal of Distributed Sensor Networks, 2013. **9**(3): p. 865154.
26. Karthikeyan, S., et al., A hybrid discrete firefly algorithm for solving multi-objective flexible job shop scheduling problems. 2015.
27. Karthikeyan, S., P. Asokan, and S. Nickolas, A hybrid discrete firefly algorithm for multi-objective flexible job shop scheduling problem with limited resource constraints. The International Journal of Advanced Manufacturing Technology, 2014. **72**(9-12): p. 1567-1579.
28. Khadwilard, A., et al., Application of firefly algorithm and its parameter setting for job shop scheduling. J. Ind. Technol, 2012. **8**(1).
29. Marichelvam, M.K., T. Prabaharan, and X.S. Yang, A discrete firefly algorithm for the multi-objective hybrid flowshop scheduling problems. IEEE transactions on evolutionary computation, 2014. **18**(2): p. 301-305.
30. Banati, H. and M. Bajaj, Performance analysis of firefly algorithm for data clustering. International Journal of Swarm Intelligence, 2013. **1**(1): p. 19-35.
31. Kaushik, K. and V. Arora, A hybrid data clustering using firefly algorithm based improved genetic algorithm. Procedia Computer Science, 2015. **58**: p. 249-256.
32. Sarma, P.N. and M. Gopi, Energy efficient clustering using jumper firefly algorithm in wireless sensor networks. arXiv preprint arXiv:1405.1818, 2014.
33. Grewal, N.S., M. Rattan, and M.S. Patterh, A linear antenna array failure correction with null steering using firefly algorithm. Defence Science Journal, 2014. **64**(2): p. 136.
34. Mohammed, H.J., et al., Design of a uniplanar printed triple band-rejected ultra-wideband antenna using particle swarm optimisation and the firefly algorithm. IET Microwaves, Antennas & Propagation, 2016. **10**(1): p. 31-37.
35. Ram, G., et al., Optimized hyper beamforming of receiving linear antenna arrays using Firefly algorithm. International Journal of Microwave and Wireless Technologies, 2014. **6**(2): p. 181-194.
36. Sharqa, A. and N. Dib, Circular antenna array synthesis using firefly algorithm. International Journal of RF and Microwave Computer-Aided Engineering, 2014. **24**(2): p. 139-146.
37. Singh, U. and M. Rattan, Design of thinned concentric circular antenna arrays using firefly algorithm. IET Microwaves, Antennas & Propagation, 2014. **8**(12): p. 894-900.
38. Ismail, M., et al. Firefly algorithm for path optimization in PCB holes drilling process. in Green and Ubiquitous Technology (GUT), 2012 International Conference on. 2012. IEEE.
39. Chen, X., et al. Global path planning using modified firefly algorithm. in Micro-NanoMechatronics and Human Science (MHS), 2017 International Symposium on. 2017. IEEE.
40. Hidalgo-Paniagua, A., et al., Solving the multi-objective path planning problem in mobile robotics with a firefly-based approach. Soft Computing, 2017. **21**(4): p. 949-964.

41. Liu, C., Z. Gao, and W. Zhao. A new path planning method based on firefly algorithm. in Computational Sciences and Optimization (CSO), 2012 Fifth International Joint Conference on. 2012. IEEE.
42. Liu, C., et al., Three-dimensional path planning method for autonomous underwater vehicle based on modified firefly algorithm. Mathematical Problems in Engineering, 2015. **2015**.
43. Wang, G., et al., A modified firefly algorithm for UCAV path planning. 2012. **5**(3): p. 123-144.
44. Patle, B., et al., On firefly algorithm: optimization and application in mobile robot navigation. 2017. **14**(1): p. 65-76.
45. Hideg, C. and D. Debnath. An introductory programming course using video game design and unity©. in 2017 IEEE International Conference on Electro Information Technology (EIT). 2017. IEEE.
46. ChePa, N., et al., Adaptive Emergency Evacuation Centre Management for Dynamic Relocation of Flood Victims using Firefly Algorithm. Journal of Telecommunication, Electronic and Computer Engineering (JTEC), 2016. **8**(8): p. 115-119.
47. Yusof, Y., et al., Firefly Algorithm for Adaptive Emergency Evacuation Center Management. INTERNATIONAL JOURNAL OF ADVANCED COMPUTER SCIENCE AND APPLICATIONS, 2016. **7**(7): p. 77-84.
48. Yang, X.-S., Nature-inspired metaheuristic algorithms. 2010: Luniver press.



# Specific Gravity-based of Post-harvest *Mangifera indica* L. cv. *Harumanis* for ‘*Insidious Fruit Rot*’ (IFR) Detection using Image Processing

N.S Khalid, S.A.A Shukor and Fathinul Syahir A.S

School of Mechatronic Engineering, Universiti Malaysia Perlis, Perlis, Malaysia  
syahirahkhalid@unimap.edu.my

**Abstract.** Bruising and internal defects detection is a huge concern for food safety supplied to the consumers. Similar to many other agricultural products, *Harumanis* cv. has non-uniform quality at harvesting stage. Traditionally, in adapting the specific gravity approach, farmers and agriculturist will estimate the absence of ‘*Insidious Fruit Rot*’ (IFR) in *Harumanis* cv. by using floating techniques based on differences in density concept. However, this method is inconvenient and time consuming. In this research, image processing is explored as a method for non-destructive measurement of specific gravity to predict the absence of ‘*Insidious Fruit Rot*’ (IFR) in *Harumanis* cv. The predicted specific gravity of 500 *Harumanis* cv. samples were used and compared with the actual result where it yielded a high correlation,  $R^2$  at 0.9055 and accuracy is 82.00%. The results showed that image processing can be applied for non-destructive *Harumanis* cv. quality evaluation in detecting IFR.

**Keywords:** Specific gravity, *Harumanis* cv., ‘*Insidious Fruit Rot*’ (IFR), image processing.

## 1 Introduction

*Mangifera indica* L., also known as mangoes, are a popular as nutritional tropical fruit which are now one of the most important fruits crops in subtropical and tropical area [1]. In Peninsular Malaysia, mangoes are grown in a limited, mixed property or orchard. According to “Fruit Crops Statistics” report produced by Department of Agriculture Putrajaya, Malaysia, the area of mango orchard in Peninsular Malaysia is rising from 5772.7 hectarage in 2015 to 6048.29 hectarage in 2017. At present, there are over 300 cultivars of mangoes with different shapes, colours, sizes, flavours, aroma and fiber contents.

One of the well-known mango cultivar in Peninsular Malaysia is *Harumanis* cv. [2]. This cultivar can be found in Perlis and this cultivar is categorized as one of the most important tropical fruits marketed throughout the world. *Harumanis* cv. is included in the national agenda as a specialty fruits from Perlis [3]. Table 1 shows Perlis exports of *Harumanis* cv. to Japan in 2010 and it is aimed for the export demand increase to 100 metric ton in 2020 [3].

**Table 1.** The target and actual export of *Harumanis cv.* to Japan .

<b>Year</b>	<b>Target</b>	<b>Export</b>
2010	3.1 metric ton	500kg
2011	3.1 metric ton	2.4metric ton
2020	100 metric ton	?

However, the increasing of this cultivar is reportedly hindered due to incidence of internal tissue breakdown known as '*Insidious Fruit Rot*' (*IFR*). This incidence is categorized as a physiological disorder and it does not show any external damage even during ripe stage or harvest time [4]. Typically, the *Harumanis cv.* quality is monitored manually and is incredibly dependent on the human visual system. Traditionally, the water displacement or floating method is applied as a method to predict internal properties or quality of the fruit by applying the density concept [5]. However, this conventional method is very time consuming and less efficient. Therefore, a fast and reliable fruit quality evaluation is needed to overcome this problem. There has been limited research application of specific gravity in *Harumanis cv.*, so the objective of this study is to apply and investigate the relationship between specific gravity and absence of *IFR* in *Harumanis cv.* using image processing techniques.

## 2 Material and Methods

### 2.1 Fruit Samples

A well-known orchard managed by Perlis Department of Agriculture , Malaysia was chosen as the source for the sample of *Mangifera indica L.*, *cv Harumanis*. All 500 optimum samples were randomly picked and supplied by Malaysia's Federal Agricultural Marketing Authority (FAMA), Perlis. They were transported on the same day to the laboratory and were determined by visualizing the position of the shoulders in relation to the position of the stem [6]. The quality of the samples was inspected by expert graders. All samples were washed and dried to completely remove water and dirt from the surface. In order to avoid degradation, image of the fruits were taken after 12 hours of inspection and the experiment was conducted in a constant laboratory temperature of 23°Celsius. Table 2 shows the fundamental characteristics data of the *Harumanis cv.* samples where SD is standard deviation and  $R^2_{SG}$  is correlation coefficient based on Pearson, R between the size and specific gravity of the sample.

**Table 2.** Fundamental characteristics data of *Harumanis cv.* samples used.

	Size (g)			Specific Gravity (g/cm <sup>3</sup> )			
	Mean	Range	SD	Mean	Range	SD	$R^2_{SG}$
<i>Harumanis cv.</i>	323.27	240-425	98.85	1.01	1.2-0.79	0.15	0.79

## 2.2 Specific Gravity Measurement by using Archimedes' Theory

The mass of *Harumanis cv.* samples were measured first by using electronic balance with high precision strain gauge sensor and the reading were recorded. Next, the samples volume was determined by water displacement method also known as Archimedes' theory. In this study, 1500mL of water was poured into the beaker and the samples were then placed into the beaker.

The volume of the sample is taken by using equation 1 and next the specific gravity of the *Harumanis cv.* samples could be calculated by using equation 2 [7] and equation 3 below. Next, the absence of the *IFR* could be predicted from the specific gravity value.

$$V_{sm} = V_{am} - V_{bm} \quad (1)$$

where

$V_{sm}$  = Volume of sample

$V_{am}$  = Volume of water after sample is submerged

$V_{bm}$  = Volume of water before sample is submerged

$$SG = \frac{weight\ in\ air \times SG\ of\ liquis}{weight\ in\ air - weight\ in\ liquid} \quad (2)$$

$$SG = \frac{\rho_{mango}}{\rho_{water}} \quad (3)$$

where

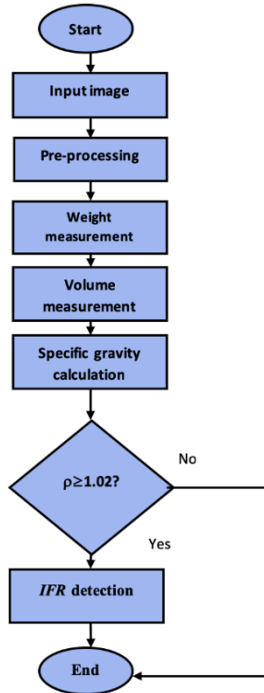
$SG$  = Specific Gravity

$\rho_{mango}$  = density of mango

$\rho_{water}$  = density of water

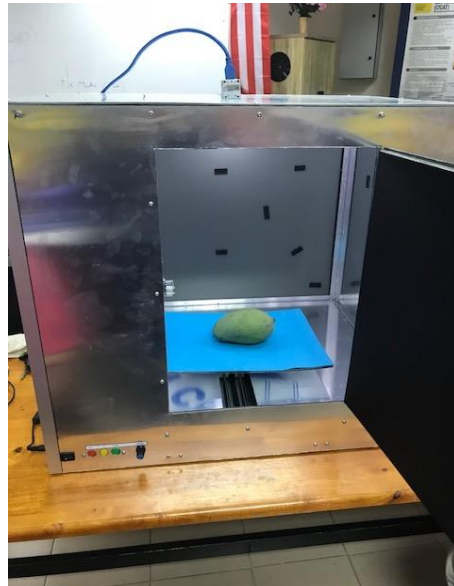
## 2.3 Proposed Method Using Image Processing

Image processing was proposed to determine the specific gravity of *Harumanis cv.* samples. The algorithm to determine the specific gravity value by using image processing is shown in Fig. 1.



**Fig. 1.** Specific gravity algorithm calculation and *IFR* prediction by using image processing.

All the images of *Harumanis cv.* samples were taken by using a Charge Coupled Device (CCD) camera at a fixed distance of 22cm from top view and connected to the personal computer via USB cable. This CCD camera was used to collect the 2D spatial information of the samples for further analysis. The image capturing platform as shown in Fig. 2 is consists of a rectangular box made of aluminum with dimension of 100 cm  $\times$  60 cm  $\times$  100 cm and an ultra-fast speed Basler CCD camera as in Fig. 3 is used for acquiring a visible image. The images of the samples were saved in BMP format for a better quality resolutions [8].



**Fig. 2.** Main frame of the platform



**Fig. 3.** Basler CCD Camera

For the pre-processing part, each picture of the RGB *Harumanis cv.* samples was converted into gray-scale by eliminating the hue and saturation information. Next, it was converted into a binary image based on whether the image pixels fall below or above the threshold value [5] as shown in equation 4. Next, the specific gravity of the samples could be calculated and the presence of *IFR* could be predicted.

$$g(x, y) = \begin{cases} 1, & \text{for } f(x, y) > T \\ 0, & \text{for } f(x, y) \leq T \end{cases} \quad (4)$$

where  $g(x, y)$  is defined as threshold image,  $f(x, y)$  is the source image and  $T$  is the threshold value.

## 2.4 Weight and Volume Estimated

The mass or weight of the *Harumanis cv.* samples can be evaluated by using mathematical equation as shown in equation 5 below [9][10] where pixel must be the entire number of all pixels in one sample.

$$\text{weight} = 0.0029 \times \text{Pixel} - 17.084 \quad (5)$$

Further analysis is continued by estimating the samples volume by using ellipsoidal equation. The analysis of ellipsoidal equation work effectively in agriculture products, since most of the fruits features appear in nearly symmetric, cylindrically or spherically [11][12]. In this study, we assumed that *Harumanis cv.* sample is in cylindrical shapes. Fig. 4 show the *Harumanis cv.* samples dimension measurement applied cylindrical algorithm while equation 6 shows the mathematical equation applied for cylindrical shape. By applying this algorithm, it is necessary to identify the value for major axis and the minor axis of the sample image, and this can be done by using region prop function in MATLAB. The value for height of the sample is from the value of major axis while for radius, the value of minor axis can be divided by 2. Fig. 5 shows the major and minor axis measured on the sample by using MATLAB software. Next, statistical analysis can been used for further analysis.

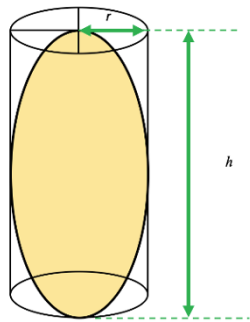


**Fig. 4.** Dimension of *Harumanis cv.* samples in cylindrical shape.

$$v = \pi r^2 h \quad (6)$$

where  $v$  is the estimated mango volume,  $r$  is the radius and  $h$  is the height.

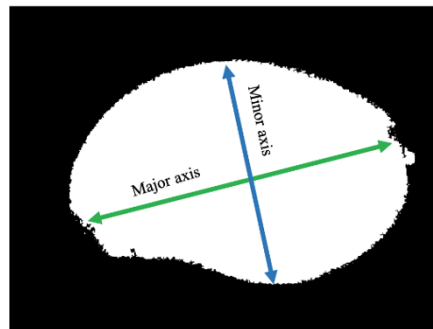


**Fig. 5.** Major and minor axis measured on the *Harumanis* cv. samples.

### 3 Results and Discussion

The analysis of the density and specific gravity measurement results using Archimedes' Theory will be discussed in this part. In this investigation, readings of mass and volume were taken, and the value of specific gravity were determined. Finally, the accuracy of the Archimedes' Theory method will be compared with image processing results.

#### 3.1 Specific Gravity Measurement Results by using Archimedes' Theory

For this part, the data for mass and volume is needed to analyze the value of specific gravity and this entire experiment was conducted by using Archimedes' Theory. Simple statistical analysis was used to investigate the relationship between mass and volume of *Harumanis* cv. as shown in Fig. 6. Based on this figure, a positive correlation was found between mass and volume.

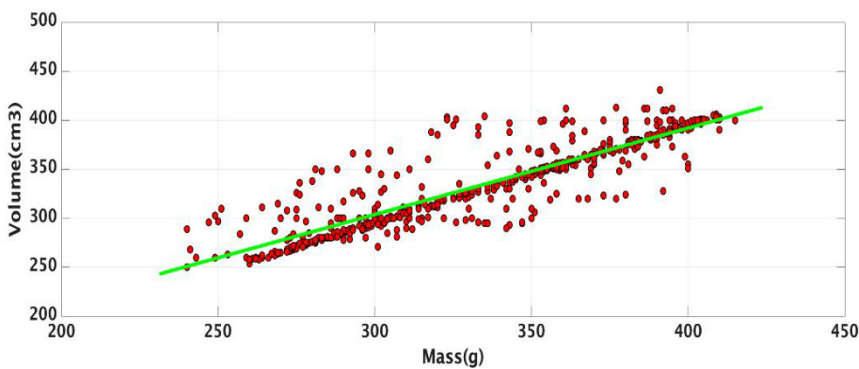


**Fig. 6.** Relationship plot between volume and mass of the 500 *Harumanis* cv. samples.

In order to predict the absence of IFR in *Harumanis* cv. samples, specific gravity value must be analyzed based on density concept by applying the mass and volume.

Fig. 7 shows the plot of the specific gravity value and prediction of *IFR* absence with respect to the number of samples. As can be seen here, the samples that are located in red circle were predicted with absence of *IFR*. This finding is in agreement with [13] which shows that the optimum matured samples have specific gravity between 1.01 and 1.02, while below 1.01 is immature and above 1.02 is considered overripe and thus, they might have internal physiological disorder.

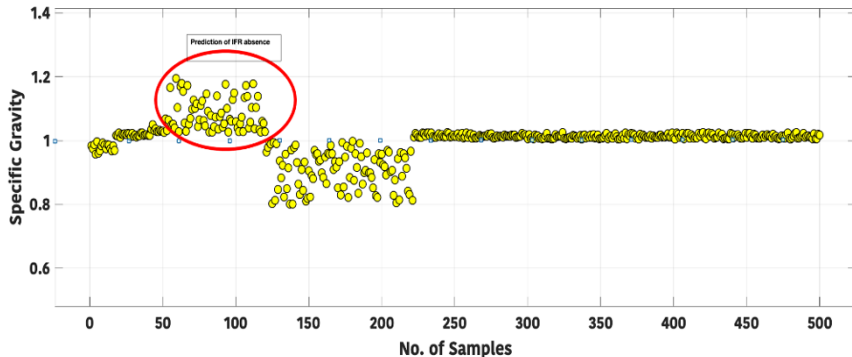


**Fig. 7.** Specific gravity of the 500 *Harumanis cv.* .with prediction of *IFR* absence

### 3.2 Specific Gravity and *IFR* Prediction Using Image Analysis

The computer vision system deployed to implement the algorithm for mass and volume estimation of *Harumanis cv.* consists of hardware and software. All captured images were transformed from RGB into binary images using threshold. Once the pre-processing is completed, the weight of the *Harumanis cv.* samples is analyzed by using equation 5. Following this, the volume was determined using major and minor axes of the samples and the predicted specific gravity can be evaluated by using equation 7. Statistical analyses are then used to analyze the data.

$$\rho = \frac{m}{V} \quad (7)$$

where  $\rho$  is the density,  $m$  is the mass and  $V$  is the volume.

The scatter plot of the predicted specific gravity of *Harumanis cv.* samples by using image analysis techniques and measured specific gravity of the samples by using Archimedes' principle are presented in Fig. 8 and a Pearson, R correlation test was used to determine their relationship.

The results obtained by using Pearson, R test revealed that there was a significant positive correlation between estimated specific gravity and measured specific gravity with the value of significant value is  $R^2$  is 0.9055 and p-value is 0.00. This means that H-null is rejected and the measured specific gravity and predicted specific gravity of the *Harumanis cv.* is positively related. The accuracy of this method is 82.00%. The predicted of the absence *IFR* can be seen from the Fig 8. as shown in the green circle.

To verify the existing or absence of this physiological disorder, the professional grader from FAMA cut the fruits to examine the interior of *Harumanis* cv.. Fig. 9 presents the *Harumanis* cv. sample that was affected by *IFR*. The experiment was successful as it was able to predict the absence of *IFR* non-destructively.

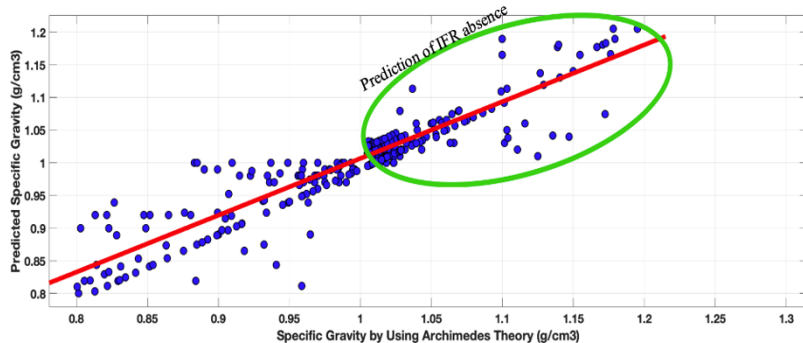


**Fig. 8.** Scatter plot of the Specific Gravity by using Archimedes Theory against Specific Gravity by using image processing.



**Fig. 9.** Sample affected by *IFR*.

#### 4 Conclusion

The non-destructive specific gravity for *IFR* prediction measurement *Harumanis* cv. using image processing techniques was successfully proposed. The process of quality inspection of *Harumanis* cv. based on density and specific gravity concept can be done automatically and it can reduce human error. Therefore, we believed that the image processing techniques can be used since it is simple, rapid and non-invasive to predict the absence of *IFR* in *Harumanis* cv.. Image processing technique has reasonable

accuracy on measuring the specific gravity of *Harumanis cv.* with correlation of determination,  $R^2$  of 0.9055 and accuracy of 82.00%. Based on this correlation, the absence of *IFR* tissue of *Harumanis cv.* can be predicted to ensure the good quality products in the market. Therefore, the image analysis has a high potential, could be applied to the fruits that having various geometrical attributes and could be applied to other type of crops as well.

## 5 Acknowledgements

Appreciation is extended to Quality Inspection Center for Agricultural Products, The Federal Agricultural Marketing Authority (FAMA), Jalan Pekeliling 4, Zon Selatan 64000, KLIA Sepang, Selangor Malaysia for samples supplied.

## References

1. Z. Li, N. Wang, G. S. Vijaya Raghavan, and C. Vigneault, "Ripeness and rot evaluation of 'Tommy Atkins' mango fruit through volatiles detection," *J. Food Eng.*, vol. 91, no. 2, pp. 319–324, 2009.
2. H. Faridah, M. Rosidah, and M. Y. Jamaliah, "Quality assessment towards VHT Harumanis mango for commercial trial to Japan," *J. Agribus. Mark.*, vol. Special Ed, pp. 77–90, 2010.
3. R. S. M. Farook *et al.*, "Agent-based decision support system for harumanis mango flower initiation," *Proc. - CIMSim 2011 3rd Int. Conf. Comput. Intell. Model. Simul.*, pp. 68–73, 2011.
4. Y. Shi, "Identification of maize southern rust using FTIR spectroscopy," pp. 0–2, 2012.
5. N. S. Khalid, A. H. Abdullah, S. A. A. Shukor, F. S. A.S., H. Mansor, and N. D. N. Dalila, "Non-Destructive Technique based on Specific Gravity for Post-harvest Mangifera Indica L. Cultivar Maturity," *2017 Asia Model. Symp.*, pp. 113–117, 2017.
6. S. Shahir and A. R. Visvanathan, "Maturity measurement of mango and banana as related to ripening," *J. Trends Biosci.*, vol. 7, no. 9, pp. 741–744, 2014.
7. J. Y. Chen, H. Zhang, Y. Miao, and R. Matsunaga, "NIR Measurement of Specific Gravity of Potato," *Food Sci Technol Res*, vol. 11, no. 1, pp. 26–31, 2005.
8. P. Mitkal, P. Pawar, M. Nagane, P. Bhosale, M. Padwal, and P. Nagane, "Leaf Disease Detection and Prevention Using Image Processing using Matlab," pp. 26–30.
9. M. Jhuria, A. Kumar, and R. Borse, "Image processing for smart farming: Detection of disease and fruit grading," *2013 IEEE 2nd Int. Conf. Image Inf. Process. IEEE ICIIP 2013*, pp. 521–526, 2013.
10. C. C. Teoh and a R. M. Syafudin, "Image processing and analysis techniques for estimating weight of Chokanan mangoes," *J. Trop. Agric. Food Sci.*, vol. 35, no. 1, pp. 183–190, 2007.
11. F. A. S. Syahir, A. y m Shakaff, A. Zakaria, M. Z. Abdullah, and A. H. Adom, "Bio-inspired vision fusion for quality assessment of harumanis mangoes," *Proc. - 3rd Int. Conf. Intell. Syst. Model. Simulation, ISMS 2012*, pp. 317–324, 2012.
12. D. J. Lee, X. Xu, J. Eifert, and P. Zhan, "Area and volume measurements of objects with irregular shapes using multiple silhouettes," *Opt. Eng.*, vol. 45, no. 2, p. 027202, 2006
13. P. Wanitchang, A. Terdwongworakul, J. Wanitchang, and N. Nakawajana, "Non-destructive maturity classification of mango based on physical, mechanical and optical properties," *J. Food Eng.*, vol. 105, no. 3, pp. 477–484, 2011.



# Reducing Climate Change for Future Transportation: Roles of Computing

Hairoladenan Kasim<sup>1</sup>, Zul-Azri Ibrahim<sup>1</sup>, Abbas M. Al-Ghaili<sup>2</sup>

<sup>1</sup>College of Computing and Informatics (CCI), Universiti Tenaga Nasional (UNITEN), 43000 Kajang, Selangor, Malaysia

<sup>2</sup>Institute of Informatics and Computing in Energy (IICE), UNITEN, Malaysia  
hairol@uniten.edu.my, zulazri@uniten.edu.my, abbas@uniten.edu.my

**Abstract.** For years, the fuels based vehicle has played a key role in the history of mankind. Such a type of vehicles has played its part not just as main transportation but also in many types of purposes as required of them. Currently, fossil fuels are the main sources of energy for the transportation mode around the world. Burning of fossil fuels will release heavy and vast amount of carbon agents into the environment which detrimental effect to the nature, surrounding and the population of earth be it humans, plants or mammals. For that a solution to reduce the gas emission from fossil fuels vehicle to prevent more ill-effect to the environment is required. New technology such as fully Electronic Vehicles (EVs) is considered as one of the best solutions to mitigate this problem. With the integration of Computing or Information and Communication Technology (ICT) can help to further improvise this future transportation and at the same time can reduce its negative impacts. This paper will review selected articles and papers published between 2001 and 2019 that contain information and terms that related climate change, global warming, environment, future transportation and computing technology. These articles were further inspected and the decision for its inclusion and exclusion were mediated to develop a comprehensive review on global warming issues that are related to transportation and how ICT can assist in mitigating them.

**Keywords:** Electronic vehicle, climate change, global warming environment, future transportation, computing technology.

## 1 Introduction

The development of speedy transportation is human's greatest accomplishment in minimizing the distances but at the same time it has also become a main cause of environmental degradation [1]. It can be treated using smart management for new futuristic transportation ways [2]. If we fly into any main city all around the world, you will be greeted by a familiar sight looking like sheen of brown smog that floats over a city. This smog comes mostly from cars and this is one of the problems caused by current modes of transportation and their fuel. Along with this smog comes carbon dioxide

(CO<sub>2</sub>), the gas that is fully responsible for the climate change. Other main sources of pollution are in the form of gas and particulate matters emissions that affect air quality causing damage to human health. As stated by [3], the most common gas includes Carbon Monoxide (CO), Nitrogen Oxides (NOX), benzene, silicon tetrafluoride and others. It is clear that very large amount of pollutants is being emitted from various forms of transport into the air that we breathe.

All of these emissions are also responsible as it affected the environment with the global warming issue. According to [4], the major types of current fossil fuels used in the transportation sector in Malaysia include natural gas, Motor gasoline, Aviation gasoline and Aviation Turbine Fuel. Diesel oil and fuel oil Natural Gas fuel make a mixture of gaseous hydrocarbons (mainly methane) which occur either in gas fields or in association with crude oil in oil fields [4]. The most noticeable way for us to achieve a reduction in pollution by motor vehicles is by reducing the emission of fumes at the source. A quick-term solution has to be made by medications to the current type of engine, maybe by improving the combustion part within the exhaust system and created a future fuel that are save for the environment and can reduce the pollution as well [4].

In addition, the current modes of transportation and their fuel have caused many problems to our environment. Transportation like cars, motorcycle and aviation industry are major users of energy and burn most of the world's fuel. With this, they are creating air pollution which includes nitrous oxides and other particulates and this is significant contributor to global warming through emission of carbon dioxide which is dangerous and harmful to environment [3]. Other than that, it also gives an impact to automobile-oriented urban sprawl which can affect the natural habitat and agricultural lands. Furthermore, even there are so many problems to environment that had been seen but still the demand on private vehicles like cars and motorcycle is still high and at the same time, the transportation industry keeps on producing new cars or other private vehicles to satisfy their customers.

Computing or Information and Communication Technology (ICT) carries an important role in the futuristic transportation mode [5]. Market of ICT has been striving and has been launching latest applications and technologies which guide and help in shifting transportation to another level while still focusing on long term and short term effects on environment [3]. ICT has a high potential to raise future technologies efficiency and at the same time it does its cause to reduce negative impacts. For example, an autonomous car will not pollute the environment as how the motor vehicle does [6]. However, these technologies would cost highly and are affordable to have frequent maintenance and would wear or tears due to insufficient monitoring and maintenance. Hence, this car will have to be controlled and monitored so any issues found would be noticed and immediately fixed and ensuring car is in a good condition as well as the surroundings. A simple graphical representation is depicted in Fig. 1 in order to provide readers a more explanation on what this paper is going to resolve such an issue.

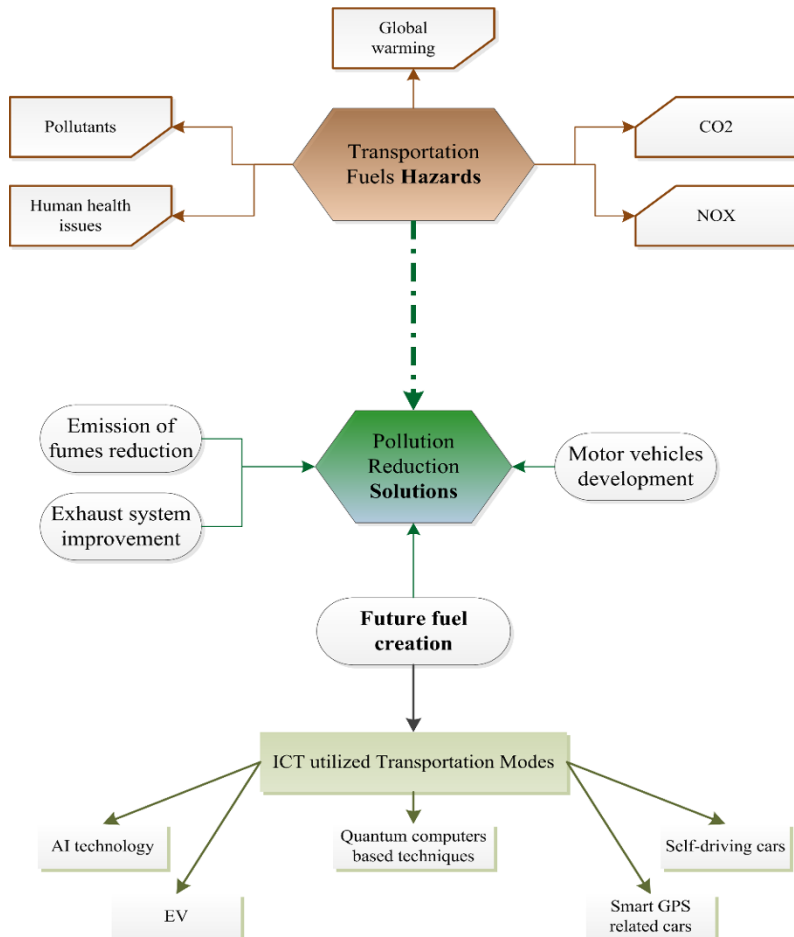


**Fig. 1.** A relationship between transportation fuels hazards and ICT-based pollution reduction solutions

The objective of this paper is to review roles of computing to mitigate climate change issues and their impact for the future transportation. Articles and papers published between years 2001 until 2019 were reviewed and selected for retrieval of paper if they were judged to include information about or containing the following terms: climate change, global warming, environment, future transportation and computing technology. From here, these articles were further inspected and the decision for its inclusion and exclusion were mediated to develop a comprehensive review on global warming issues that are related to transportation and how ICT can assist in mitigating them. The past articles used in this review were selected based on their relevance to the objective of this article. The literature review of these terms will be further elaborated in the next section of this paper.

## 2 Literature Review

### 2.1 Climate Change and Environmental Issues

The climate change issue is a global environmental issue. Climate change influences living conditions of mammals and mankind and mitigation to reduce the greenhouse gases emissions are of large scale and important for society. As stated by [7], greenhouse gases are carbon dioxide, methane nitrous oxide and others and these emissions can lead to change in climate system in longer term. This accumulation comes mainly from fossil fuels (coal and oil) and deforestation. In the last decade, carbon dioxide level in atmosphere has risen due to human activities. For instance, transportation makes a contribution to effect of greenhouse and represents heavy carbon dioxide emissions. This gas emission from transport is gradually increasing and expected to increase in future. Greenhouse emissions gases are extremely relatable issue when it comes to mean of transport.

Air pollutants are significant in urban locations as health risk. Pollutants are toxic and bestow to allergies and hypersensitivity [7]. In longer term, it can also cause cancer or other toxic effect in genetics. Road traffic caused by the transportation system is a dominant pollution source. In a case research done at certain urban area, air pollutants are a tragic factor to diseases around the area. [8] have stated that transportation mode has different characteristics that lead to different economic and environmental issues and performance. These scholars also mentioned that many countries have started focusing on small inhalable particles that exist in diesel exhaust emissions. It is necessary that emissions and their effects are measured time to time to avoid it from getting more serious in the neighborhood and nation [8].

Carbon dioxide from fossil fuels burning from the vehicles accumulates in atmosphere. Indirectly, it affects our land and oceans. As carbon dioxide enters ocean, the gas reacts with sea water to form carbonic acid. Since Industrialization era began, acidity of seawater has increased by 30 percent [7]. The world's oceans' changing chemistry is an increasing global problem. The ocean absorbs one third of man-made carbon dioxide emissions, including those from fossil fuel use, cement production and deforestation. The carbon dioxide taken into the ocean decreases pH (potential of Hydrogen) value of the ocean that changes ocean's chemistry to be more acidic [7]. This lowering pH value of seawater affects biological process such as reproduction, growth and photosynthesis of living organisms in the seawater.

The water and land taken over by transport sector, including natural areas had direct and indirect impacts. Barrier and fragmentation problems rise, the road and railways with traffic, operations and maintenance contribute to environmental impact on landscape [9]. Environmental impact depends totally on infrastructure facility design such as type of traffic and location of facility. Environmental impact of transportation on small spaces and parks in housing area caused by all ways of effect is considerably significant for recreation close to home. This access allows people to interconnect natural areas and it is a valuable feature for inhabitant in towns and rural areas. A research by [10] had proved that quantity of conventional greenhouse gases released into the atmosphere increased substantially ever since evolution of transportation industry over

the last decade. Transportation industry releases several million tons of gases every year into the atmosphere before decaying or being absorbed by chemical or biological process.

NOX and VOC emissions communicate under influence of sunlight to create ozone in air [7]. High level of ground-level ozone damages materials and plants and has heavy impact on human health. Transportation is a massive source of NO and VOC. As discovered by [11], these oxidants can irritate respiratory tracts and the eye's membrane of mucus and can potentially lead to development of cancer as well. Besides, ozone absorbs heat radiation and contributes to greenhouse effect and also degrades organic materials such as paint and plastics. In longer term, photochemical oxidants cause extensive problems with severe air pollution. [12] have stated that most of world's governments and industries from various sectors agree by now that global warming poses a serious threat to future well-being of all people and they agree that it is desirable to reduce concentration of CO<sub>2</sub> in the atmosphere by lowering our carbon emission.

## 2.2 Current Transportation Issues

Over the years, transportation has evolved so much and become an important part of a person's life. If there was no transportation, one's travelling or shipping goods can never happen. New studies and exploration were only possible due to transportation availability. Recently, there have been billions of dollars invested to enhance and improve transportation service [13]. From time to time, transportation styles and vehicles have been changing to a great degree. There are different groups of transportation e.g., sea, land and air transportation each of which plays a special role in carrying out its specific functions. Land transportation helps in covering short distances and it is the highly used mode of transportation around the world. Air transportation serves its purpose in various fields such as goods transportation, passenger transportation and weaponries or military vehicles. It allows travelers to travel around the globe at the fastest and shortest time period. On the other hand, there is sea transportation which has been used since even the ancient times. Sea path is the longest and slowest but it can transport at a huge amount that already exist everywhere in this planet.

Transportation happens throughout daily life and it is necessary for our daily living. Over half a billion commercial cars and fleet are there in the world today and it is anticipated to grow 3% annually and in the next 20 years, it will double [13]. Motor vehicles alone use one third of world oil consumption. In next two decades, it is said that global oil demand will increase and exceed demand due to large projected growth of transportation sector in developing countries. Other projections have forecasted that the petroleum global demand will keep increasing and doubled by 2020 from current level of usage that is about 75 million barrel per day [13]. Although this growth is positive to economics of technology or fossil filled countries, it will aggravate urban overcrowding, pollution of air and side impacts on economic productivity that will gradually lead to problems in human health and life quality [14].

Nowadays, our population on earth nearly 8 billion people and expected to rise even more in the coming future. Every day people are buying cars, adding planes to their arsenal and trucks transport demands from the whole wide nation. If this continues,

earth will doom and mankind will bring itself to end. Major automobile company are coming with different method of solving the problem with the most highest and greatest technology at their disposal to improve and create a better and more efficient way of executing the demand of transportation every year [15]. As for major aviation company, testing of hydrogen gas as a substitute for fossil fuel are being research and shows a great promise. The engine must be modified to suit the exponential use of hydrogen gas. As known, rockets that flew satellites to space are using the same medium for the last 10 years, introduced by National Aeronautics and Space Administration (NASA) to prevent more damage to the environment, as rocket release more mass of byproduct by launching than any automobile on earth. As a result of countless research and experiment, in order to overcome the environmental problem, mankind needs to develop a solution that is far better than the current technique used [14].

Huge carmakers recently have developed more efficient automobile with increased performance and with less amount of combustion required for a car to be driven [15]. In addition, oil companies are always supporting the car manufacturer in all aspect including designing a more efficient way of combustion that reduces carbon footprint [16]. As for now, the environment is the vital focus of the majority of people. In order to create a better future and still be gaining profit, the business model must be changed and the traditional method of combustion must be changed with a greener approach, hence most of the major car makers are now shifting to alternate fuel to gain a better and more optimized way of making transportation more eco-friendly [16]. Nevertheless, few oil companies are not happy with these initiatives, as they will disturb their business model because they depend on fossil fuel as their major selling point.

For futuristic transportation, one of the best solutions for automobile is fully Electric Vehicle (EV). This concept was merely an ideology or some sort of a dream 100 years ago, but now, it is executed excellently and now road legal [17]. Major companies like Tesla have proven to the big existing car makers that the market for electric cars is wide and available by proving the time of execution is now perfect for the ideology to be implemented [14]. Proven by the huge Gigafactory as what Elon Musk, the founder himself called it, which produces and meets the unprecedented level of demand for EV now. Major companies like Porsche, BMW, Mercedes, Toyota and Honda are now pushing their engineering teams to be able to produce cars in similar fashion, showing that they are also now in the league of EVs. The competition of inventing the most energy efficient vehicle race is now a real thing and it's going fast. It is now proven that electric is, as for now, the most prominent way of substituting with the traditional fossil fuel combustion engine [15].

### **2.3 Roles of Computing - Solutions for the future**

Nowadays, technologies are disrupting the energy use that can transform everyday life and bringing clean energy [18]. Technologies such as artificial intelligence (AI), block chain, and cloud computing are now making transportation rapidly grow. For electrical vehicle (EV), ICT can be contributed by ensuring the right time to charge the energy. Charging processes can be controlled by detection of low consumption energy. Car manufacturer should make the best possible energy supply from power grid and the

storage facilities. EV could control the energy and give feedback to the grid with it reaches its high consumption of energy [12]. The intelligent controller must know how to handle vehicles batteries carefully. Other than that, there also must be software (i.e., an embedded system) to test battery performance. It can be used if the EV needs to replace battery, so it needs intelligent controls for battery management which result can be valuable for technology in EV. Furthermore, car-charger requires a web application to monitor status information and statistics of the car battery.

Another instances is self-driving cars is fully automated with computers and does not necessarily require a man to manually use the car. Instead, the human would just have to let the car know where to go and it would bring us to our desired locations. These programs of the car are coded in a way to carry out its specified functions accordingly. It will be assisted with a navigation system; Global Positioning System (GPS) to safely and accurately bring the passenger to location. Every part of the car can be controlled from its dash screen and overall maintenance of the car too can be monitored through the screen. All of these are done using the integration of sensors in the car with its embedded system.

The roles of ICT in building the EV are wireless charging that is fully autonomous. Smart system like wireless charging can help the attributes recognized EVs that need to charge [3]. This car charging technology requires connectivity and interactivity, as the connectivity features like remote assistance and smart software upgradeability [12]. The wireless charging also requires Radio-frequency Identification (RFID) that helps to sense the car and make connectivity to smart electricity grid [19]. By that, it can transfer all of data to its web application and seeing power consumption related to battery usage. ICT also plays a crucial part for transportation to know the location if the electric car is run out of battery. This will include a processor such as Intel Atom Processor to control and support power consumption and other electronic components.

In future, there are several types of transportation that will be developed by the innovator. Innovation in the transportation industry has changed the way we travel in this century [18]. As an example, a Smart Car might already be taking its place in the industry. A Smart Car has a unique shape and size. Smart Cars use AI assistance and it can give route suggestions, be autonomous in driving, speak to you when you are driving and sometimes it can also measure your emotional expressions [20]. The development of ICT in future transportation can improve the speed, efficiency, safety and also reliability of the vehicle mobility [21]. [6] have stated that future technologies are aiming to complete the autonomous vehicles and terminals that include ports, airports, railways and road, because these technologies could give an improvement of existing modes of transportation such as automated highway systems and the creation of automated vehicles. While ICT is transforming vehicles and how the driver interacts with vehicles, at the same time, they are also improving transport infrastructures [18]. The smart infrastructure technologies or known as intelligent transportation system (ITS), are being embedded in traffic lights, car parks, toll booths, roads and bridges [19]. Hence, it will make vehicles able to communicate with each other and these innovations offer a transport infrastructure system that suffers less congestion and saves the energy.

The spreading of GPS, sensors and mobile communication technology has already resulted in great benefits in terms of improved navigation and congestion mitigation. A

network of connected and identifiable devices is calling as Internet of Things (IoT). These devices can be embedded in transportation modes and it is relied on the large volume of data that provides better support for better routing and forecast. Vehicle can then be rerouted if congestion or another form of disruption takes place. Over a million people a year are executed in street auto collisions, with many millions progressively harmed. The emergence of smart roads connected to IoT can significantly help to reduce road deaths, as IoT-enabled road sensors can instantly about best ways to avoid hazards or adverse road conditions [19]. In the future, wireless battery chargers will be found underneath roads, helping to reduce the level of air pollution and virtually eliminating the need for fossil fuels to power cars.

In terms of ICT assisting the development of these important solutions is via research, development and engineering. A proper functional system that is able to calculate the task of any machinery that is needed to assemble anything required for the production of the upcoming medium of solution is one of the methods that ICT fits in [5]. As for transport manufacturers, the implementation of AI in any algorithm or calculation is required for solutions in a faster manner; compared with normal human brain can possibly digest and calculate in a shorter period. As described by [20], machinery that existed could be upgraded with these machine learning technology in order to perform any task that is needed to be executed in a more delicate and accurate manner, also be able to operate in dangerous situation and work for a more prolonged period of time compared to a human being working the machinery itself. Undertaking these problems is not an issue as our technology now is at a definitive level that is able to create processing powers beyond the imagination of any person living 50 years ago. Technology, as we currently now using, is silicon transistors and some have predicted that the era of silicon transistors are coming to an end, at we are at the beginning of a whole new level of technology that is unimaginable even for our current generation [20]. The era of supercomputers are the thing of the past, an era traditional computers will be replaced by Quantum computers which will be able to calculate probability by using quantum bits and executing the laws in quantum physics. In an era which all probability could be calculated and examined for the best approach on doing every single thing is one could considered a power that is wielded by a group of experts.

### 3 Discussion

What is the role of ICT to assist mitigating the global warming issues? ICT can fit in these futuristic scenarios where it helps to reduce the usage of natural resources which is fossil fuels. As mentioned by [18], employing ICT in futuristic modes of transportation can make the transports more effective and efficient. The technology will develop platforms that can analyze the weather, speed limit and other innovations. It also helps in security of the transportation as well as drivers and passengers because it can help the transports to run smoothly. For instance, advanced aircraft like Autonomous Helicopters, ICT applied in verification of an estimation and control system for a helicopter ‘Slung Load System’. The estimator provides position and velocity estimates of the slung load and is designed to augment existing navigation in autonomous

helicopters. Sensor input is provided by a vision system on the helicopter that measures the position of the slung load [6]. Another example, using EVs will help passengers to not depend on fossil fuels because it uses electric to move. It is safe to use EVs paths and smart roads to reduce accidents especially when road traffic occurs [22]. Another technology in building the EVs is wireless charging that is fully autonomous. Smart system like wireless charging can help the attributes recognized electric vehicles that need to be charged. The charging technology requires connectivity and interactivity, such as remote assistance and smart software upgradeability. The wireless charging also requires RFID that helps to sense the car and make connectivity to smart electricity grid. Therefore, it can transfer data to its web application and monitor real-time power consumption on using the battery. Hence, this technology plays a crucial part for future transportation to indicate the location if the EVs require to be charged at the nearest station or electricity grid.

Smart Roads are another concept of future ICT technology that could theoretically call first responders such as the authorities to the site of an accident because they know where vehicles are and how fast they are travelling. It could also collect real-time data on road conditions and congestion data, letting drivers and self-driving cars in particular choose the route that is the most efficient and safe [22]. In addition, ICT helps to reduce accident because accident usually happens when transportations on the road are speeding or driving carelessly during bad weather conditions. Malaysia's accidents are increasing especially during festive season as cars are pack on the road [23]. So, this will threaten the safety of drivers and passengers on the road. [21] have stated that the technology will help to prevent accidents when there are technologies that can alert and warn drivers to not exceed a speed limit. Not only that, ICT also has technology that monitors the safe distance between two cars. These types of technology can save many lives while they are on the road. Integrated Roadways also envisions the system to be the backbone of a much-anticipated "nationwide 5G network" an ultra-fast wireless communication standard of the very near future without the need of additional infrastructure by sending data over an integrated fiber optic mesh [21].

An electric car engine is another example of the most promising alternative technology. One of the advantages is it relates to a lower environment such as less CO<sub>2</sub> gas emissions [17]. Even if the generation of electricity comes from a fossil fuel, EVs are less mechanically complex since they have less moving parts such as no internal combustion engine and transmission [24]. This kind of vehicles is cheaper to build and maintain, it can lower the acquisition and operating cost improves the affordability of mobility. Battery charging strategies could improve the stability of energy systems through a better coordination between the supply and the demand of electricity [24]. New materials can also be implemented on both vehicles and infrastructures.

Prevention is no longer considered as a feasible solution as the broad level of hazard is now rising at an unprecedented level. The pollution may grow greater in years to come. Hence, an aggressive approach must be executed. Major industrial titans that shape the world economics must get involved with the solution as they have the power and financial strength to do accomplish what the majority of the people aren't able to do. Creating an overall better more accomplish solution than others and ultimately

contribute to the environment without losing profit to their business. We live in an era which development occurs anywhere within. Internet is one of the major platforms that cause this transition of human knowledge to be borderless and create the opportunity for everyone to access information, anywhere at any time. By utilizing the power of the internet, people who are in need of certain information that might accomplish of what might change the world would be able to reach its climax without any knowledge and information barrier holding them back. A simple nobody today might become the pioneer of tomorrow's future by just a click of a button.

## 4 Conclusion

Eventually, it is true that transportation is an important part of a person's daily life. Transportation has evolved throughout the years and even more drastically after the industrialization began. Currently, fossil fuels are the main sources of energy for the transportation mode around the world. Due to this, as transportation need increased, fossil fuel usage too has increased gradually. Transportation has been a key player to ease the transportation of goods around the globe and it has been the key to economic growth of a nation. While transportation is serving its purpose at most definitely by easing the portability of a person or goods, the energy source that drives it is causing an incremental effect to the earth and human population. Burning of fossil fuels releases much amount of carbon agents into environment and it is bringing a detrimental effect to nature. CO<sub>2</sub> emission leads to greenhouse effect that leads several other drastic and dangerous changes to the surrounding and the global temperature. To avoid this from further depreciating our environment, efforts have already been started by corporate and government sectors but they are currently insufficient and ineffective as the demand for fossil fuel usage for transportation is still in peak. Therefore, an alternative fuel or an alternative energy source should be discovered to overcome this issue. Besides, government policies have to be improvised and enhance to promote the alternative energy source and reduce usage of fossil fuel to save the earth and its people.

In the recent times, computing has been playing a great role in industrialization of the current era. Almost every piece around is made possible through ICT service. Also, smart management is so beneficial for smart futuristic transportation ways. With this technology, alternative to fossil fuel can be discovered in the near future; even better, it will replace fossil fuel with an alternative source. For example, Tesla has been developing its product and industry fully energy efficient using hybrid battery powered to run the whole company. This is a lead for other companies to follow that fossil fuel is not the only energy source to run an industry. More corporates, government sectors and nations should work together to overcome the problem of climate change and avoid carbon footprints as much as possible to prevent heavier risks of health, land and water to fall upon us. Hence, working together will help every nation equally to save the mother earth from falling prey to carbon and greenhouse effect that will in a greater extend destroy the life of earth. Eventually, ICT creates a better system for anything the developer needed as long the processing power is there and technology of our time allows the creation of that particular thing. The world is evolving, but most of the people

mindsets are still rigid. Therefore, for us to survive in the next decades, current generation must put aside the differences and focus on the goal to create a sustainability environment for a brighter future. Humankind needs to improvise and adapt in order to survive, but now we need a transportation solution more than a prevention method, to curb the ever-growing level of climate change causes by none other than us.

## Acknowledgements

This research is funded by FRGS/1/2017/SS09/UNITEN/02/3, Ministry of Higher Education Malaysia; which is supported by Universiti Tenaga Nasional.

## References

1. X. Luo, H. Zhang, Z. Zhang, Y. Yu, and K. Li, "A New Framework of Intelligent Public Transportation System Based on the Internet of Things," *IEEE Access*, vol. 7, pp. 55290-55304, 2019.
2. A. Boukerche and R. W. Coutinho, "Crowd Management: The Overlooked Component of Smart Transportation Systems," *IEEE Communications Magazine*, vol. 57, pp. 48-53, 2019.
3. I. Dincer and C. Acar, "Smart energy systems for a sustainable future," *Applied Energy*, vol. 194, pp. 225-235, 2017/05/15/ 2017.
4. W. K. Fong, H. Matsumoto, C. S. Ho, and Y. F. Lun, "Energy consumption and carbon dioxide emission considerations in the urban planning process in Malaysia," *PLANNING MALAYSIA JOURNAL*, vol. 6, 2008.
5. L. Erdmann, L. Hilty, J. Goodman, and P. Arnfalk, *The future impact of ICTs on environmental sustainability*: European Commission, Joint Research Centre, 2004.
6. D. J. Fagnant and K. Kockelman, "Preparing a nation for autonomous vehicles: opportunities, barriers and policy recommendations," *Transportation Research Part A: Policy and Practice*, vol. 77, pp. 167-181, 2015.
7. D. J. Jacob and D. A. Winner, "Effect of climate change on air quality," *Atmospheric Environment*, vol. 43, pp. 51-63, 2009/01/01/ 2009.
8. M. J. Meixell and M. Norbis, "A review of the transportation mode choice and carrier selection literature," *The International Journal of Logistics Management*, vol. 19, pp. 183-211, 2008.
9. S. M. Abdullah. (2017, 3 Feb 2019). *Carbon dioxide emissions causing global warming*. Available: <https://www.nst.com.my/opinion/columnists/2017/12/313842/carbon-dioxide-emissions-causing-global-warming>
10. J. P. Rodrigue, C. Comtois, and B. Slack, "The geography of transport systems," *Routledge*, 2016.
11. G. Bluhm, E. Nordling, and N. Berglind, "Road traffic noise and annoyance-An increasing environmental health problem," *Noise and Health*, vol. 6, p. 43, 2004.
12. T. H. Ortmeyer and P. Pillay, "Trends in transportation sector technology energy use and greenhouse gas emissions," *Proceedings of the IEEE*, vol. 89, pp. 1837-1847, 2001.
13. A. P. Society. (2018, 8 Jan 2019). *Transportation and Energy Issues*. Available: <https://www.aps.org/policy/reports/popa-reports/energy/transportation.cfm>
14. S. Grava, *Urban transportation systems. Choices for communities*, 2003.
15. S. Chu and A. Majumdar, "Opportunities and challenges for a sustainable energy future," *Nature*, vol. 488, p. 294, 08/15/online 2012.

16. D. F. Dominković, I. Bačeković, A. S. Pedersen, and G. Krajačić, "The future of transportation in sustainable energy systems: Opportunities and barriers in a clean energy transition," *Renewable and Sustainable Energy Reviews*, vol. 82, pp. 1823-1838, 2018/02/01/2018.
17. F. Liao, E. Molin, and B. van Wee, "Consumer preferences for electric vehicles: a literature review," *Transport Reviews*, vol. 37, pp. 252-275, 2017/05/04 2017.
18. C. J. H. Midden, F. G. Kaiser, and L. T. McCalley, "Technology's four roles in understanding individuals' conservation of natural resources," *Journal of Social Issues*, vol. 63, pp. 155-174, 2007.
19. H. Menouar, I. Guvenc, K. Akkaya, A. S. Uluagac, A. Kadri, and A. Tuncer, "UAV-Enabled Intelligent Transportation Systems for the Smart City: Applications and Challenges," *IEEE Communications Magazine*, vol. 55, pp. 22-28, 2017.
20. A. Śladkowski and W. Pamuła, *Intelligent Transportation Systems – Problems and Perspectives* vol. 303: Springer International Publishing, 2016.
21. G. A. Meiring and H. C. Myburgh, "A Review of Intelligent Driving Style Analysis Systems and Related Artificial Intelligence Algorithms," *Sensors (Basel)*, vol. 15, pp. 30653-82, Dec 4 2015.
22. S. Misbahuddin, J. A. Zubairi, A. Saggaf, J. Basuni, S. A. Wadany, and A. Al-Sofi, "IoT based dynamic road traffic management for smart cities," in *2015 12th International Conference on High-capacity Optical Networks and Enabling/Emerging Technologies (HONET)*, 2015, pp. 1-5.
23. A. S. I. Almselati, R. Rahmat, and O. Jaafar, "An overview of urban transport in Malaysia," *Social Sci*, vol. 6, pp. 24-33, 2011.
24. N. Daina, A. Sivakumar, and J. W. Polak, "Modelling electric vehicles use: a survey on the methods," *Renewable and Sustainable Energy Reviews*, vol. 68, pp. 447-460, 2017/02/01/2017.



# Performance Analysis of the Level Control with Inverse Response by using Particle Swarm Optimization

I.M.Chew<sup>1</sup>, F.Wong<sup>2</sup>, A.Bono<sup>2</sup>, J.Nandong<sup>1</sup>, and K.I.Wong<sup>1</sup>

<sup>1</sup> Curtin University Malaysia, Sarawak, Malaysia

<sup>2</sup> Universiti Malaysia Sabah, Sabah, Malaysia

chewim@curtin.edu.my

**Abstract.** Boiler is an important utility system to support operations in the industry. The control of water level in the steam drum is a complicated task due to the non-minimum phase (NMP), which possibly will cause instability to the controlled water level in the steam drum. Process identification and controller design are difficult tasks for the steam drum because of non-minimum phase. Following the previous literature, this paper proposed process identification to 3<sup>rd</sup> order transfer function and optimization of Proportional-Integral-Derivative (PID) tunings of the water level by using Particle Swarm Optimization (PSO). A Graphical User Interface (GUI) has been developed to provide a direct platform to deal with these tasks. The result of PSO is compared with other tuning methods in terms of performance indicator and index. An analysis of the performance curve in 3-dimension graphs is also presented to visualize the output performance of various proportional and integral gain settings. The study has concluded that PSO provided better PI tunings for the best control of the Heat Exchanger function in the LOOP-PRO software.

**Keywords:** Non-minimum phase, PID, Process Identification, Particle Swarm Optimization, Optimum Tuning.

## 1 Introduction

In the industry, boiler plant is widely used to support the process's operation. It provides heated and pressurized steam to rotate turbines for generating electricity as well as heated steam to many downstream processes. Controlling water level is the primary objective to ensure stable operations. However, rapid changes in the steam load and feedwater supply to the steam drum causes high volatility of the water level.

When steam load has decreased, the pressure in the steam drum is increased and thus, reduces the volume of the entrained vapour bubbles and thereby decreases the water level known as the shrink effect. Whereas, the increase of the steam load causing more volume of entrained vapour bubbles and creates the swell effect.

Apart from it, feedwater load also creates the swell and shrink effect in the steam boiler drum. The increment of feedwater load causes decreasing of water's temperature and reduced the volume of entrained bubbles [1]. With the constant heat supply, the water level will start the volume of entrained bubbles increases back to be a part of the

level measurement [2]. This is known as the shrink effect. In contrast, the swell effect will happen during the decrement of feedwater load.

The swell and shrink effect exhibits the inverse response that degrades control performance of water level in the steam drum [3]. The main characteristic of inverse response is reflected by a system with the process transfer function has a positive zero meaning zero in the right half plane [4], known as Non-minimum phase, *NMP*. The inverse response curve and the closed-loop diagram are shown in Fig. 1 (a) and (b).

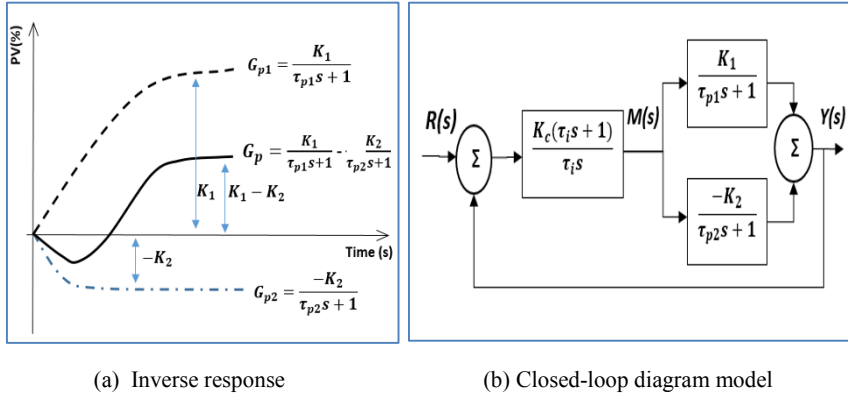


**Fig. 1.** Inverse response curve and closed-loop diagram.

$K_1$  is the process gain of the initial first order system.  $K_2$  is the process gain of the other first order system.  $\tau_{p1}$  and  $\tau_{p2}$  are the time constants of the two first order systems respectively.  $K_c$  and  $\tau_i$  are the proportional gain and integral time constant. Besides,  $Y(s)$  and  $R(s)$  are the final output and step input respectively.

$$\text{From Fig. 1 (b), } Y(s) = \left( \frac{K_1}{\tau_{p1}s+1} - \frac{K_2}{\tau_{p2}s+1} \right) u(s)$$

$$Y(s) = \frac{(K_1\tau_{p2} - K_2\tau_{p1})s + (K_1 - K_2)}{(\tau_{p1}s+1)(\tau_{p2}s+1)} \quad (1)$$

When two opposing process models interact simultaneously, the inverse response appears due to competing effects of fast dynamic to provide opposite response initially until the slow dynamic that has higher gain has grown to prevail until the new steady-state value. The inverse response is preferable to maintain positive value for both numerator and denominator of the transfer function therefore in general, value of all parameters are summarized into (2).

$$\frac{\tau_2}{\tau_1} > \frac{K_2}{K_1} > 1 \quad (2)$$

Inverse response happens in many ways in real-life applications. Dealing with inverse response is a challenging task for the process engineers and requires additional analysis in the controller's tuning. It is due to the *NMP* characteristic that causes the controller to operate on wrong information in the initial time of the transient that drives the response to the opposite direction with respect to the ultimate steady state value.

PID or known as Proportional-Integral-Derivative controller is normally used in controlling the process with an inverse response credited to its simplicity, flexibility and widely used in many industrial operations. PID tuning algorithms is based on tunable parameters and the corresponding optimal setting is normally determined by trial and error. Therefore, it is a difficult task in maintaining the stability control due to the poor tuning of PID settings. There are many deterministic approaches whereby Internal Model Control, *IMC* [5,6] and Cohen-coon, *CC* [7] methods are chosen for comparison in PID parameterization of this paper.

Particle Swarm Optimization, *PSO* is one of the bio-inspired Swarm Intelligence methods, which is greatly inspired by the social behaviour of elements in nature such as fish schooling and birds flocking [8]. *PSO* algorithm works on natural selection and survival of the fittest through many generations or iterations. When the searching algorithm is implemented, a set particle of the population is randomly selected. The random position is denoted as  $X_i$  and the random velocity is denoted as  $V_i$ . These particles are compared to the predefined fitness function for determining the initial start value of personal best,  $pbest$  and global best,  $gbest$ . Both values do not change in every iteration, but only in the condition when the new obtained particles have achieved better  $pbest$  and  $gbest$  in that iteration.  $pbest$  represents the best value of the particles while the  $gbest$  represents the goal position for the particles [9]. The velocity and position updates of *PSO* algorithm are shown in (3) and (4).

$$\text{Velocity update}, V_{id(t+1)} = WV_{id(t)} + c_1 r_1 (P_{id} - X_{id(t)}) + c_2 r_2 (P_{gd} - X_{id(t)}) \quad (3)$$

$$\text{Position update}, X_{id(t+1)} = X_{id(t)} + V_{id(t+1)} t \quad (4)$$

where,  $W$ = inertia weight,  $t$  is 1 in each interactive step,  $r_1$  and  $r_2$  are random values from the range  $[0,1]$ ,  $c_1$  and  $c_2$  are coefficient of the particle acceleration value in range  $[0,2]$ ,  $P_{id}$  is personal best position,  $P_{gd}$  is global best position,  $X_{id(t)}$  is initial position, and  $V_{id(t)}$  is initial velocity.

The optimization analysis is started by randomly identifying the initial population or particle,  $C_k = K_c K_i$ , where  $K_c = c1, c2, \dots, cn$ ,  $K_i = i1, i2, \dots, in$ . In the iteration, each population is evaluated by objective function to produce the integral error values and then it is compared to other population values. The best value is known as  $pbest$  is compared with  $gbest$  and potentially replacing  $gbest$  if the integral value is smaller than  $gbest$ . Optimization analysis operates until all iterations are completed.

This paper presents a direct approach to identify various orders of the process model and *PSO* on the PID tunings for the best performance of the controlled system. The paper is organized as followed: Section 2 explained the literature of inverse response and *PSO* analysis. Section 3 presented the used methods for process identification, *PSO* analysis, and integral measurement. Section 4 discussed the analyzed results and Section 5 concluded this research study.

## 2 Literature Study

There are many works of literature that explained the used of PID in tuning the process with an inverse response. Morari and Zafirious [6] introduced Internal Model Control, *IMC* technique for PID tunings. Alfora and Vilanova [10] used Model Reference technique to eliminate the inverse response in the PID tunings. Kadu and Sakhare designed a self-adaptive fuzzy control for the PID controller [11]. Ibrahim Kaya proposed PI-PD control for the stable process with the inverse response by approximated the dead time by using the Pade approximation theory [12]. Martinez used Model Reference technique to design a PI controller to eliminate the inverse response [13]. Mohd Irshad and Ali reviewed the PID tunings rules for the performance of underdamped SOPDT process with inverse response [14].

On the other hands, *PSO* has been introduced by Kennedy and Eberhard in 1995 [15]. Sayed et. al. proposed a new hybrid jump PSO, *HJPSO* [16]. Balamurugan et. al. developed the *PSO* for finding the duty cycle to the boost converter [17]. Ram and Rajasekar developed a global maximum power point tracking (MPPT) for Photovoltaics [18]. Adam Slowik explained in details the *PSO* with some metaheuristic belongs to this Swarm Intelligence method [8].

## 3 Methodology

### 3.1 Process Identification and Optimization using the developed GUI

This paper presents an identification method for the process with an inverse response based on the open-loop test method to determine First Order Plus Dead Time, *FOPDT*, 2<sup>nd</sup> order and 3<sup>rd</sup> order models. Parameter estimation is obtained by using the developed Graphical User Interface, *GUI* from the MATLAB simulation tool. The automated stages of the process identification include analyse the process data, estimate model parameters and displaying the dynamic performance of the process in many different types of transfer function. Each of the approximated model is compared with the real model and fitness percentage is presented to describe cross-correlation of the input and the output residual. Besides, the *GUI* is dealing with the *PSO* optimization for determining the correlation PI tunings in the closed-loop feedback control system. The *GUI* of process identification and *PSO* optimization are shown in Fig. 2.

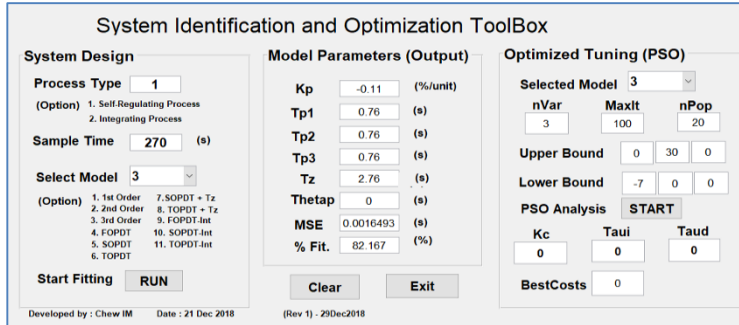


**Fig. 2.** Process Identification and PSO Optimization of the GUI.

### 3.2 Performance Measurements with Minimum Integral Error

Minimum integral error is a quantitative performance statistics measurement developed by Muriel and Smith [19]. Technically, it reflects the integral error,  $e$ , over the duration of time. The integral values from the measurement might vary from different PID controller tunings, where the least error value is desirable. The widely used minimum integral error measurement includes Integral Absolute Error,  $IAE$ , Integral Square of Error,  $ISE$ , and Integral over Time for Absolute Error,  $ITAE$ .

## 4 Analysis and Discussion

### 4.1 The Identified Process Model

During process identification, two responses happened simultaneously dynamic was only displayed by a combined response and thus it is difficult to determine individual response separately. However, it can be solved by using the developed *GUI*. Process identification was applied to produce *FOPDT*, second order and third order transfer function as depicted in Table 1.

**Table 1.** Transfer Function and Fitness Percentage.

Process Model	Transfer Function	Fitness Percentage (%)
FOPDT	$G_{p1} = \frac{-0.12(1 - 0.06s)e^{-2.59s}}{0.94s + 1}$	67.13
2 <sup>nd</sup> -order system	$G_{p2} = \frac{-0.106(1 - 2.9s)}{(1.14s + 1)(1.32s + 1)}$	73.13
3 <sup>rd</sup> -order system	$G_{p3} = \frac{-0.11(1 - 2.76s)}{(0.76s + 1)(0.76s + 1)(0.76s + 1)}$	82.34

For the *FOPDT*, the fitness percentage is only 67.13 % because it ignored the inverse response. Therefore, *FOPDT* is unable to represent the dynamic behavior for this process. For the 2<sup>nd</sup> order system, the curve response covered partially of the inverse response curve with an improvement in the fitness percentage to 73.13%. For the 3<sup>rd</sup> order system, the improved fitness percentage is 83.34% thereby is chosen for the analysis.

#### 4.2 Root Locus Gain for Stability Performance

Stability of root locus infers that the denominator should have all negative roots for the robust stability of the closed-loop system [11]. Determining the characteristic equation helps to imply the stability margin that can be obtained through the mathematic calculation of the denominator in the transfer function as  $1 + G(s)C(s) = 0$ .

$$1 + \left( \frac{-(0.3036s - 0.11)K}{(0.76s+1)^3} \right) = 0$$

Simplify it,  $0.439s^3 + 1.733s^2 + 2.28s + 1 - (0.3036s - 0.11)K = 0$

From the term  $s^1$ ,  $2.28 + 0.3036K > 0$  gives  $K > -7.5$

From the term  $s^0$ ,  $1 - 0.11K > 0$  gives  $K < 9.09$ .

As noted, stability gain,  $K$  should always have similar polarity to the process gain, the process gain obtained was a negative gain. Thereby, the range for stability should be,  $-7.5 < K < 9$ . The value of gain should have some polarity with the process gain for stability control, thereby the gain is  $-7.5 < K < 0$ . That means, the proportional gain value of the range from -7 to 0 is expected to produce asymptotically stability in the closed-loop performance.

#### 4.3 PID Controller Settings

Table 2 showed the various PID settings for different tuning methods.

**Table 2.** PID controller settings for IMC, CC, and PSO.

Controller settings	$K_c$	$K_i$	$K_d$
IMC-PI	-0.4	-0.45	0
IMC-PID	-1.089	-0.48	1.98
CC	-1.397	-0.227	0
PSO	-1.425	-0.598	0

The first three controller settings were determined by using deterministic approach, where *IMC-PID* is expected to provide more aggressive control followed by *CC* and *IMC-PI*. In addition, *PSO* is the probability approach to obtain the optimal tunings for the least inverse response, overshoots and settling time in the curve response.

#### 4.4 Unit Step Response Performance

Fig. 3 (a) illustrated the transient response of various tuning methods. It is noted that *IMC-PI* tuning performed the slowest response. *IMC-PID* tuning produced the most aggressive response. The *CC* tuning methods produced a better response as compared to both *IMC* settings. Interestingly, the *PI* settings from *PSO* analysis overall improved the transient response as the produced response has fewer oscillations with better settling time. For the inverse response, *IMC-PID* produced the sharp curve of inverse response, which was caused by the “derivative kick” of control action. *CC-PI* produced the largest inverse response whereas the *PSO* tunings produced the least inverse response.

Fig. 3 (b) showed that *PSO* provided the most balanced *PI* tunings that provides a good control to the Heat Exchanger function. *IMC-PI* tunings seemed was not much capable to mitigate the disturbance thereby produced the sluggish response. *IMC-PID* produced the largest overshoots with the longest settling time.

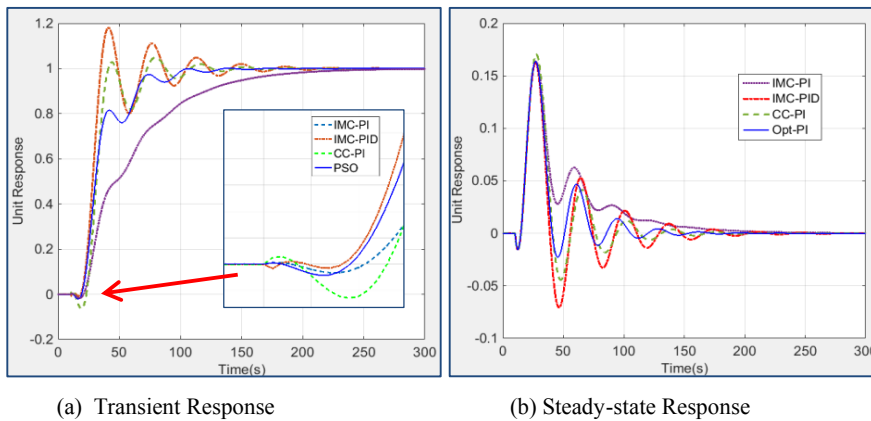


**Fig. 3.** Improved responses by using PSO analysis.

#### 4.5 Performance Indicators and Index

Table 3 showed the system performance of various PID settings. The *PSO* produced the shortest settling time and the second lowest undershoots percentage of the inverse response. The *IMC-PI* tunings produced the slowest transient response thus with the longest period of the rise time, peak time and settling time. *CC* method produced the fastest response with less overshooting but weaken in controlling the inverse response as the undershoot was 6.46%. For the performance index, *IMC-PI* and *IMC-PID* tunings produced the large integral error values. *PSO* analysis produced the smallest *I<sub>SE</sub>* and *I<sub>TAE</sub>* among three integral error measurements. It implies that *PSO* is more suitable to be used as compared to other tuning methods.

**Table 3.** Performance Indicators and Index.

Controller	Performance Indicators					Performance Index		
	Rise Time (s)	Peak Time (s)	Over-shoots (%)	Settling Time (s)	Under-shoot of IR (%)	IAE	ISE	ITAE
IMC-PI	290.01	290.01	0	142	1.62	57.85	31.01	4786.40
IMC-PID	24.79	31.26	18.1	103.2	2.876	16.83	30.60	2624.00
CC	31.02	33.78	2.8	87.17	6.462	30.46	20.36	2198.47
PSO	96.13	96.13	0	81.87	1.89	31.55	18.96	2140.82

#### 4.6 Performance Analysis of the various $K_c$ and $K_i$ values of the PID controller

The performance response of various  $K_c$  and  $K_i$  settings were analysed aimed at visualizing the impact of the applied controller settings towards the robustness, controllability of the Heat exchanger function in the LOOP-PRO software.

Figure 4 (a) and (b) depicted the relative responses by varying the  $K_c$  settings. Both the front and the rear views were shown to view responses and oscillations. The increased of  $K_c$  value enhanced the aggressiveness of the response but has increased the inverse response as well. As seen,  $K_c$  settings in between -0.3 to -0.5 is a good range that produced fewer overshoots with the small inverse response curve.

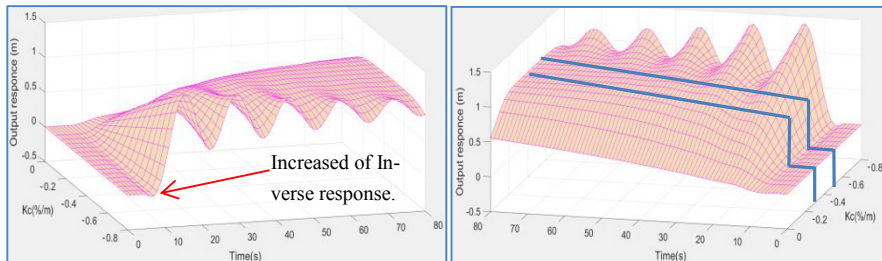
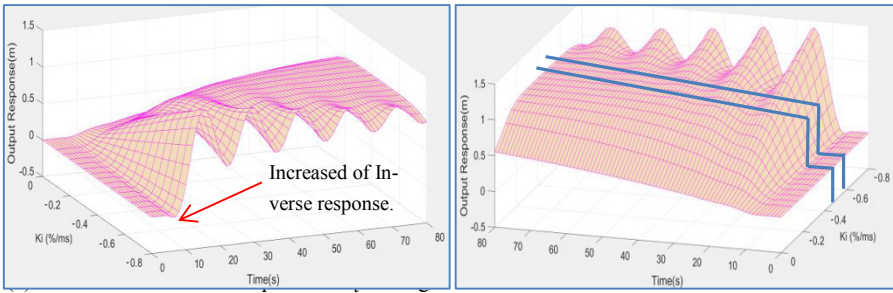
(a) Front view of curve response -  $K_c$  settings    (b) Rear view of curve response -  $K_c$  settings**Fig. 4.** Transient response of various  $K_c$  settings.

Figure 5 (a) and (b) depicted the relative response by varying the  $K_i$  values. Both the front and rear views showed the transient and inverse response curve for varying  $K_i$  settings.  $K_i$  settings are in proportional related to the aggressiveness of the response. High  $K_i$  settings cause oscillatory response whereas its low settings will cause the sluggish response. As seen from the view,  $K_i$  settings of -0.5 to -0.6 is a good range that produced a good response with a small inverse response curve.

(b) Rear view of curve response -  $K_i$  settings**Fig. 5.** Transient response of various  $K_i$  settings.

The output of both  $K_c$  and  $K_i$  tunings once again inferred the good controller settings of  $K_c = -0.425$  and  $K_i = -0.598$  by using *PSO*. It matched the *PSO*'s objective for obtaining the minimized integral error and overshoots. Therefore, the negative consequences caused by the inverse responses can be reduced when it is applied to the Heat Exchanger Function in *LOOP- PRO* software.

## 5 Conclusion

Analysis of inverse response is a critical task when designing the controller settings for enabling the stability operations in the controlled system. The process identification was carried out in various dimensions including FOPDT, 2<sup>nd</sup> order and 3<sup>rd</sup> order models. The *PSO* optimization analysis obtained the optimal PI tunings for the best curve response of the controlled process. The deterministic approaches were applied to obtain PID tunings from IMC-PI, IMC-PID and Cohen-Coon, where all the performances were discussed and compared with *PSO*. In time specification characteristic, *PSO* analysis did not produce overshoots and improves the settling time to 81.87 seconds. In terms of Performance Index, *PSO* analysis accumulated low integral error values for *IAE*, *ISE*, and *ITAE*, which reflect the great stability and controllability to the Heat Exchanger function in the *LOOP-PRO* software. The overall performance of  $K_c$  and  $K_i$  settings were also shown in 3-dimension graphics that visualise the produced curve response in various  $K_c$  and  $K_i$  settings. It has validated the obtained PI tunings of *PSO*, which concluded that  $K_c = -0.425 \text{ \%}/\text{m}$  and  $K_i = -0.598 \text{ \%}/\text{ms}$  gave the best performance due to the reduced oscillations and minimum inverse response inputs when the output systems trace each corresponding input in the desired manner.

## References

1. K.T.V.Waller, F., C.G.Nygårdas, S.:On inverse response in process control. *Ind. Eng. Chem. Fundam.* 14, 221-223 (1975).
2. M.Singh, F., D.Sakseña, S.: Parametric estimation of inverse response process comprising of order system and a pure capacitive system. *Int. J. of Infor. Tech. and Knowledge Mgmt.* 5(2), 397-400 (2012)
3. S.Arulselvi, F., G.Uma, S., M.Chidambaram, T.: Design of PID controller for boost converter with RHS Zero. *Conf. Proc. IPEMC Int. Power Electron. and Motion Ctrl. Conf.*, pp. 532-537.IEEEExplore, China (2004).
4. W.D.Zhang, F., X.M.Xu, S., Y.S.Sun, T.: Quantitive performance design for inverse-response processes," *Ind. Eng. Chem. Res.* 39, 2056-2061 (2000).
5. M.Morari, F., E.Zafirion, S.: Robust Process Control. Prentice-Hall, New York (1989).
6. I.M.Chew, F., F.Wong, S., J.Nandong, T., A. Bono, F., K.I.Wong, F.: Revisiting Cascade Control System and Experimental Analysis to PID Setting for Improved Process Control, American Scientific Publishers, 10177-10182 (2017).
7. C.A.Smith, F., A.B.Copripiو, S.: Principles and practice of automatic process control. John Wiley & Sons, USA (1985).
8. A.Slowik, F.: Natural inspired methods and their industry applications – Swarm Intelligence Algorithm. *IEEE Transactions on Ind. Infor.* 14(3), 1004-1015 (2018).
9. P.Ouyang, F., V.Pano, S.: Comparative study of DE, PSO and GA for position domain PID controller tuning. *Algorithms* 8, 697-711 (2015).
10. V.M.Alfarو, F., R.Vilanova, S.: Robust tuning of 2DoF five-parameter PID controllers for inverse response controlled processes, *J. Process Control* 23(4), 453–462 (2013).
11. C.B.Kadу, F., D.V.Sakhare, S.: Improved inverse response of boiler drum level using Fuzzy Self-Adaptive PID controller. *Int. J. of Eng. Trends and Tech.* 19 (3), 140-144 (2015).
12. I.Kaya, F.: PI-PD controllers for controlling stable processes with inverse response and dead time. *Electro. Eng.* 98, 55-65 (2016).
13. J.A.Martinez, F., O.Arrieta, S., R.Vilanova, T., J.D.Rojas, F., L.Marin, F., M.Barbu, S.: Model reference PI controller tuning for second order inverse response and dead time processes. in *IEEE Int. Conf. Emerg. Tech. Fact. Autom. ETFA*, pp. 2–6 (2016).
14. M.Irshad, F., A.Ali, S.: A review on PID tuning rules for SOPDT inverse response processes. *Int. Conf. on Intelligent Computing, Instr. & Ctrl. Tech.* pp17- 22 (2017).
15. J.Kennedy, F., C.Eberhart, S.: Particle swarm optimization. In: *Proceedings of the IEEE Int. Conf. on Neural Networks*. pp. 1942–1948, USA (1995).
16. M.Sayed, F., S. M. Gharghory, S., H.A.Kamal, T.: Gain tuning PI controllers for boiler turbine unit using a new Hybrid Jump PSO. *J. of Elect. Syst. & Info. Tech.* 2, 99–110 (2015).
17. M.Balamurugan, F., S.Narendiran, S., S.K.Sahoo, T., R.Das, F., A.K.Sahoo, F.: Application of particle swarm optimization for maximum power point tracking in PV system. In *Proc. 3rd Int. Conf. Elect. Energy Syst*, pp. 35–38, IEEE, India (2016).
18. J.P.Ram, F., N.Rajasekar, S.: A new robust, mutated and fast tracking LPSO method for solar PV maximum power point tracking under partial shaded conditions. *Appl. Energy* 201, 45–59 (2017).
19. J.B.Riggs, F., M.N.Karim, S.: Chemical and bio-process control. 3<sup>rd</sup> Edition," Pearson International Edition, USA (2006).



# 3D Keyframe Motion Extraction from Zapin Traditional Dance Videos

Ikmal Faiq Albakri<sup>1</sup>, Nik Wafiy<sup>1</sup>, Norhaida Mohd Suaib<sup>1</sup>, Mohd Shafry Mohd Rahim<sup>1</sup>, and Hongchuan Yu<sup>2</sup>

<sup>1</sup> School of Computing, Faculty of Engineering, Universiti Teknologi Malaysia, Johor, Malaysia

<sup>2</sup> National Centre for Computer Animation, Bournemouth University, United Kingdom

ikmalfaiq@yahoo.com, nikwafiy@gmail.com, {haida, shafry}@utm.my,  
hyu@bournemouth.ac.uk

**Abstract.** Capturing traditional dance motion data using motion capture technology is too expensive as it required a lot of high-priced equipment involving complicated procedures. It is also hard to find any traditional dance motion data from any open sources as the motion data always being made private and not for public use. However, the traditional dance videos can be found easily from any internet medium such as YouTube and it also free to be used by the public. Therefore, in this paper we propose a method of extracting the 3D dance motion data of Zapin traditional dance from videos instead of motion capture technology by using keyframe animation extraction method. This method works by extracting all the 3D body joints coordinates of every frame in the keyframe dance animation and reconstruct the extracted motion data into an empty character model to check whether the extracted and reconstructed 3D Zapin dance motion data is correct and efficient compare to the original dance motion in the videos.

**Keywords:** Videos, Keyframe Animation, Zapin Traditional Dance, 3D Dance Motion Data, Extraction, Reconstruction.

## 1 Introduction

As the animation industries rapidly increasing in this modern era, the demand of the motion capture technology is also increasing [1]. Motion capture is very important as the technology can captured realistic motion that later can be extracted into different form of motion data which is good for the animation industries development. However, motion capture is too expensive and time consuming making it hard to be owned by everyone. This is because motion capture required a lot of high technology camera and equipment such as body suits to track and record the movement of the motion [2]. Not to be forget it is also required a large space of area and specific talents for the process to take place [3]. Overall, it is costly for researcher to prepare the motion capture's setup in order to get the realistic motion data.

Nonetheless, this is totally different with videos as it can be found easily from the internet especially monocular videos. As it is being published publicly in the internet such as YouTube and Google, there is no problem regarding the right of ownership as everyone can download it freely and safely from patterning issues. Since the video doesn't require expensive devices and can be found literally everywhere from the internet, it can be one of the effective medium to extract the 3D motion data instead of using motion capture technology.

Conventionally, the past researchers are trying to extract the 3D motion data by using tracking method from monocular videos. With the introduction of Bayesian approach, the approach works on how to estimate the 3D articulated motion from the changing of images thus making the tracking of 3D articulated human figures from monocular video sequence possible and successful [4]. However, as the approach successfully tracked the 3D human movement from videos, there are some part of the body (usually arms) were poorly estimated due to the occlusion problem [4]. Thus making the introduced tracking approach not efficient enough if it being used to track more complicated motion such as in the traditional dance.

In this paper, we proposed a new method to extract the 3D motion data from monocular dance videos by using keyframe animation extraction method. Zapin traditional dance videos were used as the medium for the extraction of 3D motion data while conserving the Malaysia cultural heritage. As traditional dance is under threat nowadays due to the changes of culture and beliefs, extracting the traditional dance motion can be one of the initiatives to preserve the traditional dance from extinction. The objectives of the research are:

1. To extract the 3D Zapin motion data by using keyframe animation extraction method based on the monocular videos instead of motion capture.
2. To reuse and reconstruct the 3D extracted Zapin motion data into the keyframe animation.
3. To evaluate the 3D Zapin motion created using the keyframe animation reconstruction method.

With the advent of computers and the introduction of keyframe animation method, the 3D animation become more approachable as it is given a tool for the animator to completely control the specification of an animation [5]. The animator can control how to interpolate the 3D model transformations, set up the 3D model orientations or even specified how many frames for an animation to occur [5]. As the character model being represented in 3D space and visualize by the image plane in the computer, this method tends to create more realistic looking images compare to the 3D representation of a 2D drawing [6]. Therefore, by combining the feature traits of the keyframe animation with the monocular videos, this paper focussed on how to generate a new method to extract the 3D dance motion data from videos instead of capturing it by using motion capture technology.

## 2 Related Works

### 2.1 Past 3D Extraction from Monocular Video Methods

There are various researches have been carried on that emphasizing the extraction of 3D motion data from videos. Generally, the most relevant to our work is in [4], [7], where the system tracks the movement of the body joints in a 2D monocular video and combines the tracking information with a human motion model to estimate the body's motion in 3D. With the introduction of Deep Learning, the 3D monocular video tracking have getting a milestone improvement as most recent approaches have been rely on Deep Learning to estimate the 3D human pose such in [8]–[10]. The Deep Learning usually involved in the regression process to regress an image directly to the 3D joints coordinates or 2D joints locations based on which 3D coordinates are defined. As the research in [8], the system enhanced the image cues technique to the full by fusing 2D and 3D image cues to estimate the 3D human pose. Relying on two Conventional Neural Network (CNN) Deep Learning streams to jointly connecting 3D pose from 2D joint locations from the image directly, it produced an approach that merged the two streams in a more effective way. While in [9], the system used the same concept in [8] but in a real time environment. Instead of using classic physical depth reconstruction, the system focussed on several monocular image cues to estimate motion difference between images and consistency maps of temporal resolution and low spatial in real-time.

The most recent addition that emphasise the usefulness of Deep Learning to further enhance the 3D motion extraction from monocular video that closes to our work such as in [11] and [12]. The approach in [11] works by applying deformation reconstruction to the actor template mesh with a parameterized kinematic skeleton and medium-scale deformation field. With the template mesh, the deformation has been estimated to closely emulate the movement of the video input thus allowing the generation of temporally coherent surface representation of the articulated full body human motion. Then, the respective articulated human motion being gripped with 2D joints predictions to act as landmarks for the registration of 3D skeleton to the image using CNN. However, due to the lack of depth information, the estimated 3D pose is not efficient and incorrect. Therefore, another CNN has been trained by regressing 3D joints positions from monocular images. Overall, this approach managed to capture the full 3D human body movements from 2D monocular video by utilizing scattered 2D and 3D human pose detections using batch-based pose estimation with the help of two CNN. While in [12], the research produced a real time multi person 2D pose estimation system called OpenPose to track the facial, body and foot movement through key points estimation. The system works by implementing Part Affinity Fields (PAFs) to encodes both position and orientation of human body parts and associate with the individuals in the image or video. A fineness quality parses of body poses have been produced through a greedy parsing algorithm and later being combined with foot estimation to be trained using CNN with a foot dataset consisting of fifteen thousand-feet key points instances thus creating a first open source real time 2D key points image or video detection system.

Based on the research in [4], [7], the Bayesian approach managed to track the movements from a 2D monocular video and estimate the 3D motions. However, due to the

changing of lighting and contrast of the video, it causes confusion to the tracker and making the reconstruction of the 3D motion inaccurate and not efficient throughout the videos. Next, occlusion is also one of the biggest problems in video tracking method as the occluded body parts make the tracker to lose it track thus failing to reconstruct the movements correctly. The introduction of Deep Learning in [8]–[12] were able to speed up and improvise the extraction of 3D motion data from monocular videos using video tracking method by involving machine learning algorithm into the approach. Albeit the good side of Deep Learning, it required a high computation power to run CNN and it will cost a lot of money just to handle the heaviness of the process. With the costly method, it also cannot guaranteed the quality of the extraction 3D motion data as strong occlusion and fast motion will still lead to the tracking failure hence affecting the efficiency of the motion.

In general, there have been limitations on the previous research especially on the occlusion problems. The previous research trying to tackle this issue and more focussed on the image processing technique instead of the 3D animation technique. Therefore, our group have performed a new method that relies on the 3D animation technique to produce simpler but more effective 3D motion data extraction from monocular videos.

## 2.2 Keyframe Animation Creation

Keyframe animation is one of the popular approach for the character animation where the animator manually designed the pose of the character in a set of frames in the animation [13]. As the 3D computer animation tools such as Autodesk Maya become more accessible to the novice users, keyframe animation getting more attention and recognition in the animation creation industries [14]. This is because keyframe animation provide higher performance support for designing extreme poses and unusual motions [15]. Although it given a complete control for the animator to create the animation, keyframe animation is time consuming and labour intensive as the animator need to manually set the poses in every frames of the animation. However, there are past research that being done to speed up the process such as in [13], [14] by addressing the performance timing of the keyframe animation. Next, the introduction of Inverse Kinematics (IK) tools also contribute to speed up the keyframe animation process as it helps the animator to set character poses more efficiently and realistically. By further enhancing the IK in [16], the implemented approach allows the animator to take control of the inertia and center-of-mass (CM) of a character thus producing more intuitive keyframe animation.

## 2.3 Keyframe Animation Extraction

Keyframe animation contains a lot of motion data information that can be useful for the animation industries. By extracting the motion data from the keyframe animation, the motion data can be retarget, synthesis or even made reusable to be used in another animation. There are several keyframe animation extraction techniques that being introduced by the past researcher such as extraction through the keyframe animation sequences [17][18], extraction based on motion sequence represented by bone angles [19] and extraction based on joint kernel representation [20]. These extraction techniques

implemented their own unique algorithm based on the extraction operation to extract the motion data from the keyframe animation while ensuring the consistency between original motions.

### 3 Methodology

Given Zapin traditional dance videos as the input, we proposed to extract the dance motion data using the keyframe animation extraction method rather than using the image processing technique. First, we manually created the keyframe dance animation according to the videos. From the results, we devised an algorithm to extract the 3D coordinates of the body joints of every frame in the keyframe dance animation into a single XAD file. This single XAD file contained extracted motion data of the respective dance motion throughout every frame of the keyframe dance animation. Once the XAD file has been created, we applied another algorithm to reuse and reconstruct the extracted motion data into an empty model character without any animation.

#### 3.1 Keyframe Animation 3D Motion Extraction

We begin by collecting the Zapin traditional dance monocular videos from internet and split it into image sequence to act as the reference. The image sequence of the respective dance and a character model called Malcolm model were imported into the Autodesk 3D Maya. Next, each body parts of the character model were manually positioned one by one referred to the image sequence. Fig. 1 shows the process how to locate and position all the 3D coordinates of the body parts including joints in order to get similar result as the dance movement produced in the video.



**Fig. 1.** Manually positioned the body parts of the model character in Autodesk 3D Maya referred to the image sequence.

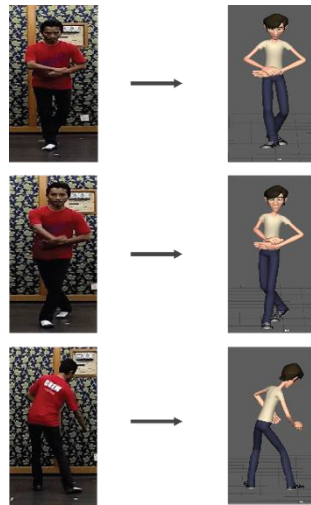


**Fig. 2.** Keyframe dance animation of Zapin Asas Dance.

Using the 3D model transformations tool provided by Autodesk 3D Maya, the orientation and location of each body parts were controlled throughout the respective Zapin dance motion. The X, Y and Z coordinates of the body parts were located precisely in order to ensure the efficiency of the motion dance. With the introduction of IK in Autodesk Maya, it allowed us to take control of the inertia and center-of-mass in the animation thus making the model character to dance more realistically and smoothly. The result of the created keyframe dance animation called Zapin Asas Dance is being showed in Fig. 2.

---

**Algorithm 1** Extraction Algorithm

---

```

1. Set Joints Name
2. Select Joints
3. Get StartFrame, Endframe
4. For (i=0; i<Joints.length; i++)
5.     Set CurrentFrame = StartFrame
6.     While (CurrentFrame != EndFrame)
7.         Get Rotation Order (Joints[i],CurrentFrame)
8.         Save to XAD file
9.         Go to next frame
10.    End While loop
11. End For Loop
12. Display Extraction Successful

```

With the keyframe dance animation has been created, the dance movement of the Malcolm model now has the valuable motion data that can be extracted out. Therefore,

we have implemented an extraction algorithm as shown in Algorithm 1 to extract the dance motion data from the keyframe dance animation. The basic idea of the extraction algorithm is to extract based on the joints representation of the model character. By selecting the joints that involved with the dance movement, all the rotations and 3D coordinates of the joints starting from the beginning of the frames until the end of the frames in the animation is being identified and extracted into a single XAD file.

### 3.2 Keyframe Animation 3D Motion Reconstruction

As we already extracted the 3D coordinates of each body joints in the form of XAD file, a new method to reuse the extracted motion data is generated. Thus, we have implemented a reconstruction algorithm as presented in Algorithm 2 to reuse and reconstruct the motion data into an empty keyframe dance animation. Similar with the idea of the extraction algorithm, we used the same concept to reconstruct the extracted motion data into an empty model character through the body joints representation.

---

#### **Algorithm 2** Reconstruction Algorithm

---

```

1. Set Joints Name
2. Select Joints
3. Set StartFrame, EndFrame
4. Read XAD file
5. Get ExtractStartFrame,ExtractEndFrame,ExtractJoints
6. If StartFrame==ExtractStartFrame && EndFrame==ExtractEndFrame
7.   For (i=0; i<Joints.length; i++)
8.     Get index of ExtractJoints where Joints[i].Name is in
9.     ExtractJoints
10.    While CurrentFrame != EndFrame
11.      Joints[i] = Set Rotation Order(ExtractJoints[index],
12.        CurrentFrame)
13.      Go to next frame
14.    End While
15.  End For Loop
16.  Display Reconstruction Successful
17. Else
18. Display Error

```

---

The reconstruction algorithm works by reading the XAD file as the input and reconstruct the 3D coordinates information into the body joints of the model character in every frames of the keyframe animation thus applying the motion movement onto the empty model character. The empty character model as shown in Fig. 3 now has been reconstructed with the Zapin dance motion data and can dance realistically just like in the original videos.



**Fig. 3.** Frame 400 before and after reconstructed the 3D coordinates of Zapin dance motion data into the empty model using the reconstruction algorithm.

## 4 Results & Discussions

### 4.1 Qualitative Analysis

Below we discussed our result using the introduced keyframe motion extraction and reconstruction from monocular videos. We have tested our method on Zapin traditional dance videos downloaded from the internet and performed a qualitative analysis to validate the accuracy of the result compared to the original dance motion from videos.

By positioning the image sequence of the Zapin dance video parallelly with the result in Autodesk 3D Maya as shown in Fig. 4 below, the result being compared frame by frame in 24 frames per second throughout the keyframe animation to check whether the extracted motion is accurately following the original motion in the Zapin dance video. This qualitative analysis is conducted on eight respondents which include three expert Zapin dancers from Yayasan Warisan Johor and five Universiti Teknologi Malaysia computer graphics and multimedia software researchers.



**Fig. 4.** The result is following the original dance motion from the video in every frame throughout the keyframe dance animation. The location and orientation of every joint such as arms, hands, legs and feet are correspondingly positioned and rotated with the joints in the dance video.

Through the observation, the respondents were provided a questionnaire and asked whether the Zapin dance animation was realistic, the efficiency of the result compared to the original Zapin dance video and how many errors or glitches can be noticed from the animation. Using the multiple choice and linear scale scoring rubric based on the respondents' questionnaire response, 100% feel the result was realistic and 87.5% agreed that the result is efficient in term of the accuracy compared to the original dance video motion with 62.5% stated no glitches can be found on the result. Therefore, this validation process managed to prove that the extraction and reconstruction of dance motion from monocular videos using our method capable to produce efficient and accurate results.

## 4.2 Summary

By tackling the most general problem of motion capture that is being too expensive and technologically intensive, we have provided an alternative method to get the same motion data just by using videos instead of motion capture technology. With the presented method, we also introduced a new way of dance motion extraction method from monocular videos that relies on keyframe animation instead of video tracking method. The extraction based on the keyframe animation is simpler yet effective in overcome the occlusion problem in tracking method that may affect the effectiveness of the motion data.

## Acknowledgement

This paper is supported by European Union H2020 under the Marie Curie Research Fellow – AniAge Project under the grant agreement No. 691215 and research grant FRGS 4F983 from the Ministry of Education (MOE), Malaysia. The authors would also like to acknowledge Universiti Teknologi Malaysia (UTM) and Bournemouth University (BU) for the opportunities and guidance especially in terms of research facilities and related support.

## References

1. Tschang, T., Goldstein, A.: Production and Political Economy in the Animation Industry: Why Insourcing and Outsourcing Occur. In: *DRUID Summer Conf.*, no. June, pp. 1–21 (2004)
2. Nogueira, P.: Motion Capture Fundamentals A Critical and Comparative Analysis on Real-World Applications. pp. 5–18 (2001)
3. Izani, M., Aishah, Eshaq, A. R., Norzaiha.: Keyframe animation and motion capture for creating animation: A survey and perception from industry people. In: *Student Conf. Res. Dev. Netw. Futur. Mind Converg. Technol. SCOReD 2003 - Proc.*, pp. 154–159 (2003)
4. Sidenbladh, H., Black, M. J., Fleet, D. J.: Stochastic tracking of 3D human figures using 2D image motion. In: *European conference on computer vision*, 2000, pp. 702–718.

5. Pullen, K. A.: MOTION CAPTURE ASSISTED ANIMATION: TEXTURING AND SYNTHESIS. no. July (2002)
6. Sturman, D.: Interactive keyframe animation of 3-D articulated models. In: *Graphics Interface '84 Proceedings*, pp. 35–40 (1984)
7. Howe, N., Leventon, M., Freeman, W.: Bayesian reconstruction of 3d human motion from single-camera video. In: *Neural Inf. Process. Syst.*, vol. 1999, p. 1 (1999)
8. Tekin, B., Marquez-Neila, P., Salzmann, M., Fua, P.: Learning to Fuse 2D and 3D Image Cues for Monocular Body Pose Estimation. In: *Proc. IEEE Int. Conf. Comput. Vis.*, vol. 2017–Octob, pp. 3961–3970 (2017)
9. Leimkuhler, T., Kellnhofer, P., Ritschel, T., Myszkowski, K., Seidel, H. P.: Perceptual Real-Time 2D-to-3D Conversion Using Cue Fusion. In: *IEEE Trans. Vis. Comput. Graph.*, vol. 24, no. 6, pp. 2037–2050 (2018)
10. Nguyen, X. T., Ngo, T. D., Le, T. H.: A Spatial- - temporal 3D Human Pose Reconstruction Framework. (1976)
11. Xu, W. *et al.*: MonoPerfCap: Human Performance Capture from Monocular Video. vol. 37, no. 2, (2017)
12. Cao, Z., Hidalgo, G., Simon, T., Wei, S.-E., Sheikh, Y.: OpenPose: Realtime Multi-Person 2D Pose Estimation using Part Affinity Fields. In: *CoRR*, vol. abs/1812.0 (2018)
13. Igarashi, T., Moscovich, T., Hughes, J. F.: Spatial keyframing for performance-driven animation. In: *Proc. 2005 ACM SIGGRAPH/Eurographics Symp. Comput. Animat.*, no. July, pp. 107–115 (2005)
14. Terra, S. C. L., Metoyer, R. A.: Performance Timing For Keyframe Animation. In: *Proc. 2004 ACM SIGGRAPH/Eurographics Symp. Comput. Animat.*, no. August, pp. 253–259 (2004)
15. Education, T., Mou, T.: Keyframe or Motion Capture ? Reflections on Education of Character Animation. vol. 14, no. 12 (2018)
16. Rabbani, A. H.: PhysIK : Physically plausible and intuitive keyframing. (2016)
17. Sen Huang, K., Chang, C. F., Hsu, Y. Y., Yang, S. N.: Key Probe: A technique for animation keyframe extraction. In: *Vis. Comput.*, vol. 21, no. 8–10, pp. 532–541 (2005)
18. Jin, C., Fevens, T., Mudur, S.: Optimized keyframe extraction for 3D character animations. In: *Comput. Animat. Virtual Worlds*, vol. 23, no. 6, pp. 559–568 (2012)
19. Xiao, J., Zhuang, Y., Yang, T., Wu, F.: An efficient keyframe extraction from motion capture data. In: *Advances in Computer Graphics*, Springer, 2006, pp. 494–501 (2006)
20. Xia, G., Sun, H., Niu, X., Zhang, G., Feng, L.: Keyframe Extraction for Human Motion Capture Data Based on Joint Kernel Sparse Representation. *IEEE Trans. Ind. Electron.*, vol. 64, no. 2, pp. 1589–1599 (2017)



# 3D Motion and Skeleton Construction from Monocular Video

Nik Mohammad Wafiy Azmi<sup>1</sup>, Ikmal Faiq Albakri<sup>1</sup>, Norhaida Mohd Suaib<sup>1</sup>, Mohd Shafry Mohd Rahim<sup>1</sup>, and Hongchuan Yu<sup>2</sup>

<sup>1</sup> School of Computing, Faculty of Engineering, Universiti Teknologi Malaysia, Johor,  
Malaysia

<sup>2</sup> National Centre for Computer Animation, Bournemouth University,  
United Kingdom

nikwafiy89@gmail.com, ikmalfaiq@yahoo.com, {haida, shafry}@utm.my,  
hyu@bournemouth.ac.uk

**Abstract.** We describe 3D motion construction as a framework for constructing a 3D motion and skeleton using a monocular video source (2D video). The processes include 3 main phases which involved in generating ground truth 2D annotation using OpenPose, generating the mesh and 3D matrices of person in the sequences of images based on 2D annotation and bounding box and lastly using the matrices to create a HIK 3D skeleton in a standalone Maya application. For the process, we highly relied on the 2D annotation using Convolution Neural Network. We demonstrate our result using a video of Malaysia Traditional Dance called zapin.

**Keywords:** Convolutional Neural Network, Human Mesh Recovery, 2D annotation, 3D annotation, Maya, Maya Standalone, HIK, Part-affinity.

## 1 Introduction

This paper is concerned with the challenge of recovering the full-body 2D human pose, and also in acquiring the anatomical keypoints on a single dance video and converting it to 3D motion data. Human pose estimation is one of the major problems which have gained lots of attention recently in the world of computer vision. The importance of human pose estimation is, it will allow us to accumulate a higher level of reasoning in terms of human-computer interaction and recognition. As for this paper, we propose a framework which will work as an alternative for the mocap technology in acquiring the 3D motion data and also 2D annotated data. Even though the quality of the mocap data is second to none, it will take lots of equipment which is expensive and also it will consume lots of time as the process need many human labours in order to control the equipments. At first we will explain the process of acquiring the 2D keypoints from the monocular video. Inferring the human pose from image sequences is not an easy task, there are several challenges that need to be addressed [3]. First, is the number of people that can appear in the image sequence. Second is the problem that originated from occlusion, contact, and limb articulations, which will induce complex spatial interference, and third

is the cost of high processing time as the number of people increase, thus making real-time performance a challenge. There are 3 main parts involved in the process of human pose estimation. First, the process starts by identifying the anatomical keypoints of the human body, it will detect and identifying every part of the body, preferably joints which can be used as tracking point in the imagery. The annotated data then will be trained. The second part is, it will joint all the keypoints to form the skeleton structure. In this process, the keypoints will be joined together based on their confidence score. Next, after all the joints are joined together, it will form a 3D representation of the skeleton structure. Human beings can be regarded as an objects composed of multiple moving parts that joined together at specific joint points. Consequently, human pose estimation aims to extract all the keypoints which represent the joints of body parts from the features of the images. By using this method, the extracted keypoints can be used to analyze or classify the motion of the human, and reconstructing the motion by applying it to full 3D mesh.

Numerous studies has been conducted towards 2D human pose estimation, and have showed significant progress since the convolutional neural networks, (CNN) has been introduced for this task. There are two approach in human pose estimation, first is bottom-up approach and the other is top-down approach. The feature in bottom-up approach is formed by collecting pieces of evidence where it directly predict the keypoints all at once to create an estimation for the pose [1]. As for top-down approach, the low level evidence are collected by obtaining human candidates using a human detector to create the estimation pose [2]. The sequences of images from the video are treated as the lowest level and human pose configuration is considered to be at higher level.

Apart of its remarkable progress of building the pose estimation, there are some notable flaws with the both approaches. The runtime of top-down approach is proportional to the number of people or performers in the image where a single-pose estimator is operating for each detection of person [3], it also very sensitive to the bounding box shifting and tightness as the network prone to get confused over annotation process [1]. Conversely, bottom-up approach greatly outperforms top-down approach in terms of computing the joint locations [4], [5] even though it takes a lot more time to connect the corresponding joints for the person



**Fig. 1.** Multi-person poses estimation and single pose estimation using OpenPose. All the body parts and keypoints that originate from person are linked together including foot.

## 2 Related Work

Human pose estimation has come a long way since its traditional approaches of adopting the techniques of pictorial structures models [4], [11], [5] and graphical models [6]. The pictorial structures model expresses the spatial correlations between parts of the body using tree-structured graphical model with kinematic which couple the connected limbs [7]. While proven to articulate the pose estimation where all the limbs of the person are visible, it prone to produce characteristic errors such as double-counting image evidence which happens because of the correlations between variables are not captured by the tree-structured model.

Sun et al. [10] propose a coarse-to-fine representation (hierarchical model) to detect and estimate the pose of body parts. Hierarchical models represent the articulate parts which have a different sizes and scales for example head, arms, legs, etc in hierarchical tree structure. The underlying consumption of these models is that the distinctive features which originated from different levels can be used to jointly improve detection performance.

There are many previous works that also heavily relied on concept that all body parts should be treated independently and use the pictorial structure framework to model spatial orientation relationship [10]. Yang et al. [11] proposed a method to capture an orientation with a flexible mixture of templates for each part. The major flaw of these methods is that the operation is dependent to the approximate inference at time of learning and testing hence they have to exchange the accuracy in modelling the spatial relationships with a simple parametric model which allow much more efficient inference.

The introduction of Convolutional Neural Networks has significantly boosted the percentage of obtaining reliable local observations of body parts which resulting the increased of accuracy on body pose estimation [8]. In comparison to fully-connected deep architectures, Convolutional Neural Networks reduces the usage of parameters which resulting to much easier training and reduces overfitting. Pfister et al. [9] used a deeper network to regress the joint confidence maps or heatmaps of the human joints. In order to capture the spatial dependencies of joints implicitly, a network with large receptive is designed. Qiang et al. [18] also make use of deep learning network to achieve a more robust and adjustable parameters for the human pose estimation based on global features. The combination between the convolutional network and the GoogLeNet does help in improving the results of low feature extraction. While in [19] the writer try to improve the accuracy of the estimation based on in-the-wild data by first explicitly encode the 2D keypoints features in heatmap which resulting the feature to contain only the depth information about the human pose, by doing so, it increase the reliability of the network to predict the 3D pose even if there are significant shift of the input between training and testing phase. Recent work of [20] also focus on improving the pose estimation efficiency by proposing a lightweight hourglass's network. The process is done by transferring the latent knowledge of the pre-trained model to a smaller target pose model.

Li et al. [13] uses a deep convolutional neural network to find the 3D human pose estimation from monocular images. There are two types of process included in this operation, first is the process of regression where the position of joints points which

relative to the root are estimated, and second is the process of detection of each joint point and local window.

The aim of detection process is to classify whether does one local window contains the specific joint or not. Both processes use bounding box images containing human subjects. Li et al.[1] used the color images with the bounding box in order to connect the joints of the candidates and form a full pose. An initial pose for each of the bounding box are acquired by performing pose parsing for every person in the image. The problems with this technique is that it prone to produce redundant poses as the same part of this one person may be visible in multiple bounding boxes. Second is the redundancy in detection which resulting to redundant poses.

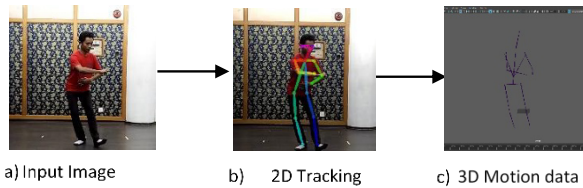


**Fig. 2.** Overall pipeline (a) an image created from a monocular video will be used as an input image, (b) OpenPose will create a bounding box of the character. For each of every frame in the video, json data which contained multiple keypoints and joints is generated.

Pishchulin et al. [15] address the problems of estimating the human body by detecting the people first and then estimating their body pose, by proposing a formula of partitioning and labelling a set of body-part hypotheses that generated with CNN-based part detectors. Even though the approach does not rely on the detection of a person, to solve the proposed integer linear programming over fully-connected graph is an NP-hard problem and lead to huge amount of processing time for a single image [3]. Wei et al. [7] proposed a Convolutional Pose Machine which is a multi-stage architecture based on sequential prediction framework that repeatedly produce 2D belief maps for every parts of the location and preserving multimodal uncertainty from previous iterations. The belief map enables the convolutional pose machine to learn rich image-dependent spatial models of the relationship between parts. While other method explicitly parse the belief map using either graphical models or specialized post-processing steps [16], [17], it learn implicit image-dependent spatial models of the relationship between parts. However, the main problem for the approach is, all the location and scale of the person of interest is given. It also needs an intermediate supervision at the end of each stage to address the problem of vanishing gradients.

### 3 Method

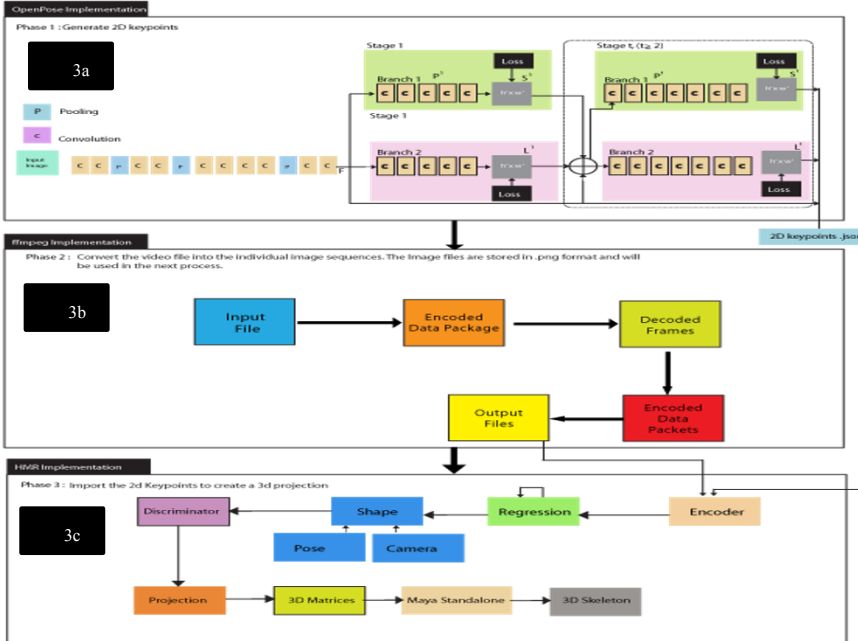


**Fig. 3.** Overall framework architecture of constructing 3D skeletons and motion data from monocular video.

Figure 3 encapsulates the overall pipeline of our method. We use OpenPose to get the bounding box of the dancer for every frame of the video. The system takes an input of image with size of  $w \times h$  and produces the 2D location of anatomical keypoints for each person in the image. The process starts with the feedforward network that make a prediction of 2D confidence maps set ' $S$ ' of body part location and also set of 2D vector fields ' $L$ ' of part affinity, which encode the degree of association between parts. The set of confidence maps defined as  $S = (S_1, S_2, \dots, S_J)$  has  $J$  confidence maps,  $J$  is the element of  $\mathbb{R}^{w \times h}$  one per part which is refined by cao et al. as  $S_j \in \mathbb{R}^{w \times h}$ ,  $j \in \{1 \dots J\}$  [3] and for the part affinities, the set  $L = (L_1, L_2, \dots, L_C)$  has  $C$  vector fields, one per limb where  $L_C \in \mathbb{R}^{w \times h \times 2}$ ,  $c \in \{1 \dots C\}$  are parsed by the greedy inference. Using the same input in the first section, the ffmpeg will turn the video input into sequence of independent image,

the output will be send into Human Mesh Reconstruction (HMR) encoder to produce the projection of 3D mesh based on the bounding box created by 2D tracking and 3D matrices generated from the images.

### 3.1 Detection and 2D Tracking Keypoints

In Figure 2(a), the input image is analyzed by the first 10 layers of VGG-19 which is a convolutional network. The network then will generate a set of feature maps for the input image. There are two branches in the network, first is the top branch which responsible in predicting set of 2D confidence maps ( $S$ ) known as body part locations. Confidence maps can be recognized as grayscale image contained high value of likelihood in one location. The second branch predicts the part affinities (PAF) which is set of 2D vector fields ( $L$ ). PAF encode degree of association between parts. At the first stage, set of confidence map  $S_1 = \rho_1(F)$  and set of part affinity fields  $L_1 = \emptyset_1(F)$ .

In each stage, the predictions which both come from top and bottom stage are concatenated along with the original image features  $F$  in order to generate refined predictions. After the iterations of PAF stages, the same process will be repeated on the confidence maps detection which starts in the most updated PAF prediction.

Two loss function are applied to interactively predict the confidence maps and PAF in both branches respectively. The loss function will also be used to address any issue which related to unfinished labelling of dataset.

$S$  is referred as the ground truth of confidence maps where  $L$  is the ground truth of part affinity vector field.  $W$  is regarded as a binary mask where  $W(p)=0$  whenever the annotation is missing from the location of image  $p$ . The importance of the mask is to avoid any penalization of true positive prediction during training. Upon this process, the vanishing gradient problem faced by [16],[17] is addressed using the intermediate concept for every stage by replenishing the gradient periodically[7].

### 3.2 Part Detection Using Confidence Maps

Each of the confidence map that generated from the annotated 2D keypoints is a 2D representation of idea that every particular part can occur at each of pixel location. There should be peak corresponding for every visible part of each person. To find the maximum value of the confidence map, the individual value of the confidence map for the person is generated first, then the max operator produces the ground truth value of confidence map which is to be predicted by the network. The reason of why the maximum value of the confidence map is taken instead average value is to create a distinct precision of close between peaks if there are multiple person involved.

After all the body parts are detected, the confidence measure of every pair of body parts are used to form the full-body poses. The confidence measure is calculated by detecting an additional midpoint between each pair of parts on a limb, and at the same time checking for any incidence between candidate part detections.

### 3.3 Creating Individual Image Sequence Based on Video

FFmpeg is a collection of libraries and tools which can be used to process any multimedia content such as video and audio files. We set the parameter of the ffmpeg to create the sequence of image based on 1 frame per every second of the video. The program then will decode every frame of the encoded data package into packets and saved into desirable format. For this process we saved the sequence of images into .png format.

### 3.4 Body Mesh Reconstruction

The next step of the process is to create a 3D projection from the annotated 2d keypoints. As the OpenPose created the bouding box for the dancer and the annotated 2d keypoints in json format. We used Human Mesh Recovery (HMR) to export the bounding box, and 2D ground truth annotations which created by the OpenPose to generate 3d parameters that corresponding to the body of real humans. Figure 3c shows how the output of image from ffmpeg and json keypoints from OpenPose are exported into HMR convolutional encoder, then all the joints reprojection error are minimized using 3D regression module which conjecture the 3D representation of human body. Later, the 3D parameters are sent to the discriminator which control whether the parameters originate from a real human shape and pose or not. A standalone maya application is hardcoded and implemented in HMR process which takes the 3D matrices produced to maya Inverse Kinematic (IK) for 3D visualization.

In order to construct a fully 3D human body from a single image, we ensure that the sequences of images that we generate from the video are already annotated with ground 2D joints. At the first phase of the process, the 3D regression will receive the convolutional features of the images, which responsible in inferring the 3D human body and projected it onto annotated 2D joints. The adversarial discriminator network will determine first whether the inferred parameter received earlier are the real meshes, this is to ensure that there are no ambiguities in these parameters. The 3D regression module is a two fully connected layer with 1024 neurons in each layer, for every layer there are a dropout layer in between which followed by final layer. The network then will implicitly learn and produce the limits of the angle for each of the joints which discouraging it from generating a model with unusual body shapes.

HMR requires the bounding box which contains the person in the image's sequences. For the best performance, we ensure that the max length of the person in the image is about 150px. Then we export the skeleton animated over time (multiple images). 3D matrices and 3D camera points are also exported. The 3D matrices are used to create or rebuild the skeleton in separate application which we will discussing later. The json directory which contain the json file of the processed video will be extracted and matched depending on

### 3.5 Maya Standalone

Maya standalone is implemented right after HMR generate the matrices from the annotated data. The motion data is generated from the maya standalone by extracting all of the matrices for each frame per person first. This information can be used to create a mocap data for one person. The mocap data is produced by creating groups from the matrices which come from the json data. In this process two additional groups are added to make sure a valid skeleton can be created by using the HIK functionality build in maya.

At first, the application will bind the group data and the skeleton data using the constraints. This will take all the translation and rotation values into account. To ensure that the start frame is located on the centre point, a matrix which can be used to transform other matrices is used, it will set the start frame of the ankle is at 0, 0, 0 in the world space. We then loop over the mocap data and the key frame from all of groups, after that, the skeleton are baked and the constraints created are removed so only the desired skeleton and HIK are left in the scene.

## 4 Results & Discussion

We test our framework on several videos contained dancing movement. Our final aim is to produce a 3D skeleton which contains the motion data from the input video. The videos are about a traditional Malaysia dance called zapin. The video consists of a single dancer performing the dance step in a controlled environment. There is no Pre-processing was done on the video, and there is also no constraint required for the video input.

The testing starts with the openpose implementation to create the bounding box from person in the video and also to create a 2D annotation, next the process moves to ffmpeg implementation in order to produce an individual image sequences which will be used in HMR in order to identify whether the annotated data and the images come from a real person. The generated matrices produced by the HMR will be exported into maya standalone application where it will produce a HIK 3D skeleton. Below are the results generated to produce 3D skeleton from monocular video.

## 5 Conclusion

In this paper, we discussed a technique of constructing a 3D motion and skeleton from a monocular video. The process including generating 2D ground truth annotation and also the bounding box for every frame in the video. Then the process continues with the mesh construction using HMR where 3D matrices are produced so that it can be exported into maya standalone program to create a 3D skeleton. What we can conclude from the process is, although the process still has a runtime complexity, and a little complex articulation due to little occlusion, we can still produce the base and important motion in 3D from a 2D video, which can be used in other kind of research such retargeting and machine learning etc.

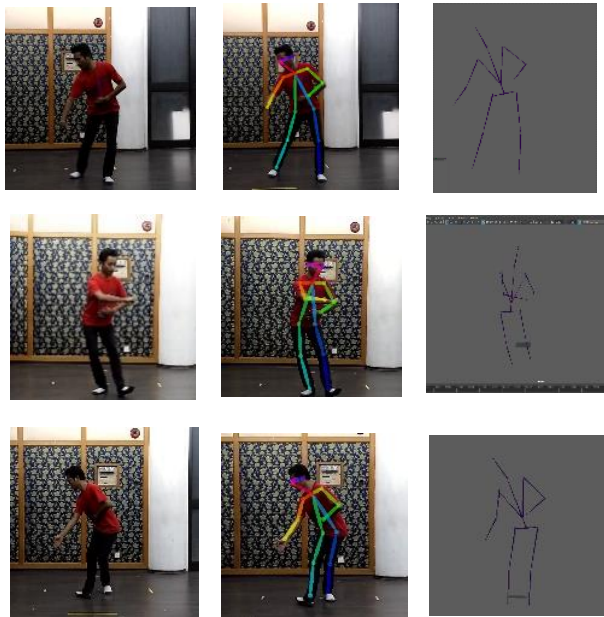


**Fig. 4.** Shows the result of generating the 3D motion from a monocular video. The tested video is a traditional Malaysia Dance called Zapin which consists of single participant.

## Acknowledgement

The authors would like to express our appreciation to Universiti Teknologi Malaysia (UTM) and Ministry of Higher Education (MOHE) for the related support and arrangements. This paper is supported by European Union H2020 under the Marie Curie Research Fellow – AniAge Project under the grant agreement No. 691215, research grant FRGS4F983 from the Ministry of Education (MOE), Malaysia and research grant GUP-Matching Grant No. 4B236 from Universiti Teknologi Malaysia (UTM).

## References

1. Li, M., Zhou, Z., Li, J., & Liu, X.: Bottom-up Pose Estimation of Multiple Person with Bounding Box Constraint. Proceedings - International Conference on Pattern Recognition, 115-120 (2018).
2. Park, S., Ji, M., & Chun J.: 2D Human Pose Estimation Based on Object Detection Using RGB-D information KSII Transactions on Internet and Information Systems, 12(2), 800-816 (2018).
3. Cao, Z., Simon, T., Wei, S. E., & Sheikh, Y.: Realtime multi-person 2D pose estimation using part affinity fields, Proceedings - 30th IEEE Conference on Computer Vision and Pattern Recognition, CVPR 2017, 1302-1310 (2017).

4. M. A. Fischler and R. A. Elschlager.: The representation and matching of pictorial structures, *IEEE Transactions on computers*, vol. 100, no. 1, pp. 67–92, (1973).
5. M. Andriluka, S. Roth, and B. Schiele.: Pictorial structures revisited: People detection and articulated pose estimation, in *Computer Vision and Pattern Recognition, CVPR 2009, IEEE Conference on IEEE*, pp 1014-1021 (2009).
6. X. Chen and A. L. Yuille.: Articulated pose estimation by a graphical model with image dependent pairwise relations, in *Advances in Neural Information Processing Systems*, pp 1736-1744 (2016).
7. Wei, S. E., Ramakrishna, V., Kanade, T., & Sheikh .. Convolutional pose machines, *Proceedings of the IEEE Computer Society Conference on Computer Vision and Pattern Recognition*, 4724-4732 (2016).
8. Newell, A., Yang, K., & Deng, J.: Stacked hourglass networks for human pose estimation, *Lecture Notes in Computer Science (Including Subseries Lecture Notes in Artificial Intelligence and Lecture Notes in Bioinformatics)*, 9912 LNCS, 483–499 (2016).
9. Pfister, T., Charles, J., & Zisserman, A.: Flowing convnets for human pose estimation in videos, *Proceedings of the IEEE International Conference on Computer Vision, International Conference on Computer Vision, ICCV*, 1913-1921 (2015).
10. Sun, M.: Technical Report: Articulated Part-based Model for Joint Object Detection and Pose Estimation, *International Conference on Computer Vision*, 7 (2010).
11. Dantone, M., Gall, J., Leistner, C., & Van Gool, L.: Human pose estimation using body parts dependent joint regressors, *proceedings of the IEEE Computer Society Conferences on Computer Vision and Pattern Recognition*, 3041-3048 (2013).
12. Karlinsky, L., & Ullman, S.: Using linking features in learning non-parametric part models. *Lecture Notes in Computer Science (Including Subseries Lecture Notes in Artificial Intelligence and Lecture Notes in Bioinformatics)*, 7574 LNCS(PART 3), 326–339 (2012).
13. Yang, Y., & Ramanan, D. (n.d.): Articulated pose estimation with flexible mixtures-of-parts, *CVPR*, 1385-1392 (2011).
14. Cai, Y., Wang, X., & Kong, X.: 3D Human Pose Estimation from RGB+D Images with Convolutional Neural Networks, 64-69 (2018).
15. Pishchulin, L., Insafutdinov, E., Tang, S., Andres, B., Andriluka, M., Gehler, P., & Schiele, B.: DeepCut: Joint Subset Partition and Labeling for Multi Person Pose Estimation, (2015).
16. Tompson, J., Goroshin, R., Jain, A., LeCun, Y., & Bregler, C.: Efficient Object Localization Using Convolutional Networks, *CoRR*, abs/1411.4 (2014).
17. A. Toshev and C. Szegedy.: DeepPose: Human Pose Estimation via Deep Neural Networks, *CVPR*, 422370 (2013).
18. Baohua Qiang, Shihao Zhang, Yongsong Zhan, Wu Xie and Tian Zhao: Improved Convolutional Pose Machines for Human Pose Estimation Using Image Sensor Data, *Sensors*, 19,718;718doi:10.3390/s19030718 (2019).
19. Habibie, I., Xu, W., Mehta, D., Pons-moll, G., Theobalt, C., Planck, M., & Campus, S. I. (n.d.) : Explicit 2D Features and Intermediate 3D Representations (2019).



# Automated Classification of Tropical Plant Species Data Based on Machine Learning Techniques and Leaf Trait Measurements

Burhan Rashid Hussein, Owais Ahmed Malik, Wee-Hong Ong, Johan Willem Frederik Slik

Faculty of Science, Universiti Brunei Darussalam, BRUNEI DARUSSALAM  
{18h8338,owais.malik,weehong.ong,johan.slik}@ubd.edu.bn

**Abstract.** The identification of plant species is fundamental for effective study and management of biodiversity. For automated plant species classification, a combination of leaf features like shapes, texture and color are commonly used. However, in herbariums, the samples collected for each species are often limited and during preservation step some of the feature details disappear making automated classification a challenging task. In this study, we aimed at applying machine learning techniques in automating herbarium species identification from leaf traits extracted from images of the families Annonaceae, Euphorbiaceae and Dipterocarpaceae. Furthermore, we investigated the application of Synthetic Minority Over-sampling Technique (SMOTE) in improving classifier performance on the imbalance datasets. Three machine learning techniques namely Linear Discriminant Analysis (LDA), Random Forest (RF) and Support Vector Machine (SVM) were applied with/without SMOTE. For Annonaceae species, the best accuracy was 56% by LDA after applying SMOTE. For Euphorbiaceae, the best accuracy was 79% by SVM without SMOTE. For inter-species classification between Annonaceae and Euphorbiaceae, the best accuracy of 63% was achieved by LDA without SMOTE. An accuracy of 85% was achieved by LDA for Dipterocarpaceae species while 91% accuracy was obtained by both RF and SVM for inter-family classification between the two balanced datasets of Annonaceae and Euphorbiaceae. The results of this study show the feasibility of using extracted traits for building accurate species identification models for Family Dipterocarpaceae and Euphorbiaceae, however, the features used did not yield good results for Annonaceae family. Furthermore, there was no significant improvement when SMOTE technique was applied.

**Keywords:** SMOTE, Species identification, Leaf measurements, Machine learning, Herbarium specimen

## 1 Introduction

In high diversity regions such as the tropics, the task of plant species identification can be difficult as the plants in the same genus are morphological similar and often difficult to distinguish. The application of machine learning in plant classification has caught

the interest of personnel in various fields given that the knowledge required by botanist can take years to train [1]. Plants have different morphological structures which are used to differentiate various species. However, one of the most important features in this regard is the leaf shape which remains unchanged over the life time of the plant and is easy to preserve in a herbarium for future studies [1]. The preserved collection of these species in herbarium contains valuable information and the digitization of the species has enhanced the access of these species for further studies.

In recent years, there have been substantial works in plant species classification using machine learning (ML) and computer vision techniques. Most of the effort in these works have been placed in fresh leaves for feature extraction [2]. Furthermore, little work have been done in identification of plant species for datasets with imbalanced distribution of classes (species) [3]. This study aimed at applying machine learning techniques namely Random Forest, Support Vector Machine and Linear Discriminant Analysis for automating plant species identification as they have been successfully applied in tropical shrub species identification in recent studies [4]. We have also applied Synthetic Minority Over-sampling Technique (SMOTE) to investigate if it could improve the classifier performance as it has proved superior and robust in other domains [5].

## 2 Datasets

Table 1 summarizes the datasets used in this study. The imbalance distribution can be observed for Annonaceae and Euphorbiaceae families.

**Table 1.** Summary of datasets collected for this study

Family	No of classes	Number of samples	Majority class sample	Minority class sample
Annonaceae	17	292	25	10
Dipterocarpaceae	63	315	5	5
Euphorbiaceae	15	399	107	10
Annonaceae + Euphorbiaceae species wise	32	691	107	10
Annonaceae + Euphorbiaceae family wise	2	691	399	292

## 3 Methodology

Figure 1 shows the steps performed for the plant species identification using the leaf measurements. The details of each stage are explained in the following sub-sections.

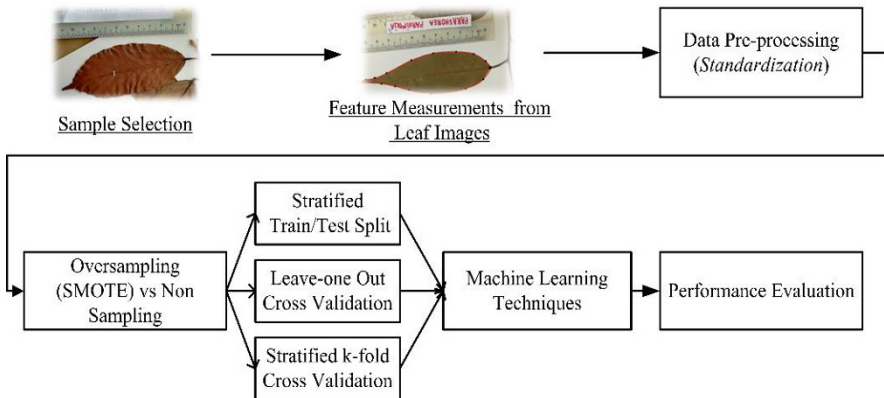


**Fig. 1.** Steps for performing plant species classification

### 3.1 Sample Selection

The leaf samples (dried leaves) used in this study were collected from Universiti Brunei Darussalam's herbarium. The images of well-developed and damage free samples of leaves were taken using a high-resolution camera and later a dedicated software (JMorph) was used to measure the leaf features.

### 3.2 Feature Measurements from Leaf Images

Fifteen leaf features for all species from our samples were collected including calibration length, outline area, angle of first vein, angle of second vein, angle of third vein, length of leaf, width of leaf, base-to-widest point width, petiole length, first vein pair distance, second vein pair distance, third vein pair distance, angle of leaf tip, angles of leaf base left and right leaf.

### 3.3 Data Preprocessing

The dataset features were standardized before applying the machine learning techniques due to different ranges of the features extracted in previous stage. For train/test split and k-fold configuration, the subsets were separately standardized while for LOOCV cross-validation, the whole dataset was standardized before training/testing.

### 3.4 Oversampling Techniques

In order to investigate the usefulness of oversampling for our class imbalance problem, oversampling technique was used to replicate more samples for the minority classes without increasing the information. Random oversampling selects the minority class randomly, duplicates its members and then appends them to the minority class set [6].

This process is repeated for several times until the desired balance in data is reached. However, following this approach may result in overfitting. To overcome the problem of overfitting, a novel technique called Synthetic Minority Oversampling Technique (SMOTE) was used [7]. The technique uses feature space to produce artificial samples of minority class rather than data space. For each instance in a minority class, a synthetic instance is generated by randomly selecting its k-nearest and compute the feature vector difference between the k-nearest neighbors and the instance. The computed feature vector difference is then multiplied by a random number between 0-1 and added to the original minority instance to generate a new artificial instance.

### 3.5 Machine Learning Techniques

In this study, we applied three different machine learning algorithms namely Random Forest (RF), Linear Discriminant Analysis (LDA) and Support Vector Machine (SVM) for classifying the plants' families/species [8].

### 3.6 Performance Metrics

Evaluating models in a multiclass problem presents a slightly different challenge than binary classification especially for the case of imbalanced dataset where the distribution of classes is not equally represented. In this study, a weighted approach for four different evaluation metrics (accuracy, weighted precision, recall and F1-measure) were used to get more intuition of the performance of ML models rather than relying on single metric due to having multiclass imbalance data sets. The formula for calculating a weighted metric is shown in Equation 1 [9]:

$$\text{Weighted Metric} = \frac{(M_{c_1} \times |c_1|) + (M_{c_2} \times |c_2|) + \dots + (M_{c_n} \times |c_n|)}{|c_1| + |c_2| + \dots + |c_n|} \quad (1)$$

Where  $M$  is a metric (Precision, Recall or F1-score),  $M_{c_1}$  up to  $M_{c_n}$  are the metrics for class 1 to class n, and  $|c_1|$  to  $|c_n|$  are the number of instances for class 1 up to class n.

## 4 Experimental Design

In this study we applied three different machine learning models under three different validation approaches including stratified train/test split (random split), leave-one-out and k-fold cross-validation. The results were evaluated before and after applying SMOTE for the imbalanced datasets. For stratified train/test split, a test size of 30% was used for all the experiments and each ML model was trained/tested 100 times for all the datasets and the average values of the evaluation metrics were reported for test data. The stratified 10-folds cross-validation was applied for all datasets except for Dipterocarpaceae family which had a maximum of 5 samples for each species. For applying

SMOTE, data balancing method was employed for training subset while imbalanced test subset was used for validating the ML models. We have used grid Search method to find the best parameters of our models.

## 5 Results and Analysis

The results and analysis of all experiments for each dataset are discussed below. We only report testing results for the case of train/test split.

### 5.1 Dipterocarpaceae

The dataset has a total of 63 species with uniform distribution of 5 samples for each species hence SMOTE was not applied. From the results (fig 2) it can be noticed that LDA showed a consistent performance with a higher accuracy of more than 10% compared to both SVM and RF models for all three cross-validation methods.

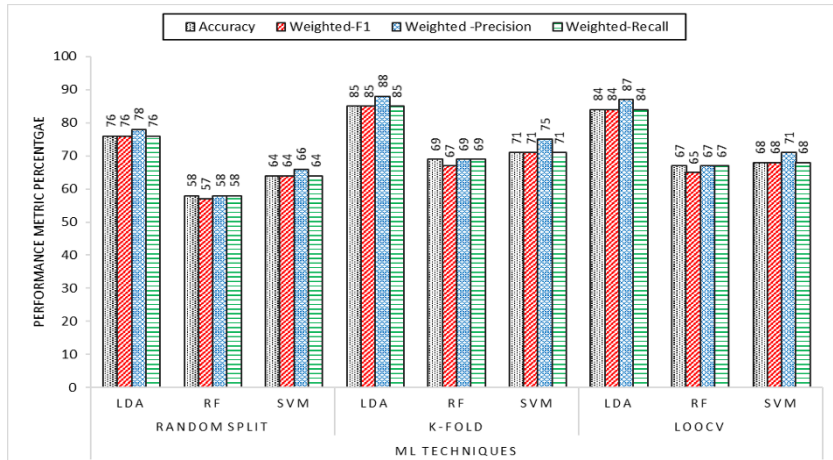


**Fig. 2.** Classification performance for Dipterocarpaceae species.

### 5.2 Annonaceae

This family has imbalanced data with the smallest group of species having a sample size of 10 and the largest group has 25 samples. Fig. 3 depicts the results of all three classifiers with different cross-validations methods without employing SMOTE. Although LDA outperformed both RF and SVM, the performance of all classifiers was found to be low and both RF and SVM classifiers ran into overfitting problem. In the next step, SMOTE was applied on the training samples of Annonaceae species dataset and imbalance test subset was used for the validation purpose. A small improvement in both accuracy (2%) and precision (4%) was noticed in LDA for k-fold cross-validation

(fig. 4). Moreover, LDA also outperformed both RF and SVM in all cross-validation methods.

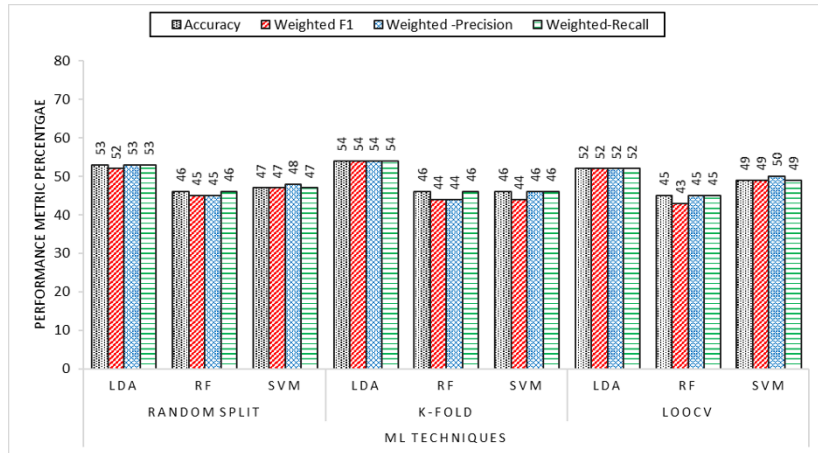


**Fig. 3.** Classification performance of Annonaceae species without SMOTE.

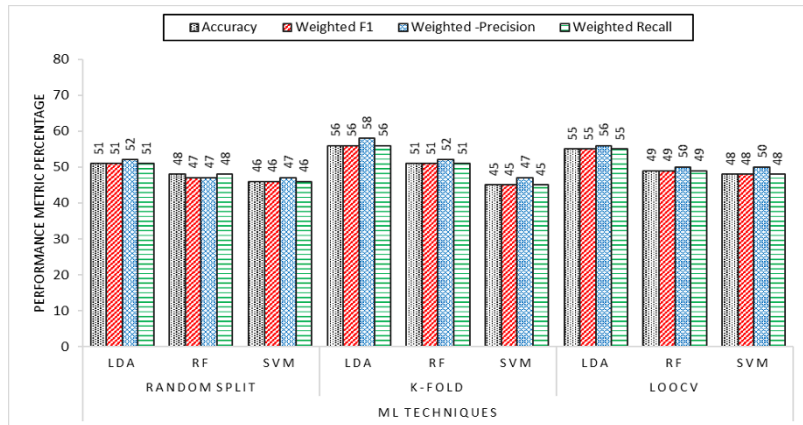


**Fig. 4.** Classification performance of Annonaceae species with SMOTE.

### 5.3 Euphorbiaceae

The class imbalance ratio in Euphorbiaceae species dataset is more than the other datasets used in this study (containing fewer number of classes than the other datasets). Before applying SMOTE analysis, all the ML classifiers had decent prediction accuracy as well as precision and SVM achieved an overall better result than RF and LDA in LOOCV (fig. 5). After applying SMOTE, significant improvement in prediction performance was observed in SVM for k-fold cross-validation with precision improving more than 10% while a smaller improvement was observed in both k-fold and LOOCV

for RF (fig. 6). There was no significant improvement in LDA performance for all cross-validation. Despite improvements observed at different cross-validation, the overall best performance was achieved by SVM (79% accuracy) without using SMOTE.

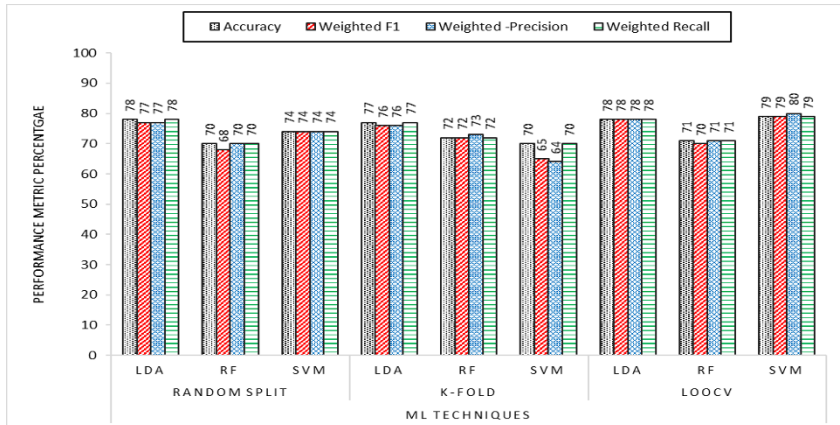


**Fig. 5.** Classification performance of Euphorbiaceae species without SMOTE.

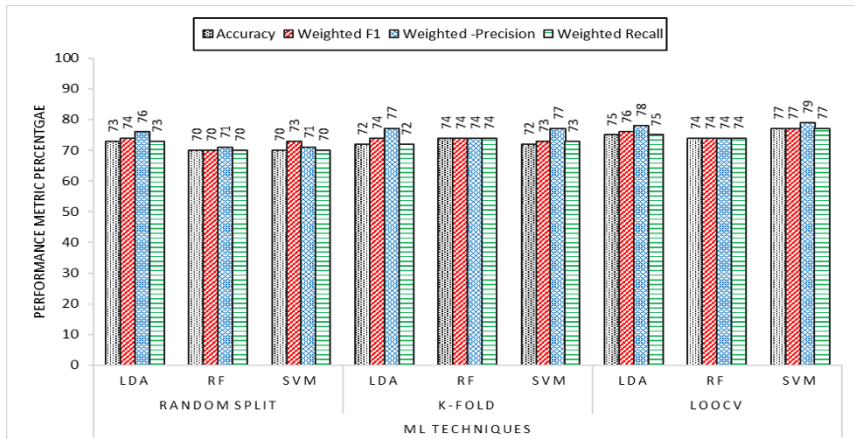


**Fig. 6.** Classification performance of Euphorbiaceae species with SMOTE

#### 5.4 Annonaceae and Euphorbiaceae Species

This dataset consisted of 32 species from two families. ML models were trained/tested for performing inter-species classification for combined species from different families. With two families, the number of samples in the dataset increased and the imbalance problem was also magnified. Without applying SMOTE analysis, LDA outperformed both RF and SVM in all cross-validation methods with RF performance being much

lower than the other two classifiers (fig. 7). After applying SMOTE, RF had a noticeable improvement in performance for all cross-validation methods while both SVM and LDA remained with little or no improvements. (fig 8). LDA was found to be the overall best classifier with both 63% accuracy and 64% precision without applying SMOTE.

### 5.5 Annonaceae and Euphorbiaceae Families

This dataset consisted of two families and ML classifiers were trained/tested for performing inter-family classification of these two families. Since the class distribution was balanced for this dataset so SMOTE was not applied. All three ML models were able to classify the instances of this dataset with an accuracy between 87-91% for different cross-validation methods (fig. 9).

Table 2 summarizes the results and presents the best performance of machine learning models for each of the dataset in term of accuracy.

**Table 2.** Summary of the best performing machine learning classifier in all datasets

Family	Prediction Accuracy	ML Technique	Cross validation	Oversampling
Annonaceae	56%	LDA	k-fold	With SMOTE
Euphorbiaceae	79%	SVM	LOOCV	Without SMOTE
Annonaceae + Euphorbiaceae species wise	63%	LDA	k-fold	Without SMOTE
Annonaceae + Euphorbiaceae family wise	91%	SVM	LOOCV	Not required
Dipterocarpaceae	85 %	LDA	k-fold	Not required

## 6 Conclusions

This work has evaluated the use of machine learning techniques applied on the extracted leaf traits and investigated the application of oversampling method for the classification of imbalanced datasets of tropical plants species. Based on the extracted leaf measurements, the prediction accuracy of the ML models considered for the given datasets were in general fair performance (63-91%) except for the family Annonaceae (56%). Although the application of SMOTE has improved the classifier performance in term of precision, most of the improvement were only noticed in RF classifier. In fact, the performance of LDA remained the same without improvement. On the other hand the application of SMOTE technique did not improve the overall performance of both LDA and SVM which could be attributed by the complexity of the data itself rather than imbalance problem as suggested by Laura et al. [10]. For the Dipterocarpaceae family with large number of species and fewer observations, the performance of LDA was still much better than both RF and SVM models. The low performance of all ML

models for Annonaceae suggests either the inadequacy of the sample size or the inability of the extracted leaf features in differentiating the species of this family. Nevertheless, these features can be used in classifying Dipterocarpaceae and Euphorbiaceae species with a fare accuracy and can well capture the family differences between Annonaceae and Euphorbiaceae.

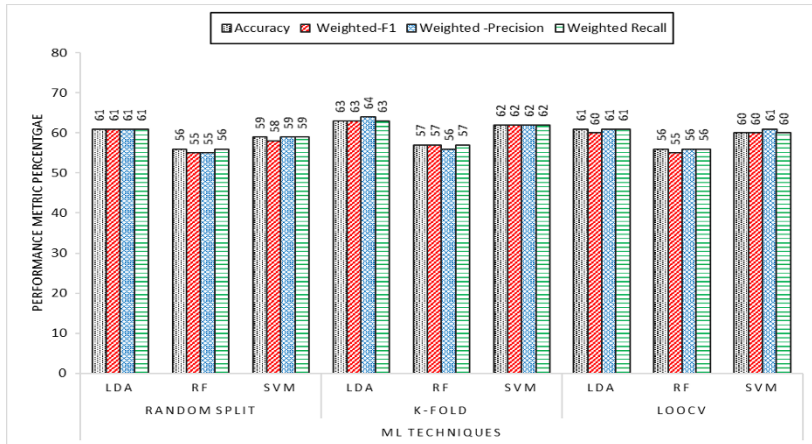


**Fig. 7.** Classification performance of combined Annonaceae and Euphorbiaceae species without SMOTE.

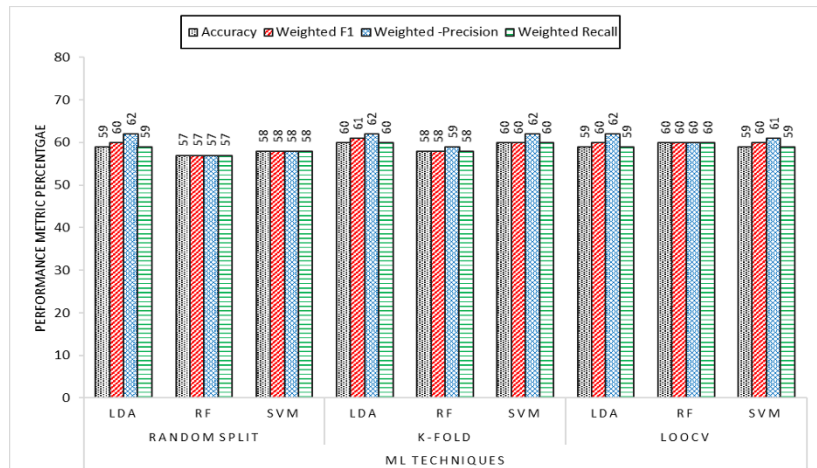


**Fig. 8.** Classification performance of combined Annonaceae and Euphorbiaceae species with SMOTE.

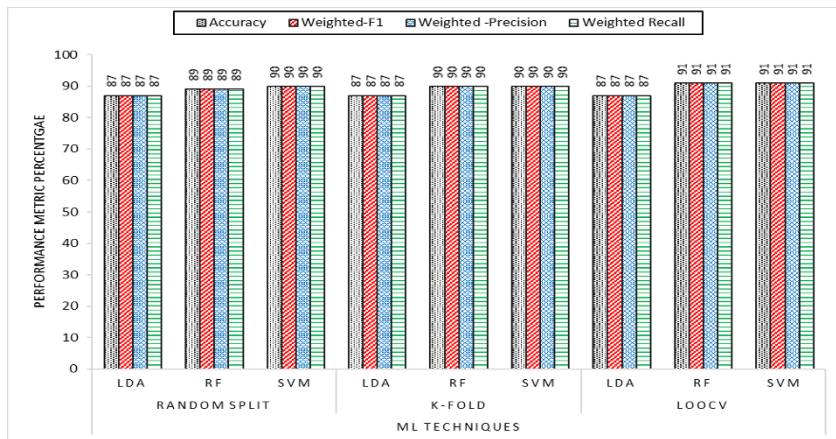


**Fig. 9.** Family wise classification performance of Annonaceae and Euphorbiaceae

## References

1. J. Wäldchen, M. Rzanny, M. Seeland, and P. Mäder, “Automated plant species identification—Trends and future directions,” *PLoS Comput. Biol.*, vol. 14, no. 4, pp. 1–19, 2018.
2. J. Wäldchen and P. Mäder, *Plant Species Identification Using Computer Vision Techniques: A Systematic Literature Review*, vol. 25, no. 2. Springer Netherlands, 2018.
3. M. S. Sainin, T. K. Ghazali, and R. Alfred, “Malaysian Medicinal Plant Leaf Shape Identification and Classification,” *Knowl. Manag. Int. Conf. Exhib. 2014*, pp. 578–583, 2014.
4. M. Murat, S.-W. Chang, A. Abu, H. J. Yap, and K.-T. Yong, “Automated classification of tropical shrub species: a hybrid of leaf shape and machine learning approach,” *PeerJ*, vol. 5, p. e3792, 2017.
5. A. Fernández, S. Garcia, F. Herrera, and N. V Chawla, “Smote for learning from imbalanced data: progress and challenges, marking the 15-year anniversary,” *J. Artif. Intell. Res.*, vol. 61, pp. 863–905, 2018.
6. A. Kasem, A. A. Ghaibeh, and H. Moriguchi, “Empirical Study of Sampling Methods for Classification in Imbalanced Clinical Datasets,” in *Computational Intelligence in Information Systems*, 2017, vol. 532.
7. K. W. P. Chawla, N.V., Bowyer,K.W., Hall, L.O., “SMOTE: Synthetic Minority Over-Sampling Technique. Journal of Artificial Intelligence Research,” vol. 16, pp. 321–357, 2002.
8. S. Shalev-Shwartz and S. Ben-David, *Understanding Machine Learning: From Theory to Algorithms*. New York, NY, USA: Cambridge University Press, 2014.
9. “sklearn.metrics.f1\_score — scikit-learn 0.20.3 documentation.” [Online]. Available: [https://scikit-learn.org/stable/modules/generated/sklearn.metrics.f1\\_score.html](https://scikit-learn.org/stable/modules/generated/sklearn.metrics.f1_score.html). [Accessed: 28-Mar-2019]
10. L. Morán-Fernández, V. Bolón-Canedo, and A. Alonso-Betanzos, “Data complexity measures for analyzing the effect of SMOTE over microarrays,” in *European Symposium on Artificial Neural Networks, Computational Intelligence and Machine Learning*, 2016.



# Human Detection and Classification using Passive Forward Scattering Radar System at Different Places

Noor Hafizah Abdul Aziz<sup>1</sup>, Liyana Nadhirah Phalip<sup>1</sup> and Nurul Huda Abd Rahman<sup>2</sup>

<sup>1</sup>Faculty of Electrical Engineering, Universiti Teknologi MARA  
Shah Alam 40450 Malaysia

<sup>2</sup>Malaysia–Japan International Institute of Technology (MJIIT), Universiti Teknologi Malaysia,  
Kuala Lumpur 54100 Malaysia  
[noor4083@uitm.edu.my](mailto:noor4083@uitm.edu.my)

**Abstract.** In military and security applications, the capability to detect human and identify their movement is progressively important. Generally, most of the radar systems are active systems, which can be easily detected by the enemy. Accordingly, passive radar is set to become an alternative to conventional active radar that offers a decisive operational advantage in that the passive radar could not be located. Passive radar does not emit any signals of its own, thus it could not be blocked. Consequently, passive radar uses many different transmission sources that are sent out from various locations to detect ground moving target especially human. The objective of this paper is to investigate the feasibility of forward scatter configuration mode using Long-Term Evolution (LTE) signal in a passive radar system for human detection and classification. This research utilized LTE frequency as a transmitter, which was a commercial telecommunication antenna. An experimental LTE based passive forward scatter radar system receiver was developed through the range of bistatic edge close to 180°. The data information of Doppler signature from human was taken at the beaches of Morib, Dungun and Port Dickson. All three places had strong LTE signal with 1.8 GHz and similar environment with that at the country borders. The human Doppler signature was analyzed, recognized and classified using the Principal Component Analysis technique. Results have shown that human of different sizes could be detected and classified based on body dimension, even at different places. This is the evolving area of research that provides a more useful outcome in improving border protection and security monitoring.

**Keywords:** Passive Radar, Forward Scatter, Human Doppler.

## 1 Introduction

Radar is a general term that is literally taken from the military. It means ‘Radio Detection and Ranging’ [1]. It is a system that is used for detection of any presence of moving object, and is also used for direction, distance or speed of objects. A typical radar system consists of a transmitter and a receiver, but sometimes the radar system could consist of a receiver only, and this type of radar is called the passive radar [2].

In this project, passive radar, or specifically, passive forward scattering radar is used to detect human. Forward Scattering Radar (FSR) that can be used for target detection and classification has a special mode of bistatic radar. FSR detects objects with an angle of detection of 180 degrees [3]. FSR provides a lot of interesting features such as generally simple hardware, an improved target radar cross section, a long coherent interval of the receiving signal, protection from stealth technology and possible operation using non-cooperative transmitter [4].

Passive radar system has advantages over the conventional radar system in many ways. For example, it is practically invisible to surveillance, it is easily transported due to its small size and it is cheaper as it does not transmit any signals [5]. Passive radar means that the radar is provided from non-radar transmission, such as broadcast, communications or radio navigation signal [6].

In the meantime, several researchers have carried out studies on passive radar with forward scatter radar mode. GPS signals could be one of the signals for passive radar system as demonstrated in [7, 8] for air target detection and in [9] for ground target detection. A research using GSM as a signal source and utilizing the forward scatter geometry for target detection is explained in [10]. Recent publications on passive forward scatter radar by exploiting the actual LTE signal transmitted through the air from the base station had classified three different vehicles into three different categories [11]. The proposed classification system in this paper provided results of excellent classification performance by using Principle Component Analysis technique, which is orthogonal transformation that looks to the direction of maximum variance in the data and is commonly used to reduce the dimensionality of the data [12]. The results from this paper can enhance the passive radar system capability by integrating the forward scatter mode onto conventional passive bistatic radar system.

## 2 Methodology

### 2.1 Human as Ground Moving Target

Twelve different persons were used as the moving targets at three different places. The information of the persons for the targets is as shown in Table 1.

**Table 1.** Information of the persons.

PLACE	PERSON	WIDTH (m)	HEIGHT (m)	DIMENSION (m <sup>2</sup> )
<b>MORIB</b>	1	0.26	1.78	0.4628
	2	0.29	1.76	0.5104
	3	0.28	1.48	0.4144
	4	0.25	1.52	0.3800
<b>DUNGUN</b>	1	0.26	1.76	0.4576
	2	0.27	1.76	0.4752
	3	0.28	1.48	0.4144
	4	0.25	1.52	0.3800
<b>PORT DICKSON</b>	1	0.24	1.76	0.4224
	2	0.32	1.76	0.5632
	3	0.23	1.77	0.4071
	4	0.25	1.52	0.3800

## 2.2 Experiment Site

The passive radar system was used as a receiver to receive a signal power strength of 1.8 GHz from the telecommunication transmitter antenna that was located 330 meters away from the radar receiver baseline. The Fig. 1(a) shows the seaside of Morib, Banting (Selangor), (2.754381, 101.441070) at the experiment site. The beach of Sura, Dungun (Terengganu), (4.728029, 103.433336) was also chosen as a location to undergo this experiment. This location was chosen because the signal transmitted from the LTE base station was strong, and as shown in the picture, it is at the seashore, which is suitable for the radar system. Before setting up the experiment, the location of an LTE base station that will act as signal transmitter must be discovered first. Then, the antenna to be used as the receiver was setup 700 meters from the commercial transmitter antenna as shown in the Fig. 1(b). The transmitter signal frequency used was 1.8 GHz. The last destination chosen for the location of the experiment was the seaside of Teluk Kemang, Port Dickson (Negeri Sembilan), (2.448141, 101.855917) as shown in the Fig. 1(c) below. The distance of the commercial transmitter antenna from the radar receiver baseline, which was also the location of the experiment, was 580 meters. The signal frequency of the transmitter was 1.8 GHz.

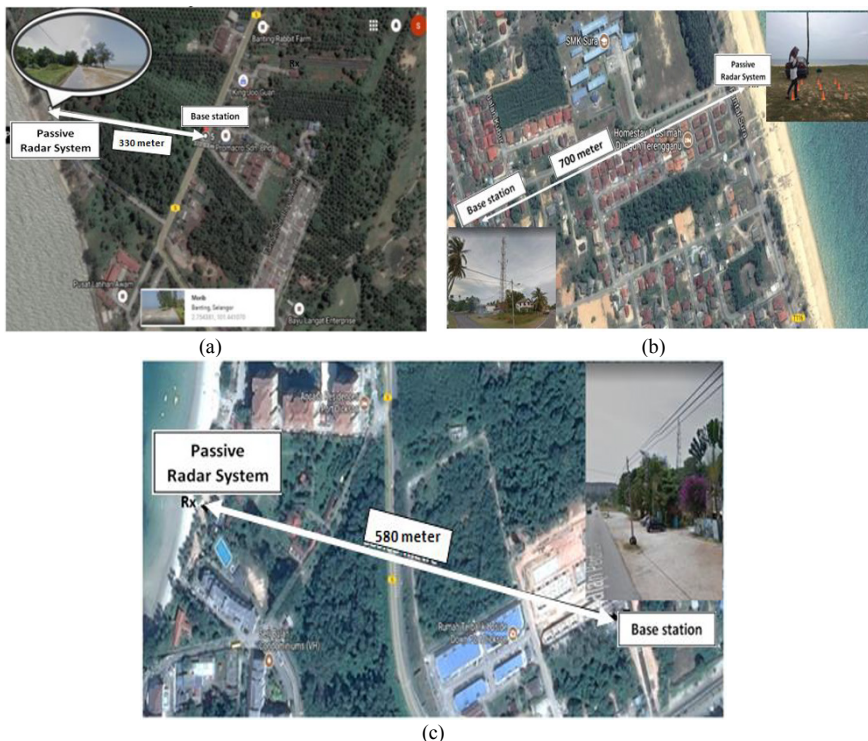


**Fig. 1.** Experiment site at (a) Morib (b) Dungun and (c) Port Dickson

From the number of sample experiments, as shown in Table 2, the receiver that acted as the passive radar will detect the presence of a human that passes through between the telecommunication transmitter and receiver antenna. The total data taken at all three places were 173 for 4 persons at Morib, 163 for 4 persons at Dungun and 145 for 4 persons at Port Dickson. The total number of samples for each person at three places were divided into training and testing process that was done to test the accuracy of classification. Here, 4 samples were taken from the total number of samples for each person for testing process. This was done to test the accuracy of the classification process. The arrangement of the baseline experiment is illustrated in Fig. 2. The figure shows that a human, as the moving target, has passed between transmitter, Tx (base station of commercial antenna) and receiver, Rx (passive radar).

**Table 2.** Number of sample experiments.

Person	Number of samples					
	Morib		Dungun		Port Dickson	
	Train-ing	Testing	Training	Test-ing	Training	Test-ing
1	31	4	33	4	34	4
2	34	4	35	4	32	4
3	20	4	33	4	33	4
4	72	4	46	4	30	4
Total	157	16	147	16	129	16
	173		163		145	

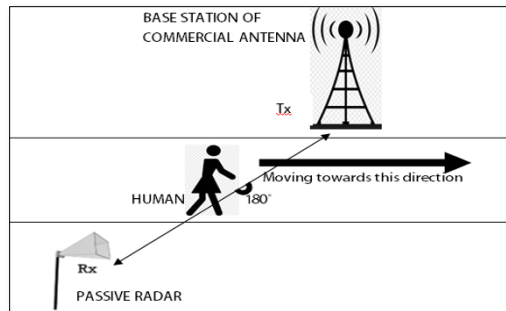


**Fig. 2.** Simple illustration of experiment site.

### 2.3 Data Processing

All of the data collected were processed and analyzed using the MATLAB software. A complete signal wave pattern was obtained by the MATLAB software and the target was classified. The steps taken for the data analysis were data selection, data segmentation, signal denoising, power spectral density, principle component analysis and

classification. The Doppler data were collected for 20 seconds, but later on during the data analysis process, it was segmented into only 2 seconds because only 2 seconds is needed to show the human Doppler signature. Then, after data segmentation is done, the noise from the raw data was removed via the denoising process. Each of the denoised data then were used to plot the Power Spectral Density (PSD) graph and later, some values are represented in the scatter plot after the Principal Component Analysis (PCA) process is done. Next, for the classification process, the cluster for the targets were done manually to determine and differentiate each of the targets. Here, the cluster will show that each of the targets are classified by their own group.

### 3 Result and Discussion

#### 3.1 Time Domain After Denoising Process

Based on the results, the Doppler signature obtained for the targets were different at Morib, Dungun and Port Dickson with respect to each person and place. The time domain plot depicted contains data that were obtained at all three places for 1 meter distance between the receiver and moving target. The received amplitude signal is in time domain, used in this passive FSR technique. As shown in Fig. 3(a), Fig. 3(b) and Fig. 3(c), the horizontal lines represent time that is proportional to the human Doppler signature. As a result, each person has different amplitudes at different distances. It also shows the time domain of signal after denoising the unwanted signal. Not all of the unwanted signals were removed, this is because it was not easy for the software to recognize and differentiate between the Doppler signature and noise.

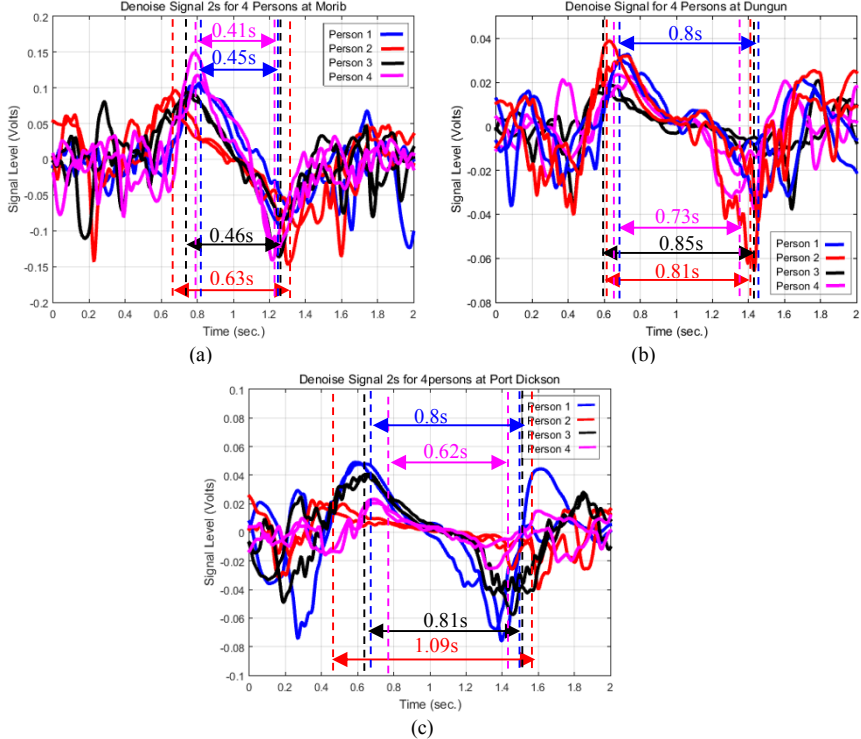
Fig. 3(a) presents the data taken in Morib. Each person had different times taken, which was 0.45 seconds for Person 1, 0.63 seconds for Person 2, 0.46 seconds for Person 3 and 0.41 seconds for Person 4. Even though the time taken were different for each person, in the case of Person 1, Person 3 and Person 4, the time taken were quite similar to each other. This can be explained by the dimensions of all three persons as in Table 1, which were  $0.4628 \text{ m}^2$ ,  $0.4144 \text{ m}^2$  and  $0.3800 \text{ m}^2$ , respectively and obviously Person 2 had the most different time taken, which was 0.63 seconds because Person 2 had the largest body build compared to the others as shown in Table 1, which was  $0.5104 \text{ m}^2$ .

Fig. 3(b) explains the time domain for all four targets at Dungun. Here the time taken for Person 1, Person 2, Person 3 and Person 4 were 0.8 seconds, 0.81 seconds, 0.85 seconds and 0.73 seconds, respectively. The reason for the similarity between the times taken for all four persons was because all of them have quite similar dimensions to each other as shown in Table 1, Person 1 was  $0.4576 \text{ m}^2$ , Person 2 was  $0.4752 \text{ m}^2$ , Person 3 was  $0.4144 \text{ m}^2$  and Person 4 was  $0.3800 \text{ m}^2$ .

Time taken for Person 1, Person 2, Person 3 and Person 4 at Port Dickson can be shown in the Fig. 3(c). Here, it is shown that there are some obvious differences between the times taken for all of the targets in Port Dickson. Time taken for Person 1 and Person 3 were nearly the same, which were 0.8 seconds and 0.81 seconds because their body dimensions were also quite similar at  $0.4224 \text{ m}^2$  and  $0.4071 \text{ m}^2$ , respectively. Person 2 had the highest time taken in Port Dickson, which was 1.09 seconds, meanwhile Person 4 had the shortest time taken for data taken in Port Dickson at 0.62

seconds. Both Person 2 and Person 4 obviously have differences in body dimensions, which were  $0.5632 \text{ m}^2$  and  $0.3800 \text{ m}^2$ , respectively.

As shown here, the human Doppler signature can be clearly seen at both ends of the signals when a human was entering and leaving the baseline, and the horn antenna that acted as the receiver started to receive the target's forward scatter lobe. As we can see, each person produced a different Doppler signature. This demonstrates that the time for a Doppler signature produced depends on the human body dimension. Body dimension increases with time domain for each person.



**Fig. 3.** Time domain at (a) Morib (b) Dungun and (c) Port Dickson.

### 3.2 Power Spectral Density of Human Detection

The signal's Power Spectral Density (PSD) for the same range of distance but of different person and places are shown in Fig 4(a), Fig. 4(b) and Fig. 4(c). It was compared between the Frequency (Hz) and normalized PSD in decibels (dB). Referring to Fig. 4(a), which is Power Spectral Density at Morib, the first main lobe for Person 1, Person 3 and Person 4, all dropped at frequency of 2.3 Hz, meanwhile Person 2 was quite different from the others that was at 2 Hz. Again, the similarities in the frequency drop can be explained by the body dimensions of each person, which can be classified as the

same size except for Person 2 because Person 2 had the largest body build. Their body dimensions were  $0.4628 \text{ m}^2$ ,  $0.5104 \text{ m}^2$ ,  $0.4144 \text{ m}^2$  and  $0.3800 \text{ m}^2$ , respectively as shown in Table 1 for Morib. Normalized power for Person 1, 2, 3 and 4 were -40 dB, -78 dB, -35 dB and -38 dB, respectively.

The Power Spectral Density in Dungun are all shown in Fig. 4(b). The first main lobe for Person 1, 2 and 3 dropped at the same frequency, which was 1.5 Hz and for Person 4, the first main lobe dropped at 1 Hz. The body dimensions for Person 1, 2, 3 and 4 were  $0.4576 \text{ m}^2$ ,  $0.4752 \text{ m}^2$ ,  $0.4144 \text{ m}^2$  and  $0.3800 \text{ m}^2$  as stated in Table 1 for Dungun. From this body build, it can be said that Person 4 had the smallest body build compared to the other targets at Dungun, whereas the others' body build were quite the same. The normalized power for Person 1, 2, 3 and 4 were -26 dB, -42 dB, -45 dB and -20 dB, respectively.

The results obtained in Port Dickson are shown in Fig. 4(c), where the normalized PSD for Person 1, 2, 3 and 4 were -57 dB, -37 dB, -22 dB and -23 dB, respectively. The PSD clearly shows the sequence of persons by body dimensions, from the biggest to the smallest, where Person 2 had the largest dimension at  $0.5632 \text{ m}^2$ . This is then followed by Person 1, which was  $0.4224 \text{ m}^2$ , meanwhile Person 3 and 4 were  $0.4071 \text{ m}^2$  and  $0.3800 \text{ m}^2$ , respectively. The first main lobe for Person 1 was 1.5 Hz, Person 2 was 1.2 Hz, Person 3 was 1.5 Hz and for Person 4, it was 2 Hz, as shown in the Fig. 4(c).

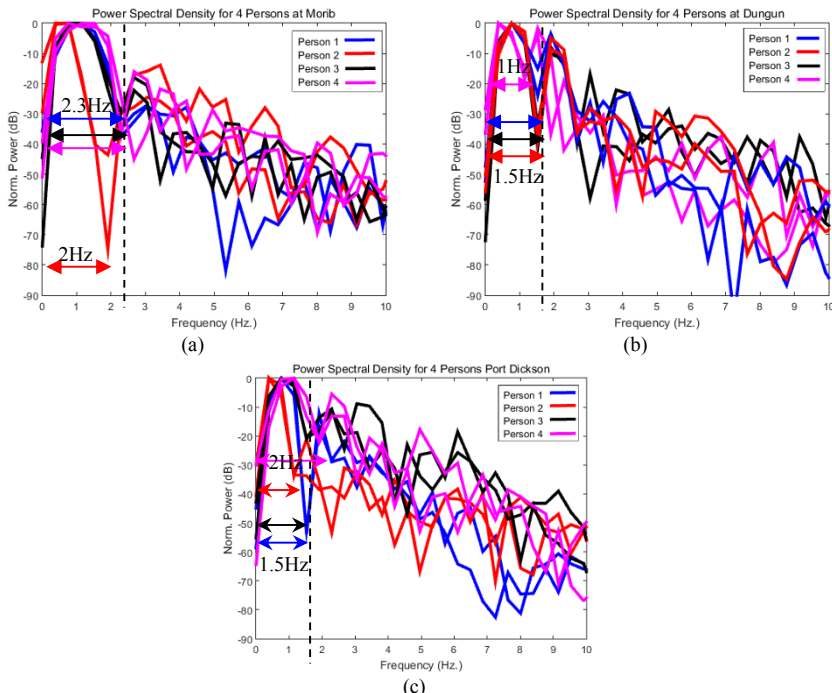


**Fig. 4.** Power spectrum density at (a) Morib (b) Dungun and (c) Port Dickson.

Also, the differences between the PSD can be explained by the distance between the passive radar system used and the commercial telecommunication transmitter antenna. As shown in the time domain of signal denoising at all three places, the difference between the distance of receiver and transmitter varied with the amplitude of signal level. The amplitude of signal level in voltage increases if the distance of the receiver and transmitter decreases.

### 3.3 Principal Component Analysis

The results of Principal Component Analysis (PCA) at Morib, Dungun and Port Dickson are shown in Fig. 5(a), Fig. 5(b) and Fig. 5(c). The purpose of this PCA is to differentiate the humans. For Person 1, 2, 3 and 4 the color is blue-diamond, red-circle, black-triangle and magenta-square, respectively. As presented in Fig. 5(a), for 1 meter at Morib, Person 2 has their own cluster located at the bottom of the graph because Person 2 had the largest body build compared to the others, which was  $0.51 \text{ m}^2$ . The cluster for Person 1 and 3 overlap one another and nearly combine as one cluster because their body dimensions were  $0.46 \text{ m}^2$  and  $0.41 \text{ m}^2$ , which is quite similar to each other, while for Person 4, half of their cluster is located at the upper right of the graph and overlaps with the clusters of Person 1 and 3. This might be because Person 4 and Person 3 were not that different in terms of body build but for sure, Person 4 and Person 1 had differences in body dimensions. For Person 1 and 3, they overlap each other because their body dimensions were almost similar, refer to Table I for Morib.

For the data taken in Dungun as shown in Fig. 5(b), the result became worse and could not be recognized because the experiment baseline was far from the transmitter antenna. This meant that, all of the targets were also far from the signals transmitted. The cluster became mixed up and overlapped but still, they have their own clusters. Refer to Table I for Dungun, the body dimensions for each person were almost the same. That is why the points in PCA are overlapping for every distance, especially for Person 1 and 2 that are located at the upper left of the graph. The difference in body dimensions between Person 1 and 2 was quite small by only  $0.02 \text{ m}^2$ . Meanwhile for Person 3 and 4, 1/5 of their clusters, which are located at the right of the graph, are overlapping with the clusters of Person 1 and 2. From this PCA, it shows that the Doppler signatures for every person can be classified and recognized. Another reason for the difficulties in classification for all the persons was because the distance of the experiment baseline and the transmitter antenna was further apart at 700 meters.

The PCA in Port Dickson is as shown in Fig. 5(c), where the clusters become more organized and can be easily classified. This is because the receiver received fully the body dimensions for each person. Person 2 and 4 have their own clusters, where most of their clusters are further apart from the others. Person 2's cluster is located on the left, while Person 4's cluster is located at the upper right. The clusters for Person 3 and 4 once again are overlapping each other, which are located at the middle bottom part of the graph. Here, as shown in Table I for Port Dickson, the body dimensions for both Person 1 and 3 were nearly similar to each other,  $0.42 \text{ m}^2$  and  $0.41 \text{ m}^2$ . This also can be proven by the distance of the experiment baseline and the commercial telecommunication antenna that was not that far apart at only 580 meters.

The performance of a classification model or classifier on a set of test data for which the true values are known was used to classify the targets. From Fig. 5(a), Fig. 5(b) and Fig. 5(c), the classification results obtained from Morib, Dungun and Port Dickson were 93.75%, 72.5% and 100%, respectively, which is classified as a success. The classification result at Dungun is the lowest because of the distance between the transmitter and the receiver was the highest among the three places, which was 700 meters. This shows that the human detection and classification using a Passive Forward Scattering Radar System at different places was successful.

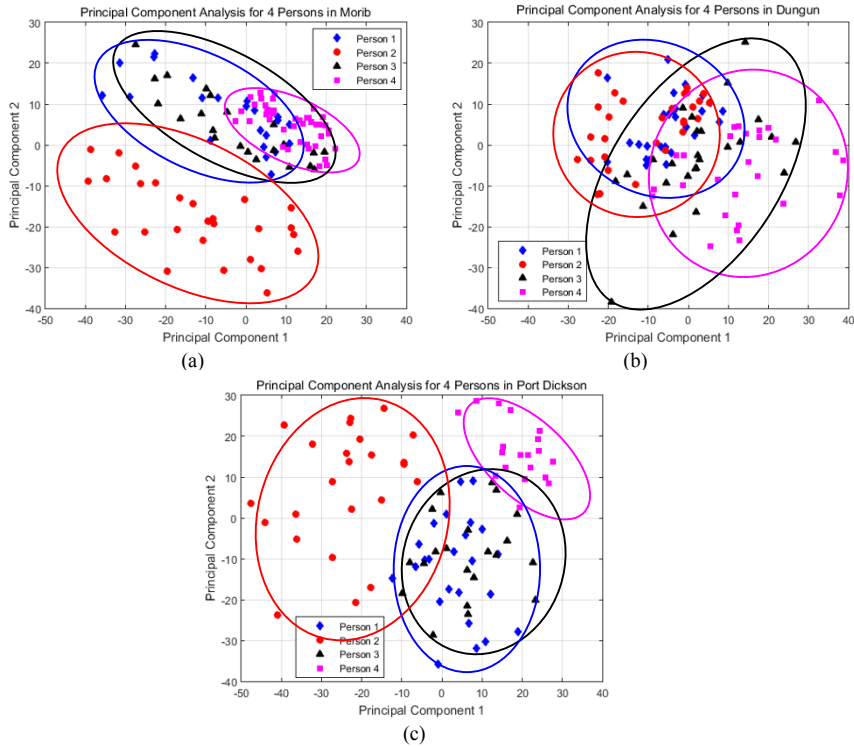


**Fig. 5.** PCA at (a) Morib (b) Dungun and (c) Port Dickson.

## 4 Conclusion

The main contribution of this paper is proof of concept by real experiment data of a passive forward scatter radar based on LTE signal for human target detection and classification. Another contribution is good feature selection of human Doppler signature by using a simple pre-processing analysis of data, which is important for classification system and algorithm. Furthermore, the detection and classification procedures were explained, by using the target's Doppler spectrum that showed good classification performance. The performance of a classification from different places showed that the

farther the distance between the LTE base station and passive forward scatter radar receiver, the tougher it was to classify the Doppler signal due to noise increment from the environment. The great potential in the passive forward scatter radar system provides a new research area in passive radar that can be used for diverse remote monitoring, including border protection, microwave fences, building monitoring, traffic surveillance, and so forth. Henceforward, future LTE based passive forward scattering radar investigations may consider air targets such as helicopters, and sea targets such as battle ships, humans and animals.

## Acknowledgement

We would like to express our sincere thanks towards UiTM and Ministry of Higher Education, Malaysia for their monetary support with FRGS grant numbered 600-IRMI/FRGS 5/3 (151/2019).

## References

1. E. F. Knott: Radar Cross Section Measurement. 1st ed. Van Nostrand Reinhold, New York (1993).
2. P. P. Iyer: Designing of radar systems for passive detection and ranging: Target acquisition without transmission. International Conference on Communication, Information and Computing Technology (ICCICT), Mumbai, pp. 1-6 (2012).
3. R.S.A. Raja Abdullah, Rasid Mohd Fadlee A. and M. Khalafa: Improvement in detection with forward scattering radar. *Science China, Information Sciences*, Vol. 54, Issue 12, pp. 2660-2672 (2011).
4. R.S.A. Raja Abdullah and A. Ismail: Forward scattering radar: Current & future applications. *International Journal of Engineering & Technology*, Vol. 3, pp. 61-67 (2006).
5. R.S.A. Raja Abdullah, A.A. Salah, A. Ismail, F. Hashim and N.H. Abdul Aziz: Experimental investigation on target detection and tracking in passive radar using Long-Term Evolution signal. *IET Radar, Sonar & Navigation*, Vol. 10, Issue 3, 577-585 (2016).
6. P. Howland: Editorial: Passive radar system. In *IEE Proceeding Radar, Sonar and Navigation*, IET, Vol. 152, pp. 105-106 (2005).
7. I. Suberviola, I. Mayordome and J. Mendizabal: Experimental results of air target detection with GPS forward scattering radar. *IEEE Geosci. Remote Sens. Lett.* 9, 47–51 (2012).
8. V. Behar, C. Kabakchiev: Detectability of air target detection using bistatic radar based on GPS L5 signals. *International Radar Symposium*, Germany, pp. 212–217 (2011).
9. C. Kabakchiev, I. Garvanov, V. Behar, P. Daskalov, H. Rohling: Study of moving target shadows using passive forward scatter radar systems. In *Proceedings of the International Radar Symposium (IRS)*, Gdansk, Poland, pp. 1–4 (2014).
10. P. Krysik, K. Kulpa, P. Samczynski: GSM based passive receiver using forward scatter radar geometry. *International Radar Symposium*, Dresden, Germany, pp. 637–642 (2013).
11. R.S.A. Raja Abdullah, N.H. Abdul Aziz, A.A. Salah, F. Hashim: Analysis on Target Detection and Classification in LTE Based Passive Forward Scattering Radar. *Sensors*, 16(10):1607 (2016).
12. L.T. Jolliffe: Principle Component Analysis. Springer Series in Statistics, 2nd ed. Springer, New York, (2002).



# An Automated Driver's Context Recognition Approach Using Smartphone Embedded Sensors

Md Ismail Hossen, Michael Goh, Tee Connie, Siong Hoe Lau and Ahsanul Bari

Faculty of Information and Science Technology, Multimedia University, Melaka, Malaysia  
{ismailmmu, ahsanulbari99}@gmail.com, {michael.goh, tee.connie, lau.siong.hoe}@mmu.edu.my

**Abstract.** Context recognition plays an important role in connecting the space between high-level applications and low-level sensors. To recognize human context, various kinds of sensors have been adopted. Among the variety of exploited sensors, smartphone internal sensors such as accelerometer and gyroscope are widely used due to convenience, non-intrusiveness and low deployment cost. Automatic detection of driver's context is a very crucial factor to determine the driver's behaviors. This paper proposes an approach to recognize driver's context which is a very specific research direction in the domain of human context recognition. The objective of this approach is to automatically detect the contexts of drivers using a smartphone's internal sensors. The proposed algorithm explores the power of a smartphone's built-in accelerometer and gyroscope sensors to automatically recognize the driver's context. Supervised machine learning k-nearest neighbor is employed in the proposed algorithm. Empirical results validated the efficiency of the proposed algorithm.

**Keywords:** Machine learning, context recognition, accelerometer, gyroscope.

## 1 Introduction

Smartphones with increased processing competencies have become popular for personal communication and computing for billions of people all over the world [1]. The newly deployed smartphones are furnished with sophisticated processing powers such as advanced operating system and integral sensors that range from GPS, cameras, Bluetooth, microphones, accelerometer, gyroscope, light sensors and magnetic sensors[2]. These kinds of smartphone internal sensors generate events that could be explored to recognize users' context automatically that facilitates the development of more responsive, powerful, intelligent and adaptive high level, mobile applications [3], [4]. One of the ubiquitous practices of smartphone integrated sensors is context recognition that is an vital task of context-aware applications which relays to automatic inference and determination of circumstantial information with a set of data captured from a variety of sensors [5]. Context recognition enables the development of advanced applications that

can adapt and respond to user's situations. Consequently, a lot of researches attention have been dedicated to design innovative and robust context-aware systems. Automatic detection of driver's context is a subset of the broader context-aware research area. In the recent development of context-aware research, driver's activity recognition is a rising new challenge [6]. Driver's context recognition can be further used for several real-time applications such as parking recognition [7], traffic estimation [8], drivers situation or behavior detection [9] and so on.

However, the majority of the existing works are conducted for basic activities such as walking, lying, sitting, dancing and talking [10]. Most of the existing works found in this domain rely on utilizing wearable sensors which cause carriage inconvenience. Besides, this kind of wearable sensors is not realized as fully context-aware due to their intrusiveness and burden for sensor positioning [5].

The goal of this work is to automatically detect driver's activities that he/she performs while parking. Throughout this paper, the study focuses to capture sensors signal and subsequently processes it to extract high-level driver's context information. In this paper, an algorithm is developed to classify driver's states (i.e. walking, running, sitting and idle) using a supervised machine learning algorithm. The contribution of this research is to propose a very specific context recognition instead of proposing in general context recognition. It focuses on a very particular domain of context recognition that is drivers' contexts while they enter into or exit out from the parking zone. The key contributions of the work comprise: (i) replacing of the wearable sensor by the power of smartphone internal sensors, (ii) addressing the problem of position-independent driver context recognition. The experimental result shows a very good convincing output in line with the research objectives.

The remainder of the paper is arranged as follows. Section 2 designates the literature reviews, section 3 illustrates the details of the proposed methodology, section 4 demonstrates the result & discussion and lastly, the paper is concluded with commenting on future works in section 5.

## 2 Literature Review

Some innovative researches have explored context recognition employing smartphone sensors. The study [4] proposed a hybrid approach that combines the wrapper method and filters considering the trade-off between accuracy and time. KNN and naïve Bayes (NB) algorithm have been applied. The data was collected with a smartphone attached to the waist of the user. This specific placement has narrowed the appropriateness of the application. [11] presented an algorithm named MBLSTM utilizing smartphone integrated accelerometer and two directional features. Features were extracted from 3-D acceleration and 2-directional vertical elements. Their experimented result showed that the proposed algorithm is effective for recognizing human activity but placement variations as well as the orientation of the phone problem were not addressed. The authors of [12] suggested an algorithm for human activity recognition free of device orientation respect to linear acceleration. They used KNN classifier for classification and showed

the effectiveness with empirical results. However, they did not consider one of the serious issues that arise with a fixed system of coordinates.

A various number of supervised and unsupervised classification algorithm can be utilized for context classification. The broadly exploited machine learning classifiers such as an artificial neural network (ANN) [13], KNN [14], NB [15], decision tree (DT) [16] and SVM [16] can be used for the classification tasks. Some of the existing works employed fuzzy logic [17], [18]. Moreover, competitive learning [19], computational intelligence [20] and spectral biclustering [21] contain exceptional properties for classification.

### 3 Method

This section introduces the proposed algorithm with details description and implementation. Fig. 1 illuminates the block diagram of the proposed system and the further particulars are delimited in the following subsections. As it is seen from Fig. 1, the proposed driver's context recognition has two main components, which are: (A) Pre-processing, and (B) Context recognition. The details of the suggested system are provided below. For data collection an android application is used where 60 fit participants performed four activities and the frequency of capturing data is set to 1 Hz.

The participants were allowed to keep the phone in any positions and orientation.

#### 3.1 Pre-processing

The input signals are the raw data that come from the user's phone. Three-axis accelerometer and gyroscope data are received from the user smartphone as an input signal. To resolve the issues such as handling missing data, removing gravity force elimination, and feature generation from an existing feature, this study has applied data pre-processing that prepares the raw data for additional processing. Firstly, the missing data were eliminated by removing the entire rows with missing values. Secondly, using the following formula gravity force effect was removed.

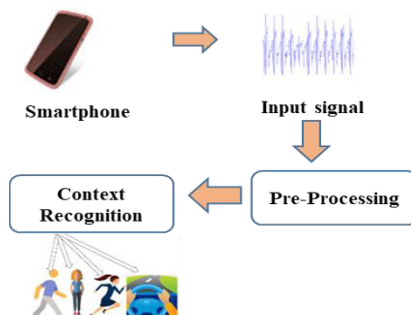


**Fig. 1.** The block diagram of the proposed system

$$\text{gravity}[n] = \text{alpha} * \text{gravity}[n] + (1-\text{alpha}) * \text{event. values}[n] \quad (1)$$

$$\text{linear acceleration}[n] = \text{event. values}[n] - \text{gravity}[n] \quad (2)$$

where the value alpha = 0.8 is a fixed value that is calculated as  $t / (t + dT)$  where  $t$  is the time constant of the low pass filter that indicates the speed assumed to respond to an input,  $dT$  is the rate of the sensor event delivery and  $n$  stands for 0, 1, 2 that represent  $x$ ,  $y$  and  $z$ -axis respectively. Sensor event represents a sensor that holds and delivers information such as sensor data and timestamp. Lastly Equation. 3 is used to construct a new feature for both the accelerometer and gyroscope.

$$std = \sqrt{\frac{1}{N} \sum_{i=1}^N (x - \bar{x})^2} \quad (3)$$

where  $N$  is the number of samples,  $x$  and  $\bar{x}$  are the value sensor reading and mean of sensor reading, respectively.

### 3.2 Context Recognition

In this paper, the driver's context means walking, driving, idle and running. These four contexts have been selected due to the association with parking action. For instance, the events that happen during parking a car is (driving → walking), on the other hand (walking → driving) occurs while a driver leaves from the parking. To recognize a driver's context, the widely used supervised machine learning is applied. In this research, KNN is selected for its high performance. A dataset collected from 60 healthy participants including 40 males and 20 females is isolated into three sets which is training, validation and testing. The training dataset is used to train the model, validation set was used for validation parameter tuning and lastly testing dataset as used to evaluate the performance of the trained model. The performance was measured based on four parameters which are *accuracy*, *precision*, *recall* and *f1-score*. The aforementioned parameters are calculated in accordance with the observation of the true positive (TP), false negative (FN), true negative (TN) and false positive (FP). The parameters used to evaluate the performance of the proposed algorithm are explained below.

**Accuracy:** It measures the correctly classifying probability for each sample and equals the samples number that is grouped correctly. Where total means the number of the total test sample. Accuracy is calculated with the following equation.

$$\text{Accuracy} = (\text{TP}+\text{FP})/(\text{TP}+\text{FP}+\text{TN}+\text{FN}) * 100 \quad (4)$$

**Precision:** Precision shows the ratio of correct positive prediction vs total positive observations. It answers to question that how many observations in the positive prediction are actually positive. Equation 5 is used to calculate the precision.

$$\text{Precision} = \text{TP}/(\text{TP}+\text{FP}) * 100 \quad (5)$$

**Recall:** Recall computes the number of actual positive predicted observations among all actual labeled classes. The recall is computed with the following formula.

$$\text{Recall} = \frac{\text{TP}}{\text{TP} + \text{FN}} * 100 \quad (6)$$

**F1-score:** It expresses the balance between recall and precision. Equation 7 calculates f1-score.

$$\text{F1-score} = \frac{2 * (\text{recall} * \text{precision})}{(\text{recall} + \text{precision})} * 100 \quad (7)$$

## 4 Results and Discussion

This section describes the experiential results achieved throughout the research. A total number of 33,454 instances are used as the training set, 3345 instances for validation, and 3346 instances for testing. The training dataset is used to train the classifiers to recognize the driver's context. The validation set is exploited to assess the model while tuning the parameters, on the other hand test data is used to evaluate the trained models. Fig.2 illustrates the test accuracy and validation accuracy are almost the same which indicates that the empirical distribution of the dataset does not differ much, and it is free from high generalization gap.

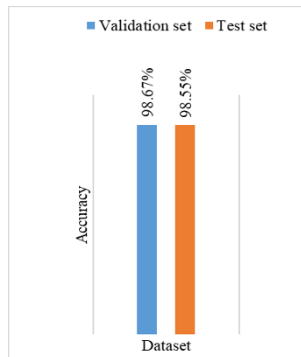


**Fig. 2.** Comparison of accuracy on test vs validation set

Additionally, to weigh the accuracy of the proposed algorithm, the level of test accuracy of each individual activity is presented in Fig. 3 that demonstrates that the proposed algorithm provides the same level of accuracy for each activity. furthermore, to examine the accuracy of the proposed system respect to different size of training and testing sample three ratios of train are experimented: test splits ratio, which is 70:30 (23417 rows for train, 10036 rows for test), 80:20 (26762 rows for train and 6691 rows for test) and 90:10 (30107 rows for train, 3346 rows for test).

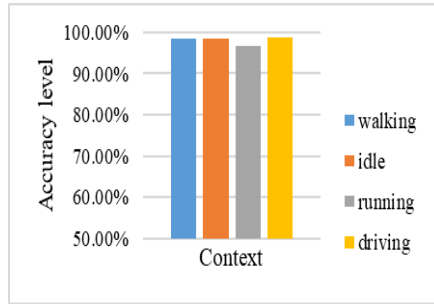


**Fig. 3.** Accuracy on individual activities

The accuracy for each classifier with the three split ratios is given in Fig. 4. Fig. 4 illustrates that all three splits provide alike accuracy. Thus, it shows that the amount of data used for training is sufficient and it can generalize to any number of unnoticed data as it performs on test data.

Apart from measuring accuracy, it has perceived the *precision*, *recall*, and *f1-score*. The result of *precision*, *recall*, and *f1-score* is 98.64%, 98.14%, 98.38%. Lastly, the cost of time to build the KNN model is measured which is 0.2243 second. To classify 3345 new unseen feature vectors, it takes only 0.1488 second which means .0000044 second for per new feature vector classification. From the experiment on time consumption it shows that it takes very little processing time.

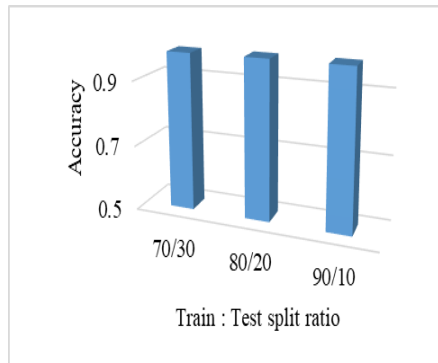


**Fig. 4.** Scores of accuracy respect to three split ratios of the train: test dataset

## 5 Conclusion and Future Work

In this paper, an algorithm has been implemented to classify driver's contexts using built-in smartphone sensors that could be further used for a variety of high-level applications. The proposed algorithm is validated with a validation and an unseen test dataset. Empirical results have been analyzed with measuring rates of accuracy, recall,

precision and time taken for classification model generating. Empirical results show that the proposed method has achieved its main objective to automatically detect the driver's context using smartphone internal sensor that does not require manual input from drivers. As a future enhancement, this work will be extended to live to test of drivers' behaviors.

## References

1. Minh, T., T. Do, Blom, J., and Gatica-Perez, D., "Smartphone Usage in the Wild : a Large-Scale Analysis of Applications and Context," *icmi*, 2011.
2. Milette, G. and Stroud, A. *Stroud, Professional android sensor programming*. John Wiley & Sons, 2012.
3. Guo, B., Zhang, D., Wang, Z., Yu, Z., and Zhou, X., "Opportunistic IoT: Exploring the harmonious interaction between human and the internet of things," *J. Netw. Comput. Appl.*, 2013.
4. Wang, A., Chen, G., Yang, J., Zhao, S., and Chang, C.-Y., "A Comparative Study on Human Activity Recognition Using Inertial Sensors in a Smartphone," *IEEE Sens. J.*, vol. 16, no. 11, pp. 4566–4578, Jun. 2016.
5. Otebolaku, A. M. and Andrade, M. T., "User context recognition using smartphone sensors and classification models," *J. Netw. Comput. Appl.*, vol. 66, pp. 33–51, May 2016.
6. Braunagel, C., Kasneci, E., Stolzmann, W., and Rosenstiel, W., "Driver-Activity Recognition in the Context of Conditionally Autonomous Driving," in *2015 IEEE 18th International Conference on Intelligent Transportation Systems*, 2015, pp. 1652–1657.
7. Hossen, M. I., Goh, M., Connie, T., Aris, A., and Pei, W. L., *A Review on Outdoor Parking Systems Using Feasibility of Mobile Sensors*, vol. 488. 2018.
8. Demissie, M. G., "Traffic Volume Estimation Through Cellular," no. July, pp. 1–16, 2013.
9. Randell, C. and Muller, H., "Context-awareness by analyzing accelerometer data," 2002.
10. Nurhanim, K., Elamvazuthi, I., Izhar, L. I., and Ganesan, T., "Classification of human activity based on smartphone inertial sensor using support vector machine," in *2017 IEEE 3rd International Symposium in Robotics and Manufacturing Automation (ROMA)*, 2017, pp. 1–5.
11. Tao, D., Wen, Y., and Hong, R., "Multicolumn Bidirectional Long Short-Term Memory for Mobile Devices-Based Human Activity Recognition," *IEEE Internet Things J.*, 2016.
12. Ustev, Y. E., Durmaz Incel, O., and Ersoy, C., "User, device and orientation independent human activity recognition on mobile phones," 2013.
13. Xiuju Fu and Lipo Wang, "Data dimensionality reduction with application to simplifying rbf network structure and improving classification performance," *IEEE Trans. Syst. Man Cybern. Part B*, vol. 33, no. 3, pp. 399–409, Jun. 2003.
14. Ezghari, S., Zahi, A., and Zenkouar, K., "A new nearest neighbor classification method based on fuzzy set theory and aggregation operators," *Expert Syst. Appl.*, vol. 80, pp. 58–74, Sep. 2017.
15. D'Angelo, G., Rampone, S., and Palmieri, F., "Developing a trust model for pervasive computing based on Apriori association rules learning and Bayesian classification," *Soft Comput.*, vol. 21, no. 21, pp. 6297–6315, Nov. 2017.
16. Hossen, M. I., Goh, M., Lau, S. H., and Bari, A., "Smartphone-Based Drivers Context Recognition," *KES Smart Innov. Syst. Technol.*, 2019.
17. (Vojislav) Kecman, V., *Learning and soft computing : support vector machines, neural networks, and fuzzy logic models*. MIT Press, 2001.

18. Sukumar, P. and Gnanamurthy, R. K., "Computer Aided Detection of Cervical Cancer Using Pap Smear Images Based on Adaptive Neuro Fuzzy Inference System Classifier," *J. Med. Imaging Heal. Informatics*, 2016.
19. Lipo Wang and Lipo, "On competitive learning," *IEEE Trans. Neural Networks*, vol. 8, no. 5, pp. 1214–1217, 1997.
20. Zurada, J. M., "Data mining with computational intelligence," *IEEE Transactions on Neural Networks*. 2006.
21. Liu, B., Wan, C., and Wang, L., "An efficient semi-unsupervised gene selection method via spectral biclustering," *IEEE Trans. Nanobioscience*, 2006.



# A Variable Sampling Interval EWMA $\bar{X}$ Chart for the Mean with Auxiliary Information

Pei Sang Ng<sup>1</sup>, Michael Boon Chong Khoo<sup>2</sup>, Wai Chung Yeong<sup>3</sup>, Sok Li Lim<sup>4</sup>

<sup>1</sup>Department of Physical and Mathematical Science, Faculty of Science,  
Universiti Tunku Abdul Rahman, 31900 Kampar, Perak, Malaysia

<sup>2</sup>School of Mathematical Sciences, Universiti Sains Malaysia, Penang, Malaysia

<sup>3</sup>School of Mathematical Sciences, Sunway University, 47500 Petaling Jaya, Malaysia

<sup>4</sup>Institute of Mathematical Sciences, Faculty of Science, Universiti Malaya, 50603,  
Kuala Lumpur, Malaysia  
sang\_ng@hotmail.com

**Abstract.** It is a well-known fact that the exponentially weighted moving average (EWMA) type control chart is very effective in detecting small and moderate shifts. To further enhance the sensitivity of the EWMA control chart in shift detection, this paper proposes the variable sampling interval EWMA chart by using a single auxiliary variable (AI) (abbreviated as VSI EWMA-AI) to monitor the process mean, where the statistic of the proposed chart is based on the information of the study and auxiliary variables. The performance of the proposed chart is evaluated by using the average time to signal (*ATS*) criterion, where the derivation of *ATS* formula is presented in this paper. Subsequently, the performance of the proposed chart is compared with the existing EWMA-AI chart in literature. The comparison shows that the VSI EWMA-AI chart has better detection ability in mean shifts than the EWMA-AI chart.

**Keywords:** Average Time to Signal, Markov Chain, Variable Sampling Interval, Exponentially Weighted Moving Average Chart.

## 1 Introduction

The use of Statistical Quality Control charts in process surveillance is prevalent in manufacturing companies. Control charts are used to ensure good quality of products and services through process monitoring, by signaling an alarm if an assignable cause is detected. Quality practitioners desire to have a quicker detection of an out-of-control (assignable cause) situation so that remedial action can be conducted immediately to prevent the cost of producing unwanted products. Therefore, control chart is one of the important tools in Statistical Process Control (SPC) and it is widely used and explored in both academic and non-academic areas. For some recent works on control charts, readers can refer to [1-5].

In 1924, Shewhart developed the first control chart, namely the  $\bar{X}$  chart [6]. The  $\bar{X}$  chart is one of the memory-less control charts. Its plotting statistic operates by only utilizing the information from current information, while the memory-type control chart

uses both past and current information in the plotting statistic. Thus, the  $\bar{X}$  chart is less sensitive compared to memory-type control charts, such as the exponentially weighted moving average (EWMA) and cumulative sum (CUSUM) charts, proposed by Roberts [7] and Page [8], respectively. Due to the main advantage of the EWMA and CUSUM charts, rooted in a quick detection of small shifts, these charts are extensively developed by the researchers in the field of quality control. See [9-11] for recent studies on memory-type control charts.

To further enhance the capability of control charts in shift detection, the auxiliary information concept was considered in the control chart's procedures in monitoring the process mean. For instance, Abbas et al. [12] developed an EWMA  $\bar{X}$  chart in the presence of auxiliary information (denoted as EWMA-AI), where the proposed EWMA-AI chart was shown to be able to detect the process shifts faster than the traditional EWMA  $\bar{X}$  chart. Subsequently, Haq et al. [13] monitored the process mean by using the EWMA  $t$  chart with auxiliary characteristics. Haq and Khoo [14] proposed the double sampling control chart using a single auxiliary variable in evaluating the chart's performance, while Ng et al. [15] presented the performance of the run sum chart by using the regression estimator in process monitoring. More recently, Haq and Khoo [16] proposed multivariate CUSUM, multivariate EWMA and double multivariate EWMA charts to monitor the process mean by using auxiliary information. Abbasi and Haq [17] developed new optimal CUSUM and adaptive CUSUM charts for the mean with auxiliary information, where all these charts were shown to surpass the auxiliary information based CUSUM chart by Abbas [18]. The objective of this paper is to improve the run length performance of the EWMA-AI chart proposed by Abbas et al. [12], by incorporating the variable sampling interval (VSI) scheme into the EWMA-AI chart.

To the best of our knowledge, the optimal design of the VSI EWMA chart with auxiliary information (denoted as VSI EWMA-AI) does not exist in the literature. Thus, this work investigates the process mean by using the VSI EWMA-AI chart. The structure of the remaining of this paper is as follows: The properties of the VSI EWMA-AI chart is presented in Section 2, where the optimal design in minimizing the out-of-control  $ATS$  ( $ATS_1$ ) of the VSI EWMA-AI chart is developed. Subsequently, Section 3 presents the optimal parameters of the VSI EWMA-AI chart and the  $ATS_1$  comparison between the VSI EWMA-AI and EWMA-AI chart. Lastly, the main observations of this research are summarized and future studies are also given in Section 4.

## 2 The proposed VSI EWMA-AI chart

### 2.1 An overview of the VSI EWMA-AI chart

Let  $(y_{r,1}, x_{r,1}), (y_{r,2}, x_{r,2}), \dots, (y_{r,n}, x_{r,n})$  be a random sample with  $n$  bivariate observations at time  $r = 1, 2, \dots$ , associated with a study variable  $Y$  and a correlated auxiliary variable  $X$ . Each pair of  $(Y_{r,k}, X_{r,k})$ , for  $r = 1, 2, \dots$  and  $k = 1, 2, \dots, n$ , is

assumed to follow a bivariate normal distribution with the population mean  $(\mu_Y, \mu_X)$ , population variance  $(\sigma_Y^2, \sigma_X^2)$  and the correlation between  $Y$  and  $X$  is denoted by  $\rho$ , i.e.  $(Y_{r,k}, X_{r,k}) \sim N_2(\mu_Y, \mu_X, \sigma_Y^2, \sigma_X^2, \rho)$ . Let the unbiased estimator of  $\mu_Y$  be [12]

$$U_{Y_r}^* = \bar{Y}_r + \rho \left( \frac{\sigma_Y}{\sigma_X} \right) (\mu_X - \bar{X}_r), \quad (1)$$

where  $\sigma_Y$  and  $\sigma_X$  are the standard deviations for the study variable  $Y$  and the correlated auxiliary variable  $X$ , respectively, while  $\bar{Y}_r = \frac{1}{n} \sum_{k=1}^n Y_{r,k}$  and  $\bar{X}_r = \frac{1}{n} \sum_{k=1}^n X_{r,k}$  are the sample mean of study variable  $Y$  and correlated auxiliary variable  $X$ , respectively.

The mean and variance of  $U_{Y_r}^*$ , denoted by  $E(U_{Y_r}^*)$  and  $\text{Var}(U_{Y_r}^*)$ , are given as

$$E(U_{Y_r}^*) = \mu_Y \quad (2)$$

and

$$\text{Var}(U_{Y_r}^*) = \frac{\sigma_Y^2(1-\rho^2)}{n}. \quad (3)$$

The plotting statistic of the proposed VSI EWMA-AI chart is shown as

$$\begin{aligned} A_0 &= \mu_{Y_0}, \\ A_r &= \lambda U_{Y_r}^* + (1-\lambda) A_{r-1}, \quad r = 1, 2, \dots \end{aligned} \quad (4)$$

where  $\mu_{Y_0}$  is the in-control population mean of the study variable  $Y$  and  $\lambda \in (0, 1]$  is the smoothing constant and  $U_{Y_r}^*$  has been explained in Eq. (1).

The upper warning limit ( $UWL$ ), upper control limit ( $UCL$ ), central line ( $CL$ ), lower warning limit ( $LWL$ ) and lower control limit ( $LCL$ ) of the proposed chart are defined as

$$\begin{aligned} UWL &= \mu_{Y_0} + W \sigma_Y \sqrt{\frac{\lambda(1-\rho^2)}{n(2-\lambda)}}, \\ UCL &= \mu_{Y_0} + L \sigma_Y \sqrt{\frac{\lambda(1-\rho^2)}{n(2-\lambda)}}, \\ CL &= \mu_{Y_0}, \end{aligned} \quad (5)$$

$$LWL = \mu_{Y_0} - W \sigma_Y \sqrt{\frac{\lambda(1-\rho^2)}{n(2-\lambda)}}$$

and

$$LCL = \mu_{y_0} - L\sigma_y \sqrt{\frac{\lambda(1-\rho^2)}{n(2-\lambda)}},$$

respectively, where  $n$  represents the sample size,  $\mu_{y_0}$  and  $\lambda$  have been defined in Eq. (4), while  $W$  and  $L$  are the design parameters that used to determine the width of the warning and control limits of the VSI EWMA-AI chart, respectively.

The VSI EWMA-AI chart operates as follows:

- Step 1: Specify  $n$ ,  $\rho$ , short ( $t_s$ ) and long ( $t_L$ ) sampling intervals.
- Step 2: Compute  $(\lambda, W, L)$  values according to the desired in-control performance.
- Step 3: Compute the charting statistic of the VSI EWMA-AI chart by using Eq. (4). Then, compute the values of  $UCL$ ,  $UWL$ ,  $LWL$  and  $LCL$  by using Eq. (5).
- Step 4: If  $A_r \in [LWL, UWL]$ , the process is in-control, thus the next sampling interval should be ( $t_L$ ).
- Step 5: If  $A_r \in (LCL, LWL) \cup (UWL, UCL)$ , the process is in-control, and thus the next sampling interval should be ( $t_s$ )
- Step 6: If  $A_r \in (-\infty, LCL] \cup [UCL, \infty)$ , the process is deemed as out-of-control. Stop the process monitoring and an immediate action should be taken to remove the assignable cause(s).

The operation of the VSI EWMA-AI chart is depicted in Fig. 1. As shown in Fig. 1, the chart is divided into central region (C.R), warning region (W.R) and out-of-control region (O.C.R).

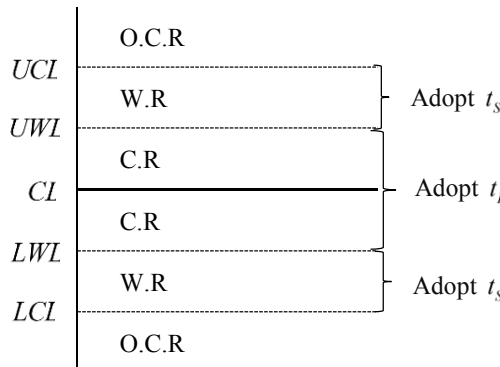


**Fig. 1.** A graphical view of the operation for the VSI EWMA-AI chart.

## 2.2 Performance measure

Since the interval between the samples of the VSI EWMA-AI chart is varied according to the values of previous charting statistic, the speed in detecting assignable cause(s) is measured by using the average time to signal ( $ATS$ ) and the standard deviation of the

time to signal (*SDTS*). The *ATS* and *SDTS* values are computed by using the Markov chain approach adopted from [19]. A brief discussion of this Markov chain procedure is given here. Assume that a Markov chain model with  $p + 1$  states is considered, where states 1, 2, ...,  $p$  are transient and state  $p+1$  is absorbing. The transition probability matrix (tpm),  $\mathbf{P}$  of this Markov chain model is shown in Eq. (6).

$$\mathbf{P} = \begin{pmatrix} \mathbf{Q} & \mathbf{c} \\ \mathbf{0}^T & 1 \end{pmatrix} = \begin{pmatrix} Q_{1,1} & Q_{1,2} & \cdots & Q_{1,p} & c_1 \\ Q_{2,1} & Q_{2,2} & \cdots & Q_{2,p} & c_2 \\ \vdots & \vdots & & \vdots & \vdots \\ Q_{p,1} & Q_{p,2} & \cdots & Q_{p,p} & c_p \\ 0 & 0 & \cdots & 0 & 1 \end{pmatrix}, \quad (6)$$

where  $\mathbf{Q}$  is a  $p \times p$  matrix of transition probabilities for the transient states,  $\mathbf{0}^T$  is a  $1 \times p$  null vector and  $\mathbf{c}$  is a  $p \times 1$  vector that satisfies  $\mathbf{c} = \mathbf{1} - \mathbf{Q}\mathbf{1}$  with  $\mathbf{1}^T$  being the  $1 \times p$  vector of all ones. In order to obtain the transition probabilities,  $Q_{i,j}$  in the tpm  $\mathbf{P}$ , first, divide the control limits *UCL* and *LCL* into  $p = 2m + 1$  subintervals. Each subinterval has the width of  $2\Delta$ , i.e.  $2\Delta = \frac{UCL - LCL}{p}$ . The midpoint of the  $j^{th}$  subinterval is represented by  $H_j$ , for  $j = -m, -(m-1), \dots, -1, 0, 1, \dots, m-1, m$ . The transition probabilities,  $Q_{i,j}$ , for  $i, j = -m, -(m-1), \dots, -1, 0, 1, \dots, m-1, m$ , of the tpm  $\mathbf{Q}$  in Eq. (7) are computed as [19]

$$Q_{i,j} = \Phi\left(\left(\frac{H_j + \Delta - (1-\lambda)H_i}{\lambda} - \delta\right)\sqrt{\frac{n}{(1-p^2)}}\right) - \Phi\left(\left(\frac{H_j - \Delta - (1-\lambda)H_i}{\lambda} - \delta\right)\sqrt{\frac{n}{(1-p^2)}}\right), \quad (7)$$

where  $\delta$  is the shift size of the process mean. Note that  $\delta$  is computed as  $\delta = \frac{|\mu_{Y_1} - \mu_{Y_0}|}{\sigma_Y}$ , where  $\mu_{Y_1}$  is the out-of-control population mean of the study variable  $Y$ .

The *ATS* and *SDTS* of the VSI EWMA-AI chart are obtained as

$$ATS = \mathbf{q}^T (\mathbf{I} - \mathbf{Q})^{-1} \mathbf{t} - \mathbf{q}^T \mathbf{t}, \quad (8)$$

and

$$SDTS = \sqrt{\mathbf{q}^T (\mathbf{I} - \mathbf{Q})^{-1} \mathbf{B} (2(\mathbf{I} - \mathbf{Q})^{-1} - \mathbf{I}) \mathbf{t} - (\mathbf{q}^T (\mathbf{I} - \mathbf{Q})^{-1} \mathbf{t})^2}, \quad (9)$$

respectively, where  $\mathbf{q}$  is a  $p \times 1$  vector of initial probabilities that contains the probabilities that correspond to the “restart state” with the  $(m+1)^{\text{th}}$  entry equals to unity and zeros elsewhere,  $\mathbf{t}$  is a  $p \times 1$  vector which consists of element  $t_L$  or  $t_S$ ,  $\mathbf{I}$  is a  $p \times p$  identity matrix and  $\mathbf{B}$  is a diagonal matrix that adopts the elements of either  $t_S$  or  $t_L$ . From Equation (8), the in-control  $ATS$  ( $ATS_0$ ) and out-of-control  $ATS$  ( $ATS_1$ ) are computed by letting  $\delta = 0$  and  $\delta \neq 0$ , respectively in Equation (7).

### 2.3 Optimal design of the VSI EWMA-AI chart

The optimal  $(\lambda, W, L)$  combination that minimize the  $ATS_1$  are computed by using the following optimization model:

$$\underset{(\lambda, W, L)}{\text{Minimize}} \ ATS_1(\delta) \quad (10)$$

subject to the constraints

$$ATS_0 = 370, \quad (11)$$

and

$$ASI_0 = 1, \quad (12)$$

where  $ASI_0$  is the in-control average sampling interval.

## 3 Numerical analysis

Table 1 presents the optimal parameters  $(\lambda, W, L)$  that minimize the  $ATS_1$  for  $\delta \in$

**Table 1.** Optimal  $(\lambda, W, L)$  combination of the VSI EWMA-AI chart, for  $n \in \{5, 7, 10\}$ ,  $\rho \in \{0.00, 0.25, 0.50, 0.75\}$  and  $\delta \in \{0.20, 0.40, 0.60, 0.80, 1.00, 1.25\}$ .

			$n = 5$			$n = 7$			$n = 10$		
$\rho$	$\delta$	$\lambda$	$W$	$L$	$\lambda$	$W$	$L$	$\lambda$	$W$	$L$	
0.00	0.20	0.05	0.621	2.491	0.09	0.640	2.673	0.09	0.640	2.673	
	0.40	0.19	0.654	2.850	0.09	0.640	2.673	0.20	0.656	2.860	
	0.60	0.34	0.660	2.942	0.19	0.654	2.850	0.37	0.662	2.951	
	0.80	0.37	0.662	2.951	0.34	0.660	2.942	0.37	0.662	2.951	
	1.00	0.37	0.662	2.951	0.37	0.662	2.951	0.37	0.662	2.951	
	1.25	0.37	0.662	2.951	0.37	0.662	2.951	0.37	0.662	2.951	
0.25	0.20	0.05	0.621	2.491	0.09	0.640	2.673	0.09	0.640	2.673	
	0.40	0.19	0.654	2.850	0.20	0.656	2.860	0.34	0.660	2.942	
	0.60	0.34	0.660	2.942	0.35	0.661	2.945	0.37	0.662	2.951	
	0.80	0.37	0.662	2.951	0.37	0.662	2.951	0.37	0.662	2.951	
	1.00	0.37	0.662	2.951	0.37	0.662	2.951	0.37	0.662	2.951	
	1.25	0.37	0.662	2.951	0.37	0.662	2.951	0.37	0.662	2.951	
0.50	0.20	0.05	0.621	2.491	0.09	0.640	2.673	0.13	0.649	2.768	
	0.40	0.19	0.654	2.850	0.20	0.656	2.860	0.34	0.660	2.942	
	0.60	0.34	0.660	2.942	0.37	0.662	2.951	0.37	0.662	2.951	
	0.80	0.37	0.662	2.951	0.37	0.662	2.951	0.37	0.662	2.951	
	1.00	0.37	0.662	2.951	0.37	0.662	2.951	0.37	0.662	2.951	
	1.25	0.37	0.662	2.951	0.37	0.662	2.951	0.37	0.662	2.951	
0.75	0.20	0.09	0.640	2.673	0.13	0.649	2.768	0.19	0.654	2.850	
	0.40	0.34	0.660	2.942	0.34	0.660	2.942	0.37	0.662	2.951	
	0.60	0.37	0.662	2.951	0.37	0.662	2.951	0.37	0.662	2.951	
	0.80	0.37	0.662	2.951	0.37	0.662	2.951	0.37	0.662	2.951	
	1.00	0.37	0.662	2.951	0.37	0.662	2.951	0.37	0.662	2.951	
	1.25	0.37	0.662	2.951	0.37	0.662	2.951	0.37	0.662	2.951	

$\{0.20, 0.40, 0.60, 0.80, 1.00, 1.25\}$  when  $t_s = 0.1$ ,  $t_L = 1.9$ ,  $n \in \{5, 7, 10\}$ ,  $\rho \in \{0.00, 0.25, 0.50, 0.75\}$ ,  $ATS_0 = 370$  and  $ASI_0 = 1$  are considered. By using the methodology presented in Section 2, the values of optimal  $(\lambda, W, L)$ ,  $ATS_1$  and  $SDTS_1$  are computed. Note that the details of selecting different combinations of  $(t_s, t_L)$  can refer to [20].

As can be observed from Table 2, when  $\rho$  increases, the  $ATS_1$  and  $SDTS_1$  values

**Table 2.** Comparison of the  $(ATS_1, SDTS_1)$  values for the EWMA-AI and VSI EWMA-AI charts when  $n \in \{5, 7, 10\}$ ,  $\rho \in \{0.00, 0.25, 0.50, 0.75\}$ ,  $\delta \in \{0.20, 0.40, 0.60, 0.80, 1.00, 1.25\}$  and  $ATS_0 = 370$ .

$\delta$	$n=5$		$n=7$		$n=10$	
	EWMA-AI	VSI EWMA-AI	EWMA-AI	VSI EWMA-AI	EWMA-AI	VSI EWMA-AI
		$\rho=0.00$		$\rho=0.25$		$\rho=0.5$
0.20	(29.9, 17.8)	(17.5, 14.4)	(23.5, 13.6)	(13.0, 11.3)	(17.9, 10.5)	(9.03, 7.63)
0.40	(10.3, 6.01)	(4.43, 4.16)	(7.80, 4.50)	(2.99, 2.88)	(5.71, 3.38)	(1.99, 2.04)
0.60	(5.13, 3.07)	(1.69, 1.91)	(3.75, 2.32)	(1.04, 1.30)	(2.63, 1.70)	(0.61, 0.89)
0.80	(2.96, 1.89)	(0.73, 1.01)	(2.07, 1.44)	(0.43, 0.69)	(1.34, 1.13)	(0.23, 0.44)
1.00	(1.83, 1.34)	(0.36, 0.61)	(1.18, 1.06)	(0.20, 0.38)	(0.64, 0.81)	(0.11, 0.21)
1.25	(1.00, 0.99)	(0.16, 0.32)	(0.53, 0.74)	(0.09, 0.17)	(0.20, 0.46)	(0.05, 0.08)
$\rho=0.25$						
0.20	(28.6, 16.8)	(16.5, 13.5)	(22.3, 13.5)	(12.1, 10.5)	(17.05, 9.8)	(8.49, 7.13)
0.40	(9.80, 5.77)	(4.10, 3.86)	(7.38, 4.30)	(2.78, 2.71)	(5.39, 3.20)	(1.83, 2.04)
0.60	(4.84, 2.91)	(1.54, 1.77)	(3.52, 2.18)	(0.95, 1.22)	(2.45, 1.62)	(0.55, 0.82)
0.80	(2.77, 1.78)	(0.66, 0.94)	(1.93, 1.37)	(0.39, 0.64)	(1.22, 1.08)	(0.21, 0.40)
1.00	(1.69, 1.27)	(0.32, 0.56)	(1.07, 1.02)	(0.18, 0.35)	(0.56, 0.76)	(0.10, 0.18)
1.25	(0.90, 0.95)	(0.15, 0.29)	(0.45, 0.69)	(0.08, 0.15)	(0.16, 0.41)	(0.04, 0.07)
$\rho=0.5$						
0.20	(24.3, 14.3)	(13.6, 10.9)	(18.9, 11.3)	(9.67, 8.20)	(14.3, 8.41)	(6.78, 5.99)
0.40	(8.13, 4.76)	(3.16, 3.03)	(6.07, 3.58)	(2.15, 2.18)	(4.39, 2.62)	(1.32, 1.57)
0.60	(3.93, 2.41)	(1.12, 1.38)	(2.82, 1.81)	(0.67, 0.96)	(1.92, 1.37)	(0.38, 0.64)
0.80	(2.19, 1.49)	(0.46, 0.73)	(1.47, 1.17)	(0.26, 0.48)	(0.86, 0.93)	(0.14, 0.28)
1.00	(1.26, 1.10)	(0.22, 0.41)	(0.73, 0.86)	(0.12, 0.24)	(0.32, 0.58)	(0.06, 0.11)
1.25	(0.59, 0.78)	(0.10, 0.19)	(0.25, 0.51)	(0.05, 0.09)	(0.06, 0.25)	(0.02, 0.05)
$\rho=0.75$						
0.20	(16.2, 9.51)	(7.94, 6.65)	(12.4, 7.18)	(5.59, 4.91)	(9.25, 5.34)	(3.78, 3.57)
0.40	(5.06, 3.02)	(1.65, 1.88)	(3.69, 2.28)	(1.02, 1.28)	(2.58, 1.69)	(0.59, 0.87)
0.60	(2.28, 1.53)	(0.49, 0.76)	(1.54, 1.21)	(0.28, 0.50)	(0.91, 0.95)	(0.15, 0.30)
0.80	(1.10, 1.03)	(0.19, 0.36)	(0.61, 0.79)	(0.10, 0.20)	(0.24, 0.51)	(0.05, 0.09)
1.00	(0.48, 0.71)	(0.08, 0.16)	(0.18, 0.44)	(0.04, 0.08)	(0.04, 0.20)	(0.02, 0.04)
1.25	(0.12, 0.36)	(0.03, 0.06)	(0.02, 0.15)	(0.01, 0.03)	(0.002, 0.04)	(0.002, 0.01)

of the VSI EWMA-AI chart decrease. For example, when  $n = 5$  and  $\delta = 0.20$ , the  $ATS_1$  ( $SDTS_1$ ) values for  $\rho = 0.00, 0.25, 0.50$  and  $0.75$  are  $17.5$  ( $14.4$ ),  $16.5$  ( $13.5$ ),  $13.6$  ( $10.9$ ) and  $7.94$  ( $6.65$ ), respectively. Noted that when  $\rho = 0.00$ , the VSI EWMA-AI chart reduces to the VSI EWMA chart. Moreover, when the sample size increases, the  $ATS_1$  decreases. From the comparison in Table 2, the VSI EWMA-AI chart significantly outperforms the existing EWMA-AI chart, for all shift levels across different values of  $\rho$ . For example, when  $n = 5$ ,  $\rho = 0.25$  and  $\delta = 0.20$ , the  $ATS_1$

values for the EWMA-AI and VSI EWMA-AI charts are 28.6 and 16.5, respectively. This indicates that the chart operating with VSI scheme detects the out-of-control situation faster than the chart operating with fixed sampling scheme.

## 4 Conclusion

This paper integrates the auxiliary information concept into the structure of the VSI EWMA-AI chart to monitor the mean of a process. By capturing the information not only from study variable but also from auxiliary variable in estimating the mean of the study variable, the VSI EWMA-AI chart becomes more sensitive to the shift detection by yielding smaller  $ATS_1$  and  $SDTS_1$  values, especially when the  $\rho$  value is large. Compared to the EWMA-AI chart, the VSI EWMA-AI chart is superior to the EWMA-AI chart, for detecting all sizes of mean shifts across different correlation levels between study and auxiliary variables. Thus, it is desirable to implement the VSI EWMA-AI chart instead of the EWMA-AI chart for process monitoring in manufacturing industries. Future research could investigate the run length performance of the variable sample size EWMA-AI chart. In addition, the research on variable sampling interval and sample size EWMA chart with auxiliary characteristics could be investigated.

## References

1. Abbas, N.: Homogeneously weighted moving average control chart with an application in substrate manufacturing process. *Computers & Industrial Engineering* 120, 460–470 (2018).
2. Cambron, P., Masson, C., Tahan, A., Pelletier, F.: Control chart monitoring of wind turbine generators using the statistical inertia of a wind farm average. *Renewable Energy* 116, 88–98 (2018).
3. Haq, A., Gulzar, R., Khoo, M. B. C.: An efficient adaptive EWMA control chart for monitoring the process mean. *Quality and Reliability Engineering International* 34(4), 563–571 (2018).
4. Lee, M. H., Khoo, M. B. K.: Double sampling  $|S|$  control chart with variable sample size and variable sampling interval. *Communications in Statistics – Simulation and Computation* 47(2), 615–628 (2018).
5. Wang, R. F., Fu, X., Yuan, J. C., Dong, Z. Y.: Economic design of variable-parameter X-Shewhart control chart used to monitor continuous production. *Quality Technology Quantitative Management* 15(1), 106–124 (2018).
6. Montgomery, D. C.: *Introduction to Statistical Quality Control*. 7th ed. New York: John Wiley & Sons (2012).
7. Roberts, S.: Control chart tests based on geometric moving averages. *Technometrics* 42(1), 97–101 (2000).
8. Page, E.: Continuous inspection schemes. *Biometrika* 41(1/2), 100–115 (1954).
9. Ali, R., Haq, A.: A mixed GWMA–CUSUM control chart for monitoring the process mean. *Communications in Statistics – Theory and Methods* 47(15), 3779–3801 (2018).

10. Cheng, X. B., Wang, F. K.: The performance of EWMA median and CUSUM median control charts for a normal process with measurement errors. *Quality and Reliability Engineering International* 34(2), 203–213 (2018).
11. Hosseini, S. S., Noorossana, R.: Performance evaluation of EWMA and CUSUM control charts to detect anomalies in social networks using average and standard deviation of degree measures. *Quality and Reliability Engineering International* 34(4), 477–500 (2018).
12. Abbas, N., Riaz, M., Does, R. J.: An EWMA-type control chart for monitoring the process mean using auxiliary information. *Communications in Statistics – Theory and Methods* 43(16), 3485–3498 (2014).
13. Haq, A., Abidin, Z. U., Khoo M. B. C.: An enhanced EWMA- $t$  control chart for monitoring the process mean. *Communications in Statistics – Theory and Methods* (in press).
14. Haq, A., Khoo, M. B. C.: A new double sampling control chart for monitoring process mean using auxiliary information. *Journal of Statistical Computing and Simulation* 88(5), 869–899 (2018).
15. Ng, P. S., Khoo, M. B. C., Saha, S., Teh, S. Y.: Run Sum Chart for the Mean with Auxiliary Information. *Journal of Testing and Evaluation* (in press).
16. Haq, A., Khoo, M. B. C.: Memory-type multivariate control charts with auxiliary information for process mean. *Quality and Reliability Engineering International* 35(1), 192–203 (2019).
17. Abbasi, S., Haq, A.: Optimal CUSUM and adaptive CUSUM charts with auxiliary information for process mean. *Journal of Statistical Computation and Simulation* 89(2), 337–361 (2019).
18. Abbas, N.: Memory-type control charts in statistical process control [PhD thesis]. Amsterdam School of Economics Research Institute (ASE-RI), Faculty of Economics and Business (FEB) (2012).
19. Zhang, L., Chen, G., Castagliola, P.: On  $t$  and EWMA  $t$  charts for monitoring changes in the process mean. *Quality and Reliability Engineering International* 25(8), 933–945 (2009).
20. Reynolds, M. R., Amin, R. W., Arnold, J. C., Nachlas, J. A.: Charts with variable sampling intervals. *Technometrics* 30(2), 181–192 (1988).



# Design of Cloud Computing Load Balance System Based on SDN Technology

Saif Al-Mashhadi, Mohammed Anbar, Rana A. Jalal, Ayman Al-Ani

National Advanced IPv6 Centre (NAv6), Universiti Sains Malaysia, 11800 Gelugor, Penang,  
Malaysia  
saifjawad@student.usm.my, anbar@usm.my, rana.jalal@yahoo.com

**Abstract.** Cloud computing is an emerging technology that came with a paradigm shift in computing and service hosting. The massive demand for cloud computing services required various techniques and new approaches to deliver reliable service efficiently and on time for users. These approaches include using new network topology, server and network virtualization, use of software-defined networks technology and network load balancing. Load balancing is an essential requirement for a fair and optimal distribution of services and bandwidth among farm servers. Various techniques for software-defined networking (SDN) architecture in load balancing are proposed. Research conducted is divided into static and dynamic load balance schemes. However, these approaches are expansive and use the same scheme for different servers. SDN is a powerful and programmable network technology. OpenFlow and OpenStack is part of SDN architecture that could provide services type, server load, and link health to a central location; thus, it provides better decision and configuration options. This research proposal explores the benefits and outcomes using SDN in cloud computing as a load balancing system.

**Keywords:** cloud computing, SDN, load balance.

## 1 Introduction

By providing on-demand scalable and pay-per-use network and computing resources, cloud computing emerged with a paradigm shift in information and communication technology (ICT) ecosystem [1]. Moreover, cloud computing eliminates up-front investment, reduces operational expenses and time required to publish application or service online. It now only needs an Internet connection and a few steps to publish services online [2]. Furthermore, it is giving more flexibility for clients to choose any required available service from various cloud computing providers and according to their computing and network needs. These services include on-demand IT-resources, which require network resources to deliver it to end user or to distribute the services within the cloud provider geographically distributed data centers network [3]. Resulted in a significant number of required network resources necessitates; thus, the cloud provider should have flexible management for it. Furthermore, both network Quality of Service

(QoS) and provided Service Level Agreement (SLA) should be high for winning the end users amongst other competitors [4].

Also, to provide efficient and cost-effective services, cloud computing vendor uses virtualization massively to separate services and application needs for each client, leading to hosting various kind of services in the same server. Furthermore, clients require access to their hosted services and application 24/7, with massive requests per day from multi-tenant clients [5]. “A tenant is a group of users who share a common access with specific privileges to the software instance” [6], which requires various load balancing approaches for reliable distribution of services, making the traditional network where network and forward planes are decoupled together are rigid and not flexible enough to cope with essential cloud services, application, and client network requirements.

In general, cloud computing vendor hosts different types of services that require different load balancing approaches. One of these approaches is having an additional and dedicated load balancer for each service which is mostly implemented using a hardware load balancer [7], a load balancing mechanism is an essential approach for incoming and outgoing traffic distribution among available servers (east-west traffic) or user's request (north-south traffic).

Load balance could be software balancers such as Microsoft network load balancing or hardware balancer. Hardware is usually expensive compared to software, and human intervention is required to configure load balancing for each service. Furthermore, the current load balancer cannot be configured to have a different scheme for each service type, so having hardware balancer is impractical and both a money and time-consuming approach.

On the other hand, programmable service type software-defined network (SDN) load balancer can allocate network resources dynamically, and on the fly for each service, application and client request independently without affecting other clients in the cloud.

This paper proposes using the SDN in cloud computing with the focus on deploying a dynamic service load balancing system by using the power of SDN, which reduces the operational and capital costs.

Before going into the details and how could it be applied, a fundamental cloud computing SDN architecture and essential components are briefly explained. This paper is organized as follows. Section 2 gives a background that covers cloud computing, SDN, cloud data center, load balance in the cloud, virtualization, and Network Function Virtualization (NFV). Section 3 the research proposal for the SDN load balance system. Finally, Section 4 gives the conclusion.

## 2 Background

### 2.1 Cloud Computing

Cloud computing, also known as the cloud, is the providing of hosted services through the Internet. Clients usually pay-per-use for getting the required services. It provides services in four main models: Software as a Service (SaaS), Platform as a Service (PaaS), Network as a Service (NaaS) and Infrastructure as a Service (IaaS) [8]. In order for the vendor to provide services for clients, cloud vendors should maintain a large-

scale data center. This data center usually includes thousands of servers which are connected using hundreds of networking devices. For instance, Amazon Web Service (AWS) operates 5000-8000 servers per data center [9]. These causes issues in scalability, management, and the ability to distribute load efficiently among different servers. Thus, researches and new inventions in load balancing are essential for the success of cloud providers.

## 2.2 Software-defined network SDN

Since it provides a lot of features and solution to network and cloud provider, the software-defined network is one of the hottest topics for discussion in networking these past years [10]. The primary goal of SDN design is the network to be open and programmable, compared to the traditional system where network control and data forwarding are in the same place (hardware). SDN achieves that by separation of network control plane (also named control plane) and data plane. Control plane in SDN is the programmable part (represented by SDN controller), and the data plane is data forwarding part (represented by switches).

Moreover, SDN architecture gives the flexibility to manage and control network resources from a central location, which is the SDN controller. The high-level architecture for SDN is illustrated in figure 1[11]. The most common protocol that used to connect the control panel with the data panel is the OpenFlow protocol; the following section will illustrate the OpenFlow protocol.

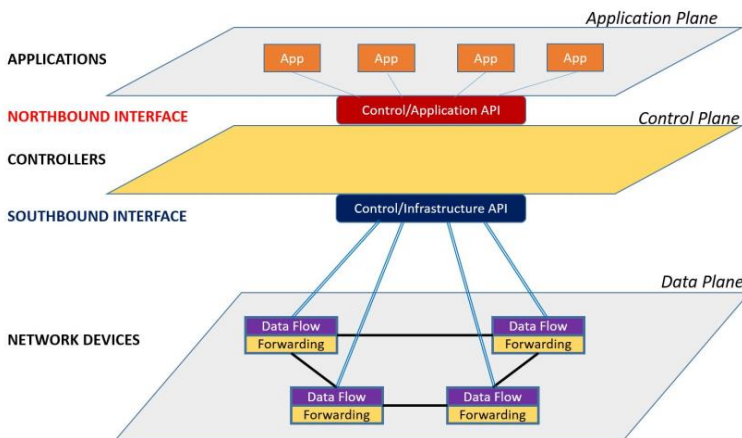


**Figure 1 - Software-Defined Networking – A high level architecture**

**Fig. 1.** High level architecture for SDN

### OpenFlow.

The separation between control logic and forwarding hardware increased the opportunities for developing new protocols by researchers and manufacturing cost-effective networking hardware. OpenFlow is the result of this separation, and it has become the standard protocol for SDN controller. It is also the base for many other controllers including Floodlight [12], NOX [13], POX [14] and OpenDaylight [15]. OpenFlow is the communication protocol between the edge network device and the SDN controller. Compared to the traditional protocol, it offers more network statistical information and could notify any change in topology. This information sent to a central place (SDN controller), giving the flexibility for the network manager to monitor the network and design the necessary action depending on data received. Moreover, this separation opens the doors for developers to develop and test a new control logic easily as long it follows the standards such as OpenFlow standard. These standards are always improved and available online for any developer [16]. However, since OpenFlow communication provides a lot of network information and management option; thus, OpenFlow communication authentication is essential to protect it [17]. On another hand, in traditional network devices, the network control logic is a property for the switch vendor and only could be developed by their own vendor developers.

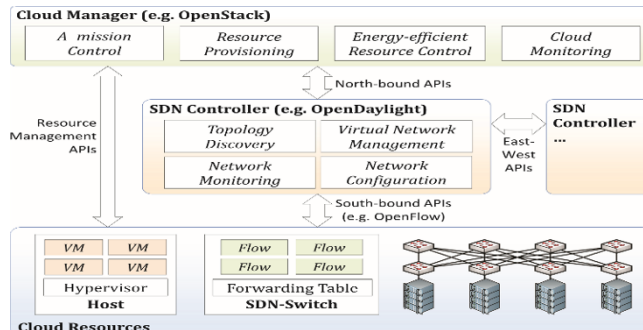


**Fig. 2.** SDN in cloud typical Architecture

### SDN in cloud architecture.

For enabling SDN in cloud computing, a typical standard architecture, as shown in Figure 2 [1] could be used. A cloud manager is required for controlling the resources and tenants. OpenStack [18] is an example of an open source cloud manager. OpenStack manage and monitor cloud computing resources. While, the networking resources and functions are provisioned by the SDN controller, including enabling dynamic load balancing and network configurations for both host and network devices. To increase network scalability and redundancy, multiple SDN controllers could function together by communicating via east-west-bound APIs. Each SDN controller manages network resources using the south-bound application programming interface (API) [1].

## 2.3 Cloud data center

As explained previously, for the cloud computing vendor to provide their service globally and efficiently, vendors usually have thousands of servers and a virtual host connected through switches, composing a data center network. A three-tier topology is a typical architecture for such network connections, which divides a network to three layers, which are core, distribution, and access. The massive number of servers and networking devices result in complexity in management, performance and scalability issues, and insufficient network bandwidth. As a solution, researchers introduced new topologies, such as fat-tree topology which is based on CLOS [19].

## 2.4 Load balance in the cloud

The enormous demand for cloud computing for Internet-delivered hosting services and applications led to a massive increase of requests per second from different users. Thus, Load balance is an essential approach for an optimized request among cloud computing services because it reduces latency and maximizes throughput. A typical architecture for load balance is illustrated in Figure 3. Furthermore, the load balance used in the cloud for the distribution of bandwidth, load, and request among servers, including virtual servers, leading to better responses time and per server utilization [20]. To distribute the load securely, the load balancer is typically installed between the firewall and the server pool. For the sake of load balancing, a lot of research and various model implementations were developed such as Application Load Balance (ALB) [21], Hardware Load Balance (HLB) [22] and Application Delivery Controller (ADC) [23]. ALB is software installed into Linux or Windows server operating systems whereas ADC is a load balancing hardware. ADC distributes the traffic to the selected servers based on the inspection of the packet header.

Furthermore, ADC checks the server's health status using a monitoring application to provide content-aware service that is used for quality of service (QoS) and security purposes. However, ADC is not able to identify the exact types of service. The importance of service-aware is essential to maximize resource utilization and optimize the time of the services processing.

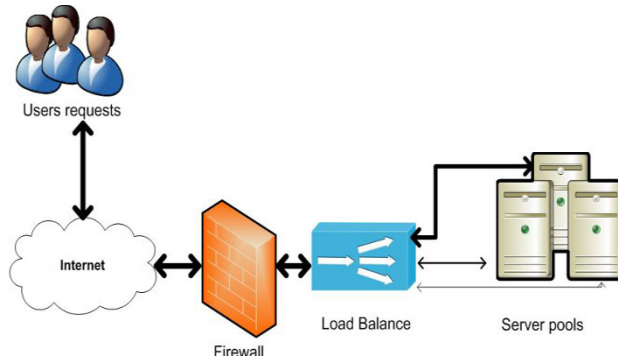


**Fig. 3.** A typical architecture for the load balance

## 2.5 Virtualization

Virtualization is the technology that allows consolidating multiple logical units into one physical unit or resource. Also, it allows one physical unit to act as a multiple physical units or resources, this leads to more agile, cost-effective system for the enterprise or the organization, besides that using virtualization lead to a maximum utilization for processing and storage resources, it also increases the utilization of network resources by reducing the number of hosts required for each service [10]. For instance, using a virtual machine (VM) permits various workloads to run on the same hardware or multiple hardware efficiently, simultaneously, and competition-free, which lead to more hardware resource utilization [24]. On the other hand, the workload could travel between different hardware independently. For instance, the hardware could be replaced or brought offline [25] for maintenance by moving the workload to the other virtualized resource. Virtualization keeps the same IP address even after network migration, which leads to more effective management and integration of network resources allocated for each service, high performance, redundant and easy to scale network resources.

## 2.6 Network Function Virtualization (NFV)

Network Function Virtualization (NFV) provides all necessary network function such as routers, load balancers, and a firewall. It gives more control over virtual machines that running different service, moreover it controlled and integrated with SDN through open flow given more central management location. NFV provides two separate virtualizations entities external and internal [18]. Each entity considered as one separate network; thus, NFV is essential to reduce cost and give more flexibility and control over network components for virtual machines.

## 3 Proposed Service-Based Load Balancing Using SDN Technology

The primary goal of the research proposal is to provide a dynamic, cost-effective service-based load balancing using SDN technology that increases server and bandwidth utilization and reduces latency. The main idea for the proposed model is similar to the principle of routing and forwarding table in a router and that map between IP address and port. In this research the table maps between services classifications, weight, and server pools that provide such services. To create this table, it essential to classify and give weight for each service, depending on service load utilization, type of service, and available link bandwidth to each server. This table will manage the network flow using SDN controller of network open flow switches.

A four-phase research methodology will be conducted according to an empirical research approach.

PHASE 1: Study SDN in cloud computing, identify the current issues and requirements regarding using SDN load balancing system.

PHASE 2: For the study and identifying the problem, several empirical experiments will be conducted, a mathematical formula for load balance will be formulated. Then the load balance mechanism based on SDN technology is proposed.

PHASE 3: A mechanism is developed that will be implemented with an appropriate SDN controller.

PHASE 4: A performance evaluation will be conducted based on various metrics and experiments. A comparison with the current load balance system will be reported and, in the end, a suggestion for future work will be discussed.

Phase 1 includes the following:

Explosive growth in network traffic and services requests results in critical issues in congestion, and overwhelmed server load. Consequently, research on load balancing for the cloud became an important research topic [26]. Various techniques to use the SDN architecture in load balancing are proposed. Conducted research could be divided into static and dynamic load balance schemes.

The static scheme is simple to implement [27]. However, it is not flexible and does not consider server usage status (CPU, RAM, and links bandwidth). For example, if the server is overloaded with task processing, it may send another task to the same server without considering the load or task side.

On the other hand, the dynamic scheme [28], takes into consideration the network node's live status, but it neglects the size and type of user request, with one algorithm for different service types [29]. Optimal load balance requires different processing scheme for each service, for instance, File Transfer Protocol (FTP) and Hyper Text Protocol (HTTP) has a different processing load, style, and the number of connections. Both dynamic and static load balance schemes are applied in dedicated hardware devices or installed inside the operating system, such as Microsoft network load balancing, which makes them costly and not dynamic for different types of services.

Besides, there are various studies using SDN technology as a load balancer for cloud computing [21]. However, these studies have not considered the service types in their approaches. OpenFlow protocol messages give the SDN controller the power to monitor different network node status and health, integrating OpenStack with NFV provides the status of server health, CPU usage, and network management [18, 30], Mixing this information with a mathematical algorithm, the researchers could have more decision in load distribution through SDN technology.

The research areas are listed below:

1. Analyzing and review SDN load balancing approaches in the cloud.
2. Propose an SDN load balancing that uses service, bandwidth, and server load classification as a base for load distribution.
3. Explore and implement the power of OpenFlow. NFV and OpenStack API to get service, bandwidth, and server load classification info and status.
4. Reduce the operational expenses (OpEx) by using, Virtual Machine (VM), NFV and OpenFlow switch instead of expensive hardware by implanting SDN technology.

Phase two and three will involve empirical experiments and tests. The mathematical formula for load balance will be created, the formula is based on different algorithms,

weighted round robin, weighted least connection algorithm and active clustering will be evaluated separately [25], Python [31] program for SDN controller based on the formula will be programmed, the approach will be tested and evaluated using Mininet [32] (an open source network emulator for SDN defined using Python language).

For empirical experiments will include OpenDayLight [18] OpenFlow SDN controller that easily could integrate with OpenStack and NFV. OpenFlow switches and Linux as the operating system, using a desktop with a minimum specification of 16Gb ram, core i7 CPU and 500GB hard disk. After which, the results will be evaluated in phase four using Mininet, Wireshark [33], and Ping tool selecting different algorithms. The proposed mechanism is illustrated in the figure. 4.

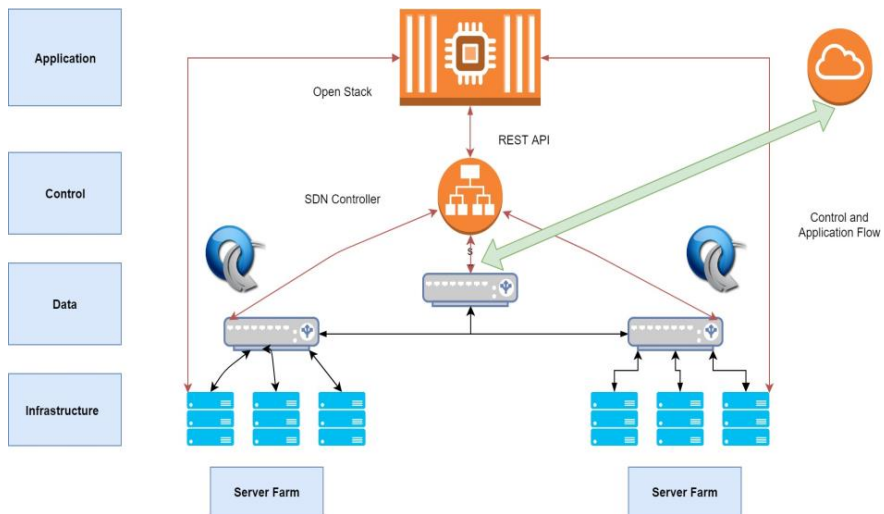


**Fig. 4.** The proposed mechanism

## 4 Conclusion

Moving toward a cloud computing model come with challenges in resources and load management, SDN as a flexible, programmed, and cost-effective is a promising solution to tackle these challenges. Moreover, integrating SDN in load balance solution will result in an agile model for cloud computing data center. However, since SDN usually manages all network resources from a central location, more researches are required to secure SDN communication between its different layers.

## Acknowledgments.

This research was supported by the Bridging Research Grant, Universiti Sains Malaysia (USM) No: 304/PNAV/6316271

## References

1. Son J, Buyya R (2018) A Taxonomy of Software-Defined Networking (SDN)-Enabled Cloud Computing. ACM Computing Surveys 51:1–36. <https://doi.org/10.1145/3190617>
2. Azodolmolky S, Wieder P, Yahyapour R (2013) SDN-based cloud computing networking. International Conference on Transparent Optical Networks 2–6. <https://doi.org/10.1109/ICTON.2013.6602678>
3. Xu Q, Li L, Liu J, Zhang J (2018) A Scalable and Hierarchical Load Balancing Model for Control Plane of SDN. Proceedings - 2018 6th International Conference on Advanced Cloud and Big Data, CBD 2018 6–11. <https://doi.org/10.1109/CBD.2018.00011>
4. Govindarajan K, Kumar VS (2017) An intelligent load balancer for software defined networking (SDN) based cloud infrastructure. Proceedings of the 2017 2nd IEEE International Conference on Electrical, Computer and Communication Technologies, ICECCT 2017. <https://doi.org/10.1109/ICECCT.2017.8117881>
5. Krebs R, Momm C, Kounev S (2012) ARCHITECTURAL CONCERNS IN MULTI-TENANT SaaS APPLICATIONS. Proceedings of the 2nd International Conference on Cloud Computing and Services Science 426–431. <https://doi.org/10.5220/0003957604260431>
6. Multitenancy. <https://en.wikipedia.org/wiki/Multitenancy>
7. Kanagavelu R, Aung KMM (2016) Software-defined load balancer in cloud data centers. Proceedings of the 2nd International Conference on Communication and Information Processing - ICCIP '16 139–143. <https://doi.org/10.1145/3018009.3018014>
8. Azodolmolky S, Wieder P, Yahyapour R (2013) SDN-based cloud computing networking. International Conference on Transparent Optical Networks 1–4. <https://doi.org/10.1109/ICTON.2013.6602678>
9. With The Public Clouds Of Amazon, Microsoft And Google, Big Data Is The Proverbial Big Deal. <https://www.forbes.com/sites/johnsonpierr/2017/06/15/with-the-public-clouds-of-amazon-microsoft-and-google-big-data-is-the-proverbial-big-deal/#205a52da2ac3>. Accessed 10 Dec 2018
10. Open Networking Foundation (2012) Software-Defined Networking : The New Norm for Networks. ONF White Paper 2:2–6
11. Hoang D (2015) Software Defined Networking – Shaping up for the next disruptive step? Australian Journal of Telecommunications and the Digital Economy 3:48. <https://doi.org/10.18080/ajtde.v3n4.28>
12. Floodlight OpenFlow Controller -Project Floodlight. <http://www.projectfloodlight.org/floodlight/>. Accessed 4 Jun 2019
13. Installing POX — POX Manual Current documentation. <https://noxrepo.github.io/pox-doc/html/>. Accessed 14 Dec 2018
14. Shalimov A, Zuikov D, Zimarina D, et al (2014) Advanced study of SDN/OpenFlow controllers. pp 1–6
15. Home - OpenDaylight. <https://www.opendaylight.org/>. Accessed 19 Dec 2018

16. Benamrane F, Ben mamoun M, Benaini R (2015) Performances of OpenFlow-Based Software-Defined Networks: An overview. *Journal of Networks* 10:. <https://doi.org/10.4304/jnw.10.6.329-337>
17. Zubaydi HD, Anbar M, Wey CY (2017) Review on Detection Techniques against DDoS Attacks on a Software-Defined Networking Controller. In: Proceedings - 2017 Palestinian International Conference on Information and Communication Technology, PICICT 2017. pp 10–16
18. Patel P, Tiwari V, Abhishek MK (2017) SDN and NFV integration in openstack cloud to improve network services and security. Proceedings of 2016 International Conference on Advanced Communication Control and Computing Technologies, ICACCCT 2016 655–660. <https://doi.org/10.1109/ICACCCT.2016.7831721>
19. Al-fares M, Loukissas A [SIGCOMM'08]A scalable, commodity data center network architecture.pdf. 63–74. <https://doi.org/10.1145/1402946.1402967>
20. Wang TS, Lin HT, Cheng WT, Chen CY (2017) DBod: Clustering and detecting DGA-based botnets using DNS traffic analysis. *Computers and Security* 64:1–15. <https://doi.org/10.1016/j.cose.2016.10.001>
21. Shang Z, Chen W, Ma Q, Wu B (2013) Design and implementation of server cluster dynamic load balancing based on OpenFlow. 2013 International Joint Conference on Awareness Science and Technology and Ubi-Media Computing: Can We Realize Awareness via Ubi-Media?, iCAST 2013 and UMEDIA 2013 691–696. <https://doi.org/10.1109/ICAwST.2013.6765526>
22. Gandhi R, Liu HH, Hu YC, et al (2014) Duet: Cloud Scale Load Balancing with Hardware and Software. *Sigcomm* 2014 27–38. <https://doi.org/10.1145/2619239.2626317>
23. Chang H, Tang X (2011) A load-balance based resource-scheduling algorithm under cloud computing environment. Lecture Notes in Computer Science (including subseries Lecture Notes in Artificial Intelligence and Lecture Notes in Bioinformatics) 6537 LNCS:85–90. [https://doi.org/10.1007/978-3-642-20539-2\\_10](https://doi.org/10.1007/978-3-642-20539-2_10)
24. Souza FR De, Miers CC, Fiorese A, Koslovski GP (2017) QoS-aware virtual infrastructures allocation on SDN-based clouds. Proceedings - 2017 17th IEEE/ACM International Symposium on Cluster, Cloud and Grid Computing, CCGRID 2017 120–129. <https://doi.org/10.1109/CCGRID.2017.57>
25. Randles M, Lamb D, Taleb-Bendiab A (2010) A comparative study into distributed load balancing algorithms for cloud computing. 24th IEEE International Conference on Advanced Information Networking and Applications Workshops, WAINA 2010 551–556. <https://doi.org/10.1109/WAINA.2010.85>
26. Handigol N, Seetharaman S (2010) Aster\* x: Load-balancing as a network primitive. 9th GENI Engineering Conference 1–2
27. Dhinesh Babu LD, Venkata Krishna P (2013) Honey bee behavior inspired load balancing of tasks in cloud computing environments. *Applied Soft Computing Journal* 13:2292–2303. <https://doi.org/10.1016/j.asoc.2013.01.025>
28. Guo Z, Su M, Xu Y, et al (2014) Improving the performance of load balancing in software-defined networks through load variance-based synchronization. *Computer Networks* 68:95–109. <https://doi.org/10.1016/j.comnet.2013.12.004>
29. Handigol N, Seetharaman S, Flajsluk M (2009) Plug-n-Serve: Load-balancing web traffic using OpenFlow. *Acm Sigcomm* 2
30. OpenStack Docs: Show usage statistics for hosts and instances. <https://docs.openstack.org/nova/rocky/admin/common/nova-show-usage-statistics-for-hosts-instances.html>. Accessed 19 Dec 2018

31. Python Networking Programming.  
[https://www.tutorialspoint.com/python/python\\_networking.htm](https://www.tutorialspoint.com/python/python_networking.htm). Accessed 26 Oct 2018
32. Mininet: An Instant Virtual Network on your Laptop (or other PC) - Mininet.  
<http://mininet.org/>. Accessed 14 Dec 2018
33. (2019) Wireshark · About. <https://www.wireshark.org/about.html>. Accessed 21 May 2018



# Analysis of Expert's Opinion on Requirements Patterns for Software Product Families Framework Using GQM Method

Badamasi Imam Ya'u<sup>1,2</sup>, Azlin Nordin<sup>2</sup>, Norsaremah Salleh<sup>2</sup>

<sup>1</sup>Abubakar Tafawa Balewa University, Bauchi

<sup>2</sup>International Islamic University Malaysia

biyau@atbu.edu.ng, badamasi.imam@live.iium.edu.my, {azlinnordin, norsaremah}@iium.edu.my

**Abstract.** Software product line engineering (SPLE), provides an opportunity to improve reuse of software artifacts through domain engineering and application engineering processes. During the domain engineering process, reuse activities of the product line are well-planned and subsequently executed in the application engineering process. This paper presents an analysis of interview result with experts in requirements engineering (RE) and software development for validating requirements pattern for software product families (RP-SPF) framework. The interview was conducted using goal questions metrics (GQM) method to define a goal and formulate research questions for conducting the interview. During the interview, 6 experts compared RP-SPF approach (systematic) with ad hoc (conventional) approach of reuse and documentation of requirements in terms of suitability, efficiency, and effectiveness in SPLE. The experts also gave their feedback on the perception of the use of RP-SPF tool. The analysis of the interview result shows that RP-SPF approach is suitable in SPLE and more efficient and effective than ad hoc approach of reuse and documentation of requirements.

**Keywords:** Software product line engineering, requirements pattern, systematic requirements reuse, expert opinion, interview.

## 1 Introduction

Software product line (SPL) is a software development paradigm that enables huge production of related software products with the aid of systematic reuse technique of software artifacts at any level of software development [1]. In SPLE, scoping is the term used to describe the requirements engineering activities in which decision is made on which organization's work product is reusable systematically and economically [2]. Up to now, product lines are the most strategic approaches that practice requirements reuse [3]. It's obvious that reuse of requirements like other software artifacts positively affects software development cost, effort and time to market [4-8]. Furthermore, research shows that the benefits of requirements reuse is not limited to requirements analysis phase but also spreads down to phases of software developments such as coding and

testing [9, 10]. This opens opportunities for practitioners to systematically reuse requirements artifacts in design, coding, and testing [11, 12]. The main contribution of this paper is a presentation of the analysis of the interview result with experts to validate RP-SPF framework based on comparison with an ad hoc approach of reuse and documentation of requirements.

The remainder of the paper presents related work in Section 2. The overview of RP-SPF framework is presented in Section 3. Section 4 presents the methodology. Result of the survey is presented in Section 5. The discussion of the result is presented in Section 6. The summary of the paper is presented in Section 7. Finally, Acknowledgement is presented in Section 8.

## 2 Related Work

This section presents related work on requirements pattern approaches. SRP is becoming a hot study subject in the SE community because of the successful nature of offering coherent structure. A common SRP method can be discovered in Withall's job to write software requirements specification [13]. Withall strategy is generic and can, therefore, be implemented and tailored to any domain, particularly the information system. Another method focusing on elicitation of demands, known as pattern-based elicitation of demands (PABRE), can be discovered in [14-16]. Some experts concentrate on particular domains using SRP templates. While others develop new requirement patterns catalog in a particular context to solve specific issues.

In the literature, we discovered that some of the suggestions for requirements patterns were in the safety context [17-21]. For instance, eight models of web security criteria were advocated [17]; the patterns were designed to assist analysts to discover a suitable safety pattern for particular purposes. Detailed steps were provided in research to organize security patterns to promote the use of patterns, particularly for a cross-reference between associated patterns [18].

On the other hand, some experts focus on requirement pattern based on a particular type of requirements. For instance (1) functional requirements [22]; (2) non-functional requirements [23]; and (3) non-technical requirements [24].

## 3 Overview of RP-SPF Framework

This section describes the RP-SPF, which is a general framework developed for systematic requirements reuse in software product line engineering (SPLE). Consequently, RP-SPF framework complies with the concepts of *design for reuse* and *design with reuse* at domain engineering and application engineering of SPLE respectively [8, 25]. To accomplish systematic reuse of requirements, RP-SPF combines requirements pattern approach, traceability and variability management of requirements through the principles and guidelines of requirements engineering (RE), SPLE and model-driven engineering (MDE).

## 4 Research Methodology

In this interview, this research applies the Goal/Question/Metric (GQM) framework, where the objectives, questions, and metrics of the interview are defined [26]. Though the GQM approach was designed initially for the improvement of software product and process, the underline ideas are all-purpose and thus can be useful to any measurement format [27]. In other words, GQM is especially helpful when research intends to define goal and metrics in specific measurement setting [28].

### 4.1 The objective of the Interview

The main aim of this interview is to validate the proposed approach, which is requirements patterns for software product family (RP-SPF) framework with the following objectives, a) To validate RP-SPF framework based its suitability, efficiency, and effectiveness in SPLE compared to the conventional approach and b) To evaluate RP-SPF tool based on a perception of use. Table 1 presents the overall goal of the interview, questions to investigate the opinions of the experts on the proposed approach and metrics to measure the responses of the respondents.

**Table 1.** GQM Definition

Goal	To discover the opinion and perception of experts regarding the suitability, efficiency and effectiveness of the proposed requirements patterns for software product family framework (RP-SPF) in requirements engineering activities of software product line engineering in the context of systematic requirements reuse.
Question	Metric
Q1. Tell me what you understand and achieve from the task you have done?	MQ1. Personal perception of the task understanding and achievement.
Q2. Tell me what your subjective impression is on the proposed RP-SPF suitability for the improvement of requirements reuse and documentation in software product line engineering compared to using a conventional approach?	MQ2. Personal opinion for the suitability of using RP-SPF in SPLE compared to using the conventional method.
Q3. Tell me what your perception is on using metamodeling strategy in facilitating software design and development?	MQ3. Personal opinion for the applicability of using metamodeling strategy by the proposed approach to improve requirements engineering in SPLE.
Q4. Tell me what your opinion is on the efficiency of RP-SPF on the reduction of the time of requirements engineering activities compared to conventional method?	MQ4. A personal opinion on the difference in the reduction of time using RP-SPF approach compared to the conventional method
Q5. Tell me what your subjective impression is on the effectiveness of the activity of reusing and producing	MQ5. A personal opinion on the correctness of the activity of reusing and producing requirements document using the proposed

	requirements document using RP-SPF compared to conventional method?	approach compared to the conventional method.
Q6.	Tell me your perception of how the structure of the requirements pattern in RP-SPF helps to manage requirements?	MQ6. Subjective opinion on proper management of requirements using RP-SPF framework.
Q6.1	What can you say on how the pattern structure assists in requirements traceability?	MQ6.1 Subjective opinion on managing requirements traceability using RP-SPF framework.
Q6.2	What is your opinion on how the requirements pattern structure helps in managing variability?	MQ6.2 Subjective opinion on managing requirements variability using RP-SPF framework.
Q7.	Tell me what your opinion is on RP-SPF tool in facilitating the reuse and documentation of requirements?	MQ7 Subjective opinion on the benefits gained using RP-SPF tool in facilitating the reuse and documentation of requirements.
Q7.1	what can say about the ease of use of RP-SPF tool?	MQ7.1 Subjective opinion on the ease of use to generate requirements document using RP-SPF tool.

## 4.2 Selecting the Interview Participants

The participants in this interview were 6 experts from software engineering, requirements engineering and software development preferably in software product line engineering. In qualitative research, the number of respondents varies from one study to another [29]. Thus, the number ranges from a sample size of 1, 2 to 30 or 40 [30]. Since the participants were experts, in this interview, a purposive sampling technique was used [31]. Thus, the experts were selected based on the following criteria:

- a) The participants have experience in software engineering/ requirements engineering.
- b) The participants have experience in software engineering/ requirements engineering within 5 years or more.
- c) The participants have experience in software development.
- d) Preferable if the participants have experienced in software product line engineering.

## 5 Results

### 5.1 Analysis of the Interview Result

During both pilot and actual interviews, all conversations were audio recorded. The recorded conversations were later transcribed in to document for analysis. The transcription of the audio was done according to the sequence of questions asked during the interview. And finally, interpretation of these data was executed using content and thematic analysis.

**Validation Questions.** In this interview, there were 7 validation questions. Since the research uses GQM, the metric used for measuring the responses of the experts (E1, E2, E3, E4, E5, and E6) was expert's opinion, which shows either positive or negative comments. For this reason, 3 types of comments were analyzed during the content analysis, which is positive (P), negative (N) and suggestion (S). During the analysis, each comment is scored either 1 or -1. For example, one positive comment (1), negative comment (-1) and suggestion comment (1).

*Suitability of RP-SPF Framework in Software Product Line Engineering.* Similarly, responses to Q2 yields a total number of 17 themes extracted from the respondent's opinions on the suitability of RP-SPF in the software product line (SPLE) especially for improving requirements reuse and documentation. Subsequently, 10 main themes and codes were formed. All the comments on the 17 themes show positive opinions of experts regarding the inquiry on the suitability of the proposed approach (see **Error! Reference source not found.1**). Overall, all the 6 respondents gave positive opinions on the suitability of RP-SPF framework to improving requirements reuse and documentation in SPLE.

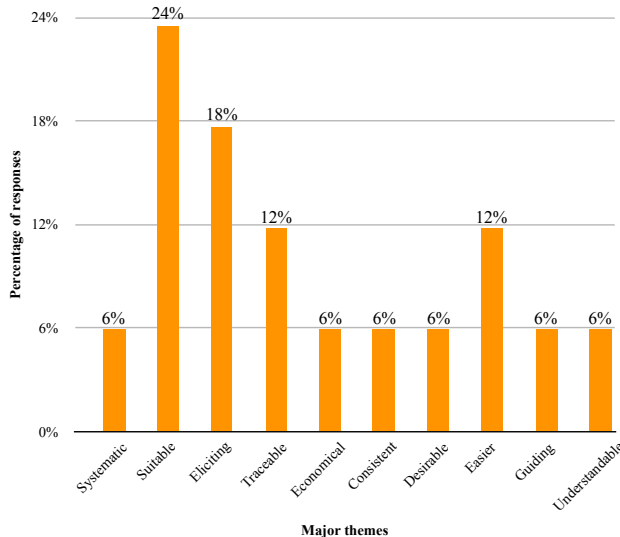


**Fig. 1.** Proportions of Themes on Suitability of RP-SPF in SPLE

*The efficiency of RP-SPF framework.* The content analysis for Q4 discovers 15 themes from the opinions of 6 respondents on the efficiency of RP-SPF approach compared to the conventional approach for reusing and documenting requirements. Considering these themes, 7 main themes and codes were composed. Furthermore, as shown in **Error! Reference source not found.2**, none of these themes represent a negative response. This means that all the opinions of the experts were positive. The overall opinion of the respondent shows that RP-SPF approach is greater in the efficiency in terms of productivity, fast and saving resources than the conventional approach.

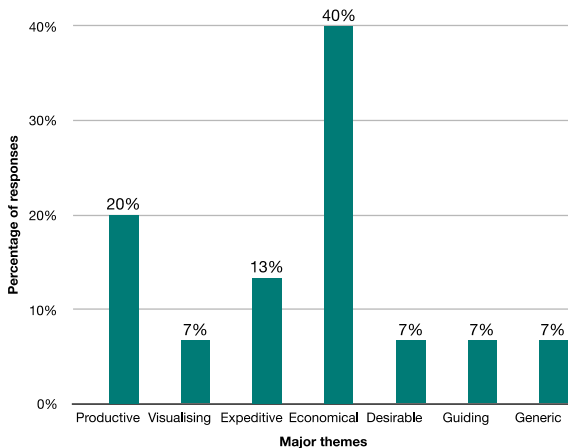


**Fig. 2.** Proportions of Themes on Efficiency of RP-SPF

*Effectiveness of RP-SPF framework.* Similarly, regarding whether RP-SPF approach is more effective than conventional approach on reuse and documentation of requirements, 19 themes were extracted from the feedback or opinions of the respondents. Subsequently, 7 main themes and codes were formulated for statistical analysis. In addition, all comments of the respondent from the 17 themes show positive opinions on the effectiveness of RP-SPF approach as illustrated in **Error! Reference source not found.3**. Thus, in comparison with the ad hoc approach of reusing and documenting requirements, RP-SPF was rated as being a more effective approach.

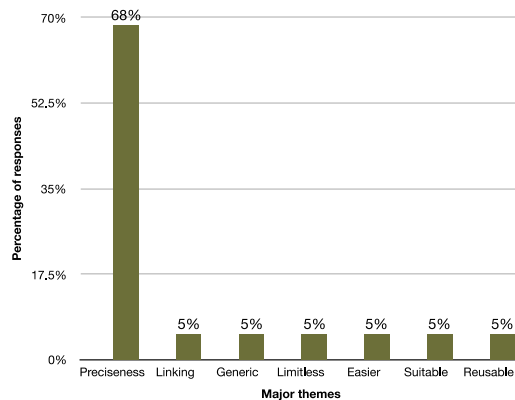


**Fig. 3.** Proportions of Themes on Effectiveness of RP-SPF

*Perception of Use of RP-SPF Tool in Facilitating the reuse and Documentation of Requirements.* The aim of this question was to investigate the usefulness of RP-SPF tool from the opinions of an expert in facilitating the reuse and documentation of

requirements. From the opinions of the respondents, 19 themes were extracted. Out of these 19, 2 themes representing 11% were negative as illustrated in **Error! Reference source not found.4**.

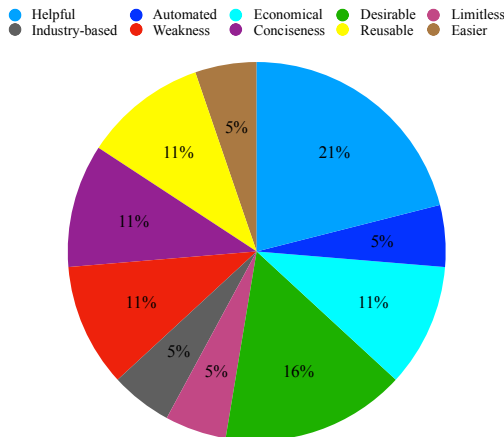


**Fig. 4.** Perception of Use of RP-SPF Tool

It is, therefore, a clear cut that the positive comments on the usefulness of RP-SPF tool accumulated to 89% of the total opinions, and thus, it can be concluded that it is essential for reusing and documenting requirements.

## 6 Discussion

Another aspect of the analysis of the result of the interview to be discussed is the reusable structure of requirements pattern that supports traceability and variability management of the requirements provided by RP-SPF. Question 6 of the interview protocol probed respondents whether the structure helps in managing traces and variations of requirements or otherwise.

*Opinions of Experts on Requirements Traceability Supported by RP-SPF.* This sub-question intends to investigate the opinion of experts regarding whether requirements pattern structure in RP-SPF assists in tracing requirements or not. From the pool of responses, 11 themes were extracted and represented by 4 main themes and codes. Within the 11 themes, 2 are negative, thus represented by a main theme ‘Weakness’ during the analysis. The proportion of the Weakness is 18%. Thus, positive opinions accrued to 82%. Therefore, it can be concluded that the structure of RP-SPF assists in requirements traceability.

*Opinions of Experts on Requirements Variability Supported by RP-SPF.* This is another sub-question that investigates the opinions of experts on whether the requirements patterns structure helps in the management of requirements variability or otherwise. From the bunch of responses, 11 themes were retrieved and subsequently, 4 main themes

were built together with their codes to enable statistical analysis. The content analysis shows that 100% of the comments were positive. From this analysis, it can be concluded that the structure of RP-SPF helps in the management of requirements variability.

*Metamodeling Strategy.* RP-SPF framework uses a metamodeling approach to integrate essential concepts such as requirements pattern, traceability, and variability to achieve systematic reuse of requirements. Thus, the respondents were asked whether the metamodeling strategy helps in the design and development of software or not.

Regarding expert's opinions on that, the respondents gave both positive and negative comments. From the content analysis, 17 themes were discovered from all responses. The negative comments were represented by 'Weakness' main theme. Although 6 positive main themes were extracted, the result shows that the proportion of the 'Weakness' from the statistical frequency analysis is the largest with 35%. Nevertheless, with 65% of total positive comments, it indicates that meta-modeling strategy is good and helps designers and developers in visualizing the internal structure of the system.

### 6.1 Threat to Validity

The validity of qualitative research is internal and external validity, which cover descriptive validity, researcher bias, interpretive validity and many more [32, 33].

*Descriptive Validity.* A source of threat to internal validity might descriptive validity in which the researcher is unable to record the data from the respondent precisely [33]. To avoid a threat to the validity of this interview, we have conducted a pilot interview with 5 Ph.D. students to test any problem that might lead to any threat to validity. Furthermore, we audio-recorded and transcribed the entire interview with all responded.

*Interpretive Validity.* This deals with the ability of the researcher to translate what exactly happened [33]. For this interview, we asked open-ended questions, which allow the respondents to best express their opinions at length without been unambiguous in some aspect.

## 7 Conclusion

This paper presents an analysis of interview with experts for the validation RP-SPF framework. Before going into the details of the interview, the paper presents related work on requirements pattern. We found that the reported approaches provided different requirements pattern templates that help in writing requirements, however, discuss mostly the implementation of requirement patterns in particular SPLE domains thus, leaving behind the practical implementation of requirement patterns in simplifying and structuring the overall requirement engineering (RE) operations taking place in SPLE. For the interview, the research uses the GQM method to state the goal and formulate research questions and metrics. 6 experts in requirements engineering and software developments from both academic and industry were the respondents. During content and thematic analysis, positive, negative and suggestions comments were discovered and formed into themes and codes to enable statistical analysis. The overall result of the analysis shows that RP-SPF approach is suitable in SPLE and is more efficient and

effective compared to ad hoc reuse and documentation of requirements. Although the experts gave recommendation for improvement of RE-SPF tool, they all express that in terms of the perception of use, RP-SPF is very useful and easy to use.

## Acknowledgment

This research was funded by the Ministry of Higher Education Malaysia under FRGS research grant (FRGS/1/2018/ICT01/UIAM/02/2).

## References

1. Karatas, E.K., B. Iyidir, and A. Birturk. Ontology-Based Software Requirements Reuse: Case Study in Fire Control Software Product Line Domain. in 2014 IEEE International Conference on Data Mining Workshop. 2014.
2. Villela, K., J. Dörr, and I. John. Evaluation of a method for proactively managing the evolving scope of a software product line. in International Working Conference on Requirements Engineering: Foundation for Software Quality. 2010. Springer.
3. Liang, P., P. Avgeriou, and C. Wang, From Architectural Knowledge to Requirements Knowledge Management. ResearchGate, 2009.
4. Benitti, F.B.V. and R.C.d. Silva, Evaluation of a Systematic Approach to Requirements Reuse. Journal of Universal Computer Science, 2013. **19**(2).
5. Chernak, Y. Requirements Reuse: The State of the Practice. in 2012 IEEE International Conference on Software Science, Technology and Engineering. 2012.
6. Goldin, L. and D.M. Berry, Reuse of requirements reduced time to market at one industrial shop: a case study. Springer-Verlag, 2013.
7. Ya'u, B.I., A. Nordin, and N. Salleh, Meta-Modeling Constructs for Requirements Reuse (RR): Software Requirements Patterns, Variability and Traceability. Malaysian Journal of Computing, 2018. **3**(2): p. 119-137.
8. Ya'u, B.I., et al. Requirements Patterns Structure for Specifying and Reusing Software Product Line Requirements in 2018 International Conference on Information and Communication Technology for the Muslim World. 2018. KICT, International Islamic University Malaysia.
9. Srivastava, S., A Repository of Software Requirement Patterns for Online Examination System. International Journal of Computer Science Issues (IJCSI '13), 2013. **3**.
10. Goldin, L., M. Matalon-Beck, and J. Lapid-Maoz. Reuse of Requirements Reduces Time to Market. in 2010 IEEE International Conference on Software Science, Technology & Engineering. 2010.
11. Liang, P., P. Avgeriou, and C. Wang, Managing Requirements Knowledge using Architectural Knowledge Management Approaches. 2011.
12. Bakar, N.H. and Z.M. Kasirun, Exploring Software Practitioners' Perceptions and Experience in Requirements Reuse A Survey in Malaysia. International Journal of Software Engineering and Technology, 2014. **1**(2).
13. Withall, S., Software requirement patterns. 2007: Pearson Education.
14. Renault, S., et al. PABRE: pattern-based requirements elicitation. in Research Challenges in Information Science, 2009. RCIS 2009. Third International Conference on. 2009. IEEE.
15. Palomares, C., C. Quer, and X. Franch, PABRE-Man: Management of a requirement patterns catalogue. 2011.

16. Palomares, C., C. Quer, and X. Franch. PABRE-Proj: Applying patterns in requirements elicitation. 2013.
17. Okubo, T. and H. Tanaka. Web security patterns for analysis and design. in Proceedings of the 15th Conference on Pattern Languages of Programs. 2008. ACM.
18. Hafiz, M., P. Adamczyk, and R.E. Johnson, Organizing Security Patterns. IEEE Software, 2007. **24**(4): p. 52-60.
19. Beckers, K., I. Côté, and L. Goeke. A catalog of security requirements patterns for the domain of cloud computing systems. in Proceedings of the 29th Annual ACM Symposium on Applied Computing. 2014. ACM.
20. Xuan, X., Y. Wang, and S. Li. Privacy requirements patterns for mobile operating systems. in 2014 IEEE 4th International Workshop on Requirements Patterns (RePa). 2014.
21. Hoffmann, A., et al. Towards trust-based software requirement patterns. in Requirements Patterns (RePa), 2012 IEEE Second International Workshop on. 2012. IEEE.
22. Palomares, C., et al. A catalogue of functional software requirement patterns for the domain of content management systems. in Proceedings of the 28th annual acm symposium on applied computing. 2013. ACM.
23. Renault, S., et al., A Pattern-based Method for building Requirements Documents in Call-for-tender Processes. International journal of computer science & applications, 2009. **6**(5): p. 175-202.
24. Palomares Bonache, C., et al., A catalogue of non-technical requirement patterns. 2012.
25. Pohl, K., G. Böckle, and F.J. van Der Linden, Software product line engineering: foundations, principles and techniques. 2005: Springer Science & Business Media.
26. Basilici, V.R., F. Shull, and F. Lanubile, Building knowledge through families of experiments. IEEE Transactions on Software Engineering, 1999. **25**(4): p. 456-473.
27. Koziolek, H., Goal, question, metric, in Dependability metrics. 2008, Springer. p. 39-42.
28. Bukhari, Z., J. Yahaya, and A. Deraman, A Conceptual Framework for Metrics Selection: SMeS. International Journal on Advanced Science, Engineering and Information Technology, 2018. **8**(6): p. 2294-2300.
29. Creswell, J.W., Educational research: planning. Conducting, and Evaluating. 2012.
30. Creswell, J.W., Research Design: Qualitative, Quantitative, and Mixed Methods Approaches. Canadian Journal of University Continuing Education, 2009. **35**(2).
31. Oates, B.J., Researching Information Systems and Computing. 2006: SAGE.
32. Maxwell, J.A., Qualitative research design: An interactive approach. Vol. 41. 2012: Sage publications.
33. Onwuegbuzie, A.J. and N.L. Leech, Validity and qualitative research: An oxymoron? Quality & Quantity, 2007. **41**(2): p. 233-249.



# A Multi-Layer Perceptron Model in Analyzing Parametric Classification of Students' Assessment Results in K12

Arman Bernard G. Santos<sup>1</sup>, Bryan G. Dadiz<sup>2</sup>, Jerome L. Liwanag<sup>3</sup>, Mari-Pearl M. Valdez<sup>3</sup>, Myen DC. Dela Cruz<sup>3</sup>, Rhommel S. Avinante<sup>4</sup>

<sup>1</sup>Asiatech-Sta. Rosa, City of Sta. Rosa, Laguna Philippines

<sup>2</sup>Technological Institute of the Philippines-Manila, Philippines

<sup>3</sup>Virgen Milagrosa University Foundation, Pangasinan, Philippines

<sup>4</sup>Cavite State University, Indang Campus, Philippines

armie\_santos@yahoo.com, bgdadiz@yahoo.com

**Abstract.** This paper focuses on assessment results based on the analysis of parametric classification with the support of the multi-layer perceptron (MLP) model. MLP is the most effective tool or model to assess and evaluate training sets, such as the score of each student, exam results, and the like. Domains are evaluated as to know the career pathing of students in the different categorical aspects. Indispensable to each categorical response are the results of the completed curriculum under the K12 educational approach. Career assessment should be administered to classify students in the different categorical domains namely: arts and design, business, information and communication technology, criminal justice and law, culinary arts, education, engineering and architecture, health care, liberal arts, math and science, and vocational respectively. MLP model has been implemented to assess students' scores and compare them to what specific categorical domain do they belong. The three main components of MLP as the computational model are the input layer, hidden layer, and the output layer. Employment of MLP in a supervised learning problem helps to pair all the training sets of input and output to train the dependence between them. This paper gives the reader the results of parametric training through associating MLP in all training datasets and the 87% accuracy results being garnered to sustain relevant parametric results.

**Keywords:** Neural Networks, Feedforward, Backpropagation, Multilayer Perceptron

## 1 Introduction

Many challenges in information age lie within the boundary of computational theory ranging from classification of objects and datasets down to giving results that entails possible solutions to each specific problem. This thrust paves the way to employ number crunching algorithms that is nearly fitting to address the concern of both mathematical and scientific explanation around the corner. One of the most useful algorithms

used to evaluate the scores in a series of test or exam administered in both academic and industry is the Multi-Layer Perceptron (MLP).

A multilayer perceptron is one of a deep learning algorithm that uses subjective numbers of hidden layers to decide or prediction. The node or the input layer obtains signals then pass through several hidden layers to come up with the accurate prediction or output. MLP learns the correlation between the set of input-output pairs and trains the parameters by adjusting the weight and biases to lessen the error. MLP uses back-propagation to make weight and bias adjustments relative to the error [1]. Some researches utilized MLP as baseline classifiers for machine learning tasks [2]-[3].

With the use of MLP, datasets can easily interpret as to analyze students' assessment results in terms of scores attained in each specific category and to give results on what domain does a student can rely on. The domains are categorized into arts and design, business, information and communication technology, criminal justice and law, culinary arts, education, engineering and architecture, health care, liberal arts, math and science, and vocational. The student in choosing his or her career shortly while currently moving forward to complete his or her K12 educational curriculum can consider different categorical domains. The MLP, on the other hand, will display and evaluate what three categorical domains that are very appropriate to choose by the student based on his or her scores attained in all career assessment categories.

Students from K12 basic education nowadays have encountered some confusion on what they are going to take in college. Some of these constraints rely on the influence of their parents or even their friends who held responsible for their personal decision. As results, students who follow courteously to those influential factors had confusingly mismatched their skills when they went to college. This problem has enlightened the researchers to create an MLP model involving the parametric classification of the results of student's scores in career exam. In parametric classification process, student's scores will be treated as raw data in the input layer followed by the hidden layer in which all the categorical domains such as arts and design, business, etc. will be then turned into a classifier. Classifiers in parametric classification are models of data with the categorical response that is built from training data (input layer) to which classifications are known. Finally, a parametric method known as Discriminant Analysis Classification will fit a parametric model to the training data and interpolate to classify test data. DAC is an approach to get the three nearest categorical domains in all listed categories.

## 2 Related Literature and Studies

Singh and Sachan emphasized the use of multilayer perceptron (MLP) on their work in machine vision. Their research paper aims to reduce the error from digitizing the handwritten or printed text from scanned images. One of the major difficulties is the irregularity of writing styles and size of the symbols. They used the MLP technique for recognizing Gurmukhi characters. Their method analyzes the symbols by training using feed-forward topology and using MLP neural network; researchers achieve the 98.96% for the proposed system in recognizing symbols [4].

Varmuza states that parametric classification is one of the categories of pattern recognition. A parametric method requires the fundamental knowledge of statistical classification problem. Selecting the most probable class in an unknown pattern helps to identify the optimum classification represented by each d-dimensional pattern space. Classification problem, on the other hand, can be made possible through estimation of training sets even if it is at large. Performing statistical boundary in each training sets helps to show exact measurement, which in turns give less optimum classification [5].

Maham Jahangir stated on his research the importance of detecting diabetes at an early stage and to prevent a possibly serious complication. Together with his co-researcher, they team up with the group medical experts to make a system that is accurate and useful in real life. They emphasized the use of multi-layer perceptron; a machine learning algorithm for precise prediction. The combination of automatic multilayer perceptron (Auro MLP) and Outlier detection method Enhanced Class Outlier Detection using distance-based algorithm to create a novel prediction framework [6].

Heazlewood and Keshishian, 2010 utilized perceptron neural systems in conjunction with the discriminant investigation to recognize the factors that describe karate competitors into high and low execution gatherings. Their investigation uncovered that both perceptron neural systems and discriminant work examination yielded a high level of exactness in classifying karate competitors into high and low execution gatherings. The creators of the present examination endeavored to reproduce Heazlewood and Keshishian's (2010) think about and apply both neural systems and discriminant work investigation to Huynh and Bedford's (2010) SATB program. Researchers used a visual based strategy to analyze skill among cricket players by evaluating verbal separation when looked with five changed kinds of knocking down some pin's conveyances. They demonstrated that master hitters were more effective than tenderfoots in distinguishing distinctive sorts of conveyances made by a specialist wrist-turn bowler. The general identification rates in this examination were fundamentally unique between national, local, and club cricket players. National players accurately distinguished 63% of conveyances, local players recognized 56%, and club players effectively distinguished 48% of general conveyances. In any case, while looking at this separation ability for kinds of conveyance, the creators found that hitters were less ready to segregate conveyances that were comparable, paying little respect to aptitude. Renshaw and Fairweather, 2000 clarified this poor separation capacity because of the conveyances that were comparative to the leg spin conveyance (i.e., topspin and reverse-pivot). Correspondingly in badminton, the wide range of shot sorts utilized have comparable appearances in execution and may for the most part just be separated amid the last couple of milliseconds preceding the racket reaching the bus [7].

Hecht-Nielsen [8] examines the likelihood of a 3-layer perceptron approximating self-assertive capacities, given proper squashing capacities at the neurons. He constructs this outcome concerning work by Kolmogorov, which expressed that any capacity could be precisely demonstrated by a multilayer organize. Kolmogorov's outcome was prefaced on suitable exchange capacities, not the same, and furthermore not smooth-at the hubs of the system. Hecht-Nielsen's investigation was discussed by Girosi and Poggio [9]. Funahashi [10] demonstrates that the multilayer perceptron

permits estimation of any persistent mapping. Hornik et al. find for 3-layer systems for approximating self-assertive Borel-quantifiable capacities, gave adequate shrouded layer neurons are available [11].

### 3 Experiments and Methodologies

This section aims to test a model for predicting the parametric classification of students' assessment in K12 on the multilayer perceptron (MLP). For modeling in this research, after conducting the experimental tests, a set of data including 1980 experimental tests on sample grades from K12 students are collected, among which 1386 train samples (70%) are selected as training data and the rest, 594 data, (30%) are selected as the test data. Additionally, three main parameters, such as general scholastic aptitude, technical vocational aptitude, and K12 courses, were used as a feature vector. These include, (SA) Scientific ability, (RC) Reading comprehension, (VA) Verbal ability, (MA) Mathematical ability, (SC) Social sciences, (CA) Clerical ability, (AG) Agriculture, (MA) Manipulative skills, (MC) Maritime criminology, (NA) Non-verbal ability, (ES) Entrepreneurial skill, (AD) Arts and Design, (BS) Business , (ICT) Information and communication technology, (CJL) Criminal Justice and Law, (CA) Culinary Arts, (ED) Education, (EA) Engineering and Architecture, (HC)Health Care, (LA) Liberal Arts, (MS) Math and Science. The target class consists of (BP) Business program, (EP) Educational Program, (ITP) Information Technology Program, (ENP) Engineering Program, and (HMP) hospitality management program. Considering the number of input data and output layers, the numbers of input and output neurons are  $N_0=1$  and  $N_j=4$ , respectively. For the neurons in the hidden layer, different experimental relations are provided based on Masters [12].

#### 3.1 Multi-Layer Perceptron

In an MLP, perceptron can compute for a single value resulting from a few inputs derived from learning weight. MLP is expressed in Figure 1. The artificial neural network-based approach MLP targets to classify the five types of parametric assessment for K12 students in the Philippines the input features are the cluster from the General Scholastic Aptitude scores, the Technical Vocational Aptitude scores, and the K12 courses scores. A Multilayer Perceptron (MLP) is a class of feed-forward artificial neural network; this model maps on a set of input data onto a set of suitable output. It acts as a directed graph, with the overall layer fully connected to the next node. Each node is a neuron, also known as the processing element that includes a nonlinear activation function [13]. The MLP architecture uses backpropagation or short for backpropagation of errors for training the network; backpropagation uses gradient descent, which produces gradient of the error functions concerning the weights of the neural network. This class of

networks is composed of multiple layers, usually reticular in a feed-forward style of a graph. In most cases, the units of these networks utilize a sigmoid activation function.

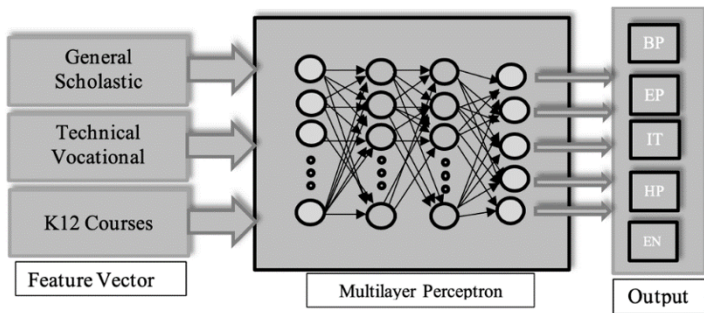


**Fig. 1.** Multilayer Perceptron Model

The artificial neural network-based approach MLP targets to classify the five types of parametric assessment for K12 students in the Philippines the input features are the cluster from the General Scholastic Aptitude scores, the Technical Vocational Aptitude scores, and the K12 courses scores. A Multilayer Perceptron (MLP) is a class of feed-forward artificial neural network; this model maps on a set of input data onto a set of suitable output. It acts as a directed graph, with the overall layer fully connected to the next node. Each node is a neuron, also known as the processing element that includes a nonlinear activation function [13]. The MLP architecture uses backpropagation or short for backpropagation of errors for training the network; backpropagation uses gradient descent, which produces gradient of the error functions concerning the weights of the neural network. This class of networks is composed of multiple layers, usually reticular in a feed-forward style of a graph. In most cases, the units of these networks utilize a sigmoid activation function.

**Back Propagation.** Run the network forward with your input data for each output node

$$\delta_k = \mathcal{O}_k (1 - \mathcal{O}_k) (\mathcal{O}_k - t_k) \quad (1)$$

for each hidden node calculate

$$\delta_j = \mathcal{O}_j (1 - \mathcal{O}_j) \sum_{k \in \text{outputs}} \delta_k W_{jk} \quad (2)$$

Update the weights and biases as follows

Given

$$\Delta W = -\eta \delta_\ell \mathcal{O}_{\ell-1} \quad (3)$$

$$\Delta \theta = \eta \delta_\ell$$

Apply

$$W + \Delta W \rightarrow W$$

$$\theta + \Delta \theta \rightarrow \theta$$

The study has considered the below termination conditions in MLP classifier:

1. The constant count of iterations.
2. When the Error falls, or the tolerance of the optimization has reached.
3. Error on a separate validation set falls below some threshold.

The value of the MLP weights is improved using a learning rule applied over a training set T on the given criterion function. The back-propagation on equation (3) is a supervised machine learning method which is applied to train the connected feedforward network that has two parts: (1)(2) propagating the activation from the input going to the output layer. The summation of all weighted inputs along with the computing outputs are propagated using a sigmoid threshold, and (3) The backward style of propagating the error between the actual observed together with the requested nominal value from the output layer that will modify the weights of nodes on the hidden layers and bias nodes (3) [14]. The errors are propagated backward by apportioning them to each unit according to the amount of the responsible unit. The weights of the network are modified going towards decreasing the square error of the output layer. Then the weight is updated for each position of the matrices, respectively. With a small random value within (-0.1, 0.1) interval is the starting weight then training will be ended when either the error reduced to less than 0.0001 or the training epochs reach up to 200. On each epoch, the training samples set are fed in random, alternating orders.

**Algorithm tuning and training.** We have trained our MLP using 26 different features from K12 assessment scores, with a five-classification dataset of 70:30 split ratio rule was applied to fetch the data for training, validation, and testing phase, which uses 70% of the student K12 scores for training and 30% for both testing and validation. Parameters are essential in machine learning algorithms. The influence of parameters is salient to the outcome of the training part. Thus, it is important that parameter tuning is examined by variating hidden layers and nodes to improve the prediction or accuracy of the exemplar [15].

Moreover, in this study it analyzes the use of some techniques to normalize the input variables to achieve these conditions 1) The mean should be zero value or minimal as the variance by comparison 2) uncorrelated 3) same variance. On this MLP analysis, it utilizes the small randomized weights to avoid diminishing the neurons. The Hidden-to-Output (HO) and Input-to-Hidden (IH) weights were customized with different configurations. The degrees of freedom are determined by the number of hidden nodes or the model's expressive power; this study experimented on different hidden neuron nodes within each hidden layer of different proposed MLP configurations [16]. For updating the weights during training uses batch training, the batch training analysis uses the true steepest descent direction with a minimum of 200 samples. Below is the summary of parameters tuned to attain the accuracy of the constructed multilayer perceptron classifier.

**Table 1.** Network parameters MLP parameters used in our analysis.

Parameters	Values/techniques used to improve MLP performance
------------	---

Activation Function	ReLU
No. of Hidden Neurons	MLP(12-8/32-32/64-64/128-128)
No. of Hidden Layers	2
Maximum Epochs	200
Error Function	MSE
Learning Rate	0.0001
Weight Updates	Mini-batch

**Performance Measures.** The MSE provides the information about the fitness of the regression line. The minimal the Mean Squared Error value, the better the fitness, it implies smaller magnitudes of error. As an example, consider the hypothetical example where every data point is in the exact regression line. This would result in residual errors of 0 for most of all the points.

*MSE (Mean Square Error).* The formula for the mean square error is:

$$MSE = \frac{1}{n} \sum_{i=0}^n (Y_i - \hat{Y}_i)^2 \quad (4)$$

Where,

$n$  this represents the number of data points

$Y_i$  this represents the observed values

$\hat{Y}_i$  this represents the predicted values

*Receiver operating characteristics (ROC).* The ideal classifier can be determined by the ROC evaluator to be examined by the user to understand the model in terms of the trade-offs between sensitivity and specificity (probability threshold). The area under the ROC curve range from 0.5 for a chance to 1.0 for the significant model.

*Classification accuracy (% Correct).* The percentage of the correct predictions also known as accuracy measure is the area covered to which the classifier or model correctly predicts the instance of unlabeled data and is summarized in the form of a table called confusion matrix. In all parts, accuracy is defined as the mean of the correctly presented diagonal part of the confusion matrix [17].

## 4 Results and Discussion

The information of the accuracies acquired with regards to this study from the K12 dataset on different multi-layer perceptron (MLP) was shown below in Table 2. The experiment on this study utilizes the ReLU activation functions on input layers and the functions of the hidden layers, and the sigmoid function is utilized for the last layer of neurons or the output layer. Table 2 shows a list of the results obtained by making ten runs in each model with 200 epochs compared in Table 1. The following table is followed by the presented graph of accuracies from Table 2 performance table that is

obtained. Noticeably, as shown in Figure 2, the nodes of the hidden layer when increased in number resulted in notable increase with its accuracy on the parametric classification of K12 students.

**Table 2.** Comparison Performance of the three different MLP networks

S. No.	Performance of the three different MLP config							
	26-12-8-5		26-32-32-5		26-64-64-5		26-128-128-5	
	A(%)	MSE	A(%)	MSE	A(%)	MSE	A(%)	MSE
1	77.99	0.23	82.34	0.17	82.81	0.17	87.89	0.11
2	78.78	0.22	82.16	0.18	83.33	0.18	87.11	0.13
3	79.69	0.2	84.22	0.16	84.77	0.15	86.33	0.14
4	78.76	0.23	83.2	0.16	85.29	0.14	86.46	0.14
5	78.91	0.22	82.16	0.17	84.38	0.17	84.77	0.15
6	79.43	0.21	83.2	0.17	85.29	0.14	88.13	0.11
7	80.47	0.19	83.02	0.16	84.51	0.15	86.87	0.14
8	79.05	0.21	82.91	0.17	83.46	0.17	87.34	0.13
9	78.91	0.22	84.01	0.14	85.78	0.14	86.78	0.13
10	80.02	0.19	82.15	0.17	84.78	0.15	87.67	0.12
Ave.	79.20	0.21	82.93	0.16	84.44	0.156	86.93	0.13

On Table 2. The results from this study experiments using the four MLP configuration are as follows: The first configuration is 26-12-8-5, the multilayer perceptron indicating twenty-six nodes for the input layer, twelve and the hidden layers adding eight nodes and five nodes for the output layer. Likewise, three remaining MLP perceptron designs with the additional nodes for the hidden layer as 26-32-32-5, 26-64-64-5, and 26-128-128-5.

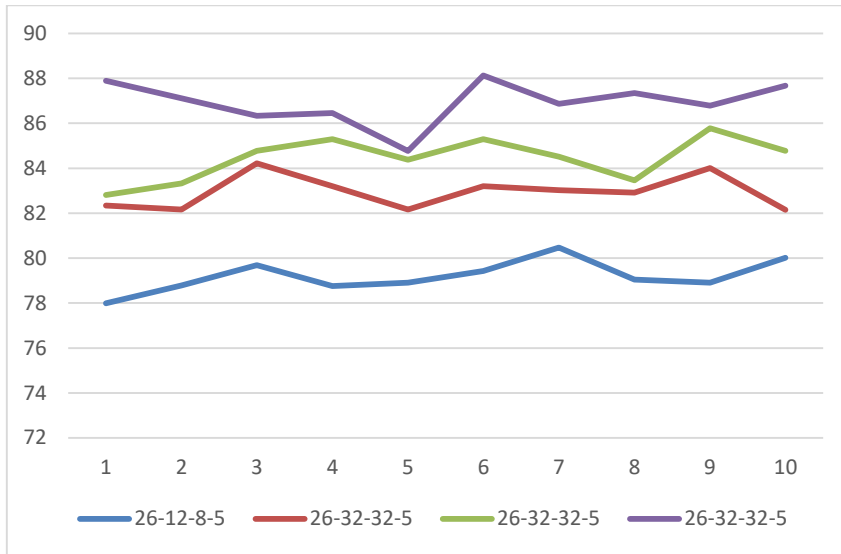


**Fig. 2.** Accuracies of the four MLP configurations.

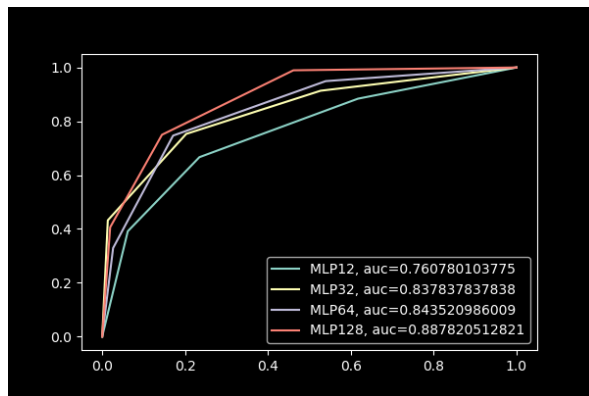


**Fig. 3.** The ROC curve of the of MLP models

Figure 2 presents the differentiation of the networks. The colors separate each MLP configuration. In Figure 3. Shows the Receiver operating characteristics (ROC) visualization. The graph shows MLP12, MLP32, MLP64, and MLP128 the models of the four different MLP configurations. This only means that MLP12 uses 12-8 nodes for the hidden layer and MLP32 uses 32-32 for two hidden layers and as well as the other two models. Moreover, it is evident that the model with configuration MLP128 shows promising results that by adding more hidden nodes makes the accuracy more desirable.

## 5 Conclusions

The researchers had finally drawn a conclusion based on the series of computations and a review from different prior published researches. This study showcased the differences of each multilayer perceptron network applied to the K12 dataset. The parametric classification of the student after senior high. Based on Table 2 from the section of results and discussion by observing the design models, it showed a great increase of accuracy by incrementing the number of nodes with the hidden layer of the MLP classifier. On this paper's finding, this work can be further optimized to arrive an accuracy of more than 87 %. Parametric classification of student can be accurately suggested with machine learning using MLP classifier. Multi-layer perceptron, as part of the artificial neural network, is being utilized for the purpose of identifying the prediction of each record or datasets with the known actual record. This research paper concluded that using MLP; researchers find light in identifying the predicted program which the students can take when they go to college. The predicted value represented by a dataset (binarized form) from the actual data were produced accurately. MLP requires the desired response to be trained based on the actual datasets given. It is concluded that MLP is effective in pattern classification because of its capability to transform datasets or input data into the most accurate and desired results. MLP layers including the input layer, hidden layer, and output layer can approximately yield desired results to solve the real problems like pattern matching, the approximation of desired results, and classify datasets according to its proper statistical results.

## References

1. DeepLearnting4J. 2017. A Beginner's Guide To Multi-Layer Perceptrons. Retrieved from <https://deeplearning4j.org/multilayerperceptron>. Copyright © 2017. Skymind. DL4J is licensed Apache 2.0.
2. Prospero, M. R., Lagamayo, E. B., Tumulak, A. C. L., Santos, A. B. G., & Dadiz, B. G. (2018, June). Skybiometry and AffectNet on Facial Emotion Recognition Using Supervised Machine Learning Algorithms. In *Proceedings of the 2018 International Conference on Control and Computer Vision* (pp. 18-22). ACM.
3. Sarmiento, A. L., Aviñante, R. R., Liwanag, J. L., & Dadiz, B. G. (2018, June). Dimension Reduction Techniques Analysis on Image Processing for Facial Emotion Recognition. In *Proceedings of the 2018 International Conference on Control and Computer Vision* (pp. 23-27). ACM.
4. Gurpreet Singh and Manoj Sachan. 2018. Multi-layer perceptron (MLP) neural network technique for offline handwritten Gurmukhi character recognition. <https://ieeexplore.ieee.org/document/7238334/authors>
5. Varmuza, Kurt. 2015. Parametric Classification Method. ISBN 978-3-642-93155-0\_5. K. Varmuza, Pattern Recognition in Chemistry © Springer-Verlag Berlin Heidelberg 2015. Retrieved from [https://link.springer.com/chapter/10.1007/978-3-642-93155-0\\_5](https://link.springer.com/chapter/10.1007/978-3-642-93155-0_5)
6. Jahangir, Maham. 2015. An expert system for diabetes prediction using auto tuned multi-layer perceptron. Department of Computer Science, University of Management & Technology, Sialkot, Pakistan. Retrieved from <https://ieeexplore.ieee.org/document/8324209/>

7. Heazlewood I.T. Keshishian H. (2010) A comparison of classification accuracy for karate ability using neural networks and discriminant function analysis based on physiological and biomechanical measures of karate athletes. In: Proceedings of the 10th Australian Conference of Mathematics in Sport, July 5-7, Darwin, Australia: 197-204.
8. Hecht-Nielsen, R. (1987, June). Kolmogorov's mapping neural network existence theorem. In Proceedings of the international conference on Neural Networks (Vol. 3, pp. 11-14). IEEE Press New York.
9. Girosi, F., & Poggio, T. (1989). Representation properties of networks: Kolmogorov's theorem is irrelevant. *Neural Computation*, 1(4), 465-469.
10. Funahashi, K. I. (1989). On the approximate realization of continuous mappings by neural networks. *Neural networks*, 2(3), 183-192.
11. Hornik, K., Stinchcombe, M., & White, H. (1989). Multilayer feedforward networks are universal approximators. *Neural networks*, 2(5), 359-366.
12. Masters, T., and M. Schwartz. "Practical neural network recipes in C." *IEEE Transactions on Neural Networks* 5, no. 5 (1994): 853-853.
13. RapidMiner Technical Support Available from: <http://docs.rapidminer.com/>
14. Bordoloi H, Sarma KK. Protein structure prediction using multiple artificial neural network classifiers. *Comp Tech Vision Sci Computational Intellig* 2012; 395: 137-146.
15. A.Deka, H.Bordoloi and K. K. Sarma, "ANN-aided Tertiary Protein Structure Prediction using Certain Coding Techniques and Known Secondary Structures", in Proceedings of International Conference on Electronics and Communication Engineering(ECE), 2012.
16. Mikaeil, Reza, Sina Shaffiee Haghshenas, Yilmaz Ozcelik, and Sami Shaffiee Haghshenas. "Development of Intelligent Systems to Predict Diamond Wire Saw Performance." *Soft Computing in Civil Engineering* 1, no. 2 (2017): 52 -69. DOI: 10.22115/SCCE.2017.49092.
17. Principe J.C., Euliano N.R, Neural and Adaptive Systems, John Wiley and Sons, 2000.



# Redefining the White-Box of k-Nearest Neighbor Support Vector Machine for Better Classification

Doreen Ying Ying Sim

Faculty of Cognitive Sciences and Human Development, University Malaysia Sarawak, Jalan  
Datuk Mohammad Musa, 94300 Kota Samarahan, Kuching, Malaysia  
[dsdoreenyy@gmail.com](mailto:dsdoreenyy@gmail.com)

**Abstract.** Distances and similarities among patterns of data points are computed by k-Nearest Neighbor methods after Principal Component Analysis is performed to the ten datasets. Weighted distances are then formulated, computed and adjusted synergistically with the Gaussian kernel width of Support Vector Machine. This is done by the proposed formulations of this research which is derived from the study on the relationships among the distances and similarities of patterns of data points as well as the kernel width of SVM. The kernel scale of Gaussian kernel width is customized and categorized by the proposed new approach. All these are known as the white-box algorithms which are to be redefined. The algorithm developed is to avoid and minimize the tradeoff and hinge loss problems of typical SVM classifications. After applying the proposed algorithms to the datasets mainly from UCI data repositories, it is shown to be more accurate in classification when compared with typical SVM classification without getting the Gaussian kernel width adjusted accordingly. Optimal kernel width from the customized kernel scale is input to the SVM classification after being computed by the proposed formulations. It is found that dimensionality reduction by PCA and distances among patterns computed by kNN and thereafter by the proposed formulations can optimally adjust the Gaussian kernel width of SVM so that classification accuracies can significantly be improved.

**Keywords:** k-Nearest Neighbor, Principal Component Analysis, Gaussian kernel width, Support Vector Machine, proposed formulations.

## 1 Introduction

### 1.1 Classical White-Box Algorithms of SVM and PCA

Support vector machine (SVM) is a stable and strong classifier [4]–[5], [9]–[12] and a supervised learning method for its classification and regression strength, while Principal Component Analysis (PCA) and k-Nearest Neighbor (kNN) are unsupervised methods. PCA is a type of dimensionality reduction techniques [1]–[3], [10]–[12] used to tune and monitor the white-box algorithms of SVM in this research. Both SVM and PCA are very popular machine learning algorithms [6]–[8], [10]–[12]. When data is visually and/or logically not easily separable, data might not be easily separated by any hard-margin, SVM usually uses a soft-margin to separate data.

## 1.2 Problem Background leading to the initiation to form kNNSVM

The biggest problem of SVM lies in the choice of its kernel, its speed during training and testing phases, as well as several key parameters that have to be set correctly in order to achieve the best generalization performance. SVM uses a hyper-plane that separates many data points, but not all data points. For SVM, misclassifications are always allowed, but at the cost of a penalty factor  $C$  [4], [9]–[12], which in this research, is fixed to have a value of 1. Hinge loss function in SVM is used for maximum margin classification [10]. SVM was developed from the theory of Structural Risk Minimization by Vapnik [4], but its classification strength decreases when the data are of much higher dimensionality [1]–[3], [5], [9]–[12]. When classifying data using SVM, its typical problems are proposed to be solved through reducing its dimension by using PCA and kNN. This is to provide a representative view on the data [5], [9]–[12]. White-box algorithms of SVM are redefined and preprocessed through the proposed new formulations after PCA and kNN are applied to the SVM classification. The proposed algorithms developed is k-Nearest Neighbor Support Vector Machine (kNNSVM) algorithms.

Weaknesses of PCA and kNN are that they are simple and powerful techniques which can be used for optimal dimensionality reduction [6]–[8], but unlike SVM, they are not sophisticated, strong and stable classifiers [10]–[12]. By using PCA-based kNN, we can reduce the number of feature variables, but concentrating on just the principal features and thus saving on the computational training time and complexity of SVM model [1]–[3], [10]–[12]. SVM is a class of algorithms which is used in many machine learning fields, so as in the kernel PCA [1]–[3]. To solve the general problem background, PCA-based kNN in this research uses a metric to measure the similarity within patterns or distance between patterns [1]–[3]. Typical SVM uses inner product (Equation (1)) as a metric. PCA does not primarily eliminate redundant features but it creates a new set of principal components [9]–[12]. PCA in this research is based on 95% confidence interval on the data.

## 2 Preliminary and Redefinitions

### 2.1 Research Assumptions and Hypotheses

A classical kernel-based SVM has a standard Gaussian kernel width which in general, is always automatically fixed or indefinite in its numerical value [2]–[4]. In addition, the box-constraint or penalty cost of SVM, i.e.  $C$ , as the regularization parameter which controls the slack variables,  $\xi$ , of SVM (see Equation (1)), can exert either stricter or more lenient separation of the hyper-plane in primal form [1]–[4].

$$\begin{aligned} \min_{w,b,\xi} \quad & \frac{1}{2} \|w\|^2 + C \sum_{i=1}^m \xi_i \\ \text{s. t.} \quad & y_i(w^T X_i + b) \geq 1 - \xi_i \quad i = 1, \dots, m, \quad \xi_i \geq 0 \end{aligned} \quad (1)$$

where  $y_i$  is the sign of hyper-plane that is shown by equation of ( $w^T X_i + b = 0$ ),  $w$  is the input vector, and  $m$  is the maximum number of elements in the class assigned.

Equation (2) shows the above SVM minimization problems to be re-written as optimization in maximizing the soft-margin SVM kernel functions in dual form [1]-[4]. All  $\alpha$  and  $y$  shown are the Lagrange multipliers and variables related to the constraints shown in Equation (1). In the kernel, denoted as  $K$ , the symbol of  $X_i$  indicates input vectors, and the symbol of  $X_s$  indicates training samples.

$$\begin{aligned} \max_{\alpha} & \sum_{i=1}^m \alpha_i - \frac{1}{2} \sum_{i,s=1}^m \alpha_i \alpha_s y_i y_s K(X_i, X_s) \\ \text{s. t. } & \sum_{i=1}^m \alpha_i y_i = 0, \quad 0 \leq \alpha_i \leq C, \quad i = 1, \dots, m \end{aligned} \quad (2)$$

1) **Research Assumptions:** Based on Equation (1) above, this research assumes that at a fixed value of 1.00, the box-constraint, i.e.  $C$ , of SVM, using PCA for optimal dimensionality reduction which is then computed accordingly by kNN and the proposed formulations of this research to adjust the Gaussian RBF kernel width of the SVM has the same pursuit as does modifying the kernel value of SVM.

2) **Research Hypothesis:** This research hypothesizes that by working out the relationships among distances in the patterns of the training samples and input vectors before input to typical SVM classification can optimally figure out Gaussian RBF kernel width which can minimize the trade-off of SVM. As such, SVM classification accuracies can significantly be improved.

## 2.2 Research Questions

The two main research questions to be researched upon are elaborated as below.

The first **RESEARCH QUESTION (RQ1)** is that to find out the correct values derived from the feature space on the distance or similarity between patterns input in a metric format by kNN that can match SVM Gaussian kernel width parameter,  $\sigma$ . This is to ensure that datasets that have been pre-processed by PCA and kNN can be optimally matched with  $\sigma$  so that classification accuracy of SVM can be improved.

The second **RESEARCH QUESTION (RQ2)** is that for each dataset applied, to reduce the trade-off loss caused by over-fitting and under-fitting, this research wishes to find out and compute the right Gaussian kernel width of SVM (in kernel scale redefined in customized fashion by this research) that can tweak and work synergistically with the weighted distance or similarity between patterns which is computed by the PCA and kNN so that SVM classification can significantly be improved.

## 2.3 Determination of the Kernel Width and Redefinitions of the Density Index

Throughout this paper, the redefinitions on the white-box algorithms are based mainly on 3 criteria. (I) The **FIRST REDEFINITION (1)** is on the standard PCA dimensionality reduction techniques which the scores from the covariance matrices as well as the principal components selected and computed by PCA are redefined as weighted distances. These weighted distances are between patterns by kNN before input to SVM classifier. In addition, to avoid bias after pre-processing by PCA but before kNN methods, a fixed number of nearest neighbors, i.e.  $k=10$ , (i.e. a fixed number of nearest neighbors for kNN) is used while applying the proposed formulations of this research to the datasets. Then, difference in weighted distances (denoted as  $d$ ) are computed based

on the average distance derived from the distances between the nearest neighbors of the patterns (denoted as  $pt$ ) after kNN method is applied to the datasets before SVM classification. The equation is denoted as  $den\_knn(\mathbf{x})$  and it is an index of density in the  $\mathbf{x}$ 's neighborhood (Eq.3). Eq.(4) (denoted as  $avg\_knn(\mathbf{x})$ ) calculates customized average index of density over the number of patterns (denoted by  $pn$ ).

$$den\_knn(\mathbf{x}) = \frac{1}{pt} \sum_i k(\mathbf{x}, \mathbf{x}_i), \quad \mathbf{x}_i \in \text{training samples or sets} \quad (3)$$

$$avg\_knn(\mathbf{x}) = \frac{1}{pn} \sum_i k(\mathbf{x}, \mathbf{x}_i), \quad \mathbf{x}_i \in \text{training samples or sets} \quad (4)$$

(II) **Determination of the range for the kernel width**, i.e. the second **REDEFINITION (2)** which is on the SVM Gaussian (mainly RBF) kernel width itself. A customized range of kernel width sizes will be built as benchmarks to the ‘automatic kernel width mode’ of a typical SVM classifier which is usually indefinite and undefined. These are redefined into THREE (3) categories of fine, medium and coarse. These 3 categories are based on the kernel scale ranges, but how to determine them? Kernel width is for range 0.01-1.00 (i.e. maximum is  $2^0$ ); medium is for range 1.01-4.00 (i.e. maximum is  $2^2$ ); and coarse is for range 4.01-10.00 (i.e. maximum is  $2^{3+2}=8+2=10$ ). Table 3 shows exact ranges of these 3 categories of  $\sigma$  or  $\sigma'$ .

(III) The third **REDEFINITION (3)** is based on the ‘**determination of the range for the kernel width**’ stated in (II) above. This redefinition is on the power of the multiples derived (such as a multiple of 2, or a multiple of 3, or etc.), i.e.  $q$ , to adjust the new kernel width  $\sigma'$ , from the difference,  $d$ , of the weighted distances before and after the dimensionality reduction by PCA and kNN methods. The power variable of  $q = 0$  applied to the  $d$  ranges from 0-0.19;  $q = 1$  to the  $d$  ranges from 0.20-0.39;  $q = 2$  to the  $d$  ranges from 0.40-0.79; and  $q = 3$  to the  $d$  ranges from 0.80-1.59.

**Determination of the Kernel Width Range and Redefinitions.** The above redefinitions are to be set as customized benchmarks so that while adjusting SVM kernel trick,  $\sigma$ , can be monitored accordingly so as to justify the matching distances between input vectors and training samples as pre-processed by kNN and PCA.

### 3 Proposed New Approaches and Formulations

#### 3.1 State-Of-The-Art Descriptions and the New Approaches

In Equation (6), the kernel scale parameter, which is called ‘lambda’, denoted as  $\lambda$  is related to how spread out, i.e. density, are the data points in the datasets. Equation (5) below shows the relationship between the kernel width and the kernel function mainly for RBF (Radial Basis Function) Gaussian kernel. If lambda is large, the kernel will fall off rapidly as the data points of input vectors,  $X_i$ , move away from training samples,  $X_s$ . If lambda is significantly reduced, the kernel will fall off slower but may need more computation time [1]–[3], [9]–[11]. Since PCA is applied to pre-process the data points by reducing the number of features and overall dimensionality, less computation needed, the values of lambda computed will be significantly smaller than those without getting

pre-processing done by PCA and kNN. Among various SVM kernels, this research uses mainly Gaussian RBF kernel, shown in Eq. (5) below [1]-[4].

$$K(X_i, X_s) = \exp\left(-\frac{\|X_i - X_s\|^2}{2\sigma^2}\right) \quad (5)$$

From Eq.(5) to Eq.(6),  $\lambda$  is inversely related to kernel functions. Since lambda will be smaller after the dimensionality reduction done by PCA and the nearest neighborhood among patterns monitored by kNN method, from inverse relationship as stated, the adjusted kernel width  $\sigma'$  will be significantly wider than the unadjusted kernel width  $\sigma$ . The index of density intensity of the data points depends on each different dataset implemented with the *k*NN method. The  $\lambda$  in Eq. (6) is the variable to be inserted with the proposed formulations so that kernel width can be adjusted.

$$K(X_i, X_s) = \exp\left(-\lambda\|X_i - X_s\|^2\right) \quad (6)$$

From Equation (5), the unadjusted,  $\sigma$ , or adjusted,  $\sigma'$ , kernel width can adapt feature space distribution. In Eq.(5) and Eq.(6), we can see that the kernel width,  $\sigma$ , is inversely related to the square root of the weighted distance,  $d$ , between patterns as well as between input vectors and training sample. Equations (7) and (8) show the relationships between the weighted distances among patterns and adjusted kernel width as well as proposed formulations of this research.

$$d = \|\Phi(x) - \Phi(y)\|^2 = \frac{2^{2q}}{\sigma'^2} \quad (7)$$

$$\sqrt{d} = \|\Phi(x) - \Phi(y)\| = \frac{2^{2q/2}}{\sigma'^{2/2}} = \frac{2^q}{\sigma'} \quad (8)$$

Substitute Eq.(8) into Eq.(5) above, replacing  $\sigma$  with  $\sigma'$ , we obtain Equation (9).

$$K(X_i, X_s) = \exp\left(-\frac{\|X_i - X_s\|^2}{2\left(\frac{2^q}{\sqrt{d}}\right)^2}\right) \quad (9)$$

Since the SVM classification used in this research is mainly for binary but not multiclass classification, this research proposes the adjusted kernel width will be increased by the multiples of 2, i.e. 2 to the power of the redefined and weighted distances among the patterns of data points pre-processed by PCA and kNN. For above,  $\|\Phi(x) - \Phi(y)\|$  in Eq.(7) and (8) are the weighted distances between patterns. From Eq.(7) to Eq.(10),  $q$  is the weighted difference in the customized index of weighted distances (as stated in REDEFINITION (3)) before and after PCA and kNN methods

during the implementation of kNN SVM algorithms.  $d$  is the weighted distance formulated from the customized index of density,  $avg\_knn'$ , as denoted in Eq.(4) above.

### 3.2 Proposed Formulations for Adjusted Kernel Width of SVM

Eq. (10) shows the newly proposed formulations to compute the Gaussian kernel (Radial Basis Function or RBF) width of SVM and  $\sigma'$  is the adjusted kernel width.

$$\sigma' = \frac{2^q}{\sqrt{d}} \quad (10)$$

It is proposed that the adjusted kernel width will be increased by mainly the multiples of 2 after working out the differences in the weighted distances between patterns before and after the distance-weighted kNN methods (as shown in Table 1 below). Hence,  $q$  in Equation (10) is used as the power of 2 in the proposed formulations while figuring out the adjusted kernel width  $\sigma'$ . The values computed for  $q$  after the PCA and kNN implementation is based on the REDEFINITION (3) on the difference of weighted distances before and after the dimensionality reduction by PCA.

## 4 Results and Discussions

### 4.1 Classification Accuracies before and after the Proposed New Approaches

**Table 1.** Details of datasets derived weighted distances and new kernel width,  $\sigma'$ .

Datasets and values acquired <b>before</b> applying proposed formulations						
	Datasets applied (from UCI data repositories and OSA actual dataset* of patients records)	No. of features or attributes	No. of tuples or rows	Average index of weighted density in kNN SVM	Weighted distances <b>before</b> PCA and kNN in kNN SVM	Weighted distances <b>after</b> PCA and kNN in kNN SVM
1	German Credit	24	1000	9.1	1.75	2.66
2	Hepatitis	19	155	5.6	2.50	3.38
3	Breast Cancer	30	569	8.7	1.12	1.31
4	Diabetes	8	768	4.7	4.05	4.91
5	Australian Credit	14	690	5.5	2.22	3.10
6	Ionosphere	34	351	9.2	0.45	1.11
7	Heart Disease	13	270	4.3	3.20	3.89
8	Liver Disorder	6	345	3.1	5.61	6.21
9	Titanic	5	1309	2.6	5.33	5.58
10	OSA actual dataset*	14	450	4.8	2.01	2.18

In Table 1, the principal components are acquired after dimensionality reduction by PCA. In Table 2, the values of principal components acquired for all the 10 datasets are all not large but fewer than 10, i.e. significant reduction in dimensionality from feature

space distribution, we just concentrate on computing the weighted distances among patterns of the data points but not on computing similarities among patterns.

**Table 2.** Details of datasets, derived differences in weighted distances and kernel widths.

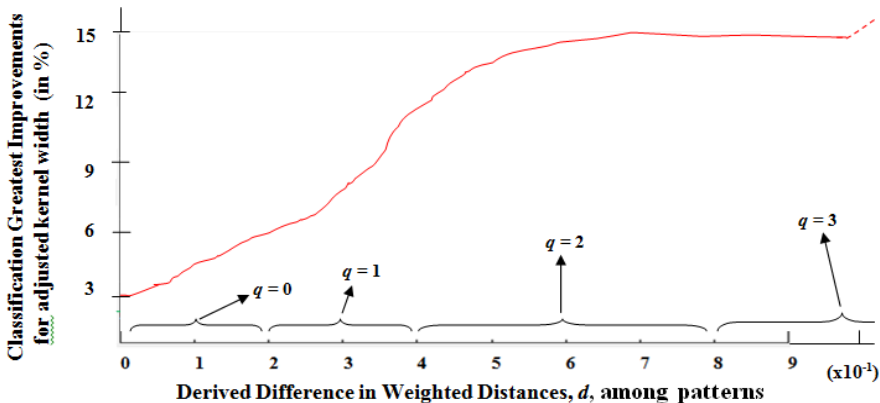
Datasets and values acquired after applying proposed formulations						
	Datasets applied (from UCI data re- positories and OSA dataset* from pa- tients' records)	Initial kernel width $\sigma$ (by de- fault)	$q$ , power obtained from the proposed formula	Principal Components, $pc$ , after PCA pre- processing before kNN SVM	Derived dif- ference in weighted distances, $d$	New kernel width $\sigma'$ (after proposed formulations)
1	German Credit	1.89	3	8	0.91	8.39
2	Hepatitis	1.91	3	5	0.88	8.53
3	Breast Cancer	2.11	0	9	0.19	2.29
4	Diabetes	1.72	3	3	0.86	8.63
5	Australian Credit	1.66	3	5	0.88	8.53
6	Ionosphere	0.98	2	9	0.66	4.92
7	Heart Disease	2.02	2	4	0.69	4.82
8	Liver Disorder	2.34	2	3	0.60	5.16
9	Titanic	1.00	1	3	0.25	4.00
10	OSA actual dataset*	0.56	0	2	0.17	2.43

Table 2 shows further experimental results after the implementation of the proposed formulations to the kNN SVM algorithms to the 10 datasets\* applied. Results showed that new kernel widths  $\sigma'$  are wider than the initial kernel widths since the derived difference in the weighted distances after kNN,  $d$ , is larger in most of the datasets applied. In other words, if weighted distances among patterns are further apart, coarse SVM kernel widths  $\sigma'$  will be allocated rather than fine kernel widths. In Table 2, the derived difference in the weighted distances,  $d$ , and the power obtained from the proposed formulations,  $q$ , are used to compute the new Gaussian kernel width  $\sigma'$  (Equation (10)). The new kernel width is on average wider than initial  $\sigma$ .

## 4.2 Validation of the Research Findings and Outcomes

Validation of the improvements in classification accuracies is measured by the significance in terms of  $p$  values. From the results shown in Figures 1 and 2, we can conclude that when there is a significant difference, i.e.  $d$ , in the weighted distances among patterns as well as between input vectors and training sample, i.e.  $q = 1$  or above for greater differences in the weighted distances among patterns before and after PCA application to the datasets (as shown in Table 1), wider SVM Gaussian kernel width can significantly improve SVM classification on the datasets applied. The results showed that the proposed formulations do work on the Gaussian kernel width sizes such that optimal kernel width match SVM classification. Figure 2 showed the generalized

Receiver Operating Characteristics (ROC) curves before and after kNNSVM algorithms on the datasets stated, with 4 different  $q$  values applied for adjusted  $\sigma'$  kernel width, against those without getting its kernel width adjusted  $\sigma$ .



**Fig. 1.** Average generalized performance of the applied 10 datasets after kNNSVM on the greatest improvements in SVM classification accuracies (in %) with derived difference in weighted distances  $d$  (in redefined scale of  $10^{-1}$  as shown in Table 2) at different adjusted kernel width  $\sigma'$  from the applied  $q$  values in proposed formulations of this research.

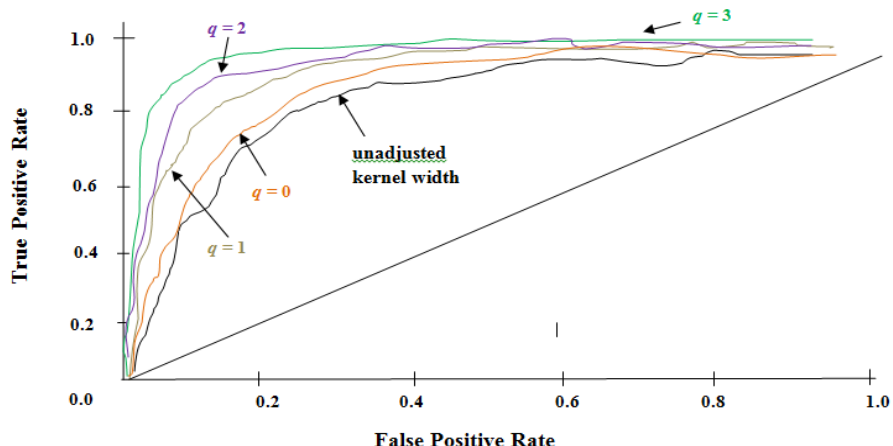


**Fig. 2.** Average generalized performance of the ROC curves applied before (by default  $\sigma$ ) and after kNNSVM algorithms ( $\sigma'$  based on  $q$  values applied) on the stated datasets.

In Table 3, the best classification accuracies are highlighted in **bold**. It shows a comparison on the classification accuracies as well as the greatest improvements (in %) achieved using default Gaussian kernel width and adjusted one after the proposed formulations stated in Eq.(10). As a comparison of SVM with the auto-default kernel

width (i.e. unadjusted), most of the datasets (except datasets of ‘Breast Cancer’ and ‘OSA actual dataset’ with shortest derived distances,  $d$ ) with adjusted SVM kernel widths fall in the category of ‘coarse kernel width’. The adjusted kernel widths,  $\sigma'$ , showed better or the best classification accuracies among the three categories.

**Table 3.** Classification accuracies based on the different assigned kernel widths applied and the greatest improvements achieved after the adjustment.

Datasets applied (from UCI repositories and OSA raw dataset)	Fine kernel width (by auto default) $\sigma=0.01\text{-}1.00$	Medium kernel width (adjusted) $\sigma'=1.01\text{-}4.00$	Coarse kernel width (adjusted) $\sigma' = 4.01\text{-}10.00$	Greatest im- provements in classification accuracies (%)
	<b>Classification Accuracy</b> based on assigned kernel width			
1 German Credit	65.9%	67.2%	<b>74.3%</b>	12.75 <sup>c</sup>
2 Hepatitis	71.9%	75.5%	<b>79.3%</b>	10.29 <sup>c</sup>
3 Breast Cancer	68.4%	<b>70.5%</b>	69.9%	3.07 <sup>a</sup>
4 Diabetes	75.3%	79.2%	<b>83.3%</b>	10.62 <sup>c</sup>
5 Australian Credit	76.5%	77.9%	<b>87.1%</b>	13.86 <sup>c</sup>
6 Ionosphere	67.6%	68.9%	<b>72.8%</b>	7.69 <sup>b</sup>
7 Heart Disease	86.1%	87.2%	<b>93.7%</b>	8.83 <sup>b</sup>
8 Liver Disorder	69.9%	75.2% <sup>d</sup>	<b>75.4%<sup>d</sup></b>	7.87 <sup>b</sup>
9 Titanic	88.7%	90.2%	<b>95.6%</b>	7.78 <sup>b</sup>
10 OSA actual dataset*	87.5%	<b>92.3%</b>	88.9%	5.49 <sup>a</sup>

<sup>a</sup>significance at  $P<0.05$ , <sup>b</sup>at  $P<0.001$ , <sup>c</sup>at  $P<0.0001$ ; <sup>d</sup> about the same classification accuracies

## 5 Conclusion and Discussions

Research questions as stated have been answered and research hypotheses of this research have been proven to be valid. Datasets of ‘Breast Cancer’ and ‘OSA actual dataset’, having the shortest  $d$ , in weighted distances among patterns, have shown the least improvements in kNN SVM classification accuracies with adjusted Gaussian kernel widths  $\sigma'$ . This is because distance-weighted kNN that applied to patterns which are further apart can adjust the kernel function which does not drop off rapidly during SVM classification. Shorter  $d$  will need a finer or narrower Gaussian kernel width. By using PCA and kNN methods before SVM classification, the proposed formulations are derived based on studying the relationships between the Gaussian kernel width of SVM and the difference between the weighted distances among the patterns after kNN method as well as the differences between the input vectors and training samples of SVM. Results showed that by reducing the number of features and overall dimensionality of the datasets by PCA, and the newly weighted distances computed by kNN method using the newly proposed formulations, overall classification accuracies can significantly be improved. Validation of the research findings and experimental outcome has been shown in the ROC curves as displayed in Figure 2, as well as in Table 3 with the level of significance of  $p$  values indicated. Results shown in Tables 1 and 2,

as well as in Figure 1, are linked with the results in Table 3, and hence have also been validated by the significance of  $p$  values.

The weaknesses of this research are that when the proposed formulations are applied to the datasets which are of too high dimensionality (e.g. over principal components of 250), if even after the PCA application, the distance-weighted kNN is still smaller than 0.10, i.e. too close among patterns of data points even after kNN methods, the proposed formulations and redefinitions will not significantly improve SVM classification. This is because the proposed wider  $\sigma'$  will not be feasible. The auto default finer  $\sigma$  which its kernel function is much better to drop off more rapidly when applied to datasets of higher density rather than more slowly to less densely distributed datasets after the pre-processing done by PCA as implemented in this research.

## Acknowledgment

All the datasets applied in this research, except those (indicated \* sign) collected from real patients' records of Obstructive Sleep Apnea (OSA) in public hospitals in Malaysia, are acquired from University of California Irvine (UCI) data repositories. Formal reference is 600-RMI (5/1/6) and the Fundamental Research Grant Scheme (FRGS) recorded and referenced as FRGS/ICT02(01)/1077/2013(23).

## References

1. Maldonado S., Merigo J., Miranda J.: Redefining support vector machines with the ordered weighted average. *Knowledge Based Systems* 148, 41–46 (2018).
2. Gao X., Hou J.: An improved SVM integrated GS-PCA fault diagnosis approach of Tennessee Eastman process. *Neurocomputing* 174, 906–911 (2016).
3. Wang W., Zhang M., Wang D., Jiang Y.: Kernel PCA feature extraction and the SVM classification algorithm for multiple-status, through-wall, human being detection. *EURASIP Journal of Wireless Communications and Networking* 151, 1-14 (2017).
4. Vapnik V., Statistical Learning Theory, John Wiley and Sons, USA (1998).
5. Qiao X., Bao J., Zhang H., Wan F., Li D.: Underwater sea cucumber identification based on principal component analysis and support vector machine. *Measurement* 133, 444–455 (2019).
6. Shihab K., Sim D. Y. Y., Shahi A. M.: Angur: A visualization system for XML documents. In: 9th WSEAS International Conference on Telecommunications and Informatics, pp. 159 – 165, WSEAS, Catania, Italy (2010).
7. Shihab K., Sim D. Y. Y.: Development of a visualization tool for XML documents. *International Journal of Computers* 4(4), 153 – 160 (2010).
8. Sim D. Y. Y.: Emerging convergences of HCI techniques for graphical scalable visualization: efficient filtration and location transparency of visual transformatio.In: 7th International Conference Information Technology in Asia, pp. 1–8, Malaysia (2011).
9. Maldonado S., Lopez J.: Synchronized feature selection for support vector machines with twin hyperplanes. *Knowledge Based Systems* 132, 119-128 (2017).
10. Barkana B. D., Sariciek I., Yildirim B.: Performance analysis of descriptive statistical features in retinal vessel segmentation via Fuzzy Logic, ANN, SVM, and classifier fusion. *Knowledge Based Systems* 118, 165-176 (2017).

11. Yang W., Si Y., Wang D., Guo B.: Automatic rrecognition of arrhythmia based on principal component analysis network and linear support vector machine. Computational Biology Medicine 101, 22–32 (2018).
12. Yang F., Wu C., Xiong N., Wu Y.: Prediction of criminal tendency of high-risk personnel based on combination of principal component analysis and support vector machine. Internatioanl Journal of Software and Hardware Research in Engineering 6(8), 1-10 (2018).



# Vehicle Classification using Convolutional Neural Network for Electronic Toll Collection

Zi Jian Wong<sup>1</sup>, Vik Tor Goh<sup>1(✉)</sup>, Timothy Tzen Vun Yap<sup>2</sup>, and Hu Ng<sup>2</sup>

<sup>1</sup> Faculty of Engineering, Multimedia University, Cyberjaya, Malaysia

<sup>2</sup> Faculty of Computing & Informatics, Multimedia University, Cyberjaya, Malaysia  
kenwongzijian@gmail.com,  
{vtgoh, timothy, nghu}@mmu.edu.my

**Abstract.** Electronic Toll Collection (ETC) is an automated toll collection system that is fast, efficient, and convenient. Transponder-based ETC's such as Malaysia's SmartTag is the most common and reliable. Transponders send identification information wirelessly and the toll fee is charged accordingly. However, it is susceptible to fraudulent transactions where transponders for more expensive vehicle classes such as trucks are swapped with vehicles from cheaper classes like taxis. As such, the toll operator must be able to independently classify the vehicle class instead of relying on information sent from potentially misused transponders. In this paper, we implement an automated video-based vehicle detection and classification system that can be used in conjunction with transponder-based ETCs. It uses the Convolutional Neural Network (CNN) to classify three vehicle classes, namely cars, trucks, and buses. The system is implemented using TensorFlow and is able to obtain high validation accuracy of 93.8% and low validation losses of 0.236. The proposed vehicle classification system can reduce the need for human operators, thus minimising cost and increasing efficiency.

**Keywords:** Vehicle classification · Computer vision · Machine learning · Tensorflow.

## 1 Introduction

Electronic Toll Collection (ETC) systems are cashless toll collection systems where payments can be made without the need to stop vehicles at toll booths. In addition to simplifying the payment process, ETCs have the added benefit of eliminating bottlenecks at toll booths, thus reducing traffic congestions and smoothing the travel. It is also more cost effective because toll booths do not need to be built, maintained, and staffed.

Most ETCs use the Automatic Vehicle Identification (AVI) system where transponders are installed in vehicles and communicate with overhead readers [?]. Upon identifying the transponder and corresponding account, a matching toll fee is charged to the driver. In Malaysia, ETC is implemented using SmartTags together with Touch 'n Go cards. Although accurate and can work in vehicles

travelling at high speeds, transponders can be easily manipulated to defraud the collection system. Most tolls charge different fees for different classes of vehicles and transponders are usually tagged to a specific vehicle class so that the correct fee is charged. However, transponders can be swapped between different classes of vehicles. For example, transponders belonging to vehicles with lower toll fees such as taxis are used in vehicles that are usually charged higher fees such as private cars and trucks.

To mitigate this problem, transponder-based system must be supplemented by other systems that can correctly classify the vehicle before the correct fee is applied. Traditionally, vehicle classification is carried out using the human visual system. In essence, a human operator is needed to explicitly set the correct fee into the collection system right before the vehicle passes through the toll. The human visual system performs exceptionally well in differentiating and highlighting key parts of an image [?] and has the highest accuracy in classifying vehicles. Despite that, relying on a human means that it is susceptible to issues such as exhaustion and accidental mistakes (e.g. human error). It also incurs additional costs due to the need for staffing and is less efficient.

In this paper, we propose an automated vehicle detection and classification system. It uses the Region-of-Interest (ROI) method to detect and extract the vehicle from a video and then applies the Convolution Neural Network (CNN) as the machine learning framework to classify the vehicle. We describe the implementation details and discuss our evaluation results.

The rest of the paper is organised as following. In Section ??, related work on vehicle detection and classification are discussed. Section ?? presents the proposed algorithm for detection and classification of vehicles. Section ?? discusses the evaluation results and Section ?? concludes the paper.

## 2 Related Work

Existing methods of vehicle type classification can generally be divided into two categories, namely sensor-based and image-based methods.

Sensor-based methods use a variety of sensors such as pneumatic pressure sensor [?], induction loop [?], magnetic sensor [?], and fiber-optic sensors [?] to differentiate one class of vehicle from another. These sensors measure the passing vehicle's physical attributes such as weight, number axles, number of wheels, height, and even magnetic field in order to obtain unique features of each class of vehicle. For example, trucks will typically weigh more than cars while buses have more axles than cars. Although sensor-based methods are accurate in classifying the vehicles, they are usually more difficult to install and maintain, oftentimes requiring the temporary closure of roads. Furthermore, sensors that have to be embedded in roads have to be replaced if the road is repaved, thus increasing costs and complexity.

On the other hand, image-based or video-based methods are usually easier to install and a single camera can capture more than just one lane of passing vehicle, thus making it more cost effective. The Automatic Number Plate Recog-

nition (ANPR) such as the one by [?], is a type of indirect vehicle classification system that uses cameras to capture images of passing vehicles in order to extract and recognise number plates using Optical Character Recognition (OCR). The number plates are then checked against a database and the driver is billed according to the registered vehicle class. Fraudsters can still defraud the system by switching or faking number plates. Additionally, this approach is less flexible because vehicles must be pre-registered with the toll concessionaire, which in turn raises privacy issues. The toll concessionaire now knows a lot of sensitive information such as vehicle type, model, location, number plate, and driver's personal information such as name and address.

As such, direct image-based methods that can actually classify vehicles using visual features such as height, width, or shape are preferable over methods that rely on number plates. According to [?], such methods exist and can generally be categorised as either model-based or appearance-based. Model-based methods compute measurable physical parameters such as width, height, and length to recover the 3D model of the vehicle. Appearance-based methods extract features such as edges and transforms to represent (as opposed to modelling the actual shape of the vehicle) the vehicle.

In our work, we focus on applying machine learning techniques to enhance the image-based vehicle classification methods. Prior work in this area include those by [?] and [?], where various machine learning methods such as decision tree,  $k$ -Nearest Neighbour ( $k$ NN), Support Vector Machine (SVM), and Neural Network (NN) are used to classify vehicle by type, colour, or class. As most of these methods are based on the vehicle's side view, we aim to apply machine learning algorithms to frontal views of the vehicles. This is consistent with our vision of an ETC system that uses transponders but is capable of automatically classifying vehicles and therefore, can prevent fraudulent transactions where transponders are swapped. Cameras will be placed on toll booths or overhead gantries, and positioned to face the front of vehicles.

### 3 Design and Implementation

The proposed video-based vehicle detection and classification algorithm consists of four components: data collection, model training, model evaluation, and model testing. Each part will be explained in detail as follows.

#### 3.1 Data Collection

The first step is to implement data into the vehicle classification system. Data collection is categorised into two sub-categories, which are data collection for model training and evaluation, and data collection for model testing. Data collection for model training and evaluation is carried out using datasets from sources such as Caltech [?], TU Graz-02 [?], and BIT-Vehicle dataset [?]. These datasets contain a large corpus of vehicles such as cars, trucks, and buses. Some samples of cars are shown in Fig. ???. A non-vehicle category is included as part

of model training so that the algorithm can differentiate vehicles from other objects.



**Fig. 1.** Sample images of cars used for training.

Therefore, we have four classes of vehicles; (1) cars, (2) trucks, (3) buses, and (4) non-vehicle, where each class has 500 images, totalling up to 2000 images. The number of images in each class is evenly distributed because unbalanced datasets could cause the CNN to be biased in its classification. Vehicles may be incorrectly classified into a class that corresponds to the larger dataset class.

On the other hand, data collection for model testing is carried out by recording videos of actual vehicles. A GoPro Hero 4 action camera is used because of its compactness, high resolution and frame rate, and ease of use. Videos of various vehicles such as cars, trucks, and buses are recorded.

### 3.2 Model Training

In model training, the GPU-enabled CNN is chosen as the classifier that classifies vehicle type. CNN is chosen because it automatically extracts features from the input data instead of having to manually perform feature extraction. Despite that, CNN is still a supervised machine learning algorithm and therefore, labelled images have to be used for model training.

The architecture of the CNN model that we use is shown in Fig. ???. Convolution layers 1, 2, and 3 are deployed to find the features of the input image through convolution, max pooling, and Rectified Linear Unit (ReLu) activation functions. This is followed by the flatten layer which ensures that its input is flattened to have the same number of features found in the convolution stage. After that, two fully-connected layers perform weight adjustments and normalisation to obtain output values between 0 and 1. Lastly, the Softmax function is applied as a normalised exponential function that generalises the input to the output class.

The training dataset consists of 2000 images categorised into four classes which are car, truck, bus, and non-vehicle. The input data of 2000 images is randomly separated into training and validation sets with a ratio of 80:20. As a

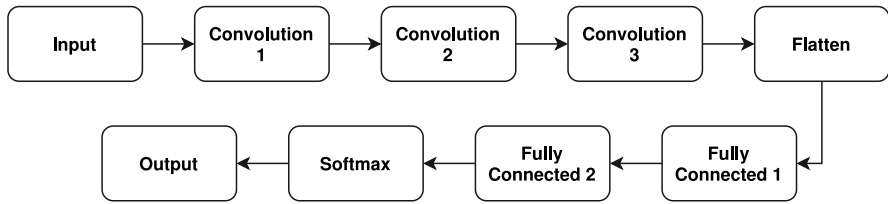


**Fig. 2.** Architecture of Convolution Neural Network (CNN).

result, 1600 images are used for training purpose while 400 images are used for validation of model. The CNN algorithm is implemented using Tensorflow, an open-sourced machine learning framework by Google and is written in both C++ and Python. The recommended parameters for CNN in Tensorflow is shown in Table ??.

For the whole training process, a laptop with Intel Core i7-4700 MQ, 8GB memory, and Nvidia GeForce GT 750M is used.

**Table 1.** Parameters for CNN layers.

Layer	Parameter	Value
Convolution 1	Filter Size	3 pixels
	Filter Width and Length	32 pixels
Convolution 2	Filter Size	3 pixels
	Filter Width and Length	32 pixels
Convolution 2	Filter Size	3 pixels
	Filter Width and Length	32 pixels
Fully Connected	Layer Size	128 pixels
Others	Learning Rate	$1 \times 10^{-4}$
	Batch Size	32

### 3.3 Model Evaluation

After the model has been trained using the training dataset, it is then evaluated using the validation dataset that was split earlier. The model's accuracy and validation loss are calculated after every epoch of training to evaluate its performance. One epoch is defined as one complete presentation of the dataset and can be calculated using (??).

$$\text{Epoch} = \frac{\text{Size of training data}}{\text{Batch size}} \quad (1)$$

where the size of training data is 1600 and the batch size is 32. The accuracy of the validation is based on the comparison between the ground truth (actual vehicle type) and predicted vehicle type of the validation data. Loss is calculated based on the cross-entropy cost function.

### 3.4 Model Testing

In order to facilitate the testing of the trained model, a GUI program as shown in Fig. ?? is used. The program is made using Tkinter, a Python-based GUI library and it operates on the videos of actual vehicles that were recorded using the GoPro camera. The program automatically extracts the Region of Interest (ROI) or more specifically, the bounding box containing only the vehicle. This is done using motion tracking and segmentation tools found in OpenCV, a computer vision library. The application determines the accuracy and robustness of the model.



**Fig. 3.** Vehicle detection and classification program.

## 4 Results and Discussions

The GUI program is used to extract the image of the vehicle from the video footage. The video footages contain various vehicle types such as cars, trucks, and buses. Fig. ?? shows the vehicle detection and segmentation process where one frame is first extracted from the video, and subsequently, the ROI containing the vehicle is identified. The results from the extracted ROI are shown in Fig. ???. The output shows that the vehicle can be correctly detected and segmented by the extraction algorithm.

The CNN is trained with different numbers of iterations. Some models are under-trained while others are over-fitted. The number of iterations used are 1000, 1200, 1500, and 2000. Generally, the accuracy for both training increases

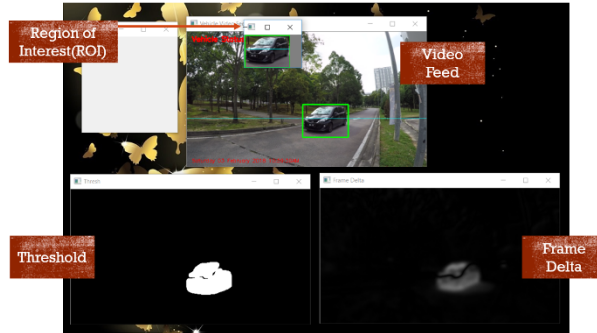


**Fig. 4.** Vehicle detection and segmentation.

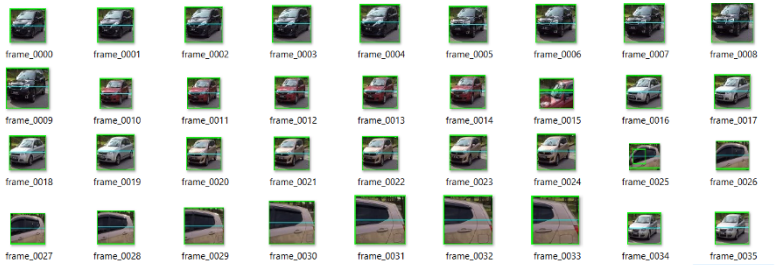


**Fig. 5.** Output of video detection and segmentation.

as the number of training epoch increases. This can be seen in Fig. ???. The figure also shows that the accuracy increases as the number of iterations increases, reaching 100% accuracy when 2000 iterations are used. However, as the number of iterations increases, so does the validation loss, resulting in poorer performance. For example, the corresponding validation loss for 2000 iterations is 0.445, which is significantly higher than those with less iterations. The results of the training are summarised in Table ??.

**Table 2.** Summary of CNN training

Number of iterations	Epoch	Training accuracy (%)	Validation accuracy (%)	Validation loss
1000	20	84.4	90.6	0.272
1200	24	90.6	93.8	0.236
1500	30	93.8	90.6	0.298
2000	40	100.0	87.5	0.445

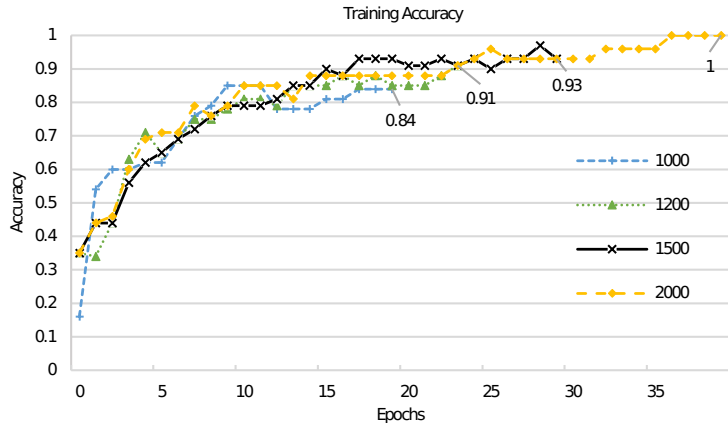


**Fig. 6.** Training accuracy for 1000, 1200, 1500, and 2000 iterations.

The most optimised model would be the one with the highest accuracy and lowest validation loss. As shown by the highlighted row in Table ??, 1200 iterations produce the best performing model. This is because it has the highest validation accuracy of 93.8% while maintaining the lowest validation loss of only 0.236. Therefore, we use the model produced by this number of iterations in our subsequent tests.

In the tests, we attempt to classify three different classes of vehicle namely cars, trucks, and buses. Each of the classes are tested using images that had not been used earlier for model training. 10 images for every class of vehicles are used and some samples of these images can be seen in Fig. ???. The accuracy of the vehicle classification system is shown in Table ??.



**Fig. 7.** Sample images used for testing.

**Table 3.** Summary of classification accuracy

Class	Correct Prediction	Accuracy (%)
Car	9/10	90.00
Truck	9/10	90.00
Bus	9/10	90.00

The tests show that an accuracy of 90% can be attained for all three classes of vehicles. We could not obtain 100% accuracy because the model had trouble differentiating one class of vehicle from another due similar visual characteristics. For example, some buses and trucks have similar frontal profiles (i.e. large and square). Some test images are also of lower visual quality, thus confusing the classifier. These issues could be mitigated by using better training datasets. Instead of relying on datasets that contain vehicles not driven in Malaysia, we could use images of actual vehicles driven in Malaysia. Despite that, the model is still sufficiently reliable and robust as a high accuracy of 90.00% could be achieved for each class of vehicle.

## 5 Conclusion

This paper shows that the convolutional neural network can be used as the machine learning framework in an automated vehicle detection and classification system for ETC. The CNN architecture is suitable to be used for model training because of its robustness, effectiveness, and high accuracy in classifying the vehicle. Overall, the work could achieve a high validation accuracy of 93.8% while maintaining low validation loss of only 0.236. In our future work, we will look into methods to further improve the accuracy of the classification system. Some possible approaches include fine-tuning the CNN's hyper-parameters, adding more layers for a deeper CNN architecture, or increase the size of the vehicle dataset. Ultimately, the classification system will improve the ETC's efficiency and reliability, thus enhancing drivers' experiences and convenience.

**Acknowledgements.** Financial support from the Ministry of Higher Education, Malaysia, under the Fundamental Research Grant Scheme with grant number FRGS/1/2018/ICT02/MMU/03/6 is gratefully acknowledged.



# Social Media, Software Engineering Collaboration Tools and Software Company's Performance

Gulshan Nematova<sup>1</sup>, Aamir Amin<sup>2</sup>, Mobashar Rehman<sup>3</sup>, Nazabat Hussain<sup>3</sup>

<sup>1,2,3</sup> Faculty of Information and Communication Technology, Universiti Tunku Abdul Rahman (UTAR), Kampar, Malaysia

<sup>2</sup> Universiti Teknologi Petronas, Malaysia  
nematova.gulshan@gmail.com, aamir@utar.edu.my,  
Mobashar@utar.edu.my, Nazabat@gmail.com

**Abstract.** Software Engineering (SE), like any other field, is utilizing Web 2.0. Within Web 2.0, Social Media (SM) is changing the landscape of Software Engineering (SE) and has the ability to improve the performance of Software Engineering Organizations (SEO). Regardless of the seeming widespread use of Social Media (SM) in SE, there is still little knowledge about the benefits or risks of SM usage as well as which SM tools could be used to enhance SE Organization's performance, and the influence they may show on the quality of software. Furthermore, in order to increase the success rate, organizations have to be able to take advantage of crisis situation as well. However, utilization of SM in CM appears as an under-studied topic and there is an emerging need of compact framework in this domain. Furthermore, so far, academic research conducted on SM, remains incomprehensive regarding its numerous purposes and subsequent influences on organizations. Same is the case for SM utilization in CM. In addition to SM, SE collaboration tools are also a vital source of improving performance. Prior literature indicates towards the need for research work on utilization of Web 2.0, especially SM and other collaboration tools, for CM in SEOs. Hence, there is a need for a thorough research on this topic. The present research aims to examine the role of social media and software engineering collaboration tools for effective crisis management and improved performance of software organizations. Based on extensive literature review and relevant theories, the present research aims to provide a conceptual framework of the use of SM and SE collaboration tools to enhance the performance of software engineering companies. Furthermore, the mediating role of crisis management is also be proposed.

**Keywords:** social media; software engineering; collaboration tools; crisis management; performance

## 1 Introduction

In present world, Web 2.0 tools function as crucial information resource for most people and have become part of our daily lives. Among these tools, the present study concerns with Social Media (SM) which is one of the widely used Web 2.0 tool. New technologies, especially SM, are gaining more popularity as a tool to assist organization

to have better contact with other businesses or public in general, causing the applications market to succeed [1], [2]. However, in order to apply SM for business purposes, an organization needs to obtain explicit information and recognize that transformation to the new era entails efforts, application and continuous adaptation to those changes. Hence, the application of SM is an element of transformation in businesses [3]. Additionally, academic studies on SM yet to be perfected in the framework of insightful investigations into the numerous uses of SM and consequent influences on organizational performances [4].

Specifically, in software engineering organizations, employees do not always have a chance for face-to-face meetings or they are not always in same place or time zone, hence Web 2.0 technologies, especially SM, are vital as they help team members to communicate and work efficiently [5]. The executives are compelled to reevaluate their businesses operations due to the increasing popularity of SM within a business [6], because crises evolving online are rather difficult to predict and can elevate fast and cause damage to organizations. SM can present opportunities as well as challenges for Crisis Management (CM) in organizations. Although, SM is a key crisis communication tool between organizations and public [7] [8], it can also quickly deliver harmful information and remarks about a crisis, causing damage to the organizational image. Additionally, whether studying about a natural disaster that took place nearby, relevant information which may modify preplanned routes of a travel journey, or simply discerning the route and urgency of an oncoming hurricane; information in real-time is critical and will allow an entity to make better informed and thorough decisions on ways to cope or alleviate risk [9]. Thus, companies are advised to efficiently use SM to control the spread of crises and converse it well with people during and after the crises [10].

Collaboration is inevitable in software engineering and the collaboration tools, similar to SM, are the only way to do it "*efficiently, consistently, and securely*" [5]. In addition, reduction in cost by discovering new, cheaper means of collaboration and communication for software companies is one of many motivating factors to research thoroughly [11]. Hence, it is pertinent to understand how software collaboration tools can enable a better crisis management and in turn an improved business performance.

## 2 Literature Review

### 2.1 Social Media (SM)

By definition, SM represents a combination of three elements: Web 2.0 technologies, content and user communities. Content means the user created content which can be anything from personal pictures to scientific articles. When users want to add any content, they can do it by stating present information or delivering an analysis of some specific product [12]. As a result, the old fashioned business dynamics have changed due to SM with the help of more efficient means such as social networks, virtual worlds, social bookmarking sites, wikis and weblogs [13]. Hence it assists the companies to reach out to individuals, dispersed across different geography, with seemingly lesser concerns [14]. What makes SM unique among all Web 2.0 innovations is the simplicity

of web-based sharing, allowing users to instantly share content among their networks by just clicking a button [15].

## 2.2 Comparison of Social Media Frameworks

	Authors	Strategies	Remarks
1	Kietzmann et. al. [16]	<ol style="list-style-type: none"> <li>1. Cognize = Recognize position within Honeycomb framework</li> <li>2. Congruity = Align strategy with overall business objective</li> <li>3. Curate = Determine resources</li> <li>4. Chase = Monitoring</li> </ol>	Provides a framework to closer look at the various functions of SM to improve BP
2	Parent et al. [17]	<ol style="list-style-type: none"> <li>1. Company = SM choice</li> <li>2. Content</li> <li>3. Control = Monitoring, Policies</li> <li>4. Community</li> <li>5. Customer = Target audience</li> <li>6. Conversation</li> </ol>	Only covers marketing aspects of BP. Only focuses on willingness to participate aspect
3	Meijer Thaens [18]	<ol style="list-style-type: none"> <li>1. Technological choice = Resources</li> <li>2. Couple SM with organization = Align tasks</li> <li>3. Objectives = Goals</li> <li>4. Arrange tasks and responsibilities</li> </ol>	Not BP aspects, only covers SM strategies of government organizations
4	Effing and Spil [19]	<ol style="list-style-type: none"> <li>1. Initiation stage = Channel choice and Target audience</li> <li>2. Diffusion stage = Policies, Resources and Goals</li> <li>3. Maturity stage = Monitoring and Content Activity</li> </ol>	Very close to Kietzmaann's framework, not much improvement

After examining the four main frameworks [16-20] on social media, Kietzmann's honeycomb framework found to be more complex and through. Additionally, there are other frameworks by Constantinides et al. [20], Wilson et al. [21], Curran et al. [22], Munar [23], Hays et al. [24], Othman et al. [25], Rodriguez-Donaire [3] and Ng et al. [26]. The majority of the frameworks also focus on advertising the offerings of a company through SM. However, there is a need for a strategy to prevent any crisis situation and to be able to use it for organizational advantage. Therefore, Honeycomb framework of Kietzmann [16] is suitable for this research.

### Honeycomb Framework of Social Media Functionalities

Many attempts have been made to describe the purpose and structure of social media with most of those classifications to be customer oriented [27], [28]. Furthermore, there are other classifications which consider the implementation aspects of social media for organizations [29] [16]. Within these classifications, the honeycomb model of social

media by Kietzmann et al. [16] is considered to be one of the most complete. The honeycomb model focuses on the functional characteristics as well as the business implications of social media tools [30]. Honeycomb framework of Kietzmann et al. [16] analyzes the impact of Web 2.0 tools by differentiating among seven SM functional blocks, as well as its impact of these functionalities on business competencies and implication of each functionality.

- Identity - It represents the degree of users' expression of their online presence.
  - H1a: Utilizing Identity functionality of SM positively effects CM and SEO's performance of the company
  - H2a: Utilizing Identity functionality of SM for CM positively effects SEO's performance
- Conversations - The examination on how SM users are interacting with one another in certain SM platforms.
  - H1b: Utilizing Conversations functionality of SM negatively effects CM and SEO's performance
  - H2b: Utilizing Conversations functionality of SM for CM negatively effects SEO's performance
- Sharing - It stands for the element of distributing exchanging and receiving content in a SM setting.
  - H1c: Utilizing Sharing functionality of SM positively effects CM and SEO's performance
  - H2c: Utilizing Sharing functionality of SM for CM positively effects SEO's performance
- Presence - It defines the degree to which SM users may get to know whether other users can be accessible via SM settings [31].
  - H1d: Utilizing Presence functionality of SM positively effects CM and SEO's performance
  - H2d: Utilizing Presence functionality of SM for CM positively effects SEO's performance
- Relationships – It associates with the plan of what an organization has to make to efficiently communicate with the users using SM.
  - H1e: Utilizing Relationships functionality of SM positively effects CM and SEO's performance
  - H2e: Utilizing Relationships functionality of SM for CM positively effects SEO's performance
- Reputation - The extent to which users can identify the status of users in a SM setting.
  - H1f: Utilizing Reputation functionality of SM positively effects CM and SEO's performance
  - H2f: Utilizing Reputation functionality of SM for CM positively effects SEO's performance
- Groups - It represent the degree to which users can form communities and sub communities.

- H1g: Utilizing Groups functionality of SM positively effects CM and SEO's performance
- H2g: Utilizing Groups functionality of SM for CM positively effects SEO's performance

### 2.3 Collaborative Development Tools (CDTs)

During software development process, it is vital for team members to be equipped with all the collaboration tools, in order to work efficiently. Any disruptive communication can cause major conflict and can directly influence the outcome of the whole project. Following are the type of CDTs [32]:

- Version-Control Systems - It is challenging at times to manage files or project related software when working in a team, this tool helps co-workers to easily distribute information or software needed among themselves.
  - Trackers - This tool helps anyone in the project to track down the information needed whenever any issue occurs with the items.
  - Build Tools - When the project is distributed amongst several teams or team members, this tool helps with build management and remote repository. It can be used for invoking test frameworks, compiling databases, arranging production systems, and sending reports to developers.
  - Modelers - It helps software engineers while creating customized software processes, artifacts and models.
  - Knowledge Centers - These tools help team members to manage contents by sharing explicit information.
  - Communication Tools - Any platform to deliver message to one another in an organization, it can be via email, web forums or some kind of corporate network.
- H4: Utilizing CDTs for CM positively effects SEO's performance.

### 2.4 SEPBO Performance

Project-based organizations are defined by their ability to support temporary projects as well as being able to distribute and sell organizations day to day products and services to either internal or external customers [33]. There are a numerous industries which operate as such, i.e. consulting firms, cultural industries, high technology [34]. In this research, we focus on Software Engineering Project-based Organizations (SEPBO). Performance is arguably the most known management and modern research dependent variable [35]. According to Smet [36], organizational performance is "*the extent to which an organization realizes its short-term objectives and prepares to realize its long-term objectives*" and can be divided into project performance and stakeholder performance.

#### Project Performance

Project performance is measured in terms of project objectives, for example, completing the project on time, not exceeding the cost planned and generating a good quality product or service [37]. Project performance is defined by three variables [38]:

- Time: Projects are required to meet the deadline given by the stakeholders. If completed before time, it might be because too many resources were put in, which is costly. On the other hand, if it is completed too late, it might be the result of inefficiency.
- Cost: Best projects are always completed within the given budget. Of course, over budgeting will bring down the overall income for the organization, but also under budgeting leads to compromises in quality.
- Quality: It is a broad term that is very subjective. Overall, the project should meet the customer's demands and satisfaction.

### **Stakeholder Performance**

According to Freeman [39], stakeholder is “*any group that can affect or be affected by the achievement of organizational objectives*”. Stakeholder can be employee, employer, buyer, seller, suppliers or even the general public. So if we want to define stakeholders in terms of SEPBO, any parties, internal or external, which is influenced by the organizational activities and outcome of the software engineering projects. Different perceptions of performance can mean different things for different stakeholders, which often lead to different attitudes towards performance [40], [41]. Organizations cannot prosper until they have a distinct interest in satisfying various stakeholders [42].

## **2.5 Crisis Management**

According to Faulkner [43], crises or disasters is “*sudden challenges which might test the organization’s ability to cope*”. CM can be characterized as the several ways a business employs to prevent or reduce the influence of the crisis [44]. According to Fink [45], crisis is an unexpected risk occurrence that leads to a critical period of difficulties. From the above given information about CM in SE, we can conclude that it is management of an unexpected occurrence with low probability and high impact risk that can result in project’s failure and requires immediate action. An entity can significantly increase its adaptability, the ability to withstand disruptions and recover operational capacity after disruptions, by enhancing its ability to quickly pinpoint and react to such events [46].

### **Phases of Crisis Management**

CM can be generally divided into three phases [47]:

- Crisis Preparedness. During this phase, the emphasis is on preventive actions that aim to reduce identified risks that could cause a crisis.
- Crisis Response. During this phase, the emphasis is on the speed and efficiency of the primary response. The effective use of Web 2.0 platforms is critical during this

phase to engage public networks to collect, analyze and broadcast information in a timely manner.

- Crisis Recovery. After the two phases there is a longer time to recover as there is no urgency of immediacy of action and there is a need to plan and support to bring the situation back to normal.

### The Role of Social Media in Crisis Management

According to Wendling [48], the new platforms of SM such as Facebook, Twitter and others were acknowledged as a company's chance to reduce the impact while a crisis occurs [48]. Wendling et al. [48] also note that until now, radio, television, newspapers and other outdated media sources were applied to convey useful information. Nonetheless, currently Web 2.0 such as Facebook and Twitter are platforms which can help an organization to distribute information to as many people as possible at the same time getting feedback and reactions from the people. The endless use of SM as a platform appears likely for the foreseeable future [49].

## 3 Proposed Framework



**Fig. 1.** Proposed Framework

## 4 Implications

### 4.1 Practical Implications

This research will help software development organizations in managing their online activities during project crisis. This research will enhance their knowledge about Web 2.0 and how to use it as a SEPBOP improvement tool. When it comes to specific examples for the framework presented, identity could help the organizations to identify their potential customers, conversations, sharing and groups can help the organizations to distribute the information about the specific product which they are producing or generally about themselves. Presence and Relationship can help the organizations to make their presence known and get closer to their customers. And lastly, reputation can determine organizational future and can even help the organizations to improve their reputation in general public.

#### 4.2 Academic Implications

Existing academic research focuses on more general or management related aspects of Web 2.0, which are less specific to SEPBOP. This research sheds the light on more technical aspect of business processes of Web 2.0, giving the organizations the thorough knowledge of better understanding the audiences' needs and wants as well as get control over software development crisis. The published work of this research can be used as a guideline to understand the problems regarding to these issues.

### 5 Conclusion

This study has proposed a framework to improve SEPBOP using Web 2.0, especially, it will help in managing online activities during crisis, enhance knowledge about Web 2.0 tools and how to use them as a SEPBOP improvement tool. The study also sheds light on more technical aspect of CM of SM, enhancing better understanding of the audiences' needs and wants as well as getting control over crisis. In future, the same framework can be assessed in other fields.

### References

1. Dutta, S. (2012). Enterprise 2.0: let the revolution begin! *Rotman Magazine*, 66-71.
2. Liu, B. F. (2010). "Distinguishing how elite newspapers and A-list blogs cover crises: Insights for managing crises online." *Public Relations Review* 36(1): 28-34.
3. Rodriguez-Donaire, S. (2012). Changing business model dynamics by means of social media. *Management of Innovation and Technology (ICMIT)*, 2012 IEEE International Conference on, IEEE.
4. Schultz, R.J., et Al., (2012). Social media usage: an investigation of B2B salespeople. *Am. J. Bus.* 27 (2), 174–194.
5. Lanubile, F., Ebert, C., Prikladnicki, R., & Vizcaíno, A. (2010). Collaboration tools for global software engineering. *IEEE software*, 27(2), 52-55.
6. Ngai, E., Tao, S.C. and Moon, K. (2015) Social media research: Theories, constructs, and conceptual frameworks. *International Journal of Information Management*, 35, 33-44.
7. Freberg, K. (2012). "Intention to comply with crisis messages communicated via social media." *Public Relations Review* 38(3): 416-421.
8. Jin, Y., et al. (2014). "Examining the role of social media in effective crisis management: The effects of crisis origin, information form, and source on publics' crisis responses." *Communication research* 41(1): 74-94.
9. Cox, S.R. and Atkinson, K., 2018. Social Media and the Supply Chain: Improving Risk Detection, Risk Management, and Disruption Recovery.
10. Wang, Y. and C. Dong (2017). "Applying Social Media in Crisis Communication: A Quantitative Review of Social Media-Related Crisis Communication Research from 2009 to 2017." *International Journal of Crisis Communication* 1(1): 29-37.
11. Lampropoulos, G. and Siakas, K., (2018). Communication in Distributed Agile Software Development: Impact of Social Media—Social Networking. *SQM XXVI*, p.43.
12. Ahlqvist, T., et al. (2008). "Social media roadmaps." Helsinki: Edita Prima Oy.

13. Curran, J. M. and R. Lennon (2011). "Participating in the conversation: exploring usage of social media networking sites." *Academy of Marketing Studies Journal* 15: 21.
14. Rodriguez, M., et al. (2012). "Social media's influence on business-to-business sales performance." *Journal of Personal Selling & Sales Management* 32(3): 365-378.
15. Beattie, A. (2011). "What is the difference between social media and Web 2.0?" *Technopedia.com*.
16. Kietzmann, J. H., et al. (2011). "Social media? Get serious! Understanding the functional building blocks of social media." *Business horizons* 54(3): 241-251.
17. Parent, M., et al. (2011). "The new WTP: Willingness to participate." *Business horizons* 54(3): 219-229.
18. Meijer, A. and M. Thaens (2013). "Social media strategies: Understanding the differences between North American police departments." *Government Information Quarterly* 30(4): 343-350.
19. Effing, R. and T. A. Spil (2016). "The social strategy cone: Towards a framework for evaluating social media strategies." *International journal of information management* 36(1): 1-8.
20. Constantinides, E., et al. (2008). Social media: a new frontier for retailers? *European Retail Research*, Springer: 1-28.
21. Wilson, H. J., et al. (2011). "What's your social media strategy?"
22. Curran, K., et al. (2012). "The role of Twitter in the world of business." *Web-Based Multimedia Advancements in Data Communications and Networking Technologies*: 169.
23. Munar, A. M. (2012). "Social media strategies and destination management." *Scandinavian Journal of Hospitality and Tourism* 12(2): 101-120.
24. Hays, S., et al. (2013). "Social media as a destination marketing tool: its use by national tourism organisations." *Current issues in Tourism* 16(3): 211-239.
25. Othman, I., et al. (2013). Facebook marketing strategy for small business in malaysia. *Informatics and Creative Multimedia (ICICM), 2013 International Conference on*, IEEE.
26. Ng, C., et al. (2013). "Best practices in managing social media for business."
27. Safko, L., Brake, D.K.: *The Social Media Bible*. John Wiley & Sons Inc., Hoboken, New Jersey (2009)
28. Cook, N.: *Enterprise 2.0*. Gower Publishing, Ltd., Aldershot (2008)
29. Helms, R.W., Booij, E., Spruit, M.R.: *Reaching out: Involving users in innovation tasks through social media*. *Reach. Out* 5, 15–2012 (2012)
30. Prodanova, J., & Van Looy, A. (2017, September). A Systematic Literature Review of the Use of Social Media for Business Process Management. In *International Conference on Business Process Management* (pp. 403-414). Springer, Cham.
31. Wollan, R., et al. (2010). *The social media management handbook: Everything you need to know to get social media working in your business*, John Wiley & Sons.
32. Carmel, E., & Agarwal, R. (2001). Tactical approaches for alleviating distance in global software development. *IEEE software*, 18(2), 22-29.
33. DeFillippi, R. J., & Arthur, M. B. (1998). Paradox in project-based enterprise: The case of film making. *California management review*, 40(2), 125-139.
34. Iftikhar, R. (2017). Crisis management in project based organizations and mega projects: an integrated approach (Doctoral dissertation, LUISS Guido Carli).
35. March, J., & Sutton, R.I. (1997). Organizational performance as dependent variable. *Organizational Science*, 8 (6): 698-706.
36. Smet, H., Lagadec, P., & Leysen, J. (2012). Disasters out of the box: a new ballgame?. *Journal of Contingencies and Crisis Management*, 20(3), 138-148.

37. De Wit, A. (1988). Measurement of Project success. *International Journal of Project Management*, 6(3): 164-170.
38. De Bakker, K., Boonstra, A., & Wortmann, H. (2011). Risk management affecting IS/IT project success through communicative action, *Project Management Journal*, 42 (3): 75-90.
39. Freeman, R. E. (1984). *Strategic Management: A Stakeholder Approach*, Boston, Pitman.
40. Agarwal, N., & Rathod, U. (2006). Defining success for software projects: an exploratory revelation. *International Journal of Project Management*, 24 (4): 358-370.
41. Shenhar, A.J., Dvir, D., Levy, O., & Maltz, A.C. (2001). Project success: a multi- dimensional strategic perspective. *Long Range Planning*, 34 (6): 699-725.
42. Ice, R. (1991). Corporate publics and rhetorical strategies: the case of union carbide's Bhopal crisis. *Management Communication Quarterly*, 4(3): 341-362.
43. Faulkner, B. (2001). "Towards a framework for tourism disaster management." *Tourism management* 22(2): 135-147.
44. Coombs, W. T. (2014). *Ongoing crisis communication: Planning, managing, and responding*, Sage Publications.
45. Fink, S. (1986). *Crisis management: Planning for the inevitable*, American Management Association.
46. Sheffi, Y. (2015) Preparing for Disruptions through Early Detection, *Sloan Management Review*, 57, 1, 31-42.
47. Chan, J. C. (2014). "The Role of Social Media in Crisis Preparedness, Response and Recovery."
48. Wendling, C., et al. (2013). "The use of social media in risk and crisis communication."
49. Anderson, J. Q. and H. Rainie (2010). The future of social relations, Pew Internet & American Life Project.



# The MMUISD Gait Database and Performance Evaluation Compared to Public Inertial Sensor Gait Databases

Jessica Permatasari, Tee Connie and Ong Thian Song

Faculty of Information Science and Technology, Multimedia University, Malaysia  
1171402368@student.mmu.edu.my, tee.connie@mmu.edu.my,  
tsong@mmu.edu.my

**Abstract.** Gait recognition is an emerging biometric method that allows an automatic verification of a person by the way he or she walks. This paper presents a new dataset for gait recognition using mobile sensors called MMUISD Gait Database that resembles the real world as closely as possible. The existing public gait databases are acquired in controlled settings. In this study, an Android application is developed to record the human gait signals through inertial measurement unit sensor such as accelerometer and gyroscope with 50 Hz fixed sampling rate. A preliminary evaluation with 80 samples of participant's data is carried out to assess the gait recognition performance using the new dataset. Time and frequency domain are used to extract gait features from the raw sensors data. The accuracy is assessed using eight classifiers with 10-fold cross validation. The results show that phone positions and orientation affect the gait recognition performance. The MMUISD dataset that introduces such variability provides a good opportunity for researchers to further investigate these challenges.

**Keywords:** Inertial Sensor, Gait Recognition, Gait Dataset.

## 1 Introduction

In recent years, studies have been conducted on human gait for physical activity recognition, especially in the areas of healthcare systems, assisted living, biometrics and security [1]. There are two types of gait analysis: video-based and sensor-based. Due to the rapid development of smartphones including embedded sensors in the smartphone, sensor-based methods have received increased attention because it is unobtrusive and user friendly. Recent studies for human gait incorporate the fusion of Inertial Measurement Unit (IMU) sensors (accelerometer and gyroscope) to analyze the gait characteristics [1][2]. It is shown that the fusion of both sensors can improve the recognition performance as they complement each other. Moreover, it has been reported in [3] that the built-in accelerometer and gyroscope are very stable in performance based on evaluation with regards to the accuracy, precision, maximum sampling frequency, sampling period jitter and energy consumption.

However, most of the previous studies analyzed the motion sensors in controlled scenarios. For instance, the experiments were conducted with fixed sensor placements and predetermined fixed orientations [1][2][4][5][6], and with particular type of outfit and shoes [7]. In fact, it is not possible to control the orientation and the sensor placement in reality. Besides, it is important to note that the data were collected using the same phone [1][2][3][4][8][9]. This makes it difficult to confirm the superiority of an algorithm on a new dataset as different smartphone manufacturers use different types of sensors in their devices. The authors in [5] had conducted a test to assess the heterogeneities of mobile sensing for activity recognition with 13 different device models from four manufacturers. Although they used various device models, the experiment was performed under fixed laboratory settings.

This paper presents a new dataset called MMUISD Gait Database. The uniqueness of this dataset includes: (1) different types of Android phones were involved, (2) different phone placements, and (3) both the accelerometer and gyroscope signals were recorded. This paper is structured as follows. Section 2 describes the related work while the data collection experiments are elaborated in Section 3. Section 4 describes data preprocessing and the performance evaluation results. Finally, in Section 5 we summarize our conclusions and future research.

## 2 Related Work

### 2.1 Existing Public Gait Databases

The authors in [1] performed data collection by fixing the sensor placement. There were only a few participants in the study, and there were age range and gender biases. A study from [2] presented the largest database for human gait inertial sensor with a large number of participants, and wide range in gender and age. They used accelerometer data from smartphone for 408 subjects out of 744 subjects while the rest is collected with the IMUZ sensors (accelerometer and gyroscope). However, the sensor placement was fixed at the waist of the participants. Furthermore, [5] and [10] only explored the motion sensor from a single body position. The number of participants was limited, and the sensor was fixed at the waist. The sensor orientation was predetermined.

A comparison of the existing public inertial sensor-based gait datasets is presented in Table 1. Overall, the gait databases were collected under controlled environment due to several constraints from the smartphone to produce a reliable and consistent data collection. Hence, there is a need to collect real life data to ensure that the wearable sensor data can be used for real practical applications.

### 2.2 Gait Recognition Methods

Some researchers performed feature extraction on the time and frequency domains and classification was conducted with machine learning classifiers [1][5][10][11][12][13]. Apart from that, template matching approach with various distance metrics was also used to extract gait templates which represent the most defining characteristic of the subjects [5].

**Table 1.** Existing Public Gait Database

Dataset	Participants (Age/ Gender variation)	Smart-phone Type	Sensor Description	Activity
Pervasive [1]	10 (males, age 25 and 30)	Samsung S2 (i9100)	Portrait left and right pocket, right upper arm, right wrist, on the belt position with belt clip (Accelerometer and Gyroscope 50 Hz)	Walking, sitting, standing, jogging, biking, walking up/down stairs (each of activities 3-4 minutes)
UCI HAR [5]	30 (age 19-48)	Samsung S2	Waist (Accelerometer and Gyroscope - 50 Hz)	Walking, walking-upstairs, walking-downstairs, Sitting, standing, laying
UCI HAPT [10]	30 (age 19-48)	Samsung S2	Waist (Accelerometer and Gyroscope - 50 Hz)	standing, sitting, lying, walking, walking downstairs and walking upstairs with Postural Transition
OU ISIR [2]	408 (age 2-78, 219 males and 189 females)	Motorola ME860	Center back waist (Accelerometer 100 Hz)	Two different level-walk sequences (entering and exiting) on flat ground
Our Dataset (MMUISD)	299 (age 18 – 28, 246 males and 53 females)	Various Android phone	Carry by hand (left and right), place in trouser pocket (left and right), backpack and handbag (Accelerometer and Gyroscope – 50 Hz)	Walking on flat ground corridor with 3 different speed (slow, normal, fast)

In [1], the authors evaluated four feature sets using nine classifiers with WEKA 3.7.10. It was found that when the individual performance of the sensor was not very high, the fusion of sensors improved the overall recognition performance. Next, in [5], 561 features in time-frequency domain and ECDF were evaluated with four classifiers and cross validation. The result of the study showed that human activity recognition performance is significantly impaired by sensor handling heterogeneities and the type of recognition technique also played an important role. Meanwhile, a study from [10] used PrSVM classifier with TFilt to evaluate 561 features data for the Activity Learning

(AL) and Activity Transition Learning (ATL). The performance of their proposed architecture was measured with the system error at different locations of the architecture pipeline and they obtained 3.64% and 3.22% for the system error for AL and ATL, respectively. On the other hand, a study from [2] used gait periodic detection from previous research study and calculate the similarity score with two normalized distance measures and two unnormalized distance measures. The magnitude of a 3D accelerometer signal was used for the evaluation since change of sensor orientation does not affect the magnitude of signal. The performance result was evaluated using receiver operating characteristic (ROC) curve and it can be concluded that the authentication performance was slightly influence by the position of the accelerometer since the acceleration depends on the location of the sensor.

### 3 Data Collection

An Android application was developed to capture the data with 50 Hz fixed sampling rate. Studies have shown that this sampling rate is sufficient for activity recognition [1]. The definition of a realistic world scenario is quite subjective so several studies have been conducted [14][15] to know how smartphone users often carry or place their phones. We also conducted an online survey to decide the sensor placement [16] based on the participants' top voted choices.

The dataset was taken in Indonesia and Malaysia. The reason for this is to have a larger dataset comprising of individuals from different races, geographies and environments which increases the diversity of habitual gait. A total of 299 undergraduate IT and Engineering students (246 males and 53 females) with ages ranging from 18 – 28 years participated in the database collection process. Informed consents were obtained for data collection for the ethical conduct as part of the regulation of Multimedia University.

The participants were formed in groups to make the data collection process more organized. Each of the participant was asked to install the application on their phones. If the participant's phone was not equipped with both sensors (some of the smartphones only have accelerometer but not gyroscope), the other group member's phone was used.

The data collection process was carried out in a corridor inside the university building. The phones were fixed at six positions, i.e. left and right pocket, in a hand carry bag, in a backpack, and in the left and right hand (see Fig. 1). Each subject performed three different walking speeds: slow walk, normal walk and fast walk. The participants were told to walk naturally for the three walking speeds without any constraints. It took around 5-8 minutes for each subject to perform all the walks at 3 different walking speeds. In the transition to change the walking speed, they were asked to stop for 3 seconds at the turning points before walking back to the initial point.

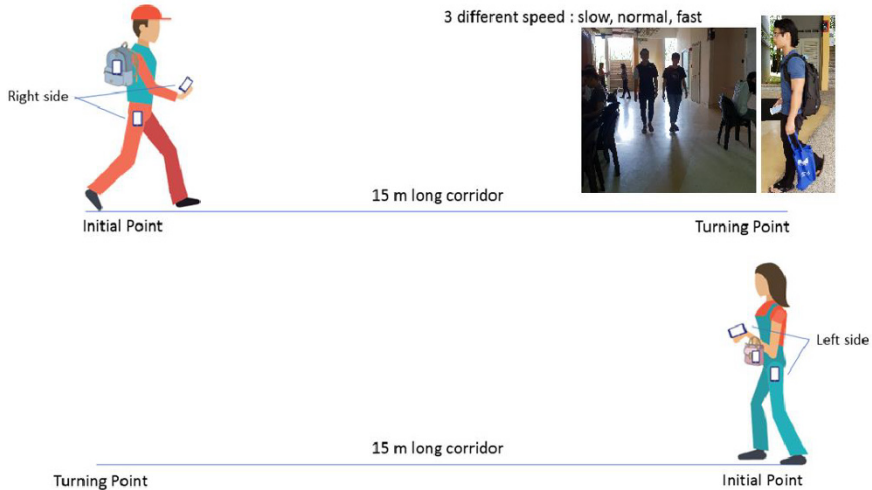


**Fig. 1.** The data collection protocol with an overview of the phone positions on a participant.

## 4 Data Preprocessing and Performance Evaluation Analysis

Eighty participant's data (40 data from Indonesia and Malaysia, respectively) were selected randomly from the MMUISD gait database for preliminary evaluation due to time constraints in preparing the data for full performance evaluation. For a fair comparison, the results are compared to the existing public gait databases using the same protocol including data preprocessing methods and classifiers (except for [5] and [10] as the datasets already contained 561 extracted features). The comparison of recognition accuracy shows the difficult level of our dataset as our dataset contains noise and orientation problems (i.e. screen rotation during walk when carried with hand or put in the handbag or backpack). Furthermore, we did not perform any algorithm to overcome the orientation problem.

### 4.1 Data Preprocessing

Some noise (abnormal spikes) occur when the application is first started. After the completion of the walking activity, some irrelevant signals also occurred due to non-gait related activity like putting the smartphones away when the application is stopped. Additionally, when the participants need to repeat the same walk and perform a turn, this also causes some noise during the transition. Therefore, some noise removal processes are required to remove the noise. First, the raw signal is segmented into three parts: slow, normal, and fast. The signal is manually segmented by observing the abnormal spikes which denotes the transition between changes in walking speed. After segmentation, the signals from the three axes of accelerometer and three axes of gyroscope are normalized with z-score as shown in Equation 1.

$$Z_i = \frac{x_i - \bar{x}}{\sigma} \quad i \in x, y, z. \quad (1)$$

$$m = \sqrt{x^2 + y^2 + z^2} \quad (2)$$

The resultant vector from the magnitudes of individual acceleration and gyroscope is calculated using Equation 2 from the normalized data in order to minimize the effect caused by orientation changes [1][17]. Thus, each sensor will have four dimensions, i.e. ( $x, y, z, magnitude$ ). A window containing 100 data points with 50% overlap is selected to extract different features which represent the characteristics of gait signal in time and frequency domain [1][18]. The extracted features include mean, standard deviation, variance, minimum value, maximum value, auto correlation mean, auto correlation standard deviation, auto covariance mean, auto covariance standard deviation, skewness, kurtosis, median absolute deviation, root mean square, interquartile, entropy, energy and sum of first five FFT coefficients. Thus, a total of 136 features were used to represent the gait signatures.

## 4.2 Performance Evaluation Analysis

The recognition performance is evaluated using eight baseline classifiers. The true positive rate given by Equation 3 is used as the evaluation metric,

$$TPR = \frac{(TP+TN)}{N} \quad (3)$$

The features data are divided into 80% training and 20% testing. Then with 10-fold CV each feature vector was randomly assigned to one of the 10 subsets. The study will classify user ID using machine learning algorithms. The classifiers used to measure the accuracy include Logistic Regression (LR), Linear Discriminant Analysis (LDA), Multi-layer Perceptron (MLP), Decision Tree (DT), Random Forest (RF), Gaussian Naive Bayesian (NB), Gradient Boosting (GB) and Support Vector Machine (SVM). The short notations for the classifiers are used for brevity henceforth.

The accuracies on the different datasets are presented in Table 2. The results reveal several important observations. First, OU ISIR dataset yields the lowest accuracy among the other dataset, this shows that the wide range of age and gender, and a larger dataset influenced the gait recognition performance. Second, Pervasive dataset yields the highest accuracy for Random Forest and Linear Discriminant Analysis classifier among the others dataset. This is possible because the number of samples is small (containing only 10 participants). Moreover, the sensor was placed at the participant's bodies thus the orientation is fixed and contains less noise. Note that this scenario is not always possible in a practical situation. Third, the classification accuracy might be improved with the total number of features (refer to UCI HAR and UCI HAPT with 561 features respectively). However, higher number of features only make the computation time longer.

In Table 2, “MMUISD Normal” trial refers to the performance evaluation of our dataset for normal walking speed using all sensor positions, which are phone in pocket, carry by hand, backpack, handbag or goody bag. Our dataset gives a relatively lower accuracy as compared to the existing public gait datasets except OU ISIR. This shows

our new dataset impose challenges for gait recognition. The reason why the results for OU ISIR is lower than MMUISD is because the OU ISIR dataset contains a much larger subjects as compared to our dataset. Besides, the OU ISIR dataset only contains accelerometer signal while MMUISD contains both accelerometer and gyroscope signals. The fusion of both sensors might also lead to better performance of the MMUISD dataset.

**Table 2.** Classification accuracy for existing public gait database.

Trial	LR	MLP	SVM	DT	RF	GB	LDA	NB
OU ISIR	16.67	1.96	0.25	4.41	<b>26.72</b>	4.17	26.23	9.07
UCI HAR	77.09	91.21	80.56	81.1	<b>92.32</b>	84.84	72.47	21.96
UCI	74.13	75.74	79.60	79.66	<b>90.21</b>	82.11	69.75	21.68
HAPT								
Pervasive	98.75	99.38	95.62	98.12	<b>99.38</b>	96.88	<b>99.38</b>	98.75
MMUISD	42.36	28.82	1.41	38.84	<b>53.87</b>	53.69	51.76	25.13
normal								

Next, we assess the performance of the MMUISD dataset by segregating the phone signals by walking speed and sensor position. Short notations as seen in Table 3 are used to represent the results in Tables 4 to 6 for each activity in the dataset collection process. For example, “Slow\_L1” refers to the data for slow walking speed with the sensor in the left of the front pocket.

**Table 3.** Short notation for walking speed and sensor position.

Notation	Description
L	Left
R	Right
1	Pants front pocket
2	Backpack
3	Hand bag or goody bag
4	Carry by hand

Tables 4 to 6 present the results for slow, normal and fast walking speed for all positions. We analyze the sensor positions for slow, normal, and fast walking speed to see which sensor position gives the best result and which classifier has the best performance. We observe that the performance trends between the left and right pocket position, and also between the left and right carry by hand position are quite similar. This result reaffirms findings in the previous studies [1]. In Tables 4 to 6, the LDA classifier shows the highest accuracy for the all sensor positions, meanwhile the lowest accuracy is reported for SVM. To the best of our knowledge, the success of the classification does not depend on the classification method, but rather on the nature of the data. For some data, one technique might perform better, for another sample it will be another technique. This finding is also consistent with the results reported by [13].

**Table 4.** MMUISD classification accuracy for the slow walking speed.

Trial	LR	MLP	SVM	DT	RF	GB	<b>LDA</b>	NB
Slow_2	58.27	11.81	0.24	38.58	49.61	33.86	<b>85.83</b>	57.48
Slow_3	40.16	11.02	0.09	23.62	33.07	19.69	<b>62.28</b>	39.37
Slow_L1	59.84	12.69	0.37	36.22	51.97	30.71	<b>86.61</b>	59.84
Slow_R1	57.48	9.45	0.28	44.09	48.82	29.13	<b>87.49</b>	51.97
Slow_L4	46.46	11.02	0.19	23.62	31.59	16.54	<b>77.17</b>	44.88
Slow_R4	53.54	14.17	0.13	33.86	43.31	32.28	<b>80.31</b>	55.12

**Table 5.** MMUISD classification accuracy for the normal walking speed.

Trial	LR	MLP	SVM	DT	RF	GB	<b>LDA</b>	NB
Normal_2	69.29	27.56	0.16	51.97	71.65	47.24	<b>83.79</b>	62.29
Normal_3	25.27	11.81	0.89	15.75	33.07	17.32	<b>66.93</b>	37.86
Normal_L1	61.42	25.98	0.76	51.18	68.59	48.03	<b>80.55</b>	59.06
Normal_R1	58.73	13.49	0.57	45.24	58.73	36.51	<b>80.48</b>	64.29
Normal_L4	52.76	19.69	0.68	33.86	42.52	33.86	<b>80.31</b>	46.46
Normal_R4	48.82	18.95	0.54	32.28	44.09	29.92	<b>81.18</b>	54.33

**Table 6.** MMUISD classification accuracy for the fast walking speed

Trial	LR	MLP	SVM	DT	RF	GB	<b>LDA</b>	NB
Fast_2	67.13	35.66	1.39	48.25	67.83	51.75	<b>86.01</b>	67.83
Fast_3	39.64	15.32	0.12	18.92	30.63	18.92	<b>66.67</b>	34.23
Fast_L1	65.77	31.53	0.91	40.54	63.96	44.14	<b>83.69</b>	52.25
Fast_R1	51.58	26.32	0.89	45.26	57.89	32.63	<b>82.11</b>	48.42
Fast_L4	50	32.54	17.46	32.54	40.48	33.33	<b>73.02</b>	39.68
Fast_R4	43.65	26.98	16.67	39.68	40.48	35.71	<b>75.4</b>	49.21

The results for handbag or goody bag yield the poorest performance as compared to the other positions. The performance result for backpack is better than goody bag or hand bag, and is almost similar to the results of the other positions. During the data collection process, the participants used their own backpack which was usually filled with belongings. This could be the reason why the performance for backpack is better than handbag or goody bag position. The movement of the sensor in the backpack is limited by other objects inside the backpack. On the other hand, the handbags and goody bags provided to the participants are empty which cause large oscillation when the participants walk. This results in undesirable patterns like spikes in the gait signal due to irrelevant movements such as swinging of the bags while walking.

#### 4.3 Discussion

There are several interesting observations from the experimental results:

- The highest accuracy was achieved for the backpack, left and right pocket sensor positions. This suggests that putting the phone in such positions (like inside the pants pocket and backpack) produces data that are easier for gait recognition. In

comparison, for the phones being carried by both the left and right hands yield poorer performance, but it performs better as compared to the sensor placed inside the hand bag or goody bag.

- Phone orientation plays an important role for the recognition performance this finding reaffirms with the previous studies in [19]. For example, result for phones placed inside the pocket is better than that carried by hands. Phones in hands are subject to higher variation in their orientations due to hand swaying movement.
- Different type of Android phone does not affect the classification performance as we observed the results from gait recognition performance in Tables 4 to 6 show almost similar pattern even though the data are from various phones. The findings also show that regardless of the walking speed, the highest accuracy achieved is still dependent on phone positions.
- The fusion of accelerometer and gyroscope helps to improve the gait recognition performance, this finding goes in line with previous study in [20]. The results for public gait database (from smartphones) containing only signal from a single sensor [2] produces inferior results compared to dataset comprising both accelerometer and gyroscope signals [1][5][10].

## 5 Conclusion and Future Work

The construction of a gait database that resembles the real world as closely as possible is described in this paper. Preliminary evaluation is conducted to compare the gait recognition performance between varying phone placements and walking speeds. The results are also compared with the benchmark gait databases. Preliminary analysis shows that the proposed dataset can contribute to the gait recognition research community to develop techniques to overcome the sensor position and orientation problems. Compared to previous works, we provide researchers with a challenging dataset to meet the demand of practical application. More samples from more volunteers will be incorporated as this research is still on-going. Further study will be performed to improve the gait recognition performance using our dataset with respect to real practical scenario.

## References

1. M. Shoaib, S. Bosch, O. Durmaz Incel, H. Scholten, and P. J. M. Havinga: Fusion of smartphone motion sensors for physical activity recognition. *Sensors (Switzerland)*, vol. 14, no. 6, pp. 10146–10176 (2014).
2. T. T. Ngo, Y. Makihara, H. Nagahara, Y. Mukaiigawa, and Y. Yagi: The largest inertial sensor-based gait database and performance evaluation of gait-based personal authentication. *Pattern Recognit.*, vol. 47, no. 1, pp. 228–237 (2014).
3. Zhizhong Ma, Yuansong Qiao, B. Lee, and E. Fallon: Experimental evaluation of mobile phone sensors. (2013).
4. K. Davis *et al.*: Activity recognition based on inertial sensors for Ambient Assisted Living. In: *19th International Conference on Information Fusion (FUSION)*, pp. 371–378 (2016).

5. A. Stisen *et al.*: Smart Devices are Different: Assessing and Mitigating Mobile Sensing Heterogeneities for Activity Recognition. *Proc. 13th ACM Conf. Embed. Networked Sens. Syst. - SenSys '15*, pp. 127–140 (2015).
6. H. Zhao *et al.*: Adaptive gait detection based on foot-mounted inertial sensors and multi-sensor fusion. *Inf. Fusion* (2019).
7. M. Muaaz and R. Mayrhofer: Smartphone-Based Gait Recognition: From Authentication to Imitation. *IEEE Trans. Mob. Comput.*, vol. 16, no. 11, pp. 3209–3221 (2017).
8. D. Anguita, A. Ghio, L. Oneto, X. Parra, and J. L. Reyes-Ortiz: A Public Domain Dataset for Human Activity Recognition Using Smartphones. *Eur. Symp. Artif. Neural Networks, Comput. Intell. Mach. Learn.*, no. April, pp. 24–26 (2013).
9. M. F. Nowlan: Human Identification via Gait Recognition Using Accelerometer Gyro Forces. *Yale Comput. Sci. http://www.cs.yale.edu/* ..., p. 8 (2009).
10. J. L. Reyes-Ortiz, L. Oneto, A. Samà, X. Parra, and D. Anguita: Transition-Aware Human Activity Recognition Using Smartphones. *Neurocomputing* (2016).
11. E. Rastegari, S. Azizian, and H. Ali: Machine Learning and Similarity Network Approaches to Support Automatic Classification of Parkinson's Diseases Using Accelerometer-based Gait Analysis. In: *Proceedings of the 52nd Hawaii International Conference on System Sciences* (2019).
12. T. T. Shiva Sharif Bidabadi, Iain Murray, Gabriel Yin Foo Lee, Susan Morris: Classification of foot drop gait characteristic due to lumbar radiculopathy using machine learning algorithms. *Gait & Posture*, vol. 71, pp. 234–240 (2019).
13. K. N. K. A. Rahim, I. Elamvazuthi, L. I. Izhar, and G. Capi: Classification of human daily activities using ensemble methods based on smartphone inertial sensors. *Sensors (Switzerland)* (2018).
14. F. Breitinger and C. Nickel: User Survey on Phone Security and Usage. *Biosig*, no. May 2010, pp. 139–144 (2010).
15. M. Redmayne: Where's your phone? A survey of where women aged 15-40 carry their smartphone and related risk perception: A survey and pilot study. *PLoS One*, vol. 12, no. 1 (2017).
16. Survey about sensor placement, <https://goo.gl/forms/HIHlcWss3SKt4BGh1%0A>, last accessed November 2018
17. T. Hoang and D. Choi: Secure and privacy enhanced gait authentication on smart phone. *Sci. World J.* (2014).
18. I.-H. Youn, K. Won, J.-H. Youn, and J. Scheffler: Wearable Sensor-Based Biometric Gait Classification Algorithm Using WEKA. *J. Inf. Commun. Converg. Eng.* (2016).
19. R. Subramanian and S. Sarkar: Evaluation of Algorithms for Orientation Invariant Inertial Gait Matching. *IEEE Trans. Inf. Forensics Secur.*, vol. 14 (2018).
20. A. Jain and V. Kanhangad: Gender classification in smartphones using gait information. *Expert Syst. Appl.* (2018).



# Brief of Intrusion Detection Systems in Detecting ICMPv6 Attacks

Adnan Hasan Bdair<sup>1</sup>, Rosni Abdullah<sup>2</sup>, Selvakumar Manickam<sup>1</sup>, and Ahmed K. Al-Ani<sup>1</sup>

<sup>1</sup> National Advanced IPv6 Centre (NAv6), Universiti Sains Malaysia, Penang, 11800, Malaysia

<sup>2</sup> School of Computer Sciences, Universiti Sains Malays, Penang, 11800, Malaysia

adnan@nav6.usm.my

**Abstract.** Network security, amongst other security issues, essentially requires implementing Internet Protocol version 6 (IPv6). Cybercriminals always hunted for methods and means to unfairly benefit from this new technology. IPv6 is an improved protocol because it has built-in security mechanisms compared to Internet Protocol version 4 (IPv4). However, IPv6 has similar susceptibilities, which are inherited from several features of IPv4. Another issue involves that the new functionalities and procedures, which are found in IPv6, depend on Internet Control Message Protocol version 6 (ICMPv6). A common vulnerability is the Denial of Service (DoS) attack. A combination of zombie hosts can form a Distributed Denial of Service (DDoS). The DoS and DDoS attacks often represent substantial hazards in today's Internet as they can cause serious damages to organizations and disrupts Internet services. This research aims to provide a brief review of the latest studies and investigates on the detection in IPv6 networks using ICMPv6 messages and DoS, as well as DDoS attacks. Moreover, this work aims to introduce the proposed techniques, which utilized the Intrusion Detection System (IDS) in an effort to combat cyber-attacks.

**Keywords:** Intrusion Detection System (IDS), IPv6, ICMPv6, DoS, DDoS, flooding, security.

## 1 Introduction

Internet users worldwide have witnessed unpredictable changes in new networking technology [1]. Connectivity, which arises from networks and new technology, has reached into many homes and businesses. However, the security systems that are implemented to protect data and privacy are not adequate. Cyber attackers have found vulnerabilities in several software applications [2]. Nowadays, cybersecurity is a new research area. Traditional TCP/IP networks are no longer the hype. New features like the Internet of Things (IoT) have, therefore, opened more vulnerabilities [3].

One of the limitations of IPv4 is the small available pool of addresses for devices. With IoT, many devices cannot be connected using IPv4. To overcome this limitation, Internet Engineering Task Force (IETF) engineers proposed IPv6 [4]. IPv6 has auto-configuration and mobility, as well as overall extensibility. IPv6 can support boundless

devices, which are connected directly to the Internet [5]. It tackles the limitations of IPv4 addressing scheme [6]. It is likely that IPv6 will become dominant as users want more connection of devices. Fig. 1 shows that in 2017, the number of clients, who used Google services via IPv6, surpassed 21% and it is expected that this percentage will increase [7].

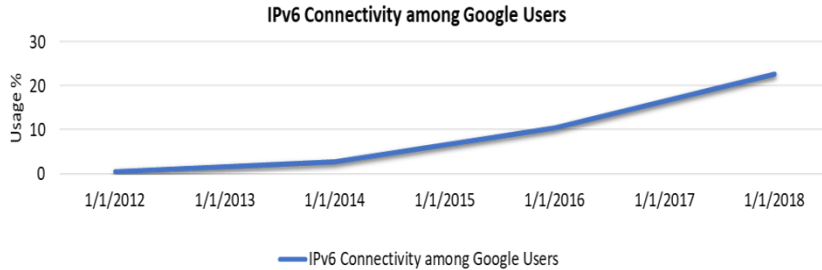


**Fig. 1.** IPv6 users on Google services

One feature called the Neighbor Discovery Protocol (NDP) was introduced by IPv6. The host's NDP is an auto-configuration, which generates its own IPv6 address for a device once the device is connected to a network [8]. Essentially, the NDP protocol uses ICMPv6 messages to detect the new device. Part of the ICMPv6's function is to detect neighbor and router discovery. It can also perform diagnostics and error reporting of packets sending [9]. What happens in a DoS attack on a node that is used for e-mail and Internet shopping is that the node is no longer able to establish the network connection. Imagine what happens to users if major online retailers are denied accessibility. Fig. 2 shows that DoS attacks constitute most of the attacks against IPv6 [10].

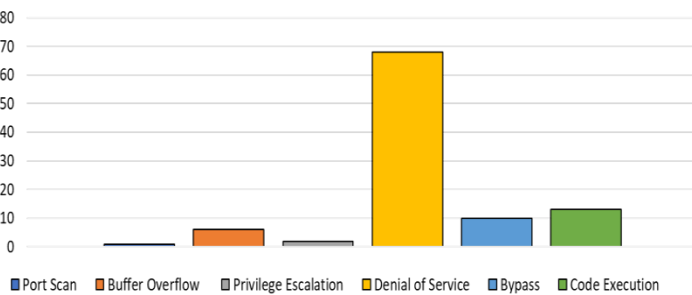


**Fig. 2.** IPv6 vulnerability classes

To overcome the DoS and DDoS vulnerability issues, [4] Prevention can be one method, which avoids the loss of business transactions caused by such attacks. Source address spoofing or preventing address stealing is through the network's policy enforcement [11]. To investigate how this spoofing takes place, a discussion on ICMPv6

is certainly needed as the ICMPv6 represents the IPv6's core. It is the protocol of communication in IPv6. Messages are sent and received via ICMPv6 from host to devices and vice-versa. Without ICMPv6, IPv6 is useless. Therefore, the vulnerabilities of ICMPv6 can be recognized and attacked [12]. Network security involves firewalls and antivirus, as well as the well-known IDS, i.e., the intrusion detection system, which aims at blocking traffic that is unpermitted. However, IDS is the most popular security technique. Generally, this technique has two groups. The first is the HIDS, i.e., the host-based IDS, whereas the second group involves the NIDS, i.e., the network-based IDS [13], [14]. In this paper, the ICMPv6 attack is highlighted and summarized. This attack is considered one of the most important protocols, and it is the backbone of IPv6. The focus is on the causes of difficulty in detection and the rate of accuracy in the discovery and what patterns and methods can solve this problem.

This research paper falls into five sections. Section 2 provides new IPv6 improvements alongside effects on the security of the network. Also, the IPv6 protocol's typical attacks are presented and explained. Section 3 discusses the significance of ICMPv6, ICMPv6-based DoS, as well as DDoS attacks, which are explained comprehensively with classification and discussion on the current DoS/DDoS attacks according to ICMPv6 messages. Section 4 reviews the intrusion detection flooding attacks, as well as the types of the intrusion detection system, particularly the task of ICMPv6 messages. Section 5 concludes this work and provides recommendations for further research.

## 2 Internet Protocol version 6 (IPv6)

The Internet has been increasingly sought-after with an ever-growing Internet penetration via smart devices that are hand-held, with the increase of Internet users and devices, additional IP addresses which are assigned, have become a necessity. A new protocol called IPv6 was introduced to enhance the issue of addressing and the communications of the network in 1998 [5]. IPv6 is supposedly more efficient in relation to the security of IPv4 due to its built-in mechanism of security such as IPsec. The Internet Society (ISOC) announced World IPv6 Launch Day on June 6, 2012. Regarding IPv6, it possesses a specific format, which involves a simpler, as well as smaller fixed header. It can achieve processing that is faster in the routers across the path's packet transmission. The IPv6 mechanism replaced the limited Option Field in the IPv4 header with Extension Headers. These headers are more flexible; they are extensible because they are not parts of the chief header. Thus, it involves a couple of extension headers, including the Authentication header, as well as the Encapsulation Security Payload [15]. Neighbor Discovery Protocol (NDP) is dependent upon the Internet Control Message Protocol version 6 (ICMPv6) protocol messages. Nevertheless, IPv6 has inherited several IPv4 features [16], [17] have made the IPv6 security a challenge for implementers. The support for IPsec in IPv6 at the specification level may look like the IPv6 mechanism is much more secure in comparison with IPv4. However, [18] this is not the real case. The in-depth analysis aims to clarify the security posture of IPv6 compared to a similar security posture of IPv4 [19], [20]. Vulnerabilities specific to IPv4 and IPv6 do exist and these are analyzed. Moreover, IPv6 networks require additional security measures

and security tools with additional capabilities to achieve a security posture at parity [21]. Numerous changes in the IPv6 protocol's specifications may result in problems of potential security. There are several attacks that are encountered by IPv6, including the DoS/DDoS flooding attack as explained in the following subsection

## 2.1 DoS/DDoS Flooding Attacks on IPv6

Flooding attacks are originated from DoS, as well as DDoS. DoS attack involves disconnecting access to the services of a machine. The attack is to suddenly swamp the target machine with as many packets as possible. Therefore, the machine won't be able to respond to users. DoS usually happens in a system or a network. The distributed DoS attack is different. Devices are remotely controlled and act like zombies, where attackers concurrently initiate attacks from these devices. It happens from many systems of networks as shown in Figure 3 [24]. Traffic patterns change when there are DoS/DDoS attacks. Network security management is to detect these attacks when anomalies in network traffic are observed. There is much diversity in the scope of the attack on the victim [25], [26] and it is difficult to detect the attackers.

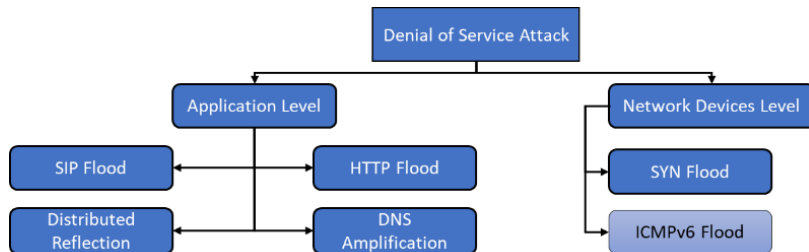


**Fig. 3.** Classification of DoS attacks

## 3 Internet Control Message Protocol version 6 (ICMPv6)

According to [24], the ICMPv6 represents a specific part of the Internet Protocol Suite in IPv6 as described by [27]. ICMPv4 messages function as diagnostic messages, which test, control purposes or error messages, and report the conditions in the operations of IP back to the original IP address. ICMPv6 copies this strategy from ICMPv4. According to [9], ICMPv6 has incorporated specific protocols, which are independent in the IPv4. The total number of messages of both versions are 256 messages. In version 4, regarding the Type of value and the message type, there is no relationship. However, version 6 error messages possess a Type value from 0 to 127 and the informational messages from 128 to 255. According to [19], ICMPv6 messages can be transported via IPv6 packets. In these packets, the IPv6 Next Header value for ICMPv6 is put to 58. The corresponding ICMPv6 equivalents to ICMPv4 messages are shown in Table 1.

ICMPv6 for the IPv6 Specification [9] uses the ICMP as defined for IPv4. In ICMPv6, the IPv6 Next Header value is set to 58 in the directly preceding header. With

the changes, every IPv6 node must implement all the behavior and messages required. These changes make ICMPv6 part of IPv6. The ICMPv6 are shown in Figure 4.

Neighbor Discovery Protocol (NDP) was introduced by IPv6. The NDP is vulnerable to exploitation [28]. It consists of five types of messages, including router advertisement (RA), router solicitation (RS), neighbor advertisement (NA), neighbor solicitation (NS), and redirect message. All the hosts in the IPv6 network can communicate via these five types of messages [29], [30]. The health of the network is made known through ICMPv6, which communicates error conditions. The servers can receive the information on the path of the network or request connection [31] through ICMPv6. The IPv6 heavily relies on the NDP, which is shown in the network in an ICMPv6 form. The IPv6 cannot operate if ICMPv6 is disabled [21], [29], [32]. Throughout auto-configuration of address in a network of IPv6 link-local, the hosts use ICMPv6 [33] message types to communicate with the neighboring hosts. However, studies [9], [34] revealed that the messages of ICMPv6 are susceptible during the process of duplicate address detection, whereby each host aims at configuring its own generated interface identifier. At this level, the attacker can misuse this process of duplication and change the content of these ICMPv6 messages.

**Table 1.** ICMPv4 vs. ICMPv6 equivalents [29]

No	ICMPv4 Message	ICMPv6 Equivalent
1	Destination inaccessible -Network unreachable (Type 3, Code1).	Destination inaccessible - No route to destination (Type 3, Code 0).
2	Destination inaccessible – Host Unable to be reached (Type 3, Code 1).	Destination inaccessible - Address inaccessible (Type 3, Code 1).
3	Destination inaccessible – Protocol Unable to be reached (Type 3, code 2)	Parameter problem unrecognized next header field (Type 4, Code 1)
4	Destination inaccessible – Port Unable to be reached (Type 3, Code 3).	Destination inaccessible – Port Unable to be reached (Type 1, Code 4).
5	Destination inaccessible – Fragmentation needed and DF set (Type 3, Code 4).	Packet Too Big (Type 2, Code 0)
6	Destination Unable to be reached-Communication with host administratively prohibited (Type 3, Code 10).	Destination Unable to be reached-Communication with destination administratively prohibited (Type 1, Code 1).
7	Source Quench (Type 4, Code 0).	This message is not implemented in IPv6.
8	Redirect (Type 5, Code 0).	Neighbor Discovery Redirect message (Type 137, Code 0).
9	Time Exceeded-TTL expired (Type 11, Code 0)	Time Exceeded-Hop Limit exceeded (Type3, Code 0).
10	Time Exceeded-Fragmentation timer expired (Type 11, Code 1).	Time Exceeded-Fragmentation timer exceeded (Type 3, Code 1)
11	Parameter Problem (Type 12, Code 0)	Parameter Problem (Type 4, Code 0 or Code 2).

DoS attacks are generally categorized into distinct groups. In [4], [35], DoS attacks have four divergent criteria, including 1) vulnerability of protocol, 2) the rate dynamics of attacks, 3) the degree of automation of the attacks, and 4) impact. First, in the exploited area of vulnerability, DoS attacks have four classes: protocol exploitation, amplification attacks, malformed packet attacks, as well as flood attacks. The second classification draws upon the rate dynamics of the attack. They are classified in accordance with exploited vulnerabilities, which are utilized in the attacks and directly related to DoS and DDoS attacks. Third, DoS attacks have three subgroups: manual and semiautomatic, as well as automatic. Fig.4 shows the categories of ICMPv6 DoS attacks.

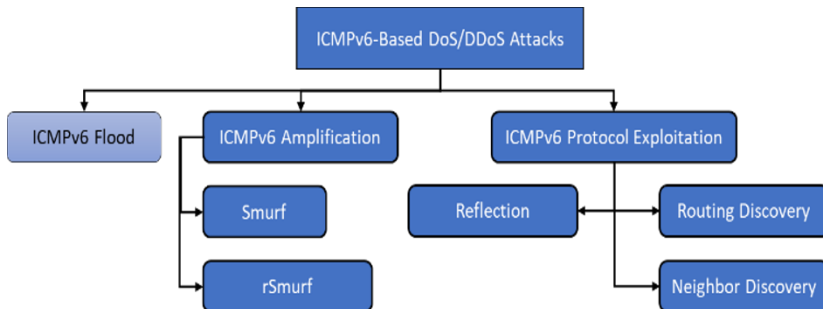


**Fig. 4.** Categories of ICMPv6-based DoS and DDoS attack

### 3.1 ICMPv6 Protocol Exploitation

This section discusses the exploitation of ICMPv6 specifications. If any node sends an ICMPv6 router advertisement (RA) packet, it can claim that it is a router. Attackers exploit this feature to perform the man-in-the-middle (MITM) attack by disguising as a router. The ICMPv6 protocol features, which can be exploited, are as follows: neighbor discovery packets that are the NS (ICMPv6 type 135) in addition to the NA (ICMPv6 type 136). For the DoS/DDoS attacks, intruders exploit the router discovery packets that are the RS (ICMPv6 type 133), the RA (ICMPv6 type 134), as well as the redirect packet (ICMPv6 type 137).

### 3.2 ICMPv6 Amplification Attacks

In ICMPv6 specifications, a defined multicast address can represent a group of IPv6 addresses [36]. An intruder needs only generate a small number of packets to create an amplification attack using the multicast feature. Currently, the amplification attack is still under research for a solution; it is shared in the IPv4 and in the IPv6 [23].

### 3.3 ICMPv6 Flooding Attack

ICMPv6 flooding attack involves swamping the node with huge traffic amounts as quickly as possible. The affected node will try to process all the requests and this, in turn, will make it unresponsive. The flooding attack is a very common attack in the IPv6 and IPv4 networks. When the bandwidth and the resources of the targeted server or the router are taken up, it will not respond to legitimate users [4], [22]. Intruders exploit traffic from ICMPv6 packets with a source address referring to another IPv6 node or to a used address [37]. Intruders can change source addresses to make it difficult to identify them. They exploit the notification messages of ICMPv6 error of the hosts, as well as the routers to distribute packets into the network. A simple tweak of ICMPv6 informational messages such as ECHO request and ECHO reply, the router advertisement (RA), the neighbor solicitation (NS), the neighbor advertisement (NA), and the multicast listener discovery messages can do the flooding [38].

Each flooding DoS attack is distinct and can be differentiated. An attack only affects the particularly targeted node, whereas other forms of attacks affect the targeted node plus other nodes. Another type of DoS attack involves creating an NS storm into the node and an NA packets' storm into the network. This will eat up the bandwidth and the system processor. The existing solutions involve a highly false-positive rate, as well as low accuracy based on the following reasons.

Firstly, it is hard to find similarities between normal traffic and abnormal packets. According to [39], flooding-based DDoS attack detection is the main challenge. These types of attacking mechanism are exploited based on huge resources between the Internet and a target server. The server should deal with all the fake requests, and this will bring it down making public users frustrated. Secondly, it is hard to detect suspicious anomalies and features in network traffic patterns.

According to [39] [40], the flooding attack is generated by ICMPv6 sending excessive numbers of packets of error messages to their destinations. Therefore, established communications are disrupted when sessions are dropped. One of the major challenges in fast network security management is detecting suspicious anomalies in network traffic patterns because of DDoS attacks that decrease the network performance.

## 4 Intrusion Detection System for ICMPv6

Intrusion detection uses a set of parameters with the aim of testing and analyzing the network traffic. The analysis should suspect network transactions. This is a software application that checks all traffic patterns and tries to highlight suspicious activities. The steps of a typical IDS involve 1) data collection, 2) data analysis, and 3) what actions that should be taken. There are two types of IDS according to the network installation position, including the NIDS (Network-based IDS), as well as the HIDS (Host-based IDS) [41], [42]. Fig.5 illustrates the steps of a typical IDS.

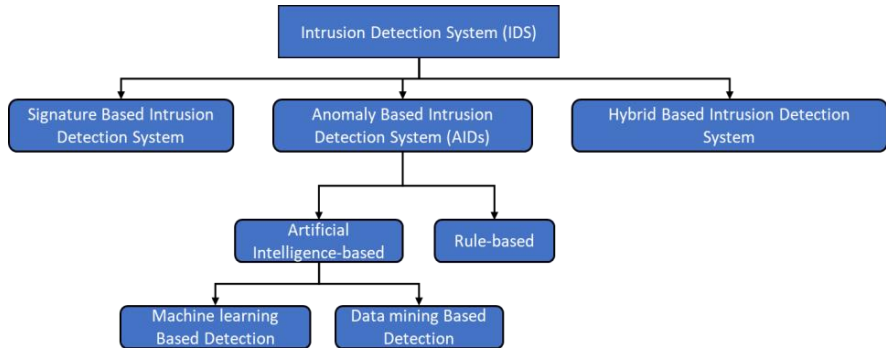


**Fig. 5.** The available IDS techniques

Based on the literature, IDS has three types: 1) signature-based, 2) anomaly-based, and 3) hybrid-based [50]. Each type is discussed in the following subsections.

#### 4.1 Signature-Based Intrusion Detection System (SIDS)

An attack has a signature or pattern. Events are compared and matched to a database. If a pattern exists in the database, then there is a match. However, new attacks cannot be detected. This requires that the new attack signature is recorded, then updated into the database. This approach involves two key disadvantages, including a) the database, which needs to be updated and b) new attacks cannot be discovered [44].

Originally [42], Snort was used in detecting IPv4 attacks and Version 2.8 is the first IPv6 version. Support continued with newer versions to include more IPv6 features. The first stage of the architecture is called the pre-processor stage, where a list of suspicious activities are identified in the network [45]. The second stage involves pattern matching and the written rules are applied in the detection engine onto the detection parameters. The original detection engine design remains the same for both IPv6 and IPv4. Only the IPv4 values are replaced with their similar IPv6 values. In Snort databases, IPv4 attack signatures are still available. Snort continues to tackle the IPv6 attacks, which are identical to the attacks that are encountered in IPv4. Therefore, Snort cannot distinguish between IPv4 and IPv6 attacks. Recently, the Snort detection engine was found to be ineffective [46] when it was tested on IPv6 attacks in an experiment by [47]. Half of these attacks that were executed, including DoS and DDoS attacks, were not detected [30].

According to [48], Snort v2.9.7 with Open Source NIDS new features, including IPv6, can detect certain attacks against IPv6-specific protocol mechanisms, i.e., DoS/DDoS attacks. Moreover, it can analyze real-time traffic, as well as packet logging on the IP networks and a rule-based attack detection mechanism can, therefore, be provided. It can also detect whether a DoS or DDoS attack is present in the network based on the behavior of DoS/DDoS as shown in Fig 6.

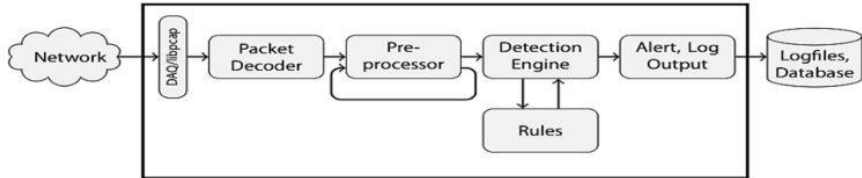


**Fig. 6.** Snort IDS architecture

The project of BRO was introduced by [49]. It is an Open Source IDS with the aim of monitoring suspicious behavior in network traffic [50]. BRO version 0.8 can support IPv6. However, BRO is used for IPv4 traffic but not IPv6. New rules cannot be specified for the characteristics of IPv6 packets, including DoS and DDoS attacks [47]. The low accuracy is the result of lacking signatures for the IPv6 attacks. BRO requires up-to-date signatures, and due to this limitation, new attacks cannot be detected. Finally, BRO is regarded as slow to respond as it requires computing resources.

## 4.2 Anomaly-Based Intrusion Detection System (AIDS)

Anomalies or events are analyzed. According to [44], the normal activity in the network is defined and any other activity that is different is identified as an intrusion [51]. What happens in this approach is there is a matching algorithm that will look at the current protocol specification with an earlier defined protocol state. This method has a higher rate of success compared to the signature-based method. The software utilizes automated learning to define a normal behavior of the system [52]. According to [30], [53], this has seen more development in anomaly-based IDS to detect IPv6 attacks. It is essential to build descriptive profiles of each normal behavior in a network. There are two main categories of AIDS which are a) Define rules for allowing or denying events and scenarios, b) Define artificial intelligence-based techniques to build the detection model.

Rule-based methods were used to build the model and profile of known attacks. There are state-based methods which exploit finite state network behaviors to identify attacks [54]. There are five subclasses of characteristics which are statistics-based, pattern-based, heuristic-based, rule-based, as well as state-based. Researchers were able to carefully streamline current intrusion detection approaches [55]. According to [43], [44] malicious activities can be detected by analyzing the unusual events happening in a network. Firstly, the normal behavior of a network is defined and then followed by comparison or no match between the current specifications with previously defined specifications. The anomaly-based method has a higher rate of detection for new attack patterns, but it has difficulties in identifying the normal region because there is an element of blurring of boundaries between the observation of normal and what is abnormal.

A simpler way to define IDS rules is by using AI-based methods. AI can learn new attack behaviors and build new rules. Therefore, new or similar attacks can be detected based on these rules [30], [53].

A study conducted by [6] used a machine learning technique, which consists of an artificial neural network and a genetic algorithm. The experimental results showed that a DDoS attack can be detected [57]. According to [58], a detector was proposed. It functions in accordance with the pattern behavior of the traffic sources. This was carried out by observing the packet arrivals that target individual cloud customers. A dynamic resource allocation strategy was proposed by the researchers to detect DDoS attacks. Through experiments with several datasets, the proposed detector was able to separate DDoS attack traffic from the flash crowd very quickly. In another study, [59] introduced an optimized intrusion detection system by utilizing a technique of soft computing with the aim of enhancing the system's performance. Techniques of soft computing, including PCA, LDA, LBP, PSO, Greedy Search, SVM, and MLP were implemented as shown in Fig 7.

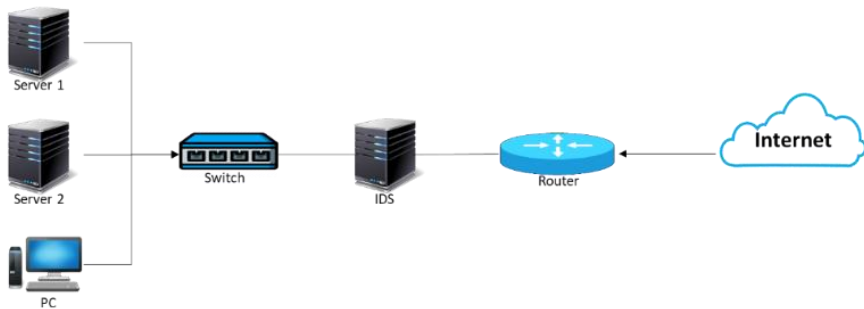


**Fig. 7. IDS Architecture**

Accordingly, the number of features was reduced, and an increase in the detection rates was obtained [44]. Finally, AI-based is easy to deploy and less costly. Security committees are encouraged to test several AI-based AIDS and select those that can achieve better detection accuracy and less manual monitoring. This approach may see more AI-based deployments.

#### 4.3 Hybrid-based Intrusion Detection System IDS (HIDS)

Another technique by researchers to overcome weaknesses in signature and anomaly-based intrusion detection is a hybrid IDS [50]. This combines both signature and anomaly-based software to detect attacks. By using Open Source tools like Snort, [60] suggested combining packet header anomaly detection (PHAD) and network traffic anomaly detection. The researchers altered the standard PHAD by modeling the protocols. This model detected an anomaly when speedy changes of the network statistics take place over a short time frame. This hybrid system incorporates power information and sensor placement (POISE). It uses the graph theory to observe the network with grid-placed sensor (GPS) algorithms. Energy consumption level anomaly is detected through the sensors in the distributed network [61] as shown in Fig 8.

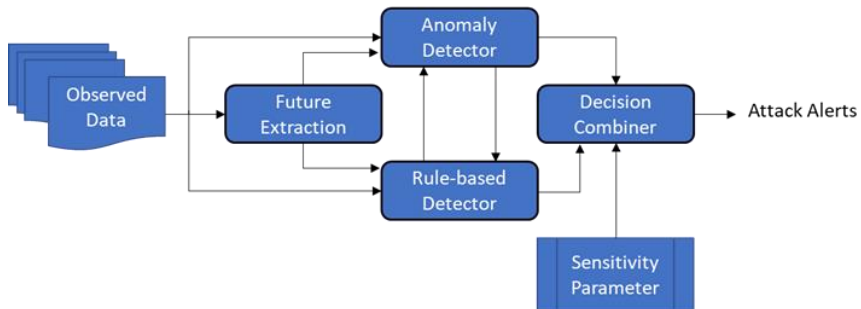


**Fig. 8.** Proposed H-IDS model

Another group of researchers developed a system by placing in parallel the anomaly-based, as well as the signature-based methods of detection. Both outputs from anomaly-based alongside signature-based detectors are combined and placed into a decision combiner unit, which will generate an attack alarm. Available for this device is a tunable sensitivity parameter. A centralized node controls the parameters of the detectors. This node is HDE, i.e., the hybrid detection engine. This intrusion detection system aims to enhance the overall DDoS attack detection performance by increasing the time of detection and accuracy [62], [63].

## 5 Conclusion

This paper has provided a brief overview of previous studies on ICMPv6-based DoS and DDoS attack detection. IPv6 can support unlimited device addresses. However, IPv6 cannot guarantee more security. ICMPv6 involves a protocol, as well as part of IPv6. Nevertheless, it has a host of vulnerabilities that can be exploited. This paper highlighted the common IPv6 attacks. The attacks occur due to exchanging unsecured ICMPv6 messages in addition to a lack of protection for the ICMPv6 protocol. This paper highlighted the intrusion detection for IPv6 based on various types of mechanisms, including anomaly, signature, as well as hybrid. Considerable interest has been shown in the anomaly-based detection area by using rule-based and AI-based techniques. Further research will focus on AI-based techniques or the ones that are easier to deploy with the lowest costs and less manual monitoring. The main problem of his work involves 1) detecting the DDOS attacks and 2) the rate of detection accuracy. Therefore, in the future work, using an Optimization Algorithm technique is proposed with the aim of reducing the number of future selections in the IDS, involving the use of special dataset IPv6, and adopting or hybridizing it with another metaheuristic algorithm to improve the intrusion detection system for detecting DDoS attacks.

## Acknowledgments

The authors would like to acknowledge the National Advanced IPv6 Centre (NAv6), Universiti Sains Malaysia (USM) for providing necessary facilities and support. The funding for this research was provided by Universiti Sains Malaysia (USM) and Iraq Airways Company (IA).

## References

- Agarwal, P., Yadav, P., Sharma, N., Uniyal, R., & Sharma, S. (2012). Network security is a key for internet users: A perspective. *Indian Journal of Engineering*, 1(1), 92-95.
- Tahir, M., Li, M., Ayoub, N., Shehzaib, U., & Wagan, A. (2018). A Novel DDoS Floods Detection and Testing Approaches for Network Traffic based on Linux Techniques. *Int. J. Adv. Comput. Sci. Appl.*, 9, 341-357.
- Al-Ani, A. K., Anbar, M., Manickam, S., & Al-Ani, A. (2019). DAD-match; Security technique to prevent denial of service attack on duplicate address detection process in IPv6 link-local network. *PloS one*, 14(4), e0214518.
- Elejla, O. E., Belaton, B., Anbar, M., & Smadi, I. M. (2017, May). A New Set of Features for Detecting Router Advertisement Flooding Attacks. In *2017 Palestinian International Conference on Information and Communication Technology (PICICT)* (pp. 1-5). IEEE.C.E.
- Al-Ani, A. K., Anbar, M., Manickam, S., Al-Ani, A., & Leau, Y. B. (2019). Preventing Denial of Service Attacks on Address Resolution in IPv6 Link-local Network: AR-match Security Technique. In *Computational Science and Technology* (pp. 305-314). Springer, Singapore.
- Deering, S., Fenner, B., & Haberman, B. Multicast listener discovery (MLD) for IPv6, October 1999. *IETF request for comments RFC2710*, 2(22), 101.I Pv6-Google, IPv6 \_ Google. 2017.
- IPv6-Google, IPv6 \_ Google. 2017.
- Narten, T., Nordmark, E., Simpson, W., & Soliman, H. (2007). *Neighbor discovery for IP version 6 (IPv6)* (No. RFC 4861).
- Conta, A., Deering, S., & Gupta, M. (2006). *Internet control message protocol (icmpv6) for the internet protocol version 6 (ipv6) specification* (No. RFC 4443). J. Ard, "Internet Protocol Version Six (IPv6) at UC Davis: Traffic Analysis with a Security Perspective," 2012.
- Mirkovic, J., & Reiher, P. (2004). A taxonomy of DDoS attack and DDoS defense mechanisms. *ACM SIGCOMM Computer Communication Review*, 34(2), 39-53.
- Elejla, O. E., Belaton, B., Anbar, M., Alabsi, B., & Al-Ani, A. K. (2019). Comparison of Classification Algorithms on ICMPv6-Based DDoS Attacks Detection. In *Computational Science and Technology* (pp. 347-357). Springer, Singapore.
- Rezvani, M. (2018). Assessment Methodology for Anomaly-Based Intrusion Detection in Cloud Computing. *Journal of AI and Data Mining*, 6(2), 387-397.
- Xue, L., Ma, X., Luo, X., Chan, E. W., Miu, T. T., & Gu, G. (2018). LinkScope: toward detecting target link flooding attacks. *IEEE Transactions on Information Forensics and Security*, 13(10), 2423-2438.
- Crainicu, B. Inside the IPsec Headers: AH (Authentication Header) and ESP (Encapsulating Security Payload). In *the Proceedings of the “European Integration-Between Tradition and Modernity” Congress*.

15. Crainicu, B. Inside the IPsec Headers: AH (Authentication Header) and ESP (Encapsulating Security Payload). In The Proceedings of the “European Integration-Between Tradition and Modernity” Congress.
16. Supriyanto, Hasbullah, I. H., Murugesan, R. K., & Ramadass, S. (2013). Survey of internet protocol version 6 link-local communication security vulnerability and mitigation methods. *IETE Technical Review*, 30(1), 64-71.
17. Elejla, O. E., Anbar, M., & Belaton, B. (2017). ICMPv6-based DoS and DDoS attacks and defense mechanisms. *IETE Technical Review*, 34(4), 390-407.
18. Joseph Klein; Sr.moderator, “Securing IPv6 Networks”, panelists Ron Broersma, Bob Scott, and Dave Rubal, panel discussion,” 2008.
19. Convery, S., & Miller, D. (2004). Ipv6 and ipv4 threat comparison and best-practice evaluation (v1. 0). *Presentation at the 17th NANOG*, 24, 16.
20. Lancaster, T. (2006). IPv6 & IPv4 Threat Review with Dual-Stack Considerations. *COMP6009: Individual Research Project, University of Southampton, Department of Electronics and Computer Science, UK*.
21. Choudhary, A. R. (2009, November). In-depth analysis of IPv6 security posture. In *2009 5th International Conference on Collaborative Computing: Networking, Applications and Worksharing* (pp. 1-7). IEEE.
22. Durdağı, E., & Buldu, A. (2010). IPV4/IPV6 security and threat comparisons. *Procedia-Social and Behavioral Sciences*, 2(2), 5285-5291.
23. Chown, T. (2008). *IPv6 implications for network scanning* (No. RFC 5157).
24. Shah, J. L., & Parvez, J. (2015). Security Issues in Next Generation IP and Migration Networks. *IOSR Journal of Computer Engineering (IOSR-JCE)*, 17, 13-18.
25. Gont, F., Liu, W., & Anderson, T. (2017). *Generation of IPv6 Atomic Fragments Considered Harmful* (No. RFC 8021).
26. Hoque, N., Bhuyan, M. H., Baishya, R. C., Bhattacharyya, D. K., & Kalita, J. K. (2014). Network attacks: Taxonomy, tools, and systems. *Journal of Network and Computer Applications*, 40, 307-324.
27. J. Postel, “Internet protocol”, Internet Eng. Task Force (IETF), Request for Comments (RFC) 791, 1981.
28. Anbar, M., Abdullah, R., Saad, R. M., Alomari, E., & Alsaleem, S. (2016). Review of security vulnerabilities in the IPv6 neighbor discovery protocol. In *Information Science and Applications (ICISA) 2016* (pp. 603-612). Springer, Singapore.
29. Anbar, M., Abdullah, R., Al-Tamimi, B. N., & Hussain, A. (2018). A machine learning approach to detect router advertisement flooding attacks in next-generation IPv6 networks. *Cognitive Computation*, 10(2), 201-214.
30. Anbar, M., Abdullah, R., Saad, R., & Hasbullah, I. H. (2017). Review of preventive security mechanisms for neighbour discovery protocol. *Advanced Science Letters*, 23(11), 11306-11310.
31. Kumar, M. A., Hemalatha, M., Nagaraj, P., & Karthikeyan, S. (2010, July). A new way towards security in TCP/IP protocol suite. In *Proceedings of the 14th WSEAS international conference on Computers: part of the 14th WSEAS CSCC multiconference* (Vol. 1).
32. Choudhary, A. R., & Sekelsky, A. (2010, November). Securing IPv6 network infrastructure: A new security model. In *2010 IEEE International Conference on Technologies for Homeland Security (HST)* (pp. 500-506). IEEE.
33. Ahmed, A. S., Hassan, R., & Othman, N. E. (2015, August). Improving security for IPv6 neighbor discovery. In *2015 International Conference on Electrical Engineering and Informatics (ICEEI)* (pp. 271-274). IEEE.

34. R. M. A. Saad; and S. R. Manickam: A Survey: Network Intrusion Detection System based on Data Mining Techniques, vol. 2, no. January 2013, pp. 145–153, 2013.
35. Al-Ani, A. K., Anbar, M., Manickam, S., Wey, C. Y., Leau, Y. B., & Al-Ani, A. (2018). Detection and Defense Mechanisms on Duplicate Address Detection Process in IPv6 Link-Local Network: A Survey on Limitations and Requirements. *Arabian Journal for Science and Engineering*, 1-19.
36. Shah, S. B. I., Anbar, M., Al-Ani, A., & Al-Ani, A. K. (2019). Hybridizing Entropy Based Mechanism with Adaptive Threshold Algorithm to Detect RA Flooding Attack in IPv6 Networks. In *Computational Science and Technology* (pp. 315-323). Springer, Singapore.
37. Douligeris, C., & Mitrokotsa, A. (2004). DDoS attacks and defense mechanisms: classification and state-of-the-art. *Computer Networks*, 44(5), 643-666.
38. Gont, F., & Liu, W. (2013). Security Implications of IPv6 options of Type 10xxxxxx. *Work in Progress, draft-gont-6man-ipv6-smurf-amplifier-03*.
39. Gao, J., & Chen, Y. (2014). Detecting DOS/DDOS Attacks Under Ipv6. In *Proceedings of the 2012 International Conference on Cybernetics and Informatics* (pp. 847-855). Springer, New York, NY.
40. Saad, R. M., Anbar, M., Manickam, S., & Alomari, E. (2016). An intelligent icmpv6 ddos flooding-attack detection framework (v6iids) using back-propagation neural network. *IETE Technical Review*, 33(3), 244-255.
41. Balasaraswathi, V. R., Sugumaran, M., & Hamid, Y. (2017). Feature selection techniques for intrusion detection using non-bio-inspired and bio-inspired optimization algorithms. *Journal of Communications and Information Networks*, 2(4), 107-119.
42. Roesch, M. (1999, November). Snort: Lightweight intrusion detection for networks. In *Lisa* (Vol. 99, No. 1, pp. 229-238).
43. Napiah, M. N., Idris, M. Y. I. B., Ramli, R., & Ahmedy, I. (2018). Compression header analyzer intrusion detection system (CHA-IDS) for 6LoWPAN communication protocol. *IEEE Access*, 6, 16623-16638.
44. Sheikhan, M., & Bostani, H. (2016, September). A hybrid intrusion detection architecture for the Internet of things. In *2016 8th International Symposium on Telecommunications (IST)* (pp. 601-606). IEEE.
45. Schütte, M. (2011). Design and implementation of an ipv6 plugin for the snort intrusion detection system. *Potsdam University Institute for Computer Science September, 1*.
46. Atlasis, A., & Rey, E. (2014). Evasion of high-end IPS devices in the age of IPv6. *BlackHat EU, 2015*.
47. Gehrke, K. A. (2012). *The unexplored impact of ipv6 on intrusion detection systems*. NAVAL POSTGRADUATE SCHOOL MONTEREY CA DEPT OF COMPUTER SCIENCE.
48. Roesch, “INTRUSION DETECTION SYSTEMS WITH THE SNORT 10,” 2014. [Online]. Available:<https://www.coursehero.com/file/p76fva1/INTRUSION-DETECTION-SYSTEMS-WITH-THE-SNORT-10-Roesch-2014-While-there-are/>.
49. Paxson, V. (1999). Bro: A system for detecting network intruders in real-time. *Computer Networks*, 31(23-24), 2435-2463.
50. Moya, M. A. C. (2008). Analysis and evaluation of the snort and bro network intrusion detection systems. *Intrusion Detection System, Universidad Pontificia Comillas*, 80, 80.
51. Jyothisna, V. V. R. P. V., Prasad, V. R., & Prasad, K. M. (2011). A review of anomaly-based intrusion detection systems. *International Journal of Computer Applications*, 28(7), 26-35.
52. Amaral, J. P., Oliveira, L. M., Rodrigues, J. J., Han, G., & Shu, L. (2014, June). Policy and network-based intrusion detection system for IPv6-enabled wireless sensor networks. In *2014 IEEE International Conference on Communications (ICC)* (pp. 1796-1801). IEEE.

53. Manninen, M. (2002). Using artificial intelligence in intrusion detection systems. *Helsinki University of Technology*.
54. Fragkiadakis, A. G., Tragos, E. Z., Tryfonas, T., & Askoxylakis, I. G. (2012). Design and performance evaluation of a lightweight wireless early warning intrusion detection prototype. *EURASIP Journal on Wireless Communications and Networking*, 2012(1), 73.
55. Sharma, S., & Gupta, R. K. (2015). Intrusion detection system: A review. *International Journal of Security and Its Applications*, 9(5), 69-76.
56. Barati, M., Abdullah, A., Udzir, N. I., Mahmud, R., & Mustapha, N. (2014, August). Distributed Denial of Service detection using a hybrid machine learning technique. In *2014 International Symposium on Biometrics and Security Technologies (ISBAST)* (pp. 268-273). IEEE.
57. Yu, S., Tian, Y., Guo, S., & Wu, D. O. (2014). Can we beat DDoS attacks in clouds? *IEEE Transactions on Parallel and Distributed Systems*, 25(9), 2245-2254.
58. Thapngam, T., Yu, S., Zhou, W., & Beliakov, G. (2011, April). Discriminating DDoS attack traffic from flash crowd through packet arrival patterns. In *2011 IEEE Conference on Computer Communications Workshops (INFOCOM WKSHPS)* (pp. 952-957). IEEE.
59. Alsdahan, A., & Khan, N. (2013). A proposed optimized and efficient intrusion detection system for wireless sensor network. *International Journal of Electrical, Computer, Energetic, Electronic and Communication Engineering*, 7(12), 1621-1624.
60. Aydin, M. A., Zaim, A. H., & Ceylan, K. G. (2009). A hybrid intrusion detection system design for computer network security. *Computers and Electrical Engineering*, 35(3), 517-526.
61. Lo, C. H., & Ansari, N. (2013). CONSUMER: A novel hybrid intrusion detection system for distribution networks in smart grid. *IEEE Transactions on Emerging Topics in Computing*, 1(1), 33-44.
62. Cepheli, Ö., Büyükcörak, S., & Karabulut Kurt, G. (2016). Hybrid intrusion detection system for ddos attacks. *Journal of Electrical and Computer Engineering*, 2016.
63. Al-Ani, A. K., Anbar, M., Manickam, S., Wey, C. Y., Leau, Y. B., & Al-Ani, A. (2018). Detection and Defense Mechanisms on Duplicate Address Detection Process in IPv6 Link-Local Network: A Survey on Limitations and Requirements. *Arabian Journal for Science and Engineering*, 1-19.



# Lake Chini Water Level Prediction Model using Classification Techniques

Lim Zee Hin and Zalinda Othman

Faculty of Information Science and Technology, Universiti Kebangsaan Malaysia, 43600 UKM Bangi, Selangor, Malaysia.  
zeehinlim@outlook.com, zalinda@ukm.edu.my

**Abstract.** Monsoon seasons in Malaysia bring uneven distribution of rainfall and eventually affect the water level at Lake Chini as flood and drought disturb the population and distribution of aquatic organisms at the lake. This study is conducted to produce Lake Chini water level prediction model by comparing several algorithms using data mining approach via classification techniques. Data from seven observation stations between 2011 and 2014 are collected from Pusat Penyelidikan Tasik Chini, Universiti Kebangsaan Malaysia and data from Melai station in particular is used for this purpose. The collected time series data is complex and high in dimensionality thus leading to low efficiency in data mining process. The analysis comprises of four phases that include data collection, data pre-processing, data mining and model development and interpretation and evaluation of patterns. To overcome high dimensional time series, dimensionality reduction approach such as Piecewise Aggregate Approximation (PAA) and Symbolic Aggregate approXimation (SAX) are applied while three classification techniques namely Decision Tree, Artificial Neural Network and Support Vector Machine are used to classify the data. Performance measures for each of the algorithms are evaluated and compared to select the most suitable model for the prediction.

**Keywords:** Time Series, Classification, Piecewise Aggregate Approximation, Symbolic Aggregate Approximation, Water Level, Lake Chini.

## 1 Introduction

Water resource is vital for daily lives and contributes to the formation of a civilization. Only one third of Earth's freshwater can be found in the surface water of lakes and rivers [1]. Lake, for instance, plays the role of a wetland ecosystem with the capability to lower the frequency of flood and erosion of the riverbanks [2]. With a surface area of 25.26 km<sup>2</sup>, Lake Chini has an important aquatic biodiversity and is Malaysia's second largest natural freshwater lake after Lake Bera. The lake is located at the southeast region of Pahang with coordinate of 3°22'30" to 3°28'00" U and 102°52'40" to 102°58'10" T. Lake Chini is formed by a combination of 12 bodies of water known as 'laut' by Chini's native, the Jakuns.

According to Malaysian Meteorological Department, monsoon seasons in Malaysia can be categorized as Southwest Monsoon (May to September) and Northeast Monsoon (November to March). Northeast monsoon brings heavy rainfall around the east coast area of Peninsular Malaysia where the lake is located. The humidity level at Lake Chini is relatively high at 80% and has the average annual temperature of 28° [3]. Hydrological analysis shows the average annual rainfall at Lake Chini is between 1487.7 mm to 3071.4 mm. The highest average rainfall ever recorded is 3071.4 mm in 1994 while the lowest is 1487.7 mm back in 1997 [4].

The water level of Lake Chini fluctuates significantly due to the monsoon seasons. Flood and drought control are necessary to protect the ecology and preserve the aquatic organism population [5]. Thus, accurate water level information is vital to prevent the flooding and drying of the lake. Water level data modelling is hard to implement due to the high complexity and high dimensionality of a time series. Time series data mining is complex as it comes with tremendous amount of data which can consume both time and space. Therefore, this paper uses time series dimensional reduction approach known as Piecewise Aggregate Approximation (PAA) and Symbolic Aggregate apProXimation (SAX) to increase the classification efficiency in data mining of Lake Chini's water level.

## 2 Background and related work

### 2.1 Time Series Representation

Time series modelling is defined as an action of predicting future by knowing the past [6]. Time series forecasting employs the collected data from the past to forecast a new value for the future. Time series can be classified as either univariate or multivariate. Univariate time series consists of one variable whereas multivariate time series has multiple variables. Time series in its discrete form can be continuous by combining them weekly, monthly or annually [7]. Most research interest on time series data mining use discretizing (symbolizing, tokenizing and quantizing) approach, however, none of the techniques allows the lower bounding of the true distance between original time series and symbolic time series. Therefore, SAX approach is used to handle the time series [8]. Time series is transformed into Piecewise Aggregate Approximation (PAA) representation before discretizing the time series into symbolic strings. There are two important functions of PAA: (1) Dimensionality reduction to be carried over to symbolic representation. (2) Lower bounding to ensure that the distance measured between symbolic time series that have been compressed is the same or near the true distance of original time series without false negative [9]. The equation 1 below explains the method of PAA in reducing dimensionality. Time series  $C$  where  $n$  is the length of time series,  $w$ , as the segment of PAA and  $\bar{c}_i$  is the average value of PAA.

$$\bar{c}_i = \frac{w}{n} \sum_{j=\frac{n}{w}(i-1)+1}^{\frac{n}{w}i} (c_j) \quad (1)$$

In short, time series with a  $n$ -dimension will be reduced to  $w$ -dimension where time series will be divided into frames with the equal size,  $w$ . Each of the frames will be calculated with an average value to become the new data-reduced representation [8].

Symbol discretization is done further after the PAA transformation to obtain a discrete representation. Since normalized time series have a Gaussian distribution, it will produce symbols with equiprobability by determining the “breakpoint” from the statistical table. SAX provides lower bounding distance measure by using the most common distance measure, i.e. Euclidean distance. By applying equation 2, a lower bounding approximation of Euclidean distance between two original time series can be found. The MINDIST function in equation 3 returns minimum distance between the original time series of two string of words as explained in [8] and has been proven by [10].

$$DR(\bar{Q}, \bar{C}) \equiv \sqrt{\frac{n}{w} \sum_{i=1}^w (\bar{q}_i - \bar{c}_i^-)^2} \quad (2)$$

$$MINDIST(\hat{Q}, \hat{C}) \equiv \sqrt{\frac{n}{w} \sum_{i=1}^w (dist(\hat{q}_i, \hat{c}_i))^2} \quad (3)$$

## 2.2 Time Series Data Mining

The most popular time series data mining in the community are indexing, clustering, classification, summarization and anomaly detection [8].

Time series data mining tasks in the past have been using stochastic model such as Autoregressive Integrated Moving Average (ARIMA). ARIMA is flexible as it represents time series as linear and follows the Box-Jenkins methodology to build time series prediction model. However, this is found to be impractical for the purpose of this study. As a stochastic time series model, ARIMA is used in short-term forecasting and checking for stationarity that occurs in the time series. It works best if a time series is constant and has little fluctuations over time, otherwise the seasonality or trend will negatively affect the calculations of ARIMA regression model. Thus, in order to preserve the accuracy of ARIMA model, differencing method is used to remove the seasonal and trend patterns of the time series. A non-stationary time series will be made stationary by mathematical formulation of ARIMA model as shown in [7]. Fluctuation of water level at Lake Chini caused by weather and monsoon leads to time series seasonality. Therefore, ARIMA model will not be further discussed as most trends will be removed under its method thus affecting the discovery of interesting time series pattern.

Meanwhile, neural network based algorithm is not applied directly toward the time series due to its time-consuming machine learning algorithms. Neural network algorithms take the input values and multiply with the individual connection weight for each node. Those values will be channeled to a hidden layer and the process is repeated until all of the calculations are done for all hidden layers. Activation function is applied to the output layer and it generates the result that consists of the predicted value by the network. NN-based algorithm is time consuming if the high dimensionality of the time series has not been lowered. Thus, this research is using PAA approach to compress the

time series and SAX approach to discretize the time series for further data mining process in order to increase the data mining efficiency.

For the most part, Artificial Neural Network (ANN) has been a success in hydrology-related field such as rainfall-runoff modelling, streamflow forecasting and reservoir operations [11]. Multi-layer perceptron (MLP) algorithm in ANN with feed-forward topology, feeds in or learn from past value and calculates the weigh to predict the new value. ANN approach is optimized in classification of data, determining new patterns and prediction. ANN has been proven to be more efficient and accurate from previous research [12, 13, 14, 15].

On the other hand, Support Vector Machine (SVM) is a type of machine learning formation built by Vapnik in 1960s for the use of telecommunication. SVM builds a hyperplane in a high dimensional space feature that maximizes the margin between two classes. Margin is defined as the distance between separating hyperplane and the nearest points on either side of two classes [16]. Sequential Minimal Optimization (SMO) is the SVM algorithm that will be used in this study. Researchers compare SVM with ANN in their previous research and found that SVM has a better accuracy in classification, built a better prediction model and overcome the overfitting issue of ANN [17, 18, 19].

In addition, Decision Tree (DT) with its J48 algorithm is one of the popular classification techniques in data mining. DT is represented in hierarchy and its rules or reasoning are easier to understand compared to other techniques [20]. From the research paper proposed by [21], DT succeeds in classifying symbolic representation of time series. [22] used the same approach to extract the pattern from rainfall time series and worked on Random Forest after clustering the discretize symbols.

Besides, result on PAA and SAX can be applied on different data mining approach such as Ant Colony Optimization as proposed in [23]. The summary of related works is shown in Table 1. This paper focuses on the dimensionality reduction of water level time series and comparison of classification method to build a prediction model.

### 3 Research Method

This research was conducted in four phases. The first phase consisted of identification of issue and data collection from *Pusat Penyelidikan Tasik Chini* (PPTC). The next phase was data pre-processing in which data cleaning, transformation and integration were carried out. Time series dimensionality reduction by PAA and symbolic representation by SAX were also discussed in this phase. Thirdly, the building of data mining model from the pre-processed data using three classification techniques; ANN, SVM and DT. The last phase was the comparison of data mining model by evaluating the performance measurement of each model. The best model will be selected to be Lake Chini's water level prediction model.

**Table 1.** Summaries of related works

<b>Refer- ence</b>	<b>Models</b>	<b>Summary</b>
[12]	ANN, ARMA(ARMAX)	ANN has better accuracy with difference of 1.87cm from original value 303.42cm
[13]	ARIMA, ANN	ANN has lower MSE (0.00674) compare to ARIMA (0.01246).
[14]	ANN, Statistical model	ANN prediction is more accurate with RMSE (0.92), R (0.97), $R^2$ (0.95) AND D (1.00).
[15]	ANN, ARMA(ARMAX)	ANN with R (0.999) is higher than ARMAX (0.997).
[17]	ANN, SVM(SVR)	SVR has lowest MSE (0.0080) in Lake Van and MSE (0.0054) in Lake Egirdir. SVR able to overcome overfitting problem of ANN.
	ANN, SVM	ANN is more accurate with RMSE (0.177), $R^2$ (0.9626) and E (0.8391) for short term prediction. SVM is more accurate with RMSE (0.134), $R^2$ (0.9235) and E (0.7343) for long term prediction. SVM is more stable due to principle of structural risk minimization
[18]		SVR obtained more promising result than ANN.
[19]	ANN(WANN), SVM(SVR)	
[21]	J48, ADTree, PART, JRip	PART has highest accuracy but JRip is more suitable (high accuracy, shorter reasoning)

### 3.1 Data Pre-processing and Representation

In data collection phase, Lake Chini's water level data were collected from the seven observation stations at *Pusat Penyelidikan Tasik Chini* (PPTC). Out of these stations, the data from Melai station was selected to be studied. The time series ranged from 2011 to 2014.

Pre-processing on raw data is essential in order to generate quality data to build accurate data mining model. This is followed by data integration to combine similar data from different databases. In this case, the data from Melai station was separated into monthly Microsoft Excel sheets and recombined into a single annual Excel sheet. Then, the annual sheets were integrated to become an overall water level data for Melai station. Table 2 shows the total instances for each year and overall total instances for Melai station.

**Table 2.** Total amount of instances

<b>Year</b>	<b>No. of instances</b>
2011	28419
2012	19015
2013	35040
2014	31584

Total	<u>114048</u>
-------	---------------

Data cleaning is a process to remove or correct the inconsistent, redundant and missing data. Discrepancy inspection is done by filtering out the error by observation and missing data are replaced by average value from the overall datasets. Irrelevant data is deleted after seeking advice from the experts. Data transformation in this research is focused on dimensionality reduction of water level time series. PAA and SAX transformation are used to reduce the enormous datasets and convert the real-valued time series into symbolic representation. By applying PAA transformation, 114048 datasets from Melai station between 2011 to 2014 were compressed into 10 segments and each of the data points was the average value of the segment as shown in Table 3. SPMF software created by [24] provides visual representation of PAA in Fig. 1.

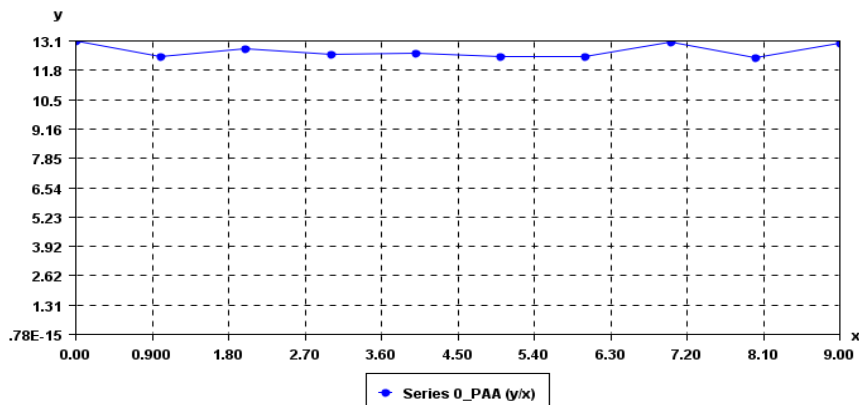


**Fig. 1.** Melai time series in PAA representation

**Table 3.** Average data points for 10 segments

Data point	Average value
0	13.08
1	12.40
2	12.71
3	12.49
4	12.51
5	12.38
6	12.39
7	13.00
8	12.33
9	12.96

SAX transformation discretizes the PAA average value to symbolic representation according to the breakpoint table. SPMF provides the discretization by assigning the symbols to the average value in each segment in Table 4.

**Table 4.** Discretization of symbols

Segment Interval	Symbol
[-∞, 12.07]	a
[12.07, 12.46]	b
[12.46, 12.79]	c
[12.79, 13.19]	d
[13.19, ∞]	e

Therefore, the string of words from SAX transformation for 10 segments were “dbcccbdbd” for Melai station. The range of discretization for the segment interval is based on the normalized value of the water level in the breakpoint table and each point of the segment discretization is based on the number of segments assigned after the dimensionality reduction.

### 3.2 Time Series Data Modelling

WEKA was applied in this study to carry out time series data mining. Water level data were imported into WEKA in Comma-Separated Value (CSV) format. First, *PropositionalToMultiInstance* filter was used to collect the rows of water level data with the same Time attribute, i.e. “2014-01-01” and combined it into a single line of dataset for each day. In short, the value of the same Time attribute will be bagged together and returned to the water level data as a single row as shown in Table 5. Each water level value was separated by “\n”.

*SAXTransformer* filter undergoes a symbolic discretization to the data. A compression rate can be set to determine the percentage of the dimension reduction to be done on the data. In this study, a default value of 100 was used and five symbols were set as the maximum symbols to be discretized. Table 6 shows the SAX transformation by discretizing the water level values into symbols according to the breakpoint table in *SAXTransformer* filter. For example, “e, {0.96}” where ‘e’ was the symbol and “{0.96}” was the compression rate set by the filter.

Since the result of *SAXTransformer* was not in the form of string of words (separated by “{}” and “\n”), therefore *OneDimensionTimeSeriesToString* filter was used to combine the words or symbols in each row of data as shown in Table 7. Next, *StringToWordVector* filter identified the frequency of the word pattern that can be found in the strings and gave a new set of attributes for the word pattern. This filter has the same *Bag-of-Words* approach as what was proposed by Pavel et al. [25]. For each row of data, frequency for each word pattern was calculated and *n-grams* parameter was tuned to determine the size of the word patterns generated. In Table 8, the frequency for b, c and d was 1.0 since the string of words for “2014-01-01”, “bcd” contained these symbols.

Before the *AddCluster* filter was applied, Time attribute had been removed to enable WEKA to generate new cluster. *AddCluster* filter underwent clustering for each row of

word patterns frequency. *SimpleKMeans* was simple to use thus it became the algorithm in clustering the rows of data. Two clusters were assigned and the data were clustered as *cluster1* and *cluster2*. This text clustering approach has also been used in [26]. Following that, the process of classification using ANN, SVM and DT techniques as well as data mining models were carried out. The performance measure for each model was tested by using 10-fold cross validation as well as classification accuracy, *Mean Absolute Error* (MAE) and *Root Mean Squared Error* (RMSE).

**Table 5.** Bagging by *PropositionalToMultiInstances* filter

Time	Water level (m)	Time	Bag
2014-01-01	12.84	2014-01-01	12.84\n12.45\n12.63
Bag			
2014-01-01	12.45		
2014-01-01	12.63		
2014-01-02	12.75	2014-01-02	12.75\n12.74\n12.74
2014-01-02	12.74	Bag	
2014-01-02	12.74		

**Table 6.** *SAXTransformer* application

Time	Bag	Time	Bag
2014-01-01	12.84\n12.45\n12.63	2014-01-01	d,{0.96}\nb,{0.96}\nc,{0.96}
S		A	
2014-01-02	12.75\n12.74\n12.74	2014-01-02	c,{0.96}\nc,{0.96}\nc,{0.96}
X		→	

**Table 7.** *OneDimensionalTimeSeriesToString* filter application

Time	Bag
2014-01-01	d,{0.96}\nb,{0.96}\nc,{0.96}
2014-01-02	c,{0.96}\nc,{0.96}\nc,{0.96}



Time	String of words
2014-01-01	dbc
2014-01-02	ccc

**Table 8.**

*StringToWordVector* filter application

Time	a	b	c	cc	ccc	d	e
2014-01-01	0.0	1.0	1.0	0.0	0.0	1.0	0.0

**Table 9.** 2014-01-02 0.0 0.0 1.0 1.0 1.0 0.0 0.0

AddCluster filter application									AddClus-
No.	a	b	c	cc	ccc	d	e	Clus-	ter
1	0.0	1.0	1.0	0.0	0.0	1.0	0.0	cluster1	
2	0.0	0.0	1.0	1.0	1.0	0.0	0.0	cluster2	

## 4 Result and Discussion

The results from three algorithms were compared in this section. The performance measure was tested using 10-folds cross validation. The cross validation in WEKA split the data samples into 10 parts. Next, nine portions of the data samples were used as training set whereas one portion was used as testing set. The iteration continued, and the process of training and testing were repeated for 10 times. Final result was generated after taking the average value from all 10 results and the performance measurement models were compared based on time taken to build the model, classification accuracy, MAE and RMSE. Classification accuracy is the ratio of correctly predicted instances to total predictions, in which 100% is the highest accuracy that can be achieved for one classification technique. Classification accuracy is shown with two labels, i.e. *Correctly Classified Instances* and *Incorrectly Classified Instances*. On the other hand, MAE measures how close is a predicted value to the eventual outcome while RMSE measures the differences between values (sample and population values) predicted by a model or an estimator and the values that are actually observed. Both MAE and RMSE with a small value give a better prediction result.

**Table 10.** Results for 10-folds cross validation

Performance Measure	Station		
	SMO	Melai	J48
Time taken	0.14	103.31	0.25
Classification Accuracy	98.75	99.00	97.84
MAE	0.225	0.0166	0.223
RMSE	0.2771	0.0744	0.1131

Table 10 shows the result for Melai station after 10-folds cross validation. Apparently, SMO algorithm took the shortest time to build the model at 0.14 seconds. However, MLP had the highest accuracy overall (99.00%) followed by SMO (98.75%) and J48 (97.84). The classification accuracy for these algorithms do not have significant differences. MLP algorithm even scored the lowest MAE and RMSE at 0.0166 and 0.0744 respectively. Although MLP exceeds others in terms of accuracy and performance measure, the time taken for MLP to build its model is longer (103.31 seconds)

and it may not be efficient in some cases. In the study of [12] and [15], RMSE and MAE for ANN were relatively lower than other algorithms.

## 5 Conclusion and Future Works

In this research, the water level time series from Melai station in Lake Chini from 2011 to 2014 were studied. Dimensionality reduction was applied to the time series using Piecewise Aggregate Approximation (PAA) approach whereas Symbolic Aggregate approXimation (SAX) approach converted the real-valued time series into symbols. To classify the water level, three classification algorithms from data mining techniques were used, i.e. MLP, SMO and J48. The 10-folds cross validation results showed that MLP performed better by obtaining the highest accuracy and lower value of RMSE and MAE compared to SMO and J48. However, the time taken to build the MLP model was time consuming. At the clustering stage after the *StringToWordVector* filter was applied, the label for the clusters generated such as cluster1, cluster2 and cluster3 had yet to be specified. Lake Chini experts can study the pattern for each cluster and determine their characteristics. The scope for those clusters can be grouped as water level indicator such as safe, high and critical level. This idea was proposed by [21] for rainfall prediction. Lkhagva et al. [27] proposed that *Extended SAX* (ESAX) to increase the symbolic strings representation by a higher dimensionality reduction compared to SAX. Tamura et al. [28] conducted the research based on clustering of time series by application of *moving average convergence divergence (MACD)-histogram-based SAX* (MHSAX) and *k-medoid*. The accuracy of Euclidean distance in distance measure between time series has improved thus increasing the accuracy of clustering using *k-medoids*.

## Acknowledgment

This research is conducted with the support of Universiti Kebangsaan Malaysia Grant GGP-2017-025 and Pusat Penyelidikan Tasik Chini.

## References

1. Das, J., Acharya, B. C.: Hydrology and Assessment of Lotic Water Quality in Cuttack City, India. *Journal Water, Air and Soil Pollution* 150, 163–175 (2003).
2. Shuhaimi Othman, M., Lim Eng Chong, Mushrifah Idris & Shaharudin Idrus.: Kualiti Air Dan Logam Berat di Tasik Chini, Pahang. Prosiding Seminar IRPA RMK8, Kategori EAR (2), 216-220 (2005).
3. Nurul Syazwani Ab Rani, Mohd Ekhwan Hj Toriman, Mushrifah Hj Idris, Nor Rohaizah Jamil & Mohd Khairul Amri Kamarudin.: Muatan Sedimen Terampai dan Perkaitannya dengan Penghasilan Muatan Sedimen pada Musim Kering dan Hujan di Tasik Chini, Pahang. Bangi: *eBangi*. 4(1), 70-83 (2009).
4. Muhd Barzani Gasim, Mohd. Ekhwan Hj. Toriman, Ahmad Abas, Mir Sujaul Islam & Tan Choon Chek.: Water Quality of Several Feeder Rivers between Two Seasons in Tasik

- Chini, Pahang (Kualiti Air di antara Dua Musim Beberapa Sungai Pembekal di Tasik Chini, Pahang). Bangi: Sains Malaysiana 37(4), 313–321 (2008).
- 5. Nor Rohaizah Jamil, Mohd Ekhwan Toriman, Mushrifah Idris, Ng Lee How.: Analisis ciri-ciri luahan Sungai Chini dan Sungai Paya Merapuh Tasik Chini, Pahang bagi waktu normal, waktu basah dan selepas banjir. Jurnal Sains Sosial dan Kemanusiaan 7(1), 1-16 (2012).
  - 6. Raicharoen, T., Lursinsap, C., Sanguanbhoki, P. 2003. Application of critical support vector machine to time series prediction, Circuits and Systems. *Proceedings of the 2003 International Symposium* 5(25-28): 741-744.
  - 7. Ratnadip, A. & Agrawal, R. K.: An Introductory Study on Time Series Modeling and Forecasting. LAP Lambert Academic Publishing, Germany (2013).
  - 8. Lin, J., Eamonn, K., Stefano, L. and Chiu, B.: A Symbolic Representation of Time Series, with Implications for Streaming Algorithms. Proceedings of the 8<sup>th</sup> ACM SIGMOD Workshop on Research Issues in Data Mining and Knowledge Discovery (2003).
  - 9. Wang Xiaoyue, Hui Ding, Goce Trajcevski, Peter Scheuermann, Eamonn Keogh.: Experimental Comparison of Representation Methods and Distance Measures for Time Series Data. *Data Mining and Knowledge Discovery* 26(2), 275-309 (2013).
  - 10. E. Keogh, K. Chakrabarti, M. Pazzani, and S. Mehrotra. Dimensionality Reduction for Fast Similarity Search in Large Time Series Databases. *Journal of Knowledge and Information Systems*. vol. 3. pp. 263-286 (2001).
  - 11. Rao S. G.: Artificial Neural Networks in Hydrology. I: Preliminary Concepts. *Journal of Hydrologic Engineering* 5(2), (2000).
  - 12. Abdusselam, A.: Forecasting Surface Water Level Fluctuations of Lake Van by Artificial Neural Networks. *Water Resources Management* 21(2), 399-408 (2007).
  - 13. Siti Hajar Arbain, Antoni Wibowo: Time Series Methods for Water Level Forecasting of Dungun River In Terengganu Malaysia. *International Journal of Engineering Science and Technology* 4(4), 1803-1811 (2012).
  - 14. Shilpi Rani & Dr. Falguni Parekh.: Application of Artificial Neural Network (ANN) for Reservoir Water Level Forecasting. *International Journal of Science and Research* 3(7) (2014).
  - 15. Young, Chih-Chieh & Liu, W.-C & Hsieh, W.-L.: Predicting the Water Level Fluctuation in an Alpine Lake Using Physically Based, Artificial Neural Network, and Time Series Forecasting Models. *Mathematical Problems in Engineering*. (2015).
  - 16. Wang, W. C., Chau, K. W., Cheng, C. T. & Qiu, L.: A comparison of performance of several artificial intelligence methods for forecasting monthly discharge time series. *Journal of Hydrology* 374: 294–306 (2009).
  - 17. Cimen, M. & Kisi, O.: Comparison of two different data-driven techniques in modeling lake level fluctuations in Turkey. *Journal of Hydrology* (378), 253-262 (2009).
  - 18. Mohsen, B., Keyvan A., Emery A. Coppola Jr.: Comparative Study of SVMs and ANNs in Aquifer Water Level Prediction. *Journal of Computing in Civil Engineering* 24(5) (2009).
  - 19. Karran, Daniel & Morin, Efrat & Adamowski, Jan.: Multi-step streamflow forecasting using data-driven non-linear methods in contrasting climate regimes. *Journal of Hydroinformatics* 16, 671-689 (2015).
  - 20. Rokach, L. & Maimon O.: *Data Mining with Decision Trees: Theory and Applications*. World Scientific Publishing Co., New Jersey (2014).
  - 21. Zulaiha Ali Othman, Noraini Ismail, Abdul Razak Hamdan, Mahmoud AhmedSammour: Klang Valley Rainfall Forecasting Model Using Time Series Data Mining Technique. *Journal of Theoretical and Applied Information Technology* 92(2), pp. 372-379 (2016).

22. Taib, S. M., Abu Bakar, A., Hamdan, A. R., & Syed Abdullah, S. M. Classifying weather time series using featurebased approach. International Journal of Advances in Soft Computing and its Applications 7(SpecialIssue3), 56-71 (2015).
23. Syaidatul Nadia Sabri and Rizauddin Saian. Predicting Flood in Perlis Using Ant Colony Optimization. Journal of Physics: Conference Series (855) (2017).
24. Fournier V. P., Lin, C.W., Gomariz, A., Gueniche, T., Soltani, A., Deng, Z., Lam, H. T.: The SPMF Open-Source Data Mining Library Version 2. Proc. 19th European Conference on Principles of Data Mining and Knowledge Discovery (PKDD 2016) Part III 9853: 36-40 (2016).
25. Pavel Senin, Sergey Malinchik. 2013. SAX-VSM: Interpretable Time Series Classification Using SAX and Vector Space Model. Proceedings – IEEE International Conference on Data Mining (2013).
26. Anisha, M.T., Resmipriya M.G.: An Efficient Text Classification Scheme Using Clustering. Procedia Technology 24, 1220-1225 (2016).
27. Lkhagva, B., Suzuki, Y., and Kawagoe, K.: New time series data representation ESAX for financial applications. IEEE 22nd International Conference on Data Engineering Workshops, x115-x115 (2006).
28. Tamura K., Ichimura T.: Clustering of time series using hybrid symbolic aggregate approximation. IEEE Symposium Series on Computational Intelligence (SSCI), Honolulu, HI, pp. 1-8 (2017).



# Development of a Bi-level Web Connected Home Access System using Multi-Deep Learning Neural Networks

K. Y. Tham, T. W. Cheam, H. L. Wong and M. F. A. Fauzi

Faculty of Engineering, Multimedia University, Persiaran Multimedia,  
63100 Cyberjaya, Selangor, Malaysia  
[h1wong@mmu.edu.my](mailto:h1wong@mmu.edu.my)

**Abstract.** Home entrance is a vital entry point that should be secured at all times. A bi-level home access system was designed and developed using face authentication and hand gesture recognition. The system's mainframe runs on a Raspberry Pi 3 minicomputer. The board serves as the computing platform to process various deep learning algorithms for face authentication and hand gesture recognition. It also serves as a communication hub which allows registered users to communicate with the system remotely via mobile application. Home occupants may also register emergency contacts such as their neighbours' for quick response at their property. An Android mobile application was developed for remote user interface. Google Firebase platform was used to store user profile and historical data. The face authentication consists of two steps, namely face detection and face recognition. The Multi-task Cascaded Convolutional Neural Network (MTCNN) was employed for face detection, while the Inception ResNet was used for face recognition. Upon successful face authentication, the system proceeds to read the user's hand gesture. First, the system detects the hand using Single Shot MultiBox Detector (SSD) that runs on a Convolutional Neural Network (CNN). Next, a sequence of hand pose is recognised using the conventional CNN method. Based on experiments, the average detection/recognition accuracy under normal operating conditions using real face and real-video captured by the system is approximately 95.7%. An occupant needs approximately 7s to complete the process to enter the house.

**Keywords:** Face Authentication, Hand Gesture Recognition, Deep Learning, Embedded System, Raspberry Pi, Android Mobile Apps, Google Firebase.

## 1 Introduction

Security is always a concern to the house occupants. With the advancement of technology, we can utilize artificial intelligence and the internet to enhance home security. Based on Malaysia crime and safety report [1], Kuala Lumpur was identified as a high-threat city for crime. Those crimes include snatch theft, burglary and abductions. The frequency of residential breaks-ins was also high. In urban area, most people work during the day and leave their houses unguarded. The residents usually return home at different times. Due to the high cost of living, some parents have to allow their teenage

school or college-going children to return home by themselves. Nevertheless, older children may also be vulnerable to indirect or direct threats [2].

A bi-level home entry security system was proposed to deter break-ins and prevent trespassing through close monitoring and faster response by the locally connected community. The system can be installed at the main door of the house. With such a system, the house occupant can monitor the returning of other occupants remotely. Parents will have more peace of mind in letting their teenage child to return home alone, as they could monitor the child remotely. In an event that a returnee is forced by knife-point to open the door, the returnee can wave a secret panic gesture without alarming the abductor. Then, a warning alert is sent to the nearby contacts, which may include the neighbours, security guards or police.

The paper is organised as follows. A background study is presented in section 2. Then, the system design which includes the hardware, the networks employed and the firmware will be discussed in section 3. The results are presented and discussed in section 4. Finally, the conclusions and future recommendations are given in section 5.

## 2 Background Study

Eight types of lock system were discussed in [3]. The mechanical lock system, password lock system and Radio Frequency Identification (RFID) lock system requires keys or card, which do not verify the authority of the person holding it. Thus, the security level is low. Lock systems that operate using One Time Password (OTP) or Near Field Communication (NFC) are slightly more secure. OTP-based systems require a mobile device to connect to a server in order to obtain the generated OTP while the NFC method requires the mobile phone to have the feature itself [4]. These mechanisms are harder to be hacked. However, the need of carrying a mobile device may pose as a downside because one may not carry a mobile phone at all times, especially children. Biometric lock system grants access by verifying the user's unique physical or behavioural characteristics. However, physical characteristics such as fingerprints may be duplicated, and it remains unique throughout one's life. On the other hand, face appearance can change, and hand gesture can be altered. Development of home access system integrated with face authentication and hand gesture recognition on embedded systems is still at its infancy.

The results from different classification techniques for face recognition, namely the Support Vector Machine (SVM), Convolutional Neural Network (CNN) and Artificial Neural Network (ANN) with Bag of Words (BoW), Histogram of Gradients (HOG) and image pixels were studied by [5]. From the literature, image pixels with CNN and ANN yielded the highest accuracy. With suitable training, direct face image combined with neural network methods also gave the lowest time spent. Hand gesture recognition is primarily used to understand sign language and is also applied in human-computer/robot interaction. Hands can be segmented by using hand contour and its silhouette [6]. Convexity defects and convex hull have been employed by [7] for hand gesture recognition. Both methods require a clean binary image of the hand gesture in order to capture the concavity and convexity locations. The locations are modelled mathematically

in order to classify different hand gestures. Even though the accuracy reported is on the high-side of 98%, the need to define each hand pose can be tedious if more gestures have to be added in a long run. Feedforward multilayer ANN with back-propagation training was developed to distinguish four different gestures of post-processed hand images [8]. The method yielded an accuracy of 88.7%. Max-pooling CNN with six hidden layers for hand gesture recognition was presented by [9]. The authors also compared it with SVM classifier and a tiled-CNN. The proposed max-pooling CNN achieved the highest classification rate of 96.8%.

A recent review on Deep Learning (DL) based vision system was presented by [10]. The authors discussed various vision applications, which include object detection, recognition and tracking. They discussed the following DL architectures: Deep Boltzmann Machine (DBM), Deep Belief Networks (DBN), Stacked Auto-Encoders, CNN and Deep Residual Learning (DRL). According to their survey, CNN implementations remained the most popular at 66.7%. Although DL accuracies can be high, the challenges will be setting-up dataset for efficient network training as well as achieving computation efficiency for real-time system applications.

Our proposed design is closely related to the concept given in Faceture ID [11]. A Leap motion controller (LMC), which is mainly used for virtual reality, was employed. It was used in recognising hand gesture motion that represents digits. The digits are OTP sent to the user after the user's face was recognised. CNN was employed in their recognition processes. However, their proof of concept was done on a computer. The LMC alone is an expensive device compared to our proposed system. Moreover, the Faceture ID required one to have a mobile device at the entry point in order to receive the OTP.

### 3 System Design

The goal of this project was to design and develop a full ecosystem for a home entrance access system that allows interconnectivity with home occupants and the local community with real-time updates through mobile application and a cloud database. Fig. 1 shows an overview of the system.

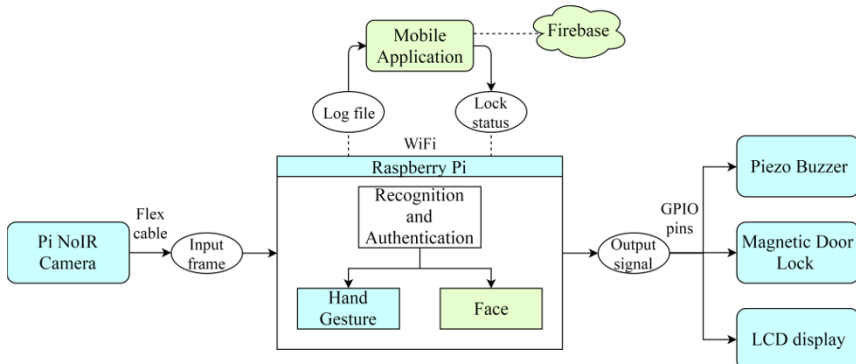


**Fig. 1.** System overview of the home access system

The Raspberry Pi 3 Model B+ is a single board computer employed as the central processing unit and the communication hub. It runs on quad-core with a 64-bit SoC processor at 1.4GHz with 1GB SDRAM. Its powerful processing capability allows execution of machine learning libraries, which were used in this project. Besides that, the board has built-in 802.11ac Wi-Fi that helps interconnectivity with the mobile application and cloud database. The board also comes with multi-purpose GPIO pin-outs, which were used with on-site interfacing units. They are the piezo buzzer, a 16 x 2 LCD display module and a relay switch. The Pi board can only drive 3.3V and 5V. Thus, the relay was applied to control the electromagnetic door lock which was driven by a 9V supply. A Raspberry Pi NoIR camera module was connected through the CSI port to capture the image frames for face authentication and hand gesture recognition. The CSI bus is capable of transferring data at extremely high speed, up to 2Gbps. It has a fixed focused lens with native resolution of 5 megapixels. Table 1 gives the summary of the GPIO connections.

**Table 1.** Raspberry Pi 3 GPIO connection to hardware peripherals.

GPIO number	Connection	Function
2	Vcc pin of LCD module and relay	5V power supply
39	Ground pin of LCD module, relay and negative terminal of piezo buzzer	Ground
3	SDA of LCD module	I <sup>2</sup> C communication
5	SCL of LCD module	I <sup>2</sup> C communication
16	Signal pin of relay	GPIO
18	Positive terminal of piezo buzzer	GPIO

With a small form factor of 85mm x 56mm x 20mm, weighing at only 50g, the Raspberry Pi 3 can be easily packaged together with the other hardware peripherals and installed at the door entrance. The system's flow is described in Fig. 2.

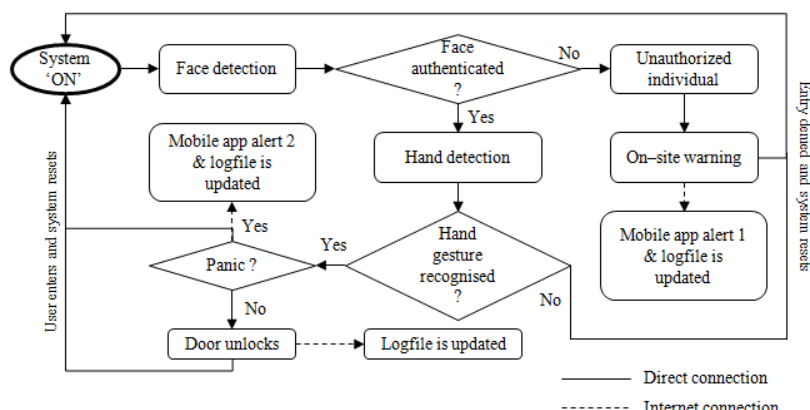


**Fig. 2.** System flow of the home access system

### 3.1 Face Authentication

The face authentication consists of two parts, namely the face detection and its recognition.

Initially, the system actively scans for a face. Each frame is converted from RGB to grayscale before the detection commences. The Multi-task Cascaded Convolutional Neural Network (MTCNN) [12] was employed for the purpose of face detection and alignment. MTCNN is a deep cascaded multi-task framework that explores the inherent correlation between detection and alignment to optimize its performance. It consists of three layers, which are the proposal network (P), refinement network (R) and output network (O). Firstly, the face is detected through the P-network. Then, rejection of a large number of false candidates is performed. Calibration with bounding box regression is done in R-network. Finally, the O-network identifies the face bounding box and its facial landmarks. 3x3 kernels were used in the 2D-convolution filters and max pooling except for their last layers in the R-network and O-network, which utilized 2x2 kernels. Finally, the detected face is segmented and normalized to 162 x 162 pixels while its features are preserved in a 128-dimensional feature vector.

The Inception ResNet v1 CNN classifier [13] was applied to identify the house occupants. Initially, a segmented face goes through a series of 2D-convolution layers and max pooling with 3x3 kernels before being fed into three Inception ResNet blocks. Each Inception network has residual connections between each layer of output that reduces the loss of computation resources between layers. These networks utilized combinations of 1x1, 1x3, 3x1, 3x3, 1x7, 7x1 convolution kernels. Later, average pooling was done using a kernel size of 8x8 before being fed into the dropout layer. Dropout is used to prevent model over-fitting and the value employed was 0.2. Finally, the softmax layer enables the model to distinguish more than two different users. The trained classifier output ( $q$ ) is compared with the numerical result from MTCNN ( $p$ ) using equation (1). The acceptance threshold was set at 95%.

$$d(p, q) = \sqrt{\sum_{i=1}^n (p_i - q_i)^2} \quad (1)$$

### 3.2 Hand Gesture Recognition

Hand gesture recognition consists of two parts, namely the hand detection and hand pose recognition. A sequence of correct hand poses will yield the correct hand gesture recognition as entry or panic password.

An open source real-time hand detection using neural networks from [14] was adopted. Single Shot MultiBox Detector (SSD) [15] approach was implemented in the algorithm. The SSD approach is based on a feed-forward CNN that produces bounding boxes and scores for the presence of an object class. Thus, recognition of multiple desired objects in a single frame is possible. In this case, the network was trained to detect the human hand. The convolution process decreases the input size progressively to allow detections at multiple scales. 3x3 sized kernels were used for its 2D-convolution

and max pooling layers. The model used for transfer learning of the neural network is the SSD Mobilenet v1 Common Objects in Context (COCO) model.

Later, the hand is segmented and normalized to 200 x 200 pixels. The background is subtracted by detecting skin color via thresholding done in the HSV color space, namely the hue ( $H$ ), saturation ( $S$ ) and value ( $V$ ) components. The threshold employed in this project is given in equation (2). The binary image then goes through a series of morphological process to reduce the noise caused by threshold as shown in Fig. 3.

$$\begin{aligned} 0 \leq H &\leq 30 \\ 50 \leq S &\leq 200 \\ 80 \leq V &\leq 255 \end{aligned} \quad (2)$$

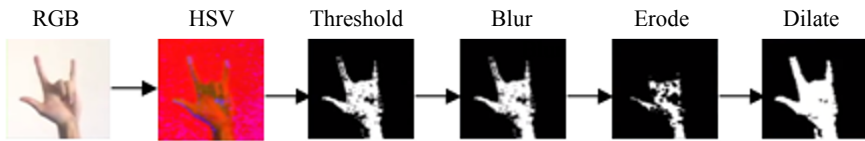


**Fig. 3.** Pre-processing steps for hand contour segmentation

The Convolutional Neural Network (CNN) [16] and adaptation given in [17] was employed to recognise static hand pose. The CNN is originally made to recognise digits and handwritings. Since the segmented hands important features are their edges and positions, the same network is suitable to recognise hand pose as well. The post-processed binary image is fed into the CNN, which consists of twelve layers. 3x3 kernels for 2D-convolution and 2x2 kernels for max pooling were implemented. The dropout value applied was 0.5. Eight classes of hand pose were trained, as tabulated in Fig. 4. All classes except ‘nothing’ were used to recognise hand gesture. The ‘nothing’ class denotes binary images which do not fall under the seven other classes. In this project, a sequence of three hand-poses makes up for a set of hand gesture password for entry or panic code. The sequence can be defined by the user.

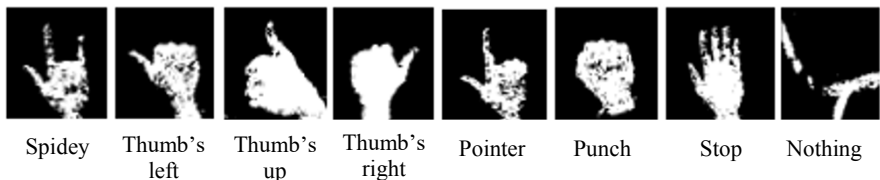


**Fig. 4.** Hand pose classes trained by CNN

### 3.3 Firmware

Raspbian 9 serves as the operating system for the Raspberry Pi 3 board. The OpenCV image processing library was installed on the board and used for preprocessing steps such as color conversions and morphological operations. Besides that, the machine

learning library, Keras, which is backed by TensorFlow, was also installed on the board. The Python programming language was used to develop the codes for image processing and deep learning. For developmental purpose, a similar setup was put in place on a notebook running on Ubuntu. CNN models training and data collection were done using the notebook. Then, the trained models were exported to the Raspberry Pi 3 board for implementation and their processing speeds were observed.

**Google Firebase.** The services utilized in this project are Firebase authentication, real-time database and cloud messaging. All user login credentials are stored in Firebase authentication. This allows users to access the home system using their mobile devices. An authorized user can also register a new user by entering the email address and password. The Firebase database is used to store all historical data of the home access system. During a successful or failed attempt, a real-time data stamp along with its status and user ID is logged. The data can be checked via a mobile application. The database was divided into three tables. All activities are stored in the first table. Second table holds this latest entry data. A user can send signal to lock or unlock the door remotely through a third table. The Firebase cloud messaging is used to send notification or alert to the mobile application. A python script was created to invoke the messaging service during an emergency, such as foiled attempt to enter the house or panic gesture signaled by an occupant.

**Mobile Application.** For proof of concept, an Android-based mobile application was developed. The application communicates with Firebase and Raspberry Pi 3 board. Login page, new user registration page, historical data browser and door lock/unlock interface were created. Therefore, the system's activities logged in Firebase can be viewed remotely. Two Python scripts were coded for communication. Firstly, is to update the status of the Firebase database whenever there is an attempted entry. Secondly, is to allow the Raspberry Pi 3 to read the database and respond accordingly. Fig. 5 shows screenshots of the mobile interface developed.

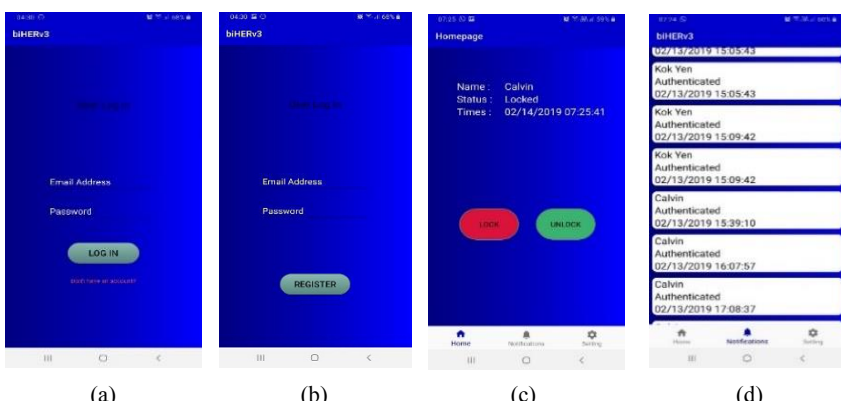


**Fig. 5.** Mobile application interface (a) Login page; (b) New user registration; (c) Remote lock/unlock buttons and (d) View historical data

## 4 Results & Discussions

The face authentication was tested with the LFW face image database, which consists of 13233 images of 5749 different human subjects [18]. The dataset was divided into two parts. 80% of the dataset were used for model training while the remaining 20% were used for validation. Validation showed an accuracy of 100% for face detection using MTCNN and 98.6% for face recognition using the Inception ResNet v1.

Later, the face authentication was tested using real-video of five individuals captured by the camera. To register a user for model training, the video of the user's face moving and tilting slightly was taken for 10s. Then, the frames grabbed from the video were used for training. The model was able to recognise individuals when the head is slightly tilted, different facial expressions and vaguely occluded. Few positive results are shown in Fig. 6. On the other hand, the recognition failed when the face is turned ~90° to the left or right and when the face is severely occluded. However, this case is unlikely in real-application scenario as an authorized user would naturally face the camera during the home access process.



**Fig. 6.** Sample frames of successful face recognitions

The hand pose recognition model using CNN was trained using a total of 23136 pre-processed binary hand segmented images, containing eight classes. The training set was randomly split into 80% for training and 20% for validation. Different rotation, translation and distance of hand pose images were introduced to the training set to increase its robustness. The validation results showed an accuracy of 99.7%. The hand pose recognition for the eight different classes mentioned was then tested on real-video that went through preprocessing on the spot. The hand pose recognition accuracy was slightly lower as tabulated in Table 2. The accuracy drop was due to lighting direction, hand angle and background variations invoked to the test video, which effect the binary image produced (*see* Fig. 7).



**Fig. 7.** Effects of lighting to the preprocessing stage.

Execution time for each process is evaluated on the Raspberry Pi 3 board as tabulated in Table 2. Accuracies of each process are shown as well. Since a sequence of three hand poses are needed to recognise a set of hand gesture password, the processing time for hand gesture recognition is threefold the time of a single hand pose recognition process. Based on the experimental data, a person needed about 7s to enter the house, assuming there is no error in between processes.

**Table 2.** Accuracy and speed for face authentication and hand pose recognition processes

Process	Data source	Number of training images	Accuracy	Time per frame
Face detection (MTCNN)	LFW	10586	100%	0.13s
Face recognition (Inception ResNet-CNN)	Self-captured	1912	95%	1s
Hand detection (SSD-CNN)	Self-captured	3840	94.4%	1s
Hand segmentation	Self-captured	-	-	0.04s
Hand pose recognition (CNN)	Self-captured	23136	93.4%	1s

The Raspberry Pi 3 minicomputer can perform extensive algorithm for home entry purpose. The board was also capable of driving the hardware peripherals, sending and retrieving data from cloud. However, the authors noticed that the board heated up easily during high computing operations. A heat sink can be attached to the board's main processor to reduce the temperature.

## 5 Conclusion & Future Work

A home access system with face authentication and hand gesture recognition had been designed and developed on the Raspberry Pi 3 single board computer. Besides being able to process computing intensive algorithms, the board can also communicate with Android-based mobile device and the Google Firebase cloud computing platform. The home access system was tested to simulate real-operating environment. Since the home occupants are able to set emergency contacts, the setup implicitly encourages neighbours to work with each other to keep the local community safe. Thus, the neighbours and local security could reach the property faster in the event of danger. Four CNN variants had been implemented on the Raspberry Pi 3. The MTCNN and Inception ResNet v1 were used for face authentication. The SSD-CNN and a conventional CNN were utilized for hand pose recognition. Those Deep Learning models yielded high accuracies and were able to perform at acceptable speed for home accessing purpose. In order to increase the robustness of the models, the training sets can be expanded by introducing more variations. Application of artificial image noise to increase lighting tone and direction variations may be used to expand the training set. On the other hand, the pre-processing before the face authentication and hand gesture recognition can be improved further through adaptive filtering based on the recent environment lighting condition.

## References

1. Malaysia 2018 Crime & Safety Report, <https://www.osac.gov/>, last accessed 2019/04/15.
2. Malaysian Police Reveals That On Average, 4 Children Go Missing Every Day in Our Country, <https://www.worldofbuzz.com/>, last accessed 2019/04/15.
3. Divya, R. S., Mathew, M.: Survey on various door lock access control mechanisms. In: 2017 International Conference on Circuit, Power and Computing Technologies (ICCPCT), pp. 1-3. IEEE, Kollam (2017).
4. Hung, C., Bai, Y., Ren, J.: Design and implementation of a door lock control based on a near field communication of a smartphone. In: 2015 IEEE International Conference on Consumer Electronics, pp. 45-46. IEEE, Taipei (2015).
5. Islam, K. T., Raj, R. G., Al-Murad, A.: Performance of SVM, CNN, and ANN with BoW, HOG, and image pixels in face recognition. In: 2nd International Conference on Electrical & Electronic Engineering, pp. 1-4. IEEE, Rajshahi, (2017).
6. Passarella, R., Fadli, M., Sutarno: Hand gesture recognition as password to open the door with camera and convexity defect method. In: 1st International Conference on Computer Science and Engineering, pp. 63-73. ICON-CSE, Palembang (2014).
7. Mesbahi, S. C., Mahraz, M. A., Riffi, J., Tairi, H.: Hand gesture recognition based on convexity approach and background subtraction. In: International Conference on Intelligent Systems and Computer Vision, pp. 1-5. IEEE, Fez (2018).
8. Tasnuva, A.: A neural network based real time hand gesture recognition system. International Journal of Computer Applications 59(4), 17-22 (2012).
9. Nagi, J., Ducatelle, F., Di Caro, G. A., Cireşan, D., Meier, U., Giusti, A., Nagi, F.: Max-pooling convolutional neural networks for vision-based hand gesture recognition. In: IEEE International Conference on Signal and Image Processing Applications, pp. 342-347. IEEE, Kuala Lumpur (2011).
10. Abbas, Q., Ibrahim, M. E.A., Jafar, M.A. A comprehensive review of recent advances on deep vision systems. Artificial Intelligence Review 52(1). 39-76 (2019).
11. Aleluya, E. R. and T. Vicente, C. : Faceture ID: face and hand gesture multi-factor authentication using deep learning. Procedia Computer Science 135, 147-154 (2018).
12. Zhang, K., Zhang, Z., Li, Z., Qiao, Y.: Joint face detection and alignment using multitask cascaded convolutional networks. IEEE Signal Processing Letters 23(10), 1499-1503 (2016).
13. Szegedy, C., Ioffe, S., Vincent. V.: Inception-v4, Inception-ResNet and the Impact of Residual Connections on Learning. In: 31<sup>st</sup> AAAI Conference on Artificial Intelligence, pp. 4278-4284. AAAI, San Francisco (2017).
14. Victor Dibia, Real-time Hand-Detection using Neural Networks (SSD) on Tensorflow, (2017), GitHub repository, <https://github.com/victordibia/handtracking>, last accessed 2019/03/30.
15. Liu, W., Anguelov, D., Erhan, D., Szegedy, C., Reed, S., Fu, C. Y., Berg, A. C.: SSD: Single shot multibox detector. In: European Conference on Computer Vision, pp 21-37. Springer-LNCS, Amsterdam (2016).
16. LeCun, Y., Kavukcuoglu, K. and Farabet, C.: Convolutional networks and applications in vision. In: IEEE International Symposium on Circuits and Systems, Paris, pp. 253-256. IEEE, Paris (2010).
17. Keras Tutorial: The Ultimate Beginner's Guide to Deep Learning in Python, <https://elitedatascience.com/keras-tutorial-deep-learning-in-python>, last accessed 2018/11/05.
18. Labeled Faces in Wild Home, <http://vis-www.cs.umass.edu/lfw/>, last accessed 2018/11/30.



# Portrait of Indonesia's Internet Topology at the Autonomous System Level

Timotius Witono<sup>1,2(✉)</sup> and Setiadi Yazid<sup>1(✉)</sup>

<sup>1</sup> Faculty of Computer Science, Universitas Indonesia,  
Depok, Indonesia

[setiadi@cs.ui.ac.id](mailto:setiadi@cs.ui.ac.id), [timotius.witono@ui.ac.id](mailto:timotius.witono@ui.ac.id)

<sup>2</sup> Faculty of Information Technology, Maranatha Christian University,  
Bandung, Indonesia

[timotius.witono@it.maranatha.edu](mailto:timotius.witono@it.maranatha.edu)

**Abstract.** Internet topology research at the AS-level is generally carried out globally, while lesser research focuses on certain regional topologies. The motivation of this research is to provide a portrait of Indonesia's Internet topology at the AS-level over the past ten years, from 2009 to 2018; with datasets taken from APNIC and CAIDA. Analysis of ten years consecutive data shows that the number of ASNs allocated for Indonesia has increased by around 114 new ASNs per year, while the average network diameter and path length has been quite constant over the past ten years. The growth in the number of AS nodes and links occurs linearly with a ratio of nodes:links around 1:2.5. Indonesia's Internet topology at the AS-level has scale-free property, with the presence of hubs in the topology; this results in a robust topology against random attacks with a critical threshold above 90% but still susceptible to targeted attacks.

**Keywords:** Internet Topology, Autonomous System, Complex Network, Graph Theory

## 1 Introduction

Internet topology is an interesting area of research that attracts many researchers to gain many insight from research in this area. The most prominent research are in the level of autonomous system (AS) because of its highest granularity level in the Internet and its easiness to collect the data of AS [1]. One of the most cited paper in this research area is from Faloutsos *et al* [2], they stated that topology of the Internet does follow the rules of power-law distributions. Willinger and Roughan divide motivations in network topology research into four categories as follows: scientific, adversarial, managerial, and informational [3]. Internet structure is very important to be known by researcher and engineer, because structure affect its function and can also be used to predict future developments [4]. An accurate representative topology will also enable engineer to enhance the quality of services, estimating delays, and enhancing effective traffic [5]. Many researcher use Border Gateway Protocol (BGP) table dump to generate a graph that represent the Internet topology on the level of AS, or at least

a part of AS-topology in the Internet. A **node** represents an AS-Number (ASN) and an **edge** represents a link between nodes [3]. Many researcher use BGP table dump from Route Views (RV) and Routing Information Service (RIS) as their sources of experiment, but there are also another sources that can be obtained; such as from traceroute-like probe or from Internet Routing Registry (IRR) [6]. Although there have been many attempts to obtain the AS-level Internet topology, efforts to obtain a complete topology are very difficult and even almost impossible [7].

AS topology is mainly discussed and measured in the scope of global Internet topology, while fewer articles discuss about specific regional or country level of AS topology. Berenguer and Pintor discuss about Internet AS topology in Latin America and the Caribbean (the LAC region) [8]. Çakmak and Aydin analyzed about 43 thousand active AS from 25 selected countries and found non-uniformity in their interconnection ecosystem; while Gregori *et al* found that African AS-level ecosystems are heterogeneous in terms of culture, development, and economy [9, 10]. Another study on global African inter-domain topology conducted by Fanou *et al*, they collected data from 2013 to 2016 while improving their measurement infrastructure by installing more vantage points [11]. Wählisch *et al* inspected their home country of Germany for its AS-structure and made a detailed analysis of it; while another study from Siritana *et al* discussed the relationship between AS in Thailand [12, 13].

The motivation of this research is to photograph Indonesia's Internet topology at the AS-level over the past ten years, from 2009 to 2018. The specific purpose of this research is to measure the development of the Indonesia's Internet topology at the AS-level in the last ten years; whereas from the general view, a representative model of regional Internet topology will give opportunities for researchers and stakeholders to diagnostics network, optimize performance, improve service and policy. We retrieve datasets from *Asia Pacific Network Information Centre* (APNIC) and *Center for Applied Internet Data Analysis* (CAIDA) as the first step, then we store them to the **Neo4j** as a graph database, furthermore we layout and analyze the stored-data with **Gephi**. We choose a simple undirected graph layout to represent the topology, therefore graph algorithm is used to analyze the collected data. Because the data analyzed is static data, we use several *topological metrics* which focus on measuring connectivity between complex network components. We arrange this paper as follows: *Section 2* provide outline about related works in the area of Internet topology, *Section 3* explain about the data and methodology that we use to represent and analyze, *Section 4* discuss about the results of representation and analysis, while *Section 5* conclude the research and also propose some future works.

## 2 Related Work

AS-graph is a logical Internet topology where nodes represents the AS and edges reflects the relationship between AS [3]. ASes use BGP to exchange routing information on the Internet, each BGP-speaking router has a table which contains

*IP-prefix-to-AS* mappings to show its reachability against other ASes by creating path vector to each connected AS; AS-graph can be obtained directly from this BGP data. There are two repository projects that collect and archive BGP routing table, they are Route Views (RV) of the University of Oregon and Routing Information Service (RIS) of RIPE NCC [6]. Dhamdhere and Dovrolis examines the evolution of the AS for 12 years –*between 1998 and 2010*– with data sources derived from historic dataset belonging to RV and RIS. They state that BGP table dump from RV and RIS are not enough to infer the evolution of peering links or more commonly called Peer-to-Peer (P2P), so they focus on the evolution of Customer-to-Provider (C2P) links. There are several conclusions mentioned in their research, namely: there are two phases of AS' growth which can be concluded from a span of 12 years –*an exponential increase until 2001 and a slower exponential growth thereafter*–, the average of path length on the Internet remains stable, and AS growth in Europe is faster and more dynamic than in the United States [14]. Trajković writes that the trend of Internet topology mapping has been changed from generating random graph to the mining of ASes data from public dataset. The conclusions of this study are: power-law exponents on both the dataset in 2003 and 2008 remain similar –*regardless of the growth of the Internet, the addition of users, and the addition of new elements to the network*–; but the spectral properties analysis finds some new trends and important changes to the AS-graph [15]. Research from Oliveira *et al* shows that topologies at the AS-level which are generated only from a single data snapshot from a BGP-based public dataset, usually having a low quality of accuracy and completeness [7]. The main problem in the process of inferring Internet topology in the form of AS-graph from BGP table dumps dataset is the presence of missing data, especially information of edges missing in significant numbers; missing information of edges can be supplemented by adding the dataset from other parties, such as from Regional Internet Registry (RIR) and looking glass from Internet eXchange Point (IXP) [16].

There are many graph metrics that have been defined in regard to complex network analysis, among them is a technical paper which is written by Hernandez and Mieghem. On this paper, they focused on general graph metrics which are unweighted and undirected; these metrics can be used as tools for analyzing, discriminating, and synthesizing complex networks. A complex network can be studied merely in the light of its topology, focus on nodes and their interconnection, a graph  $G$  defined as a set of nodes  $N$  connected by links  $L$  [17]. Jamakovic *et al* defines topological metric in their research article. A network can be represented as an undirected graph  $G = (N, L)$  with  $n = |N|$  nodes and  $m = |L|$  links. Here are some topological metrics that are relevant to the literature on computer networks: **Basics**, **Degree**, **Distance**, **Clustering**, **Centrality**, **Coreness** and **Robustness** [18]. **Eigenvector Centrality** is the process of measuring the centrality of a node based on the prestige level of neighboring nodes; a node is considered increasingly central if it has prestige neighbors. **Betweenness Centrality** measures the centrality of a node from how many other nodes are connected through that node; the more a node is passed as a path between

the other nodes, the more central the node is. **Degree centrality** measures the level of centrality of a node by calculating the number of edges connected to that node; the more edges on a node, then the node is considered increasingly central [19]. **Scale-free** property of complex networks were introduced by Barabási *et al* from their research on the World Wide Web (WWW), they found that the degree distribution of WWW topology was not random but followed power law distribution on a *log-log* scale. They define *scale-free* network as "*a network whose degree distribution follows a power law*", in contrast to random network whose degree distribution follows the Poission distribution. The main difference between random network and *scale-free* network is that there are hubs on *scale-free* network which effectively forbidden in random network that normally have comparable degrees on most nodes. *Scale-free* network is naturally robust to the removal of random nodes in the percolation process, critical threshold in *Equation (1)* is a critical value that will make a network fragmented if the value is reached ( $f_c$ : critical threshold,  $\langle k \rangle$ : average degree,  $\langle k^2 \rangle$ : second moment of degree) [20].

$$f_c = 1 - \frac{1}{\frac{\langle k^2 \rangle}{\langle k \rangle} - 1} \quad (1)$$

### 3 Data and Methodology

In this section we explain the research steps that we have taken to present the Indonesia's Internet AS topology in AS-graph representation; the sequence of research steps is described in *Figure 1*.

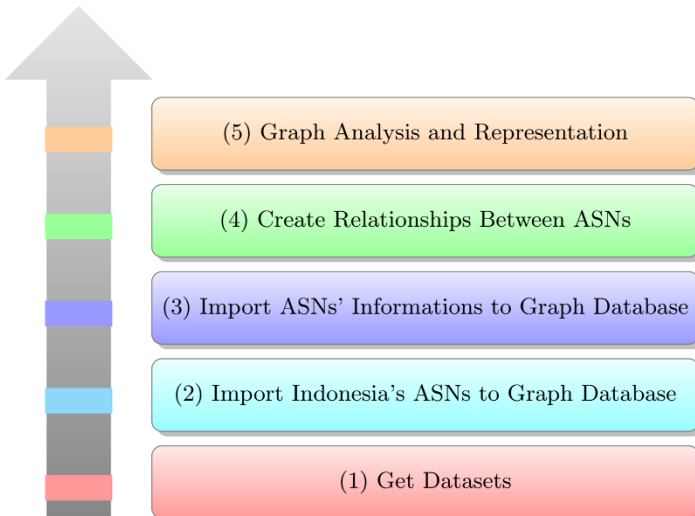


**Fig. 1.** Research steps

These are the detail of research steps in *Figure 1*:

1. Get Datasets

We retrieve Autonomous System Numbers (ASNs) of Indonesia from *Asia Pacific Network Information Centre* (APNIC) [21]. There were 1452 ASNs allocated by APNIC for Indonesia until 2018, first ASN was allocated in 1994. We retrieve *AS Organizations* datasets (*AS Org*) from *Center for Applied Internet Data Analysis* (CAIDA) [22]. We also use *AS Relationships* datasets (*AS Rel*) from CAIDA as a source of relations between AS [23].

2. Import Indonesia's ASNs to Graph Database

ASNs dataset from APNIC is converted from text (TXT) to comma-separated values (CSV) format, then loaded to Neo4j as the graph database for this research. ASNs of each year between 2009 to 2018 are imported to Neo4j as nodes, all nodes have *label:AsYY* (YY: year) with *property:ASN* as their properties.

3. Import ASNs' Informations to Graph Database

After all nodes *label:AsYY* have been created with *property:ASN*, another properties are added to all nodes regarding the ASN, based on CAIDA *AS Organizations* dataset. As the result of this step, *label:AsYY* nodes have additional properties as follow *properties: ASN, ASname, ORGID, ORGName, Country, Source*.

4. Create Relationships Between ASNs

On this step, links are created between related nodes based on relationship information from CAIDA *AS Relationships* dataset. In accordance with the information held by the dataset, each pair of ASNs in the dataset is matched with the data on the graph database.

5. Graph Analysis and Representation

We use Gephi as a tool to analyze and represent the Indonesia's Internet AS topology as a simple undirected graph. Several undirected topological metrics which we use for analysis are degree, distance, centrality, density, and robustness.

## 4 Result and Discussion

*Figure 2* shows the number of *Allocated ASN* for Indonesia from APNIC, which increased linearly from 2009 to 2018. The number of ASNs in Indonesia increased significantly from only 404 in 2009 to 1452 in 2018. The biggest increase was in 2018 and 2011, where there were 203 and 200 new ASNs respectively; while the smallest increase occurred in 2012 with only 13 new ASNs allocated by APNIC. In total, there are 1141 new ASNs allocated for Indonesia in the last 10 years, or around 114 new ASNs per year. The percentage of *Connected Nodes* which can be inferred with CAIDA's *AS Relationship* is between 65% to 78% of the amount of APNIC's *Allocated ASNs*, or around 72% on average; while the number of *Detected Links* each year is around 234% to 274% when compared to *Detected Nodes* in the same year. In the comparison seen from the right-side box in *Figure 2*, the number of nodes and links increases linearly from 2009 to 2018.

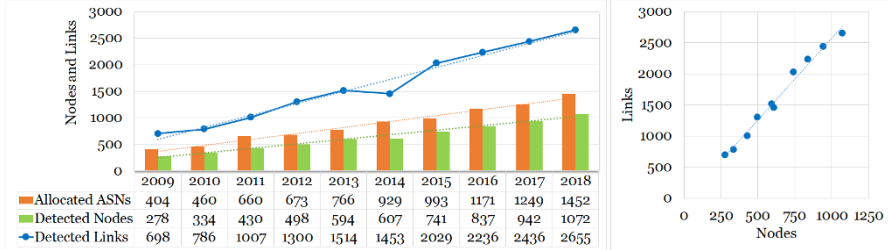


**Fig. 2.** Number of nodes and links of Indonesia's AS-Graph between 2009 to 2018

The *diameter* of Indonesia's Internet AS topology in the past ten years is constant between 6 to 8, with an *average diameter* of 7. The *average path length* in *Figure 3* is quite constant in ten years, with 2.985 being the lowest and 3.302 being the highest; this is in line with the results of research on Internet topology globally [14]. The *graph density* of Indonesia's Internet AS topology is always sparse and it is getting more sparse from year to year, as seen from the right-side box in *Figure 3*.

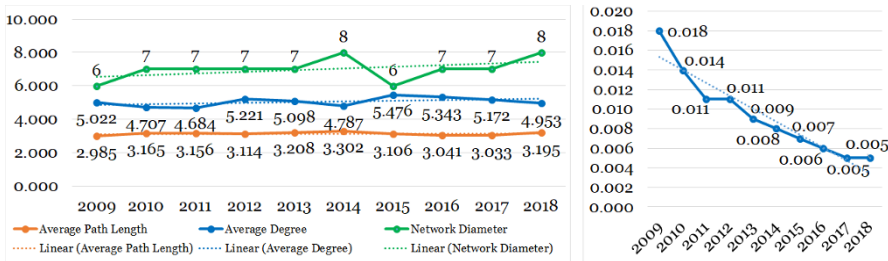


**Fig. 3.** Network diameter, average degree, average path length (*left-side box*) and graph density (*right-side box*) of Indonesia's AS-graph between 2009 to 2018

We choose ForceAtlas2 [24] layout algorithm in *Figure 4* to represent the Indonesia's Internet AS topology in 2018; with scaling node-size according to each *eigenvector centrality* and different node-color according to each *coreness*. Details of the topological metric of Indonesia's Internet topology in 2018 are listed in *Table 1*.

**Table 1.** Topological metric of Indonesia's Internet AS topology in 2018

Metric	Value	Metric	Value
Nodes	1072	Maximum Degree	279
Links	2655	Average Degree	4.953
Network Radius	4	Average Path Length	3.195
Network Diameter	8	Average Clustering Coefficient	0.339
Maximum Coreness	6	Graph Density	0.005

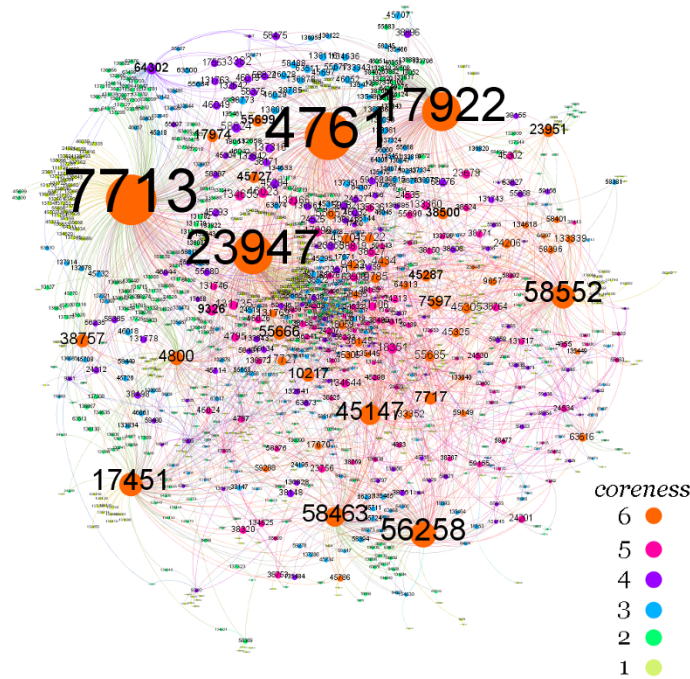


**Fig. 4.** ForceAtlas2 layout of Indonesia's Internet AS topology in 2018 (*node-size: eigenvector centrality, node-color: coreness, node-label: AS-Number*)

The most prominent ASN in Indonesia's Internet AS topology in 2018 is AS7713, it has the highest influence values in terms of *eigenvector centrality*, *betweenness centrality*, and *degree centrality*. AS4761 is the second leading ASN on the AS-graph, while AS23947 gets the third position in the value of *eigenvector centrality* and *degree centrality*. Ranking of the top ten ASNs in the Indonesia's Internet AS topology in 2018 is listed in *Table 2*.

**Table 2.** AS ranking of Indonesia's Internet AS topology in 2018

Ranking	ASN	Eigenvector Centrality	ASN	Betweenness Centrality	ASN	Degree Centrality
1	AS7713	1.00	AS7713	0.28	AS7713	279
2	AS4761	0.94	AS23947	0.22	AS4761	197
3	AS23947	0.80	AS4761	0.16	AS23947	195
4	AS17922	0.76	AS58552	0.12	AS17922	169
5	AS56258	0.49	AS17451	0.11	AS58552	120
6	AS58552	0.46	AS56258	0.09	AS17451	104
7	AS17451	0.45	AS45147	0.07	AS58463	104
8	AS45147	0.39	AS17922	0.07	AS56258	103
9	AS58463	0.37	AS4800	0.05	AS4800	91
10	AS4800	0.25	AS58463	0.04	AS45147	87

The degree distribution *Figure 5* shows that the Indonesia's Internet AS topology is *scale-free*, because there are hubs in the tail of the log-log plot; this shows that in general Indonesia's Internet AS topology has criteria similar to global Internet topology [2]. Preferential attachment –*preference of new nodes to attach with nodes that are more connected than those that are less connected*– does not apply absolutely to the Indonesia's Internet AS topology; while three of the top ten ASNs in 2018 experienced significant growth from 2009 (AS7713, AS4761, AS2397), AS45147 did not grow significantly in the number of degrees from 2009 to 2018.

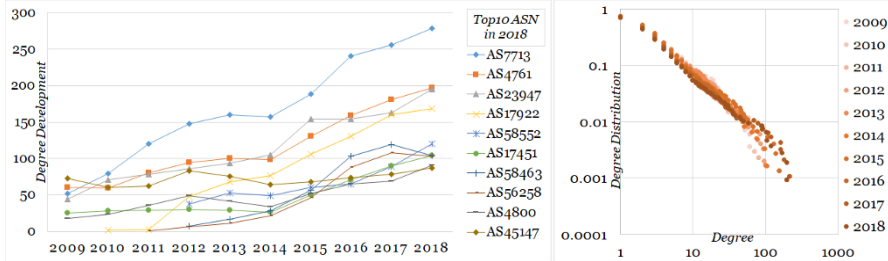


**Fig. 5.** Development of the degree over the last ten years of the top ten ASNs in 2018 (left-side box) and degree distribution of Indonesia's Internet AS topology in Complementary Cumulative Distribution Function (CCDF) format (right-side box)

Indonesia's Internet topology as a *scale-free* network is robust to perturbation, *Figure 6* shows that its critical threshold increased from 0.9460 to 0.9812 in the last ten years. As a consequence, Indonesia's Internet topology at the AS-level is robust against random attacks, but is vulnerable to attacks targeted at prominent nodes.

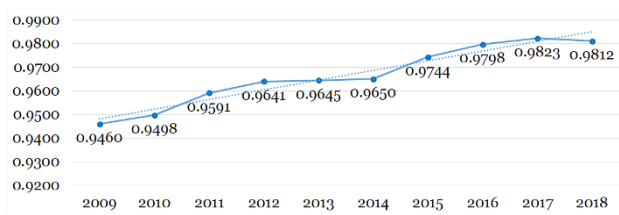


**Fig. 6.** Critical threshold

## 5 Conclusion and Future Work

Indonesia's Internet topology at the AS-level has developed linearly over the last ten years –*2009 to 2018*–, with an average growth of 114 new ASNs per year.

CAIDA's *AS Relationship* can connect around 72% of the total ASN allocated by APNIC; the number of *links* each year is an average of 2.5 times the number of AS *nodes* that are connected. The *network diameter* of Indonesia's Internet AS topology is quite constant for ten years, with a range varying from 6 to 8; the *average path length* is also constant, with a range of 2.985 to 3.302. *Graph density* of Indonesia's Internet AS topology has become more sparse over the past ten years; while has *scale-free* property, so it is resilient to random attacks with critical limits above 90%.

One of the limitations in this research is the ambiguity of multigraph existence because the process of combining twelve monthly *AS Relationship* data for each year AS-Graph; the solution taken in this research is to use the latest link information and ignore the previous one. Another drawback of this research is the incompleteness of the links, because there are a fair amount of P2P-links that are not detected in the datasets.

## Acknowledgements

This research was funded by Universitas Indonesia's PITTA-B-2019 research grant.

## References

1. He, Y., Siganos, G., Faloutsos, M.: Internet Topology. Springer New York, New York, NY (2009), [https://doi.org/10.1007/978-0-387-30440-3\\_293](https://doi.org/10.1007/978-0-387-30440-3_293)
2. Faloutsos, M., Faloutsos, P., Faloutsos, C.: On Power-law Relationships of the Internet Topology. SIGCOMM Comput. Commun. Rev. 29(4), 251–262 (Aug 1999), <http://doi.acm.org/10.1145/316194.316229>
3. Willinger, W., Roughan, M.: Internet Topology Research Redux. ACM SIGCOMM (2013), <http://sigcomm.org/education/ebook/SIGCOMMeBook2013v1.pdf>
4. Accongiagioco, G.: Modeling and Analysis of the Internet Topology. Ph.D. thesis, IMT Institute for Advanced Studies, Lucca (2014), <http://e-theses.imtlucca.it/id/eprint/140>
5. Tozal, M.E.: Policy-Preferred Paths in AS-level Internet Topology Graphs. Theory and Applications of Graphs 5(1) (Mar 2018), <https://doi.org/10.20429/tag.2018.050103>
6. Huffaker, B., Fomenkov, M., claffy, k.: Internet Topology Data Comparison. Tech. rep., Cooperative Association for Internet Data Analysis (CAIDA) (May 2012), <https://www.caida.org/publications/papers/2012/topocompare-tr/>
7. Oliveira, R., Pei, D., Willinger, W., Zhang, B., Zhang, L.: The (In)Completeness of the Observed Internet AS-level Structure. IEEE/ACM Transactions on Networking 18(1), 109–122 (Feb 2010), <https://doi.org/10.1109/TNET.2009.2020798>
8. Berenguer, S.S., Pintor, F.V.: Radiography of internet autonomous systems interconnection in Latin America and the Caribbean. Computer Communications 119, 15–28 (Apr 2018), <https://doi.org/10.1016/j.comcom.2018.01.008>
9. Çakmak, G., Aydin, M.N.: A country-specific analysis on internet interconnection ecosystems. In: 2017 9th International Congress on Ultra Modern Telecommunications and Control Systems and Workshops (ICUMT). pp. 232–237 (Nov 2017), <https://doi.org/10.1109/ICUMT.2017.8255151>

10. Gregori, E., Imrota, A., Sani, L.: On the african peering connectivity revealable via BGP route collectors. In: e-Infrastructure and e-Services for Developing Countries. AFRICOMM 2017. Lecture Notes of the Institute for Computer Sciences, Social Informatics and Telecommunications Engineering. vol. 250. Springer, Cham (2018), [https://doi.org/10.1007/978-3-319-98827-6\\_35](https://doi.org/10.1007/978-3-319-98827-6_35)
11. Fanou, R., Francois, P., Aben, E., Mwangi, M., Goburdhan, N., Valera, F.: Four years tracking unrevealed topological changes in the african interdomain. Computer Communications 106, 117–135 (Jul 2017), <https://doi.org/10.1016/j.comcom.2017.02.014>
12. Wählisch, M., Schmidt, T.C., De Brün, M., Häberlen, T.: Exposing a nation-centric view on the German internet - A change in perspective on AS-Level. In: Passive and Active Measurement. PAM 2012. Lecture Notes in Computer Science. vol. 7192, pp. 200–210. Springer, Berlin, Heidelberg (2012), [https://doi.org/10.1007/978-3-642-28537-0\\_20](https://doi.org/10.1007/978-3-642-28537-0_20)
13. Siritana, H., Kitisin, S., Gertphol, S.: A study of autonomous system relationships within Thailand. In: 2011 Eighth International Joint Conference on Computer Science and Software Engineering (JCSSE). pp. 7–11 (May 2011), <https://doi.org/10.1109/JCSSE.2011.5930077>
14. Dhamdhare, A., Dovrolis, C.: Twelve Years in the Evolution of the Internet Ecosystem. IEEE/ACM Transactions on Networking 19(5), 1420–1433 (Oct 2011), <https://doi.org/10.1109/TNET.2011.2119327>
15. Trajković, L.: Analysis of Internet Topologies. IEEE Circuits and Systems Magazine 10(3), 48–54 (Aug 2010), <https://doi.org/10.1109/MCAS.2010.937882>
16. Roughan, M., Willinger, W., Maennel, O., Perouli, D., Bush, R.: 10 Lessons from 10 Years of Measuring and Modeling the Internet’s Autonomous Systems. IEEE Journal on Selected Areas in Communications 29(9), 1810–1821 (Oct 2011), <https://doi.org/10.1109/JSAC.2011.111006>
17. Hernández, J.M., Van Mieghem, P.: Classification of Graph Metrics. Tech. rep., Delft University of Technology (2011), [https://www.nas.ewi.tudelft.nl/people/Piet/papers/TUDreport20111111\\_MetricList.pdf](https://www.nas.ewi.tudelft.nl/people/Piet/papers/TUDreport20111111_MetricList.pdf)
18. Jamakovic, A., Uhlig, S., Theisler, I.: On the relationships between topological metrics in real-world networks. In: Proceedings of the 4th European Conference on Complex Systems (ECCS’07) (Oct 2007), <http://resolver.tudelft.nl/uuid:efe2e862-71dc-4d8d-9aff-b097264a5a34>
19. Bloch, F., Jackson, M.O., Tebaldi, P.: Centrality Measures in Networks. SSRN Electronic Journal (June 2017), <https://dx.doi.org/10.2139/ssrn.2749124>
20. Barabási, A.L., Pósfai, M.: Network Science. Cambridge University Press (2016), <http://networksciencebook.com/>
21. Asia Pacific Network Information Centre: APNIC delegated internet number resources , available online: <https://ftp.apnic.net/stats/apnic/delegated-apnic-latest> (*accessed on March, 2019*)
22. Center for Applied Internet Data Analysis: The CAIDA AS Organizations Dataset (1999-2018), available online: <http://www.caida.org/data/as-organizations/> (*accessed on March, 2019*)
23. Center for Applied Internet Data Analysis: The CAIDA AS Relationships Dataset (1999-2018), available online: <http://www.caida.org/data/as-relationships/> (*accessed on March, 2019*)
24. Jacomy, M., Venturini, T., Heymann, S., Bastian, M.: ForceAtlas2, a Continuous Graph Layout Algorithm for Handy Network Visualization Designed for the Gephi Software. PLoS ONE 9(6), 1–12 (Jun 2014), <https://doi.org/10.1371/journal.pone.0098679>



# Low Latency Deep Learning Based Parking Occupancy Detection By Exploiting Structural Similarity

Chin-Kit Ng, Soon-Nyeon Cheong and Yee-Loo Foo

Faculty of Engineering, Multimedia University, 63000 Cyberjaya, Selangor, Malaysia  
chinkitng@yahoo.com, sncheong@mmu.edu.my, ylfoo@mmu.edu.my

**Abstract.** Proliferation of vehicle traffic and increasing demands for parking resources in metropolitan areas have induced the frustration of finding parking among motorists. This paper put forward a novel structural similarity (SSIM) decision scheme to realize low latency outdoor parking occupancy detection that serve as an integral part in smart parking framework by providing parking availability information in real time. An SSIM decision module is added on top of the conventional trained Convolutional Neural Network (CNN) classifier to greatly reduce the reaction time in identifying the occupancy status of parking space images extracted from live parking lot camera feeds. The proposed SSIM based parking occupancy detection has been implemented and deployed at an outdoor carpark in Multimedia University, Malaysia to assess its performance in term of detection accuracy and computation time. Assessment results show that the incorporation of SSIM decision module does not deteriorate the accuracy of parking occupancy classification with an overall accuracy of 99%. The computation time of detection application is shortened by more than six times when compared to the pure CNN classification approach when there is only a single instance of parking occupancy change, registering a processing time of 0.45 second when running on a Raspberry Pi 3 single board computer.

**Keywords:** Convolutional Neural Network, Deep Learning, Parking Occupancy Detection, Structural Similarity.

## 1 Introduction

Rapid urbanization induces the proliferation of vehicle traffic in downtown areas of metropolis. The increasing demands for parking resources worsen urban mobility due to immense number of motorists who are cruising for parking. Difficulty of finding parking spaces has caused several adversities such as traffic congestion, illegal parking, traffic accidents, etc. In fact, a study by Boston Consulting Group in 2017 reported that drivers in the capital city of Malaysia spend around 25 minutes every day to search for parking space [1]. This worrying circumstance requires the pressing need of smart parking technology to mitigate the frustration of finding parking. In recent years, rising trend of using computer vision approaches for identifying the occupancy status of parking spaces is observed due to its cost-effectiveness when compared to sensor-based systems. Among the diverse computer vision algorithms proposed for parking

occupancy detection, deep learning method has gained great interest in both research and industrial fields because of its capability to provide high accuracy results. Nonetheless, deep learning-based approaches trade off their processing speed for accurate detection and require expensive computing hardware to ensure real-time performance. To enable more scalable and reliable solution, a distributed system is often preferable where embedded devices with relatively low computational power are used for running occupancy detection locally.

This paper introduces a novel approach of combining deep learning with structural similarity algorithms to realize real-time parking occupancy detection performance on single board computer. A decision module based on structural similarity index is added as preprocessing stage to determine potential changes of occupancy status at each parking space. Subsequently, only parking space images with significant changes in structural information are fed into a binary classifier to confirm whether there is a change in occupancy status. The reasoning behind the addition of decision module to minimize the detection latency is because not all parking space will experience a change in occupancy status simultaneously no matter how busy a parking area is. Therefore, the more computationally intensive image classification stage should only be performed on parking space images that are determined to have potential changes in between successive detection cycles when an image of parking area is retrieved from surveillance camera. The authors have implemented and evaluated the proposed low latency parking occupancy detection scheme at a university carpark in Multimedia University, Malaysia. Assessment results evidence that the novel approach can accelerate the reaction time to reflect change of occupancy status at a single parking space up to six times faster as compared to perform the image classification stage on all parking space images at each detection cycle.

## 2 Related Work

Over the years, increasing researches and developments have been carried out on the use of computer vision method for parking occupancy detection due to its high applicability in outdoor parking environment. Majority of vision-based approaches rely on handcrafted visual features extracted from parking lot images to train classifiers or vehicle detectors to realize occupancy detection. For example, Peng et al. proposed the use of vehicle color feature, local gray-scale variant feature and corner feature extracted from individual parking space image namely to train a Support Vector Machine (SVM) classifier for differentiating occupied and empty parking spaces [2]. However, hand-crafted features exhibit the limitation of being susceptible to varying illumination and weather conditions which may deteriorate the detection accuracy [3]. The ability of deep CNN to overcome such drawbacks by learning features which optimally characterize the image content has inspired its application for accurate outdoor parking occupancy detection [4].

The work by Valipour et al. proved the practicality of using deep CNN for parking occupancy detection whereby a trained classifier based on VGGNet-F has achieved over 99% overall detection accuracy [5]. The classifier can run on a Raspberry Pi 3

single board computer with inference time of 0.22 seconds per parking space image. In the previous work by the authors, a simplified version of AlexNet with only three convolutional layers is used to train a binary classifier for occupancy status classification [6]. The performance benchmark based on self-collected testing dataset also demonstrated high detection accuracy of over 99%. In term of inference time, the classifier can process 23 parking space images in about 5 seconds on a Raspberry Pi 3 Model B single board computer (i.e. approximately 0.22 seconds per image). Both the aforementioned works simply perform images classification on all parking spaces during every detection iteration regardless whether or not there is parking activity going on. Although the reported inference time is considered relatively short even when running on resource-constrained embedded devices, significant latency would still present especially when the camera view covered large number of parking spaces, thus slowing down the reaction time to reflect parking occupancy changes in real time.

In a more recent work by Acharya et al. [7], image features extracted by the ImageNet-VGG-f CNN model is used to train an SVM classifier for greater generalizing ability in parking occupancy detection. The detection results showed a high transfer learning accuracy of 96% on an isolated testing dataset. Nonetheless, the use of rather complex CNN model as feature extractor that originally meant for large scale image classification requires GPU support to achieve real-time detection performance. Nurullayev et al. proposed a novel dilated CNN known as CarNet that can integrate global contextual image information with less computational cost for detecting occupancy status of parking spaces [8]. Evaluation results verified the proposed CarNet can generalize well when apply to images from different parking scenario. The reported accuracy outperforms previous works in term of generalization property. Unfortunately, the authors did not assess the processing speed of CarNet and its feasibility to run on embedded devices. Another smart parking solution proposed by H. Bura et al. employed Raspberry Pi single board computer as an interface to stream camera feeds to Nvidia Jetson TX2. The embedded AI computing device powered by Nvidia GPU runs parking space classification algorithm based on a custom-designed neural network with just one convolutional layer [9]. The edge-based solution can provide high detection accuracy and able to process 50 parking space images within 355 milliseconds. However, it requires a more costly GPU-enabled computing device to achieve such real-time performance.

In this paper, a lightweight deep neural network named Mobilenet [10] is chosen as the CNN model for training a binary classifier for outdoor parking occupancy detection. A low latency preprocessing stage based on SSIM algorithm is added as a decision scheme to determine structural changes at each parking space. This is to make sure that only images that exhibit significant variation are fed to the more computationally intensive CNN classifier for parking occupancy detection. SSIM was first introduced by Wang et al. for image quality assessment as inspired by human visual perception that comply with structural information extraction from a scene [11]. Therefore, by measuring the variation in structural information, a perceived image distortion (i.e. a change in parking scene in this case) can be reliably estimated within fractions of a second even on resource limited embedded devices.

### 3 System Design

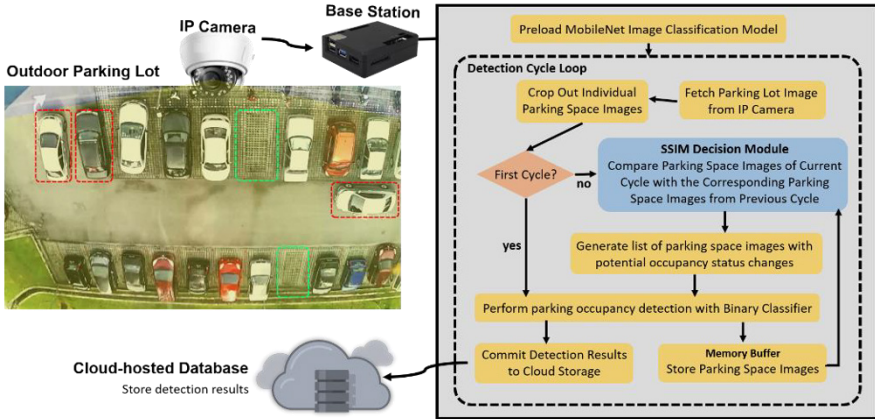


**Fig. 1.** System architecture of SSIM-based Parking Occupancy Detection

A system overview of the proposed low latency parking occupancy detection is shown in Figure 1. A base station which functions as the detection unit is locally connected to an IP camera monitoring an outdoor parking lot. In order to obtain an image classification model retrained for parking occupancy detection, parking lot images are collected for two weeks period under different weather circumstances. From all the collected parking lot images, regions of individual parking space are cropped out based on a pre-configured annotations file containing the boundary coordinates of each parking space. Subsequently, all parking space images are manually categorized into two classes (i.e. occupied and empty) according to the presence of vehicle and serve as the training dataset. A lightweight deep neural network named MobileNet is selected for the transfer learning process due to its ability to run with low computational requirements on resource-constrained embedded device and still offering real-time performance. The structure of MobileNet model is built based on depthwise separable convolutions which factorize standard convolution into depthwise and pointwise convolution to greatly reduce the computation requirements for mobile and embedded vision applications. Altogether, the MobileNet has 28 convolution layers including the first full convolution layer, each of which is followed by a batchnorm and ReLU nonlinearity. The resulting model which have been trained specifically for parking occupancy classification is then moved to the base station.

At the base station, the trained MobileNet image classification model is preloaded into the memory when the detection application is initialized. During each detection cycle, parking lot image is fetched from the IP camera and images of individual parking space are cropped out. At the first cycle, all parking space images are fed into the binary classifier to determine their corresponding occupancy status based on the preloaded model. All the parking space images are then stored in a memory buffer for later use. In each subsequent detection cycle, all the cropped parking space images are passed

through the SSIM decision module and get compared to the respective images from the previous cycle in the memory buffer. The decision module computes the SSIM index for each pair of parking space images from current and previous cycle to determine whether significant changes in structural information is presence in each parking space with reference to a threshold value. The threshold value is preset based on the SSIM index of a group of parking space image sequences that exhibits vehicle parking and leaving activities. A parking space is considered to have potential occupancy status change if the computed SSIM index is less than the threshold value (i.e. SSIM index of 1 means the image pair is exactly identical to each other whereas a value of 0 indicates no structural similarity between them). A list of parking space images from current cycle that have potential occupancy changes is generated as the output of SSIM decision module and fed into the binary classifier to confirm the presence of vehicle. With such implementation, only parking spaces that exhibit significant structural changes will be passed to the more computationally intensive classification process. This will minimize the total processing time of each detection cycle when there is no parking activities since only the fast SSIM computation will be performed. More importantly, the reaction time to detect occupancy change at any parking space can be greatly shorten and hence achieve real-time performance even on embedded platform. At the end of each detection cycle, only classification results from the list of parking space images outputted by SSIM decision module are committed to the cloud storage.

## 4 System Implementation



**Fig. 2.** Image samples of training dataset: empty (first row) and occupied (second row)

The proposed low latency parking occupancy detection approach is implemented at the parking lot of Faculty of Engineering in Multimedia University. A Foscam FI9800P outdoor IP camera is used to collect parking lot images (covering 22 parking spaces) by taking snapshot from the third floor of faculty building at ten minutes interval for ten working days (i.e. 8am to 7pm on each day). From each parking lot image, 22 parking space images are cropped out using OpenCV Python library based on the cropping boundaries preconfigured with the LabelImg image annotation tool. Approximately 7k image samples for each of the two classes (i.e. occupied and empty) are obtained as the

training image dataset. Some image samples from each of the two classes are shown in Figure 2. The minimal version of MobileNet (i.e. MobileNet\_v1\_025\_128) has its width multiplier set to 0.25 and input resolution of 128. In total, it has only 15 million Multi-Adds computations and 0.2 million parameters which are 38 times and 16 times less than the respective value of baseline MobileNet (i.e. MobileNet\_v1\_100\_224). The minimal MobileNet is downloaded from Tensorflow github repository and used for transfer learning process. The training operation based on the prepared training dataset is performed using the Tensorflow v1.9 machine learning framework on a desktop computer equipped with NVIDIA GeForce GTX1080 GPU. The minimal MobileNet model is trained for 4000 iterations with RMSprop optimizer and 0.01 initial learning rate. The training process is completed within 4 minutes with 100% train and validation accuracy. The image classification model is obtained in the form of a trained computational graph.

The base station is realized with a Raspberry Pi 3 Model B+ single board computer running on Raspbian Stretch OS and installed with Tensorflow packages. The parking occupancy detection application is coded in Python language and the SSIM index computation is performed with the *compare\_ssim* function available in the Python-Skimage library. Ten instances of parking activities (i.e. parking space image sequences that experience vehicle entering or leaving event) are utilized to determine the optimal threshold value for the SSIM decision module by inspecting the computed SSIM index between successive frames of a parking space image sequence with vehicle movement. The authors found that the value of 0.7 provides a good sensitivity level to identify parking space images that show significant change in structural information without triggering too many false alarms (e.g. minor variations due to shadow patterns, debris, stray cats or dogs, etc.). The threshold value of 0.7 is chosen with respect to the setting such that one parking lot image is retrieved every second. For more frequent retrieval rate of parking lot image, higher threshold value should be used as the changes between adjacent image frames will be less significant. Tensorflow module is imported to consume the image classification model for classifying the occupancy status of parking space images shortlisted by the SSIM decision module. Detection results are committed to the Firebase Realtime Database for storage in JSON format only when there are occupancy changes to minimize the data traffic.

## 5 Results and Discussions

Eight hours of parking lot video recordings are independently collected for each of the three sessions (i.e. 24 hours of video recordings in total), namely morning (8am to 12noon), afternoon (12noon to 4pm) and evening (4pm to 7pm) to serve as the testing dataset for detection accuracy assessment. The video recordings in testing dataset are purposely selected such that they exhibit interferences due to changing weather conditions such as sunny, cloudy and rainy circumstances. Image frames are extracted from each video recording at a rate of one frame per second and the occupancy status of each parking space are manually annotated to establish the ground truth. False Negative Rate (FNR), False Positive Rate (FPR) and Average Detection Accuracy (ADA) are used as

the evaluation metrics to quantitatively represent the assessment results. Their respective formulae are stated as in equation (1), (2) and (3). A false negative (FN) means empty space is classified as occupied whereas a false positive (FP) means occupied space is classified as empty. True negative (TN) and true positive (TP) indicate correct classification of occupied space and empty space respectively.

$$FPR = \frac{FP}{FP + TN} \quad (1)$$

$$FNR = \frac{FN}{FN + TP} \quad (2)$$

$$ADA = \frac{TP + TN}{TP + TN + FP + FN} \quad (3)$$

All the parking lot image frames extracted from video recordings in testing dataset are processed with the SSIM based parking detection application as well as the conventional pure CNN classifier approach. This is to examine whether the addition of SSIM decision module will negatively affect detection accuracy. Evaluation results evidence that the presence of SSIM decision module does not degrade the detection accuracy when compared with the pure CNN classifier approach. The computed evaluation metrics in Table 1 show that high accuracy is demonstrated across all the three sessions of testing dataset with overall ADA of 99.98%. There is only one instance of false positive being identified in the afternoon sessions on a black-colored vehicle due to the error of occupancy status classification by the binary classifier.

**Table 1.** Accuracy of parking occupancy detection.

Testing Dataset	No. of test samples		Evaluation Metrics		
	empty	occupied	FNR	FPR	ADA
Morning (8am - 12pm)	23065	610535	0	0.0000	1.0000
Afternoon (12pm - 4pm)	88479	545121	0	0.0006	0.9995
Evening (4pm - 7pm)	222325	411275	0	0.0000	1.0000
Total/Overall	333869	1566931	0	0.0002	0.9998

In order to evaluate the performance of SSIM module in identifying parking spaces that have potential change in parking occupancy status, two evaluation metrics namely precision rate (PR) and recall rate (RR) are adopted. Their formulae are given in equation (4) and (5). A true positive (TP) means parking space image is shortlisted due to significant changes triggered by vehicle parking activity. A false negative (FN) means the SSIM module fails to identify parking space image that is undergoing vehicle parking activity. A false positive (FP) signifies the parking space image is shortlisted due to false alarms. Assessment results in Table 2 prove that the SSIM decision module can successfully identify all parking spaces which experience parking occupancy changes with overall RR of 1.0. Perfect precision rate is observed in the morning session in

which all the 35 parking image sequences shortlisted by SSIM decision module are indeed having a change in occupancy status. For afternoon and evening sessions, their PR drop significantly to 0.85 and 0.87 respectively following an increase in the number of parking activities during lunch hours (i.e. 12pm to 2pm) and when people get off work after 5pm. The drop in PR is mainly due to the false alarms triggered by drivers walking through the adjacent parking space to get in or get out their cars which is inevitable. Another noticeable source of false alarms is due to water droplets during heavy rain condition. Such flaw can be potentially mitigated by performing Gaussian normalization on the parking images before applying SSIM computation to filter out the high frequency noise introduced by rain droplets in the expense of increase processing time.

$$PR = \frac{TP}{TP + FP} \quad (4)$$

$$RR = \frac{TP}{TP + FN} \quad (5)$$

**Table 2.** Performance of SSIM Decision Module.

Testing Dataset	No. of Shortlisted Parking Space Im- age Sequence	Evaluation Metrics				
		TP	FN	FP	PR	RR
Morning (8am - 12pm)	35	35	0	0	1.000	1.000
Afternoon (12pm - 4pm)	59	50	0	9	0.847	1.000
Evening (4pm - 7pm)	75	65	0	10	0.867	1.000
Total/Overall	169	150	0	19	0.888	1.000

Table 3 illustrates the increase in computation speed of the proposed SSIM based parking occupancy detection in comparison to the pure CNN classifier approach. The time taken to perform SSIM computation on all the 22 parking space image pairs is around 332 milliseconds. This means when there are no parking activities in the parking lot, the detection cycle can be completed in less than 0.4 second. This implies that the detection is 8 times faster as compare to pure CNN classifier approach which takes around 3 seconds for each detection cycle. In addition, a single instance of parking occupancy change can be detected in less than half a second, registering a speed-up factor of 6.4 with respect to the computation time of pure CNN classification. Even with ten simultaneous changes in parking occupancy status, the proposed detection method can still offer up to 1.65 times speed up. In extreme case where all the 22 parking spaces are shortlisted by SSIM decision module (although hardly possible), only a minimum delay of 0.33 second will be added to the overall processing time.

To sum up, the addition of SSIM decision module to the parking occupancy detection application can greatly shorten the computation time of each subsequent detection cycle as compared to pure CNN classifier approaches in [5, 6]. This makes the proposed solution a suitable candidate to realize low latency parking occupancy detection on resource-constrained embedded device meanwhile maintaining high detection accuracy.

Besides, such implementation represents a more cost-effective solution than the work described in [7] as it can offer real-time performance without GPU hardware acceleration. The detection mechanism which is enabled through a single board computer base station attached to an IP camera also supports horizontal scalability for distributed system. By just adding another set of detection unit (i.e. the base station and IP camera), the proposed solution can be easily extended to cover more parking areas. More importantly, since the parking occupancy detection is carried out at the endpoints, no additional processing burden will be imposed on the cloud server. This will ensure timeliness delivery of the parking occupancy information to the cloud storage which is indispensable in real-time application.

**Table 3.** Computation speed of parking occupancy detection with SSIM decision module.

No. of Simultaneous Parking Space Images Shortlisted	SSIM Computation Time on 22 parking space image pairs (ms)	Classification Time of Parking Space Images (ms)	Total Processing Time (SSIM + Image Classification) in seconds	Total Processing Time of Pure CNN Classification on 22 parking space images (seconds)	Speed-up Factor w.r.t. Pure CNN Classification
0		0.0	0.3324		8.77
1		122.2	0.4546		6.41
2		243.9	0.5763		5.06
3	332.4	361.0	0.6934	2.9152	4.20
5		621.6	0.9540		3.06
10		1438.2	1.7706		1.65

## 6 Conclusion

A novel low latency deep learning based parking occupancy detection approach is presented in this paper by exploiting the structural similarity between parking space image pairs from successive detection cycles. The inclusion of SSIM decision module as pre-processing stage can accelerate the computation speed of the detection application tremendously without causing deterioration of the detection accuracy. Consequently, a base station can detect and reflect any instance of parking occupancy changes in a timelier fashion or perform the occupancy detection for wider coverage of parking lot within a fixed duration. Moreover, the proposed system architecture leverages on the local artificial intelligence (AI) capability of embedded devices to enable a decentralized solution. This is often preferable for mass deployment due to its scalability and protection against single point of failure. In future work, multithreading mechanism can be incorporated into the detection application by exploiting the multicore architecture of single board computer to further speed up the computation especially for the more time-consuming image classification process.

**Acknowledgments.** The authors thankfully acknowledge the financial supports provided by the Telekom Malaysia Research and Development Grant (No. RDTC170946) to successfully implement the proposed system at Multimedia University (Cyberjaya, Malaysia).

## References

1. The Boston Consulting Group, BCG.: *Unlocking Cities: The impact of ridesharing in South-east Asia and beyond.* (November 2017).
2. C. Peng, J. Hsieh, S. Leu, C. Chuang.: Drone-Based Vacant Parking Space Detection. In: 2018 32<sup>nd</sup> International Conference on Advanced Information Networking and Applications Workshops (WAINA), Krakow, pp. 618-622. (2018).
3. Chen, Y., Yang, X., Zhong, B., Pan, S., Chen, D., Zhang, H.: CNNtracker: Online discriminative object tracking via deep convolutional neural network. *Applied Soft Computing* (38), 1088-1098. (2016).
4. Donahue, J., Jia, Y., Vinyals, O., Hovtman, J., Zhang, N., Tzeng, E., Darrell, T.: Decaf: A deep convolutional activation feature for generic visual recognition. In: International Conference on Machine Learning, pp. 647-655. (2014).
5. Valipour, S., Siam, M., Stroulia, E., Jagersand, M.: Parking-stall vacancy indicator system, based on deep convolutional neural networks. In: 2016 IEEE 3rd World Forum on Internet of Things (WF-IoT), pp. 655-660. (2016).
6. Chin-Kit Ng, Soon-Nyeon Cheong.: Cost-Effective Outdoor Car Park System with Convolutional Neural Network on Raspberry Pi. *Journal of Engineering and Applied Sciences* (13), pp. 7062-7067. (2018).
7. Acharya, Debaditya, Weilin Yan, Kourosh Khoshelham.: Real-time image-based parking occupancy detection using deep learning. *Research@Locate* (2018).
8. Nurullayev, S., Lee, S. W.: Generalized Parking Occupancy Analysis Based on Dilated Convolutional Neural Network. *Sensors* 19(2) (2019).
9. H. Bura, N. Lin, N. Kumar, S. Malekar, S. Nagaraj, K. Liu.: An Edge Based Smart Parking Solution Using Camera Networks and Deep Learning. In: 2018 IEEE International Conference on Cognitive Computing (ICCC), San Francisco, CA, pp. 17-24. (2018).
10. Howard, A. G., Zhu, M., Chen, B., Kalenichenko, D., Wang, W., Weyand, T., Adam, H.: Mobilenets: Efficient convolutional neural networks for mobile vision applications. *arXiv preprint arXiv:1704.04861* (2017).
11. Wang, Z., Bovik, A. C., Sheikh, H. R., Simoncelli, E. P.: Image quality assessment: from error visibility to structural similarity. *IEEE transactions on image processing* 13(4), 600-612. (2004).



# Sequential Constructive Algorithm incorporate with Fuzzy Logic for Solving Real World Course Timetabling Problem

Tan Li June<sup>1</sup>, Joe H. Obit<sup>2</sup>, Yu-Beng Leau<sup>3</sup>, Jetol Bolongkikit<sup>4</sup> and Rayner Alfred<sup>5</sup>

<sup>1</sup> Universiti Malaysia Sabah Labuan International Campus, Malaysia

<sup>2</sup> Knowledge Technology Research Unit, Universiti Malaysia Sabah, Malaysia, Jalan UMS,  
88400 Kota Kinabalu, Sabah, Malaysia

lijunetan93@gmail.com, joehenryobit@gmail.com, lybeng@ums.edu.my  
jetol@ums.edu.my, ralfred@ums.edu.my

**Abstract.** Sequential constructive algorithm is one of the popular methods for solving timetabling problems. The concept of the algorithm is to assign event based on their difficulty value by using different sequential heuristic. The most common sequential heuristics are largest enrolment, largest degree and saturation degree. Each sequential heuristic has its own criteria to obtain events' difficulty value. Instead of single sequential heuristic, this paper presents to use fuzzy logic to consider multiple sequential heuristics in order to obtain the difficulty value of the events. The proposed method will be used to generate feasible solution as well as improve the quality of the solution. Another objective of this paper is to tackle a real world course timetabling problem from Universiti Malaysia Sabah Labuan International Campus (UMSLIC). Currently, UMSLIC generates course timetable manually which is very time consuming and ineffective. The experimental results show that the proposed method is able to produce better quality of solution less than one minute. In terms of quality of timetable and efficiency, the proposed method is outperforming UMSLIC's manual method.

**Keywords:** Sequential Constructive Algorithm, Fuzzy Methodology, Course Timetabling Problem.

## 1 Introduction

A general definition of course timetabling problem is known as scheduling of a given set of courses to a limited number of timeslots and room under certain criteria and requirements [1]. Every institution has its own set of criteria and requirements and they are often known as a set of constraints in timetabling problem. Basically, constraints can be categorized into two groups: hard and soft constraints. A feasible solution must not involve in hard constraint violation. Although different institutions have different sets of constraints, however there are some hard constraints that commonly used in course timetabling problem. For instance, no student is assigned to attend

more than one lecture concurrently. On the other hand, soft constraints are not necessary to be solved but it is highly desirable when soft constraints violation can be reduced in order to improve the quality of the solution. For instance, a student should not be assigned to only attend a lecture a day. Normally, the feasibility and quality of a timetable is measured by using cost function which indicates the degree of hard and soft constraints violation.

An enormous number of studies have been done with different approaches to solve course timetabling problems since the early of 1960's. For example, methods that are used to generate feasible solution such as sequential constructive algorithm [1], [2] and constraint programming [3], [4]. While metaheuristic algorithms are popular in improving solution such as Great Deluge [5], [6], Simulated Annealing [7], [8], Tabu Search [9], [10] and so forth.

This paper aims to solve course timetabling problems of Universiti Malaysia Sabah Labuan International Campus (UMSLIC). In UMSLIC, the course timetable is generated by timetabling officer manually. The timetabling process is time consuming as it needs to go through several times of amendments in order to produce a feasible timetable. Therefore, this paper proposes to develop an algorithm which integrates sequential constructive algorithm with fuzzy logic [11] to solve UMSLIC course timetabling problems. In this paper, there are two different phases of experiments: construction and improvement phase. The development of algorithm will be further discussed in Section 4.

## 2 Related Work

### 2.1 Sequential Constructive Algorithm

Sequential constructive algorithm was first introduced by [12] to solve examination timetabling problems. The idea of the algorithm is to assign those “difficult” events into timetable first. It is very difficult for those difficult events to fit themselves in the timetable when most of the timeslots and rooms are occupied by other events. There are some common sequential heuristics used to generate feasible solution such as Largest Degree (LD), Largest Enrolment (LE), Least Saturation Degree (SD), Largest Colored Degree (LCD) and Weighted Largest Degree (WLD).

However, in [13], the algorithm was unable to produce feasible solution for large instance from benchmark dataset by [14]. Therefore, many researchers introduced modified version of sequential constructive algorithms in order to improve the performance of the algorithms.

In [15], a hyper-heuristic framework which employed Tabu search to search for permutations of graph heuristic to solve both examination and course timetabling problems. The framework utilized the Tabu search to store all the possible permutations and select the most suitable heuristic to construct timetable. Any move that is not able to assign course into feasible slot and room will be stored in a Tabu list.

While paper [16] proposed a framework to hybridize sequential heuristics with local search and Tabu search. The framework is composed by three processes which each of them has different objective to achieve. The experimental results showed that

the proposed method able to generate feasible solutions for benchmark datasets [14] and ITC 2002 datasets [17]. However, none of them outperformed in terms of efficiency. For instance, the heuristic produced the best quality of timetable would taking longer time than the others.

## 2.2 Fuzzy Methodology applied in different area of research

In real world situation, most of the knowledge is ambiguous in nature and human reasoning is usually based on fuzzy information. Besides, decision making often involves considering multiple factors simultaneously. The concept of fuzzy logic was introduced is to handle such imprecise information and deal with multiple aspects at the same time. In present, fuzzy logic had been widely applied in variety of real world applications [18], [19] such as washing machines, air conditioners, and even timetabling problem particularly. For instance, fuzzy logic was applied to consider more than one heuristic ordering simultaneously to determine the difficulty value of a course.

In [11], LD, LE and SD were used to incorporate with fuzzy methodology to generate three different fuzzy combinations: Fuzzy LDLE, Fuzzy SDLE and Fuzzy SDLD. The proposed method was tested with examination timetabling benchmark datasets by [20]. The results showed that the proposed approach was able to produce comparable results in literature and overall, Fuzzy SDLE produced the best result among the fuzzy heuristic orderings.

The research on fuzzy heuristic orderings was extended to compare with non-fuzzy heuristic ordering in terms of algorithm performance in [21]. Basically, the non-fuzzy heuristic ordering refers to the single heuristic ordering which are LD, LE and SD. With the same examination benchmark datasets by [20], results showed that scheduling a list of courses based on fuzzy heuristic orderings is way more effective than only based on single heuristic ordering.

## 3 Fuzzy System and Fuzzy Sets Theory

### 3.1 Introduction

In 1965, Zadeh introduced fuzzy logic to deal with imprecise information with the idea of fuzzy set [22]. The basic idea of fuzzy logic is to use a fuzzy set to represent a class of events with degrees of membership. The general framework is to translate a fuzzy set into linguistic variable which will be assigned value in the range of zero and one by using membership function  $f_A(X)$ . A fuzzy set can also be known as an extended version of classical set theory. A membership function quantifies the linguistic variable of the fuzzy set based on its membership degree. This paper illustrates the form of fuzzy set by using room temperature as an example. For instance, the statement of “it is cold if the temperature is below 10°C” can be controversial due to its ambiguous status. In classical set theory, the membership function of the set of temperature is presented as below:

$$f_A(x) = \begin{cases} 1, & \text{if } x \leq 10^\circ\text{C} \\ 0, & \text{if } x > 10^\circ\text{C} \end{cases} \quad (1)$$

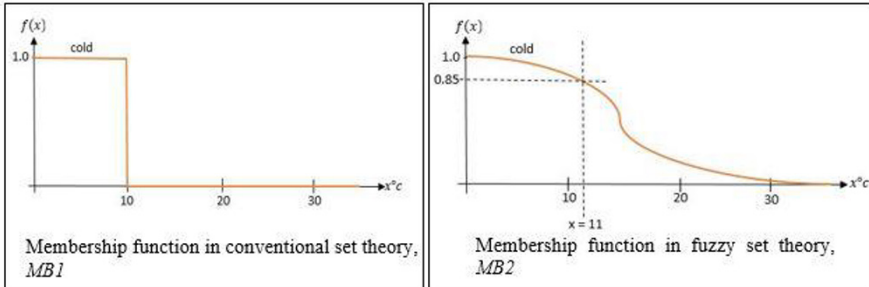


**Fig. 1.** Different membership function

Fig 1 shows the different membership functions are plotted based on conventional and fuzzy set theory. In  $MB1$ , all temperature above  $10^\circ\text{C}$  do not considered as cold such as  $11^\circ\text{C}$  because the degree of membership of  $11^\circ\text{C}$  is zero which is not really accurate.

In fuzzy set theory, “temperature” is used as a linguistic variable and assigned with linguistic value which is “cold”. Unlike conventional set theory, which is only either “cold” or “not cold”, fuzzy control system assigns value to the linguistic variable in the range of zero and one to the room temperature using membership function  $f_A(x): X \rightarrow [0,1]$  before evaluating the temperature. In  $MB2$ , the degree of membership of  $11^\circ\text{C}$  is 0.85 which is still considered as cold but with slightly less than  $10^\circ\text{C}$ . The result indicates that  $11^\circ\text{C}$  is still considered as cold but not as cold as  $10^\circ\text{C}$ .

The framework of a fuzzy system consists of four processes: fuzzification, a set of “IF...THEN...” rules, inference engine and defuzzification. Fuzzy set theory employs “IF...THEN...” rule to link input variables to output variables. In a rule, “IF” plays a role as “antecedent” while “THEN” to produce the output variables as “consequent” [11]. A set of rules is generated based on the number of inputs and outputs, and the pre-defined feature of the system.

## 4 Methodology

### 4.1 Generate Feasible Solution

This paper considers two sequential heuristics simultaneously with the implementation of fuzzy system to determine the difficulty values of a given set of courses. The three main sequential heuristics that used in this paper are:

1. **Largest Degree (LD):** Courses are listed in descending order based on the number of courses in conflict. For instance, a course with higher number of courses in conflict will be scheduled into timetable first.

2. **Largest Enrolment (LE):** Courses are listed in descending order based on the total number of students who take the particular course. For instance, a course with greater number of students will be scheduled into timetable first.
3. **Saturation Degree (SD):** Courses are listed in ascending order based on the number of available slot for the particular course. For instance, a course with fewer number of available slots will be scheduled into timetable first.

Hence, there will be three different combinations of multiple sequential heuristics which are: fuzzy largest degree and largest enrolment (LDLE), fuzzy saturation degree and largest enrolment (SDLE) and fuzzy saturation degree and largest degree (SDLD). Table 1 summarizes the hard and soft constraints for UMSLIC course timetabling problem:

**Table 1.** Hard constraints and soft constraints of UMSLIC course timetabling problem.

Hard constraints	Soft constraints
<ol style="list-style-type: none"> <li>1. No students and lecturers are assigned to attend more than one course simultaneously.</li> <li>2. A course must be assigned into a room that is able to fit all the students of that certain course.</li> <li>3. Cannot assign more than one into a room in every timeslot.</li> <li>4. There are certain courses must be assigned into specific timeslot.</li> </ol>	<ol style="list-style-type: none"> <li>1. Students and lecturers should not attend more two courses consecutively.</li> <li>2. Students and lecturers should not attend course at the last time slot of the day.</li> <li>3. Students should not only attend a single course in a day.</li> <li>4. Extra room space should be reduced.</li> </ol>

This section will take largest degree (LD) and largest enrolment (LE) as an example to discuss the process of generating fuzzy multiple sequential heuristics. In this scenario, largest degree (LD) and largest enrolment (LE) will act as linguistic variables with three different linguistic values: small, medium and large. A set of “IF...THEN...” rules will be applied to link the linguistic variable and generate a single output variable which is named as courseweight, refers to the difficulty value of a course. There are total nine rules for fuzzy LDLE used for fuzzy reasoning and only three of them will be used to illustrate the process as below:

Rule 1: IF (LD is small) and (LE is medium) THEN (courseweight is small).

Rule 2: IF (LD is medium) and (LE is medium) THEN (courseweight is medium).

Rule 3: IF (LD is medium) and (LE is large) THEN (courseweight is large).

To determine the linguistic values for LD and LE, first thing is to normalize the input values of LD and LE by using a formula as follow:

$$val' = \frac{val - minValueOfTheList}{maxValueOfTheList - minValueOfTheList} \quad (2)$$

From equation (2),  $val'$  is the normalized value while  $val$  is each of the values from the list in the range of  $[\text{minValueOfTheList}, \text{maxValueOfTheList}]$ . For example, a set of courses with the LD [4, 90] and LE [1, 176], and assume LD and LE for a course is 33 and 101 respectively. In this scenario, 33 and 101 will be treated as input values and normalized by using equation (2). Therefore, the normalized value of LD and LE are 0.34 and 0.57 respectively.

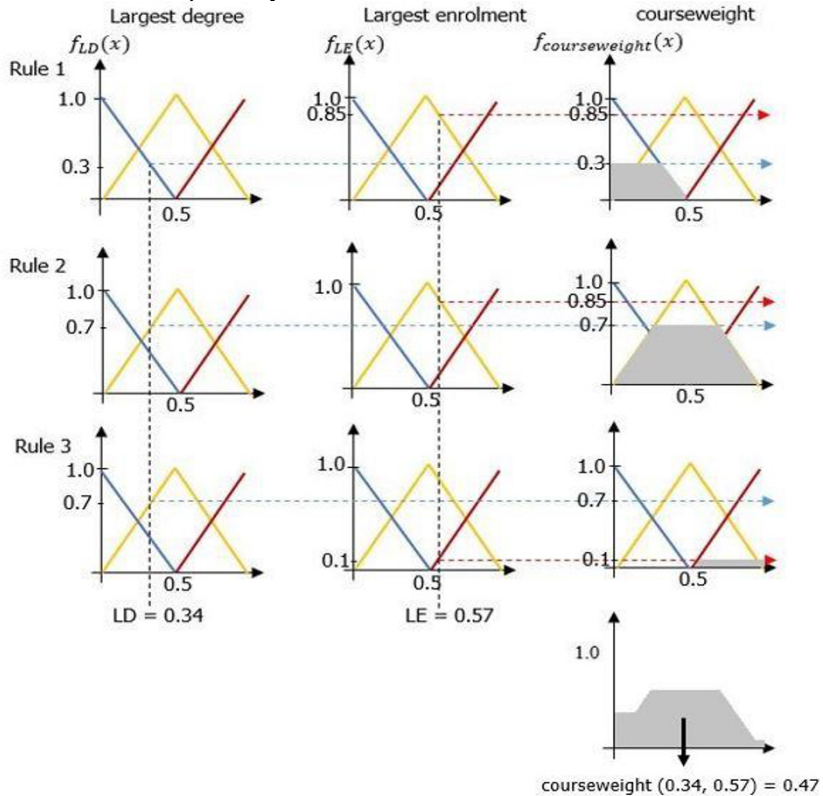


**Fig. 2.** Illustrate using the Mamdani Inference process to generate courseweight

Fig. 2 shows how to generate an output value, courseweight by using fuzzy rules based system with the three rules stated above.

The output linguistic value from the rules will be transformed into crisp value by using Centre of Gravity (COG) which finds the centroid of a planar figure. From Fig. 2, a value 0.47 is obtained from fuzzy system which indicate the course has 0.47 as difficulty values based on LD and LE criteria.

The scheduling process starts after the list of course is reordered by using fuzzy multiple sequential heuristic and it is named as *unscheduledCourses*, *UC*. A course with highest *courseweight* will be selected first and assign into a random feasible timeslot and room. If a course fails to fit into any timeslot and room, it will be moved from the *UC* to the *failScheduledCourses*, *FC*. Meanwhile, it is important to note

that LD and LE are known as static sequential heuristics which remain the difficulty value of a course unchanged until the end of the process. While SD is a dynamic heuristic ordering which will always calculate and update the difficulty value for the unscheduled courses throughout the whole scheduling process. Therefore, there will be an extra calculation on slot available for fuzzy SDLE and fuzzy SDLD. This step terminates if there is no course left in unscheduled courses. If there is at least one course in the *FC*, it will trigger *reschedulingProcess* to disturb the solution. The whole scheduling process will be terminated when all courses are managed to assign into timetable. The number of hard and soft constraints violation will be calculated as penalty cost to evaluate the feasibility and quality of timetable. The construction phase is presented in pseudocode as shown in Fig. 3:

```

Select a fuzzy multiple sequential heuristic and generate a list of unscheduled courses, UC,
while (UC is not empty)
| select a course c with highest courseweight;
| while (c is not removed from UC)
| | select an empty timeslot t and room r at random ;
| | if (t and r are feasible for c) then
| | | assign c into t and r;
| | | move c from UC to scheduledCourses, SC;
| | end
| | if (no feasible slot and room available for c) then
| | | move c from UC to failScheduledCourses, FC;
| | | break;
| | end
| end
| if (fuzzy multiple sequential heuristics consists of SD) then
| | recalculate the timeslot and room availability for every course
| | reorder the list of course based on the fuzzy multiple sequential heuristic criteria
| end
| end
| while (FC is not empty)
| | reschedulingProcess = false ;
| | while (reschedulingProcess is not true)
| | | select an assigned course c from timeslot t and room r ;
| | | select an empty timeslot t* and room r* at random ;
| | | if (t* and r* are feasible for the c) then
| | | | swap c from t and r to timeslot t* and room r* respectively ;
| | | | reschedulingProcess = true ;
| | | end
| | end
| | end
| | select an unassigned course c, an empty timeslot t and room r at random ;
| | if (t and r are feasible for the c) then
| | | assign c into t and r;
| | | move c from FC to SC;
| | end
| end

```

**Fig. 3.** Pseudocode of construction phase

#### 4.2 Improve Solution

The process starts with reordering the set of courses into a list, *RescheduledCourses*, *RC* by using the same fuzzy multiple sequential heuristics applied in construction phase. This process is set to run for 10000 iterations as the algorithms do not produce any significant difference after 9000 iterations. At each iteration, a course with highest *courseweight* will be rescheduled to other timeslot and room which lower the soft constraints violation for the course. After reschedul-

ing, *RC* will remove the course and the whole timetable will be re-evaluated and employs hill climbing with monte carlo to accept or reject the new solution. In order for algorithm to accept the new solution, one of these criteria must be achieved: 1. If penalty cost of the new solution is lower than current solution or 2. Accept worse solution within certain probability, it is known as Exponential Monte Carlo. If fuzzy SDLE or fuzzy SDLD is implemented in this experiment, the timetable need to be evaluated every iteration to update *RC* as they are composed of dynamic sequential heuristic. Improvement phase is presented in pseudocode as shown in Fig. 4.

```

Reorder the list of courses as RescheduleCourses, RC by using the fuzzy multiple sequential
heuristic applied in construction phase
S = current solution ;
f(S) = penalty cost of current solution ;
while (iteration < 10000)
| if (RC is not empty) then
| | select a course c with highest courseweight from timeslot t and room r ;
| | move c to a feasible timeslot t* and room r* which cause the lowest soft constraints
| | violation for c and form a new solution S* ;
| |  $\beta = f(S^*) - f(S)$  ;
| | if (f(S^*) < f(S)) then
| | | S  $\leftarrow S^*$ 
| | end
| | else if (f(S^*) > f(S)) or (exponential(- $\beta$ ) > rand[0,1]) then
| | | S  $\leftarrow S^*$ 
| | end
| | else if (f(S^*) is zero) then
| | | break ;
| | end
| | remove c from RC ;
| end
| else
| | recreate RC ;
| end
end

```

Fig. 4. Pseudocode of improvement phase

## 5 Experimental Results

Java based applications and the fuzzy logic reasoning system generated by [23] are implemented in the research. The dataset semester 1 session 2016/2017 of UMSLIC is used to conduct the experiments. The experiments run 50 times to obtain the average penalty costs. Table 2 presents penalty costs of real world timetable and experimental results.

Table 2. Results comparison between real world application and proposed algorithms

Approach	UMSLIC	Fuzzy LDLE	Fuzzy SDLE	Fuzzy SDLD
Hard constraint	86	0	0	0
Soft constraint	2313	4719	4637.17	5026
Soft constraint (improved)	-	368.17	276.67	274.83

Improvement rate	-	92.14	94.02	94.58
------------------	---	-------	-------	-------

In order to generate a feasible solution, the penalty cost of hard constraint must be zero. In construction phase, the proposed algorithms only focus on generating a feasible solution without considering soft constraints. This explains why the proposed algorithms have higher penalty cost for soft constraints violation. Although UMSLIC timetable has the lowest penalty cost for soft constraints violation among the approaches, but it has penalty cost of 86 for hard constraints violation. This indicates that no matter how low the soft constraints violation is, the timetable is still not feasible and practical. Therefore, students who retake subject and clash with their main subjects, they have to deal with the lecturer personally. Besides, the duration for UMSLIC to produce a timetable can be up to three months. While the proposed algorithm can generate a feasible timetable less than one minute. This indicates that the proposed algorithm performs much more effective than UMSLIC's manual method. Among the fuzzy multiple sequential heuristics, Fuzzy SDLE outperformed in construction phase as it has the lowest average penalty cost for soft constraints violation. While Fuzzy SDLD performed better in improving solutions. It has the lowest average penalty cost for soft constraints violation 274.83 and it is able to improve the quality of feasible solutions up to 94.58%. The overall results show that the proposed algorithm is way more effective than UMSLIC method for solving the course timetabling problem.

## 6 Conclusion

In conclusion, this paper has proposed the implementation of fuzzy logic to consider more than one sequential heuristic simultaneously. The paper compares the performance of different fuzzy multiple sequential heuristics with UMSLIC real world timetable. The experimental results proved that the proposed methods performed well in both construction and improvement phase for solving real world course timetabling problem. This motivates the research to work further by implementing multi-agent system. By doing so, the three fuzzy multiple sequential heuristics will communicate with each other in order to generate and improve the solution.

## References

1. Syariza A. R., Andrej B., Burke E. K., Ozcan E,: Construction of Examination Timetables Based on Ordering Heuristics. 2009 24th International Symposium on Computer and Information Sciences, pp. 680-685 (2009).
2. S. R. Runa Ganguli,: A Study on Course Timetable Scheduling using Graph Coloring Approach. International Journal of Computational and Applied Mathematics, vol. 12, pp. 469-485 (2017).
3. Y. J. Kuan, J. H. Obit , A. Rayner,: A Constraint Programming Approach to Solve University Course Timetabling Problem (UCTP). Ameircan Scientific Publishers, pp. 400-407 (2016).

4. June T. L., J. H. Obit, Yu-Beng L., Jetol B.; Implementation of Constraint Programming and Simulated Annealing for Examination Timetabling Problem, Computational Science and Technology 2018 (ICCST 2018), pp. 175-184 (2018).
5. D. Landa-Silva, J. H. Obit; Great Deluge with Non-linear Decay Rate for Solving Course Timetabling Problems, IEEE, pp. 11-18 (2008).
6. D. Landa-Silva, J. H. Obit; Evolutionary Non-linear Great Deluge for University Course Timetabling, Springer-Verlag Berlin Heidelberg, pp. 269-276 (2009).
7. Y. J. Kuan, H. O. Joe and A. Rayner; Comparison of Simulated Annealing and Great Deluge Algorithms for University Course Timetabling Problems (UCTP), American Scientific Publishers, vol. 4, pp. 400-407 (2015).
8. Abramson D., Krishnamoorthy M., Dang H.; Simulated Annealing Cooling Schedules for the School Timetabling Problem, Asia Pacific Journal of Operational Research, pp. 1-22 (1999).
9. A. S. Luca Di Gaspero; Tabu Search Techniques for Examination Timetabling, International Conference on the Practice and Theory of Automated Timetabling, pp. 104-117 (2000).
10. Adeyanju I., Arulogun T., Omidiara E., Omotosho O. i.; University Examination Timetabling Using Tabu Search, International Journal of Scientific and Engineering Research, vol. 5, no. 10 (2014).
11. Asmuni H., Burke E. K., Garibaldi J. M.; Fuzzy Multiple Heuristic Ordering for Course Timetabling".
12. S. Broder; Final Examination Scheduling, Communication of the ACM, pp. 494-498 (1964).
13. Salwani A., Burke E. K., McCollum B.; An investigation of variable neighborhood search for university course timetabling (2005).
14. Socha K., Knowles J., Sampels M.; A max-min ant system for the university course timetabling problem., Proceedings of the 3rd International Workshop on Ant Algorithms, ANTS 2002, Springer Lecture Notes in Computer Science, vol. 2463, no. 10, pp. 1-13 (2002).
15. Burke E. K., McCollum B., Meisels A., Petrovic S., Qu R.;A graph-based hyper-heuristic for educational timetabling problems," European Journal of Operational Research , pp. 177-192 (2007).
16. D. Landa-Silva, J. H. Obit; Comparing Hybrid Constructive Heuristics for University Course Timetabling, pp. 222-225 (2011).
17. International timetabling competition 2002. Metaheuristic Network, <http://www.idsia.ch/Files/tcomp2002/>.
18. S. C. Pappis C.P., "Fuzzy Reasoning," Burke and Kendall, pp. 437-474 (2005).
19. P. Gupta; Applications of Fuzzy Logic in Daily life, International Journal of Advanced Research in Computer Science, pp. 1795-1800 (2017).
20. Carter M. W., Laporte G., Lee S. Y.; Examination Timetabling: Algorithmic Strategies and Applications, Journal of the Operational Research Society, pp. 373-383 (1996).
21. Asmuni H., Burke E. K., Garibaldi J. M.; A Comparison of Fuzzy and Non-Fuzzy Ordering Heuristics for Examination Timetabling, Proceeding of 5th International Conference on Recent Advances in Soft Computing, pp. 288-293 (2004).
22. L. Zadeh; Fuzzy Sets, Information and Control, pp. 338-353 (1965).
23. J. A.-F. Pablo Cingolani; jFuzzyLogic: A Robust and Flexible Fuzzy-Logic Inference System Language Implementation, 2012 IEEE International Conference on Fuzzy Systems, pp. 1-8 (2012).

24. Asmuni H., Burke E. K., Garibaldi J. M., McCollum B.; An investigation of fuzzy multiple heuristic orderings in the construction of university examination timetables, *Computers & Operations Research*, pp. 981-1001 (2009).
25. Y. J. Kuan, H. O. Joe and A. Rayner.; A Constraint Programming Approach to Solve University Course Timetabling Problem (UCTP), American Scientific Publishers, vol. 4, pp. 400-407 (2016).



# An Investigation of Generality in two-layer Multi-agent Framework towards different domains

Kuan Yik Junn<sup>1</sup>, Joe Henry Obit<sup>1</sup>, Rayner Alfred<sup>2</sup>, Jetol Bolongkikit<sup>1</sup> and Yu-Beng Leau<sup>2</sup>

<sup>1</sup> Universiti Malaysia Sabah Labuan International Campus, Malaysia

<sup>2</sup> Knowledge Technology Research Unit, Universiti Malaysia Sabah, Malaysia, Jalan UMS, 88400 Kota Kinabalu, Sabah, Malaysia

[kyj\\_anderson@hotmail.com](mailto:kyj_anderson@hotmail.com), [joehenryabit@ums.edu.my](mailto:joehenryabit@ums.edu.my),  
[ralfred@ums.edu.my](mailto:ralfred@ums.edu.my), [jetol@ums.edu.my](mailto:jetol@ums.edu.my), [lybeng@ums.edu.my](mailto:lybeng@ums.edu.my)

**Abstract.** This paper proposes a two-layer multi-agent communication in two different environments. The communications in both layers of the framework are studied in order to determine the relevancy of agents to manage themselves towards different constraints across several domains. In this context, the generality of the multi-agent framework is measure by how well the agents improve the quality of solution compared with existing meta-heuristics. The two domains considered are university course timetabling and examination timetabling problems in Universiti Malaysia Sabah. The results are then compared with meta-heuristics introduced in previous studies using the same domains.

**Keywords:** Multi-agent System, University Course Timetabling Problems, Examination Timetabling Problems.

## 1 Introduction

In the field of Artificial Intelligence, various intelligent approaches are introduced into scheduling problems. By definition, scheduling is the highly sophisticated process of assigning various tasks into limited as well as restricted resources within given computational time [1]. Dealing with scheduling problems needs to consider on the constraints for the problem domain itself. Generally, the hard constraints are the requirements that need to be satisfied in any circumstances in order to achieve solution feasibility while soft constraints are related with the quality of a particular solution, satisfying most of the users' needs [2]. Low-level heuristics are the most common methods use in searching. However, the tendency for the search to trap in the local optima is very high due to its greedy behavior. The capabilities of meta-heuristics which allow accepting worse solution based on certain conditions provide flexibility to explore different region of search space, hence giving opportunity to find a better solutions in the next cycle of searches [3] which proved to be more effective comparing with low-level heuristics. The drawback of meta-heuristics required adjusting the parameters which need to be study comprehensively in order to yield the best results

for a specific domain. Therefore, the search strategy is more domain-dependent. Despite the significant implementation of meta-heuristics, the studies on optimization are increasingly shifted towards the paradigm of hyper-heuristics. The fundamental knowledge of hyper-heuristics is based on the search space of heuristics instead of the problem solutions which aim on reducing the reliability towards the domain knowledge [3], proving that hyper-heuristics required minimum parameter tuning. Multi-agent System (MAS) is also gaining popularity among researchers due to its advantages in terms of reliability, robustness and scalability [4]. Agents can act independently by their own and may interact with other agents to accomplish specific tasks. The motivation of conducting MAS is due to the uniqueness in the agent itself having multiple characteristics and the ability to perform multiple tasks in real-time environment. Agents exhibit its cognitive behavior to adapt into the environment, and perceive its own way to react towards the external factors. In this research, three types of agents are used: Heuristic Agents (HA), Cooperative Agents (CA) and Mediator Agent (MA). The roles of each type of agents are described in Section 4. The proposed framework of MAS is divided into two layers. The first layer involves agents communication between HA and CA while the second layers involves distribution of solutions between CA and MA.

The outline of this paper is presented as follow: Section 2 discusses on related work using MAS in timetabling problem, Section 3 elaborates on the problem background in the domain of this study while Section 4 highlights the main approach of this research using MAS framework. Section 5 presents the experimental results comparing MAS with existing meta-heuristics methods and Section 6 concludes the research along with future works.

## 2 Related Works

In [5], proposed a model consist of Central Agent which help to coordinates the tasks performed by Scheduling Agent. The experimental results revealed that sophisticated heuristic is required for Central Agent to communicate more effectively in order to achieve the objective. Similarly, the work [6] is used in real-world distributed timetabling problems, compromising Central Agent and Scheduling Agent. Unlike the existing distributed timetabling algorithms whereby the agent is linked to central agent, the multiply sectioned constraint networks [7] keep the timetable of all agents privately.

The proposed agent model [8] performed examination with mobile agent which consists of two types of agents. The system model is further improvised [9] using four different types of agents such as Course, Interface, Publisher and Signboard Agents whereby each of the agent have their own tasks and objectives but communicating with other agents through viable means of constructed solutions. A set of rules is established in order to simplify the negotiation between agents. Their model shows that it is able to guide the search into flexible and acceptable solutions in timetabling problem. Aside from that, a general solution model is successfully improvised using agent technology [10]. The model tackles two main issues in course timetabling problem. Those issues are dynamic constraint issues and application-specific issues. Whereas

agent model in [11] focused solely on the evaluation of the communication in its architecture using interaction diagram. The model is potentially allows the agents to perform negotiation when the conflict is exist. The implementation of Multi-agents for class timetabling also have been applied by [12]. Their research used steepest ascent hill climbing algorithm to find optimal solution, assisted by *CombinationGenerator* agent which produced all the possible combination for timetable. At the same time, another agent called *MinFinder* is tasked to search the best combination with minimum valuation for further improvement.

While some researchers represent the algorithm as agent to improve the solution, the multi-agent architecture [2] used three cooperating agents which represent the entity from the domain itself. Commonly, the architecture consist of solver which produces solution based on faculty department, a negotiator agent to communicate and negotiate worthy solution to be deliver to other agents and a manager agent which updates the needed information for the solver and negotiator agent to handle the tasks correctly. In similar condition, [13] proposed automated timetabling using department or faculties as agents which used their own algorithms and communicate with central system to obtain permission for a certain resources based on a set of request. For instance, by studying the attributes obtained from the problem domain, agents can identify the proper methods and communicate with other agents which have sufficient knowledge on the particular problem. This can be seen in framework proposed [3] consist of Mediator Agent which acts a coordinator among other agents and Timetabling Agent, which performs global and local scheduling.

### 3 Problem Background

This research investigated two types of domains: University Course Timetabling Problems and Examination Timetabling Problems. The study highlighted the real-world problem of both domains in Universiti Malaysia Sabah Labuan International Campus (UMSLIC). The instances are obtained from Academic Service Division (ASD) of UMSLIC. The hard constraints for course timetabling are as follow:

1. ( $Hc_1$ ) Each student is not allowed to attend more than one event at the same time. This condition also applied towards lecturer whereby they are not allowed to lecture more than one class at a time.
2. ( $Hc_2$ ) Event must be scheduled into rooms that can fit the size of the event.
3. ( $Hc_3$ ) There must be no sharing of room at the same timeslot among events.
4. ( $Hc_4$ ) Event must be assigned based on the predefined timeslots.

The soft constraints for the UMSLIC course timetabling are as follow:

1. ( $Sc_1$ ) Each student is discouraged to attend more than two classes consecutively.
2. ( $Sc_2$ ) The room capacity should be utilized by having events with the size close to the room capacity.

The following table 1 summarized the total number of student, courses, timeslots and rooms for each of the instances.

**Table 1.** Summary of datasets for course timetabling in UMSLIC.

Datasets	Students	Courses	Timeslots	Rooms
Sem 2 s2014/2015	2248	112	35	18
Sem 1 s2015/2016	2371	125	35	18
Sem 1 s2016/2017	2264	211	35	18

Meanwhile, the examination timetabling involved the exams taken by the student based on the course enrollment. Similar with course timetabling, the real-world instance are obtained from ASD of UMSLIC and usually the timetable is published on CELCAT system. The hard constraints for examination timetabling are:

1. ( $Hc_1$ ) Each student is not allowed to sit for more than one exam at a time.
2. ( $Hc_2$ ) The room capacity must not be exceeded throughout the exam period.
3. ( $Hc_3$ ) There must be no mixed duration of exams in a period.

The soft constraints for the UMSLIC examination timetabling are as follow:

1. ( $Sc_1$ ) Each student is discouraged to sit for more than one exam consecutively.
2. ( $Sc_2$ ) Exams with many students should be held into earlier period of timetable.

The table 2 below describes the summary of datasets based on total number of students, courses, exams, periods and rooms.

**Table 2.** Summary of datasets for examination timetabling in UMSLIC.

Datasets	Students	Courses	Exams	Periods	Rooms
Sem 2 s2014/2015	2248	112	92	35	18
Sem 1 s2015/2016	2371	125	98	35	18

Technically, the constraints are identified after having several rounds of interviews with ASD officer in charge dealing with timetabling in UMSLIC. After the constraints are identified, the evaluation of cost function is calculated based on formulation model constructed in previous studies [14, 15, 16, 17, 18 and 19]. The cost function is the penalty given for each violation in soft constraints (both course timetabling and examination timetabling) subject to neither any hard constraints as mentioned above are violated. The performance of MAS is compared with the methods implemented in previous studies using the same domain. In course timetabling problem, the performance is compared with enhanced Great Deluge [15], Simulated Annealing [16] and modified Genetic Algorithm [17]. The preliminary results of Multi-agent framework proposed in [18] is set as benchmark quality, whereby the framework implemented in this research is further improvised in the aspect of communication

(message sending and receiving). As for examination timetabling problem, the results are compared with existing method proposed in [19] in the same domain (UMSLIC).

## 4 Proposed framework

### 4.1 Motivation of Multi-agent

The motivation of implementing Multi-agent is heuristics and meta-heuristics or any evolutionary algorithms can be represented as an agent. The only concern is the design of agents' interaction and giving tasks and responsibilities to them. It is believed that agent is much more reliable [20] when working in distributed environment due to single agent failure will not affect the entire system. In this research, the novelty in the proposed framework is highlighted based on two components:

1. The framework is divided into two layers whereby the first layer focus on neighborhood movements from heuristics agent to produce feasible solution while the second layer involve improving solution process which communicate with a mediator agent to obtain solution from a pool of feasible solutions;
2. Aside from distributing and managing the pool of solution, mediator agent has another critical role to improve the pool of solution itself using genetic operators.

In this framework, there are three different types of agents and each agent consists of different heuristic or meta-heuristics. The agent types are listed as follow:

- HA – entities represent low-level heuristic. Based on the current solution regardless of feasibility, it performs neighborhood movements which change the solution into a new solution.
- CA – play the roles of improving solution in meta-heuristics. It communicates with both HA and MA. It provides solutions to HA in order to perform local search and receive solution from MA for improvement.
- MA – act as a coordinator to distribute solutions to CA. At the same time it improves the global best solution from the pool of solution.

The implementation of Multi-agent framework is developed using Java Agent Development (JADE) platform. The agent communication is more object-oriented with Foundation of Physical Intelligent Agent (FIPA), whereby the establishing communication between agents needs to align in according to FIPA standard.

### 4.2 First layer of Multi-agent framework

In this framework, the communication of agent is defined by Agent Communication Language (ACL). The first layer involves several communication attempts between HA and CA. An initial solution is created by several HA and perform INFORM message to be deliver towards CA. The purpose of HA perform the search is to disturb the solution. CA may perform REQUEST towards HA for a new solution. Each HA re-

plies back to CA with their messages either AGREE or CANCEL. It is important to note that not every attempt performed by HA is successful. This is due to high conflict occurs in the solution which limits the movement of HA. If the move is successful done by any HA, it will return the new solution to CA. The HA consist of:

- Simple move – select an event (or exam) at random from the timetable solution and move it to another feasible region of empty resources (timeslot and room). This local search represents HA for both course timetabling and examination timetabling.
- Swap move - select two events (or exams) at random from the timetable solution and exchange their respective timeslot and room between those events. This local search represents HA for both course timetabling and examination timetabling.
- Swap timeslot – select two timeslots at random from the timetable solution and swap all the events in that timeslot to the other timeslot and vice-versa. This local search represents HA for course timetabling problem.
- Cyclic timeslot – select two timeslots (mark as timeslot A and timeslot B) at random from the timetable solution and move all the events in timeslot A to the next timeslot. All the events in that timeslot will move to the following timeslot and so on until it reaches timeslot B. Finally, all the events in timeslot B will move to timeslot A. This movement is used as HA for course timetabling problem.

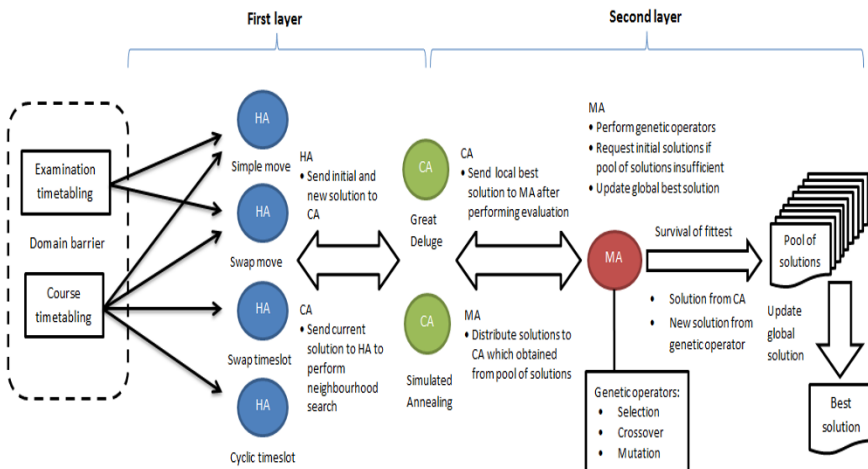
The CA consists of meta-heuristics search techniques that evaluate the solutions from HA and determine whether to accept the solution based on certain conditions. In this framework, Great Deluge and Simulated Annealing are used as CA. The solution is accepted if new solution received from HA is improved. Else, the acceptance criteria from either GD or SA are used to determine whether the solution will be accepted. The detailed implementation of SA and GD can be referred to previous work in [16].

### 4.3 Second layer of Multi-agent framework

The second layer of the framework involves communication between several CA and a MA. At first the CA sends initial solutions to MA with INFORM performative. The MA receives initial solutions and allocate into a pool of solutions. The pool size is set to 50 as indicated from previous work [18]. If the initial solutions in the pool are insufficient, MA will perform REQUEST performative to CA to generate a new initial solution which takes place in the first layer of the framework. Else, the search begins with CA sending REQUEST to MA to obtain a solution from the pool.

The MA in this framework performs several tasks as mentioned in Table 3. There is only one MA in the framework which plays an important role to produce the overall best solution through the searches outcome. The advantage of this newly introduced MA is the ability to exhibit concurrent behavior (while it selects random solutions from the pool to be distributed towards CA, it also performs genetic operators by manipulating the solutions in the pool). The stages in genetic operator include:

- Selection – selecting two solutions from the pool. One of the solutions is selected randomly from the top 25 while the other is selected randomly from the bottom 25. This is to ensure more variance in the pool.
- Crossover – two solutions that have been selected will perform one-point crossover. The crossover point is randomly selected based on the total number of events (or exams). The starting event until the crossover point event will switch their timeslot with the timeslot from the other solution. If the particular event unable to switch timeslot due to infeasibility occurred, it proceeds to the next event. In the end, only one new solution is produced while the other is discarded.
- Mutation – occurs at the probability of less than one percent. If mutation occurs, the new solution will undergo simple move or swap move several times. This is to generate different variant from the parents' solution.
- Survival of fittest – the new solution is evaluated in terms of its fitness (quality). If the cost function of the solution is much better than one of the solution in the pool, it replaced the worst solution in the pool.

**Fig. 1.** Multi-agent framework**Table 3.** Specification of agent's knowledge and responsibilities

Agent type	Acquaintances	Responsibilities
Heuristic (HA)	Cooperative	<ol style="list-style-type: none"> <li>1. Perform local search move. (i.e. simple move, swap move)</li> <li>2. Forward the new solution to CA after performed move.</li> </ol>
Cooperative (CA)	Heuristic, Mediator	<ol style="list-style-type: none"> <li>1. Sends current solution to HA and receives the new solution after HA performed the move.</li> <li>2. The new solution is evaluated based on the quality and acceptance criteria from Simulated Annealing and Great Deluge.</li> <li>3. Send the current local best solution to MA after evaluation.</li> </ol>

Mediator (MA)	Cooperative	<ol style="list-style-type: none"> <li>1. Receive initial solutions from CA to form a pool of solutions. It will request more solutions from CA until the pool is full.</li> <li>2. Distribute solutions to CA for improvement if requested.</li> <li>3. Accepts the local best solution from CA if the quality of the solution is better than either one of the solutions from the pool. Then, the worst solution from the pool will be eliminated.</li> <li>4. Update the global best solution from the pool.</li> <li>5. Perform genetic operators using the solution pool and introduce the new solution into the pool through survival of fittest.</li> </ol>
------------------	-------------	--

## 5 Experimental Results

In this experiment, two different domains are used. First, the proposed framework is compared with the past results of meta-heuristic approaches [17] in course timetabling problem. Next, the proposed framework is then compared with the work done in [19] using the examination timetabling problem. Therefore, the datasets used are based on the same semester tested in [14, 15, 16, 17, 18 and 19], session 2014/2016 semester 2 and session 2015/2016 semester 1. Based on the previous experimental outcome [18], increasing number of agents in the complex system will leads to increasing message pending in queue to be processed, hence will indirectly slow down the speed of processor and this will result in taking longer time to improve the best solution. Through this problem, the current framework will only be using four HA, two CA and an MA.

The experiments are conducted with 30 runs for both course timetabling and examination timetabling instances. The average cost in Table 4 and Table 5 indicates the average cost function in the 30 runs while the improvements show the percentage of reduction in cost function in average based on initial solution produced. The algorithm used in course timetabling denotes GA as Genetic Algorithm, GD as Great Deluge, SA as Simulated Annealing, MAS as Multi-agent System and CP and SA as Constraint Programming and Simulated Annealing. The stopping criterion for the searches is based on two following conditions: the process stop once the iteration reached 100, 000. The amount is considered as the parameter testing suggested that too low iteration did not yield optimum results as the search can be further improve while iteration higher than that did not bring much significant different as the standard deviation is lower at this point; the process stop based on time setting with maximum time allowed is five minutes

The experiments for course timetabling shown in Table 4 previously recorded the best result using GA approach [17] in both semesters, outperform GD and SA. As of the latest work done in this research using MAS, the communication between agents is proven successful, improving the solution more than 40 percent for both semesters. Besides, the average cost function in semester 2 session 2014/2015 is 19921 (MAS), 3926 lower than GA while semester 1 session 2015/2016 the proposed framework with average cost of 21786 manage to beat the results of GA, difference of 2896.

**Table 4.** Experimental results of UMSLIC course timetabling problem.

Experiment	Semester 2 Session 2014/2015				Semester 1 Session 2015/2016			
	GA	GD	SA	MAS	GA	GD	SA	MAS
Algorithm	23847	29081	30139	19921	24682	29400	30475	21786
Average cost								
Improve (%)	37.67	25.87	23.62	43.55	35.33	25.44	22.41	40.02

Meanwhile, the performance of MAS managed to produced slight competitive results compared with CP and SA technique whereby MAS produced better quality of solutions in semester 2 session 2014/2015 but unable to outperform CP and SA in semester 1 session 2015/2016 although the average cost is not much significant difference between them. This shown that MAS managed to find better solution in semester 2 session 2014/2015 with more than 25 percent improvement from initial solution but perform poorer in semester 1 session 2015/2016 with only 15.5 percent improvement.

**Table 5.** Experimental results of UMSLIC examination timetabling problem

Experiment	Semester 2 Session 2014/2015		Semester 1 Session 2015/2016	
	CP & SA	MAS	CP & SA	MAS
Algorithm	6848.0	6013.1	11695.6	12343.7
Average cost				
Improve (%)	21.30	25.62	16.12	15.50

These experiments proves that the proposed framework is more effective compared with the previous version [18] as the agents are reduced to optimum level to yield the best result. The improvement rate is increased if compared to existing results in the past as shown in Table 5 and Table 6. The ability to produce good results in course timetabling problems and competitive results in examination timetabling problems best described the generality in the proposed framework.

## 6 Conclusion

Scheduling is proved to be difficult task to solve, which is considered a NP-hard problem. Different domain may have different constraints from one another as discussed in section 3. In order to compensate the weaknesses in meta-heuristics technique, a multi-agent framework is proposed to produce satisfying solutions in multiple domains. Although the results show that the proposed framework does not produce the best solution in every instance, the performance is rather competitive compared with methods done in previous work [14, 16 and 18].

For future work, the proposed framework will be implemented in benchmark timetabling domains. So far, the implementation of the proposed framework is prove successfully producing good solutions in real-world problem but the conflict density in benchmark problems are much higher comparing with real-world problem. Hence, the performance of the proposed framework can be measured in terms of quality with the results from existing state-of-art in the literatures. Three types of instances are considered namely International Timetabling Competition 2002 (ITC2002), International

Timetabling Competition 2007 (ITC2007) and Socha (2002) instance while ITC2007 is considered for examination timetabling problem.

## References

1. Wren, A.: Scheduling, timetabling and rostering—a special relationship?. In: International conference on the practice and theory of automated timetabling, pp. 46-75. Springer, Berlin, Heidelberg (1995).
2. Di Gaspero, L., Mizzaro, S., Schaerf, A.: A multiagent architecture for distributed course timetabling. In: Proceedings of the 5th International Conference on the Practice and Theory of Automated Timetabling (PATAT-2004), pp. 471-474. (2004).
3. Obit, J.H., Landa-Silva, D., Ouelhadj, D., Vun, T.K., Alfred, R.: Designing a multi-agent approach system for distributed course timetabling. In: Hybrid Intelligent Systems (HIS), 2011 11th International Conference, pp. 103-108. IEEE (2011).
4. Strnad, D., Guid, N.: A multi-agent system for university course timetabling. Applied Artificial Intelligence 21(2), 137-153 (2007).
5. Kaplansky, E., Kendall, G., Meisels, A., Hussin, N.: Distributed examination timetabling. In: Proc. of the 5th International Conference of the Practice and Theory of Automated Timetabling (PATAT), pp. 511-516. Pittsburgh, USA (2004).
6. Meisels, A., Kaplansky, E.: Scheduling agents—distributed timetabling problems. Practice and Theory of Automated Timetabling IV, 166-177 (2003).
7. Xiang, Y., Zhang, W.: Distributed University Timetabling with Multiply Sectioned Constraint Networks. In: FLAIRS Conference, pp. 567-571 (2008).
8. Yang, Y., Paranjape, R., Benedicenti, L.: An examination of mobile agents system evolution in the course scheduling problem. In: Canadian Conference on Electrical and Computer Engineering 2004 (IEEE Cat. No. 04CH37513), vol. 2, pp. 657-660. IEEE (2004).
9. Yang, Y., Paranjape, R., Benedicenti, L., Reed, N.: A system model for university course timetabling using mobile agents. Multiagent and Grid Systems 2(3), 267-275 (2006).
10. Yang, Y., Paranjape, R., Benedicenti, L.: An agent based general solution model for the course timetabling problem. In: Proceedings of the fifth international joint conference on Autonomous agents and multiagent systems, pp. 1430-1432. ACM (2006).
11. Oprea, M.: MAS\_UP-UCT: A multi-agent system for university course timetable scheduling. International Journal of Computers Communications & Control 2(1), 94-102 (2007).
12. Nandhini, M., Kanmani, S.: Implementation of class timetabling using multi agents. In: 2009 International Conference on Intelligent Agent & Multi-Agent Systems, pp. 1-2. IEEE (2009).
13. Pedroso, J.P.: A multi-agent system for automated timetabling with shared resources. Faculdade de Ciencias da Universidade do Porto Departamento de Ciencia de Computadores Rua do Campo Alegre, 8234150-180 (2003).
14. Obit, J.H., Junn, K.Y., Alfred, R.: A Performance Comparison of Metaheuristics Search for University Course Timetabling Problems. Advanced Science Letters 23(11), 11012-11015 (2017).
15. Obit, J.H., Junn, K.Y., Alfred, R.: Performance comparison of linear and non-linear great deluge algorithms in solving university course timetabling problems. Advanced Science Letters 23(11), 11027-11030 (2017).

16. Junn, K.Y., Obit, J.H., Alfred, R.: Comparison of simulated annealing and great deluge algorithms for university course timetabling problems (UCTP), *Advanced Science Letters* 23(11), 11413-11417 (2017).
17. Junn, K.Y., Obit, J.H., Alfred, R.: The Study of Genetic Algorithm Approach to Solving University Course Timetabling Problem. In: *International Conference on Computational Science and Technology*, pp. 454-463. Springer, Singapore (2017).
18. Junn, K.Y., Obit, J.H., Alfred, R., Bolongkikit, J.: A Formal Model of Multi-agent System for University Course Timetabling Problems. In: *Computational Science and Technology*, pp. 215-225. Springer, Singapore (2019).
19. June, T.L., Obit, J.H., Leau, Y.B., Bolongkikit, J.: Implementation of Constraint Programming and Simulated Annealing for Examination Timetabling Problem. In: *Computational Science and Technology*, pp. 175-184. Springer, Singapore (2019).
20. Yang, Y., Paranjape, R.: A multi-agent system for course timetabling. *Intelligent Decision Technologies* 5(2), 113-131 (2011).



# $\mu^2$ : A Lightweight Block Cipher

Wei-Zhu Yeoh, Je Sen Teh\*, and Mohd Ilyas Sobirin Bin Mohd Sazali

Universiti Sains Malaysia, Penang, Malaysia

\*jesen\_teh@usm.my

**Abstract.** This paper presents a 64-bit lightweight block cipher,  $\mu^2$  with a key size of 80-bit.  $\mu^2$  is designed based on well-established design paradigms, achieving comparable performance and security when compared against existing state-of-the-art lightweight block ciphers.  $\mu^2$  is based on the Type-II generalized Feistel structure with a round function,  $F$  that is a 16-bit ultra-lightweight block cipher based on the substitution-permutation network. Security evaluation indicates that  $\mu^2$  offers a large security margin against known attacks such as differential cryptanalysis, linear cryptanalysis, algebraic attack and others.

**Keywords:** Cryptanalysis, Feistel, IoT, lightweight block cipher, SPN

## 1 Introduction

In recent years, the rise of Internet-of-Things (IoT) devices with constrained computing capability has been prominent. These devices have not only widely used in everyday life but are also interconnected to form a network to provide unobtrusive services to the consumers. However, this interconnectivity poses a range of security risks. Thus, lightweight block ciphers have been proposed in response to those concerns, such as PRESENT [9], LED[14] and CHAM [18]. These lightweight block ciphers have been meticulously designed to have simple structures and high throughput for their implementation. PRESENT is the currently the ISO/IEC standard [16] for 64-bit lightweight block ciphers. Despite its simple design based on the substitution-permutation network (SPN), it has been shown to resist various cryptanalytic attacks over the years. Although there exists recently proposed lightweight block ciphers [14,4,18], they have yet to undergo sufficient cryptanalysis to be considered state-of-the-art.

In this paper, we propose  $\mu^2$ , a new 64-bit block cipher based on the Type-II generalized Feistel structure (GFS). Unlike regular ciphers, its round function  $F$  is in itself a 4-round ultra-lightweight cipher (ULC) is based on SPN. Embedding another block cipher within the design still maintains design simplicity and ease of analysis. The inspiration of the cipher's name  $\mu^2$  comes from the metric multiplicative prefix micro,  $\mu$  which often associated with a very tiny value whereas the power of 2 implies the use of a two ciphers.  $\mu^2$  has shown to be more efficient than PRESENT, with comparable security margins. Therefore, it serves as a suitable lightweight block cipher candidate for resource-constrained devices. In addition, this work is in line with Malaysia's National Cryptography

Policy (NCP) [1] and National Cyber Security Policy (NCSP) [2], which supports cryptographic research and development towards self-reliance.

## 2 Specification of $\mu^2$

### 2.1 Main Structure of $\mu^2$

$\mu^2$  is a lightweight block cipher with 15 rounds. It has a block length of 64 bits and a key length of 80 bits. The design of  $\mu^2$  is based on a Type-II GFS as shown in Figure 1.  $\mu^2$  uses a new ULC with a block size of 16 bits, which is based the

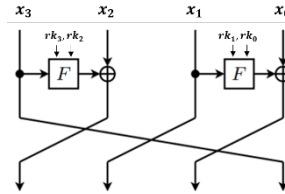


Fig. 1:  $\mu^2$  Structure

SPN and Even-Mansour construction [11]. This ULC is detailed in Section 2.2. Four rounds of the ULC will be used for each  $F$ -function.  $\mu^2$  uses PRESENT's 4-bit s-box for encryption and key generation as shown in Table 1.

Table 1: Substitution Box

$x$	0	1	2	3	4	5	6	7	8	9	A	B	C	D	E	F
$S[x]$	C	5	6	B	9	0	A	D	3	E	F	8	4	7	1	2

The design of the key schedule (key generation algorithm) of  $\mu^2$  is based on PRESENT which can be summarized as

1. Initialize an 80-bit register with the 80-bit secret key.
2. Left rotate the register by 61 bits.
3. Substitute the four most significant bits (MSBs) and  $64^{th}$  to  $67^{th}$  bits using the substitution box (s-box).
4. XOR the  $15^{th}$  to the  $18^{th}$  bits with a round counter.
5. Extract the 64 MSBs as the round key,  $RK$

or mathematically defined as

1.  $[k_{79}k_{78}\dots k_1k_0] = [k_{18}k_{17}\dots k_{20}k_{19}]$

2.  $[k_{79}k_{78}k_{77}k_{76}] = S[k_{79}k_{78}k_{77}k_{76}]$
3.  $[k_{67}k_{66}k_{65}k_{64}] = S[k_{67}k_{66}k_{65}k_{64}]$
4.  $[k_{18}k_{17}k_{16}k_{15}] = [k_{18}k_{17}k_{16}k_{15}] \oplus \text{round\_counter}$

Unlike PRESENT, the *round\_counter* is only 4 bits because  $\mu^2$  only has 15 rounds, and is initialized to 0 at the beginning. Another change made is to feed 4 more distinct bits of value through the same s-box in due to the reduced rounds of the key schedule compared to PRESENT. The round key,  $RK$  is divided into four sub-round keys,  $RK = \{rk_3, rk_2, rk_1, rk_0\}$ .  $rk_3$  and  $rk_2$  are used in the left  $F$ -function whereas  $rk_1$  and  $rk_0$  are used in the right  $F$ -function as shown in Figure 1. New round keys are generated by repeating the same key generation algorithm. This is performed once after each round of  $\mu^2$ . Note that the very first round key is directly extracted from the secret key prior to transformation.

## 2.2 Ultra-lightweight Cipher ( $F$ -function)

As previously mentioned, the  $F$ -function of  $\mu^2$  is a 16-bit block cipher based on the SPN and Even-Mansour construction. The sub-round keys are XOR-ed with the 16-bit input before and after the completing four rounds of the SPN. To break symmetry between each round, round constants are introduced,  $con_i = \{0x1000, 0x2000, 0x3000, 0x4000\}$ . To break the symmetry between each instance of the  $F$ -function, the ULC also includes a counter,  $F_{count}$  which is incremented after computing each  $F$ -function. Thus, each round of  $\mu^2$  will increment  $F_{count}$  by 2.  $F_{count}$  is initialized to 0 at the beginning.

The substitution layer consists of four 4-bit s-boxes defined in Table 1. This is followed by a bitwise permutation,  $\pi$  designed to maximize the number of active s-boxes (AS) defined as

$$\pi[b_{15}b_{14}\dots b_1b_0] = [b_3b_6b_9b_{12}b_7b_{10}b_{13}b_0b_{11}b_{14}b_1b_4b_{15}b_2b_5b_8], \quad (1)$$

where  $b_i$  is the  $i^{th}$  bit of the 16-bit data block. The effect of  $\pi$  on the number of AS is described in Section 4.1. A visual depiction of the entire SPN is as shown in Figure 2 whereas the block diagram of the  $F$ -function is as shown in Figure 3.

## 3 Design Choices

### 3.1 Intended Uses and Goals

The goal is to construct a new robust lightweight block cipher that is suitable for adoption and deployment by highly-constrained computing devices while maintaining the efficiency on 16/32/64-bit processors. This newly proposed cipher should not only be comparable with various existing proposals of similar intent but also outperforms the previous proposal in some aspect while maintaining the design and implementation simplicity.

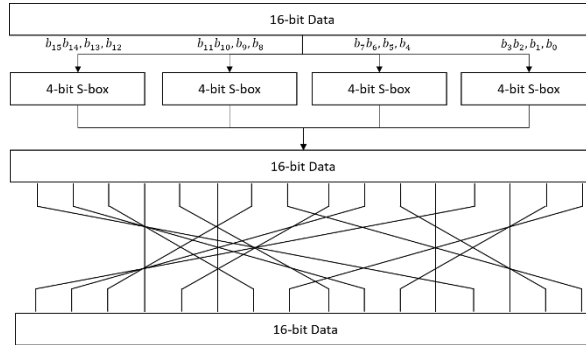
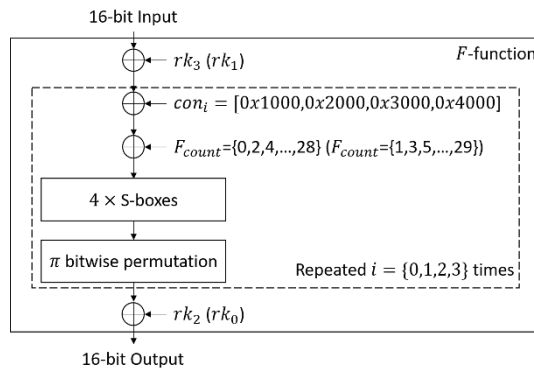


Fig. 2: Substitution-Permutation Network

Fig. 3:  $F$ -function

### 3.2 Structure of the $\mu^2$

The Type-II GFS structure of  $\mu^2$  and the choice of a more elaborate  $F$ -function is quite similar to that of the 4-branch version of the Simpira V2 permutation [13]. Unlike Simpira which uses AES [20] as its  $F$ -function, we proposed a new 16-bit ULC as the replacement that is suitable for constrained devices. We have also chosen the same number of rounds as Simpira to ensure sufficient bit diffusion.

The ULC constituting the  $F$ -function can be seen as a mini-PRESENT variant with 16-bit block size due to the fact that it uses the s-box from PRESENT and also adopts a similar bitwise approach to its permutation albeit with a different pattern. The choice of resemblance is explained in the following section.

### 3.3 Substitution Layer (S-box) and Permutation Layer (P-layer)

In order to maximize the efficiency of the algorithm, a single strong 4-bit to 4-bit S-box,  $S : \mathbb{F}_2^4 \rightarrow \mathbb{F}_2^4$  is chosen as the non-linear substitution layer. Compared with larger size 8-bit s-box featured prominently in U.S. encryption standard AES [20], a 4-bit s-box is much more compact and advantageous when implemented in resource-constrained devices.  $\mu^2$  cipher adopted the s-box defined in the PRESENT which is well-studied and thoroughly investigated and thus is able to provide reasonably strong resistance against well-established attack due to its excellent nonlinearity, differential probability and algebraic order.

The permutation layer is chosen to maximize efficiency while providing adequate security. As such, a simple bitwise permutation layer was selected because of its simplicity and efficiency when implemented. Due to the simple nature of the bit permutation, it also allows clear and precise security analysis to be made in the later section.

### 3.4 Key Schedule and Even-Mansour Scheme

The key schedule of the cipher is a straightforward modification of the PRESENT key schedule. The robust yet simple key schedule defined by PRESENT has a minimal impact on the overall performance while providing some increased security against various type of cryptanalysis attack. There is some study on the strength of the PRESENT key schedule [15] but the investigation indicates that the 80-bit key schedule shows no significant exploitable weakness. The modification of the round counter bit and the inclusion of an extra non-linear s-box per round is in direct respond to the lower number of round of the proposed cipher.

The double-key Even-Mansour scheme [11] is used to introduce secret key information. Although there is a notable security proof [10] that shows single-key Even-Mansour scheme has the same security lower bound as the double-key scheme. The use of the double-key variant allows direct utilization of the modified PRESENT key schedule with minimal modification. The key schedule produces a 64-bit round key for each round which can be divided equally into two pairs of 16-bit keys to be used for the two F-functions respectively.

## 4 Security Analysis

### 4.1 Differential and Linear Cryptanalysis

For differential and linear cryptanalysis, the minimum number of AS,  $AS_{min}$  determines the cipher's security margin. For  $\mu^2$  the following observations that can be made by examining the permutation layer in conjunction with the s-boxes of  $F$ -function:

1. The input to an s-box comes from four distinct s-boxes and the output of an s-box goes into four different s-boxes.
2. An input with a one-bit difference will always lead to an output difference of two bits or higher.

3. S-box activation patterns of  $1 - 1 - 1$  and  $1 - 2 - 1$  cannot occur.
4. When there is a non-zero difference entering the 4-round ULC, the  $1 - 2 - 2 - 1$  pattern will have the least number of AS because any other patterns with fewer AS will violate observations 3 and 4.
5. If there are any other cases whereby any one of the rounds contains three or four AS, there will be at least six or more AS in total.

As stated above,  $AS_{min} = 6$ . The GFS structure has a minimum of 14 differentially activated  $F$ -function in 15 rounds. Thus, 15 rounds of  $\mu^2$  will have a minimum of  $14 \times 6 = 84$  AS. The maximum differential probability of the s-box is  $2^{-2}$ . Based on these criteria, the probability of a single path differential is upper-bounded by  $2^{-168}$ . A successful attack would have a data complexity of  $2^{168}$  which exceeds the available message space of  $2^{-64}$ . Hence,  $\mu^2$  has a large security margin against differential cryptanalysis [7].

Next, we analyze  $\mu^2$ 's security against linear cryptanalysis. The maximum bias of the s-box is  $2^{-2}$  and based on the previous analysis, each round of  $\mu^2$  has  $AS_{min} = 6$ . By applying the piling-up lemma [19],

$$\epsilon = 2^{(14 \times 6) - 1} \times (2^{-2})^{14 \times 6} = 2^{-85}.$$

The data complexity of the linear attack can be calculated as

$$N_L = \frac{1}{\epsilon^2} .$$

Hence for 15 rounds of  $\mu^2$ , the data complexity of a linear attack is estimated to be  $2^{170}$  which exceeds the message space of  $2^{64}$ .

## 4.2 Integral Attacks

Integral attacks [17] are known to be more applicable to the analysis of ciphers with word-like structures. However, there have been some attempts to use integral attack to analyze bit-based cipher [22,23] but the attack is not particularly detrimental to the overall strength of the cipher security. Any word-like structure of  $\mu^2$  will be disrupted by bit-wise operation of ULC. Hence, it is believed that integral attack poses no threat to  $\mu^2$ .

## 4.3 Algebraic Attacks

Extending from the work by PRESENT, the s-box of the PRESENT can be described by 21 quadratic equations in eight input/output-bit variables over binary field,  $GF(2)$ . Each round of the cipher consist of 34 s-boxes (encryption and key generation). Therefore, the entire proposed system can be expressed by  $34 \times 15 \times 21 = 10710$  quadratic equations in 4080 variables. These numbers tend to indicate that  $\mu^2$  exhibits a high level of immunity against algebraic attack.

#### 4.4 Key Schedule Attacks

The most successful attacks on the key scheduling are the slide attack [8] and related-key attack [6]. These attacks rely on the relationship between each subsequent rounds. Since the key schedule of the  $\mu^2$  cipher is nearly identical to that of the PRESENT, some of the existing analysis can be easily extended. The relationship and symmetry of each round are broken up by the introduction of the round-dependent counter. Furthermore, the key is further scrambled using nonlinear s-box. The presence of  $F$ -function counter and ULC round counter also contribute towards the overall strength against these types of attacks as well. The combined efforts should thwart the attacker from mounting a successful slide or related-key attack on the key schedule.

#### 4.5 Statistical Analysis

The NIST statistical test suite [21] was used to test the number sequences generated from the cipher to ensure that they resemble pseudorandom sequences with no statistical defects. A 1000-Mbit sample of number sequences was tested whereby the number sequences were generated by encrypting plaintext that was incremented by 1 for each block starting at 0 while the key is fixed at 0. The number sequences are considered to be random when the test results have a  $P$ -value of  $\geq 0.01$  and passing ratio  $\geq 9.8056$ . Based on the acquired results illustrated at Table 2, the  $\mu^2$  cipher indeed approximates a pseudorandom function which is one of the desirable traits of a block cipher.

Table 2: NIST Test Result

Test	$P$ -value	Passing Ratio	Result
Frequency	0.073	0.989	Pass
Block frequency	0.372	0.987	Pass
Cumulative sums	0.391	0.990	Pass
Runs	0.055	0.987	Pass
Longest run	0.365	0.992	Pass
Rank	0.514	0.989	Pass
FFT	0.575	0.989	Pass
Nonoverlapping templates	0.056	0.992	Pass
Overlapping templates	0.036	0.991	Pass
Universal	0.587	0.997	Pass
Approximate entropy	0.637	0.990	Pass
Random excursions	0.713	0.987	Pass
Random excursions variant	0.454	0.990	Pass
Serial	0.321	0.983	Pass
Linear complexity	0.997	0.988	Pass

## 5 Performance and Comparision

To illustrate that the performance of  $\mu^2$ 's software implementation is comparable to existing proposals, performance measurements from various lightweight ciphers including  $\mu^2$  were measured using the same computing device. Their performance were benchmarked using the Intel Skylake I5-6600K @ 3.5GHz CPU. The implementations for existing lightweight ciphers, PRESENT and SKINNY [3] were taken from existing resources made available by other researchers who have optimized the algorithm with respect to the target platform [24,12,5]. The acquired results are shown in Table 3. It can be seen that  $\mu^2$  achieved a comparable throughput when compared to other well-known lightweight block ciphers.

Table 3: Software implementation throughput of  $\mu^2$ , PRESENT and SKINNY

Cipher	Throughput $Mb/s^{-1}$	Reference
$\mu^2 - 80^*$	148.28	This
PRESENT-80*	133.77	[9][24]
SKINNY-64*	121.23	[5][3]

\* The implementations used do not represent the best possible optimized version.

## 6 Conclusion

In this paper, we presented a new lightweight block cipher  $\mu^2$  which has a block length of 64-bit and an 80-bit key. It is specifically designed to provide high security margins while maintaining good performance for constrained devices. A variant of Type-II GFS is used as the design foundation for the cipher with a SP-network based ULC as its 16-bit round function. The use of a single 4-bit s-box and bit permutation layer contribution towards the overall efficiency of the cipher which exceeds well-known lightweight ciphers such as PRESENT and SKINNY. Based on the security evaluation and the preliminary cryptanalytic results of  $\mu^2$ , it is shown that  $\mu^2$  achieved sufficient security margin against well-known attacks. However, more security analysis still needs to be conducted to verify the security of the proposed cipher even further.

## Acknowledgements

This work has been partially supported by Universiti Sains Malaysia under Grant No. 304/PKOMP/6315190.

## References

1. Malaysia National Cryptography Policy. <http://www.parlimen.gov.my/files/hindex/pdf/DN-09122013.pdf>, [https://cnii.cybersecurity.my/main/ncsp/policy\\_thrusts.html](https://cnii.cybersecurity.my/main/ncsp/policy_thrusts.html)
2. Malaysia National Cyber Security Policy. [https://cnii.cybersecurity.my/main/ncsp/policy\\_thrusts.html](https://cnii.cybersecurity.my/main/ncsp/policy_thrusts.html), [https://cnii.cybersecurity.my/main/ncsp/policy\\_thrusts.html](https://cnii.cybersecurity.my/main/ncsp/policy_thrusts.html)
3. SKINNY family of block ciphers. <https://sites.google.com/site/skinnycipher/home>
4. Banik, S., Pandey, S.K., Peyrin, T., Sasaki, Y., Sim, S.M., Todo, Y.: GIFT: A Small Present. In: Fischer, W., Homma, N. (eds.) *Cryptographic Hardware and Embedded Systems – CHES 2017*, vol. 10529, pp. 321–345. Springer International Publishing, Cham (2017). [https://doi.org/10.1007/978-3-319-66787-4\\_16](https://doi.org/10.1007/978-3-319-66787-4_16)
5. Beierle, C., Jean, J., Kölbl, S., Leander, G., Moradi, A., Peyrin, T., Sasaki, Y., Sasdrich, P., Sim, S.M.: The SKINNY Family of Block Ciphers and Its Low-Latency Variant MANTIS. In: Robshaw, M., Katz, J. (eds.) *Advances in Cryptology – CRYPTO 2016*, vol. 9815, pp. 123–153. Springer Berlin Heidelberg, Berlin, Heidelberg (2016). [https://doi.org/10.1007/978-3-662-53008-5\\_5](https://doi.org/10.1007/978-3-662-53008-5_5)
6. Biham, E.: New types of cryptanalytic attacks using related keys. *Journal of Cryptology* **7**(4) (1994). <https://doi.org/10.1007/BF00203965>
7. Biham, E., Shamir, A.: Differential cryptanalysis of DES-like cryptosystems. *Journal of Cryptology* **4**(1), 3–72 (1991). <https://doi.org/10.1007/BF00630563>
8. Biryukov, A., Wagner, D.: Advanced Slide Attacks. In: Goos, G., Hartmanis, J., van Leeuwen, J., Preneel, B. (eds.) *Advances in Cryptology — EUROCRYPT 2000*, vol. 1807, pp. 589–606. Springer Berlin Heidelberg, Berlin, Heidelberg (2000). [https://doi.org/10.1007/3-540-45539-6\\_41](https://doi.org/10.1007/3-540-45539-6_41)
9. Bogdanov, A., Knudsen, L.R., Leander, G., Paar, C., Poschmann, A., Robshaw, M.J.B., Seurin, Y., Vikkelsoe, C.: PRESENT: An Ultra-Lightweight Block Cipher. In: Paillier, P., Verbauwhede, I. (eds.) *Cryptographic Hardware and Embedded Systems - CHES 2007*, vol. 4727, pp. 450–466. Springer Berlin Heidelberg, Berlin, Heidelberg (2007). [https://doi.org/10.1007/978-3-540-74735-2\\_31](https://doi.org/10.1007/978-3-540-74735-2_31)
10. Dunkelman, O., Keller, N., Shamir, A.: Minimalism in Cryptography: The Even-Mansour Scheme Revisited. In: Hutchison, D., Kanade, T., Kittler, J., Kleinberg, J.M., Mattern, F., Mitchell, J.C., Naor, M., Nierstrasz, O., Pandu Rangan, C., Steffen, B., Sudan, M., Terzopoulos, D., Tygar, D., Vardi, M.Y., Weikum, G., Pointcheval, D., Johansson, T. (eds.) *Advances in Cryptology – EUROCRYPT 2012*, vol. 7237, pp. 336–354. Springer Berlin Heidelberg, Berlin, Heidelberg (2012). [https://doi.org/10.1007/978-3-642-29011-4\\_21](https://doi.org/10.1007/978-3-642-29011-4_21)
11. Even, S., Mansour, Y.: A construction of a cipher from a single pseudorandom permutation. *Journal of Cryptology* **10**(3), 151–161 (Jun 1997). <https://doi.org/10.1007/s001459900025>
12. Gong, Z., Hartel, P., Nikova, S., Zhu, B.: Towards Secure and Practical MACs for Body Sensor Networks. In: Hutchison, D., Kanade, T., Kittler, J., Kleinberg, J.M., Mattern, F., Mitchell, J.C., Naor, M., Nierstrasz, O., Pandu Rangan, C., Steffen, B., Sudan, M., Terzopoulos, D., Tygar, D., Vardi, M.Y., Weikum, G., Roy, B., Sendrier, N. (eds.) *Progress in Cryptology - INDOCRYPT 2009*, vol. 5922, pp. 182–198. Springer Berlin Heidelberg, Berlin, Heidelberg (2009). [https://doi.org/10.1007/978-3-642-10628-6\\_13](https://doi.org/10.1007/978-3-642-10628-6_13)
13. Gueron, S., Mouha, N.: Simpira v2: A Family of Efficient Permutations Using the AES Round Function. In: Cheon, J.H., Takagi, T. (eds.) *Advances in Cryptology*

- ASIACRYPT 2016, vol. 10031, pp. 95–125. Springer Berlin Heidelberg, Berlin, Heidelberg (2016). [https://doi.org/10.1007/978-3-662-53887-6\\_4](https://doi.org/10.1007/978-3-662-53887-6_4)
14. Guo, J., Peyrin, T., Poschmann, A., Robshaw, M.: The LED Block Cipher. In: Hutchison, D., Kanade, T., Kittler, J., Kleinberg, J.M., Mattern, F., Mitchell, J.C., Naor, M., Nierstrasz, O., Pandu Rangan, C., Steffen, B., Sudan, M., Terzopoulos, D., Tygar, D., Vardi, M.Y., Weikum, G., Preneel, B., Takagi, T. (eds.) Cryptographic Hardware and Embedded Systems – CHES 2011, vol. 6917, pp. 326–341. Springer Berlin Heidelberg, Berlin, Heidelberg (2011). [https://doi.org/10.1007/978-3-642-23951-9\\_22](https://doi.org/10.1007/978-3-642-23951-9_22)
15. Hernandez-Castro, J.C., Peris-Lopez, P., Aumasson, J.P.: On the Key Schedule Strength of PRESENT. In: Hutchison, D., Kanade, T., Kittler, J., Kleinberg, J.M., Mattern, F., Mitchell, J.C., Naor, M., Nierstrasz, O., Pandu Rangan, C., Steffen, B., Sudan, M., Terzopoulos, D., Tygar, D., Vardi, M.Y., Weikum, G., Garcia-Alfaro, J., Navarro-Arribas, G., Cuppens-Boulahia, N., de Capitani di Vimercati, S. (eds.) Data Privacy Management and Autonomous Spontaneous Security, vol. 7122, pp. 253–263. Springer Berlin Heidelberg, Berlin, Heidelberg (2012). [https://doi.org/10.1007/978-3-642-28879-1\\_17](https://doi.org/10.1007/978-3-642-28879-1_17)
16. International Organization for Standardization: ISO/IEC 29192-2:2012 Information technology – Security techniques – Lightweight cryptography – Part 2: Block ciphers (2019)
17. Knudsen, L., Wagner, D.: Integral Cryptanalysis. In: Goos, G., Hartmanis, J., van Leeuwen, J., Daemen, J., Rijmen, V. (eds.) Fast Software Encryption, vol. 2365, pp. 112–127. Springer Berlin Heidelberg, Berlin, Heidelberg (2002). [https://doi.org/10.1007/3-540-45661-9\\_9](https://doi.org/10.1007/3-540-45661-9_9)
18. Koo, B., Roh, D., Kim, H., Jung, Y., Lee, D.G., Kwon, D.: CHAM: A Family of Lightweight Block Ciphers for Resource-Constrained Devices. In: Kim, H., Kim, D.C. (eds.) Information Security and Cryptology – ICISC 2017, vol. 10779, pp. 3–25. Springer International Publishing, Cham (2018). [https://doi.org/10.1007/978-3-319-78556-1\\_1](https://doi.org/10.1007/978-3-319-78556-1_1)
19. Matsui, M.: Linear Cryptanalysis Method for DES Cipher. In: Helleseth, T. (ed.) Advances in Cryptology — EUROCRYPT ’93, vol. 765, pp. 386–397. Springer Berlin Heidelberg, Berlin, Heidelberg (1994). [https://doi.org/10.1007/3-540-48285-7\\_33](https://doi.org/10.1007/3-540-48285-7_33)
20. National Institute of Standards and Technology: Advanced encryption standard (AES). Tech. Rep. NIST FIPS 197, National Institute of Standards and Technology, Gaithersburg, MD (Nov 2001). <https://doi.org/10.6028/NIST.FIPS.197>
21. Rukhin, A., Soto, J., Nechvatal, J., Smid, M., Barker, E.: A Statistical Test Suite for Random and Pseudorandom Number Generators for Cryptographic Applications. Tech. rep., BOOZ-ALLEN AND HAMILTON INC MCLEAN VA (May 2001)
22. Wu, S., Wang, M.: Integral Attacks on Reduced-Round PRESENT. In: Hutchison, D., Kanade, T., Kittler, J., Kleinberg, J.M., Mattern, F., Mitchell, J.C., Naor, M., Nierstrasz, O., Pandu Rangan, C., Steffen, B., Sudan, M., Terzopoulos, D., Tygar, D., Vardi, M.Y., Weikum, G., Qing, S., Zhou, J., Liu, D. (eds.) Information and Communications Security, vol. 8233, pp. 331–345. Springer International Publishing, Cham (2013). [https://doi.org/10.1007/978-3-319-02726-5\\_24](https://doi.org/10.1007/978-3-319-02726-5_24)
23. Z’aba, M.R., Raddum, H., Henricksen, M., Dawson, E.: Bit-Pattern Based Integral Attack. In: Nyberg, K. (ed.) Fast Software Encryption, vol. 5086, pp. 363–381. Springer Berlin Heidelberg, Berlin, Heidelberg (2008). [https://doi.org/10.1007/978-3-540-71039-4\\_23](https://doi.org/10.1007/978-3-540-71039-4_23)
24. Zhu, B.: An efficient software implementation of the block cipher PRESENT for 8-bit platforms: Bozhu/PRESENT-C (Feb 2019)



# Tweet sentiment analysis using deep learning with nearby locations as features

Wei Lun Lim, Chiung Ching Ho, and Choo-Yee Ting

Faculty of Computing & Informatics, Multimedia University, 63100 Cyberjaya,  
Selangor, Malaysia  
lynerlwl@gmail.com, ccho@mmu.edu.my, cyting@mmu.edu.my

**Abstract.** Twitter classification using deep learning have shown a great deal of promise in recent times. Many works had been performed on twitter sentiment analysis but there has not been much work done investigating the effects of location on twitter sentiment analysis. In this study, we concatenated text and location features as a feature vector for twitter sentiment analysis using a deep learning classification approach specifically Convolutional Neural Network (CNN). The achieved results show that using location as a feature alongside text has increased the sentiment analysis accuracy.

**Keywords:** sentiment analysis, location analysis, natural language understanding, deep learning, convolutional neural network

## 1 Introduction

Sentiment analysis analyzes people's opinion on what they feel on something. Mostly, people will make a comment on social media or leave a review on the product page to let the public know what they are thinking. Through those feedback, company or authorities can respond and further improve their product and services. Sometimes only an event is not enough to let people have the effort to open their account and share their feelings. We hypothesize that a person's surrounding locations could affect their emotions. In this study, we have investigated the effects of a person's location on the sentiment of their Tweet content. Sentiment analysis of tweets is performed using a combination of text and nearby location categories as a feature vector.

## 2 Related Works

The usage of Twitter for analytics has been well established in recent times. Twitter has been mined for purposes ranging from analyzing the users of Twitters [1], ecological research [2], rare-health event detection [3], and so forth. One recent development in Twitter analytics is the move towards incorporating data outside of Twitter to enrich the data, e.g. image and video data alongside text in a Twitter post. Apart from this, the geotagged nature of a Tweet also suggests that mining location associated with a

Tweet could bear exciting results. The mining of location has been used to predict business locations [4, 5], and business sales prediction [6]. Recent works relating work the mining of Tweets and locations have focused on the relationship between locations and products [7], and demographics [8], emotions [9], and estimation of Twitter user location [10]. All these works suggest that there is value in investigating the effects of location on sentiment.

Natural Language Processing (NLP) can extract text features from text data, but the sentiment might be wrong without considering the context at the sentence level [11]. By using CNN, the convolution layer can extract useful features that enable better performance. CNN has performed better in term of classification accuracy compare to traditional feature-based method [12]. Prior works have used CNN for sentiment analysis on text [13,14]. However, these works only have text as input.

### 3 Methodology

The methodology used for this study can be divided into distinct phases. The first phase involved activities related to data acquisition, pre-processing and sentiment labeling. Subsequently, the second phase of this study consist of the convolutional neural network architecture design and empirical experiments performed to elicit sentiments of tweets using a combination of word vectors and location vectors. Each phase is described in detail in its corresponding subsection.

#### 3.1 Dataset preparation, data preprocessing and sentiment labeling

In this study, the dataset used was modified from the Geo-tagged Microblog Corpus [15] which contains geotagged tweets. The original dataset contained 377616 tweets, from which a subset of 10000 tweets was created via random sampling. In this study, we only consider text information for the elicitation of sentiment. The preprocessing steps which were performed included the removal of Unicode Strings, Numbers, Website links and URLs, Retweet and Mentions symbols, Hashtag symbols, Punctuation, as well as White Spaces. After the tweets are pre-processed, the sentiment score was calculated using pattern matching of phrases implemented in the TextBlob [16] library. Each tweet was categorized to positive when the score is more than zero, and negative when the score is less than zero as shown in Algorithm 1. 250 samples of positive and negative labelled tweets were used to form a dataset of 500 geotagged tweets with the sentiment.

**Algorithm 1:** Categorization of tweets to positive or negative sentiment

---

```

Data: tweets
Result: categorize tweets sentiment to 0 or 1 based on sentiment score
while not at end of this document do
    read current;
    if score > 0 then
        | label sentiment as 1;
    else
        | label sentiment as 0;

```

---

Subsequently, the categories of the location nearby every tweet was acquired. In this study, we used the Geonames Find Nearby Web Services [17] and the Google Places Nearby Search [18] to extract the categories of locations nearby every tweet. Nearby locations were extracted within a 300 meters radius of every tweet. The returned result was then appended to their corresponding tweet.

### 3.2 Convolution neural network architecture design

In this phase, the focused is on designing the convolution neural network (CNN) to be used to perform sentiment classification using word and location feature vectors. The baseline model shown in Fig. 1 was created by only using word embeddings as the initial input to the CNN. The text representation was learned using 3 embedding methods: one-hot, word2vec (w2v), and GloVe. For w2v, the pre-trained model that was trained on 100B Wikipedia data [19, 20] was used. For GloVe, the pre-trained model that was trained on 6B Wikipedia data and 27B Twitter data [21] were used. A deep learning CNN model is then used to train and classify the sentiment of each tweet.

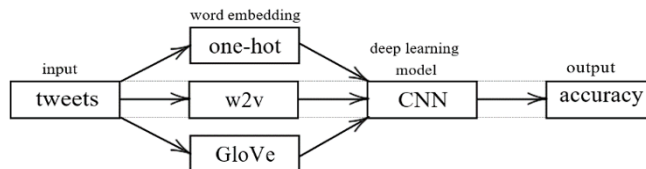


**Fig. 1.** Tweet sentiment analysis using word embeddings and CNN

The baseline CNN model is composed of one embedding layer, three convolution layers, one flattens layer, two dropout layers, and two dense layers. The sigmoid activation function is used as the output only contains 0 or 1. Losses are computed using binary cross entropy and Adam is used to optimizing the learning rate. The architecture is shown in Fig. 2.

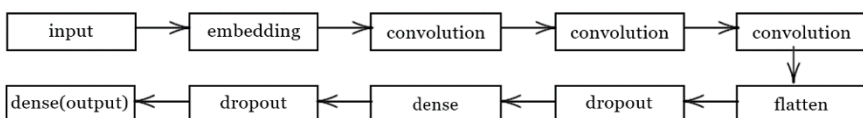


**Fig. 2.** CNN architecture used

Fig. 3 shows our proposed method which used a combination of vectorized text and vectorized location features to perform sentiment analysis. The text is concatenated with the vectorized categories of nearby locations to form an array as the input. We used 2 ways to generate the vectorized categories of nearby locations, namely one-hot encoding and count. The one-hot nearby location categories encoding transformed the nearby location categories into a binary vector consisting of the occurrences of said location category. Using the count method, nearby location categories were converted into a numeric vector of occurrences, which has the value ranging from zero(non-occurrence) to N (where N is the number of occurrences).

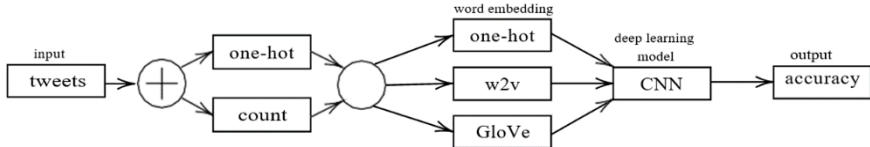


**Fig. 3.** Tweet sentiment analysis using a combination of word embeddings and vectorized nearby location categories

The overall architecture used to perform tweet sentiment classification with Geonames location features using a CNN with vector dimension of 50 is shown in Fig. 4. The architecture of CNN is the same for all experiments. The only changes are on the text vectors depends on whether the input is only text which shown in Fig. 1 or text with location features which shown in Fig. 3.

## 4 Experiments

The dataset used for the tweet sentiment classification experiments conducted in this study consisted of 250 positive and 250 negative tweets. Only 500 tweets were sampled to be used in the experiment due to the cost of calling the web services to determine the nearby locations. The 500 tweets, were divided into the training and testing set, using a 90:10 training to testing set split. This ratio was chosen as the dataset contained an average of 60 words after the pre-processing stage, and classification of short text is difficult due to sparsity and lack of common words [22]. As such, a higher training to testing set ratio may combat the sparsity inherent in short text. For all experiments, a seed value was set to ensure reproducibility of results. All pre-processed tweets are padded to a length of 25, as that is the maximum length of tweets after it has been integer encoded. Subsequently, the only variable which changes in each of the experiments is the dimensions of the embedding layer.

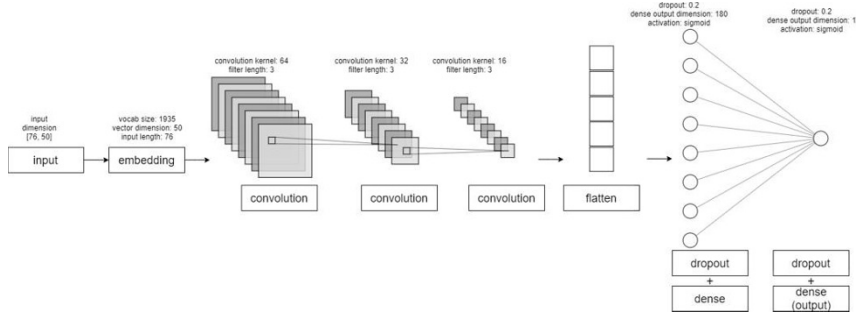


**Fig. 4.** CNN architecture for tweet sentiment classification using a combination of text and nearby location category features

After the text is concatenated with the nearby location categories, with the resultant length of the input vector being 76 and 125, depending on nearby locations extracted using Geonames and Google Places web services respectively. This length reflects the total categories returned by the Geonames (51 categories) and Google Places (100 categories) web services. The vector structure of text concatenate with Geonames is (500, 76) while for text concatenate with Google is (500, 125).

For the one-hot embedding text experiment, the grand mean approach is performed whereby the experiment is repeated 30 times for each vector dimension and the result is the average accuracy. This is because unlike the pre-trained w2v and GloVe which have an embedding matrix as an initializer, the one-hot method is using a random initializer, which hampers reproducibility of results.

#### 4.1 CNN with one-hot embedding

The results for the tweet sentiment classification experiment for the CNN model using the one-hot embedding as an embedding is shown in Table 1. This approach resulted in the highest accuracy of 63.9% when using only text features with 200 dimensions embedding vector, while the highest accuracy of 69.7% is achieved by using a combination of text and one-hot nearby location categories features.

#### 4.2 CNN using pre-trained 100B w2v model

The results for the tweet sentiment classification experiment for the CNN model using the pre-trained 100B w2v model for embedding is shown in Table 2. The highest accuracy of this model is 66.0% when using text features only, while the highest accuracy of 78.0% is achieved using a combination of text and count of nearby location categories features.

**Table 1.** Accuracy of CNN model using one-hot embedding

Embedding vector dimension	Text only feature	Text & One-hot Geonames features	Text & One-hot Google Places features	Text & Count of Geonames features	Text & Count of Google Places feature
50	62.1	62.8	66.4	62.7	63.1
100	62.7	61.9	<b>69.7</b>	65.9	67.7
200	<b>63.9</b>	65.9	66.9	66.5	68.4
300	61.7	62.7	69.4	67.5	69.2

**Table 2.** Accuracy of CNN model using pre-trained word2vec Wikipedia 100B embedding

Embedding vector dimension	Text only feature	Text & One-hot Geonames features	Text & One-hot Google Places features	Text & Count of Geonames features	Text & Count of Google Places feature
300	<b>66.0</b>	70.0	78.0	71.9	<b>78.0</b>

### 4.3 CNN using pre-trained 6B GloVe model

The results for the tweet sentiment classification experiment for the CNN model using the pre-trained GloVe 6B model for embedding is shown in Table 3. The highest accuracy of this model is 74.0% when using text features only with an embedding vector dimension of 200, while the highest accuracy of 78.0% is achieved using a combination of text and count of nearby location categories features.

**Table 3.** Accuracy of CNN model using pre-trained GloVe Wikipedia 6B embedding

Embedding vector dimension	Text only feature	Text & One-hot Geonames features	Text & One-hot Google Places features	Text & Count of Geonames features	Text & Count of Google Places feature
50	56.0	56.0	52.0	60.0	54.0
100	58.0	56.0	68.0	56.0	63.9
200	<b>74.0</b>	76.0	74.0	74.0	<b>78.0</b>
300	73.9	75.9	73.9	73.9	75.9

**Table 4.** Accuracy of CNN model using pre-trained GloVe Twitter 27B embedding

Embedding vector dimension	Text only feature	Text & One-hot Geonames features	Text & One-hot Google Places features	Text & Count of Geonames features	Text & Count of Google Places feature
50	81.9	79.9	80.0	81.9	78.0
100	74.0	76.0	75.9	78.0	75.9
200	<b>83.9</b>	77.9	83.9	79.9	<b>84.0</b>

## 5 Discussion

Out of the 11 experiments conducted (w2v experiments are excluded because only 300 vector dimensions are used), experiments with an embedding vector dimension of 200 generated the highest accuracy consistently. For the nearby location categories, usage of Google Places resulted in better results as compared to the usage of Geonames, as Google have 100 categories of place while Geonames has only 51 categories. Based on the four types of embedding methods experiment, using location by count achieve higher testing accuracy than using one-hot as shown in Table 5.

**Table 5.** Comparison of accuracy on location embedding methods

Embeddings	One-hot	Count
One-hot	69.7	69.2
Word2Vec	78.0	78.0
Glove 6B	75.9	78.0
Glove 27B	83.9	84.0

A comparison of testing accuracy before and after location feature is added is shown in Table 6. Overall the location feature does increase the testing accuracy. The increment percentage depends on the architecture of the word embeddings used.

**Table 6.** Comparison of accuracy using combination of text and location features

Embeddings	Text Only	Text and Location	Increase
One-hot	63.9	69.7	5.8
Word2Vec	66.0	78.0	12.0
Glove 6B	74.0	78.0	4.0
Glove 27B	83.9	84.0	0.1

## 6 Conclusions

In this study, we have proven that using location as a feature will improve the accuracy of tweet sentiment classification. The accuracy increased as the location feature improved the vector representation of words. The vector representation of tweets is sparse and by concatenating the location feature it allows the CNN to find better representation. To use location as a feature, we have attempted to vectorize the location via a one-hot and count operation. Vectorization of location by count resulted in slightly better accuracy as compared to the one-hot operation. This study has also shown that higher embedding vector dimension will result in higher accuracy for the concatenated text and location feature (in this study, a dimension of 200 consistently provide the highest accuracy). Currently the radius of nearby entities being used in this research is 300m, and the change in radius will be investigated further. We also will use other deep learning model like LSTM to perform the classification. Other embedding methods on location feature and text will be explored. We also will use more data as in this study we only used 500 tweets. We could also try using more sentiment levels as the current approach is using binary classification (positive or negative).

## Acknowledgments

This project is partially supported by Artificial Intelligence Research Unit (AiRU).

## References

1. Ong Kok Chien, Poo Kuan Hoong, and Chiung Ching Ho. A comparative study of hits vs pagerank algorithms for twitter user's analysis. In 2014 International Conference on Computational Science and Technology (ICCST), pages 1–6. IEEE, 2014.
2. Adam G Hart, William S Carpenter, Estelle Hlustik-Smith, Matt Reed, and Anne E Goodeough. Testing the potential of twitter mining methods for data acquisition: Evaluating novel opportunities for ecological research in multiple taxa. *Methods in Ecology and Evolution*, 9(11):2194–2205, 2018.
3. Ari Z Klein, Abeed Sarker, Haitao Cai, Davy Weissenbacher, and Graciela Gonzalez-Hernandez. Social media mining for birth defects research: a rule-based, bootstrapping approach to collecting data for rare health-related events on twitter. *Journal of biomedical informatics*, 87:68–78, 2018.
4. Jeremy YL Yap, Chiung Ching Ho, and Choo-Yee Ting. Analytic hierarchy process (ahp) for business site selection. In AIP Conference Proceedings, volume 2016, page 020151. AIP Publishing, 2018.
5. Hui-Jia Yee, Choo-Yee Ting, and Chiung Ching Ho. Optimal geospatial features for sales analytics. In AIP Conference Proceedings, volume 2016, page 020152. AIP Publishing, 2018.
6. Choo-Yee Ting, Chiung Ching Ho, Hui Jia Yee, and Wan Razali Matsah. Geospatial analytics in retail site selection and sales prediction. *Big data*, 6(1):42–52, 2018.
7. Amita Jain and Minni Jain. Location based twitter opinion mining using common-sense information. *Global Journal of Enterprise Information System*, 9(2), 2017.
8. Prabhsimran Singh, Ravinder Singh Sawhney, and Karanjeet Singh Kahlon. Sentiment analysis of demonetization of 500 & 1000 rupee banknotes by indian government. *ICT Express*, 4(3):124–129, 2018.
9. Hyo Jin Do and Ho-Jin Choi. Sentiment analysis of real-life situations using location, people and time as contextual features. In 2015 International Conference on Big Data and Smart Computing (BIGCOMP), pages 39–42. IEEE, 2015.
10. Xin Zheng, Jialong Han, and Aixin Sun. A survey of location prediction on twitter. *IEEE Transactions on Knowledge and Data Engineering*, 30(9):1652–1671, 2018.
11. Shiyang Liao, Junbo Wang, Ruiyun Yu, Koichi Sato, and Zixue Cheng. Cnn for situations understanding based on sentiment analysis of twitter data. *Procedia computer science*, 111:376–381, 2017.
12. Yuebing Zhang, Zhifei Zhang, Duoqian Miao, and Jiaqi Wang. Three-way enhanced convolutional neural networks for sentence-level sentiment classification. *Information Sciences*, 477:55–64, 2019.
13. Aliaksei Severyn and Alessandro Moschitti. Twitter sentiment analysis with deep convolutional neural networks. In Proceedings of the 38th International ACM SIGIR Conference on Research and Development in Information Retrieval, pages 959–962. ACM, 2015.
14. Tao Chen, Ruirong Xu, Yulan He, and Xuan Wang. Improving sentiment analysis via sentence type classification using bilstm-crf and cnn. *Expert Systems with Applications*, 72:221–230, 2017.

15. Jacob Eisenstein, Brendan O'Connor, Noah A Smith, and Eric P Xing. A latent variable model for geographic lexical variation. In Proceedings of the 2010 conference on empirical methods in natural language processing, pages 1277–1287. Association for Computational Linguistics, 2010.
16. Advanced usage: Overriding models and the blobber class. [https://textblob.readthedocs.io/en/dev/advanced\\_usage.html#sentiment-analyzers](https://textblob.readthedocs.io/en/dev/advanced_usage.html#sentiment-analyzers).
17. Geonames.org: Geonames web service documentation. [http://www.geonames.org/ export/web-services.html](http://www.geonames.org/export/web-services.html).
18. Google.com: Place search | places api. <https://developers.google.com/places/web-service/search>.
19. Google.com: Google code archive - long-term storage for google code project hosting. <https://code.google.com/archive/p/word2vec/>.
20. Tomas Mikolov, Kai Chen, Greg Corrado, and Jeffrey Dean. Efficient estimation of word representations in vector space. arXiv preprint arXiv:1301.3781, 2013.
21. Jeffrey Pennington, Richard Socher, and Christopher D. Manning. Glove: Global vectors for word representation. In Empirical Methods in Natural Language Processing (EMNLP), pages 1532–1543, 2014.
22. PC Rafeeqe and S Sendhilkumar. A survey on short text analysis in web. In 2011 Third International Conference on Advanced Computing, pages 365–371. IEEE, 2011.



# Quantifying attractiveness of incomplete-information multi-player game: case study using DouDiZhu

Yuxian Gao<sup>1</sup>, Wanxiang Li<sup>1</sup>, Mohd Nor Akmal Khalid<sup>1</sup>, and Hiroyuki Iida<sup>1</sup>

School of Information Science, JAIST, Nomi, 923-1211, Japan  
[{gaoxyexian,wanxiang.li,akmal,iida}@jaist.ac.jp](mailto:{gaoxyexian,wanxiang.li,akmal,iida}@jaist.ac.jp)

**Abstract.** This paper explores the nature of DouDiZhu which is an incomplete-information multi-player game and the most popular card game in China. While there are many DouDiZhu-like card games in the world, standard DouDiZhu card game is particularly characterized by its harmonic combination of several factors including the number of players, player's roles such as landlord and peasant, the number of decks, and score system to determine the winner. However, a study on such factors in relation to DouDiZhu game sophistication and attractiveness is not yet established. As such, this paper conducts such study by building the artificial intelligence (AI) player of DouDiZhu game with different levels, conducting simulations of self-play among the AI players, and employing the game refinement measure to assess and identify the attractive settings of this game. The results obtained show that standard DouDiZhu has provided the most sophisticated game setting for various AI players, which is analogous to actual human players of various levels.

**Keywords:** multiplayer game · incomplete information game · game refinement theory · DouDiZhu card game.

## 1 Introduction

DouDiZhu, also called ‘Fighting Landlord’, ‘Landlords’ or ‘2 against 1’, is commonly considered as the most popular computer card game in China [12]. In 2017, download amount of DouDiZhu network client reaches 1.13 billion <sup>1</sup>. “Happy DouDiZhu”, one of the game platforms, has 200 million players playing over 8 hours online per day <sup>2</sup>. At the end of 2017, “Happy DouDiZhu” was awarded as “Best mobile casual game of the year” on China’s game rankings <sup>3</sup>.

The game DouDiZhu is played by three players, where two of them play as peasants, the other one plays as the landlord. A game lasts about one to three minutes. On the player side who plays out the first cards, wins the game. Peasants share half of the income or loss while landlord bears alone, twice as the peasants. Strategy and luck are two essential aspects of an interesting game. The rules of DouDiZhu are not difficult, however the winning needs strategies and skills.

---

<sup>1</sup>[youxitao.com/articles/13003/](http://youxitao.com/articles/13003/)

<sup>2</sup>[questmobile.com.cn/research/report-new/32](http://questmobile.com.cn/research/report-new/32)

<sup>3</sup>[games.qq.com/a/20180118/028654](http://games.qq.com/a/20180118/028654)

The initial hands after dealing almost decide the possibility of winning or losing the game. In a good game, the winning would depend on strategy, but also necessary adding a certain element of random luck. This paper tries to find out a proper explanation of why this game has been so popular using the game refinement theory. We analyze the process of DouDiZhu, finding the game length and branching factor, and then conducted simulations of the game by giving a simple version of the game in which the session of bidding to be a landlord is skipped.

The content of this paper is as follows. Related research with respect to the paper's context is given in Section 2. Section 3 discusses the methods to analyze the game. Then, the procedure of the simulation experiment is described where the data are collected and analyzed in Section 4. Lastly, Section 5 concludes the paper.

## 2 Related Works

Card games have a history of thousands of years which dates back to the ancient Chinese records. The earliest appearance of card game in history can be traced back to the Tang dynasty, called “leaves play (ye zi xi)”, which is considered to be the ancestor of Poker, character cards, and Mahjong [10]. Since the works on poker games in 1995 started [2], scholars have focused on card games with incomplete information. Different from the complete information game, participants can only observe part of the information in the game process. At the same time, solving incomplete information game also requires dealing with randomness, risk management, opponent modeling, fraud, and information unreliability.

Many scholars have conducted research on related theories about the Texas Hold'em card game and bridge card game that focuses mainly on artificial intelligence (AI) solutions such as algorithms and its game engine. An optimal strategy theory had been proposed to solve the problem of two-person limited bet which showed a high game performance level in Texas Hold'em card game [3]. Another concept that focuses on virtual Regret using the Regret Minimization approach had been proposed to solve large-scale gaming problems [15]. In 2017, an AI for a card game called *Libratus* was designed by the Carnegie Mellon University, had won over 1.76 million in chips against human professional players because it can determine the strategy of playing cards by balancing the risks and benefits.

Another school of incomplete information studies is conducted on the bridge card since the 1960s. The development of computer bridge is mainly divided into a strategy that either human-based [1] or computer search-based [5]. The study automates bridge play by reducing the search space by independently considering sub-problems of different suit combinations and analyzing the problem of incomplete information in expert texts. Since the year 1996, the American Contract Bridge League established an official World Computer-Bridge Championship, to be run annually as an international bridge event ([bridgebotchampionship.com](http://bridgebotchampionship.com)) where it has attracted more attention from people from all walks of life.

DouDiZhu is a typical incomplete information game among Chinese people, which got its name from the Movement of Land Reform during the initial period of establishment of China. It was invented from Hubei Province in China around the 90s, where the initial version was Winner (named of "Paodekuai") and the name was changed to DouDiZhu on 1995. Since DouDiZhu has very strong Chinese characteristics, most studies in China mainly focused on why DouDiZhu is popular in China from the perspectives of historical causes (see works by [4] and [6]). As more and more games are being conquered by AI, researchers have now begun to study the aspects of algorithms of DouDiZhu AI. The characteristics of DouDiZhu game was analyzed and regarded as a two-person zero-sum game system where a variety of search strategies were designed [8]. The learning function of the DouDiZhu game system was also theoretically realized where the reasoning algorithm, the learning algorithm and other relevant theoretical knowledge of dynamic fuzzy logic were analyzed and applied it to the game of DouDiZhu [9].

The performance of a cheating UCT agent with a determined UCT agent was compared by the previous study, called Mini DouDiZhu [11]. The most effective method of narrowing the gap between complete information and incomplete information only has little impact on the strength of the AI agents. The concept of coequal hand quality for solving the fairness problem in compound DouDiZhu competition had also been presented [14]. The classification method based on the probability distribution has been proven to provide better classification effect than the statistical method.

To this end, more scholars are paying attention to this field where most of them are focusing on technical or historical facts of DouDiZhu game. To the best of our knowledge, this study is the first to reasonably explain the reason for this game popularity from the perspective of a game designer. As such, this study proposes a method to examine sophisticated levels of the DouDiZhu game where different settings are examined to measure the attractiveness of the game as well as determining the best setting for the game.

### 3 Methodology

#### 3.1 Game refinement theory

Game refinement (GR) theory was put forward by Iida et al. [7], which has been applied to evaluate the attractiveness or sophistication of different kinds of games. From the perspective of the player, with more information game outcome become more predictable when close to the end. In the DouDiZhu game, information or certainty of the game outcome can be nearly considered as a linear process accumulated with time  $t$ , i.e. almost linear approximation, that is  $x(t)$  in Equation (1).

$$x'(t) = \frac{n}{t}x(t) \quad (1)$$

The constant  $n$  is a parameter determined by the differences of skill between players of the game. Let  $D$  be the total moves of the game. Assume  $x(0) = 0$  and  $x(D) = B$ , noting that  $0 \leq t \leq D$ ,  $0 \leq x(t) \leq B$ . Then, the rate of game outcome certainty  $x'(t)$  can be determined, which is proportional to  $x(t)$ , as given in the Equation (2). Deriving the Equation (2) twice, the accelerated velocity of the solved uncertainty along the game process can be deduced.

$$x(t) = B\left(\frac{t}{D}\right)^n \quad (2)$$

$$x''(t) = \frac{B}{D^n} n(n-1)t^{n-2} \quad (3)$$

In the process of DouDiZhu game, the uncertainty will last till the last move, at  $t = D$ . And the equation becomes as in Equation (4). The measure  $\frac{\sqrt{B}}{D}$  could reflect some aspects of the attractiveness of games where  $B$  stands for the average number of possible moves and  $D$  stands for the average game length. This measure had been verified by many games where the sophistication of games have the same degree of informational acceleration value ( $GR \in [0.07, 0.08]$ ) [7], as shown in Table 1.

$$x''(D) = \frac{B}{D^2} n(n-1) \quad (4)$$

**Table 1.** Measure (GR) of game refinement for board games where  $B$  is the average branching factor,  $D$  is the average game length, and  $GR$  is the game refinement value

Games	$B$	$D$	$GR$
Chess	35	80	0.074
Shogi	80	115	0.078
Go	250	208	0.076

### 3.2 Versions of DouDiZhu game

DouDiZhu game has only about 30 years of development. According to record, the rules have not changed much since then. Yet, its popularity from the game implied that the rules have changed in some details over time. In this section, the variants and changes of the DouDiZhu game are chronologically reviewed and analyzed (summarized as in Table 2).

DouDiZhu was originated from *Winner* (in Chinese “Zhengshangyou” or “Paodekuai”), which is a kind of poker game, where the first one to play out all hands will be the winner. Main differences of *Winner* and classic DouDiZhu is in the number of players where *Winner* can play at least by two players (usually not more than eight) where each player fights on their own, using two decks

**Table 2.** Versions of DouDiZhu games

DouDiZhu Version	N	Players	Competition	Cards	Initial Hands
Classical	3	2 vs. 1	54	(20,17,17)	
Winner	2-8	Each other	52-108	Equal distribution*	
Big Two	4	Each other	54	(13,13,13,13)	
2-person	2	1 vs. 1	54	(20,17)	
4-person	4	3 vs. 1	108	(33,25,25,25)	

\* Initial hands of 2 players, 3 players, and 4 players, will be (20,20), (18,18,18), and (13,13,13,13) getting rid of two jokers, respectively.

of cards when more than 4 players<sup>4</sup>. The classical DouDiZhu is the most popular version of the game in China, played by three players. The valid card categories include single, pairs, straights, triplets, wings, planes, bombs and rocket, in which the triplets, planes, and bombs also can be played with kickers (see Table 3).

**Table 3.** Categories of Cards

Category	Description	LS*	HL**
Single	one card	3	JOKER
Straight	at least 5 consecutive single cards	34567	34567890JQKA
Pair	2 same cards	33	22
Wings	at least 3 consecutive pairs	334455	556677889900JJQQKKAA
	3 same cards	333	222
Triplet	3 same cards & a single kicker	3334	222A
	3 same cards & a pair kicker	33344	222AA
Plane	at least 2 triplets	333444	JJJQQKKKAAA88990022
Bomb	4 of a kind	3333	2222
Rocket	JOKER and joker		

\*:Lowest & shortest rank; \*\*:Highest & longest rank; Note:'0' represents for card '10'.

Another version, called the *Big Two*, is commonly played by four players. Each player plays on their own. The main difference between *Big Two* and DouDiZhu is on the valid card combination. *Big Two* can play flushes, while DouDiZhu does not care about the suit. In *Big Two* the straight can only consist of exactly five cards, while DouDiZhu's straight can consist of five to 12 cards. Another two variants are the two players and the four players DouDiZhu. The rules are the same with classic DouDiZhu but the players are limited to two people and utilize two decks of cards, respectively. In addition, four-player DouDiZhu is three versus one. One player plays as the landlord while the remaining player plays as the peasants.

<sup>4</sup>[https://en.wikipedia.org/wiki/Winner\\_\(card\\_game\)](https://en.wikipedia.org/wiki/Winner_(card_game))

### 3.3 Assessment methods employed for DouDiZhu game versions

In this study, the bidding phase is skipped and the assignment of the landlord to the player is random. In the game, 54 cards are split randomly between three players where the cards number is (20,17,17) and the one who gets 20 cards is the landlord. As such, players with cards of (20,17,17) will be separated in a manner of  $(L, P1, P2)$ . The landlord ( $L$ ) is one side, fighting for his own while peasant 1 ( $P1$ ) and peasant 2 ( $P2$ ) are other sides that cooperate to fight against  $L$ . The first side who play out all card hands wins the game.

The gameplay can be divided into two categories, initiative play or passive play. After dealing the cards, the landlord will play the first card or combination (initiative play). Alternatively,  $P1, P2, L$ , can play bigger-force card to follow last player's cards one by one (passive play). If they do not have bigger cards or they decide to skip, it called a *pass*. Two players in a row choose to pass will end the round. Then, the third player can initiate play with any cards as he wants and begin the next round. For instance,  $L, P1, P2$  play card in turns as  $L(33), P1(55), P2(PASS), L(AA), P1(PASS), P2(22), L(PASS), P1(PASS)$ , then  $P2$  will start a new round and initiate the card plays. The game ends until any one of the three players has played all the cards. To collect data, *game length* ( $D$ ) of DouDiZhu is the number of the total moves of the three players.

The possible options are counted as follows. When a player initiates a play, the number of options is estimated by the number of possible regular combinations at the player hand estimated from the card that is left. In example, the card pile of  $P1$  is “2221K999888633”, possible options  $P1$  can play 1 card are either 3, 6, 8, 9, k, 1, 2, which is seven in total; and so on until the possible option  $P1$  can play 10 cards is “8889992233”, which is only one. Counting all options together,  $7 + 4 + 3 + 18 + 9 + 1 + 4 + 12 + 4 + 1$ , the final number of  $P1$  options at this turn is 63. When a player plays passively, the number of options will be limited as the same type of the last played cards. For example,  $P2$  played “66633”, the card left for  $L$  is “22”, so the option for  $L$  is only “pass”, which is only a single option. Since peasants need to cooperate, sometimes they will “pass” even when they have cards to play. And sometimes they do not want to split bigger-force combinations thus they may also “pass”. In short, they can “pass” anytime when they play cards passively.

## 4 Simulation and Data Analysis

### 4.1 Simulation

The simulation was conducted for 10,000 times for each of the game settings. Assuming the number of game players as  $n$ , number of landlord as  $l$ , number of the peasants as  $p$ , hands allocation will be showed as  $(h_1, h_2, \dots, h_n)$ , a game setting will be showed as  $DDZ[(n, l, p)(h_1, h_2, \dots, h_n)]$ . Classical DouDiZhu has  $n = 3$  players in the game where a player is randomly assigned to be the landlord at the beginning of the game. Shuffled cards are dealt with the landlord, peasant 1 and peasant 2, respectively, where 20, 17, 17 cards are the initial state.

For each player's turn, the options a player can play will be calculated as the *branchfactors* ( $B$ ). The landlord always initiates play in the first round. Then, followed by peasant 1, peasant 2, and so on. All the players can pass even when they have bigger-force cards (this rule is the opposite in Winner; see Table 2). When there is two "Pass" in a row, a new round is declared. Each time a player moves, it is called a *hand*. A round will be several hands while at least 3 initiative card plays, and two "Pass". Once there is a player who plays out all the hands, the game is over.

Such simulation utilizes the classical DouDiZhu rules as an example to simulate other versions of DouDiZhu game considered for this study. In the case of classical DouDiZhu, setting showed as  $DDZ[(3, 1, 2)(20, 17, 17)]$ . The DouDiZhu AI program can realize dealing cards and playing cards, during which cooperation between peasants should work as intelligent as possible. Thus, different card categories are provided with a different numeric value according to the game rules, as shown in Table 4. An optimal strategy for the simulation is described as follows:

**Table 4.** Numerical value of the card categories in the simulation

Categories	Description	Numeric values	Examples
Single	3 (Joker)	1-15	'3' = 1, 'K' = 11
Straight	Sum of single	15-78	'456789' = 2 + 3 + 4 + 5 + 6 = 20
Pair	single * 2	2-30	'66' = 4 × 2 = 8
Wings	sum pair	12-110	'66778899' = 8 + 10 + 12 + 14 = 44
Triplet	single*3 + length	6-44	'KKK55' = 11 × (3 + 5) = 38
Plane	sum triplet	17-191	'JJJQQQKKK854' = 31 + 34 + 37 = 72
Bomb	single *200	200-3000	'5555' = 3 × 200 = 600
Rocket		5000	'JOKER+joker' = 5000

- For initiative playing, preferentially play categories as a sequence of plane, wings, straight, triplet, pairs and single. Among the same category, firstly play the smaller-force cards.
- For passive playing, among the optional strategies, firstly play the smaller-force cards.
- The landlord plays his cards at all costs. Peasants play cards bigger than landlord at all costs.
- Peasant 1 will play card bigger than peasant 2 when card force is smaller than 50; Otherwise, he will *pass*. Likewise for peasant 2.

The simulation is conducted with three AI levels: *strong*, *fair*, and *weak*. A *strong* AI always follows the optimal strategy aforementioned above. For a *fair* AI, peasants cooperate with each other, whereas either one of the peasant's cards always chooses *pass* while landlord's play a card as long as they have bigger cards. For a *weak* AI, the three players play bigger cards randomly. They play *pass* only when they don't have bigger cards.

## 4.2 Data Collection and Analysis

The game data was manually observed and counted for a small sample of about 100 games which is given in Table 5. The average possible options ( $B$ ) of classical DouDiZhu is 5.166, and its average game length ( $D$ ) is 29.71. As such, the  $GR$  measure of the classical DouDiZhu is 0.0765. According to the game refinement theory, a good and sophisticated games always find the balance between chance and skill as they changed over time. Since the sophisticated zone of game refinement value for most popular games has been verified to be  $GR \in [0.07, 0.08]$  [7], the classical DouDiZhu game is found to be the most sophisticated game version among the three DouDiZhu games on the manual simulation. In addition, the classical DouDiZhu game obtained the  $GR = 0.0765$  which is within the sophistication zone, thus probably offered a reasonable interpretation to the popularity of the classical DouDiZhu game in China.

**Table 5.** Manually data analysis of DouDiZhu game where  $B$  is the average possible options,  $D$  is the average game length, and  $GR$  is the game refinement value

DouDiZhu version	$B$	$D$	$GR$
Classical	5.166	29.71	0.0765
4-person	12.670	59.23	0.0601
2-person	2.789	17.89	0.0934

Analyzing further, DouDiZhu game has an interesting score system. In the simulation, skipping the step of bidding to be the landlord, the basic points are settled as 1, 2 or 3 in real gameplay. In this study, the basic score point is given as 3. Every time there is a player playing a *bomb* or *rocket*, the score will be doubled. For instance, if there are a total of three *bomb* in a game and the landlord wins the game, the landlord will gain 24 points while the peasants lose 12 points, respectively. Considering that this game is about cooperation and competition, the average scores in each setting could help us identify the fairness of the game setting. The possible score of Landlord and Peasants in different settings are given in the Table 6.

Typical DouDiZhu game setting is denoted as  $DDZ[(3, l, p)(20, 17, 17)]$ . In reality, human players have emotions and they tend to make decisions and consider different strategies based on their experience and preferences that often produces an unexpected outcome. Hence, considering the cooperation between two computer peasant's performance is corresponds with such real situation. The simulation with different settings are conducted, which is shown in Table 7.

We could find that among different card settings,  $DDZ[(3, 1, 2)(20, 17, 17)]$  is still the with the highest game refinement value. The measure of game refinement would decrease as the additional cards that landlord possesses. It could be inferred that the landlord have more advantage than the peasant at the initial game state and the game would be more dependent on skill.

**Table 6.** Possible score of Landlord and Peasant in different game settings

Setting	Win			Average rocket & bomb		Score		
	L	P1	P2			ratio	L	P
DDZ[(3,1,2)(20,17,17)]	0.317	0.388	0.295		0.222	1.222	2.32	2.5
DDZ[(3,1,2)(18,18,18)]	0.491	0.309	0.2		0.215	1.215	3.58	1.85
DDZ[(3,1,2)(22,16,16)]	0.078	0.55	0.372		0.273	1.273	0.6	3.5
DDZ[(3,1,2)(24,15,15)]	0.019	0.632	0.349		0.459	1.459	0.2	4.3
DDZ[(3,0,3)(18,18,18)]	0.356	0.315	0.329		0.207	1.207	0.9	-
DDZ[(2,0,2)(21,17)]	0.508	0.492	-		0.089	1.089	1.7	1.6

\*L score =  $6 \times L$  win  $\times$  score ratio, P score =  $3 \times (P1 \text{ win} + P2 \text{ win})$

**Table 7.** The simulation results at different settings

Setting	B	D	GR
DDZ[(3, 0, 3)(20, 17, 17)]	7.3440	45.4180	0.0597
DDZ[(3, 1, 2)(20, 17, 17)]	8.1980	40.0320	0.0715
DDZ[(3, 1, 2)(18, 18, 18)]	7.6440	40.6960	0.0680
DDZ[(3, 1, 2)(22, 16, 16)]	10.0150	39.0700	0.0810
DDZ[(3, 1, 2)(24, 15, 15)]	14.3730	37.8100	0.1000

Different level of the players would affect the sophistication and balancing of the game [13]. After collecting the data and analyzing further the setting of  $DDZ[(3, 1, 2)(20, 17, 17)]$ , there was another interesting discovery. Weak AI has no cooperation; thus, the player fight among themselves giving the fairest winning ratio. Strong AI with a high level of cooperation can also maintain balanced benefits of two sides (landlord versus peasants).

Cooperation strategy which can keep DouDiZhu game at a relatively fair level may critically affect the game sophistication in the multiplayer cooperative game. The  $GR$  measure decreases when cooperation strategy is prioritized. This implies that the game will be difficult for most players. In other words, the game is less interesting to a new player when considering the cooperation. Similarly, with a higher sense of cooperation, the game would be more challenging.

## 5 Concluding remarks

This study had conducted both manual and computer simulation to test different aspects of the Chinese most popular card game, DouDiZhu. The simulation results revealed some trends of DouDiZhu game. Manual and further simulations found that the game is sophisticated like other popular games and requires cooperation strategy to maintain the game fairness among the players. It was found that the most sophisticated game setting for the DouDiZhu game is the

*DDZ*[(3, 1, 2)(20, 17, 17)], which was refined with both fairness and sophistication. In addition, it could be inferred from the simulation results that cooperation can be an influencing factor that greatly effects the sophistication of a game. In addition, a scoring system was used as a measuring factor to explore the fairness of this game. Nevertheless, the complicated score system of DouDiZhu game was rather simplified compared to a real-world DouDiZhu game scenario. A future study could investigate how scores will affect the attractiveness of the game and explores further cooperation factors in term of improving the game entertainment experience.

## References

1. Berlin, D.L.S.: Span: Integrating problem-solving tactics. In: International Joint Conference on Artificial Intelligence. pp. 1047–1051 (1985)
2. Billings, D.: Computer poker. University of Alberta. Department of Computing Science (1995)
3. Billings, D., Burch, N., Davidson, A., Holte, R.C., Schaeffer, J., Schauenberg, T., Szafron, D.: Approximating game-theoretic optimal strategies for full-scale poker. In: International Joint Conference on Artificial Intelligence. pp. 661–668 (2003)
4. Cai, X.: Why do chinese people like playing "doudizhu"? Party life: jiangsu (2011)
5. Frank, I., Basin, D.: Search in games with incomplete information: a case study using Bridge card play. Elsevier Science Publishers Ltd. (1998)
6. Hu, C.: A brief analysis of the phenomenon of "doudizhu". The enterprise culture (8), 79 (2000)
7. Iida, H., Takahara, K., Nagashima, J., Kajihara, Y., Hashimoto, T.: An application of game-refinement theory to mah jong. Proceedings of Iccg Ndhoven **3166**, 333–338 (2004)
8. Lin, J.: The application of game tree searching technology in card online game (2009)
9. Liu, X.: Research and its application on dynamic fuzzy relational learning algorithm (2010)
10. Wang, S.: The spread and change of ye zi xi. Literature and history knowledge (5), 56–60 (1995)
11. Whitehouse, D., Powley, E.J., Cowling, P.I.: Determinization and information set monte carlo tree search for the card game dou di zhu. In: 2011 IEEE Conference on Computational Intelligence and Games (CIG'11). pp. 87–94. IEEE (2011)
12. Wikimedia: Dou dizhu. [https://en.wikipedia.org/wiki/Dou\\_dizhu](https://en.wikipedia.org/wiki/Dou_dizhu) (2019), last accessed April 2019
13. Xiong, S., Li, W., Xinting, M., Iida, H.: Mafia Game Setting Research using Game Refinement Measurement (12 2017)
14. Zhang, Y., Chen, Z., Zheng, L., Zhang, Z., Ding, M., Meng, K., Li, S.: Research on hand discrimination for doudizhu game. In: 4th International Conference on Education, Management, Arts, Economics and Social Science (ICEMAESS 2017). Atlantis Press (2017). <https://doi.org/10.2991/icemaess-17.2017.97>
15. Zinkevich, M., Johanson, M., Bowling, M., Piccione, C.: Regret minimization in games with incomplete information. In: International Conference on Neural Information Processing Systems. pp. 1729–1736 (2007)



# An Improvement of Computing Newton's Direction for Finding Unconstrained Minimizer for Large-Scale Problems with an Arrowhead Hessian Matrix

Khadizah Ghazali<sup>1</sup>, Jumat Sulaiman<sup>1</sup>, Yosza Dasril<sup>2</sup> and Darmesah Gabda<sup>1</sup>

<sup>1</sup> Faculty of Science and Natural Resources, Mathematics with Economics Programme, Universiti Malaysia Sabah, 88400 Kota Kinabalu, Sabah, Malaysia.

<sup>2</sup> Faculty of Electronic and Computer Engineering, Universiti Teknikal Malaysia Melaka, 76100 Melaka, Malaysia.

khadizah@ums.edu.my, jumat@ums.edu.my, yosza@utem.edu.my,  
darmesah@ums.edu.my

**Abstract.** In large-scale problems, classical Newton's method requires solving a large linear system of equations resulting from determining the Newton direction. This process often related as a very complicated process, and it requires a lot of computation (either in time calculation or memory requirement per iteration). Thus to avoid this problem, we proposed an improved way to calculate the Newton direction using an Accelerated Overrelaxation (AOR) point iterative method with two different parameters. To check the performance of our proposed Newton's direction, we used the Newton method with AOR iteration for solving unconstrained optimization problems with its Hessian is in arrowhead form and compared it with a combination of the Newton method with Gauss-Seidel (GS) iteration and the Newton method with Successive Over Relaxation (SOR) iteration. Finally, comparison results show that our proposed technique is significantly more efficient and more reliable than reference methods.

**Keywords:** Newton method, AOR iteration, Unconstrained optimization problems, Large-scale optimization, Arrowhead matrix.

## 1 Introduction

We consider large-scale unconstrained minimization problem

$$\min_{\mathbf{x} \in \mathbb{R}^n} f(\mathbf{x}) \quad (1)$$

where the objective function  $f : \mathbb{R}^n \rightarrow \mathbb{R}$  is smooth with at least twice continuously differentiable and  $n$  is large. These problems appear in a wide range of applications, including electric power systems for the nonlinear large mesh-interconnected system [1], discrete-time optimal control [2], the DNA reproduction process [3] or even in the sign recurrent neural network [4]. Therefore, developing an efficient method to solve problems (1) is a significant and vigorous scientifically research area.

There are various methods listed in [5] to solve unconstrained minimization, and Newton's method is listed as one of the best-known methods that possess the fast quadratic rate of convergence with excellent performance when the initial point is chosen correctly. However, if it involves a large-scale problem, computation and storage of the Hessian for the classical Newton method are too costly to be practical. For that reason, many researchers have modified this classical Newton's method to overcome its disadvantages, such as in [6-10].

Shen et al. [6] presented a new regularized Newton method for solving unconstrained minimization problems by using the modified Cholesky factorization algorithm to replace the objective function's Hessian. On top of that, they used a first-order method to find the first-order stationary point and only mention that the algorithms can be extended to second-order algorithms by the help of negative curvature. Grapsa [7] proposed modification on Newton's direction for solving unconstrained optimization using the gradient vector modification at each iteration, while Tahera et al. [8] combined two types of descent direction to propose a new algorithm for solving unconstrained optimization problems. Recently, Abiodun and Adelabu [9] investigated the performance of the Newton method and compared it with two iterative modification of Newton's method for solving unconstrained minimization problems. However, they concluded that the computational numerical result obtained was depend on the nature of the objective function.

Thus, we modified the classical Newton method via its Newton's direction, and this modification is different from the existing combination of Newton's method with other methods, as stated in the previous paragraphs. This Newton's direction is obtained by solving a linear system that involves the Hessian matrix and the gradient. Therefore, solving it using the direct method for large-scale problems is not a smart choice. On the other hand, we used the AOR point iteration. This AOR iteration has been introduced by Hadjidimos in [11] using a two-parameter generalization of the SOR method and classified as one of the most straightforward and powerful techniques for solving any linear systems.

As a result, in this paper, motivated by the advantages of the classical Newton method, we proposed the AOR point iteration to find the Newton direction and then solve problem (1) using Newton's method. We called this method as Newton-AOR method. This improvement is a new contribution to the large-scale unconstrained optimization problem where the Hessian is in the arrowhead matrix form. To verify the performance of the improved Newton direction, we used a combination of Newton's method with Gauss-Seidel iteration and a combination of Newton's method with SOR iteration as reference methods, and they are called as Newton-GS method and Newton-SOR method respectively.

The rest of this paper is organized as follows. In the next section, we described the Newton scheme with an arrowhead Hessian matrix, while in section 3, we formulated the AOR iteration for computing Newton's direction. In section 4, we presented our numerical experiment and result. Lastly, the conclusion is stated in section 5.

## 2 Newton Iteration with an Arrowhead Hessian Matrix

In this section, we began with a second-order quadratics Taylor approximation;

$$f(\underline{\mathbf{x}}) \approx \underbrace{f(\underline{\mathbf{x}}^{(k)})}_{\text{Constant}} + \underbrace{\left[ \nabla f(\underline{\mathbf{x}}^{(k)}) \right]^T (\underline{\mathbf{x}} - \underline{\mathbf{x}}^{(k)})}_{\text{Linear term}} + \underbrace{\frac{1}{2} (\underline{\mathbf{x}} - \underline{\mathbf{x}}^{(k)})^T \nabla^2 f(\underline{\mathbf{x}}^{(k)}) (\underline{\mathbf{x}} - \underline{\mathbf{x}}^{(k)})}_{\text{Quadratic term}} \quad (2)$$

Therefore, to compute a local minimizer of  $f(\underline{x})$  around the current point  $\underline{x}^{(k)}$ , we replace the function  $f(\underline{x})$  in problem (1) by its approximation (2) to have the next point  $\underline{x}^{(k+1)}$ . Instead of solving problem (1), we solve

$$\min_{\mathbf{x} \in \mathbb{R}^n} f(\underline{\mathbf{x}}^{(k)}) + \left[ \nabla f(\underline{\mathbf{x}}^{(k)}) \right]^T (\mathbf{x} - \underline{\mathbf{x}}^{(k)}) + \frac{1}{2} (\mathbf{x} - \underline{\mathbf{x}}^{(k)})^T \nabla^2 f(\underline{\mathbf{x}}^{(k)}) (\mathbf{x} - \underline{\mathbf{x}}^{(k)}) \quad (3)$$

and get the minimizer of problem (3) by solving the following linear system (also known as the Newton equation);

$$\mathbf{H}(\underline{\mathbf{x}}^{(k)}) \underline{d}^{(k)} = -\nabla f(\underline{\mathbf{x}}^{(k)}) \quad (4)$$

where,  $\mathbf{H}(\underline{\mathbf{x}}^{(k)}) = \nabla^2 f(\underline{\mathbf{x}}^{(k)})$  as the Hessian matrix of second partial derivatives of  $f(\underline{\mathbf{x}})$  and  $\underline{\mathbf{d}}^{(k)} = \underline{\mathbf{x}}^{(k+1)} - \underline{\mathbf{x}}^{(k)}$  as the search direction call Newton's direction. This Newton's direction can formally define by;

$$\underline{d}^{(k)} = - \left[ \mathbf{H}(\underline{\mathbf{x}}^{(k)}) \right]^{-1} \nabla \underline{f}(\underline{\mathbf{x}}^{(k)}) \quad (5)$$

The Newton iteration can obtain the estimation of the problem (3) from equation (4) as;

$$\underline{\mathbf{x}}^{(k+1)} = \underline{\mathbf{x}}^{(k)} - \left[ \mathbf{H}(\underline{\mathbf{x}}^{(k)}) \right]^{-1} \nabla f(\underline{\mathbf{x}}^{(k)}). \quad (6)$$

As a particularly interesting case, in this study we considered problems with Hessian of an arrowhead (up or down) matrix of order  $n$  with the general form given by [12];

$$\mathbf{H}(\underline{x}^{(k)}) = \begin{bmatrix} \frac{\partial^2 f}{\partial x_1^2} & \frac{\partial^2 f}{\partial x_1 \partial x_2} & \frac{\partial^2 f}{\partial x_1 \partial x_3} & \dots & \frac{\partial^2 f}{\partial x_1 \partial x_n} \\ \frac{\partial^2 f}{\partial x_2 \partial x_1} & \frac{\partial^2 f}{\partial x_2^2} & 0 & \dots & 0 \\ \vdots & 0 & \ddots & \ddots & \vdots \\ \frac{\partial^2 f}{\partial x_n \partial x_1} & 0 & \dots & 0 & \frac{\partial^2 f}{\partial x_n^2} \end{bmatrix} @ \mathbf{H}(\underline{x}^{(k)}) = \begin{bmatrix} \frac{\partial^2 f}{\partial x_1^2} & 0 & \dots & 0 & \frac{\partial^2 f}{\partial x_1 \partial x_n} \\ 0 & \ddots & \ddots & \vdots & \vdots \\ \vdots & \ddots & \frac{\partial^2 f}{\partial x_{n-2}^2} & 0 & \frac{\partial^2 f}{\partial x_{n-2} \partial x_n} \\ 0 & \dots & 0 & \frac{\partial^2 f}{\partial x_{n-1}^2} & \frac{\partial^2 f}{\partial x_{n-1} \partial x_n} \\ \frac{\partial^2 f}{\partial x_n \partial x_1} & \dots & \frac{\partial^2 f}{\partial x_n \partial x_{n-2}} & \frac{\partial^2 f}{\partial x_n \partial x_{n-1}} & \frac{\partial^2 f}{\partial x_n^2} \end{bmatrix}$$

### 3 Formulation of the proposed Newton's Direction

We noted that for large-scale problems, one of the difficulties in finding newton's directions is solving the inverse of the Hessian matrix. Therefore, we are not looking for the Newton direction using equation (5), but instead, we used equation (4). This equation (4) in abstract form is nothing but a linear system. Thus, for simplicity, we rewrite equation (4) as in the general form;

$$\mathbf{A}\underline{d} = \underline{f} \quad (7)$$

where,

$$\mathbf{A} = \begin{bmatrix} b_1 & c_1 & c_2 & \cdots & c_{n-1} \\ a_2 & b_2 & 0 & \cdots & 0 \\ a_3 & 0 & b_3 & \ddots & \vdots \\ \vdots & \vdots & \ddots & \ddots & 0 \\ a_n & 0 & \cdots & 0 & b_n \end{bmatrix} @ \mathbf{A} = \begin{bmatrix} b_1 & 0 & \cdots & 0 & c_1 \\ 0 & b_2 & \ddots & \vdots & c_2 \\ \vdots & \ddots & b_3 & 0 & \vdots \\ 0 & \cdots & 0 & \ddots & c_{n-1} \\ a_2 & a_3 & \cdots & a_n & b_n \end{bmatrix}, \underline{d} = \begin{bmatrix} d_1 \\ d_2 \\ d_3 \\ \vdots \\ d_n \end{bmatrix}, \underline{f} = \begin{bmatrix} f_1 \\ f_2 \\ f_3 \\ \vdots \\ f_n \end{bmatrix}$$

To express the Gauss-Seidel iteration, we decomposed matrix  $\mathbf{A}$  in equation (7) as a sum of three matrices as follows [13];

$$\mathbf{A} = \mathbf{D} - \mathbf{L} - \mathbf{U} \quad (8)$$

where  $\mathbf{D}$  is the nonzero diagonal matrix of  $\mathbf{A}$ ,  $\mathbf{L}$  and  $\mathbf{U}$  are strictly lower and upper triangular matrices of  $\mathbf{A}$ , respectively. By applying the decomposition in equation (8) into a linear system (7), the iterative formulation of the Gauss-Seidel method stated in vector form as [13, 14];

$$\underline{d}^{(k+1)} = (\mathbf{D} - \mathbf{L})^{-1} \mathbf{U} \underline{d}^{(k)} + (\mathbf{D} - \mathbf{L})^{-1} \underline{f} \quad (9)$$

Similarly, the SOR method with the implementation of the relaxation factor,  $\omega$  in vector form stated as [15, 16];

$$\underline{d}^{(k+1)} = (\mathbf{D} - \omega \mathbf{L})^{-1} (\omega \mathbf{U} + (1-\omega) \mathbf{D}) \underline{d}^{(k)} + \omega (\mathbf{D} - \omega \mathbf{L})^{-1} \underline{f} \quad (10)$$

where  $\omega \in [1, 2)$  and selected based on the smallest number of inner iterations. By using the same analogy as the SOR method, the AOR method with two different parameters expressed as follows [11]:

$$\underline{d}^{(k+1)} = (\mathbf{D} - \gamma \mathbf{L})^{-1} ((\omega - \gamma) \mathbf{L} + \omega \mathbf{U} + (1-\omega) \mathbf{D}) \underline{d}^{(k)} + \omega (\mathbf{D} - \gamma \mathbf{L})^{-1} \underline{f} \quad (11)$$

where  $\gamma$  is the acceleration parameter and  $\omega$  is the overrelaxation parameter. Next, the implementation of AOR point iterations with concerning the type of Hessian, produce the component  $d_i^{(k+1)}$  in the form that can be computed as

$$\begin{aligned} d_i^{(k+1)} &= (1-\omega) d_i^{(k)} + \frac{\omega}{b_i} \left( f_i - \left( \frac{\gamma - \omega}{\omega} \right) a_i d_{i-1}^{(k)} - \left( \frac{\gamma}{\omega} \right) a_i d_{i-1}^{(k+1)} - \sum_{j=1}^{n-1} c_j d_{i+1}^{(k)} \right), i = 1 \\ d_i^{(k+1)} &= (1-\omega) d_i^{(k)} + \frac{\omega}{b_i} \left( f_i - \left( \frac{\gamma - \omega}{\omega} \right) a_i d_1^{(k)} - \left( \frac{\gamma}{\omega} \right) a_i d_1^{(k+1)} \right), i = 2, 3, \dots, n \end{aligned} \quad (12)$$

for the problem involves with arrowhead up Hessian, and as

$$\begin{aligned} d_i^{(k+1)} &= (1-\omega)d_i^{(k)} + \frac{\omega}{b_i} \left( f_i - \left( \frac{\gamma-\omega}{\omega} \right) c_i d_n^{(k)} - \left( \frac{\gamma}{\omega} \right) c_i d_n^{(k+1)} \right), i = 1, 2, \dots, n-1 \\ d_i^{(k+1)} &= (1-\omega)d_i^{(k)} + \frac{\omega}{b_i} \left( f_i - \left( \frac{\gamma-\omega}{\omega} \right) c_i d_{i-1}^{(k)} - \left( \frac{\gamma}{\omega} \right) c_i d_{i-1}^{(k+1)} - \sum_{j=2}^{n-1} a_j d_{i-1}^{(k+1)} \right), i = n \end{aligned} \quad (13)$$

for the problem involves with arrowhead down Hessian. Noted that for  $\omega = \gamma = 1$ , equation (11) is reduced to the Gauss-Seidel method and if  $\omega = \gamma$ , then equation (11) coincides with the SOR method. This equation (12) and equation (13) are an improved way to calculate the Newton direction according to its type of Hessian either arrowhead up or arrowhead down. Using these two equations, we proposed an improved Newton's method with AOR iteration (call as Newton-AOR) for finding unconstrained minimizer for large-scale problems with an arrowhead hessian matrix. Thus, we proposed the following algorithm for solving problem (1).

---

**Algorithm 1:** Newton-AOR with an Arrowhead Hessian Matrix Scheme

---

- i. Initialize – Set up the objective function  $f(\underline{x})$ ,  $\underline{x}^{(0)} \leftarrow \underline{0}^n$ ,  $\varepsilon_1 \leftarrow 10^{-6}$ ,  $\varepsilon_2 \leftarrow 10^{-8}$  and  $n \leftarrow \underline{0}$
  - ii. Assign the optimal value of  $\omega$  and  $\gamma$ .
  - iii. For  $j = 1, 2, \dots, n$  implement
    - a. Set  $\underline{d}^{(0)} \leftarrow \underline{0}$
    - b. Calculate  $f(\underline{x}^{(k)})$
    - c. Identify the Hessian type as arrowhead up or arrowhead down, then calculate the approximate value of  $d_i^{(k+1)}$  using either equation (12) or equation (13).
    - d. Check the convergence test  $\|\underline{d}^{(k+1)} - \underline{d}^{(k)}\| \leq \varepsilon_2$ . If yes, go to step (e). Otherwise, go back to step (b)
    - e. For  $i = 1, 2, \dots, n$  calculate;  $\underline{x}^{(k+1)} \leftarrow \underline{x}^{(k)} + \underline{d}^{(k)}$
    - f. Check the convergence test  $\|\nabla f(\underline{x}^{(k)})\| \leq \varepsilon_1$ . If yes, go to (iii). Otherwise, go back to step (a)
  - iv. Display approximate solutions
- 

## 4 Numerical Experiments and Results

In this section, numerical experiments are performed using Algorithm 1 for illustrating its competence, and all the numerical calculation are compiled using C language with double precision arithmetic. Five unconstrained optimization test functions from the collection collected in [17-19] are used and stated in Table 1. The selection of all these test functions is based on its Hessian type, which is an arrowhead Hessian matrix. Three different initial points were selected with its standard initial point (a) is as suggested in [17-19], while for the selection of a nonstandard initial point (b) and (c) are chosen randomly from a range surrounding the standard initial point. Also, all these test cases

were run five times using five different order of Hessian matrix as  $n = \{1000, 5000, 10000, 20000, 30000\}$ . Thus, this gives the total number of test cases is 75 cases.

As the first order necessary for  $\underline{\mathbf{x}}^{(k)}$  to be a minimum of  $f(\underline{\mathbf{x}})$  is  $\|\nabla f(\underline{\mathbf{x}}^{(k)})\| = 0$ , therefore we decide to terminate the minimization algorithm with  $\underline{\mathbf{x}}^{(k)}$  as an estimate of  $\underline{\mathbf{x}}^*$ , if  $\|\nabla f(\underline{\mathbf{x}}^{(k)})\| \leq 10^{-6} = \varepsilon_1$ . This convergence tolerance decision is the same as what was posted by Moyi and Leong in [20]. Besides that, a tolerance of  $10^{-8} = \varepsilon_2$  was chosen to terminate the inner iteration. Through the numerical experiments, five parameters were observed, such as the number of inner iterations, number of outer iterations, execution time (in seconds), function value (at the iterate where execution terminated) and maximum error. Results generated by Algorithm 1 are compared with the reference methods. Thus, we report the computational result of the Newton-GS (NGs), Newton-SOR (NSOR), and Newton-AOR (NAOR) in Table 2. All values tabulated in Table 2 are rounded up to two decimal places. Therefore, all maximum error values are smaller than the convergence tolerance,  $\varepsilon_1$ .

**Table 1.** Test functions used in the numerical experiment.

Test Number	Test Name, Algebraic Expression, local optimal value and optimal point	Initial point, $\mathbf{x}^{(0)}$		
		(a) Standard	(b) Nonstandard 1	(c) Nonstandard 2
1	LIARWHD $f(\underline{\mathbf{x}}) = \sum_{i=1}^n 4(-x_i + x_i^2)^2 + \sum_{i=1}^n (x_i - 1)^2$ $f^* = 0$ and $\mathbf{x}^* = (1.0, 1.0, \dots, 1.0)$	(4.0, 4.0, ..., 4.0)	(1.5, 1.5, ..., 1.5) (3.3, 3.5, ..., 3.3, 3.5)	
2	NONDIA $f(\underline{\mathbf{x}}) = (x_1 - 1)^2 + \sum_{i=2}^n 100(x_i - x_{i-1}^2)^2$ $f^* = 0$ and $\mathbf{x}^* = (1.0, 1.0, \dots, 1.0)$	(-1.0, -1.0, ..., -1.0)	(2.0, 2.0, ..., 2.0) (2.0, 1.5, ..., 2.0, 1.5)	
3	DIAG-AUP1 $f(\underline{\mathbf{x}}) = \sum_{i=1}^n 4(x_i^2 - x_i)^2 + (x_i^2 - 1)^2$ $f^* = 0$ and $\mathbf{x}^* = (1.0, 1.0, \dots, 1.0)$	(4.0, 4.0, ..., 4.0)	(1.5, 1.5, ..., 1.5) (3.3, 3.5, ..., 3.3, 3.5)	
4	Schwefel 2.4 $f(\underline{\mathbf{x}}) = \sum_{i=1}^n (x_i - 1)^2 + (x_i + x_i^2)^2$ $f^* = 0$ and $\mathbf{x}^* = (1.0, 1.0, \dots, 1.0)$	(0.0, 0.0, ..., 0.0)	(2.0, 2.0, ..., 2.0) (3.0, 2.0, ..., 3.0, 2.0)	
5	ARWHEAD $f(\underline{\mathbf{x}}) = \sum_{i=1}^{n-1} (-4x_i + 3) + (x_i^2 + x_n^2)^2$ $f^* = 0$ and $\mathbf{x}^* = (1.0, 1.0, \dots, 1.0, 0.0)$	(1.0, 1.0, ..., 1.0)	(-1.0, -1.0, ..., -1.0) (2.0, -1.0, ..., 2.0, -1.0)	

Noted that in Table 2, test function 5 shows its approximate value are the optimal value for all three methods. Therefore, the selection of a good initial point can influence the efficiency of the new search process. It is observable that the number of inner iteration and the execution time (in seconds) for our proposed method reduces well compared from the referenced method. Thus, to have well understood for the efficiency of the reductions, we presented Table 3 and Table 4 using computational results from Table 2. Table 3 indicated the decrement percentage of the number of inner iterations for the Newton-AOR and Newton-SOR compared to Newton-GS, while Table 4 reported the comparison of speed ratio for the Newton-AOR method with both the reference methods. Moreover, in Table 4, we used the total execution time in seconds for every test case.

## 5 Conclusion

An improved calculation of finding Newton's direction for solving unconstrained optimization in large-scale problem with an arrowhead Hessian has been developed by AOR iteration. As expected, through the implementation of two parameters ( $\gamma$  and  $\omega$ ) in the AOR method can indicate that the approach we proposed is more superior compared to reference methods. This fact can be explained in Table 3 and Table 4. From Table 3, the decrement percentage of the number of inner iteration is in the range 29.11%-99.20%, and 1.25%-98.83% correspond to Newton-AOR and Newton-SOR methods compared to Newton-GS method. A comparison of the speed ratio in Table 4 reveals that our proposed method is significantly faster than the Newton-SOR method with speed ratio is up to 2.46 times and more rapidly than the Newton-GS method with speed ratio is up to 332.96 times. Thus, it can be concluded that our proposed iterative method can show significant improvement in the number of iterations and execution time compared to Newton-GS and Newton-SOR iterative methods. For further study, we plan to develop an algorithm on the same problems here base on 4-point explicit group block iterative approach as done by Ghazali et al. [21] for tridiagonal Hessian type.

**Acknowledgment.** The authors are grateful for the fund received from Universiti Malaysia Sabah upon publication of this paper (GUG0160-2/2017).

## References

1. Lin, S.Y., Lin, C.H.; An efficient method for unconstrained optimization problems of non-linear large mesh-interconnected systems, IEEE Transaction on automatic control 40(3), 490-95 (1995).
2. Ng, C.K., Liao, LZ., Li, D.: A Globally Convergent and Efficient Method for Unconstrained Discrete-Time Optimal Control, Journal of Global Optimization 23, 401-421 (2003).

3. Zang, W., Zhang, W., Zhang, W., Liu, X.: A Genetic Algorithm Using Triplet Nucleotide Encoding and DNA Reproduction Operations for Unconstrained Optimization Problems. *Algorithms* 10, 76 (2017). <http://dx.doi.org/10.3390/a10030076>
4. Maratos, N.G., Moraitis, M.A.; Some results on the Sign recurrent neural network for unconstrained minimization, *Neurocomputing* 287, 1-21 (2018).
5. Sun, W., Yuan, Y.: *Optimization Theory and Methods-Nonlinear Prog.* Springer, United States (2006).
6. Shen, C., Chen, X., Liang, Y.: A regularized Newton method for degenerate unconstrained optimization problems. *Optimization Letters* 6, 1913–1933 (2012).
7. Grapsa, T.N.: A Modified Newton Direction for Unconstrained Optimization, *Optimization* 63(7), 983-1004 (2014).
8. Taheri, S., Mammadov, M., Seifollahi, S.: Globally convergent algorithms for solving unconstrained optimization problems. *Optimization* 64(2), 249-263 (2015).
9. Abiodun, T.L., Adelabu, O.A.: A Comparison of Newton's Method and Two of its Modifications for the Solution of Nonlinear Optimization Problems. *International Journal of Educational Sciences* 17(1-3), 116–128 (2017).
10. Bogg, P.T., Byrd, R.H.: Adaptive, Limited-Memory BFGS Algorithms for Unconstrained Optimization, *SIAM Journal on Optimization* 29(2), 1282-1299 (2019).
11. Hadjidimos, A.: Accelerated Overrelaxation Method. *Mathematics of Computation* 32(141), 149–157 (1978).
12. Stanimirovic, P.S., Katsikis, V.N., Kolundzija, D.: Inversion and pseudoinversion of block arrowhead matrices. *Applied Mathematics and Computation* 341, 379-401 (2019)
13. Varga, R.S.: *Matrix iterative analysis*. Springer, Berlin (2000).
14. Ghazali, K., Sulaiman, J., Dasril, Y., Gabda, D.: Newton method with explicit group iteration for solving large scale unconstrained optimization problems. *Journal of Physics: Conference Series*. 1132, 012056 (2018).
15. Sulaiman, J., Hasan, M.K., Othman, M., Karim, S.A.A.: Numerical solutions of nonlinear second-order two-point boundary value problems using half-sweep SOR with Newton method. *Journal of Concrete and Applicable Mathematics* 11(1), 112–120 (2013).
16. Young, D. M.: Iterative methods for solving partial difference equations of elliptic type. *Transactions of the American Mathematical Society*. 76(1), 92-111 (1954).
17. Andrei, N.: Test functions for unconstrained optimization. Research Institute for informatics. Center for Advanced Modeling and Optimization, 8-10, Averescu Avenue, Sector 1, Bucharest, Romania, 1-15 (2004).
18. Andrei, N.: An unconstrained optimization test function collection. *Advanced Modeling and Optimization. An Electronic International Journal*. 10(1), 147-161 (2008).
19. Jamil, M., Yang X.: A literature survey of benchmark functions for global optimization problems. *Int. J. Mathematical Modelling and Numerical Optimisation*. 4(2), 150-194 (2013).
20. Moyi, A.U., Leong, W.J.: A sufficient descent three-term conjugate gradient method via symmetric rank-one update for largescale optimization, *Optimization* 65(1), 121–43 (2016).
21. Ghazali, K., Sulaiman, J., Dasril, Y., Gabda, D.: Application of Newton-4EGSOR Iteration for Solving Large Scale Unconstrained Optimization Problems with a Tridiagonal Hessian Matrix. In: Alfred, R., Lim, Y., Ibrahim, A., Anthony P. (eds) *Computational Science and Technology. Lecture Notes in Electrical Engineering*. 481 Springer, Singapore (2019).

**Table 2.** Computational result of the Newton-GS, Newton-SOR, and Newton-AOR.

Test No. (initial point)	n	Number of inner iterations			Number of outer iterations			Execution time (seconds)			Function value at the iterate where execution terminated			Maximum error		
		N <sub>GS</sub>	N <sub>SOR</sub>	N <sub>AOR</sub>	N <sub>GS</sub>	N <sub>SOR</sub>	N <sub>AOR</sub>	N <sub>GS</sub>	N <sub>SOR</sub>	N <sub>AOR</sub>	N <sub>GS</sub>	N <sub>SOR</sub>	N <sub>AOR</sub>	N <sub>GS</sub>	N <sub>SOR</sub>	N <sub>AOR</sub>
1(a)	1000	1567	376	368	38	14	14	0.04	0.01	0.01	2.40E-13	1.47E-14	7.02E-15	9.90E-07	3.16E-07	9.45E-07
	5000	2194	408	396	52	17	17	0.38	0.05	0.05	2.35E-13	6.00E-16	7.00E-16	9.72E-07	6.63E-07	8.33E-07
	10000	2509	443	435	58	17	17	0.63	0.09	0.08	2.23E-13	1.60E-15	8.76E-16	9.46E-07	4.64E-07	5.79E-07
	20000	2821	507	429	63	18	16	1.46	0.19	0.19	2.40E-13	1.00E-15	2.26E-15	9.80E-07	2.31E-07	8.55E-07
1(b)	30000	2899	549	213	65	21	19	2.07	0.33	0.31	2.45E-13	2.00E-16	2.35E-18	9.91E-07	2.89E-07	6.68E-07
	1000	1013	207	177	32	10	8	0.03	0.02	0.01	2.31E-13	2.16E-16	9.13E-16	9.70E-07	6.40E-07	6.73E-07
	5000	1039	232	211	46	8	7	0.21	0.03	0.02	2.21E-13	3.33E-14	5.76E-14	9.41E-07	3.66E-07	7.24E-07
	10000	1022	232	215	36	20	9	0.35	0.06	0.05	2.48E-13	2.51E-18	1.64E-14	9.97E-07	3.94E-07	9.81E-07
1(c)	20000	1038	232	206	52	8	12	0.65	0.18	0.11	2.48E-13	1.38E-17	1.39E-15	9.97E-07	6.88E-07	8.44E-07
	30000	1042	236	214	58	15	9	0.97	0.31	0.16	2.31E-13	2.78E-15	2.55E-14	9.61E-07	6.97E-07	3.23E-07
	1000	1556	394	349	37	17	15	0.04	0.03	0.01	2.42E-13	3.29E-17	9.86E-17	9.93E-07	6.73E-07	8.32E-07
	5000	2131	415	391	50	15	23	0.27	0.07	0.05	2.47E-13	3.98E-17	1.27E-17	9.95E-07	5.66E-08	6.92E-07
2(a)	10000	2384	460	425	57	23	25	0.56	0.18	0.11	2.25E-13	9.64E-18	6.71E-18	9.50E-07	9.14E-07	9.65E-07
	20000	2553	538	515	61	20	19	1.19	0.32	0.25	2.49E-13	5.98E-17	8.01E-17	9.99E-07	3.31E-07	8.84E-07
	30000	2593	580	556	33	23	24	1.64	0.50	0.42	2.39E-13	5.97E-18	2.30E-18	9.78E-07	1.85E-07	9.67E-07
	1000	22986	1079	838	7528	124	25	1.34	0.03	0.02	2.47E-15	2.40E-18	4.25E-13	1.00E-06	9.72E-07	8.30E-07
2(b)	5000	52084	1883	1350	28374	225	248	18.95	0.26	0.26	2.47E-15	2.39E-15	2.25E-15	1.00E-06	9.55E-07	7.06E-08
	10000	128743	2633	1473	96881	320	67	123.63	0.66	0.44	2.47E-15	1.06E-15	4.74E-12	1.00E-06	6.73E-07	9.47E-07
	20000	243256	3308	2133	209648	319	338	518.18	1.58	1.55	2.47E-15	2.67E-15	2.99E-15	1.00E-06	3.12E-07	7.73E-07
	30000	351492	4129	2809	326806	669	709	1182.51	3.70	3.27	2.47E-15	7.13E-18	7.33E-18	9.99E-07	8.80E-07	9.68E-07
2(c)	1000	38789	2762	2692	7536	214	211	1.55	0.08	0.07	2.50E-15	1.12E-17	1.15E-17	9.99E-07	9.81E-07	9.96E-07
	5000	168711	7024	6745	45606	526	532	37.86	0.82	0.78	2.50E-15	1.95E-18	1.94E-18	1.00E-06	9.99E-07	9.87E-07
	10000	302950	10346	9897	98059	747	757	152.13	2.44	2.36	2.50E-15	1.02E-18	1.00E-18	1.00E-06	9.99E-07	9.89E-07
	20000	557276	14252	13653	209806	1537	1479	621.94	7.45	7.27	2.50E-15	6.70E-19	5.70E-19	1.00E-06	9.99E-07	9.95E-07
3(a)	30000	799141	17081	16839	326742	2134	1766	1194.97	14.71	14.00	2.50E-15	5.49E-19	3.85E-19	9.99E-07	9.97E-07	9.95E-07
	1000	38695	2810	2790	7535	110	69	1.18	0.06	0.08	2.50E-15	2.35E-18	4.78E-16	1.00E-06	9.07E-07	3.35E-07
	5000	173806	6905	6486	45606	652	70	33.15	0.84	0.63	2.50E-15	2.77E-18	1.60E-13	1.00E-06	9.95E-07	8.92E-07
	10000	302014	10989	10551	98058	656	270	129.24	3.28	2.14	2.50E-15	7.40E-19	1.99E-16	1.00E-06	9.96E-07	5.48E-07
3(b)	20000	554369	14569	14497	209808	1769	811	522.01	7.72	6.84	2.50E-15	9.80E-19	3.78E-19	1.00E-06	9.95E-07	9.97E-07
	30000	796433	17818	16863	326742	1446	1163	1193.60	13.17	12.48	2.50E-15	3.09E-19	4.61E-19	9.99E-07	9.94E-07	9.96E-07
	1000	412	185	161	17	15	13	0.03	0.01	0.00	4.69E-14	4.01E-17	3.21E-17	8.70E-07	6.74E-07	4.39E-07
	5000	452	184	150	20	17	11	0.05	0.03	0.01	4.95E-14	4.03E-18	2.24E-18	8.90E-07	4.85E-07	3.39E-08
3(c)	10000	463	187	147	21	17	10	0.11	0.08	0.05	5.79E-14	1.94E-18	9.08E-17	9.63E-07	4.84E-07	3.40E-07
	20000	470	188	142	23	17	13	0.20	0.14	0.09	5.32E-14	1.73E-18	7.80E-19	9.23E-07	6.50E-07	3.27E-07
	30000	473	188	144	24	18	13	0.27	0.23	0.14	4.54E-14	4.58E-19	6.22E-18	8.53E-07	4.09E-07	9.86E-07
	1000	279	105	67	13	10	7	0.01	0.00	0.00	4.66E-14	1.81E-17	1.51E-19	8.67E-07	4.55E-07	4.69E-08
3(d)	5000	284	106	69	17	10	7	0.07	0.04	0.01	5.70E-14	1.64E-18	6.81E-18	8.57E-07	4.03E-07	4.39E-08
	10000	286	108	71	19	10	8	0.07	0.06	0.03	4.63E-15	1.23E-18	4.33E-20	8.61E-07	1.85E-07	8.01E-08
	20000	287	107	71	20	10	8	0.14	0.11	0.05	5.90E-14	2.40E-18	1.52E-19	9.72E-07	4.20E-07	1.94E-07
	30000	289	107	71	21	10	8	0.19	0.15	0.07	5.66E-14	2.81E-18	2.71E-19	9.52E-07	9.54E-07	3.09E-07
3(e)	1000	404	176	153	16	12	13	0.01	0.01	0.00	5.94E-14	4.51E-17	5.24E-17	9.79E-07	7.57E-07	4.92E-07
	5000	434	170	155	20	14	13	0.05	0.03	0.02	4.65E-14	5.95E-18	2.35E-17	8.64E-07	3.91E-07	9.71E-07
	10000	441	172	155	22	15	15	0.09	0.08	0.05	4.09E-14	9.36E-19	4.00E-18	8.09E-07	3.46E-07	4.64E-07
	20000	444	178	156	23	16	15	0.18	0.16	0.10	4.11E-14	9.74E-19	6.87E-18	8.11E-07	4.74E-07	8.56E-07
4(a)	30000	446	176	156	24	16	16	0.28	0.24	0.15	5.64E-14	3.81E-19	9.82E-19	9.50E-07	3.80E-07	4.09E-07
	1000	104	64	64	16	6	5	0.02	0.01	0.00	1.13E-15	4.89E-17	4.53E-16	9.57E-07	3.92E-07	9.00E-07
	5000	88	61	61	23	8	7	0.06	0.04	0.01	1.24E-16	9.51E-18	1.13E-16	9.98E-07	3.91E-07	9.71E-07
	10000	84	57	57	27	8	8	0.10	0.06	0.02	8.22E-17	1.03E-17	1.03E-17	9.11E-07	6.19E-07	6.19E-07
4(b)	20000	81	52	52	30	3	3	0.17	0.09	0.04	4.09E-17	1.21E-14	1.21E-14	8.09E-07	2.22E-07	2.22E-07
	30000	79	56	56	31	7	7	0.20	0.12	0.06	3.37E-17	5.74E-18	5.46E-18	8.99E-07	6.82E-07	6.82E-07
	1000	447	144	94	19	6	7	0.03	0.01	0.00	7.99E-15	3.02E-14	9.41E-17	8.03E-07	9.75E-07	4.74E-08
	5000	462	162	117	26	7	7	0.11	0.05	0.02	1.78E-16	9.09E-16	1.39E-16	8.44E-07	2.90E-07	6.25E-07
4(c)	10000	464	163	125	29	10	7	0.19	0.07	0.04	8.75E-17	1.42E-16	3.98E-16	8.37E-07	9.18E-07	9.55E-07
	20000	461	167	129	32	12	8	0.32	0.15	0.07	5.80E-17	9.77E-18	3.33E-16	9.64E-07	5.36E-08	5.94E-07
	30000	464	165	129	34	6	8	0.54	0.20	0.11	2.97E-17	9.84E-14	3.82E-16	8.51E-07	9.36E-07	5.09E-07
	1000	561	171	159	21	8	8	0.04	0.01	0.00	8.80E-15	3.81E-16	1.11E-14	8.43E-07	2.60E-07	7.82E-07
5(a)	5000	664	219	200	29	12	7	0.15	0.08	0.02	1.84E-16	6.48E-16	1.75E-14	8.59E-07	4.82E-07	5.01E-12
	10000	688	237	223	30	11	11	0.25	0.11	0.06	9.99E-17	8.65E-17	2.45E-15	8.95E-07	5.33E-07	3.41E-07
	20000	710	245	237	33	15	12	0.49	0.21	0.12	4.59E-17	2.53E-17	3.82E-16	8.57E-07	5.22E-07	7.17E-07
	30000	718	256	245	35	15	12	0.68	0.28	0.18	3.02E-17	1.52E-17	4.25E-16	8.51E-07	4.28E-07	1.84E-07
5(b)	1000	41	39	21	6	6	6	0.01	0.00	0.00	1.00E+00	1.00E+00	1.00E+00	1.09E-12	2.69E-07	2.64E-10
	5000	41	39	21	6	6	6	0.02	0.01	0.01	1.00E+00	1.00E+00	1.00E+00	5.77E-12	8.53E-07	5.01E-12
	10000	41	40	21	6	7	6	0.03	0.02	0.01	1.00E+00	1.00E+00	1.00E+00	1.15E-11	8.87E-08	1.00E-11
	20000	41	40	21	6	7	6	0.04	0.04	0.02	1.00E+00	1.00E+00	1.00E+00	2.31E-11	1.77E-07	2.00E-11
5(c)	30000	41	40	21	6	7	6	0.08	0.05	0.03	1.00E+00	1.0				

**Table 3.** Decrement percentage of the number of inner iterations for the Newton-AOR and Newton-SOR compared to Newton-GS.

Test No. (initial point)	Number of inner iteration (%)	
	N <sub>SOR</sub>	N <sub>AOR</sub>
1(a)	76.01-82.34	76.52-92.65
1(b)	77.30-79.57	78.96-82.53
1(c)	74.68-80.70	77.57-82.17
2(a)	95.31- <b>98.83</b>	96.35- <b>99.20</b>
2(b)	92.88-97.86	93.06-97.89
2(c)	92.74-97.76	92.79-97.88
3(a)	55.10-60.25	60.92-69.79
3(b)	62.24-62.98	75.17-75.99
3(c)	56.44-61.00	62.13-65.02
4(a)	29.11-38.46	<b>29.11</b> -38.46
4(b)	63.77-67.79	72.02-78.97
4(c)	64.35-69.63	65.88-71.76
5(a)	2.44-4.88	48.78
5(b)	13.79-14.04	54.39-55.17
5(c)	<b>1.25</b>	58.75

**Table 4.** Comparison of speed ratio for the Newton-AOR method with Newton-GS method and Newton-SOR method.

Test No. (initial point)	Total execution time (seconds)			Speed ratio		
	N <sub>GS</sub> (I)	N <sub>SOR</sub> (II)	N <sub>AOR</sub> (III)	I II	I III	II III
1(a)	4.58	0.67	0.65	6.84	7.05	<b>1.03</b>
1(b)	2.21	0.60	0.35	3.68	6.31	1.71
1(c)	3.70	1.10	0.84	3.36	4.40	1.31
2(a)	1844.61	6.23	5.54	<b>296.09</b>	<b>332.96</b>	1.12
2(b)	2008.45	25.50	24.49	78.76	82.01	1.04
2(c)	1879.18	24.17	22.15	77.75	84.84	1.09
3(a)	0.66	0.49	0.30	1.35	2.20	1.63
3(b)	0.48	0.36	0.16	1.33	3.00	2.25
3(c)	0.61	0.52	0.32	<b>1.17</b>	<b>1.91</b>	1.63
4(a)	0.55	0.32	0.13	1.72	4.23	<b>2.46</b>
4(b)	1.19	0.48	0.24	2.48	4.96	2.00
4(c)	1.61	0.69	0.38	2.33	4.24	1.82
5(a)	0.18	0.12	0.07	1.50	2.57	1.71
5(b)	0.19	0.08	0.06	2.37	3.17	1.33
5(c)	0.23	0.14	0.08	1.64	2.88	1.75



# Semantic Segmentation of Herbarium Specimens Using Deep Learning Techniques

Burhan Rashid Hussein, Owais Ahmed Malik, Wee-Hong Ong and Johan Willem Frederik Slik

Faculty of Science, Universiti Brunei Darussalam, BRUNEI DARUSSALAM  
{18h8338, owais.malik, weehong.ong, johan.slik}@ubd.edu.bn

**Abstract.** Automated identification of herbarium species is of great interest as quite a number of these collections are still unidentified while others need to be updated following recent taxonomic knowledge. One challenging task in automated identification process of these species is the existence of visual noise such as plant information labels, color codes and other scientific annotations which are mostly placed at different locations on the herbarium mounting sheet. This kind of noise needs to be removed before applying different species identification models as it can significantly affect the models' performance. In this work we propose the use of deep learning semantic segmentation model as a method for removing the background noise from herbarium images. Two different semantic segmentation models, namely DeepLab version three plus (DeepLabv3+) and the Full- Resolution Residual Networks (FRNN-A), were applied and evaluated in this study. The results indicate that FRNN-A performed slightly better with a mean Intersection of Union (IoU) of 99.2% compared to 98.1% mean IoU attained by DeepLabv3+ model on the test set. The pixel -wise accuracy for two classes (herbarium specimen and background) was found to be 99.5% and 99.7%, respectively using FRNN-A model while the DeepLabv3+ was able to segment herbarium specimen and the rest of the background with a pixel-wise accuracy of 98.4% and 99.6%, respectively. This work evidently suggests that deep learning semantic segmentation could be successfully applied as a pre-processing step in removing visual noise existing in herbarium images before applying different classification models.

**Keywords:** semantic segmentation, herbarium images, DeepLabv3+, plant species, deep learning.

## 1 Introduction

With the continuing effort of large scale digitization of herbarium specimens, automating the process of plant species identification using machine learning and image processing techniques has also gained a huge momentum [1]. One of the common pre-processing step in plant species identification or automatic feature extraction is the segmentation process where the task is to remove the background noise of the target specimen before applying different machine learning algorithms [2]. Most of the studies

have used different image segmentation algorithms which have existed prior to deep learning approach like clustering, edging, graph partitioning methods and thresholding [3]. One present challenge in building an automated plant species identification system for herbarium images is the existence of visual noise such as plants labels, color codes and collector information which are randomly placed on the herbarium mounting sheet. Removing this kind of visual noise, even with robust thresholding segmentation methods, remains difficult and therefore makes the fully automated species identification task significantly challenging [4,5].

The application of semantic segmentation using deep learning has been one of the major computer vision tasks alongside image classification, object detection and localization together with instance segmentation and has been successfully applied in different domains such as in medical diagnosis, agricultural field and autonomous driving [6]. The development and use of these models are growing fast with either improving existing techniques or finding new domain area for applications.

In this study we aimed at applying deep learning semantic segmentation technique in order to remove the visual background noise from the collection of herbarium specimens. Different studies have expressed the need to deal with such noise, although to present, these studies have applied simple cropping technique as a way to remove or reduce such noise [7]. Simple cropping of the herbarium images does not guarantee effective removal of the visual noise such as the labels that are often randomly placed and sometimes present at the center of the images. Furthermore, this cropping technique may discard certain parts of the specimens containing well-structured and useful visual representation of the specimen.

Therefore, in this study we proposed the use of deep learning semantic segmentation technique as an alternative solution in removing background noise from herbarium specimens. This work could be taken as an important pre-processing step towards building herbarium plant species identification systems. Since plant species identification for herbarium accounts for the whole herbarium specimen, proper specimen segmentation is required in cases where specimens have other background noise which must be removed before applying classification models. Through this method, a full herbarium specimen could be well utilized as all the background noise has been suppressed.

## 2 Methodology

The proposed method is depicted in Figure 1 below. The steps are explained in the following sections.

### 2.1 Dataset and Annotation

Universiti Brunei Darussalam Herbarium (UBDH) contains information about more than 8000 plant species samples from the tropical region [8]. Currently, a digital repository of these species is being created and images of the dried leaves have been collected using a high-quality camera and a scanner. For this study, we selected 395 species samples images from UBDH in order to conduct our experiments. We used an image labeler

application from MATLAB 2018 software for creating ground truth labels for the image dataset. The ground truth labels consist of two classes as either a herbarium specimen (leaves/stems) or the background (everything other than the specimen). After exporting our ground truth labels from MATLAB software, we applied a median filter to improve the labels by reducing any noise during labeling process.

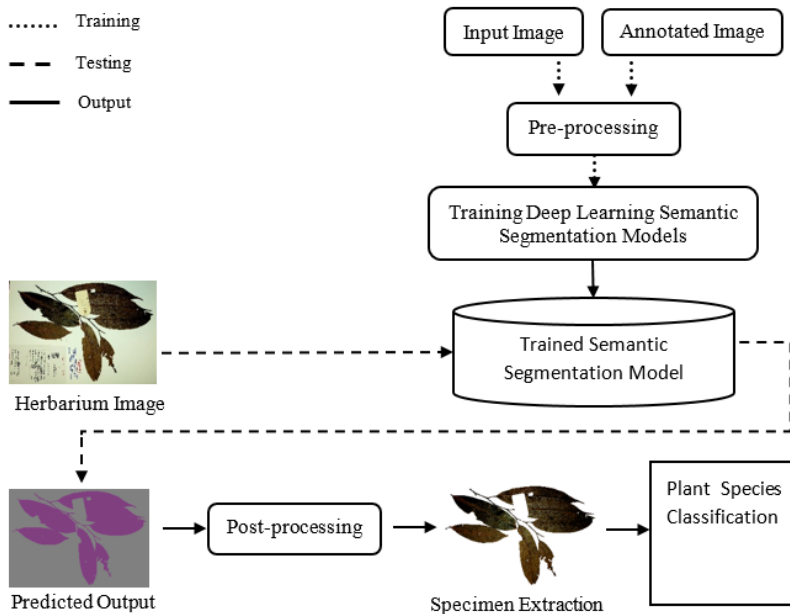


**Fig. 1.** Semantic Segmentation Model for Herbarium Specimens

## 2.2 Pre-processing

Since deep learning models are computationally expensive and require same size input, all inputs images and their annotation were downsampled and then cropped to  $512 \times 512$  size [5]. We applied data augmentation techniques in both original images and their corresponding annotated images such as horizontal and vertical flipping, rotation and brightness changes to improve network regularization and number of samples in our network. [9].

## 2.3 Training Deep Learning Semantic Segmentation Models

The dataset was divided into 80% training set, 10% validation set and 10% test set. We trained two different models and the results were compared. DeepLabv3+ used the pre-trained weights while second model (FRRN-A) was trained from scratch.

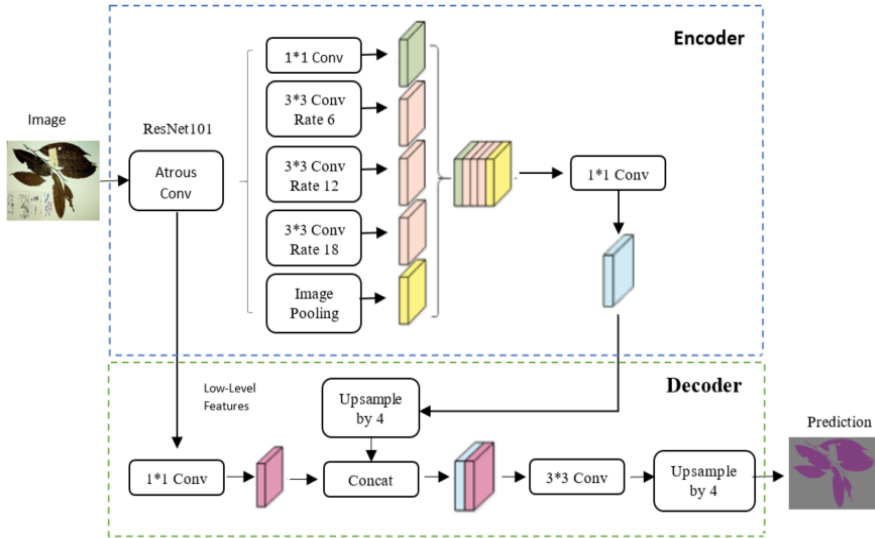


**Fig. 2.** DeepLabv3+ architecture (Conv = Convolutional layer)

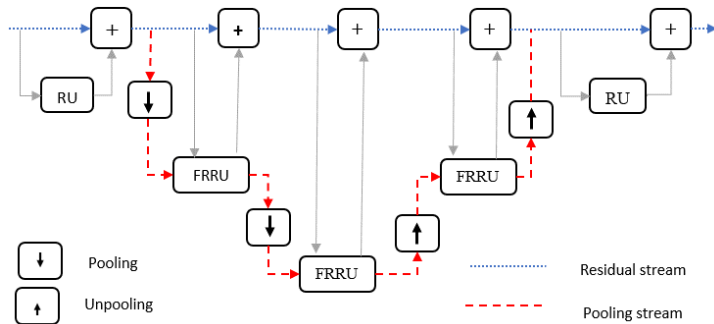


**Fig. 3.** Abstract structure of full-resolution residual network.

The network shown in Fig.3. has two process streams. The residual stream (blue) stays at full image resolution, pooling stream (red) undergoes a sequence of pooling and unpooling operations. The two process are coupled using full-resolution residual units (FRRUs).

### DeepLabv3+ Architecture

DeepLabv3+ architecture extends the architecture of its predecessor DeepLabv3 by adding an effective decoder module to recover object boundaries. Furthermore, the

spatial pyramid pooling applied in the network structure results in faster and stronger encoder-decoder network since the training is done at multiple rates while capturing multi-scale contextual information. Figure 2 shows the flow of DeepLabv3+ encoder-decoder pathway to achieve a precise object boundary. This architecture have been explained in more detail in the original paper by Chen et al. [10]. We decided to use this network as it's one of the current state of art on Pascal VOC leaderboard for image segmentation[11].

### **Full-Resolution Residual Networks**

Full-resolution residual networks architecture uses two separate streams to capture both features and location of the objects/classes in an image [12]. Figure 3 depict the abstract structure of the network. Pooling stream undergoes a series of pooling and unpooling operations to handle high level semantic information for high classification accuracy while residual stream handles the low-level pixel information at full image resolution and enable a precise segment boundary for high localization accuracy. The two streams are coupled together using full-resolution residual units (FRRUs) to produce a strong recognition and localization performance for semantic segmentation. In this work we used FRRN-A which is a lighter version of the FRRN that works with lower input resolution images [12] .

### **Networks Training**

After conducting experiments with different hyperparameter settings, we have reported the hyperparameters that have given the best results. We have used a batch size of 1 for FRRN-A which was trained from scratch. For DeepLabv3+ model we have used a batch size of 3 with pretrained ResNet101 trained from ImageNet. It has been shown in various studies that the earlier layers of deep learning neural networks deal with generic features which indicates that they can be useful for other computer vision tasks instead of random weight initialization [13]. In both networks we have used the Adam optimization method with the learning rate of 0.00005. All networks were trained using sigmoid cross entropy loss function (due to a binary class problem) for 100 epochs.

This study was implemented using TensorFlow deep learning framework [14] and we used a dell G7 equipped with an Intel i7 and NVIDIA GeForce GTX 1060 for training our networks running on Windows 10 system.

#### **2.4 Post-processing**

In this step, the output labels from semantic segmentation network were converted into image masks. Later these masks were applied to the original images in order to suppress the background noise by using bitwise operation and finally converting the output images to a white background. Since most of the herbarium images contain dark color dried leaves, hence changing to a white background helped to improve the network performance.

## 2.5 Performance Evaluation

Different studies have proposed numerous metric for evaluation of semantic segmentation models [6]. One metric which is commonly used along other metrics is the Intersection over Union (IoU). This metric quantifies the percentage overlap between the target label and the predicted label for each class and also provides a global mean scores (MIoU) by averaging IoU of all classes. MIoU calculates the ratio of true positives over the sum of true positive, false positive and false negative. Equation 1 shows how MIoU is calculated.

$$MIoU = \frac{1}{N} \sum_{x=1}^N \frac{N_{xx}}{\sum_{y=1}^N N_{xy} + \sum_{y=1}^N N_{yx} - N_{xx}} \quad (1)$$

Where  $N$  is the total number of classes,  $N_{xx}$  is the true positives pixels,  $N_{xy}$  is the false positive pixels and  $N_{yx}$  is the false negative pixels.

## 3 Results and Discussion

All deep learning models were trained on 315 images of the training set and evaluated on both validation and test set containing 40 images each. Several experiments were conducted with different hyperparameters setting and the best hyperparameters of the models were reported in section 2.3 on the network training subsection. The performances of the models were evaluated using various metrics as shown in Table 1. Both models performed well on validation and test sets with a MIoU of above 98% although FRRN-A performed slightly better with both validation and test MIoU above 99%. It was also be observe that in terms of pixel-wise accuracy of both classes, FRRN-A also outperformed DeepLabv3+ model for both validation and test sets.

From figure 4 and 5, both loss curves show a gradual decrease in loss and increase in both MIoU and accuracy as the training progress. This behavior is observed until epoch 80 where no further significant improvement (flatness) is observed for both loss, accuracy and MIoU curves which indicate the convergence of our networks. Another observation to be noted is that, the loss, accuracy and MIoU plots of the FRRN-A are not as smooth as for the DeepLabv3+ model, even though for both models the same learning rate was used. For example, this behavior can be noticed between epochs 20 and 40 where there is a jagged behavior for both classification accuracy and MIoU for FRRN-A (figure 5) which is not the case for the DeepLabv3+. This behavior maybe attributed by the random weight initialization used in training the FRRN-A model. Nevertheless, the performance of the FRRN-A model progressively improved and eventually produced better results.

Figures 6 and 7 show a sample output of the predicted labels by the models versus the ground truth labels from the test data set. These results show that most of the specimen's leaves were correctly segmented by both models. The difference of the two models can be observed on specimen's stem in which case the output of the FRRN-A model is slightly better than the DeepLabv3+ output.

In general, the predicted labels and ground truth labels were almost identical which indicates that these models have learned the visual features of the herbarium specimens as expected and ignored any other background noise.

**Table 1.** Deep Learning model's performance comparison

Evaluation Metrics	Validation set		Testing set	
	DeepLabv3+	FRRN-A	DeepLabv3+	FRRN-A
Specimen accuracy	98.8%	99.6%	98.4%	99.5%
Background accuracy	99.6%	99.7%	99.6%	99.7%
Average precision	99.5%	99.7%	99.3%	99.7%
Average Recall	99.5%	99.7%	99.3%	99.7%
Average F1-score	99.5%	99.7%	99.3%	99.7%
Mean IoU	98.6%	99.3%	98.1%	99.2%

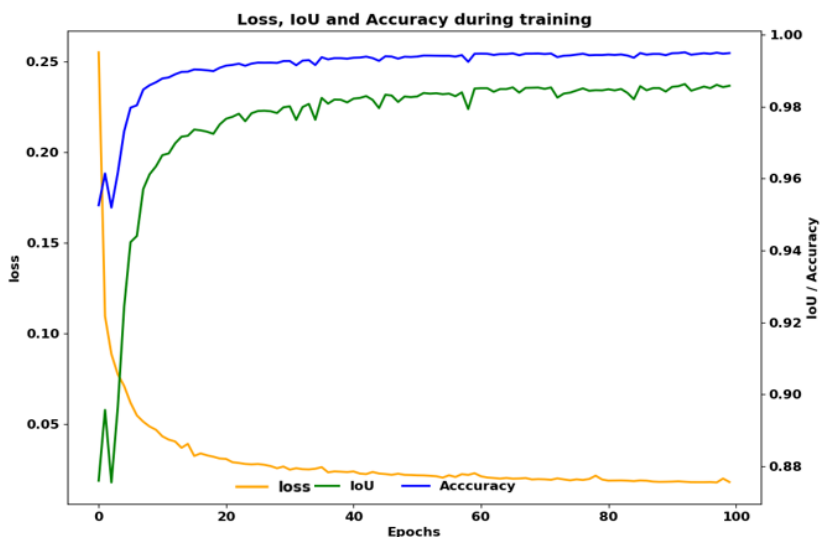


**Fig. 4.** Loss, IoU and Accuracy during training for DeepLabv3+ model

Although the dataset used in this study was small in relation to the most of the deep learning architectures, both models were still able to achieve a very good performance. The effectiveness of the DeepLabv3+ in term of parameters and computational efficiency was observed as the network trained much faster and with larger batch size than FRRN-A. This study therefore shows the feasibility of applying this technique as a pre-processing step in removing background noise from herbarium images for building plant species identification systems.

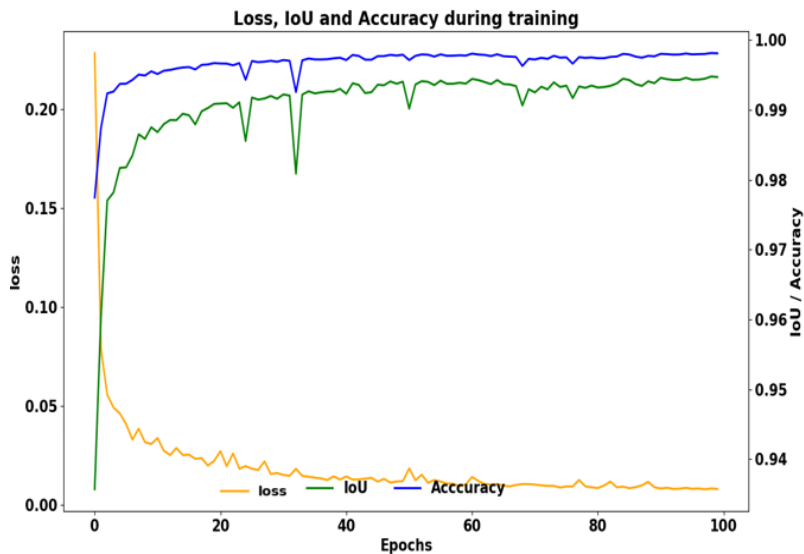


**Fig. 5.** Loss, IoU and Accuracy during training for FRRN-A model

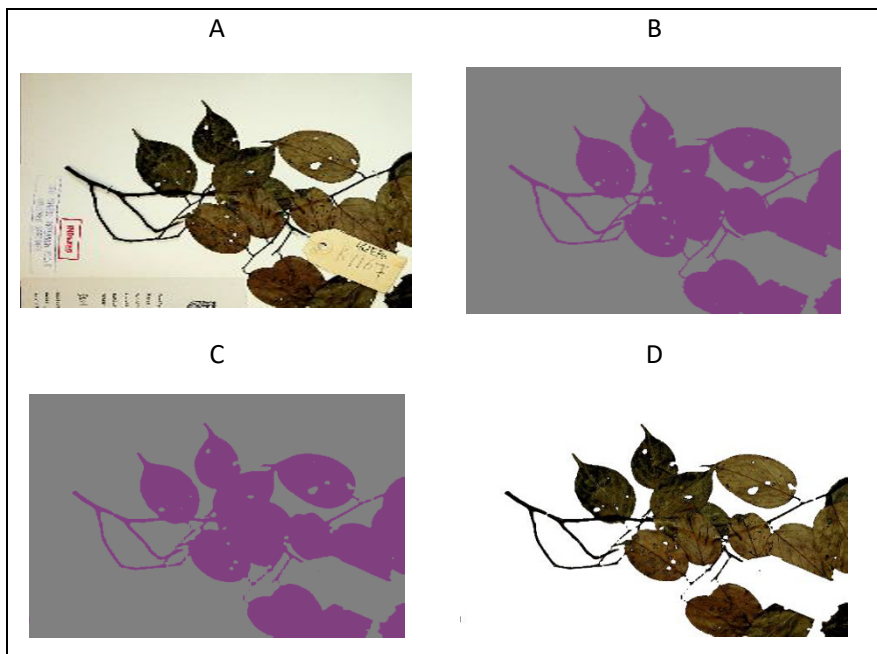


**Fig. 6.** Sample of the test set using DeepLabv3+ model, (A) Original images, (B) Annotated label, (C) Predicted label, (D) Output image after masking with the predicted label.

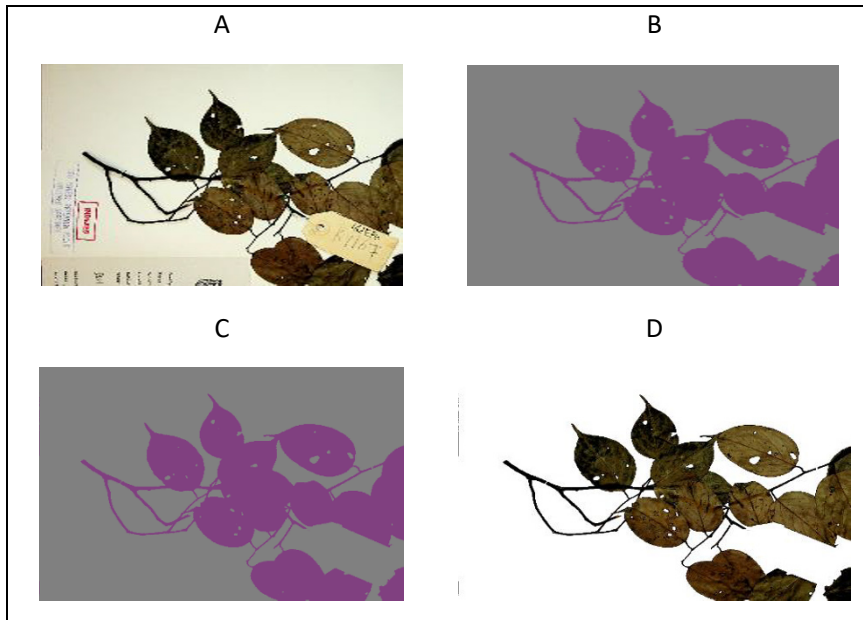


**Fig. 7.** Sample of the test set using FRRN-A model, (A) Original images, (B) Annotated label, (C) Predicted label, (D) Output image after masking with the predicted label.

#### 4 Conclusions and Future Work

In this study we proposed a method of using deep learning semantic segmentation models for removing background noise in herbarium images as a pre-processing step before applying classification models. Both of the applied models achieved a MIoU above 98% on test set. The proposed solution is more effective than the current practice of image cropping as none of the specimen is discarded hence making a full utilization of the current available herbarium collections. With this solution, the same herbarium image can be cropped at different location since none of the background noise exist and use these cropped images for training different classification models. We also showed that these models can achieve good performance even when trained on a smaller dataset although this is not usually the case for most of deep learning tasks as it may depend on the problem at hand. On the other hand, this approach could prove more robust in cases where thresholding methods struggle due to complex visual noise that may exist in the images. In future we intend to extend this work by utilizing our proposed method in building herbarium species identification system.

## Acknowledgement

We acknowledge Universiti Brunei Darussalam for sponsoring this research under the research grant UBD/RSCN/1.4/FICBF(b)/2018/011.

## References

1. J. Wäldchen, M. Rzanny, M. Seeland, and P. Mäder, “Automated plant species identification—Trends and future directions,” *PLoS Comput. Biol.*, vol. 14, no. 4, pp. 1–19, 2018.
2. M. Rzanny, M. Seeland, J. Wäldchen, and P. Mäder, “Acquiring and preprocessing leaf images for automated plant identification: Understanding the tradeoff between effort and information gain,” *Plant Methods*, vol. 13, no. 1, pp. 1–11, 2017.
3. A. Taneja, P. Ranjan, and A. Ujjlayan, “A performance study of image segmentation techniques,” *2015 4th Int. Conf. Reliab. Infocom Technol. Optim. Trends Futur. Dir. ICRITO 2015*, pp. 1–6, 2015.
4. D. Corney, J. Y. Clark, H. L. Tang, and P. Wilkin, “Automatic extraction of leaf characters from herbarium specimens,” *Taxon*, vol. 61, no. 1, pp. 231–244, 2012.
5. J. Carranza-Rojas, H. Goeau, P. Bonnet, E. Mata-Montero, and A. Joly, “Going deeper in the automated identification of Herbarium specimens,” *BMC Evol. Biol.*, vol. 17, no. 1, p. 181, 2017.
6. F. Lateef and Y. Ruichek, “Survey on Semantic Segmentation using Deep Learning Techniques,” *Neurocomputing*, 2019.
7. S. Younis *et al.*, “Taxon and trait recognition from digitized herbarium specimens using deep convolutional neural networks,” *Bot. Lett.*, vol. 165, no. 3–4, pp. 377–383, 2018.
8. G. Polgar, T. U. Grafe, H. Y. K. Pang, A. Brahim, D. Cicuzza, and J. W. F. Slik, “The universiti Brunei darussalam biological collections: History, present assets, and future development,” *Raffles Bull. Zool.*, vol. 66, no. May, pp. 320–336, 2018.
9. C. Zhang, S. Bengio, M. Hardt, B. Recht, and O. Vinyals, “Understanding deep learning requires rethinking generalization,” 2016.
10. L. C. Chen, Y. Zhu, G. Papandreou, F. Schroff, and H. Adam, “Encoder-decoder with atrous separable convolution for semantic image segmentation,” *Lect. Notes Comput. Sci. (including Subser. Lect. Notes Artif. Intell. Lect. Notes Bioinformatics)*, vol. 11211 LNCS, pp. 833–851, 2018.
11. M. Everingham, S. M. A. Eslami, L. Van Gool, C. K. I. Williams, J. Winn, and A. Zisserman, “The pascal visual object classes challenge: A retrospective,” *Int. J. Comput. Vis.*, vol. 111, no. 1, pp. 98–136, 2015.
12. T. Pohlen, A. Hermans, M. Mathias, and B. Leibe, “Full-resolution residual networks for semantic segmentation in street scenes,” in *Proceedings of the IEEE Conference on Computer Vision and Pattern Recognition*, 2017, pp. 4151–4160.
13. J. Yosinski, J. Clune, Y. Bengio, and H. Lipson, “How transferable are features in deep neural networks?,” in *Advances in Neural Information Processing Systems 27*, Z. Ghahramani, M. Welling, C. Cortes, N. D. Lawrence, and K. Q. Weinberger, Eds. Curran Associates, Inc., 2014, pp. 3320–3328.
14. J. D. Dignam, P. L. Martin, B. S. Shastry, and R. G. Roeder, “TensorFlow: A System for Large-Scale Machine Learning,” *USENIX Symp. Oper. Syst. Des. Implement.*, vol. 101, no. C, pp. 582–598, 2016.



# Development of Variable Acoustic Soundwave for Fire Prevention

Maila R. Angeles<sup>1</sup>, Jonrey V. Rañada, Dennis C. Lopez, Jose Ross Antonio R. Apilado, Ma. Sharmaine L. Carlos, Francis John P. David, Hanna Joy R. Escario, Andrea Isabel P. Rolloda, Irish Claire L. Villanueva

College of Engineering, National University, Manila, Philippines  
mrangeles@national-u.edu.ph

**Abstract.** Abstract. Fire is one of the most fundamental issues known to man. It easily interacts and devours anything such as buildings, machineries, and establishments creating danger to life and properties. Fire is considered a threat thus fire protection companies continue to find solutions and means for effective techniques in controlling conflagration. Today, the traditional fire extinguisher has a lot of drawbacks because it leaves chemical residues in the area and can cause health problems such as skin allergy and eye irritations. Another method of extinguishing fire is using acoustic fire extinguisher. This study was conducted to eliminate fire by using a low frequency sound wave thereby eliminating any chemicals. Different experiments with frequency ranges between 14 – 90 Hz were conducted in this study. The revisions made were the range of frequency, and the wattage used in order to suppress a much larger fire as compare to the existing acoustic fire extinguisher. It has a built-in fire alarm that can automatically create a sound once the device detected the fire. The acceptability of the project is determined through testing and evaluation. The 4 and 3.8 on the evaluation result of the respondents show that the project was acceptable as an alternative device to extinguish the fire. The design is environment friendly and simple to operate, minors can use it in case of emergency.

**Keywords:** fire extinguisher, low frequency, acoustic wave, fire, vortex cannon.

## 1 Introduction

Fire safety is a big concern in most of the countries because it can cause heavy damage to their surroundings including humans by combustion, heat, smoke, and/or gas that produced from fire [1]. It is important that the government requires to install a fire extinguisher at home and in the industry [2]. It would be used as prevention if the size of the fire is minimal. The traditional fire extinguishers are divided into different types, based on different kinds of fires. All these types leave chemical residue to extinguish the fire which could harm to the person and the environment. This chemical with various health problems, particularly those persons suffering from pre-existing medical conditions and ailments [3]. Hence it is important that the user must be aware for the

potential health effects of chemical used in these devices. In the Philippines the fires and fire-related casualties are generally unstudied and seen to be continual problem [4]. Most of the times the fire exists because of faulty electrical wiring and neglected open flames. Also, there are hundreds of sky-high buildings or establishments developed using a variety of combustible materials producing concern in fire safety. Right now, some fire protection experts hypothesize that an ordinary person untrained in the operation of a fire extinguisher will not use the device effectively. Also, these same experts often speculate that, even if the untrained person chooses to operate the fire extinguisher, he or she would be unfit to do as such securely [5].

Because of this, the need for new fire extinguishing techniques is ideal. The recent study developed a new generation fire extinguisher that eliminates flames by playing a heavy bass. Excessive boost in the bass region will make the music sound boomy. Sounds travels at a specific speed and has properties of frequency and wavelength. The soundwave below 200 Hz are acoustic or bass. It has a great annoyance potential, and that some people seem to react adversely to even the levels just above their hearing threshold. The different sounds have different frequency and the human ear is most sensitive from the range of 20 Hz to 20 KHz. The frequency is cycled as the number of wave cycles that occur in one second. Contrasted with high frequencies, low frequencies propagate for long distances as shown in Figure 1. Low frequencies will also pass through walls and windows with little attenuation [6]. The speed of sound varies greatly depending upon the medium it is traveling through. This are mathematically related as:

$$\text{Velocity of sound} = \text{Frequency} * \text{Wavelength} \quad (1)$$

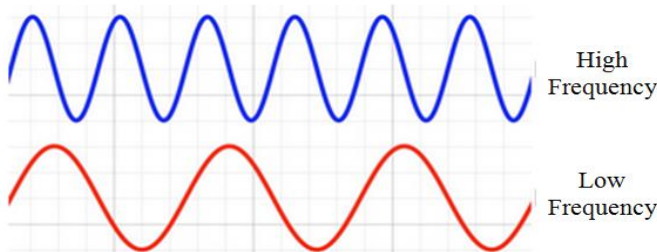


**Fig. 1.** Wavelength Comparison for High and Low Frequency

In year 2015 the Engineering students in Visvesvaraya Technological University, Belgaum was developed an acoustic sound wave device to prevent the fire. The existing study namely wave extinguisher uses the bass frequency in suppressing the flame [7]. The wave extinguisher has created using function generator and travel into amplifier that will use to boost the signal [8]. The pressure in the acoustic wave from the amplifier is compressed through the vortex cannon that serves as the pathway and this explain how the flames put off. As the pressure wave goes back and forth, it stimulates where the air is. That space is enough to keep the fire for reigniting.

The flame extinguishing during their testing was conducted to the 12 inches pan. There project can suppress the fire at a maximum distance of 14 inches with the frequency of 20 to 40 Hz. The result and the sample screenshot during their testing were shown in Figure 2 [9].

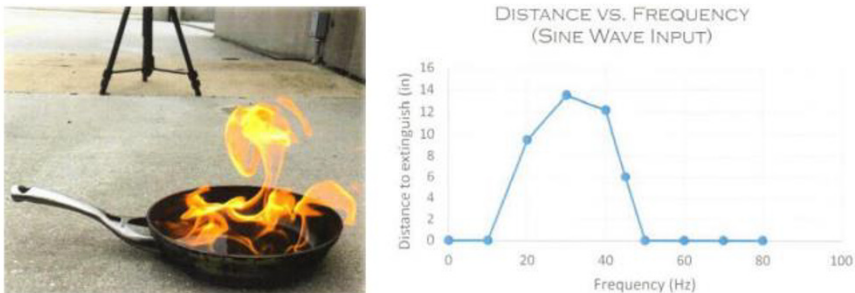
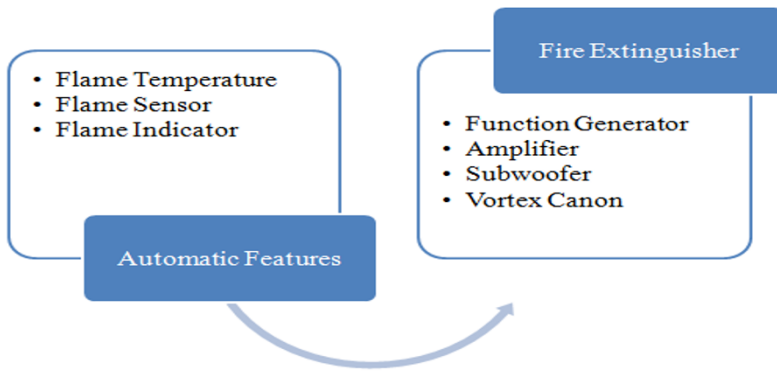


Fig. 2. Wave extinguishing sample screenshot for testing and result

This project is conceptualized after the wave extinguisher. The primary objective is to provide an alternative device to prevent the fire. It is eco-friendly because it uses a sound wave in preventing the fire. To make the advantage with the existing the large amount of wattage and a wider range of frequency from 14-90 Hz must be included on the design. The high wattage can douse a much larger fire while a much lower frequency can further the distance of prevention. Aside from that this project can set either automatic or manually operated. For automatic operation, the device has a built-in flame sensor which will run and produce sound waves once it detects the fire. To check the effectiveness of this project testing and evaluation were conducted. During the testing a large amount of fire and a much more distance of extinguishing has considered as compare to the existing.

## 2 Methodology

In order to conceptualize the development of this project that has shown in Figure 3, the two main components of the device were created. These are the project itself and the automatic features.



**Fig. 3.** The architecture of the project

The main components of the project are divided into four parts these are function generator, amplifier, subwoofer, and vortex cannon. First is the function generator the frequency of 14-90 Hz was considered. The below 20 Hz frequency also includes in order to check if it still extinguishes the fire. The output frequency from function generator produce a higher intensity soundwave and perform different function as compare to the other sounds or frequencies [10]. The signal from the frequency generator will be intensified to the amplifier. Then, the subwoofer, it will used convert the frequency into soundwave. The powerful 12 inches subwoofer was designed. The 12 inches device can produce a high-power bass due to its large cone that can suppress a wide area of fire.

Lastly is the vortex cannon that attached in the subwoofer, it will maximize the intensity of the signal and serve as a pathway for soundwave. In order to produce a sound proof material that compress the sound from subwoofer the vortex canon is made of insulation foam covered by cardboard [11] [12]. This will help to avoid any losses during propagation of sound wave. The size of this part is large enough for the sound to travel in a much longer distance. The insulation foam is much cheaper and easily to design as compare to the fiber glass.

The second part of the architecture design is the automatic features. These are flame sensor, flame indicator, and the liquid crystal display (LCD). The flame sensor detects the existence of fire together with the temperature. This temperature computes the velocity of sound waves once they sense the heat from fire, then the light indicator will turn on and the fire extinguisher will open automatically. The LCD is the guide of the user to know the velocity and the presence of fire. All of the features were developed using the Arduino software that has shown in Figure 4. The Arduino is a microcontroller that is used to join the components in one place [13]. This project took the advantage of this controller because it is less expensive, and the programming code is easy.

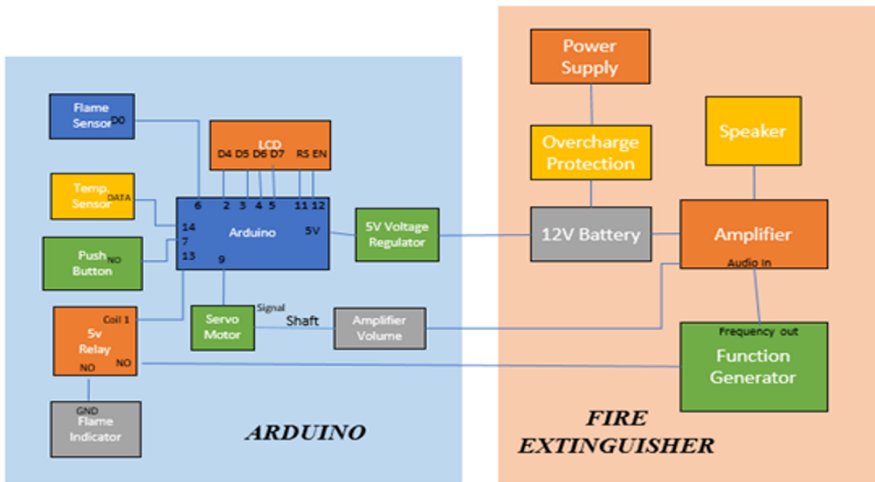


**Fig. 4.** Wiring assembly for automatic and main feature

Figure 4 shows the interconnection of each component to form an Acoustic Fire Extinguisher. This project was developed in electronic based therefore it needs a power supply as a source to operate the device. The rechargeable battery is use as a power source this idea was based from the charging concept of emergency light which is always unplug when it is needed.

For the main features the 12V rechargeable battery was used to supply the main part of the project. While for the automatic parts it needs a 5V regulator to supply the Arduino. The regulator is an electronic device that will stabilize the voltage to a desired value. On this part the regulator it will step down the voltage to 5V.

The Arduino was used to drive the different sensor in automatic part. The temperature sensor is for the measurement of ambient temperature through an electrical signal. While the flame sensor is for detecting the fire which also provides high signal upon the detection. The Arduino will now read the signal through 5V relay and provides alert by turning the flame indicator.

This project has the capability to produce a sound alarm in order to notify someone near the facility once it detects a fire. It can automatically extinguish the fire. The device will automatic produce a sound once the sensor detects a fire. The chances of preventing the fire depends on the size of fire and the distance of the device to the fire. If the person notice that it needed someone to extinguish the fire. The person will manually turn on the device and direct the extinguisher to the fire.

The evaluation and testing are also included on the study. The purpose of the evaluation is to know the satisfaction of the respondents in using this project while the testing is to check if this project can prevent a large amount of fire as compare to the wave extinguisher using much wider range of frequency.

### 3 Results and Discussion

The low frequency fire extinguisher was used on this project in order to prevent a startup fire from spreading without damaging the health or the surroundings. This project can operate either manual or automatic. The system design using bass frequency ranges from 14-90 Hz. These frequencies will amplify and transfer to a 12 inches subwoofer that attached before the vortex tube. The vortex canon is made up of insulation foam. In order to produce a sound proof material this foam was fitted neatly and covered by cardboard.

The project operates in a dc source that can be charged every time it will not be in use. The overcharge protection was also included that gives the battery a protection for excessive charging. When the device detects a fire the flame indicator will automatically light up and the frequency generator will start. The frequency generator will provide a fix or variable frequency with an LCD that displays the frequency selected. The user can also set the device into manual operation by turning on the switch.

The actual design of this project is shown in Figure 5. The researchers came up with this design because of the following reasons: First, for the ease of use of the user. Second the size of the vortex canon was considered in order to have a good quality of the sound compression. Third, the circuit enclosed using a fiber glass that can easily remove in order to troubleshoot the device just in case of malfunction.

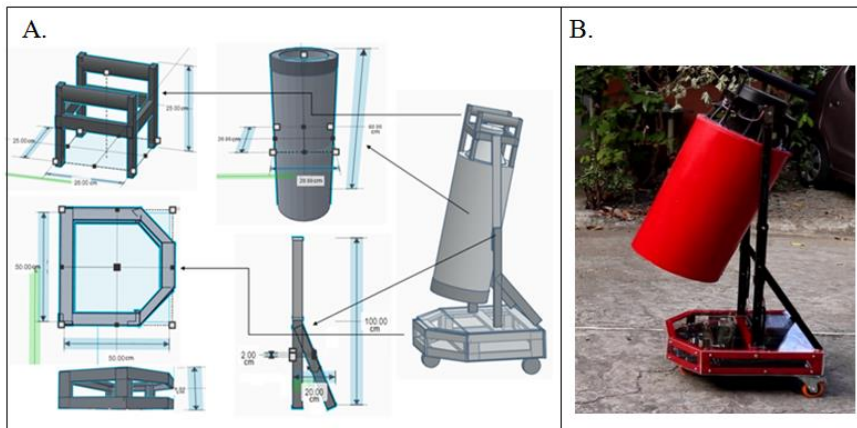


**Fig. 5.** Project design. (A) 3D , (B) actual layout

The acceptability of the project was determined to the evaluation result. The 48 respondents were involved on this part. The purpose of the evaluation is to check the quality of the project and the satisfaction of the respondents in using the project. Figure 6 shows the average rating scale of the respondents in terms of ease of use, adaptability and satisfaction. Based on the survey, the three parts got an above average rating. On which 3.83 for the adaptability and 4 for the ease of use and satisfaction.

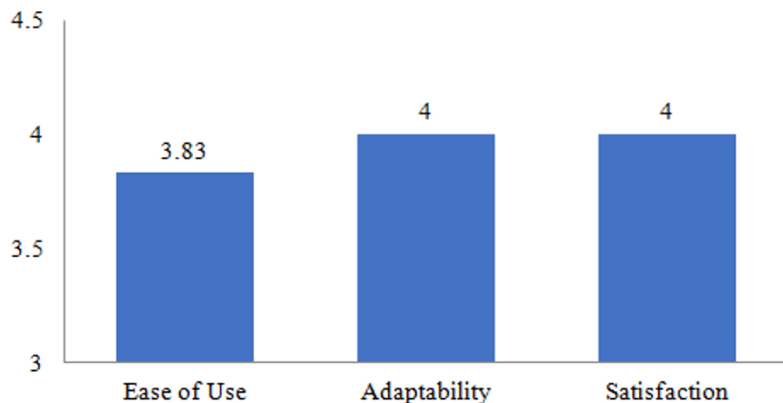


**Fig. 6.** Average rating scale of the respondents in ease of use, adaptability, and satisfaction for the project.

During the testing the flame that need to be extinguished was located at the 40 cm pan. It was assured that the amount of fire has been equal all throughout the testing. Based on the testing that has been made as shown in Figure 7, all the frequencies that were included in function generator from 14-90 Hz can extinguish the fire with the distance of 1.5 m from vortex canon to the flame. It was found out also that the 85Hz frequency is the most efficient frequency because it can extinguish the fire from minimal distance of 0.5 m up to maximum distance of 1.5 m within a shortest possible time.

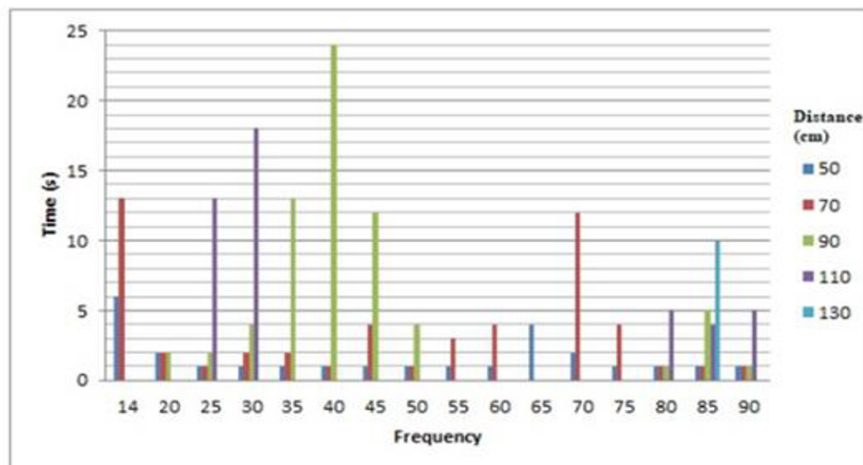


**Fig. 7.** Testing result for every frequency with respect different distance

## 4 Conclusions

The objective of this study is to provide an alternative way of preventing the fire. The objective was achieved through positive result of testing and evaluation and based on a comprehensive review of the existing study, comprehensive design of the project and development. It was successfully developed an acoustic wave fire extinguisher which is user-friendly and does not leave any residue or harmful chemicals in the blazing area. It can also prevent a large amount of fire as compare to the exiting with 16 inches fire diameter at a distance of 130 centimeters from fire extinguisher within 10 seconds using 85 Hertz frequency. The researchers recommend for further improvements in the design of the prototype. It is also recommended to implement the concept of low frequency fire extinguisher as a firewall.

## Acknowledgements

Foremost, we give our deepest sense of gratitude to the ECE faculty in National University for their guidance and support to make this project possible. We gratefully acknowledge Engineer Francisca Jayectin for proof reading our documents. Finally, we owe more than thanks to our family and friends, who contributed to our work with encouragement.

## References

1. Morgan, A. B., & Gilman, J. W. (2012). An overview of flame retardancy of polymeric materials: application, technology, and future directions. *Willey Online Library*, 37(4), 1.
2. Chan, E. Y., Yue, J., Lee, P., & Wang, S. S. (2016). Socio-demographic Predictors for Urban Community Disaster Health Risk Perception and Household Based Preparedness in a Chinese Urban City. *Public Library of Science*, 1.
3. Kelchner, L. (2017, July 27). *Health Risk of Exposure of Fire Extinguisher Chemicals*. Retrieved May 20, 2019, from <https://healthfully.com>
4. Velasco, G. N. V. (2013). *Epidemiological Assessment of Fires in the Philippines, 2010-2012*. Retrieved May 20, 2019, from <https://www.econstor.eu/handle/10419/126941>
5. Poole, B., Hicks, W. D., Notarianni, K. A., Hanks, C., Harris, R., & Gorbett, G. E. (2012). *Ordinary People and Effective Operation of Fire Extinguishers*. Retrieved March 28, 2018, from <https://www.femalifesafety.org>
6. Waye, K. P. (2011). Noise and Health - Effects of Low Frequency Noise and Vibrations: Environmental and Occupational Perspectives. *Elsevier*, 2, 240-253.
7. Sarji, A., Ramrk, M., & R, U. H. (2016). *Development of Portable Fire Extinguisher Using Acoustic Waves*. Karnataka State Council for Science and Technology (KSCST).
8. Ejiofor, O. S., & Ahanonu, S. C. (2015). Design and Construction of a 300 Watt Audio Amplifier. *International Journal of Emerging Multidisciplinary Research*, 5(6), 9-14.
9. Robertson, S., Tran, V., & Mark, B. (2015, 2015-2016). *Wave Extinguisher*. Retrieved June 3, 2019, from <https://ece.gmu.edu>
10. Sculthorpe, N., Herbert, P., & Grace, F. (2015). Low Frequency and High-Intensity Interval Training is an Effective Method to Improve Muscle Power in Lifelong Sedentary Aging Men: A Randomized Controlled Trial. *Journal of American Geriatrics Society*, 63(11).

11. Sculthorpe, N., Herbert, P., & Grace, F. (2015). Low Frequency and High-Intensity Interval Training is an Effective Method to Improve Muscle Power in Lifelong Sedentary Aging Men: A Randomized Controlled Trial. *Journal of American Geriatrics Society*, 63(11).
12. Perry, B., & Gee, K. L. (2014). The Acoustically Driven Vortex Canon. *The Physics Teacher*, 52(3), 1.
13. Mowad, M. A. E.-L., Fathy, A., & Hafez, A. (2014). Smart Home Automated Control System Using Android Application and Microcontroller. *International Journal of Scientific and Engineering Research*, 5(5), 935-939.



# Cryptoanalysis of Lightweight and anonymous three-factor authentication and access control protocol for real-time applications in wireless sensor networks

Jihyeon Ryu<sup>1</sup>, Youngsook Lee<sup>2</sup>, and Dongho Won<sup>3,\*</sup>

<sup>1</sup>Department of Platform Software, Sungkyunkwan University  
jhryu@security.re.kr

<sup>2</sup>Cyber Security, Howon University,  
ysooklee@howon.ac.kr

<sup>3</sup>Department of Computer Engineering, Sungkyunkwan University  
dhwon@security.re.kr

**Abstract.** Wireless sensor networks are used to monitor various environmental conditions such as temperature, sound, pollution level, humidity, wind and so on. Therefore, fast and secure authentication is important and requires a lightweight protocol that is secure. AmirHosein et al. proposed a 3-factor protocol in wireless sensor networks, but we found that the protocol in the wireless sensor network had some weaknesses. Firstly, it is a weakness in smart card deodorization. And it is also vulnerable to user impersonation. Moreover, it is possible to attack the session key. In this paper, we describe this weakness and prove AmirHosein et al.'s scheme is insecure.

**Keywords:** Remote user authentication · Wireless sensor network · Biometric

## 1 Introduction

Wireless sensor networks (WSNs) represent the communication between wireless sensors with various sensors and are one of the core technologies used in modern IoT. WSNs use many industrial and consumer applications such as temperature monitoring, environmental conditions like temperature, sound, pollution level, humidity, wind and so on.

The WSN consists of the following three elements: (1) User interface (2) Gateway node (*GW*) (3) Sensor node (*SN*). The user interface provides the user with an environment to access the *GW* and *SN*. The *GW* enables communication between the user *U* and the sensor node *SN*, and the *SN* measures the

---

\* Corresponding author.

physical environmental condition. WSN should provide users with fast speeds and simple protocols, and of course safety must also be satisfied. Accordingly, various types of user authentication paper have recently been proposed in the WSN [2–4].

Wong et al [6]. proposed a 2-factor user authentication scheme in a lightweight, dynamic hash-based WSN for the first time in 2006. However, this technique has problems such as Replay attack and forgery attack, so in 2007, Tseng et al. proposed a new authentication scheme that complements it [7]. However, this also has problems such as Replay attack and MITM attack, and Vaidya et al proposed a robust dynamic user authentication scheme [8]. This has the problem of DoS and forgery attack [9]. There have also been many user authentication papers on wireless sensor networks [10–14]. The Das model [15] was also a frequently cited 2-factor user authentication in WSN. However, the scheme of Das proposed a scheme of He et al [16]. and Khan et al [17]. due to the lack of mutual authentication and key exchange and vulnerability to impersonation attack. However, Kumar et al [18]. found that [16] is vulnerable to information leaking attacks, does not guarantee user anonymity, and [17] does not provide mutual authentication and does not guarantee the confidentiality of their messages.

In 2016, Gope et al [5]. propose a novel two-factor lightweight anonymous authentication protocol in WSN that uses a database to overcome the previous vulnerabilities. However, AmirHosein et al [1]. argue that their protocol is vulnerable to side-channel attacks because they are 2-factors, and session keys are also vulnerable. To overcome these drawbacks, in 2019, AmirHosein et al. proposed a new 3-factor authentication protocol in WSN. We confirmed that the scheme of AmirHosein et al. is still vulnerable.

The rest of the paper is summarized as follows. We provide some preliminary knowledge such as hash function, fuzzy extractor in section 2. In Section 3, we review AmirHosein et al.’s protocol of [1]. Moreover, we specify some vulnerabilities in AmirHosein et al.’s protocol [1] in section 4. At last, the conclusion is shown in Section 5.

## 2 Preliminary Knowledge

This section describes the basic knowledge of the hash function and contents of the fuzzy extractor used in AmirHosein et al.’s scheme [1].

### 2.1 Hash function

A hash function maps data of arbitrary length to fixed length data, and is useful for fast data retrieval and fast encryption. The hash function has the following three properties [19].

**preimage-resistance** When there is an output, it is computationally infeasible to find the input that hashes it. i.e. to find any preimage  $x'$  such that  $h(x') = y$  when given any  $y$  for which a corresponding input is not known.

**2nd-preimage resistance** It is computationally infeasible to find another input with the same output for a particular input. i.e. to find a 2nd-preimage  $x' \neq x$  such that  $h(x) = h(x')$ .

**collision resistance** It is computationally impossible to find two inputs with the same hashing result. i.e. any two distinct inputs  $x, x'$  which hash to the same output. such that  $h(x) = h(x')$

## 2.2 Fuzzy Extractor

Handling the user's biometric information should be very careful and accurate. However, the biometric information may not be recognized exactly the same. The fuzzy extractor uses error tolerances to solve this. Based on [20], the fuzzy extractor works in the following:

$$Gen(B) \rightarrow \langle x, y \rangle \quad (1)$$

$$Rep(B^*, y) = x \text{ if } B^* \text{ is information similar to } B \quad (2)$$

$B$  represents biometric information of the user, and  $B^*$  represents information similar to biometric information of the user.  $Gen$  is a probabilistic algorithm using biometric input  $B$ , and extracts string  $x \in \{0, 1\}^k$  and assistance string  $y \in \{0, 1\}^*$ .  $Rep$  is a deterministic algorithm that recovers  $\alpha$  from  $y$  and any vector  $B^*$  that is similar to  $B$ .

## 3 Review of the target protocol

This section describes AmirHosein et als's protocol [1]. The scheme consists of three phases as follows: registration, login, authentication, and password change. The notation for the target paper [1] is written in Table 1.

### 3.1 Registration Phase

In the registration phase, the user and gateway nodes in the private channel exchange secret information about the smart card. This allows confidential information to be stored in the database used by the smart card and gateway nodes when the user authenticates.

1. User  $U$  chooses his/her identity  $U_{id}$  and sends the registration request  $U_{id}$  and Personal credential to the gateway node  $GW$  in the secure channel.

**Table 1.** Notations used in AmirHosein et al. protocol.

Notations	Description
$U$	The user
$GW$	Gateway node
$SN$	Sensor node
$\mathcal{A}$	The malicious attacker
$U_{id}$	Identity of user
$U_{psw}$	Password of user
$U_b$	Biometric information of user
$AU_{id}$	Disposable identity of user
$SU_{id}$	Shadow identity of user
$GW_{id}$	Identity of gateway node
$SN_{id}$	Identity of the sensor node
$SC$	Smart card
$DB$	Database
$w$	Private key of gateway node
$APM$	A set of user $U$ 's access privilege masks
$G$	A set of user $U$ 's group ids
$KEM_{ug}$	Secret emergency key between user and gateway
$Sk_{ug}$	Secret key between user and gateway
$Sk_{gs}$	Secret key between gateway and sensor node
$SK$	Session key between user and sensor node
$Ts_{ug}$	Transaction sequence values
$h(\cdot)$	One-way hash function
$X \parallel Y$	Concatenate operation
$\oplus$	Bitwise XOR operation

2. The gateway node  $GW$  generates random number  $n_g$ , unique random number used to identify a particular access group  $G_j$ , random number user access privilege mask  $APM_j$  and random sequence number  $Ts_{ug}$ . After that group the created variables  $G = \{G_1, G_2, \dots\}$ ,  $APM = \{APM_1, APM_2, \dots\}$ . After obtaining the registration request from user  $U$ ,  $GW$  calculates  $Sk_{ug} = h(U_{id} \parallel n_g) \oplus GW_{id}$ ,  $sid_j = h(U_{id} \parallel r_j \parallel Sk_{ug})$ ,  $SU_{id} = \{sid_1, sid_2, \dots\}$ ,  $KEM_{ug} = h(U_{id} \parallel sid_j \parallel r'_j)$ ,  $G = \{G_1, G_2, \dots\}$  and  $APM = \{APM_1, APM_2, \dots\}$ . Also  $GW$  computes  $U_{id}^\# = U_{id} \oplus h(GW_{id} \parallel w \parallel Ts_{ug})$ ,  $Sk_{ug}^\# = Sk_{ug} \oplus h(GW_{id} \parallel U_{id} \parallel w)$ ,  $G_j^\# = G_j \oplus h(GW_{id} \parallel U_{id} \parallel w)$ ,  $APM_j^\# = APM_j \oplus h(GW_{id} \parallel U_{id} \parallel w)$ ,  $Sk_{gs}^\# = Sk_{gs} \oplus h(GW_{id} \parallel w \parallel SN_{id})$  and  $KEM_{ug}^\# = KEM_{ug} \oplus h(GW_{id} \parallel U_{id} \parallel w)$  using its secret key  $w$ . And save the data  $\langle Ts_{ug}, (SU_{id}, KEM_{ug}^\#), Sk_{ug}^\#, Sk_{gs}^\#, U_{id}^\#, G^\#, APM^\# \rangle$  in  $DB$ .  $GW$  sends  $\langle Sk_{ug}, (SU_{id}, KEM_{ug}), Ts_{ug}, G_U, h(\cdot) \rangle$  to user  $U$  in  $SC$ .
3. After user  $U$  takes  $SC$  from the  $GW$ , chooses his/her  $U_{id}$ , password  $U_{psw}$ , imprints the biometric  $U_b$  and then computes  $Gen(U_b) = (RS_U, P_U)$ ,  $Sk_{ug}^* = Sk_{ug} \oplus h(h(U_{id}) \oplus h(U_{psw}) \oplus h(RS_U))$ ,  $KEM_{ug}^* = KEM_{ug} \oplus h(h(U_{id}) \oplus h(U_{psw}) \oplus h(RS_U))$ ,  $SU_{id}^* = SU_{id} \oplus h(h(U_{id}) \oplus h(U_{psw}) \oplus h(RS_U))$ ,

$G^* = G \oplus h(h(U_{id}) \oplus h(U_{psw}) \oplus h(RS_U))$ ,  $f_U^* = h(h(Sk_{ug}) \oplus h(U_{id}) \oplus h(U_{psw}) \oplus h(RS_U))$ . And save the data  $\langle Sk_{ug}^*, f_U^*, (SU_{id}^*, KEM_{ug}^*), Ts_{ug}, G^*, P_U, Gen(\cdot), Rep(\cdot), h(\cdot) \rangle$  in  $SC$ .

### 3.2 Login Phase

The user enters his/her confidential information into the smart card and requests login in the login phase.

1.  $U$  inserts the smart card and enters  $U_{id}$ ,  $U_{psw}$  and  $U_b$ . The smart card computes  $RS_U = Rep(U_b, P_U)$ ,  $Sk_{ug} = Sk_{ug}^* \oplus h(h(U_{id}) \oplus h(U_{psw}) \oplus h(RS_U))$  and checks the condition  $f_U = h(h(Sk_{ug}) \oplus h(U_{psw}) \oplus h(U_{id}) \oplus h(RS_U)) \stackrel{?}{=} f_U^*$ . If it holds, the smart card ensures that the user successfully passes the verification process. Otherwise, this phase terminates immediately.
2. After verification successfully, user  $U$  generates random number  $N_u$  and computes  $N_x = Sk_{ug} \oplus N_u$ ,  $G = G^* \oplus h(h(U_{id}) \oplus h(U_{psw}) \oplus h(RS_U))$ ,  $AU_{id} = h(U_{id} \parallel Sk_{ug} \parallel N_u \parallel Ts_{ug})$ ,  $G'_j = G_j \oplus N_u$ ,  $V_1 = h(AU_{id} \parallel G'_j \parallel Sk_{ug} \parallel N_x \parallel SN_{id})$ . In case of loss of synchronization, user  $U$  selects one of the unused pair of  $(sid_j^*, KEM_{ug_j}^*)$  from  $(SU_{id}^*, KEM_{ug}^*)$  and surrenders his/her  $U_{id}$ ,  $U_{psw}$ ,  $RS_U$  and computes  $sid_j = sid_j^* \oplus h(h(U_{id}) \oplus h(U_{psw}) \oplus h(RS_U))$ ,  $KEM_{ug} = KEM_{ug}^* \oplus h(h(U_{id}) \oplus h(U_{psw}) \oplus h(RS_U))$ ,  $AU_{id} = sid_j$  and  $Sk_{ug} = KEM_{ug_j}$ .
3.  $U$  sends the login request messages  $M_{A_1} = \{AU_{id}, G'_j, N_x, Ts_{ug}(ifreq), SN_{id}, V_1\}$  to  $GW$ .

### 3.3 Authentication Phase

In the authentication phase, the gateway node verifies the user with the login message received from the user, and sends a new message containing the secret information to the sensor node. The sensor node and user share their keys and exchange secret information.

1. After receiving the login request messages  $M_{A_1}$  from user  $U$ , the  $GW$  first checks the validity of the transaction sequence number  $Ts_{ug}$ .  $GW$  computes  $N_u = Sk_{ug} \oplus N_x$  and  $G_j = G'_j \oplus N_u$ , and also computes  $h(GW_{id} \parallel U_{id} \parallel w) = G_j^\# \oplus G_j$ ,  $APM_j = APM_j^\# \oplus h(GW_{id} \parallel U_{id} \parallel w)$  that  $G_j^\#$  and  $APM_j^\#$  are in  $DB$ . After that,  $GW$  calculates  $AU_{id} = h(U_{id} \parallel Sk_{ug} \parallel N_u \parallel Ts_{ug})$ ,  $V_1 = h(AU_{id} \parallel G'_j \parallel Sk_{ug} \parallel N_x \parallel SN_{id})$  and checks if  $AU_{id}$  and  $V_1$  is valid. If successfully verification of  $AU_{id}$  then continue calculates. Otherwise,  $GW$  terminates the session.  $GW$  generates a session key  $SK$  and time stamp  $T$ , calculates  $SK' = h(Sk_{gs}) \oplus SK$ ,  $APM'_j = h(Sk_{gs}) \oplus APM_j$  and  $V_2 = h(AU_{id} \parallel APM'_j \parallel SK' \parallel T \parallel Sk_{gs})$ . Finally,  $GW$  sends the messages  $M_{A_2} = \{AU_{id}, APM'_j, SK', T, V_2\}$  to the sensor node  $SN$ .

2. Upon getting the message  $M_{A_2}$ ,  $SN$  checks  $T$  whether it is valid or not. If this does not hold,  $SN$  disconnects the session. Then  $SN$  also verifies  $V_2 \stackrel{?}{=} h(AU_{id} \parallel APM'_j \parallel SK' \parallel T \parallel Sk_{gs})$ . If it does not satisfy,  $SN$  disconnects also.  $SN$  computes  $APM_j = APM'_j \oplus h(Sk_{gs})$  and generates new time stamp  $T'$ .  $SN$  continues to calculate  $SK = h(Sk_{gs}) \oplus SK'$ ,  $V_3 = h(SK \parallel Sk_{gs} \parallel SN_{id} \parallel T')$ ,  $K_{gs_{new}} = h(Sk_{gs} \parallel SN_{id})$  and  $Sk_{gs} = K_{gs_{new}}$ . At last,  $SN$  transmits  $M_{A_3} = \{T', SN_{id}, V_3\}$  to  $GW$ .
3. The gateway node  $GW$  checks the time stamp  $T'$  and  $V_3 \stackrel{?}{=} h(SK \parallel Sk_{gs} \parallel SN_{id} \parallel T')$ . If not, it terminates the connection.  $GW$  generates a random number  $Ts_{ug_{new}}$  and calculates  $Ts = h(Sk_{ug} \parallel U_{id} \parallel N_U)$ ,  $SK'' = h(Sk_{ug} \parallel U_{id} \parallel N_U) \oplus SK$ ,  $V_4 = h(SK'' \parallel N_U \parallel Ts \parallel Sk_{ug})$ ,  $K_{ug_{new}} = h(Sk_{ug} \parallel U_{id} \parallel Ts_{ug_{new}})$ ,  $Sk_{ug} = K_{ug_{new}}$ ,  $K_{gs_{new}} = h(Sk_{gs} \parallel SN_{id})$  and updates  $Sk_{ug} = K_{ug_{new}}$  and  $Sk_{gs} = K_{gs_{new}}$ . If  $GW$  cannot get  $Ts_{ug}$  in  $M_{A_1}$ ,  $GW$  generates a random number  $K_{ug_{new}}$  and calculates  $x = h(U_{id} \parallel KEM_{ug_j}) \oplus K_{ug_{new}}$ . And then,  $GW$  updates  $Sk_{ug} = K_{ug_{new}}$  after that sends the messages  $M_{A_4} = \{SK'', Ts, V_4, x\}$  to the user  $U$ .
4. After user  $U$  obtains the message  $V_4 = h(SK'' \parallel N_U \parallel Ts \parallel Sk_{ug})$  checks its validity. If there is no abnormality, proceed to the next step or end it. And  $U$  computes  $SK = h(Sk_{ug} \parallel U_{id} \parallel N_U) \oplus SK''$ ,  $Ts_{ug_{new}} = h(Sk_{ug} \parallel U_{id} \parallel N_U) \oplus Ts$ ,  $K_{ug_{new}} = h(Sk_{ug} \parallel U_{id} \parallel Ts_{ug_{new}})$  and then updates  $Sk_{ug} = K_{ug_{new}}$  and  $Ts_{ug} = Ts_{ug_{new}}$ .
5.  $U$  and  $SN$  successfully shared  $SK$ . The  $SN$  responds user  $U$ 's query according to  $APM_j$  stored for user  $U$  using session key  $SK$ . Finally, at the end of this phase, the  $SN$  removes  $APM_j$  from storage due to security reasons.

### 3.4 Password and Biometrics Change Phase

Follow the steps below to change the user's password:

1.  $U$  puts his/her smart card into the terminal and inserts  $U_{id}$ , previous password  $U_{psw}$  and previous biometric  $U_b$ . And inputs the new password  $U_{psw}^*$ , new biometric  $U_b^*$ .
2. Smart card computes  $RS_U = Rep(U_b, P_U)$  and retrieve  $Sk_{ug}, KEM_{ug}, SU_{id}$ ,  $G$  and  $f_U$  as follows.  $Sk_{ug} = Sk_{ug}^* \oplus h(h(U_{id}) \oplus h(U_{psw}) \oplus h(RS_U))$ ,  $KEM_{ug} = KEM_{ug}^* \oplus h(h(U_{id}) \oplus h(U_{psw}) \oplus h(RS_U))$ ,  $SU_{id} = SU_{id}^* \oplus h(h(U_{id}) \oplus h(U_{psw}) \oplus h(RS_U))$ ,  $G = G \oplus h(h(U_{id}) \oplus h(U_{psw}) \oplus h(RS_U))$  and  $f_U = f_U^* \oplus h(h(Sk_{ug}) \oplus h(U_{psw}) \oplus h(U_{id}) \oplus h(RS_U))$ .
3. Smart card computes  $Gen(U_b^*)$ ,  $Sk_{ug}^{**}$ ,  $SU_{id}^{**}$ ,  $KEM_{ug}^{**}$ ,  $G^{**}$  and  $f_U^{**}$  as below.  $Gen(U_b^*) = (RS_U^*, P_U^*)$ ,  $Sk_{ug}^{**} = Sk_{ug} \oplus h(h(U_{id}) \oplus h(U_{psw}) \oplus h(RS_U^*))$ ,  $SU_{id}^{**} = SU_{id} \oplus h(h(U_{id}) \oplus h(U_{psw}) \oplus h(RS_U^*))$ ,  $KEM_{ug}^{**} = KEM_{ug} \oplus h(h(U_{id}) \oplus h(U_{psw}) \oplus h(RS_U^*))$ ,  $G^{**} = G \oplus h(h(U_{id}) \oplus h(U_{psw}) \oplus h(RS_U^*))$ ,  $f_U^{**} = h(h(Sk_{ug}) \oplus h(U_{psw}) \oplus h(U_{id}) \oplus h(RS_U^*))$ .
4. Finally, smart card will replace  $Sk_{ug}^*$  with  $Sk_{ug}^{**}$ ,  $SU_{id}^*$  with  $SU_{id}^{**}$ ,  $KEM_{ug}^*$  with  $KEM_{ug}^{**}$ ,  $G^*$  with  $G^{**}$ ,  $f_U^*$  with  $f_U^{**}$  and  $P_U$  with  $P_U^*$ .

## 4 Analysis of the target protocol

We prove that AmirHosein et al.'s protocol [1] has some security exposure in this section. The details are as follows.

### 4.1 Loss of Smart card information

Attacker  $\mathcal{A}$  can decrypt the information on the  $SC$  equally in the following two cases. First case is insider attack in the registration phase and the second case is loss of synchronize in the login phase. Insider attack is a stronger attack, but it can be considered when there is no case of loss of synchronize.

**Insider attack** In registration phase, Attacker  $\mathcal{A}$  extract the smart card  $SC$  when  $GW$  sends to  $U$ . He/she can get the  $SC$  information  $\{Sk_{ug}, SU_{id}, KEM_{ug}, Ts_{ug}, G, h(\cdot)\}$  that are not encrypted.

### Loss of synchronize

1. An attacker  $\mathcal{A}$  steals the  $U$ 's smart card  $SC$ , the inside information is  $\langle Sk_{ug}^*, f_u^*, (SU_{id}^*, KEM_{ug}^*), Ts_{ug}, G^*, P_U, Gen(\cdot), Rep(\cdot), h(\cdot) \rangle$ .
2. And in loss of synchronize case,  $\mathcal{A}$  can thus get user's login message  $M_{A_1} = \{AU_{id}, G'_j, N_x, Ts_{ug}(ifreq), SN_{id}, V_1\}$ .  $\mathcal{A}$  computes  $h(h(U_{id}) \oplus h(U_{psw}) \oplus h(RS_U)) = AU_{id} \oplus SU_{id}^*$ . The obtained information  $h(h(U_{id}) \oplus h(U_{psw}) \oplus h(RS_U))$  can be calculated  $Sk_{ug} = Sk_{ug}^* \oplus h(h(U_{id}) \oplus h(U_{psw}) \oplus h(RS_U))$ ,  $KEM_{ug} = KEM_{ug}^* \oplus h(h(U_{id}) \oplus h(U_{psw}) \oplus h(RS_U))$ ,  $G = G^* \oplus h(h(U_{id}) \oplus h(U_{psw}) \oplus h(RS_U))$ .

### 4.2 User Impersonation Attack

An attacker  $\mathcal{A}$  can make a user impersonation attack, and the victim is assumed to be  $U$ . The details are as follows.

1.  $\mathcal{A}$  generates random numbers  $N_{\mathcal{A}}$  and computes  $N_{x\mathcal{A}} = Sk_{ug} \oplus N_{\mathcal{A}}$ ,  $G'_{j\mathcal{A}} = G_j \oplus N_{\mathcal{A}}$ ,  $AID_{\mathcal{A}} = h(U_{id} \parallel Sk_{ug} \parallel N_{\mathcal{A}} \parallel Ts_{ug})$  and  $V_{1\mathcal{A}} = h(AU_{id} \parallel G'_{j\mathcal{A}} \parallel Sk_{ug} \parallel N_{\mathcal{A}} \parallel SN_{id})$  that  $Sk_{ug}$  and  $G_j$  obtained from stolen smart card attack.
2.  $\mathcal{A}$  transmits the login request  $M_{\mathcal{A}1} = \{AID_{\mathcal{A}}, G'_{j\mathcal{A}}, N_{x\mathcal{A}}, Ts_{ug}, SN_{id}, V_{1\mathcal{A}}\}$  to the gateway node  $GW$ .
3. After  $GW$  obtains the login request from the  $\mathcal{A}$ , first, verifies  $Ts_{ug}$  and calculates  $N_{\mathcal{A}} = Sk_{ug} \oplus N_{x\mathcal{A}}$ ,  $G_j = G'_{j\mathcal{A}} \oplus N_{\mathcal{A}}$  and  $h(GW_{id} \parallel U_{id} \parallel w) = G_j^\# \oplus G_j$ ,  $APM_j = APM_j^\# \oplus h(GW_{id} \parallel U_{id} \parallel w)$  that  $G_j^\#$  and  $APM_j^\#$  are in  $DB$ . And  $GW$  computes  $AID_{\mathcal{A}} = h(U_{id} \parallel Sk_{ug} \parallel N_{\mathcal{A}} \parallel Ts_{ug})$ ,  $V_{1\mathcal{A}} = h(AU_{id} \parallel G'_{j\mathcal{A}} \parallel Sk_{ug} \parallel N_{\mathcal{A}} \parallel SN_{id})$  and checks if  $AID_{\mathcal{A}}$  and  $V_1$  is valid.  $GW$  does not detect attackers. Unfortunately,  $GW$  still misunderstand to communicate with  $U$ .

As a result, the attacker  $\mathcal{A}$  will be verified as  $GW$  by user  $U$ . Therefore, the user impersonation attack is succeed.

### 4.3 Session Key Attack

Assume that Attacker  $\mathcal{A}$  has access to the  $DB$ . At this time, Attacker  $\mathcal{A}$  can extract the session key  $SK$  of user  $U$  and sensor node  $SN$  as follows.

1. Assume that the attacker  $\mathcal{A}$  can access to the database  $DB = \langle Ts_{ug}, (SU_{id}, KEM\#_{ug}), Sk_{ug}\#, Sk_{gs}\#, U_{id}^\#, G\#, APM\# \rangle$ . He/she will use the data  $Sk_{ug}\#$ .
2. Attacker  $\mathcal{A}$  calculates  $h(GW_{id} \parallel U_{id} \parallel w) = Sk_{ug} \oplus Sk_{ug}\#$ ,  $APM_j = APM_j^\# \oplus h(GW_{id} \parallel U_{id} \parallel w)$  and extract the message  $M_{\mathcal{A}_2} = \{AU_{id}, APM'_j, SK', T, V_2\}$ . And then,  $\mathcal{A}$  computes  $h(Sk_{gs}) = APM'_j \oplus APM_j$  and  $SK = h(Sk_{gs}) \oplus SK'$ . Now, attacker  $\mathcal{A}$  successfully seized the session key  $SK$ .

As a result, this result shows that AmirHosein et al.'s protocol does not satisfy session key.

## 5 Conclusions

In this paper, we revisited AmirHosein et al.'s three-factor user authentication protocol for wireless sensor networks, and pointed out that insider attack and loss of synchronize attack are possible in AmirHosein et al.'s protocol. The stolen smart card attack could be used to extract critical user's information. Consequently, It enables attacks on escape of session key and user impersonation attack. For these reasons, their protocol cannot assure the security of authentication. Finally, our further research would propose an improved user authentication protocol which can handle with these problems.

## Acknowledgements

This work was supported by the National Research Foundation of Korea(NRF) grant funded by the Korea government(MSIT) (No. 2019R1A2C1010159)

## References

1. Adavoudi-Jolfaei, A., Ashouri-Talouki, M., Aghili, S. F.: Lightweight and anonymous three-factor authentication and access control scheme for real-time applications in wireless sensor networks. *Peer-to-Peer Networking and Applications*, **12**(1), 43–59. (2019)
2. Gope, P., Das, A. K., Kumar, N., Cheng, Y.: Lightweight and Physically Secure Anonymous Mutual Authentication Protocol for Real-Time Data Access in Industrial Wireless Sensor Networks. *IEEE Transactions on Industrial Informatics*. (2019)
3. Li, X., Peng, J., Obaidat, M. S., Wu, F., Khan, M. K., Chen, C.: A Secure Three-Factor User Authentication Protocol With Forward Secrecy for Wireless Medical Sensor Network Systems. *IEEE Systems Journal*. (2019)

4. Rani, R., Kakkar, D., Kakkar, P., Raman, A.: Distance based enhanced threshold sensitive stable election routing protocol for heterogeneous wireless sensor network. In Computational Intelligence in Sensor Networks, Springer, Berlin, Heidelberg. 101–122. (2019)
5. Gope, P., Hwang, T.: A realistic lightweight anonymous authentication protocol for securing real-time application data access in wireless sensor networks. IEEE Transactions on industrial electronics, **63**(11), 7124–7132. (2016)
6. Wong, K. H., Zheng, Y., Cao, J., Wang, S.: A dynamic user authentication scheme for wireless sensor networks. In IEEE International Conference on Sensor Networks, Ubiquitous, and Trustworthy Computing (SUTC'06) **1**(8). (2006)
7. Tseng, H. R., Jan, R. H., Yang, W.: An improved dynamic user authentication scheme for wireless sensor networks. In IEEE GLOBECOM 2007-IEEE Global Telecommunications Conference. 986–990. (2007)
8. Vaidya, B., S Silva, J., Rodrigues, J. J.: Robust dynamic user authentication scheme for wireless sensor networks. In Proceedings of the 5th ACM symposium on QoS and security for wireless and mobile networks. 88–91. (2009)
9. Faye, Y., Niang, I., Guyennet, H.: A user authentication-based probabilistic risk approach for Wireless Sensor Networks. In 2012 International Conference on Selected Topics in Mobile and Wireless Networking. 124–129. (2012)
10. Ryu, J., Lee, H., Kim, H., Won, D.: Secure and Efficient Three-Factor Protocol for Wireless Sensor Networks. Sensors, **18**(12), 4481. (2018)
11. Moon, J., Lee, D., Lee, Y., Won, D.: Improving biometric-based authentication schemes with smart card revocation/reissue for wireless sensor networks. Sensors, **17**(5), 940. (2017)
12. Jung, J., Moon, J., Lee, D., Won, D.: Efficient and security enhanced anonymous authentication with key agreement scheme in wireless sensor networks. Sensors, **17**(3), 644. (2017)
13. Chung, Y., Choi, S., Lee, Y., Park, N., Won, D.: An enhanced lightweight anonymous authentication scheme for a scalable localization roaming service in wireless sensor networks. Sensors, **16**(10), 1653. (2016)
14. Nam, J., Choo, K. K. R., Han, S., Kim, M., Paik, J., Won, D.: Efficient and anonymous two-factor user authentication in wireless sensor networks: achieving user anonymity with lightweight sensor computation. Plos one, **10**(4), e0116709. (2015)
15. Das, M. L.: Two-factor user authentication in wireless sensor networks. IEEE transactions on wireless communications, **8**(3), 1086–1090. (2009)
16. He, D., Gao, Y., Chan, S., Chen, C., Bu, J.: An Enhanced Two-factor User Authentication Scheme in Wireless Sensor Networks. Ad hoc and sensor wireless networks. **10**(4), 361–371. (2010)
17. Khan, M. K., Alghathbar, K.: Cryptanalysis and security improvements of 'two-factor user authentication in wireless sensor networks'. Sensors. **10**(3), 2450–2459. (2010)
18. Kumar, P., Lee, H. J.: Cryptanalysis on two user authentication protocols using smart card for wireless sensor networks. In 2011 Wireless Advanced. 241–245. IEEE. (2011)
19. Katz, J., Menezes, A. J., Van Oorschot, P. C., Vanstone, S. A.: Handbook of applied cryptography. CRC press. (1996)
20. Dodis, Y., Reyzin, L., Smith, A.: Fuzzy extractors: How to generate strong keys from biometrics and other noisy data. In International conference on the theory and applications of cryptographic techniques. 523–540. Springer, Berlin, Heidelberg. (2004)



# Ultimate Confined Compressive Strength of Carbon Fiber-Reinforced Circular and Rectangular Concrete Column

Jason Ongpeng, Isabel Nicole Lecciones, Jasmine Anne Gardupe and Daniel Joshua Buera

Civil Engineering Department, De La Salle University, 2401 Taft Avenue, 0922 Manila, Philippines  
jason.ongpeng@dlsu.edu.ph

**Abstract.** Retrofitting circular and rectangular concrete columns with Carbon Fiber Reinforced Polymer (CFRP) has been proven to be a method of increasing the ultimate confined compressive strength  $f'_{cc}$ . The present study uses a hybrid of Analytic Hierarchy Process (AHP) and Backpropagation Artificial Neural Networks (BP) that assesses the strength performance of circular and rectangular columns confined with CFRP, steel ties and a hybrid method using both materials. The data used for the modeling came from available references in journal articles. The process of AHP was first used in determining the best set of independent parameters which are as follows: unconfined concrete strength  $f'_{co}$ , ultimate CFRP strength  $f_{CFRP}$ , volumetric ratio of CFRP  $\rho_{CFRP}$ , and steel transversal strength ( $f_s$ ). Additional independent parameters such as the diameter (D) and corner radius (r) were also included since these were found to have the highest significance on circular columns and rectangular columns, respectively. After utilizing AHP, BP was used as a tool for modeling the  $f'_{cc}$  as an output parameter. From this, two best models were produced for circular and rectangular columns out of twenty BP that were trained, validated and tested. These models were selected based on the Pearson's correlation coefficient (R) which performed better compared to previous existing models from past literature. The BP models attained were C\_5\_520\_5 for circular columns and NC\_5\_415\_6 for rectangular columns. Additionally, a parametric study of the BP models was done to determine the effect of the important input parameter  $f'_{co}$  with the output parameter  $f'_{cc}$ .

**Keywords:** Artificial Neural Network (ANN), Analytic Hierarchy Process (AHP), Carbon Fiber Reinforced Polymer (CFRP), Concrete.

## 1 Introduction

Over the years, retrofitting has been put into practice by civil engineers as it has been observed to enhance the performance of reinforced concrete on existing structures while also being sustainable and cost-effective. Oftentimes, retrofitting is the optimal

solution to restore minimal defects or pre-existing damages on these structures. In retrofitting columns, confinement is common and the purpose of it is to prevent concrete columns from expanding laterally. Back then, the idea of lateral pressure was adopted where transverse reinforcement would be used either on columns in the form of steel ties or by retrofitting these columns with steel tubes [11]. According to Oreta and Ongpeng [25], confining concrete is also called passive confinement because it is only useful when the concrete is subjected to lateral dilation, causing an increasing in volume. Due to the increasing demand of adopting advanced technology in the construction environment, simulation of the designs has been done to anticipate possible defects and analyze the behavior of the affected structures. The use of CFRP has proven its capability on strengthening different columns that have circular or rectangular cross-sections. Columns with circular cross-sections are the most common which could be seen in studies from Ongpeng [25] and Guler and Ashour [13] where CFRP were retrofitted. However, in most cases, circular columns are not constructed since it does not architecturally provide the optimal space for end users. Therefore, rectangular columns are mostly designed in construction. On that note, the focus of this study is to analyze the data obtained from previous studies in generating new models that would assess the capabilities of CFRP confinement, steel ties and hybrid of both steel ties and CFRP on circular and rectangular columns. A decision-making method, that is the AHP, would be used to determine the best set of data from the given parameters. Such method was utilized to lessen researchers' bias and to allow the consideration of other parameters commonly ignored that may have an actual contribution on the strength of columns. After which, a data processing system called the BP was adopted to determine the ultimate confined compressive strength of the concrete columns.

## 2 Methodology

Three phases were done to obtain the appropriate models for columns with circular and rectangular cross-sections as seen in Figure 1. In collecting the relevant data, careful selection, sorting and normalization were carried out. During the classification of data, AHP was utilized. Utilizing AHP allows the division of data into components in a decision hierarchy layout form. Analytic Hierarchy Process (AHP) ranks the top-most criteria down to the least important ones. This would lead to a more effective model since AHP minimizes the bias in selecting which parameters to be used. After which, BP was used in data analysis and modeling. This phase is where the best models were selected by comparing it to different models.

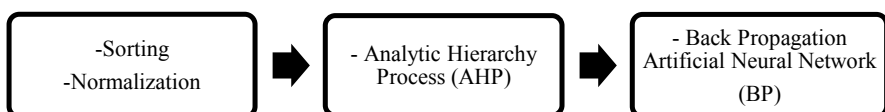


**Fig. 1.** Methodology of the study.

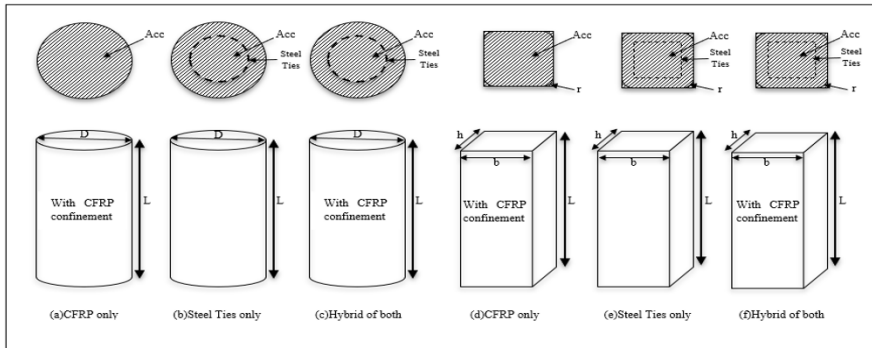


**Fig. 2.** Six Conditions (a and d) CFRP, (b and e) Steel Reinforcement, (c and f) Hybrid confinement.

Figure 2 shows three types of circular columns and three types of rectangular columns when it is subjected to different conditions - CFRP confinement, steel ties reinforcement and a combination of both. All the independent and dependent parameters are presented before proceeding with AHP. Eighteen independent parameters including the mechanical properties of the materials and geometric properties of the concrete were considered. The independent variables are as follows: cross-section diameter of concrete column,  $D$ , cross-section base of concrete column,  $b$ , cross-section height of concrete column,  $h$ , corner radius,  $r$ , length of concrete column,  $L$ , area of concrete core,  $A_{cc}$ , unconfined concrete strength,  $f'_{co}$ , number of layers,  $n$ , thickness of CFRP,  $t_{CFRP}$ , modulus of elasticity of CFRP,  $E_{CFRP}$ , ultimate jacket strength of CFRP,  $f_{CFRP}$ , maximum elongation of CFRP,  $\varepsilon_{CFRP}$ , volumetric ratio of CFRP,  $\rho_{CFRP}$ , diameter of steel ties,  $d_s$ , transversal strength of steel ties,  $f_s$ , modulus of elasticity of steel ties,  $E_s$ , number of steel ties,  $n_s$ , spacing between steel ties,  $s$ , and the dependent variable, confined concrete strength,  $f'_{cc}$ .

### 3 Results

Data collection was done by analyzing the data gathered from past studies where journals were related to CFRP and steel ties in reinforcing concrete columns were considered. The data collected should have a uniaxial compression test with no cyclic loading. Overall, a sum of 520 and 415 datasets were obtained for circular and rectangular columns, respectively. Table 1 shows the summary of references used in alphabetical order. The hierarchy was divided into three categories, namely, concrete specifications, CFRP, and steel, with different assigned weights. The weights were based on the fundamental scale from a study by Saaty (1987). In AHP, assigning the weights are subjective since it depends on the preference of the decision maker. The best set of input parameters generated after AHP process are those parameters with the highest weights/ranks as shown highlighted in Figure 3 and Figure 4.

The BP was done by splitting the normalized data into three, which are the training, testing and validation sets. In the present study, the researchers used a 70/15/15 rule where seventy (70) percent was used for the training set, fifteen (15) percent for testing set and the remaining fifteen (15) percent used for validation set. Twenty BP models were developed, ten for the circular columns and other ten for the rectangular columns. From the twenty, only two BP models were chosen as the best: one model for the circular columns and one for the rectangular columns. The variation of BP models had varying hidden nodes ranging from one (1) to ten (10). The resulted Mean Squared Error (MSE) and Regression (R) values were compared to select the best model. The MSE is defined as the average squared difference between outputs and targets while R-value measures the correlation between outputs and targets. The model with the MSE closest to zero and Regression R-value nearest to one were selected as the best model. For identification purposes, each BP model was notated as follows: first letter signified the cross-section of the columns where C represented circular columns while NC represented non-circular, or in this case, rectangular columns. An example of a BP model is the C\_5\_520\_5 that signifies that it is a circular column with five (5) input parameters considered and 520 data samples with five (5) hidden nodes.

The best BP models for circular and rectangular columns are C\_5\_520\_5 for circular columns with an ultimate confined compressive  $f'_{cc}$  as the target data, the R-value was 0.89182. For the rectangular columns with the ultimate confined compressive strength  $f'_{cc}$  as the target data, the BP model NC\_5\_415\_6 with six (6) hidden nodes was chosen to yield better results as it had the highest R-value and MSE value of 0.94533 and 0.00324, respectively. The transfer function for the hidden and output function for both models is shown as sigmoid and linear functions, respectively.

In comparing with existing models in Figure 5, the comparison of models did not consider the model by Mander, Priestley & Park [24] since the study only considered columns in cyclic loading. From the findings of the present study, the R-value of the developed model in this paper is higher than the analytical model by Mander, Priestley & Park [24] since it had a larger number of data considered. As shown in Figure 6, the graph had an R-squared value of 0.6494 thus giving an R-value of 0.8059. For the developed BP model, the R-squared value obtained was 0.8689 thus giving an R-value of 0.9321.

**Table 1.** Summary of Database of Circular Columns.

Researchers	No. of Data	D mm	L mm	Concrete		CFRP		Steel		
				f <sub>co</sub> MPa	f <sub>cc</sub> MPa	f MPa	ρ <sub>CFRP</sub> %	ds mm	f <sub>s</sub> MPa	s mm
[2] Aire, C., Casas, J., Gettu, R., & Marques, S. (2010)	8	150	150	42-69	46-217	3900	0.32-3.74	0	0	0
[5] Benzaid, R. & Mesbah, H. (2014)	18	160	320	26-63	26-100	450	2.50-7.50	0-8	0-235	0
[6] Benzaid, R., Mesbah, H., & Chikh, N. (2010)	18	160	320	26-63	40-101	4300	0.33-0.98	0-8	0-235	0-140
[8] Chastre, C. & Silva, M. (2010)	48	160	320	20-200	24-296	3200	0-3.30	0	0	0
[9] Chen, G., He, Y., Jiang, T. & Jin, C. (2016)	4	150	750	35	51	3339	0.89-1.34	0	0	0
[11] De Lorenzis, L., Micelli, F., & La Tegola, A. (2002)	44	150	300	33-44	55-97	2600-4025	0.29-0.88	0	0	0
[12] Elsanadedy, H., Al-Salloum, Y., Al-sayed, S. & Iqbal, R. (2011)	6	55-150	110-300	38-43	43-67	1028	1.00-1.20	0	0	0
[13] Guler, S. & Ashour, A. (2015)	12	50-150	100-300	41-54	76-146	846	2.66-8.00	0	0	0
[14] Huang et. al (2002)	4	100	200	159	169-235	3950	2.80-7.00	0	0	0
[15] Ilki, A., Peker, O., Karamuk, E., Demir, C., & Kumbasar, N. (2008)	3	200-300	600-900	27-31	27-31	0	0	0	0	0
[16] Issa, C., Chami, P., Saad, G. (2008)	18	250	500	9-27	9-94	0-3430	0-1.32	8	476	50-145
[17] Jiang, T. & Teng, J. (2007)	27	150	300	31	30-76	3450	0.34-1.02	0	0	0
[18] Karabinis, A. & Rousakis, T. (2002)	18	152	305	38-48	48-161	1908-3078	0.29-3.58	0	0	0
[20] Lam, L., Teng, J., Cheung, C. & Xiao, Y. (2006)	6	152	305	39-41	53-79	3754-3800	0.43-0.87	0	0	0
[21] Leuterio, C., Monzones, A., & Almeda, J. (2006)	6	177-179	497-501	27	34-53	4100	0.27-0.54	0	0	0
[22] Lim, J. & Ozbakkaloglu, T. (2014)	10	63	126	52-128	96-157	4370	0.71-1.41	0	0	0
[23] Lin, C.-T. & Li, Y.-F. (2003)	27	100-150	200-300	17-25	37-105	4170	0.29-1.32	0	0	0
[27] Ozbakkaloglu, T. & Vincent, T. (2013)	53	4-302	150-305	35-103	39-141	3800	0.31-1.85	0	0	0
[29] Pan, Y., Guo, R., Li, H., Tang, H., & Huang, J. (2017)	32	110	200	16-23	16-61	4412	0-0.81	0	0	0

[30] Park, T., Na, U., Chung L., & Feng, M. (2008)	16	150	300-600	21-27	28-41	2000	0.53-1.60	0	0	0
[34] Shehata, I., Carneiro L., Shehata, L. (2001)	6	150	300	26-30	26-72	3550	0-0.88	0	0	0
[36] Tamuzs, V., Valdmanis, V., Gylloft, K., & Tepfers, R. (2008)	18	150	300-1500	21-49	27-75	4500	0.91-1.81	0	0	0
[38] Theriault, M., Neale, K. & Claude, S. (2004)	5	51-304	102-1824	37	64-70	3481	0.87-1.29	0	0	0
[44] Zhou, J., Bi, F., Wang, Z. & Zhang, J. (2016)	69	70-310	140-620	22-28	22-127	3500	0-2.86	0	0	0
[45] Zhou, Y., Liu, X., Xing, F., Cui, H., & Sui, L. (2016)	27	150	300	13-41	13-87	3844.4	0-1.34	0	0	0
[46] Ziaadiny, H. & Abbasnia, R. (2013)	2	150	300	32-47	67-82	3943.5	0.94	0	0	0
<b>TOTAL</b>	<b>520</b>									

**Table 2.** Summary of Database of Rectangular Columns.

Researchers	No. of Data	b mm	h mm	r mm	L mm	Concrete		CFRP		Steel		
						f <sub>co</sub> MPa	f <sub>cc</sub> MPa	f <sub>CFRP</sub> MPa	ρ <sub>CFRP</sub> %	ds mm	fs MPa	s mm
[1] Al-Salloum, Y. (2006)	8	150	150	5-50	500	27-32	41-64	935	3.20	0	0	0
[3] Belouar, A., Laraba, A., Benzaid, R. & Chikh, N. (2013)	24	140	140	0	280-1000	25-70	25-82	4300	0-1.11	0-8	0-235	0
[4] Benzaid, R. & Mesbah, H. (2013)	78	140	140	0	100-560	24-64	24-80	450	0-8.57	0-8	0-235	0
[5] Benzaid, R. & Mesbah, H. (2014)	18	140	140	0	280	25-64	25-80	450	0-8.57	0-8	0-235	0
[10] Chen, L. & Ozbakkaloglu (2016)	16	113-150	150-225	10-20	300	39	32-65	4370	0-0.89	0	0	0
[14] Huang et. al (2002)	14	200-300	200-300	0	600-900	24-31	26-36	0	0	0-12.7	0-342	0-187
[15] Ilki, A., Peker, O., Karamuk, E., Demir, C., & Kumbasar, N. (2008)	37	150-250	250-300	10-40	500	10-30	10-60	0-3430	0-1.65	0-8	0-476	0-200
[19] Lam, L. & Teng, J.-G. (2003)	12	150	150-225	15-25	600	24-42	35-95	4519	0.44-2.20	0	0	0
[26] Ozbakkaloglu, T. (2013)	24	113-150	150-225	15-30	300	77-78	42-114	3800	1.87-3.12	0	0	0



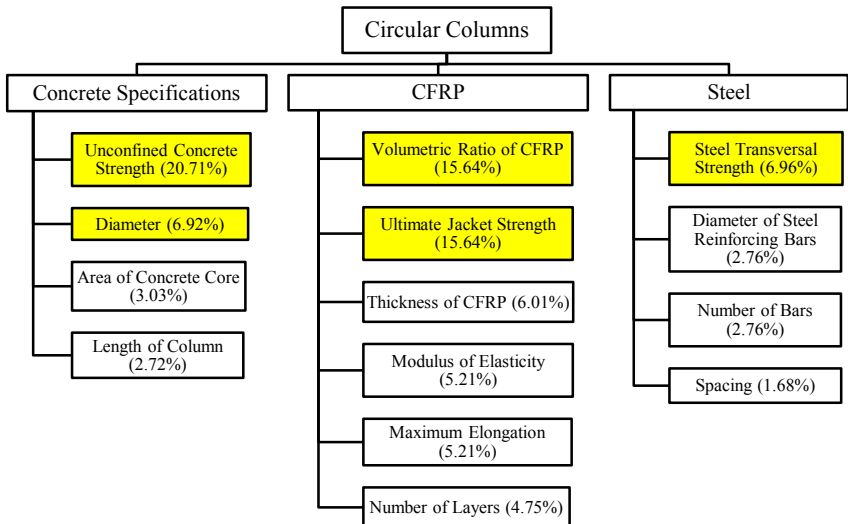


**Fig. 3.** Final Weights of Circular Columns.

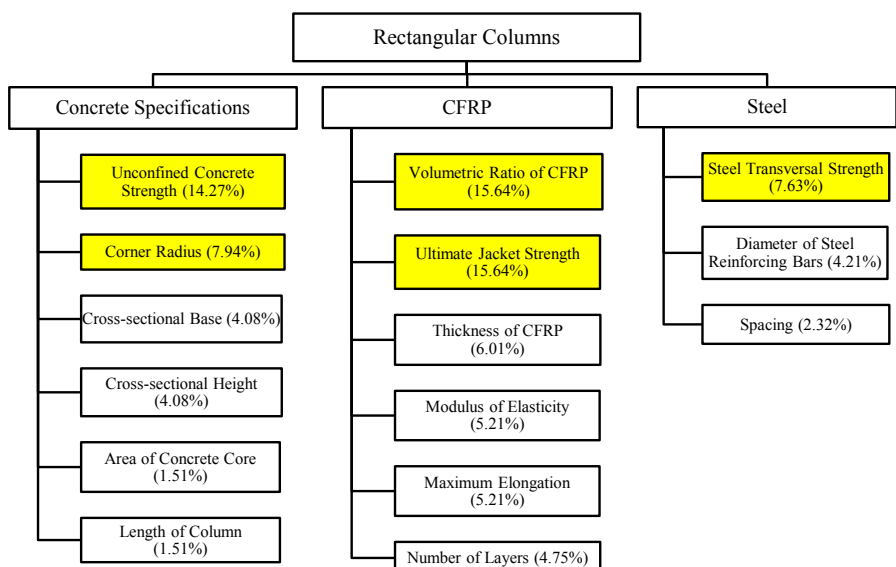


**Fig. 4.** Final Weights of Rectangular Columns.

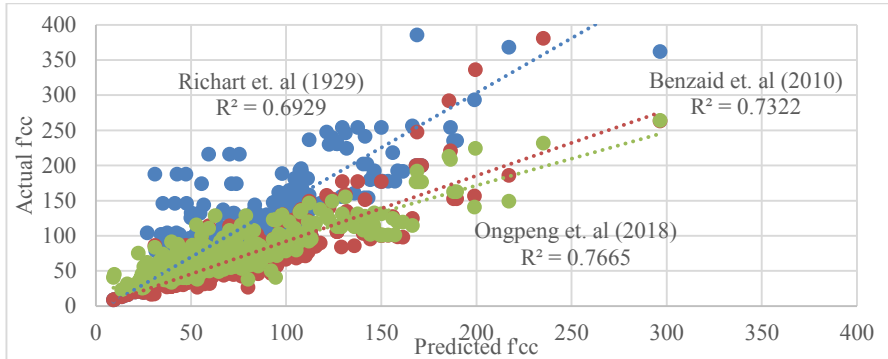


**Fig. 5.** Actual versus Predicted  $f_{cc}$  for circular columns.

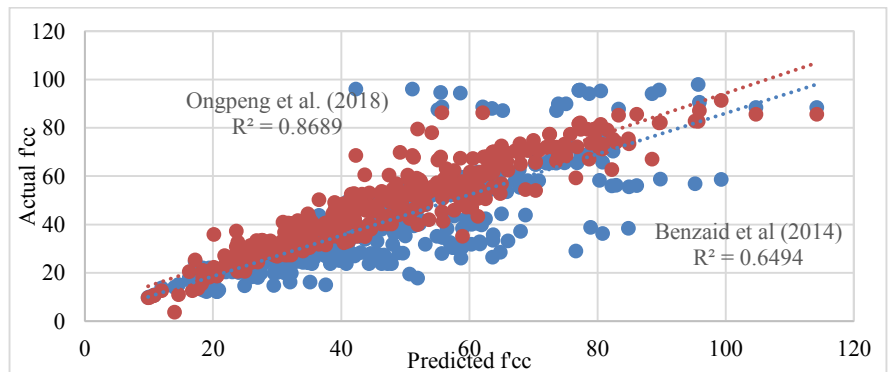


**Fig. 6.** Actual versus Predicted  $f'_{cc}$  for rectangular columns.

#### 4 Conclusions and Recommendations

Retrofitting circular and or rectangular columns have been essential for rural and urban areas where earthquakes are prone to occur. Data gathered from past journals related to CFRP and steel ties in reinforcing concrete columns were considered, where a total of 520 and 415 datasets were obtained for circular and rectangular columns, respectively. Through the Analytic Hierarchy Process (AHP), five input parameters that were proven to be significant that are: the unconfined  $f'_{co}$ , ultimate CFRP strength ( $f_{CFRP}$ ), volumetric ratio of CFRP ( $\rho_{CFRP}$ ), steel transversal strength ( $f_s$ ) and diameter ( $D$ ) for circular columns while corner radius ( $r$ ) for rectangular columns. The two best models using Backpropagation Artificial Neural Networks (BP) in predicting the ultimate confined compressive strength  $f'_{cc}$  were the C\_5\_520\_5 and NC\_5\_415\_6 for circular and rectangular column, respectively. Such models were proved better findings than the analytical models from past studies. Additionally, for model C\_5\_520\_5, the trend of

the parametric study showed significant increase in compressive strength compared to model NC\_5\_415\_6.

## References

1. Al-Salloum, Y. (2006). Influence of edge sharpness on the strength of square concrete columns confined with FRP composite laminates. Composites Part B: engineering, 38, 640-650.
2. Aire, C., Casas, J., Gettu, R., & Marques, S. (2010). Concrete laterally confined with fibrereinforced polymers (FRP) experimental study and theoretical model. Materiales de Construcción, 60(297), 19-31.
3. Belouar, A., Laraba, A., Benzaid, R. & Chikh, N. (2013). Structural performance of square concrete columns wrapped with CFRP sheets. Procedia Engineering, 54, 232-240.
4. Benzaid, R., & Mesbah, H. (2013). Strength model for square concrete columns confined by external CFRP sheets. Engineering Structures, 30, 1632-1646.
5. Benzaid, R., & Mesbah, H. (2014). The confinement of concrete in compression using CFRP composites – effective design equations. Journal of Civil Engineering and Management, 20(5), 632-648.
6. Benzaid, R., Mesbah, H., & Chikh, N. (2010). FRP-confined concrete cylinders: axial compression experiments and strength model. Journal of Reinforced Plastics and Composites, 29(16), 2469-2488.
7. Berthet, J., Ferrier, E., & Hamelin, P. (2004). Compressive behavior of concrete externally confined by composite jackets. part A: experimental study. Construction and Building Materials, 20, 338-347.
8. Chastre, C., & Silva, M. (2010). Monotonic axial behavior and modelling of RC circular columns confined with CFRP. Engineering Structures, 32, 2268-2277.
9. Chen, G., He, Y., Jiang, T., & Jin, C. (2016). Behavior of CFRP-confined recycled aggregate concrete under axial compression. Construction and Building Materials, 111, 85-97.
10. Chen, L., & Ozbakkaloglu, T. (2016). Corner strengthening of square and rectangular concrete filled FRP tubes. Engineering Structures, 117, 486-495.
11. De Lorenzis, L., Micelli, F., & La Tegola, A. (2002). Influence of specimen size and resin type on the behaviour of FRP-confined concrete cylinders. Advanced polymer composites for structural applications in construction, 231-239.
12. Elsanadedy, H., Al-Salloum, Y., Alsayed, S., & Iqbal, R. (2011). Experimental and numerical investigation of size effects in FRP-wrapped concrete columns. Construction and Building Materials, 29, 56-72.
13. Guler, S., & Ashour, A. (2015). Review of current design guidelines for circular FRP-wrapped plain concrete cylinders. Journal of Composites for Construction, 20(2), 1-20.
14. Huang et al. (2002). Axial load behavior of stiffened concrete-filled steel columns. Journal of Structural Engineering, 128(9), 1222-1230.
15. Ilki, A., Peker, O., Karamuk, E., Demir, C., & Kumbasar, N. (2008). FRP retrofit of low and medium strength circular and rectangular reinforced concrete columns. Journal of Materials in Civil Engineering, 20(2), 169-188.
16. Issa, C., Chami, P., & Saad, G. (2008). Compressive strength of concrete cylinders with variable widths CFRP wraps: Experimental study and numerical modeling. Construction and Building Materials. 23(6), 2306-2318.
17. Jiang, T., & Teng, J. (2007). Analysis-oriented stress-strain models for FRP-confined concrete. Engineering Structures, 29(11), 2968-2986.

18. Karabinis, A., & Rousakis, T. (2002). Concrete confined by FRP material: a plasticity approach. *Engineering Structures*, 24, 923–932.
19. Lam, L., & Teng, J.-G. (2003). Design-oriented stress-strain model for FRP-confined concrete in rectangular columns. *Journal of Reinforced Plastics and Composite*. 22(13), 1149-1186.
20. Lam, L., Teng, J., Cheung, C. & Xiao, Y. (2006). FRP-confined concrete under axial cyclic compression. *Cement and Concrete Composites*, 28(10), 949-958.
21. Leuterio, C., Monzones, A., & Almeda, J. (2006). Confinement effect of CFRP and/or steel ties in circular RC columns 35 MPa concrete strength (Undergraduate's thesis). De La Salle University, Manila, Philippines.
22. Lim, J., & Ozbakkaloglu, T. (2014). Investigation of the influence of the application path of confining pressure: tests on actively confined and FRP-confined concretes. *Journal of Structural Engineering*, 141(8), 1-12.
23. Lin, C.-T., & Li, Y.-F. (2003). An effective peak stress formula for concrete confined with carbon fiber reinforced plastics. *Canadian Journal of Civil Engineering*, 30(5), 882-889.
24. Mander, J., Priestley, M. & Park, R. (1988). Theoretical stress-strain model for confined concrete. *Journal of Structural Engineering*, 114(8), 1804-1826.
25. Ongpeng, J. (2006). Retrofitting RC circular columns using CFRP sheets as confinement. Paper presented at the Symposium on Infrastructure Development and the Environment 2006, University of the Philippines-Diliman, 7-8 December (pp. 1-20).
26. Ozbakkaloglu, T. (2013). Axial compressive behavior of square and rectangular high-strength concrete-filled FRP tubes. *Journal of Composites for Construction*, 17(1), 151-161.
27. Ozbakkaloglu, T., & Vincent, T. (2013). Axial compressive behavior of circular high-strength concrete-filled FRP tubes. *Journal of Composites for Construction*, 1-11.
28. Ozcan, O., Binici, B., & Ozcebe, G. (2007). Improving seismic performance of deficient reinforced concrete columns using carbon fiber-reinforced polymers. *Engineering Structures*, 30(6), 1632-1646.
29. Pan, Y., Guo, R., Li, H., Tang, H., & Huang, J. (2017). Analysis-oriented stress-strain model for FRP-confined concrete with preload. *Composite Structures*, 166, 57-67.
30. Park, T., Na, U., Chung L., & Feng, M. (2008). Compressive behavior of concrete cylinders confined by narrow strips of CFRP with spacing. *Composites Part B: Engineering*, 39(7-8), 1093-1103.
31. Richart, F., Brandtzaeg, A., & Brown, R. (1929). The failure of plain and spirally reinforced concrete in compression. *Illinois Engineering Experiment Station*, 26(31).
32. Rochette, P., & Labossiere, P. (2000). Axial testing of rectangular column models confined with composites. *Journal of Composites for Construction*, 4(3), 129-136.
33. Saaty, R. (1987). The Analytic hierarchy process—what it is and how it is used Mathematical Modelling, 9(3-5), 161-176.
34. Shehata, I., Carneiro L., Shehata, L. (2001). Strength of short concrete columns confined with CFRP sheets. *Materials and Structures*, 35(1), 50–58.
35. Sheikh, S., & Uzumeri, S. (1982). Analytical model for concrete confinement in tied columns. *Journal of the Structural Division*, 108, 2703-2722.
36. Tamuzs, V., Valdmanis, V., Gylltoft, K., & Tepfers, R. (2008). Stability analysis of CFRP-wrapped concrete columns strengthened with external longitudinal CFRP sheets. *Mechanics of Composite Materials*, 44(3), 199–208.
37. Tao, Z., Yu, Q., & Zhong, Y.-Z. (2008). Compressive behaviour of CFRP-confined rectangular concrete columns. *Magazine of Concrete Research*, 60(10), 735-745.

38. Theriault, M., Neale, K., & Claude, S. (2004). Fiber-reinforced polymer-confined circular concrete columns: investigation of size and slenderness effects. *Journal of Composites for Construction*, 8(4), 323-331.
39. Wang, D., Wang, Z., Smith, S., & Yu, T. (2016). Size effect on axial stress-strain behavior of CFRP-confined square concrete columns. *Construction and Building Materials* 118, 116-126.
40. Wang, L.-M., & Wu, Y.-U. (2007). Effect of corner radius on the performance of CFRP-confined square concrete columns: test. *Engineering Structures*, 30(2), 493-505.
41. Wang, Z., Wang, D., Smith, S. & Lu, D. (2012). CFRP-Confined square RC columns. I: experimental investigation. *Journal of Composites for Construction*, 16(2), 150-160.
42. Wu, Y.-F., & Wei, Y.-Y. (2009). Effect of cross-sectional aspect ratio on the strength of CFRP-confined rectangular concrete columns. *Engineering Structures*, 32(1), 32-45.
43. Yan, Z., & Pantelides, C. (2010). Concrete column shape modification with FRP shells and expansive cement concrete. *Construction and Building Materials*, 25(1), 396-405.
44. Zhou, J., Bi, F., Wang, Z. & Zhang, J. (2016). Experimental investigation of size effect on mechanical properties of carbon fiber reinforced polymer (CFRP) confined concrete circular specimens. *Construction and Building Materials*, 127, 643-652.
45. Zhou, Y., Liu, X., Xing, F., Cui, H., & Sui, L. (2016). Axial compressive behavior of FRP-confined lightweight aggregate concrete: an experimental study and stress-strain relation model. *Construction and Building Materials*, 119, 1-15.
46. Ziaadiny, H. & Abbasnia, R. (2013). Experimental investigation and strength modeling of CFRP-confined concrete rectangular prisms under axial monotonic compression. *Materials and Structures*, 48(1-2).



# Examining Machine Learning Techniques in Business News Headline Sentiment Analysis

Seong Liang Ooi Lim, Hooi Mei Lim, Eng Kee Tan, Tien-Ping Tan\*

School of Computer Sciences, Universiti Sains Malaysia, 11800 Penang, Malaysia  
tienping@usm.my

**Abstract.** Sentiment analysis is a natural language processing task that attempts to predict the opinion, feeling or view of a text. The interest in sentiment analysis has been rising due to the availability of a large amount of sentiment corpus and the enormous potential of sentiment analysis applications. This work attempts to evaluate different machine learning techniques in predicting the sentiment of the readers toward business news headlines. News articles report events that have happened in the world and expert opinions. These are factors that will affect market sentiment, and a headline can be considered as a summary of an article in a single sentence. In this study, we constructed a sentiment analysis corpus which consists of business news headlines. We examined two different approaches, namely text classification and recurrent neural network (RNN) in predicting the sentiment of a business news headline. For text classification approach, multi-layer perceptron (MLP) classifier, multinomial naïve Bayes, complement naïve Bayes and decision trees were experimented. On the other hand, for the RNN approach, we evaluated the typical RNN architecture and the encoder-decoder architecture in predicting the sentiment.

**Keywords:** sentimental analysis, text classification, recurrent neural networks, business/finance news.

## 1 Introduction

Sentiment analysis is a natural language processing (NLP) task that attempts to predict the opinion, feeling or view of a text. Thus, it is sometimes also referred to as opinion mining. The interest in sentiment analysis has been rising due to the availability of a large amount of sentiment corpus and the enormous potential of sentiment analysis applications, such as tracking the political inclination of the public [1], reviewing customer satisfaction toward a product or service [2], improving customer relationship management, and detecting the well-being of the people. Sentiment prediction is done by either assigning a category, such as positive, negative or neutral, or a value to a text.

Sentiment analysis can be performed at three different levels. Document-level sentiment analysis treats individual document such as a review post as a basic data unit to assign with a sentiment class. However, it does not work well with documents which contain comparisons of different items and aspects. Sentence-level sentiment analysis predicts the sentiment of sentences in a document, while aspect-/feature-/phrase-level

sentiment analysis works with even more granular data units, which are words or phrases that carry the opinion.

While many works related to sentiment analysis attempted to predict the sentiments of the authors, we are interested in analyzing the sentiments of the readers. See examples in Table 1. This work focuses on business/finance news headlines. A headline can be seen as the summary of an article in a sentence. Often, business news headlines also describe experts' opinion on a certain issue. Events that happen in the world and expert opinions are factors that will affect market sentiment. Market sentiment is the overall emotion of traders and investors toward a particular security or market. When the market sentiment is bullish/positive, stock prices may go up, and on the other hand, when the market sentiment is bearish/negative, the opposite is likely to happen. Thus, business news headlines are good indicators to predict the direction of the market.

**Table 1.** Examples of news headlines and their sentiment

Sentence	Sentiment
1. Palm oil may fall more into of 2,162-2,178 ringgit range	Negative
2. Genting Malaysia 's growth prospects still seen positive despite us setback	Positive
3. Wall Street extends rally, tech leads S&P, Nasdaq to record highs	Positive
4. Ecoworld aware of women 's influence in the workplace	Neutral

## 2 Sentimental Analysis

Sentiment analysis usually involves several essential steps, namely data collection, data pre-processing, feature extraction, feature selection, and sentiment classification. Data collection involves acquiring textual data from the relevant sources, which could be review websites, blogs, microblogs or datasets [3]. Web scraping can be used to collect these data which are later stored in the database. Some data are already annotated with sentiment information, such as text on hotel booking, product satisfaction, etc., but some collected data require manual annotation. Sentiment annotation can be carried out by assigning each text a sentiment class, which can be either positive, negative, neutral or conflict [3], or it can be assigned a value. Next, the raw data will be pre-processed using NLP techniques. Tokenization is employed to split up the texts into tokens by eliminating whitespaces and unwanted punctuations. Normalization is used to convert all the characters to lowercase or uppercase. Stemming extracts fixed parts of the words, while stop word removal removes common words such as "a", "an", "the", and etc.

Depending on the sentiment analysis approach used, feature extraction may or may not be applied. For machine learning approaches that use the bag-of-words model such as naïve Bayes, decision tree, and support vector machine (SVM), feature extraction is required. On the other hand, approaches that use artificial neural networks may not need to perform feature extraction, but word embedding. During feature extraction, potentially useful features such as term frequency, term co-occurrence such as n-grams, part of speech (POS) information, opinion words based on relevant lexicon and syntactic dependency are identified and extracted. Additional features used in [4] for aspect-

based sentiment analysis include Word-Aspect Association Lexicon which links opinion words to the aspects which they usually describe. Besides, negation words such as “not” and “never” must be considered so that words appearing in a negated context are not processed wrongly. The extracted features can be filtered through feature selection to reduce the size of the feature vector and thus enhance performance. Information gain, odd ratio, term frequency-inverse document frequency (TF-IDF) and POS can be used for feature weighting mechanisms. Moreover, ablation analysis can be conducted to find out which features contribute to the highest accuracy gains.

Once the features are obtained, sentiment modelling can be carried out using machine learning techniques. There are two types of machine learning: supervised and unsupervised. In supervised machine learning, the data must be annotated with the appropriate class. The most commonly used classifiers are naïve Bayes, SVM, and maximum entropy. Classification is done based on the selected features extracted from the text. The most commonly used features are: frequency of term, part of speech, and negation. Naïve Bayes shows better precision compared to the other classifiers [5].

On the other hand, deep learning approaches use multiple layers of processing units for modelling; lower layers learn simple features while higher layers will learn more complex features from features derived by lower layers. The most commonly used approaches in deep learning are convolutional neural network (CNN) and recurrent neural network (RNN) [5]. A neural network consists of 3 main layers, which are the input/embedding layer, hidden layer, and output layer. Word embedding layer is used to learn and capture the semantic and the relationship of words. It can be trained by using neural networks or matrix factorization. Then, the word vector will be input to the hidden layer for feature extraction and the output layer will have an activation function such as Softmax function for final classification. A very comprehensive study on deep neural networks in sentiment analysis was carried out by Zhang et al. [6].

There are also other sentiment modeling approaches that do not use machine learning technique. One approach uses a sentiment lexicon in predicting the sentiment of a text. Sentiment lexicon contains a list of words, each with a score that indicates the sentiment polarity. First, the scores of subjective words are summed up separately according to positive, negative, and neutral classes. The overall polarity of a text is determined by the class with the highest score. For example, if a text contains more positive words, then its polarity will be positive [3]. There are three methods to construct a sentiment lexicon: manual construction, dictionary-based approach, and corpus-based approach. Manual construction requires experts to manually create the lexicon which is very time-consuming. In a dictionary-based approach, first, a small set of opinion words known as the seed list is collected manually. It is used to search for their synonyms and antonyms to expand the lexicon. The new words will be added into the seed list and the iteration will continue until no new word is found. However, this approach has a limitation, i.e. it cannot search for opinion words in a domain-specific orientation. Finally, in a corpus-based approach, a seed list is expanded via the help of a corpus text. Thus, it can help to search for domain-specific and oriented opinion words.

The works on sentiment analysis in business/finance news focus on using domain knowledge in the analysis. Godbole et al. (2007) investigated sentiment lexicon construction and analysis on news and blog [7]. The sentiment lexicon was initialized

through a seed list of polarity words, followed by the expansion of the seed list through synonym and antonym using WordNet. On the other hand, Ruiz-Martínez et al. (2012) proposed financial sentiment annotation using ontological resources with natural language processing resources [8]. The financial ontology was manually created for stock market domain. The open-source software GATE was used to annotate the sentiment using sentiment gazetteers developed to mark up all sentiment words and associated entities in our ontology. Another approach based on financial ontology was proposed by Salas-Zárate et al. [9]. Different from the previous approach, the polarity of each feature was identified based on the position of it within the text, words around the feature, and SentiWordNet. The sentiment polarity of the document was calculated by summing up all the scores from the features.

### 3 Methodology

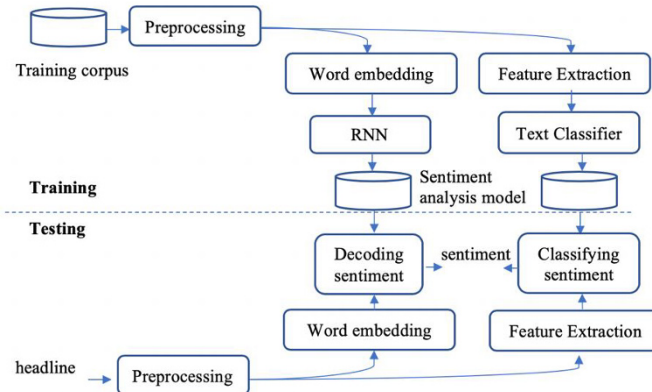


**Fig. 1.** Sentiment analysis steps

We examined two different types of approach for sentiment analysis: text classification approaches and recurrent neural networks (RNN). Both approaches went through similar preprocessing steps, but the text classification approaches required the text to be converted to a feature vector, while RNN required input in the form of word embedding vector before subsequent training/testing could be carried out. Fig. 1 shows the general process to perform sentiment analysis through machine learning.

Pre-processing was performed so that the relevant features could be extracted from the given texts. The preprocessing steps involved tokenization, part-of-speech (POS) tagging, lemmatization, stop words removal, and normalization. The tokenizer split each headline sentence into words using white spaces and punctuations as delimiters [10]. After tokenization, POS tagging of the tokens in each headline was optionally carried out for later use in lemmatization, which is an optional step that converts each token into its base word. This step helped to reduce the number of features by grouping similar words into the same base word form and ensured that the classifier generalizes better to other word forms which were not found in the training data but appeared in

the test data. Stop words were removed from the list of tokens, and normalization was performed by converting each token into lowercase, and numbers were converted to a tag using regular expressions.

Feature	No Lemmatisation					With Lemmatisation				
	a-g	...	malls	...	zwiipe	a-g	...	mall	...	zwiipe
Boolean Feature	⋮	⋮	⋮	⋮	⋮	⋮	⋮	⋮	⋮	⋮
	0	...	1	...	0	0	...	1	...	0
	⋮	⋮	⋮	⋮	⋮	⋮	⋮	⋮	⋮	⋮
	0	...	0	...	0	0	...	0	...	0
	a-g	...	malls	...	zwiipe	a-g	...	mall	...	zwiipe
Frequency	⋮	⋮	⋮	⋮	⋮	⋮	⋮	⋮	⋮	⋮
	0	...	2	...	0	0	...	2	...	0
	⋮	⋮	⋮	⋮	⋮	⋮	⋮	⋮	⋮	⋮
	0	...	0	...	0	0	...	0	...	0
	a-g	...	malls	...	zwiipe	a-g	...	mall	...	zwiipe
Probability	⋮	⋮	⋮	⋮	⋮	⋮	⋮	⋮	⋮	⋮
	0	...	0.154	...	0	0	...	0.154	...	0
	⋮	⋮	⋮	⋮	⋮	⋮	⋮	⋮	⋮	⋮
	0	...	0	...	0	0	...	0	...	0
	a-g	...	malls	...	zwiipe	a-g	...	mall	...	zwiipe

**Fig. 2.** Snippets of feature matrices generated by various combinations of pre-processor and feature vector

In the feature extraction step, the bag-of-words model was used to represent the news headlines by treating each of them as a collection of words or tokens. Before such feature vector could be built, the vocabulary used, which is the set of unique words or tokens which appear in the headlines, must be learned from the training data first. The size of the vocabulary determines the dimension of the feature vector used to represent each headline. Each value in the feature vector corresponds to a unique word in the vocabulary. The value can be a Boolean feature (indicating whether the word appears in the headline sentence), a frequency value (indicating how many times the word appears in the headline sentence) or a probability value (indicating the probability of occurrence of the word in headline sentence, i.e. the frequency of the word divided by the total number of words in the headline sentence). Fig 2 shows snippets of the feature matrices for text classification. Four types of text classification model were experimented, namely multilayer perceptron (MLP) classifier, naïve Bayes classifier, decision tree classifier and support vector machine (SVM) classifier. Two types of naïve Bayes classifier, namely multinomial naïve Bayes classifier and complement naïve Bayes classifier were used as they are known to be suitable models for text classification [11]. These models were trained by passing in the feature vectors of the training data as well as the corresponding target vector of sentiment values.

On the other hand, for RNN, each token in a sentence was converted to a word embedding vector instead of a feature vector. First, each word is converted into an integer index which represents its frequency in the training dataset. Then, the Embedding layer in RNN will compute its vector representation.

## 4 Experiment and discussion

We are interested in predicting the sentiment of readers on business news headlines. To construct the sentiment corpus, we collected the data from the Internet. We used a web crawler to collect news headlines from *The Edge Markets*, one of the leading business news websites in Malaysia that many investors and traders read. We collected 60,000 headlines from the year 2014 until 2018. We applied a crowdsourcing approach to annotate the headlines. Each annotator would annotate the headline as either positive, negative or neutral. A headline is annotated as positive if it describes a positive sentiment about a company, security or market, and vice versa. On the other hand, a headline is annotated as neutral if it is neither positive nor negative. We managed to annotate 22,000 headlines: 20,000 headlines for training, 1,000 headlines for development and another 1,000 headlines for testing. Table 2 shows the distribution of the data.

**Table 2.** Distribution of different sentiments in the training and testing data

Sentiment	Training Data		Development Data		Testing Data	
	Count	Percentage	Count	Percentage	Count	Percentage
Positive	8,901	44.5%	546	54.6%	439	43.9%
Neutral	6,838	34.2%	217	21.7%	305	30.5%
Negative	4,261	21.3%	237	23.7%	256	25.6%

Several libraries were used, including Natural Language Toolkit (NLTK) [10] for NLP tasks such as tokenization, POS tagging as well as lemmatization and Scikit-Learn [11] for text classification approaches. Table 3 shows the results from development set for each classifier based on the pre-processing and feature extraction steps used. Among them, multinomial naïve Bayes classifier yields the best accuracy of 66.6% when lemmatization is not applied and Boolean feature is used. In terms of accuracy, complement naïve Bayes classifier is as good as multinomial naïve Bayes classifier, followed by SVM classifier, while MLP classifier and decision tree classifier perform badly. It is worth noting that MLP classifier and decision tree classifier may generate different results when they are rerun as they incorporate some elements of randomness in their implementation, although their results are unlikely to differ much from time to time.

In general, the accuracy of the classifiers improves when lemmatization is applied. This shows that lemmatization is a useful step in ensuring that the trained model generalizes better to unseen data. In terms of features, Boolean and frequency features yield similar accuracies regardless of the type of classifier. This is probably due to their similar values as most tokens occur only once in a headline sentence. However, probability feature yields distinct results when they are used with different types of classifier. For instance, it yields the worst accuracy of 55.5% when it is used with MLP classifier. Also, multinomial naïve Bayes and SVM classifiers yield significantly lower accuracies when it is used, suggesting that it may not be suitable to be used with these classifiers. We selected the best model based on our development data result, the multinomial naïve Bayes classifier to evaluate the testing data. The classifier yields an accuracy of **63.8%**.

**Table 3.** Accuracy (development data) of text classification approaches using different types of features in sentiment analysis

Pre-Processing	No Lemmatization			With Lemmatization			
	Feature	Bool.	Freq.	Prob.	Bool.	Freq.	Prob.
MLP Classifier		58.2%	57.1%	<b>55.5%</b>	60.7%	57.8%	57.9%
Multinomial Naïve Bayes		<b>66.6%</b>	65.4%	60.1%	65.6%	65.2%	60.8%
Complement Naïve Bayes		65.9%	65.8%	65.7%	66.4%	65.6%	66.4%
Decision Tree		57.2%	58.1%	57.1%	59.8%	58.2%	57.0%
SVM		62.2%	62.7%	58.9%	64.4%	64.4%	60.1%

Several strategies were attempted to improve the accuracy of the classifiers. One of such strategies is feature selection, which reduces the number of features by retaining only a subset of features that have the best discriminatory ability. The scoring of the features is done through chi-squared ( $\chi^2$ ) test which determines the independence between each individual feature (token) and the sentiment class. Features that are not related to the sentiment class are removed from the feature vectors to improve the efficiency of the classifiers and hopefully their accuracy since the retained features are now more relevant and have better discriminatory ability.

For implementation, a built-in feature selector class in Scikit-Learn was used to select the  $k$  best features in terms of their  $\chi^2$  scores from the initial feature vectors. Consequently, the dimensions of the feature vectors were reduced from  $n \times 14,352$  (no lemmatization) and  $n \times 12,287$  (with lemmatization), where  $n$  is the number of headlines, to  $n \times k$ . Table 4 shows the results of applying  $k$ -best feature selection on the feature vectors before classification. Generally, the accuracies of multinomial and complement naïve Bayes classifiers gradually decrease as  $k$  decreases. This may be because as the number of features decreases, it becomes increasingly difficult for the classifiers to extract features from the given headlines. Nevertheless, complement naïve Bayes classifier achieves the highest accuracy of 66.8% when  $k = 6,000$ , and its corresponding accuracy from test set is **65.4%**, while MLP and SVM classifiers achieve particularly high accuracy when  $k$  is the lowest. This suggests that feature selection can still improve the accuracy of certain types of classifiers.

Another method of feature selection is to select only the tokens with document frequency above a certain threshold value. Document frequency refers to the number of documents (headline sentences) in which the token appears. This step helps to remove rare words that usually do not carry any sentiment information, and thus prevents the model from overfitting. Table 5 shows the results of applying minimum document frequency (min-DF) filter to the feature vectors before classification, which reduces the size of the feature vector to 8,200 (no lemmatization) and 6,983 (with lemmatization) respectively. Generally, applying minimum document frequency filter reduces the accuracy of all the classifiers, except MLP classifier whose accuracy increases slightly. Nevertheless, complement naïve Bayes classifier achieves the highest accuracy of 65.7% among all the models where minimum document frequency filter is applied. When evaluated using the testing data, this model yields an accuracy of **65.3%**.

**Table 4.** Accuracies (development data) of the classifiers using  $k$ -best feature selection

Classifier	$k$	No Lemmatization			With Lemmatization		
		Bool.	Freq.	Prob.	Bool.	Freq.	Prob.
MLP Classifier	All	58.2%	57.1%	55.5%	60.7%	57.8%	57.9%
	10,000	59.7%	57.9%	59.0%	60.8%	60.9%	59.6%
	6,000	55.8%	57.1%	57.7%	60.2%	59.0%	60.3%
	2,000	57.7%	60.7%	60.2%	58.5%	61.9%	59.1%
Multinomial Naïve Bayes	All	66.6%	65.4%	60.1%	65.6%	65.2%	60.8%
	10,000	66.5%	66.1%	59.9%	65.7%	65.4%	60.3%
	6,000	63.9%	63.9%	60.1%	64.7%	64.4%	61.1%
	2,000	63.0%	63.2%	60.1%	64.5%	64.1%	60.8%
Complement Naïve Bayes	All	65.9%	65.8%	65.7%	66.4%	65.6%	66.4%
	10,000	65.8%	64.9%	65.0%	66.6%	66.4%	65.8%
	6,000	63.6%	63.0%	64.3%	65.4%	65.3%	<b>66.8%</b>
	2,000	63.1%	63.7%	62.5%	64.3%	64.0%	64.4%
Decision Tree	All	57.2%	58.1%	57.1%	59.8%	58.2%	57.0%
	10,000	57.7%	57.1%	55.9%	55.8%	58.0%	59.5%
	6,000	58.0%	57.2%	55.9%	57.6%	58.1%	57.8%
	2,000	56.9%	56.8%	55.4%	57.0%	56.2%	55.5%
SVM	All	62.2%	62.7%	58.9%	64.4%	64.4%	60.1%
	10,000	63.1%	63.5%	58.4%	64.9%	64.6%	59.9%
	6,000	60.2%	60.8%	58.2%	64.4%	64.2%	59.2%
	2,000	64.0%	64.2%	57.7%	65.0%	66.0%	59.5%

**Table 5.** Accuracies (development data) of the classifiers using min-DF filter of 2

Classifier	Min-DF	No Lemmatization			With Lemmatization		
		Bool.	Freq.	Prob.	Bool.	Freq.	Prob.
MLP Classifier	None	58.2%	57.1%	55.5%	60.7%	57.8%	57.9%
	2	58.5%	58.1%	57.9%	60.0%	59.1%	58.3%
Multinomial Naïve Bayes	None	<b>66.6%</b>	65.4%	60.1%	65.6%	65.2%	60.8%
	2	64.7%	64.5%	61.2%	64.5%	64.2%	61.7%
Complement Naïve Bayes	None	65.9%	65.8%	65.7%	66.4%	65.6%	66.4%
	2	64.8%	64.5%	63.9%	65.1%	64.3%	<b>65.7%</b>
Decision Tree	None	57.2%	58.1%	57.1%	59.8%	58.2%	57.0%
	2	55.9%	58.8%	54.1%	59.0%	57.6%	57.6%
SVM	None	62.2%	62.7%	58.9%	64.4%	64.4%	60.1%
	2	62.3%	61.7%	58.7%	64.4%	64.1%	60.4%

For testing the recurrent neural networks approach, we used the same data for training, testing and development. We examined two types of RNN architecture. One using a typical RNN architecture, and another applied the encoder-decoder architecture [12]. In both the architectures, a specialized RNN cell, which is the long-short term memory (LSTM). The typical RNN architecture consists of 4 hidden layers of LSTM cell. The first, second, third and fourth layer consists of 128, 64, 32, and 16 states correspondingly. The Softmax activation method is used in output layer since this is a multiclass classification. We also tested the LSTM encoder-decoder architecture that is normally used for sequence-to-sequence modelling such as neural machine translation [13]. The encoder uses a bidirectional cells with attention. Both the encoder and decoder consists of one hidden layer, and 128 states. The output layer of the decoder is also using the Softmax activation method. The result is presented in Table 6. The result shows that the encoder-decoder architecture is slightly better than the typical RNN architecture in sentiment analysis. If we compare both the results of text classification approach and the RNN approach, we can see that the encoder-decoder approach is slightly better.

**Table 6.** Accuracies (test data) of RNN approaches

RNN	No Lemmatization	With Lemmatization
LSTM (4 layers)	63.9%	64.1%
Bidirectional LSTM encoder-decoder with attention	<b>66.9%</b>	-

## 5 Conclusion

In this work, we collected and annotated a sentiment analysis corpus that consists of business news headlines. We evaluated two different approaches, namely the text classification approach and recurrent neural networks in modelling and predicting the sentiments of headlines. In the text classification approach, we tested the MLP classifier, multinomial naïve Bayes, complement naïve Bayes and decision trees approaches. The complement naïve Bayes approach with k-best feature selection gave the highest accuracy at 65.4% on the test data using the feature vector that consists of lemma and probabilities. The recurrent neural network approach using bidirectional encoder-decoder architecture with attention on the other hand obtained an accuracy of 66.9%. Thus, in term of accuracy, the neural network approach has a slight lead. The second advantage of RNN approach is it does not need any intervention in feature selection. Thirdly, the syntactic information has been removed in the bag of word approach, but not in the RNN approach. Thus, we foresee if more annotated data is available, the RNN approach will perform even better. However, in term of time used for modeling and testing, the RNN approach took a longer time than the text classification approach even using GPU.

## Acknowledgement

This work is funded by Universiti Sains Malaysia through the Bridging grant scheme 304.PKOMP.6316283.

## References

1. Kušen, E., Strembeck, M.: Politics, sentiments, and misinformation: An analysis of the Twitter discussion on the 2016 Austrian Presidential Elections. *Online Social Networks and Media* 5: 37-50 (2018).
2. Miranda, M. D., José Sassi, R.: Using sentiment analysis to assess customer satisfaction in an online job search company. *Lecture Notes in Business Information Processing* 183: 17-27 Springer Cham (2014).
3. Kaushik A., Kaushik A., Naithani S.: A Study on Sentiment Analysis: Methods and Tools. *International Journal of Science and Research (IJSR)* 4, 287-292 (2015).
4. Kiritchenko S., Zhu, X., Cherry, C., Mohammad, S. M.: Detecting aspects and sentiment in customer reviews. In: 8th International Workshop on Semantic Evaluation (SemEval), pp. 437-442, ACL, Dublin (2014).
5. M. Alharbi, A. M., de Doncker, E.: Twitter sentiment analysis with a deep neural network: An enhanced approach using user behavioural information. *Cognitive Systems Research* 54, pp. 50-61 (2019).
6. Zhang, L., Wang, S., Liu, B.: Deep learning for sentiment analysis: A survey. *Wiley Interdisciplinary Reviews: Data Mining and Knowledge Discovery* (2018).
7. Godbole, N., Srinivasaiah M., and Skiena, S.: Large-scale sentiment analysis for news and blogs. In: ICWSM'2007, Boulder (2007).
8. Ruiz-Martínez, J. M., Valencia-García, R., García-Sánchez, F.: Semantic-based sentiment analysis in financial news. In: 1st International Workshop on Finance and Economics on the Semantic Web, pp. 38–51, Heraklion (2012).
9. Salas-Zárate, M. P., Valencia-García, R. Ruiz-Martínez, A., Colomo-Palacios, R.: Feature-based opinion mining in financial news: An ontology-driven approach. *Journal of Information Science* 43(4): 458-479 (2017).
10. Bird, S., Loper, E., Klein E.: Natural Language Processing with Python. O'Reilly Media Inc., Sebastopol (2009).
11. Pedregosa F., Gaël, V., Alexandre, G., Vincent, M., Bertrand, T., Olivier, G., Mathieu, B., Peter, P., Ron, W., Vincent, D., Jake, J., Alexandre, P., David, C., Matthieu, B., Matthieu, P., and Édouard, D.: Scikit-learn: Machine Learning in Python. *Journal of Machine Learning Research*: 12: 2825-2830 (2011).
12. Géron, A.: Hands-on machine learning with scikit-learn and tensorflow: concepts, tools, and techniques to build intelligent systems, O'Reilly Media, California (2017).
13. Bérard, Alexandre, Olivier Pietquin, Christophe Servan, and Laurent Besacier.: Listen and translate: A proof of concept for end-to-end speech-to-text translation. In: NIPS: pp. 1-5, Barcelona (2016).



# A 2×1 Microstrip Patch Array Rectenna with Harmonic Suppression Capability for Energy Harvesting Application

Nur ‘Aisyah Amir<sup>1</sup>, Shipun Anuar Hamzah<sup>1</sup>, Khairun Nidzam Ramli<sup>1</sup>, Shaharil Mohd Shah<sup>1</sup>, Mohamad Shamian Zainal<sup>1</sup>, Fauziahanim Che Seman<sup>1</sup>, Nazib Adon<sup>1</sup>, Mohamad Sukri Mustapa<sup>2</sup>, Mazlina Esa<sup>3</sup>, Nik Noordini Nik Abd Malik<sup>3</sup>

<sup>1</sup> Faculty of Electrical and Electronic Engineering, Universiti Tun Hussein Onn Malaysia, 864000 Parit Raja, Johore Malaysia

<sup>2</sup> Faculty of Mechanical and Manufacturing Engineering, Universiti Tun Hussein Onn Malaysia, 864000 Parit Raja, Johore Malaysia

<sup>3</sup> School of Electrical Engineering, Faculty of Engineering, Universiti Teknologi Malaysia, 813000 Johore Bahru, Johore Malaysia  
shipun@uthm.edu.my

**Abstract.** This paper presents a microstrip patch array rectenna for radio frequency (RF) energy harvesting at 2.45 GHz. The rectenna configuration consists of a 2×1 rectangular patches and seven stages Hillard voltage multiplier circuit, respectively. The antenna is designed to have high gain and able to capture the 2.45 GHz signal while the rectifier circuit is used to convert that RF signal into direct current (DC) power supply. The antenna is designed and simulated using the Computer Simulation Technology (CST) Microwave Studio software. The rectifier is designed and simulated using Advanced Design System (ADS) software. The antenna is fabricated and tested with measured gain of 5 dB is obtained. Then, the rectifier circuit prototype is measured and the results indicate that it can convert a signal into 2.5 V DC power supply. Finally, the integration of the array antenna and the rectifier circuit is performed which successfully produces 0.3 V power supply. The tested result in anechoic chamber verifies that the rectenna is able to capture and convert the 2.45 GHz signal into a DC power supply.

**Keywords:** Energy harvesting, 2x1 array rectenna, DC voltage

## 1 Introduction

Microstrip patch array rectenna has the potential to be applied as the radio frequency (RF) energy harvesting systems. The rectenna has the capability to capture the RF signal and converts it into a direct current (DC) output efficiently. The design includes an array antenna integrated with EBG-stubs filter and rectifier circuit that have been reported in [1]. References in [1-9] discuss the latest approach to implement array rectenna operates at 2.45 GHz for DC power supply application.

In [2], the authors proposed a rectenna by using a 2.45 GHz hexagonal  $2 \times 1$  patch array and a rectifier circuit. The antenna measured gain is 5 dBi while the total dimension is  $47.2 \times 45$  mm $^2$ . Two HSMS 2860 *Schottky* diodes, resistor and capacitor have been used in the rectifier circuit. The rectenna produced 0.4 V (from the simulation).

A  $4 \times 1$  patch array rectenna is presented in [3]. It used an antenna with a simulated gain of 11 dB. This rectenna configuration has no matching network since the ASI 3486 silicon Schottky diode is directly mounted at the feed point of the antenna. It generates 2.7 V of DC voltage when the input power is 20 dBm.

An innovative rectenna is published in [4]. It consists of a  $2 \times 1$  patch array with a simulated gain of 8.422 dBi. In their work, the authors studied two design of rectifier circuits namely, bridge rectifier and voltage doubler. In the first rectifier circuit, they employed a HSMS-8101 microwave Schottky diode while in the second circuit they used two HSMS-2852 zero bias Schottky detector diodes, respectively. The first rectenna produces 5 V of DC voltage and the second rectenna produces 2.91 V, respectively.

In [5], an array rectenna using 4-element of cascaded patch antenna operates at 2.45 GHz is proposed. The total dimension is  $200 \times 200$  mm $^2$ . The antenna measured gain is 13.4 dBi. The rectifier circuit used HSMS-282c diode. The rectenna successfully generates a DC voltage of 18.5 Volts.

One of the latest works on rectenna array design is presented in [6]. The authors proposed a  $3 \times 3$  patch array antenna with a high simulated gain of 9.14 dBi. In the rectifier circuit, they used a HSMS-2820 Schottky diode. The rectenna output is 7.02 V.

In [7], a good configuration rectenna is presented. The rectenna consists of a  $4 \times 1$  patch array antenna with a simulated gain of 10.85 dB. A 2-stage cascaded Cockcroft Walton multiplier with Schottky diodes HSMS-2820 is designed as a rectifier circuit. Finally, the rectenna output is 2.1 Volts with a transmitted power of 0.8 W.

A circular rectenna array is presented in [8]. It used a  $3 \times 2$  circular array antenna that operates at 2.65 GHz. Seven units of Shottky diode SMS7621-079F are used in the rectifier circuit. The rectenna output is 0.14 V when the transmitted power of 3 dBm is used.

In [9], a  $8 \times 9$  array dipole at 2.45 GHz is proposed. The dimension is  $50 \times 50$  cm $^2$  with an antenna gain of 5.2 dBi (single dipole). In total, 72 units of HSMS-282 Schottky diode have been used in this work. The rectenna output is 10 V with 20 dBm as the input power. Others work on development of an array rectenna are reported in [10-12].

This paper presents a developmental work of microstrip patch array rectenna that operates at 2.45 GHz. It has a capability to suppress the harmonic frequencies. The antenna's design has been discussed in detail as reported in [13]. The rectifier circuit employs a Villard circuit due to its effectiveness. The proposed design together with the results and discussion are presented in Section 2 and Section 3, respectively. Finally, Section 4 concludes the work.

## 2 Development of Rectenna

The geometry of the proposed 2.45 GHz patch array rectenna is shown in Figure 1. There are three stages in designing the rectenna. The first stage is receiving antenna which is 2x1 patch array with EBG-stub filter. The antenna is the harmonic suppression array antenna that are discussed in [13]. The antenna used EBG-stub filter to eliminate the unwanted frequencies as well as to increase the gain to 5.8 dB. The second stage is about the rectifier circuit. The function is to convert the RF signal to a direct current (DC) power supply. The rectifier circuit used in the design is a seven-stage Hillard voltage multiplier. In this work, a HSMS-2860 Schottky detector diode is selected. Finally, the third stage is the integration of the receiving array antenna and rectifier circuit. The antenna is fabricated on a FR-4 substrate with a relative permittivity,  $\epsilon_r$  of 4.6, loss tangent,  $\tan \delta$  of 0.0019 and thickness,  $h$  of 1.6 mm.

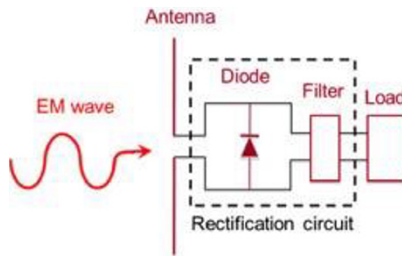


**Fig. 1.** Block diagram of the RF energy harvesting system [1].

### 2.1 2x1 Array Antenna with EBG and Filter

Figure 2 shows the layout of a 2x1 rectangular inset feed array antenna with EBG structure and filter. The corresponding parameters and dimensions are tabulated in Table 1. Figure 3 shows the comparison of reflection coefficients between the simulation and measurement. It is shown from the figure that by implementing the EBG and filter, the harmonic frequencies above 4.6 GHz are suppressed which make the antenna operates at a single frequency of 2.45 GHz.

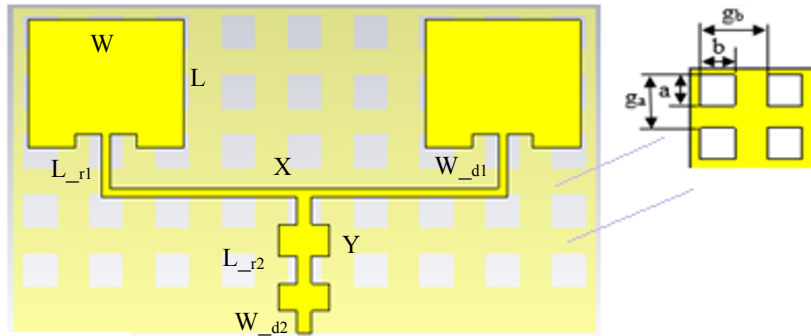


**Fig. 2.** Prototype of a  $2 \times 1$  rectangular inset feed array antenna with EBG structure and filter.

**Table 1.** Dimensions of the  $2 \times 1$  rectangular inset feed array antenna with EBG structure and filter

Parameters	Dimension	Parameters	Dimensions
L	29.16 mm	X	88.32 mm
W	37.61 mm	Y	5 mm
L_r1	5.5 mm	G_a	15 mm
L_r2	15.7 mm	G_b	15 mm
W_d1	0.71 mm	a	7 mm
W_d2	4.13 mm	b	7 mm

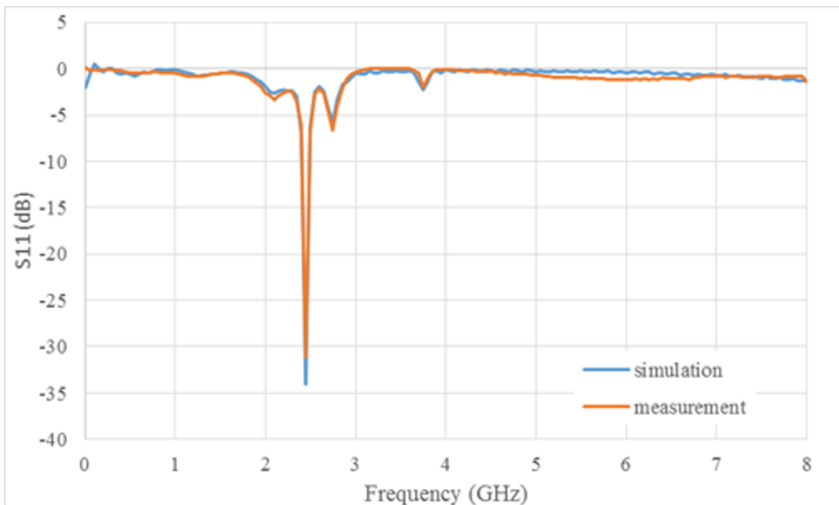


**Fig. 3.** Comparison of reflection coefficients between the simulation and measurement.

Figure 4 (a) and (b) show the radiation patterns of 2×1 rectangular inset feed array antenna with EBG structure and filter at 2.45 GHz. In E-plane, the main lobe magnitude is 5.34 dB at direction 0°. The angular width at 3 dB is 36.9° which is narrower as compared to a single antenna. In H-plane, the main lobe magnitude is 5.83 dB at direction 345°. The angular width at 3 dB is 72.2°.

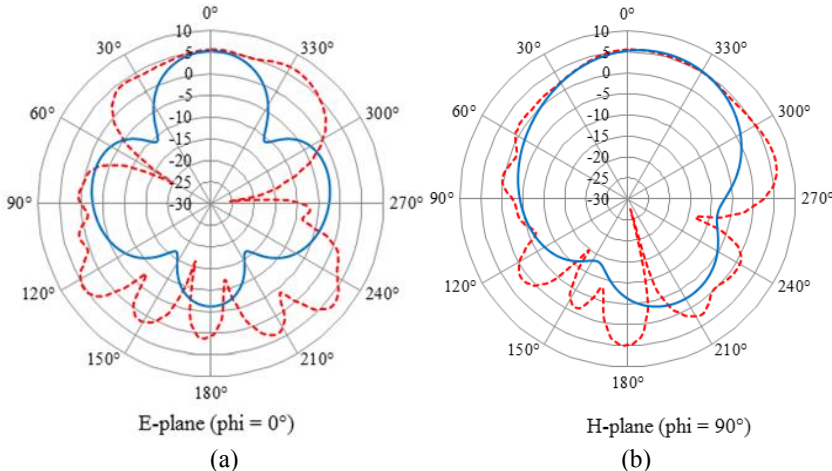


**Fig. 4.** Simulated (blue color) and measured (red color) radiation pattern of 2×1 rectangular inset feed array antenna with EBG structure and filter, (a) E-plane and (b) H-plane.

## 2.2 Rectifier Circuit Design

The seven-stage Villard voltage multiplier circuit can double up the input signal voltage towards the ground at a single output and can be cascaded to form a voltage multiplier with an arbitrary output voltage and its design simplicity as can be seen in Figure 5. From the figure, there is a RF signal source at the bottom of the circuit followed by the first stage of voltage multiplier circuit. Each stage is stacked onto the previous stage. Stacking is done from left to right for simplicity instead of conventional stacking from bottom to top such as Grainacher voltage doubler circuit. The circuit uses 7 pairs of Agilent HSMS-2850 zero-bias Schottky surface-mount diode. The other component associated with the circuit is the stage capacitor. The capacitors used for this circuit are the through-hole type, which make it easier to modify for optimization. The circuit design uses a capacitor across the load to store and provide DC leveling of the output voltage and its value only affects the speed of the transient response. Without a capacitor across the load, the output is not a good DC signal, but more of an offset AC signal. Besides, the most interesting feature about this circuit is the fact that these stages are connected in series. This method behaves similarly as the principle of stacking batteries in series to get more voltage at the output [14]. Due to this distinctive feature, succeeding stages in the circuit can gain more voltage than the previous stages. If a second stage is added on top of the first multiplier circuit, the only waveform that the second

stage receives is the noise of the first stage. This noise is then doubled and added to the DC voltage of the first stage. Therefore, the more stages that are added, theoretically, more voltage will come from the system regardless of the input.

Figure 6 shows the output versus input voltages for a single and seven-stage Villard voltage multiplier circuit. From Figure 6, as can be seen, the rectifier circuit has successfully rectified the input voltage of each type of voltage multiplier circuit. However, the single voltage multiplier circuit can only rectify approximately 100 mV which is from 500 mV to 608.63 mV. On the other hand, the seven-stage voltage multiplier circuit rectifies approximately five times from the input voltage to 2.5 V. This shows that the seven-stage Villard voltage multiplier circuit can rectify more input power source than a single stage.

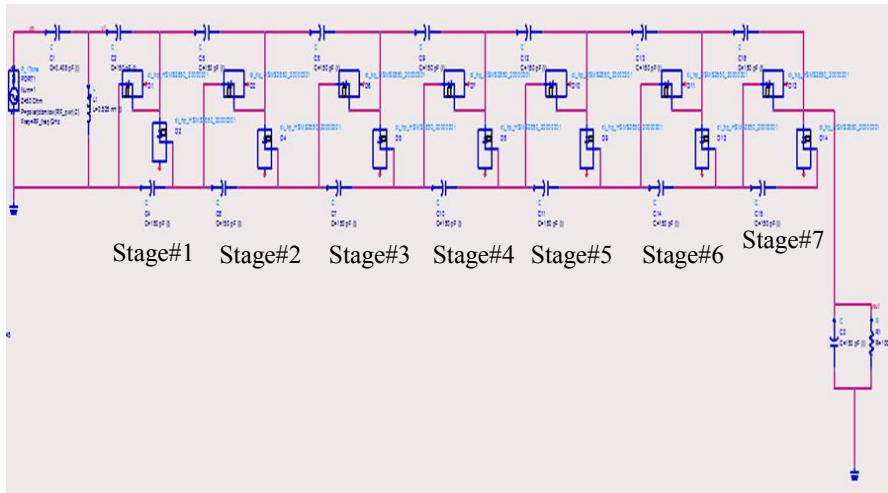


**Fig. 5.** Seven-stage Villard voltage multiplier circuit

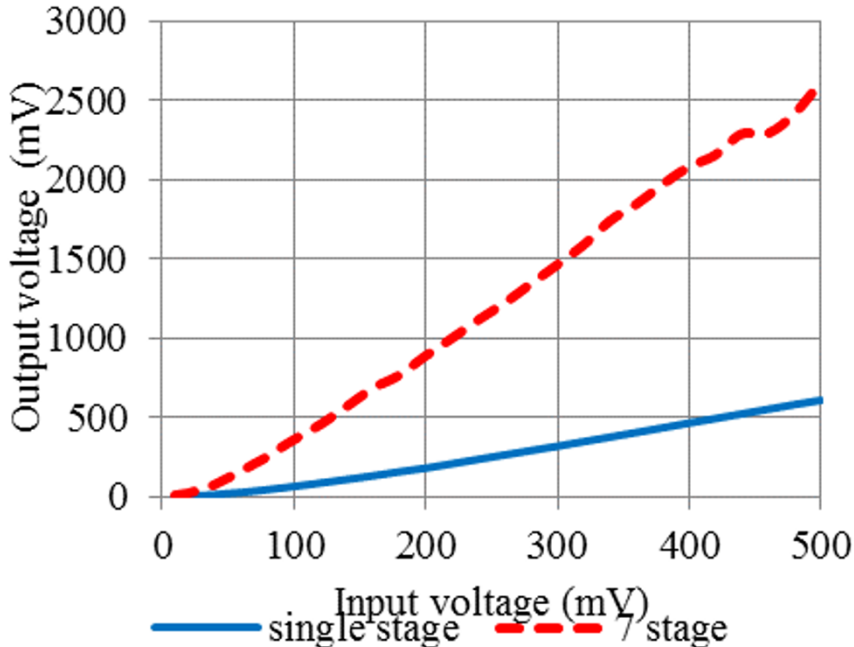


**Fig. 6.** Output versus input voltages of a single and seven-stage Villard voltage multiplier circuit

### 3 Rectenna Measurement and Analysis

The rectenna measurement is based on a standard experiment measurement setup where the proposed  $2 \times 1$  array antenna is connected to the rectifier circuit via a cable with the horn antenna connected to the spectrum network analyzer on the other side. In this work, the input power supply to horn antenna is varied from -10 dBm to 10 dBm. The distance, R from the transmitting and receiving antenna are 60 cm and 100 cm based on the far field formula. The measurement setup is shown in Figure 7. The performance of the rectenna system has been observed with a  $2 \times 1$  antenna.

Based on the comparison in Figure 8, it can be seen that the distance of 60 cm gives higher output voltages as compared to 100 cm. It can be seen that when the transmitting and receiving antenna is nearer, the power losses decreases. This will affect the performance of the antenna and produces higher output voltages. As can also be seen from the figure, the highest output voltage for 60 cm is 300 mV while for 100 cm, the output voltage is only 152 mV. Nevertheless, the results show that the rectenna system has successfully rectified the input signal from the horn antenna.

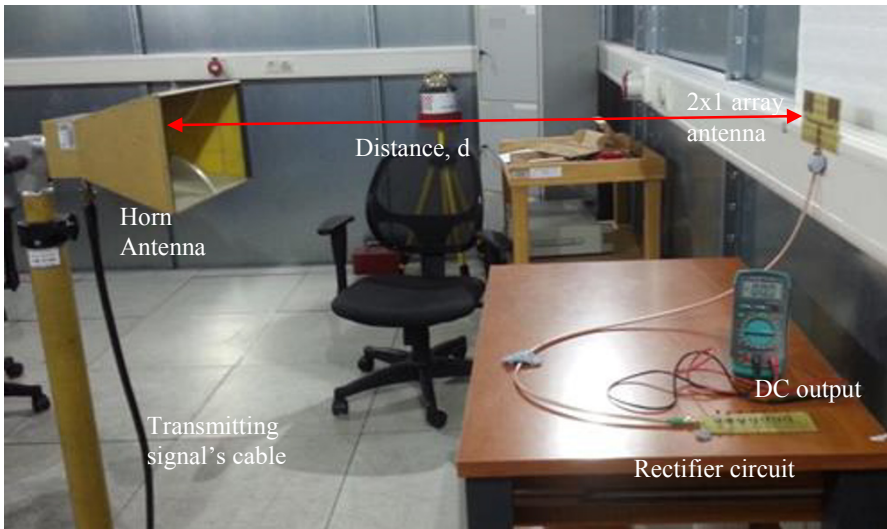


**Fig. 7.** Rectenna measurement setup

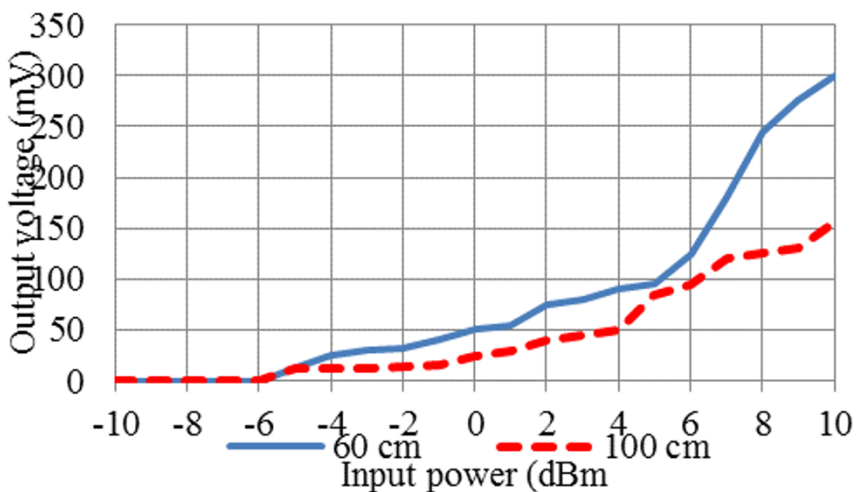


**Fig. 8.** Comparison of a  $2 \times 1$  rectenna output voltages between 60 cm and 100 cm of distance between the transmitting and receiving antennas

## 4 Conclusion

In this paper, an array patch rectenna system is designed, measured, analyzed and discussed. The rectenna system consists of two main parts which are the receiving antenna and rectifier circuit. Each part contributes to a different role in order to improve the performance of the rectenna system. Before combining the receiving antenna and rectifier circuit, each part is designed and analyzed separately. The complete rectenna system is a combination of a 2x1 array receiving antenna and rectifier circuit. The distance used for the measurement between the transmitting antenna (horn antenna) and rectenna are 60 cm and 100 cm. Based on the results, the shorter the distance, the higher the output power. Finally, the proposed rectenna system has successfully converted 10 dBm input power to 0.3 V output voltage.

## Acknowledgement

The work is supported by the Universiti Tun Hussein Onn Malaysia (UTHM) under the Tier 1 Grant Scheme (Vote No: H169). The measurements are performed at the Research Center for Applied Electromagnetics (EMCenter), UTHM.

## References

1. N. Amir.: Microstrip patch array rectenna with harmonic suppression capability for energy harvesting application. M. Eng. dissertation, Dept. Elect. Eng., UTHM, Malaysia, (2018).
2. H. Nugroho, S.H. Pramono, E.Yudaningtyas. Desain dan implementasi rectenna hexagonal patch array pada frekuensi 2.4 GHz. Journal EECCIS. 10(2), 39-44 (2016).
3. A.Mueed, M. N. Jafri, S. I. Butt. Integrated design of rectenna using microstrip patch for wireless power transfer at 4.3 GHz. In: 6<sup>th</sup> International Bhurban Conference on Applied Sciences and Technology 2009, pp. 19-22, IST, Islamabad (2009).
4. S. Shawalih, K.N. Abdul Rani, H. A Rahim. 2.45 GHz wearable rectenna array design for microwave energy harvesting. Indonesian Journal of Electrical Engineering and Computer Science.14(2). pp. 1-4 (2019).
5. X. Li, L. Yang, L. Huang. Novel design of 2.45 GHz rectenna element and array for wireless power transmission. IEEE Access. vol 7. pp. 28356-28362 (2019).
6. M. A. Sennouni, J. Zbitou, B. Abboud, A. Tribak and M. Latrach. Efficient rectenna design incorporating new circularly polarized antenna array for wireless power transmission at 2.45GHz. In: International Renewable and Sustainable Energy Conference (IRSEC) 2014. pp. 1-5, IEEE, Ouarzazate (2014).
7. G.N. Tan, X.X. Yang, H. Mei, Z. L. Lu. Study on millimeter-wave vivaldi rectenna and arrays with high conversion efficiency . Jurnal Hindawi. Vol. 2016. pp. 1-8 (2016).
8. J.J. Trad, B.A. Zeb, K.P. Esselle and M.U. Afzal. Preliminary investigations into a simple and effective rectenna for RF energy harvesting. In: 2017 IEEE International Symposium on Antennas and Propagation & USNC/URSI National Radio Science Meeting. pp. 1095-1096 , IEEE, San Diego (2017).
9. J. Zhang, Y. Huang and P. Cao. Harvesting RF energy with rectenna arrays. In: 6th European Conference on Antennas and Propagation (EUCAP), pp 365-367, IEEE, Prague (2011).

10. W. Huang, B. Zhang, X. Chen, K. Huang, C. Liu. Study on an S-band rectenna array for wireless microwave power transmission. Jurnal PIER. Vol. 135. pp. 747-758 (2013).
11. J. Zhang. Rectennas for RF Wireless Energy Harvesting. PhD. dissertation, Dept. Elect. and Electronic Eng., University of Liverpool, United Kingdom (2013).
12. K. Nishida, Y. Taniguchi, K. Kawakami, Y. Homma, H. Mizutani, M. Miyazaki, H. Ikematsu and N. Shinoharaa. 5.8 GHz high sensitivity rectenna array. In: International Microwave Workshop Series on Innovative Wireless Power Transmission: Technologies, Systems, and Applications (MTT-S), pp. 19-22, IEEE, Kyoto (2011).
13. N.A. Amir, S.A. Hamzah and K.N. Ramli. 2x1 microstrip patch array antenna with harmonic suppression capability for rectenna. Advanced in Science, Technology and Engineering Systems Journal. 6(2). pp. 267-271 (2017).
14. Schottklydiode. [online]. Available:[https://en.wikipedia.org/wiki/Schottky\\_diode](https://en.wikipedia.org/wiki/Schottky_diode). (last accessed 2019/06/16)



# Towards Computer-Generated Cue-Target Mnemonics for E-Learning

James Mountstephens, Jason Teo Tze Wi, and Balvinder Kaur Kler

Universiti Malaysia Sabah, 88400 Kota Kinabalu, Sabah, Malaysia.  
james@ums.edu.my, jtwteo@ums.edu.my, balvinder@ums.edu.my

**Abstract.** A novel method to generate memory aids for general forms of knowledge is presented. Mnemonic phrases are constructed using constraints of phonetic similarity to learning material, grammar, semantics, and factual consistency. The method has been implemented in Python using the CMU Pronouncing Dictionary, the CYC AI knowledge base, and Kneser-Ney 5-gram probabilities built from the large-scale COCA text corpus. Initial tests have produced encouraging output.

**Keywords:** Mnemonics, e-learning, n-grams, cue-target.

## 1 Introduction

It is no exaggeration to claim that memory is crucial to life and to learning [1] and that education depends on the successful transfer of learning material to student memory. Although human memory is powerful, its imperfections have long motivated people to develop and use devices to improve it, known generally as ‘mnemonics’. For example, to remember the colours of the rainbow {red, orange, yellow, green, blue, indigo, violet} people often use the mnemonic ‘Richard of York Gave Battle In Vain’, which has the same initials as the list to be remembered and can help trigger their recall. More technically, within the domain of human learning and memory, mnemonics are “cognitive strategies designed to enhance the encoding of information” in order to facilitate storage and retrieval [2]. A wide range of techniques exist that are suitable for different types of information. Research in education and psychology indicates that when used properly, mnemonics can improve memory and learning [2-4] but also that their general application can be limited by the time, imagination, and creativity required to generate them.

Modern computing techniques could be used to automatically generate mnemonics and could therefore overcome this barrier to widespread usage, with the potential to aid education at all levels. Modules for generating effective mnemonics could become part of e-learning systems allowing individual learners to request mnemonics on demand for learning material that they felt required them. A successful computer-aided mnemonic system would be able to take in learning material, automatically generate and output effective mnemonics most appropriate to the student and to the learning domain and might also explain the processes used so that students could develop the skills for

themselves. Despite this potential, computer-aided mnemonics are currently under-studied. As will become clear presently, one reason for this is that the problem is extremely challenging and requires input from most domains in AI. To date, systems have only been developed to help remember login passwords based on sentences extracted from text corpora [5], to learn foreign language vocabulary using keywords with phonetic similarity [6], and to memorise information presented as lists using formal grammars, genetic algorithms, and corpus-derived n-gram frequencies [7,8]. These systems have proven encouragingly effective within their respective limited types of learning material. However, no existing system is able to generate mnemonics for what is known in memory studies as cue-target pairs, a much more general form of knowledge. The acquisition of much basic knowledge can be viewed as learning the correct target for a given cue. For example, in learning capital cities of the world, the cue “Senegal” should trigger recall of the target “Dakar” in the learner. Or when learning the formulas for chemical compounds, the cue “hydrochloric acid” should trigger the target “HCl”. The list of factual domains where this form of knowledge is found is vast: football teams, dates of battles, and many, many more.

The key principle for cue-target mnemonics (CTMs) is to identify or to construct a memorable link between cue and target so that the presented cue strongly suggests the unseen target. This link could be based on visual (orthographic), auditory (phonetic), and meaningful (semantic / factual) properties. When no direct link can be identified, an indirect link may be constructed using intermediate objects which instead form a chain of links between cue and target. Some examples are shown in figure 1 below. To link “positive ion” to “cation” we can observe that ‘positive’ is represented as a ‘+’, which looks like the “t” in “cation” (but not anion). Or to remember that in a neuron, the axon provides output, we can observe that output means action and action sounds like axon. As a more complex example, to remember that the 2nd amendment to the US constitution is the right to bear arms, we can imagine a bear raising its 2 arms as an intermediate object with visual and semantic properties that link cue and target.

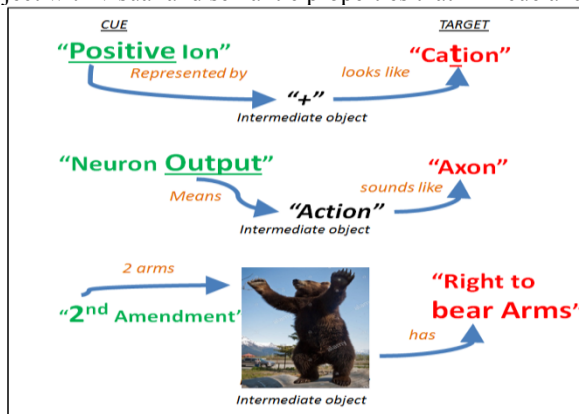


**Fig. 1.** Examples of CTMs made by constructing links between cue, intermediate object, and target.

Developing a machine to automatically identify and generate these kinds of memorable links between cue and target is technically and theoretically challenging. In effect, it requires a simulation of human-level knowledge and creativity, and the use of all the senses. The work presented here constitutes the first steps towards the wider goal of generating CTMs and attempts to make initial progress by extending the good features of the few existing computer mnemonic systems. More specifically, it will generate CTMs by combining phonetic similarity and constructed mnemonic phrases. For example, to remember that the country “Senegal” (cue) has the capital city “Dakar” (target) the CTM “Sun Is Gone Darker” is a semantically and factually consistent phrase whose parts sound like the syllables of the cue and target pair. To better understand the approach developed here, the existing systems will be examined in more detail.

## 2 Related Work

### 2.1 Keyword Mnemonics and Transphoner

Stanford’s Transphoner system [6] is a computer implementation of the established ‘keyword’ mnemonic system [2] used primarily for learning foreign language vocabulary, which can be seen as a highly restricted form of cue-target learning using a keyword as an intermediate object. Using the keyword system to learn the native meaning  $t$  of a foreign cue word  $c$  is done in two stages: i) find a keyword  $k$  in the native language phonetically similar to  $c$ , ii) vividly visualise a scene where keyword  $k$  is somehow related to  $t$ . As an example, the Spanish word ‘lago’ means ‘lake’ in English. ‘Lago’ (pronounced ‘log-oh’) sounds like the English word ‘log’ and ‘log’ could be visualised as floating on a lake. So, when a learner says the word ‘lago’ they hear ‘log’ and see it on a ‘lake’. Note that many keywords are phonetically similar to the cue (eg. ‘logo’ or ‘lager’) but that ‘log’ is a good choice because it is semantically consistent with ‘lake’. This chain of association linking source and target vocabulary has been shown to be effective in foreign language learning [1,2].

The key mechanisms used here are a transformative encoding of the foreign word into a phonetic equivalent and then the semantic visualisation by the user of some way to connect the keyword and target. Transphoner is able to automate the first mechanism and attempts to do so in such a way that is suitable for the second. As an example of Transphoner in action, the French word ‘Ratatouille’ which means ‘vegetable dish’ is Transphoned into the keywords ‘Rat Tattoo’ which sound strongly like the cue and are vividly imageable. It is important to note that Transphoning can split a single cue word into multiple keywords that sound like the cue’s individual syllables (Ratatouille → Rat Tattoo). As described later, this one-to-many relationship will be exploited by the CTM system developed here.

Space precludes a detailed account of the implementation of Transphoner but its basic components include databases of phonetic transcriptions for all words under consideration (using the IPA phoneme set), metrics for determining phonetic distance (using ALINE and Levenshtein distance) and semantic relatedness functions (based on Wordnet semantic hierarchies). Transphoner has been tested and found to improve the recall of German vocabulary by English speakers.

It is an impressive system. However, Transphoner (and the keyword method itself) may not be suitable to create general cue-target pairs for all learners. Recall that making CTMs involves constructing a chain of links between cue and target. Transphoner phonetically links cue to keyword but it does not explicitly link keyword to target. This last link still requires creativity, visualisation skills, and effort from the learner, which may be challenging for some. Referring to the ‘Ratatouille’ example just given, ‘Rat Tattoo’ certainly sounds like the cue but it is entirely unrelated to the target ‘vegetable dish’ and because of this, the user may have a hard job of visualising a scene that links them. To put it another way, the intermediate object that Transphoner generates (the keyword) does not contain any direct ‘trace’ of the target – that connection must be established mentally by the learner. In contrast, the CTM system developed here will generate an intermediate object that i) contains traces of both cue and target and ii) fully describes a scene, requiring no effort of imagination from the learner. Inspired by Transphoner, our system will find phonetic substitutes for both cue and target and bind them together. This method of binding is derived from the next existing system for computer-aided mnemonics.

## 2.2 Elaborated Acronyms

Mountstephens [7,8] developed a computer system to generate mnemonics for information presented in lists or, more generally, items in a sequence. Like Transphoner, this system was based on an existing mnemonic technique: the method known as Elaborated Acronyms [2]. Standard acronyms, which use list initials are popular memory aids (eg FIFO, RAM, RAID) which work well when the list initials are pronounceable. However, this is not always the case and more generally, Elaborated Acronyms (EAs) can be used. The most common type of EA is a sentence with the same initials and number of words as those in the list to be memorised. Classic examples for some common lists are: ‘My Very Excellent Mother Just Sent Us Nachos’ for the eight planets {Mercury, Venus, Earth, Mars, Jupiter, Saturn, Uranus, Neptune} and ‘Every Good Boy Deserves Food’ for the notes on the musical stave {E, G, B, D, F}.

EAs work because they bind the unrelated items in a list together into a single unit. A list may lack formulaic relation between elements that would allow deduction of the next item, but sentences are intimately bound together with long-range grammatical and semantic dependencies that constrain the possible options. If a sentence starts with “the cat...”, the words following must be grammatically correct and factually consistent, such as “sat on the mat” but neither “on mat the sat” nor “sat on the moon”. Achieving this binding by computer is challenging because it requires somehow enforcing grammar, semantics, and factual knowledge in broad domains. The biggest problem in the previous work was to evaluate this grammatical and semantic consistency in a candidate EA. For a given list  $L$  of  $n$  words, a candidate EA is a sequence also of  $n$  words and with the same initials as  $L$ . Clearly, a vast number of candidate EAs are possible and most of them will be neither memorable nor even grammatical phrases. For example, candidate EAs for the list {Red, Orange, Yellow, Green, Blue, Indigo, Violet} might include "Real Off Yes Guzzling Bust Igloo" and "Riding On Yachts Gets Better In Venice". While both sequences meet the basic constraints, the second is

clearly more memorable than the gibberish of the first. Note how the second sequence forms a grammatical phrase and how its elements are factually consistent: yachts do provide rides on water, and Venice is known for its water.

In the previous work, this task of generating EAs was framed as an optimisation problem with an objective function for evaluating the memorability of different candidate EAs. The particular search method used was that of Genetic Algorithms (GAs), which are known to efficiently identify maxima in large search spaces. Criteria for success were modelled as a function of grammaticality and coherent meaning by using context-free grammars (CFGs) and n-gram frequencies extracted from large text corpora [11]. The generated EAs were tested on human subjects and found to produce a significant increase in recall performance on list information over learning by simple repetition [10]. This method will be adapted here to generate CTMs.

### 3 System Concept, Design, and Implementation

#### 3.1 System Concept

At first glance, EAs are not appropriate for cue-target pairs since the former are whole sentences and the latter are just two words. However, if we recall that Transphonener can split single words into multiple phonetic substitute words then Transphoning both the cue and target can produce enough words to be bound into a memorable phrase in the same way that EAs bind a list of words by initial. The resulting intermediate object will then have strong links in all parts of the chain. An example will elucidate the approach. Imagine that a learner was trying to memorise the names of American Football teams and wanted to generate a CTM for the “Cincinnati Bengals”. In their raw form, Cincinnati (cue) and Bengals (target) are unrelated words. It is hard to see any way to link them directly. But if we allow phonetic links then other words can be chosen that do suggest each other but are still linked to the original words by sound. One possibility is the phrase “Since You’re Nasty, Bang Guns!”.

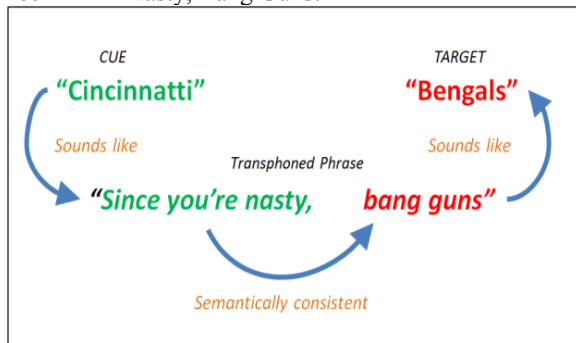


**Fig. 2.** Example of CTM by Transphoning cue and target and generating phrase from syllable substitutes.

When the user reads and says the cue “Cincinnati” in their head, it sounds like “since you’re nasty”, and being nasty suggests (or is at least strongly consistent with) “bang guns”, which in turn sounds like the target “Bengals”. Unlike Transphonner, a complete chain of links is built from cue to target. Semantic and factual consistency bridges the gap between the Transphoned cue and Transphoned target. Phonetic similarity enables us to relate cue and target to the left and right sides of the phrase, respectively. Admittedly, this example is no Shakespearean sentence. And ‘banging guns’ may not inevitably be associated with being nasty (the reader is unlikely to imagine that phrase naively). But it does fit and, once seen and heard, should be easy to bring to mind. It noted again that finding any link at all meeting phonetic and semantic constraints is challenging. Though clearly derivative of existing mnemonic designs, this approach has not been formalised in the memory literature nor implemented on computer before. The specific steps required to produce CTMs with this approach are given next.

### 3.2 Design and Implementation

Given a cue and target word pair ( $c, t$ ), the main processes to generate a CTM using the system presented here are as follows. This system design and its processes have been implemented using an overall platform of Python with additional Java code. Several existing libraries and databases were used and interfaced with custom code. To help illustrate the stages, the cue-target pair “Senegal” and “Dakar” will be used as an example.

#### Find phonemes for cue and target

The input words ( $c, t$ ) must first be phonetically transcribed. The CMU Pronouncing Dictionary [9], which contains over 134,000 transcriptions was used here. CMU uses the ARPABET phoneme set, and each phoneme can consist of multiple characters, as seen in the transcriptions for “Senegal” and “Dakar” which are [S EH N AH G AO L] and [D AA K AA R], respectively. Some preprocessing was carried out before use. First, stress information required for pronunciation but not needed here was stripped out. Then multiple character phonemes were converted to single characters to easily support the Levenshtein edit distance function. Finally, all preprocessed transcriptions were entered into a custom trie data structure in Python by Levenshtein distance to facilitate fast search for phonetically similar words in later stages.

#### Group phonemes into syllables

Since there may be many phonemes for a given word (7 and 5 for our example words above) and our intention is to replace phonetic representations with substitute words, this could lead to sentences too long to memorise. Syllables are natural places to break a word into subwords and are less than or equal in number to the number of phonemes. Identifying syllable boundaries within CMU phonemes was done using heuristics developed by [10] which have a Python implementation. For the phonemes just obtained, syllable groupings would be [S EH N] [AH] [G AO L] and [DAA] [KAAR].

### **Derive all possible syllable groups**

Even after grouping phonemes into syllables, the resulting units may still yield a large number of short words, for which it may be difficult to find similar sounding substitutes and/or to fit into sentences. Deriving all possible groupings of syllables gives more options for similar sounding substitute words and provides more flexibility in sentence structure. For the syllables of “Senegal” the possible groupings are: [S EH N] [AH] [G AO L]; [S EH N AH] [G AO L]; [S EH N] [AH G AO L]; and [S EH N AH G AO L].

### **Find phonetic substitute words for syllable groups**

A search using a suitable distance function is conducted for words that sound similar to each syllable group. Here, the trie constructed at the start based on Levenshtein distance was used to find words within a permitted phonetic distance. A tremendous number of phonetically similar words may exist for each syllable group. For example, [S EH N] (“sen”) differs from [S UH N] (“sun”) and [T EH N] (“ten”) by only one phoneme and can be considered phonetically similar. Depending on the distance function used, shorter and longer words might also be considered similar: [S EH N] (“sen”) and [S EH N S] (“sense”), for instance. As an edit distance, Levenshtein distance will consider the latter example to have a distance of 1 (i.e. very similar). These possible substitutes are the raw material for the candidate phrases to be evaluated.

### **Combine phonetic substitutes for both cue and target into candidate sequences**

Each set of phonetic substitutions for each syllable group is concatenated to yield sequences that may (but more likely will not) be grammatical and meaningful sentences. Using the table above, a few possible sequences are “Sin He Goal Darker”, “Ten Is Cool Barker”, “Sun Is Gone Darker”. Python’s itertools library allows efficient generation of all possible combinations of words into candidate sequences.

### **Evaluate candidate sequences and select the most coherent and memorable**

Clearly, most candidate sequences will be neither grammatically correct nor semantically and factually consistent. An objective function must be used that takes into account grammar, semantic consistency, and world knowledge in order to select the most memorable sentence. Phonetic similarity to source words should be included also. There are both implicit and explicit methods to evaluate these criteria. Grammatical consistency can be evaluated explicitly by using a natural language parser. In this project, a link parser from the Python Natural Language Toolkit (nltk) library was used to assign a score for the grammatical correctness of a candidate sequence. Factual consistency might be identified explicitly using Cyc [12], a comprehensive ontology and knowledge base spanning the common sense concepts and heuristics about how the world works. Cyc contains millions of manually-entered factual assertions using an extended form of first order logic (FOL). For example: dogs can jump, cats can eat; cars drive on roads; human skin is living, contains blood, and is something we wash. Implicit grammatical and factual knowledge can be captured by n-gram probability models derived from large text corpora [11,13]. N-grams are contiguous sequences of  $n$  items found in a text. Example bigrams (when  $n=2$ ) might include ‘at home’ and ‘apple

hermit'. It should seem reasonable that the first example would have a higher frequency than the latter and this information can be used to evaluate candidate sentences. Note that factual compatibility of objects is captured because objects spoken about together are often found together and that local grammatical regularities are captured since the grammatical noun phrase "car on the road" would have higher probability than ungrammatical sequence "car road on the". Here, the Python nltk library was used to build a 5-gram Kneser-Ney probability model [11] built on n-grams from the 560-million word COCA corpus [13]. 5-grams were chosen after initial experiments with shorter sequences ( $n=2,3,4$ ) yielded unbalanced sentences.

### **Manual clean up**

Currently, subject-verb agreement and punctuation must be done manually

## **4 Experiments**

Using the method just described, CTMs were generated for a set of 32 cue-target pairs for NFL American Football teams. This domain was chosen since the NFL is not well known outside of the US and future testing can be less biased by existing knowledge. Almost all cues and targets have minimal direct linkage, making them challenging to learn and to develop CTMs for.

Arizona Cardinals	Dallas Cowboys	Los Angeles Rams	Philadelphia Eagles
Atlanta Falcons	Denver Broncos	Miami Dolphins	Pittsburgh Steelers
Baltimore Ravens	Detroit Lions	Minnesota Vikings	San Diego Chargers
Buffalo Bills	Green Bay Packers	New England Patriots	San Francisco 49ers
Carolina Panthers	Houston Texans	New Orleans Saints	Seattle Seahawks
Chicago Bears	Indianapolis Colts	New York Giants	Tampa Bay Buccaneers
Cincinnati Bengals	Jacksonville Jaguars	New York Jets	Tennessee Titans
Cleveland Browns	Kansas City Chiefs	Oakland Raiders	Washington Redskins

**Fig. 3.** List of 32 American Football team cue-target pairs.

### **4.1 Explicit Factual Consistency: Cyc**

Cyc was explored to discover whether it could explicitly identify factual relations between the elements in candidate CTM sequences, rating them higher. The nltk link parser was used to identify all content words in a candidate sequence (ie noun, verb, adjective, adverb) and to then query Cyc using its Java API for assertions involving each possible pair. A higher number of assertions involving word pairs was taken to mean greater factual consistency between them. As an example of success, after "Washington Redskins" was broken into syllable groups [wash] [ing] [ton] [red] [skins], the parser identified [wash] as a verb and [skins] as a noun. Cyc was queried and found to contain an assertion that "All personal washing affects pieces of skin.", which is Cyc's way of saying that "we wash skin". This may seem trivial to a human but it is common-sense knowledge that is found in no other AI system. It is in fact a direct link between cue and target – a CTM that could be used without Transphoning. However, few other usable

assertions were found in these experiments which may be due to our inexperience with devising Cyc queries. More work will be carried out in the future but for the present purposes, implicit measures of semantic and factual consistency will be used.

#### 4.2 Implicit Factual Consistency: n-Grams

Using the nltk link parser to evaluate grammar and the KN 5-gram probability model to evaluate factual consistency, the following 10 usable CTMs were obtained. Mnemonic phrases for the remaining 22 NFL teams were manually rejected as being too close to gibberish to be effective.

1 <u>Arizona Cardinals</u> A Rich Owner's Car Dies Now	6 <u>Chicago Bears</u> The Car Goes There
2 <u>Atlanta Falcons</u> Fat Santa Shall Come	7 <u>Cincinnati Bengals</u> Since You're Nasty, Bang Guns
3 <u>Baltimore Ravens</u> Boil Tea More Bravely	8 <u>Dallas Cowboys</u> Dad Loves Cowboys
4 <u>Buffalo Bills</u> Blood Follows Kills	9 <u>Houston Texans</u> Huge Stones Take Tons
5 <u>Carolina Panthers</u> Cow Runs Like A Panther	10 <u>Jacksonville Jaguars</u> Packs Some Kill Jaguars

**Fig. 4.** 10 usable CTMs for American Football teams

It can be seen that the proposed method was able to construct a small number of phrases that do simultaneously meet the requirements of phonetic similarity to cue and target, reasonable grammatical correctness, and semantic and factual consistency. And although not intended, each phrase rhymes with the combined cue and target, which may aid memorability. However, there are clearly instances where compromises were made in the competing constraints. For example, “Bravely” does not really sound like “Ravens” and boiling tea does not usually require bravery; “Packs” and “Jaguars” are factually consistent, but the overall sentence does not make much sense. It is worth noting that in several instances, phrases using the raw target (without phonetic substitution) were rated highest by the system and this may be a useful feature to promote in future since it forces the right hand side of the sentence (which corresponds to the cue and is seen during testing) to conform to the left hand side (which is unseen during testing and needs the most help to recall).

### 5 Conclusion

The work presented here has only scratched the surface of this method to improve memory and learning. Greater refinement of the system and testing on actual learners

must be carried out before conclusions about effectiveness can be made. Both are currently in progress. However, the results obtained here are encouraging.

## Acknowledgements

This work was funded by Universiti Malaysia Sabah under SGPUMS Grant SBK0363-2017.

## References

1. Schwartz, B.L.: Memory: Foundations and Applications. 3rd edn. SAGE (2017).
2. Worthen, J.B. and Hunt, R.R.: Mnemonology: Mnemonics for the 21st Century. Essays in Cognitive Psychology. New York, NY, US. Psychology Press. (2011)
3. Carney, R. N., & Levin, J. R.: Delayed mnemonic benefits for a combined pegword-keyword strategy, time after time, rhyme after rhyme. *Applied Cognitive Psychology*, 25, 204-211. (2011).
4. Seay, S.S.: The Use/Application of Mnemonics As a Pedagogical Tool in Auditing, Academy of Educational Leadership Journal 14 (2). (2010).
5. Jeyaraman,S., Topkara, U.: Have the cake and eat it too - Infusing usability into text-password based authentication systems. In Proceedings of ACSAC '05 Proceedings of the 21st Annual Computer Security Applications Conference. Pages 473 – 482. (2005).
6. Savva, M., Chang, A.X., Manning, C., Hanrahan, P.: TransPhoner: Automated Mnemonic Keyword Generation. In Proceedings: ACM Conference on Human Factors in Computing Systems. (2014).
7. Mountstephens, J.: Towards Computer-Generated Mnemonic Phrases: Experiments with Genetic Algorithms and N-Grams. *Journal of Engineering and Applied Sciences*. Vol 9, Issue 9. (2014).
8. Mountstephens, J.: Computer-Generated Mnemonics Can Improve Student Memory, Advanced Science Letters, in press.
9. <http://www.speech.cs.cmu.edu/cgi-bin/cmudict>
10. <https://github.com/kylebgorman/syllabify>
11. Bird, S., Klein, E., Loper, E.: Natural Language Processing with Python: Analyzing Text with the Natural Language Toolkit. Beijing: O'Reilly. (2009).
12. <https://www.cyc.com/>
13. <https://www.english-corpora.org/coca/>



# Data Integration for Smart Cities: Opportunities and Challenges

Subashini Raghavan<sup>1</sup>, Boung Yew Lau Simon<sup>1\*</sup>, Ying Loong Lee<sup>1</sup>, Wei Lun Tan<sup>1</sup>, Keh Kim Kee<sup>2</sup>

<sup>1</sup>Lee Kong Chian, Faculty of Engineering and Science, Universiti Tunku Abdul Rahman, Bandar Sungai Long, Malaysia

<sup>2</sup>School of Engineering and Technology, University College of Technology Sarawak, Sibu, Malaysia  
simonlau@utar.edu.my

**Abstract.** Current modern cities are equipped with sensors generating huge amounts of data waiting to be tapped for “smart” decision making such as smart grid, smart transportation, smart buildings and smart healthcare. However, these data are not readily analyzable due to the heterogeneity of data types and formats from “vertical silos” smart city systems. In this paper, the existing related work in progress of smart city data sharing and integration are enumerated and the key technical challenges and limitations are identified and highlighted. We propose a bottom-up publish/subscribe data sharing and integration model to overcome the technical challenges and limitations in cross-domain integration of smart city data. A data representation scheme and Application Programming Interface (API) based prototype application are currently under development. The proposed model shows a promising prospect for facilitating smart city data sharing and extraction, transformation and loading when fully implemented.

**Keywords:** Smart City, Internet of Things, Data Sharing and Integration, Heterogeneity

## 1 Introduction

It has been estimated that 55% of the world’s population lives in urban areas, a proportion that is expected to increase to about 68%, by 2050 [1]. Such an increase necessitates the need for creating a modern, sustainable living environment for urban citizens. However, city decision makers need to have a holistic view of the scenarios of physical infrastructure, buildings, vehicles and human flow in cities in real time to have a timely response. As such, there is a rising call for the use of emerging technologies such as the Internet of Things (IoT), machine learning (ML) algorithms and Big Data Analytics (BDA) to make modern cities “smarter” [2]. In Malaysia, a number of smart city initiatives such as the Greater Kuala Lumpur, Iskandar Malaysia, Smart Selangor and Putrajaya Smart City have been proposed under the 11th Malaysia Plan to tackle problems

arisen from rapid urbanization, such as environmental pollution, traffic congestion, flood, waste disposal, water shortage, and rising healthcare / medical costs [3, 4].

The Institute of Electrical and Electronics Engineers (IEEE) has physically defined a “smart city” as a suite of smart applications bringing together technologies, governments and societies to enable characteristics such as smart healthcare, smart transportation, smart home, smart building, etc designed and developed to manage assets and resources more efficiently [5]. “Smart cities” in this context refer to the development of technology-based urban systems integrating information and communication technology (ICT) with various physical devices (sensors) which are interconnected, forming the so-called Internet of Things (IoT) for driving efficient city management and economic growth [6, 7]. The next generation of smart city applications heavily depends on the ubiquitous sensing capabilities of wirelessly connected sensors and actuators to observe, measure, reason and act in the physical world. The continuous and ubiquitous sensing of environment results in a huge volume of data presented in diverse formats [8, 9]. These data are valuable assets to the cities waiting to be explored for better decision making. The ability to collect, clean, integrate, transform and analyse sensor data streams from disparate sources would provide actionable insights [10].

Notwithstanding the promising prospect, innovative solutions, which exploit these data to create better public services, are constantly being hampered by the lack of visibility, accessibility and compatibility among these data [11]. At present, most of the smart city sensor data are stored and secured in proprietary storage or in electronic devices, undisclosed to the public. Smart city systems which work in “silos”, are closed, designed and developed by specific vendors using proprietary technologies, and dedicated for a particular need of a home, a company or a few persons rather than contributing to the common good of the cities. They cannot be easily combined or extended with third-party components or services due to the heterogeneity of structure and formats [12]. Hence, there is an increasing need for a new tool or platform to facilitate the collection, integration and assimilation of smart city data to support what a “smart” city could do.

The objectives of the paper are to 1) identify the key limitation of current data sharing and integration methods in bridging the “interoperability gap” of smart city data from the aspects of data sharing and integration is enumerated; 2) devise a model to overcome the current technical challenges. The key contributions of this paper is a model to enable cross-domain sharing, integration and analysis of smart city IoT data.

The rest of this paper is organized as follows. Section 2 describes the key distinguishing characteristics of smart city sensor data. Section 3 discusses the existing methods in data sharing and integration. Section 4 identifies the key technical challenges faced in data sharing and integration. Lastly, Section 5 proposes a data sharing and integration model and provides several future research directions.

## 2 Characteristics of Smart City IoT Data

In the context of a smart city, data are generated from humans and machines. The human-generated data include 1) social data coming from crowd-sourced citizens; 2)

document files and enterprise data generated by the authorities, governments as well as businesses and enterprises. Meanwhile, with the current advent of IoT, more machine-generated data are streamed generated from various sensing devices installed everywhere in the city working round-the-clock, exists mostly in the form of text or video images. Due to the exponential increase in the number of sensors deployed in the physical environment, the machine-generated data far outgrow the human-generated data. Hence, the real untapped value of “smart” information in a city lies in the machine-generated data (also termed as IoT data) based on their sheer volume, velocity and variety. Based on an application domain-based taxonomy [13], the sensor types are further mapped to smart city domains.

**Table 1.** Mapping of the key sensor parameters with key Smart City domains

Smart City Domains		Building	Mobility/ Transport	Energy & Environ- ment	Human Bi- ology/ Health
Sensor Type	Motion	Vibration <sup>6</sup> Door <sup>2</sup> Movement <sup>1,6,7</sup>	Acceleration <sup>6</sup> Volume <sup>6</sup> Load <sup>6,7</sup> Shock <sup>6</sup> Velocity <sup>4,6,7</sup> Front Screen <sup>4</sup>	Vibration <sup>7</sup> Move- ment <sup>6,7</sup>	Vibration <sup>8,9</sup> Weight <sup>9</sup> Activity <sup>7,8,9</sup>
	Position	Location <sup>6</sup> Proximity <sup>6</sup>	Location <sup>4</sup> Proximity <sup>6</sup>	Location <sup>5,6</sup>	Tilt <sup>8,9</sup> Location <sup>7,9</sup> Proximity <sup>6</sup>
	Environment	Smoke <sup>4</sup> Lightning <sup>1,2,3,6</sup> Tempera- ture <sup>1,3,6,7</sup> Gas <sup>4,6</sup> Pressure <sup>7</sup> Water <sup>4</sup> Humidity <sup>3,6</sup> Acoustic <sup>6</sup> Moisture <sup>1</sup> Voltage <sup>4,7</sup> Current <sup>4,7</sup> Power <sup>4</sup>	Temperature <sup>6</sup> Acoustic <sup>6</sup>	Tempera- ture <sup>4,5,6,7</sup> Voltage <sup>7</sup> Current <sup>7</sup> Power Humid- ity <sup>4,5,6,7</sup> Pres- sure <sup>4,5,6,7</sup> Volume <sup>6</sup> Rain <sup>4</sup> Water <sup>7</sup> pH <sup>7</sup> Sound <sup>7</sup> CO <sub>2</sub> <sup>6,7</sup> CO <sup>4,5,6</sup> O <sub>3</sub> <sup>4,6</sup> SO <sub>2</sub> <sup>4,6</sup> NO <sup>4,6</sup> Noise <sup>4</sup> Acoustic <sup>6,7</sup> Flow <sup>7</sup> Light <sup>5</sup> Dust Parti- cles <sup>4,5</sup> Wind speed <sup>4</sup>	Pressure <sup>6,8,9</sup> Tempera- ture <sup>6,8,9</sup> Magnet <sup>8</sup> CO <sub>2</sub> <sup>9</sup> Radiation <sup>6</sup>

Biosensor				Heart rate <sup>6,8</sup> , Pulse <sup>8</sup> , Oxygen <sup>8,6</sup> , Blood Glucose <sup>8</sup> , Blood pressure <sup>6,8</sup> , EEG <sup>8</sup> ;ECG <sup>8</sup> , EMG <sup>8</sup> EOG <sup>8</sup>
-----------	--	--	--	--

Note: index 1: ref [32], 2:[33], 3:[34], 4:[35], 5:[36], 6:[37], [7:38], [8:39]

To analyze these raw sensor data, the first step is to make the data accessible. Secondly, the data are turned into a processable and analyzable form for insight and decision making. Generally, sensors deployed in smart cities are attached to private homes, buildings, transportation vehicles, energy infrastructures, etc to capture the motion, position and environmental parameters related to the smart city appliances while biosensors are also deployed to measure human biological parameters such as heart rate, blood pressure, oxygen level, etc as summarized in Table 1.

The sensor data normally originate from closed, isolated, single-purpose, task-specific, “vertically silo” applications such as smart lighting, smart parking, traffic and security monitoring. As standalone systems, the data collected rarely satisfy all the data quality standard required by an ideal system which includes accuracy, consistency, completeness and timeliness [12].

For instance, Figures 1 and 2 illustrate the presence of inconsistency and incompleteness / missing data in two different but related smart city sensor datasets available on Kaggle and UCI Machine Learning Repository respectively. In Figure 1, the set of parameters collected for both datasets are inconsistent and lacking standard semantics even though both are addressing the air quality issue. Parameters such as Ground Truth hourly averaged concentrations for CO, Non Metanic Hydrocarbons, Benzene, Total Nitrogen Oxides ( $\text{NO}_x$ ) and Nitrogen Dioxide ( $\text{NO}_2$ ) were collected for assessing the Italy Air Quality in dataset 1 while different parameters such as Sulphur dioxide, Nitrogen dioxide, Respirable Suspended Particulate Matter, etc. were recorded on the other dataset. In addition, some Distance data of the first dataset are missing as well.

Similarly, in Figure 2, the date format for two wearable tracking devices are inconsistent. The day, month and year of the SenseWear Pro are of the same order as the FitBits but separated using a backlash, “/” instead of a hyphen, “-“. Moreover, the date format within the dataset in SenseWear Pro has a different order in displaying the year as “yy” and “yyy”. Other than that, the distance in which the activity occurred in the SenseWear Pro are recorded with a full stop, “.” to separate the number from its decimal places whereas in the FitBits it is separated using a comma, “,”. In addition, in both cases in Figures 1 and 2, certain sections of the data are incomplete. For instance, the column Respirable Suspended Particulate Matter (rspm), suspended particulate matter (spm), location monitoring station and particulate matter 2.5 (pm2.5) of the Hyderabad India Air Quality data, are recorded as “not available”, i.e., “NA” and the first 5 rows of the SenseWear Pro data, despite an activity occurred, the distance recorded was 0.

**Italy Air Quality**

Date	Time	CO(GT)	PT08 S1(CO)	NMHC(GT)	C6H6(GT)	PT08 S2(NMHC)	NOx(GT)	PT08 S3(NOx)	NO2(GT)	PT08 S4(NO2)	PT08 S5(O3)	T	RH	AH
10/03/04	18:00:00	2	1292	112	9.4	955	103	1174	92	1559	972	13.3	47.7	0.7258
10/03/04	19:00:00	2	1292	85	9.0	955	131	1145	114	1555	972	13.3	47.7	0.7252
10/03/04	20:00:00	2	1292	80	9.2	948	172	1092	122	1584	1203	11.0	60.0	0.7867
10/03/04	21:00:00	2	1292	51	6.5	936	131	1205	116	1490	1110	11.2	59.6	0.7868
10/03/04	22:00:00	1.6	1272	38	4.7	930	89	1205	96	1593	1049	11.2	59.6	0.7868
10/03/04	0:00:00	1.2	1193	31	3.6	690	62	1462	77	1333	733	11.3	56.8	0.7603
10/03/04	1:00:00	1.2	1185	31	3.6	690	62	1453	76	1333	730	10.7	60.0	0.7702
10/03/04	2:00:00	0.9	1094	24	2.3	699	45	1579	60	1276	1037	10.7	60.0	0.7464
10/03/04	3:00:00	0.6	1010	19	1.7	561	-200	1705	-200	1235	501	10.3	60.2	0.7517
10/03/04	4:00:00	2.00	1011	14	1.3	527	21	1818	34	1197	445	10.1	60.5	0.7465
10/03/04	5:00:00	2.07	1066	8	1.1	512	16	1818	26	1182	412	11.2	59.8	0.7368
10/03/04	6:00:00	0.7	1052	8	1.6	553	34	1738	48	1221	472	10.5	58.1	0.7353
10/03/04	7:00:00	1.1	1144	29	3.2	667	98	1629	82	1339	730	10.2	59.8	0.7417
10/03/04	8:00:00	2	1333	64	6.0	900	174	1136	112	1317	1023	11.2	59.8	0.7408
10/03/04	9:00:00	9.9	4941	a7	na	na	na	na	na	na	na	na	na	na

<b>India Air Quality</b>										<b>1. Incomplete Air Quality Parameter</b>			<b>2. Missing data</b>		
stn_code	sampling_da	state	location	agency	type	so2	no2	rspm	spm	location	mo	pm2.5	date		
150	February	M Andhra Prad	Hyderabad	NA	Residential, I	4.8	17.4	NA	NA	NA	NA	NA	01/02/90		
151	February	M Andhra Prad	Hyderabad	NA	Industrial	3.1	6.2	28.6	NA	NA	NA	NA	01/02/90		
152	February	M Andhra Prad	Hyderabad	NA	Residential, I	6.3	14.7	NA	NA	NA	NA	NA	01/03/90		
153	March	M Andhra Prad	Hyderabad	NA	Industrial	4.7	7.4	NA	NA	NA	NA	NA	01/03/90		
152	March	M03 Andhra Prad	Hyderabad	NA	Residential, I	6.4	25.7	NA	NA	NA	NA	NA	01/03/90		
150	April	MO41 Andhra Prad	Hyderabad	NA	Residential, I	5.4	17.1	NA	NA	NA	NA	NA	01/04/90		
151	April	MO41 Andhra Prad	Hyderabad	NA	Industrial	4.7	8.7	NA	NA	NA	NA	NA	01/04/90		
152	April	MO41 Andhra Prad	Hyderabad	NA	Residential, I	4.2	23	NA	NA	NA	NA	NA	01/04/90		
151	May	M0511 Andhra Prad	Hyderabad	NA	Industrial	4	8.9	NA	NA	NA	NA	NA	01/05/90		
152	May	M0511 Andhra Prad	Hyderabad	NA	Residential, I	3.6	18.6	NA	NA	NA	NA	NA	01/05/90		
150	June	M0611 Andhra Prad	Hyderabad	NA	Residential, I	3.9	14.1	NA	133	NA	NA	NA	01/06/90		
151	June	M0611 Andhra Prad	Hyderabad	NA	Industrial	5.6	11.8	NA	82	NA	NA	NA	01/06/90		
152	June	M0611 Andhra Prad	Hyderabad	NA	Residential, I	3.3	19.3	NA	111	NA	NA	NA	01/06/90		
150	July	M0719 Andhra Prad	Hyderabad	NA	Residential, I	3.9	8.2	NA	118	NA	NA	NA	01/07/90		

Fig. 1. Inconsistent and incomplete data collected from Italy Air Quality and India Air Quality

**SenseWear Pro**

Date	StartTime	Duration	Activity	ActivityType	LogType	Steps	Distance	ElevationGai	Calories
10/01/17	12:21:10	5172000	Walk	90013	auto_detect	5768	0	0	508
10/03/17	19:14:12	1792000	Walk	90013	auto_detect	2257	0	39.624	199
10/03/17	23:19:57	1787000	Walk	90013	auto_detect	2334	0	3.048	171
10/05/17	18:37:24	1075000	Walk	90013	auto_detect	175	0	0	136
10/09/17	10:55:51	7936000	Walk	90013	auto_detect	10588	0	341.376	860
10/10/17	11:27:42	5446000	Hike	90012	tracker	519	4.46707	188.976	730
10/10/17	13:16:03	4309000	Hike	90012	tracker	5477	3.71722	187.452	626
10/10/17	15:18:13	7886000	Hike	90012	tracker	15992	7.9415	185.014	1144
10/12/17	7:22:00	1178000	Walk	90013	auto_detect	1247	0	6.096	100
10/12/17	9:20:43	9736000	Walk	90013	auto_detect	1328	0	18.288	118
10/13/17	1:22:00	3520000	Walk	90013	auto_detect	482	0	9.14	343
10/13/17	13:52:22	2766000	Walk	90013	auto_detect	4147	0	243.84	357
10/14/2017	8:32:58	1587000	Walk	90013	auto_detect	2352	0	9.144	173
10/15/2017	18:11:03	1740000	Walk	90013	auto_detect	2065	0	18.288	209
10/17/2017	8:30:12	1076000	Walk	90013	auto_detect	1640	0	15.24	141
10/21/2017	19:01:08	2166000	Run	90009	tracer	5760	6.465203	46.33	460
10/21/2017	19:50:14	1126000	Walk	90013	auto_detect	2015	0	21.336	166

Data	Calories burned	Steps	Distance	Plan	Minutes of sedentary activity	Minutes of light activity	Minutes of moderate activity	Minutes of intense activity	Activity Calories
08-05-2015	1.934	905	0.00		0	1.355	46	0	0
09-05-2015	3.631	18.925	14.11		4	611	316	61	60
10-05-2015	3.204	14.224	10.57		1	602	226	14	7.119
11-05-2015	2.671	6.775	4.00		8	749	180	23	4
12-05-2015	2.495	5.02	3.75		1	876	171	0	7.26
13-05-2015	2.76	7.75	5.29		15	726	172	34	18
14-05-2015	2.687	5.614	4.17		2	782	216	13	1
15-05-2015	2.793	8.169	6.07		14	801	218	8	9.983

Fig. 2. Inconsistent and incomplete data collected from SenseWear Pro and FitBits.

Apparently, the raw sensor data such as those shown in Figures 1 and 2 are mostly semi-structured or unstructured. They exist in the forms of XML, CSV or JSON or in other markup languages that are attached with some latent meanings or descriptions which are normally incomplete and not readily understood by a computer of what it represents. Besides, they also do not conform to the formal structure of data models associated with the ontology of the smart city context. All of these collectively results in the technical barrier in combining the data for further analysis.

In the following sections, the current key data sharing and integration techniques are described and the respective limitations and weaknesses are discussed. This paper aims to highlight that the true value of smart cities can only be derived when firstly, the owner or the provider of data are willing and able to publish and share the data in a way

that is easy and secure to themselves while sufficiently meaningful to the users of the data. Secondly, the technical aspect of collating data shared from multiple sources cannot be easily achieved without the help of a data integration intermediary that extracts out the technical detail of data extraction, transformation and loading in an integrated database for analysis.

### 3 Data Sharing: Open Data Portal and Data Exchange or Marketplace

Currently, IoT data in the smart city context are generally published and shared via open data portals and data exchanges or marketplace.

#### 3.1 Open Data Portal

Open data portals allow data owners to publish and share either full data sets or metadata from multiple sources into huge, searchable databases or archives of different types of machine-readable media [14]. To date, several cities have begun to offer open data to citizens and businesses via open data portals. The open data portal approach takes the form of search tools that allow human users to filter and search the data relevant to their problems. It has been found that most of the current Open Data Initiatives are from the European Union Member States such as Brussels [15], Barcelona [16], Florence [17], Helsinki [18], Lisbon [19], and Dublin [20]. These open data portals present a broad range of downloadable “data dump” in the form of comma separated values (CSV), eXtensible Markup Language (XML), JavaScript Object Notation (JSON) open XML spreadsheet (XLXS) files or web service API access. These open data portals serve as the platforms for smart city solution providers to access data with minimal costs to develop next-generation applications [14]. Smart city open data portals with the respective data formats available and smart city applications served are summarized in Table 2.

**Table 2.** Common found data format on smart city open data portals

Smart City Domain	Data Format	Source
<b>Energy and Environment</b>	CSV, MAT, JSON, KML, FGDB, DWG, API	<a href="https://archive.ics.uci.edu/ml/datasets/Air+Quality">https://archive.ics.uci.edu/ml/datasets/Air+Quality</a> <a href="https://www.kaggle.com/shrutibhargava94/india-air-quality-data">https://www.kaggle.com/shrutibhargava94/india-air-quality-data</a> <a href="https://data.amsterdam.nl/datasets/Jlag-G3UBN4sHA/">https://data.amsterdam.nl/datasets/Jlag-G3UBN4sHA/</a> <a href="https://openei.org/datasets/dataset/uk-co2-nox-and-pm10-emissions-from-local-authorities-operations-2008-09">https://openei.org/datasets/dataset/uk-co2-nox-and-pm10-emissions-from-local-authorities-operations-2008-09</a>
<b>Mobility/Transportation</b>	CSV, Excel, GeoJSON, Fi-ware NGSI, TTL, JSON, GeoJSON, shapefile, KML	<a href="http://iot.ee.surrey.ac.uk:8080/datasets.html#traffic">http://iot.ee.surrey.ac.uk:8080/datasets.html#traffic</a> <a href="http://kolntrace.project.citi-lab.fr/#trace">http://kolntrace.project.citi-lab.fr/#trace</a> <a href="https://www.kaggle.com/sohier/uk-traffic-counts#Traffic-major-roads-km.csv">https://www.kaggle.com/sohier/uk-traffic-counts#Traffic-major-roads-km.csv</a> <a href="https://www.cs.dartmouth.edu/~dfk/papers/rawassizadeh-datasets.pdf">https://www.cs.dartmouth.edu/~dfk/papers/rawassizadeh-datasets.pdf</a> <a href="https://old.datahub.io/dataset/dft-road-traffic-counts">https://old.datahub.io/dataset/dft-road-traffic-counts</a>

<b>Building</b>	CSV, Excel	<a href="https://repository.lboro.ac.uk/articles/REFIT_Smart_Home_dataset/2070091">https://repository.lboro.ac.uk/articles/REFIT_Smart_Home_dataset/2070091</a> <a href="https://lig-getalp.imag.fr/en/health-smart-home-his-datasets-2/">https://lig-getalp.imag.fr/en/health-smart-home-his-datasets-2/</a> <a href="http://archive.ics.uci.edu/ml/datasets/energy+efficiency">http://archive.ics.uci.edu/ml/datasets/energy+efficiency</a> <a href="https://archive.ics.uci.edu/ml/datasets/UJIIndoorLoc">https://archive.ics.uci.edu/ml/datasets/UJIIndoorLoc</a>
<b>Biology/Health</b>	CSV	<a href="https://github.com/webscale/Rbitfit">https://github.com/webscale/Rbitfit</a> <a href="http://archive.ics.uci.edu/ml/datasets/Daily+and+Sports+Activities">http://archive.ics.uci.edu/ml/datasets/Daily+and+Sports+Activities</a> <a href="https://courses.media.mit.edu/2004fall/mas622j/04.projects/home/">https://courses.media.mit.edu/2004fall/mas622j/04.projects/home/</a>

### 3.2 Data Exchange or Marketplace

A data exchange or marketplace is the channel through which companies can buy and sell IoT sensor data collected [21]. Current data exchanges available in the market include Synchronicity [22], Databroker DAO [23] and Copenhagen's City Data Exchange [24]. The data can be accessed on-demand by buyers such as application developers to create new and useful services.

## 4 Data Integration Through Open Standards

The key approaches towards supporting data interoperability for IoT concentrate on the formulation of open data models and schema to encode sensor data for integration purposes. Relevant standardization efforts include the IPSO Alliance Smart Objects [25], the Sensor Model Language (SensorML) [26], the Semantic Sensor Network (SSN) ontology [27], the Web of Things Thing Description [28] and the JSON-LD [29]. However, the existence of these standards does not automatically result in interoperable systems due to the fact that the models require deliberate efforts by individual IoT systems to change their internal design to conform to the standards. The need for hooking up legacy systems with the proprietary design is also not addressed. Furthermore, without strict enforcement of any one of the many standards as the sole global standard, the IoT implementation scene remains inherently fragmented with varying standards being adopted by different practitioners.

## 5 Smart City IoT Data Sharing and Integration Model

Sampling of the abovementioned open data portals and data marketplaces found that all of them require a substantial amount of manual efforts in searching, understanding the data representation and locating the right data to be used. Moreover, additional efforts are needed to overcome the format incompatibility among the data from various sources. Among the technical challenges in sharing and integrating smart city sensor data identified are 1) the lack of a standard vocabulary to describe IoT sensor parameters in the context of smart city applications; 2) syntactic differences in the data representation format such as the date/time standard, conflict of measurement units and difference in schema; 3) missing data, redundant data and data errors. A complete and detailed discussion on the technical challenges and limitations pertaining to the existing smart city sensor data is beyond the scope of this paper.

Conventional top-down standard-based approaches dictate that the design of individual proprietary IoT systems must strictly adhere to a global data model in order for its data to be compatible and usable for data analytics on a global scale. The approach requires a tedious revamp of the design of the existing systems for standard adherence and it is unable to resolve legacy system issues. We propose to address the limitation by employing a bottom-up, publish/subscribe architecture where proprietary systems are given the liberty to maintain the original design of their systems while being able to publish and share the types of data via a standard web API such as a “REST-ful” web service. The suitability of a publish/subscribe protocol for the distribution of sensor and control data to end-users and external services is evidenced in existing IoT design [30, 31]

In this paper, an open smart city IoT sensor data sharing and integration model underpinned by an API-based cloud architecture are proposed. This model consists of the data sensing layer, the data access layer (publishing and sharing), the data integration layer and the data analysis layer, as depicted in Figure 3.

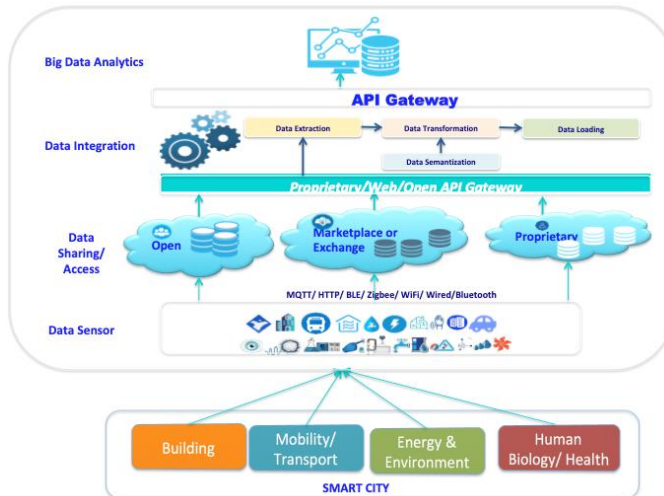


**Fig. 3.** Smart City IoT Data Sharing and Integration Model

**Data Sharing and Extraction.** The data extraction layer is responsible to extract and collate sensor data from heterogeneous sources through API. API design guideline would guide data publishers the type of data to be published such as basic metadata to describe the data they made public such as the name of the parameters, units of measurement used and acceptable ranges of continuous or nominal value(s) with minimal effort expended in changing their existing design. These data shared would then be accessed, downloaded, consolidated and stored in a central data store. The consolidated data may vary in format and complexity based on the metadata, the data type and the amount of data which will be addressed in the data transformation layer.

**Data Transformation.** The extracted data are integrated and semanticized before they are ready for high-level analysis: a) During the integration process, data from various different sources would be examined for similarities and discrepancies as well as the possible presence of data error. Duplications may be present and have to be gleaned while discrepancies are consolidated. The data are manipulated in such a way that duplicates are filtered, missing data are imputed, sorted and finally translated based on a standard format. b) After the data integration process, data is semantized by annotation with mark-ups and special properties such as tags and labels. A smart city ontology representing smart city domain knowledge and context information would be embedded with the sensor data for further processing.

**Data Loading.** The integrated and semantized data would be published via a web API for use in a data analytics software tool.

## 6 Conclusion

In this paper, the existing related work currently under progress for smart city data sharing and integration are enumerated, and the key technical challenges and limitations are identified and highlighted. A bottom-up publish/subscribe data sharing, and integration model is proposed to overcome the technical limitations in cross-domain integration of smart city data. The proposed model and architecture show a promising prospect for facilitating smart city data sharing and extraction, transformation and loading when fully implemented. A data representation scheme which is able to integrate different datasets in the raw format into a consolidated form is currently being further developed as a proof-of-concept.

## References

1. United Nation Department of Economic and Social Affairs, <https://www.un.org/development/desa/en/news/population/2018-revision-of-world-urbanization-prospects.html>, last accessed 2018/05/16.
2. Allam, Z., & Dhunny, Z. A.: On big data, artificial intelligence and smart cities. In: *Cities*, 89(November 2018), pp. 80–91. <https://doi.org/10.1016/j.cities.2019.01.032> (2019).
3. Silva, B. N., Khan, M., & Han, K.: Towards sustainable smart cities: A review of trends, architectures, components, and open challenges in smart cities. In: *Sustainable Cities and Society*, 38(August 2017), pp. 697–713. <https://doi.org/10.1016/j.scs.2018.01.053> (2018).
4. No. S. Kassim, “Smart City Initiative,” Plan Malaysia, [https://www.mcmc.gov.my/skmmgovmy/media/General/pdf/Sesi-5-Rangkakerja-Berteraskan-Aspek-Informasi-\(PLANMalaysia\).pdf](https://www.mcmc.gov.my/skmmgovmy/media/General/pdf/Sesi-5-Rangkakerja-Berteraskan-Aspek-Informasi-(PLANMalaysia).pdf), last accessed 2018/09/04.
5. Yau, K. L. A., Lau, S. L., Chua, H. N., Ling, M. H., Iranmanesh, V., & Kwan, S. C. C.: Greater Kuala Lumpur as a smart city: A case study on technology opportunities. In: 2016 8th International Conference on Knowledge and Smart Technology, KST 2016, (February), pp. 96–101. <https://doi.org/10.1109/KST.2016.7440496> (2016).
6. Villanueva-Rosales, N., Garnica-Chavira, L., Larios, V. M., Gómez, L., & Aceves, E.: Semantic-enhanced living labs for better interoperability of smart cities solutions. In: IEEE

- 2nd International Smart Cities Conference: Improving the Citizens Quality of Life, ISC2 2016 - Proceedings, pp. 1–2, <https://doi.org/10.1109/ISC2.2016.07580775> (2016).
- 7. Peris-Ortiz, M., Bennett, D., Yábar, D.: Sustainable Smart Cities: Creating Spaces for Technological, Social and Business Development. 1st ed. Springer, ISBN 9783319408958 (2017).
  - 8. Gubbi, J., Buyya, R., Marusic, S., & Palaniswami, M.: Internet of Things (IoT): A vision, architectural elements, and future directions. In: Future Generation Computer Systems, 29(7), pp. 1645–1660. Elsevier B.V, <https://doi.org/10.1016/j.future.2013.01.010> (2013).
  - 9. ATIS Data Sharing Framework for Smart Cities Report, <https://www.atis.org/smart-cities-data-sharing/>, last accessed 2019/04/20.
  - 10. Khan, Z., Anjum, A., & Kiani, S. L.: Cloud based big data analytics for smart future cities. In: Proceedings - 2013 IEEE/ACM 6th International Conference on Utility and Cloud Computing, UCC 2013, pp. 381–386. <https://doi.org/10.1109/UCC.2013.77> (2013).
  - 11. Ahlgren, B., Hidell, M., & Ngai, E. C. H.: Internet of Things for Smart Cities: Interoperability and Open Data. In: IEEE Internet Computing, 20(6), pp. 52–56. <https://doi.org/10.1109/MIC.2016.124> (2016).
  - 12. Karkouch, A., Mousannif, H., Al Moatassime, H., & Noel, T.: Data quality in internet of things: A state-of-the-art survey. In: Journal of Network and Computer Applications, 73, pp. 57–81. <https://doi.org/10.1016/j.jnca.2016.08.002> (2016).
  - 13. Rozsa, V., Denisczwiecz, M., Dutra, M., Ghodous, P., Ferreira da Silva, C., Moayeri, N., ... Figay, N.: An application domain-based taxonomy for IoT sensors. In: *Advances in Transdisciplinary Engineering*, 4, 249–258. <https://doi.org/10.3233/978-1-61499-703-0-249> (2016).
  - 14. Wang, X., Fang, Y., Liu, Y., & Horn, B.: A Survey on the Status of Open Data and Its Future. In: 4th IEEE International Conference on Universal Village 2018, UV 2018, 1–4. <https://doi.org/10.1109/UV.2018.8642128> (2019).
  - 15. Data Mobility Brussels, <https://data-mobility.brussels/>, last accessed 2019/04/20.
  - 16. Barcelona Digital City CityOS, <https://cityos.io/>, last accessed 2019/04/20.
  - 17. Open data Municipality of Florence, <http://opendata.comune.fi.it>, last accessed 2019/04/20.
  - 18. Helsinki Region Infoshare, <http://www.hri.fi/en>, last accessed 2019/04/20.
  - 19. Lisboa Aberta, <http://dados.cm-lisboa.pt/>, last accessed 2019/04/20.
  - 20. Smart Dublin, <https://data.dublinked.ie/dataset>, last accessed 2019/04/20.
  - 21. Park, J. S., Youn, T. Y., Kim, H. Bin, Rhee, K. H., & Shin, S. U. Smart contract-based review system for an IoT data marketplace. Sensors (Switzerland), 18(10), 1–16. <https://doi.org/10.3390/s18103577> (2018).
  - 22. Synchronicity IoT Data Marketplace, <https://iot-data-marketplace.com>, last accessed 2019/04/20.
  - 23. Databroker dao, [https://databrokerdao.com/](https://databrokerdao.com), last accessed 2019/04/20.
  - 24. Copenhagen Solution Labs, <https://cphsolutionslab.dk/content/2-what-we-do/3-data-platforms/3-city-data-exchange/1-learnings-from-the-city-data-exchange-project/city-data-exchange-cde-lessons-learned-from-a-public-private-data-collaboration.pdf>, last accessed 2019/04/20.
  - 25. J. Jimenez, M. Kostery and H. Tschofenig, “IP for Smart Objects - IPSO Objects,” in Iot Semantic Interoperability Workshop 2016, pp. 1-7, (2016)
  - 26. OpenGIS Sensor Model Language (SensorML) Implementation Specification, [https://portal.opengeospatial.org/files/?artifact\\_id=7927](https://portal.opengeospatial.org/files/?artifact_id=7927), last accessed 2018/09/03.
  - 27. Semantic Sensor Network Ontology, <https://www.w3.org/TR/vocab-ssn/#overview-of-classes-and-properties>, last accessed 2018/09/03.

28. Web of Things (WoT) Thing Description, W3C, <https://w3c.github.io/wot-thing-description/>, last accessed 2018/09/03.
29. W3C JSON-LD, W3C, <http://www.w3.org/TR/json-ld/>, last accessed 2018/09/03.
30. Daniel H., Niels K., Thomas M., & Vlado H.: Meeting IoT Platform Requirements with Open Pub/Sub Solutions, In: *annals of telecommunications*, 72(1-2), pp. 1-11, <http://doi.org/10.1007/s12243-016-0537-4> (2016)
31. Vavassori S., Soriano J., & Fernández R.: Enabling Large-Scale IoT-Based Services throughElastic Publish/Subscribe, In: *Sensors* 17(9), pp. 1-19, <http://doi.org/10.3390/s17092148> (2017)
32. Plageras, A. P., Psannis, K. E., Stergiou, C., Wang, H., & Gupta, B. B. Efficient IoT-based sensor BIG Data collection processing and analysis in smart buildings. *Future Generation Computer Systems*, 82, 349–357. <https://doi.org/10.1016/j.future.2017.09.082> (2018).
33. Linder, L., Vionnet, D., Bacher, J. P., & Hennebert, J. Big Building Data-a Big Data Platform for Smart Buildings. *Energy Procedia*, 122, 589–594. <https://doi.org/10.1016/j.egypro.2017.07.354> (2017).
34. Shah, J., & Mishra, B. Customized IoT Enabled Wireless Sensing and Monitoring Platform for Smart Buildings. *Procedia Technology*, 23, 256–263. <https://doi.org/10.1016/j.protcy.2016.03.025> (2016).
35. Rathore, M. M., Paul, A., Hong, W. H., Seo, H. C., Awan, I., & Saeed, S. Exploiting IoT and big data analytics: Defining Smart Digital City using real-time urban data. *Sustainable Cities and Society*, 40(August 2017), 600–610. <https://doi.org/10.1016/j.scs.2017.12.022> (2018).
36. Csaji, B. C., Kemeny, Z., Pedone, G., Kuti, A., & Vancza, J. Wireless Multi-Sensor Networks for Smart Cities: A Prototype System with Statistical Data Analysis. *IEEE Sensors Journal*, 17(23), 7667–7676. <https://doi.org/10.1109/JSEN.2017.2736785> (2017).
37. Rozsa, V., Denisczwiecz, M., Dutra, M., Ghodous, P., Ferreira da Silva, C., Moayeri, N., ... Figay, N. An application domain-based taxonomy for IoT sensors. *Advances in Transdisciplinary Engineering*, 4, 249–258. <https://doi.org/10.3233/978-1-61499-703-0-249>, (2016).
38. Hancke, G. P., de Silva, B. de C., & Hancke, G. P. The role of advanced sensing in smart cities. In *Sensors* (Switzerland) (Vol. 13). <https://doi.org/10.3390/s130100393> (2013).
39. Haghi, M., Thurow, K., & Stoll, R. Wearable devices in medical Internet of things: Scientific research and commercially available devices. *Healthcare Informatics Research*, 23(1), 4–15. <https://doi.org/10.4258/hir.2017.23.1.4> (2017).



# Estimating Material Parameters Using Light Scattering Model and Polarization

Hadi A. Dahlan<sup>1</sup>, Edwin R. Hancock<sup>2</sup> and William A. P. Smith<sup>2</sup>

<sup>1</sup>National University of Malaysia, 43600 UKM Bangi, Selangor, Malaysia

<sup>2</sup>University of York, Deramore Lane, York YO10 5GH, UK

had86@ukm.edu.my, edwin.hancock@york.ac.uk,

william.smith@york.ac.uk

**Abstract.** When rendering the 3D graphics object in the computer vision and graphics fields, the parameter values, such as the surface roughness, refractive index, and light absorption are used for modeling realistic light scattering rendering behavior of a material. Most of these values were usually obtained from different literature or online sources. In general, a specific measuring tool is needed when acquiring the measurement, but, what if we could use an alternative method of measuring when the tools are not available? The idea is to use the light scattering model to estimate the parameter measurement values of material by doing the inverse rendering of the capture polarization image of the object's light scattering. In this paper, we investigate whether we can estimate four different measurements, using ARLLS model. We captured the object's degree of polarization (DOP) to be fitted and compare with the model to investigate the relationship between the two by doing the correlation test between the object measurement DOP and the model parameters to see whether the estimations are in agreement with each other (e.g. by reference or by the practical characteristics of the object). Furthermore, the test will be conducted using materials with varying degree of properties (e.g. very rough surface; highly chromatic).

**Keywords:** Light scattering model, Measurement estimation, Light polarization, Correlation test

## 1 Introduction

In computer vision and graphics, the light scattering modeling is one of the main studies done by these fields. It is a study where generally a 3D object is rendered using specific parameter values to create a realistic light scattering behavior when applying on a specific model. It is mainly used for either simulation or entertainment purposes. The light scattering model might consist of one or more parameters based on the authors aim for the model. However, most authors referred different sources for the parameter values when using it with their light scattering model; sources such as from other literature or the internet. Most of the parameters that they used for their models, such as the surface roughness, refractive, and light absorption have to use multiple different measuring tools which can be difficult due to unavailability or cost. It would be interesting to

estimate these measurements using the light scattering model in an inverse manner. If the estimation of the measurements is closely accurate to the real measurements, this can be an alternative method of measuring the values without the use of specializing measuring tools. The possible application of this method of measurements is that for certain materials, researcher will not need to extract some part of material to be measured - such as when measuring the refractive index of a substance like human skin; the researcher would not need to do it *in vitro* (e.g. extracted cell from the skin), instead, the researcher can directly measure the skin value of the refractive index using the light scattering model. In this paper, we aim to investigate whether our light scattering model, which is the absorptive rough laminar light scattering model (ARLLS), whether it can estimate an accurate measurement of four chosen parameters (surface and sub-surface roughness; light absorption; and refractive index). However, due to equipment and resource limitation, the author decided to use the degree of polarization (DOP) of the materials to compared and analyzed the agreement between the measurements and the estimated parameter. The relationship between the two is compared and analyzed by first completing a correlation test between the object measurement (DOP) and the model parameters to see whether the estimations are in agreement with each other (e.g. by reference or by the practical characteristics of the object).

## 2 Literature Review

Before attempting on using a model for estimating a material characteristic, it is crucial to know first about the light reflectance/scattering model. In past decades, authors from the computer vision and graphics fields have designed many different light reflectance/scattering models based on statistical and analytic discoveries. This helps current animators tremendously in their efforts to render realistic looking objects (and even human) in their films. Most of these models need specific parameter(s) values for them to produce the desired radiance output. These values were usually obtained by either measured directly or based on other literature.

The purpose of the general reflectance model is to characterize the directional distribution of the reflectance of a certain material using physical models that are suitable for the design of efficient global illumination computation algorithms. Reflection is a process during which an electromagnetic power flux travels incidentally towards a point of a surface and leaves that point without any change in frequency. The function that is used to model this phenomenon is called the Bidirectional Reflectance Distribution Function (BDRF) [1-3]. The BRDF is the ratio of the quantities of the reflected light from the outgoing direction, to the amount of incident light that reaches the point at the surface from the incoming direction. However, in the real world, the light reflection depends on the characteristics of the light, and the composition of the material, and its physical traits.

In modeling natural reflectance, there are many properties that need to be considered, such as retro-reflection, occluding, isotropic or anisotropic surface, and conservation of energy. It is difficult to design a model that covers all of the properties that affect the behavior of light. So, most authors design their model to focus on a specific goal

instead, each with their own formulation, conditional setup, and applicability [1, 4-8].

Ragheb and Hancock (R-H) [7] first attempted to create a light scattering model based on the Beckmann–Kirchhoff model for moderately rough surfaces by adding the Fresnel term to describe the subsurface scattering effects for surfaces of intermediate roughness. R-H used two variant correlation functions, the Gaussian and the Exponential, to derive closed-form solutions for the process of light scattering from random rough surfaces. R-H continued to test their model in [9], where they showed that their modified model was able to give a good estimation of the surface roughness parameters for dielectric surfaces using the pixel brightness measurements obtained from a digital camera.

Later, R-H further improved their model in [10] by extending their previous modified model from [7, 9] so that it would work on rough, laminar surfaces for dielectrics. Here, the model scattering geometry of the material is split into two layers, namely the surface layer and the subsurface layer.

Afterward, Hadi–Hancock extended the R-H model even further to include a light absorption function, in which we will name it here as the absorptive rough laminar light scattering (ARLLS) model [11]. The authors designed it for the purpose of observing the effectiveness of the model as a light scattering model when light absorption term is included and also to compare it with the previous R-H model [10]. In this paper, the ARLLS model will be used to conduct our experiment, which is to observe whether we can estimate multiple different measurements close to the material physical properties; using a light scattering model as an alternative to the standard measuring tools.

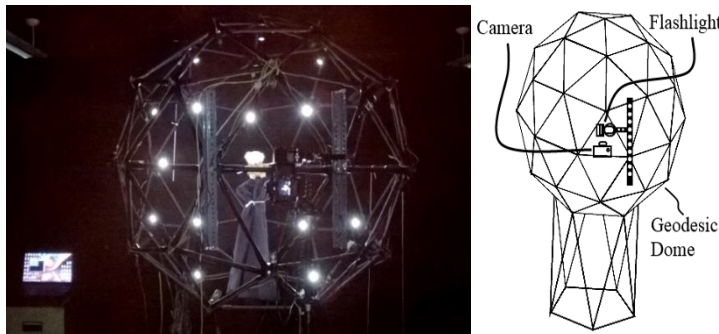
### 3 Methodology

The selected parameters of the ARLLS model need to have a rational relationship with the sample materials. Due to the difficulty of obtaining real measurements such as the surface roughness (need roughness measuring instrument), a different comparing method is used. This is done by comparing the light scattering with that of the material's polarization state. It was known that polarization is directly related to how a material scatters light. The material properties such as surface roughness, subsurface roughness, and light absorption can directly affect how the polarization of the material will behave [12-17]. To validate the model parameter relation with the material's known measurement, the author decided to use the degree of polarization (DOP) as the material's measurement. The relationship between the two is analyzed by doing a correlation test. Furthermore, the test will be conducted using materials with varying degree of properties (e.g. very rough surface; highly chromatic). This is to observe whether the model can estimate the parameters as closely as the material physical properties (logically) and for varying type of materials. Table 1 shows how the model parameters can be related to the material. Here, the test will be conducted on all RGB channels because the model does depend on the light wavelength.

**Table 1.** The ARLLS model parameters relation to the subject material.

Parameter	Relation
<b>Surface slope (<math>\sigma/T</math>) and Subsurface slope (<math>\sigma'/T'</math>)</b>	Both are the components of surface and subsurface texture. They are quantified by the deviations in the direction of the normal vector of a real surface from its ideal form.
<b>Refractive index (<math>n</math>)</b>	Value calculated from the ratio of the speed of light in a vacuum to that in a second medium of greater density; used for a particular substance, confirm its purity or measure its concentration.
<b>Balance Parameter (<math>\beta</math>)</b>	The parameter $\beta$ control which two components (surface or subsurface) scatter the light the most. In the physical term, this parameter basically describes how the light incident is scattered either by the surface or through subsurface interactions.
<b>Light absorption (<math>a</math>)</b>	The intensity of light absorbed after it passes through a sample.

In this test, the DOP is calculated using Zhang and Hancock's comprehensive polarization reflectance model [18]. Furthermore, to obtain the necessary angle measurements from the object material, the diffuse normal map is captured using the Ma et al. [19] spherical gradient illumination technique and a geodesic dome light stage. Here, two light sources were used, namely a) ultra-bright white LEDs and b) a flash lamp. A thorough setup can be referred to [19, 20]. Figure 1 shows an image of the geodesic light stage used for this experiment and its diagram.

**Fig. 1.** The geodesic dome light stage used in the experiment (left) and its diagram (right).

### 3.1 The ARLLS model

The absorptive rough laminar light scattering model (ARLLS) is a modified version of the R–H model [10] and have been proposed in [11]. The authors for the R–H model defined two different correlation functions models, which are: 1) the Gaussian correlation function and 2) the Exponential correlation function. Here, only the Exponential will be used for this experiment. The ARLLS model extends the R–H model by adding an absorption term; defining it using the conservation of energy for light transmission,

reflectance, and absorption. Moreover, the absorption parameter is unit-less and can be used as an alternative representation for light absorption in a dielectric. For the model equations, the surface scattering equation for the ARLLS model is similar to the R–H model [10]. However, the subsurface scattering component for the ARLLS model version added an absorption equation in which it extends the R–H model subsurface scattering component. The ARLLS subsurface radiance when the correlation function is Exponential is then given by:

$$L_E^{sb}(\theta_i, \theta_s, \phi_s, \sigma'/T', n) = L_E^{sf}(\theta_i, \theta_s, \phi_s, \sigma'/T') \\ \times [1 - f(\theta_i, n) - Ab(a, \theta_i)] \left[ 1 - f\left(\theta'_s, \frac{1}{n}\right) - Ab(a, \theta_{s2}) \right] d\omega' \quad (1)$$

The ARLLS model's thorough equation description and definition can be referred from the paper [11].

### 3.2 Comprehensive polarization reflectance model

In the field of computer vision, Fresnel Theory is generally used to predict how polarized light interacts with a surface. The theory has other applications, such as reflectance component separation, surface analysis and surface normal recovery [18, 19, 25, 26]. The equation for the DOP curve here is referred from Zhang and Hancock [18]. The standard equation for the degree of polarization (DOP)  $\rho$  is:

$$\rho = \frac{I_{max} - I_{min}}{I_{max} + I_{min}} \quad (2)$$

Here,  $I_{min}$  and  $I_{max}$  denote the minimum and maximum intensity values in the polarised images. In the experiment,  $I_{min} = I_{cross-polarized}$  and  $I_{max} = I_{co-polarized}$ . The  $I_{cross-polarized}$  is an image of an object captured when the light source (camera flash) polarizer filter oriented in  $0^\circ$  angle and the camera polarizer filter oriented in  $90^\circ$ , while the  $I_{co-polarized}$  is when both the light source and the camera polarizer filter are oriented in  $0^\circ$  angle. Another to note that  $I_{cross-polarized} = I_{diffuse}$  and  $I_{co-polarized} = I_{diffuse} + I_{specular}$ , where  $I_{diffuse}$  and  $I_{specular}$  are the diffuse and specular reflectance components of the image respectively. Each object was illuminated in the camera viewing direction. To obtain the polarization curve, the  $I_{min}$  and  $I_{max}$  in equation 2 need to be replaced with the Fresnel coefficients as to relate the  $\rho$  to the zenith angle  $\theta$ . Giving that  $L_1 = L_{specular} \frac{R_{||}(n,\theta)}{R_{\perp}(n,\theta) + R_{||}(n,\theta)}$  and  $L_2 = L_{diffuse} \frac{R_{||}(1/n,\theta) - R_{\perp}(1/n,\theta)}{R_{\perp}(1/n,\theta) + R_{||}(1/n,\theta) - 2}$ , the new polarization model (referring from [18]) then becomes:

$$\rho = \frac{L_1 + L_2}{L_{diffuse} + L_1} \quad (3)$$

The zenith angle is required for the calculation of the material's  $\rho$ . For this, we used the Ma et al. [19] normal maps acquisition method. The incident and viewing angles

are calculated by converting the material's estimated normal map vectors into angles using [9] conversion. Both the light source and the camera were positioned to be the same. These angles are later used in the model data fitting for estimating the material's scattering parameters and also the  $\rho$ .

### 3.3 Comprehensive polarization model fitting procedure and the refractive index estimation.

There are sixteen samples captured for this experiment. Most of them are color samples with medium to rough surface and some of the leaves are multilayered. To obtain the material's DOP curve for the correlation test, Zhang–Hancock model [18] is used to fit the DOP data of the material, which is first calculated using the  $I_{co-polarized}$  and  $I_{cross-polarized}$  (see Equation 2). Figure 2 shows the several DOP samples images calculated using the green channel. In Zhang–Hancock model, there are three parameters need to be considered: the two radiance  $L_{specular} = L_s$  and  $L_{diffuse} = L_d$ , and the refractive index  $n$  (see Equation 3). Since the total radiance is a sum of specular and diffuse radiance  $L_s + L_d = 1$ , the author presumed that the specular radiance  $L_s = 1 - L_d$ . The fitting process is completed using the Matlab's nonlinear least square function with 25 maximum evaluation while using the trust-region-reflective algorithm as the optimization option. The test was done on each RGB channels; using 1100 random data points with selected angles between  $0^\circ - 75^\circ$ . Selected data with similar angles were averaged before the normalization process. Using the exhaustive method, the search for the best-fit is done by minimizing the root-mean-squared error  $\Delta_{RMS\rho}$  by varying the parameters of  $L_d$  and  $n$ . The ranges for the parameters used in the experiment are  $L_d$  which ranges from (0 to 1) and  $n$  which range from (1 to 2.5). The RMS fitting error for the  $\rho$  is given by:

$$\Delta_{RMS\rho} = 100 \times \frac{1}{K} \left\{ \sum_{k=1}^K [\rho_m(\theta^k) - \rho_p(\theta^k, L_d, n)]^2 \right\}^{\frac{1}{2}} \quad (5)$$

where  $\rho_m$  is the normalized data,  $\rho_p$  is the normalized DOP from the model prediction and  $k$  runs over the index number of the measurements used ( $K$ ).



**Fig. 2.** The  $\rho$  images for three samples. Start from the left: Apple; Clay Pot; and Grapefruit. Calculated from the green channel of the images.

There were several limitations when conducting the experiment. The first is that the data samples  $> 75^\circ$  angles were not included in the test due to the high measurement error that exists on most of the collected samples. Additionally, due to a high error measurement for the wood sample, resulting from human error, it was not included in the correlation test.

## 4 Results

### 4.1 The refractive index result and discussion

Comparing the estimated refractive index  $n$  with the reference data, it was observed that some samples were estimated over or under the reference range values (see Table 2). If the lowest point of the curve decreases or increases in value, so does the estimation of  $n$ . The estimation of  $n$  using the Zhang–Hancock model can result in some discrepancies between the reference value and the estimated refractive index when dealing with rough surfaces, translucence and/or color coated materials. Most of the samples used for this experiment featured one or more of these characteristics.

**Table 2.** The refractive index  $n$  estimation using the comprehensive polarization model.

Samples	$n_{ref}$	$n_r$	$n_g$	$n_b$
Blue Rubber Ball	1.50-1.59 [27]	1.39	1.27	1.28
Orange Plastic Ball	1.49-1.50 [28]	1.05	1.08	1.30
White Polystyrene	1.55-1.59 [29]	1.47	1.38	1.34
Wood Cube	1.47-1.48 [28]	2.14	2.30	2.42
Brown Clay Teapot	1.47-1.68 [30]	1.14	1.11	1.32
Brown Cloth	1.51-1.71 [31]	1.15	1.17	1.45
Big Leaf 1	1.41-1.60 [32-34]	1.51	1.35	1.81
Big Leaf 2	1.41-1.60 [32-34]	1.12	1.02	1.29
Big Leaf Dry 1	1.41-1.60 [32-34]	1.16	1.23	1.55
Big Leaf Dry 2	1.41-1.60 [32-34]	1.15	1.16	1.35
Banana	1.41-1.60 [32-34]	1.25	1.38	1.61
Green Apple	1.41-1.60 [32-34]	1.50	1.46	1.83
Small Leaf	1.41-1.60 [32-34]	2.15	1.97	2.33
Small Leaf Dry	1.41-1.60 [32-34]	1.20	1.21	1.55
Small Leaf Hydrate	1.41-1.60 [32-34]	1.23	1.03	1.49
Yellow Grapefruit	1.41-1.60 [32-34]	1.25	1.30	1.63

### 4.2 The model parameter estimation results

The estimated  $n$  from the DOP model was used in the new scattering model fitting test. In circumstances where the  $n$  is not in the range of the reference, the proposed model is not particularly sensitive to the choice of the refractive index, so using the estimated values is acceptable. Additionally, for this test, the roughness parameters for the upper and lower boundaries of the scattering model are assumed identical  $\sigma/T = \sigma'/T'$ . Table 3 shows the ARLLS model  $\Delta_{RMS}$  and their estimated parameters for 15 samples (wood was excluded due to high data variance), when performed on red, green and blue channels.

**Table 3.** Estimated Parameters for the ARLLS model (Here the surface slope  $\sigma/T = \sigma'/T'$ ). The rows highlighted in gray are samples that obtained  $\Delta_{RMS} < 0.15$  for all color channels.

Samples	Red				Green				Blue			
	$\Delta_{RMS}$	$\sigma/T$	$\beta$	$a$	$\Delta_{RMS}$	$\sigma/T$	$\beta$	$a$	$\Delta_{RMS}$	$\sigma/T$	$\beta$	$a$
Blue Rubber Ball	0.208	0.440	0.505	0.743	0.206	0.566	0.396	0.935	0.238	1.218	0.266	0.718
Orange Plastic Ball	0.233	1.804	0.378	0.767	0.125	0.600	0.902	0.836	0.081	0.340	0.290	0.972
White Polyester	0.176	0.471	0.384	0.718	0.172	0.486	0.323	0.783	0.161	0.493	0.287	0.821
Brown Clay Teapot	0.178	0.623	0.302	0.894	0.168	0.383	0.317	0.893	0.174	0.456	0.480	0.596
Brown Cloth	0.314	0.674	0.502	0.678	0.293	0.648	0.352	0.832	0.250	0.652	0.289	0.849
Big Leaf 1	0.152	0.470	0.380	0.782	0.286	0.430	0.495	0.789	0.180	0.507	0.251	0.901
Big Leaf 2	0.128	0.718	0.430	0.771	0.222	1.750	0.127	0.075	0.119	0.694	0.315	0.812
Big Leaf Dry 1	0.223	0.800	0.452	0.655	0.238	0.549	0.447	0.809	0.084	0.480	0.300	0.850
Big Leaf Dry 2	0.311	1.606	0.127	0.858	0.319	1.533	0.154	0.866	0.235	0.959	0.292	0.934
Banana	0.174	1.156	0.310	0.768	0.156	0.900	0.406	0.740	0.093	0.691	0.318	0.890
Green Apple	0.118	0.402	0.276	0.731	0.115	0.520	0.188	0.937	0.125	0.396	0.243	0.307
Small Leaf	0.193	0.773	0.352	0.862	0.181	0.892	0.301	0.929	0.190	0.794	0.339	0.832
Small Leaf Dry	0.164	0.983	0.361	0.664	0.146	0.672	0.396	0.758	0.150	0.634	0.292	0.712
Small Leaf Hydrate	0.057	0.712	0.432	0.617	0.091	0.834	0.477	0.471	0.109	0.764	0.286	0.452
Yellow Grapefruit	0.077	0.556	0.313	0.841	0.070	0.486	0.304	0.846	0.077	0.425	0.282	0.398

**Table 4.** Correlation between the DOP  $\rho$  and the estimated parameters for the model at five specific angle range.

Parameters	$0^\circ - 15^\circ$	$16^\circ - 30^\circ$	$31^\circ - 45^\circ$	$46^\circ - 60^\circ$	$61^\circ - 75^\circ$
$\sigma/T$	-0.276	-0.267	-0.242	-0.238	-0.327
$\beta$	-0.273	-0.255	-0.214	-0.203	-0.252
$a$	0.068	0.071	0.075	0.075	0.091

Table 4 shows the correlation results. In practice, surface roughness and absorption can cause depolarization to polarized incident light. It would hypothesize that the model's roughness parameter  $\sigma/T$  should have a negative relationship with the sample's  $\rho$  value since increasing roughness would likely depolarize polarized light even more. Interestingly, evidence of this behavior did emerge from the measurement. For example, a smooth surface apple with low  $\sigma/T$  (small scattering of light) was shown to have higher  $\rho$ , while a less smooth surface, like grapefruit, having high  $\sigma/T$  than the apple (wide scattering of light) was shown to have lower  $\rho$ . This suggests that the behavior of the model's  $\sigma/T$  parameter is in agreement with the surface roughness effects on the material's DOP [12-17]. Meanwhile, the model's absorption,  $a$ , should have a positive relationship with the sample's  $\rho$  value, because high absorption levels would produce low diffuse radiance. Even though  $a$  and  $\rho$  have a positive correlation for the model, the correlation coefficients result are not significant ( $p > 0.2$ ). The correlation between  $\beta$  and  $\rho$  suggested a negative correlation, which means that as the model's lower boundary component becomes more dominant (e.g.  $\beta > 0.5$ ), the  $\rho$  value will become lower. This result follows the diffuse polarization process state from [6], which asserts that incident light that penetrates a surface material will result in internal scattering and, later, refract back into the air, ultimately becoming partially polarized (hence lower  $\rho$ ). The significant here is that table 3 and 4 also provide means to validate the literature regarding light scattering (and polarization) behavior on most dielectric material, such as the strength of the polarization effects due to the different

in surface roughness of the material [12-17] and will especially help in the accurate diagnosis and simulation of various biological material such as plants and skin.

## 5 Conclusion

The results of this experiment regarding correlation have suggested that the parameters of the proposed scattering model can be related to the sample measurements and physical characteristics. These parameters are the roughness parameter  $\sigma/T$ , the balance parameter  $\beta$ , and the absorption parameter  $a$ . Moreover, the results from Table 3 and 4, have shown that the model parameter estimation of leaves and fruits samples obtained  $\Delta_{RMS} < 0.2$ , indicating that the new models can be used to estimate parameters for biological type samples quite accurately. This is important when trying to estimate parameters for biological samples for the purpose of statistical analysis. Meanwhile, the refractive index  $n$  estimate values are different when compare with the reference of the selected materials. This may be due to the differences in measuring/estimating the materials refractive index. The reference obtained their measurements by using a refractometer on a small part of the material separated from the whole (e.g. *in vitro*), while the model estimation of the material's  $n$  is done directly on the material (e.g. *in vivo*). In overall, this study shows a possible implication for future study on the alternative method of measuring and also the study of the acquisition of parameter values for light scattering/reflectance models.

## References

1. Montes, R., & Urea, C. (2012). An overview of BRDF models. University of Grenada, Technical Report LSI-2012, 1.
2. Chen, C. H. (2015). Handbook of pattern recognition and computer vision. World Scientific.
3. Wynn, C. (2000). An introduction to BRDF-based lighting. Nvidia Corporation.
4. Thompson, W., Fleming, R., Creem-Regehr, S., & Stefanucci, J. K. (2016). Visual perception from a computer graphics perspective. AK Peters/CRC Press.
5. Kurt, M., & Edwards, D. (2009). A survey of BRDF models for computer graphics. ACM SIGGRAPH Computer Graphics, 43(2), 4.
6. Wolff, L. B. (1994). Diffuse-reflectance model for smooth dielectric surfaces. JOSA A, 11(11), 2956-2968.
7. Ragheb, H., & Hancock, E. R. (2006). Testing new variants of the Beckmann Kirchhoff model against radiance data. Computer Vision and Image Understanding, 102(2), 145-168.
8. Guarnera, D., Guarnera, G. C., Ghosh, A., Denk, C., & Glencross, M. (2016, May). BRDF representation and acquisition. In Computer Graphics Forum (Vol. 35, No. 2, pp. 625-650).
9. Ragheb, H., & Hancock, E. R. (2007). The modified Beckmann Kirchhoff scattering theory for rough surface analysis. Pattern Recognition, 40(7), 2004-2020.
10. Ragheb, Hossein, and Edwin R. Hancock. "A light scattering model for layered dielectrics with rough surface boundaries." International Journal of Computer Vision 79.2 (2008): 179-207.
11. Dahlan, Hadi A., and Edwin R. Hancock. "Absorptive scattering model for rough laminar surfaces." Pattern Recognition (ICPR), 2016 23<sup>rd</sup> International Conference on. IEEE, 2016.

12. Konnen, G. P., & Knennen, G. P. (1985). Polarized light in nature. CUP Archive.
13. Barron, L. D. (2009). Molecular light scattering and optical activity. Cambridge University Press.
14. Perez, J. J. G., & Ossikovski, R. (2016). Polarized light and the Mueller matrix approach. CRC press.
15. Kerker, M. (2016). The Scattering of Light and Other Electromagnetic Radiation. Elsevier.
16. Goldstein, D. H. (2017). Polarized Light. CRC Press.
17. Bohren, C. F., & Huffman, D. R. (2008). Absorption and scattering of light by small particles. John Wiley & Sons.
18. Zhang, L., & Hancock, E. R. (2012, November). A comprehensive polarisation model for surface orientation recovery. In Proceedings of the 21st International Conference on Pattern Recognition (ICPR2012) (pp. 3791-3794). IEEE.
19. Ma, Wan-Chun, et al. "Rapid acquisition of specular and diffuse normal maps from polarized spherical gradient illumination." Proceedings of the 18th Eurographics conference on Rendering Techniques. Eurographics Association, 2007.
20. Dutta, Abhishek. "Face Shape and Reflectance Acquisition using a Multispectral Light Stage." Diss. University of York, 2010.
21. Jensen, J. R. (2009). Remote sensing of the environment: An earth resource perspective 2/e. Pearson Education India.
22. Lillesand, T., Kiefer, R. W., & Chipman, J. (2014). Remote sensing and image interpretation. John Wiley & Sons.
23. Govaerts, Y. M., Jacquemoud, S., Verstraete, M. M., & Ustin, S. L. (1996). Three-dimensional radiation transfer modeling in a dicotyledon leaf. Applied Optics, 35(33), 6585-6598.
24. Stimson, H. C., Breshears, D. D., Ustin, S. L., & Kefauver, S. C. (2005). Spectral sensing of foliar water conditions in two co-occurring conifer species: *Pinus edulis* and *Juniperus monosperma*. Remote Sensing of Environment, 96(1), 108-118.
25. Zhang, L., & Hancock, E. R. (2013). Robust estimation of shape and polarisation using blind source separation. Pattern Recognition Letters, 34(8), 856-862.
26. Atkinson, G. A., & Hancock, E. R. (2006). Recovery of surface orientation from diffuse polarization. IEEE transactions on image processing, 15(6), 1653-1664.
27. McPherson, A. T., & Cummings, A. D. (1935). Refractive index of rubber. Rubber Chemistry and Technology, 8(3), 421-429.
28. Mikhail Polyanskiy. RefractiveIndex.INFO - Refractive index database. <https://refractiveindex.info>, 2018. [Online; accessed March 26, 2018].
29. Index of Refraction. <http://hyperphysics.phy-astr.gsu.edu/hbase/Tables/indrf.html>, 2018. [Online; accessed March 26, 2018].
30. Mukherjee, S. (2013). Physical Properties of Clay and Soil Mechanics. In The Science of Clays (pp. 54-68). Springer, Dordrecht.
31. Perry, D. R., Appleyard, H. M., Cartridge, G., Cobb, P. G. W., Coop, G. E., Lomas, B., ... & Farnfield, C. A. (1985). Identification of textile materials.
32. Woolley, J. T. (1971). Reflectance and transmittance of light by leaves. Plant physiology, 47(5), 656-662.
33. Forest B. H. Brown. (1920). The Refraction of Light in Plant Tissues. Bulletin of the Torrey Botanical Club, 47(6), 243-260. doi:10.2307/2480396
34. Gausman, H. W., Allen, W. A., & Escobar, D. E. (1974). Refractive index of plant cell walls. Applied optics, 13(1), 109-111.



# Workplace Document Management System Employing Cloud Computing and Social Technology

Alfio I. Regla and Praxedis S. Marquez

Technological Institute of the Philippines, 363 P. Casal St., Quiapo, Manila  
alibanalreal6@gmail.com, p.marquez@tip.edu.ph

**Abstract.** This study is focused on implementing a document management system for Romblon State University, Cajidiocan Campus, Romblon, Philippines. To date, most Higher Education Institution like the Romblon State University generates the bulk of documents of several types like feedback reports, minutes of the meeting, syllabi, lesson plans, policies, memos, and other circulars. These documents are often stored in filing cabinets and are used as compiled evidence for accomplishment reports or accreditation purposes. With such, the school is faced with problems like storage space, document security and sharing of documents when needed. For such reasons, this study will support the facilitation of easy access to documents using social technology across the academic organization as well as providing a larger storage space through cloud computing. Furthermore, the study was designed to 1] track, manage and store documents digitally, 2] to keep records of various versions which were created or revised by different users and 3] to employ social technology to increase staff collaboration skills and work efficiency. To construct the study, the researchers made use of several fact-finding techniques and an Agile methodology. It used a total population of purposive sampling to attain 100% confidence in evaluating the performance of the system through user-acceptance testing. Through evaluation, the respondents scored the developed system with a mean of 4.94, which exhibits that the respondents strongly agree with the capabilities of the developed system and that it is responsive to their needs. It was then concluded that the study was able to allow users to manage their documents socially and provide larger space of storage.

**Keywords:** Document Management System, Cloud Computing, Control Versioning, Social Technology, Tracking System

## 1 Introduction

One factor that would increase productivity and promote fast solutions in a workplace is when employees intend to work together. To date, mobility is important for professionals to accomplish everyday tasks alongside with the capability to access important files and documents. These maybe in the form of collaborative activity feedback reports, approved policies, memos, requests, payrolls and applications. In most entities, documents are the building blocks of daily operations which entail reviews and

approval administrative functions. It does play a central role in administering proper delivery of services as well as operational decision making. In a learning institution like the Romblon State University (RSU) in Romblon, Philippines, management of documents is as important as delivering services to students and other stakeholders. However, like other entities, problems of file organization, storage, security and tracking are also experienced by RSU. Such constraint often causes loss of documents, working on wrong versions and other data privacy issues. To address such issues, the developed system aims to 1] track, manage and store documents digitally, 2] to keep records of various versions which were created or revised by different users and 3] to employ social technology to increase staff collaboration skills and work efficiency.

This study will support easy access to documents using social technology across the academic organization as well as providing a larger storage space through cloud computing. The social technology that was utilized will upkeep the need of every Department Heads and Unit Officers to collaborate in creation, reviewing and approval of documents. It will provide the opportunity to users to share files, to work together, to participate and to communicate their ideas. Also, the study will provide security features such as allowing different levels of access to specific documents for ensuring that sensitive information are safe. In conjunction, the system will allow users to preserve versions of created documents for historical tracking thus, reducing the occurrence of working on the wrong versions of files.

Moreover, the development of a document management system for a workplace like Romblon State University will help speed up their workflow, improve staff productivity, secure information, reduce storage spaces and improve customer services.

## 2 Related Works

### 2.1 Document Management

In the study of [5], developed a web-based document management system use as a repository and to tracks the required thesis document submitted by the graduating students. This online database system was motivated by the previous paper-based submission process. The system is significant for the graduating students to search and tracks the requirement process and its dateline for submitting processes. Moreover, for the faculty, as the administrator can update the status of a submission, can send a notification, create and delete the announcement.

In the study of [6], proposed a prototype of a document management system that utilized a cloud as storage. This is to help the validation of any scientific paper made by the faculty at the University of Udayana. The designed prototype provides a central repository of the faculty and university level work file. Moreover, the system challenges to solve the validation of a document with efficient management on the storages medium.

In the study of [3], proposed the “Intranet-Based Document Management and Monitoring System” exclusively in National University was based on the response of the target users. The feature of the system allowed the Institution to store, manages, update and securely monitors documents that go in and out of the office. The web-based

document management system designed by [7], provides access to authorized users anywhere, anytime using any device as long as there is an Internet connection. The features offered by the system are document uploading, file versioning, metadata creation that maintain redundancy of file and security. The document management system (DMS) by [8] designed for the small and medium storage which do not have enough funds to develop a regular functional DMS. The system utilized the use of Open Source Software components in the development and can offer low-cost web services. The system is basically written in Japanese as the initial target is an Institution in Japan.

## 2.2 Document Revision Control

Version control system (VCS) is significant features for software development and document management [10]. In the study of [11], explains the importance of document version control which the modification detection is in managing document. This study shows reasons probably happen on modifying the content of the document. As the content changes possible also to change document size, it's either grow or reduce, second if the document content changes new version of the same document is created.

## 2.3 Social Technology in Document Handling

In the study of [12], shows that an integration of social technology like collaboration system helps to monitors users' participations and publishes this interaction among authorized members most likely on doing a group project works. The document editor program on the study of [13], provides a collaborative user environment. This editor integrated relevant functional features for the user to do collaborative documents. It also provides a monitoring function for the users every time there is modification to the collaborative document. This monitoring feature provides the authors timely update and accurate status every time there is a modification on the document.

To sum-up, in order for the researcher to achieve the objectives of the study, the researchers gathered several literatures and studies related to the topic. Based on the gathered related literatures, document management systems are usually crafted using several tools and technology. One of the tools mentioned, is the use of Internet-based technology and cloud computing technology. Cloud computing technology is a computer resource that provides a vast digital storage area for files or documents. This will help the researcher provide solutions in terms of document storage for Romblon State University (RSU).

Also, to seek answers on several challenges in the existing procedures of document handling, the researchers considered the use of document version control features to keep track of modifications made by the user on each document and to provide several level of user accesses for data privacy. A social technology was also adopted by researchers in order to facilitate collaboration among users when participating on document reviews and approval. The developed system shall provide a document editor to realize the said system feature.

To achieve the development of study, the researchers benchmarked on existing studies made. These similar studies were made as point of references in designing a

document management system that would provide solutions to current issues of file organization, storage, security and tracking. An agile methodology was adopted for the research design in order to help researchers manage the construction of the proposed system efficiently.

### 3 Methodology

This chapter discusses the methods used in this study. Methodology is a way to determine solutions to a given research problem and to accurately plan, analyze, design and develop the research.

The proponents made use of the Agile methodology in constructing the proposed system. Agile method is used in project management to pool the right resources according to priority and need. It is an approach to software development which solutions progress through collaboration of teams and end users. The researchers choose Agile method because it helps the researchers in anticipating changes and it allows more flexibility in the development of the research.

During initiation phase, the proponents conducted several fact-finding techniques in order to fully understand the workflow of document management for Romblon State University. With such, the proponents conceptualized the system architecture of the study and the context diagram to properly illustrate the designed solutions for the research. These are shown on the following figures.

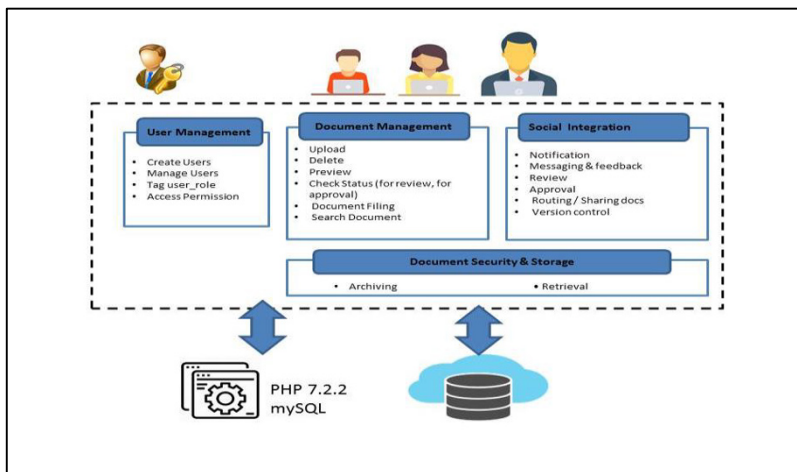


**Fig. 1.** System Architecture

Fig. 1 shows the system architecture of the research. The system is divided into following modules: 1] User Management, 2] Document management, 3] Social Integration, 4] Document Storage & Security. As illustrated, created documents and

transactions will be archived in a cloud. The developer will use PHP and MySQL as languages to construct the code of the system.

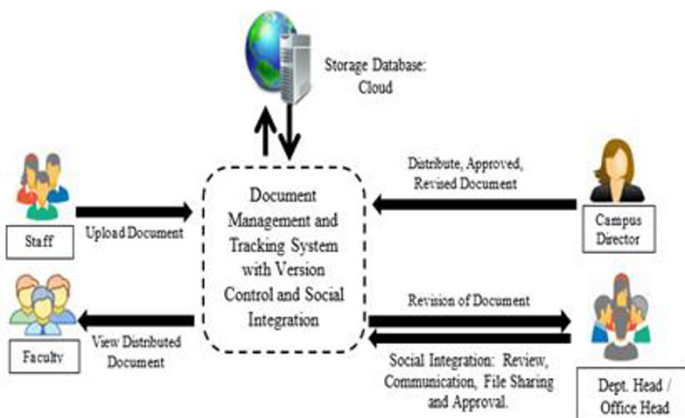


**Fig. 2.** Context Diagram

Fig. 2 depicts the distinct functionalities of the designed system. In this study, users are able to carry out various tasks including searching, editing, sending, attaching, routing and approval of documents through its social integration feature. Archiving and retrieval functions using the cloud technology were also applied to provide a better storage capacity of documents for the organization.

The developed system has been used and evaluated by 40 users in different departments of Romblon State University (RSU). Data gathered were interpreted using a 5-Point Likert Scale. The developed system was evaluated in terms of efficiency, reliability, user-friendliness, interoperability, functionality, compatibility, usability, security, maintainability and portability.

The researchers applied the total population purposive sampling since the intended user of the proposed system has a small size of 40 employees. According to [15], total population sampling, researchers choose to study the entire population because of the size of the population that has the particular set of characteristics that are typically very small.

**Table 1.** Profile of the Respondents

Position	Frequency	Percentage
Department Heads/Office Heads	8	0.08
Faculty	27	0.27
Office Assistants	5	0.05
Total	40	.40

Table 1 shows the demographic information of the respondents. These are the employees of RSU -Cajidiocan Campus and are the users of the developed system

## 4 Results and Discussion

### 4.1 User Management Module

The User Management Module provides functionality to manage user accounts. It implements authentication of username and password. It also allows System Administrator to tag user roles for each client and to provide access permission to the system.

### 4.2 Document Management

In the developed system, documents are managed into several ways. It includes deleting, viewing and uploading of documents as seen in Fig. 3. Every department in the organization may also search and retrieve a document using the following parameters: filename, file type, category or description. It also allows user to send documents to the different users. In addition, each user may be able to track document status whether pending, for review or for approval. In terms of file organization, the system provides a venue for the user to organize files into folder or category.

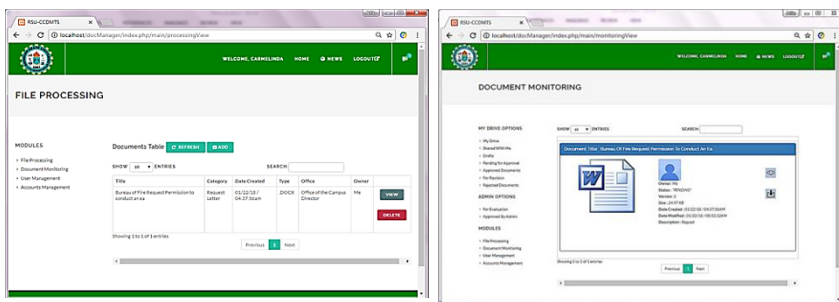


**Fig. 3.** Uploading, deletion and document status monitoring interfaces

### 4.3 Social Integration

The social integration component permits the collaborative work among users. It allows documents to be retrieved, reviewed and revised by authorized users as seen in Fig. 4. Additional tasks that include social integration are as follows:

- Notification.** This feature enables the user to identify alerts of incoming messages.
- Messaging.** This task allows multiple users to establish communication with each other and quickly exchange messages.
- Review, Approval and Routing.** This task permits users to actively collaborate with members and work on the same documents. Users may send comments, do

approval and share documents to each other. With this, business workflow is made easy and it results to work efficiency.

- d. **Version Control.** The version control module helps the user maintain different versions of the document and may check changes made to the documents. With such utility, the user may contrast early version of the documents made from the adopted revisions of users. The user may follow versions of documents by using file details such as file size, type, author and date created.

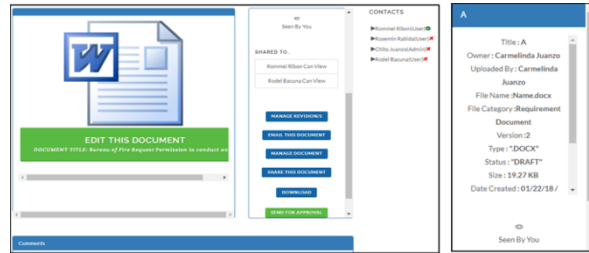


**Fig. 4.** Social Integration Module

#### 4.4 Document Storage and Security

By utilizing cloud technology for archiving and retrieval of documents, the study was able to answer the need for storage space for each department and employees of Romblon State University (RSU). In addition, with the security features of cloud computing in terms of document privacy and access, it increased the confidence of keeping documents confidential and that only authentic users had access on the right information. To measure the performance of the developed system, the proponents conducted a unit testing and a user-acceptance testing evaluation. Table 2 shows the summary of results of the user-acceptance testing evaluation.

**Table 2.** Overall mean of software evaluation

Criterion	Mean	Interpretation	Criterion	Mean	Interpretation
Efficiency	4.91	Very good	Compatibility	4.95	Very good
Reliability	4.88	Very good	Usability	4.96	Very good
User – Friendliness	4.96	Very good	Security	4.94	Very good
Interoperability	4.94	Very good	Maintainability	4.94	Very good
Functionality	4.93	Very good	Portability	4.96	Very good
GRAND MEAN	4.94	Very good			

The respondents strongly agree that the developed system performs well which was exhibited by a mean score of 4.94. The result of the software evaluation shows that the work process of the developed system has been efficient, reliable, user-friendly, interoperable and functional. With such results, it exhibits that the developed system was able to attain the goals of study for RSU – Cajidiocan Campus. The developed system was able to help the organization improve its processes in handling documents.

To ensure that the developed application would work well and that it will fit the need of each user, the proponent conducted a unit testing aside from a user-acceptance testing. The unit testing was a method used to individually test parts of the source code if the study performs according to the expected result. Below is the summary results of the unit testing conducted.

**Table 3.** Summary results of unit testing

Test Case #	Test Case Description	Passed	Failed
1	Authentication of the system.	✓	
2	Sending and receiving of messages.	✓	
3	Receiving, viewing, hiding and deleting of notifications.	✓	
4	Adding, editing, and removing user.	✓	
5	Adding, viewing document and its metadata, document naming, managing revisions, downloading, sending document for approval and to e-mail, approving and rejecting document.	✓	
6	Viewing the segregated files and status of files.	✓	
7	Backup document to local computer and to the cloud	✓	
8	Searching of specific document	✓	
9	Authentication of the system.	✓	

Based on the results, it shows that all modules are 100% working and that the system was able to deliver the expected outcome for the user.

#### 4.5 Research Implication

This study provides an innovation on document handling to integrate some features such as version control, tracking system, and social integration facility. The designed system helps to improve the document handling in the selected institution. Moreover, suggest other organization with similar issues about the business operational workflow toward shifting from manual to automated safekeeping and managing of files, document management, retrieving and preparing files for later use like accreditation. It shows that users strongly agree on the designed system. Therefore, it gives the selected institution the opportunity to shift from manual to automated document management system.

### 5 Conclusion and Future Works

The study employs social media integration in document handling through the designed notifications for users, messaging for communication, and sharing, reviews, and approval of documents. Moreover, the system applied version control of the documents created so that it will be easy to monitor the users who contributed to the revisions of the document's content. Based on the results of the software evaluation, the respondents graded the system with a grand mean of 4.94 which implies that the respondents

strongly agree that the system is efficient, user-friendly, interoperable, reliable, functional, usable, secure, compatible in executing multitasks, maintainable, and portable. Based on the results of the unit testing done by the developer it has a 100% rating which indicates that all the modules achieved the intended goal. The study was able to achieve its desired objectives and served as a stepping stone to maximizing technology innovation in RSU -Cajidican Campus. Hence, the developed system was able to allow employees of the institution to manage documents at any time easily and practically to do a more efficient workflow process through social integration feature that gives a venue for collaboration among users. The designed Document Management System is more accurate in providing details to the document to be uploaded to make a smooth retrieval in search modules; make the system available online as to facilitate the full capacity of the cloud-based. However, recommendations are presented to future researchers, to the selected University. First, add features for the system that allows students as the user of the system but only for request and monitoring of requested documents of the students. Second, improve the design of the system with consideration to the background and graphics. Third, add another feature of the social media such as reactions to the documents in messaging and viewing of documents and improve the search function of the system that allows searching as well as the content of the document. Lastly, provides users the capacity to affix the digital signature to the document that needs approval.

## References

1. Williams, M., Peterson, G. M., Tenni, P. C., Bindoff, I. K., & Stafford, A. C. (2012). DOCUMENT: a system for classifying drug-related problems in community pharmacy. *International journal of clinical pharmacy*, 34(1), 43-52.
2. Malaney, S., Kulkami, P., Viswanathan, K., Malaney, V., & Evans, J. (2012). U.S. Patent No. 8,176,004. Washington, DC: U.S. Patent and Trademark Office.
3. Miñon, J. D. F., Lim, C. M. A., Morano, J. A. L., Fajutagana, R. F., & Fabito, B. S. (2016, November). An Intranet-based Document Management and Monitoring System framework: A case for the National University Quality Management Office. In *Region 10 Conference (TENCON), 2016 IEEE* (pp. 2262-2267). IEEE.
4. Falk, R. J., & Radi, R. J. (2011). U.S. Patent No. 7,962,385. Washington, DC: U.S. Patent and Trademark Office.
5. Rakfukfon, K., Siraphaibool, S., Rattanadechaphitak, S., & Chiravirakul, P. (2017, May). MySRT management system for senior project document repository and tracking. In *2017 6th ICT International Student Project Conference (ICT-ISPC)* (pp. 1-4). IEEE.
6. Muliantara, A., Sanjaya, N. A., Widiarth, I. M., & Setiawan, I. M. A. (2015, September). Prototype of cloud based document management for scientific work validation. In *2015 International Conference on Information & Communication Technology and Systems (ICTS)* (pp. 237-240). IEEE.
7. Mary, J. S., & Usha, S. (2015, November). Web based document management systems in life science organization. In *Green Engineering and Technologies (IC-GET), 2015 Online International Conference on* (pp. 1-3). IEEE
8. Lee, T., & Iio, J. (2015, September). Document Management System Based on ISAD (G). In *Network-Based Information Systems (NBiS), 2015 18th International Conference on* (pp. 685-689). IEEE.

9. Mary, J. S., & Usha, S. (2015, November). Web-based document management systems in life science organization. In *Green Engineering and Technologies (IC-GET), 2015 Online International Conference on* (pp. 1-3). IEEE
10. Lass, M., Leibenger, D., & Sorge, C. (2016, November). Confidentiality and Authenticity for Distributed Version Control Systems-A Mercurial Extension. In *Local Computer Networks (LCN), 2016 IEEE 41st Conference on* (pp. 1-9). IEEE.
11. Sonawane, V. R., & Rao, D. R. (2015). A Comparative Study: Change Detection and Querying Dynamic XML Documents. *International Journal of Electrical and Computer Engineering*, 5(4), 840.
12. Kass, A., Shettigar, S., Yelisetty, S., & Ergueta, M. P. (2017). *U.S. Patent No. 9,560,091*. Washington, DC: U.S. Patent and Trademark Office.
13. Parker, J. R., Singh, S., Prickril, G., & Chan, W. (2018). *U.S. Patent Application No. 10/015,215*.
14. Ambler, S. W., & Lines, M. (2012). Disciplined agile delivery: A practitioner's guide to agile software delivery in the enterprise. IBM Press.
15. Lund Research Ltd. (2012 ). Retrieved March 16, 2018, from <http://dissertation.laerd.com/purposive-sampling.php#total>



# The Development of an Integrated Corpus for Malay Language

Normi Sham Awang Abu Bakar

International Islamic University Malaysia, Kuala Lumpur, Malaysia  
nsham@iium.edu.my

**Abstract.** Generally, a corpus serves as the source of data for various types of research. As such, there are several Malay corpora being developed to support the needs of the researchers. However, the various corpora of Malay text are distributed and not integrated, where some words are not included or missing in some corpora. The focus of this paper is to develop an integrated corpus that will combine four most comprehensive Malay corpora. The intention is to provide comprehensive coverage of Malay corpora which would be beneficial for any relevant work.

**Keywords:** Malay corpora, Web crawler, Mobile application, Sentiment analysis

## 1 Introduction

The Malay language is used by more than 200 million speakers and most of speakers reside in the South East Asia region [1]. Despite it's popularity, it's advancement in the text processing area is still scarce. For instance, there are more than 10 text corpora listed for English language and several of them have more than 425 million words in them. One important usage of these text corpora is in the area of Sentiment Analysis (SA). Essentially, a text corpus is a collection of written or spoken text which are in machine readable form [1]. In general, the usage of text corpora as the source of information has been widely accepted by researchers from wide range of research areas [2]. Hence, the research on the Malay language corpora can provide insight into the opinion mining and analysis among Malay speaking population in the world.

The main objective of this paper is to discuss the development of an integrated Malay corpus that combines four of the most comprehensive Malay language text corpora. The focus of the discussion is the methodology used to develop the integrated corpus. This paper is arranged as follows: Section 2 elaborates the background of the study, while Section 3 discusses the prior related work. In addition, the methodology used for developing the system is presented in Section 4, and Section 5 explains the conclusion and future work.

## 2 Background of Study

Essentially, there have been several research work that explores the usage of various Malay corpora. Moreover, several researchers have attempted to develop their own Malay corpus as the source of their data, as presented in Table 1:

**Table 1.** Malay text corpora

Corpus	Context	Application	Provider
sealang.net	General	Collocation analysis Concordance Provide with example sentences from multiple sources	CRCL and University of Wisconsin-Madison <a href="#">Center for Southeast Asian Studies</a> (CSEAS)
<a href="https://glosbe.com">https://glosbe.com</a>	General/ education	Online dictionary. Almost all languages available, millions of translations.	Glosbe
Mcp.anu.edu.au (Malay concordance project)	Education	Concordance	Australian National University
MyBaca.org	Education	To find words whether it is capable in starts, end or middle of the sentences	School of educational studies
<a href="https://www.lexilogos.com/english/malay_dictionary.htm">https://www.lexilogos.com/english/malay_dictionary.htm</a>	Education	Malay-English dictionary	Lexilogos project
<a href="http://prpm.dbp.gov.my/">prpm.dbp.gov.my/</a> (Pusat Rujukan Persuratan Melayu)	Education	Define and provide detailed meaning of word.	Dewan Bahasa dan Pustaka

### 2.1 SEAlang

Resources that can be found in SEAlang include [3]:

- Bilingual and monolingual dictionaries
- Monolingual text corpora and aligned bi-text corpora
- Tools for manipulating, searching, and displaying complex scripts
- Specialized reference works, including historical and etymological dictionaries

## 2.2 Malay Concordance Project (MCP)

The project aims to help scholars share resources for the study of classical Malay literature. In the last year it has been consulted by scholars from more than 30 countries world-wide, who made over 20,000 searches [4].

These texts can be searched on-line to provide useful information about:

- contexts in which words are used,
- where terms or names occur in texts,
- patterns of morphology and syntax.

## 2.3 MyBaca

The online system contains the common words that occur in the Malay language textbooks used in Malaysian schools and the related linguistic information. Users could conduct word search according to six primary linguistic features, which include frequency of occurrence, word length, phoneme length, number of syllables, type of syllable, and word category [5].

## 2.4 Pusat Rujukan Persuratan Melayu, Dewan Bahasa dan Pustaka (DBP)

This corpus is managed by the Dewan Bahasa dan Pustaka and among the services offered are word search, synonym and antonym. The search engine enables users to find information across all the databases determined by DBP [6].

## 2.5 Malay Online Virtual Integrated Corpus (MOVIC)

The individual corpus presented in Table 1 indicates that the development of each corpus is on a standalone mode and not even connected to one another. This brings us to the issue of getting the data from multiple sources might waste the time for the researcher. Instead, if the various corpora can be integrated, the researchers can go to just one place to search for the needed information, thus, we can reduce the time to collect the data, and can focus on the analysis, which is more important for the research.

Therefore, the Malay Online Virtual Integrated Corpus (MOVIC) is essential to address the issue of lack of integrated corpus. The source of data for MOVIC would come from the above-mentioned corpora, which later, will be integrated in one application.

Generally, MOVIC can be used in any research domain that uses Malay terms regardless of the nature of the research. It is hoped that the users of MOVIC can benefit from services provided.

## 3 Prior related work

Most of the work in the usage of Malay corpora are for sentiment analysis and investigating the social media to collect sentiment data. Al-Safar et al proposed a Malay sentiment analysis classification model to improve classification performances based on

the semantic orientation and machine learning approaches [7]. In a similar line, Al-Molsmi presents the effects of the common-used feature selection methods (Information Gain, Gini Index, and Chi-squared), and three machine learning classifiers (SVM, Naive Bayes, and K-nearest neighbor) for Malay sentiment classification [8]. Furthermore, the work in [9] aims to identify the opinion mining and sentiment analysis components for extracting both English and Malay words in Facebook. Later, information, in terms of texts, are extracted and clustered into emotions.

Similarly, Hulliyah et al discuss the overview of past and recent research on emotion detection as well as some approaches and techniques used and shows the link between both sentiment analysis and emotion recognition [10]. The development of a *Twitter corpus known as the Malay Chat-style Corpus (MCC)* was discussed in detail in [11]. In the article, Saloot et al investigate aspects of the Twitter messages corpus to build a reliable Tweet corpus from the Web. Interestingly, they conducted multiple analysis on MCC, including words frequency, collocation frequency, ranks of frequency, metadata analysis, and the usage of the automatic language identification tool to identify Malay language tweets on Twitter [12].

Similarly, Baldwin and Awab [13] present an open source toolkit for Malay, that includes a word and sentence tokeniser, a lemmatiser and a partial part-of-speech (POS) tagger. Furthermore, the work of Noor Ariffin and Tiun [14] attempted to design and implement a non-standardised Malay POS model for tweets and performs assessment based on the word tagging accuracy of test data of unnormalised and normalised tweet texts.

The work of Gossen et al [15] investigate the usage of an integrated focus crawler to gather Web and Social Media content. The work of Myers and McGuffee [16] discusses an open-source web-crawling platform implemented in Python. This platform utilizes regular expressions to extract relevant data from geographically targeted websites. From the web crawler development point of view, Boldi et al [17] discuss the development process of BUBiNG, a web crawler built upon the experience with their previous web crawler, UbiCrawler. They discuss the fetching logic of BUBiNG and the architecture used to develop the crawler.

Similarly, Di Pietro et al [18] discuss the implementation of a focused web crawler to gather data from several websites. The work of Mei and Frank [19] suggests using a self-guiding web crawler to gather data from extremist websites. Shemsadi et al [20] explores the possibility of creating a set of tools to capture Internet of Things (IoT) data from a set of data sources. They present the framework of the crawler engine called ThingSeek, together with the specifications of the collected datasets.

From the literature, they show that the corpora are not-integrated, and users need to spend longer time to search through all possible corpora for the various information they need. The objectives for this research are a) to develop a comprehensive, integrated corpus of Malay words which will be combined from multiple sources/corpora, and b) to display in a user-friendly way using the web and mobile version the combined information from the different corpora, i.e. the meaning, concordance, etc.

## 4 Movic Development

Essentially, the main aim of the Movic development is to integrate the various corpora to become a centre for the Malay corpora reference. There are two versions of Movic, the web and mobile version.

Previously, users of the Malay corpora must go to each corpus separately to find the information they need. For example, if they want to get the concordance and collocation analysis, they need to go to the SEALang website, and if they want to know about contexts in which words are used or where particular terms or names occur in texts, they can go to the Malay Concordance Project (MCP).

Moreover, from MyBaca website, users could conduct word search according to six primary linguistic features, which include frequency of occurrence, word length, phoneme length, number of syllables, type of syllable, and word category. Lastly, the DBP website offers the services of word search, synonym and antonym search.

The motivation to develop Movic is to provide a “one-stop centre” for Malay word search. For example, if the user search for the word “*baca*”, Movic will crawl from all four sources (SEALang, MyBaca, MCP and DBP). The results displayed in Movic will include all the information from all four sources. Users do not need to go to separate sources anymore, because that information will be collected by Movic using its intelligent crawler function. The details of how the crawler works will be discussed in the next section.

### 4.1 4.1 Movic Crawler Engine

The crawling process in Movic is divided into several components, as depicted in Fig. 1.

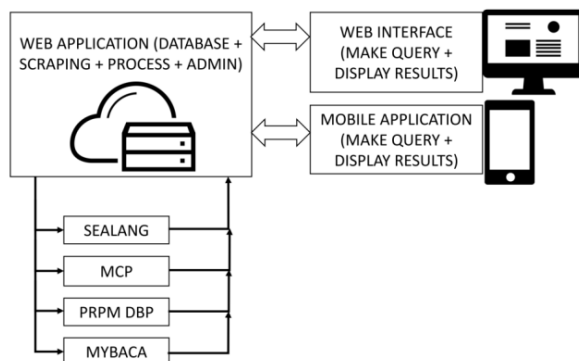


**Fig. 1.** Movic Crawler Engine

The steps used to obtain the required results from the various Malay corpora are as follows:

- 1) Generate full request to URLs - In this first step, a web crawler query is sent to the selected Malay corpora, i. e. Sealang, MCP, PRPM DBP and MyBaca. The queries were written in PHP Simple HTML Dome, and Wordpress.org (Fig. 2). The queries are sent to the websites to locate the required information.

```

function display ($search) {
    // $search input will receive from user query
    // each query different for corpus

    // generate url for PRPM DBP
    $url = "http://prpm.dbp.gov.my/cari?keyword=". $search;
}

```

**Fig. 2.** Generate full request to URLs

- 2) Read page contents - The next step is a reader function will read the selected part of the page (Fig. 3). Once the relevant information is found in the target websites, the crawler will read the content of the page.

```

$html = file_get_html($url);

// file_get_html() is scrapping function call from Simple
// HTML DOM library all content from request url will be
// scrap

```

**Fig. 3.** Read page contents

- 3) Restructure data - The data source for this system are from multiple websites, and each one keeps the data in different structures. Thus, it is necessary to restructure the data to standardize the output in MOVIC, especially to make it more mobile friendly.
- 4) Merge data for each source - In this phase, the data from each source are kept separately until all data are refined, then merged in a container (Fig. 4).
- 5) Integrate data from all sources - Then, the collected data from selected sources are integrated and stored on a database.
- 6) Display results - Finally, the integrated data are displayed in a web and mobile friendly display page.

```

function allcorpus() {
    function scraping_generic($search) {
        display_mybaca($search);
        $return = false;
        display_prpm($search);
        $return = false;
        display_sealang($search);
        $return = false;
        display_mcp($search);
        return $return;
    }
}

```

**Fig. 4.** Merge data for each source

## 4.2 Movic search results

In general, the web crawler is designed to collect the contents from multiple corpora and then, display them in a dashboard, as shown in Fig. 5. The search results are displayed in both web and mobile version.

Furthermore, the results are displayed in the format reported in the original website, for example, the for MyBaca corpus, information displayed are: Frequency in corpus, source of word, word category, word structure and word category. In addition, the results from Pusat Rujukan Persuratan Melayu (by DBP) gives the definition of words in different contexts, while results from SEALang display the distinct leading collocation e.g. “*di baca*” and trailing collocation e.g. “*baca cerita*”. Lastly, the Malay Concordance Project shows the results on the context where the word is used, the location where the word appear in texts, and the word morphology.

**Fig. 5.** Search results: Mobile version

To test for the robustness of Movic, we have simulated 200 users to use Movic simultaneously using a testing tool called Blazemeter. The result of the testing shows

that, the performance of MOVIC remains stable even though the number of users increase.

### 4.3 Challenges

The effort to integrate the Malay corpora is not without challenge. One of the biggest challenges to get the content from the multiple corpora is, the structure of each corpus is different from one another. Hence, we need to select the relevant content manually and later, execute the script to access the intended information.

Another challenge is to find the library to do the information scraping. Due to the lack of work done in Malay language development, the library to do the scrapping for Malay corpora is scarce. In addition, because of the existence of the irrelevant data in the selected corpora, several levels of pre-processing are required.

Lastly, two corpora, SEALang and MCP require longer processing time due to the extensive information in their respective websites. Therefore, we need to eliminate the delay by having two levels of execution time to improve the performance of the crawler.

## 5 Conclusions

The main purpose of MOVIC is to have an integrated corpus for Malay language. Currently, different corpora host different sets of information for the same word. Therefore, to ease the tasks of searching in multiple corpora for the needed information, there is a need for an integrated corpus to provide different aspects of descriptions for the search keywords. The main challenges in the development are mainly attempting to write the script to crawl the multiple corpora and the main hindrance is the different structure of the corpora. In addition, the performance of the web crawler is a complex issue to solve, and to solve the problem, we had to perform two levels of processing to improve the performance. The future work include building a more comprehensive corpus that can include the work in sentiment analysis in Malay language. This can be achieved by integrating with the social media database to collect the sentiment analysis data.

## Acknowledgment

This research is fully funded by the International Islamic University's RIGS grant, ID: RIGS-17-156-0731.

## References

1. Medhat, W., Hassan, A. and Korasky, H.: Sentiment analysis algorithms and applications: A survey. *Ain Shams Engineering Journal*, Vol. 5, pp 1093-1113 (2014).
2. Asyafi'ie, M. A., Harun, M., Shapiai, M. I. and Khalid, P. I.: Identification of phoneme and its distribution of Malay language derived from Friday sermon transcripts. In *2014 IEEE Student Conference on Research and Development (SCoReD)*, (pp. 1-6) (2014).
3. SEALang Homepage, [sealang.net](http://sealang.net), last accessed 15/05/2019

4. Malay Concordance Project Homepage, <https://mcp.anu.edu.au>, last accessed 15/05/2019
5. MyBaca Homepage, [mybaca.org](http://mybaca.org), last accessed 15/05/2019
6. Pusat Rujukan Persuratan Melayu, [prpm.dbp.gov.my](http://prpm.dbp.gov.my), last accessed 15/05/2019
7. Al-Saffar, A., Awang, S., Tao, H., Omar, N., Al-Saiagh, W., & Al-bared, M.: Malay sentiment analysis based on combined classification approaches and Senti-lexicon algorithm. *PloS one.* (2018)
8. Al-Moslmi, T., Gaber, S., Al-Shabi, A., Albared, M., and Omar, N.: Feature Selection Methods Effects on Machine Learning Approaches in Malay Sentiment Analysis, *The 1st ICRIL-International Conference on Innovation in Science and Technology (IICIST 2015)*, 444-447.
9. Zamani, N.A., Abidin, S.N., Omar, N., & Abiden, M.Z.: Sentiment Analysis : Determining People's Emotions in Facebook. *Applied Computational Science*, 111-116 (2014)
10. Hulliyah, K., Bakar, N.S., & Ismail, A.R.: Emotion recognition and brain mapping for sentiment analysis: A review. *2017 Second International Conference on Informatics and Computing (ICIC)*, 1-5.(2017).
11. Saloot, M. A., Idris, N., Aw, A. and Thorleuchter, D.: Twitter corpus creation: The case of a Malay Chat-style-text Corpus (MCC). *Digital Scholarship in the Humanities*, Vol. 31, No. 2, pp 227-240.
12. Saloot, M. A., Idris, N. and Mahmud, R.: An architecture for Malay Tweet normalization, *Information Processing & Management*, 50(5), pp.621-633, (2016).
13. Baldwin, T. and Awab, S.: Open source corpus analysis tools for Malay, *Proceedings of the Fifth International Conference on Language Resources and Evaluation (LREC'06)*, Genoa, Italy (2006).
14. Noor Ariffin, S. N. A. and Tiun, S.: Part-of-Speech tagger for Malay Social Media Texts. *GEMA Online Journal of Language Studies*, Vol. 18(4), pp. 124-142, (2018).
15. Gossen, A., Demidova, E., Risse, T.: iCrawl: Improving the freshness of web collections by integrating social web and focused web crawling, *Proceedings of the 15th ACM/IEEE-CS Joint Conference on Digital Libraries*, pp. 75-84, (2015).
16. Myers, A. and McGuffee, J. W.: Choosing Scrapy, *Journal of Computer Sciences in Colleges*, Vol 31 (1), (2015).
17. Boldi, P., Marino, A., Santini, M. and Vigna, S.: BUbiNG: Massive crawling for the Masses. *ACM Transaction on the web (TWEB)*, vol. 12 (2), (2018).
18. Di Pietro, A., Aliprandi, C., De Luca, A. E., Raffaelli, M., Soru, T.: Semantic Crawling: an Approach based on Named Entity Recognition, *IEEE/ACM International Conference on Advances in Social Networks Analysis and Mining*, (2014).
19. Mei, J. and Frank, R.: Sentiment Crawling: Extremist content collection through a sentiment analysis guided web-crawler. *IEEE/ACM International Conference on Advances in Social Networks Analysis and Mining*, (2015).
20. Shemshadi, A. A., Sheng, Q. Z. and Qin, Y.: ThingSeek: A crawler and search engine for the Internet of Things. *Proceedings of the 39th International ACM SIGIR conference on Research and Development in Information Retrieval*, (2016)



# Word Embedding for Small and Domain-specific Malay Corpus

Sabrina Tiun<sup>1</sup>, Nor Fariza Mohd Nor,<sup>2</sup>, Azhar Jalaludin,<sup>2</sup>, Anis Nadiah Che Abdul Rahman,<sup>2</sup>

<sup>1</sup> ASLAN Lab, CAIT, Faculty of Technology and Information System, Universiti Kebangsaan Malaysia.

<sup>2</sup> Faculty of Science Social and Humanities, Universiti Kebangsaan Malaysia  
sabrinatiun@ukm.edu.my

**Abstract.** In this paper, we present the process of training the word embedding (WE) model for a small, domain-specific Malay corpus. In this study, Hansard corpus of Malaysia Parliament for specific years was trained on the Word2vec model. However, a specific setting of the hyperparameters is required to obtain an accurate WE model because changing one of the hyperparameters would affect the model's performance. We trained the corpus into a series of WE model on a set of hyperparameters where one of the parameter values was different from each model. The model performances were intrinsically evaluated using three semantic word relations, namely; word similarity, dissimilarity and analogy. The evaluation was performed based on the model output and analysed by experts (corpus linguists). Experts' evaluation result on a small, domain-specific corpus showed that the suitable hyperparameters were a window size of 5 or 10, a vector size of 50 to 100 and Skip-gram architecture.

**Keywords:** Corpus linguistic, Malay corpus, Word2vec, word embedding

## 1 Introduction

The word embedding (WE) model is a neural network based on the distributional semantic model (DSM). The distributional hypothesis states that semantically similar words tend to have similar contextual distributions [1-2]. This distributional hypothesis relies on a structuralist conception of meaning similarity. In the WE context, if two words have similar vectors, then they have the same distribution; thus, they have a similar meaning because a word is represented as a vector in the semantic space [1]. DSM is an old concept in corpus linguistics; however, corpus linguists are interested in using WE, in addition to other approaches in performing corpus analysis because of its success in many natural language processing applications [7-8].

Even though WE models have been successfully trained on large corpora, such as Google Web 2.0 [6] and Wikipedia WE [6], the training of the WE model in small and domain-specific corpus is potentially useful, such as in the work of [3]. A small and domain-specific trained corpus for the WE model tends to exhibit bias knowledge.

However, such bias is useful when the corpus WE is utilised to represent word knowledge; bias knowledge will avoid issues regarding word problems, such as polysemy or homonym [1]. In small and domain-specific corpora, word senses will unlikely encounter the same words that have more than one meaning or have the same form. Ref. [1] stated that the trained WE model will make sense regardless of the corpus size. The use of the WE model in the corpus study for a small corpus will aid corpus linguistics in performing an intensive and a different way of analysing corpus.

However, the main issue is the selection of a suitable (accurate) WE model given a specific corpus-based task. Setting the hyperparameters, such as, vector size (density), window size, negative sampling and frequency cut-off appropriately is important to obtain an accurate model. This is because by changing any of the hyperparameters would affect the model's performance (accuracy).

This study aims to create an accurate distributional or WE model for a small corpus that is suitable for linguistic analysis.

## 2 Related Work

The three most popular WE models are Word2vec<sup>1</sup>, GloVe<sup>2</sup> and fastText<sup>3</sup>. These models exhibit their own strengths for a certain kind, size and purpose of corpus. Apart from the types of WE model, the model itself possesses its own variant, such as Word2vec, which consists of two architectures, namely, continuous bag-of-words (CBOW) and Skip-gram. The model needs to be created on the basis of the task and size to obtain a suitable and accurate WE model.

In creating a WE model, such as Word2vec, for the corpus study, the decision of using either CBOW or Skip-gram should be carefully considered. CBOW should be used instead of Skip-gram when finding/predicting related words given the context terms [1]. Ref. [6] mentioned that the use of Skip-gram instead of CBOW is suggested for a small corpus if the task concerns one target word. By contrast, CBOW is best used with tasks that involve many target words.

In [2], various window and vector sizes were combined to obtain the optimal distributional model for Bangla corpus. The size corpus contained 2 million words with 500K unique ones. The finding showed the optimal model with fastText Skip-gram compared with other models (e.g. fastText-CBOW and Word2vec-tensor flow).

Ref. [3] evaluated the specific-domain WE model and their hypermeter setting. Two models were evaluated on the basis of Word2vec with the variants of Skip-gram and CBOW. The hyperparameters are vector size (density), window size, negative sampling and frequency cut-off. The used dataset was the oil and gas corpus, which contains 8 million sentences with 47 K documents.

The model and various parameters (hyperparameters) were tested in [1]. The study explored the variation between the models trained with changing parameters (architecture, window size, vector dimensions and context type). The aforementioned study

---

<sup>1</sup> <https://code.google.com/archive/p/word2vec/>

<sup>2</sup> <https://nlp.stanford.edu/projects/glove/>

<sup>3</sup> <https://fasttext.cc/>

concluded that changing even just one parameter could result in a massive effect on the model semantic space. In the study, sizeable corpora, namely, BNC and ACL, were used.

In this study, the Word2vec model is chosen because the corpus linguists aim to use the WE as a tool to mine relations amongst words in the corpus. Further analysis with other linguistic tools can be conducted by mining the word semantic relations.

### 3 Dataset and Method

In this work, a WE model on Hansard corpus of Malaysia Parliament for specific years needed to be created. A small corpus was trained for the WE model. The following three main stages of processing were involved in creating an accurate WE model: (i) cleaning the corpus, (ii) training the corpus for the WE model and (iii) manually assessing the WE model to select a suitable WE model. Details on the dataset and the stages of processing (Fig. 1) will be explained in the following subsections.

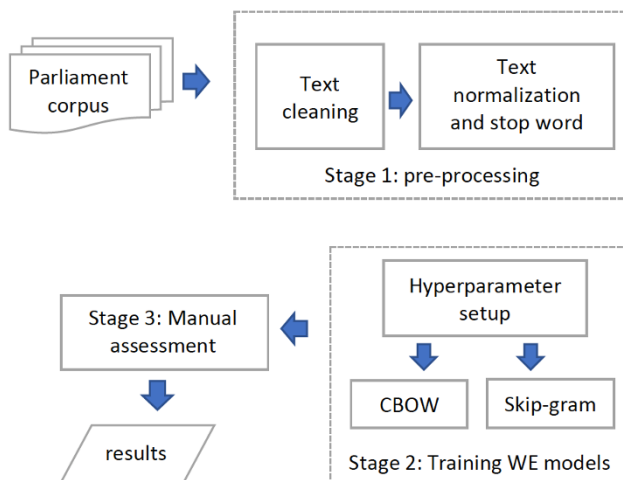


**Fig. 1.** Process of developing a suitable WE model for Hansard corpus (Malaysia Parliament)

#### 3.1 Dataset

In this study, Hansard corpus of Malaysia Parliament (years 1982–1985)<sup>4</sup> is developed on the Word2vec WE model. A detailed description of this corpus is presented in Table 1.

<sup>4</sup><https://www.parlimen.gov.my/hansard-dewan-rakyat.html>

**Table 1.** Cleaned raw corpus description

Item	Total
Number of tokens (N)	14,099
No. of files	256
Size	50.7 K

### 3.2 Method

**Stage 1.** The pre-processing phase consisted of two processes: i) Text cleaning and (ii) text normalisation and stop word removal. In the text cleaning, we removed symbols, characters and numbers that were unimportant for this study. Considering that the parliament usually begins after the prayer, we take only the content after the word ‘DOA’ was found. The content segmentation is easy because the ‘DOA’ was written in a separate line before the content text of a parliament session.

**Stage 2.** Training WE models with a hyperparameter setting: The hyperparameters and types of architectural models need to be appropriately selected to determine the suitable WE model for the corpus linguists.

- a. *Architectural models (CBOW and Skip-gram).* In this work, the Word2vec from the Gensim library is used. Ref. [9] reported that the prediction task is suitable for the Word2vec model even though many WE models are presented. The Word2vec model is chosen because one of the possible tasks that will be performed using the WE model is word analogue, which is the prediction task. Both types of the Word2vec architectures are chosen to be trained on our small corpus; since different applications, have different kind of WE model. For example, mentioned in [9], Skip-gram predicts less accuracy than CBOW for word analogy task.
- b. *Hyperparameter setting.* In our evaluation method, the frequency cut-off (min\_count) was set to two. Certain vocabulary words will not be captured in the model if the value is higher than two because the size is small. This case is particularly true for the word analogy prediction task. Negative sampling (neg) is ignored in this study. Ref. [3] reported that this parameter has no impact on the similarity tasks performed on a developed WE model from the domain-specific corpus. Therefore, only two hyperparameters are considered: (i) vector (dim) and (ii) context window (win) sizes. The WE models are trained using these parameters, and the outputs are assessed by experts (corpus linguists).

**Table 2.** Hyperparameter setting

WE model	Window size (win)	Vector size (dim)	Min. frequency
Word2vec-CBOW	3,5,10	20,50,100	2
Word2vec-skip-gram	3,5,10	20,50,100	2

**Stage 3.** The WE training model is an unsupervised task. The result can be objectively evaluated in a specific way. The optimal evaluation method involves directly evaluating

the intended task of the WE [4]. Therefore, we evaluated our Word2vec model on the basis of the task that the corpus linguists will use on the WE model. The developed WE model will be used for linguistic analysis. An example of linguistic analysis is to find related words of a term or discover any knowledge insight given by any relation that has been uncovered amongst the words. We assume that the developed WE model can propose similar words that are semantically related either negatively (dissimilar) and positively and reasonable analogy words to assess whether the model is suitable and can be used for accurate analysis. In this study, three types of word relations were studied: (i) the top 10 most similar words (positive distance); (ii) the top 10 most dissimilar words (negative distance) and (iii) word analogy.

The developed models were evaluated or assessed by three experts (corpus linguists) considering that the WE model will be used by this type of experts to perform corpus analysis. The models were manually assessed to select the suitable WE model. The experts were asked to choose the most similar and dissimilar words related to the chosen target word. The similar words are the top 10 words that have the closest distance to the target one in the WE model. By contrast, the top 10 words with the farthest distance from the target word are selected for dissimilar words. Examples of similar and dissimilar words related to the target word are listed in Table 3.

**Table 3.** Output example generated by the WE model for the manual evaluation

Tasks	Output words
Similar words	'percaya', 0.9998050332069397) 'pihak', 0.9997930526733398) 'memberikan', 0.9997929334640503) 'mengambil', 0.9997841119766235) 'malaysia', 0.9997739791870117 'kemelesetan', 0.9997662305831909) 'hasil', 0.999764084815979) 'menggunakan', 0.9997577667236328) 'berharap', 0.999757707118988) 'peringkat', 0.9997556209564209
Dissimilar words	'piagam', 0.4672910273075104) 'kelas', -0.1163417249917984) 'portfolio', -0.14977161586284637) 'anggap', -0.8345522284507751) 'luhat', -0.8362379670143127) 'rebat', -0.947994589805603) 'meringankan', -0.9482786059379578) 'matahari', -0.9486640691757202) 'menggiatkan', -0.9544367790222168) 'punya', -0.9546446800231934)
Word analogy	Kampung : perladangan :: bandar : <b>pengangkutan</b> Bank : pinjaman :: pelabur : <b>giat</b>

In the assessment of the WE model in terms of predicting word analogy, the experts were asked to choose the outputs that have the most sensible word analogy relation. Following the same parallelogram model of analogue as in *king* (*x*) : *queen* (*y*) :: *man* (*a*) :? (*b*) in Fig. 2, the WE model is given values *x*, *y* and *a*, and value *b* is the predicted one. In the example of Table 1, the word ‘pengangkutan’ is the value of *b*, given the value of *a* = ‘bandar’, *x* = ‘kampung’ and *y* = ‘perladangan’.

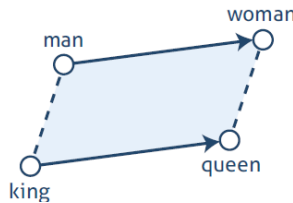


**Fig. 2.** Parallelogram on the word analogue model for *king*:*queen*::*man*:*woman* [6]

Word analogy is included in the evaluation because it is a potential analysis tool that linguists can use to infer relations amongst words by reasoning unfamiliar word relations given the familiar ones.

The assessment performed by the linguists on the developed models is based on an agreement with regard to which models produced acceptable outputs. Agreement was achieved through a discussion and by running the corpus on WordSmith 5.0<sup>5</sup> to see the sample usage of the given words (words for evaluation) from the corpus.

## 4 Result and Discussion

The three top models (Table 4) for word similarity output are selected on the basis of the experts’ evaluation. In Table 4, ‘sg = 0’ refers to CBOW architecture, and ‘sg = 1’ refers to Skip-gram architecture.

**Table 4.** Top WE models for the corpus

Evaluation	Architecture and hyperparameter
Word similarity	Model 1: vector size=50, window size=10, min. count=2, sg=1
	Model 2: vector size=100, window size=10, min. count=2, sg=1
	Model 3: vector size=100, window size=5, min. count=2, sg=0
Word dissimilarity	Model 4: vector size=100, window size=3, min. count=2, sg=1

<sup>5</sup><https://wordsmith-tools.software.informer.com/5.0/>

Only one model needs to be chosen; thus, the model that gives the highest number of similar words was chosen. Model 1 in Table 4 was chosen (Word2vec of Skip-gram, window size = 10, vector size = 50, minimum frequency count = 2).

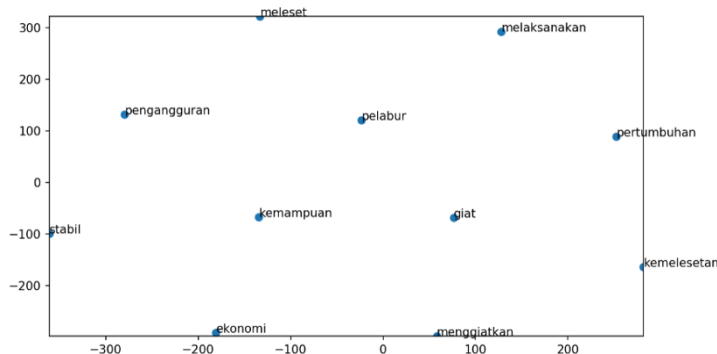


**Fig. 3.** Output of the top 10 most related words from the chosen WE model

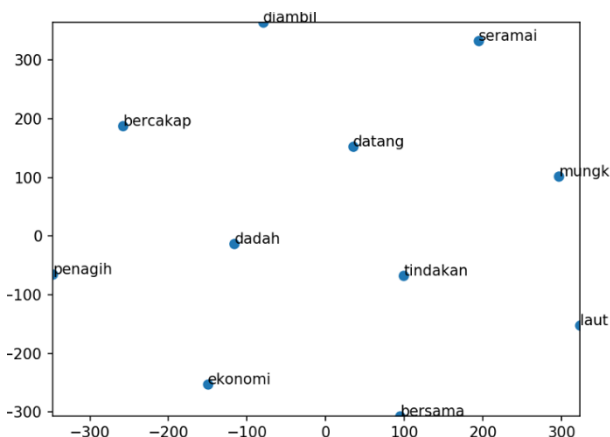


**Fig. 4.** Output of the top 10 most unrelated words from the chosen WE model

The output examples from the WE model with the set hyperparameters are visualised in Fig. 3 (top 10 most similar words) and Fig. 4 (top 10 dissimilar words) for the test word ‘ekonomi’ (*economy*). In Fig. 3, the output is valid because the words related to ‘ekonomi’ (*economy*) are commonly associated with various terms, such as ‘pelabur’ (*investor*) and ‘stabil’ (*stable*).

The output example for word analogue is depicted in Table 5. The word analogue that runs on a small WE model, which consists of word pairs ‘bank-institusi’ (*bank-institution*) and ‘perlaburan-diputuskan’ (*investment-decided*), do make sense. The connection of the word pair with the same magnitude or parallelogram can provide clues

to corpus linguists to do further investigate on the word pair relation with different approaches.

**Table 5.** Example of word analogues from the chosen WE model

No.	Examples
1.	ekonomi (x) : pinjaman (y) :: bank (a) : <b>institusi</b> (b)
2	ekonomi (x) : meleset (y) :: pelaburan (a) : <b>diputuskan</b> (b)

## 5 Conclusion

In this study, we conducted experimental work on developing a WE model for a small Malay corpus, which is a domain-specific corpus that contains dialogue during a parliamentary session. Setting the suitable hyperparameters is essential to obtain an accurate WE model. A series of WE models is trained for the corpus. The outputs of those models are then evaluated. The evaluation is manually performed by the corpus linguists considering that the model will be used by them as another approach in studying the corpus. The small corpus is best trained for the WE model with hyperparameters of vector size = 50, window size = 10 and Skip-gram architecture on the basis of three intrinsic word relations, namely; word similarity, dissimilarity and analogy.

## Acknowledgement

This works is supported by Universiti Kebangsaan Malaysia (Research Code: GGPM-2017-025)

## References

1. Desagulier, G. Can Word Vectors help corpus linguists? <https://halshs.archives-ouvertes.fr/halshs-01657591v2/document>, last accessed 2019/05/01.
2. Ritu, Z. S., Nowshin N., Nahid M. M. H., Ismail, S. Performance Analysis of Different Word Embedding Models on Bangla Language. In: International Conference on Bangla Speech and Language Processing (ICBSLP), IEEE: Sylhet, Bangladesh (2018).
3. Nooralahzadeh F., Øvreliid L., Lønning J. T. Evaluation of Domain-Specific Word Embeddings Using Knowledge Resources. In: Calzolari N. et al (eds.) the 11th International Conference on Language Resources and Evaluation (LREC 2018), pp.1438-1445, ELRA, Miyazaki, Japan (2018).
4. Řehůrek R. Word2vec Tutorial. <https://rare-technologies.com/word2vec-tutorial/#app>, last accessed 2019/01/30.
5. Chen, D., Peterson, J.C., Griffiths, T.L. Evaluating vector-space models of analogy. In: The Proceedings of the 39th Annual Conference of the Cognitive Science, Cognitive Science Society: London, UK. (2017)
6. Word2vec. <https://code.google.com/archive/p/word2vec/>, last accessed 2019/05/30.

7. Hamilton, W.L., Leskovec, J., & Jurafsky, D. (2016). Diachronic Word Embeddings Reveal Statistical Laws of Semantic Change. In: Proceedings of the 54th Annual Meeting of the Association for Computational Linguistics, ACL: Berlin, Germany (2016).
8. Nina Tahmasebi, N. A Study on Word2Vec on a Historical Swedish Newspaper Corpus. In: Proceedings of the Digital Humanities in the Nordic Countries 3rd Conference, Helsinki, Finland (2018).
9. Mikolov T., Chen K, Corrado G., Dean J. Efficient Estimation of Word Representations in Vector Space. In: Proceedings of Workshop at ICLR 2013, Microtome Publishing: Scottsdale, AZ, USA (2013).



# Blood Glucose Classification to Identify a Dietary Plan for High-Risk Patients of Coronary Heart Disease Using Imbalanced Data Techniques

Monirah Alashban<sup>1</sup> and Nirase Fathima Abubacker<sup>2</sup>

<sup>1</sup>DCU @ Princess Nourah bint Abdulrahman University, Saudi Arabia

<sup>2</sup>Dublin city University, Dublin, Ireland

nirase.fathimaabubacker@dcu.ie, mmalashban@pnu.edu.sa

**Abstract.** Coronary heart disease (CHD) is a deadly disease that affects people around the world, yet early prevention can help to decrease mortality numbers. An increase in total blood glucose levels is one of the high-risk factors for CHD occurrence. Therefore, it is important to control glucose regulation and slow down the development of diabetes. Advances in the machine learning approach helps to create a multiclass classifier capable of categorising patients as normal, prediabetic or diabetic based on blood glucose levels. In addition, a modifiable diet based on the classified patient's glucose levels aids in reducing the risk of developing heart disease. This study aims to classify blood glucose levels for CHD risk factors using the highly imbalanced Framingham Heart Study dataset and to identify a suitable dietary plan that reduces the risk of developing CHD. The efficiency of classification depends on the balanced dataset; hence, the proposed study aims to apply effective imbalanced data techniques such as Random Oversampling, SMOTE, SMOTENNN and SMOTETomek to enhance the classification performance. Various imbalanced data techniques with different classifiers are used for investigation. The results suggest that the voting ensemble classifier with the random oversampling technique recorded the highest balanced accuracy, outperforming other classifiers with AUC (73%), specificity (77.45%), sensitivity (72%), F1 measures (78%) and balanced accuracy (67.94%). The proposed study suggests a suitable dietary plan, including preventive tips for normal patients, a low glycaemic diet for prediabetes and a diabetic diet for diabetes patients, which help to reduce the development of CHD risk factors.

**Keywords:** Classification algorithms, machine learning, random oversampling, SMOTE, SMOTENNN, SMOTETomek, logistic regression, support vector machine, random forests, multilayer perceptron, voting ensemble classifier.

## 1 Introduction

Cardiovascular Disease (CVD) is one of the deadliest diseases in the world. The most common type of cardiovascular disease is Coronary Heart Disease (CHD), which results in over 350,000 deaths yearly [1]. Fortunately, it is possible to prevent coronary heart disease and reduce mortality if those at high risk are identified well in advance of an

adverse coronary event [1]. Intervention experiments have shown that lowering risk factors decreases the CHD rate and other CVDs [2]. Risk factor accumulation is the main cause of CHD, while diabetes is a major risk factor for its occurrence [3]. The 10-year mortality rate from CHD is significantly related to high blood glucose levels [4]. Thus, it is important to control glucose regulation and slow down the development of diabetes in order to reduce the mortality incidence from CVDs [3].

Dietary management of high-risk CHD patients depends not only on the stage of the disease but also on other conditions, such as blood glucose levels and other risk factors [2]. In this study, the main focus is on blood glucose levels to identify a suitable diet plan for high-risk CHD patients. Dietary management of high-risk CHD patients relies on the current stage of blood glucose levels. There are three stages of glucose levels: normal, prediabetes and diabetes. Up to the prediabetes stage, patients do not have a high risk for CHD. Hence, patients in the normal and prediabetes stages may not require strict dietary controls. However, at the diabetes stage, patients require very strict dietary controls to avoid developing CHD. A special eating routine, such as the glycaemic diet [5] and diabetes diet [6], is important for controlling the disease and preventing further deterioration of the disease. Glycaemic and Diabetes diet plans are special eating routines for prediabetes and diabetes patients, respectively.

Machine learning is a motivating field of research that is being used to make important decisions based on the results of the analysis. Classification techniques can be used with medical data to diagnose the target class for each data piece. Automated classification using machine learning techniques will help doctors to diagnose patients as normal, prediabetic or diabetic based on blood glucose levels, and they suggest a diet plan for classified patients. This study addresses how recent advances in machine learning can be applied to create a multiclass classifier capable of diagnosing patients as normal, prediabetic or diabetic.

## 2 Literature Review

The classification procedure identifies the target class for every piece of data. Classification is likewise utilised to determine blood potassium level and identify a suitable diet plan for the patient [7]. Wickramasinghe et al. [7] applied different algorithms such as multiclass decision jungle, multiclass decision forest, multiclass neural network and multiclass logistic regression to classify the potassium zone. The results show that a multiclass Random Forest algorithm gives a better result than other classification algorithms. The utilisation of classification algorithms was examined by Govindarajan et al. [8] to classify a stroke that combines data mining tools and machine learning algorithms using artificial neural networks, as well as to support vector machines, boosting and bagging, and random forests. The obtained results have illustrated that the artificial neural networks succeeded in outperforming other algorithms with a smaller standard deviation and a higher classification accuracy.

Class-imbalanced data is a challenging issue in supervised learning as standard classification techniques are designed to handle balanced class distributions. While various strategies exist to solve this problem, methods that generate data to obtain a balanced

class distribution are more varied than modifications to the classification algorithm [9]. Douzas et al. [9] applied the simple and effective oversampling method SMOTE, which avoids the generation of noise and effectively overcomes imbalances between and within classes. Many algorithms have been proposed, but most are complex and tend to generate unnecessary noise.

Empirical results of extensive experiments with various datasets show that training data oversampled with the proposed method improves classification results. Bach and Werner [10] examined undersampling and oversampling methods when analysing imbalanced data related to osteoporosis; they found that the most efficient combination was SMOTE with the Random Forest classifier. Batista, Prati and Monrad [11] undertook research into different datasets and demonstrated that oversampling methods offer good performance in datasets with a low number of positive examples. They specifically noted that random oversampling methods performed well with datasets that had a relatively large quantity of majority examples. These researchers also offered a pair of SMOTEEEN and SMOTETOMEK methods and analysed their behaviour in comparison with resampling techniques used to deal with imbalanced datasets. Comparative experimentation demonstrates that oversampling offers greater accuracy than undersampling with consideration to the area below the ROC curve (AUC). Both methods offered excellent outcomes when employed with datasets having a low quantity of positive examples. Liu et al. [12] proposed a novel method for oversampling minority classes. Results from experiments demonstrate that this method improved AUC by 37.83% (from 0.513 to 0.707), which provided the highest AUC for the imbalanced temporal clinic brain magnetic resonance imaging dataset.

### 3 Dataset

The Framingham Heart Study dataset is collected from a cardiovascular study on residents of the town of Framingham, Massachusetts. It is publicly available on the Kaggle website [13]. There are over 4,000 unique patients with 16 different attributes related to risk factors of heart disease. Each attribute is a potential risk factor, including demographic, behavioural and medical risk factors. It is a highly imbalanced dataset, meaning that the number of instances is different in each class. Due to the imbalanced dataset, several imbalanced data techniques have been applied. Table 1 shows the attributes of this dataset.

### 4 Methodology

#### 4.1 Data Preprocessing

The data preprocessing step is essential because real-world data is generally noisy, incomplete and inconsistent. The missing values are handled by implementing a single imputation method [14]. The categorical variables are imputed by a mode and continuous variables imputed by median. Min-max normalisation is used to scale numeric

attributes values so that they can fall within a particular range. Categorical attributes have been transformed into a format that uses one hot encoding to improve work with classification algorithms. The continuous glucose column in this dataset has been converted to a categorical variable based on three classes—normal, prediabetes and diabetes [15]—to identify a suitable dietary plan for each category after building the classification model [7]. The main reason for converting glucose column to a categorical variable is to obtain a more accurate solution for the most suitable diet plan for the patient, which can be identified using the predicted classification result [7]. Feature selection and Principal Component Analysis (PCA) techniques have been applied in this study to improve the performance of the classifiers. The significant features used are PrevalentHyp, PrevalentStroke, BMI, DiaBP, Age, TotChol, SysBP and HeartRate.

**Table 1.** Attributes description.

ATTRIBUTE	DESCRIPTION	TYPE
Sex	Male or Female.	Categorical
Age	Age of the patient.	Numerical
Education	Education levels.	Categorical
CurrentSmoker	Whether or not the patient is a current smoker.	Categorical
CigsPerDay	The number of cigarettes smoked per day.	Numerical
BPMeds	Whether or not patient was on blood pressure medication.	Categorical
PrevalentStroke	Whether or not the patient had previously had a stroke.	Categorical
PrevalentHyp	Whether or not the patient was hypertensive.	Categorical
Diabetes	Whether or not the patient had diabetes.	Categorical
TotChol	Total cholesterol level.	Numerical
SysBP	Systolic blood pressure.	Numerical
DiaBP	Diastolic blood pressure.	Numerical
BMI	Body Mass Index.	Numerical
HeartRate	Heart rate.	Numerical
10yearCHD	The 10-year risk of coronary heart disease.	Categorical
Glucose	Glucose level.	Numerical

## 4.2 Dealing with an Imbalanced Dataset

To cope with class imbalances, the most frequently used data level approach is sampling. The sampling process modifies the training set to promote a more balanced distribution of classes. Sampling methods fall into different approaches such as under-sampling and oversampling. Under-sampling takes a few examples out of the majority class, while oversampling creates new synthetic examples and adds them to the minority class at the training stages. Variations on these standard techniques can be employed to combine both of them [11].

### Oversampling Techniques

Oversampling techniques [11] offer replications of minority class values, either randomly or as an element of an informative process. Increasing the number of minority instances is intended to create a better balance for the classes, but the generation of new instances brings with them a risk of overfitting. A number of methods have been created

with the purpose of making the oversampling method more informative and to lower the possibilities of overfitting. The advantage of oversampling techniques is that no information losses are involved.

*Random Oversampling (ROS):* ROS technique [11] operates through the replication of a randomly chosen collection of examples in the minority class to prevent the majority class disproportionately affecting training processes. As random sampling is used, the decision function finds it problematic in distinguishing borders between classes. Thus, although it is a standard method, random oversampling may not be effective in causing large improvements to minority class recognition. Possible problems with oversampling are that the classifier training time may be increased and overfitting may appear as class imbalance ratios worsen with the duplication of minority class examples.

*Synthetic Minority Oversampling Technique (SMOTE):* SMOTE technique [11] creates artificial data on the basis of similarities in feature space between existing minority classes through the introduction of minority classes that are not replicated that does not lead to loss of information [16]. Introducing new examples is an effective way of changing learner bias and creating more general bias, chiefly in terms of minority classes. The k-NN algorithm is employed for the extrapolation and creation of new minority examples from present imbalances in the minority classes. The k-NN neighbours are selected at random on the basis of the quantity of oversampling that is needed. Adding synthetically generated minority class examples creates more balance within the class distribution.

### **Hybrid Over- and Undersampling Techniques**

The hybrid methodology [17] is intended to balance training data as well as to take out noisy instances that are found on the wrong side of decision borders. To clean up the data, the most commonly employed methods are Edited the Nearest Neighbours (ENN) and Tomek link. Two good-to-go samplers are provided by imbalanced-learn, which are SMOTE with Tomek link and SMOTE with ENN techniques.

*SMOTE with Tomek link (SMOTETomek):* SMOTETomek technique [17] combines over- and undersampling using SMOTE and Tomek link. Class oversampling is performed using SMOTE and cleaning it using Tomek link. While oversampling may balance out class distribution in minority class instances, it does not solve other problems that generally appear with datasets that have skewed class distributions. There is often a lack of definition for class clusters when a number of majority class instances invade the space of the minority class. If classifiers are induced in such situations, overfitting may result. For the creation of class clusters, it is proposed that Tomek links should be applied to oversampled training sets to be employed as a data cleaning or undersampling method.

*SMOTE with Edited the Nearest Neighbours (SMOTEENN):* SMOTEENN technique [17] combines over- and undersampling using SMOTE and Edited Nearest Neighbours. Class oversampling is performed using SMOTE and cleaned using ENN. The motivation for using the SMOTEEN methodology is similar to the motivation for employing

the SMOTETomek methodology. ENN tends to remove a greater number of instances than the Tomek links. ENN is employed for the removal of instances in all classes and so any instance which undergoes misclassification from all three Nearest Neighbours will be taken out of the training set.

### 4.3 Modelling

Different machine learning models with different data mining techniques are used in this step. Hyperparameter tuning entails selecting a set of optimal hyperparameters for a learning algorithm. Hyperparameter optimisation has been applied using GridSearchCV to select the best parameters for the classification models.

#### **Logistic Regression**

Logistics regression (LR) is used for modelling relationships between one or more independent variables ( $X$ ) and a dependent variable ( $Y$ ) by estimating probabilities.

#### **Support Vector Machine**

Support Vectors Machines (SVM) [18] are a method for the classification of linear and non-linear data. They work by transforming the original data into a higher dimension. The SVM then searches for a hyperplane (decision boundary) that separates the tuple of one class from the others. The model is employed for non-linear classification using custom kernels and for mapping data through a higher dimensional space.

#### **Random Forest**

Random Forest (RF) [18] is an ensemble method which combines predictions from a multiplicity of Decision Tree (DT) algorithms to produce predictions that have a higher accuracy than any individual model. RF employs the classification from each tree to make an overall classification. The RF will choose the class of instances presented to it that has the most votes.

#### **Multilayer Perceptron**

Multilayer Perceptron neural networks (MLP) [18] represent one of the most important models for artificial neural networks. The structure of the MLP comprises an input layer, one or more hidden layers and an output layer. The input nodes pass on values to the initial hidden layer, and the nodes of the initial hidden layer pass values on to the second layer and so forth until the output is produced.

#### **Voting Ensemble**

Voting is one of the simplest ways in an ensemble learning technique to combine two or more algorithms to raise the accuracy of the classification model. It works by creating two or more individual models from the training dataset. A voting classifier considers the models as one model and averages the predictions of the sub-models to make predictions for new data. Voting classification is a good way when one classifier algorithm's defects can be a benefit for another classifier. The outputs of each classifier are combined, and extremely predicted classes are chosen that attain the best accuracy rate

[19]. The voting ensemble model is trained using the LR, SVM, RF and MLP models and then combines them to predict the final output. These classifiers were pitted against each other and the best-performing classifier was selected by voting using the voting classifier.

## 5 Results

The classification algorithms LR, SVM, RF, MLP and voting ensemble have been applied to the dataset using Python programming language. Different metrics have been considered rather than focusing only on balanced accuracy such as recall (sensitivity), specificity, F1, ROC Curve and AUC. The generalised comparison of the experiments is illustrated in Table 2 below.

**Table 2.** Balanced accuracy performance.

	<b>ROS</b>	<b>SMOTE</b>	<b>SMOTEENN</b>	<b>SMOTE Tomek</b>	<b>Original Imbalanced Dataset</b>
<b>LR</b>	64.00%	64.63%	65.00%	63.00%	58.00%
<b>SVM</b>	63.25%	64.47%	64.19%	63.33%	58.00%
<b>RF</b>	62.71%	65.00%	64.00%	65.00%	33.33%
<b>MLP</b>	62.65%	64.00%	61.32%	61.00%	33.29%
<b>Proposed Voting Ensemble</b>	<b>67.94%</b>	66.29%	67.55%	65.55%	<b>53.93%</b>

The comparison given in Table 2 aims to conclude the effect of sampling techniques on the imbalanced dataset with five classification models using balanced accuracy measures. It illustrates that the balanced accuracy performance of this dataset has improved for all the classifiers when using sampling techniques. In particular, it is observed from Table 2 that the balanced accuracy performance of LR (65.00%), SVM (64.47%), RF (65.00%), MLP (64.00%) and voting ensemble (67.94%) were improved when using sampling techniques compared with the original imbalanced dataset performance that obtained LR (58.00%), SVM (58.00%), RF (33.33%), MLP (33.29%) and voting ensemble classifier (53.93%). The performance of the classifiers using the balanced and imbalanced dataset is also shown in Fig.1.

From Fig.1, it is observed that the classifiers LR, SVM, RF, MLP and the voting ensemble with different sampling techniques outperformed the classifiers using the imbalanced dataset. To understand the significant performance of sampling techniques, Table 3 provides the performance results of sampling techniques in terms of AUC, specificity, sensitivity and F1 using different classification models.

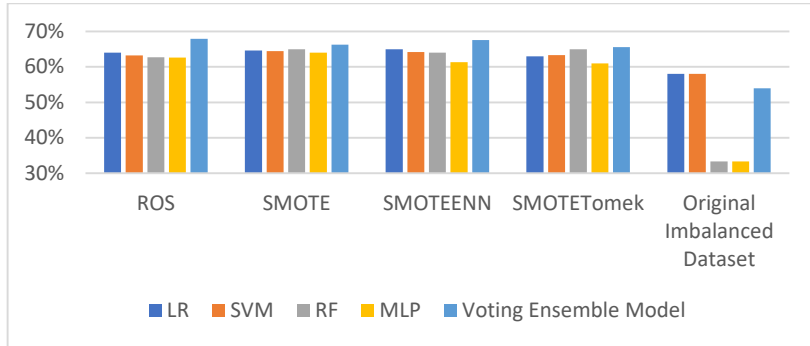


**Fig. 1.** The performance of the classifiers using balanced and original imbalanced dataset.

**Table 3.** The performance of sampling techniques ROS, SMOTE, SMOTENN, SMOTETomek.

		ROS	SMOTE	SMOTENN	SMOTE Tomek
LR	AUC	70.00%	70.00%	70.00%	69.00%
	Specificity	75.37%	74.75%	75.25%	74.42%
	Sensitivity	63.16%	61.48%	61.61%	61.74%
SVM	F1	71.67%	70.31%	70.38%	70.51%
	AUC	69.00%	71.00%	70.00%	69.00%
	Specificity	74.24%	76.60%	74.90%	75.05%
RF	Sensitivity	67.44%	61.74%	54.47%	58.63%
	F1	74.67%	70.76%	64.61%	68.18%
	AUC	68.00%	70.00%	69.00%	70.00%
MLP	Specificity	74.00%	75.47%	74.81%	75.50%
	Sensitivity	64.33%	63.42%	62.91%	71.08%
	F1	72.51%	71.88%	71.51%	77.39%
Proposed Voting Ensemble	AUC	69.00%	70.00%	67.00%	68.00%
	Specificity	74.68%	75.25%	72.28%	74.12%
	Sensitivity	67.44%	64.07%	39.43%	62.13%
	F1	74.78%	72.31%	49.90%	70.86%
	AUC	<b>73.00%</b>	70.00%	72.00%	71.00%
	Specificity	<b>77.45%</b>	76.38%	76.21%	75.89%
	Sensitivity	<b>72.00%</b>	72.00%	58.11%	72.00%
	F1	<b>78.00%</b>	78.00%	67.49%	78.00%

The comprehensive comparison given in Table 3 aims to conclude the efficient classification model with sampling methods that achieve the goal using specificity, sensitivity, F1 and AUC measures. It illustrates that the best performance of LR, SVM, RF,

MLP and the voting ensemble classifier is recorded with ROS, SMOTE, SMO-TETomek, SMOTE and ROS, respectively. More specifically, it is observed from Table 3 that the voting ensemble classifier with ROS followed by SMOTE obtained the highest value of AUC, specificity and sensitivity metrics, outperforming the other classifiers. Overall, voting ensemble outperformed other classifiers with ROS, which has AUC (73.00%), specificity (77.45%), sensitivity (72.00%) and F1 (78.00%). The performance of sampling techniques with classification models in terms of AUC, specificity, sensitivity and F1 is also shown in Fig. 2.

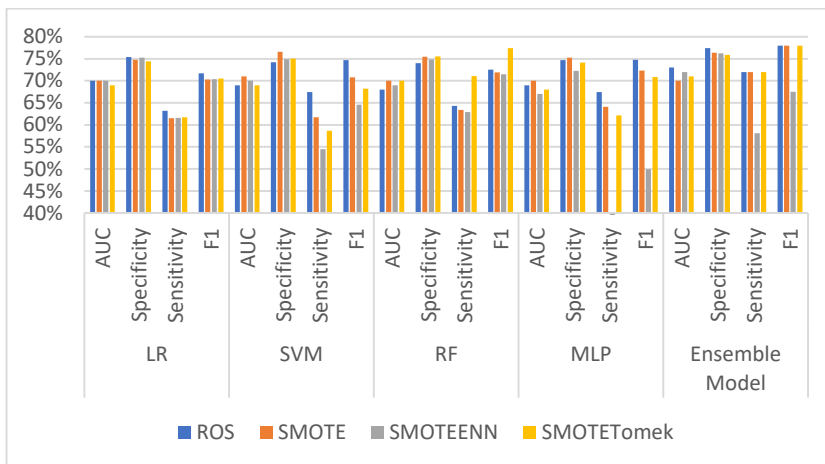


**Fig. 2.** The performance of sampling techniques with classification models in terms of AUC, specificity, sensitivity and F1.

Fig. 2 demonstrates that the voting ensemble classifier using random oversampling technique has outperformed other classifiers in terms of AUC, specificity, sensitivity and F1.

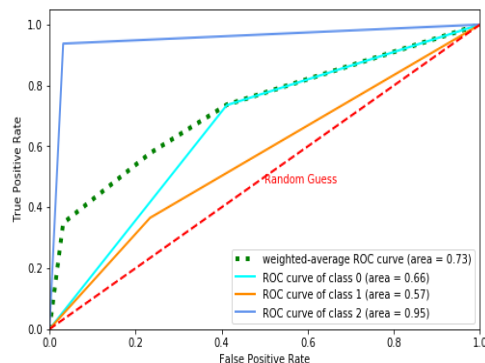


**Fig. 3.** Weighted average ROC score for the voting ensemble model using ROS technique.

Fig. 3 shows that the weighted average ROC score for the three classes is 73%. This clearly indicates that the voting ensemble classifier with ROS is good at distinguishing between diabetes, prediabetes and normal classes. We will also discuss the comparison of the proposed work with other works that are in the same domain with a different dataset. Kazlauskaitė et al. [20] examined Self-Monitored Blood Glucose (SMBG) performance. The data collected copies of SMBG diaries and concluded that a patient's self-assessment of his or her diary's sensitivity was 63% and specificity 56%. Moreover, Kumari et al. [21] designed a classification model for the detection of diabetes with better performance. The Pima Indian diabetic dataset has been utilized and concluded that the SVM could be successfully used for diagnosing diabetes disease with specificity (76.5%). Hence, the effective voting ensemble classifier in this study outperforms the others in terms of sensitivity (72%) and specificity (77.45%).

## 6 Conclusion

Blood glucose classification can be modelled as a multi-class classification problem. This analysis solves this problem by using five classical methods of machine learning with four sampling techniques. Experimental results derived from the highly imbalanced dataset offer insights into oversampling and hybrid over- and under sampling techniques. The performance of the dataset was improved when using sampling techniques. All classification models outperformed the original imbalanced dataset. Overall, the voting ensemble classifier with random oversampling recorded the highest performance, thus outperforming the other classifiers with AUC (73%), specificity (77.45%), sensitivity (72%), F1 measures (78%) and balanced accuracy (67.94%). Based on the classification of classes, the proposed work also suggests a suitable dietary plan, including low glycaemic [5] and diabetic [6] diet plans for prediabetes and diabetes patients, respectively. Furthermore, the proposed work suggests preventive tips for normal patients. Hence, the proposed diet plans for each type of patient will help to reduce the development of CHD risk factors.

## References

1. M. Dogan, S. Beach, R. Simons, A. Lendasse, B. Penaluna, and R. Philibert, "Blood-Based Biomarkers for Predicting the Risk for Five-Year Incident Coronary Heart Disease in the Framingham Heart Study via Machine Learning," *Genes (Basel.)*, vol. 9, no. 12, p. 641, 2018.
2. W. P. Castelli, "Epidemiology of coronary heart disease: the Framingham study," *Am. J. Med.*, vol. 76, no. 2, pp. 4–12, 1984.
3. M. Sun et al., "Efficacy and Safety of Ginkgo Biloba Pills for Coronary Heart Disease with Impaired Glucose Regulation: Study Protocol for a Series of N-of-1 Randomized, Double-Blind, Placebo-Controlled Trials," *Evidence-Based Complement. Altern. Med.*, vol. 2018, 2018.
4. K. Pyörälä, "Relationship of glucose tolerance and plasma insulin to the incidence of coronary heart disease: results from two population studies in Finland," *Diabetes Care*, vol. 2, no. 2, pp. 131–141, 1979.

5. “Glycemic Diet.” [Online]. Available: <https://www.mayoclinic.org/healthy-lifestyle/nutrition-and-healthy-eating/in-depth/glycemic-index-diet/art-20048478>. [Accessed: 19-May-2019].
6. “Enjoy-Food.” [Online]. Available: <https://www.diabetes.org.uk/guide-to-diabetes/enjoy-food>. [Accessed: 19-May-2019].
7. M. Wickramasinghe, D. M. Perera, and K. Kahandawaarachchi, “Dietary prediction for patients with Chronic Kidney Disease (CKD) by considering blood potassium level using machine learning algorithms,” in Life Sciences Conference (LSC), 2017 IEEE, 2017, pp. 300–303.
8. P. Govindarajan, R. K. Soundarapandian, A. H. Gandomi, R. Patan, P. Jayaraman, and R. Manikandan, “Classification of stroke disease using machine learning algorithms,” *Neural Comput. Appl.*, pp. 1–12.
9. G. Douzas, F. Bacao, and F. Last, “Improving imbalanced learning through a heuristic oversampling method based on k-means and SMOTE,” *Inf. Sci. (Ny.)*, vol. 465, pp. 1–20, 2018.
10. M. Bach, A. Werner, J. Żywiec, and W. Pluskiewicz, “The study of under-and over-sampling methods’ utility in analysis of highly imbalanced data on osteoporosis,” *Inf. Sci. (Ny.)*, vol. 384, pp. 174–190, 2017.
11. G. E. Batista, R. C. Prati, and M. C. Monard, “A study of the behavior of several methods for balancing machine learning training data,” *ACM SIGKDD Explor. Newsl.*, vol. 6, no. 1, pp. 20–29, 2004.
12. R. Liu, L. O. Hall, K. W. Bowyer, D. B. Goldgof, R. Gatenby, and K. Ben Ahmed, “Synthetic minority image over-sampling technique: How to improve AUC for glioblastoma patient survival prediction,” in 2017 IEEE International Conference on Systems, Man, and Cybernetics (SMC), 2017, pp. 1357–1362.
13. “Framingham Heart Study Dataset.” [Online]. Available: <https://www.kaggle.com/amanajmeral1/framingham-heart-study-dataset>. [Accessed: 2019].
14. Z. Zhang, “Missing data imputation: focusing on single imputation,” *Ann. Transl. Med.*, vol. 4, no. 1, 2016.
15. “American Diabetes Association.” [Online]. Available: [Diabetes.org/diabetes-basics/diagnosis/](https://www.diabetes.org/diabetes-basics/diagnosis/). [Accessed: 19-May-2019].
16. R. Akbani, S. Kwek, and N. Japkowicz, “Applying support vector machines to imbalanced datasets,” in European conference on machine learning, 2004, pp. 39–50.
17. C. Tantithamthavorn, A. E. Hassan, and K. Matsumoto, “The impact of class rebalancing techniques on the performance and interpretation of defect prediction models,” *IEEE Trans. Softw. Eng.*, 2018.
18. I. Choubey, “Machine Learning Techniques for Automatic Modulation Classification.” San Diego State University, 2017.
19. U. K. Kumar, M. B. S. Nikhil, and K. Sumangali, “Prediction of breast cancer using voting classifier technique,” in 2017 IEEE International Conference on Smart Technologies and Management for Computing, Communication, Controls, Energy and Materials (ICSTM), 2017, pp. 108–114.
20. R. Kazlauskaitė, S. Soni, A. T. Evans, K. Graham, and B. Fisher, “Accuracy of self-monitored blood glucose in type 2 diabetes,” *Diabetes Technol. Ther.*, vol. 11, no. 6, pp. 385–392, 2009.
21. V. A. Kumari and R. Chitra, “Classification of diabetes disease using support vector machine,” *Int. J. Eng. Res. Appl.*, vol. 3, no. 2, pp. 1797–1801, 2013.
- 22.



# A Review of An Interactive Augmented Reality Customization Clothing System Using Finger Tracking Techniques as Input Device

Feng, Liying<sup>1</sup>, Ng, Giap Weng<sup>2</sup>, Ma, Liyao<sup>3</sup>

<sup>1</sup>Hainan Vocational University of Science and Technology,  
Haikou City, 571126 Hainan Province, China

<sup>2</sup>Faculty of Computing and Informatics, Universiti Malaysia Sabah, Jalan UMS,  
88400 Kota Kinabalu, Sabah, Malaysia

<sup>3</sup>Faculty of Art and Design, University of Hainan, Haikou City,  
570228 Hainan Province, China

547772180@qq.com, nggiapweng@ums.edu.my, 576126427@qq.com

**Abstract.** This paper mainly focuses on the review of applications in Augmented Reality (AR) technology in the field of clothing customization using finger tracking techniques as input device. Review the influence and role of AR technology in the clothing customization industry. A comparative analysis of the technological advances and technical deficiencies embodied in the virtual fitting software developed by the world in the past 10 years using AR technology. Through research and comparison, a personalized clothing customization system based on AR technology is proposed. The system can enhance people's experience and interaction with the fashion design process and improve the satisfaction of clothing customization using finger techniques as input device.

**Keywords:** Augmented Reality, Interactivity, Experiencing, Custom Clothing, Finger Tracking.

## 1 Introduction

Since the invention of electronic computer technology, human's lives has been divided into two parts by computer technology: the physical and the digital world. The physical world is touchable and offers life pleasure. The digital world is a virtual world created through computer technology. Hence, how do we combine the real and virtual world? This is the magical effect of Augmented Reality (AR) technology, to superimpose virtual digital content in the real world and enhance the content. AR allows people to touch the real world and maintain a connection with real-time physical. At present, AR technology is leading the development of the times and will gradually integrate into all aspects of our lives, including business, art, culture and entertainment, and industry. Finger tracking is a high-resolution technique that is employed to know the consecutive position of the fingers of the user and therefore represent objects in 3D. The finger tracking technique is used as a tool of the computer that act as an external device in the

computer that is also similar to a keyboard and a mouse. In this application, users will interact with the application with mouse and finger to interact with the application. This application will detect and track user's finger through the finger track device which is the Leap Motion/Kinect and users can directly interact with the application. In each level of this application, instructions will be given.

## 2 Motivation

The goal of Augmented Reality is to enhance a person's perception of the surrounding world. The AR system will provide a better means for clothing customization which can enhance people's experience and interaction with the fashion design process and improve the satisfaction of clothing customization using finger techniques as input device. Creating suitable representation of the clothing customization in a rich context using AR interfaces will allow users to promote reflection of the metacognitive processes, where users could see the real world and virtual imagery, augmenting the real world with additional information in clothing customization with finger tracking as input device environment.

## 3 The Impact and Role of Augmented Reality Technology in the Clothing Customization Industry

### 3.1 AR Technology Can Meet People's Needs for the Interaction of Clothing in the Personalized Design Process

The style design, colour matching and fabric selection of the clothing are important elements of fashion design link. They are the entry point for designers to realize the design of clothing and the basic point for users to make personalized requirements. The colouring function, effect rendering function and real-time 3D effect display function in AR technology can provide consumers and designers with an uninterrupted interactive platform to meet human interaction needs in the personalized design process. It can effectively solve the designer's troubles. For example, the communication between designer and consumer may not be smoothly understood, the effect of low satisfaction result, 2D picture is not realistic, design time is time consuming and the cost of the sample production could be high.

### 3.2 AR Technology Can Meet People's Experiential Needs for Clothing Effects

In today's era, human's pursuit of material has gradually improved, and the standards of brand, quality and characteristics have been more clearly defined. People are more eager to obtain experiential services, also known as experiential consumption. According to Alibaba's vice president Jing Jie (2016): "The distance between the brand and the consumer is not the channel, but the experience"<sup>[1]</sup>. The AR virtual fitting mirror is

the most representative technical application of AR technology in the apparel industry, and it is also a hot spot for technology research and development. AR virtual fitting products can provide consumers with an immersive, authentic try-on experience to meet the consumer's experiential needs and increase the sales profit of the clothing. According to the sales data of the Chinese online sales platform "Tmall" after using the virtual fitting products in 2017, "AR technology can effectively enhance the purchasing confidence of users. By using the virtual fitting room customers, their average stay time on the website is increased from 2 minutes to more than 10 minutes, even to 50 minutes or more, and their average purchase rate is 5% increased to 15%"<sup>[2]</sup>. The designer brand store "Broadcast" launched a virtual fitting room function in Shanghai stores, achieving a year-on-year increase of 22.7% in turnover<sup>[3]</sup>. It can be seen that through the application and development of AR technology, the virtual fitting product can effectively meet the experiential demand of people for the try-on effect of the garment and achieve the commercial goal of increasing the sales of the garment.

### **3.3 AR Technology Leads the Intelligent and Diversified Development of the Garment Industry**

Although the current AR technology has a single application in fashion design, clothing display, clothing marketing, the development content is not profound, but in the future, AR technology not only represents a single application of smart technology in certain fields, but also represents a kind of new lifestyles, like smartphones, change people's entertainment, life and work. As AR technology matures, future applications will present in a variety of ways. Therefore, AR technology will focus on all aspects of real life in the field of apparel applications, enabling intelligent technology to serve people's application purposes, and this is also the development trend of AR technology leading the future garment enterprises to be intelligent and diversified.

## **4 The Comparative Analysis of the Application Effect of Typical AR Products in the Garment Industry**

Virtual fitting software and colouring technology are typical products developed by AR technology, and are also hotspots for AR product development in recent years. Virtual fitting software has changed the traditional clothing sales method with its realistic rendering effect, convenient try-on function and rich clothing resources, forming a clothing sales system integrating display appreciation, try-on experience, online purchase and other functions. It provides people with a more convenient and broader consumption space, and also creates greater commercial value for the seller. AR colouring technology was widely used in the development of children's paper books in the early days. Two years ago, AR colouring technology has been gradually developed and applied in apparel design. To date, the article is based on an in-depth analysis of the application of the above two types of products.

## 4.1 Functional Analysis of AR Virtual Fitting Software

### The Effect of the Model.

*Display Real-time Human Body Model.*

The mannequin is the main part of the fitting period, and the effect of the mannequin directly affects the appearance of the fitting effect. According to the virtual fitting software data in the past ten years, at present, real-time data collected by the camera (such as kinect) can be realized, and the user's 3D human body model, motion, and expression can be displayed in real time on the display screen. For example, the product "Vss For In-Store Retail" developed by Zugara in the United States in 2009<sup>[4]</sup>, the product "Swivel" developed by Ultra-Realistic Company in 2011<sup>[5]</sup> and the product "AR Door Kinect" developed by Russian AR Door Company, in 2012, NDP Company of Japan developed the product "UNIQLO Magic Mirror"<sup>[6]</sup>, the product "Trylive" developed by Total Immersion in France in 2013 and the product "Virtual wardrobe" developed by Microsoft, United States in 2014<sup>[7]</sup>. These products can achieve real-time mannequin display effects. This human body model reflects the characteristics of the model itself to a great extent, giving people a sense of realism like a mirror. It has won people's acceptance and love, but it has not been reflected in the personalization of makeup and hair style and needs of further development.



Fig. 1. NDP-UNIQLO Magic Mirror



Fig. 2. Total Immersion- Trylive

*Configuring a Standardized Human Body Model.*

With the development of time, AR virtual fitting technology has gradually improved, and 2016-2018 is the rapid development stage of China's development of AR virtual fitting software. China's well-known online sales platforms such as Tmall, Jingdong, and Alibaba have successively launched the AR virtual fitting function. The fitting software developed by these sales platforms has chosen to use a fixed-configuration standard model instead of the user's own real-time image. This fixed standard model can achieve maximum access to user data by modifying body characterization data. Taking a dressed mannequin as an initial condition, a virtual try-on is achieved by mapping the geometric relationship between the original garment and the human body to a new human body model<sup>[8]</sup>. Now, better Chinese software, such as the fitting system developed by Good Buying Co., can rebuild the 3D virtual fitting body model in 20 seconds, with an average error of less than 1.5 cm in each dimension<sup>[9]</sup>. The fixed model can also

realize the function of replacing the facial image, that is, the system recognizes the facial features of the user according to the 2D picture provided by the user, performs intelligent extraction of the facial features, and reconstructs the 3D face model. The face model can also add facial features, hair styles, hair color and other details to make the overall human body model more aesthetic. From another point of view, although this model has an aesthetic adjustment function, but if the user cannot correctly and objectively set his skin color and body value, it will bring about a difference in the actual clothing try-on effect, resulting in try-on. The effect of the difference between the effect and the real effect.

### **The Effect of Clothing.**

In the virtual fitting software, in addition to prepare a high-quality human body model, factors that affect the fitting effect, such as whether the garment has a realistic fabric simulation effect, the size of the viewing angle, whether the garment is displayed with a 3D model, clothing and human body, whether the model positioning point has a high degree of fit and whether the garment can be automatically scaled according to different body sizes. At present, through the comparative analysis of the fitting software, most of the software that implements the user's own model, most of their clothing models are represented by 3D effects. Moreover, in the 3D clothing model products, about half of the fitting software can achieve 360-degree observation angles, such as the "UNIQLO Magic Mirror" developed by NDP in Japan in 2012, and the "Trylive" product developed by Total Immersion in France in 2013. The two softwares implemented the above functions earlier and enabled the system to automatically recommend the appropriate clothing based on the size of the experiencer. Producing a large number of 3D clothing models requires high costs. For example, complex clothing costs about several thousand yuan, and data storage requires high storage space. Therefore, in order to reduce development costs, some virtual fitting systems use 2D clothing and A combination of 3D mannequins. For example, in 2014, the product "Virtual wardrobe" developed by Microsoft Corporation of the United States was used by people in the High Street store. The device, hailed as 'every woman's dream invention', uses Microsoft's motion sensing technology, Kinect 3D<sup>[9]</sup>.

### **Human-Computer Interaction and Other Auxiliary Functions.**

At present, all kinds of fitting software have shown a very friendly and beautiful interactive interface. Most of these software systems use Kinect's somatosensory camera to collect human body data, perceive the user's gestures and sounds, and give corresponding responses in time. Fully experience the AR technology to bring intuitive and real-time interaction and experience to the customer, so that the user liberates the hands. Get rid of the mouse, touch screen and other media, and return to the most real physical movements of people. On the basis of friendly somatosensory interaction function, individual fitting software continues to develop more powerful auxiliary functions, such as accessory display, online purchase, effect photography, advertising and other auxiliary functions are gradually developed and applied. The product "Swivel" developed

by Ultra-Realistic, shown below, is the first virtual fitting software that integrates the accessory functions into the system [5].



**Fig. 3.** Virtual fitting mirror developed by Ultra-Realistic

Another example is the virtual fitting product developed by China Gooda Company in 2018. It can not only realize auxiliary functions such as taking photos, online purchase, advertising, but also build a mature 3D clothing wisdom platform with intelligent face recognition and intelligent human body, model building, smart clothing 3D, automatic body measurement, smart clothing matching recommendation, system API interface, virtual try-on sharing and other functions. The company currently has the world's original intelligent anthropometric technology, using image recognition, artificial intelligence and other algorithms, automatically calculate the user's body size and other key data, can achieve the acquisition of 80 body data in 0.5 seconds. These advanced accessibility features give users a more convenient and intuitive experience.



**Fig. 4.** Gooda's 3D clothing smart system

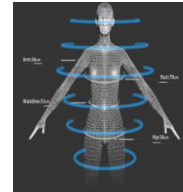


**Fig. 5.** Human data collection

NO.	year	Country	Company	product name	Representative partner	Real human model	interactive mode	2D/3D	Perspective	Accessories	photos and share	online sale	ad
1	2009	America	Zugara	Webcam Social Shopping/WSS For Web WSS For Kiosks VSS For In-Store Retail	PayPal	/	gesture	2D	180	x	✓	✓	✓
2	2009	America	Cisco	Video of future shopping mode		/	gesture	3D	180	x	✓	x	✓
3	2010	Japan	FURUTANI	Magic mirror	CRYSTA	/	~	2D	180	x	✓	✓	~
4	2011	~	Ultra-Realistic	Swivel	Face Cake	/	gesture	2D	180	/	✓	~	✓
5	2011	Russia	AR Door	AR Door Kinect	Topshop	/	gesture	3D	180	x	~	~	✓
6	2012	Japan	NDP	UNIQLO Magic Mirror	UNIQLO	/	gesture	3D	360	x	✓	~	~
7	2013	Franch	Total Immersion	Trylive	MISTET SPEX	/	gesture	3D	360	/	✓	✓	~
8	2013	Japan	Digital Fashion	Active Lab		~	/	gesture	3D	~	x	~	~
9	2014	America	Intellabs	augmented reality dressing room		~	x	gesture	2D	~	x	x	~
10	2014	America	Microsoft	Virtual wardrobe	High Street 商店	/	gesture	3D	360	x	✓	x	~
11	2016	China	HAOMAYI	Good Match Box	TMALL	x	touch	2D	180	x	✓	✓	✓
12	2018	China	JingDong		INMAN	x	touch	3D	360	x	✓	✓	✓
13	2018	China	Gooda		Alibaba	x	touch	3D	360	x	✓	✓	✓

**Fig. 6.** Development of virtual fitting technology

## 4.2 Functional Analysis of AR Colouring Technology

As another mature application of augmented reality, AR colouring technology has gradually gained favour and application in the clothing industry by virtue of self-design and self-filling. At present, China's more mature fashion design product "Huafu Small Dwelling" can realize the individualized design of clothing colour to meet the user's self-design and self-appreciation experience. This is the barrier between the fashion designer and the user. For this reason, applying AR technology to the clothing design and clothing customization can effectively improve the satisfaction of the design effect.

Through the technical comparison of the virtual fitting software for nearly 10 years, we can clearly know that although various countries are striving to develop new products, the virtual fitting software developed by AR technology is still immature. Such as clothing and mannequin movements are delayed. There is less software that uses the real-time real-life model as the main body of the fitting, and it has not yet reached the stage of popularization. In terms of apparel design, customized products that can be self-designed are also very rare. Therefore, designing a clothing customization system that uses a human model and uses finger tracking technology as an input device can effectively reduce the cycle of the garment from design to finished product. This can make large-scale personalized clothing customization possible. At the same time, virtual fitting will help merchants reduce the cost of advertising and reduce clothing consumption, which has a good effect on business operations. Therefore, the research on the related technology of the clothing customization system with the virtual fitting function has high practical application significance and commercial value.

## 5 The Design of Clothing Customization System Based on AR Technology

Haute couture clothing originated in France in the 20th century, and today it has become a popular fashion trend in the world [9]. Traditional Haute Couture focuses on superb craftsmanship and advanced fabrics and is a representative of the luxury of high society. So, nowadays, how can more people enjoy the luxury service of high-end customization, and can meet the needs of people's self-design? To this end, the development of a clothing customization system based on AR technology is very research-oriented. On the one hand, through the comprehensive development and application of the colouring technology and virtual fitting technology in AR technology, the user can realize the intelligent design of self-design, self-matching colour and self-testing effect. On the other hand, the traditional high-end custom hand-made process is preserved for manual measurement, manual pattern making, cutting and hand-made. This design system not only allows users to experience the advanced product design environment, but also allows users to experience the traditional hand-customized production process and enjoy the traditional custom-retained luxury service.

Based on the above analysis, the following two parts of the system function modules are proposed:

- (1) **Intelligent interactive design module:** This module mainly solves two problems of style design and virtual try-on of clothing. The design of clothing style includes clothing style design, pattern design, colour matching and costume 3D model construction. The fittings include the construction of the human body model, the realization of the virtual fitting and the rendering of the clothing effect.
- (2) **Traditional manual custom module:** This module mainly realizes three functions of size measurement, pattern making, tailoring and sewing of garments, and each part needs manual operation by professional personnel.

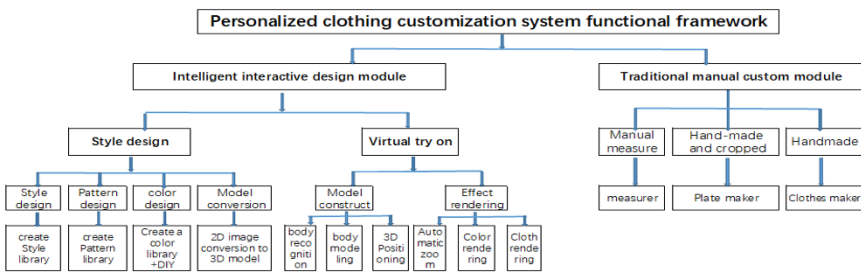


**Fig. 7.** The specific system architecture diagram

## 6 Interaction Technique of Augmented Reality System

The interaction technique in an AR system can be divided into at least six categories which are 3D pointing where devices like mouse is used, gesture recognition where hand-worn trackers or hand-mounted camera is used, gaze tracking where tiny camera is used to track gaze direction, speech recognition where microphones and earphones are used, text input where keyboard, keypads of hand-held devices or pen-based handwriting recognition system is used and lastly context awareness where information of users' position and orientation is required for manipulation of AR system interface<sup>[10]</sup>.

There are many types of display technique, tracking technique and interaction technique. However, the types which are suitable to be employed in AR system are highly depending on several aspects either within the system or external factors. External factor which determined the types of technique being employed are the allocation of resources, i.e time, money and human resources. In the AR system, the types of display technique, tracking technique and interaction technique are interdependent. If the display technique chosen need high computational power and a device like HMD is used, then the tracking technique which need high computational power like natural features based tracking can be used.

## 6.1 Way of Interaction

There are three categories of interaction which are positioning, moving and controlling. In positioning, users able to directly interact with the book by placing some AR element into the environment by using tangible interfaces as for a trigger to activate some event such as start an animation. In second category which is moving, users will able to have direct interaction with the environment by moving certain AR element from one place to another place. As for controlling, users will able to have indirect interface with the environment by controlling some AR element of the environment through interface provided on the screen of display devices or virtual button.

## 6.2 Finger Tracking

The finger tracking system is focused on user-data interaction, where the user interacts with virtual data, by handling through the fingers the volumetric of a 3D object that we want to represent [11]. This system was born based on the human-computer interaction problem. The objective is to allow the communication between them and the use of gestures and hand movements to be more intuitive. These systems track in real time the position in 3D and 2D of the orientation of the fingers of each marker and use the intuitive hand movements and gestures to interact.

## 6.3 Finger-Based Concept

Touch screen-based interaction seems intuitive because it conforms to regular smart phone interaction with almost all common applications (including most current commercial mobile AR programs) [12]. However, it only allows to remotely control the tri-dimensional augmented reality via 2D input on the touch screen. If we track the users' index finger when their hand is moved in front of the device (i.e. when it appears in the live video on the screen), we can realize a finger-based interaction where the tip of the finger can be used to directly interact with objects, i.e., select and manipulate the object. In the ideal case, we can track the finger in all three dimensions and thus enable full manipulation of objects in 3D. However, since 3D tracking with a single camera is difficult and noisy (especially on a mobile phone with a moving camera and relatively low processing power), we restrict ourselves to 2D interactions in this study. In order to avoid influences of noisy input from the tracking algorithm, we also decided to use a robust marker-based tracking approach where users attach a small sticker to the tip of their index finger. Object selection is done by "touching" an object (i.e., holding the finger at the position in the real world where the virtual object is displayed on the screen) until an associated progress bar is filled. Menu entries can be selected in a similar fashion. In translation mode, objects can be moved by "pushing" them. For example, an object is moved to the right by approaching it with the finger from the left side and pushing it rightwards. Clicking anywhere on the touch screen places the object at its final position and leaves translation mode.



**Fig. 8.** Finger-Based Concept

## 7 Conclusion

In summary, the main purpose of this project is to study and exposed people to the usage of finger tracking techniques in an interactive augmented reality experience-based personalized clothing customization system. Human's pursuit and awareness of beauty has gradually improved, personalized and distinctive clothing has become a mainstream goal pursued by human. Consumers' demand for products no longer stays in terms of function, quality, quality but to the pursuit of experiential services at the psychological level. What human's need is to experience the feeling of pleasure in the process of consumption, hence the personality customization has become the norm of modern consumers. Participatory and interactive experiential consumption has become the next generation market highland of e-commerce. Therefore, using AR technology to provide users with a participatory and interactive experience-based personalized clothing customization system has important research significance for promoting the breakthrough of AR technology and exploring the trend of personalized clothing customization.

## References

1. Tianxia Business Network: Tmall Interactive Alliance was established in 2017. Tmall merchants customized exclusive consumer experience for buyers, <http://www.chinaz.com/biz/2016/1221/631173.shtml> (2016).
2. Chinese clothing circle: UNIQLO did not make a virtual fitting, good buy clothes: let Inditex Group take the lead, [https://www.sohu.com/a/129802918\\_386972](https://www.sohu.com/a/129802918_386972) (2017).
3. Zinc Finance: From the line to the line, how does the virtual fittings break through the retail border? Retrieved from <http://mini.eastday.com/a/180316102452559.html>.
4. Zhiyun.: Virtual test clothes comparable to shopping malls: Interview with the US ZUGARA company product marketing department Deputy General Manager JACK BENOFF. Cultural monthly,(1),50—53 (2013).
5. Yamin, W., Ying, F.: Augmented reality technology in the field of clothing. Woolen Technology,46(05),57-61 (2018).
6. Chunlong,J.: Kinect-based 3D virtual fitting system. Xidian University of Electronic Technology (2014).
7. Winter, Katy: Every woman's new best friend? Hyper-realistic new virtual mirror lets you to try on clothes at the flick of the wrist and instantly share the images online[N]. Daily Mail, 21 May 2014.

8. Li , J. , Ye, J. , et al. Fitting 3D garment models onto individual human models. *Computers & graphics*, 34(6), 742-755 (2013).
9. Siying,C.: Creative Design of Cheongsam in High-end Clothing Customization. GuangZhou University (2018).
10. Van, Krevelan, Poelman, R.: A Survey of Augmented Reality Technologies, Applications
11. and Limitations. System Engineering Section, Delft University of Technology Jaffalaan 5, 2628BX Delft, The Netherlands (2010).
12. Goebl, W., Palmer, C.: Balasubramaniam, Ramesh, ed. “Temporal Control and Hand Movement Efficiency in Skilled Music Performance”.PLoS ONE. 8(1): e50901.doi:10.1371/journal.pone.0050901. PMC 3536780. PMID 23300946 (2013).
13. Wolfgang, H, Casper, V.W.: Gesture-Based Interaction via Finger Tracking for Mobile Augmented Reality. Volume 62, Issues 1, pp.233-258. Retrieved from <https://link.springer.com/article/10.1007/s11042-011-0983-y> (2013).



# Classifying Emotion based on Facial Expression Analysis using Gabor Filter: A Basis for Adaptive Effective Teaching Strategy

Anna Liza A. Ramos<sup>1\*</sup> Bryan G. Dadiz<sup>2</sup> Arman Bernard G. Santos<sup>3</sup>

<sup>1</sup> Saint Michael's College of Laguna , Binan , Philippines

<sup>2</sup> Technological Institute of the Philippines, Manila, Philippines

<sup>3</sup> Asiatech-Sta. Rosa, City of Sta. Rosa, Laguna Philippines

annakingramos@yahoo.com.ph, bryan.dadiz@tip.edu.ph,  
armie\_santos@yahoo.com

**Abstract.** Emotion is equivalent to mood or state of human emotion that correlates with non-verbal behavior. Related literature shows that humans tend to give off a clue for a particular feeling through nonverbal cues such as facial expression. This study aims to analyze the emotion of students using Philippines-based corpus of a facial expression such as fear, disgust, surprised, sad, anger and neutral with 611 examples validated by psychology experts and results aggregates the final emotion, and it will be used to define the meaning of emotion and connect it with a teaching pedagogy to support decisions on teaching strategies. The experiments used feature extraction methods such as Haar-Cascade classifier for face detection; Gabor filter and eigenfaces API for features extraction; and support vector machine in training the model with 80.11% accuracy. The result was analyzed and correlated with the appropriate teaching pedagogies for educators and suggest that relevant interventions can be predicted based on emotions observed in a lecture setting or a class. Implementing the prototype in Java environment, it captured images in actual class to scale the actual performance rating and had an average accuracy of 60.83 %. It concludes that through aggregating the facial expressions of students in the class, an adaptive learning strategy can be developed and implemented in the classroom environment.

**Keywords:** emotions, facial expression, Gabor filter, adaptive learning, facial expression, emotion detection, teaching pedagogy

## 1 Introduction

Emotion elicits stimuli such as happy, fear, neutral, angry, disgust, sad, which provides the signal to individuals to make strategic actions and decision making [1]. Decision making is significant to the educational setting environment in terms of how they develop students' and teachers' self-regulation [2] thus improve academic achievement [3]. Emotion is now being observed and given so much attention [4] to transform

learner's values and behavior [5], motivate learning [6] and creates different classroom contexts, [7].

Furthermore, emotion influenced individual intrapersonal, interpersonal and social, cultural and political dimensions [8] In fact teachers are encouraged to read the facial expression of students' in order to assess the level of understanding [9] educators are also help to strengthen knowledge acquisition through employing an engaging environments [10], consider emotion through integration of experience to the academic study [11] and [12] stated that it is vital to detect one's emotion before applying mitigation technique. On the other hand, emotion influence teachers' decisions about their delivery of instruction together with its content in facilitating learning [13] and it revealed that teachers understand the aims of education by giving importance on creating positive-student teachers relationship to support student development both academically and socially [14]. There are several studies conducted to observe the leaner's emotional behavior as the basis for employing interventions and teaching strategies. A study revealed that the active participation of students in the class connotes happiness which means that the students showed interest in their studies [15] A teaching strategy is to adapt either these two approaches by asking the students or proceed to the next level of discussion. With regards to student's avoidance of discussion and absence of engagement, it connotes the fear emotion [16], [10] The strategy is to employ group activities [17]. In a collaborative approach, students create a project in a group to elicit interactions among the members of the group [18], [19]. Application of real-world engagement and connection in concepts and experiences [20] encouragement of students to respond question and provides them investigative techniques that apply inquiry approach [21] [22] and recognizing prior knowledge, an integrative approach [23] and the application of inquiry or constructivist approach [24], These approaches are applied to elicit learning. According to UNESCO, an effective pedagogy holistically develops learners. However, it was found out that social and emotional pedagogy is not a core set of things that teachers know instead they perform within the rhythms of their work in terms of considering the student emotions and social positionalities through their planning instructional practices [25].

Through the advancement of technology, detection of emotion is one the emerging research field in affective computing. There are application and tools being using computer vision learning analytics and machine learning [26]. Several, studies conducted focusing on the emotion that implements different approaches and applied best-suited algorithms. Emotion analysis using feature dimensionality techniques, [27][28] Some of the studies are analyzing the sentiments of the customer [29], recognizing the malicious intention through gesture [30], detecting the stress level of a person [31] determining student emotion in computer programming activities [32] , assessing the emotion of participants interacting the computer interfaces activities [30], identifying the level of student engagement in Java Programming activity [33] and capturing emotion expressed in mobile phone and internet to activate and express emotion [34]. Majority of these studies are utilizing the Cohn Kanade and JAFEE databases. In this study, it attempted to build a Filipino-based facial expression corpus to localize the detection and recognition methods.

Furthermore, to test the efficiency and effectiveness of the experiment by applying the best-suited algorithms to achieve higher accuracy to be implemented in the prototype model. The model can be useful for educators to assess the emotion of the students in a classroom setting environment. Moreover, this study provides discovery to analyze further the first build datasets based on Filipino features. Initial experiments were conducted on the previous paper from the average accuracy result from the still images [35]. The objectives of this paper include a) to build and analyze the Filipino based facial features using OpenCV with Haar Cascade Classifier for detection, Gabor Filter, and Eigenfaces API for features extraction, Support Vector Machine for classification and Euclidean distance for recognition b) to formulate teaching pedagogy based on the types of emotion c) to develop a prototype model that will be able to classify the emotion, aggregated the detected emotion which processed different type of formats and finally d) to test the recognition accuracy of the prototype model.

## 2 Methodology

This study applied an experimental approach where facial expression emotion of the subject is captured in supervised learning, utilization of the best suited algorithms for face detection, features extraction and face recognition and classification of facial features, the formulation of proposed teaching pedagogy based on the aggregated emotion and the testing of the developed prototype model which are able to accommodate different of formats such as still images, real-time video and video file for processing the images.

### 2.1 Building the training dataset

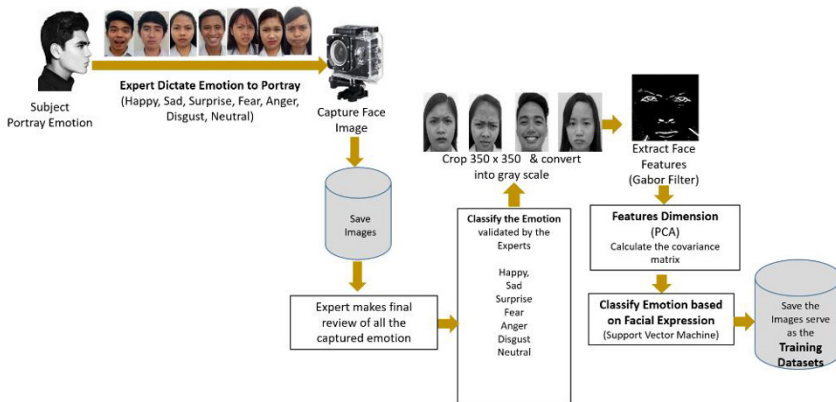


**Fig. 1.** Annotation of Emotions from Images by Psychologist

Fig. 1, the study built the training datasets with the assistance of the experts in validating and verifying the portrayed facial expressions of the subjects. The validation applied two approaches, first is to instruct the topic by providing a sample image on how to describe the required emotion. However, among the emotions, specifically "fear" emotion was the difficult emotion to be portrayed, it needs assistance for the experts to institute a scenario or provide a role play for the subject act the required emotion. All 1 images were reviewed again by the experts after taking the images to ensure the accuracy of the portrayed emotion. Their total images are total of 611 images composed of 281 images of female and 331 images of male subjects ages from 18 to 20 years old portraying the emotions on " Happy," "Fear," "Neutral," " Sad," "Surprised," "Disgust" and "Anger." This presentation of images is not balanced due to the elimination of incorrect emotion portrayed from 1024 images down to 611. To determine the accuracy, the images are fed into Weka tool to balance the features and utilize Rapid Miner tool to check the classification accuracy.

**Table 1.** Filipino based Facial Features Datasets

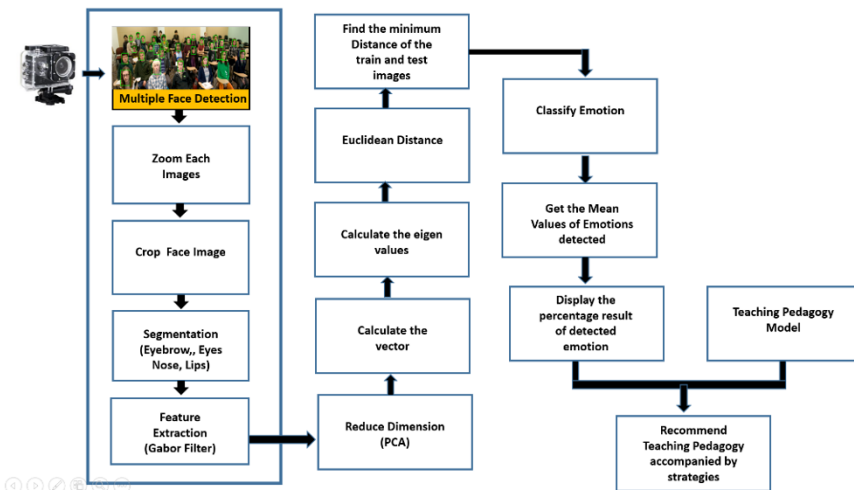
Emotion	Female	Male	Total
Happy	44	60	104
Fear	30	31	61
Neutral	44	54	98
Sad	37	43	80
Surprised	43	46	89
Disgust	42	43	85
Anger	41	53	94
<b>Total</b>	<b>281</b>	<b>331</b>	<b>611</b>

Table 1 shows the number of emotions portrayed by the subjects ages 18 to 20 years old. These images are not balanced due to the elimination of incorrect emotion portrayed from 1024 images down to 611. These images are fed into Weka tool to balance the features which will be used to check the classification accuracy using Rapid Miner tool.

## 2.2 Processing the images

Fig. 2, the prototype model was developed in JAVA and utilized an OpenCV for face image detection. The model detects multiple face images using Haar Cascade Classifier. Once detected, the images were zoomed using Bicubic interpolation and Replication algorithm. Then, these images would then, be cropped and converted into grayscale for the extraction of the features using Gabor Filter and Principal Component Analysis to optimize the search space. The facial features are classified using Support Vector Machine. For recognition purpose, the new input image will be compared to the training datasets using Euclidean distance finding its closest image vector. All detected emotions are aggregated every 20 seconds. The result of the aggregated would be then the basis for determining the recommended teaching strategies according to conditions set

in this study focusing the negative emotions composed of "Anger," "Disgust," "Sad," "Fear" and "Surprise." If one of these emotions marked the highest percentage, and if all these emotions are equal in percentage, then the prototype will aggregate as the basis for teaching strategies recommendation. Moreover, the prototype model is capable of processed features extraction by producing a pixel value of the image and generate a histogram. Also, the model allows uploading of video file format limited to 500m only, enable the teacher to set up a class schedule and generate PDF file report indicating the number of faces detected, teaching strategies recommendation and the histogram of detected emotion.



**Fig. 2.** Conceptual Framework

### 2.3 Formulation of the Teaching Pedagogy Matrix

The survey was facilitated where the respondents were asked to rank the teaching strategies according to each emotion. The survey questionnaire was formulated from various sources and validated by experts. The questionnaire was composed of two parts: (1) the profile of the respondents and the teaching pedagogies/approaches identified such as Constructivism, Integrative, Reflective, Inquiry-Based, and Collaborative. The survey questionnaires were answered by 15 educators with master's and Doctorate in Education. The respondents ranked the five teaching pedagogy approaches by writing 1 is the best, and 5 is the least teaching pedagogy to be applied for a particular emotion. The data was tabulated based on the weighted mean and the frequency count. The result was ranked. Accordingly, the lowest number of count means represent the priority pedagogy for a certain emotion. The matrix was based on the pedagogy approaches which is equally distributed by 20% and with regards to the color-coding assignment of each pedagogy was based from sources where Orange color refers to Collaborative, Green color refers to Constructivism, Yellow color refers to Inquiry-based, Gray color refers to Integrative and Blue refers to Reflective.

### 3 Results and Discussion

Table 2. the Filipino based facial features were analyzed using different types of classification algorithms which among the algorithms provide higher accuracy as the basis for the implementation in the prototype model. Based on the results, the Support Vector Machine outperformed other algorithms specifically, the algorithm marked excellent performance on emotion such as "Disgust", "Fear" and "Happy" while the "Neutral and Sad" marked little difference in percentage because of the similarity in some facial features of the subject except for the lip area where the subject is advised to make pouty lips . It is same with the "Anger" and "Surprise" emotion were the features are difficult to distinguish because there are some facial features looked like Anger even it is not, particularly in the eyebrow and eye part.

**Table 2.** Classification Result based on Various Algorithms

EMOTION	SVM	Decision Tree	KNN	Naïve Bayes	Neural Networks	AVERAGE Accuracy
Anger	78.43%	70.59%	77.45%	82.18%	83.33%	78.39%
Disgust	100%	17.65%	85.29%	90.20%	47.06%	68.04%
Fear	100%	0%	72.55%	100%	62.75%	67.06%
Happy	100%	57.84%	91.18%	94.57%	92.16%	87.15%
Neutral	47.06%	1.96%	40.22%	62%	12.75%	32.79%
Sad	58.82%	0%	49.02%	79%	17.65%	40.89%
Surprise	76.47%	8.82%	95.10%	83.24%	78.43%	64.42%
<b>ACCURACY</b>	<b>80.11%</b>	<b>22.41%</b>	<b>72.97%</b>	<b>80.07%</b>	<b>56.31%</b>	

Table 2. the Filipino based facial features were analyzed using different types of classification algorithms which among the algorithms provide higher accuracy as the basis for the implementation in the prototype model. Based on the results, the Support Vector Machine outperformed other algorithms specifically, the algorithm marked excellent performance on emotion such as "Disgust", "Fear" and "Happy" while the "Neutral and Sad" marked little difference in percentage because of the similarity in some facial features of the subject except for the lip area where the subject is advised to make pouty lips . It is same with the "Anger" and "Surprise" emotion were the features are difficult to distinguish because there are some facial features looked like Anger even it is not, particularly in the eyebrow and eye part.

**Table 3.** Prototype Model Recognition Result in Different Formats

Format	Detected Images	Percentage
Still Images	24/35	68.57%
Uploaded Video File	3/5	60%
Real-Time Video	7/13	53.84%
<b>Average</b>		<b>60.83%</b>

Table 3. showed the results of the three (3) different formats applied in the experiment focusing the frontal view. And to, re-assure the accuracy of the prototype since it will not produce 100% accuracy due to the limitation of the datasets, the experts checked the performance of the proto-type In the first experiment using still images there were about 11 out of 35 or 31.42 % emotions are detected incorrectly composed of 1 image for "Anger" emotion, 2 images for "Happy" emotion, 4 images for "Neutral" emotion , 2 images for "Disgust" emotion and 2 images for "Sad" emotion. This is due to resolution and distance issues. Some of the face images processed in the prototype model are too near; thus, it looks big-ger than the other images. In the experiment no. 2 using an uploaded video file format captured in a 16-megapixel resolution from cellular phone camera there are two subjects that are not into frontal view which greatly affect the result of the recognition. And for the third experiment, the real-time video format was used where the prototype is installed with a native built-in camera of a laptop. There were about 48 images captured; however, only 13 images are in frontal view 7 of which are correctly detected and labeled accordingly. The results are affected due to some issue on distance and blurry images.

**Table 3.** Emotion Classification Result based on Actual Classroom Environment

Emotion	Class1 (Earth Science)	Class 2 (Stat & Probabil- ity)	Class 3 (Physics)	Class 4 (Programming Class)
Anger	2/18 or 11%	3/42 or 7%	2/26 or 8%	4/30 or 13%
Disgust		2/42 or 55%		3/30 or 10%
Fear				2/30 or 7%
Happy		1/42 or 2%	1/26 or 4%	
Neutral	8/18 or 44%	5/42 or 12%	7/26 or 27%	4/30 or 13%
Sad	8/18 or 44%	26/42 or 62%	13/26 or 50%	5/30 or 17%
Surprise		5/42 or 12%	3/26 or 12%	8/30 or 27%
PEDAGOGY	INTEGRATIVE	REFLECTIVE	INTEGRATIVE	CONSTRUCTIVISM

Table 4. shows the result of classified emotion per class. The class provides exercises dealing with problem-solving activities. Based on the observation of the researcher and the teacher, the students, therefore, find difficulty in solving the provided activity. With the used of the prototype model, the prototype resulted a "Sad" emotion marked the highest percentage in three (3) classes for Earth Sciences, Stat & Probability, and Physics while in programming it generates an emotion "Surprise." This result validates the initial assessment of the teachers and the sentiments of the students as well because most of the students got the lower score in this experiment activity



**Fig. 3.** Prototype Model Capture

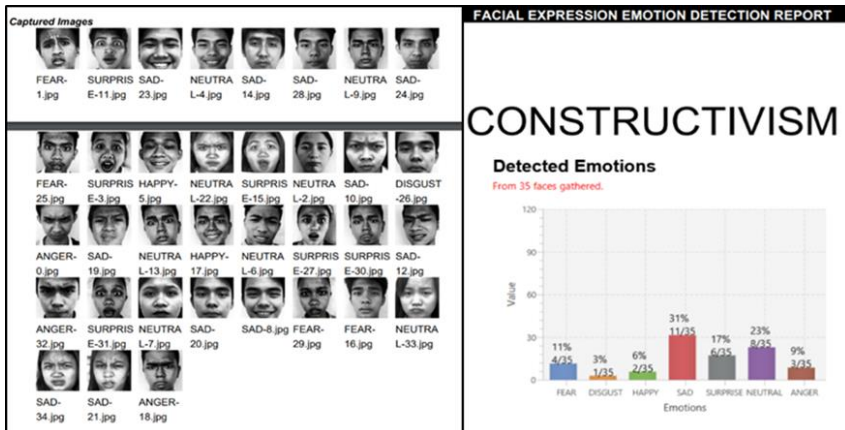


**Fig. 4.** Prototype Model Capture

In Fig. 4 and 5, the developed prototype model provides a panel to view the captured video, it also provides label "the continuous quality improvement (CQI)" result, the histogram of the detected emotion, the number of faces detected and generation of PDF report which contains the class information, the histogram of detected emotions and the teaching strategies recommendation. Moreover, the prototype can re-simulate the captured video. This prototype can be helpful for educators to visually view the student emotion and utilize the detected emotion report for further assessment or may address some issues and concerns.

## 4 Conclusion and Recommendations

Based on the result, it indeed provides good results even though the images are captured in various formats which marked an average result of 60.83 % and recorded 80.11% for classification accuracy utilizing the new build Filipino features. The build features are then recommended for utilization. Furthermore, the study can be useful for educational institutions to assess the emotional state of the students that will possibly affect students learning performance. This prototype model can be a great of help for the educators to manage the class more productively and effectively. To achieve the efficiency of the recognition and to strengthen appropriate teaching strategies recommendation applicable based on emotion. This study would like to recommend the following. Educators should develop an empirical study to identify what appropriate teaching strategies of an emotion which is suitable and applicable based on the topics and activities conducted. Utilize state-of-the-art resources for better detection and recognition. Consider algorithms which provide great performance in image processing. Consider building datasets in different angles, distance, and lighting concerns to increase the accuracy. Utilization resources that could provide a high-end camera for better detection and recognition. Apply other algorithms that will more improve the recognition accuracy and can efficiently optimize the image processing. Consider building datasets in different angles, distance, and lighting concerns to increase the accuracy.

## References

1. Lerner, J. S., Li, Y., Valdesolo, P., & Kassam, K. S. (2015). Emotion and decision making. *Annual review of psychology*, 66, 799-823.
2. Pekrun, R., & Goetz, T. (2002). Positive emotions in education. Beyond coping: Meeting goals, visions, and challenges. E. Frydenberg.
3. Rienties, B., & Rivers, B. A. (2014). Measuring and understanding learner emotions: Evidence and prospects. *Learning Analytics Review*, 1, 1-28.
4. Pitt, A. J., & Brushwood Rose, C. (2007). The significance of emotions in teaching and learning: On making emotional significance. *International journal of leadership in education*, 10(4), 327-337.
5. Türkkahraman, M. (2012). The role of education in societal development. *Journal of educational and instructional studies in the world*, 2(4).
6. Demetriou, H., Wilson, E., & Winterbottom, M. (2009). The role of emotion in teaching: are there differences between male and female newly qualified teachers' approaches to teaching?. *Educational studies*, 35(4), 449-473.
7. Meyer, D. K., & Turner, J. C. (2002). Discovering emotion in classroom motivation research. *Educational psychologist*, 37(2), 107-114.
8. Fried, L., Mansfield, C., & Dobozy, E. (2015). Teacher emotion research: Introducing a conceptual model to guide future research.
9. Mangurian, L. P. (2007). Learning, Emotion, and their Application for Teaching. In ACRL Thirteenth National Conference (pp. 1-10).
10. Shuck, B., Albornoz, C., & Winberg, M. (2013). Emotions and their effect on adult learning: A constructivist perspective.

11. Felten, P., Gilchrist, L. Z., & Darby, A. (2006). Emotion and Learning: Feeling Our Way toward a New Theory of Reflection in Service-Learning. *Michigan Journal of Community Service Learning*, 12(2), 38-46.
12. Tabbasum, H, Emaduddin, S, M., Awan Agsa & Ullah, R. (2019). Multi-Class Emotion Detection using Textual Analysis. *The International Journal of Emotional Education*. Vol 9, Number 1 pp. 85-98
13. McCaughtry, N. (2004). The emotional dimensions of a teacher's pedagogical content knowledge: Influences on content, curriculum, and pedagogy. *Journal of Teaching in Physical Education*, 23(1), 30-47.
14. Reeves, J., & Le Mare, L. (2017). Supporting Teachers in Relational Pedagogy and Social Emotional Education: A Qualitative Exploration. *International Journal of Emotional Education*, 9(1), 85-98.
15. Kimura, Y. (2010). Expressing emotions in teaching: Inducement, suppression, and disclosure as a caring profession. *Educational Studies in Japan*, 5, 63-78.
16. Essel, G., & Owusu, P. (2017). Causes of students' stress, its effects on their academic success, and stress management by students. Seinäjoki University of Applied Sciences, West Finland.
17. Marshall, E., Mann, V., & Wilson, D., (2016). Maths anxiety: A collaboration. HEA STEM conference, Nottingham
18. Reed, Z, A., (2014). Collaborative Learning in the Classroom. Center for Faculty Excellence, United States Military Academy, West Point, New York
19. Roselli, N. D. (2016). Collaborative Learning: Theoretical Foundations and Applicable Strategies to University. *Journal of Educational Psychology-Propósitos y Representaciones*, 4(1), 251-280.
20. Villanueva, M. G. F. (2010). Integrated teaching strategies model for improved scientific literacy in second-language learners (Doctoral dissertation).
21. Adams, P., & Findlay, C. (2015). Transforming Pedagogy and Practice Through Inquiry-Based Curricula: A Study of High School Social Studies. *One World* (04750209), 3(2).
22. Preston, L., Harvie, K., & Wallace, H. (2015). Inquiry-Based Learning in Teacher Education: A Primary Humanities Example. *Australian Journal of Teacher Education*, 40(12), n12.
23. Akpan, J. P., & Beard, L. A. (2016). Using Constructivist Teaching Strategies to Enhance Academic Outcomes of Students with Special Needs. *Universal Journal of Educational Research*, 4(2), 392-398.
24. Guthrie, K. L & McCracken, H., (2010). Reflective Pedagogy: Making Meaning in Experiential Based Online Courses. *The Journal of Educators Online*, Volume 7, Number 2,
25. Ferry, M., McCaughtry, N., & Kulina, P. H. (2011). Social and emotional pedagogy: Rhythm and junctures. *Journal of Teaching in Physical Education*, 30(1), 13-30.
26. Bosch, N., D'Mello, S., & Mills, C. (2013, July). What emotions do novices experience during their first computer programming learning session? In *International Conference on Artificial Intelligence in Education* (pp. 11-20). Springer, Berlin, Heidelberg.
27. Sarmiento, A. L., Aviñante, R. R., Liwanag, J. L., & Dadiz, B. G. (2018, June). Dimension Reduction Techniques Analysis on Image Processing for Facial Emotion Recognition. In *Proceedings of the 2018 International Conference on Control and Computer Vision* (pp. 23-27). ACM.
28. Prospero, M. R., Lagamayo, E. B., Tumulak, A. C. L., Santos, A. B. G., & Dadiz, B. G. (2018, June). Skybiometry and AffectNet on Facial Emotion Recognition Using Supervised Machine Learning Algorithms. In *Proceedings of the 2018 International Conference on Control and Computer Vision* (pp. 18-22). ACM.

29. Cambria, E. (2016). Affective computing and sentiment analysis. *IEEE Intelligent Systems*, 31(2), 102-107.
30. Greene, S., Thapliyal, H., & Caban-Holt, A. (2016). A survey of affective computing for stress detection: Evaluating technologies in stress detection for better health. *IEEE Consumer Electronics Magazine*, 5(4), 44-56.
31. Choi, J., Lee, S., Lee, C., & Yi, J. (2001). A real-time face recognition system using multiple mean faces and dual mode fisherfaces. In ISIE 2001. 2001 IEEE International Symposium on Industrial Electronics Proceedings (Cat. No. 01TH8570) (Vol. 3, pp. 1686-1689). IEEE.
32. D'Mello, S., & Calvo, R. A. (2013, April). Beyond the basic emotions: what should affective computing compute?. In CHI'13 Extended Abstracts on Human Factors in Computing Systems (pp. 2287-2294). ACM.
33. Ramos, A. Flor, J. & Casabuena , M., (2017). Face Expression Emotion Detection using Eigenfaces, Fisherfaces & Local Binary Histogram Algorithm towards Predictive Analysis of Students Emotion in Programming. 8<sup>th</sup> Euro Conference on Big Data and Applications, Gwangeong Korea
34. Serrano-Puche, J. (2015). Emotions and digital technologies: Mapping the field of research in media studies.
35. Ramos A. L. A. and Dadiz B. G., (2018). A Facial Expression Emotion Detection using Gabor Filter and Principal Component Analysis to identify Teaching Pedagogy. 1-6. 10.1109/HNICEM.2018.8666274.



# A Perspective Towards NCIFA and CIFA in Named-Data Networking Architecture

Ren-Ting Lee, Yu-Beng Leau, Yong Jin Park and Joe H. Obit

Faculty of Computing and Informatics, Jalan UMS, 88400, Universiti Malaysia Sabah, Sabah,  
Malaysia

LRT@JOSHLRT.COM, lybeng@ums.edu.my, yjp@ieee.org,  
joehenryobit@gmail.com

**Abstract.** Named-Data Networking (NDN) is the most promising architecture in the future Internet. NDN ensure high availability of contents and security of the data packet. However, it may disturb the stability and security in NDN routing such as Interest Flooding Attack (IFA). There are many existing detection and mitigation technique about IFA which labelled a non-collusive type of routing threats where it causes the PIT resources to exhausted and legitimate request could not perform in communication. Unfortunately, all the existing counter-measure mechanism could not defend the Collusive Interest Flooding Attack (CIFA). The attacks initiated with a satisfying interest and malicious data producer will reply to the corresponding request before the expiry of existing PIT entries in NDN router along the path. CIFA is classified as low rate intermittent attack which is very difficult in distinguish with legitimate requests. Thus, CIFA is more vulnerable and threatens than previous NCIFA. Moreover, there is no benchmark datasets or any public datasets to perform further experiments on detecting CIFA. Thus, there is a need to produce reliable datasets for future investigation in detection or mitigation relevant attacks in NDN.

**Keywords:** Gaming AI, Android Game Development, 3rd Person Shooting Game, Artificial Intelligence

## 1 Introduction

### 1.1 Internet Trending

The world is changing at a fast pace; The Internet had a shift from client-server based application to multiple clients with client application working with a distributed server. The trending of getting something from the internet such as searching over Google, Baidu and Amazon had become the most common things among the netizen. As the traffics and bandwidth is getting larger, the equipment that deploys classified as high-end which will be costly and it is the key for the whole solution in managing requests in data processing [1]. As the number of devices and users had increased tremendously, availability and security of data are taking for concern.

Future Internet architecture as described is an Information-Centric Networking (ICN) could using naming as request as the name is unique at its own, it can be creating at infinite. Besides that, the data content or the packet is secured in a distributed networking with digital signature or certificate [2]. One of the most promising solutions among the ICN is Named-Data Networking (NDN), fully funded by the U.S. National Science Foundation (NSF) under the Future Internet Architecture (FIA) program [3].

The aims are to solve the host-client IP based limitation in parallel to the growth of Internet networking, the increasing number of new devices appeared in both online services and applications especially in the Internet of Things (IoT) related solution [4]. The comparison of both architectures is shown in Fig. 1.

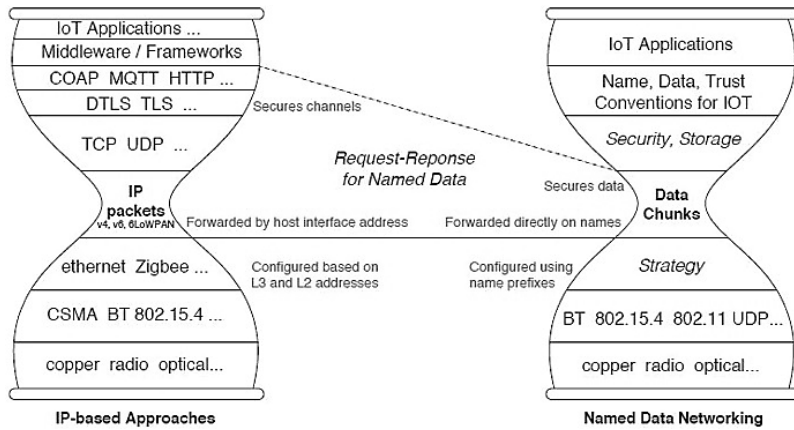


**Fig. 1.** Internet Architecture of IP-based Approaches versus Named-Data Networking

Fig. 1 shows a comparison between IP-based approaches and Named-Data Networking. The architecture shown in hourglass diagram clearly shown the differences of TCP/IP architecture is using destination address and source address for identification of host and client while NDN using name or data to identify the source rather than channel based communication. NDN is fitted into relevant network operations which traditionally available in IP-based approaches provided within the network layer.

## 2 Background

### 2.1 NDN Overview

NDN communication is driven by receivers such as data consumers via the exchange of packets in terms of interest and data [5]. These packets carry an identity which is a name that can be transmitted in a single data packet as shown in Fig. 2. There are 2 types of packets, interest packet is defined by consumer sends it over network and router will forward this name to data producer. Once interest reaches the data requesting node,

the data contains both the name with its content in the data packet will return to the consumer in a reverse path [6].

The NDN router consists of 3 major data structure:

1. Forwarding Interest Base (FIB) maps name prefixes to one or multiple physical network interfaces, specifying directions to which interest could be forwarded.
2. Pending Interest Table (PIT) holds all unsatisfied interests that have been sent upstream toward potential data origins. Each PIT entry contains an interest packet and one or multiple incoming physical network interfaces indicating multiple downstream consumers. NDN routers can achieve the reverse path data forwarding and multicasting without requiring the consumer to acquire a network address.
3. Content Store (CS) which is a temporarily buffers data packets that pass through NDN router which allowing prompt response for different consumers requesting the same data.

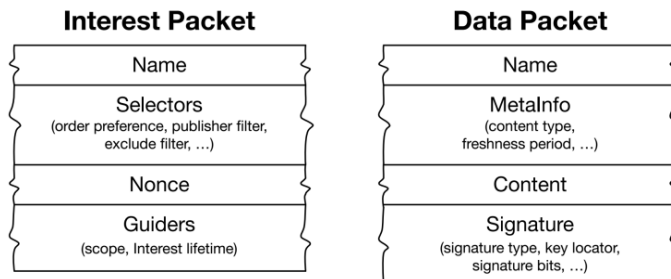


**Fig. 2.** Packets in NDN Architecture

Fig. 2 shows the packet contents in NDN architecture. There are two types of packets which is interest and data. The packet is basically to store or hold information which to apply or retrieves in upon request methods.

## 2.2 The Overview of Internet Attacks

The availability of the internet had been available than 3 decades and yet the Denial-of-Service (DoS) or Distributed Denial-of-Service (DDoS) attacks are still available and constitute an active hazard threat within the internet society. The attacks of DDoS occurs in multiple systems flooding of bandwidth or resources of a target victim was tracked at 600 Gbps during peak DDoS Attack in 2017 and 1.7 Tbps in 2018 [7]. The DDoS attack usually happens at the application layer caused by thousands and more compromising PC to attack to web server or website which launches on an operating system or network resources and results the service will be down, loss and purloined of data as shown in Fig. 3 [8-10].

Fig. 3 below shows the attack model in DDoS classified into 3 groups. Group A is a botnet attack where the attacker will remote command malware-infected computers to

send large packets to the victim. Group B is an individual attacker that sending malicious packets to victim and Group C is clean user where they couldn't send or receive a reply from the victim (server) due to the resources is overwhelmed.

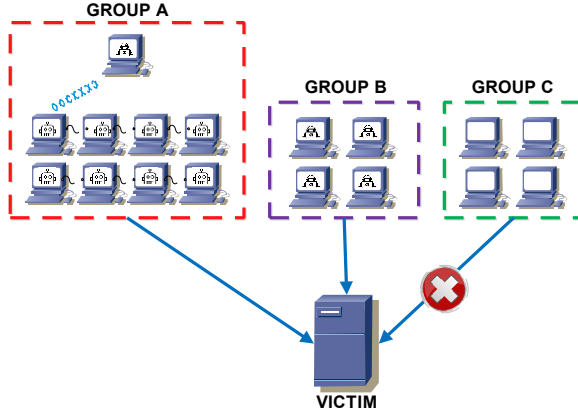


**Fig. 3.** DDoS Attack Model

As the trend of DDoS is getting serious and increasing in current Internet architecture, NDN as the future Internet architecture must provide better mitigation and detection technology to prevent these attacks. In NDN, the attacker usually sends huge and unsatisfied interests with spoofed names to NDN network. The large interests will cause the requested bandwidth of the whole NDN network increased and cause the NDN router memory exhausted.

Routing attacks generally happens in all networks and vulnerable to perform at anywhere and anytime [11]. The routing attacks in NDN could be further derived into Pending Interest Table (PIT) oriented attacks and Forwarding Information Base (FIB) oriented attacks. Both attacks are classified into DDoS and spoofing attacks where the attacks will exhaust the resources in the cycle of time due to bulk interests are sent in a short period of time overload the router. A typical variation of DDoS in NDN is the Interest Flooding Attack (IFA) [12, 13].

### 2.3 Overview of NCIFA and CIFA

IFA is an attack that is easy to launch and difficult to prevent in NDN. It had been identified very first in [14] and classified into Non-Collusive based and Collusive based Interest Flooding Attack (IFA). Both attacks will create damages in the existing network by exhaust NDN router resources and then shut down the content provider. It could last until the NDN router cache is free for the malicious interest attack through flooding. This is a DDoS attack in general and could be a launch without knowledge of a content distributed environment. It affects network performance, stability and security. The nodes in the network suffered from dropping legitimate requests and responding to the IFA [13, 15, 16].

NCIFA attacks send unsatisfied interest to overwhelm PIT. Once the PIT entries are full, there are no more resources for new interests. The router then responds to the attack by forwarding the request to the data producer and cause network traffic congestion as

shown in Fig. 4. As this continues to happen, new PIT entry will be generated each time a new interest is packet in NDN router is received and legitimate request could not be handled and cause a long delay [14, 17-20].

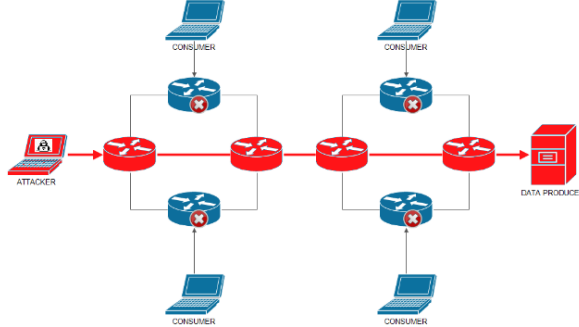


**Fig. 4.** Interest Flooding Attack Model

Fig. 4 shows the attack model in Interest Flooding Attack. An attacker can be anywhere at the edge of any NDN router. When an attacker launch attack, the interests are sent to the nearest NDN router with unique and unsatisfied interest. The interests will be logged in NDN router and generate entries in PIT. The router responds to the attack and forwarding to data producer to request content. As a result, the PIT entries will full and it could not accept any new coming interest before the timeout of unsatisfied interest. This cause the legitimate consumer could not request content from a nearby router.

In another phenomenon, malicious client and server collude together to generate interest flooding. In precise, malicious clients send long unique satisfying interest to request contents and it could only be satisfied by a malicious server. The malicious server responds to the attack by generating successive replies to the data packets corresponding to the PIT entries. This results in entries flood in PIT of the router along the network path. Once the malicious server replies the data in reverse path before PIT entries expired. This cause overload in PIT on the same path of the router and forced to drop all legitimate interest packets [21, 22], this attack named as CIFA as shown in Fig. 5.

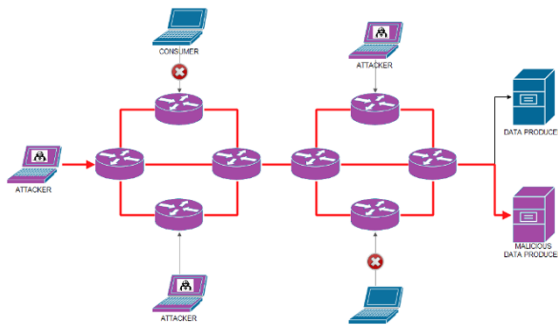


**Fig. 5.** Collusive Interest Flooding Attack Model

Fig. 5 shows CIFA attack model. In the example, 3 attackers sending satisfied interest request from edge NDN router along with the network. All NDN router will respond to the content requested from the malicious content provider. The attacks consider as a legitimate request where NDN router could not differentiate it is a legal request or an attack request as all interests appeared to be valid. Each time the attacker sends unique interest through the NDN router and the malicious content provider will push back data to the nearest router and the valid content can go to the attacker in reverse path. All request is done in a short time and cause PIT router to be full before time out. Once the PIT of router full, the clean legitimate user which is consumer could not request any content until the PIT entries expired.

Based on the above phenomenon which is NCIFA and CIFA, both of the resources will be exhaust which causes the NDN routers to shut down and stop service as a node. Moreover, the path infiltration could be happened by distributing copies of content in many untrusted locations, it causes the validation of origins contents is difficult due to the existing path is inaccessible and attack announce an invalid route but claim them as a trusted path.

### **3 Countermeasure of Non-Collusive Interest Flooding Attack (NCIFA)**

Detection of NCIFA and countermeasure had been proposed through several types of research and all of the findings involved different knowledge and technique to either detect and mitigate the attacks. The first IFA had been discussed by Gasti et al.[23], they proposed a statistical approach in detecting the attack. Push back mechanism is applying to the router after IFA is confirmed to the incoming routers. The proposed method is the lack of analysis of IFA and countermeasure performance. Besides that, J. Tang et al. [24] proposed a technique to detect compromised prefixes in IFA[24]. There are 2 phases of detection. In rough detection simply identifies using ratio method and then accurate detection using interests' expiry ratio, if any exceed the threshold consider an attack. By applying the configuration of the threshold is fair enough to identify the attacker location and the countermeasure happens once the router which closet to the attacker is identified. This technique had a drawback where it takes longer time and resources than the usual detection mechanism. Some research focus on rate limit where interest acceptance can be enforced based on the different parameter, Kai Wang et al. had proposed mitigation technique based on security management mechanism [25] and FIB-records [26]. The proposed method can ensure the legitimate consumer exist at same area even IFA is detected but it responds to retrieving content in time. H. Dai et al. [27] propose a mitigation strategy by Interest Traceback, based on and it responds to attacks with spoofed data. Amin [28] had stated that the method is not efficient as it may cause network overhead and stored with spoofed contents. If any short arriving long unsatisfied interests, it could flood the router above normal usage and it will decrease legitimate interests being forwarded from the interface. Amin applying improved RBF and PSO method where it known as proactive detection and adaptive reaction, it could respond quickly and effectively to mitigate IFA. There are also approach using

machine learning which is Naveen Kumar [29]. Naveen proposed a technique with identified features to be evaluated in IFA and also the attack detection with a different algorithm in a hybrid model such as MLP with BP, RBF with PSO, RBF with TLBO and etc. The overall approach of Naveen provides a comprehensive solution in detecting and mitigate NCIFA with better accuracy compared with existing work.

All the mitigation techniques are good at detecting NCIFA. They could be detecting malicious interest by criteria such as threshold, patterns and traceback. By design of mitigation algorithm, they consider good in the detection and fair enough to mitigate the attack in simulated model with either standard topology on a small scale and large scale.

## 4 Countermeasure of Collusive Interest Flooding Attack (CIFA)

The attack is first mentioned by M. Wahlsch [30] about the scenario of CIFA and the attack model. The previous countermeasure for NCIFA is considered adversaries flood with unsatisfied interest packet by an attacker while CIFA is flooded with satisfied interest by an attacker. Existing CIFA countermeasure technique could not be mitigated based on any NCIFA approach and they do not consider CIFA. There are proposed technique by Cesar et al. [31] considering remove PIT in order to avoid IFA but this may bring down the performance of the overall NDN architecture and it could lead to security issue as the interests do not store or keep within NDN router. Currently, there is not much approach in existing technique to mitigate CIFA. A better approach by retaining the current architecture and keep the PIT in NDN router, Hani Salah et al. evaluate and mitigate CIFA with CoMon framework [18, 21]. CoMon is efficient in detect and mitigate attacks in coordinated method via aggregation of timely evidence in the state of forwarding. In details, attacks can be detecting and mitigate at early phase by implementing the routers in a strategic position working along with a controller of domain based on monitoring of PIT changes. The solution is simulated extensively and shows that it is effective in maintaining the low overhead of signalling against CIFA, it works well for NCIFA but it does not ensure load balancing, fault tolerance and detections over multi-domains. Besides that, Yonghui et al. [22] proposed wavelet analysis in the detection of CIFA. The proposed mechanism will extract the signal in attack band using a Discrete Wavelet Transform algorithm and its feasibility and effectiveness with proposed work against the CIFA is evaluated. The overall performance is kept within computational time and low complexity with high accuracy. Lastly, the latest work in detect CIFA had proposed by Shigeyasu et al. [32], a distribution approach to detect CIFA. The approach will keep detecting any security attack and unsatisfied interest for discarding from original data producer for every second based on statistical information. Once it discarded, malicious attackers will send next interest within the second and this defence mechanism will keep loop until it is complete the detection. The proposed mechanism had the acquisition rate of the legitimate consumer over NDN at a low rate of malicious users but still can be improved as the content acquisition rate is rated below 50% currently.

The difficulty in CIFA compared to NCIFA is the attacks is seem like legitimate, the attacks are done by a satisfied interest but with a malicious provider. Most authors had claimed that the NCIFA has been extensively researched based on email conversations or survey conducted among the authors corresponding to their detection or mitigation technique but not CIFA. There are not many recent works to detect CIFA due to no benchmark datasets or relevant public datasets to perform further experiments. The detection of CIFA could be improvised in term of content acquisition rate as most of the approach mentioned is to detect security attack and invalid discarding interest of last reviewed statistical information.

## 5 Conclusion

This paper discussed a perspective of attack towards Interest Flooding in non-collusive attack and collusive attack for named-data networking. Existing research focus on countermeasure in NCIFA cannot apply in CIFA. CIFA is a lower rate intermittent characteristic of attack as it is very similar like a legitimate request (satisfied interest) with the malicious content provider but for NCIFA, the attack is purely by attackers in the network by generating unsatisfied interests towards NDN router forwarded along the path. Besides that, there is no benchmark dataset is available for CIFA detection. Thus it is difficult to compare the results across different research works. The upcoming research will propose a reliable dataset for CIFA detection in order to standardize the simulated parameters and open for future detection and mitigation usage in NDN.

## Acknowledgement

The authors would like to thank Universiti Malaysia Sabah for funding this research project entitled “Designing a Rule-based Mechanism to Detect the Flash Crowd Attacks During Flash Events” under the SGPUMS-SPBK grant (SBK0359-2017).

## References

1. Broberg, J., Rajkumar Buyya, Zahir Tari, *MetaCDN: Harnessing Storage Clouds for high performance content delivery*. Journal of Network and Computer Applications, 2009: p. pp.1012-1022.
2. Ganesh, V., *IoT: Architectures and Security P2P vs ICN*, 2017, Aalto University.
3. J. Pan, S.P., and R. Jain, *A survey of the research on future internet architectures*. 2011(IEEE Communications Magazine).
4. M. Amadeo, C.C., A. Iera, and A. Molinaro, *Named data networking for iot: an architectural perspective*. European Conference on Networks and Communications (EuCNC), 2014(IEEE): p. pp. 1-5.
5. Cheng Yi, A.A., Ilya Moiseenko, Lan Wang, Beichuan Zhang, Lixia Zhang, *A case for stateful forwarding plane*. Computer Communications, 2013. **36**(7): p. pp. 779-791.

6. p. Konstantina, A.K., C. Joseph, C. Augustin G.Phillipa, *Named Data Networking*. ACM SIGCOMM Computer Communication Review, 2014. **44**(3): p. 67.
7. Cisco, *Cisco Visual Networking Index: Forecast and Trends, 2017–2022*, 2019, Cisco Public: United State.
8. Gligor, V.D., *A note on denial-of-service in operating systems*. IEEE Transactions on Software Engineering, 1984. **3**: p. pp. 320–324.
9. Needham, R.M., *Denial of service: an example*. Communications of the ACM, 1994. **11**: p. pp. 42–46.
10. Reo, J. *Small DDoS Attacks Cause Big Problems*. 2016 [cited 2018 12 December]; Available from: <https://www.corero.com/blog/740-small-ddos-attacks-cause-big-problems.html>.
11. Eslam G. AbdAllah, H.S.H.a.M.Z., *A Survey of Security Attacks in Information-Centric Networking*. IEEE COMMUNICATION SURVEYS & TUTORIALS, 2015. **17**(3): p. pp. 1441-1454.
12. Eslam G AbdAllah, H.S.H., Mohammad Zulkernine, *A Survey of Security Attacks in Information-Centric Networking*. IEEE COMMUNICATION SURVEYS & TUTORIALS, 2015. **17**(3): p. pp. 1441 - 1454.
13. François-Xavier Aguessy, F.R., Théo Combe, Edgardo Montes de Oca, Wissam Mallouli, Guillaume Doyen, Tan Nguyen, Rémi Cogranne, Thibault Cholez, Xavier Marchal, *Security analysis of the virtualized NDN architecture*. Deployment and securisation of new functionalities in virtualized networking environments, 2016.
14. V. Jacobson, D.K.S., J. D. Thornton, M. F. Plass, N. H. Briggs, R. L. Braynard. *Networking named content*. in *5th international conference on Emerging networking experiments and technologies*. 2009. ACM.
15. Lauinger, T., *Security & scalability of content-centric networking*, 2010, TU Darmstadt.
16. M. Wahlsch, T.C.S., M. Vahlenkamp, *Lessons from the past: Why data-driven states harm future information-centric networking*. IFIP Networking Conference, 2013: p. pp. 1-9.
17. Tan N. Nguyen, R.C., Guillaume Doyen and Florent Retraint ', *Detection of Interest Flooding Attacks in Named Data Networking using Hypothesis Testing*. IEEE International Workshop on Information Forensics and Security (WIFS), 2015.
18. Hani Salah, J.W., Thorsten Strufe, *Coordination Supports Security: A New Defence Mechanism Against Interest Flooding in NDN*. 40th Annual IEEE Conference on Local Computer Networks, 2015: p. pp. 73-81.
19. L. Zhang, D.E., J. Burke, V. Jacobson, J. D.Thornton, D. K. Smetters, B. Zhang, G. Tsudik, D. Massey, C. Papadopoulos et al., *Named data networking (NDN) project*, in *Relat'orio T'ecnico NDN-0001/2010*, Xerox Palo Alto Research Center-PARC.
20. Tan NGUYEN, R.C., Guillaume DOYEN, *An Optimal Statistical Test for Robust Detection against Interest Flooding Attacks in CCN*. IFIP/IEEE International Symposium on Integrated Network Management (IM2015), 2015: p. pp. 253-260.
21. Hani Salah, T.S., *Evaluating and Mitigating a Collusive Version of the Interest Flooding Attack in NDN*. IEEE Symposium on Computers and Communication (ISCC), 2016.
22. Yonghui Xin, Y.L., Wei Wang, Weiyuan Li, Xin Chen, *Detection of collusive interest flooding attacks in named data networking using wavelet analysis*. IEEE Military Communications Conference (MILCOM), 2017.

23. Paolo Gasti, G.T., Ersin Uzun, Lixia Zhang, *DoS & DDoS in Named-Data Networking*, in *Computer Science - Networking and Internet Architecture, Cryptography and Security2012*, Harvard University.
24. J. Tang, Z.Z., Y. Liu, and H. Zhang, *Identifying Interest flooding in Named Data Networking*. Green Computing and Communications and Cyber, Physical and Social Computing, 2013(IEEE): p. pp. 306-310.
25. K. Wang, H.Z., Y. Qin, J. Chen, and H. Zhang, *Decoupling malicious interests from pending interest table to mitigate interest flooding attacks*. Globecom Workshops (GC Wkshps), 2013: p. pp. 963-968.
26. K. Wang, H.Z., H. Luo, J. Guan, Y. Qin, and H. Zhang, *Detecting and mitigating interest flooding attacks in content-centric network*. Security and Communication Networks, 2014. 7(4): p. pp. 685-699.
27. H. Dai, Y.W., J. Fan, and B. Liu, *Mitigate DDoS attacks in NDN by interest traceback*. IEEE INFOCOM, 2013(NOMEN Workshop).
28. Amin Karami, M.G.-Z., *A hybrid multiobjective RBF-PSO method for mitigating DoS attacks in Named Data Networking*. Neurocomputing, 2015(Elsevier): p. pp. 1262-1282.
29. Naveen Kumar, A.K.S.a.S.S., *Evaluating Machine Learning Algorithms for Detection of Interest Flooding Attack in Named Data Networking*. International Conference on Security of Information and Networks, 2017. **10**.
30. M. Wahlisch, T.C.S., M. Vahlenkamp, *Backscatter from the data plane–threats to stability and security in information-centric network infrastructure*. Elsevier Computer Networks, 2013.
31. Cesar Ghali, G.T., Ersin Uzun, Christopher A. Wood, *Living in a PIT-less World: A Case Against Stateful Forwarding in Content-Centric Networking*, in *Computer Science - Networking and Internet Architecture2015*, Cornell University.
32. Shigeyasu, T., Sonoda, Ayaka, *Distributed Approach for Detecting Collusive Interest Flooding Attack on Named Data Networking*. International Conference on Network-Based Information Systems (NBiS), 2019. **21**.



# Augmented Reality for Learning Calculus: A Research Framework of Interactive Learning System

Md Asifur Rahman, Lew Sook Ling and Ooi Shih Yin

Faculty of Information Science and Technology, Multimedia University, Melaka, Malaysia  
asifchanchal@gmail.com, sllew@mmu.edu.my, syooi@mmu.edu.my

**Abstract.** The traditional classroom has been evolving with the implementation of technology in and outside the classroom environment. There has been a significant implementation of technology for learning mathematics. Augmented Reality stands out as part of the visualization of spatiality related contents. Technology implementation has caused changes in interactivity of students with system and also with their fellow peers and teachers. This paper provides a systemic literature review of studies that analyzed the effects of human-human and human-system interactivity in students' learning experiences and learning performances and proposes a research framework of an interactive learning system for learning calculus through the implementation of augmented reality.

**Keywords:** Augmented Reality, Interactive Learning System, Interactivity, Learning Experience, Learning Performance, Calculus.

## 1 Introduction

Learning is no longer just confined into a traditional classroom environment where the instructor is the one mainly talking, and students are absorbing the lesson being delivered. This one-way traditional teaching style is inefficient as it is considered as spoon feeding [1]. In traditional classroom environment, there exists a problem of student participation which has caused students performing poorly especially in Science, Technology, Engineering and Mathematics subjects [2]. According to the report of Programme for International Students Assessment, (PISA) Malaysian student's performance is still below the average. PISA evaluates international education system in three aspects of Reading, Mathematics, and Science. Malaysia scored 421 and 443 in PISA ranking of 2012 and 2015 for Mathematics respectively while the world average was 494 and 490 [3] [4]. Researches identify that the abstract concept in Mathematics requires spatial thinking, visualization and imagination in order to have a better understanding [5].

However, there is lack of interactive system that allows students in understanding abstract concept of Mathematics. For example, understanding solid of revolution, based on the 2D materials printed on books or projected on slide creates a barrier for students to conceptualize and therefore, resulting in poor academic performance.

We found that although there are some researches that are addressing the issues of student interaction with the system, there is still lack of teacher-student or student-

student interaction in interactive learning system [1]. We also explored the reasons for difficulties in understanding abstract concept of Mathematics and found that visualization plays a significant role. Students face difficulties in understanding solid of revolution based on 2D medium.

Hence, this paper proposes a research framework that includes 3D visualization through Augmented Reality (AR) as part of system-human interaction and a discussion platform for human-human interactivity. The contributions of this paper are systemic review on implementation of Interactive Learning System and Augmented reality in education and the research framework.

## 2 Literature Review

### 2.1 Interactive Learning System

A technological revolution in the 21<sup>st</sup> century has transformed the academic sector from a traditional classroom environment to a digital learning environment. Different technologies have been implemented in classroom with the aim of creating an interactive learning environment that will assist in performance increment for examples: game-based learning, augmented reality, and virtual reality. According to study in [6] pedagogical technology can be divided into two categories including synchronous and asynchronous. Synchronous technology is used for interactivities running simultaneously and asynchronous is for the assistance in self-learning mechanism e.g. downloading text contents and video. In class, synchronous interactive technology allows students to interact with the system and also with the personnel present at that time.

**Table 1.** Comparison of different pedagogical study on interactive learning system

Interactivity	Sources
Teacher-Student	[1], [2], [7], [8]
Student-Student	[7], [9]
Interactive System	[1], [7], [8], [9], [10], [11], [12], [13], [14], [15], [16]

Based on the research studied, interactive learning was the most common factors found in 6 studies [2, 10, 12, 11, 13, 14, 11]. Enhancing interactivities of human-system and human-human can be considered as two main strengths in the field of human computer interaction [7, 8]. As part of interactivity, many researchers have emphasized on game-based learning. There were five studies that have implemented game-based learning systems, which are directly or indirectly related to interactive learning [10, 9, 14, 15, 16]. Game-based learning can promote system thinking [14], improve math performance [9], affect learning outcome [15]. From the findings of literature review, we summarize that interactive learning system can vary from study to study, but the implementation purpose remains same, which is to promote interactivity among the learners. The research frameworks proposed that affective and cognitive are the two domains that get affected by interactivities. Interactivities promoted by the system have impacted the affective domain which is related to learners' behavior in interacting with peers or

teachers [15, 17, 2, 1, 12]. Other researches have emphasized the cognitive effects of proposed systems in terms of knowledge acquisition, learning outcome, learning performance or achievements [7, 13, 15, 9, 10, 8, 16, 14]. It can be observed from the study that most of the studies have followed quasi-experimental methods [7, 13, 15, 9, 2, 1, 10, 8, 16]. Additionally, some have also emphasized on experimental design method as these studies discussed mostly the designing principles of interactive learning systems [17, 11, 14, 12]. Among the weaknesses identified, very few studies have implemented both interactivities as part of their researches [7, 8]. Besides mobility, longer implementation time, lack of quantitative results is some of the other limitations found from the review [1, 10, 12].

## 2.2 Augmented Reality

Augmented Reality (AR) is a 3D representation of an object which combines real and virtual world together to allow a real-time interaction [18]. Augmented reality allows versatility and creativity by integrating real and virtual environment [19]. The study by [20] has illustrated three main attributes of enhanced reality including integration of real and virtual environment, real-time interaction, ensuring three-dimensional space of real environment. These attributes can also be considered as attributes of augmented reality based on the similarities defined by other researchers [18, 19, 21]. The study of [19] suggests that AR provides flexibility of interacting with virtual content for understanding the theory subjects that require more practical and experimental interaction. Additionally, visualization of complicated structure, real-time projected augmentation, understanding of abstract concept and interaction are the benefits of AR [18, 20].

When it comes to pedagogy, AR implementation has been done in terms of interactive books or system. A closed interactive book shows images printed on the books in a real-world situation whereas, open content allows the students to draw 3D structure in book which can be visualized through AR application later [18]. In terms of interactive system, AR has assisted learners with 3D view of shapes that are difficult to conceptualize [18, 22]. From existing papers, the present study summarizes that studies have focused on the affective outcome of this immersive technology, for example, motivation [23, 24, 25]. Some have studied the cognitive aspects focusing on knowledge acquisition and retention [24, 23, 21]. On the other hand, some have analyzed spatial visualization [18, 26]. Interactivity through this system has allowed the students to learn in an immersive environment. Among the researches reviewed, quasi-experimental study was the most common methodology, followed by experimental study which were used by five [24, 27, 28, 18, 23] and four researches [26, 21, 29, 25] respectively. Although all the researches have focused on human-system interactivity, human-human interactivity was not a focus on the studies conducted. Among the AR studies, mobility of the system was implemented on several studies [28] [18] [25] [30] [27] [23] [26] while some were not mobile [22] [29] [31] [21] [24]. The major weakness of reviewed articles is not having human-human interactivity as part of the system developments. Besides, small sample size and limited implementation duration are also mentioned in studies [24, 23, 29, 25].

### 3 Methodology

The current paper has carried out a systemic literature review (SLR) where relevant sources have been searched in Multimedia University Library Integrated Access (MULiA) 3.0 based on keywords. This paper adopted six step SLR method mentioned in [32]. Firstly, queries were developed based on research questions including interactive learning, interactive learning system, augmented reality for learning mathematics, math Performance, and learning experience. The searches have been conducted from August 15, 2017, to May 7, 2019 based on search strategies. Thirdly, the relevant and recent article were selected based on the selection criteria. After that, titles and abstracts were analyzed to ensure the quality assessment of the displayed articles. Data were extracted from the studies to form a group of categories to identify the characteristics of selected articles as part of the fifth step. At last, data were synthesized to provide an easy understanding of shared characteristics among the selected articles. The analysis is presented as part of literature review and result.

### 4 Result

By being motivated with the implementation of augmented reality in learning, this study proposes that human-human interaction and human-system interaction, incorporated through an interactive learning system affects learning experience which results in affecting the performance of learning Mathematics. Fig 1 portrays the research framework adopted by the current study.

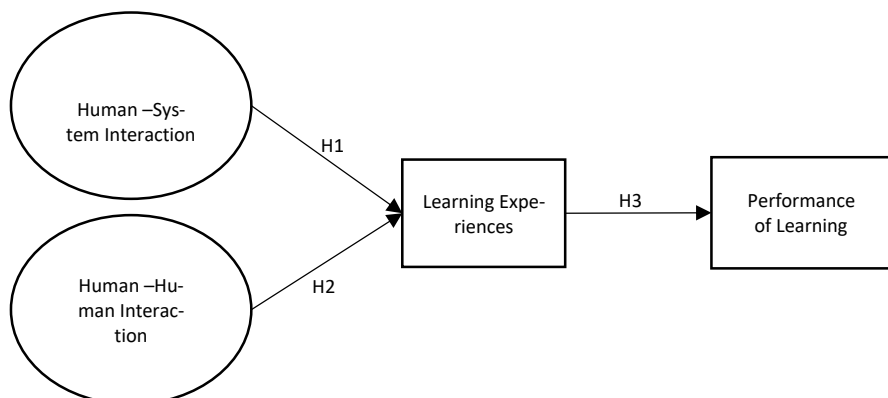


**Fig. 1.** Research framework

#### 4.1 Interactivity

Interactivity simply refers to the interaction of more than one person or entity. In learning, interactivity occurs by means of verbal communication or nonverbal communication among human [33]. Technology is considered as interactive when it allows interpersonal interaction and creates a social presence of others [8]. In an interactive learning environment, interactivity can be categorized into two sectors including Human-System and Human-Human [7]. Human-Human interaction can be categorized into Teacher-Student and Student-Student when it comes to pedagogy [7]. Hence interactive learning system can be defined as a form of learning that facilitate interaction between students and teachers and vice versa, through multiple hardware and software. Studies suggest that interactivity plays a very vital role in students learning efficiency [7, 8]. The study of [34] suggests that the traditional way of teaching need to be evolved especially for science, technology, engineering and mathematics courses where students should comprehend through interaction and participation.

Interactivity does not only allow learner to learn from human, but it also gives a platform for conceptualizing the learning concept through discussion with teachers or peers. The present study considers the interaction of teachers and students as part of Human-Human interaction and hypothesizes:

H1: Increment in Human-Human Interaction Enhance Students' Learning Experiences

#### 4.2 Interactive Learning System

The constraints in traditional teaching have motivated the implementation of technology to make learning available for everyone through e-learning which eventually deviated to M-learning [1]. Over time, implementation of interactive learning system has become a necessity to make learning experience more interactive as it is suggested that the appropriate implementation of technology enhance the teaching and learning experience [6]. Thus, an interactive technology should facilitate the interaction among the students where formation of a conducive learning environment comes along the way. Many studies have proposed different types of games as part of interactive system for children's education. For example, an implementation of gesture-based interactive learning system has increased the coordination among students [15]. Additionally, interactive learning system has not only assisted the conventional students, it has also become an important tool for the students with special ability [8]. Another study suggests that human-system interactivity results in active participation in learning process which eventually improve learning outcomes and better instructional understanding [24]. In implementing the human-system interaction effectively, design of system, use of multimedia including animation and sounds play a significant role in capturing student's attention [26].

In educational context, interactive system has become a crucial tool which should provide with sufficient human-system interaction and mediate the human-human

interaction through the functions incorporated inside the system. As such this study proposes the following hypothesis:

H2: Human-System Interaction Enhance Students' Learning Experiences

#### 4.3 Learning Experience

Learner's experience comes from the formed environment of institution. Learning experience can be defined as the learner's experience throughout the learning period in a particular institution [35]. Each student has their own learning styles in understanding a certain lesson. Among different learning styles, students mostly process information via visual and auditory channel [36] [21]. Thus, visualization plays a very important role in understanding the content. AR not only allows students to view the 3D objects printed in 2D medium but also to interact with the physical objects in a virtual manner [25]. Thus, AR assists in creating a conducive learning environment.

Active engagement and collaboration are the two factors that engage students in learning and this active engagement affect students' performance of learning [34] [37]. A study by [38] suggests that, implementation of information technology can affect students' learning experience. In ubiquitous learning platform, collaborative learning as part of learning experience provides learners a platform to discuss and explore. The attribute of collaborating learning enhances learning experience and eventually contribute to students' performance.

So, it can be said that learning experience through interactivity has a significant impact on the students' performance of learning. Hence, this study hypothesizes:

H3: Improvement of Learning Experience Improves Performance of Learning

### 5 Recommendation

The current paper proposes an interactive learning system by implementing mobile augmented reality for learning calculus. The system intends to adopt the mechanism of marked base close content interactive book which promotes interactivity. In line with the research framework adopted by this paper, the application function is categorized into two main interactivities including human-system and human-human interaction. The application proposes to include 3D content based on the chapter "Application of Define Integral" by implementing augmented reality. This will allow the users to interact with interactive content and provide an exclusive human-system interaction. The second function of application intends to provide a discussion platform for the students and teacher to promote collaborative learning and eventually resulting in human-human interaction. Both of these application functionalities will assist in creating a learning experience by providing visualization and interaction facilities. Thus, the application will assist in moderating the third factor of the research framework. As students' performance in calculus course highly depends on understanding the abstract problems which can be achieved through a conducive learning experience, therefore, the

proposed application should affect students' performance by initiating that designated learning experience.

## 6 Conclusion

An interactive learning system can improve learning performance by providing a conducive learning experience for the learner. This paper proposes a research framework with three hypotheses which intends to implement mobile augmented reality for learning calculus. The factors of human-human and human-system interactions through the proposed application should affect learning experiences and eventually affecting the performance of learning.

## References

1. W. H. Lee, M. C. Kuo and C. C. Hsu, "An In-classroom Interactive Learning Platform by Near Field Communication," in 2015 8th International Conference on Ubi-Media Computing (UMEDIA): 360 - 364, 2015.
2. S. Krusche, A. Seitz, J. Börstler and B. Bruegge, "Interactive Learning – Increasing Student Participation through Shorter Exercise Cycles," in ACE '17, January 31-February 03, 2017, Geelong, VIC, Australia, 2017.
3. OECD, "PISA 2012 Results in Focus," Programme for International Student Assessment, 2014.
4. OECD, "PISA 2015 Results in Focus," Programme for International Student Assessment, 2016.
5. E. Quintero, P. Salinas, E. González-Mendivil and H. Ramírez, "Augmented Reality app for Calculus: A Proposal for the Development of Spatial Visualization," in 2015 International Conference on Virtual and Augmented Reality in Education, 2015.
6. H. C. Lucas, "Technology and the failure of the university," in Communications of the ACM, 2017.
7. L. Blasco-arcas, I. Buil, B. Hernández-ortega and F. J. Sese, "Using clickers in class . The role of interactivity , active collaborative learning and engagement in learning," Computers & Education 62 (2013) 102–110, pp. 102-110, 2013.
8. H.-c. Lin, Y.-h. Chiu, Y. J. Chen, Y.-p. Wuang, C.-p. Chen, C.-C. Wang, C.-L. Huang, T.-M. Wug and W.-H. Hob, "Continued use of an interactive computer game-based visual perception learning system in children with developmental delay," International Journal of Medical Informatics, pp. 76-87, 2017.
9. A. King, "Using Interactive Games to Improve Math Achievement Among Middle School Students in Need of Remediation," ProQuest Dissertations and Theses, 2011.
10. T.-y. Lin, C.-f. Chen, D.-y. Huang, C.-w. Huang and G.-d. Chen, "Using Resource of Classroom and Content of Textbook to build Immersive Interactive Learning Playground," in 2014 IEEE 14th International Conference on Advanced Learning Technologies, 2014.
11. M. Phadung, "Interactive E-Book Design and Development to Support Literacy Learning for Language Minority Students," in World Congress on Sustainable Technologies (WCST-2015), 2015.

12. X. Zhong, H. Fu, Y. Yu and Y. Liu, "Interactive learning environment based on knowledge network of geometry problems," in 2015 10th International Conference on Computer Science & Education (ICCSE), 2015.
13. P. X. Contla, H. Kamada and D. Takago, "Visual Interactive Learning System Using Image Processing About Multiple Programming Languages," in 2016 IEEE 5th Global Conference on Consumer Electronics, 2016.
14. R. S. Vishkaie and R. M. Levy, "Bubble Play : an Interactive Learning Medium for Young Children," in 2015 International Conference on Cyberworlds, 2015.
15. H.-s. Hsiao and J.-c. Chen, "Using a gesture interactive game-based learning approach to improve preschool children 's learning performance and motor skills," Computers & Education, vol. 95, no. January, pp. 151-162, 2016.
16. M. K. Pedersen, A. Svenningsen, N. B. Dohn, A. Lieberoth and J. Sherson, "DiffGame : Game-based mathematics learning for physics," in 2nd International Conference on Higher Education Advances, HEAD'16, 21-23 June 2016, València, Spain, 2016.
17. H.-S. Kim and K.-O. Jeong, "A Study on the Flipped Instructional Model to Support Active and Interactive Learning," in IEEE, 2016.
18. E. G. de Ravé, F. J. Jiménez-Hornero, A. B. Ariza-Villaverde and J. Aguas-Ruiz, "DiedricAR: a mobile augmented reality system designed for the ubiquitous descriptive geometry learning," Multimedia Tools and Applications, pp. 9641-9663, 2016.
19. M. T. Coimbra, T. Cardoso and A. Mateus, "Augmented Reality: an Enhancer for Higher Education Students in," in 6th International Conference on Software Development and Technologies for Enhancing Accessibility and Fighting Infoexclusion (DSA1 2015), 2015.
20. T. Jeřábek, V. Rambousek and M. Prokýšek, "PARAMETERS OF AUGMENTED REALITY AND ITS USE IN EDUCATION," Journal on Efficiency and Responsibility in Education and Science, pp. 232-244, 2013.
21. P. Sommerauer and O. Müller, "Augmented reality in informal learning environments: A field," Computers & Education, p. 59e68, 2014.
22. J. Purnama, D. Andrew and M. Galinium, "Geometry Learning Tool for Elementary School using Augmented Reality," in IAICT 2014, Bali 28-30 August 2014, 2014.
23. A. Estapa and L. Nadolny, "The Effect of an Augmented Reality Enhanced Mathematics," Journal of STEM Education 16. 40. , 2015.
24. A. Cascales-Martínez, M.-J. Martínez-Segura, D. Pérez-López and M. Contero, "Using an Augmented Reality Enhanced Tabletop System to Promote Learning of Mathematics: A Case Study with Students with Special Educational Needs," EURASIA Journal of Mathematics Science and Technology Education 13(2), pp. 355-380, 2017.
25. C.-h. Yu, Y.-T. Liao and C.-C. Wu, "Using Augmented Reality to Learn the Enumeration Strategies Of Cubes," in 2016 IEEE International Conference on Teaching, Assessment, and Learning for Engineering (TALE), 2016.
26. P. Salinas and E. González-Mendivil, "Augmented Reality and Solids of Revolution," International Journal for Interactive Design and Manufacturing (IJIDeM), p. 829–837, 2017.
27. R.-c. Chang and Z.-s. Yu, "Application of Augmented Reality Technology to Promote Interactive Learning," in Proceedings of the 2017 IEEE International Conference on Applied System Innovation IEEE-ICASI 2017 - Meen, Prior & Lam (Eds), 2017.
28. A. G. D.Corrêa, A. Tahira, J. B. Ribeiro Jr. and R. K. I. T. Y. Kitamura, "Development of an interactive book with Augmented Reality for mobile learning," in 2013 8th Iberian Conference on Information Systems and Technologies (CISTI), , 2013.
29. H.-Q. Le and J.-I. Kim, "An augmented reality application with hand gestures for learning 3D geometry," in 2017 IEEE International Conference on Big Data and Smart Computing (BigComp), 2017.

30. S. M. Banu, "Augmented reality system based on sketches for geometry education," in ICEEE, 2012.
31. T. G. Kirner, F. M. V. Reis and C. Kirner, "Development of an Interactive Book with Augmented Reality for Teaching and Learning Geometric Shapes," in 7th Iberian Conference on Information Systems and Technologies (CISTI), 2012, 2016.
32. L. Sook-Ling and a. Y. Yee-Yen, "Information Infrastructure Capability and Organizational Competitive Advantage: A," Australian Journal of Basic and Applied Sciences, vol. 8, no. 3, pp. 126-139, 2014.
33. S. N. Y. K. S. Baktygul Abykanova, "The Use of Interactive Learning Technology in Institutions of Higher Learning," INTERNATIONAL JOURNAL OF ENVIRONMENTAL & SCIENCE EDUCATION, vol. 11, no. 18, pp. 12528-12539, 2016.,
34. S. Freeman, S. L. Eddy, M. McDonough, M. K. Smith, N. Okoroafor, H. Jordt and M. P. Wenderoth, "Active learning increases student performance in science, engineering, and mathematics," Proceedings of the National Academy of Sciences, pp. 8410-8415, 2014.
35. K. Nakakoji, K. Yamada, Y. Yamamoto and M. Morita, "A conceptual framework for learning experience design," in Proceedings - 1st Conference on Creating, Connecting and Collaborating Through Computing, C5 2003, 2003.
36. R. Hussein Ibrahim and D. A.-r. Hussein, "Assessment of visual, auditory, and kinesthetic learning style among undergraduate nursing students," International Journal of Advanced Nursing Studies, vol. 5, p. 1, 2015.
37. Z. Zerihun, J. Beishuizen and W. van Os, "Student learning experience as indicator of teaching quality," in Educational Assessment, Evaluation and Accountability, 2012.
38. S. Krishnasamy, L. Sook-Ling and C.-K. Tan, "Information Technology Capabilities for Mathematics Education in High School: Conceptual Framework.,," Advanced Science Letter, pp. 8013-2016, 2017.



# Development of a Rain Sensing Car Speed Limiter

Efren Victor Jr. N. Tolentino, Joseph D. Retumban, Jonrey V. Rañada, Harvey E. Francisco, Johnry Guillema, Gerald Mel G. Sabino, Jame Rald G. Dizon, Christian Jason B. Gane, and Kristian G. Quintana

National University, 1008 Manila, Philippines  
evntolentinojr@national-u.edu.ph

**Abstract.** The Rain Sensing Car Speed Limiter is a system device that is installed and integrated in a vehicle to determine the rain condition and automatically limit the speed of the vehicle according to the rain condition level. It coincides with the automatic brake system that decreases the speed of the vehicle if it exceeds the speed limit. The speed is measured using a Hall Effect sensor that is installed in the vehicle's wheel while the rain condition is measured using a moisture sensor. The Arduino attached in the control box processes the data and produces a response which is divided into three categories: (a) Extreme Rainfall, (b) Heavy Rainfall, and (c) Light Rainfall. The system is designed to determine the volume of the rainfall and a corresponding response on the vehicle speed will be instigated by the system based on the coded data. The functionality of the system tested is fully working. The system device is developed to minimize road accidents during rainy seasons.

**Keywords:** Rain Sensing, Road Safety, Speed Limiter.

## 1 Introduction

The World Health Organization (WHO) ranked Road Traffic Injuries 8th in Top 10 Global Cause of Deaths in 2016. In the Philippines, the number of death-related road incident was increased by 45.76% from 2006 to 2015 according to the Philippine Statistics Authority (PSA).

One of the main causes of road accident is over-speeding on public roads. Although the respective departments in the government are doing the necessary actions to maintain road safety such as the control and traffic monitoring using different advanced vehicle speed measuring devices including radar and laser gun [1], such efforts are inadequate. Such technologies only work within line-of-sight to accurately measure the speed and is affected by inclement weather aside from it being operated by a personnel. A better solution is to prevent over-speeding before it even happens. A system that automatically checks and limits the speed of the vehicle when it exceeds the speed limit should is a crucial invention.

This study focuses on automatically controlling the speed of the vehicle when driving in the rain. The advantage of the system is that it does not have an interaction unit

for the user in terms of activating the program of the speed limiter. This is made to address the concern of the traffic safety specifically for local use, knowing the fact that drivers cannot avoid natural disasters on highways.

The researchers aim to develop a safer means of transportation using a system that can detect the speed of the vehicle and the rain condition by using sensors and microcontroller.

### 1.1 Background of the Study

Southeast Asia has become one of the most progressive regions in the world. Contributing to this is the growth of automotive market due to the increase in demand. One of the leading countries in the automotive industry is the Philippines. Some of the foreign companies even have an automotive assembly plants built in the country. As of 2018, the National Statistics Office (NSO) recorded a total of 9,251,565 registered motor vehicle in the Philippines, an increase of 1.259% from the 2012 data of 7,138,700 registered motor vehicles. Safety is the number one priority when driving. With the increasing number of automotive vehicles in the Philippines, the number of traffic incidents becomes proportional. There are numerous road accidents because of irresponsible drivers who neglect to follow traffic rules. Moreover, road accidents also happen due to natural disasters.

The relationship between weather and road traffic flow has been studied for over 6 decades now. The beginning of the study has been started by Tanner [2], which investigates the connections of traffic flow to the weather. Various studies have been performed from time to time [3-7] focusing into the negative effects of weather to traffic parameters. According to Zsolt [8], rainfall has the most significant impact on traffic parameters compared to other weather events because rainfall can cause poor visibility for the driver, increase the probability of aquaplaning of the tires, and decrease the traction between the road and the vehicle.

Since the Philippines is a tropical country and given its geographical location, rain is a normal phenomenon that occurs all throughout the year. The outpour of rain makes a slippery and wet roadway; thus, contributes to one of the leading causes of road accidents.

### 1.2 State of the Art

Speed monitoring, speed control, and rain sensing in vehicles have been used for different methods to ensure that the vehicle's speed is below safe speed. Such developments are summarized below.

**RF Based Automatic Speed Limiter by Controlling Throttle Valve.** The study [9] focused on designing a system that limits the speed when a vehicle enters a specific area by using a Radio Frequency Identification that will control the vehicles' speed based on the data that is coming from the Radio Frequency transceivers that are positioned in traffic signal posts.

Two methods to control the throttle system by using a system Based on Drive by wire that is installing an additional throttle valve were defined. It is controlled by a micro-controller to limit the maximum speed of the vehicle. Another system was based on Electronic throttle which controls the maximum speed of the vehicle automatically by using a program to the vehicles' Engine Control or Engine Control Module.

**Automatic Vehicle Speed Control System Using Wireless Fidelity.** The study [10] focused on the location of the vehicle approaching critical zones. It also monitors the speed at a safe value using Wireless technology such as Frequency Modulation (FM) and Wireless Fidelity as a transmitter and installs the receiver in the vehicle. The system automatically alerts the driver to reduce the speed according to the area it approaches.

**Automatic Speed Control and Accident Avoidance of Vehicle Using Multi-Sensors.** The study [11] proposed a system that uses eye blink sensors for the driver and ultrasonic sensors for the measurement of distance from another vehicle.

The eye blink sensor detects if the eye did not blink or the drivers' eye is closed for thirty seconds. The system automatically controls the speed of the vehicle and gives alarm to the driver. The ultrasonic sensor system is responsible for continuous monitoring any obstacle or another vehicle. The system automatically send signal to the driver and control the sped of the vehicle.

**GPS and GSM Enabled Embedded Vehicle Speed Limiting Device.** The study [12] developed a system that uses Global Positioning System (GPS) and Global System for Mobile communication (GSM) to control the speed of a vehicle. The system was integrated in the vehicle and the speed and location is being monitored by the authority using GPS. It offers a simple and effective solution for controlling the speed of the vehicle based on its GPS coordinates and an emergency switch using GSM communication which helps in emergency condition. The governing body will display a caution in the form of visual display integrated in the driver's vehicle or auditory advises if the driver of the vehicle is driving beyond the maximum speed allowed. It also involved adjusting the speed to a particular limit.

### 1.3 Objectives of the Study

The study aims to develop a system integrated in automotive vehicle that will monitor rain condition and measure speed, thus limiting the speed of a vehicle based on the rain condition. Specifically, it aims to (a) develop a system that can measure the speed of the vehicle and recognize the intensity of the rain, (b) develop a speed limit system if the rainfall is determined to be present, and (c) establish rain condition levels and speed limit action for the vehicle using the automatic brake system and throttle controller according to these levels.

## 2 Methodology

### 2.1 Project Design

The system consists of five main components: (a) the DC supply from the car battery which has an output of 12V, (b) the switch-mode power supply voltage regulator which regulates the output power of the battery to give an output of 5V, (c) the Hall Effect sensor which measures the speed of the vehicle by counting the rotation of the wheel, (d) the rain sensor which is a moisture sensor to detect and determine the volume of the rain, and (e) the Arduino microcontroller. Fig. 1 shows the design of the system component.

Both the Hall Effect sensor and the rain sensor output were programmed in the Arduino, which serves as the central processing unit of the system. The Arduino provides the speed reading, the moisture level and the rain condition level if rain is present. It is also responsible for the speed limit of the vehicle based on the corresponding level of the rain condition and the control to the throttle inhibitor and automatic brake system if it exceeds the speed limit on a specific rain condition level.

### 2.2 Project Development

**Software.** The microcontroller used in the project is the Arduino Microcontroller. The hardware components are much cheaper compared to other microcontroller and the programming language is much easier to understand because it uses C++ compared to other microcontroller having complex programming language.

The software is done using Arduino programming language consisting of two parts: (a) the first part is the detection of rainfall, and (b) the second part is the car speed measurement. For the first part, the presence or absence of rainfall determines the main input data for the program. If rainfall is not present, the software will not produce any output process. For the second part, a Hall Effect sensor is utilized to measure the car's speed. If rain is present and is categorized to a level where it exceeds the maximum speed, the software will produce an output that will lower down the car's speed according to the speed limit set to that particular rainfall condition. In short, if the Hall Effect sensor detects that the vehicle is running beyond the set speed limit, the device will trigger the automatic brake and inhibit the throttle body.

**Rainfall Categorization.** Table 1 below shows the different levels of rainfall, the rainfall intensity, and the corresponding trigger for it to be categorized in a level. The data for the rainfall intensity was obtained from the Philippine Atmospheric, Geophysical and Astronomical Services Administration (PAGASA).

The rainfall level was patterned from the rainfall level of PAGASA. The classification was 2.5 liters per square meter per hour for Light Rain, 7.57 liters per square meter per hour for Heavy Rain, and 15.14 liters per square meter per hour for Extreme Rain.

The Trigger value was calculated based on Eqn. (1):

$$\text{Trigger} = \text{Rainfall Intensity} \times \text{Moisture Percentage} \quad (1)$$

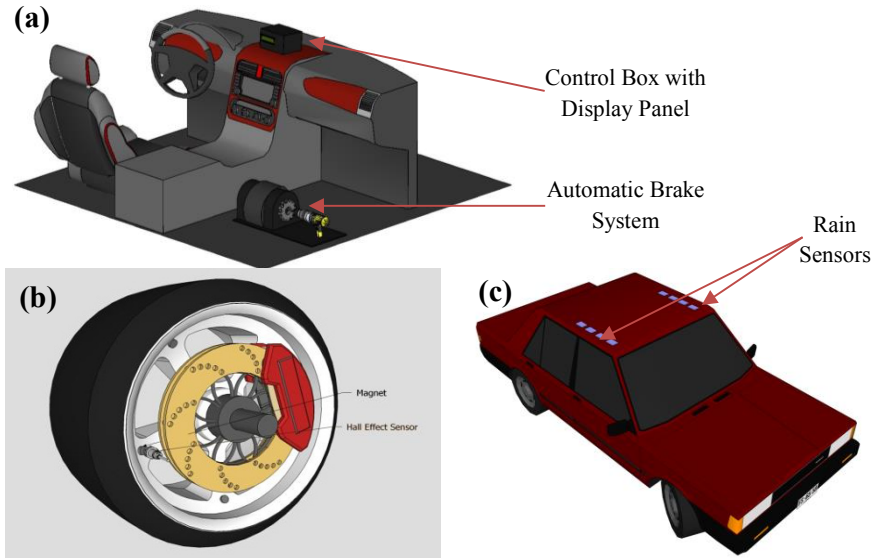


**Fig. 1.** Design of (a) the vehicle's interior, (b) the Hall Effect Sensor, and (c) the Rain sensors.

From the formula, the value of Light Rainfall was calculated to be 0.125 liters per hour, Heavy Rainfall was 1.590 liters per hour, and Extreme Rainfall was 4.240 liters per hour. The calculated data was patterned to the standard that was set by PAGASA. From the calculated volume of rain per time, the Rain Intensity was given by Eqn. (2) below.

$$\text{Rainfall Intensity} = (\text{Volume}/\text{time}) \div \text{Moisture Percentage} \quad (2)$$

From Eqn. (2), the Trigger value for the device was calculated and the corresponding output of the device was formulated. Table 2 gives a summary of the Trigger values for the different Rainfall conditions as well as the corresponding output for the particular Rainfall level.

**Table 1.** PAGASA Rainfall Level

Level of Rainfall	Rainfall Intensity (per square meter)	Trigger
Light	5 to 20% Moisture Level (2.50 L/hr)	0.125 liters in an hour
Heavy	21 to 27% Moisture Level (7.57 L/hr)	1.590 liters in an hour
Extreme	Greater than 28% Moisture Level (15.14 L/hr)	4.240 liters in an hour

**Table 2.** Calculated Rainfall Level and Corresponding Output

Level of Rainfall	Rainfall Intensity (per square meter)	Trigger	Output
Light	5 to 20% Moisture Level (2.50 L/hr)	1.3 milliliters per second	Automatic decrease in speed not greater than 80 kph
Heavy	21 to 27% Moisture Level (7.57 L/hr)	16.8 milliliters per second	Automatic decrease in speed not greater than 60 kph
Extreme	Greater than 28% Moisture Level (15.14 L/hr)	44.8 milliliters per second	Automatic decrease in speed not greater than 40 kph

**Project Testing and Evaluation.** To evaluate the effectiveness of the project, a functionality test was done. The test was comprised of several functions wherein the system can (a) recognize the presence of rainfall using the moisture sensor, (b) read the speed of the vehicle and match it to the value to the vehicle's speedometer, (c) determine the intensity level as well as the condition of the rainfall, and (d) apply the automatic brake system and throttle inhibitor after determining which speed limit should be applied to the vehicle after classifying the rainfall level and condition.

For the evaluation of the system's effectiveness, it must satisfy the process flowchart as illustrated in Fig. 2. The first part is the rain detection. If there is no rainfall, there will be no speed limit action. If it satisfies a certain rainfall category, it will produce an output of speed limit according to the rainfall condition and trigger the automatic brake system and throttle inhibitor.

### 3 Results and Discussion

#### 3.1 Project Technical Description

The project was composed of three sections: the design of the system, programming codes in Arduino, and prototyping. The design of the project was roughly sketched using a computer program called SketchUp. The programming codes were done in Arduino. The physical design of the project was made from 3D printed gears for the automatic brake system and the control box house by an acrylic case to avoid short circuit and to minimize space.

The Hall Effect Sensor was placed on the vehicles' suspension while the magnet was placed on the wheel to monitor accurate speed of the vehicle. The multiple moisture sensors were placed on the vehicles' roof to monitor the rain condition. The Automatic Brake System was placed in the parking brake of the vehicle with a motor and a gear that will control the brake. The control box contains the Arduino which acts as the CPU of the system that detects the presence of rainfall and the corresponding condition, a voltage regulator for the supply of the system, and a Liquid Crystal Display (LCD) that

show the rain condition, moisture level and the current speed of the vehicle. Fig. 3 shows some photos of the actual prototype.

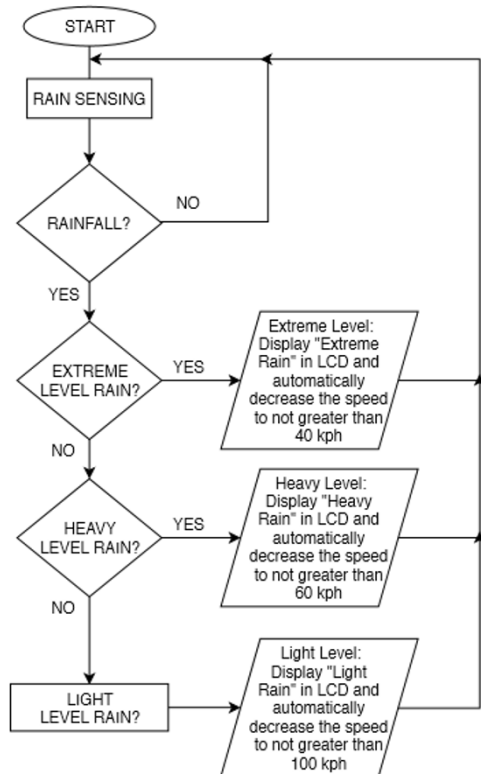


**Fig. 2.** The process flowchart of the system for evaluation of its effectiveness.

### 3.2 Results

**Testing in Light Rain Condition.** The original speed is the speed of the vehicle without the presence of rainfall. A Light Rain Condition was simulated with an appropriate speed limit of 80 kph. If the driver exceeds the speed limit, the system will activate and it will only release if the speed is less than 10 kph of the speed limit. On the first trial, the original speed was 98 kph, when the rain was simulated, the speed limit system was activated for 5.4 seconds until it reached the speed of 68 kph before releasing the accelerometer and stopping the automatic brake system. On the second trial, the original speed was 87 kph and when the rain was simulated the speed limit system activated for 3.8 seconds until it reached the speed of 69 kph before releasing the accelerometer and stopping the brake system. On the last trial, the original speed was 75 kph and when

the rain was simulated, the system did not activate because it did not exceed the speed limit. These results were shown in Table 3 below.

**Table 3.** Testing in Light Rain Condition with 80 kph Speed Limit

Level of Rainfall	Original Speed	System Activated (Time)	System Release (Speed)
Trial 1	98 kph	5.4 secs	68 kph
Trial 2	87 kph	3.8 secs	69 kph
Trial 3	75 kph	-	-

**Testing in Heavy Rain Condition.** On the first trial, the original speed was set to 85 kph. When the rain was simulated, the speed limit system activated for 6.9 seconds until it reached the speed of 48 kph before releasing the accelerometer and stopping the automatic brake system. On the second trial, the original speed was 72 kph and when the rain was simulated, the speed limit system activated for 4.8 seconds until it reached the speed of 48 kph before releasing the accelerometer and stopping the brake system. On the last trial, the original speed was 60 kph. When the rain was simulated, the system did not activate because it did not exceed the speed limit. Table 4 shows the summary of the results.

**Table 4.** Testing in Heavy Rain Condition with 60 kph Speed Limit

Level of Rainfall	Original Speed	System Activated (Time)	System Release (Speed)
Trial 1	85 kph	6.9 secs	48 kph
Trial 2	72 kph	4.8 secs	48 kph
Trial 3	60 kph	-	-

**Testing in Extreme Rain Condition.** For the first trial, the original speed was set to 80 kph. When the rain was simulated, the speed limit system activated for 8.7 seconds until it reached the speed of 32 kph before releasing the accelerometer and stopping the automatic brake system. On the second trial, the original speed was 60 kph and when the rain was simulated the speed limit system activated for 4.8 seconds until it reached the speed of 30 kph before releasing the accelerometer and stopping the brake system. On the last trial, the original speed was 40 kph and when the rain was simulated, the system did not activate because it did not exceed the speed limit. The results were shown in Table 5 below.

**Table 5.** Testing in Extreme Rain Condition with 40 kph Speed Limit

Level of Rainfall	Original Speed	System Activated (Time)	System Release (Speed)
Trial 1	80 kph	8.7 secs	32 kph
Trial 2	60 kph	4.8 secs	30 kph
Trial 3	40 kph	-	-

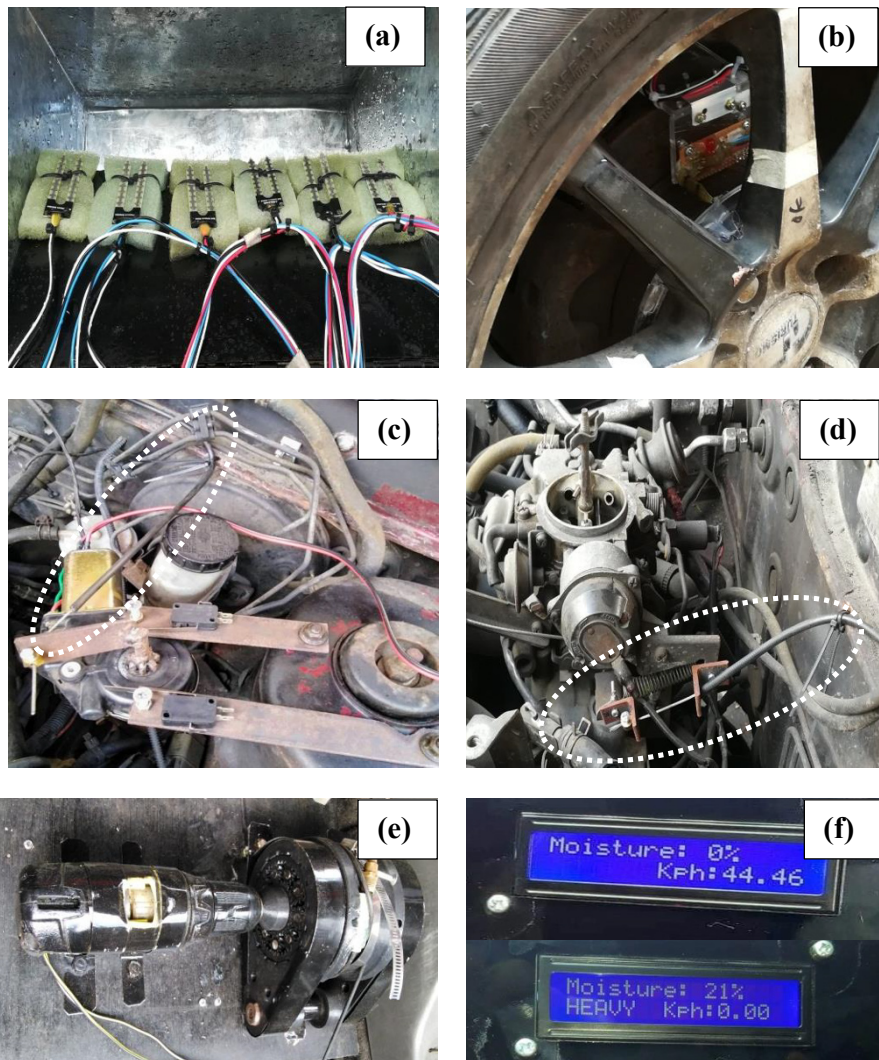


**Fig. 3.** Actual prototype of the project and the functionality during operation and testing. (a) moisture sensor; (b) Hall Effect sensor; (c) cable puller and (d) throttle body with installed cable; (e) automatic brake system; and (f) LCD display of the output.

## 4 Conclusion

This research aims to develop a system that limit the car speed of the vehicle when it detects a rainfall for safety purposes. The functionality of the system tested is fully working as desired. Moreover, the system displays the current speed and the type of rain condition. The system also establishes rain condition levels and automatically limits the speed of the vehicle on each level.

## References

1. Adnan, M. A., Sulaiman, N., Zainuddin, N. I., & Besar, T. B. (2013). Vehicle Speed Measurement Technique Using Various Speed Detection Instrumentation. *IEEE Business Engineering and Industrial Applications Colloquium (BEIAC)*, 641-645.
2. Tanner. (1952). Weather and Road Traffic Flow.
3. Changnon, S. (1996). Effects of Summer Precipitation on Urban Transportation.
4. Hogema, J. (1996). Effects of Rain on Daily Traffic Volume and On Driving Behaviour. Netherlands.
5. Keay K, S. I. (2005). Road Accidents and Rainfall in a Large Australian City.
6. Chung et al. (2005). Does Weather Affect Highway Capacity?
7. Alhassan, H. M., & Ben-Edigbe, J. (2011). *Highway Capacity Loss Induced by Rainfall*.
8. Zsolt, S. (2014). How does the rainfall influence the. *Conference on Effective Road Safety Campaigns*, (pp. 42-51). Budapest.
9. Savignesh, H., Mohamed, S. M., Nagaraj, M., Dr. Shamila, B., & Nagaraja, P. M. (2015, January). *RF Based Automatic Vehicle Speed Limiter by Controlling Throttle Valve*. Retrieved from Research & Reviews: <http://www.rroij.com/open-access/rf-based-automatic-vehicle-speed-limiter-bycontrolling-throttle-valve.php?aid=50080>
10. Sai Chaitanya, P., Vikram, V., & Kalesh, B. (2014). *Automatic Vehicle Speed Control System Using Wireless fidelity*. Retrieved from International Journal of Advance Electrical and Electronics Engineering (IJAEEE): [http://www.irdindia.in/journal\\_ijae/ijae/pdf/vol3\\_iss4/8.pdf](http://www.irdindia.in/journal_ijae/ijae/pdf/vol3_iss4/8.pdf)
11. Bhavanam, N. (2014, July). *Automatic Speed Control and Accident Avoidance Of vehicle using Multi Sensors*. Retrieved from Research Gate: [https://www.researchgate.net/publication/266393877\\_Automatic\\_Speed\\_Control\\_and\\_Accident\\_Avoidance\\_Of\\_vehicle\\_using\\_Multi\\_Sensors](https://www.researchgate.net/publication/266393877_Automatic_Speed_Control_and_Accident_Avoidance_Of_vehicle_using_Multi_Sensors)
12. Priyadarshni, V., Gopi Krishna, P., & Sreenivasa Ravi, K. (2016, May). *GPS and GSM Enabled Embedded Vehicle Speed*. Retrieved from Indian Journal of Science and Technology: <http://www.indjst.org/index.php/indjst/article/viewFile/93045/69581>



# Implementation of the 4EGKSOR for Solving One-Dimensional Time-Fractional Parabolic Equations with Grünwald Implicit Difference Scheme

Fatihah Anas Muhiddin<sup>1</sup>, Jumat Sulaiman<sup>2</sup>, and Andang Sunarto<sup>3</sup>

<sup>1</sup> Faculty of Computer and Mathematical Sciences, Universiti Teknologi MARA, Malaysia

<sup>1,2</sup> Mathematics with Economics Program, Universiti Malaysia Sabah, Malaysia

<sup>3</sup> Faculty of Economic and Islamic Business, IAIN Bengkulu, Indonesia

fatihah.anas@uitm.edu.my, jumat@ums.edu.my, andang99@gmail.com

**Abstract.** Solving one-dimensional time-fractional parabolic equations using numerical technique will require some iterative solver to solve the generated large and sparse linear systems. Thus, by considering the advantages of the Explicit Group iteration technique together with the Kaudd SOR (KSOR) iterative method, this paper examines the efficiency of the four-point Explicit Group Kaudd SOR (4EGKSOR) iterative method to solve the approximation equations generated from discretization of one-dimensional time-fractional parabolic equations using the finite difference scheme with the second order Grünwald Implicit difference scheme. In addition, the formulation and implementation of the proposed method to solve the problem are also presented. Numerical result and comparison with four-point Explicit Group Gauss-Seidel (4EGGS) method are given to illustrate the efficiency of the proposed method.

**Keywords:** Time-Fractional Parabolic equation, Grünwald derivative, Implicit Finite Difference, 4EGKSOR iteration.

## 1 Introduction

Fractional differential equations (FDEs) have profound applications in the fields of sciences, engineering and economics [1-3]. Some of the benefits of fractional derivatives have been mentioned in many researches. It is said to be better in describing some type of real-life phenomena [4] since users have freedom to select the order of the derivative [5] as compared to the ordinary derivative. This also made it useful in problem solving related to non-Markovian random walk [6], which involves systems with long-term memory.

In this study, we considered inhomogeneous Time-fractional parabolic equations (TFPE) which can be defined in general form as follows

$$\frac{\partial^\alpha U}{\partial t^\alpha} + p(x) \frac{\partial U}{\partial x} = q(x) \frac{\partial^2 U}{\partial x^2} + f(x, t), \quad a \leq x \leq b, \quad 0 \leq t \leq T, \quad 0 < \alpha \leq 1, \quad (1)$$

where the function  $f(x, t)$  is a source term and note that for  $\alpha=1$ , equation (1) is the classical parabolic partial differential equation.

There are plenty of recent development in numerical approach for solving problem (1) could be found in literatures, such as refer [7]-[10]. Numerical treatment of TFPDE will generate approximation equations with a character of large and sparse system of linear equations (SLE). So, in order to reduce the computational complexity, our interest is to solve the generated SLEs using iterative method. Previously, similar studies to us could be found such as [11]-[12]. However, in most of their studies, the fractional derivatives are defined in the sense of Caputo, while in this study we discretized problem (1) using Grünwald fractional operator and implicit difference scheme. The definition of Grünwald fractional derivative we used in this study is defined by [13]-[14].

**Definition 1** The Grünwald fractional derivative of order  $\alpha$  of a function  $f(t)$  is defined as

$$D_G^\alpha f(t) = \frac{1}{(\Delta t)^\alpha} \lim_{N \rightarrow \infty} \sum_{k=0}^j g_{\alpha,k} f(t - k\Delta t), \quad 0 < \alpha < 1 \quad (2)$$

where the Grünwald weights are  $g_{\alpha,k} = \frac{\Gamma(k-\alpha)}{\Gamma(-\alpha)\Gamma(k+1)}$ .

One of the well-known classical point-iterative method is the Gauss-Seidel (GS) method. To accelerate the convergence rate even further, Evans [15] introduced the Explicit Group (EG) method, which have been investigated extensively over the past years. Recently, inspired by the same objective, Youssef [16] have introduced a new method which is called as Kaudd Successive Over-Relaxation (KSOR) iterative method. This method is a modification of the classic SOR iterative method, which the difference lies on the values of the relaxation parameter allowed. Recently, the effectiveness of the KSOR method has also been discussed to solve the integral equation [17] and two-point boundary value problem in [18].

Thus, in this paper our focus is to investigate the effectiveness of the four-point Explicit Group (4EG) method together with the KSOR iterative method, in solving problem (1) since none of the previous researches have employed this technique to solve such fractional equation problem before. Throughout this paper, we will refer this iterative method as 4EGKSOR method. For simplicity purposes, the solution domain (1) is assumed to be uniformly divided into  $N = 2^p$ ,  $p \geq 2$  in directions of  $x$  and  $t$ , which the subintervals are denoted as  $\Delta x$  and  $\Delta t$  respectively and defined as

$$\Delta x = \frac{(b-a)}{N} = h, \quad n = N-1, \quad \Delta t = \frac{T}{M} \quad (3)$$

This paper is outlined as such. Next section we discuss the derivation of second-order Grunwald implicit approximation equations for problem (1) followed by the formulation of 4EGKSOR iterative method in Section 3. In Section 4, numerical re-

sults associated with the respective tested examples are presented and the performances are discussed. Finally, conclusion is given in Section 5.

## 2 Formulation of Explicit Group Grünwald Implicit Finite Difference Approximation

This section briefly discussed the discretization of problem (1). To facilitate us in discretizing problem (1), first let the mesh point  $x_i = \alpha + ih$ , where  $i = 0, 1, \dots, N-1, N$  and  $h = \Delta x$  as in equation (2), denotes the uniform step-size. By using formulation of the Grünwald fractional derivative in time and central difference scheme in space the general discrete equation of problem (1) can be written as follows

$$\frac{1}{(\Delta t)^\alpha} \sum_{k=0}^j g_{\alpha,k} U_{i,j-k} + \frac{p(x)}{2\Delta x} (U_{i+1,j} - U_{i-1,j}) + \frac{q(x)}{(\Delta x)^2} (U_{i+1,j} - 2U_{i,j} + U_{i-1,j}) = f_{i,j} \quad (4)$$

which can be simplified into

$$\alpha_i U_{i-1,j} + \beta_i U_{i,j} + \gamma_i U_{i+1,j} = F_{i,j} \quad (5)$$

by letting

$$G_k = \frac{g_{\alpha,k}}{(\Delta t)^\alpha}, \quad a_i = \frac{p(x)}{2\Delta x}, \quad b_i = \frac{q(x)}{(\Delta x)^2}$$

where

$$\alpha_i = b_i - a_i, \quad \beta_i = G_0 - 2b_i, \quad \gamma_i = b_i + a_i,$$

and

$$F_{i,j} = \begin{cases} f_{i,1} - G_1 U_{i,0} & j=1 \\ f_{i,j} - \sum_{k=1}^j G_k U_{i,j-k} & j=2, 3, \dots, M \end{cases}$$

Whereas, the diverse form of computational molecules for equation (5) is as illustrated in Figures 2 (a) and (b). Here, the illustrations are for time levels  $j=1$  and  $j=2$  respectively.

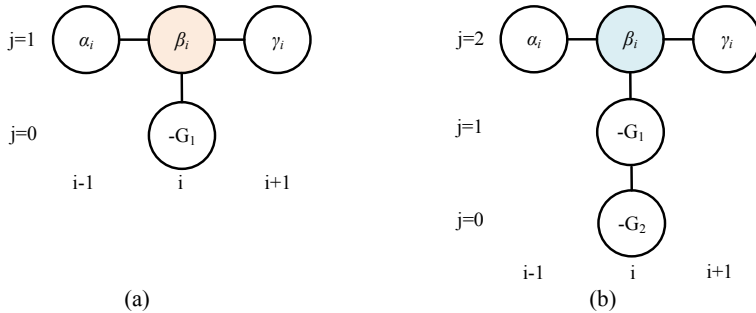


**Fig. 1.** (a) The computational molecule for Grünwald time-fractional parabolic approximation equation at time level  $j=1$  and (b) The computational molecule for Grünwald time-fractional parabolic approximation equation at time level  $j=2$ .

Then, equation (5) can be expressed in a matrix form as

$$AU_j = F_j \quad (6)$$

where

$$A = \begin{bmatrix} \beta_1 & \gamma_1 \\ \alpha_2 & \beta_2 & \gamma_2 \\ & \alpha_3 & \beta_3 & \gamma_3 \\ & & \alpha_4 & \beta_4 & \gamma_4 \\ & & O & O & O \\ & & & \alpha_{m-2} & \beta_{m-2} \gamma_{m-2} \\ & & & \alpha_{m-1} & \beta_{m-1} \end{bmatrix}_{(m-1) \times (m-1)},$$

$$\underline{U}_j = [U_{1,j} \ U_{2,j} \ U_{3,j} \ K \ U_{m-2,j} \ U_{m-1,j}],$$

$$\underline{F}_j = [F_{1,j} - \alpha_1 U_{0,j} \ F_{2,j} \ F_{3,j} \ K \ F_{m-2,j} \ F_{m-1,j} - \gamma_{m-1} U_{m,j}],$$

and

$$\alpha_i = b_i - a_i, \quad \beta_i = G_0 - 2b_i, \quad \gamma_i = a_i + b_i.$$

Based on SLE (6), the characteristic of the coefficient matrix  $A$  has large-scale and sparse.

### 3 Derivation of Four-Point EGKSOR Iterative Method

This section discussed the implementation of 4EGKSOR iterative method in solving linear system generated from discretization of the problem (1). Based on equation (6) above, let the coefficient matrix  $A$  be decomposed into the form of

$$A = D + L + V \quad (7)$$

where  $D$ ,  $L$  and  $V$  are the diagonals, lower triangulation and upper triangulation matrices respectively.

To formulate the 4EGKSOR iterative method, let us recall the KSOR iterative method states in general form as [17]

$$\underline{U}_j^{(k+1)} = \left( ((1+\omega)D - \omega L)^{-1} (D + \omega V) \right) \underline{U}_j^{(k)} + \left( ((1+\omega)D - \omega L)^{-1} (\omega F_j) \right) \quad (8)$$

where the relaxation parameter  $\omega$  is extended to  $R - [-2, 0]$  for KSOR iterative method. Recall that, relaxation parameter for the classical SOR iterative method is  $0 \leq \omega < 1$ .

Next, we consider a group of four points ( $4 \times 4$ ). Figure 4 depicted the finite grid that is used to construct the approximation equations, where the 4EGKSOR iterative method are applied onto each four- and three-point block until convergence is met.

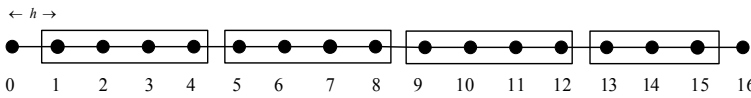


**Fig. 2.** the distribution of uniform node points for 4EGKSOR at the solution domain for  $N=16$ .

Then, based on the approximation equation (5) and Figure 4, the four-point blocks for  $i = 1, 5, 9, 13, \dots, N-7$ , can generally be written as follows

$$\begin{bmatrix} b_i & 1 & 0 & 0 \\ a_{i+1} & b_{i+1} & 1 & 0 \\ 0 & a_{i+2} & b_{i+2} & 1 \\ 0 & 0 & a_{i+3} & b_{i+3} \end{bmatrix} \begin{bmatrix} U_{i,j} \\ U_{i+1,j} \\ U_{i+2,j} \\ U_{i+3,j} \end{bmatrix} = \begin{bmatrix} S_1 \\ S_2 \\ S_3 \\ S_4 \end{bmatrix} \quad (9)$$

where

$$\begin{aligned} S_1 &= U_{i,j} - a_i U_{i-1,j}, & S_2 &= U_{i+1,j}, \\ S_3 &= U_{i+2,j}, & S_4 &= U_{i+3,j} - U_{i+4,j}. \end{aligned}$$

and

$$a_i = \frac{\alpha_i}{\gamma_i}, \text{ and } b_i = \frac{\beta_i}{\gamma_i}.$$

Then, by determining the inverse matrix of equations (9) and adding one weighted parameter  $\omega$ , the formulation of 4EGKSOR method can be stated in general as

$$\begin{bmatrix} U_{i,j} \\ U_{i+1,j} \\ U_{i+2,j} \\ U_{i+3,j} \end{bmatrix}^{(k+1)} = \frac{1}{1+\omega} \begin{bmatrix} U_{i,j} \\ U_{i+1,j} \\ U_{i+2,j} \\ U_{i+3,j} \end{bmatrix}^{(k)} + \frac{\omega}{\beta_i} \begin{bmatrix} b_i & 1 & 0 & 0 \\ a_{i+1} & b_{i+1} & 1 & 0 \\ 0 & a_{i+2} & b_{i+2} & 1 \\ 0 & 0 & a_{i+3} & b_{i+3} \end{bmatrix}^{-1} \begin{bmatrix} S_1 \\ S_2 \\ S_3 \\ S_4 \end{bmatrix} \quad (10)$$

Meanwhile, the last three-point block at  $i = N - 3$  as in Figure 4 can generally be written as follows

$$\begin{bmatrix} b_{n-2} & 1 & 0 \\ a_{n-1} & b_{n-1} & 1 \\ 0 & a_n & b_n \end{bmatrix} \begin{bmatrix} U_{n-2,j} \\ U_{n-1,j} \\ U_{n,j} \end{bmatrix} = \begin{bmatrix} S_{n-2} \\ S_{n-1} \\ S_n \end{bmatrix} \quad (11)$$

where

$$S_{n-2} = U_{n-2,j} - a_{n-2}U_{n-3,j}, \quad S_{n-1} = U_{n-1,j}, \quad S_n = U_{n,j} - U_{n+1,j+1}.$$

and

$$a_i = \frac{\alpha_i}{\gamma_i}, \text{ and } b_i = \frac{\beta_i}{\gamma_i}.$$

Again, by determining the inverse matrix of coefficients in equation (10), the three-point block (3EGKSOR) method with weighted parameter  $\omega$  can be stated in general as

$$\begin{bmatrix} U_{n-2,j} \\ U_{n-1,j} \\ U_{n,j} \end{bmatrix}^{(k+1)} = \frac{1}{1+\omega} \begin{bmatrix} U_{n-2,j} \\ U_{n-1,j} \\ U_{n,j} \end{bmatrix}^{(k)} + \frac{\omega}{\beta_i} \begin{bmatrix} b_{n-2} & 1 & 0 \\ a_{n-1} & b_{n-1} & 1 \\ 0 & a_n & b_n \end{bmatrix}^{-1} \begin{bmatrix} S_{n-2} \\ S_{n-1} \\ S_n \end{bmatrix} \quad (12)$$

Thus, the implementation of four- and three-points block 4EGKSOR and 3EGKSOR method is as summarized in algorithm 1.

#### **Algorithm 1:** 4EGKSOR scheme

- i. Initialize  $\underline{U}_j^{(0)} \leftarrow 0$  and  $\varepsilon \leftarrow 10^{-10}$
- ii. Assign the optimal value of  $\omega$ ,
- iii. For  $i = 1, 5, 9, \dots, N - 7$ , calculate equation (10) for any complete group case  
For  $i = N - 3$ , calculate equation (12) for the ungroup case
- iv. Perform the convergence test,  $\left| \underline{U}_{i,j}^{(k+1)} - \underline{U}_{i,j}^{(k)} \right| \leq \varepsilon = 10^{-10}$ . If yes, go to step (v).  
Otherwise repeat step (iii).
- v. Display approximate solutions.

## 4 Numerical Experiments

In order to verify the effectiveness of the proposed methods, several numerical tests were carried out on the following one-dimensional time-fractional parabolic equations problem. In comparison, the 4EGGS method acted as control method. Three criteria which are the number of iterations, execution time and maximum absolute error will be considered to access the performance. In the following examples, the tolerance error is set to  $\varepsilon = 10^{-10}$ .

**Example 1** [19] Consider the following one-dimensional linear inhomogeneous time-fractional parabolic equation

$$\frac{\partial^\alpha U(x,t)}{\partial t^\alpha} + \frac{\partial U(x,t)}{\partial x} - \frac{\partial^2 U(x,t)}{\partial x^2} = \frac{2t^{2-\alpha}}{\Gamma(3-\alpha)} + 2x - 2, \quad t > 0, x \in R, 0 < \alpha \leq 1,$$

with  $p(x) = 1$  and  $q(x) = -1$  and subject to the initial condition,  $U(x,0) = x^2$ .

The exact solution is  $U(x,t) = x^2 + t^2$ .

**Example 2** [20] Consider the following one-dimensional linear inhomogeneous time-fractional parabolic equation

$$\frac{\partial^\alpha U}{\partial t^\alpha} - \frac{\partial^2 U}{\partial x^2} = \frac{2t^{2-\alpha}}{\Gamma(3-\alpha)} \sin(2\pi x) + 4\pi^2 t^2 \sin(2\pi x), \quad t > 0, x \in R, 0 < \alpha \leq 1,$$

with  $p(x) = 0$  and  $q(x) = -1$  and subject to the initial condition,  $U(x,0) = 0$ .

The exact solution is  $U(x,t) = t^2 \sin(2\pi x)$ .

**Example 3** [21] Consider the following one-dimensional linear inhomogeneous time-fractional equation

$$\frac{\partial^\alpha U}{\partial t^\alpha} - \frac{\partial^2 U}{\partial x^2} = \frac{2e^x t^{2-\alpha}}{\Gamma(3-\alpha)} - t^2 e^x, \quad t > 0, x \in R, 0 < \alpha \leq 1,$$

with  $p(x) = 0$  and  $q(x) = -1$  and subject to the initial condition,  $U(x,0) = 0$ .

The exact solution is  $U(x,t) = t^2 e^x$ .

The numerical results of the examples are recorded in Tables 1 to 3 by considering five different mesh sizes (128, 256, 512, 1024 and 2048).

**Table 1.** Comparison of iteration numbers (k), the computation time (seconds) and maximum errors (Max Error) for the iterative methods at  $\alpha=0.333, 0.666, 0.999$  for Example 1

M	Method	$\alpha=0.333$			$\alpha=0.666$			$\alpha=0.999$		
		k	t	Max Error	k	t	Max Error	k	t	Max Error
128	4EGGS	4972	2.78	2.59720E-02	2426	2.26	1.30650E-02	752	1.95	1.24800E-03
	4EGKSOR $(\omega=2.1266)$	202	1.86	2.59720E-02 $(\omega=2.1902)$	141	1.85	1.30650E-02 $(\omega=2.3802)$	82	1.84	1.24800E-03
256	4EGGS	18330	10.41	2.59720E-02	8961	7.02	1.30650E-02	2775	4.67	1.24780E-03
	4EGKSOR $(\omega=2.0616)$	403	3.83	2.59720E-02 $(\omega=2.0911)$	277	3.77	1.30650E-02 $(\omega=2.1759)$	163	3.72	1.24800E-03
512	4EGGS	67144	57.81	2.59720E-02	32949	32.15	1.30650E-02	10247	15.03	1.24780E-03
	4EGKSOR $(\omega=2.0305)$	801	8.07	2.59720E-02 $(\omega=2.0447)$	551	7.82	1.30650E-02 $(\omega=2.0844)$	320	7.67	1.24800E-03
1024	4EGGS	243927	380.3	2.59750E-02	120277	195.6	1.30670E-02	37654	71.65	1.24540E-03
	4EGKSOR $(\omega=2.0152)$	1593	17.42	2.59720E-02 $(\omega=2.0222)$	1095	16.53	1.30650E-02 $(\omega=2.0414)$	633	15.73	1.24800E-03
2048	4EGGS	877170	2734.98	2.59810E-02	435091	1381.74	1.30740E-02	137347	460.19	1.23760E-03
	4EGKSOR $(\omega=2.0076)$	3172	40.44	2.59720E-02 $(\omega=2.0111)$	2175	36.98	1.30650E-02 $(\omega=2.0206)$	1249	33.66	1.24800E-03

**Table 2.** Comparison of iteration numbers (k), the computation time (seconds) and maximum errors (Max Error) for the iterative methods at  $\alpha=0.333, 0.666, 0.999$  for Example 2

M	Method	$\alpha=0.333$			$\alpha=0.666$			$\alpha=0.999$		
		k	t	Max Error	k	t	Max Error	k	t	Max Error
128	4EGGS	3934	2.51	3.4737E-04	1967	2.15	5.2938E-04	647	1.93	4.5596E-04
	4EGKSOR $(\omega=2.1245)$	183	1.9	3.4734E-04 $(\omega=2.1799)$	126	1.88	5.2936E-04 $(\omega=2.3791)$	75	1.87	4.5594E-04
256	4EGGS	13369	8.09	2.0170E-04	6761	5.96	3.8495E-04	2280	4.48	3.1275E-04
	4EGKSOR $(\omega=2.0587)$	360	3.81	2.0159E-04 $(\omega=2.0859)$	247	3.81	3.8484E-04 $(\omega=2.1601)$	141	3.7	3.1268E-04
512	4EGGS	44065	35.66	1.6560E-04	22678	22.26	3.4916E-04	8161	12.99	2.7697E-04
	4EGKSOR $(\omega=2.0289)$	712	7.9	1.6516E-04 $(\omega=2.0419)$	489	7.72	3.4872E-04 $(\omega=2.0811)$	255	7.49	2.7686E-04
1024	4EGGS	138660	184.92	1.5780E-04	73432	111.38	3.4137E-04	29511	55.91	2.6774E-04
	4EGKSOR $(\omega=2.0142)$	1366	16.77	1.5606E-04 $(\omega=2.0218)$	920	16.05	3.3968E-04 $(\omega=2.0409)$	526	15.53	2.6793E-04
2048	4EGGS	404251	1033.52	1.6068E-04	239463	702.79	3.4029E-04	106790	335.17	2.6379E-04
	4EGKSOR $(\omega=2.0074)$	2680	37.71	1.5379E-04 $(\omega=2.0102)$	1907	35.57	3.3744E-04 $(\omega=2.0202)$	1019	32.51	2.6571E-04

**Table 3.** Comparison of iteration numbers (k), the computation time (seconds) and maximum errors (Max Error) for the iterative methods at  $\alpha=0.333, 0.666, 0.999$  for Example 3

M	Method	$\alpha=0.333$			$\alpha=0.666$			$\alpha=0.999$		
		k	t	Max Error	k	t	Max Error	k	t	Max Error
128	4EGGS	5135	2.74	1.1757E-03	2481	2.25	2.5780E-03	765	1.95	2.2070E-03
	4EGKSOR $(\omega=2.1253)$	207	1.9	1.1757E-03 $(\omega=2.1894)$	145	1.89	2.5780E-03 $(\omega=2.3806)$	84	1.87	2.2070E-03
256	4EGGS	18947	10.25	1.1748E-03	9174	6.89	2.5772E-03	2823	4.71	2.2063E-03
	4EGKSOR $(\omega=2.0610)$	412	3.83	1.1750E-03 $(\omega=2.0905)$	287	3.77	2.5773E-03 $(\omega=2.1759)$	167	3.71	2.2064E-03
512	4EGGS	69492	55.9	1.1742E-03	33771	31.05	2.5765E-03	10433	14.73	2.2056E-03
	4EGKSOR $(\omega=2.0301)$	820	8.04	1.1748E-03 $(\omega=2.0444)$	562	7.83	2.5772E-03 $(\omega=2.0844)$	330	7.65	2.2063E-03
1024	4EGGS	252870	364.78	1.1723E-03	123456	186.85	2.5746E-03	38376	68.84	2.2036E-03
	4EGKSOR $(\omega=2.0150)$	1634	17.13	1.1748E-03 $(\omega=2.0220)$	1117	16.3	2.5771E-03 $(\omega=2.0416)$	651	15.49	2.2062E-03
2048	4EGGS	911194	2617.93	1.1650E-03	447405	1306.02	2.5670E-03	140180	441.11	2.1957E-03
	4EGKSOR $(\omega=2.0075)$	3254	39.86	1.1748E-03 $(\omega=2.0110)$	2223	36.18	2.5771E-03 $(\omega=2.0206)$	1288	33.3	2.2062E-03

**Table 4.** Reduction percentage of the number of iterations (Iter) and computational time for the 4EGKSOR compared to 4EGGS iterative method.

Example		$\alpha=0.333$	$\alpha=0.666$	$\alpha=0.999$
1	Iter	95.94–99.64%	94.19–99.50%	89.10–99.10%
	Time	33.09–98.52%	18.14–97.32%	5.64–92.69%
2	Iter	95.35–99.34%	93.60–99.20%	88.41–99.05%
	Time	24.30–96.35%	12.56–94.94%	3.11–90.30%
3	Iter	95.97–99.64%	94.16–99.50%	89.02–99.08%
	Time	30.66–98.48%	16.00–97.23%	4.10–92.45%

From the numerical results in Tables 1 to 3, the reduction percentage of 4EGKSOR iterative method in comparison to the 4EGGS iterative method for examples 1 to 3 are summarized in Table 4. From the result, 4EGKSOR method manage to reduce the 4EGGS iteration numbers. In addition, as the mesh size increases, the computational time has also improved. This clearly shows that 4EGKSOR iterative method is more efficient compared to 4EGGS iterative method.

## 5 Conclusion

In previous section, we presented the formulation of 4EGKSOR using second-order implicit finite difference scheme with Grünwald fractional derivative operator. From the numerical results recorded in Tables 1 to 3, it is observed that, 4EGKSOR iterative method has outperform the 4EGGS iterative method performance in terms of the iteration numbers and computational time. This is because of the existence of the optimal relaxation parameter  $\omega$ , which have been appropriately selected so that the convergence rate is optimum. Meanwhile, in terms of accuracy, numerical solutions of 4EGKSOR iterative method are in good agreement with the 4EGGS iterative method. For future work, this study will be continued to investigate on the use of half-sweep iteration concept as discussed in [18], which inspired by Abdullah (1991) as an alternative approach to speed up the execution time for solving one-dimensional time-fractional parabolic partial differential equations.

## References

1. Xu, Q., Xu, Y. Extremely low order time-fractional differential equation and application in combustion process. Communications in Nonlinear Science and Numerical Simulation 64, 135–148 (2018).
2. Edeki, S., Ugbebor, O., Owoloko, E. Analytical solution of the time-fractional order Black-Scholes model for stock option valuation on no dividend yield basis. International Journal of Applied Mathematics 47(4), (2017).
3. Paradisi, P. Fractional calculus in statistical physics: the case of time fractional diffusion equation. Communications in Applied and Industrial Mathematics e-530, 1–25, (2015).
4. Sontakke, B. R., Shelke, A. S. Approximate Scheme for Time Fractional Diffusion Equation and Its Applications. Global Journal of Pure and Applied Mathematics 13(8), 4333–4345 (2017).

5. Almeida, R., Bastos, N. R., Monteiro, M. T. Modeling some real phenomena by fractional differential equations. *Mathematical Methods in the Applied Sciences* 39(16), 4846–4855 (2015).
6. Gaspar, F. J., Rodrigo, C. Multigrid Waveform Relaxation for the Time-Fractional Heat Equation. *SIAM Journal on Scientific Computing*, 39(4), A1201–A1224 (2017).
7. Ghaffari, R., Ghereishi, F. Reduced spline method based on a proper orthogonal decomposition technique for fractional sub-diffusion equations. *Applied Numerical Mathematics*, 137, 62–79 (2019).
8. Gunzburger, M., Wang, J. A Second-Order Crank-Nicolson Method for Time-Fractional PDES. *International Journal of Numerical Analysis and Modeling* 16(2), 225–239 (2019).
9. Wang, Y. M., Ren, L. A high-order L<sub>2</sub>-compact difference method for Caputo-type time-fractional sub-diffusion equations with variable coefficients. *Applied Mathematics and Computation* 342, 71–93 (2019).
10. Wu, L., Zhao, Y., Yang, X. Alternating Segment Explicit-Implicit and Implicit-Explicit Parallel Difference Method for Time Fractional Sub-Diffusion Equation. *Journal of Applied Mathematics and Physics* 6(5), 1017–1033 (2018).
11. Sunarto, A., Sulaiman, J., Saudi, A. (2016). Caputo's Implicit Solution of Time-Fractional Diffusion Equation Using Half Sweep AOR Iteration. *Global Journal of Pure and Applied Mathematics* 12(4), 3469–3479 (2016).
12. Sunarto, A., Sulaiman, J., Saudi, A. SOR method for the implicit finite difference solution of time-fractional dif-fusion equations. *Borneo Science (The Journal of Science & Technology)* 34, 34–42 (2014).
13. Podlubny, I. *Fractional Differential Equations*. Academic Press, San Diego (1999).
14. Zahra, W. K., Elkholy, S. M. Cubic spline solution of fractional bagley-torvik equation. *Electronic Journal of Mathematical Analysis and Applications* 1(2), 230–241 (2013).
15. Evans, D. J. Group explicit iterative methods for solving large linear systems. *International Journal of Computer Mathematics* 17(1), 81–108 (1985).
16. Youssef, I. K. On the Successive Overrelaxation Method. *Journal of Mathematics and Statistics* 8(2), 176–184 (2012).
17. Radzuan, N. Z. F. M., Suardi, M. N., Sulaiman, J. KSOR iterative method with quadrature scheme for solving system of Fredholm integral equations of second kind. *Journal of Fundamental and Applied Sciences* 9(5S), 609–623 (2017).
18. Suardi, M. N., Radzuan, N. Z. F. M., Sulaiman, J. Cubic B-spline Solution of Two-point Boundary Value Problem Using HSRSOR Iteration. *Global Journal of Pure and Applied Mathematics* 13(11), 7921–7934 (2017).
19. Uddin, M., Haq, S. RBF's approximation method for time fractional partial differential equations. *Communications in Nonlinear Science and Numerical Simulation* 16(11), 4208–4214 (2011).
20. Jiang, Y., Ma, J. High-order finite element methods for time-fractional partial differential equations. *Journal of Computational and Applied Mathematics* 235(11), 3285–3290 (2011).
21. Ma, Y. Two implicit finite difference method for time fractional diffusion equation with source term. *Journal of Applied Mathematics & Bioinformatics* 4(2), 125–145 (2014).
22. Abdullah, A.R. The Four Point Explicit Decoupled Group (EDG) Method: A Fast Poisson Solver. *International Journal of Computer Mathematics*, 38, 61–70 (1991).



# Particles Aggregation Using Flexural Plate Waves Device

Wan Nur Hayati Wan Husin<sup>1</sup>, Norazreen Abd Aziz<sup>1</sup>, Muhamad Ramdan Buyong<sup>2</sup>,  
and Siti Salasiah Mokri<sup>3</sup>

<sup>1</sup> Centre of Advanced Electronic and Communication Engineering, Universiti Kebangsaan  
Malaysia, 43600 Bangi, Selangor, Malaysia

<sup>2</sup> Inst. Of Microengineering and Nanoelectronic, Universiti Kebangsaan Malaysia, 43600  
Bangi, Selangor, Malaysia

<sup>3</sup> Centre for Integrated Systems Engineering and Advanced Technologies, Universiti  
Kebangsaan Malaysia, 43600 Bangi, Selangor, Malaysia  
[norazreen@ukm.edu.my](mailto:norazreen@ukm.edu.my)

**Abstract.** Particles aggregation has wide applications especially in the areas of medical, biology and biochemical analysis. Several on-chip methods have been used to manipulate particles such as surface acoustic wave (SAW), bulk acoustic wave (BAW), magnetophoresis and dielectrophoresis. Other aggregation methods such as ultracentrifugation and mass spectrometry are inconvenient to be used as they require high-tech equipment and relevant specialists. In this work, on chip aggregation method by flexural plate waves (FPW) device provided an automated and fast response process. This paper describes an aggregation procedure of 6.42  $\mu\text{m}$  polystyrene particles using FPW device. Experiment was conducted using two FPW devices with two different diameter of the smallest annular interdigitated transducer (AIDT). The operation frequency for both devices was 30.6 MHz while the RF power supply was 100 mW. The efficiency of particle aggregation was analysed based on the number of particles at the pressure nodes (quantitative results). This contactless aggregation method was seen suitable for microfluidic applications or to be more specific for on-chip cell biology co-culture that does not affect the physical condition of cells.

**Keywords:** Aggregation, AIDT, FPW device, Microfluidics

## 1 Introduction

Particles aggregation is of great interest in many applications such as biomedical, biology and biochemical. Specifically, the aggregation of particles is used for analysing DNA, testing cancerous blood cells as well as in co culture cell biology. Particles aggregation is a type of lab-on-chip (LOC) technique that does not perturb the condition of cells involved [1-2].

The are many techniques that can be used to manipulate particles such as surface acoustic wave (SAW) bulk acoustic wave (BAW), magnetophoresis, dielectrophoresis, ultracentrifugation (AUC) and mass spectrometry. These noninvasive and contactless manipulation of suspended microparticles has received a huge interest among researchers [3-9]. Controllable acoustic force involved in those meth-

ods produce causes no damage to the viability and functional of biological cells. To be specific, acoustic manipulation in microfluidic channels has emerged as an effective tool in microfluidics to control micron-sized objects for chemical, physical and biological applications. In contrast to acoustic manipulation, AUC and mass spectrometry techniques use advanced technology equipment that require well-trained operators to handle them.

Acoustic wave devices are widely applied for various purposes, among them are for radio frequency (RF) communication, chemical and biochemical detectors and optical modulators. Recently, acoustic waves technology has been involved in creating standing acoustic-wave field to generate acoustic pressure trap for capturing/trapping, transporting or sorting suspended microparticles or biological cells in microfluidics channel [10-13].

Surface acoustic wave, bulk acoustic and plate wave or commonly known as flexural plate wave are among the prominent techniques used in on-chip particles separation. Flexural plate mode (FPW) is a complex vibration wave that propagates in parallel with the entire surface and is generated when the substrate thickness is smaller or comparable to the wavelength. There are several factors that affect the efficiency of the acoustic wave device in the process of micro particle alignment. Among the influencing factors are force, time, frequency, size, acoustic contrast factor, density and compression of micro-particles. Whereas the forces that influence the particle alignment process using acoustic waves are acoustic propagation force, diffusion, drag, float and gravitational forces [14].

On chip aggregation method by FPW device provides an automated and fast response process. Furthermore, this device operates at low power supply and can also be developed using the low-cost MEMS technology. This work presents the efficacy of particles aggregation using flexural plate wave device for microfluidic applications. In this paper, the theory of FPW and the principles of using FPW device for particles aggregation are presented. It was observed that the aggregation process using FPW was affected by several parameters namely size, density, particles concentration, time, frequency and forces [15].

## 2 Theory

Flexural plate waves (FPW) are considered as complex vibrational waves that propagate parallel to the test surface throughout the thickness of the material [16]. These waves are generated when the thickness of the substrate is smaller than or comparable to the wavelength of the waves. The propagation of FPW device depends on the density and elastic material characteristics of a component. With FPW, a number of modes of particle vibration are possible, but the two most common are the symmetrical and asymmetrical modes as shown in Figure 1 and Figure 2. When the exciting force is parallel to the plates, the wave motion in the symmetrical mode will be highly generated.

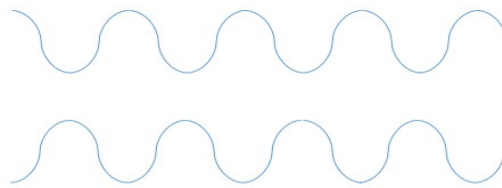


**Fig. 1.** Symmetry mode waves

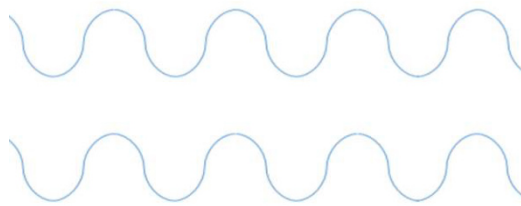


**Fig. 2.** Asymmetry mode waves

The use of micro channel in particles aggregation and manipulation has been described in the previous literature [17]. However, this method requires a hydrodynamic force to aggregate the particles. Hydrodynamic force is generated when a core stream is flowed in an inlet micro channel among symmetric side micro channels that have flowed sheath streams. FPW device introduces the direct technique of aggregation particles, which does not require micro channel and hydrodynamic forces. Using FPW device, the aggregation particles only occur in the droplet.

The behaviour of micro particles can be predicted from various forces including the acoustic radiation force, viscous drag force, diffusion force, gravitational force and buoyant force. However, the gravitational force and buoyant force cancel each other due to the densities of both particles and the suspending media that are almost balanced where both forces are have same value but in different direction [18]. Figure 3 shows the direction of force in the particles.

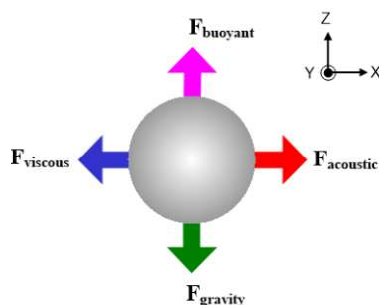


**Fig. 3.** Forces acted on particles

Acoustic contrast factor is the determinant of particle movement in particle alignment process [19]. Acoustic contrast factor determines the movement of micro particles either through the pressure node or anti-node pressure. If the acoustic contrast factor has a positive value, it will move towards the pressure of the node and when the acoustic contrast factor has a negative value. Acoustic propagation,  $F_R$  is divided into two; primary acoustic propagation force and the secondary acoustic propagation force. Acoustic propagation power is generated by a stationary surface acoustics wave (SSAW). Meanwhile, secondary acoustic propagation forces are caused by acoustic waves scattered from particles. The primary acoustic radiation force is given by:

$$F_{ac} = - \left( \frac{\pi p_o^2 V_c \beta_w}{2\lambda} \right) \emptyset(\beta, \rho) \sin(2kx) \quad (1)$$

$$\emptyset = \frac{5\rho_c - 2\rho_w}{2\rho_c + \rho_w} - \frac{\beta_c}{\beta_w} \quad (2)$$

Where  $p_o$ ,  $V$ ,  $\beta_w$ ,  $\beta_c$  &  $k$ ,  $x$ ,  $\rho_c$ ,  $\rho_w$  are the acoustic pressure amplitude, volume of particle, compressibility of medium, compressibility of particle, wavelength, wave number, particle distance from the pressure node, density of the particles and density of medium [20]. Acoustic contrast factor is the determinant of particle movement in particle aggregation or separation process. The contrast factor ( $\emptyset$ ) is derived from both the particles density and compressibility. The movement of the particles either towards the pressure nodes or anti pressure nodes is determined by the acoustic contrast factor ( $\emptyset$ ). The particles that have ( $\emptyset$ )  $> 0$  will be attracted to the pressure nodes and the particles that have ( $\emptyset$ )  $< 0$  will move toward the opposite direction.

The drag is the resistance force acting on the particles in the direction opposite to the acoustic radiation force. The drag force is derived from the Stoke law, which explains the sphere of movement in the viscous liquid at a specific velocity given by

$$F_v = 6\pi\eta rv \quad (3)$$

where  $F_v$ : drag force,  $\eta$ : liquid viscosity,  $r$ : particle radius and  $v$ : velocity between particles and medium.

Drag force cannot be ignored even though the acoustic propagation force is more powerful than drag force. The micro particles will have a net power proportional to the micro particle radius ( $r$ ), resulting in acoustic propagation force proportional to  $r^3$  while the drag force is proportional to  $r$ . This results in the greater the size of the micro particles as they move faster towards the pressure nodes.

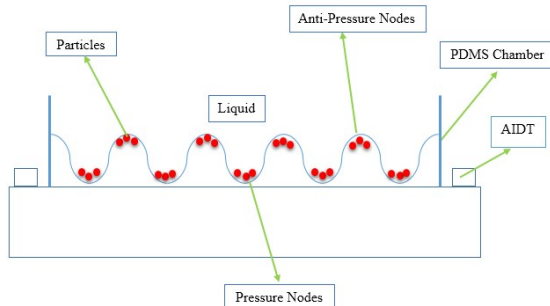
### 3 Methodology

Aggregation experiment was conducted using two FPW devices with various diameters of the smallest AIDT, which named as device A and device B. Both devices operated at a frequency of 30.6 MHz and RF power supply at 100 mW (20 dBm). The mixture of polystyrene particles and deionised water at various concentration was formed as shown below.

**Table 1.** Concentration ratios of polystyrene particles and deionised water

Ratio, ( $\mu\text{L}$ )	Concentration (%)
1:3	0.25
1:5	0.17
1:10	0.09
1:20	0.05
1:30	0.03

3 $\mu\text{L}$  of this mixture was injected in PDMS chamber located at the centre of the device at angle 90° before generated the AIDT at the RF power of 20 dBm and frequency of 30.6 MHz. This experimental process was applied for device A and device B. The diameter of aggregation spatial for device A was 1.5 mm while the diameter of aggregation spatial for device B was 2 mm. The PDMS chamber used in this experiment depends on the diameter of aggregation spatial. The PDMS chamber with a diameter of 1.5 mm was used for device A and PDMS chamber with 3 mm in diameter was used for device B. The size of PDMS chamber must be equal or a little bit bigger than diameter of aggregation spatial for particles to be successfully aligned at the pressure nodes. Figure 4 illustrates how the particles align at the pressure nodes in chamber.

**Fig. 4.** Particles aggregation at pressure nodes

## 4 Results and Discussion

Experiments for each concentration ratio of both devices were recorded in the form of video. MATLAB software was used to convert video to image clipping so that the data analysis can be implemented easily and accurately. On average, at least 500 photo clippings can be extracted from each experimental video. Six different measurement locations on the same pressure nodes were firstly identified to ensure the accuracy of calculation of the number of particles counted. Each image clip was analysed using Particle Analysis ImageJ. The number of particles on the image was calculated and \ recorded in the Microsoft Excel software. These steps were carried out for every location identified.

From observation, device A contained 8 pressure nodes while device B contained 16 pressure nodes. Figure 5 shows the particles that have successful aggregated at pressure nodes for device A at concentration percentage of 0.25, 0.09 and 0.03. Table 2 displays the total number of particles suspended on pressure nodes for device A. Based on the experiment for device A, higher concentration ratio of particles can allow more particles to be successful aggregated at pressure nodes.

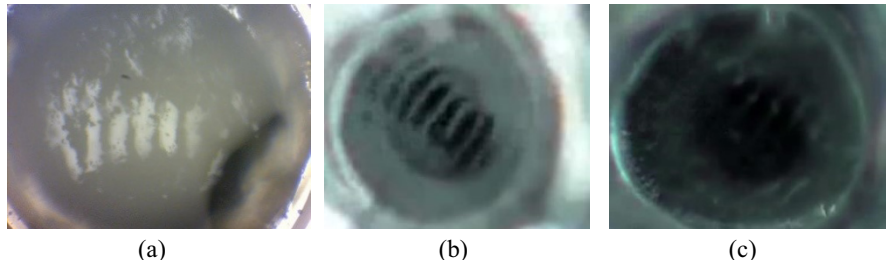


**Fig. 5.** Aggregated polystyrene particles at the pressure nodes for device A with the concentration of (a) 1:3, (b) 1:10 and (c) 1:30

**Table 2.** Number of particles aggregated at pressure node in device A.

Concentration (%)	No of Particles
0.25	5271088
0.17	2790400
0.09	1887168
0.05	1129280
0.03	930192

Based on observation from experimental work, device B formed 18 pressure nodes. Figure 6 shows the particles that have successfully aggregated at pressure nodes for device B at concentration percentage of 0.25, 0.09 and 0.03.

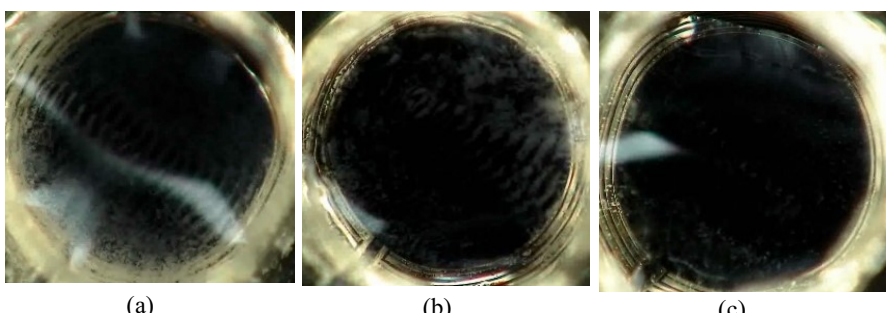


**Fig. 6.** Particles that have successfully aggregated at the pressure nodes for device B with the concentration of (a) 1:3, (b) 1:10 and (c) 1:30

Particles that have successfully aggregated at pressure nodes was counted using ImageJ software. Table 3 shows the total number of particles suspended on pressure nodes for device B. Based on the experiment for device B, the higher the ratio concentration of particles, the more the particles that can successful aggregate at pressure nodes.

**Table 3.** Number of particles aggregated at pressure node in device B.

Concentration (%)	No of Particles
0.25	4456620
0.17	4148424
0.09	3776544
0.05	1352268
0.03	1142856

Based on both Table 1 and Table 2, the number of particle count for device A was higher than that of device B for concentration ratio of 1:3, but lower for other ratios. Figure 5 and figure 6 display that more particles were aligned at device A compared to device B. Figure 7 shows the normalised particles aggregation efficiency ( $\eta$ ) for both devices.

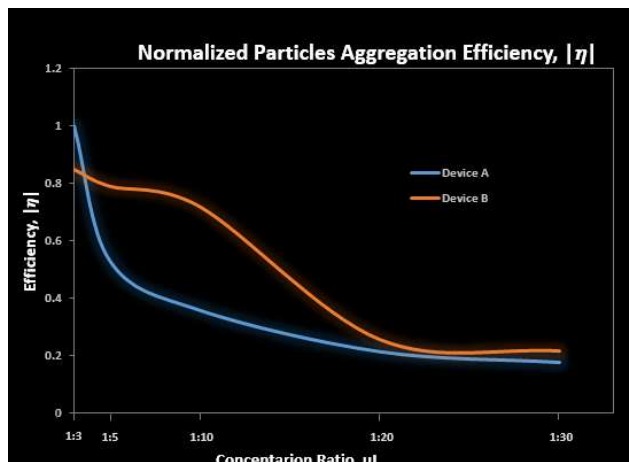


**Fig. 7.** Normalised particles aggregation efficiency ( $\eta$ ) for device A and device B

## 5 Conclusion

In conclusion, the aggregation process of 6.42  $\mu\text{m}$  polystyrene particles using two types of flexural plate wave device with similar frequency and power (RF) has been demonstrated. Aggregation efficiency was influenced by spatial size, concentration of microparticles in fluid, frequency and power supply. The acoustic plate mode waveform (FPW) produced better particle alignment than magnetophoresis, dielectrophore-

sis ultracentrifugation (AUC) and mass spectrometry. This aggregation method will be very useful in biological and medical applications especially for molecular biology study.

## Acknowledgement

The authors gratefully acknowledge that this work was financially supported by the Research University Grant of Geran Galakan Penyelidik Muda (Project No: GGPM-2017-035), Universiti Kebangsaan Malaysia.

## References

1. Devendran, C., Gunasekara, N.R., Collinsb, D.J. & Neild, A. 2016. Batch Process Particle Separation using Surface Acoustic Waves (SAW): Integration of Travelling and Standing SAW. *RSC Advances* 6(7): 5856–5864.
2. Gossett, D.R., Weaver, W.M., Mach, A.J., Hur, S.C., Tse, H.T. K., Lee, W., Amini, H. & Carlo, D.D. 2010. Label-Free Cell Separation and Sorting in Microfluidic Systems. *Analytical and Bioanalytical Chemistry* 397(8):3249–3267.
3. Luong, T.D. & Nguyen, N.T. 2010. Surface Acoustic Wave Driven Microfluidics – A Review. *Micro and Nanosystems* 2(3): 1-9.
4. Li, H., Friend, J.R. & Yeo, L.Y. 2007. Surface Acoustic Wave Concentration of Particle and Bioparticle Suspensions. *Biomed Microdevices* 9(5):647–656.
5. Nam, J., Lim, H. & Shin, S. 2011. Manipulation of Microparticles using Surface Acoustic Wave in Microfluidic Systems: A Brief Review. *Korea-Australia Rheology Journal* 23(4): 255-267.
6. Destgeer, G.; Hyung, J.S. 2015. Recent advances in microfluidic actuation and micro-object manipulation via surface acoustic waves. *Lab Chip*, 15: 2722–2738.
7. Endo,A.,Yanagimoto,M., Asami,T. & Miura,H. 2015. Non contact atomization of droplets using an aerial ultrasonic source with two vibrating plates. *Jpn. J. Appl. Phys.*, 54: 07-13.
8. Greenhall, J., Guevara Vasquez, F. & Raeymaekers, B. 2016. Ultrasound directed self-assembly of user-specified patterns of nanoparticles dispersed in a fluid medium. *Appl. Phys. Lett.*, 108, 103103.
9. Collins, D.J., Devendran, C., Ma, Z., Ng, J.W., Neild, A.& Ai, Y. 2016. Acoustic tweezers via sub-time-of-flight regime surface acoustic waves. *Sci. Adv.*, 2,:1600089.
10. Hsu, J.-C.; Huang, Y.-W.; Hsu, C.-H. Transportation control of microfluidic particles using mode switching between surface acoustic waves and plate waves. *Jpn. J. Appl. Phys.* 2017, 56.
11. Ng,J.W., Devendran,C. & Neild,A. 2017. Acoustic tweezing of particles using decaying opposing traveling surface acoustic waves (DOTSAW). *Lab Chip*, 17, 3489–3497
12. Barnkob, R., Nama, N., Ren, L., Huang, T.J., Costanzo, F.& Kähler, C.J. 2018. Acoustically driven fluid and particle motion in confined and leaky systems. *Phys. Rev. Appl.*, 9, 014027.
13. Hsu, J.C., Hsu, C.H. & Huang Y. W. 2019. Acoustophoretic Control of Microparticle Transport Using Dual-Wavelength Surface Acoustic Wave Devices *Micromachines* 10 (52):1-19
14. Johansson, L., Enlund, J., Johansson, S., Katardjiev, I. & Yantchev, V. 2012. Surface Acoustic Wave Induced Particle Manipulation in A PDMS Channel—Principle Concepts for Continuous Flow Applications. *Biomed Microdevices* 14(2):279–289.

15. Jo, M.C. 2013. An Acoustic-based Microfluidic Platform for Active Separation and Mixing. Degree of Doctor of Philosophy, Department of Mechanical Engineering College of Engineering University of South Florida
16. Weinberg, M. S., Cunningham, B. T., and Clapp. C. W. 2000. Modeling Flexural Plate Wave Devices Journal of Micromechanical Systems. 9 (3): 370-379
17. Guldiken, R., Jo, M.C., Gallant, N.D., Demirci, U. & Zhe, J. 2012. Sheathless Size-Based Acoustic Particle Separation. Sensors 12(1): 905-922.
18. Soliman, A.M., Eldosoky, M.A. & Taha, T.E. 2015. Modelling and Simulation of Microparticles Separation using Standing Surface Acoustic Waves (SSAWs) Microfluidic Devices for Biomedical Applications. International Journal of Computer Applications 129(9): 30-38.
19. Moradi, K. 2015. Acoustic Manipulation and Alignment of Particles for Applications in Separation, Micro-Templating and Device Fabrication. Degree of Doctor of Philosophy, Department of Mechanical Engineering of Florida International University.
20. Muller, P. B., Barnkob, R., Jensen, M. J. H. & Bruus, H. 2012. A numerical study of microparticle acoustophoresis driven by acoustic radiation forces and streaming-induced drag forces. Lab on a Chip, 12(22), 4617.



# A User Mobility-Aware Fair Channel Assignment Scheme for Wireless Mesh Network

Bander Ali Saleh Al-rimy, Maznah Kamat\*, Fuad A. Ghaleb, Mohd. Foad Rohani, Shukor Abd Razak, Mohd Arief Shah

Faculty of Computing, Universiti Teknologi Malaysia, Skudai, Johor, Malaysia  
kmaznah@utm.my, bnder321@gmail.com, fuadeng@gmail.com,  
foad@utm.my, shukorar@utm.my, shah@gmail.com

**Abstract.** Wireless Mesh Networks (MR-WMNs) are characterized by having multiple radio interfaces with which, node can send/receive data to/from multiple nodes. This feature increases the network capacity and improves data delivery rate. However, interference between the co-located channels is one of the main constraints that hinder such networks from achieving the optimal utilization of the available resources such as bandwidth and transmission routes. Bottleneck is one of the consequences of such limitation, which leads to network fragmentation and performance degradation especially in the critical links shared by multiple paths connecting the nodes with the gateway. Although several studies have been conducted to address such limitation, they were all built on the premise of stationary topology, which does not hold for real world WMNs that include mobile users in addition to backbone nodes and routers. To this end, this paper proposes a user mobility-aware channel assignment algorithm based on weighted link ranking to fairly allocate the channels and minimizes the interference, thus improves the capacity of the network. Multiple criteria were used to rank those links before applying the channel assignment algorithm. Those criteria were obtained from traffic and network topology such as distance from the gateways, interference index, and traffic load. The results from numerical simulation demonstrate that the proposed scheme has reduced the interference which, consequently, improved the network capacity.

**Keywords:** Channel assignment; fairness; interference matrix; weighted link ranking.

## 1 Introduction

Wireless mesh networks (WMN) are multi-radio wireless nodes connected using redundant paths in order to provide robust, fault-tolerant and flexible network. As such, WMNs are able to support real-time applications which are challenging in conventional wireless networks [1]. With such characteristics, WMNs can provide broadband network access to the centralized resources such as Internet, traffic information, and healthcare systems. In recent years, some new application scenarios have emerged in WMNs such as smart grids and intelligent transportation systems [2]. Different radio

technologies are used in WMN including IEEE 802.11 (a/b/g/n) and 802.16 [3]. Such variety makes WMN flexible to support many manufacturing standards. Moreover, the ability to integrate with other technologies like wireless ad-hoc networks makes it easy to combine WMNs into the existing infrastructure and provide the nodes with the ability to share and exchange the data over Internet. Client meshing is one of the important characteristics that distinguish WMNs from conventional wireless ad-hoc networks [4]. WMN consists of a collection of stationary mesh routers that provide connectivity to mesh clients to access network resources through gateways [5]. The gateways transfer the information from and to the mesh network. The backbone of mesh networks provides routing functionality as well. The flexibility, auto-configuration, self-organization and cost-effectiveness make WMNs suitable for a wide range of applications such as Internet access, smart grids and healthcare systems that provide the aid for emergency cases [3]. For more discussion about the potential WMN applications, the reader is referred to these surveys [3, 6].

To send/receive data between wireless nodes, the sender and receiver need to share same radio channel. However, at any time, only single node can use a channel. On other word, if two or more nodes send data packets on the same channel concurrently, those packets would collide result in unsuccessful sending/receiving process. Furthermore, the increase number of competing nodes adversely affects the performance of the entire network [7]. As such, supporting the concurrent transmission is imperative for reliable wireless networks.

By providing multiple radio interfaces that could work on different channels, Wireless Mesh Networks (WMNs) enable wireless nodes to send and/or receive data concurrently [8]. That is, the node with multiple radio interfaces can send/receive data from multiple nodes at the same time. For instance, a wireless node with three radio interfaces can be paired with three other nodes each of which uses one radio interface. As such, the node can send/receive data to/from three nodes simultaneously. However, overlapping channels can interfere with one another causing degradation to network capacity [9, 10]. To avoid such interference, orthogonal channels need to be assigned to neighboring links [11]. Nevertheless, IEEE 802.11b/g protocol that support WMN has only three non-overlapping channels. For instance, having channel 1 assigned to one link, the node has channels 6 and 11 remain to be used by neighboring link without causing interference to each other. Such constraint renders channel assignment among WMN nodes an NP-Hard problem in which, the optimal solution cannot be found [12].

Several studies have been conducted to address channel assignment issue and provide effective algorithms that decrease the interference between communication links while maintaining high network capacity and preserving its connectivity. However, unfair distribution of channels between the links is the main limitation of those algorithms due to the lack of mechanism in distinguish between the links given network topology [2, 11]. That is, existing solutions deal with all links equally regardless of whether they are critical, which might cause bottlenecks in the network. Such bottlenecks hinder the ability of WMNs to achieve the best possible throughput of the topology. Although the scheme proposed by [11] addressed such issue based on three criteria: the proximity of the link to the gateway, interference index and traffic load, the proposed scheme assumes that the topology is stationary, which does not hold for MWNs whose topologies

change as a result of mobile users who usually join/leave the network. Such dynamics in the topology renders existing assignment suboptimal. Consequently, the bottleneck could unpredictably move from one link to another, causing degradation to network capacity. To this end, this paper addresses this issue by proposing a topology changing-aware weighted link ranking scheme for fair channel assignment in WMNs. The proposed scheme overcomes the limitation of existing works by involving the interference caused by channels connected to mobile nodes (users) and dynamically cope with the topological changes that those nodes cause to the network.

The rest of this paper is organized as follows. Section 2 reviews the related work. Section 3 describes the proposed algorithm. Section 4 illustrates the performance evaluations and comparison with the related works. The paper is concluded in Section 5.

## 2 Related Work

Several studies have been conducted to address channel assignment issues and provide effective algorithms that decrease the interference between communication links while maintaining high network capacity and preserving its connectivity. Furthermore, those studies proposed different strategies to allocate the best possible channel for each pair of WMN nodes. Several channel assignment algorithms considered the channel assignment as edge coloring problem [2, 13, 14]. The links are ranked based on specific criteria such as interference, capacity, and frequency of use. Then, each link is given a channel based on its ranking value, which means a high ranked link is given a lower interference channel. However, the link fairness which aims to equity distribute the quality of the channel was ignored which make single criteria is not effective to utilize the capacity of the network. A multi-criterion link ranking scheme was proposed by [10]. The scheme used five criteria to rank the link. Although the link fairness was considered, the proposed algorithm assumes stationary environment where the mesh client is fixed.

In their study, [15] proposed a collaborative-learning automata scheme, which conducts channel assignment while preserving the network topology. The proposed scheme deploys learning automata into nearest mesh routers that collaborate with each other and share information and data transmission. Channel utilization factor (CUF) was used as a channel selection criterion. By employing the topology control and link interference weight, Multi-Radio Multi-Channel (MRMC) assignment algorithm was proposed by [16]. The topology control was adopted to preserve the transmission power of WMN nodes. Then, the weight was calculated for each link based on the expected load in each network node. Topology control approach was also adopted by [17] to develop CLICA, a greedy heuristic-based channel assignment algorithm, to find connected; low-interference topologies within the original WMN network. Graphic theory and Integer Linear Programming were utilized to guide the assignment process and obtain the lower bound for optimum. MesTic strategy was proposed by [18], which combines mesh traffic pattern with connectivity issues in order to assign the channels in a way that minimizes the interference within WMNs. The scheme employs a ranking function that

calculates link weights based on the traffic, proximity to the gateway (in terms of number of hops) and number of radio interfaces per node.

Most of the aforementioned approaches assume stationary environment which makes them limited to static scenarios. In addition, those schemes have not considered the fairness for channel assignment. Although the scheme presented in [10] have considered the link fairness into account, the static assumption of mesh clients is the main limitation of this algorithm. In this paper, a dynamic channel assignment is presented where the user mobility and link fairness have been taken into account during design.

### 3 The Proposed S Channel Assignment Algorithm

Maintaining high capacity is the ultimate aim of channel assignment algorithms for WMNs. Several factors govern such capacity like traffic patterns, interference and topological connectivity. In this section, the proposed scheme is described along with the methods and techniques used in building its different components. As shown in Figure 1, two main components constitute the proposed scheme: links ranking and channel assignment.

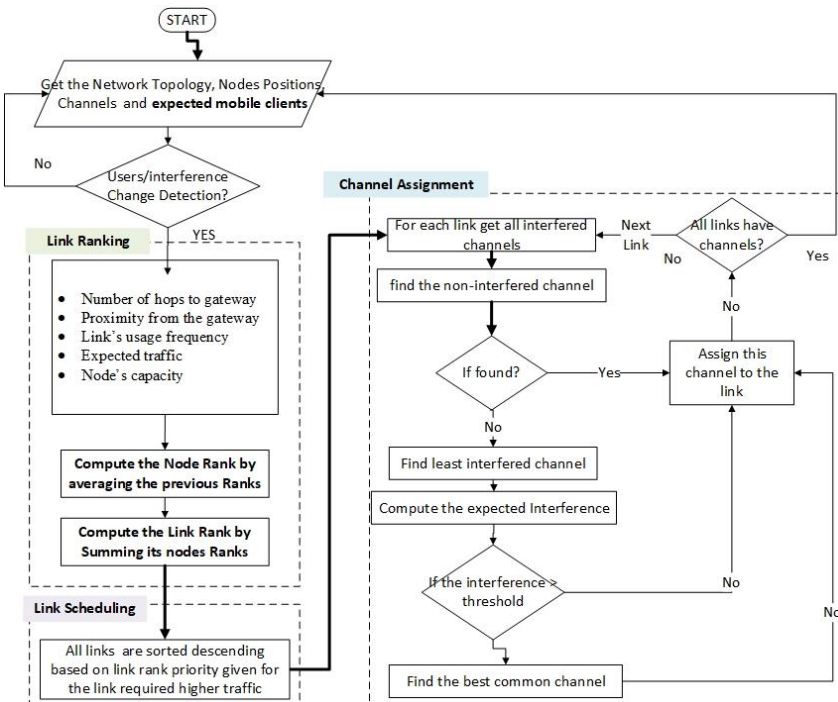


**Fig. 1.** General architecture of the proposed scheme

### 3.1 Links ranking

During link ranking phase, each link is weighted based on several criteria like number of hops to gateway, proximity from the gateway, link's usage frequency, expected traffic, and node's capacity. Dijkstra's algorithm, a well-known graph-based shortest path finding algorithm [21] was employed to find the number of hops to gateway while the Euclidian distance was employed to determine the length of the link between two nodes. The lower the number of radios, the higher the priority in channel assignment. These criteria were calculated based on network topology and traffic information. As such, the proposed scheme can fairly allocate the channels into different links within WMNs and maximize the concurrent transmission without compromising overall capacity. The details of those criterion can be found in our previous publication [11]. As was proposed in [11], the final link score is calculated according to the aforementioned criterion. To prevent the bias ranking, each criterion was normalized by dividing by the maximum obtained rank. Then, the scores of all links emerged from the node were added up into one value which represents node's rank. Having calculated the ranking of each node, the link's ranking was determined by adding up those whose nodes share that link.

### 3.2 Links Scheduling

After links ranks are calculated, the links scheduling procedure starts as follows. For each node, the links are sorted in a descending order such that link with the highest score takes the least available interfered channel. Similar to [11] the proposed dynamic channel assignment scheme uses the concept of least interfered channel as elaborated in Section 3.3. Contrary to [11], the proposed scheme keeps monitoring topology changes in the network, which invalidates the expected traffic calculation due to user mobility. That is, when mobile users move from one MR to another, expected traffic on both MRs changes accordingly. Such change of topology triggers expected traffic recalculation. Consequently, channel assignment algorithm conducts a new assignment (as shown in Fig. 1).

### 3.3 Dynamic Channel Assignment using Least Interfered Channel

Having calculated links rankings, the proposed scheme allocated the channels to each one of those links based on least interfered channel approach. Unlike greedy approach which visits the links first and looks for the nodes within that link, the least interfered channel approach visits the nodes and gives the priority to the links attached to that node. Moreover, every link was visited based on its order. For each link  $l$ , the interference from neighboring links is identified according to conflicting graph and interference model (to be explained later). When assigning a channel to neighboring link, the scheme records the link along with the assigned channel into a variable ( $N_c$ ), which contains the list of neighboring channels. Then, one of non-overlapping channels is assigned to the link  $l$  and loop to the next link. If non-overlapping channels are not

available, search for the least interfered channel, which is determined using the interference model.

After assigning channels to all links in the network, the proposed scheme keeps monitoring the topology. If a change to network topology is detected, the proposed scheme triggers channel assignment process. Therefore, the scheme becomes aware of the changes in the network due to user mobility that invalidates existing assignment.

**Table 1.** Overlapping Ratio

Channels	1	2	3	4	5	6	7	8	9	10	11
1	1	0.77	0.55	0.32	0.09	0	0	0	0	0	0
2	0.77	1	0.77	0.55	0.32	0.09	0	0	0	0	0
3	0.55	0.77	1	0.77	0.55	0.32	0.09	0	0	0	0
4	0.32	0.55	0.77	1	0.77	0.55	0.32	0.09	0	0	0
5	0.09	0.32	0.55	0.77	1	0.77	0.55	0.32	0.09	0	0
6	0	0.09	0.32	0.55	0.77	1	0.77	0.55	0.32	0.09	0
7	0	0	0.09	0.32	0.55	0.77	1	0.77	0.55	0.32	0.09
8	0	0	0	0.09	0.32	0.55	0.77	1	0.77	0.55	0.32
9	0	0	0	0	0.09	0.32	0.55	0.77	1	0.77	0.55
10	0	0	0	0	0	0.09	0.32	0.55	0.77	1	0.77
11	0	0	0	0	0	0.09	0.32	0.55	0.77	1	1

The proposed interference model relies on the IEEE 802.11b channels which has 11 channels with only three orthogonal (non-overlapping) channels. Thus, each channel overlaps with three other neighboring channels in the frequency spectrum. According to the standard, only channels 1, 6, and 11 are not overlapped. To obtain the least interfering channel, the proposed scheme employs the interference factor (I-Factor) [22] to calculate the ratio of the overlapping area such that, the channel with the lowest overlapping area was selected. For instance, as shown in Table 1, channel 1 has 77% overlapping area with channel 2 and has 55% overlapping area with channel 3.

To assign a channel to a link, the proposed scheme selects the channel with the lowest interference effect on the neighboring channels. To avoid assigning high overlapping channels, certain overlapping threshold is considered during channel assignment. Figure 3 shows the pseudo code of the proposed scheme.

**Input:** network topology, nodes positions, channels, expected mobile clients  
**Output:** channels assigned to links

---

```

1: for each node n:
2:    $rg_n \leftarrow$  rank based on number of hops to gateway
3:    $re_n \leftarrow$  rank based on Euclidean distance from gateway
4:    $rf_n \leftarrow$  rank based on frequency of use to reach the gateway
5:    $rt_n \leftarrow$  rank based on expected traffic
6:    $ri_n \leftarrow$  rank based on expected interference
7:    $r_n \leftarrow$  average( $rg_n, re_n, rf_n, rt_n, ri_n$ )
8: for each link m connecting two nodes,  $n_1$  ;  $n_2$ :
9:    $rl_m \leftarrow r_{n_1} + r_{n_2}$ 
10: sort all links descendent
11: for each link:
12:    $C_i \leftarrow$  get all interfered channels
13:    $C_n \leftarrow$  find non-interfered channels
14:   if length( $C_n$ ) = 0:
15:     find least interfered channel
16:     compute the expected interference
17:     if expected interference > threshold:
18:       Find the best common channel
19:       assign this channel to the link
20:     if all links have channels:
21:       switch to monitoring mode
22:   else:
23:     assign this channel to the link
24:   if all links have channels:
25:     switch to monitoring mode

```

---

**Fig. 2.** Pseudocode for the Proposed Algorithm

## 4 Performance Evaluation

In this section, the performance of proposed channel assignment scheme is evaluated and compared with the related work. The baseline algorithm starts assigning channels to nodes arranged in descending order of the number of hops to the gateway [15, 19]. This algorithm may not provide fair allocation of channels in the most sensible area of a WMN like nodes far from gateway. Since the direction of the traffic is towards the gateway, bottleneck may occur anywhere in that path causing network fragmentation and capacity degradation. Instead of relying on single criterion, the proposed algorithm employed multiple criteria to calculate link rankings based on which the channels were allocated to those links. Python's network library was utilized to implement the simulation of both algorithms, i.e. the proposed and baseline algorithms for simulating network as a conflicted graph. This kind of simulation is widely accepted for numerical evaluation of channel distribution in the field of channel assignment algorithms.

To conduct the evaluation, two performance measures were used, i.e. Network Capacity (NC), and Fractional Network Interference (FNI). NC is the total concurrent transmission in the network after channel assignment algorithm while FNI is the ratio between network interference and the total conflicting links in the network. FNI is also defined as the number of conflicts that remain after channel assignment relative to the number of conflicts in a single channel network. It is the remaining ratio of interference

after applying the channel assignment algorithm. To analyze the impact of interference between the links, different scenarios were implemented each of which with different number of nodes, namely 10, 20, 30, 40, and 50. With each scenario, many random topologies were generated and tested. All parameters used in this experiment were chosen according to the common practice in the field of channel assignment algorithms.

Figures 3(a), 3(b), 3(c), 3(d), 3(e) and 3(f) show an example of the graphical representation of a WMN network. Figure 3(a) shows a representation of network topology

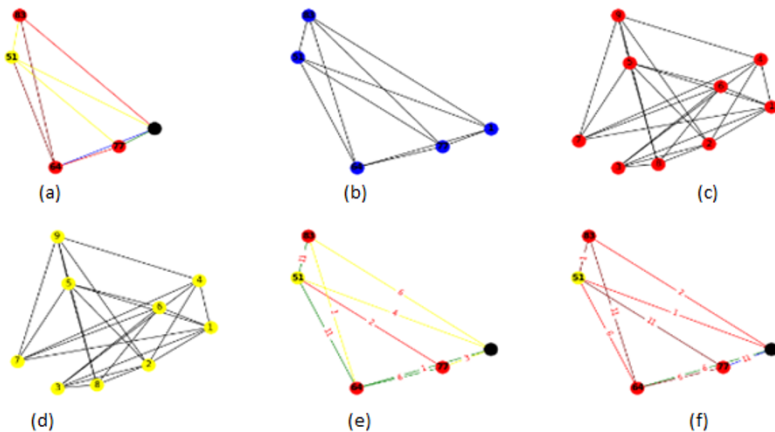


**Fig. 3.** Graphical Representation of a WMN Network of Channel Assignment

in which the nodes represent the mesh routers and the edges represent the required link. Figure 3(b) represents the possible interference between those nodes where the communication range of the nodes are overlapped. The mesh routers may not be located in the range of each other, however, their links can still interfere with each other. To consider such fact in the proposed channel assignment algorithm the conflicted graph was used. This property has been overlooked in the previous schemes, they only consider the interference among nodes and not the links. Figure 3(c) represents the conflict graph where the links were represented as nodes and the edges represent the overlapping status of two links. Accordingly, Figure 3(d) represents the potential interference between the links. By the help of this representation, the channel assignment algorithm uses this graph to assign the channels with the least interference., channel assignment results of static approach and channel assignment results of dynamic approach respectively. Figure 3(e) shows the result of the channel assignment of the existing baseline scheme where Figure 3(f) shows the results of the channel assignments as obtained from the proposed scheme.

As shown in Figure 3(a), the network is composed of five mesh routers (nodes) each of which is represented as an vertices, while each link in the topology are represented as edge. The link is a connection between two network interfaces in the corresponding

vertices that form the edge. Thus, each link in the graph needs a dedicated channel which is assigned by the channel assignment algorithm. The interference graph in Figure 3(b) depicts the potential interference range that each node causes on the other nodes. If two nodes are located in the interference range of each other, an interference link is added between them. This representation is used to show how nodes interfere with each other's. In Figure 3(c), the vertices in the conflict graph represent the links while the edges represent the mesh routers that make the links. The graphical representation of link interference is shown in Figure 3(d) shows the interference that each link inflicts on the other links. This representation is more effective than using the node interference representation in Figure 3(b). This is because the node based representation overlooks the potential interference between the adjacent links in the graph. Figure 3(e) shows the result of channel assignment process using the static approach while Figure 3(f) shows the results of channel assignment using the dynamic approach.

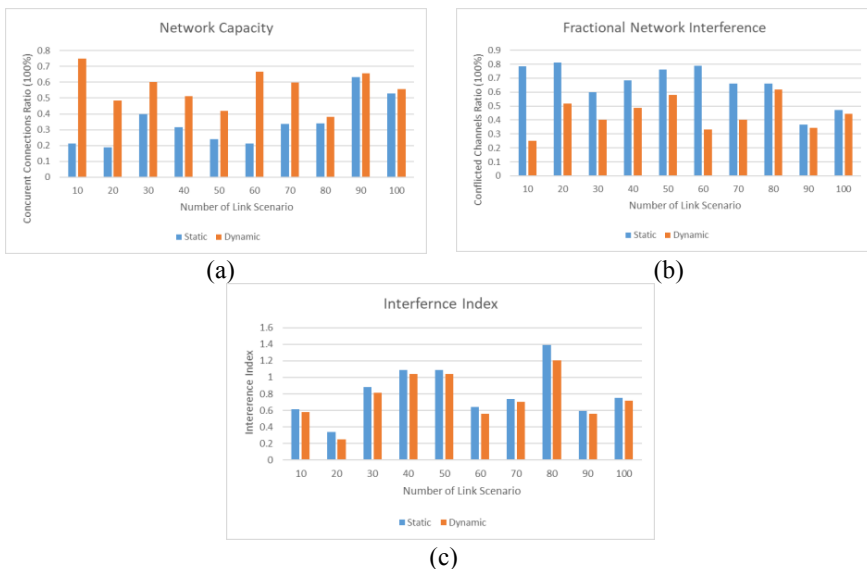


**Fig. 4.** Results Comparative (a) network capacity, (b) fractional network interference, (c) interference index.

Figures 4(a), and 4(b), show the performance of the proposed algorithm in terms of the Network Capacity (NC) and Fractional Network Interference (FNI) as function of number of links in each simulated scenario, respectively. Figure 4(c) illustrates the average interference index. As shown in Figure 4(a), the proposed channel assignment scheme outperforms the related approach in terms of concurrent connections in all scenarios. On average, the network capacity (measured by number of concurrent connections) increases from 34% to 56% as compared to [11]. This is attributed to the dynamic approach that the proposed scheme employs, which enables it to detect and react to the changes in network topology. Moreover, Figure 4(c) shows that, for all scenarios, the proposed scheme decreases the interference index. On average, the interference

between the selected channels decreases from 81% to 74% compared to existing work. Similarly, Figure 4(b) shows that the average fractional network interference decreases from 65% to 43% compared to related work. This is attributed to the ability of proposed scheme to detect the changes in network topology causes by mobile nodes which enables it to redistribute the channels among conflicting links accordingly.

These results clearly show that the proposed dynamic channel assignment scheme leads to improve the network performance during user movement, as compared to the static algorithm. T-Test results show a significant improvement in the number of concurrent connections and fractional network interference. Also, the proposed dynamic channel assignment can preserve the link fairness as compared to the static one which has a shorter duration to keep link fairness. In the proposed algorithm, the use of common channel when two links can heavily interfere with each other leads to reduce the interference and further improved fairness in medium access and hence, increase the number of concurrent connections.

## 5 Conclusion

In this paper, a novel channel assignment algorithm is proposed based on user mobility and multiple weighted criteria. Unlike the existing channel assignment algorithms which assume a stationary topology of the WMNs, the proposed algorithm accounts for user mobility that causes network topology to change partially or entirely and maintains high capacity and connectivity during the WMN lifetime. The proposed algorithm employs multi-criteria to rank the links within WMN based on which, the fair channel allocation is carried out. The simulation results show an improvement in the network performance as well as stable capacity compared to the related algorithms. Future work, further analysis and evaluation of the performance of the proposed algorithm in terms of network throughput as well as optimizing criteria coefficients selection using heuristic methods such as the genetic algorithm to search for the best possible weights.

## Acknowledgement

This work is supported by the Ministry of Higher Education (MOHE) and Research Management Centre (RMC) at the Universiti Teknologi Malaysia (UTM), under research grant Trans-disciplinary Research Grant Scheme (TRGS) with VOT R.J130000.7828.4L852.

## References

1. Cheng, H., et al., *Links organization for channel assignment in multi-radio wireless mesh networks*. Multimedia Tools and Applications, 2013. **65**(2): p. 239-258.
2. Khan, U.U., et al., *Fairness in Cognitive Radio Networks: Models, measurement methods, applications, and future research directions*. Journal of Network and Computer Applications, 2016. **73**: p. 12-26.

3. Islam, A.B.M.A.A., et al., *Channel Assignment Techniques for Multi-Radio Wireless Mesh Networks: A Survey*. IEEE Communications Surveys & Tutorials, 2016. **18**(2): p. 988-1017.
4. Shi, W.-X., K.-Q. Cui, and Y. Chai, *Routing and Channel Assignment for Multicast in Multi-Channel Multi-Radio Wireless Mesh Networks*. Journal of Communications, 2016. **11**(11).
5. Kanagasabapathy, A.A., A.A. Franklin, and C.S.R. Murthy, *An Adaptive Channel Reconfiguration Algorithm for Multi-Channel Multi-Radio Wireless Mesh Networks*. IEEE Transactions on Wireless Communications, 2010. **9**(10): p. 3064-3071.
6. Avallone, S., I.F. Akyildiz, and G. Ventre, *A Channel and Rate Assignment Algorithm and a Layer-2.5 Forwarding Paradigm for Multi-Radio Wireless Mesh Networks*. IEEE/ACM Transactions on Networking, 2009. **17**(1): p. 267-280.
7. Kumar, N. and J.H. Lee, *Collaborative-Learning-Automata-Based Channel Assignment With Topology Preservation for Wireless Mesh Networks Under QoS Constraints*. IEEE Systems Journal, 2015. **9**(3): p. 675-685.
8. Moreno, J., et al., *Design of Indoor WLANs: Combination of a ray-tracing tool with the BPSO method*. IEEE Antennas and Propagation Magazine, 2015. **57**(6): p. 22-33.
9. Cardieri, P., *Modeling interference in wireless ad hoc networks*. IEEE Communications Surveys & Tutorials, 2010. **12**(4): p. 551-572.
10. Roh, H.T. and J.W. Lee, *Channel assignment, link scheduling, routing, and rate control for multi-channel wireless mesh networks with directional antennas*. Journal of Communications and Networks, 2016. **18**(6): p. 884-891.
11. Ghaleb, F.A., et al. *Fairness of Channel Assignment Algorithm Based on Weighted Links Ranking Scheme for Wireless Mesh Network*. in *Proceedings of the Fourth International Conference on Engineering & MIS 2018*. 2018. ACM.
12. Wang, J. and W. Shi, *Partially overlapped channels- and flow-based end-to-end channel assignment for multi-radio multi-channel wireless mesh networks*. China Communications, 2016. **13**(4): p. 1-13.
13. Qu, Y., B. Ng, and M. Homer, *Optimising channel assignment to prevent flow starvation and improve fairness for planning single radio WMNs in built environments*. Computer Networks, 2017. **129**: p. 215-231.
14. Mogabel, H.A., et al., *Review of channel assignment approaches in multi-radio multi-channel wireless mesh network*. Journal of Network and Computer Applications, 2016. **72**: p. 113-139.
15. Kumar, N. and J.-H. Lee, *Collaborative-learning-automata-based channel assignment with topology preservation for wireless mesh networks under QoS constraints*. IEEE Systems Journal, 2015. **9**(3): p. 675-685.
16. Zhao, X., et al., *A Multi-Radio Multi-Channel Assignment Algorithm Based on Topology Control and Link Interference Weight for a Power Distribution Wireless Mesh Network*. Wireless Personal Communications, 2018. **99**(1): p. 555-566.
17. Marina, M.K., S.R. Das, and A.P. Subramanian, *A topology control approach for utilizing multiple channels in multi-radio wireless mesh networks*. Computer Networks, 2010. **54**(2): p. 241-256.
18. Skalli, H., et al., *Channel assignment strategies for multiradio wireless mesh networks: Issues and solutions*. IEEE Communications Magazine, 2007. **45**(11).



# Tweep: A System Development to Detect Depression in Twitter Posts

Chempaka Seri Abdul Razak<sup>1</sup>, Muhammad Ameer Zulkarnain<sup>1</sup>,  
Siti Hafizah Ab Hamid<sup>1</sup>, Nor Badrul Anuar<sup>1</sup>, Mohd Zalisham Jali<sup>2</sup>, Hasni Meon<sup>3</sup>

<sup>1</sup> Fac. of Computer Science & Information Technology, University of Malaya, Malaysia

<sup>2</sup> Fac. of Science and Technology, Universiti Sains Islam Malaysia, Malaysia

<sup>3</sup> Fac. of Communication Visual Art & Computing, Universiti Selangor, Malaysia

chempakaseri@siswa.um.edu.my, ameerzulkarnain@siswa.um.edu.my,  
sitihofizah@um.edu.my, badrul@um.edu.my, zalisham@usim.edu.my,  
hasni@unisel.edu.my

**Abstract.** This paper presents a system development named Tweep that enables a consumer to analyze depression status using Machine Learning based on personal Twitter posts. In order for the consumer to curb mental illness, Tweep does not only analyze Twitter users' personal depression status, but also that of the people they follow on Twitter i.e. their 'following'. This project is the first work that practices a user-friendly interface system that analyzes depression status for public use. The system uses rule-based Vader Sentiment Analysis and two Machine Learning techniques namely Naive Bayes and Convolutional Neural Network. The output of the system is the percentage of the positive and negative posts of the Twitter users and of their followings.

**Keywords:** Depression, Twitter, Machine Learning, Emotion

## 1 Introduction

Depression or depressive disorder is a common mental health illness and the largest contributor to suicide which involves a total number of 322 million (4.4% of the world's population) people worldwide [1]. Among the causes of depression are poverty, unemployment, death of a loved one, relationship break-up, physical illness and alcohol and drug abuse. Depression is a huge burden to all communities, it is a complex social issue that is hard to be curbed, what more when the public is still unaware of the symptoms and some even deny of having such illness. Although traditional methods are available, they are not always practical; they are time consuming, questionable and expensive. Social media is seen to be a suitable platform to not only detect early symptoms but also to prevent depression from occurring altogether.

Social media applications such as Facebook, Instagram, and Twitter encourage the users to share experiences, opinions, knowledge and locations. Since the major component of mental health research requires the study of behavior, which may be based on

ones' interaction and communication with family and friends, using social media applications to detect, analyze and treat patients with depression is believed to be effective and promising. Many researches have been done to detect depression posts from the patients, analyze the usage of depressive words on social media and diagnose patients through their social media posts in the long run. However, the existing works only focus on improving and validating the accuracy of the result.

This project aims to develop a user-friendly system, Tweep to analyze one's Twitter posts as well as that of his followings. The output of the system displays the percentage of positive and negative posts. The percentage becomes an indicator of his mental health status. Tweep acts as a simple self-diagnosis using one's past Twitter posts. In comparison to other existing works that merely focus on improving the accuracy of methods to detect depression posts on Twitter, this work focuses on the development of the system for the public's benefits.

## 2 Related Works

Works on analyzing and detecting depression via Twitter have started in 2013 by Choudhury et al. [2] where they predicted the risk of depression from Twitter post using user's activities by SVM and estimated the depressive tendencies of the populations. They applied crowdsourcing as the main method in collecting data where they devised a questionnaire to gather information from Twitter users. Tsugawa et al. [3] continued the research by applying the method to a more large-scale data focusing on Japanese speaker Twitter users. The accuracy they achieved was 69% as compared to [2] which was 70%. Reavley and Pilkinson [4] used hashtags to monitor Twitter users' attitude towards depression. However, their method was limited to very specific hashtags only. The work was unable to detect other than the hashtags provided in the rules. The same method was applied by Mowery et al. [5] where they used particular words to analyze depressive symptoms on Twitter. Based on the words specified, the findings show the frequency of depressive words used by the users. However, it did not analyze the depression status of the users who posted the words. Meanwhile, works by Reece et al. [6] and Coopersmith et al. [7, 8] focused on analyzing the correlation between the patients' conditions with their twitter posts. Their findings helped to improve the accuracy of the diagnosis. Only Julius Jacobson's [9] work was closed to the present work, where it detected depressed Twitter users based on their posts. However, her work was limited to Korean language users only.

## 3 Methodology

### 3.1 Data Preprocessing

In this study, a python Twitter crawler is used to query data from Twitter. Tweepy library is used as the python Twitter API wrapper in the script. The script is given a 'seed' account from the user and it acts as the starting point. The method of crawling is based on the Depth-First Search mechanism and techniques. The script goes in-depth

by taking the followers list of the seed (depth 0) and continues the seed's follower will be at Depth 1. Next, the script gets the list of followers from the user in Depth 1 and performs crawling for Depth 2 and continues until Depth 3. The data is stored in JSON file. The dataset is then cleaned where quotes, extra spacing and symbols are removed from the tweets. Then, the dataset is split into training set and test set.

### 3.2 Text Classification Techniques

Tweep employs a Rule-based approach (VADER Sentiment) and Machine Learning approach (TextBlob and Convolutional Neural Network).

#### Rule-based Approach

Rule-based approaches classify text into organized groups by using a set of linguistic rules. These rules train the system to use semantically relevant elements of a text to identify relevant categories based on its content. Each rule consists of a pattern and a predicted category.

#### *VADER Sentiment Analysis*

Valence Aware Dictionary and sEntiment Reasoner (VADER) is a lexicon and rule-based sentiment analysis tool that is specifically attuned to sentiments expressed in social media. VADER uses a combination of qualitative and quantitative methods that construct and validate a list of lexical features which are specifically tuned to sentiment in microblog-like contexts.

```
@app.route('/api/sentiment/nltk', methods=['GET'])
```

#### Machine Learning Based Approach

Machine Learning systems learn to make classification based on past observations. By using pre-labeled examples as training data, a machine learning algorithm can learn. The different associations between pieces of text and a particular output are expected for a particular input.

#### *Naïve Bayes*

The Naïve Bayes classifier is the simplest and most commonly used classifier. Naïve Bayes classification model computes the posterior probability of a class, based on the distribution of the words in the document. The model works with the BOWs feature extraction which ignores the position of the word in the document. It uses Bayes Theorem to predict the probability that a given feature set belongs to a particular label.

TextBlob is a simplified text processing that provides API for common natural language processing tasks such as sentiment analysis. The tool implements Naïve Bayes text classification technique that returns a named tuple of the form Sentiment (polarity, subjectivity). For the system, we only take the polarity scores that float within the range [-

1.0, 1.0] where -1.0 is negative and 1.0 is positive. TextBlob has an accuracy of 70%. The tool is used via API.

```
@app.route('/api/sentiment/blob', methods=['GET'])
```

#### *Convolutional Neural Network (CNN)*

CNN extracts key features from the training data. It grasps contextual local features from a sentence and after several convolutional operations, it forms a global feature vector out of the local features. Features extracted by CNN can be used as they carry more useful information. The architecture of proposed CNN model for text classification consists of word embedding as the input layer, 1-Dimension convolutional layer, 1-Dimension pooling layer, and output layer. The system accesses the CNN model through the API.

```
@app.route('/api/v1/sentiment', methods=['GET'])
```

## 4 System Requirement

### 4.1 Functional System Requirement

1. The system shall allow the user and the administrator to login to the system via Twitter.
2. The system shall be able to display the user's followers and following profiles.
3. The system shall be able to display the user, his or her followers, and his or her following tweets.
4. The system shall be able to visualize the analyzed data in chart and table manner.
5. The sentiment module shall be able to receive Twitter data from the Twitter API
6. The sentiment module shall be able to calculate tweets sentiment score
7. The system shall allow the administrator to view users that have registered to the system
8. The system shall allow the administrator to delete registered user from the system

### 4.2 Non-functional System Requirement

#### Interoperability

1. The system is able to connect to Twitter database via the Twitter API
2. The system is able to communicate to three Python Application via REST API

## 5 System Development

Tweep is the system that is being developed in the present study. The system uses rule-based Vader Sentiment Analysis and two Machine Learning techniques namely Naive Bayes and Convolutional Neural Network. The output of the system is the percentage of the positive and negative posts of the Twitter users and of their followings. Figure 1 below shows the Use Case Diagram for the system. As the users log in to the system, they are able to analyze their tweet sentiment. It also enables them to analyze their followers' or followings' tweets sentiment.

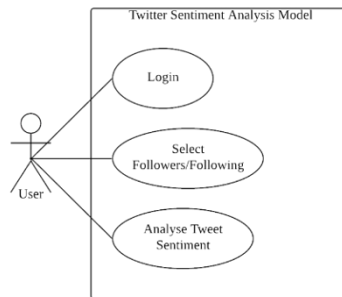


**Fig. 1.** Use Case Diagram of the System

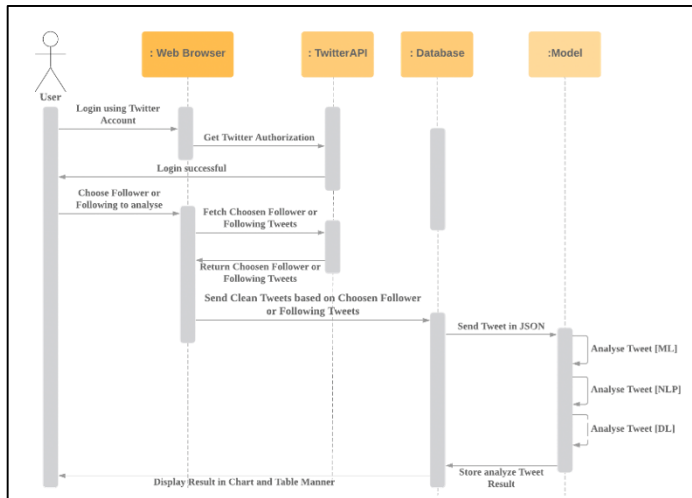


**Fig. 2.** Sequence Diagram of the System

The system starts by asking the end-user to log in to the system using their Twitter account. This process is needed for verification and redirection to Twitter API and database control. As shown in Figure 3, as the user clicks on the 'Sign in with Twitter' button, they are redirected to the system using Twitter API.

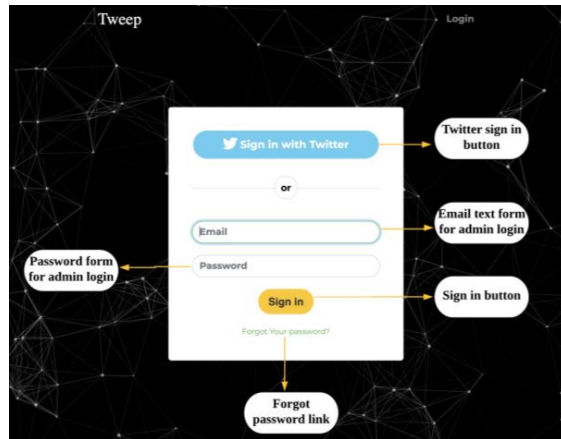


**Fig. 3.** Login page on the system and redirect to the Twitter Account Login

After a successful login, the system redirects the user to the main page of the system as shown in Figure 4. The system displays the user's Twitter information and user's followers and following lists.

No	Twitter Name	Description	Followers	Following	Tweets
1	mellowparenikin	goin back to my old acc @AidelGerrardo	56	80	16
	zanaashop	Pre Order: 11 Jun - 18 Jun // Batik & Lace straight from jakarta! 🌟	139	294	104
	ainadif	21. A servant of Allah.	76	191	5560
	dahlaacinta1	15	114	97	829
	dahlaacinta		396	121	772
6	HanaRicq0	Fighting!! Always trust Allah!*	4	141	22

**Fig. 4.** The main page of the system

As the user clicks on the 'Analyze your Tweets' button, the system is redirected to the Tweets Sentiment page as shown in Figure 5. The system displays the user tweets in graph based on their positive and negative tweets. When the user chooses one of their followers, the system will display the percentages of their followers' positive and negative tweets as depicted in Figure 6.

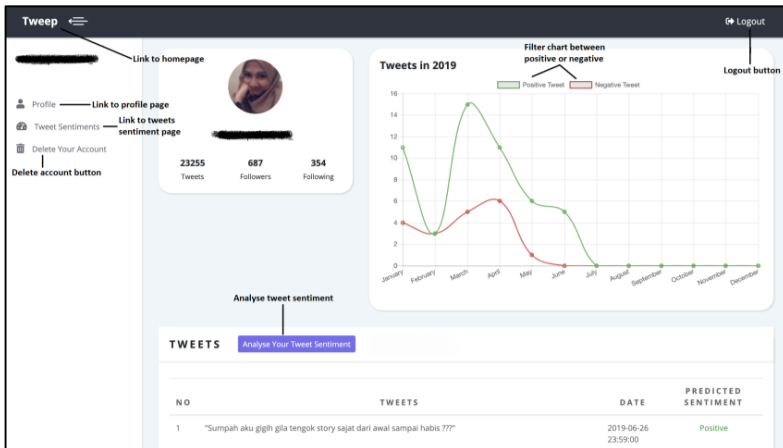


Fig. 5. User Tweets Sentiment page

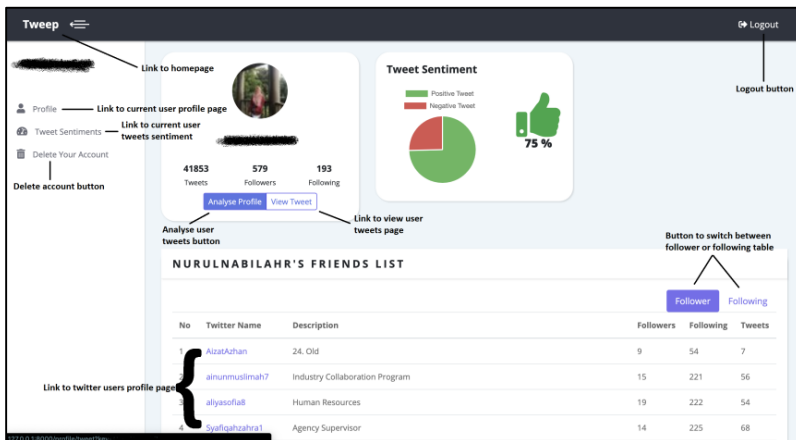
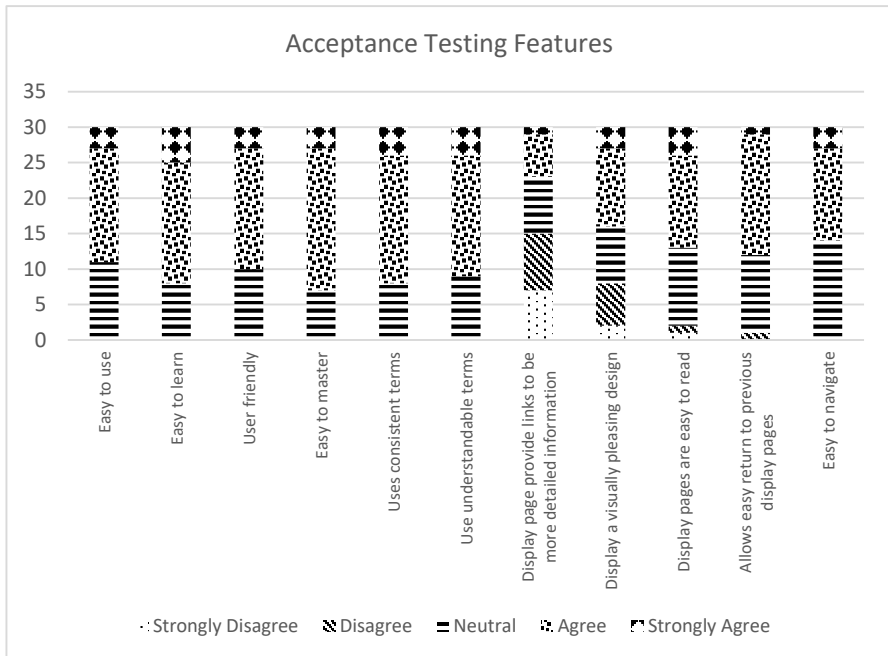


Fig. 6. Follower's Tweet Sentiment

Then, the system sends the tweets in JSON to be analyzed and stores the results in the database. The tweets are analyzed in all three models. The system returns the predicted sentiments which are Positive, Negative or Neutral. When the system returns two Positive results and one Negative or Neutral result, the system takes the Positive predicted sentiment as the Overall Predicted Sentiment, same goes when there are two Negative results and two Neutral results.

## 6 Results

The system is evaluated based on Acceptance Testing that covers two main purposes, Features and Actions. Acceptance Testing based on Features evaluates the perceived ease of use, ease of understanding and ease of finding.



**Fig. 3.** Acceptance Testing Features

Figure 6 shows the results of the evaluation survey that has been conducted on 30 people. Perceived ease of use of the system is shown in Question 1 to Question 4. Question 5 to Question 9 focus on the ease of understanding of the system to the user. Meanwhile, Question 10 and Question 11 cover the ease of finding for the user that use the system. Most of the respondents feel neutral and agree that the system is user friendly. As for the ease of understanding, the system uses consistent and understandable terms that most respondents are familiar with. 15 respondents claim that the system does not provide links that feed more information and 8 respondents figure that the system does not have a pleasing design. On the other hand, 28 respondents feel neutral and agree that the system is easy to be maneuvered. In addition, the ease of finding states that most of the respondents are neutral and agree that the system is easy to be operated which also points to the fact that the system is able to return to previous page easily.

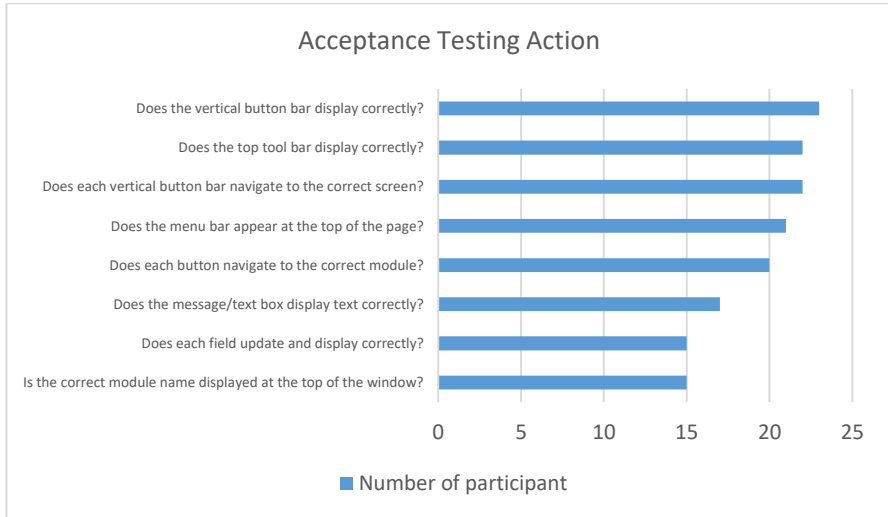


**Fig. 4.** Acceptance Testing Action

Figure 7 shows the results for the Acceptance Testing based on Actions. The respondents are asked to test the system; whether the system runs accordingly. More than 20 respondents agree that the vertical menu button bar runs correctly and navigates to the correct page. A total of 22 respondents find that the number of top tool bar is displayed correctly. Half of the respondents opine that a correct module name is displayed at the top of the window and that each field updates and displays correctly. In summary, most of the respondents are satisfied with the system, though few of them claim that it could use some improvements. The system ought to stress on the user friendliness feature which includes having a pleasing design and more alert functions that can assist the user in using Tweep.

## 7 Conclusion

This paper presents a system that enables to analyze depression status using Machine Learning based on personal Twitter posts. The purpose of this system, Tweep is to provide a user-friendly interface to analyze the user's depression status. With Tweep, Twitter users with high chance of depression can be identified at early stages. Technically, the system uses three different existing models to analyze the tweets from two different approaches namely Rule-based approach and Machine Learning approach. However, most of the models are limited to English language only. It proves that it is least effective with data in Malay language. For future research, the model should produce a more reasonable result on Malay language tweets or tweets that contain more than one language. Another factor that may affect the results are tweets that contain different number of punctuation marks, or words that contain all capital letters (e.g. SUKA), words with character flooding (e.g. sukaaaa), emojis and negation words. Next, more accurate

techniques, such as robust tokenization and stemming methods or any reliable methods can be applied to improve the quality of the input text. Finally, tweets that contain words that have a negative meaning but brings a positive vibe (e.g. savage, which can be translated as someone who is unpredictable) to a particular community should be taken in context as they do not necessarily convey negativity.

## Acknowledgement

This work is partly supported by Malaysian FRGS research grant; FP001-2017A.

## References

1. T. S. Portal Statistics and Studies, "Social Media Usage Worldwide," (2019): <https://www.statista.com/statistics/272014/global-social-networks-ranked-by-number-of-users/>
2. Munmun De Choudhury, Michael Gamon, Scott Counts, & Eric Horvitz, "Predicting Depression via Social Media," *ICWSM* (2013).
3. Sho Tsugawa, Yusuke Kikuchi, Fumio Kishino, Kosuke Nakajima, Yuichi Itoh, & Hiroyuki Ohsaki. "Recognizing Depression from Twitter Activity." In *Proceedings of the 33rd Annual ACM Conference on Human Factors in Computing Systems (CHI '15)*. ACM, New York, NY, USA (2015): 3187-3196.
4. Nicola J. Reavley, & Pamela D. Pilkington, "Use of Twitter to Monitor Attitudes towards Depression and Schizophrenia: An Exploratory Study," *PeerJ*, 2 (2014): doi:10.7717/peerj.647.
5. Andrew G. Reece, Andrew J. Reagan, Katharina L. M. Lix, Peter Sheridan Dodds, Christopher M. Danforth, & Ellen J. Langer, "Forecasting the Onset and Course of Mental Illness with Twitter Data," *Scientific Reports* (2016): doi:10.1038/s41598-017-12961-9.
6. Mowery D., Smith H., Cheney T., Stoddard G., Coppersmith G., Bryan C., & Conway M., "Understanding Depressive Symptoms and Psychosocial Stressors on Twitter: A Corpus-Based Study," *Journal of Medical Internet Research*, 19(2) (2017): doi:10.2196/jmir.6895
7. Glen Coopersmith, Mark Dredze, & Craig Harman, "Quantifying Mental Health Signals in Twitter," *Workshop on Computational Linguistics and Clinical Psychology. ACL* (2014): 51-60.
8. Glen Coppersmith, Mark Dredze, Craig Harman, & Kristy Hollingshead, "From ADHD to SAD: Analyzing the Language of Mental Health on Twitter through Self-Reported Diagnoses," In *Proceedings of the 2nd Workshop on Computational Linguistics and Clinical Psychology. NAACL* (2015): 1-11.
9. Julius Jacobson, "Detecting Language from Depressed Users with Korean Twitter Data," Seoul National University (2018).



# Measuring the Application of Anthropomorphic Gamification for Transitional Care; A Goal-Question-Metric Approach

Nooralisa Mohd Tuah<sup>1</sup> and Gary B. Wills<sup>2</sup>

<sup>1</sup>Universiti Malaysia Sabah, Jalan UMS, 88400, Kota Kinabalu, Sabah, Malaysia

<sup>2</sup>University of Southampton, Highfield Campus, Southampton, SO17 1BJ, United Kingdom  
aelise@ums.edu.my, gbw@ecs.soton.ac.uk

**Abstract.** The gamification of anthropomorphic interfaces is one of technology interventions in health. Applying them into transitional care may encourage a patient to learn about their condition, so that they are able to self-manage. This research is based on the researcher's previous developed framework to develop a rigorous scale that assesses the applicability of anthropomorphic interfaces gamification for transitional care in an application. By measuring, it may inform the software developer or designer of the design requirement for the application. We adopt a Goal-Question-Metric (GQM) approach to develop a new measurement instrument. The GQM offered a stepwise approach to refine a theoretical perspective of anthropomorphic gamification for transition care into measurable values. Thus, this research presents how the measurement items can be created using GQM. Later, these items will be grouped together as an instrument called Transitional Anthropomorphs Gamification Scale (TAGS). This instrument needs for further validation, ensuring they measured the right construct.

**Keywords:** Anthropomorphic Interfaces, Gamification, Transition Care, Goal-Question-Metric.

## 1 Introduction

Technology interventions such as gamification for healthcare become more challenging when structure, function, and design in a game become more complex and dynamics [1, 29, 31, 32]. A healthcare gamified application, particularly in a transitional care process requires an informed design that could help the designers or developers to understand the suitability of a game used for a transitional care process. The suitability includes the application of anthropomorphic interfaces in gamification for transitional healthcare.

A human-like representation in computer applications that is designed with the human qualities of something that is not a human is referred to as anthropomorphic interfaces [23]. Applying game elements into a non-gaming context like healthcare is known as gamification [8, 13]. Gamification also refers to as a process that offer a playful

environment that contains motivating features for the users to maintain their engagement [5, 29, 33]. Moving a patient from one care to other cares and, from one stage of condition to a better stage of condition are referred as a transitional care process in healthcare setting [11, 21, 35]. Providing a gamified application as a platform or a tool to support the transition process, will help the patients to learn about their condition and allow them to self-manage. With this in mind, a measurement tool is required to measure the extent of how anthropomorphic interfaces in gamification are applied within games and how transitional care is adapted within the games. By measuring this, it will inform the developer or designer of the design requirements for the of anthropomorphic interfaces in gamification for transitional healthcare. Also, by measuring it will help the potential user to understand the suitability of the game used in a transitional process.

Measurement is commonly practiced in the computer science field, such as software engineering, as a process to quantify a concept, so that it can be more visible, understandable, and controllable [15, 24]. Measuring also seen as a way to gain more insight and to increase understanding of real-world phenomenon [12, 15]. To this end, research on measuring game design and its effect have been explored extensively [6, 12, 34]. However, measuring a gamified application for transition care has yet to be developed. Thus, this paper would like to develop a metrics use to measure the application of anthropomorphic interfaces (A) in gamified application (G) for transitional healthcare (T), referred as Transitional-Care Anthropomorphs Gamification Scale (TAGS).

This research presents how the items of TAGS can be developed using a Goal-Question-Metric (GQM) approach. The GQM was introduced by Basili [4], is a systematic approach which can be adopted to a different setting and purpose [16]. It will support the definition and scope of a newly developed TAGS. Besides, GQM is tailored to achieve a specific requirement of a software product, process, or project [4]. Other than software, the GQM also offers a practical approach for any measurement problems [4]. As the TAGS instrument is yet to be developed, the GQM approach is adopted to create a new metric for the TAGS instrument. Therefore, we begin by discussing how an anthropomorphic interface of gamified application is measured. Follow by the gamification of transition care within games, and the adoption of a GQM approach to generate suitable metrics for TAGS.

## 2 Related Works

Gamification was introduced as one of a motivational solution in addressing motivational problem, whether in learning, healthcare, or business contexts [5, 28]. Implementing anthropomorphic interfaces within interactive applications such as game and gamified application, is expected to increase the motivation of the player [5]. Anthropomorphic interfaces in gamification offer player's identification and personalisation whereby this will directly involve the players and motivate their engagement. With this in mind, patients who are in a transitional care process, transfer from hospital care to self-manage, from one stage of condition to a better stage of condition, required an

additional tool to support them in learning and in maintaining to motivate their engagement throughout the process [11, 21]. The involvement of technology which are fun and playful, imparted learning through playing games seems could support and motivate the patients in health [28, 29] as well as in transitional care [35].

To this end, there is no game or web-based application available in the market that practically used to support the transitional process. As Sailer [28] argues that a gamified application should be well designed and should be derived from an established framework or models, this research work follows the similar approach.

This research sought to develop an instrument that able to assess the design of anthropomorphic gamification for transitional healthcare application. The instrument provides generalizability for the design of anthropomorphic interface application in a gamification of transitional care. Particularly, on facilitating the users to acquire knowledge of his/her health condition to self-management.

## **2.1 Measuring Anthropomorphic Interfaces Gamification for Transition care**

Measuring a game is deem necessary when a game is used to predict future directions of game design, or users playing patterns and behaviour, or the effects of playing a game [such as in 2, 7, 18, 34]. To measure the intended cause, an appropriate response could be taken accordingly. By measuring, subjective measures could be quantified and by obtaining quantitative evidence, any uncertainty could be reduced based on one or more observations [15]. Previous research in human and computer interaction could involve measuring usability [16], user engagement [26], and affective interfaces [14]. In gamification, the measures usually involved users' engagement [6, 33], motivation [5, 28], enjoyment [10, 12] and experiences [2, 18, 19]. Meanwhile, gamification in healthcare was research mainly focuses on sustaining patients' motivation and behaviour change [17, 28, 35]. Anthropomorphic interfaces in healthcare was research on motivation and users' behaviour [5, 17, 28], non-player character [20], and as a user's health representation [26, 31]. To this end, no significant research has been found that measure the design of anthropomorphic interfaces gamification for transitional care application.

This research work is a continuation of researcher's previous work on Anthropomorphic Interfaces Gamification for Transitional Care (TAG) in [22]. Following the framework, a comprehensive metric addressing the extent of how anthropomorphic interfaces gamification for transitional care is designed. The related elements and their relationship are scrutinized and summarised as the basis to develop the measures. This metric will able to inform the software developer or designer of the design requirements for TAG and thus, will help them to understand the suitability of the game used for transitional process. We first discussed the application of anthropomorphic interfaces gamification in transitional care.

## **2.2 Anthropomorphic Interfaces Gamification in transitional care**

Anthropomorphic interfaces in computer applications were applied in different degree of human-like representation. In the previous conducted research, the implementation

of anthropomorphic interface could be perceived as an avatar or an interface agent in different degrees of anthropomorphic designs. A spectrum of anthropomorphic interfaces was developed in [23] and there were five different degrees of anthropomorphic interfaces generally applied in an application. These anthropomorphic interfaces have to be designed with human characteristics that practically presence and able to respond. Their application in a game varies depending on the purpose of the game. The purpose could be as a player's representation, game strategies, or non-player character. Gamifying them required a strategy on how to design and apply the game mechanics in a gamified application.

Meanwhile, in general, a transitional care is a process of transfer of one's health condition into a better stage. It also refers transferring a patient who lives with a long-term condition (e.g. diabetes, kidney transplant, asthma) from hospital care into self-care [11, 21, 35]. It is a period of process of a patient improving their health condition by adapting it well into their life. So that they can leave the hospital care and try to self-care. Transitional care is one of the healthcare issues that requires specific attention specifically in managing patient engagements during the process of transfer [35]. Wilson [35] suggests that with gamification, it can help to encourage a positive behaviour, such as following instructions and medication adherence, among the young children patients in a transitional care process. Wilson's model adapted the current process of transitional care in England. By modelling how gamification can be implemented in the process, each completed task will be given a point, a successful level will be awarded with a bonus point and a badge, different level with a different point score, and patients who is doing well progression will be given a trophy. Basically, Wilson's gamification model was designed specifically following the checklists for transition care process rather than a gamified application that help the patient to learn and adapt their condition through the transfer process. Current research, such as Klaassen et. al [20], Hwang et. al [17], and Schmeil et. al [30], they worked only related to one specific condition such as diabetes, that help the patient to monitor their condition and learn at the same time.

As gamification for transitional care is still in its infancy stage, various applications of gamification for transitional care should be designed thoroughly. Following TAG framework in [22], anthropomorphic interfaces gamification is suggested for its application in transitional care. In TAG, the framework was intended to provide a fundamental element for creating a gamified application that uses anthropomorphic interfaces as patient's self-representation, to motivate the patient in learning and adapt to their condition. So that they can be able to self-manage. Also, in TAG, motivational elements play a significant role to indicate the effect of anthropomorphic interfaces gamification to support the patient to learn about their condition. Most importantly, the elements will expose how the patients could give their attention to the learning material, relate the game content to previous experience and personal interest, confidence in making choices, and value after completing something in the game.

The above discussion of anthropomorphic interfaces gamification for transitional care summarised the TAG framework. Following TAG, we describe each element for inclusion in the metrics development for the instrument.

### 3 Metrics Development

In previous established measurement instrument in game research, the methods to develop an instrument are varied. An instrument to measure user's engagement in gameplay by Brockmyer et. al [6] and an instrument to measure the relationship between a player and their avatar by Banks [2], were created based on their developed conceptual framework. Meanwhile, an instrument to measure play experience in a game by O'Brien [25] and an instrument that measures a gameful experience in gamification by Eppmann et. al [9], were created based on the examination and analysis of concept in gaming literature. One assessment model called MEEGA [27] was developed using a goal-question-metric (GQM) approach to evaluate educational games that is used for teaching a software engineering class. GQM was used to systematically analyze a question derive from literature, so that the goals can be achieved. Meanwhile, in usability research, study by Hussain et. al [16] employed GQM to develop a usability metric for measuring usability of mobile applications. From these studies, it is plausible to summarise that developing an instrument is deriving from a theoretical construct such as literature, model, or framework. Except that, the GQM method has a structured way of measuring intended constructs. Thus, employing both methods will help to build the instrument systematically.

Other than the GQM, Basili [4] also compared it with another method used for measuring software quality which are software quality measurement (SQM) and quality function deployment (QFD). Both the SQM and QFD were considered not suitable in this research as it is not tailorable to be used for other purposes, other than for quality measurement. Besides, they focus more on measuring the final product rather than the process to achieve the final product. Meanwhile, Kassou [36] compared GQM with Goal-Argument-Metric (GAM) and Balanced-Scorecard Framework (BSc) in order to develop a security metric. Following his comparison, we believed GAM and BSc shared the same approach which is goal-oriented methodology. However, each approach has a different way of defining the goal and ways to achieve it. In this view, we believed the GQM approach provide a clear guideline and steps in developing the instrument for this research. To practically applied the GQM method, the following Figure 1 will show the process of developing the metrics. Following the GQM method, metrics for TAG will be developed. These metrics will be group together and identified as the Transitional-Care Anthropomorphs Gamification Scale (TAGS).

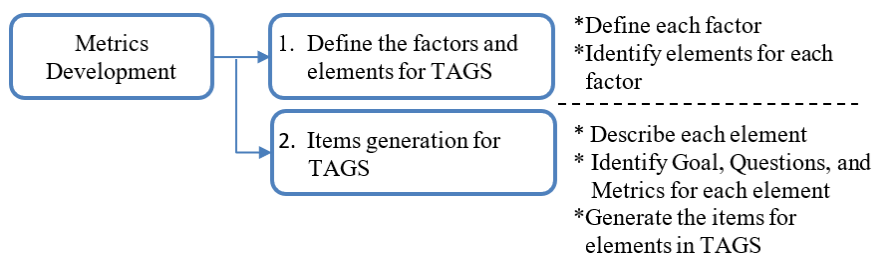


**Fig. 1.** Metrics Development Process

### 3.1 Measurement Elements

In TAG framework, four factors were identified and within these factors, there are fifteen (15) elements derived from it. The elements are grouped within their respected factor, as in the framework. Each of the element must be defined first as to state the scope and describe its purposes in order to develop the instrument. All elements are selected for inclusion in the new measurement instrument and their description are summarized in table 1.

**Table 1.** TAGS Elements Description

Factors	Elements	Descriptions
<b>Anthropomorphic Interfaces</b>	Anthropomorphic Interface Design	User's representation in an application
	Design Purpose	The purpose of applying an anthropomorphic character in an application. It could be either as personalization or as part of a strategy in an application
	Social Response	An anthropomorphic interface should be able to offer responses in an application
	Social Presence	An anthropomorphic interface that exhibit the presence of a user in an application
	Accessibility	the anthropomorphic interface accessibility options in an application
<b>Gamification</b>	Reward System	the applicability of reward systems in a gamified application, particularly, how the anthropomorphic interfaces are part of it. The reward system includes points, badges, and trophies.
	Leaderboard	The user's information and their achievement in a board, that includes how anthropomorphic interfaces may represent users in the Leaderboard
	Levels	the applicability of levels in gamified applications and how the anthropomorphic interfaces are implemented at levels.
<b>Motivation</b>	Attention	the ways in which the user's attention can be grabbed, so that he/she gets absorbed into the gamified applications. the elements of excitement, support, and surprise

	Relevance	the ways in which the content of a gamified application relates to a user's interests. the elements of relatedness to previous experience and personal interest
	Confidence	what the users expect to experience in the application, in order for the users to become confident in completing the given task. the elements of opportunity, expectation, learning outcome, and confidence in choice making
	Satisfaction	The feel of satisfied when accomplished certain task. the elements of outcomes, experiences, feedback, and value after achieving something.
<b>Transition Care</b>	Stage of transition	the stages of the transition are applied in the application.
	Health Condition	which of the health condition is being addressed in a gamified application
	Self-Management	the application supports user's self-management for a change in their behavior

To this end, there is no specific instrument that measure the application of anthropomorphic interfaces gamification for transitional care. Developed instruments in previous research that might be related to the TAG, were in isolation. For example, earlier research by Bartneck et. al [3] developed instrument that related to the design of anthropomorphism for human-robot interaction and quite recent research by Banks [2] measures player-avatar interaction in a player-avatar relationship, are not suitable for measuring the application of anthropomorphic interfaces for TAG.

As of gamification, one latest developed instrument is GAMEX [9], where it measures the gameful experiences when users engage with the gamified application. Another research in games such as Fu et. al [12], Wiebe et. al [33], and Fang et. al [10], respectively measure the level of users' enjoyment of e-learning games, user's engagement in playing games, and flow experiences in a gameplay. In our research, gamification elements should measure on how game elements should be designed and how anthropomorphic interfaces are part of the gamification. As we reviewed, the developed instrument for gamification were not suitable for TAG.

Meanwhile, in a transitional care research, there is one specific tool that measures patient's clinical/hospital readiness moving from one care to another, known as TRAQ [30]. Even though it is comprehensive in term of ensuring that the patient has mastered their condition and able to take care of themselves, it is not relevant to measure anthropomorphic interfaces gamification for TAG.

### 3.2 The GQM method

A GQM, introduced by Basili et. al [4] is a systematic approach which can be used to define a measurement framework or to solve any measurement problem [16, 27]. This includes measuring any processes, products (software/system/tools), or resources in a project. Since, there is no instrument yet to measure anthropomorphic interfaces gamification for transitional care, a systematic approach like GQM could be adopted to create a new measurement metric. To adopt the GQM, it is worth to review how it works. There are three levels in generating a metric in GQM. They are; 1) conceptual level (goal), 2) operational level (question), and 3) quantitative level (metrics). The GQM using a top-down procedure. First, a specific goal for a product, process, or a viewpoint has to be identified in the conceptual level. Then, in the operational level, a set of question is developed to describe how to assess and achieve the identified goal. Lastly, in the quantitative level, a metric is developed to answer the respective questions associated with the goal. Figure 2 illustrates the structure of GQM.

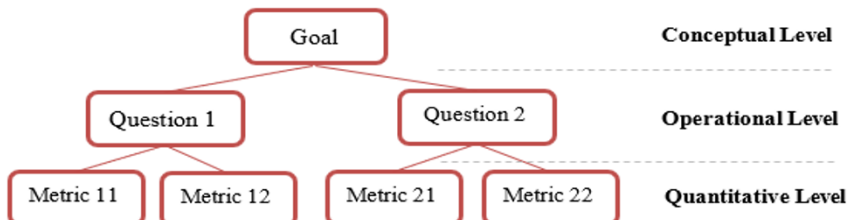


**Fig. 2.** GQM's Structure

### 3.3 Items Generation

Previous studies by Savi [38] and Rais [37] implemented GQM to formulate their questionnaire. By following the same concept, metrics for TAGS are developed. In TAGS, the metrics are the items in the instrument as it can quantify the participants' opinions or their relation to the condition being measured. Thus, for inclusion in TAGS, the elements described in Table 1 is the viewpoint which measure is taken. Thus, we defined the goal for each element. Followed by developing related questions and then, the metrics. These metrics become the measurement items for TAGS. In Table 2, we present one example of the TAG's element, showing the generated metrics for the design purpose of an anthropomorphic interface. The element of design purpose is related to the application of anthropomorphic interfaces in an application. In TAG, the purpose of anthropomorphic interfaces could be a personalisation tool or as a game strategy. Thus, the goal is set as to understand the purposes of using or applying anthropomorphic interfaces in an application. Two questions could be asked, 1) why they are applied and 2) how they are used. Based on that, metrics to measure these questions is generated.

**Table 2.** GQM Approach for Design Purpose Element

<b>Element</b>	<b>Design Purpose</b>
<b>Goal</b>	To understand the purposes of using or applying anthropomorphic interfaces in an application.
<b>Questions</b>	<b>Metrics</b>
Q1. How anthropomorphic character is applied? (Ease of character customization)	1. I can easily customize my own character 2. I can easily customize my character's environment (for example; house, car, office, garden, etc.) 3. I normally use my character as a tactic to confuse other characters or opponents 4. I normally do not choose a character as a strategy to win
Q2. How are the anthropomorphic interfaces used in an application? (As a strategy to win)	5. I am allowed to upgrade my character to be more powerful or meaningful as the application progresses

The same concept presented for DEP was applied to generate all metrics for TAGS. A 5-point Likert scale is used to gather participants' responses of the TAGS instrument, ranging from 1- strongly disagree to 5- strongly agree. We believed, 5-point Likert scale could provide just enough choice, straightforward, and manageable for the participant to use it. In this context of study, the participant will be a software or game developer, or a designer. They are the suitable person who can give responses in informing the application of anthropomorphic interfaces gamification in transitional care.

## 4 Conclusion

In this research, we present the development of measurement instrument for anthropomorphic interfaces gamification for transitional care application. The instrument adopting a Goal-Question-Metric (GQM) approach. We defined the transitional anthropomorphs gamification elements for inclusion in transitional anthropomorphs gamification scale (TAGS), using the TAG framework as a reference. GQM was adopted as a solution to systematically derive a suitable instrument for TAGS. Whereby using GQM, goal for each element was set, questions were developed to achieve the set goal, and metrics were generated to answer the questions. The developed metrics for TAGS can be applied to assess the extent of anthropomorphic interfaces applicability in gamified application for transitional care. TAGS can be useful for software developers and designers to; i) inform the design requirements for TAG, ii) assess the suitability of the game/applications that can be used for transitional process, iii) apply where appropriate to improve user's motivation in self-care/management. This instrument required validation to assure that the items measured the right content. We will report the result of our validation study in due time. Nevertheless, this research has contributed to the way an instrument can be developed using the GQM approach in HCI, gamification, and healthcare research.

## References

1. Alahäivälä, T., & Oinas-Kukkonen, H. (2016). Understanding persuasion contexts in health gamification: A systematic analysis of gamified health behavior change support systems literature. *International Journal of Medical Informatics*, 96, 62–70.
2. Banks, J., & Bowman, N. D. (2016). Emotion, anthropomorphism, realism, control: Validation of a merged metric for player–avatar interaction (PAX). *Computers in Human Behavior*, 54, 215–223.
3. Bartneck, C., Kulić, D., Croft, E., & Zoghbi, S. (2009). Measurement Instruments for the Anthropomorphism, Animacy, Likeability, Perceived Intelligence, and Perceived Safety of Robots. *International Journal of Social Robotics*, 1(1), 71–81. <http://doi.org/10.1007/s12369-008-0001-3>
4. Basili, V., Caldiera, G., & Rombach, H. (1994). Goal Question Metric Approach. *Encyclopedia of Software Engineering*, 1, 98–102.
5. Birk, M. V., Atkins, C., Bowey, J. T., & Mandryk, R. L. (2016). Fostering Intrinsic Motivation through Avatar Identification in Digital Games. *Proceedings of the 2016 CHI Conference on Human Factors in Computing Systems - CHI '16*, 2982–2995.
6. Brockmyer, J. H., Fox, C. M., Curtiss, K. A., McBroom, E., Burkhart, K. M., & Pidruzny, J. N. (2009). The development of the Game Engagement Questionnaire: A measure of engagement in video game-playing. *Journal of Experimental Social Psychology*, 45(4), 624–634.
7. Dahl, G., & Kraus, M. (2015). Measuring how game feel is influenced by the player avatar's acceleration and deceleration. In *Proceedings of the 19th International Academic Mindtrek Conference on AcademicMindTrek '15* (pp. 41–46). <http://doi.org/10.1145/2818187.2818275>
8. Deterding, S., Dixon, D., Khaled, R., & Nacke, L. (2011). From game design elements to gamefulness: defining gamification. In *Proceedings of the 15th International Academic MindTrek Conference: Envisioning Future Media Environments* (pp. 9–15). Tampere, Finland: ACM. <http://doi.org/10.1145/2181037.2181040>
9. Eppmann, R., Bekk, M., & Klein, K. (2018). Gameful Experience in Gamification: Construction and Validation of a Gameful Experience Scale [GAMEX]. *Journal of Interactive Marketing*, 43(2018), 98–115. <http://doi.org/10.1016/j.intmar.2018.03.002>
10. Fang, X., Zhang, J., & Chan, S. S. (2013). Development of an Instrument for Studying Flow in Computer Game Play. *International Journal of Human-Computer Interaction*, 29(7), 456–470. <http://doi.org/10.1080/10447318.2012.715991>
11. Field, S. (2014). From the pond into the sea. Children's transition to adult health services. *Care Quality Commission*, (June), 1–12.
12. Fu, F. L., Su, R. C., & Yu, S. C. (2009). EGameFlow: A scale to measure learners' enjoyment of e-learning games. *Computers and Education*, 52(1), 101–112. <http://doi.org/10.1016/j.compedu.2008.07.004>
13. Hamari, J., Koivisto, J., & Sarsa, H. (2014). Does Gamification Work? A Literature Review of Empirical Studies on Gamification. In *Proceedings of 47th Hawaii International Conference on System Sciences (HICSS)* (pp. 3025–3034). Waikoloa, HI: IEEE. <http://doi.org/10.1109/HICSS.2014.377>
14. Hsu, Y. (2012). Affective Interfaces of Embodied Conversational Agents. *International Journal of Affective Engineering*, 12(2), 71–78.
15. Hubbard, D. W. (2014). *How to Measure Anything: Finding the Value of Intangibles in Business* (2nd Editio). Hoboken, New Jersey: John Wiley & Sons.

16. Hussain, A., & Ferneley, E. (2008). Usability metric for mobile application: a goal question metric (GQM) approach. *Proceedings of the 10th International Conference on Information Integration and Web-Based Applications and Services (iiWAS '08)*, 567–570. <http://doi.org/http://doi.acm.org/10.1145/1497308.1497412>
17. Hwang, M., & Mamykina, L. (2017). Monster Appetite : Effects of Subversive Framing on Nutritional Choices in a Digital Game Environment. In *CHI '17: Proceedings of the 2017 CHI Conference on Human Factors in Computing Systems* (pp. 4082–4096). Denver, CO, USA: ACM. <http://doi.org/10.1145/3025453.3026052>
18. Kao, D., & Harrell, D. F. (2015). Exploring the impact of role model avatars on game experience in educational games. *Proceedings of the 2015 Annual Symposium on Computer-Human Interaction in Play*, 571–576. <http://doi.org/10.1145/2793107.2810291>
19. Karadimitriou, K., & Roussou, M. (2011). Studying Player Experience in a Collaborative Embodied Interaction Game. In *2011 Third International Conference on Games and Virtual Worlds for Serious Applications* (pp. 199–206). Athens: IEEE. <http://doi.org/10.1109/GAMES.2011.51>
20. Klaassen, R., Bul, K. C. M., Op Den Akker, R., Van Der Burg, G. J., Kato, P. M., & Di Bitonto, P. (2018). Design and evaluation of a pervasive coaching and gamification platform for young diabetes patients. *Sensors (Switzerland)*. <http://doi.org/10.3390/s18020402>
21. Marape, M. (2013, December). Adolescent Transition Care. *Royal College of Nursing*, 1–25.
22. Mohd Tuah, N., Willis, G. B., & Ranchhod, A. (2018). The Application of Anthropomorphic Gamification within Transitional Healthcare: A conceptual framework. *EAI Endorsed Transactions on Game-Based Learning*, 4(14), e2. <http://doi.org/10.4108/eai.4-1-2018.153530>
23. Mohd Tuah, N., Wills, G., & Ranchhod, A. (2016). The Characteristics and Application of Anthropomorphic Interface: A Design Spectrum. In IT (Ed.), *ACHI 2016: The Ninth International Conference on Advances in Computer-Human Interactions* (pp. 398–402). Venice, 24-28 Apr 2016, 24-28 Apr 2016: ThinkMinds.
24. Norman, E. F., & Shari, L. P. (1997). *Software Metrics; A Rigorous & Practical Approach*. Boston, USA: ITP.
25. O'Brien, H. L., & Toms, E. G. (2010). The Development and Evaluation of a Survey to Measure User Engagement. *Journal of The American Society for Information Science and Technology*, 61(1), 50–69. <http://doi.org/10.1002/asi>
26. Orji, R., Tondello, G. F., & Nacke, L. E. (2018). Personalizing Persuasive Strategies in Gameful Systems to Gamification User Types. In *Proceedings of the 2018 CHI Conference on Human Factors in Computing Systems - CHI '18* (pp. 1–14). <http://doi.org/10.1145/3173574.3174009>
27. Petri, G., Gresse von Wangenheim, C., & Borgatto, A. F. (2018). MEEGA+, Systematic Model to Evaluate Educational Games. In *Encyclopedia of Computer Graphics and Games*. [http://doi.org/10.1007/978-3-319-08234-9\\_214-1](http://doi.org/10.1007/978-3-319-08234-9_214-1)
28. Sailer, M., Hense, J. U., Mayr, S. K., & Mandl, H. (2017). How gamification motivates: An experimental study of the effects of specific game design elements on psychological need satisfaction. *Computers in Human Behavior*, 69, 371–380. <http://doi.org/10.1016/j.chb.2016.12.033>
29. Sardi, L., Idri, A., & Fernández-Alemán, J. L. (2017). A systematic review of gamification in e-Health. *Journal of Biomedical Informatics*, 71, 31–48. <http://doi.org/10.1016/j.jbi.2017.05.011>
30. Sawicki, G. S., Lukens-Bull, K., Yin, X., Demars, N., Huang, I. C., Livingood, W., & Wood, D. (2011). Measuring the transition readiness of youth with special healthcare needs:

- Validation of the TRAQ - Transition readiness assessment questionnaire. *Journal of Pediatric Psychology*, 36(2), 160–171. <http://doi.org/10.1093/jpepsy/jsp128>
31. Schmeil, A., & Suggs, S. (2014). “ How am I Doing?” - Personifying Health through Animated Characters. Design, User Experience, and Usability. User Experience Design for Everyday Life Applications and Services, The Series of Lecture Notes in Computer Science. DUXU2014., 8519, 91–102. [http://doi.org/10.1007/978-3-319-07635-5\\_10](http://doi.org/10.1007/978-3-319-07635-5_10)
  32. Theng, Y.-L., Lee, J. W. Y., Patinadan, P. V., & Foo, S. S. B. (2015). The Use of Videogames, Gamification, and Virtual Environments in the Self-Management of Diabetes: A Systematic Review of Evidence. *Games for Health Journal*. <http://doi.org/10.1089/g4h.2014.0114>
  33. Werbach, K. (2014). (Re)defining gamification: A process approach. Lecture Notes in Computer Science (Including Subseries Lecture Notes in Artificial Intelligence and Lecture Notes in Bioinformatics), 8462 LNCS, 266–272. [http://doi.org/10.1007/978-3-319-07127-5\\_23](http://doi.org/10.1007/978-3-319-07127-5_23)
  34. Wiebe, E. N., Lamb, A., Hardy, M., & Sharek, D. (2014). Measuring engagement in video game-based environments: Investigation of the User Engagement Scale. *Computers in Human Behavior*, 32, 123–132. <http://doi.org/10.1016/j.chb.2013.12.001>
  35. Wilson, A. S., & McDonagh, J. E. (2014). A Gamification Model to Encourage Positive Healthcare Behaviours in Young People with Long Term Conditions. *EAI Endorsed Transactions on Game-Based Learning*, 1(2). <http://doi.org/10.4108/sg.1.2.e>
  36. Kassou, M., & Kjiri, L. (2013). A Goal Question Metric Approach for Evaluating Security in a Service Oriented Architecture Context. Retrieved from <http://arxiv.org/abs/1304.0589>
  37. Rais, A. E., Sulaiman, S., & Syed-Mohamad, S. M. (2011). Game-based approach and its feasibility to support the learning of object-oriented concepts and programming. *2011 5th Malaysian Conference in Software Engineering, MySEC 2011*, 307–312. <http://doi.org/10.1109/MySEC.2011.6140689>
  38. Savi, R., Wangenheim, C. G. Von, & Borgatto, A. F. (2011). A model for the evaluation of educational games for teaching software engineering. *Proceedings - 25th Brazilian Symposium on Software Engineering, SBES 2011*, (September), 194–203. <http://doi.org/10.1109/SBES.2011.27>



# An Integration of Image Processing Solutions for Social Media Listening

Dr. Christine Diane L. Ramos, Ivana Koon Yee U. Lim, Yuta C. Inoue, John Andrew Santiago and Nigel Marcus Tan

De La Salle University, Taft Manila, Philippines  
christine.diane.ramos@dlsu.edu.ph, ivana\_lim@dlsu.edu.ph,  
yuta\_inoue@dlsu.edu.ph, john\_andrew\_santiago@dlsu.edu.ph,  
nigel\_tan@dlsu.edu.ph

**Abstract.** Social media has become the core platform in the modern digital marketing of today, thus it is crucial for business organizations to strategically utilize such channels for decision-making and customer relationship management. Given that there is a disparity of contextualizing marketing insights obtained from social media listening using text data solely, this study explores the use of images in order to capture the image context to gain a better understanding of marketing insights. By integrating different existing image processing tools and services (Google Cloud Vision and Microsoft Cognitive Services) and aggregating the image analysis data, relevant contextual insights can be captured through data visualization reports of the system. Social media listening proponents such as marketing researchers, brand advocates, product managers, and other individuals involved in the marketing business functions may find this study to be significant as the current social media listening tools are mostly text-based and image analysis is still a relatively young field in social media analytics.

**Keywords:** Social Media Listening; Social Listening, Social Media Images, Image Processing, Google Cloud Vision, Microsoft Cognitive Services, Instagram

## 1 Introduction

The rise of social media channels has been rampant since the past decade with the rise of new websites such as Facebook, YouTube, Twitter, Instagram, and many more. While these innovations may have changed the way computers handle large volumes of data, they may have changed how individuals live as social media streams have now been incorporated into everyday use and activities. As of 2013, there are more than 16 billion photos posted on Instagram since its launch in October 2010 which attracted more than 150 million active users, and Instagram has an average of 95 million photos and videos being shared by users daily [4]. In the 2016 press release of Instagram (2016), there are almost a million new posts per day by Instagram users, and according to Chaffey (2016), the rate of new users entering into Instagram has surpassed the counterpart social networking sites Twitter, YouTube, LinkedIn, and even Facebook. In

order for companies to keep track of all the things happening in social media, with regards to the products and brands they promote, social media listening—the method of identifying and assessing what is being said about a company, individual, product or brand on the Internet—connects firms to all available market information, and using social media listening, data in the context of the perceptions of customers with regards to a brand can be acquired which “greatly improve customer service, and create a strong online community” [4].

Over the past decade, Instagram has substantially grown prevalent amongst individuals, as it is the most popular photo and video sharing app for people to share their everyday moments, after all a myriad of data points is the worth of an image [4]. Moreover, Ha [3] explains that a hashtag can be defined as a word or phrase preceded by a hash or pound sign (#) and used to identify messages on a specific topic. Because of this structure and functionalities, businesses have explored using user-generated content in understanding their market, and in identifying user groups that they should focus on, as well as formulating different strategies in launching online marketing campaigns. However, there are still scarcely any studies that explore the content of images that are posted in the feeds of Instagram public accounts especially with relation to social media listening; there is scant attention from the academic literature and the research community when it comes to the domain of image-based social media listening on top of the text. Obtaining knowledge of what is being said of a company, product or brand by users and other stakeholders in terms of the images posted can shed some light into how other Instagram users perceive a particular organization and much more context can be revealed for actionable insights with the use of images; nevertheless, there is little research focused on this particular field of study in the present day. As such, this study explores the use of images in order to capture the image context to gain a better understanding of relevant contextual marketing insights by integrating different existing image processing tools and services, and through data visualization reports of the system. Individuals in the digital marketing field will find this study highly beneficial as the current social media listening tools are mostly text-based and image analysis is still a relatively young field in social media analytics.

## 2 Related Literature

According to Lee [6], social media analytics refers to “the practice of gathering data from social media platforms and analyzing the data to help decision-makers address specific problems.” Various individuals such as social scientists, business managers, and medical professionals from different industrial sectors make use of social media analytics as social media in itself is wide-range by nature. Compared to traditional media analysis wherein data collection is oftentimes manual and the analysis is labor-intensive, automating social media analytics is more cost-effective in analyzing social media data to gain insights with the sentiments of customers to further improve customer relationships. Additionally, social media analytics is being employed by many Fortune 500 including McDonald’s, Pepsi, and Marriott in order to gain a competitive advantage [6].

Social media platforms involve an abundance of user-generated content, having a wide range of data types and data volumes, and hence, a great deal of attention from researchers are attracted to social media sites with relation to analyzing market performance. Furthermore, Lee presents that social media analytics in itself consists of multiple technologies and methods, namely: sentiment analysis, social network analysis, statistical methods, image analysis, and video analysis, to which the first three are mostly being utilized; image and video analysis is still a relatively young field of technological development. Lee also provides a framework for managing the processes of social media analytics, stage 1 being developing key social media metrics such as brand awareness, increasing website visits, enhancing corporate reputation, etc. Stage 2 encompasses the social media platforms that are chosen for monitoring and listening. Moreover, stage 3 is performing social media analytics followed by the last stage which is building social media intelligence [6].

## 2.1 Social Media Listening

Chumwatana & Chuaychoo [2] defines social media listening as the “process of monitoring the websites on the internet or social media channels to see what’s being said about the brand, business and other topics related to products.” Chumwatana and Chuaychoo proposed a technique for social media listening (Fig. 1) which encompasses the following stages: data collection, data cleaning, data storing (in databases), querying the data, and data reporting through data visualizations.

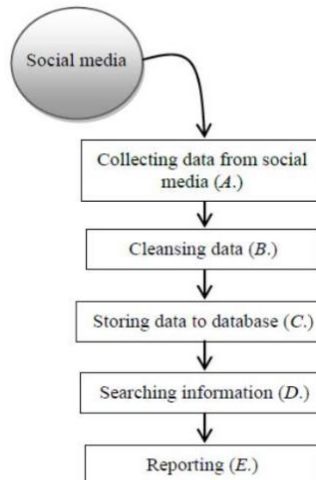


**Fig. 1.** Social Media Listening Process [2].

Actionable insights from social media listening are usually the end goal, and it is what differentiates listening from social media monitoring as the latter mainly focuses on compiling data rather than “looking forward to determining future actions” [8].

Additionally, social media listening is more specifically explained by Sprout Social as “the process of tracking conversations around specific topics, keywords, phrases, brands or industries, and leveraging insights to discover opportunities or create content for those audiences.” According to Jackson [5], social media listening differs from social media monitoring in that it extracts key insights that contribute to the overall strategy of a business, and it requires analysis and integration of data; listening is more of “seeing the forest through the trees (monitoring).”

## 2.2 Microsoft Cognitive Services (Vision)

Microsoft's Cloud Cognitive Services in Azure offer their very own Computer Vision API. Similar to some of Google's feature set, one of its features is image content analysis. It provides tags and descriptions for each entity found, as well as identify color schemes and adult content. Another feature is text extraction through Optical Character Recognition (OCR). It can extract text from human penmanship or digital text. Additionally, there are features such as personality recognition (celebrities), and landmark recognition. Apart from sending an image resource file, it can also accept a video file and make its own analysis. The way it works is that it will extract individual frames from the video and treat them as individual images. Lastly, it offers a thumbnail generation that outputs space efficient image files with varying sizes and styles based on the user's requirements [7].



**Fig. 2.** Microsoft Face API

Apart from the Computer Vision API, Microsoft's Vision Cognitive Services also offer Face API. It can detect faces and identify several elements from such like facial attributes (hair, baldness, hair colors), smile level, head pose, gender, age, facial hair attributes (moustache, beard, sideburns), glasses (returns No Glasses/Glasses), makeup (eye makeup and lip makeup), emotion (anger, contempt, disgust, fear, happiness, neutral, sadness, and surprise), and other photographic properties (occlusion, blurriness

level, exposure levels, and noise levels). From the JSON response, it returns the said elements with a confidence level for each. One example of the elements returned are emotions like anger, annoyance, fear, happiness, neutral, sadness, and surprise. Another example is the face attributes of the face detected such as the smile level, hairstyle, hair color, glasses, makeup, and accessories. It can also detect photographic elements such as blur levels, exposure levels, noise levels, and shadow occlusions on the objects [7].

### 2.3 Google Cloud Platform (Cloud Vision API)

Google Vision API is a cloud service that was released on the 2nd of December 2015. According to Casalboni [1], the API utilizes a RESTful interface that is said to be simpler in terms of its processing algorithms thus, providing more accurate results. The author also mentioned in the article that the API provides 6 key features which are: label detection, text detection, face detection, landmark detection, logo detection, and safe search detection.

Label detection simply gives out tags or keywords that can be perceived from the image together with their corresponding confidence levels (percentage values) to the image uploaded. Text detection performs Optical Character Recognition (OCR) that extracts the text recognized by the tool from the image. Face detection is not the usual concept that just boxes out faces, it detects facial key points, emotional likelihood, and the other facial properties like roll, tilt, and pan of the face. Landmark detection basically gives out a result of what a known landmark has been detected from the image together with its confidence (percentage value). Logo detection is much like landmark detection, it gives out the detected logo/s from the image together with its confidence level. Lastly, safe search detection detects if an image contains any explicit, negative, or violent content from predefined categories by the tool which is: adult, spoof, medical, violence, and racy.

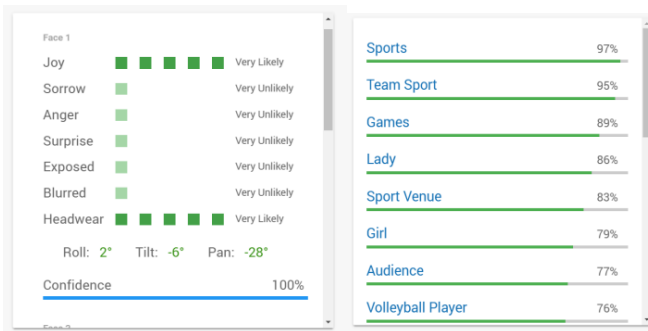


**Fig. 3.** Facial Recognition (left) and Label (right) Results

The feature set of both services are almost on par. However, the processing of Google's Cloud Vision API is all around better in terms of accuracy, quantity, processing time, and most especially relevance. Google's service captures more tags that are more relevant to the image, and that it also provides confidence levels per tag. Microsoft's

service only provides confidence results to some tags. The only thing Google's service falls short compared to Microsoft's is in terms of facial recognition and analysis.

**Table 1.** Comparative Table of Image Analysis Tools

Features	Microsoft Cognitive Services	Google Cloud Vision API
Text Recognition	✓	✓
Facial Recognition	✓	✓
Landmark	✓	✓
Recognition	✓	✓
Description labels	✓	✓
Emotion Percentage	✓	✓
Gender	✓	✗
Age	✓	✗
Adult content	✓	✓
Racy content	✓	✓
Categorization	✓	✓
Dominant Colors	✓	✓
Logo detection	✗	✓
Video	✓	✗

As shown in the table, it provides important facial attributes, emotions, accessories, and such. Apart from that, Google's image analysis service provides better and more relevant results that will be more useful for the group's project. Having everything considered, the group plans to utilize Google's Cloud Vision API, specifically its, label detection and safe search detection, altogether with the Microsoft Face API to provide the necessary information required by the group in processing such images.

### 3 Methodology

In the social media image listening engine, the marketing campaign process by the De La Salle University Office for Strategic Communications (DLSU STRATCOM) was employed which composed of pre-event campaigning stage, during the event, and after the event was transpired. The proponents were also able to interview target users of the system, which are marketing officers and other individuals in the marketing domain, and both the Gap Analysis and Ishikawa Fishbone Diagram were utilized in determining where the social media listening process can fit into the marketing event campaign process of STRATCOM.

The architecture of the social media listening engine initiates first with a hashtag input of the user in the web application of the project, and it is limited to only a single hashtag per search. This hashtag input can be the username of an organization or a related hashtag, to which the scraper tool will use in order to retrieve all the necessary information such as the likes, comments, and the image source URLs of a certain post or a group of posts. These pieces of information are all retrieved by returning a JSON file together with the scraped image files from the scraper tool. These images will then be used for the image analysis services from existing tools such as the Google Cloud Vision API and the Microsoft Cognitive Services in order to produce the necessary data which are tags and their corresponding confidence levels. These outputs will then be further processed to generate confidence reports that will be represented in any form of visualization like graphs, charts, etc.

### **3.1 Scraping Process and Image Collection**

The scraper tool collects images with the hashtag caption included in the images. These images (from the image URL) collected by the scraper tool only select images posted by public Instagram user accounts. The scraper tool also produces a JSON response that would include detailed information as previously mentioned such as the identification of the image by Instagram, the caption of the image itself, the number of likes of the image, timestamp, etc. The main output, however, will simply be the images scraped through its URL.

### **3.2 Integration Module**

The integration module comprises of the outputs from the image scraper tool and once the scraping process is complete, the data is saved in a NoSQL namely MongoDB, and the data processing step can begin. The engine will access services that provide image analysis such as Microsoft Cognitive Services and Google Cloud Platform which provides outputs in JSON format that contains descriptions such as “person,” “women,” “games,” etc. and is also saved into the database. After the information processing in the integration module, the engine can then present information through visualization and reports.

### **3.3 Visualization Module**

The last component is the visualization module. Several reports would be generated from the data aggregated through the services used to perform image analysis. These reports would show the aggregated data of age, gender, emotions, category classification, and label results. A picture can be classified into a friend, food, gadget, captioned picture, pet, activity, selfie, and fashion [4]. The tallying of labels and tags would be presented using a word cloud to easily identify which labels or tags are most associated with the specified hashtag.

## 4 Results and Discussion

The engine comprises a dashboard that presents the images that were collected from Instagram, as well as other information such as the total number of likes, number of detected brand logos, trend of images posted over time, and the participation of each image category (Fig. 4). The charts are also drillable to see the specific images for each data point (Fig. 4).

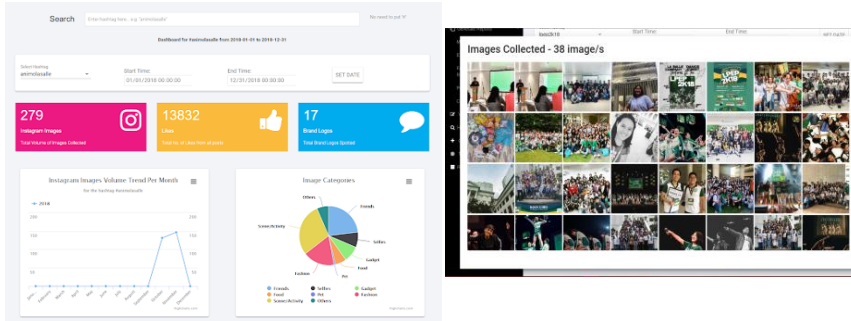


**Fig. 4.** Dashboard Visualization (left) and Images from Drill Down Charts (right)

The Face Analysis page caters only to the images that contain faces. The first chart shows a half donut chart for the male and female genders and their respective percentages, and the histogram shows the distribution of the age detected from the faces in the images. The Emotion recognition bar chart uses Microsoft Face API to retrieve the recognized faces in the image. There are 7 emotions identified by the API which are the following: Anger, Contempt, Disgust, Fear, Happiness, Neutral, Sadness, and Surprise. These emotions are represented by the confidence level. The system would calculate the total confidence level of each face recognized and divided it by the number of faces to get the percentage of each emotion.

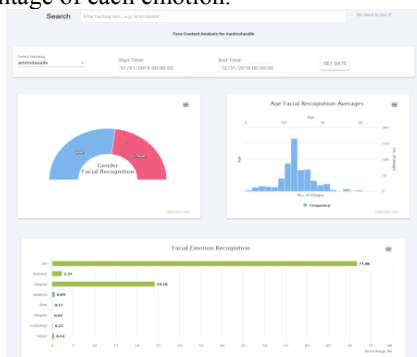


**Fig. 5.** Facial and Emotion Recognition Report

Given the difficulty in contextualizing or validating marketing insights obtained from social media listening using only text, we investigate the use of images to complement the text insights and display it via charts that are categorized by the type of analysis that the charts show per page. The following table summarizes the UAT results in terms of total passed and failed tests per user.

**Table 2.** Data Retrieved from the Scraper

User	No. of Passed Tests	No. of Failed Tests	Total No. of Tests
1	83	1	84
2	83	1	84
3	83	1	84

#### 4.1 Multiple Hashtags for an Event

The limitation of having 1 hashtag per event is that the user must create multiple events for a different hashtag. This would mean that the user has to repeat the “create calendar” process multiple times to keep track of the event through multiple hashtags. The advantages of having a single hashtag, on the other hand, means that there will be no duplicating issues due to the current database structure of the system. The current system’s database structure uses the IG post’s ID as the primary key of the collection and prevents any duplicate posts, thus not being able to track multiple hashtags in one event. We recommend that for the future development of the system, necessary modifications to the database structure has to be made by adding a new collection that keeps track of the hashtags to events so that there is no need to drastically change the structure of the database.

#### 4.2 Maximum Images Scrapped Per Search

Another limitation lies with fetching at a maximum of only 1000 Instagram images from posts. This limitation is not from the Graph API, but from the scraper being used. The Graph API does not have a limit, but it has a rate of how much the scraper can collect within a period of time. The more the scraper collects, the slower it would become to gather the posts and eventually the scraper would lose the network connection with the API. Another limitation of the scraper being able to scrape 1000 images is that if a hashtag contains more than 1000 posts, the scraper cannot collect posts before the 1000th most recent post. The scraper would stop the collection process once it has detected the previous latest post’s Instagram ID, thus making it not possible to scrape posts before the previous search. Currently, the Graph API does not have a function where it can return posts with specific criteria. It is recommended to increase the scraper’s collection capacity to accommodate more than 1000 images.

## 5 Conclusion

In this study, various existing solutions for image analysis were reviewed, and the image processing solutions—specifically the Microsoft Cognitive Services and Google Cloud Platform Services APIs—were integrated into the system. The resulting content characterizations from analyzed images from the different image analysis tools were then presented through visualizations. The system was able to meet its goal, which was to capture the image context to gain a better understanding of marketing insights in order to aid in contextualizing these marketing insights obtained from social media listening. The proponents of the system recommend future audiences that the system can be further improved in terms of its extensibility by scaling more in terms of the social media platforms it supports aside from the Instagram social media site. This can be achieved by integrating APIs from each social media platform into the system. Another avenue to improve upon the system would be multiple hashtag search functionality and video analysis features. With regards to the visualizations and how the image analysis results are presented, further research into suitable information architecture would be recommended as well.

## References

1. Casalboni: A. Build powerful applications that see and understand the content of images with the Google Vision API page, <https://cloudacademy.com/blog/google-vision-api-image-analysis>, last accessed 2018/03/14.
2. Chumwatana, T., Chuaychoo, I.: Using social media listening technique for monitoring people's mentions from social media: A case study of thai airline industry. In: 2nd International Conference on Knowledge Engineering and Applications, pp. 103-106. (2017).
3. Ha, A.: An Experiment: Instagram Marketing Techniques and Their Effectiveness (Unpublished bachelor's thesis). California Polytechnic State University (2015), <https://digital-commons.calpoly.edu/comssp/185>, last accessed 2018/03/28.
4. Hu, Y., Manikonda, L., Kambhampati, S.: What we instagram: A first analysis of instagram photo content and user types. In: 8th International Conference on Weblogs and Social Media, ICWSM 2014 pp. 595-598. The AAAI Press (2014).
5. Jackson, D. (2017, September 20). What is social listening & why is it important? (2017), <https://sproutsocial.com/insights/social-listening>, last accessed 2018/04/16.
6. Lee, I.: Social media analytics for enterprises: Typology, methods, and processes. Business Horizons, pp. 61, 199-210 (2018).
7. MVP Award Program Beyond the obvious with API vision on cognitive services page,
8. <https://blogs.microsoft.com/mvpawardprogram/2018/03/20/api-vision-cognitive-services>, last accessed 2018/03/25.
9. Newberry, C.: Social listening: What it is, why you should care, and how to do it well (2017). <https://blog.hootsuite.com/social-listening-business>, last accessed 2018/04/15.



# On the trade-offs of Proof-of-Work algorithms in blockchains

Zi Hau Chin, Timothy Tzen Vun Yap, Ian K. T. Tan

Multimedia university, Persiaran Multimedia, 63100 Cyberjaya, Malaysia  
[zihau27@gmail.com](mailto:zihau27@gmail.com), [timothy@mmu.edu.my](mailto:timothy@mmu.edu.my), [ian@mmu.edu.my](mailto:ian@mmu.edu.my)

**Abstract.** There are many different protocols that regulate the way in which each node on a blockchain network is able to reach consensus that a newly created block is valid. One of the protocols, Proof-of-Work (PoW) gained popularity when it was implemented in a blockchain-based cryptocurrency known as Bitcoin. However, there are inherent deficiencies in its current implementation. This paper discusses these deficiencies, as well as the parameters that directly and indirectly affect its efficacy and performance so that possible enhancements to the protocol can be investigated.

**Keywords:** Proof-of-Work, Blockchain, Bitcoin, Difficulty

## 1 Introduction

A blockchain is based on a distributed, decentralized and public digital ledger technology that is used to record data over numerous computers. By storing data across its peer-to-peer network, the data is not owned or controlled by a single entity, hence it is decentralized and distributed. It is a growing list of records known as “blocks” that are linked together using cryptography. Each block is linked back, referring to the previous block or parent block by including the cryptographic hash of the previous block in the chain. The linked blocks then form a chain, thus any included record cannot be altered without the modification of every following block, which will require consensus of the network majority. Blockchain consensus protocols are keeping all the nodes on a network synchronized, in which the nodes agree on a same state of the blockchain.

## 2 Blockchain

The idea behind blockchain was originally described by Haber and Stornetta as “a cryptographically secured chain of blocks” [1]. Bayer, Haber and Stornetta then implemented Merkle trees into the previous design in order to improve its efficiency and reliability by allowing multiple documents to be collected into one block [2]. However, the blockchain technology as we know it today was conceptualized by a pseudonymous Satoshi Nakamoto in the Bitcoin white paper during 2008 [3].

The most interesting features of blockchain are immutability and decentralization. Data stored in blockchain is secured using cryptography. Particularly in Bitcoin, a Secure Hash Algorithm 256 (SHA256) cryptographic hash function is applied twice to the block header of each block which contains data such as the cryptographic hash of the previous block, transaction data, timestamp, etc. The output is a 32-byte hash known as the “block hash” or “block header hash” which acts as the primary identifier of a block due to its ability to identify a block unambiguously and uniquely. Additionally, a cryptographic hash function is designed with a one-way function in mind, which means that it is unfeasible to invert, thus contributing to the blockchain’s immutability.

In Bitcoin, a distribution computation system known as “Proof-of-Work (PoW)” algorithm is used in order to achieve the state of being completely decentralized. Unlike centralized system or network that require all data to pass through central server, Bitcoin passes all data through a distributed, peer-to-peer (P2P) network, where all nodes are equal and there are no nodes with special rights. Every 10 minutes, a vote will be conducted in order for the nodes to reach consensus about the state of the Bitcoin network.

Dywork and Naor presented the concept of PoW in 1993 to combat junk mail and control access to a shared resource [4] but the term PoW first originated from a 1999 paper by Jakobsson and Juels [5]. The concept is that in order to acquire access to a shared resource, the user is required to compute a moderately hard but feasible function, thus preventing ill-conceived usage of the shared resource. Bitcoin’s PoW is actually based on Back’s version of HashCash’s PoW [6].

### 3 Literature Review

#### 3.1 Pricing via Processing for Combatting Junk Mail

The main idea introduced by Dywork and Naor is that a computation of a moderately hard but feasible function is required by the user in order to acquire access to a shared resource to prevent frivolous use of the shared resources [4]. Previously, legislation and usage fees have been used to restrain the access to a resource. However, the authors wished to avoid a system where sending an email between friends and families would cost as much as sending a postal mail. Thus, such approaches were deemed to be underutilizing the electronic medium and is unsuitable to act as a discouragement for sending junk email. So instead of charging the “cost of using the medium plus the profit to the provider”, they wished to impose a type of cost on the transmission where it will discourage the act of sending junk email while not interfering with the normal usage of the system.

A function known as the pricing function that requires the sender of an email to compute a somewhat expensive but feasible function of the message plus some other additional information was proposed. Additionally, a shortcut would be used by the resource manager to allow cheap access to the resource that will bypass the control mechanism. The idea of a shortcut is the same as

the trapdoor one-way permutation proposed by Diffie and Hellman [7], where in this case, a shortcut would allow a pricing function to be computed easily. Using email as an example, the shortcut would allow the email service provider to “permit bulk mailings at a price chosen by the service provider”, thus lowering the cost of sending emails as compared to computing the pricing function for each recipient. The system was assumed to be in an environment where computers were connected to a communication network and it did not require human participation. The system would be consisted of a pricing function  $f_s$ , a shortcut  $c$  and a hash function  $h$ . The pricing function and shortcut would be determined by an “authority” and all users must obey the authority. A hash function was used so that only the hash value of a pricing function would be applied to a message instead of pricing function which may be too long. The hash function  $h$  and pricing function  $f_s$  were known to all users, but the shortcut  $c$  would be known only by the authority and any number of trusted agents chosen by the authority.

In order to send a message  $m$ , at time  $t$ , to destination  $d$ , the sender was required to compute the following pricing function:

$$y = f_s(h(< m, t, d >)) \quad (1)$$

Then proceed to send  $< y, m, t >$  to destination  $d$ . The email client of the recipient will verify that  $y = f_s(h(< m, t, d >))$ . The message would be discarded when the verification fails or time  $t$  is notably different from the current time, and the sender might or might not be notified that the transmission failed. On the other hand, the message would be sent to the recipient successfully if the verification succeeded and the time  $t$  was not significantly different from the current time.

### 3.2 Bitcoin: A Peer-to-Peer Electronic Cash System

Nakamoto published the Bitcoin whitepaper in 2008 [3] but the actual Bitcoin client was released in 2009. The vision of Nakamoto is to create a “purely peer-to-peer digital cash that would allow one party to send the online payment to another party without going through a financial institution”. The idea is to define a digital signature chain as an electronic coin. A coin owner will transfer the coin to the new owner by signing and adding a “hash of the previous transaction and the public key of the new owner” to the end of coin. Verification of the ownership of the chain can be done by a payee by verifying the signatures. To ensure that the owners of the coin did not double-spend without a trusted central authority, transactions need to be announced publicly. Additionally, the participants must follow the same timeline in order for everyone to agree on a single order history in which transactions are received.

A PoW system similar to Hashcash [6] was utilized to implement the distributed peer-to-peer timestamp server in Bitcoin. Roughly speaking, participants or also known as miners are expending their computational power to find the solution to a PoW puzzle, this process is called mining. The goal of the PoW

puzzle is to find a value or nonce by incrementing it, that when hashed with a cryptographic hash function such as SHA-256 will output a block hash with the required number of leading zero bits. Every time a solution is found, a new block will be generated and attached to the existing blockchain.

### 3.3 Revisiting Difficulty Control for Blockchain Systems

In Bitcoin, although the expected time taken to mine a block or also known as block time is set to 10 minutes, the block time is actually determined by the *difficulty* ( $D$ ) of the PoW. As time goes by, the efficiency of hardware and number of nodes will cause the hash rate (computational power) to increase, thus the time taken to mine a block will decrease. If the current block time is less than 10 minutes, the difficulty will be increased (harder to mine a block) in order to maintain the 10 minutes block time. The difficulty will be adjusted once every 2016 blocks or roughly 2 weeks ( $2016 * 10 \text{ minutes} = 20160 \text{ minutes} = 2 \text{ weeks}$ ). But there is an adjustment limit of how much the difficulty can increase or decrease per difficulty readjustment. The new difficulty can only increase up to 4 times of the current difficulty, and can only decrease by 1/4 times of the current difficulty. The adjustment limit exists in order to prevent drastic changes to the difficulty of the whole Bitcoin network. The *target* ( $T$ ) is a value that determines the number of leading zeros required from the computed SHA-256 block hash. The block hash must be smaller than or equal to the current target in order for the newly generated block to be valid and accepted by the network.

There is a relationship between the difficulty and target, where if the difficulty increases (harder to mine), the target will decrease (as the target becomes smaller, it will be harder to find a block hash that is smaller than or equal to it) and vice versa. The equation to calculate the new target  $T$  in Bitcoin can be summarized as:

For every  $N$  blocks ( $N = 2016$ )

$$T_{i+1} = T_i * \frac{X_N}{N * B} \quad (2)$$

$X_N$  is the actual time taken to mine  $N$  number of blocks while  $B$  is the expected block time (10 minutes in Bitcoin). The formula to calculate the new difficulty  $D$  can be defined as:

$$D_{i+1} = \frac{1}{T_{i+1}} \quad (3)$$

However, the difficulty readjustment algorithm can be exploited in order to maximize a miner's profit. The *coin-hopping attack* can be summarized as following:

- We assume that miner  $X$  can mine at least 2 possible cryptocurrencies ( $C1$ ,  $C2$ ) with the same profitability.
- $X$  is currently mining  $C1$  before the start of an epoch  $E1$ . At the beginning of  $E1$ ,  $X$  switched to mine  $C2$ .

- The total hash rate (mining power) of  $C1$  dropped because  $X$  is not contributing his computational power to mine  $C1$ .
- Then at the beginning of epoch  $E2$  that is right after epoch  $E1$ , the difficulty of  $C1$  decreased. So now  $X$  switched back to mine  $C1$  because the lower difficulty mean it has a higher profitability.

Bitcoin is vulnerable to such attack because Bitcoin's difficulty readjustment algorithm is not suitable to deal with a sudden increase or decrease in hash rate [8]. If the hash rate is constant, the difficulty readjustment algorithm is able to maintain the expected block time. But if the hash rate is growing exponentially, it will not be able to maintain the expected block time. Meshkov, Chepurnoy and Jansen state that an ideal difficulty readjustment algorithm must:

- (i) be resistant to known difficulty manipulation-based attacks such as the coin-hopping attack.
- (ii) be able to maintain the expected block time even with the random increase or decrease in the network hash rate.

A new difficulty readjustment algorithm called *linear algorithm* that is based on linear least square method [9] was proposed. To obtain a more accurate prediction, rather than using only 1 cycle (previous 2016 blocks) of the actual time taken to mine a block, multiples cycles of 2016 blocks can be used instead. Three different simulation of the proposed algorithm was performed. The first is to observe how well the proposed algorithm is able to deal with exponential difficulty growth. A fixed increase of 10% in the hash rate was applied to every epoch.

From the observations, the difficulty calculated by the Bitcoin algorithm is always lower than the real difficulty and the linear algorithm. Thus, the average block time from the original Bitcoin algorithm is approximately 9 minutes and 5 seconds, which is about 10% lower than the expected 10 minutes. On the other hand, the difficulty calculated by the linear algorithm is closer to the real difficulty, albeit still lower with the average block time of about 9 minutes and 45 seconds. The linear algorithm has an average error of roughly 1.9% while the Bitcoin algorithm is sitting at about 9.1%.

The last simulation measured how well the algorithms deal with the coin-hopping attack. To manipulate the difficulty, the attacker repeatedly turned on and off his mining equipment. Difficulty calculated by the Bitcoin algorithm is always in antiphase with the real difficulty and the average block time is 10 minutes 10 seconds, while the average block time for linear algorithm is 10 minutes 5 seconds.

### 3.4 Fast(er) Difficulty Adjustment for Secure Sidechains

During the Scaling Bitcoin workshop in Milan 2016, Friedenbach proposed few solutions regarding the Bitcoin difficulty adjustment algorithm [14]. Friedenbach at first, suggested to adjust the difficulty more frequently, or at least every  $N$  blocks where  $N < 2016$ . By adjusting the difficulty earlier, Bitcoin will be able to

respond to sudden event such as sudden increase or decrease in hash rate more quickly. However, when the difficulty adjustment interval increases, the error rate also increases. This is due to fact that the algorithm is not reacting fast enough to sudden shifts in hash rate. In addition, when the difficulty adjustment interval is very low, the error rate actually increases exponentially, because the algorithm is overreacting to some lucky blocks (blocks are mined within few seconds or minutes). Thus adjusting the difficulty every block is actually not recommended.

In the second suggestion, the sliding window is decoupled from the adjustment frequency. Currently in Bitcoin where the difficulty will readjust once every 2016 blocks, the actual time taken to mine the previous 2016 blocks were used in order to calculate the new difficulty. Friedenbach proposed to treat the interval of difficulty adjustment and the size of sliding window (actual time taken to mine  $X$  blocks) as two independent parameters to tweak. Last but not least, suggestion to change the control algorithm was also made as Bitcoin is currently using a simple and naive control algorithm.

### 3.5 On the Security and Performance of Proof of Work Blockchains

Gervais, Karame, Wüst, Glykantzis, Ritzdorf and Capkun studied the extent to which consensus and network parameters such as block size, block time, network propagation and etc., affect the performance and security of PoW blockchains [10]. Ever since the release of Bitcoin in 2009, it has been forked multiple times. All the forks include fine tuning the consensus parameters of Bitcoin (block time and hash function) and network parameters (block size and information propagation mechanism) in order to improve the efficiency of blockchain. For example, two of the most well-known forks of Bitcoin, Dogecoin and Litecoin implemented the block time of 1 minute and 2.5 minutes respectively instead of 10 minutes.

Even though many different consensus protocols such as PoS, Practical Byzantine Fault Tolerance (pBFT), PoB, and etc. were introduced, PoW is still the main consensus protocols that many new cryptocurrencies choose to implement. Although the security of Bitcoin has been studied in depth, but that is not the case for other variants of PoW blockchains. A new framework was proposed in order to analyze the relationship between performance and security of various network and consensus parameters of PoW blockchains. The framework proposed by Gervais et al. has two key components: i) a PoW blockchain instance and ii) a blockchain security model.

Bitcoin, Litecoin, Dogecoin and Ethereum were instantiated as blockchain instances with their default network and consensus parameters. A simulator that is able to mimic the blockchain instances are designed and implemented in order to obtain a more realistic result. The PoW blockchain instances will output measured or simulated stale block rate, block propagation times and throughput. The proposed framework enables Gervais et al. to measure the security and performance of PoW blockchains when considering different consensus and net-

work parameters. However, as this paper main focus is on the performance of PoW blockchain, only the performance component is reviewed.

Stale blocks are undesirable because they cause chain forks to happen, and it could affect the performance and security of blockchain. Bitcoin, Litecoin and Dogecoin are all PoW-based blockchain and are using the same propagation system but with different block time and block sizes [11]. Table 1 suggests that block interval (block time) and block sizes heavily affect the stale block rate. For instance, Bitcoin which has larger average block size (534.8KB) but 4 times longer block interval (10 minutes) as compared to Litecoin (6.11 KB & 2.5 minutes) results in a higher stale block rate of 0.41% vs 0.273%. On the contrary, the difference in stale block rate between Litecoin and Dogecoin is mainly caused by the block interval (2.5 minutes vs 1 minute) as their average block size was roughly the same (6.11 KB vs 8KB). In Ethereum, stale blocks are known as uncle blocks. The stale block rate of Ethereum is 6.8% as compared to Bitcoin 0.41%. Although it has the smallest average block size of 1.5KB, but the block interval is also the lowest (10 – 20 seconds) and the number of available public nodes are also higher than both Litecoin and Dogecoin. Based on the observation, we can infer that a very low block interval is not necessarily the best as seen from the example of Dogecoin and Ethereum.

**Table 1.** Impact of different blockchain parameter choices on the network propagation times/median block propagation time ( $t_{MBP}$ ). Stale block rate ( $r_s$ ) and average block size ( $S_B$ ) were measured over the last 10000 blocks [10].

	Bitcoin	Litecoin	Dogecoin	Ethereum
Block interval (mins)	10	2.5	1	1/6 to 2/6
Public nodes	6000	900	600	4000
Mining pools	16	12	12	13
$t_{MBP}$ (sec)	8.7	1.02	0.85	0.5 0.75
$r_s$ (%)	0.41	0.273	0.619	6.8
$S_B$ (KB)	534.8	6.11	8	1.5

**Impact of block interval** Multiple simulations with different block interval ranging from 25 minutes to 0.5 seconds were performed to investigate the effects of the block interval on  $t_{MBP}$  and  $r_s$ . Four different cases of block request management system method were also defined for the simulation, including:

1. Standard block request management
2. Standard block request management + unsolicited block push from miners
3. Standard block request management + unsolicited block push from miners + relay network
4. Sendheaders mechanism with unsolicited block push and relay network

With unsolicited block push, miner is able to broadcast their mined blocks without advertisement. Whereas in relay network, blocks are propagated immediately

after the verification. A lower block size can be achieved because transactions are reference with a 2 bytes transaction ID. On the contrary, Bitcoin adopted sendheaders mechanism since version 0.12. Peers can receive future *block headers* directly from their peers, skipping usage of *inv* messages, thus reducing latency and bandwidth overhead. Each simulation was run for 10000 blocks, for each block request management system method.

From Table 2, the  $r_s$  for block interval of 10 minutes with the standard request management method was 1.85%, which is relatively close to the 1.69% reported by Decker and Wattenhofer [11]. On the other hand, the  $r_s$  significantly dropped when unsolicited block push for miners were added to the method (Case 2). Unsolicited block push profit the miners since miners were interconnected and the first node with faster propagation method was able to reach the network majority faster. However,  $r_s$  is not significantly affected by the addition of the relay network (Case 3). In contrast, the addition of the relay network (Case 3) significantly reduced the  $r_s$  when the block size was bigger than 2 MB as shown in Table 3. Gervais et al. stated that although the impact of the sendheader mechanism was limited, it was able to mitigate the partial eclipse attacks [12].

**Table 2.** Impact of block interval ranging from 25 minutes to 0.5 seconds on  $t_{MBP}$  and  $r_s$ . Block size was fixed to the current block size of Bitcoin (1MB) [10].

	Case 1		Case 2		Case 3		Case 4	
Block interval	$t_{MBP}$ (s)	$r_s$ (%)						
25 mins	35.73	1.72	25.66	0.16	22.50	0.03	22.44	0.02
10 mins	14.7	1.51	10.65	0.13	9.41	0.14	9.18	0.13
2.5 mins	4.18	1.82	2.91	0.16	2.60	0.16	2.59	0.15
1 mins	2.08	2.15	1.34	0.35	1.30	0.25	1.27	0.29
30 secs	1.43	2.54	0.84	0.45	0.84	0.51	0.84	0.52
20 secs	1.21	3.20	0.67	0.86	0.69	0.85	0.68	0.82
10 secs	1.00	4.77	0.35	1.73	0.33	1.41	0.53	1.59
5 secs	0.89	8.64	0.37	2.94	0.45	2.99	0.44	3.05
2 secs	0.84	16.65	0.40	6.98	0.39	7.28	0.38	7.10
1 secs	0.82	26.74	0.53	12.44	0.38	12.59	0.37	12.52
0.5 secs	0.82	38.15	0.61	20.62	0.49	20.87	0.36	21.10

**Impact of Block size** Simulations with a fixed block interval of 10 minutes and ranging block sizes from 0.1 MB to 8 MB were performed to investigate the effects of block size on the performance. From Table 3, the  $t_{MBP}$  increased linearly whenever the block size increased, but when block size was equal to 8 MB,  $t_{MBP}$  and  $r_s$  actually increased exponentially. With an efficient network propagation mechanism, it is actually able to decrease the  $t_{MBP}$  and  $r_s$ . But in Case 2, the  $t_{MBP}$  is worse than that from the standard block request management

(Case 1) with block size of 8 MB. Thorough analysis of the results in Tables 1 to 3 can be found in [10].

**Table 3.** Impact of block size ranging from 0.1 MB to 8 MB on  $t_{MBP}$  and  $r_s$ . Block interval was fixed to the current block interval of Bitcoin (10 minutes) [10].

	Case 1		Case 2		Case 3		Case 4	
Block size	$t_{MBP}$ (sec)	$r_s$ (%)						
0.1 MB	3.18	0.32	2.12	0.03	2.02	0.03	2.02	0.2
0.25 MB	7.03	0.88	4.93	0.11	4.49	0.05	4.46	0.17
0.5 MB	13.62	1.63	9.84	0.13	8.65	0.05	8.64	0.06
1 MB	27.67	3.17	20.01	0.38	17.24	0.07	17.14	0.07
2 MB	57.79	6.24	44.6	1.12	35.49	0.08	35.38	0.1
4 MB	133.30	11.85	126.57	5.46	78.01	0.12	78.40	0.13
8 MB	571.50	29.97	875.97	15.64	555.49	0.43	550.25	0.4

## 4 Discussions and Conclusion

Although the PoW algorithm allows blockchains to achieve consensus in a distributed manner and achieve security without the need of a central authority, it is not without its deficiencies. It is lacking in speed, limiting the throughput blockchains are able to achieve. In addition, the PoW difficulty adjustment in Bitcoin is not responsive to sudden event or differences in hash rate. If there is a loss of this hash rate just after a difficulty adjustment (worst case), it would take months for the miners to slowly grind until the next difficulty adjustment. This will result in several difficulty adjustment cycles to level out the discrepancies due to the adjustment limit.

From this study, we will be proposing a solution to the inherent trade offs of PoW through the consideration of learning models such as expectation maximization and dynamic Bayesian network through reparameterization of the PoW scheme. The need to identify the parameters of the scheme is challenging as the blockchain itself has many facets to its framework, such as network, storage, view (data structure of the full ledger), sidechain as well as consensus [15]. In addition, key parameters that actually significantly alters the performance of the scheme has to be ascertained as well, and they need to fit the optimization performed by the learning models.

## 5 Acknowledgement

Financial support from the Ministry of Higher Education, Malaysia, under the Fundamental Research Grant Scheme with grant number FRGS/1/2018/ICT02

/MMU/03/6, as well as the Multimedia University Mini Fund with Project ID MMUI/180239, are gratefully acknowledged.

## References

1. Haber, S., & Stornetta, W. S. (1990, August). How to time-stamp a digital document. In Conference on the Theory and Application of Cryptography (pp. 437-455). Springer, Berlin, Heidelberg.
2. Bayer, D., Haber, S., & Stornetta, W. S. (1993). Improving the efficiency and reliability of digital time-stamping. In Sequences II (pp. 329-334). Springer, New York, NY.
3. Nakamoto, S. (2008, October 31). Bitcoin: A Peer-to-Peer Electronic Cash System. Retrieved April 25, 2019, from <https://nakamotoinstitute.org/bitcoin/>
4. Dwork, C., & Naor, M. (1993). Pricing via Processing or Combatting Junk Mail. Advances in Cryptology - CRYPTO'92: Lecture Notes in Computer Science, 740, 139-147.
5. Jakobsson, M., & Juels, A. (1999). Proofs of Work and Bread Pudding Protocols(Extended Abstract). In IFIP — The International Federation for Information Processing (pp. 258-272). Springer.
6. Back, A. (2002). Hashcash - A Denial of Service Counter-Measure. Retrieved April 30, 2019, from [https://www.researchgate.net/publication/2482110\\_Hashcash\\_-A\\_Denial\\_of\\_Service\\_Counter-Measure](https://www.researchgate.net/publication/2482110_Hashcash_-A_Denial_of_Service_Counter-Measure)
7. Diffie, W., & Hellman, M. E. (1976). New directions in cryptography. IEEE Transactions on Information Theory, 22(6), 644-654.
8. Meshkov, D., Chepurnoy, A., & Jansen, M. (2017). Short Paper: Revisiting Difficulty Control for Blockchain Systems. In Data Privacy Management, Cryptocurrencies and Blockchain Technology (pp. 429-436). Oslo, Norway.
9. Lawson, C. L., & Hanson, R. J. (1974). Solving Least Squares Problems.
10. A. Gervais, G. O. Karame, K. Wüst, V. Glykantzis, H. Ritzdorf and S. Capkun, "On the Security and Performance of Proof of Work Blockchains," in CCS '16 Proceedings of the 2016 ACM SIGSAC Conference on Computer and Communications Security, Vienna, Austria, 2016.
11. Decker, C., & Wattenhofer, R. (2013). Information propagation in the Bitcoin network. IEEE P2P 2013 Proceedings. Trento, Italy: IEEE.
12. Gervais, A., Ritzdorf, H., Karame, G. O., & Capkun, S. (2015). Tampering with the Delivery of Blocks and Transactions in Bitcoin. CCS '15 Proceedings of the 22nd ACM SIGSAC Conference on Computer and Communications Security (pp. 692-705). Denver, Colorado, USA: ACM.
13. Investing.com. (n.d.). All cryptocurrencies. Retrieved from Investing.com: <https://www.investing.com/crypto/currencies>
14. Friedenbach, M. (2016, October 9). Scaling Bitcoin workshop : Milan 2016 - Fast difficulty adjustment. Retrieved from Scalingbitcoin: <https://scalingbitcoin.org/transcript/milan2016/fast-difficulty-adjustment>
15. Croman, K., Decker, C., Eyal, I., Gencer, A. E., Juels, A., Kosba, A., Miller, A., Saxena, P., Shi, E., Sirer, E. G., Song, D. & Wattenhofer, R. (2016, February). On scaling decentralized blockchains. In International Conference on Financial Cryptography and Data Security (pp. 106-125). Springer, Berlin, Heidelberg.



# Ideal Combination Feature Selection Model for Classification Problem based on Bio-Inspired Approach

Mohammad Aizat Basir<sup>1</sup>, Mohamed Saifullah Hussin<sup>1</sup> and Yuhanis Yusof<sup>2</sup>

<sup>1</sup>School of Informatics and Applied Mathematics, Universiti Malaysia Terengganu, Malaysia.

<sup>2</sup>School of Computing, Universiti Utara Malaysia, Malaysia.

aizat@umt.edu.my, saifullah@umt.edu.my, yuhanis@uum.edu.my

**Abstract.** Feature selection or attribute reduction is a crucial process to achieve optimal data reduction for classification task. However, most of the feature selection methods that were introduced work individually that sometimes caused less optimal feature being selected, subsequently degrading the consistency of the classification accuracy rate. The aim of this paper is to exploit the capability of bio-inspired search algorithms, together with wrapper and filtered methods in generating optimal set of features. The important step is to idealize the combined feature selection models by finding the best combination of search method and feature selection algorithms. The next step is to define an optimized feature set for classification task. Performance metrics are analyzed based on classification accuracy and the number of selected features. Experiments were conducted on nine (9) benchmark datasets with various sizes, categorized as small, medium and large dataset. Experimental results revealed that the ideal combination is a feature selection model with the implementation of bio-inspired search algorithm that consistently obtains the optimal solution (i.e. less number of features with higher classification accuracy) on the selected dataset. Such a finding indicates that the exploitation of bio-inspired algorithms with ideal combination of wrapper/filtered method can contribute in finding the optimal features to be used in data mining model construction.

**Keywords:** Feature Selection, Bio-Inspired, Classification.

## 1 Introduction

Real world data set usually consists of a large number of attributes. It is common that some of those attributes are irrelevant and consequently affect the data mining model. In situations where a rule has too many conditions, having a large number of attributes, makes the rule becomes less interpretable. Based on this understanding, it is important to reduce the number of features to be used in data mining model construction. In practical situations, it is recommended to remove the irrelevant and redundant dimensions to reduce the processing time and labor cost. [1] stated that the data set with large number of attributes is known as a data set with high dimensionality. The high dimensionality data set leads to a phenomenon known as the curse of dimensionality where computation time is an exponential function of the number of the dimensions. There are

also cases where the extraction of the features in the model contain redundancy. This issue is very much related to the high dimension of search space. Possible solution is to reduce the dimension, without compromising to prevent losing essential information in the data. Large number of attributes in each possible rules will caused vague representation, thus difficult to comprehend, utilize and exercise. Hence, the complexity of the attribute should be reduced by decreasing the number of attributes and eliminating insignificant attributes that will improve the processing time and improve storage efficiency.

The key problem for attribute complexity reduction is the risk of losing information. There are two critical aspects of attribute reduction problems, which are the degree of attribute optimality (in terms of subset size and corresponding dependency degree) and time required to achieve this attribute optimality. For instance, previous methods such as Entropy-Based Reduction (EBR) and Quick Reduct which was created by [2] performed reduction quickly but does not guarantee a minimal size of subset in many cases [2]–[4]. Combination (hybrid) methods such as Rough Set-Based Attribute Reduction (RSAR) and swarm algorithms such as GenRSAR proposed by [1] and AntRSAR, Particle Swarm Optimization (PSORSAR) and BeeRSAR developed by [3] improved the accuracy but require large processing time [5].

Feature selection, also known as attribute selection is the process of selecting a subset of relevant features (attributes) to be used in model development. It is the process of choosing a subset of important features so that the feature space is optimally reduced to evaluation criterion. The reduction of data and computational complexity can be done with feature selection process. In general, it can be viewed as search problem where every state in the search space represents a subset of possible features. For example, examining all subsets in small search area at any order and search will complete in short minimal time. Conversely, the search space is usually not small, typical data mining application is large ( $N > 20$ ) (where  $2^N$  the number of possible solutions for problem of dimensions N). Concerning this problem, it is vital to identify the best search strategy in order to discover near-optimal subsets of features that further refine the quality of the data mining process.

## 2 Related Works

Ant Colony Optimization (ACO) algorithm was applied to find the optimum features for breast cancer diagnosis of Raman-based cancer [6]. The result shows that ACO feature selection improves the diagnostic accuracy of Raman-based diagnostic models. Likewise, a hybrid approach for feature subset selection using ACO and multi-classifier ensemble was proposed by [7]. In the research, ACO was used to enhance the predictive accuracy of filters method. Extensive experimentation indicates that the proposed method has the ability to generate small subsets and attained higher classification accuracy.

New Independent RSAR with Artificial Bee Colony (ABC) has been presented by [5]. In this research, dataset instances have been grouped based on decision attributes. Next, Quick Reduct Algorithm proposed by [8] has been applied to discover the

reduced feature set for each class. Once the reduct sets are discovered, they utilized ABC algorithm to select a random number of attributes from each set, based on the RSAR model, to find the final subset of attributes. An experiment was carried out on five different datasets from the UCI machine learning [9] and compared to six different algorithms which are general RSAR, Entity-based Reduct by [2], GenRSAR and AntRSAR by [1] and Particle Swarm Optimization based RSAR and BeeRSAR by [3]. They found that the proposed method can obtain more minimal reduct than other existing methods.

New nature-inspired feature selection technique based on bats behavior has been proposed by [10]. The technique implemented wrapper approach that combines the power of exploration of the bats together with the speed of the Optimum-Path Forest classifier [11]. [10] claimed that the proposed technique can find the set of features that maximizes the accuracy in a validating set. Their experiment employed five public datasets to accomplish this task, in which Bat Algorithm has been compared against Binary Firefly Algorithm [12] and Binary Gravitational Search Algorithm [13]. They claimed that the proposed algorithm out-performed the compared techniques in 3 out of 5 datasets, being the second best in the remaining two datasets.

Cuckoo Search Algorithm which as introduced by [14] has also been used to solve feature selection problem. For instance, modified cuckoo search algorithm with rough sets has been proposed by [15]. This modified cuckoo search algorithm imitates the obligate brood parasitic behavior of some cuckoo species in combination with the Levy flight behavior of some birds. The proposed algorithm shows the capability to reduce the number of features in reduct set while considering the classification quality into account. Also, [16] proposed a prediction method based on Cuckoo Search algorithm. Two algorithms namely Cuckoo Search Algorithm and Cuckoo Optimization Algorithm were used during subset generation and results show that both algorithms have selected significantly a smaller number of features as well as improved prediction accuracy on selected datasets.

In 2010, Yang created the Firefly Algorithm and it was employed in many areas and this includes feature selection application. For example, Firefly Algorithm Based Wrapper-Penalty Feature Selection method for cancer diagnosis has been developed by [17]. The developed method explored the inclusion of a penalty function to the existing fitness function promoting the Binary Firefly Algorithm. This reduces the feature set to an optimal subset while increasing the classification accuracy. In addition, [18] proposes feature selection in Arabic text classification based on Firefly Algorithm. The proposed algorithm has been successfully applied in different combinatorial problems and obtained high precision value in improving Arabic text classification.

Inspired by existing work in feature selection, the goal of this paper is to present a model for obtaining the optimal number of attributes for the employed datasets. The model consists of the best arrangement (combination) of reduction algorithms and search methods. To produce the model of reduction set, ideal combination of many algorithms' methods are experimented together with different attribute selection search methods. Thereafter, optimization method using bio-inspired search algorithms have been applied to obtain the best reduction set of the attribute tested with nine (9) data sets.

### 3 Methodology

The methodology is shown in form of algorithm in Table 1. It consists of four main steps: (1) Data Selection various size of dataset; (2) Data Pre-processing; (3) Dimensionality Reduction; (4) Formulate best combination; the expected output from phase 1 is a model which consists of the best arrangement (combination) of search methods and reduction algorithms.

**Table 1.** Algorithm for Ideal Combination Feature Selection Model

<i>Start</i> 1. Load Dataset [small, medium, large] 2. Handling missing values
• Remove insignificant columns with majority missing values • Replace with ‘0’ for missing values • Dataset discretization (Instance Supervised filters)
3. Dimensionality Reduction
• Reduction algorithm (Wrapper & Filtered) + BIO-INSPIRED Search Method • Parameter setting: <ul style="list-style-type: none"> <li><input type="checkbox"/> Ant {evaporation rate, pheromone rate, heuristic rate}</li> <li><input type="checkbox"/> Bat {frequency, loudness}</li> <li><input type="checkbox"/> Bee {radius damp, radius mutation}</li> <li><input type="checkbox"/> Cuckoo {pa rate, sigma rate}</li> <li><input type="checkbox"/> Firefly {beta zero, absorption coefficient}</li> </ul> • Get the minimal attribute reduct achieved + high classification accuracy.
4. Formulation the best combination for each category of dataset [small, medium, large].
<i>End</i>

Step 1 (Data Selection): All the data set (refer Table 2) were selected from UCI Machine Learning Repository. These data sets consist of various sizes (small, medium, large) in order to examine the capability of algorithms to perform attribute selection.

Step 2 (Data Pre-processing): Data set that has missing values has been pre-processed in order to make sure that data set is ready to be experimented. In this step, data set that has missing value (denoted as ‘?’ in original dataset) can be replaced either with 0 or mean value. Both approaches have been tested and results show no significant difference in terms of performance. This research opts to replace missing value with “0”.

Step 3 (Dimensionality Reduction): Five (5) bio-search methods and two (2) reduction algorithms have been used in order to search for the optimal attributes. With these two search, [19] claimed that for efficient space searching, balance of exploitation and exploration need to be achieved. The reduction algorithms and bio-search methods are used in data mining studies by [20][21][22][23]. Three (3) learning algorithms have been used with wrapper methods which are Naïve Bayes, K-nearest Neighbor and Decision Tree.

Step 4 (Formulate the best combination): For this step, various combinations of bio-inspired search methods and reduction algorithms were tested with selected attributes to acquire the best combination list for the model. Optimal numbers of reductions with good classification accuracy are the criteria for choosing the best combination list of the model.

**Table 2.** Data Set Characteristics

Category Size	Data set	#Attr	#Inst	#Classes
Small	Breastcancer	9	367	2
Small	Parkinson	22	197	2
Small	Ozone	72	2536	2
Medium	Clean1	166	476	2
Medium	Semeion	265	1593	2
Medium	Cnae	865	1080	9
Large	Emails	4702	64	2
Large	Gisette	5000	13500	2
Large	Arcene	10000	900	2

**Table 3.** Experimentation Parameters Setting

Algorithm	Population Size	#Iteration	Mutation Probability	Others
Ant	20	20	0.01	Evaporation rate: 0.9, Pheromone rate: 2.0, Heuristic rate: 0.7
Bat	20	20	0.01	Frequency: 0.5, Loudness: 0.5
Bee	30	20	0.01	Radius Damp: 0.98, Radius Mutation: 0.80
Cuckoo	20	20	0.01	Pa rate: 0.25, Sigma rate: 0.70
Firefly	20	20	0.01	Beta zero: 0.33, Absorption Coefficient: 0.001

Parameter values used was the default setting for this experiment.

## 4 Results and Discussion

Table 4 shows the performance of filtered and bio-search algorithm with wrapper for selecting the optimal number of features (attributes). It can be seen that filtered method has the capability to reduce the attributes for seven (7) data sets (Ozone, Clean1, Semeion, Cnae, Emails, Gisette, Arcene) except for Breastcancer and Parkinson data sets where the original attributes is maintained. However, the reduction of attributes using filtered approach does not confirm the optimal selection compared to bio-search algorithm with wrapper method. The wrapper method with five (5) bio-search algorithms

achieved better reduction results for all data sets. Furthermore, all bio-search algorithms succeeded to reduce the attributes better than filtered approach. This result approved the suitability of bio-search algorithm with wrapper methods to perform optimal features selection. Also, the ability of random search function that exists in the bio-search algorithms gives more advantages to select the best optimum features. For reduction purposes, it can be concluded that bio-search algorithms with wrapper method can be used to reduce attributes from all sizes of data.

**Table 4.** Results using Filtered/Wrapper with Bio-search Algorithms

Data set	#Attr	#Attr	# Attr [Reduction (Wrapper + Bio Search)]				
	Original	Filtered (Info Gain)	Ant	Bat	Bee	Cuckoo	Firefly
Breastcancer	9	9	<b>8</b>	<b>7</b>	<b>7</b>	<b>8</b>	<b>6</b>
Parkinson	22	22	<b>7</b>	<b>5</b>	<b>7</b>	<b>6</b>	<b>4</b>
Ozone	72	65	<b>6</b>	<b>7</b>	<b>3</b>	<b>4</b>	<b>4</b>
Clean1	166	132	<b>73</b>	<b>60</b>	<b>41</b>	<b>63</b>	<b>73</b>
Semeion	265	105	<b>39</b>	<b>30</b>	<b>33</b>	<b>35</b>	<b>38</b>
Cnae	865	112	<b>79</b>	<b>83</b>	<b>70</b>	<b>71</b>	<b>77</b>
Emails	4702	56	<b>14</b>	<b>18</b>	<b>13</b>	<b>14</b>	<b>17</b>
Gisette	5000	745	<b>278</b>	<b>222</b>	<b>177</b>	<b>232</b>	<b>257</b>
Arcene	10000	2227	<b>449</b>	<b>433</b>	<b>191</b>	<b>530</b>	<b>604</b>

**Table 5.** Classification Accuracy of Best Reduction Set

Data set	Acc(%) [Be- fore Reduction ]	Acc (%) Filtered (Info Gain)	Acc (%) [Reduction (Wrapper + Bio Search)]				
			Ant	Bat	Bee	Cuckoo	Firefly
Breastcancer	96.2	96.2	<b>96.2</b>	<b>96.2</b>	<b>96.2</b>	<b>96.2</b>	<b>96.6</b>
Parkinson	84.8	84.8	<b>89.4</b>	<b>87.9</b>	<b>89.4</b>	<b>89.4</b>	<b>84.8</b>
Ozone	93.3	93.3	<b>93.9</b>	<b>93.9</b>	<b>93.9</b>	<b>93.9</b>	<b>93.9</b>
Clean1	85.8	85.8	84.6	<b>92</b>	85.1	<b>87.7</b>	85.2
Semeion	94.5	94.5	<b>95.2</b>	<b>97.8</b>	<b>97.2</b>	<b>96.1</b>	<b>97</b>
Cnae	87.5	87.7	85.6	<b>88.8</b>	84.2	86.6	<b>88.3</b>
Emails	72.7	72.7	<b>81.8</b>	<b>90.9</b>	<b>72.7</b>	<b>86.4</b>	<b>77.23</b>
Gisette	91.5	91.5	<b>91.8</b>	91.2	90.3	89.4	90.9
Arcene	70.6	70.6	<b>79.4</b>	67.6	<b>85.3</b>	<b>76.5</b>	<b>76.5</b>

Table 5 shows the classification results of best reduction set. The classification results for filtered approach achieved similar results to the original data sets. Conversely, this result is still not the best since the number of reductions using filtered approach is

not optimal. Nevertheless, all bio-search algorithms with wrapper method performed better than filtered approach in terms of classification accuracy. All five (5) algorithms (ant, bat, bee, cuckoo and firefly) proved to have good classification accuracy for small size of data sets (Breastcancer, Parkinson and Ozone). Reduct data sets using bat algorithms achieved good classification results for medium data sets (Clean1, Semeion, Cnae). This is most likely due to global search features in bat algorithms that has been utilized for selecting optimal attributes. Furthermore, ant algorithms were found to have good classification result for large data sets (Emails, Gisette, Arcene). This result demonstrated ant algorithms utilized the advantages of random walk function in order to reach optimum feature selection.

**Table 6.** Ideal Combination

Data set size	Reduction Algorithm	Bio-search Algorithm
Small [1-100]	Wrapper	Ant, Bat, Bee, Cuckoo, Firefly
Medium [101-1000]	Wrapper	Bat
Large [1001-10000]	Wrapper	Ant

Table 6 shows the best combination list of reduction algorithms with suitable bio-search algorithms for various sizes of data sets. This result can be a guideline for searching optimal number of attributes based on data set size where suitability matches of the combination between reduction algorithm and bio-search algorithm.

## 5 Conclusion and Future Work

The contribution of this paper in the area of data mining is significant as it provides insight of manipulation of bio-inspired algorithms in exploration and exploitation of the search space in reducing size of feature set. This paper explores feature selection method where five (5) attribute selection search methods and two (2) reduction algorithms were compared and tested on nine (9) data sets. The obtained model (combination of search methods and reduction algorithm) has generated good classification accuracy with relevant features. Determining the parameter setting of the bio-inspired search algorithms can be considered for future work in order to determine the best setup to acquire more promising results.

## Acknowledgement

The authors gratefully acknowledge use of service and facilities of Universiti Malaysia Terengganu (UMT), Universiti Utara Malaysia (UUM) and Kementerian Pendidikan Malaysia (KPM). This research was funded by the Ministry of Higher Education Malaysia under TAPE-RG research grant (Vot No. 55133).

## References

1. R. Jensen and Q. Shen, "Finding rough set reducts with ant colony optimization," in *Proceedings of the 2003 UK workshop on Computational Intelligence*, 2003, vol. 1, no. 2, pp. 15–22.
2. R. Jensen and Q. Shen, "A rough set-aided system for sorting WWW bookmarks," *Lect. Note Comput. Sci.*, pp. 95–105, Oct. 2001.
3. N. Suguna and K. Thanushkodi, "A novel rough set reduct algorithm for medical domain based on bee colony," *J. Comput.*, vol. 2, no. 6, pp. 49–54, 2010.
4. Z. Zhao and H. Liu, "Searching for interacting features," in *IJCAI International Joint Conference on Artificial Intelligence*, 2007, pp. 1156–1161.
5. N. Suguna, K. G. Thanushkodi, and T. Nadu, "An independent rough set approach hybrid with artificial bee colony algorithm for dimensionality reduction," *Am. J. Appl. Sci.*, vol. 8, no. 3, pp. 261–266, 2011.
6. O. Fallahzadeh, Z. Dehghani-Bidgoli, and M. Assarian, "Raman spectral feature selection using ant colony optimization for breast cancer diagnosis," *Lasers Med. Sci.*, pp. 1–8, Jun. 2018.
7. W. Shahzad, A. Ellahi, and A. Naseer, "A hybrid approach for feature subset selection using ant colony optimization and multi-classifier ensemble," *Int. J. Adv. Comput. Sci. Appl.*, vol. 9, no. 1, pp. 306–313, 2018.
8. A. Chouchoulas and Q. Shen, "Rough set-aided keyword reduction for text categorization," *Appl. Artif. Intell.*, vol. 15, no. 9, pp. 843–873, 2001.
9. N. K. Ibrahim, R. S. A. R. Abdullah, and M. I. Saripan, R. S. A. R. Abdullah, and M. I. Saripan, "Artificial neural network approach in radar target classification," *J. Comput. Sci.*, vol. 5, no. 1, pp. 23–32, Jan. 2009.
10. R. Y. M. Nakamura, L. a. M. Pereira, K. a. Costa, D. Rodrigues, J. P. Papa, and X.-S. Yang, "BBA: a binary bat algorithm for feature selection," *2012 25th SIBGRAPI Conf. Graph. Patterns Images*, pp. 291–297, Aug. 2012.
11. J. P. Papa, A. X. Falcão, V. H. C. De Albuquerque, and J. M. R. S. Tavares, "Efficient supervised optimum-path forest classification for large datasets," *Pattern Recognit.*, vol. 45, no. 1, pp. 512–520, 2012.
12. R. Falcon, M. Almeida, and A. Nayak, "Fault identification with binary adaptive fireflies in parallel and distributed systems," in *2011 IEEE Congress of Evolutionary Computation, CEC 2011*, 2011, pp. 1359–1366.
13. E. Rashedi, H. Nezamabadi-Pour, and S. Saryazdi, "BGSA: binary gravitational search algorithm," *Nat. Comput.*, vol. 9, no. 3, pp. 727–745, 2010.
14. X. S. Yang and S. Deb, "Cuckoo search via Levy flights," in *2009 World Congress on Nature and Biologically Inspired Computing, NABIC 2009 - Proceedings*, 2009, pp. 210–214.
15. M. A. El Aziz and A. E. Hassanien, "Modified cuckoo search algorithm with rough sets for feature selection," *Neural Comput. Appl.*, vol. 29, no. 4, pp. 925–934, Feb. 2018.
16. A. M. Usman, U. K. Yusof, and S. Naim, "Cuckoo inspired algorithms for feature selection in heart disease prediction," *Int. J. Adv. Intell. Informatics*, vol. 4, no. 2, p. 95, Jul. 2018.
17. R. Sawhney, P. Mathur, and R. Shankar, "A firefly algorithm based wrapper-penalty feature selection method for cancer diagnosis," *Lect. Note Comput. Sci.*, pp. 438–449, May 2018.
18. S. Larabi Marie-Sainte and N. Alalyani, "Firefly algorithm based feature selection for arabic text classification," *J. King Saud Univ. - Comput. Inf. Sci.*, 2018.
19. M. Montazeri, H. R. Naji, and A. Faraahi, "A novel memetic feature selection algorithm," in *The 5th Conference on Information and Knowledge Technology*, 2013, pp. 295–300.

20. M. Aggarwal, "Performance analysis of different feature selection methods in intrusion detection," *Int. J. Sci. Technol. Res.*, vol. 2, no. 6, pp. 225–231, 2013.
21. M. Hall and G. Holmes, "Benchmarking attribute selection techniques for discrete class data mining," *IEEE Trans. Knowl. Data Eng.*, vol. 15, no. 6, pp. 1437–1447, Nov. 2003.
22. M. Hall, E. Frank, G. Holmes, B. Pfahringer, P. Reutemann, and I. H. Witten, "The WEKA data mining software," *ACM SIGKDD Explor. Newsl.*, vol. 11, no. 1, p. 10, Nov. 2009.
23. A. Masilamani, M. Anbarasi, and E. Anupriya, "Enhanced prediction of heart disease with feature subset selection using genetic algorithm," *Int. J. Eng. Sci. Technol.*, vol. 2, no. 10, pp. 5370–5376, 2010.



# Comparison of Ensemble Simple Feedforward Neural Network and Deep Learning Neural Network on Phishing Detection

Gan Kim Soon, Liew Chean Chiang, Chin Kim On, Nordaliela Mohd Rusli and Tan Soo Fun

Knowledge Technology Research Unit, Faculty of Computing and Informatics, Universiti Malaysia Sabah, Jalan UMS, 88400 Kota Kinabalu, Sabah.  
kimonchin@ums.edu.my, daliela@ums.edu.my, soofun@ums.edu.my

**Abstract.** Phishing attack is one of wide spread cybercrimes due to the advancement of the Internet. There are many forms of phishing attack and the most common one is through email. The attacker tries to pretend by sending email from an official organization or body to deceive the user in giving in their credential user name and password. The username and password are then used for malicious purpose. Many methods have been used to detect these phishing attacks; however, the attack evolved too quickly to be solved by manual approach. Therefore, automated phishing detection through artificial intelligence approach would be more feasible. In this paper, a comparison study for phishing detection between two neural networks which are the feedforward neural network and the deep learning neural network is carried out. The result is empirically evaluated to determine which method performs better in phishing detection.

**Keywords:** Phishing Attack, Feedforward Neural Network, Deep Learning Neural Network,

## 1 Introduction

Phishing has become one of the escalating threats due to Internet advancement [1]. Due to the sharing of personal information in social media, attacker can easily gather victim's personal information and plan for an attack. With this information, attacker can produce personalized and believable email tailored to specific victim.

Social engineering technique is one of most common techniques used to deceive the victim in providing personal information [2]. The attacker can spoof by constructing email from recognized organization and body to deceive victim in providing personal credential information. The advance attacker might even spoof the entire website just to acquire the victim's username and password [3].

Many methods and activities have been introduced including training sessions and specialized team to monitor and detect these emails [3]. However, the manual approaches are still prone to human error and more importantly it is very costly. Email filtering system using blacklisted-based methods might solve the problem temporary,

but, it will become inflexible when the attacker changes the email or keyword used. Therefore, an efficient and cost less solution is needed to encounter the problem.

Artificial Intelligence (AI) methods have been proven of its effectiveness and efficiency in many researches area such as gaming, image recognition, stock price forecasting, etc [4-10]. Machine learning algorithms are one of the most commonly adopted AI methods for detecting phishing attack, particularly using Artificial Neural Network (ANN) [11]. ANN is a biological model with high adaptability on changes. It has the ability to learn and model non-linear and complex relationships. ANN has shown to perform well in many information processing in various fields [11,12]. There are many types of ANN architecture including multilayer network architecture, feedforward neural network and recurrent neural network, amongst others. The most famous learning algorithm for ANN would be backpropagation algorithms [12]. It is a supervised learning algorithm to reduce the learning error by comparing the predicted output with targeted output and adjust the weight based on the errors reported.

In this paper, the ANN is adopted to detect the dynamic changing phishing emails. Two ANN methods are adopted in the experiment namely 1) ensembled feedforward neural network (EFFNN) and 2) deep learning neural network (DLNN). DLNN has been proven to be superior in many research areas. However, thus far no one has confirmed the DLNN performance in phishing attack. Hence, it motivates us to compare the performance of both ANNs.

## 2 Related Works

There are three types of phishing attacks namely the spear phishing, whaling phasing and clone phishing. Spear phishing is normally targeted on specific individual or organization. Whaling phishing targets the high profile or powerful individual in the companies to retrieve confidential information of the organization whilst clone phishing is to deceive the victim with a cloned version of an original website. Researchers have developed few automated phishing detection techniques that is divided into content-based approaches, non-content-based approaches and visual similarity approach. Content-based approaches is based on the contents or features of the phishing message. The features used include message size, embedded links, abnormal URL, spelling errors and others. One of example is the SpoofGuard tool [13]. SpoofGuard is a client-site defence tool acts as a plugin for IE browser to defend against phishing attack. A threshold value is used to evaluate the message features to determine the phishing message.

On the contrary, the non-content-based approaches is based on URL and host information. A blacklist method is utilized as a basic control mechanism and as a database list. PhishNet is one of the non-content-based approach [14]. PhishNet is composed of two components to detect the phishing messages which use the URL prediction and pattern matching of the URL components. The pattern matching mechanism utilizes both hasp map together with regular expression. Besides, a white list is used to maintain a list of good websites. Two of the lists are used together to lower the false positive rate.

The visual similarity approach compares the website features such as website layout, colour schemes, and others. The goal is to determine if the two suspicious websites are similar. The earth move distance is used to calculate the similarity between two websites [15]. Machine learning is applied to determine the threshold for the earth move distance for the similarity. BaitAlarm is a tool that utilize the CSS based comparison to determine the phishing attack [16]. AI methods have been adopted in detecting phishing attacks since a decade ago. Chadrasekaran derived a set of message features to detect phishing from the email dataset [17]. The experiment derived 25 features including 18 functional words and 7 marker attributes and styles. ANN was used to train on 200 email datasets where 100 out of the dataset was phishing emails and the result showed a better performance when the functional word is unique to emails. Fernando used a sender-centric approach to detect the phishing email [18]. He used a two-step system to detect the phishing email. The first step was to segregate legitimate and phishing email messages by using a SVM classifier whilst the second step was to determine sender-related information by using a set of heuristic rules. Three different fields of email were used which include the email account from public email service providers, sender geographical locations and the authorized sender. The dataset used in the research had 1001 phishing message, 1400 message from EasyHam corpus, 50 phishing and 10 legitimate banking messages. Two groups of experiments were conducted in the research. The first group consisted of the performance of SVM classifier to differentiate banking and non-banking messages whilst the second group comprises the performance of rules to identify phishing messages from legitimate banking messages. Both experiments achieved more than 90% accuracy results.

Abu-Nimeh had conducted a machine learning comparison for phishing detection too [19]. Six different machine learning techniques were used in the comparative study namely logistic regression (LR), classification and regression tree (CART), random forest (RF), neural network (NNet), SVMs and Bayesian additive regression trees (BART). A total of 43 features were used in the study. The dataset of the experiment contains a total of 2,889 emails where 1,718 were of legitimate emails and the remaining 1,171 were of phishing emails. The 10-fold cross-validation was to validate the experimental result and the result shows that ANN performed well in the experiment.

Moving on, Rami had performed a phishing detection study by using backpropagation FFNN using MATLAB [20]. A total of 18 features were used to differentiate phishing and legitimate message. It is a three-layer architecture with two hidden neurons in the hidden layer. The learning rate used was 0.7. MSE was used to evaluate the experimental result. The dataset used for the experiment contained 2,000 phishing email and 2,000 ham emails. 3,000 messages were used as the training dataset and 1,000 messages were used as the testing set. The experiment claimed to achieve 99% of accuracy rate. Similarly, Zhang & Yuan used 18 features to detect the phishing email with FFNN [21]. A huge dataset was used, it contained a total of 4,202 ham emails and 4,560 phishing emails. Ghazi and Loay also used FFNN to detect the phishing email [22] where 18 features were extracted from the header and body of the email. The experiment was carried out with different number of hidden neurons used.

The result showed that FFNN achieve an accuracy of 98.72% and 0.0053% false positive rate.

### 3 Methodology

In this study, there are two experiments involved. First experiment used EFFNN. The ensemble method is a combination of outputs of many NNs which gives a more accurate prediction and significantly improve generalization ability than any of the single network [23]. In the ensemble methods, the ensemble outputs of the NNs are calculated either by selecting most votes or averaging all the outputs. The activation function used is sigmoid function. Ensemble methods used are capable to improve performance and the generalisation ability of the NNs. DLNN, on the other hand, is also in feed forward pattern which composed of at least two or more hidden layers. The advantages of DLNN is that it performs better when processing unstructured data. It has the ability to deduce new features in more sophisticated feature set. The gradient descent technique is used in changing the weights in every iteration to minimize the cost function. In this work, the whole process of the experiment involves the set features determination, pre-processing the dataset, and training with EFFNN and DLNN. The pre-processing steps include dataset cleaning and extracting the dataset into binary form. The email in dataset is parsed with email content and header by using the quopri python library. The content is then parsed further with depth-first traversal order. There are 18 features used in the experiments and it is listed as in Table 1 below.

**Table 1.** 18 features used for phishing detection

No	Features
1	Existence of HTML code embedded within email
2	The number of pictures used as link is more than 2
3	The number of different domains in the email is more than 3
4	The number of embedded links in the email is more than 3
5	The message has HTML code included <form> tag
6	“From” domain is not equal to “ReplyTo” domain
7	The message size less than 25KB
8	The message has JavaScript Code
9	Nonmatching between target and appeared text of URLs in the email
10	Email message has a link like the IP address
11	The message has one of the words “click here”, “click”, or “here”, or “login” in text part of links
12	The number of dots in the domain is more than 3
13	The message has @ symbol in URL
14	The URL in the message has a port value other than 80 or 443
15	The domain of any embedded links in the HTML body is not equal to sender’s domain
16	If https:// is used instead of http://
17	Existence of hexadecimal numeric representation in the links
18	The email is classified as spam by SpamAssassin 3.2.3.5 Win 32.

The CSDMC2010 SPAM corpus dataset is adopted in this study. This dataset has been used in data mining competition associated with ICONIP 2010. The dataset contains 4,327 messages with 2,949 ham emails and 1,378 phishing emails. The settings for the two NNs are discussed in next section.

## 4 Experimental Setup

The EFFNN used has combined and averaged several NN outputs in order to predict new output. A simple two-layer FFNN architecture is adopted with the neurons 18-10-1. Backpropagation is adopted as the learning algorithm. The sigmoid transfer function is used in the training. The learning rate of 0.1 and iterations of 1000 are used in the experiment.

The DLNN is different from EFFNN as it does not aggregate output from multiple learning and it has an extra hidden layer compared to FFNN. The DLNN used has the same 18 input neurons as FFNN but with two hidden layers used. Each layer has 10 hidden neurons. The output layer is same as FFNN setting which contains only one output neuron. The other settings are same as EFFNN experiment setting. Table 2 shows the default parameter setting used for both EFFNN and DLNN.

**Table 2.** Default Parameter Setting for EFFNN and DLNN

Descriptions	EFFNN Setting	DLNN Setting
Input Layer Neuron	18	
Hidden Layer Neuron	(input neurons + output neurons) / 2	
Output Layer Neuron	1	
Number of Hidden Layer	1	2
Number of Networks	2	1
Transfer Functions	Sigmoid Function	
Learning Algorithm	Backpropagation	
Epoch	1000	
Learning Rate	0.1	
Batch Size	NIL	100
Total Experiments	10	10

The first run of EFFNN and DLNN experiments had shown that the results generated very low success rate. It might be happened due to unsuitable parameter setting used in the experiments. We were unable to benchmark any parameter setting due to lack of research published using similar algorithm. Hence, a series of preliminary experiments had been carried out to fine tune the NNs parameters in order to obtain a better combination of fine-tuning parameters values and its results.

The EFFNN tuning processes involved number of NNs used, number of hidden neurons used, range of epochs, and range of learning rate. The DLNN tuning processes involved number of hidden layers, number of hidden neurons, number of epochs, batch size and range of learning rate. Tables 3 and 4 have shown the range of parameters used in the tuning experiments.

**Table 3.** Tuning Parameters used in EFFNN.

Tuned Parameters	Values
Number of neural networks	2 - 10
Number of hidden neurons	1 - 10
Number of epochs	250, 500, 750, 1000
Learning rate	0.001 – 0.009, 0.1 – 0.9

**Table 4.** Tuning Parameters used in DLNN

Tuned Parameters	Values
Number of hidden layers	2 - 10
Number of hidden neurons	1 - 10
Number of epochs	250, 500, 750, 1000
Batch size	64, 128, 256, 512
Learning rate	0.001 – 0.009, 0.1 – 0.9

## 5 Results and Discussions

### 5.1 EFFNN Tuning Experiment Results and Discussions

The EFFNN experiment results are shown in Tables 5, 6, 7, 8 and 9. Table 5 has shown that the average test accuracy rate is higher with three NNs used and Table 6 has shown that each NN should acquire two hidden neurons in order to generate high average test accuracy rate. Thus, the number of hidden neurons required in training the EFFNN topology is lower if we compared to the single FFNN experiment that discussed in [8]. The learning time is shortened with a smaller number of hidden neurons used.

**Table 5.** Result for Different Number of NNs used

No. of Neural Networks	Average Acc
2	93.11%
3	<b>93.77%</b>
4	93.55%
5	92.89%
6	93.33%
7	93.55%
8	93.55%
9	93.33%
10	93.55%

**Table 6.** Result for Different Number of Hidden Neurons used

No. of Hidden Neurons	Average Acc
2	<b>94.44%</b>
3	93.55%
4	93.55%
5	92.55%
6	93.78%
7	93.33%
8	93.11%
9	93.11%
10	93.55%

Tuning learning rate tasks is much more difficult compared to other tuning experiments. Most of the references had suggested that the learning rate used in the learning process should be very low, in the rage of 0.001 – 0.1 [7,8]. However, Table 7 has shown that the EFFNN performed better with 0.05 learning rate used.

**Table 7.** Result with Different Learning Rate used

Learning Rate	Average Acc	Learning Rate	Average Acc
0.01	94.21%	0.001	84.89%
0.02	93.77%	0.002	86.67%
0.03	93.55%	0.003	88.89%
0.04	94.44%	0.004	91.11%
0.05	<b>94.67%</b>	0.005	93.77%
0.06	93.99%	0.006	93.99%
0.07	94.22%	0.007	93.77%
0.08	93.99%	0.008	93.99%
0.09	93.44%	0.009	94.44%
0.1	93.44%		

Table 8 has shown the experimental results obtained for tuning with different number of epochs. It is clearly showing that the EFFNN were over trained if the number of epochs used is more than 500.

**Table 8.** Result for Different Number of Epochs used

Epochs	Average Test Accuracy
250	94.67%
500	<b>94.89%</b>
750	94.22%
1000	93.77%

**Table 9.** Summary of Parameter Tuning for EFFNN experiments

Training Parameters	Value
Number of Neural Network	3
Number of Hidden Neuron	2
Epoch	500
Learning Rate	0.05

Table 9 has shown the summary of EFFNN parameter tuning results. The EFFNN performed better with aggregation of three NNs used, two hidden neurons for each hidden layer, maximum 500 training epochs and 0.05 learning rate.

## 5.2 DLNN Tuning Experiment Results and Discussions

The DLNN tuning experimental results are tabulated in Tables 10, 11, 12, 13, and 14. Tables 10 and 11 have shown that the DLNN performed optimal with 6 hidden layers and 10 hidden neurons used. This has proven that the training dataset used is complex and the DLNN took more training time compared to the EFFNN.

Table 12 has shown that the DLNN needs more training iteration in order to generate optimal success rate and the overall testing accuracy has been increased with the increment of epochs used. Furthermore, Table 13 has shown that the batch size involved should be 128. Increment of binary batch used has reduced the average success rate of the training. Table 14 has shown that the DLNN could generate optimal success rate with 0.002 of learning rate. This is contradicted to the EFFNN experiment as the EFFNN could generate high accuracy rate with larger learning rate used.

**Table 10.** Result for Different Number of Hidden Layers used

No. of Hidden Layers	Average Test Accuracy
2	92.22%
3	92.89%
4	92.44%
5	91.56%
6	<b>94.22%</b>
7	93.77%
8	73.11%
9	93.33%
10	66.00%

**Table 11.** Result for Different Number of Hidden Neurons used

No. of Hidden Neurons	Average Test Accuracy
2	93.99%
3	92.88%
4	93.77%
5	93.99%
6	93.55%
7	93.99%
8	93.78%
9	93.78%
10	<b>94.21%</b>

**Table 12.** Result for Different Number of Epochs used

Epochs	Average Test Accuracy
250	84.00%
500	84.44%
750	85.11%
1000	<b>93.11%</b>

**Table 13.** Result for Different Number of Batch Size Involved

Batch Size	Average Test Accuracy
64	92.67%
128	<b>93.78%</b>
256	89.37%
512	66.00%

**Table 14.** Result for Different Learning Rate used

Learning Rate	Average Test Accuracy
0.01	92.89%
0.02	93.11%
0.03	92.66%
0.04	92.89%
0.05	92.44%
0.06	93.11%
0.07	84.00%
0.08	83.99%
0.09	84.22%
0.1	84.89%

Learning Rate	Average Test Accuracy
0.001	92.22%
0.002	<b>93.55%</b>
0.003	93.11%
0.004	92.67%
0.005	93.11%
0.006	93.33%
0.007	92.89%
0.008	93.33%
0.009	93.33%

As a summary, the DLNN experimental results had showed that the DLNN could perform optimal with 6 hidden layers, 10 hidden neurons in each hidden layer, 1000 epochs, 0.002 of learning rate, and batch size of 128.

The parameter tuning results are then used to rerun the EFFNN and DLNN training and testing. The results are shown in Table 16. It can be observed that the EFFNN has performed slightly better than the DLNN for this phishing study case. This has proven

that the combination of few FFNN would provide more accurate prediction and improve the generalization ability. The other reasons might be due to the dataset used which can be considered as structured data compared to unstructured data such as images and videos where the DLNN used to perform better.

**Table 15.** Accuracy Comparison between EFFNN and DLNN.

Neural Networks	Average Test Accuracy (10 runs)
Ensemble Feedforward Neural Network (EFFNN)	94.41%
Deep Learning Neural Network (DLNN)	94.27%

## 6. Results and Discussions

This study investigates the use of NNs in phishing detection. There were two types of NNs used in this investigation which are Ensemble Feedforward Neural Network (EFFNN) and Deep Learning Neural Network (DLNN). The CSDMC2010 SPAM corpus dataset were used in the experiments. There were 18 unique features used to distinguish between SPAM and HAM messages. Besides, a series of parameter tuning experiments were also conducted to fine tune the NNs parameters setting in order to generate optimal solutions and high accuracy rate. The results have shown that the EFFNN performed slightly better than the DLNN due to the nature of the dataset and the generalization ability of ensemble.

## Acknowledgment

This project is partially supported by university SBK0366-2017 research grant.

## References

1. Vayansky, I., Kumar, S.L.: Phishing—challenges and solutions. Computer Fraud & Security (1), 15-20 (2018).
2. Gupta, B. B., Tewari, A., Jain, A. K., Agrawal, D. P.: Fighting against phishing attacks: state of the art and future challenges. Neural Computing and Applications 28(12), 3629-3654 (2017).
3. Gupta, B. B., Arachchilage, N. A., Psannis, K. E.: Defending against phishing attacks: taxonomy of methods, current issues and future directions. Telecommunication Systems 67(2), 247-267 (2018).
4. Chin, K. O., Chang, K. T., Teo, J., Alfred, R., Cheng, W., Tan, T. G.: Self-Evaluation of RTS Troop's Performance. Journal Teknologi. UTM Press. 76(12), 119–126 (2015).
5. Tan, T. G., Yong, Y. N., Chin, K. O., Teo, J., Alfred, R.: Automated Evaluation for AI Controllers in Tower Defense Game Using Genetic Algorithm. CCIS 378, Springer-Verlag Berlin Heidelberg, 135–146 (2013).
6. Ian, K. W., Chin, K. O., Alfred, R., Asri A. A. A., Tan, T. G., Anthony, P.: A Review of Computer Vision Methods for Fruit Recognition. Advanced Science Letters 24(2), 1538-1542 (2018).

7. Connie, L., Chin, K. O., Anthony, P.: A Review of Automatic License Plate Recognition System in Mobile based Platform. *Journal of Telecommunication, Electronic and Computer Engineering* 10(3-2), 77-82 (2018).
8. Chin, K. O., Teo, K. Y., Alfred, R., Teo, J., Anthony, P., Cheng, W.: Backpropagation Neural Ensemble for Localizing and Recognizing Non-Standardized Malaysia's Car Plates. *International Journal on Advanced Science, Engineering and Information Technology* 6 (2016).
9. Chang, S. V., Chin, K. O., Gan, K. S., Alfred, R., Anthony, P.: External Constraints of Neural Cognition for CIMB Stock Closing Price Prediction. UPM Press (2017).
10. Phang, W. S., Tan, L. I., Anthony, P., Chin, K. O.: Improving the Accuracy of Stock Price Prediction Using Ensemble Neural Network 24(2), 1524-1527 (2018).
11. Gupta, N.: Artificial neural network. *Network and Complex Systems* 3(1), 24-28 (2013).
12. Chang, S. V., Gan, K. S., Chin, K. O., Alfred, R., Anthony, P.: A review of stock market prediction with Artificial neural network (ANN). In 2013 IEEE International Conference on Control System, Computing and Engineering, pp. 477-482. IEEE (2013).
13. Teraguchi, N. C. R. L. Y., Mitchell, J. C.: Client-side defense against web-based identity theft. Computer Science Department, Stanford University (2004).
14. Prakash, P., Kumar, M., Kompella, R. R., Gupta, M.: Phishnet: predictive blacklisting to detect phishing attacks. In 2010 Proceedings IEEE INFOCOM, pp. 1-5. IEEE (2010).
15. Fu, A. Y., Wenyin, L., Deng, X.: Detecting phishing web pages with visual similarity assessment based on earth mover's distance (EMD). *IEEE transactions on dependable and secure computing* 3(4), 301-311 (2006).
16. Mao, J., Li, P., Li, K., Wei, T., Liang, Z.: BaitAlarm: detecting phishing sites using similarity in fundamental visual features. In 2013 5th International Conference on Intelligent Networking and Collaborative Systems, pp. 790-795. IEEE (2013).
17. Chandrasekaran, M., Narayanan, K., & Upadhyaya, S.: Phishing email detection based on structural properties. In NYS cyber security conference (Vol. 3). (2006).
18. Sanchez, F., Duan, Z.: A sender-centric approach to detecting phishing emails. In 2012 International Conference on Cyber Security, pp. 32-39. IEEE (2012).
19. Abu-Nimeh, S., Nappa, D., Wang, X., Nair, S.: A comparison of machine learning techniques for phishing detection. In Proceedings of the anti-phishing working groups 2nd annual eCrime researchers summit, pp. 60-69. ACM (2007).
20. Mohammad, R., McCluskey, T. L., Thabtah, F. A.: Predicting phishing websites using neural network trained with back-propagation. World Congress in Computer Science, Computer Engineering, and Applied Computing. (2013).
21. Zhang, N., Yuan, Y.: Phishing detection using neural network. Department of Computer Science, Department of Statistics, Stanford University. CA (2013).
22. Jameel, N. G. M., George, L. E.: Detection of phishing emails using feed forward neural network. *International Journal of Computer Applications* 77(7). (2013).
23. Hansen, L. K., Salamon, P.: Neural network ensembles. *IEEE Transactions on Pattern Analysis & Machine Intelligence*, (10), 993-1001 (1990).



# Design and Development of Multimedia and Multi-Marker Detection Techniques in Interactive Augmented Reality Colouring Book

Angeline Lee Ling Sing, Awang Asri Awang Ibrahim, Ng Giap Weng, Muzaffar Hamzah, Wong Chun Yung

Faculty of Computing and Informatics, Universiti Malaysia Sabah,  
88400 Kota Kinabalu, Sabah, Malaysia  
[lingsing@hotmail.com](mailto:lingsing@hotmail.com), [nggiapweng@ums.edu.my](mailto:nggiapweng@ums.edu.my)

**Abstract.** The aim of this paper is to the design and develop multimedia and multi-markers detection techniques in interactive Augmented Reality (AR) colouring book application for aquarium museum. This study is conducted to create entertaining AR colouring mobile application on Android Operating System which allows users to express, create and interact with their creativity through colouring activities. It allows users to engage and relish the stimulating colouring book content by switching between a reality and augmented world. Conversely, users may tend to lose interest in the colouring activities, but with AR technology it keeps colouring relaxing and inspiring. The design and development of this project was carried out using Unity3D integrates with Vuforia Engine. The multimedia and multi-markers scripting was written in C# programming language.

**Keywords:** Augmented Reality, Multimedia, Multi-Markers, Colouring book.

## 1 Introduction

A colouring book is a type of book containing line art targeting user especially children to add colour using either crayons, colour pencils, marker pens, water colour paint or any form of artistic media. Colouring book is a platform for user to express their imagination, creativity, emotional-feeling as well as opinions in daily life. Creating entertaining and educational books not only requires visually stimulating content but also means for students to interact, create, and express themselves [1]. Nowadays, children are captivated in using electronic devices for many purposes either for fun playing or learning. Hence, children tend to divert to 3D objects AR colouring application compared to conventional way of colouring book which expose only 2D images. Contrary, implementing AR into colouring book is deem as a way for user to learn new method, discover a new perception of reality, curiosity, and develop a sense of patience and calmness in daily life.

In today's technology hype, colouring has evolved from physical book to mobile colouring application. For example, SMASHINGMAG, Monochromatic Scheme, Mandala drawing app, Colorfly (Coloring Books for adults), and Family Coloring Pages.

Users can start colouring and drawing using variety colours options provided in the application anytime and anywhere without the need to carry a book and colour pencils. Nevertheless, some of the colours may not be suitable to all the user's interest as users may be limited to certain colour choices offered in the system. Hence, when users are done with the colouring in the application, there is no further interaction, and this made the colouring application become less fun and attractive. Therefore, by designing and developing finger motion features in AR colouring book would certainly benefit user to gain a whole new experience, knowledge and cognitive-emotional curiosity.

## 2 Problem Statement

Conventional colouring book however do not have further interaction that can be seen through 3D from the screen. Attentively, colouring book is a book which contains art where user can add colour such as coloured pencil, water colour and marker pens onto the book. User may tend to get uninterested seeing the same colouring design and there is no uniqueness to the colouring design. Hence, the colouring book will eventually lose its attention to the user. Consequently, to make image ‘pop-up’ through mobile screen is by implementing AR in the colouring book app. With AR, it supports users to understand art experientially, appreciate art in a new perspective and getting user excited about checking out the art museum and gallery [2]. However, the interaction only happened to the physical touch screen of the mobile device, limited interaction where user can interact with the object that overlay on the screen. The interaction within AR application are still limited [3] and not advanced like allowing the user to touch and interact with the object so that it will change its colour or turn it into others object.

AR helps create interactive and experiential art, users get to interact and be creative with the art that will creates a memorable experience [4]. Furthermore, AR is the perfect approach to creativity. With AR technology there are infinite number of ways to alter user's environment. This technology is suitable to enhance user creativity and imagination [5]. Therefore, by designing and develop multimedia and multi-markers features in AR colouring book will add other features from the previous and existing AR colouring book.

## 3 Objective and Scope of Study

The objective of study is to design and develop multimedia and multi-markers detection techniques in AR colouring book. User is required to scan the colouring book using their mobile cameras. Subsequently, the colour chart options and interaction buttons will pop-out once the markers are detected. The application will display the virtual content in real environment. Human Computer Interaction (HCI) principles are applied as guidelines for designing the interface process and system flow of the colouring application.

## 4 Methodology

### 4.1 System Development Model

The Rapid Application Development Model (RAD) method is utilised in this study. According to Ghahrai (2018), the advantage of this RAD model is that the development time is reduced and can increase the reusability of components [6]. There are four phases involved in RAD Model which consists of requirements planning, user description, construction and evaluation.

**Requirements Planning.** The requirements planning definition require developer to identify the objectives and the requirements of the study based on the technical review. During this phase, developers determine the goals and expectations for the project as well as current and potential issues that would need to be addressed during the buildup.

**User Description.** During this phase, developer needs to gather design information survey which comprise the design component from user's perception before implementing it on a working prototype.

**Construction.** The development of the mobile application system is compelling to coding, testing, system design and implementation to ensure the system is developed smoothly. The system phase breaks down into several process which include designing user interface application; create 3D objects for the application; coding use for interaction of 3D coloured image; and finally, the system integration and testing.

**Evaluation.** Lastly, evaluation will be performed to evaluate the mobile colouring application. Developer will conduct the system usability testing and collect feedback from users regarding the system to find problems. Figure 1 shows the process of RAD Model.

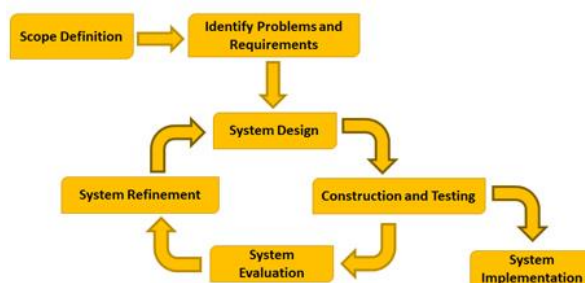


**Fig. 1.** Rapid Application Development Model (RAD)

## 4.2 Software

**Unity.** Unity is a closed-source, cross platform game development application. Unity creates game by manipulating objects in 3D and attaching various components together. Even 2D games must be manipulated in 2D/3D. Scripts are written in C#, Boo or Unity script and attached to 3D objects as component. This application software can be used in different platforms such as iOS, Android, VR, desktop and TV. Besides, Unity provides high-end visuals, audio, animation, physics and simulation which allows user to create any type of games. It is a powerful and ideal software to develop AR colouring book and Android platform in this study.

**Vuforia Augmented Reality SDK.** Vuforia is an augmented reality software development kit (SDK) for mobile devices that enables creation of augmented reality applications. It uses computer vision technology to recognize and track planar images (Image Targets) and simple 3D objects, such as boxes in real time. Vuforia works by using computer vision technique whereby it will detect image or marker and display the 3D virtual object relative to the image or marker position and camera position. In this study, Vuforia is imported to Unity as a plugin to Unity software.

## 4.3 Conceptual Design

For conceptual design application, user must first point the web camera towards the image target. Once the image is recognised by the system, the colour which is coloured by user on the colouring book will be extracted accordingly with the texture extracted and be mapped on the surface of the 3D model. After mapping the texture onto the 3D model, the model will be augmented on the colouring application where the texture of the 3D model is exactly look like how the user colour the 2D representation of the 3D model on the colouring book. After successfully augmenting the 3D model on the colouring book, user can choose to take photo or make the texture of the 3D model permanent instead of real-time texturing. When user aims to take photo, the system will lead user to another screen where the augmented 3D model will appear in the middle of the screen and is able to be manipulated by fingers for rotating, translating or scaling the 3D model. Finally, user can press capture button to capture a photo where the photo will be blending the augmented object in real environment. Figure 2 displays the flowchart of the system process.

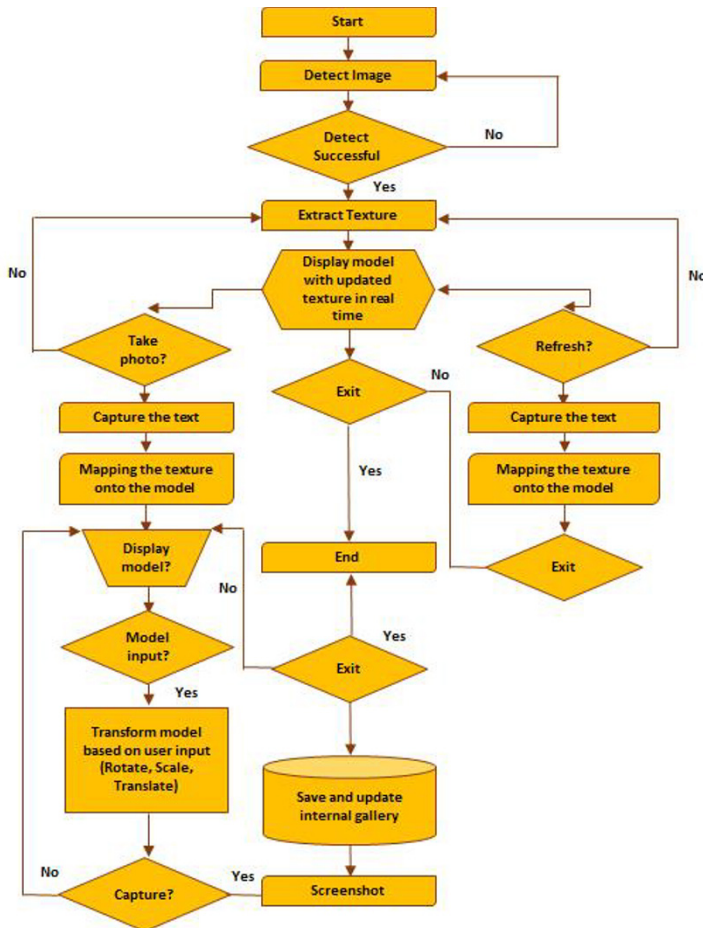


**Fig. 2.** Flow chart of the system process

#### 4.4 Data Flow Diagram of Development Process

Figure 3 shows the overview data flow diagram of the development process with the implementation of Vuforia Engine in Unity. The initial step of the development process is uploading image target into target management system in Vuforia Engine Developer Portal. Once the image target is successfully uploaded, the file will be available for download in unity editor format and import the target image unity package into unity project. The next step is to load image target into the unity project scene and add content in the target such as 3D model, user interface and multimedia content. Furthermore, the inspector panel in Unity3D is used to control the game object settings, configure component attributes and the connection between game object and image target.

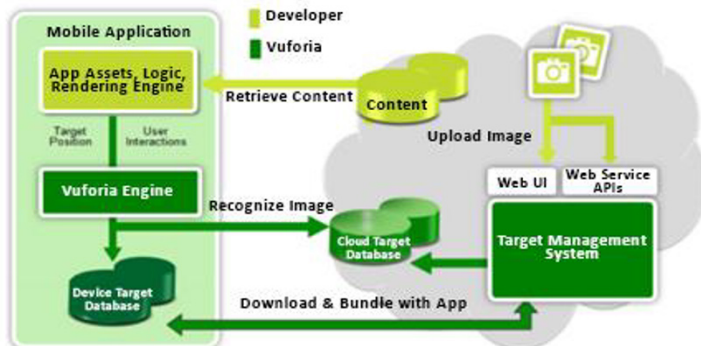


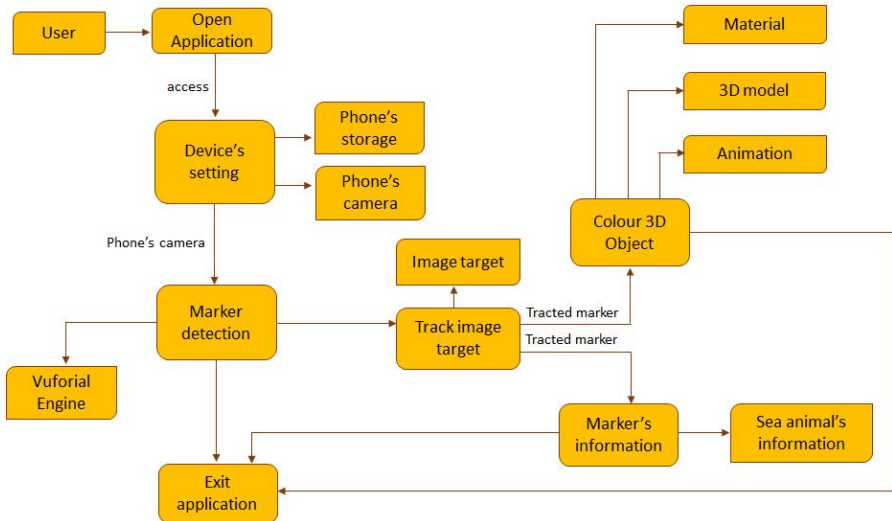
**Fig. 3.** DFD of development process

#### 4.5 Data Flow Diagram of AR Colouring Book

Figure 4 depicts the data flow diagram of the Mobile AR Colouring Book application. The data flow of this application shows in the following: First, user will open the application on their device. The application will request permission from user to access the device's camera and storage when the application is launched for the first time. Rejecting permission to access the camera will result in failure to use the application, as the camera is important for image tracking.

Once the user is allowed by the application to access the device camera, it will instantly display the camera interface. User will navigate the camera for image or marker detection, and the application will track the image target. Image target is a visual image where Vuforia Engine can detect and track. In addition, image targets do not need special black and white regions such as barcode or QR code to be recognized. Image target is detected based on the features that is found in the image itself by comparing the features in live camera image. Once image target is recognized by Vuforia Engine, the content on the image target will be available as long as the detected image target is in the camera's field of view. A good image target must have a lot of features that is rich in details, good contrast and no repetitive patterns that could confuse the image tracking. Furthermore, after the image target or marker is tracked, two options will appear under the image target which are the 3D colouring and information option.

When user picks 3D colouring option, it will redirect user to the selected 3D colouring scene. In 3D colouring scene, user can interact with the 3D object by selecting colour on the colour selector on the top left of the application and touch the 3D object to apply colour on it. User can control the 3D object by clicking the scaling and rotate button that is available on the screen. Besides, user can see the 3D motion by clicking the play button to activate the animation. When user clicks on the information button that is available below the image target, the information about the selected image target will pop-out on the screen for educational purpose. Not only user can have fun with the application, but also learn the interesting facts about the sea animals.

**Fig. 4.** DFD of AR Colouring Book

#### 4.6 Marker Design

This AR project experiment-based study is using multi-markers detection techniques (Marker-based AR). Marker-based AR uses camera to capture marker then produce the result on the screen. The marker design could be a quick response to code (QR code), barcode or images. These markers will be uploaded and stored in Vuforia Developer Portal.

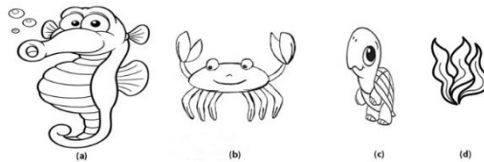
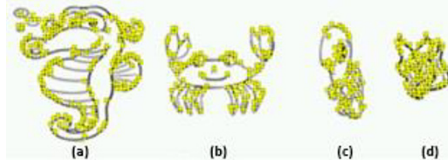
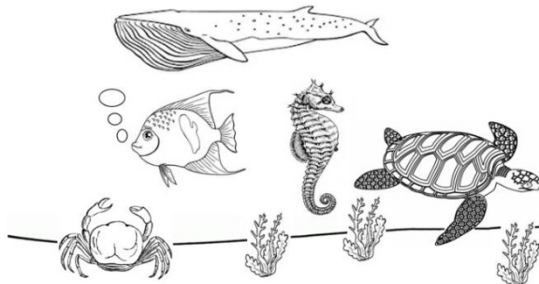
**Fig. 5.** 2D Objects

Figure 5 above illustrates four different 2D drawing. Each of the drawing from (a) to (d) represent as a unique marker. There will be three stages of marker recognition process. First, the image conversion where the image will be converted to binary image. Next, from the binary image it will compute the features point (see Fig. 6) below and finally markers identification. It shows that each marker has a unique features point.

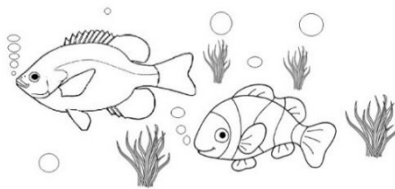
**Fig. 6.** 2D Objects Features

Sources: Vuforia Developer Portal – Markers uploaded to target manager

#### 4.7 Colouring Book Design



**Fig. 7.** AR Colouring Book Design No.1



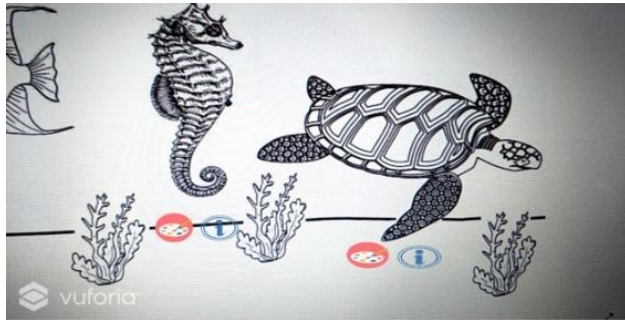
**Fig. 8.** Colouring Book Design No.2

Figure 7 and Figure 8 illustrate the sample of black and white colouring book objects design. This application is developed specifically for Aquarium & Marine Museum, University Malaysia Sabah (UMS). Hence, the theme of the colouring book is relating to the sea animals. Each of the sea animals or objects above represent a unique marker, where user will use their device to track the mural design in order to trigger the interaction in the application.

#### 4.8 User Interface Design

Once the application has been launched, the first things user should see after the application is fully loaded is the AR camera. User is required to point the camera to colouring book design in order to interact with it. If the AR camera recognize the marker on the colouring book, the colour and information button will appear on the screen below the marker. The colour buttons allow user to colour the 3D object with

their choice of preference, example of colour options (see Fig. 9). The information button will appear detail descriptions pertaining the selected marker for education purposes.



**Fig. 9.** Augmented Reality Camera Interface

Figure 10 represents the colour selector that is used to choose a variety choice of colour for 3D object.

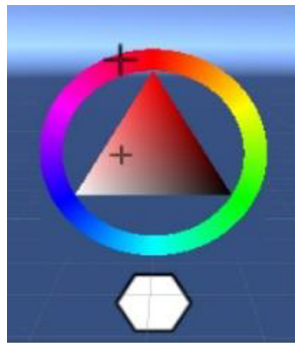


**Fig. 10.** Colour Selector

## 5 Scripting C# to Control Unity Game Object

### 5.1 Scale, Rotate and Navigate Scene with Button

As shown in figure 11 below, there are a total of five buttons available for user to interact. From the top right corner, the button is used to scale up, down 3D model and activate animation while the button on the top left corner is to navigate going back to the main scene and button next to it, is for rotating 3D modelling.



**Fig. 11.** The User Interface of 3D Colouring Scene

```
public void ScaleUpButton()
{
    GameObject.FindWithTag("Model").transform.localScale += new Vector3(scalingSpeed, scalingSpeed, scalingSpeed);
}

public void ScaleDownButton ()
{
    GameObject.FindWithTag ("Model").transform.localScale += new Vector3 (-scalingSpeed, -scalingSpeed, -scalingSpeed);
}
```

**Fig. 12.** Scale Up and Down C# Script

```
public void SceneLoader(int SceneIndex)
{
    SceneManager.LoadScene(SceneIndex);
}
```

**Fig. 13.** Navigate Scene C# Script

```
public void RotationRightButton ()
{
    GameObject.FindWithTag ("Model").transform.Rotate (0, -rotationSpeed * Time.deltaTime, 0);
}
```

**Fig. 14.** Rotation C# Script

## 5.2 5.2 3D Models

The 3D models used in this project are imported from CadNav. CadNav is a website that provide 3D models with permissive licence to use freely for commercial or non-commercial purposes. It contains all kind of 3D models ranging from furniture to character, decoration, plant, animals and others. Figure 15 shows a sample of 3D model of a seahorse with details description.



**Fig. 15.** 3D Model Details

Figure 16 shows all the 3D models that are used in this project. These 3D models do not have any texture colour on it. The purpose of using white texture in these 3D models is to allow user to colour the 3D models based on personal choice of preference.

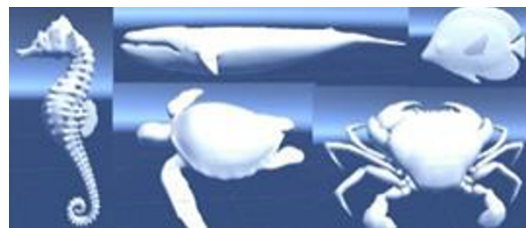


**Fig. 16.** Sea Animal 3D Models

## 6 Discussion and Conclusion

This colouring mobile application is created with a repetitive technique to assist user to express colouring creativity and appreciate content by interacting with 3D augmented object. This experimental-based study is solely focus on cooperating the methods involvement to design and develop AR colouring application. The strengths of this app are, it contains colouring interaction by overlying content on image target in real time environment; it is educational, as user is able to acquire information object; the multiple image target detection allows user to track more than one marker or object simultaneously. However, the drawbacks of AR colouring is the operating system only support Android Operating System and the ability to track marker depends on the sensitivity distance between the marker and camera.

## 7 Conclusion

There is room for improvement for new features which are to be experimented such as video content and images capture. Visual appearance interface system can be improved to maximize usability and user experience. To date, current application supports only android operating system device. Hence, more supported platforms such as IOS device will be developed in the near future.

## References

1. Clark, A & Duenser, A.: An interactive augmented reality coloring book. IEEE Symposium on 3D User Interfaces 2012, 3DUI 2012 - Proceedings. 7-10. 10.1109/3DUI.2012.6184168 (2012).

2. Kendall, J.: *How Augmented Reality will make street art come to life*. Retrieved from bighink: <https://bigthink.com/jonathan-kendall/how-augmented-reality-will-revolutionize-the-art-world>, last accessed 2018/5/2.
3. Speicher, M., Brian, D. H., Yu, Ao., Zhang, B., Zhang, H., Nebeling, J. & Nebeling, M.: XD-AR: Challenges and Opportunities in Cross-Device Augmented Reality Application Development. Proceedings of the ACM on Human-Computer Interaction, Vol. 2, No. EICS, Article 7.10.1145/3229089 (2018).
4. GreenBuzz.: *Art, Museums, And Augmented Reality*. Retrieved from GreenBuzz: <http://greenbuzzagency.com/art-museums-augmented-reality/>(2017).
5. Roylance, W.: *Augmented Reality: A Holistic Approach to Creativity*. Retrieved from diplomaticourier: <https://www.diplomaticourier.com/2017/05/03/augmented-reality-holistic-approach-creativity/> (2017).
6. Ghahrai, A.: What is the RAD Model. Retrieved from <https://www.testingexcellence.com/rapid-application-development-rad/>(2018).



# From A Shared Single Display Application to Shared Virtual Space Learning Application

Gary Loh Chee Wyai<sup>1</sup>, Cheah Waishiang<sup>2</sup>, Muhammad Asyraf Bin Khairuddin<sup>2</sup> and Chen Chwen Jen<sup>2</sup>

<sup>1</sup>School of Computing, University College of Technology Sarawak, 96000, Sibu, Sarawak, Malaysia

<sup>2</sup>Faculty of Computer Science & IT, UNIMAS, Kota Samarahan, Sarawak, Malaysia  
wscheah@unimas.my

**Abstract.** Shared single display support the learning environment through multiple devices like mouse, keyboard or mobile phone. To what extend it is useful for university learning? We had identified some challenges in using shared single display. This paper reports the challenges in using a shared single display for learning activity in university. From the challenges, we explored a shared virtual space and the finding is reported in this paper. It is interesting to claim that shared virtual space is more promising in term of learning activities and development. The shared virtual space is easy to manage. However, creating sustainable and collaborative, scalable learning virtual space is a challenge and worth to explore in future.

**Keywords:** Gaming AI, Android Game Development, 3rd Person Shooting Game, Artificial Intelligence

## 1 Introduction

The computer-supported collaborative learning (CSCL) is a software application developed to support collaborative learning. It can enhance student's skills, receive supports by peers, serve as communication medium etc. [3]. They are several kinds of CSCL. Among them, a shared single display (SSD) groupware is used in a classroom setting [4]. SSD enables a group of users to share the same concurrent display (which can be a large display or just a monitor), where each member will have his or her own input device to simultaneously interact with the system. This allows collaborators to benefit from the advantages of face-to face interactions as they are co-located; as well as be able to observe the non-verbal communication among members such as excitement and enthusiasm of the collaborating parties. With the multi-mice setting, students can work individually or collaboratively. The students will work within their own region or in a shared single display. Each region allows the students to provide the answer accordingly by clicking on the button provided or drag and drop the entire answer. The question is presented at the left handle corner of the screen. In this case, the students require to fill in the answers based on the questions given. Each player needs to provide an answer(s) when given a question. The students need to answer each question and

submit all the answers before proceeding to the next question. This is important to engage the students during the answering session.

It has been reported that shared single display is useful for primary schools, but can it benefit the university students? This paper investigates the adoption of a shared single display technology for learning the programming concept. A single shared display is developed in this study to create a collaborative learning environment in the tutorial room. In this case, a group of students will use a computer to answer a set of tutorials and learn collaboratively. The effectiveness of this technology is presented in this paper. In addition, the issues and limitation of this technology are presented in this paper. The results from this finding has introduced a new insight for collaborative system development in a classroom to learn programming concept in which a virtual shared space is investigated and reported.

Section 2 presents the works on shared single display through multi-mice technology. It covers the findings of experimenting shared single display in learning the concept of Data structure and Algorithm. Section 3 presents the proposed shared virtual space as an alternative method for learning technology. The findings of both experiments are presented in Section 4. The paper is concluded in Section 5.

## 2 Shared Single Display



**Fig. 1.** Multi-mice shared single display application

This section presents the experiment setting for the research on shared single display. Multi-mice technology is adopted to develop a shared single display among the under-graduate students, as shown in Figure 1. The subject of the experiment is TMF1434, Data Structure and Algorithm (DSA). This is one of the subjects that seem to be difficult to deliver due to the complexity and time constraint. It is always a challenge to conduct this course as students need to learn a new programming concept (e.g. Object-oriented framework) within the first two weeks of a semester. Meanwhile, students failed to relate the theory of DSA to the problem-solving due to much times were taken to understand the theory of DSA. Although students can consult lecturers after every classes or tutorials, the clarification of the topics only limited to a small number of students. Furthermore, there are many students feel hesitant to discuss with their lecturers or ask questions in the class or tutorials. They would prefer to consult their friends on the

topics that they do not understand. As a result, students are unable to fulfil the learning outcome of this course for most of the times.

The content of the experiment is based on the syllabus from a reference book, “C++ early object” and other relevant references. Also, the syllabus is used during the first three weeks on this subject (TMF1434). The experiment is done in the week 8 after the students had their midterm. Hence, these students were exposure to this programming language, which is C++ and have a similar background on this programming language. Students will be given 15-20 minutes to sit in a group to answer the exercises. The questions are in multiple choices. Due to the small size of the screen, each Single Display Group (SDG) session will cover only four students. The evaluation is conducted to identify the performance of the students in term the score of the individual test (pre-test); score of collective tests; score of SDG test; individual post-test.

The evaluation techniques used for this experiment are observation, the group exercise results and the post-test of every individual results. Observation is conducted among the researchers to understand the student interaction in using the collaborative system. Finally, discussion is conducted among the students to understand the usefulness of multi-mice application in learning. The pre-test and post-test for face to face interaction is conducted in the class. Then for the multi mice experiment, it was conducted in the research lab.

## 2.1 Results of the evaluation

We conducted two experiments for this study. The first experiment consists of 39 participants among the DSA students on April and May 2017. The second experiment is conducted among the new batch of 47 DSA students from November – December 2017. The following describe the overall observation based on both group of DSA students.

*Observation 1:* For the first week, most of the groups spent a long time to do it because most of them had discussion when they were doing the questions. Basically, they discuss when they had basic knowledge for the current shown questions in the computer. They will simply choose one of the answers when all of them had no idea on how to do it. For the second week, it is almost the same situation as the first week.

*Observation 2:* For the third week, one of the groups (consist of all the Malays) had did the answering very fast. It seems like they did not have more discussions for the questions. The other group (consist of all the Chinese and male) also did it fast. They will only have their discussions when they encounter a problem. Another group (two Chinese females and two Malay females), will only have their discussions with each other and within the same race. The time they spent to do the questions are shorter than the week before.

*Observation 3:* It seems the students like to discuss when they know certain topic. They will simply choose an answer without discussion if they do not understand the question.

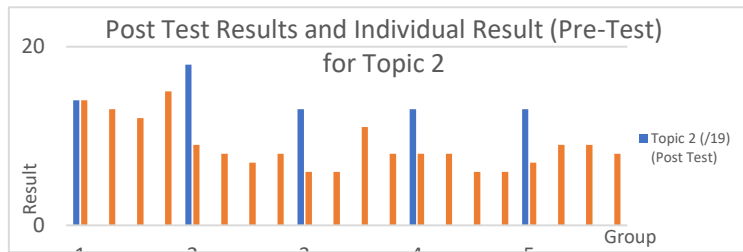


**Fig. 2.** Results from the experiment, group performance versus individual performance through SDG

We present various aspects of the analysis results in the following description and figures. Figure 2 presents collective results and individual results for SDG. The collective results are derived in each SDG. In this case, students answer a set of paper-based questions after each SDG. One set of the paper is given to the group. Then, they answer the questions with or without discussion.

From the results in Figure 2, it is interesting to find that the collective performance is better than the individual performance. There are two interesting observation based on the individual results through single display experiment as shown in Figure 3. In the first experiment, the students tend to have a similar score in almost every test. In the second experiment, the students had different scores. As we gave the students to choose their member, they tend to form the group with their friends. Hence, the tendency to follow their friends' answers was there. On the other hand, the member from experiment two is done randomly. Hence, the students tend to work on their own during the test.

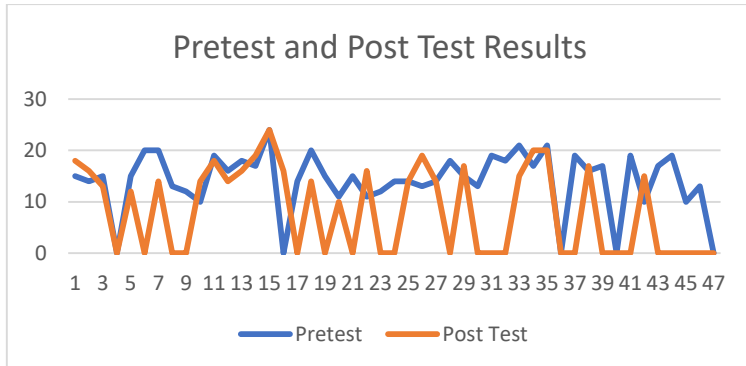


**Fig. 3.** The marks distribution among the group members for the first and second experiment.

Figure 3 shows the score among the group member for the 1<sup>st</sup> experiment and the 2<sup>nd</sup> experiment. In Figure 3 (left), the chart presents an individual performance on two series of SDG. Both students in the pilot test were scoring almost the same marks. In Figure 3 (right), the chart presents an individual performance on three series of SDG test. For example, student1 score 6 marks for test1; 7 mark for test2 and 5 mark for

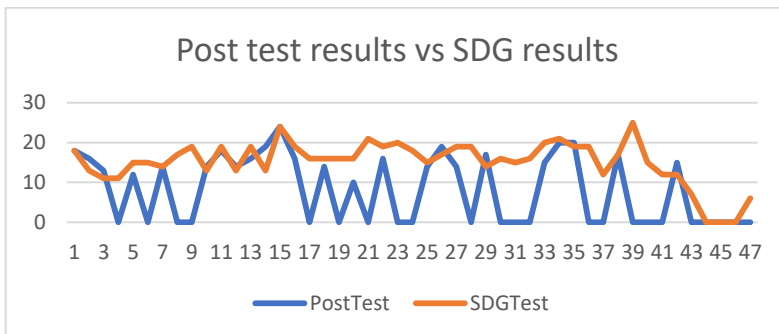
test3. The similar pattern is applied to all the test group for 1<sup>st</sup> experiment and 2<sup>nd</sup> experiment.

Figure 4 shows the pretest results from 2<sup>nd</sup> experiment. It is interesting to view that, none of the students have scored full mark in the experiment although they have the basic knowledge of C++. The student scored with zero value are those who absent in the experiment. The post-test results are lower as compared to the pretest results. Only 10/24 of the students can score slightly higher as compared to the pre-test.



**Fig. 4.** The results of pre-test and post-test

Figure 5 shows the post-test results versus the SDG results. The results present the accumulative of three tests under SDG setting. The SDG test results are scored higher as compared to the actual post-test results. Three students were absent from the SDG experiment and thus their scored is zero. The highest mark for the SDG result is 25 and the lowest mark for SDG result is 10. On the other hand, the highest mark for the post-test is 24 and the lowest mark for post-test is 12. Although the question sets are the same, the students fail to score full marks. This indicate that the SDG failed to support knowledge retention.



**Fig. 5.** Post-test results versus SDG results

Multi-mice application can engage and promote interaction among the students. As the SDG do require the contribution from each member thus the students need to commit in order to complete the experiments. However, the longer the deployment, the less discussion happen among the group members. As shown in the results, the post-test results are lower as compared to the pre-test results. Among the reason may be caused by confusion after some interviews with the students. As the members are randomly selected, they do not really trust each other in the group. They were certain time all the group members agreed on the answers but instead of fill in the agreed answer, the member chooses a different answer for the entire question. Meanwhile, it may be a case in which the students received a wrong concept after the discussion. The more discussion, the more confusion among the students.

The SDG results scored higher as compared to post-test results. This is known as cheat sheet effect in which, the members tend to follow the answers among the group member. We have identified the following design challenge in dealing with collaborative learning technology for learning programming. In general, the challenges are partner selection; inter-cultural issue; dominance case; fear of negative evaluation; and information overloaded.

*Partner selection:* One of the challenges in collaborative design is partner selection. Issue like missing partner happened in the experiments if we allowed the grouping to be flexible after a fixed time. We can foresee a challenge to maintain the entire group. Due to the inconsistent member, it will affect the overall finding. To overcome this challenge, marks will be given to SDG test for attendance. Hence, students are more aware on their slots and the attendance.

*Inter-cultural in collaborative learning design:* The inter-cultural has played an important factor in the collaboration learning. From the finding, the inter-cultural has affected the interaction among the students, as stated in one of the observations. The SDG can bridge the communication gaps among the members and promote discussion among them.

*Dominance:* One or a few individual members may dominate group discussions and monopolies the group's time; (not happened during discussion but it happens during the face to face collaborative setup. There are cases in which one or two students will take the lead to answers the questions and the rest of the members will continue their work without participant in the group discussion.

*Fear of negative evaluation:* As marks are given during the SDG experiment, students are more aware of the experiment. Cases like members withdraw from the experiment and avoid participating in the group discussions seldom happen.

*Information overloaded:* Higher volumes of information generated during the group discussion process created a condition where information is overload for the individual members. Even with this condition happened, so far, all the students had answered all the questions but cannot score with full mark. Perhaps this is one of the factors that lead to the poor performance from the students themselves.

*Type of question:* Due to a small screen of the SDG for each member, it is a challenge to include a complex question like a complete programming in the question bank.

Hence, the higher order of thinking questions like structure question and writing program is not supported in the experiment.

We present the findings upon using the shared single display technology for university learning. Some insufficiency of the adoption of a shared single display technology is presented and there is a need to have an alternative technology based on the findings given. In the following section, a shared virtual space is investigated and reported.

### 3 Shared Virtual Space

#### 3.1 Shared virtual space through Virtual Reality (VR) technology

Virtual Reality (VR) is developed to guide the Mandarin learning course at Faculty of Language Studies, UNIMAS. In this VR application, the lessons and corresponding game-like exercises are provided. Through the uses of this application, the students will be able to gain knowledge, recognize the Mandarin character and know the meaning of the character as well. Besides that, the students can learn this language without an internet connection and can be learnt by themselves without the involvement of lecturer or others. According to Bell and Fogler [10], VR as an educational tool can pull the user to the real like environment and this can make the students become enthused and interested in its contents. Therefore, learning through mobile VR application will be more effective compared to learn through ordinary mobile application because of the 3D images that make the virtual environment real and the user can have an immersive learning.

In the application, the student is exploring to immersive environment. Students will learn Mandarin character with the aid of audio pronunciation and the respective 3D images that can help in memorizing the words. The student can move and look around the virtual environment and look at the objects to learn the words and listen to the correct pronunciation. There are total of 3 virtual environments based on the themes for the learning lessons. The themes are Family Members, Foods and Numbers. After the student completed a lesson, the student can test their understanding by entering the respective game like a quiz. For the game like quiz, there might be question appearing, for example, the word ‘father’ in front of the player, then the player needs to find out the correct object from the environment. The second lesson is locked until the player done the quiz of the first lesson, means that to unlock a lesson, the player must complete the previous lesson and quiz. This lock and unlock feature can ensure the player learn something from the system.

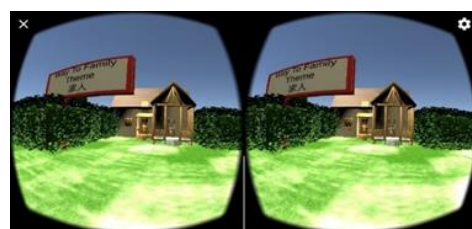


**Fig. 6.** Homepage of Learning Language in Virtual Reality Environment



**Fig. 7.** VR view for family lesson

Figure 6 above shown the family theme in VR system. In the Family Lesson, the user will immerse in a house. Inside this virtual environment, he or she can learn the pronunciation and the mandarin characters of the family members with the aid of the 3D models. The family members that can be learned through the lesson are father, mother, elder brother, elder sister, younger brother and younger sister. The mandarin character will only display when the VR pointer pointing to the 3D character as shown in Figure 7 and then the pronunciation audio of the corresponding character can be played if the user clicks on the Button B of the controller. Figure 8 presents the quiz view upon entering to the quiz model in the VR application.

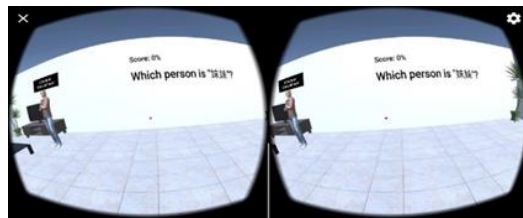


**Fig. 8.** The quiz zone

VR is introduced in education as the new teaching and learning method. A fun and effective learning environment can be created through VR, so the students will be attracted to use it. Other than that, VR can make the user totally immerses in the virtual world which is isolated from the surrounding environment, so the user will have the real sensation of being inside the virtual world. If using AR, the user may be losing focus when learning because the user is not isolated from the real world since the virtual objects overlay to the real world. There is some limitation during the class time, for example, students need to have an imaginary about the objects that are unapproachable from the lessons. With the uses of VR, students can experience and interact with the “real thing” and not just an imaginary.

We introduce two shared virtual space technology for learning Mandarin. Usability studies were conducted in using both technology among students for Mandarin learning. In brief, 100% of them think that this VR application can be used to enhance their language learning and they will recommend their friends to try out and use this application during their learning.

## 4 Discussion

Comparing the technology for shared virtual space with the shared single display, the findings are following. These findings can serve as research challenge when exploring both technology for learning technology development. Shared single display through multi-mice is tighten to hardware limitation. As the display is shared through a white screen, the usage is limited to number of students. Hence, having a whole class activity is no easy to achieve. Although, we can adopt technology like shared single display through smart phone, it is tightening to the number(s) of connection to wireless shared single display devices. While using the shared single technology, shared single display is suitable in classroom and shared virtual space is suitable for open learning environment. The scalability of a shared single display technology is an issue. As most of the shared single display technology require hardware, hence it is very hard to increase the number of students in using the shared single display technology. Within the virtual space, students can explore to virtual word, to explore the virtual objects, having the undiscovered experience. However, it is a challenge to create a real object within the virtual world. Lots of expertise are required to create those models. From the findings, the post tests for students scored lower than pre-test, this shown the negative effect of collaborative learning. We can conclude that the more collaboration and discussion will create more conflict on certain topics. Hence, post discussion is needed upon the collaboration activities.

It is easy to develop a collaboration learning through a shared single display technology with multi-mice system. Theoretically, we can adopt the notion of collaboration within the shared virtual space. However, it is a technical challenge to allow concurrent users within a shared virtual space. Meanwhile, scalability of the users in a shared virtual space is yet to be explored.

## 5 Conclusion

This paper presents a challenge to develop a collaborative system through a shared single display to shared virtual space. From the experiment of a shared single display, students feel comfortable to do the exercise without the supervision or appearance of the instructors. The shared single display can capture individual performance as well as group performance. The finding from this paper leads to the following implication. With shared single display, groups are more effective and objective in evaluation and error detection tasks. The group member can gain more knowledge with a proper guidance and setting. The interactions among the group members lead to synergies. The group member spends more time to discuss the question as compared to work individually. However, the correction of the question and confusion of the answers need to handle indeed. None of the students scored with full mark. This may be due to a higher volume of information generated during the group process creates a condition of information overloaded for the individual member. However, some design challenges in using a shared single display are discovered. They are 1) methods of groupwork on a project 2) decision making in collaborative work 3) when and how to communicate

with the other group members 4) what types of roles the various group members can have and what related responsibilities each member should assume 5) how to plan and distribute the different tasks of the project among the group members. On the other hand, working on a shared virtual space is promising. However, embedded the notion of collaborative element in a shared virtual space is challenging and need to further explore. How to allow the users to work in a shared virtual space collaboratively seemlessly? How to control the crowd while users can hop in and hop out easily in the shared virtual space? How to prevent the negative factors when users try to sabotage the learning? Working on the collaborative learning in virtual reality has started to receiving attention in [11]. In future, more works are needed to explore into this area. For example, embedded collaborative learning in a shared virtual space; comparing the results with the benchmark data. Meanwhile, it is interesting to investigate the negative effect of the collaboration learning as discovered in this paper.

## References

1. Blake, C and Scanlon, E (2013) Design for Collaboration. *Journal of Interactive Media in Education*, 2013(2): 10. DOI: <http://dx.doi.org/10.5334/2013-10>
2. Daradoumis, T., Xhafa, F., Marquès, J. M (2002) A methodological framework for project-based collaborative learning in a networked environment. *International journal of continuing engineering education and life-long learning*, 12, pp. 389-402.
3. Kordaki, M., Siempos, H., & Daradoumis, T (2011) Collaborative learning design within open source e-learning systems: lessons learned from an empirical study. In *E-Infrastructures and technologies for lifelong learning: Next generation environments*, pp. 212-233, IGI Global.
4. Rohse, S. & Anderson, T. (2006) Design patterns for complex learning. *Journal of Learning Design* 1(3).
5. Rice, S., & Gregor, M. N. (Eds.). (2016) *E-Learning and the Academic Library: Essays on Innovative Initiatives*. McFarland.
6. Deokar, A. V., Kolfschoten, G. L., & de Vreede, G. J. (2008). Prescriptive workflow design for collaboration-intensive processes using the collaboration engineering approach. *Global Journal of Flexible Systems Management*, 9(4), pp. 11-20.
7. Terrenghi, L., & Hilliges, O. Design for Collaboration on a Table-top Display in the Home. Ubiquitous information access through distributed user interfaces and ontology-based service-discovery.
8. Peters, E., Heijligers, B., de Kievith, J., Razafindrakoto, X., van Oosterhout, R., Santos, C., & Louwerse, M. (2016). Design for collaboration in mixed reality: Technical challenges and solutions. In *2016 8th International Conference on Games and Virtual Worlds for Serious Applications (VS-GAMES)*, IEEE, pp. 1-7.
9. Akkerman, S. F., Bronkhorst, L. H., & Zitter, I. (2013). The complexity of educational design research. *Quality & Quantity*, 47(1), pp. 421-439.
10. Bell, J. T., & Fogler, H. S. (1995). The investigation and application of virtual reality as an educational tool. In *Proceedings of the American Society for Engineering Education Annual Conference*, pp. 1718-1728.
11. Abdullah, J., Mohd-Isa, W. N., & Samsudin, M. A.: Virtual reality to improve group work skill and self-directed learning in problem-based learning narratives. *Virtual Reality*, (2019), pp. 1-11.



# Towards a Character-based Meta Recommender for Movies

Alia El Bolock<sup>12</sup>, Ahmed El Kady<sup>1</sup> Cornelia Herbert<sup>2</sup>, and Slim Abdennadher<sup>1</sup>

<sup>1</sup> German University in Cairo, Computer Science, Cairo, Egypt

<sup>2</sup> Ulm University, Applied Emotion and Motivation Psychology, Ulm, Germany

**Abstract.** Improving user experience through personalization is one of the current research trends in HCI. This includes recommendations that suit the preferences of all users (not only the majority) as dictated by their character, i.e. all aspects that influence human behaviors; including personality traits, affective states, socio-cultural embeddings and individual beliefs to name but a few. The aim of this paper is developing a recommender system for movies , that is adaptive in the way it recommends selections on the basis of the user's character. We present an architecture for a generic module-based recommendation platform that uses the user's character to choose a recommendation algorithm for each user. We deployed a movie recommendation application to determine the relation between recommender algorithm preference and (1) the user's personality, (2) background and (3) gender. Based on the data collected from 84 participants, high correlation between the user's personality (Openness, Extraversion and Conscientiousness) and gender and the recommender algorithm that they prefer.

## 1 Introduction

With the emergence of the fields of Ubiquitous Computing, Big Data and Affective Computing, the abundance of data available has opened up new approaches on how to personalize and thus enhance the user experience. A perfect example of an application that can take advantage of this opportunity is recommender systems. Recommender systems are utilized in many different areas of our daily lives, ranging from which ads or notifications to display for the user to where to go on vacation; or which movie to watch. Recent work in Personality Computing [27, 26] such as [23], tested the hypothesis that incorporating user personality into recommendation systems can improve the recommendations quality. Most users favored personality-based recommender systems over state of the art counterparts. This highlights that recommendations cannot follow one approach for all users. All previously proposed solutions tackled this by including the personality traits in the recommendation process itself. Not only the recommendations should be based on the user personality, but the algorithm should differ from one user to the other. In this work, we propose the recommender for recommenders concept which chooses one recommender algorithm from a pool of algorithms,

based on the current user. By giving each user an algorithm tailored to their own preference mechanism dictated by their character, the user experience and recommendation accuracy is bound to increase. Based on Personality and Affective Computing human-centric algorithms started taking human personality or affect into consideration. Character Computing [9, 11, 8, 12, 18] expands this further to include the whole character. The user's character represents all the defining features of an individual; including the appearance, stable *personality* traits, variable *affective*, cognitive and motivational states as well as history, morals, beliefs, skills and socio-cultural embeddings, to name a few. For the purpose of this work, we consider a subset of character components (personality traits, gender and background) to investigate whether it affects the preference of recommendation styles. As a proof of concept, we chose movies as our medium for recommendation for its accessibility. Based on the results we suggest a generic module-based architecture for a recommender for recommenders. Section 2 will represent the related work. Section 3 will give an overview of the architecture of the followed approach. Section 4 will present the conducted study and its results and their evaluations in **Sections 5** and **6**, respectively. The conclusion and possible future plans will be given in Section 7.

## 2 Related Work

In this section, we give a brief overview of the related work focusing on personalization in recommendation algorithms. Wu *et al.*[29] provides an extensive review of recommendation techniques with their strengths and weaknesses. Most used techniques can be clustered into 1) collaborative filtering algorithm based on item or user similarity, 2) back to higher recommendation, 3) hot recommendation and 4) fresh recommendation, concluding that algorithm preference varies from one person to the other, which further motivates our work. When talking about personality and personalization, the majority of the existing work relies on the five-factor model (FFM) of personality [2] (also known as OCEAN and the big five), which classifies personality into five traits: openness to experience (O), conscientiousness (C), extraversion (E), agreeableness (A), and neuroticism (N). These traits can either be acquired implicitly (through questionnaires e.g. [14] and expert interviews) or explicitly (through different techniques e.g. social media [15], ubiquitous computing and sensors [10] or behavior analysis [30, 1]) (see [27]). Ferwerda *et al.* [13] showed a relation between music listening behaviors and preference and inferred personality traits from social media. Nalmpantis *et al.* [23] combined personality traits with movie genre preference for movie recommendations. Results from previous work on genre preference according to personality were used. New recommendations were made based on the user's value for genre preference and the predicted movie rating using a k-NN algorithm, favoring the expected preferred genre. Their results showed an improvement in user experience to state of the art algorithms. Hu *et al.* [20] investigate the acceptance of using personality traits when recommending something from the perspective of the user. Hu [19] also tackled the idea of how to

link the user personality with the characteristics of the item being recommended. Hauger *et al.* [17] discussed the two main shortcomings of collaborative filtering algorithms: 1) the cold start predictions problem and 2) the user-bias problem. The proposed solutions were based on using the user profiles. It was concluded that users with similar mindsets are more likely to like the same items. Potash *et al.* [24] implemented a recommender system that incorporated NLP-based inferred user personality into the recommendations. While most work relies only on the personality, it is clear that other components need to be included. Although it has been inferred in some papers, only one work [23] investigated including the user's personality on the meta-level to help in choosing the recommendation style itself.

### 3 Recommender for Recommenders

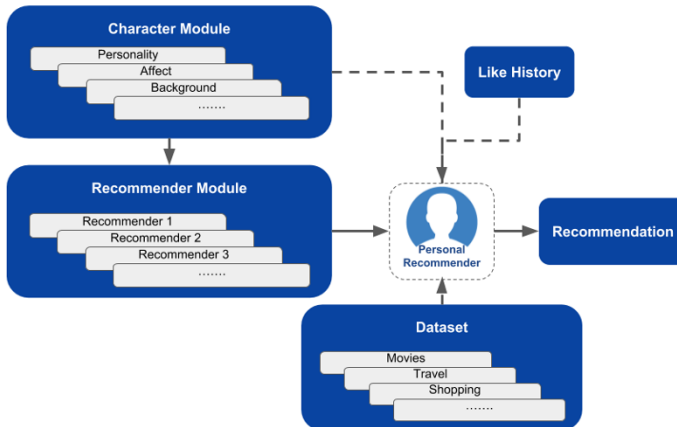


**Fig. 1.** Modules of the generic meta recommender platform.

The recommendation algorithm liked by the majority is not necessarily the one that suits everyone (as will be shown from Fig. 3a). The focus of most recent research is to improve the user experience, which means every user and not only the majority. That is why personalization plays an integral role in trending research as investigated by Affective, Personality and character Computing. Building on the results shown by our pilot study we present an architecture for a generic recommender system that suits the preferences of all users not only the majority, by including the recommendation algorithms themselves in the personalization process. The idea of creating a recommender system for choosing the recommender algorithm based on character, benefits from being a generic one as it can be applied on many different fields. In this section the architecture

of the main character-based recommender systems platform is described. When using the platform each user is presented with the recommendations resulting from the recommendation algorithm most suitable to the user's character. We propose a module-based model that can be described as plug and play, as it can be used in any field that uses recommender systems. For example, if we changed movies to music this meta level recommender will still work. This can be done by exchanging or extending any of the modules. Fig. 1 illustrates the architecture of the recommender for recommenders platform. The Character Module is used to calculate the values for the relevant components of the user's character. In the implemented web application presented in Chapter 4 for example, this module contained a short version of the big five personality test to calculate the personality as well as a short questionnaire to collect background information. The Recommender Dataset can contain any number of recommender algorithms depending on the developed preference and the recommendation domain. As proof of concept we used three simple variations of collaborative filtering as our recommendation algorithms in the implemented web application. The Character Module uses the output of the Character Profile to decide which recommender algorithm to choose from the Recommender Dataset. The Character Module needs to first be trained using labeled data of user preferences to be able to select the most fitting recommendation technique. Alternately, its preferences can be set or verified by personality psychology experts. After a recommender  $X$  is chosen, the remainder of the platform proceeds similar to any other recommender system, with the difference being able to include the user's character in the final recommendation process as well, as shown in as shown in [20, ?]. The chosen dataset from the Dataset Module is then used as input for the chosen recommender  $X$ , alongside the current user's liking history. The dataset used in the implemented web application was the MovieLens one (movies and their rating) thus resulting in a movie recommendation application. This dataset can be interchanged with any other one, depending on the recommendation domain. Based on this information the recommender algorithm presents the user with a new recommendation. Upon the user's evaluation of the recommendation it is either added to the "Like History" of the user or discarded and marked to be devalued the next time the algorithm runs. In the future, the recommender algorithm itself can utilise the user's character. This architecture allows for our approach to be universal as none of the modules depend on one specific application domain, character component, assessment method or recommendation algorithm.

## 4 Experiment: Character Components and Recommendation Preference

To answer research question of the ability to predict the preferred recommendation style based on character, we developed a web application for movie recommendation based on different recommender algorithms (for an overview see Fig 2). The aim of deployed version of the recommender was two-fold: (1) test the

hypothesis whether there is a correlation between recommendation technique preferences and character and (2) collect a dataset of user character and recommender preference. 84 users (46 males and 38 females, age:  $MEAN = 22$  and  $SD = 2.9$ ) participated in our study, after giving a written informed consent. With the help of the web application we recorded a subset of user character profiles (big five personality, background info and gender), preferred movies per user and score of each recommender per user. All data was fully anonymized. The web platform recorded 812 instances of users liking a recommender over a period of one month. We collected a dataset containing all the required parameters to train our model. Although giving consent prior to participating, the main purpose behind the collected data was reported after the study to avoid affecting their preferences while using the application.



**Fig. 2.** Overview of the flow of the data collection process resulting from the user's interaction with the movie recommender application.

#### 4.1 Movie Recommender Web Application

To investigate the correlation between user personality traits and different recommender algorithms, movies were chosen as the recommendation medium for its ease of use. To the users, the implemented movie recommendation web application is like any other; requiring the user to sign up, select initial preferences and then ask for movie recommendations which he/she can then evaluate. We made use of the MovieLens [16] dataset which contains 100,000 ratings on 9,000 movies by 700 users. Three different recommendation algorithms were implemented and integrated in the web platform so participants can get recommendations from all three of them without knowing the source algorithm of the recommendations or that there are even different recommendation techniques involved. To sign up to the application participants were asked to sign a consent form, fill in their demographic information (gender, nationality, age, occupation and relationship status) as well as the percentages of their five personality traits<sup>3</sup>. The platform then displayed three recommended movies, each resulted from one of the algorithms in the recommender dataset. The participants were asked to choose the movie they like the most without knowing that each recommendation resulted from a different algorithm. To avoid any biases the results of the three recommenders were randomly shuffled and thus displayed in a different location each

<sup>3</sup> <http://www.personalityassessor.com/bigfive/>

time. The chosen movies are automatically added to the list of the participant's favorite movies.

## 4.2 Recommender Algorithms

The deployed data collection application recommended movies using three different variants of the collaborative filtering algorithm using K-nearest neighbor (k-NN) (for a comprehensive survey see [25]). The k-NN algorithm we used took into consideration the z-score normalization for each user. The *first recommender* relies on a most recently liked algorithm. It calculates the nearest neighbor to the movie the user liked last. The recommendation is done using the k-NN algorithm on that movie and then the recommendation is presented to the user. This algorithm has a volatile memory as it only keeps track of the most recent movie the user liked. The *second recommender* obtains the movie closest the last ten movies the user watched using k-NN. This was followed by doing an intersection between the lists and presenting the movie nearest to the ten movies to the user. The *third recommender* (Algorithm 1) starts by getting the genre of movies the user prefers from their list of liked movies before applying collaborative filtering using k-NN to the movies of the user by this genre(similar to [23]).

---

### Algorithm 1 Recommender Three.

---

```

1: procedure RECOMMENDER3( User )
2:   Movies  $\leftarrow$  MoviesLikedByUser(User)
3:   Genre  $\leftarrow$  MostCommonGenre(Movies)
4:   FilterMoviesByGenre ( Movies, Genre )
5:   k  $\leftarrow$  1
6:   for each m  $\in$  Movies do
7:     Recommendations  $\leftarrow$  kNN(m, k)
8:   end for
9:   FilterMoviesByGenre ( Recommendations, Genre )
10:  r  $\leftarrow$  getItemRandom(Recommendations)
11:  return r
12: end procedure

```

---

## 4.3 Recommender Scoring System

To distinguish between the preferences of each individual participant, a scoring system to rate the recommender algorithms for each participant was implemented. The scoring system was not visible to the participants and only served to further annotate the collected dataset to be able to later train the model for the recommender for recommenders. As mentioned above, after the user is presented with the three recommendations they are prompted to choose which movie they liked the most. This translates that on this occasion this specific user preferred the recommender that recommended the movie they favored. The movie

recommendations are all presented to the user together in a single page but the position of the three recommendations are randomized each time as to remove any bias or behavior that might influence the user's choice. The system then records specific user points for this recommender based on a streak system. This means if the user preferred the same recommender more than once consecutively the recommender gets more points. The effect of by chance decisions and false positives is initially not considered as it was manually controlled by monitoring the participants through feedback interviews. In the future, we need to introduce measures to control for false positive, for base rate and for by chance decisions.

## 5 Results

The aim of the experiment was to collect a dataset from the usage of our test platform including the three recommenders, to analyze it and answer our research question. Fig. 3a shows the distribution of the recommender preference among the users of the web application. Of the 84 users 17 preferred the first algorithm, 27 preferred the second and the remaining 40 chose the third. While these numbers might show that the third algorithm was the best, the 17 or 27 preferring the other algorithms should also be taken into consideration, as together they make up more than half the participants. This fact highlights the motivation for our research, where recommendation should suit the preferences of all users not only the majority. Upon filtering the users by gender, the recommender preferences gain a clear pattern. We found a statistically significant difference at  $p < 0.05$  (2-tailed  $p = 0.019$  and  $t = -2.4$ ) between females and males with respect to recommender preference. For females the preference is distributed equally among the three recommenders. The majority of males prefer the third recommender with a count of 26 followed by the second recommender while less than a handful of men prefer the first one.

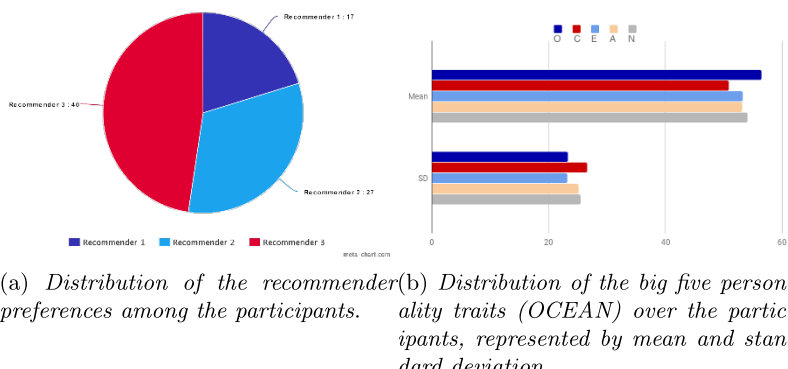


**Fig. 3.** A figure representing the recommender preference and personality distributions.

The five personality traits are normally distributed for the participants. Fig. 3b shows the means and standard deviations of each trait. We can assume no bias introduced by the personality distributions. We applied logistic regression on the collected dataset to train a model to predict recommender preference based on each personality trait. The prediction accuracy for each different parameter (with and without gender) is shown in Table 1. When considering each trait on its own, Conscientiousness yielded the highest accuracy, which is still low.

**Table 1.** Accuracy of predicting recommender preferences using logistic regression using different parameters.

	trait only	trait + female	trait + male
Openness	57.1	62.5	75
Conscientiousness	61.9	12.5	83.3
Extraversion	47.6	37.5	75
Agreeableness	52.4	50	75
Neuroticism	52.5	25	58.3

Accuracy %	O	E	A	C	N
Openness	62.5	80	60	40	70
Conscientiousness	40	20	40	12.5	30
Extraversion	80	37.5	40	20	30
Agreeableness	60	40	50	40	40
Neuroticism	70	30	40	30	25

**Table 2.** Accuracy of intersecting trait pairs for female participants.

Accuracy %	O	E	A	C	N
Openness	75	75	75	40	70
Conscientiousness	40	20	40	83.3	30
Extraversion	75	75	40	20	30
Agreeableness	75	40	75	40	40
Neuroticism	70	30	40	30	58.3

**Table 3.** Accuracy of intersecting trait pairs for male participants.

Openness to experience gave 57.14% accuracy, while Extraversion gave 47.61%. Agreeableness and Neuroticism each produced a slightly higher accuracy of 52.38%. Conscientiousness on the other hand gave the highest score with 61.90%. Adding gender as a parameter improved some of the results, such as Openness, while worsening others, such as Extraversion, Conscientiousness and Neuroticism (see Fig. 4a). When training the models using trait pairs for females, the most accurate model obtained was that of combining Openness with Extraversion which gave a considerable increase to 80%. The rest of the results are shown below in Fig. 2. The heat-maps showing Pearson's correlation coefficient between Recommender liking and Openness and Extraversion in females are shown in Fig. 4b and 4c, respectively. The same was done for the male participants but yielded no improvement. Combining Conscientiousness with any of the other traits produced the highest accuracy of 83.33%, which is identical to the accuracy obtained

from Conscientiousness alone. The rest of the results can be found in Table 3. Upon adding more than two traits no increase in accuracy was observed.

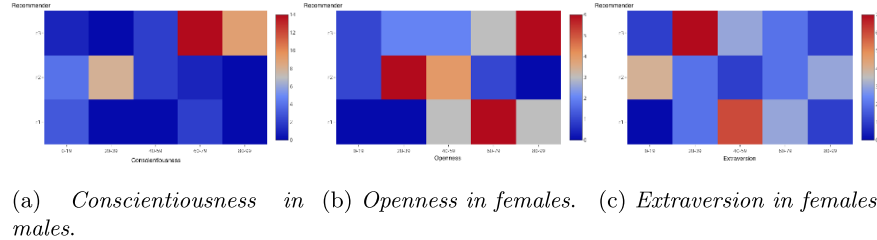


**Fig. 4.** Heat maps representing the interesting Pearson correlations between gender and some of the big five traits. The x-axis represents the percentile range of the personality trait, the y-axis represents the recommender and the z-axis represents the user count at each intersection.

## 6 Discussion

The obtained results show that incorporating certain character components in the recommendation process is promising. A difference between the genders and the recommender preferences (see [28]) was found, which aligns with the gender stereotypes related to movie preferences, explaining the bias of males to the third recommender. As the dataset contains 1545 movies that are listed with the genre romance, which is stereotyped as a genre that females like, 924 of these movies are also labeled as drama, however a total of 4365 movies in our dataset are likewise labeled as drama as the most prominent genre. This means if a female user likes the romance genre the algorithm might have a high chance of marking this user's favorite genre as drama which can then recommend an action/drama movie which the user will not like. This can be solved in the future by using a more discriminating database or integrating a confidence scoring system for genres in the recommendation algorithm. The other interesting finding is the varying correlation between the personality traits and recommender preference. From the heat-map in Fig. 4a we can clearly see the clustering of male users across the values of Conscientiousness, users with high Conscientiousness chose *Recommender 3*, while users with low Conscientiousness went for *Recommender 2*. Heat-maps that present the correlations for females in Fig. 4b and 4c, show that female participants preferring *Recommender 1* have moderately high Openness and relatively high Extraversion<sup>4</sup>. For *Recommender 2* the users had low values in both openness to experience and Extraversion, while *Recommender*

<sup>4</sup> Most female participants had relatively lower Extraversion values than males.

$\beta$  had very high values in openness to experience and in Extraversion it was relatively in between. Openness to experience trait is linked to unusual ideas, curiosity, and variety of experience [3], explaining why such open individuals preferred a recommender with volatile memory while the others were biased towards *Recommender 2*. Users with high Conscientious prefer adventure, and science fiction movies [6, 28] causing them to prefer *Recommender 3*. The results show that Extraversion, Openness and Conscientious are the traits most contributing to recommendation preferences. This can be explained by considering the personality style graphs resulting from the NEO-PI five factor personality questionnaire [22]. These traits contribute to interest, activity and learning styles.

## 7 Conclusions and Future Work

In this paper, we showed how certain character components can be used to improve the recommendation process by personalizing the recommender style not only the recommendation itself. As proof of concept, we tested this by deploying a movie recommendation web application running on three different recommendation algorithms. The application was used to collect the necessary data and find correlations between preferred recommendation algorithms and character (personality, gender and background for starters). A difference in recommender algorithm preference related to personality and gender was found. Accordingly, we proposed a generic module-based recommendation framework for enhancing the user experience and increasing the prediction accuracy. The recommendation platform chooses recommendation algorithms compatible with the user's character components to generate domain specific recommendations.

In the future, we will include more character components in the recommender recommendation process, such as affect [4] and socio-cultural [5]. We are also implementing multiple recommendation applications in different domains with different recommendation algorithms to gather the big dataset needed for the generic platform. The applications should be tested on a larger scale and for an extended period of time. A large scale usability and user preference study is to be conducted. The platform will also be tested for more diverse state of the art recommendation algorithms depending on the application domains. Another important investigation is also how to include other factors from the Character Module in the recommender selection process as well as the recommendation process [21]. This can be done in a variety of ways as being investigated in both Personality and Character Computing. Popular approaches include using social network profiles to build a character model and mining behaviour and usage patterns from the phone [10, 31, 7].

## References

1. Adel, M., El Bolock, A., Abdennadher, S.: Music = me : A character computing application for extracting user characteristics from music listening behavior.

- In: Second Workshop on Character Computing, 17th International Conference on Mobile and Ubiquitous Multimedia. ACM (2018)
- 2. Allport, G.W., Odber, H.S.: Trait-names: A psycho-lexical study. *Psychological monographs* **47**(1), i (1936)
  - 3. Ambridge, B.: Psy-Q: You know your IQ - now test your psychological intelligence. EBL-Schweitzer, Profile (2014)
  - 4. Andjelkovic, I., Parra, D., O'Donovan, J.: Moodplay: Interactive mood-based music discovery and recommendation. In: Proceedings of the 2016 Conference on User Modeling Adaptation and Personalization. pp. 275–279. ACM (2016)
  - 5. Barza, S., Memari, M.: Movie genre preference and culture. *Procedia-Social and Behavioral Sciences* **98**, 363–368 (2014)
  - 6. Cantador, I., Fernandez-tobias, I., Bellogin, R.: Relating personality types with user preferences in multiple entertainment domains (2013)
  - 7. Chittaranjan, G., Blom, J., Gatica-Perez, D.: Mining large-scale smartphone data for personality studies. *Personal and Ubiquitous Computing* **17**(3), 433–450 (2013)
  - 8. El Bolock, A.: Defining character computing from the perspective of computer science and psychology. In: Proceedings of the 17th International Conference on Mobile and Ubiquitous Multimedia. pp. 567–572. ACM (2018)
  - 9. El Bolock, A.: Character Computing, chapter: What is Character Computing. HumanComputer Interaction Series, Springer (2019)
  - 10. El Bolock, A., Amr, R., Abdennadher, S.: Non-obtrusive sleep detection for character computing profiling. In: International Conference on Intelligent Human Systems Integration. pp. 249–254. Springer (2018)
  - 11. El Bolock, A., Salah, J., Abdelrahman, Y., Herbert, C., Abdennadher, S.: Character computing: Computer science meets psychology. In: 17th International Conference on Mobile and Ubiquitous Multimedia. pp. 557–562. ACM (2018)
  - 12. El Bolock, A., Salah, J., Abdennadher, S., Abdelrahman, Y.: Character computing: challenges and opportunities. In: Proceedings of the 16th International Conference on Mobile and Ubiquitous Multimedia. pp. 555–559. ACM (2017)
  - 13. Ferwerda, B., Schedl, M.: Personality-based user modeling for music recommender systems. In: Berendt, B., Bringmann, B., Fromont, É., Garriga, G., Miettinen, P., Tatti, N., Tresp, V. (eds.) *Machine Learning and Knowledge Discovery in Databases*. pp. 254–257. Springer International Publishing, Cham (2016)
  - 14. Goldberg, L.R.: The development of markers for the big-five factor structure. *Psychological assessment* **4**(1), 26 (1992)
  - 15. Habib, S., El Bolock, A., Abdennadher, S.: Character-based behavior analysis through facebook within a multimodal data collection platform. In: 2nd Workshop on Character Computing, 17th International Conference on Mobile and Ubiquitous Multimedia. ACM (2018)
  - 16. Harper, F.M., Konstan, J.A.: The movielens datasets: History and context. *ACM Trans. Interact. Intell. Syst.* **5**(4), 19:1–19:19 (Dec 2015)
  - 17. Hauger, S., Tso, K.H.L., Schmidt-Thieme, L.: Comparison of recommender system algorithms focusing on the new-item and user-bias problem. In: Preisach, C., Burkhardt, H., Schmidt-Thieme, L., Decker, R. (eds.) *Data Analysis, Machine Learning and Applications*. pp. 525–532. Springer Berlin Heidelberg (2008)
  - 18. Herbert, C.: Character Computing, chapter: An Experimental-Psychological Approach for the Development of Character Computing. HumanComputer Interaction Series, Springer (2019), <https://www.springer.com/us/book/9783030159535>
  - 19. Hu, R.: Design and user issues in personality-based recommender systems. In: Proceedings of the Fourth ACM Conference on Recommender Systems. pp. 357–360. RecSys '10, ACM, New York, NY, USA (2010)

20. Hu, R., Pu, P.: Acceptance issues of personality-based recommender systems. In: Proceedings of the Third ACM Conference on Recommender Systems. pp. 221–224. RecSys '09, ACM, New York, NY, USA (2009)
21. Kedar, S., Bormane, D.: Automatic personality assessment: A systematic review. In: International Conference on Information Processing (ICIP). pp. 326–331. IEEE (2015)
22. McCrae, R.R., Costa, Jr, P.T., Martin, T.A.: The neopi3:a more readable revised neo personality inventory. *Journal of personality assessment* **84**(3), 261–270 (2005)
23. Nalmpantis, O., Tjortjis, C.: The 50/50 recommender: A method incorporating personality into movie recommender systems. In: Boracchi, G., Iliadis, L., Jayne, C., Likas, A. (eds.) *Engineering Applications of Neural Networks*. pp. 498–507. Springer International Publishing, Cham (2017)
24. Potash, P., Rumshisky, A.: Recommender system incorporating user personality profile through analysis of written reviews. ACM (2015)
25. Shi, Y., Larson, M., Hanjalic, A.: Collaborative filtering beyond the user-item matrix: A survey of the state of the art and future challenges. *ACM Computing Surveys (CSUR)* **47**(1), 3 (2014)
26. Vinciarelli, A., Mohammadi, G.: More personality in personality computing. *IEEE Transactions on Affective Computing* **5**(3), 297–300 (July 2014)
27. Vinciarelli, A., Mohammadi, G.: A survey of personality computing. *IEEE Transactions on Affective Computing* **5**(3), 273–291 (2014)
28. Whr, P., Lange, B.P., Schwarz, S.: Tears or fears?comparing gender stereotypes about movie preferences to actual preferences. *Frontiers in Psychology* **8**, 428 (2017)
29. Wu, W., He, L., Yang, J.: Evaluating recommender systems. In: Seventh International Conference on Digital Information Management (ICDIM 2012). pp. 56–61 (Aug 2012)
30. Wu, W., Chen, L.: Implicit acquisition of user personality for augmenting movie recommendations. In: International Conference on User Modeling, Adaptation, and Personalization. pp. 302–314. Springer (2015)
31. Zhang, Y., Olenick, J., Chang, C.H., Kozlowski, S.W., Hung, H.: Teamsense: Assessing personal affect and group cohesion in small teams through dyadic interaction and behavior analysis with wearable sensors. *Proceedings of the ACM on Interactive, Mobile, Wearable and Ubiquitous Technologies* **2**(3), 150 (2018)



# A Framework for Automatic Analysis of Essays Based on Idea Mining

Azreen Azman<sup>1</sup>, Mostafa Alksheri<sup>2</sup>, Shyamala Doraisamy<sup>1</sup>, Razali Yaakob<sup>1</sup>, and Eissa Alshari<sup>3</sup>

<sup>1</sup> Universiti Putra Malaysia, 43400 Serdang, Selangor, Malaysia

[azreenazman@upm.edu.my](mailto:azreenazman@upm.edu.my)

<sup>2</sup> Elmergib University, Libya

<sup>3</sup> IBB University, Yemen

**Abstract.** Assessing essays in online and open learning environment can be problematic as the number of submission increases with the increase of enrolment. A tool to automatically analyse those essays is required to assist instructor in the assessment process. The aim of this study is to propose a framework for automatic analysis of essays by identifying idea within the text in order to assist instructor in the assessment. The framework incorporates an idea mining model to identify and measure idea from text and proposes analysis method based on the calculated scores. A simulation of potential application of the framework is provided to show how a tool implemented based on that can be used for automatic and interactive assessment of essays.

**Keywords:** Online learning, Essay assessment, Idea mining, Text mining, Analysis tool

## 1 Introduction

The use of online learning tools in education has become a necessity in order to improve the effectiveness of content delivery and assessment. Online Learning Management System (LMS) such as Moodle has been deployed in many institution of higher learning to facilitate better learning environment for instructors and students. Recently, the Massive Open Online Course (MOOC) initiative allows unlimited enrolment and open access into online courses to the public through Web based platform such as the OpenLearning platform. As such, the class can become really huge as it is no longer limited by the physical facilities.

One of the challenges of any online-based learning is the assessment of student learning. For instance, it is problematic to assess student essay submitted through an online platform. Many text analysis methods have been used to assist instructor in the process such as text similarity between submission to check on the plagiarism, keywords identification or word counts to check on the usage of important keywords in the essay *et cetera*.

Idea mining has been proposed as a method to identify potential new idea written in a text. The aim is to discover part of the text (*student essay*) to contain novel idea based on another text (*context text*) as the context for measuring the idea. This paper attempts

to propose a framework for assessing novelty of student essay based on idea mining. As such, an automatic analysis of essay can be implemented to discover novelty in essay.

### 1.1 Problem Definition

In a typical setting, an instructor may use many materials in learning sessions with the students about a particular topic. The materials can be of different types and format, such as texts, images or videos. Later, the students are given an assignment to write an essay about the learned topic. By assuming that the students used the learned materials as the basis for the essay and incorporate new idea onto it, the quality of the submitted essay can be measured by how much new idea being discussed. In this paper, only textual materials are considered.

More specifically, let  $D = \{d_i\}$  be a set of student essays on a given topic and  $C$  be the context text, containing all common information about the topic covered throughout the learning session with all students. The problem is to rank  $D$  with respect to  $C$ , such that  $d_i$  is ranked higher than  $d_j$  if  $idea(d_i, C) > idea(d_j, C)$ , where the function  $idea(d_i, C)$  calculates a score reflecting the amount of new idea being written in  $d_i$  with respect to the context text  $C$ . The context text  $C$  may be the concatenation of all textual information about the given topic extracted from the lecture notes, academic papers, online materials and *et cetera*.

### 1.2 Idea Definition

An approach for mining idea from text was probably first proposed by Thorleuchter *et al.* in [18]. An idea is defined as an association between two or more entities [13], or a pair of attributes called *mean* and *purpose*. In short, an idea is a pair of text phrases representing the *mean* and *purpose* that co-occur in a text within the same context.

As an example, a text “*A transistor is a semiconductor device. It can be used to amplify or switch electronic signals.*” can be defined as idea where the text phrase “***a transistor is a semiconductor device.***” represents the *mean* and “***it can be used to amplify or switch electronic signals.***” represents the *purpose*, and both text phrases are related or connected within the same context.

The model proposed in [18] focuses on the identification of novel idea within the text. Given that the text “*A transistor is a semiconductor device. It can be used to amplify or switch electronic signals.*” is known to the reader, he/she will find a new idea on another text “*A nanomagnet is a miniaturized magnet that can be used to amplify or switch electronic signals.*”. In this context, the text phrase “***A nanomagnet is a miniaturized magnet***” represents the *mean* and “***that can be used to amplify or switch electronic signals.***” represents *purpose*. While the *purpose* is known to the reader, the *mean* appears to be unknown. As such, the combination of unknown *mean* and known *purpose* is more likely to contain new idea to the reader. In general, a novel idea is a pair of ***known mean*** and ***unknown purpose*** or ***unknown mean*** and ***known purpose*** that appear within a text. In [1, 18], the model is simplified to discover pair of related/connected known and unknown text phrases within text to avoid the problematic modeling of *mean* and *purpose* in text.

## 2 Related Work

### 2.1 Automated Essay Assessment Systems

Essays are considered as a useful tool to assess student learning, to guide the learning process and to evaluate the progress. While manual grading of student essays is a time-consuming process, the key issue is the rater reliability because the assessment by human raters will involve subjective judgments [5]. In learning sessions, the same assignments may be taken by over a number of students at a time where the marks differ significantly, the marks may be arbitrated by an instructor. More recently, statistical evaluations of rater severity have been applied instead of an arbitrator, leading to situations where the final mark could be higher or lower than the mark assigned by either grade.

In the past, a number of systems that automate the analyzing of essays have been developed. Those systems are vary according to their methodology and in the nature of the essays that can be analyzed. There are many automated systems for assessment of free text answers available either commercially or as a result of research [19]. According to [22], four commercial systems, Project Essay Grade, E-rater, Intelligent Essay Assessor and IntelliMetric, are predominance in this field. An automated evaluation engine with both compiled and source code was designed by [10] as a tool for non experts in a variety of purposes, including essay assessment. A number of different methodologies are represented, the major ones being: the use semantic analysis (Intelligent Essay Assessor), natural language processing (Electronic Essay Rater), neural networks (Intelligent Essay Marking Systems) and text classification (Bayesian Essay Test Scoring System) [2].

### 2.2 Text Mining in Essay Assessment

In recent years, text mining have been applied to different fields, including learning assessments [20]. While it is difficult to build knowledge with text mining alone, the authors in [9] tried to extract students' knowledge by using text mining and qualitative content analysis at the same time. Authors in [9, 6] suggested that essay content can be imported into a computer, classified the same clauses used in essays when broken into words, and classified the words into parts of words. Then, after analyzing the features of the classified words, frequently occurring words and keywords were extracted, and their frequency and simultaneous occurrence relationships were analyzed. Finally, analysis of the characteristics of the words, connections between words, and essay content were analyzed in concert with the results of qualitative data analysis.

## 3 Idea Mining Framework

The aim of this paper is to propose a framework for automatic analysis of student essay for novel idea. It is based on the idea mining model in [1] which is an improvement of the original model proposed in [18]. While both models ranks text phrases within a piece of text based on its likelihood to contain new idea, the proposed framework

attempts to rank documents or a set of *student essays* based on how much new idea has been written.

The framework expects two types of text, the *student essay* consists of the original submission of a particular topic in which the new idea to be discovered and measured, and the *context text* consists of common learning materials about the topic in textual form which have been used in teaching such as worksheets, presentations or any supporting resources for student learning. The framework consists of several steps which are pre-processing, text pattern creation, term vector formation, term vector similarity, idea mining measurement, essay measurement and ranking, as depicted in Fig. 1.

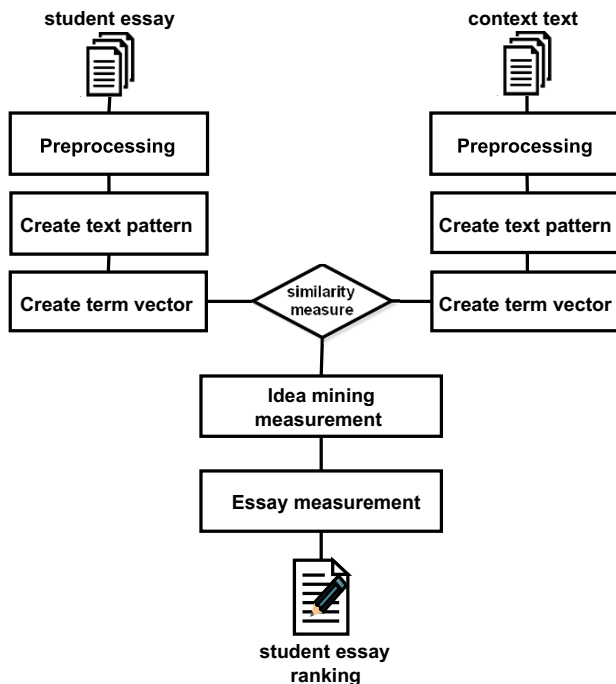


**Fig. 1.** Students' essay assessment framework

### 3.1 Data Preparation and Preprocessing

In the pre-processing step, both texts (*student essay* and *context text*) are transformed into appropriate format for further processing [4]. First, the text is cleaned to remove scripting code, punctuation, as well as specific characters. Next, the texts are tokenized to split them into tokens (terms). The terms that appear only once or twice are also discarded. According to Zipf's Law [21], those terms carry less meaning and removing them will reduce the size of the vocabulary. Finally, the well-known Porter stemmer

algorithm [11] is applied to the tokens and related terms with the same stem are grouped for further processing.

### 3.2 Text Pattern

In both [1, 18] models, the text is splitted into several *text patterns*, which are used to represent text phrases within the text. It is a heuristic approach to slice the text based on overlapping set of consecutive terms in the text by using predefined stop words following the algorithm described in [1]. This step extracts text patterns from both the *student essay* and *context text*. As a results, both *student essay* and *context text* will further be represented by a set of extracted text patterns. Next, each text pattern of the *student essay* is paired with each text pattern of the *context text* and the similarity of the pair is calculated to rank the pair based on its relatedness.

### 3.3 Term Vector

In information retrieval (IR), bag-of-words is a common method to represent unstructured text as vector [7]. In this framework, the extracted text patterns from *student essay* and *context text* are represented as term vectors before the similarity between them is calculated. In the vector, a weighting scheme is used where the occurrence of a term in the text pattern will be given a non-zero value and the absence of a term in the text pattern will be given a zero value. The dimension of the vector is defined by the total number of unique words for the whole *student essay* and *context text*.

The common terms weighting scheme proposed by [12] is used to calculate; how many times a term occurs in a *text pattern* (the term frequency  $tf_{(t,d)}$ ), how many times the term occurs in all text patterns (the document frequency  $df_t$ ), and the total number of text patterns (inverse document frequency  $idf_t$ ). The highest weights are assigned when the terms occur more times within a small number of text patterns and occur fewer times in all text patterns. The *text patterns* discovered from the *student essay* are compared to the *text patterns* from the *context text* to find the top similar pairs. As such, term vectors in vector space model are created to represent every *text pattern*.

### 3.4 Similarity Measure

In order to compute the similarity between two vectors, a frequently used distance measure, the *Euclidean distance*, is suited for idea mining implementation [8, 3]. In practice, this similarity measure considered as a proper predictor for vector (word) similarity calculation. In more recent studies for mining ideas [15, 16, 14], the term vector from *student essay* are compared to all vectors from *context text* using similarity measures, and then only the top similar pairs more than a threshold value is considered for idea mining measurement. The similarity between two text patterns indicates the relatedness of the text phrases it represents. As such, only the top ranked pairs of *text patterns* are considered as candidates for the idea mining measurement.

### 3.5 Idea Mining Measurement

Now that the pairs of related text patterns are discovered, the next step is to measure those pairs based on their potential to contain new idea. In Section 1.2, a text is considered to contain new idea if it comprises of known and unknown related text phrases within the same context. In this framework, the *context text* [14] is the source of known text phrases (due to the fact that it is made known to the students through lectures or any learning sessions) and the *student essay* is the source for unkown text phrases written by the students.

Traditionally, the extraction of a new idea depends on the *context text* where text patterns representing known ideas occur [14]. This is further simplified as finding part of a text that potentially contains both terms (or words) that are *known*, refers to the intersected terms in *student essay* and *context text*, and *unknown*, refers to the terms solely in *student essay*. This is visualized in the Venn diagrams of Figure 2 in which the intersection of these documents shows the overlapping terms to produce the *known* and *unknown* terms which will be used for the idea extraction measurements.

Idea mining measure is used to predict a new idea based on the balancing between the number of *known* terms and the number of *unknown* terms in a text pattern, and by considering both, the frequency of *known* terms appear in *context text* and the frequency of *unknown* terms appear in the *student essay*. In addition, specific terms as calculated in [17, 16] can represent the characteristic of a new idea. However, in this study the measure of calculating the specific terms are omitted. As such, the idea mining is measured based on:

- the number of *known* and *unknown* terms is well balanced,
- *known* terms occur more frequently in *context text* than other terms,
- *unknown* terms occur more frequently in *student essay* than other terms, and
- specific terms occur, which are characteristic for a new idea.

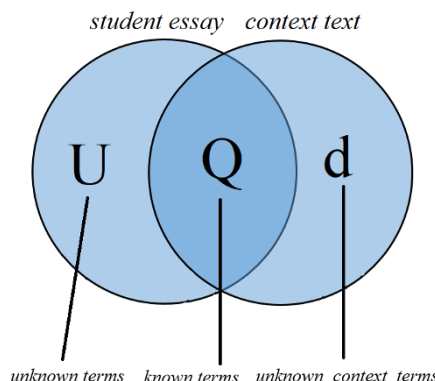


**Fig. 2.** The venn diagram for the overlapping of terms in *student essay* and *context text*

Based on [18], the measurement of idea in the paired *text patterns*,  $m_{idea}$ , is by combining all parameter's values as follows:

$$m_{idea} = \begin{cases} m_b + m_{f_Q} + m_{f_U} + m_c & (p \neq q) \\ 0 & (p = q) \end{cases} \quad (1)$$

where  $m_b$  measures for the balance of *known* and *unknown* terms distribution,

$$m_b = \begin{cases} \frac{2(p-q)}{p} & q \geq \frac{p}{2} \\ \frac{2q}{p} & q < \frac{p}{2} \end{cases} \quad (2)$$

and  $p$  is the number of *unknown* terms exists in *student essay*,  $p = |U|$ , and  $q$  is the number of *known* terms exists in both *student essay* and *context text*,  $q = |Q|$ . The other parameters are measured as follows:

- $m_{f_Q}$  as the number of frequently *known* terms occur in *idea text* over the number of all *known* terms in *context text*,
- $m_{f_U}$  as a measure for frequently of *unknown* terms occur in the *idea text*,
- $m_c$  a set of characteristic terms (e.g. quicker, better, higher etc.).

Therefore, each paired *text patterns* is assigned with a probabilistic score such that  $0.0 \leq m_{idea} \leq 1.0$ , and higher  $m_{idea}$  indicates a higher likelihood of the *text pattern* to contain new idea.

### 3.6 Essay Measurement and Ranking

As a results of the previous steps, each essay  $d_i$  will comprise of a set of text patterns and each text pattern is assigned with a probabilistic score reflecting the likelihood of that text pattern to contain novel idea. As such, each essay can be measured by the scores of those text patterns it contained. Based on the previous work on idea mining, it is more effective to only consider the top- $k$  text patterns in calculation. As such, the text patterns should be ranked.

In a simple statistical approach, the essay can be measured by calculating the *average* and *maximum* of the top- $k$  scores to summarized the score for the essay  $d_i$ . Therefore, those essays can be ranked in the order of their likelihood to contain more idea comparatively. In the case of the maximum of the top- $k$ ,  $\max_k$ , the essays will be ranked based on the highest of the best idea being written, while the average of the top- $k$ ,  $\text{average}_k$ , will measure the highest of the overall idea being written.

## 4 Application

The aim of this paper is to propose a framework for analysis of essay based on idea mining. The framework will evaluate the text to identify novel idea written in the essay based on a predetermined context text. Such tool can be used for automatic analysis of essay for ranking or grading, as well as interactive setting for detailed analysis.

#### 4.1 Automatic analysis

In an automatic setting, the tool can be used to rank essays based on the  $average_k$  or the  $max_k$  scores to provide indication of the novelty quality of those contents. Ranking is suitable since the scores represent relative measurement rather than objective measurement of those content. Based on the ranking of essays, an instructor can devise an assessment instrument such as based on rubric or checklist to assign marks.

Alternatively, the tool can produce the *average max min chart* on the  $average_k$ ,  $max_k$  and  $min_k$  scores such as in Fig. 3 to give an overall quality of the essays. The chart will provide flexibility to the instructor in evaluation. For instance, if an assessment is focused on the highest in novelty, an instructor may consider *essay3* as the best, but if it also concern on the least of minimum score, *essay1* may be selected.

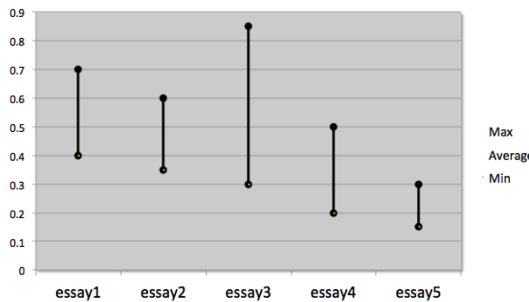


**Fig. 3.** Example for Average Max Min Chart of the idea mining scores

#### 4.2 Interactive analysis

Any automatic tools suffer from bias in the algorithm especially concerning subjective measurement. As such, alternative interactive tool can be provided to the instructor in order to give him/her more control in the assessment. In this context, the tool can provide an interface to display the content of the essay highlighted with the part in which novel idea is identified and is tagged with the computed idea mining scores, such as depicted in Fig. 4. It is similar to the document viewer on the Turnitin system where part of the text is highlighted to indicate similarity with other documents.

---

### Introduction

In computer science and software engineering in general, any systems that we build, it requires some form abstract frameworks and libraries. Irrelevant of size, complexity, type or language, these applications are build based on data. And **these data requires abstract representations, and these abstract representations is what data structure** is all about. Data structure is crucial in being the structure **to develop as well as maintaining efficient and scalable systems** (Azan & Alebicito, 2016). Data structure is a form abstraction in itself, as it hides the true implementation of system from an end user, which means developers could build a whole library and frameworks, without the user even knowing about it, which in itself hides the implementation internally. Data structure **provides patterns to solve problems, so data structure allows** developers to create a solution to solve said problems efficiently and elegantly. So in other words, data structure helps developers **to understand a certain problem by enabling a certain patterns** on those problems, and then create ways or solution to solve them.

**Fig. 4.** Example for Average Max Min Chart of the idea mining scores

Such view will give an instructor to inspect the quality of the highlighted part of the text with respect to the idea being written. The instructor may accept or reject the suggestion by the tool and any changes (acceptance or rejection) can be used to recalculate the ranking of the essays. In addition, interactively, the instructor can assign mark to the essay as he/she inspect the text.

## 5 Conclusion

The aim of the framework proposed on this paper is to measure an essay for novelty in its content calculated against a predefined context text representing prior knowledge. Based on the calculated scores, those essays can be ranked to assist instructor in assessment. In an interactive setting simulation, the instructor is given control to accept or reject suggestion by the tool. As such, the analysis to can provide assistance to the instructor to assess student's essay on online learning system.

Next, an extensive evaluation of the framework will be conducted on real dataset of students' essay. The evaluation should be conducted interactively in which actual instructors are selected as expert to use the tool to evaluate essays of his/her students. In addition, the framework can be extended to include import keywords of the chosen topic to improve the measurement of idea.

## References

1. Mostafa Alksher, Azreen Azman, Razali Yaakob, Eissa M Alshari, Abdul Kadir Rabiah, and Abdulmajid Mohamed. Effective idea mining technique based on modeling lexical semantic. *Journal of Theoretical and Applied Information Technology*, 96(16):5350–5362, 2018.
2. David Callear, Jennifer Jerrams-Smith, and S Victor. Bridging gaps in computerised assessment of texts. In *Proceedings IEEE International Conference on Advanced Learning Technologies*, pages 139–140. IEEE, 2001.

3. Emad Elabd, Eissa Alshari, and Hatem Abdulkader. Semantic boolean arabic information retrieval. *arXiv preprint arXiv:1512.03167*, 2015.
4. Weiguo Fan, Linda Wallace, Stephanie Rich, and Zhongju Zhang. Tapping the power of text mining. *Communications of the ACM*, 49(9):76–82, 2006.
5. Raphael Gamaroff. Rater reliability in language assessment: The bug of all bears. *System*, 28(1):31–53, 2000.
6. Linda Goodwin, Michele VanDyne, Simon Lin, and Steven Talbert. Data mining issues and opportunities for building nursing knowledge. *Journal of biomedical informatics*, 36(4-5):379–388, 2003.
7. Djoerd Hiemstra. Information retrieval models. *Information Retrieval: searching in the 21st Century*, pages 1–17, 2009.
8. Andreas Hotho, Andreas Nürnberger, and Gerhard Paaß. A brief survey of text mining. In *Ldv Forum*, volume 20, pages 19–62, 2005.
9. Tomoya Itatani, Kyoko Nagata, Kiyoko Yanagihara, and Noriko Tabuchi. Content analysis of student essays after attending a problem-based learning course: Facilitating the development of critical thinking and communication skills in Japanese nursing students. In *Healthcare*, volume 5, page 47. Multidisciplinary Digital Publishing Institute, 2017.
10. Elijah Mayfield and Carolyn Penstein Rosé. An interactive tool for supporting error analysis for text mining. *Proceedings of the NAACL HLT 2010 Demonstration Session*, pages 25–28, 2010.
11. Martin F Porter. An algorithm for suffix stripping. *Program*, 14(3):130–137, 1980.
12. Gerard Salton, James Allan, and Chris Buckley. Automatic structuring and retrieval of large text files. *Communications of the ACM*, 37(2):97–108, 1994.
13. DR Swanson. Literature-based discovery? the very idea. *Literature-based discovery*, pages 3–11, 2008.
14. Dirk Thorlechter, Sarah Herberz, and Dirk Van den Poel. Mining social behavior ideas of przewalski horses. In *Advances in Computer, Communication, Control and Automation*, pages 649–656. Springer, 2011.
15. Dirk Thorlechter and Dirk Van den Poel. Extraction of ideas from microsystems technology. *Advances in Computer Science and Information Engineering*, pages 563–568, 2012.
16. Dirk Thorlechter and Dirk Van den Poel. Web mining based extraction of problem solution ideas. *Expert Systems with Applications*, 40(10):3961–3969, 2013.
17. Dirk Thorlechter, Dirk Van den Poel, and Anita Prinzie. Extracting consumers needs for new products-a web mining approach. In *Knowledge Discovery and Data Mining, 2010. WKDD'10. Third International Conference on*, pages 440–443. IEEE, 2010.
18. Dirk Thorlechter, Dirk Van den Poel, and Anita Prinzie. Mining ideas from textual information. *Expert Systems with Applications*, 37(10):7182–7188, 2010.
19. Salvatore Valenti, Francesca Neri, and Alessandro Cucchiarelli. An overview of current research on automated essay grading. *Journal of Information Technology Education: Research*, 2(1):319–330, 2003.
20. Pernille Warrer, Ebba Holme Hansen, Lars Juhl-Jensen, and Lise Aagaard. Using text-mining techniques in electronic patient records to identify adr from medicine use. *British journal of clinical pharmacology*, 73(5):674–684, 2012.
21. Jianping Zeng, Jiangjiao Duan, Wenjun Cao, and Chengrong Wu. Topics modeling based on selective zipf distribution. *Expert Systems with Applications*, 39(7):6541–6546, 2012.
22. Kaja Zupanc and Zoran Bosnić. Automated essay evaluation with semantic analysis. *Knowledge-Based Systems*, 120:118–132, 2017.



# Advanced Fuzzy Set: An Application to Flat Electroencephalography Image

Suzelawati Zenian<sup>1\*</sup>, Tahir Ahmad<sup>2,3</sup>, Amidora Idris<sup>3</sup>

<sup>1</sup> Department of Mathematics with Computer Graphics, Faculty of Science and Natural Resources, Universiti Malaysia Sabah, Jalan UMS, 88400 Kota Kinabalu, Sabah, Malaysia

<sup>2</sup> Centre for Sustainable Nanomaterials, Ibnu Sina Institute for Scientific and Industrial Research, Universiti Teknologi Malaysia, 81310 UTM Johor Bahru, Malaysia

<sup>3</sup> Department of Mathematical Sciences, Faculty of Science, Universiti Teknologi Malaysia, 81310 UTM Johor Bahru, Malaysia

\*suzela@ums.edu.my

**Abstract.** Epileptic seizures refer to temporary disturbance in the electrical activity of the brain. The real time electrical activities of the cortical and subcortical neuronal activity are recorded by using Electroencephalogram (EEG) whereby few specific electrodes are placed on the scalp. EEG measures the differential voltage fluctuations resulting from ionic current flows within the neurons of the brain and can detect the changes over milliseconds. In this study, the image form of the EEG signals known as Flat EEG image is carried out. The advanced fuzzy techniques namely intuitionistic fuzzy set (IFS) and type-2 fuzzy set are explored to enhance the image of Flat EEG. The parameter in intuitionistic fuzzy image is optimized using intuitionistic fuzzy entropy. Whereas Hamacher t-conorm is applied for type-2 fuzzy enhancement. Experimental results on Flat EEG input images at two different time show that type-2 produced better output images compared to intuitionistic fuzzy methods.

**Keywords:** Flat EEG; intuitionistic fuzzy set; type-2 fuzzy set; uncertainty; image enhancement.

## 1 Introduction

The existence of uncertainty in our daily life is an essential and unavoidable. The uncertainty occurs in the precision that we seek. Therefore, there is a strong relationship between precision and uncertainty. In 1965, Zadeh introduced fuzzy set theory which is a fundamental approach in modeling uncertainty and provides a formal way in describing real world phenomena. Zadeh [1] mentioned that in the real world, the membership values for the classes of objects are not always precisely defined. Thus, there exists sets which do not have exact determined boundary. Since then, it has enlivened the notion to explore more on powerful tools in order to deal with uncertainties and imprecision.

The ordinary (type-1) fuzzy set considers only one uncertainty which is the membership function that is user defined. Different results are obtained by different

membership functions. Thus, there is uncertainty involved in defining the membership function. That is why the extension of ordinary fuzzy set is introduced to represent the uncertainty in a better way. The emergence of advanced fuzzy set is to consider more or different types of uncertainties. In 1975, Zadeh introduced type-2 fuzzy set which considered the uncertainty in the membership function of type-1 fuzzy set. Thus, the membership function is not a single value but rather than an interval [2]. Meanwhile, the intuitionistic fuzzy set considers more uncertainties in terms of membership and non-membership functions. The intuitionistic fuzzy set was introduced by Atanassov in 1983 [3].

One of the applications of fuzzy set is in image processing. Image processing is used to enhance visual appearance of images since the pixel values of an image may not be precise as uncertainty arises within the gray values of an image due to several factors. Prewitt is probably the first person to realize the importance of incorporating fuzzy theory in image processing. Pioneer research on the applications of fuzzy set theory in image processing was carried out by Pal et al. and Rosenfeld in the 1980s [4].

In this study, the uncertainties might occur during the process of imaging and transformation such as Flat EEG since the regions of clusters in Flat EEG are not always defined. The digital Flat EEG itself is a fuzzy object which has been proven in details by Abdy [5]. Hence, the boundary area of the epileptic foci which is represented in the shades of gray is not well-defined. Therefore, the main aim of this work is to handle the uncertainty and improve the visibility of the clusters centres by using two different approaches of advanced fuzzy set. Both approaches have different concepts in determining the uncertainty. Previous work on enhancing the Flat EEG images by using different techniques has been done by Suzelawati et al. [6-7].

## 2 Basic Concepts

Fuzzy Research Group of Universiti Teknologi Malaysia (UTM) developed Flat EEG since 1999 which has been used purely for visualization. The main scientific value lies in the ability of flattening method to preserve information recorded during seizure. The data sources is based only on the data collected from epileptic patients from Hospital Kuala Lumpur (HKL) and Hospital Universiti Sains Malaysia (HUSM) Kubang Kerian, Kelantan.

### 2.1 Flat EEG

Zakaria [8] has formulated fundamental ideas to describe an epileptic seizure as a system that is represented by its motion or a dynamic physical process. The Flat EEG is a method to flatten EEG signals (see Fig. 1) from a high dimensional signal into a low dimensional signal. Thus, the EEG signals can be viewed on the Cartesian plane as depicted in Fig. 2. The ‘jewel’ of the method is that EEG signals can be compressed and analyzed. The EEG coordinate system (see Fig. 3a) is defined as

$$C_{EEG} = \left\{ ((x, y, z), e_p) : x, y, z, e_p \in \Re \text{ and } x^2 + y^2 + z^2 = r^2 \right\} \quad (1)$$

where  $r$  is the radius of a patient head. Furthermore, the mapping of  $C_{EEG}$  to a plane is defined as follows:

$S_t : C_{EEG} \rightarrow MC$  (see Fig. 3b) such that

$$S_t((x, y, z), e_p) = \left( \frac{rx + iy}{r+z}, e_p \right) = \left( \frac{rx}{r+z}, \frac{ry}{r+z} \right)_{e_p(x, y, z)} \quad (2)$$

where  $MC = \{( (x, y)_o, e_p ) : x, y, e_p \in R\}$  is the first component of Fuzzy Topographic Topological Mapping (FTTM). FTTM is a non-invasive technique for solving neuromagnetic inverse problem. It is based on mathematical concepts namely topology and fuzzy. It aims to accommodate static simulated, experimental magnetoencephalography (MEG), and recorded electroencephalography signals [9]. Both  $C_{EEG}$  and  $MC$  were designed and proven as 2-manifolds. Meanwhile  $S_t$  is designed to be a one to one function as well as being conformal. Details of proofs are contained in [8].

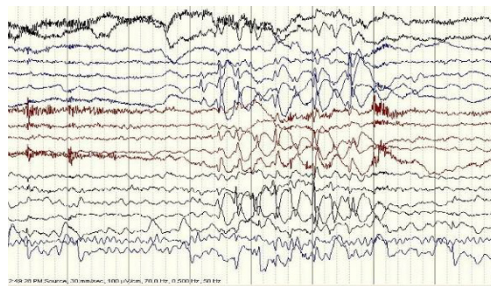


Fig. 1. EEG signal

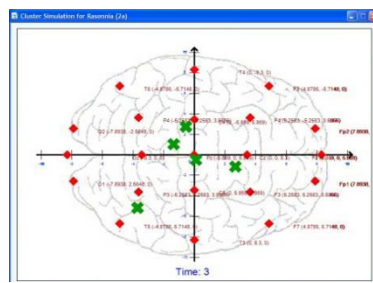
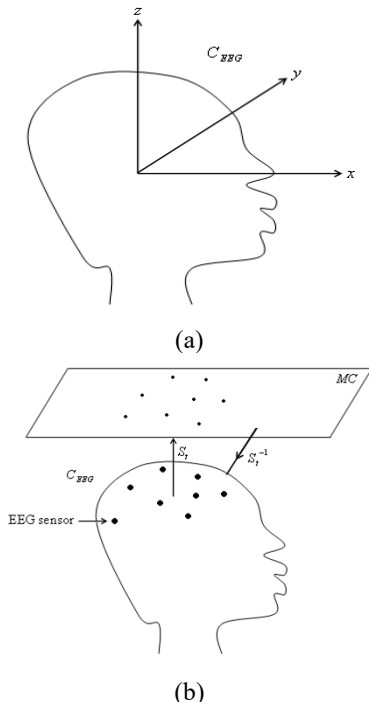


Fig. 2. Flat EEG



**Fig. 3.** (a) EEG Coordinate System, (b) EEG Projection

## 2.2 Digital Flat EEG

Flat EEG that is obtained via the flattening method has to be digitized in order to convert it to a form that can be stored in a computer. It has been successfully done by Abdy [5,10] whereby the Flat EEG is transformed into images by using fuzzy approach. There are three main steps that are involved in the transformation of Flat EEG into images as follows:

- a) Flat EEG is divided into pixels (see Fig. 4)

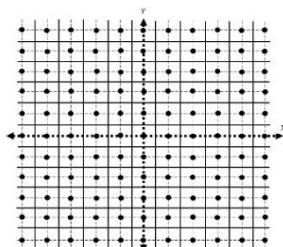


**Fig. 4.** Flat EEG pixels.

- b) The membership value for each pixel is determined in a cluster centre and the maximum operator of fuzzy set is implemented (see Fig. 5)

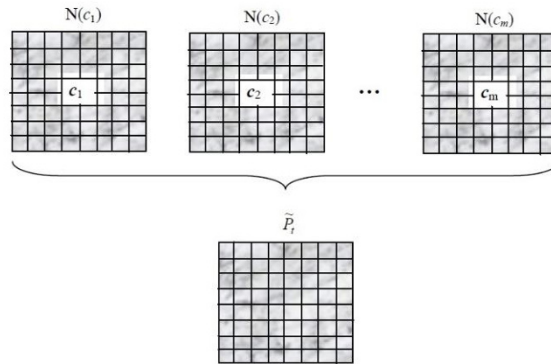


**Fig. 5.** Fuzzy neighborhood of each cluster centre  $c_j$  of a Flat EEG.

- c) The membership value of pixel is transformed into image data.

### 3 Methodology

In this section, image enhancement using two distinct advanced fuzzy techniques are discussed, namely intuitionistic fuzzy enhancement and type-2 fuzzy enhancement. In this work, the intuitionistic fuzzy method applied the entropy-based enhancement method. For the type-2 approach, it implemented enhancement using Hamacher t-conorm. The type-2 fuzzy set represents membership function in an interval range with upper and lower membership levels. The methods are described as the followings [2, 11, 12]:

#### 3.1 Type-2 Fuzzy Enhancement

1. The entire input image is initially fuzzified by using

$$\mu(g) = \frac{g - g_{\min}}{g_{\max} - g_{\min}} \quad (3)$$

2. The upper and lower membership values are computed as

$$\begin{aligned} \mu^{upper}(g) &= [\mu(g)]^\alpha \\ \mu^{lower}(g) &= [\mu(g)]^{1/\alpha}, \quad 0 < \alpha \leq 1 \end{aligned} \quad (4)$$

where  $\mu(g)$  is the fuzzified image.

3. The new membership function is computed using Hamacher t-conorm as

$$\mu_{enh}(g) = \frac{\mu^{upper}(g) + \mu^{lower}(g) + (\lambda - 2) \cdot \mu^{upper}(g) \cdot \mu^{lower}(g)}{1 - (1 - \lambda) \cdot \mu^{upper}(g) \cdot \mu^{lower}(g)} \quad (5)$$

where  $\lambda$  is the average of the image.

### 3.2 Entropy-Based Intuitionistic Fuzzy Enhancement Method

1. An image is initially fuzzified by using Eq.3
2. The intuitionistic fuzzy membership function is calculated as follows

$$\mu_{IFS}(g; \lambda) = 1 - (1 - \mu(g))^{\lambda-1} \quad (6)$$

3. The non-membership function is given as

$$\nu_{IFS}(g; \lambda) = (1 - \mu(g; \lambda))^{\lambda(\lambda-1)} \quad (7)$$

4. The hesitation degree is

$$\pi_{IFS}(g; \lambda) = 1 - \mu_{IFS}(g; \lambda) - \nu_{IFS}(g; \lambda) \quad (8)$$

5. The optimum value of  $\lambda$  that corresponds to the maximum value of the entropy values is obtained using intuitionistic fuzzy entropy given by

$$E = \frac{1}{M \times N} \sum_{j=0}^{N-1} \sum_{i=0}^{M-1} \frac{2\mu(g)\nu(g) + \pi^2(g)}{\pi^2(g) + \mu^2(g) + \nu^2(g)} \quad (9)$$

$$\lambda_{opt} = \max(IFE(A_{IFS}; \lambda)) \quad (10)$$

6. In the intuitionistic fuzzy domain, the image is represented as  $A_{IFS\_opt} = \{g, \mu_A(g; \lambda_{opt}), \nu_A(g; \lambda_{opt}) | g \in 0, \dots, L-1\}$ . Atanassov's operator as given in Eq.11 is applied to  $A_{IFS\_opt}$  to deconstruct the intuitionistic image into fuzzy image

$$D_\alpha(A_{IFS\_opt}) = \{x, \mu_A(x) + \alpha\pi_A(x), \nu_A(x) + (1-\alpha)\pi_A(x) | x \in X\} \quad (11)$$

7. The optimum value of  $\alpha$  is computed as

$$\alpha'_{opt} = \frac{\sum_{g=0}^{L-1} h_A(g) \pi_A(g; \lambda_{opt}) (1 - 2\mu_A(g; \lambda_{opt}))}{2 \sum_{g=0}^{L-1} h_A(g) \pi_A^2(g; \lambda_{opt})} \quad (12)$$

$$\text{where } \alpha_{opt} = \begin{cases} 0 & , \alpha'_{opt} < 0 \\ \alpha'_{opt} & , 0 \leq \alpha'_{opt} \leq 1 \\ 1 & , \alpha'_{opt} > 1 \end{cases}$$

8. The enhanced image in gray-level domain is written as  

$$g' = (L-1)\mu_{D_{\alpha_{opt}}(A_{opt})}(g)$$

## 4 Results and Discussion

The aforementioned advanced fuzzy methods are implemented on Flat EEG images during epileptic seizure at time  $t = 3$  and  $t = 4$  of size 201 x 201. Table 1 shows the data of the cluster centres that are transformed into image form as given in Fig. 6 and Fig. 7, respectively. The input image in Fig. 6 shows that there are two cluster centres whereas there are three cluster centres that can be observed in Fig. 7. The brightness of the vague boundaries represents the strength of the electrical potential for Flat EEG image.

**Table 1.** Position and electrical potential of the cluster centres at two different time

Time (second)	Position		Electrical potential ( $\mu V$ )
	$x$	$y$	
3	1.6918	-0.2614	40.0578
	-4.3997	0.2275	195.1227
4	-2.9509	-0.8576	112.0698
	3.2332	-1.7782	66.8746
	-0.2821	2.1374	12.4553

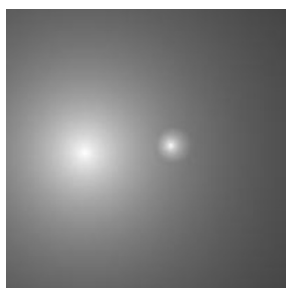


**Fig. 6.** Input image at  $t = 3$

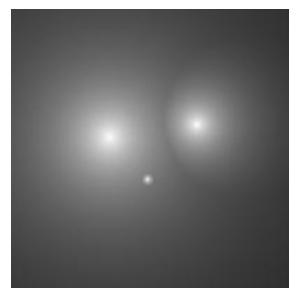


**Fig. 7.** Input image at  $t = 4$

The output images at  $t = 3$  and  $t = 4$  using type-2 fuzzy set and intuitionistic fuzzy set are given in Fig. 8. It can be observed that both methods are able to preserve the information of the cluster centres. However, the vague boundaries of the foci seem

brighter and spread wider by implementing the intuitionistic fuzzy technique in both input images. On the other hand, type-2 shows darker boundaries of the epileptic foci compared to intuitionistic fuzzy enhancement.

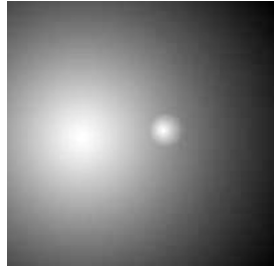
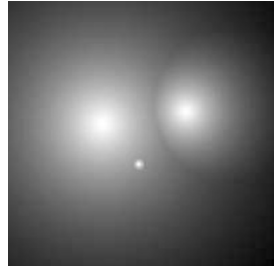
Furthermore, two error metrics are used to measure image quality between the input and output images which are mean squared error (MSE) and peak-signal-to-noise-ratio (PSNR). The MSE and PSNR are pixel based difference measures. The MSE is the average squared difference between input and output images as given in Eq. 13. Lower values of MSE indicates lower error between input and output images.

$$MSE = \frac{1}{N} \sum_{i=1}^N (x_i - y_i)^2 \quad (13)$$

PSNR is used in calculating the ratio between maximum pixel intensity value and MSE. It shows the measure of peak error. The formula is given as follows:

$$PSNR = 10 \log_{10} \frac{L^2}{MSE} \quad (14)$$

where  $L$  is the highest possible pixel intensity value in the image. A higher PSNR value provides a higher quality of the image. A small value of PSNR implies high numerical differences between input and output images [13-14]. Table 2 shows performance comparison for both advanced fuzzy methods using PSNR and MSE. From the results, it shows that type-2 gives higher PSNR and lower MSE values compared to IFS, which represents that type-2 gives better performance compared to IFS.

Time (sec- ond)	Type-2	IFS
3 <sup>rd</sup>		
4 <sup>th</sup>		

**Fig. 8.** Flat EEG output using type-2 and IFS at different time

**Table 2.** Performance evaluation.

Time (second)	PSNR		MSE	
	Type-2	IFS	Type-2	IFS
3 <sup>th</sup>	21.2232	19.7192	490.6362	693.6767
4 <sup>th</sup>	22.2888	16.0786	383.8826	1.6040e+03

## 5 Conclusions

This paper implemented two types of advanced fuzzy set namely type-2 and intuitionistic fuzzy sets to enhance the image of Flat EEG. Experimental results show that type-2 performs better than the intuitionistic fuzzy method. Performance comparisons are carried out using PSNR and MSE to measure the image quality.

## Acknowledgments

The authors would like to express heartfelt thanks to Universiti Malaysia Sabah for providing financial support under UMS Research Grant (SLB0154-2017).

## References

1. Zadeh, L.A.: Fuzzy Set. *Information and Control*, vol. 8, pp. 338-353 (1965).
2. Chaira, T.: *Medical Image Processing: Advanced Fuzzy Set Theoretic Techniques*. CRC Press (2015).
3. Atanassov, K.T.: Intuitionistic Fuzzy Sets. *J. Fuzzy Sets and Systems*. 20, 87-96 (1986).
4. Chaira, T., Ray, A.K.: *Fuzzy Image Processing and Applications with MATLAB*. CRC Press, Inc. (2010).
5. Abdy, M.: Fuzzy Digital Topological Space and Image of Flat Electroencephalography during Seizure. Ph.D thesis, Universiti Teknologi Malaysia (2014).
6. Suzelawati, Z., Tahir, A., Amidora, I.: Revised Selected Papers, *Communications in Computer and Information Science*, Springer, vol. 545 (2015).
7. Suzelawati, Z., Tahir, A., Amidora, I.: Edge Detection of Flat Electroencephalography Image via Classical and Fuzzy Approach, *Revised Selected Papers, Communications in Computer and Information Science*. pp 247-255. Springer (2016).
8. Zakaria, F.: Dynamic Profiling of EEG Data during Seizure using Fuzzy Information. Ph.D thesis, Universiti Teknologi Malaysia (2008).
9. Ahmad, T., Ahmad, R.S., Zakaria, F., Yun, L.L.: Development of Detection Model for Neurromagnetic Fields. Proceeding of BIOMED, pp. 119-121. Kuala Lumpur (2000).
10. Abdy, M., Ahmad, T.: Transformation of EEG Signals into Image Form during Epileptic Seizure. *Int. J. of Basic and Appl. Sc.* 11, 18-23 (2011).
11. Ensafi, P., Tizhoosh, H.R.: Type-2 Fuzzy Image Enhancement. In *International Conference Image Analysis and Recognition*. Springer, Berlin, Heidelberg, 159-166 (2005).
12. Chaira, T.: Construction of Intuitionistic Fuzzy Contrast Enhanced Medical Images. *IEEE Proceedings of 4<sup>th</sup> International Conference on Intelligent Human Computer Interaction*. 1-5 (2012).
13. Dosselmann, R., Yang, X.D.: Existing and Emerging Image Quality Metrics. In *Canadian Conference on Electrical and Computer Engineering*. IEEE. 1906-1913 (2005).
14. Hore, A., Ziou, D.: Image Quality Metrics: PSNR vs. SSIM. In *20<sup>th</sup> International Conference on Pattern Recognition (ICPR)*. IEEE. 2366-2369 (2010).



# Impact Assessment of Large-Scale Solar Photovoltaic integration on Sabah Grid System

Myjessie Songkin, N. N. Barsoum, Farrah Wong

Faculty of Engineering, Universiti Malaysia Sabah, 88400 Kota Kinabalu, Sabah, Malaysia  
myjc2009@gmail.com, nader@ums.edu.my and farrah@ums.edu.my

**Abstract.** The integration of large scale solar photovoltaic (LSSPV) in Peninsular Malaysia and Sabah is on the increasing trend, with many government incentives introduced for the past few years. The availability of solar energy and its generation outputs are depended on weather conditions. As the penetration level increases and becomes a significant portion in the generation mix, the solar output fluctuations could pose reliability risks to the grid system. This paper extensively reviews the present research on large-scale solar photovoltaic (LSSPV) power generation in Sabah Grid System, discusses the modelling and simulation methods of LSSPV and explores impacts of LSSPV integration on dynamic and static characteristics of power systems stability. Additionally, this paper also evaluated the reactive power capabilities of the LSSPV and tested for compliance with the Grid Code for Sabah and Labuan. Power quality assessments, Fault (low-voltage) ride through capability and frequency response of the LSSPV were also performed to verify LSSPV compliance.

**Keywords:** Large Scale Solar Photovoltaic, Power System Stability, Impact of Solar PV Integration, Sabah Grid System

## 1 Introduction

The renewable energy generally includes solar photovoltaic, wind, hydroelectric, biomass, biogas, tidal and geothermal power generations. Of the various forms of renewable energies, the hydroelectric, biomass, biogas, tidal and geothermal power generations store the primary energy, and their generation are controllable (despatchable) and similar to conventional fossil fuel generators.

Unlike the above renewable energies, the availability of solar energy and their generation outputs are dictated by weather conditions. As the penetration level increases and becomes a significant portion in the generation mix, the solar output fluctuations could pose reliability risks to the grid system. The high penetration of solar generations could also result in increased load-following duties of conventional generation plants [1-5]. Contrasting the fully despatchable conventional power plants, uncertainty in the solar generation outputs poses a challenge in incorporating them in the long-term generation capacity planning analysis. Their full rated capacity cannot be effectively used, and the reliability calculations such as reserve margin and Loss of Load Expectation (LOLE) may not be determined accurately.

This paper basically reviewed the present research and development of large-scale solar photovoltaic power generation in Sabah Grid System. The associated plant component parameters, study methodology, modelling basis, results and findings are also presented. The study was done by using commercial software PSSE version 33. There were two load cases of the grid (peak and light load) were performed for the year of 2018, based on which a numbers of operation scenarios and study cases were built including steady-state analyses, such as power flow, N-1 and N-2 contingency analysis, and fault level study to evaluate the impact of the large scale solar photovoltaic (LSSPV) on the Sabah grid. The reactive power capabilities of the LSSPV were evaluated and tested for compliance with the Grid Code for Sabah and Labuan [6]. Power quality assessments, Fault (low-voltage) Ride Through capability and Frequency Response were also performed to verify its compliance by simulating a number of events according to the Sabah Grid Reliability Standard (SGRS) [7].

## 2 LSSPV System Modelling and Simulation

### 2.1 Steady State Model

The LSSPV with a capacity of 48MW located in North of Sabah has been modelled in detail using the inverter model provided by HUAWEI. This LSSPV plant is exporting its power generation to the Sabah Grid System via 132kV transmission line. The LSSPV plant model has been constructed with key parameters as shown in Table 1 below:

**Table 1.** Steady State Model Parameters of the LSSPV

Elements	Unit	Resistance(R)	Reactance (X)
i. 132kV Underground Cable	1kM	2.706e-4pu/km	1.000e-43 pu/km
ii. 132/33/11kV Transformer	60MVA	0.0035 pu	0.105 pu
iii. STATCOM	20MVAr	0.0 pu	99999 pu
iv. Inverter Transformer	2.5 MVA	0.0092 pu	0.065 pu
v. Inverter	2.303MVA	0.0 pu	99999 pu

### 2.2 Dynamic Model

The dynamic model provided by the solar inverter manufacturer Huawei are WECC Generic Model [8] with recommended inverter parameters settings in PSSE version 33. In general, the WECC model for PV plant includes REGC\_A module, REEC\_B module and REPC\_A module, as illustrated in Fig. 1 below.

REGC\_A module represents the inverter interface with grid, REEC\_B module represents the electrical controls of the inverters and REPC\_A module represents the plant controller. The dynamic model provided by Huawei includes REGC\_A module and REEC\_B module. The WECC plant control model REPC was built based on Grid Code requirement.

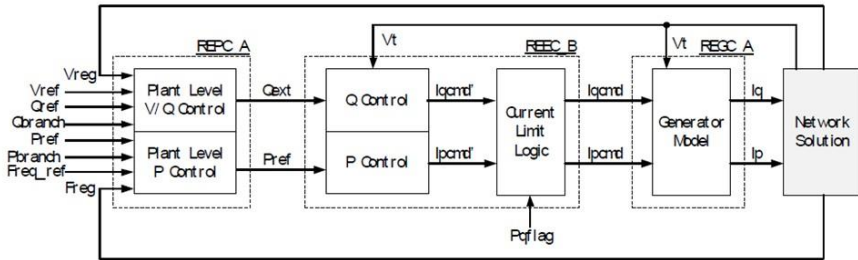


**Fig. 1.** Dynamic Model of PV Inverter

Each dynamic model will be used to represent combined 2MW string inverters and connected with inverter transformers of 33/0.48kV. In total, 24 dynamic models are used to represent the dynamic behaviors' of 48MW PV plant. The model parameters have been customized to meet the Grid Code requirements. The dynamic model used for the STATCOM is shown in Fig. 2.

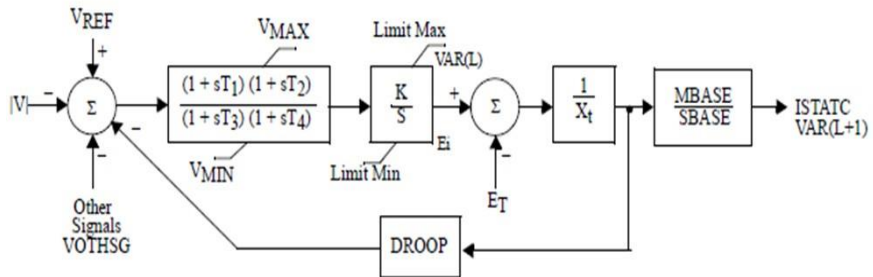


**Fig. 2.** Dynamic Model of STATCOM [9]

### 2.3 Scenario cases

**1) Operating cases:** Two load cases (2018) were given (peak load and light load). For each connection option, a total of six (6) scenarios were defined from combinations of grid load levels and the LSSPV plant output levels as tabulated in Table 2.

**Table 2.** Scenario Cases

LSSPV Power Output	Peak Load	Light Load
100% (48Mwac)	S5	S6
50% (24Mwac)	S3	S4
0% (0Mwac)	S1	S2

Study results of scenario S1 and S2 form the bases of peak load and light load condition, and the impact of the LSSPV plant at peak load condition can be quantified by comparing the results of S3 and S5 with that of S1. Similarly, the differences between

results of S2 and that of S4 and S6 indicate the impact of the LSSPV plant at system light load condition.

**2) Scenario for Steady State Assessment:** Steady state Power Flow, N-1 and N-2 contingency analyses were performed with all the six (6) scenarios for each connection option. N-1 Contingency exemplified by contingencies such as single generator, single transformer or single line outages. On a double circuit or multi-circuit line, a Single Contingency or N-1 Contingency shall mean loss of only one circuit, and not the entire structure. The N-2 Contingency means that a double contingency such as the simultaneous loss of two lines connected to the same circuit breaker or a unit(s) outage in a substation or both circuits of a double circuit line. A less severe double contingency category allows for system readjustment after outage of the first element. The reactive power capability assessments include both active-reactive Power (PQ) relationship and voltage-reactive power (VQ) relationship analysis, and are not specifically related to an operation scenario. Scenario S5 has been taken as the base to achieve the required 1.0pu voltage at point of common connection (PCC) for PQ analysis, 0.9pu and 1.1pu voltages at PCC for VQ analysis but with necessary modifications. The power quality analyses were performed with S6 due to the grid system has highest source impedances during light load condition with the least number of online generators and loads. The power quality assessment results represent the worst-case scenario.

**3) Scenario for Transient Stability Assessment:** It is a common practice to perform the studies on the scenario with the most severe impact to the grid. Hence, the fault current studies and transient stability study were performed with the peak-load base case and S5 for comparison purpose. In case of unstable test, the same test will be performed on original grid model without the LSSPV plant, so as to identify whether the issue is attributed to the connection of the LSSPV plant. Based on the study guideline at the vicinity of the PCC, following stability tests have been identified for this study. *Category '1'* events up to two buses away from interconnection point, i.e. 3-phase faults with 150ms clearing followed by loss of the faulty element. The applicable events are tabulated in Table 3 below:

**Table 3.** Category 1 Events

Case code	Transmission line	Fault location	Fault Clearing time
B1FR	KDAT132---MGRS132 Line 1	KDAT132	150ms
B1T0	KDAT132---MGRS132 Line 1	MGRS132	150ms
B2FR	KDAT132---MTGG132 Line 1	KDAT132	150ms
B2T0	KDAT132---MTGG132 Line 1	MTGG132	150ms
B3FR	MTGG132---MGRS132 Line 1	MTGG132	150ms
B3T0	MTGG132---MGRS132 Line 1	MGRS132	150ms
B4FR	MGRS132---KBLD132 Line 1	MGRS132	150ms
B4T0	MGRS132---KBLD132 Line 1	KBLD132	150ms
B5FR	KBLD132---DGUN132 Line 1	KBLD132	150ms

*Category '2'* events up to two buses away from interconnection point, i.e. single or three phase faults with 150ms clearing followed by loss of the parallel lines. The applicable events are tabulated in Table 4 below:

**Table 4.** Category 2 Events

Case code	Transmission line	Fault location	Fault Clearing time
C1FR	MGRS132--5BLD132 Line 1 & Line 2	MGRS132	150ms
C1T0	MGRS132--KBLD132 Line 1 & Line 2	KBLD132	150ms
C2FR	KBLD132--DGUN132 Line 1 & Line 2	KBLD132	150ms

### 3 Impacts of LSSPV Integration to the Sabah Grid System Stability

Based on the simulations of the stated scenarios above, the impact of the integration of LSSPV to the Sabah Grid system stability is as follows:

#### 3.1 Steady State Study Analysis

**Power Flow:** Calculated with all six (6) cases for each connection option. The calculation results were checked on 132kV and 275kV subsystems:

- Voltage checks for all buses based on criteria of  $[0.95\text{pu} \leq \text{VBUS} \leq 1.05\text{pu}]$ ; and monitor the voltage of buses at the vicinity of the interconnection point.
- Loading checks for branches above the current rating; and monitor the loading of branch elements at the vicinity of the interconnection point.
- To achieve 48MW at PCC, the required inverter power is:  $P_{\text{Inverter}} = 48.96 \text{ MW}$  (losses of 2%).

Voltage performance check found none of the bus voltages is out of the range  $[0.95\text{pu} \leq \text{VBUS} \leq 1.05\text{pu}]$  before and after the LSS connection. Bus voltages at the vicinity of the PCC with and without the LSSPV are tabulated in Table 5, from which one can conclude that the LSSPV plant has little impact on the voltage performance of the grid at the vicinity of PCC. Connection of the LSSPV does not pose voltage performance issue to the grid under steady state operation for all operating scenarios.

**Table 5.** Comparison of Bus Voltages (p.u) near the PCC with and without LSSPV (light and peak load)

Bus No.	Light Load				Peak Load			
	S2	S4	S5	$\Delta S6-2$	S1	S3	S5	$\Delta S6-1$
52005	1.037	1.040	1.039	0.003	1.009	1.010	1.010	0.001
52002	1.041	1.048	1.048	0.008	1.007	1.011	1.012	0.005
52004	1.040	1.046	1.046	0.006	1.008	1.011	1.012	0.004
991001	1.041	1.048	1.049	0.008	1.007	1.012	1.012	0.005

Loading of transmission elements were checked based on their current rating and it was observed that none of transmission elements are loaded above 100.0 % of their current rating for the total of 6 cases.

All transmission elements at the vicinity of the PCC are loaded within their ratings. The connection of LSSPV does not cause additional overload of transmission elements at the vicinity of the PCC.

**N-1 Contingency:** The N-1 contingencies were set up by SINGLE BRANCH IN SUBSYSTEM 'TRANSALL', which was defined by KVRANGE 132.000 500.000. The reporting criteria for ACCC runs are as follows to comply the Sabah Grid Reliability Standard (SGRS):

- i. Branch loading more than 100% of current rating, overloaded branches in base case ignored.
- ii. Bus voltage is either less than 0.95pu or greater than 1.05pu.
- iii. Bus voltage deviation exceeds limits of Drop more than 5% or Rise more than 10%.

No overload is found during N-1 contingency analysis under peak and light load. There are 39 violations under light load condition and 6 violations under peak load condition identified from N-1 analysis.

However, under Light load condition for S4 and S6, thirty (30) of them already existed in S2. For the other nine (9) cases, all the initial voltages are close to 1.05 and with very small changes (0.001-0.002 pu) in N-1 causing the overvoltage ( $\Delta = 0.001$  pu). Those buses in the nine (9) voltage violation cases are connected with very long transmission lines with very low loading factor and suggested to add shunt reactors to overcome the voltage issues. The six (6) voltage violations under Peak load condition exist with the same magnitude regardless whether the LSSPV is at 0% (S1) or 100% (S5) output. These violations are not triggered or worsen by the connection of the LSSPV.

**N-2 Contingency:** The N-2 contingencies were set up by PARALLEL BRANCH IN SUBSYSTEM 'TRANS132', 'TRANS275' and 'TRANS500', which is defined by KV 132.0, KV275 and KV 500.0. The reporting criteria for ACCC runs are as follows to comply the Sabah Grid Reliability Standard (SGRS):

- i. Branch loading >100% of Rating A, overloaded branches in base case ignored.
- ii. Bus voltage <0.9pu or >1.1pu.
- iii. Bus voltage deviation exceeds limits of Drop>10% or Rise >10%.

No overload is found during N-2 contingency analysis under Peak and Light load condition and no voltage violated cases are found under Light load condition (S2, S4 and S6). One (1) voltage violation is found under Peak load condition and occur with the same magnitude regardless whether the LSS is at 0% (S1) or 100% (S5) output, This violation is not triggered or worsens by the connection of the LSSPV.

**Reactive Power Capabilities Study:** Huawei SUN2000-42KTL inverter (PWM, current source) has Reactive Power Capability of half circle in the quadrant 1 and quadrant 2 as shown in Fig.3. The inverters are rated 2.303MVA ( $47\text{kVA} \times 49$ ) with nominal terminal voltage of 480V, or in other words, the nominal current  $\text{IN} = 2770\text{A}$ . SUN2000-42KTL allows its terminal voltage from 0.8pu (384V) to 1.15pu (552V), to which its MVA rating is proportional. STATCOM rated capacity is 20MVar. Evaluations of the LSSPV plant's PQ capability were performed as follows:

- i. The main transformer's OLTC to regulate the main 33kV bus voltage between 1.045pu and 1.06pu during lagging Power Factor and 0.97 to 0.99 during leading Power Factor.
- ii. PV generator active power PGen is set from 0.0 to 1.0pu in 20 steps, ramp the reactive power QGen from 1.2pu to 0.0 in 100 steps, until (inverter current  $\leq$  its nominal) and ( $0.9 \leq$  inverter Vterm  $\leq 1.1$ ) and (main transformer loading  $\leq$  its rating).
- iii. Record the P and Q at PCC, inverter current and terminal voltage, the tap position of main step up transformer.

The Reactive Power capability tests were performed with and without 20MVar STATCOM for compliance with the Grid Code for Sabah and Labuan requirements. The VQ capability tests were performed with the LSS at 100% output and the PCC voltage of 0.9pu and 1.1pu for compliance with the Grid Code for Sabah and Labuan requirements.

**PQ and VQ studies:** The PQ and VQ capability runs were performed with and without compensation, of which the results are compared with Grid Code requirements. The results obtained with 20MVar STATCOM installed, the plant's PQ capability fulfils the Grid Code requirements. The plant's reactive capacity at PMAX: -36.02Mvar (lead) to 3275Mvar (lag), fulfils the Grid Code requirements of -15.64Mvar (lead) to 29.74Mvar (lag) for 48MW LSSPV plant. Similar to PQ studies the VQ capability curves of the LSSPV plant with 20MVar STATCOM fulfils the Grid Code requirements.

**Fault Level Study:** Short-circuit current calculations were performed according to IEC 60909 [10], with a  $C_{\text{factor}}$  of 1.1 applied. The breaking capacities of circuit breakers are assumed as 31.5kA for 132kV and 40kA for 275kV, respectively. With the inverter's current limiting nature, fault current contribution from the LSSPV plant is very minor to three-phase short circuit faults in the transmission system. The zero sequence paths are isolated between the LSS PV 33kV side and the 132kV transmission system with the  $Y_d$  connected main step up transformer. However, with the 132/33kV  $YN_d$  transformer high-voltage side neutral solid grounded, the transformer does contribute Single-Line-to-Ground (SLG) fault current at PCC. Fault current contribution from the LSSPV plant is very minor to three-phase fault and no issue is found on the three-phase short-circuit fault calculation. Due to the transformer setting,  $Y_d$  connection and no earth grounding path, all SLG fault current at 132kV and 275kV are zero. Isolated

132kV neutral is recommended for the main step up transformer, so as to limit the single line to ground fault current contribution from the plant.

**Power Quality Study:** The impact of LSSPV on the grid system in terms of power quality is closely related to the emission level of the LSSPV inverters and the strength of the grid system as view from the PCC. The strength of the grid system as view from the PCC can be quantified by effective short-circuit ratios (SCR), calculated at Bus PCC 51078 [BCHG132 132.00]. Viewed from the effective SCR at PCC, the grid system is super strong in comparison with the LSSPV is shown in Table 6.

**Table 6.** Strength of the Grid System at PCC

Load case	Short-Circuit Power (MVA)	LSS Rated Power (MVA)	Effective Short- Circuit Ratio
Peak Load	662.39	55.272	11.98
Light Load	619.98	55.272	11.21

### 3.2 Transient Study Analysis

Stability tests were performed with both *Category '1'* and *'2'* events. The former is ‘three-phase fault, 150ms clearing followed by loss of single transmission element’ the latter is ‘one or three phase fault on parallel lines, 150ms clearing followed by loss of two or more transmission elements’. Angle Spread, Frequency deviation, Voltage at both ends of the Line, Powers to the PCC, and Powers from the PV Inverter are monitored.

#### a. Stability Tests with Category 1 Events and Category 2 Events

For all the tests, the Grid System and LSSPV successfully withstood the contingencies, and regained a state of equilibrium after the faulty element was isolated from the system. The contingency ‘B1FR’ was identified as the worst case for Category 1 and ‘C1FR’ was identified as the worst case for Category 2, of which the frequency deviation went through a modal analysis for calculation of damping ratios. Test results shown are positive on all cases, where the angle spread is less than 180° and the worst-case damping factor is more than 5% (limit stated in SGPS requirement). A system with positive damping is called to be dynamically stable.

#### b. Fault-Ride-Through-Test

A total of eight cases have been tested by varying the fault impedance, which is a function of the Thevenin impedance (from ASCC result) at the PCC and the targeted per unit residual voltage,  $U_r$ , i.e. the fault impedance  $Z_F = Z_{\text{Thevenin}} * U_r / (1 - U_r)$ .

*Successful Fault-Ride-Through:* The residual voltage magnitudes were obtained from Grid Code for Sabah and Labuan requirements, the following combinations of residual voltages at PCC and fault durations were tested: [0pu, 0.15s], [0.1pu, 0.3s], [0.2pu, 0.45s], [0.3pu, 0.6s], [0.5pu, 0.9s], [0.7pu, 1.2s], [0.9pu, 1.5s], [0.92pu, 3s]. For

all the eight testing cases, the LSSPV inverter rode successfully through the fault (low voltage) events, and provided reactive support during the low-voltage period.

*Tripped Due to Prolonged (+0.5s) Low Voltage:* A second test was performed with prolonged (+0.5 second) low-voltage, i.e. the following combinations of residual voltages at PCC and fault durations were tested: [0pu, 0.15+0.5s], [0.1pu, 0.3+0.5s], [0.2pu, 0.45+0.5s], [0.3pu, 0.6+0.5s], [0.5pu, 0.9+0.5s], [0.7pu, 1.2+0.5s], [0.9pu, 1.5+0.5s], [0.92pu, 3+0.5s]. With the prolonged 0.5s, the LSSPV inverter provided reactive support at the first part of the low-voltage period. However, the built-in protection tripped the inverter when the low-voltage period is longer than the settings.

### c. Frequency Response Test:

The LSSPV's frequency response is tested according to Grid Code for Sabah and Labuan. It's impractical to achieve large over frequency with the Sabah Grid model; therefore this test is performed by connecting the detail LSSPV plant to a two-machine power system in PSSE version 33. The over frequency reduction capability of LSSPV plant is verified by sudden reduction of the load at bus 201, which results in increasing the system frequency above 51Hz. The inverter parameters have been set to reduce active power 0.4pu/Hz when frequency exceeds 50.5Hz, and will return to its pre-disturbed state only if the frequency went below 50.5Hz.

## 4 Conclusion

Based on the study performed, it was observed that no transmission element is overloaded under normal grid condition due to 48MW LSSPV connection. The grid system is strong in comparison with the LSSPV and the effective short-circuit ratio at PCC is around 11. The LSSPV is also capable of operating continuously within the stipulated range of grid voltage variations. A number of voltage violations were found in N-1 and N-2 contingency analysis. However, these violations are not triggered by the connection of LSSPV. With the installation of 20MVAr STATCOM, the LSSPV fulfils the reactive power requirement as required by the Grid Code of Sabah and Labuan. All transient stability tests of category 1 and 2 events at the vicinity were passed with acceptable damping.

Power quality assessment with the LSSPV observed that the worst-case harmonic distortion, flicker and voltage unbalance results are within the limit of Sabah Grid Reliability Standards. The LSSPV inverter also successfully rode through the fault (low voltage) events, and provided reactive support according to the Grid Code of Sabah and Labuan settings. It is also observed that the LSSPV inverter response to grid system over frequency correctly according to Grid Code requirements.

## References

1. Widén, Joakim & Åberg, Magnus & Henning, Dag, "Impacts of Large-Scale Solar and Wind Power Production on the Balance of the Swedish Power System", 851-858. 10.3384/ecp11057851,2011.

2. Shaker, Hamid & Zareipour, Hamidreza & Wood, David, "Impacts of large-scale wind and solar power integration on California's net electrical load", Renewable and Sustainable Energy Reviews. 58. 761-774. 10.1016/j.rser.2015.12.287, 2016.
3. D. Wang, X. Yuan, M. Zhao and Y. Qian, "Impact of large-scale photovoltaic generation integration structure on static voltage stability in China's Qinghai province network," in The Journal of Engineering, vol. 2017, no. 13, pp. 671-675, 2017.
4. L. Bird and M. MilliganJ., "Lesson from Large-Scale Renewable Energy Integration Study", 2012 World Renewable Energy Forum, Denver, Colorado, May 13-17, 2012.
5. A. Mills et. al, "Integrating Solar PV in Utility System Operations", Argone National Laboratory, ANL/DIS-13/18.
6. Grid Code for Sabah and Labuan (Electricity Supply Act 1990 (Act 447)), version 2, 2017.
7. Sabah Grid Reliability Standard, Version 1.0, March 2015.
8. Generator Model data sheet, Siemens, PSSE Model Library, October 2013.
9. WECC Renewable Energy Modeling Task Force, WECC PV Power Plant Dynamic Modeling Guide, April 2014.
10. Short-circuit currents in three-phase a.c. systems - Part 0: Calculation of currents, IEC 60909-0:2016



# i-BeeHOME: An Intelligent Stingless Honey Beehives Monitoring Tool Based On TOPSIS Method By Implementing LoRaWan – A Preliminary Study

Wan Nor Shuhadah Wan Nik<sup>1</sup>, Zarina Mohamad<sup>1</sup>, Aznida Hayati Zakaria<sup>1</sup> and Abdul Azim Azlan<sup>2</sup>

<sup>1</sup>Faculty of Informatics and Computing, Universiti Sultan Zainal Abidin (UniSZA),  
Besut Campus, 22200 Besut, Terengganu, MALAYSIA

<sup>2</sup>University Malaysia of Computer Science & Engineering (UNIMY),  
63000 Cyberjaya, Selangor, MALAYSIA  
wnshuhadah@unisia.edu.my, zarina@unisia.edu.my,  
aznida@unisia.edu.my, azimazlan4@gmail.com

**Abstract.** This paper describes a preliminary study on the development of an intelligent bee hives monitoring tool called *i-BeeHOME*. This tool benefits LoRa and LoRaWan (LoRa in low power WANs) technology. This intelligent tool is capable to collect crucial information on bee colony hives in real-time despite of its remote location. The capability as a smart device of *i-BeeHOME* is further advanced when these information is then analyzed using one of the most well-known multi-criteria decision making (MCDM) method, i.e. TOPSIS. Therefore, it is realized that the capability of *i-BeeHOME* is three-fold, i.e. (1) collects and retrieves crucial information from beehives despite of its remote/rural location where WiFi/BLE based networks are ineffective by using LoRa technology, (2) analyzes information collected to predict the conformity of bee hives location for high quality of honey production by using TOPSIS method, and (3) tracking the geographical location of beehives in protecting it from being stolen/lost by using LoRaWAN technology. It is expected that the development of this tool will not only help the beekeepers to monitor honey beehives with minimum effort, but also implicitly allows further investigation on how to promote high quality of honey production by stingless bees.

**Keywords:** Internet-of-Things (IoT), Smart Farming, Multi-Criteria Decision Making (MCDM), TOPSIS Method.

## 1 Introduction

In natural habitat, stingless bees usually nest in tree trunks and branches, underground cavities, or rock crevices. However, in agricultural industry, it is common for beekeepers to keep the bees in their original log hive or transfer them to a wooden box, as this makes it easier to control and monitor the hive. This industry requires a smart invention that takes advantage of advance technology to help beekeepers to monitor stingless honey beehives with minimum effort despite of its nature of remote/rural location. A

real time monitoring of beehives is crucial to allow analysis and further investigation to ensure high quality of honey production.

Keeping stingless bees has been very popular in the last few years, especially in tropical and subtropical regions of the world. Although stingless bee keeping seems to be straight forward, there are two main issues that could hinder the success, i.e. (1) how to monitor the beehives despite of its nature of remote/rural location, and (2) how to protect the beehives from being stolen/lost.

By realizing the potential benefits on the commercialization of the honey from Stingless Honey Bee, the advancement in a way of evaluating a suitable location of the bee to nest together with the tracking and monitoring of Stingless Bee Hives is needed. This way, the beekeeper can predict the best geographical area to place the box and attract the bees to nest in it and further produce a good quality honey. Further, the advancement also should be able to ease the beekeeper to track and monitor the hives and further protect the honey from being stolen or lost.

Therefore, this paper addresses these issues by providing an intelligent stingless honey beehives monitoring tool that take advantage of LoRaWan (LoRa in low power WANs) technology called *i-BeeHOME*. While LoRa devices and wireless radio frequency technology is described as a long range, low power wireless platform that has become an important technology for Internet-of-Things (IOT) networks worldwide, LoRaWan is capable on exploiting transmitted packages to calculate the current position without the use of current GPS or GSM. The synergy of these two technologies offers an efficient, flexible and economical solution to real world problems in predicting a precise location of rural/remote area and indoor use cases, where cellular and WiFi/BLE based networks are ineffective. Further, this tools is equipped with an intelligent analysis engine that exploit one of the most well-known Multi-Criteria Decision Making (MCDM) method i.e. TOPSIS. This analysis engine considers set of an important criteria that directly affect the quality of honey production by stingless bees, i.e. temperature, humidity, level of noise and reach of lights in the area of beehives location. From the analysis of these criteria, this tool is capable to predict the conformity of bee hives location for high quality of honey production.

In summary, it is realized that the aim of this project can be described as follows: (1) to propose the implementation of LoRa / LoRaWAN technologies to monitor the location of the beehives and tracking a real-time location of beehives, and (2) to propose the use of the Multi-Criteria Decision Making (MCDM) method, i.e. TOPSIS method, to predict the conformity of the area to place the beehives.

## 2 Literature Review

The advancement of LoRa / LoRaWan technologies has become a de facto for the emerging of Internet-of-Things (IoT) paradigm in a world of smart societies nowadays [1], [2], [3], [4]. Research in [5] studied the use of LoRaWan technology in agriculture industry, with the advancement of this technology can be considered to be pioneered by SemTech [6]. In [5], the agriculture system based on LoRaWan network for data transmission from sensor nodes to cloud services has been developed. The system allows data analytics by utilizing data streams within their cloud services by using a case

study from a grape farm. The study proved that the IoT agricultural system can benefit LoRaWan services.

For a specific discussion on the advantages of LoRa / LoRaWan technologies in beehives monitoring, [7] has developed a remote beehive monitoring using LoRa. This system monitors the temperature and weight of beehives in order to predict the potential health status of bees which directly affect the quality of honey production. However, this project does not specifically discuss the analytics part when data are collected from the rural area where bees are kept.

Undoubtedly, some existing products are available which can help beekeepers to monitor their beehives [8], [9], [10]. However, none of these product descriptions specifically discuss the analytics part on how data collected from their system is analyzed in order to achieve good decision on the best location to place the beehives to ensure high quality of honey production.

### 3 Motivations

Beehives monitoring system is gaining more attention in agriculture domain as it allows automatic monitoring of beehives despite of remote beehives locations in nature. This project aims to help beekeepers to choose the best location to locate their beehives based on each criteria value that affect the quality of honey production. Undoubtedly, there are many beehives monitoring systems that are available in the market such as in [11], [12], [13] and [14] with most of them are equipped with GPS (Global Positioning System) technology to trace the location of beehives. However, it is arguable that the use of GPS, especially in small devices with limited power capability, can cause battery power drainage in their systems [1], [2], [3]. Comparatively, *i-BeeHOME* is developed by exploiting LoRaWan (LoRa in low power WANs) technology which can better save battery power consumption. Furthermore, to the best of our knowledge, none of these systems are capable to suggest the best beehive location for beekeepers to place their beehives in order to obtain a good quality of honey produced by stingless bees. Most of these systems only send notifications on data collected from beehives to beekeepers and leave the decision on finding the best location to locate their beehives to the beekeepers. *i-BeeHOME* on the other hand, is intelligent enough to evaluate data collected from beehives and suggest the best location to place the beehives in order to get good quality of honey produced by stingless bees.

### 4 Methodology and Project Framework

The proposed methodology and project framework can be divided into two (2) main phases, i.e. Phase 1: Predicting the conformity of the potential geographical location to place the beehives for high quality honey production, and Phase 2: Tracking and monitoring the location of the beehives.

#### **PHASE 1:**

In this phase, data collected from sensors at beehives are analyzed by using TOPSIS method. This method is one of the well-known MCDM technique to make decision when multiple criteria need to be considered simultaneously. In our case, set of criteria that directly affect the health of bees and further the quality of honey production by these bees were determined, i.e. temperature, humidity, level of noise and reach of sunlight. Steps involved in this phase are described as follows:

**Step 1:** Determine a set of criteria that need to be considered when determining the best location to place the beehives.

**Table 1.** An example of criteria set value for the best geographical location to place the box (beehives)

Location ID	Temperature	Humidity	Level of noise	Reach of sunlight
1	10	3.4	0.70	3
2	6	2.7	0.40	9
3	10	5.6	0.37	2
4	15	6.4	0.25	7

**Step 2:** Enter each criteria value collected from sensor nodes located at beehives into TOPSIS method and retrieve the best location to re-arrange and place the beehive.

**Algorithm** *LocationSelection*

**BEGIN**

1. **FOR** each beehives location  $R_i \in \Re^N$  **DO**
2.     Evaluate  $temperature_{R_i}$ ,  $humidity_{R_i}$ ,  $noise_{R_i}$  and  $sunlight_{R_i}$
3. **ENDFOR**
4. Construct a decision matrix  $D$
5. WeightAssignment ( $temperature_{R_i}$ ,  $humidity_{R_i}$ ,  $noise_{R_i}$ ,  $sunlight_{R_i}$ )
6. Normalize  $D$  with elements are defined by  $z_{ij} = f_{ij} / \sqrt{\sum_{i=1}^m f_{ij}^2}$ ,  $i=1, \dots, m$ ;  $j=1, \dots, n$ .
7. Formulate the weighted normalized decision matrix whose elements are  $x_{ij} = w_j z_{ij}$ ,  $i=1, \dots, m$ ;  $j=1, \dots, n$ .

8. Determine the positive ( $a^+$ ) and the negative ( $a^-$ ) ideal beehive locations as follows:

$$a^+ = \{(\min_i x_{ij} \mid j \in J) \mid i = 1, \dots, m\} = \{x_1^+, x_2^+, \dots, x_n^+\}$$

$$a^- = \{(\max_i x_{ij} \mid j \in J) \mid i = 1, \dots, m\} = \{x_1^-, x_2^-, \dots, x_n^-\}$$

9. Calculate the separation measures for ideal and negative ideal locations of each beehive location as follows:

$$R_i^+ = \sqrt{\sum_{j=1}^n (x_{ij} - x_j^+)^2}, \quad i = 1, \dots, m$$

$$R_i^- = \sqrt{\sum_{j=1}^n (x_{ij} - x_j^-)^2}, \quad i = 1, \dots, m$$

10. Calculate relative closeness of each beehive location to the ideal beehive location as follows:

$$cl_i^+ = R_i^- / (R_i^- + R_i^+), \quad 0 \leq cl_i^+ \leq 1 \text{ and } i = 1, \dots, m.$$

11. Rank the beehive location based on the magnitude of closeness  $cl_i^+$ .

12. **IF** ( $cl_i^+ > cl_j^+$ ) **THEN**

$R_i$  is preferred to  $R_j$ .

13. **ENDIF**

14. **END LocationSelection**

---

**Fig. 1.** Beehive location selection algorithm

In order to run an algorithm shown in Fig. 1, a set of criteria that give significant effect on the quality of honey production first need to be determined, i.e. temperature, humidity, level of noise and reach of sunlight. These criteria are considered based on [15] and [16]. In step 1 to 3, the algorithm evaluates real values of each criterion captured from each location of beehives. Then in step 4, the decision matrix  $D$  is constructed as follows:

$$D = \begin{bmatrix} C_1 & C_2 & \cdots & C_n \\ R_1 & f_{11} & f_{12} & \cdots & f_{1n} \\ R_2 & f_{21} & f_{22} & \cdots & f_{2n} \\ \vdots & \vdots & \ddots & \ddots & \vdots \\ R_m & f_{m1} & f_{m2} & \cdots & f_{mn} \end{bmatrix} \quad (1)$$

with  $W = (w_1, w_2, \dots, w_n)$ , where  $w_j$  is the weight of the criterion  $C_j$  satisfying  $\sum_{j=1}^n w_j = 1$ .  $R_i$  denotes the alternative beehive locations  $i$ ,  $i=1, 2, \dots, m$ ;  $C_j$  represents the  $j^{th}$  criterion,  $j = 1, 2, \dots, n$  related to  $i^{th}$  location, and  $f_{ij}$  is a crisp value indicating the real value of each beehive location  $R_i$  with respect to each criterion  $C_j$ . Further in step 5, weight is assigned for each criteria considered before the value in decision matrix  $D$  is normalized in step 6 and weighted normalized decision matrix D is formulated in step 7. The essence of TOPSIS method relies on the construction of a positive and a negative ideal beehive location as shown in step 8. The construction of these two locations are very important as the algorithm needs to calculate the separation measures for ideal and negative ideal locations of each beehives location as shown in step 9. Finally, in order to determine the best location to place the beehive, the algorithm first calculate relative closeness of each beehive location to the ideal beehive location based on the equation shown in step 10 to allow the construction of their ranking (step 11). The location on the first rank is considered as the best place to locate the beehive (step 12 to 13).

### **PHASE 2:**

In this phase, the available and current technologies to monitor the beehives is studied and further implemented in this project, i.e. LoRa / LoRaWan technologies. Fig. 2 below shows the framework of *i-BeeHOME* project that implements the LoRa / LoRaWan technology.

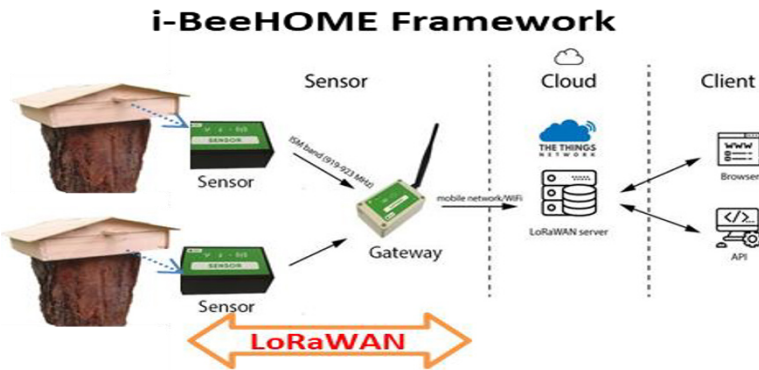


**Fig. 2.** The framework of i-BeeHOME project

In this framework, the physical layer of the system is based on LoRa architecture while LoRaWan protocol takes place in the communication part. LoRaWan is a powerful technology especially in obtaining the geographical locations of a physical entity, where its long range capabilities can be reached up to 15km due to its sensitivity of the receivers [1]. As compared to GPS or GSM technologies which can easily drain the battery power of devices implementing it due to its high energy consumption, LoRaWan uses low power technology of LoRa to calculate the geolocation by applying an algorithm on the gateways timestamps from received packages. This way, the geographical location of beehives can be determined with minimal power consumption from the battery installed in the beehives.

## 5 Conclusion

It is hoped that this project can be tested and further implemented in the real environment of the beehives to further benefits the beekeeper and its commercialization industry. The advantages of LoRa / LoRaWan technologies is synergize with TOPSIS method to be implemented as an intelligent stingless honey beehives monitoring tool.

## Acknowledgement

This work is financially supported by a Collaborative Research Grant (Grant No: UniSZA/2017/PKP/01) (R0021) under Universiti Sultan Zainal Abidin (UniSZA) and Universiti Malaysia Pahang (UMP), Universiti Malaysia Terengganu (UMT) and Universiti Utara Malaysia (UUM).

## References

1. Fargas, B.C. and M.N. Petersen. GPS-free geolocation using LoRa in low-power WANs. in 2017 Global Internet of Things Summit (GloTS). 2017.
2. Barro, P.A., et al., A Smart Cities LoRaWAN Network Based on Autonomous Base Stations (BS) for Some Countries with Limited Internet Access." 11, no. 4: 93.. Future Internet, 2019. 11: p. 4-93.
3. Ram, P. LPWAN, LoRa, LoRaWAN and the Internet of Things. 2018; Available from: <https://medium.com/coinmonks/lpwan-lora-lorawan-and-the-internet-of-things-aed7d5975d5d>.
4. Subashini, S., R. Venkateswari, and P. Mathiyalagan. A Study on LoRaWAN for Wireless Sensor Networks. 2019. Singapore: Computing, Communication and Signal Processing. Advances in Intelligent Systems and Computing, Springer.
5. Davcev, D., et al. IoT agriculture system based on LoRaWAN. in 2018 14th IEEE International Workshop on Factory Communication Systems (WFCS). 2018.
6. LoRa Applications - Smart Agriculture. 2019; Available from: <https://www.semtech.com/lora/lora-applications/smart-agriculture>.
7. Kaufman, D. Remote Beehive Monitoring Using Low power Radio (LoRa). 2018; Available from: <https://contest.techbriefs.com/2018/entries/electronics-sensors-iot/9054>.
8. Pierre and Juan. OpenHiveScale: A Mechanical and OpenSource Scale for Remote Beehives Monitoring. [cited 2019; Available from: <http://www.openhivescale.org/>.
9. Beehive Monitoring. 2019]; Available from: <https://www.digitalmatter.com/Solutions/Smart-Farming-AgTech/Beehive-Monitoring>.
10. Reading Beehives: Smart Sensor Technology Monitors Bee Health and Global Pollination. 2015; Available from: <http://www.libelium.com/temperature-humidity-and-gases-monitoring-in-beehives/>.
11. Markham, D. High tech monitor helps beekeepers track bee activity and colony health in realtime. 2015; Available from: <https://www.treehugger.com/gadgets/high-tech-monitoring-system-helps-beekeepers-track-bee-activity-and-colony-health-realtime.html>.
12. Bento, M. APiS Tech: Smart Hive Monitor for Every Beehive. 2019; Available from: <https://www.indiegogo.com/projects/apis-tech-smart-hive-monitor-for-every-beehive#/>.
13. OSBeehives. 2019; Available from: <https://www.osbeehives.com/pages/tech-specs>.
14. Beepro. 2018; Available from: <http://beepro.ch/en/>.
15. Castle, D. Factors Affecting Global Bee Health. May 2013; Available from: <https://croplife.org/wp-content/uploads/2014/05/Factors-Affecting-Global-Bee-Health-June-2013.pdf>.
16. Bett, C.K., Factors Influencing Quality Honey Production. International Journal of Academic Research in Business and Social Sciences, 2017. Vol. 7, No. 11.



# Optimizing Parameters Values of Tree-Based Contrast Subspace Miner using Genetic Algorithm

Florence Sia and Rayner Alfred

Knowledge Technology Research Unit, Faculty of Computing and Informatics  
Universiti Malaysia Sabah, Jalan UMS, 88400, Kota Kinabalu, Sabah, Malaysia  
[florence.sfs@ums.edu.my](mailto:florence.sfs@ums.edu.my), [ralfred@ums.edu.my](mailto:ralfred@ums.edu.my)

**Abstract.** Mining contrast subspace finds contrast subspaces or subspaces where a query object is most similar to a target class but different from other class in a two-class multidimensional data set. Tree-based contrast subspace miner (TB-CSMiner) which employs tree-based likelihood contrast scoring function has been recently introduced to mine contrast subspaces of a query object by constructing tree from a subspace that is data objects in a subspace space are divided into two nodes recursively with respect to the query object until the node contains only objects of same class or a minimum number of objects. A query object should fall in the node that has higher number of objects belong to the target class against the other class in a contrast subspace. The effectiveness of TB-CSMiner in finding contrast subspace of a query object relies on the values of several parameters involved which include the minimum number of objects in a node, the denominator of tree-based likelihood contrast scoring function, the number of relevant features for tree construction, and the number of random subspaces for contrast subspace search. It is difficult to identify the values of these parameters in a straightforward way based on the conventional analysis. As a consequence, this paper proposes a genetic algorithm based method for identifying the parameters values of TB-CSMiner in which sets of parameters values are treated as individuals and evolved to return the best set of parameters values. The experiment results show that the TB-CSMiner with parameters values identified through the genetic algorithm outperformed those identified through the conventional analysis in most of the cases.

**Keywords:** Mining Contrast Subspace, Contrast Subspace, Genetic Algorithm.

## 1 Introduction

Given a two-class multidimensional data set, a target class, and a query object, mining contrast subspace aims to find subspaces in which the query object is most similar to the target class but dissimilar to the other class [1-2]. Those subspaces are subsets of features from the full feature set of the data set and known as contrast subspaces. A query object can be any object of great interest which its contrast subspaces wanted to be discovered. There are real life applications of mining contrast subspace over many domains such as medical, insurance, banking, science, and etc. For example, a medi-

cal doctor wants to diagnose a patient with Hepatitis A disease. Hence, the doctor may want to know in what subspace the patient's symptoms are most similar to Hepatitis A disease but dissimilar to Hepatitis B disease. This can reduce diagnostic error and makes sure proper treatment can be provided to the patient. Another example is an analyst in an insurance field wants to investigate a fraud claim, thus the analyst may want to know what subspace that makes the fraud claim most similar to fraudulent cases but dissimilar to normal cases. The discovered contrast subspace can be used to determine further investigations and actions that need to be taken.

Tree-based contrast subspace miner (TB-CSMiner) which uses tree-based likelihood contrast scoring function has been developed to mine contrast subspace without affected by the dimensionality (i.e. number of features) of subspaces in multidimensional numerical data set of two classes [3]. Fig. 1 illustrates the process of TB-CSMiner.

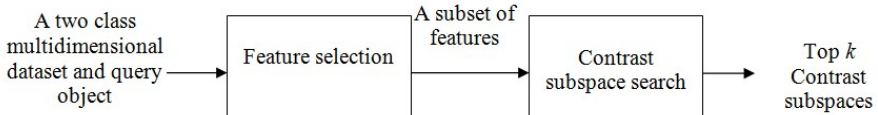


**Fig. 1.** The TB-CSMiner process.

TB-CSMiner mines contrast subspaces of a query object by first identifying a subset of relevant features with respect to a query object based on the tree-based likelihood contrast scoring function from the full feature set given in a data set. A series of random subspace searches based on the tree-based likelihood contrast scoring function is then performed on the selected subset of relevant features to find contrast subspaces of a query object. For a subspace, the tree-based likelihood contrast scoring function constructs a half binary tree by recursively partitioning data objects into two nodes with respect to a query object and terminates the partitions when the node contains all objects belong to the same class or a minimum number of objects. A contrast subspace of a query object is where the query object resides in the node that has higher number of target objects (i.e. objects belong to the target class) against other objects (i.e. objects belong to the other class). TB-CSMiner requires four important parameters which including the minimum number of objects in a node, the denominator of tree-based likelihood contrast scoring function, the number of relevant features for tree construction, and the number of random subspaces for contrast subspace search. The effectiveness of TB-CSMiner depends highly on the values of these parameters. However, the best parameters values for TB-CSMiner in mining contrast subspace cannot be determined directly from the conventional analysis of TB-CSMiner performance.

This paper proposes a genetic algorithm based method for effectively identifying the best parameters values of TB-CSMiner. It generates a population that contains various sets of the parameter's values. For each set of parameters values, the TB-CSMiner uses the parameters values to find contrast subspaces of a query object. Then, the classification task is performed on the identified contrast subspace space. The classification accuracy is assessed and assigned to the used set of parameters

values. After examining all sets of parameters values in the population, a subgroup of the sets of parameters values which have high classification accuracy are selected for evolving process via crossover and mutation operations. At the end, only good sets of parameters values are returned and taken as the best possible sets of parameters values for TB-CSMiner to achieve optimal performance.

Experiments are carried out to evaluate the effectiveness of the genetic algorithm based method in identifying the best parameters values of TB-CSMiner on real world numerical data set. The effectiveness of the genetic algorithm based method in improving the accuracy is compared to the conventional analysis method.

The rest of this paper is organized as follows. We provide the discussion of related works in Section 2. The detailed description of TB-CSMiner is presented in Section 3. Section 4 presents the framework of the genetic algorithm based parameters values identification method. The experimental setup and results are presented in Section 5. Lastly, the conclusion of this work is drawn in Section 6.

## 2 Related Work

Given a two class multidimensional data set, a target class, and a query object, mining contrast subspace is a process of discovering contrast subspaces of the query object in the data set. A contrast subspace is a subspace or subset of features where the given query object is most similar to the target class but dissimilar to other class. To the best of our knowledge, there are only few methods have been developed for mining contrast subspace.

CSMiner (Contrast Subspace Miner) is the first method proposed to mine contrast subspace of a query object in multidimensional data set of two classes [1]. It employs a density-based likelihood scoring function to estimate the likelihood of a query object to the target class and the other class in a subspace. Based on this, CSMiner uses a density-based likelihood contrast scoring function which is the ratio of probability density of target objects to probability density of other objects to measure the likelihood of a query object to the target class against other class in a subspace. CSMiner searches subspace set in depth-first search manner and prunes subspaces from the search space using the upper bound of probability density of target objects. However, CSMiner is inefficient for high dimensional data as the size of search space increase exponentially with the dimensionality (i.e. number of features) of data.

CSMiner-BPR has been introduced to improve the efficiency of the mining contrast subspace by CSMiner [2]. It uses the  $\varepsilon$ -neighbourhood of a query object to create the upper bound of probability density of target objects and the lower bound of probability density of other objects. The subspaces in the search space are pruned based on the upper and lower bound conditions. Thus, the mining process can be accelerated through saving the time of computing the objects outside of  $\varepsilon$ -neighbourhood. Nevertheless, the density-based likelihood scoring function of the abovementioned methods tends to decrease when the dimensionality of subspace increases. This affects the comparison among the different dimensionality of subspaces leading to result inaccurate contrast subspaces for the given query object.

Recently, TB-CSMiner (Tree-Based Contrast Subspace Miner) has been proposed which employs the tree-based likelihood contrast scoring function that is not affected by the dimensionality of subspace [3]. TB-CSMiner is inspired by the divide-and-conquer concept of decision tree method used for classification task. It attempts to gather query object with the target objects but separate it from the other objects in group. The tree-based likelihood contrast scoring function is estimated by the ratio of target objects and other objects in a subspace. TB-CSMiner requires predefined some parameters values which determine the effectiveness of this method.

### 3 Tree-Based Mining Contrast Subspace

Tree-based Contrast Subspace Miner (TB-CSMiner) employs tree-based likelihood contrast scoring function to mine contrast subspaces of a query object in a two-class multidimensional data set [3]. Given a two class  $d$ -dimensional numerical data set  $O$  comprised of  $O_+$  objects belong to class  $C_+$  and  $O_-$  objects belong to class  $C_-$ , a target class  $C_+$  and a query object  $q$ . For a subspace  $S$ , the tree-based likelihood contrast scoring function begins by constructing a half binary tree from the subspace space. Fig. 2. shows the first level of a half binary tree construction process. The tree construction involves the process of selecting a feature  $f$  with highly discriminating value  $a$  such as  $f \leq a$  and  $f > a$ , to partition the data objects in the subspace space into left node that containing a subset of objects with  $f$  has value at most  $a$  and right node that containing a subset of objects with  $f$  has value greater than  $a$ . Information gain function is used to find this highly discriminating value of a feature corresponds to value that is good on distinguishing objects from different classes [4-5]. The values of features being considered are first sorted in ascending order and then the information gain for each mid-value of every two subsequent values is computed. A mid-value with maximum information gain is chosen for the data partition. This partition process continues at the node that has the query object recursively and terminates when all objects in the node having the same class or reaching a user predefined minimum number of objects threshold  $n$ . The node that cannot be partitioned further is called

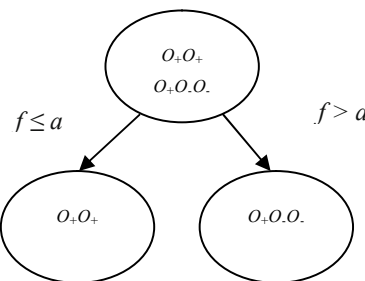


**Fig. 2.** First level of a half binary tree construction.

leaf node of the tree. Finally, the tree-based likelihood contrast score of  $S$  with respect to  $q$  is computed as follows:

$$\text{Tree-LC}_S(q) = \frac{\text{freq}(C_+, X_{\text{leaf}})/|O_+|}{N} \quad (1)$$

with

$$N = \begin{cases} \text{freq}(C_-, X_{\text{leaf}})/|O_-|, & \text{freq}(C_-, X_{\text{leaf}}) > 0 \\ \varepsilon, & \text{freq}(C_-, X_{\text{leaf}}) = 0 \end{cases}$$

where  $\text{freq}(C_+, X_{\text{leaf}})$  denotes the number of target objects in the leaf node,  $|O_+|$  is the number of target objects in the data set,  $\text{freq}(C_-, X_{\text{leaf}})$  is the number of other objects in the leaf node,  $|O_-|$  is the number of other objects in the data set and  $\varepsilon$  is a small constant value. High tree-based likelihood contrast score of subspace signifies that query object is more likely belong to the target class against the other class in the subspace.

The TB-CSMiner consists of two main phases which are the feature selection and the contrast subspace search phase. In feature selection phase, the tree-based likelihood contrast score for each feature or one-dimensional subspace of the full feature set in the data set with respect to a query object is estimated using Eq. (1). A subset of highly scored  $m$  one-dimensional subspaces is selected as a subset of relevant features for contrast subspace search in the next phase. The value of  $m$  is defined by a lower limit 2 and an upper limit is the dimensionality of data. In contrast subspace search phase, the tree-based likelihood contrast score of a random subspace with respect to a query object is estimated. A random subspace constitutes features which are randomly picked from the subset of relevant features. This procedure is repeated for user predefined  $t$  random subspaces and the top  $k$  highly scored random subspaces in their tree-based likelihood contrast scores are taken as the contrast subspaces of the query object.

TB-CSMiner requires four important parameters which are the minimum number of objects in a node, the denominator of tree-based likelihood contrast scoring function, the number of relevant features for tree construction, and the number of random subspaces for contrast subspace search. The values of these parameters are determined through a conventional analysis. Herein, the conventional analysis attempts to find the values of the parameters on which the TB-CSMiner is able to mine contrast subspace effectively. The effectiveness of TB-CSMiner is evaluated in terms of the classification accuracy performed on the contrast subspace. Specifically, mining contrast subspace of query object is performed using TB-CSMiner with various values of the parameters on several data sets. For a contrast subspace of a query object obtained from the TB-CSMiner with a set of parameters values, different types of classification task are performed on the contrast subspace space and the resulting classification accuracy is assigned to the set of parameters values. The higher the classification accuracy indicates the higher the accuracy of the contrast subspace. After examining all sets of parameters values, the effect of the minimum number of objects and the denominator based on the classification accuracy with the rest of the parameters having fixed values is assessed to find the optimal values of those parameters. This is followed by assessing the effect of the number of relevant features and the number of random subspaces with other parameters having fixed values to find the optimal val-

ues of those parameters. These optimal values of the parameters are taken as the best parameters values of TB-CSMiner.

Since TB-CSMiner does not involve any distance computation, TB-CSMiner has shown ability to mine contrast subspace process without affected by the dimensionality of the subspaces. However, the effectiveness of TB-CSMiner in mining contrast subspace relies on the pre-determined values of the above mentioned parameters. The conventional analysis is not able to identify the best values for the parameters of TB-CSMiner by considering the correlation among all values of the parameters in a straightforward way.

## 4 Genetic Algorithm Based Parameters Values Identification Method

This paper proposes a novel method for identifying values of the parameters of TB-CSMiner by using genetic algorithm [7-10]. The identification process is performed on a pre-determined list of values of each parameter. Fig. 3 below illustrates the flow chart of the genetic algorithm used to find the best parameters values of TB-CSMiner. The details of the process involved are described as follows:

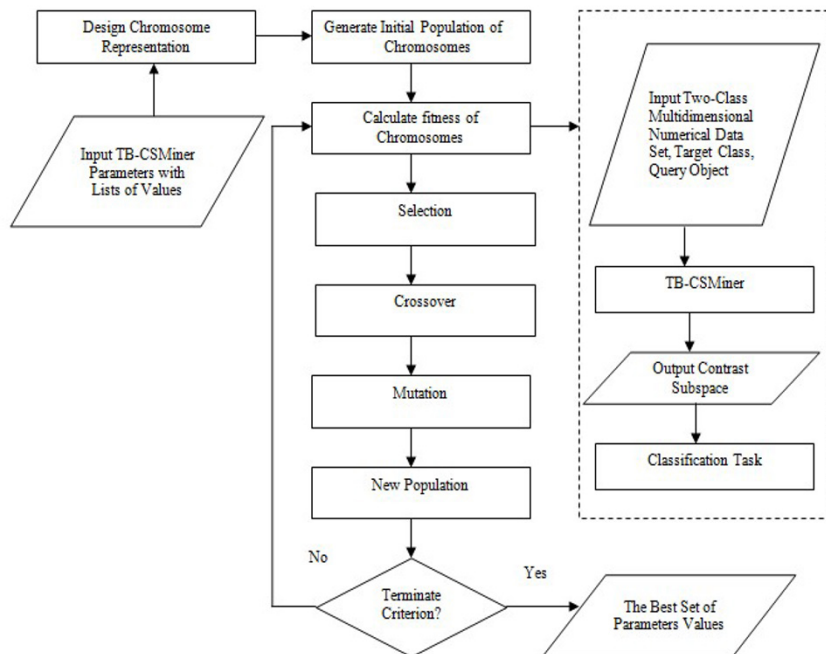


**Fig. 3.** The flow chart of parameters values of TB-CSMiner identification using genetic algorithm.

First, a chromosome representation is designed to carry information about the minimum number of objects in a node  $n$ , the denominator of tree-based likelihood contrast scoring function  $\varepsilon$ , the number of relevant features for tree construction  $m$ , and the number of random trees for contrast subspace search  $t$ . Based on this, a chromosome consists of genes which each gene is assigned to the value of one of those parameters. Instead of using the actual parameters values, the values of the genes correspond to the index position of the parameter's values in the pre-determined list of values of the parameters. An example of chromosome representation used in this work is shown in Fig.4.

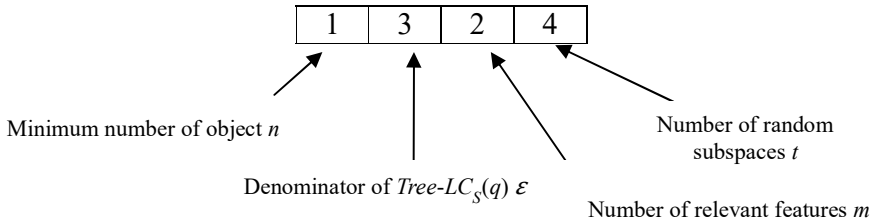


**Fig. 4.** An example of chromosome representation.

Given the minimum number of objects  $n \in \{0.2, 0.3, 0.4, 0.5\}$ , the denominator  $\varepsilon \in \{0.1, 0.01, 0.001\}$ , the number of relevant features  $m \in \{2, 3, 4, 5\}$ , and the number of random subspaces  $t \in \{10, 20, 30, 40\}$ , thus the chromosome in Fig.4 represents a set of parameters values  $n=0.1$ ,  $\varepsilon=0.001$ ,  $m=3$ , and  $t=40$ .

Second, an initial population of  $l$  random chromosomes is created. Each random chromosome takes the value of each parameter randomly from the pre-determined list of values of the parameter.

Third, the fitness of each chromosome in the population is evaluated based on the effectiveness of the TB-CSMiner using the parameters values extracted from the chromosome. As aforementioned in the previous section, the effectiveness of TB-CSMiner is assessed in terms of the classification task performed on the contrast subspace. Hence, the classification accuracy is assigned to the chromosome as fitness score.

Next, a simple yet practical roulette wheel selection technique is used to select chromosomes from the population into new population [11]. A roulette wheel with each slot represents the selection probability defined by the proportion of a chromosome's fitness to the total fitness values of whole population is created. The wheel is spin and the slot where the pointer stops corresponds to the chromosome being selected. This spinning process repeats until there are  $l$  chromosomes in the new population. The roulette wheel selection allows chromosomes with above average fitness values are more likely to be chosen.

After that, the most frequently used one-point crossover operation with a probability of crossover  $p_c$  is performed on those selected chromosomes to produce new chromosomes. A pair of parent's chromosomes is first chosen randomly from the new population and followed by a crossover point is picked from 1 to total genes-1 at random. The fragments of the parent's chromosomes after the crossover point are then

interchanged. This produces two new chromosomes which replace the current parents chromosomes in the new population. The mutation operation with a probability of mutation  $p_m$  is subsequently performed on the selected chromosomes. During the mutation process, the value of a parameter in a parent chromosome is changed to other value randomly chosen from the pre-determined list of values of the parameter.

Accordingly, a new population of chromosomes is generated, and the fitness evaluation is carried out on the chromosomes of the new population. A series of selection, crossover, and mutation is performed iteratively to generate new populations. The population generation process is terminated when the number of iterations  $\mu$  is met.

## 5 Experimental Setup

An experiment is carried out to evaluate the effectiveness of the proposed genetic algorithm based method in identifying the best values of the parameters of TB-CSMiner by comparing to the conventional analysis. In this experiment, a list of minimum number of objects  $n \in \{0.02, 0.04, 0.06, 0.08, 0.10, 0.12, 0.14, 0.16, 0.18, 0.20, 0.25, 0.30, 0.35, 0.40\}$ , a list of denominator of tree-based likelihood contrast scoring function  $\varepsilon \in \{0.1, 0.01, 0.001\}$ , a list of number of relevant features  $m \in \{2, 3, \dots, d\}$ , and a list of number of random subspaces  $t \in \{50, 100, 150, 200, 250, 300, 350, 400\}$ , are used. These values of the parameters are selected by referring to other related works that already exist [12-14]. Besides, this experiment uses the population size  $l=50$ , the probability of crossover  $p_c=0.6$ , the probability of mutation  $p_m=0.01$ , and the number of iterations  $\mu=100$ , which are frequently used in another optimization works [15]. The proposed genetic algorithm based method is implemented in Matlab 9.2 programming language.

These experiments are carried out on five real world multidimensional numerical data sets from UCI machine learning repository which have been used as benchmark in recent works [16]. The five data sets include the Breast Cancer Wisconsin (BCW) data, the Wine data, the Pima Indian Diabetes (PID) data, the Glass Identification (Glass) data and the Climate Model Simulation Crushes (CMSC) data. Table 1 provides the details of these data sets. All non-numerical features and all objects having missing values are removed from the data sets.

**Table 1.** Details of five real world data sets.

Data Set	Number of Objects	Number of Features
BCW	699	9
Wine	178	13
PID	768	8
Glass	214	9
CMSC	540	21

The effectiveness of the parameter's values identification methods are assessed based on the accuracy of the contrast subspace obtained from the TB-CSMiner using

the identified best values of the parameters. That is the contrast subspace accuracy is evaluated in terms of the classification accuracy on the contrast subspace space. The classification accuracy of the contrast subspaces obtained from the TB-CSMiner with the best parameter's values identified through the conventional analysis is used as the benchmark to evaluate the effectiveness of the proposed genetic algorithm based method.

For each data set, the genetic algorithm based method is performed to identify the best values of the parameters. During the fitness evaluation, each object in the data set is taken as the query object and the class of the query object is the target class. The TB-CSMiner is run to find the contrast subspaces of a query object. Only the top one scored contrast subspace is considered, and the data set is then projected onto the contrast subspace with respect to the query object. After that, the contrast subspace space is fed into three classifiers which include J48 (decision tree), NB (naive bayes), and SVM (support vector machine), in WEKA to perform the classification task [17]. The classification accuracy based on 10-fold cross validation is measured. This evaluation process repeats for the rest of the query objects of the data set. For each classifier, the classification accuracy of the contrast subspace for all query objects is averaged and assigned to the currently being considered set of parameters values. Hence, each set of parameters values has three fitness scores corresponds to the accuracy of the three classifiers respectively. At the end of the identification process, the top ten highly scored sets of parameters values are taken from each classifier thus there are total 10 sets X 3 classifiers =30 best sets of parameters values for the data set. Lastly, due to the different characteristic of data sets, these sets of parameters values are generalized to find the best set of parameters values for TB-CSMiner particularly for the data set.

The following Table 2 shows the results of TB-CSMiner using parameters values obtained by conventional analysis and genetic algorithm based method for three classifiers on five real world data sets. It can be seen that the TB-CSMiner with parameters values obtained from the proposed genetic algorithm based method has higher classification accuracy than the conventional analysis for all classifiers on BCW data. The TB-CSMiner with parameters values obtained from the proposed method shows higher classification accuracy for NB and SVM on Wine, Glass, and CMSC data. Meanwhile, the TB-CSMiner with parameters values identified using the proposed method shows higher classification accuracy for J48 and NB on PID data. The improvement is not significant according to the paired-sample T-test at the level of  $p < 0.05$  but the proposed method outperformed the conventional analysis on 11 out of 15 cases in overall. This superior performance shows that the proposed method is able to identify the best parameters values of TB-CSMiner well compared to the conventional analysis.

On the whole, the conventional analysis produces better accuracy on only 4 out of 15 cases. This poor performance from the fact that the conventional analysis examines parameters values separately which may lead to losing important information regarding to the relation among parameters values. Hence, the empirical studies show that the TB-CSMiner with the parameters values identified through the proposed genetic algorithm based method demonstrates good performance in mining contrast subspaces of query objects on real world data sets.

**Table 2.** Average classification accuracy (%) on five real world data sets.

Dataset	Conventional Analysis			Genetic Algorithm		
	J48	NB	SVM	J48	NB	SVM
BCW	98.62	99.41	97.97	<b>98.77</b>	<b>99.50</b>	<b>98.23</b>
Wine	95.93	97.57	94.61	95.75	<b>97.58</b>	<b>96.30</b>
PID	93.87	95.63	85.12	<b>95.19</b>	<b>96.43</b>	83.99
Glass	96.29	96.86	91.90	96.09	<b>96.93</b>	<b>92.72</b>
CMSC	93.85	96.87	94.04	92.88	<b>96.95</b>	<b>94.10</b>

## 6 Conclusion

A genetic algorithm based method has been proposed for effectively identifying the best parameters values of TB-CSMiner. The mining contrast subspace using TB-CSMiner requires four parameters which include the minimum number of objects in a node, the denominator of tree-based likelihood contrast scoring function, the number of relevant features for tree construction, and the number of random subspaces for contrast subspace search. Relevant values of these parameters are necessary in order for TB-CSMiner to mine accurate contrast subspaces of a query object. An experiment has been carried out to evaluate the effectiveness of the genetic algorithm based method and compared to the conventional analysis. The experiment results demonstrate that the TB-CSMiner with the parameters values obtained from the genetic algorithm based method performed better than the conventional analysis in most of cases. Thus, the proposed genetic algorithm based method is capable to find the best parameters values for TB-CSMiner.

## Acknowledgement

The authors gratefully acknowledge that this work was financially supported by the Research University Grant of Skim Penyelidikan Bidang Keutamaan (SPBK) (Project No: SBK0428-2018), Universiti Malaysia Sabah.

## References

1. Duan, L., Tang, G., Pei, J., Bailey, J., Dong, G., Campbell, A., Tang, C.: Mining contrast subspaces. In: Pacific-Asia Conference on Knowledge Discovery and Data Mining, pp. 249-260, Springer, Cham (2014).
2. Duan, L., Tang, G., Pei, J., Bailey, J., Dong, G., Nguyen, V., Tang, C.: Efficient discovery of contrast subspaces for object explanation and characterization. Knowledge and Information Systems, 47(1), 99-129 (2016).
3. Sia, F., Alfred, R.: CSMiner-TBM: Tree-Based Mining Contrast Subspace. International Journal of Advances in Intelligent and Informatics. 5(2), (Nov 2019).

4. Kotsiantis, S. B.: Decision trees: a recent overview. *Artificial Intelligence Review*, 39(4), 261-283 (2013).
5. Aggarwal, C. C.: Data mining: the textbook. Springer, (2015).
6. Kumar, M., Husian, M., Upreti, N., Gupta, D. Genetic algorithm: Review and application. *International Journal of Information Technology and Knowledge Management*, 2(2), 451-454 (2010).
7. Hiassat, A., Diabat, A., Rahwan, I.: A genetic algorithm approach for location-inventory-routing problem with perishable products. *Journal of Manufacturing Systems*, 42, 93-103 (2017).
8. Ho-Huu, V., Nguyen-Thoi, T., Truong-Khac, T., Le-Anh, L., Vo-Duy, T.: An improved differential evolution based on roulette wheel selection for shape and size optimization of truss structures with frequency constraints. *Neural Computing and Applications*, 29(1), 167-185 (2018).
9. Yin, Z. Y., Jin, Y. F., Shen, S. L., Huang, H. W.: An efficient optimization method for identifying parameters of soft structured clay by an enhanced genetic algorithm and elastic-viscoplastic model. *Acta Geotechnica*, 12(4), 849-867 (2017).
10. Cachón, A., Vázquez, R. A.: Tuning the parameters of an integrate and fire neuron via a genetic algorithm for solving pattern recognition problems. *Neurocomputing*, 148, 187-197 (2015).
11. Shi, Z., Li, Q., Zhang, S., Huang, X.: Improved crow search algorithm with inertia weight factor and roulette wheel selection scheme. *International Symposium on Computational Intelligence and Design*, pp. 205-209 (2017).
12. Zhou, Z. H., Chen, K. J., Dai, H. B.: Enhancing relevance feedback in image retrieval using unlabeled data. *ACM Transactions on Information Systems (TOIS)*, 24, 219-244 (2006).
13. Banfield, R. E., Hall, L. O., Bowyer, K. W., Kegelmeyer, W. P.: A comparison of decision tree ensemble creation techniques. *IEEE Transactions On Pattern Analysis And Machine Intelligence*, 29(1), 173-180 (2006).
14. Laguzet, F., Romero, A., Gouiffès, M., Lacassagne, L., Etiemble, D.: Color tracking with contextual switching: real-time implementation on CPU. *Journal of Real-Time Image Processing*, 10, 403-422 (2016).
15. Chiroma, H., Abdulkareem, S., Abubakar, A., Zeki, A., Gital, A. Y. U., Usman, M. J.: Correlation study of genetic algorithm operators: crossover and mutation probabilities. In: *Proceedings of the International Symposium on Mathematical Sciences and Computing Research*, pp. 6-7 (2013).
16. UCI repository of machine learning databases, <http://www.ics.uci.edu/~mlearn/MLRepository.html>, last accessed 2019/6/13.
17. Bouckaert, R. R., Frank, E., Hall, M., Kirkby, R., Reutemann, P., Seewald, A., Scuse, D.: WEKA manual for version 3-9-1, University of Waikato, Hamilton, New Zealand. (2016).



# Development of a Self-sufficient Ad Hoc Sensor to Perform Electrical Impedance Tomography Measurements from Within Imaged Space

Abbas Ibrahim Mbulwa<sup>1</sup>, Ali Chekima<sup>1</sup>, Jamal Ahmad Dargham<sup>1</sup>, Yew Hoe Tung<sup>1</sup>,  
Renee Chin Ka Yin<sup>1</sup> and Wong Wei Kitt<sup>2</sup>

<sup>1</sup> Universiti Malaysia Sabah, 88400 Kota Kinabalu, Sabah, Malaysia

<sup>2</sup> Curtin University, 98009 Miri, Sarawak, Malaysia  
aibramai3@gmail.com

**Abstract.** Electrical Impedance Tomography (EIT) is an ill-posed problem whereby there are insufficient measured data to solve for a large amount of unknowns (finite elements). Conventionally, EIT measurements are performed on the boundary of an object or a process vessel. This results in a lower spatial resolution in central regions far off the conventional periphery electrodes. This paper presents the development of a self-sufficient EIT sensor with an aim to obtain EIT measurements from any locality within the object or the process vessel. An ad hoc EIT sensor that performs the current injection and voltage measurement around two pairs of electrodes is developed. The sensor consists of a current source, voltage amplifier, multiplexers, and microcontroller. Tests were conducted on a phantom tank. The sensor successfully performs localized voltage measurements from the interior of the imaged space with channel SNR average of 15dB.

**Keywords:** Electrical Impedance Tomography, Howland current source, EIT sensor.

## 1 Introduction

Electrical Impedance Tomography (EIT) is a simple solution to obtaining information about the interior of an object or a process through electrical excitation and measuring of voltage, whereby interior conductivity distribution within an object or a process vessel can be reconstructed in a form of tomograms. EIT has shown potential over existing imaging modalities [1], however, the main drawback has been its low spatial resolution towards the center of the imaged space. The favorable effort to solve this problem has been increasing the number of measurements by increasing the number of conventional electrodes available [2]. Various conventional electrode arrangements such as; ring, linear and matrix arrangements are explored in [3]. Multiple rings and semicircle have also been used [4]. One of the limitations of conventional arrangements is that the electrodes are usually located around the periphery of the object under test, hence limiting where the changes in conductivity in the medium can be detected and measured.

Several studies [5-8] have investigated the feasibility of integrating internal electrodes to perform measurements from within the imaged space. Murphy et al [9] used electrodes mounted on a rotating impeller to further extend the number of measurements of a conventional EIT system. The electrodes mounted on the rotating impeller were only used as current sinks. Chin et al [10] employed voltage sensor nodes to acquire localized measurements within the imaged space. Each sensor node is equipped with two electrodes that only function to acquire voltage difference measurements, similar to those obtained using wall-mounted electrodes. The authors reported overall improvement of sensitivity across the medium, however, there was a lack of new information collected within the central regions. This is attributed to the fact that electric excitation is limited to wall-mounted electrodes while the internal electrodes acted only as a voltage measuring electrodes. Additionally, Zhang et al [11] used an array of long steel-cased boreholes as electrodes to detect oil-water distribution in oil fields. Bai et al [12] used borehole-to-surface as electrodes to detect ground anomalies. In both cases, the electrodes are fixed at one side of the imaged space, therefore, limiting detection of anomalies located far off the electrodes [13].

This paper presents the development of a self-sufficient ad hoc EIT sensor that is equipped with two pairs of electrodes which act as a current source and voltage measuring system. This allows for current injection (source and sink) and voltage measurements to be performed from any location within the imaged space. This paper consists of four sections. Section 2 describes the methods of developing a four-electrode self-sufficient EIT sensor. Section 3 presents simulation and experimental results for the current source and voltage measurements. The prototype is tested on a process vessel containing tap water with and without inserted anomaly. Conclusions are presented in Section 4.

## 2 Method

The sensor design modules include a current source, an analog switch and selection, a voltage sensor, and a microcontroller that handles analog-to-digital conversion and communication. The term ‘self-sufficient’ means the EIT sensor consists of its own current source and a voltage sensing circuit. This is to enable the EIT sensor to perform current injection and localized voltage measurement from “any” interior location using four electrodes attached around a small 3D structure made of non-conducting material. Fig. 1 presents the system architecture of the self-sufficient EIT sensor.

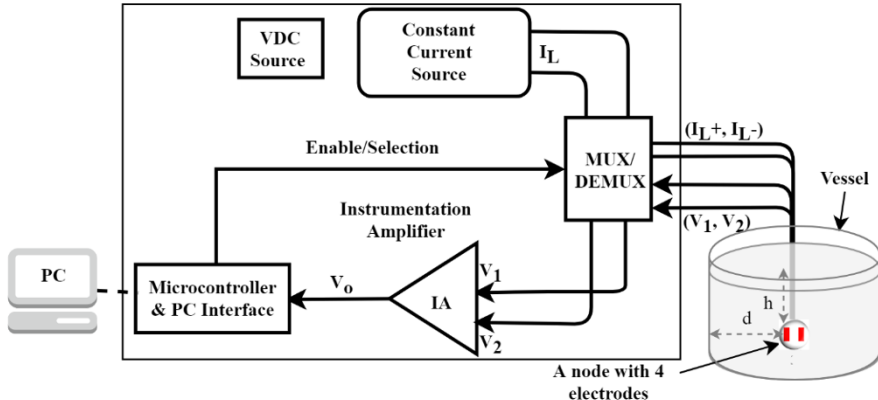


Fig. 1. Self-sufficient EIT sensor architecture.

EIT system requires a constant current source, whereby a dependent source such as voltage-controlled current source (VCCS) fed with an alternating voltage signal from a voltage signal generator is used [14]. For a DC-based EIT system, a VCCS fed with a VDC is used [15].

## 2.1 Howland Current Source

Howland current technique is a preferred solution for EIT systems due to its ability to produce constant current from simple implementation [16]. Some studies have investigated the characteristics and performance of Howland Current Source (HCS) in different configurations [17]. In this work, the improved Howland current source is chosen over a basic Howland configuration. Fig. 2 presents the schematic of the improved Howland current source.

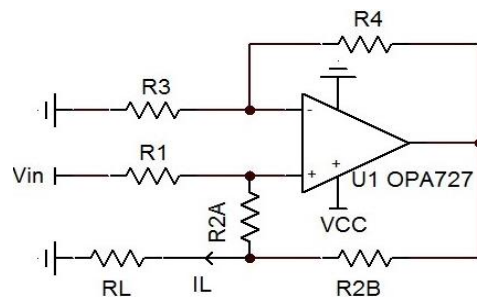


Fig. 2. Schematic of the improved Howland current source.

When resistor matching condition is achieved (1), the load current  $I_L$  is proportional to the differential input voltage of the operational amplifier and it's independent of the

load voltage  $V_L$ , provided  $R_{2B}$  is fixed and the ratio  $R_4/R_3$  is constant [17]. The load current  $I_L$  is given by (2).

$$\frac{R_{2A} + R_{2B}}{R_1} = \frac{R_4}{R_3} \quad (1)$$

$$I_L = \left( \frac{V_{in+} - V_{in-}}{R_{2B}} \right) \frac{R_4}{R_3} \quad (2)$$

The improved Howland current configuration generally solves the inefficiency in resistor matching and output stability problem that exists in basic Howland configuration. Various researchers [18-21] have implemented improved Howland configuration in their EIT system design.

## 2.2 Current Pattern and Voltage Measurement

The adjacent current pattern method suggested by Brown and Segar [22] is used. In the adjacent current pattern, an EIT system sequentially applies electric current into the domain by using a pair of adjacent electrodes (pair drive) where one electrode is a current source, and another is a current sink. While the current is applied to the domain, a voltage measurement is performed on the remaining pair of electrodes by using the adjacent voltage measurement strategy where the differential voltage is measured on the adjacent electrodes pair. This strategy is superior in comparison to other strategies [23]. The adjacent strategy yields a total of  $L(L - 3)$  measurements (including reciprocal pairs), where  $L$  represents a total number of electrodes. In a multiple ad hoc sensors system, other current patterns e.g. opposite [24] and other measurement strategies [23] are worth investigating.

Table I shows a measurement sequence for the four-electrode EIT sensor using the pair drive and differential voltage measurement through adjacent strategy. A total of four full measurements are obtainable from a single sensor.

**Table 1.** Pair drive measurement sequence for a four-electrode EIT sensor with address selection bits.

Measurement Number	Address Bits			Current Injection Electrode Pair	Voltage Sensing Electrode Pair
	A1	A0	EN		
	x	x	0	None	None
1	0	0	1	E1,E2	E3,E4
2	0	1	1	E2,E3	E4,E1
3	1	0	1	E3,E4	E1,E2
4	1	1	1	E4,E1	E2,E3

Voltage measurement is implemented using instrumentation amplifier INA128. The INA128 operates on as low as  $\pm 2.25$  V supply voltage, it offers a CMRR of 120 dB minimum, and gain ranging 1 – 1000 V/V set by the external gain resistor. To alternate current injection (source and sinking) and voltage measurement, two 4:1 bidirectional

analog multiplexers (CD74HC) are used. CD74HC operates at as low as 2 V and has 7 Ω on-resistance, it is digitally controlled through address bits that alternate role of the two electrode pairs as shown in Table 1.

### 2.3 Microcontroller and system integration

The microcontroller handles the issuance of address bits and transfer of measured voltage to PC after analog-to-digital conversion (ADC). There is a trade-off between the size of a microcontroller IC and the resolution of its built-in ADC. Most microcontrollers of a smaller size such as 8bits mid-range PIC or ATtiny AVR, having eight or less pin count, offer up to 10 bits ADC resolution, while microcontrollers with larger pin counts of more than sixteen offer 12 bits ADC or more. In this work, the ad hoc sensor uses 4 pins; 2 for address bits (GPIO pins) and 2 for transmitter/receiver. A PIC12F1840 is used. PIC12F1840 is an 8-bits low power microcontroller with an internal flexible ADC and oscillator. It has 256 bytes RAM which is sufficient for handling ADC and communication for one sensor. Fig. 3 shows the integrated system showing module connectivity excluding PC communication components. The sensor prototype is constructed and tested on a phantom vessel.

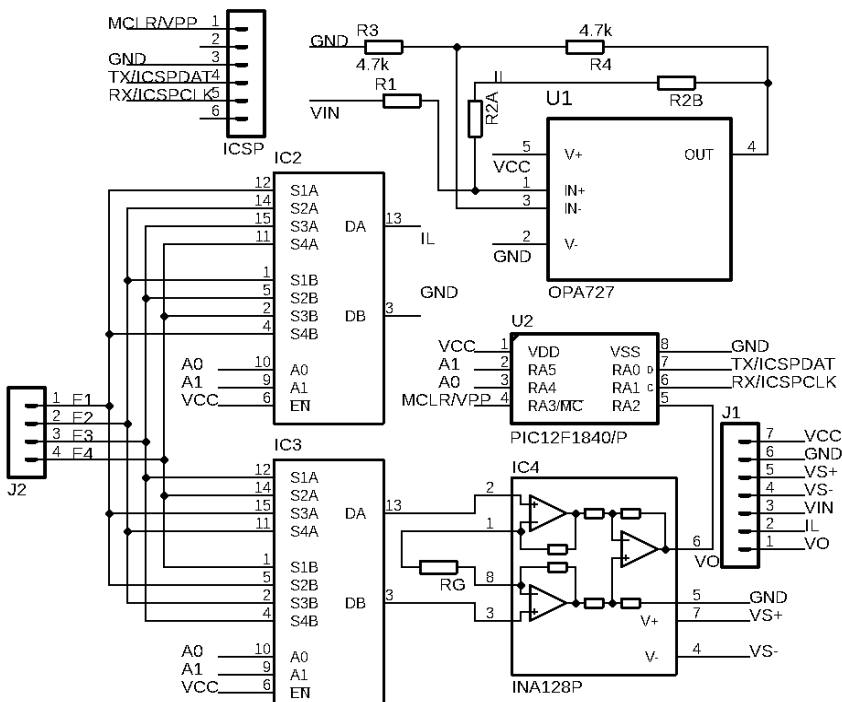


Fig. 3. EIT ad hoc sensor system schematic, excluding PC communication components.

### 3 Results and discussion

#### 3.1 Current Source

Simulation of the current source (Fig. 2) is performed using TINA-TI software. The range of load impedance for which the load current is stable and constant was determined through trimming of resistor R2A so that  $R2A + R2B$  balances with R1 (2). R2A was set to 0.47 k $\Omega$ . All resistors are set with 1% tolerance.

Figure 4 shows the simulation of the load current over a variety of load impedance where the current is constant and stable at 1 mA for load impedance variation of up to 2.2 k $\Omega$ . For load impedance variation above 2.2 k $\Omega$ , the current drops instantaneously. This indicates that a stable current over a wider range of load impedance is achievable with current requirements of less than 1 mA. The output impedance was simulated using a method presented in [25], where the output impedance of 35 M $\Omega$  is achieved.

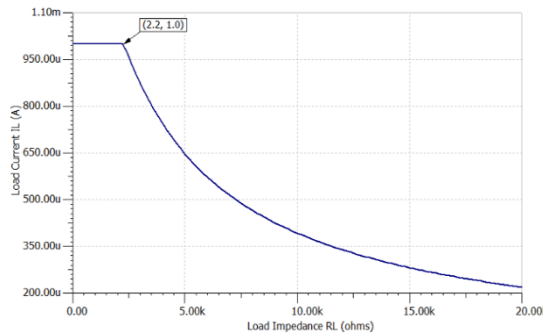
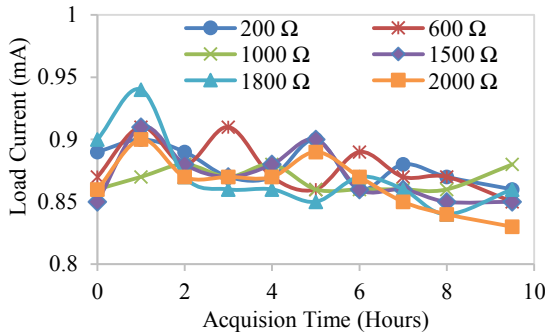


Fig. 4. Simulated load current over load impedance.

Figure 5 shows the experimental results. In experiments, the load current was determined by measuring the output voltage across load impedance  $R_L$ . To investigate the stability of the current source, measurement of the load current was performed using six load impedances namely; 200  $\Omega$ , 600  $\Omega$ , 1000  $\Omega$ , 1500  $\Omega$ , 1800  $\Omega$  and 2000  $\Omega$  for a period of approximately 10 hours of continuous operation, where the load impedance was changed after an interval of approximately one hour. Measurements were performed using *Sanwa-CD800a* digital multimeter. It can be observed in Fig. 5 that a fairly constant current of approximately 0.9 mA is achieved for a load variation of up to 2 k $\Omega$ . The results demonstrate that the sensor can be used in mediums of various conductivities without greatly affecting current source performance.



**Fig. 5.** Measured load current over time for various load.

### 3.2 Localized voltage measurements inside a filled vessel

This section discusses the experimental measurements of voltage on various localities inside the process vessel filled with tap water. The phantom setup is shown in Fig. 1. The sensor node is placed at a radial and height position  $d$  and  $h$  successively, where a full measurement set from four injections is acquired using the two electrode pairs of the sensor. The measurement strategy is presented in Table I. Measurements were obtained at a temporal resolution of 50 samples per second with four sequential current injections at every 200 samples (readings). 200 samples per injection is a good compromise between reaching the static conditions on each measurement and having a fast data acquisition rate. Only samples recorded before electrode switching effects and after the static conditions reached are taken into account in calculating the final four voltage data set (full measurement from one sensor). The final value of the voltage is obtained by finding the mean value of the samples within the mentioned conditions. Fig. 6 shows the localized voltage data measured from inside homogeneous tap water.

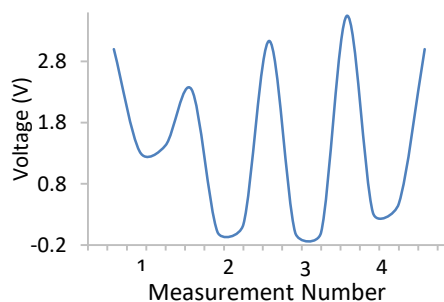


**Fig. 6.** Full measurement from single locality inside a vessel filled with homogeneous tap water.

Measurements were repeated for various locations within the medium to determine the signal-to-noise ratio (SNR). Fig. 7 shows SNR for all four measurement channels for

measurements obtained from different locations within the medium. A relatively higher SNR is achieved on the first measurement channel where current is injected on electrodes (E1, E2) and voltage is measured on electrodes (E3, E4). SNR decreased on the second measurement. Third and fourth measurements have shown reciprocity to the first and second measurement channels. With reciprocity, only half of the full measurements are unique i.e.  $L(L - 3)/2$  [23].

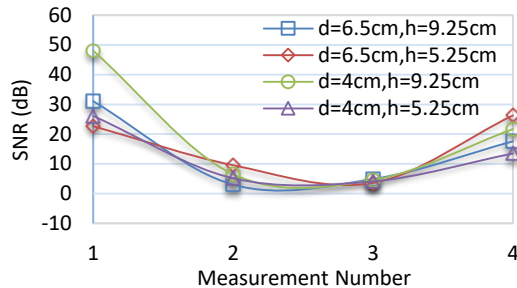


**Fig. 7.** SNR for measurements acquired from four localities inside a vessel filled with tap water.

To evaluate the sensor, experiments to detect anomalies were conducted. A conductive anomaly and a non-conductive anomaly were inserted in an imaged space and measurement were performed successively. Fig. 8 shows measurements obtained from a homogeneous (without anomaly inserted) and inhomogeneous imaged space. The sensor is able to detect and distinguish between conductive and non-conductive anomaly. The magnitude of measurements taken from imaged space with an inserted anomaly, relative to that without anomaly, shows a slight increase as the sensor-anomaly displacement decreases. This implies that the sensor well detects anomaly located in its vicinity than those far located.

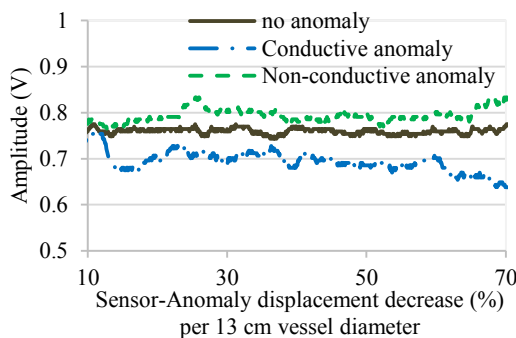


**Fig. 8.** Measured voltage from imaged spaced with and without anomaly

The results obtained from the experiments demonstrate that localized EIT measurements can be acquired from any location interior of the imaged space using an ad hoc EIT sensor. This measurement especially from central location contains information that is not readily obtainable using periphery electrodes mounted on the wall of the process vessel.

## 4 Conclusion

This paper presents the development of a self-sufficient ad hoc EIT sensor that is deployed within the imaged space to perform constant current injection and differential voltage measurement from any locality within the imaged space. The sensor implements an improved Howland current technique and two 4:1 bidirectional analog multiplexer to alternate constant current injection and differential voltage measurement using its four electrodes. The results obtained show that localized EIT measurements can be acquired from any location interior of the imaged space using an ad hoc EIT sensor. The advantages of this approach are: (a) the internal electrodes perform both current injection and voltage measurements (b) miniature, low-cost and low-power EIT hardware design. Furthermore, this approach can be used to extend conventional EIT or formulate a novel ad hoc EIT system.

## References

1. Holder, D. S.: Electrical Impedance Tomography Methods, History and Applications. Institute of Physics, Bristol (2005).
2. Chin, R. K., York, T. A.: Improving spatial resolution for EIT reconstructed images through measurement strategies. In: IEEE International Conference on Signal and Image Processing Applications 2013, pp. 5-10. IEEE (2013).
3. Schlebusch, T., Leonhardt, S.: Effect of electrode arrangements on bladder volume estimation by electrical impedance tomography. In Journal of Physics: Conference Series. 434(1), 012080, (2013).
4. Ayati S. B., Kaddour B. M, Kerr D.: In vitro localization of intracranial haematoma using electrical impedance tomography semi-array. Med Eng Phys (2014).
5. Lyon, G. M., Oakley, J. P.: A simulation study of sensitivity in stirred vessel electrical impedance tomography. Tomography techniques for process design and operation, pp. 137-146. (1993).
6. Heikkinen, L. M., Vauhkonen, M., Savolainen, T., Leinonen, K., Kaipio, J. P.: Electrical process tomography with known internal structures and resistivities, Inverse Problems in Engineering 9(5), 431-454 (2001).
7. Kim, K. Y., Kang, S. I., Kim, M. C., Kim, S., Lee, Y. J., Vauhkonen, M.: Dynamic image reconstruction in electrical impedance tomography with known internal structures. IEEE Transactions on Magnetics 2002, vol. 38(2), pp. 1301-1304. IEEE (2002).
8. Ijaz, U. Z., Khambampati, A. K., Lee, J. S., Kim, K. Y., Kim, M. C., Kim, S.: Electrical Resistance Imaging of Two-Phase Flow Through Rod Bundles. In AIP Conference Proceedings, vol. 914(1), pp. 844-849. AIP (2007).
9. Murphy, S. C., Chin, R. K. Y., York, T. A.: Design of an impeller-mounted electrode array for EIT imaging. Measurement Science and Technology 19(9), 094009 (2008).

10. Chin, R.K.Y., Wright P., York T.A.: Electrical Tomography Using Ad Hoc Wireless Sensors. In 6th World Congress on Industrial Process Tomography, Beijing, China (2010).
11. Zhang, Y. Y., Liu, D. J., Ai, Q. H., Qin, M. J.: 3D modeling and inversion of the electrical resistivity tomography using steel cased boreholes as long electrodes. *Journal of Applied Geophysics* 109, 292-300 (2014).
12. Bai, Z., Tan, M. J., Zhang, F. L.: Three-dimensional forward modeling and inversion of borehole-to-surface electrical imaging with different power sources. *Applied Geophysics*, 13(3), 437-448 (2016).
13. Wang, Y., Ren, S., Dong, F.: A transformation-domain image reconstruction method for open electrical impedance tomography based on conformal mapping. *IEEE Sensors Journal*, 19(5), 1873-1883 (2018).
14. Frounchi, J., Dehkhoda, F., Zarifi, M. H.: A Low-Distortion Wideband Integrated Current Source for Tomography Applications. *European Journal of Scientific Research* 27(1) 56-65 (2009).
15. Russo, S., Nefti-Meziani, S., Carbonaro, N., Tognetti, A.: Development of a high-speed current injection and voltage measurement system for electrical impedance tomography-based stretchable sensors. *Technologies* 5(3), 48-58 (2017).
16. Ross, A. S., Saulnier, G. J., Newell, J. C., Isaacson, D.: Current source design for electrical impedance tomography. *Physiological measurement* 24(2), 509-516 (2003).
17. Hammond, G. D., Speake, C. C., Stiff, M.: Noise analysis of a Howland current source. *International Journal of Electronics* 95(4), 351-359 (2008).
18. Bertemes-Filho, P., Felipe, A., and Vincence, V. C.: High accurate Howland current source: Output constraints analysis. *Circuits and Systems* 4(07), 451-158 (2013).
19. Goharian, M., Soleimani, M., Jegatheesan, A., Chin, K., Moran, G. R.: A DSP based multi-frequency 3D electrical impedance tomography system. *Annals of biomedical engineering* 36(9), 1594-1603 (2008).
20. Lee, J. W., Oh, T. I., Paek, S. M., Lee, J. S., Woo, E. J.: Precision constant current source for electrical impedance tomography. In *Engineering in Medicine and Biology Society, Proceedings of the 25th Annual International Conference of the IEEE*, vol. 2, pp. 1066-1069. IEEE (2003).
21. Mahnam, A., Yazdanian, H., Samani, M. M.: Comprehensive study of Howland circuit with non-ideal components to design high performance current pumps. *Measurement* 82, 94-104 (2016).
22. Brown, B. H., Seagar, A. D.: The Sheffield data collection system. *Clinical Physics and Physiological Measurement*, 8(4A), 91-97 (1987).
23. Graham, B. M., Adler, A.: Electrode placement configurations for 3D EIT. *Physiological measurement* 28(7), S29-S44 (2007).
24. Hua, P.: Effect of the measurement method on noise handling and image quality of EIT imaging. In: *9th Int. Conf. IEEE Eng. In Med. And Bioi. Society*, vol. 9, pp. 1429-1430. IEEE (1987).
25. Bertemes Filho, P.: Tissue characterisation using an impedance spectroscopy probe, Doctoral dissertation. University of Sheffield (2002)



# Malaysian Road Accident Severity: Variables and Predictive Models

Choo-Yee Ting<sup>1</sup>, Nicholas Yu-Zhe Tan<sup>1</sup>, Hizal Hanis Hashim<sup>2</sup>, Chiung Ching Ho<sup>1</sup>, and Akmalia Shabadin<sup>2</sup>

<sup>1</sup> Faculty of Computing and Informatics, Multimedia University, Malaysia

<sup>2</sup> Malaysian Institute of Road Safety Research, Malaysia

[cyyting@mmu.edu.my](mailto:cyyting@mmu.edu.my); [nicholas.290696@gmail.com](mailto:nicholas.290696@gmail.com); [hizalhanis@miros.gov.my](mailto:hizalhanis@miros.gov.my);  
[ccho@mmu.edu.my](mailto:ccho@mmu.edu.my); [akmalia@miros.gov.my](mailto:akmalia@miros.gov.my)

**Abstract.** Road accident refers to an incident where at least one land vehicle with one or more people injured or killed. While there are many variables attributed to road accident, ranging from human to environmental factors, the work presented in this paper focused only on identifying predictors that could potentially lead to fatality. In this study, the raw dataset obtained from the Malaysian Institute of Road Safety Research (MIROS) was firstly preprocessed and subsequently transformed into analytical dataset by removing missing values and outliers. Such transformation, however, resort to large feature space. To overcome such challenge, feature selection algorithms were employed before constructing predictive models. Empirical study revealed that there were 26 important predictors for predicting accident fatality and the top five variables are month, speed limit, collision type, vehicle model and vehicle movement. In this work, six predictive models constructed were *Random Forest*, *XG-Boost*, *CART*, *Neural Net*, *Naive Bayes* and *SVM*; with *Random Forest* outperformed the rest with an accuracy of 95.46%.

**Keywords:** Accident Severity · Optimal Feature Set · Predictive Model.

## 1 Introduction

Road accident imposes public road safety, road repair cost and psychological effect to the immediate and indirect victims. World Health Organization (WHO) reported an estimate of 1.25 million fatal road accidents occurs every year worldwide [1]. Fatal road accident has also been reported to be the main contributor for death among teenagers aged between 15 to 29 years old.

Recent work has demonstrated the use of predictive analytics as an alternative way to combat the increasing rate of road accident. Predictive analytics could reduce road accident by forecasting future accidents, which in turn enables relevant agencies to take preventive measures and decisions. One of the most commonly deployed techniques is the *logistic regression* model. Research has shown that variables related to accident can be categorised into five main categories: *offending driver*, *vehicle condition*, *tunnel characteristics*, *environmental*

*conditions and crash information* [2]. Phillips & Sagberg [3] have included *sleep* or *tiredness* when constructing a predictive model. Xie and colleagues proposed a method to model the likelihood of a real-time crash based on freeway loop data through eigenvectors and eigenvalues of the spatiotemporal schematics [4].

Despite the fact that accident differs from one country to another, over 90% of road accident death occurred among low-income and middle-income countries [1]. Low-income and middle-income countries contributed to 54% of worldwide vehicles [5]. In Malaysia, the total number of road accidents that occurred in Malaysia has reached its peak at 489,606 in the year 2015 and was steadily increased from the year 1997 to 2015. The number of road fatality in the year 2013 is 6915 but the number of road fatality in the year 2014 dropped to 6674. No significant difference between year 2014 and 2015 in terms of the number of road fatality while the mortality rate in Malaysia had steadily decreased from year 1997 to 2015. Road accident requires serious attention as it is one of the top five causes of death in Malaysia according to Institute for Health Metrics and Evaluation [6]. Therefore, a system that can predict the severity of road accident should be deployed to lower the occurrence of the road accident in Malaysia. It will indirectly improve the economy and make the road safer for the citizen. Accident severity prediction can benefit several agencies to help them make smarter decision and save lives [7]. Furthermore, a better understanding of the relationship between accident severity and accident factors can curb the economic impact of crashes and also reduce the number of fatal crashes (Jeong et al., 2018). By lowering the fatal accidents, it is also one of the goal of the national strategy of Toward Zero Deaths [9]. In this light, this study aimed to investigate on variables that have high impact towards fatality and subsequently utilizing the variables to construct a predictive model. The work presented in this study had scoped to accidents in Malaysia, with the raw data supplied by Malaysia Institute of Road Safety Research (MIROS).

## 2 Related Work

This section discusses variables (attributes) related to accidents, feature selection techniques, and predictive modeling that commonly found in literature.

### 2.1 Variables related to Accidents

Finding the important variables contributed to accident is crucial before construction of predictive models. Researchers have investigated variables related to accidents, which can be categorized into five different components: *road* , *demographic* , *environment* , *vehicle*, and *accident* .

Road characteristic has variables related to the road itself. *Number of lanes* [10][11], *degree of curve* [12][11] and *speed limit* [13] [11] are under the *road* component. The *Road* component should be considered when constructing model due to the condition of the road have some direct impact on the number of

road accident occurred. Variables in road characteristic are more consistent as compared to others [11].

*Area type* [14] [11], age [10] [11] and *rule violation* [15][16] are under demographic characteristic. Demographic characteristic might play a role in predicting road accident as driver age will affect reaction time, or the violation of the traffic rules might endanger another driver on the road. Variables of demographic characteristic are able to provide more information regarding the people involved in a road accident or the area around the road itself.

*Time* [10][14], *weather* [14][11], and *day* [16] are under environment component. The environmental variables should be considered when constructing model due to most of the environmental characteristics are hazardous as they will affect the driver sight or the vehicle condition. Environmental characteristic is different from country to country as the variables will have different value based on each country. Variable time will also affect the occurrence of road accident as daytime will have higher chances of road accident occur compared to night time [17].

*Traffic speed* [18][19] and *vehicle type* [16][10] are under the *vehicle* component. Vehicle characteristic is one of the important factors as a vehicle can have a direct effect on the occurrence of a road accident. The traffic speed is statistically a significant predictor for the occurrence of road accident [4]. The different type of vehicle will also affect the occurrence of road accident as a heavy vehicle are having higher chances to involved in a road accident as compared to lighter vehicles [17].

*Accident severity*[21][20], *crash type* [10][14], and *number of vehicles involved in accident*[16][17] are under accident component. *Accident* is itself an interesting component when several researchers have used accident-related variables to predict road accident itself. The different crash types will resort to different severity of road accident.

*Road characteristic* has the highest number of variables, but the most used category is from environmental characteristic which the variables are being used 38 times by researchers and for the variables used in road characteristic, demographic characteristic, vehicle characteristic and accident characteristic have a total of 34, 32, 20 and 18 respectively. Most of the variables used by researchers are because their research method used these variables to construct their models.

## 2.2 Feature Selection

Feature selection is the process of selecting important variables that represent the domain problem. Feature selection is commonly a pre-requisite to predictive model construction, mainly because most machine learning methods are having difficulty when dealing with the large number of features [22]. With feature selection, not only the model constructed provides higher predictive accuracy, but also improve model training time and space complexity particularly when noise has been removed [23]. While there are many different feature selection techniques, this paper has scoped to only Recursive Feature Elimination (RFE) technique due to space limitation.

### 2.3 Modeling Techniques

Lloyd & Forster used Multivariate Regression Model because more than one dependent variables involved in the modeling task [24]. Jiang and colleagues used five different categories of variables which were *offending driver*, *vehicle condition*, *tunnel characteristics*, *environmental conditions* and *crash information* with all having categorical data type [2]. Gitelman and colleagues used Classification Tree because the *road infrastructure indicators* were considered as a candidate for classification because all the variables are in categorical data type [25]. In this study, classification algorithms from different family were explored during data modelling section. The findings shall be reported subsequent section.

## 3 Dataset

**Table 1.** Components of MIROS Accident Dataset

Dataset Component	Variables
Road	Road_Geometry, Road_Type, Road_Width, Shoulder_Width, Road_Surface_Condition, area_type, Road_Surface_Type, Quality_Of_Surface, Road_Condition, Lane_Marking, Shoulder_Type, Road_Defect, Light_Condition, Traffic_System, Location_type, Speed_Limit, Control_Type
Demographic	Age, kelas_pengguna, driver_occupation, Sex, licanse_type, InjuryRace, driver_qualification, drinking_drive, license_status
Environment	Month, Hour
Vehicle	Veh_Model, Veh_Modification, Veh_Movement, Veh_Defect, Veh_Ownership, foreign_veh, c_Veh_Type
Accident	Accident_Severity, Collision_Type, animal_fault, tempat_kejadian

The raw dataset used in this study was accident records for year 2015 provided by MIROS. The dataset was separated into three files: the accident info file has 485872 rows and 63 columns, while the car driver info file has 565236 rows and 32 columns and injury info file has 570131 rows and 16 columns. There is a total of 40 variables that are identified by MIROS expert that are deemed important. After extracting the important variables, the resulting dataset consists of a total of 40 columns and 1621239 rows. The detail description about the variables of the final transformed dataset is shown in Table 1. There are five components namely *road*, *demographic*, *environment*, *vehicle*, and *accident*.

## 4 Method

---

**Algorithm 1** Analytical Dataset Preparation

---

**Require:**  $D_{\text{raw}}$

**Ensure:**  $D_{\text{train}}, D_{\text{test}}, F_{\text{best}}$

- 1:  $D_{\text{removedDamage}} \leftarrow \text{remove-DamageOnly}(D_{\text{removedNA}})$
- 2:  $D_{\text{discretized}} \leftarrow \text{discretize}(D_{\text{removedDamage}})$
- 3:  $D_{\text{latlon}} \leftarrow \text{obtainLatLon}(D_{\text{removedDamage}})$
- 4:  $D_{\text{imputed}} \leftarrow \text{imputation}(D_{\text{latlon}})$
- 5:  $D_{\text{preprocessed}} \leftarrow \text{location-weather-profile}(D_{\text{imputed}})$
- 6:  $F_{\text{best}} \leftarrow \text{featureSelection}(D_{\text{preprocessed}})$
- 7:  $D_{\text{train}}, D_{\text{test}} \leftarrow \text{split}(D_{\text{preprocessed}})$

---

The algorithm above shows the overall steps in analytical data preparation. Let  $D$  denote the dataset while  $F$  denote the feature set. In algorithm 1, the first step is to transform the blank spaces and null to NA. The next step is to remove accidents that are damage only as this paper only focus on accident that involved injured people. The resulting dataset has 40166 rows and 40 columns. After imputation, the weather information is obtained from Dark Sky API (Dark Sky API, 2018). Latitude, longitude, day, month and time columns will be transformed into the format that Dark Sky API required. Temperature data has also obtained from Dark Sky API together with weather data. The column day will be removed after obtaining weather and temperature data. The next step is to obtain the number of each place that is provided by Google Places API by providing latitude and longitude data (Google Places API, 2018). Google Places API will return 90 different types of places and the number of each place around that particular accident location. The returned data will then merged with existing dataset and the number of columns will increase from 41 to 133. Column synagogue is removed from the dataset as the value it contains is all zero. Column latitude and longitude are then removed as location data already obtained from Google Places API. The resulting total number of columns reduced from 133 to 129.

The next step was to perform feature selection method, namely RFE. The refined dataset was then split into training ( $D_{\text{train}}$ ) and testing ( $D_{\text{test}}$ ) dataset before model construction phase.

---

**Algorithm 2** Predictive Model Construction

---

**Require:**  $D_{\text{train}}, D_{\text{test}}, F_{\text{best}}$

**Ensure:**  $M_{\text{best}}$

- 1:  $M_{\text{trained}} \leftarrow \text{train}(D_{\text{train}}, F_{\text{best}})$
- 2:  $D_{\text{predictOutput}} \leftarrow \text{predict}(M_{\text{trained}}, D_{\text{test}})$
- 3:  $M_{\text{best}} \leftarrow \text{evaluate}(M_{\text{predictOutput}}, M_{\text{trained}}, D_{\text{test}})$

---

In this study, classifiers were deployed to train models by using the variables importance produced by RFE. The models were evaluated to obtain the optimal. The selected packages to run data modelling are *randomForest*, *xgBoost*, *caret* (CART), *nnet*, *e1071* (Naive Bayes) and *e1071* (Support Vector Machine). The classifier families from which the six classifiers were chosen are *Bayesian*, *Neural Networks*, *Support Vector Machines*, *Decision Trees*, *Boosting* and *Random Forests*. The reason to choose classifiers from different families was that each family performs differently from each other. Another reason is that because *Random Forest*, *SVM*, *Neural Net*, *XGBoost* are the top four families for classification tasks [12]. *Naive Bayes* and *CART* are commonly used as benchmark predictive models in many research work. The equation for accuracy measurement is as follow:

$$\text{Accuracy} = \frac{TN + TP}{TP + TN + FP + FN}$$

## 5 Findings and Discussion

### 5.1 Feature Selection

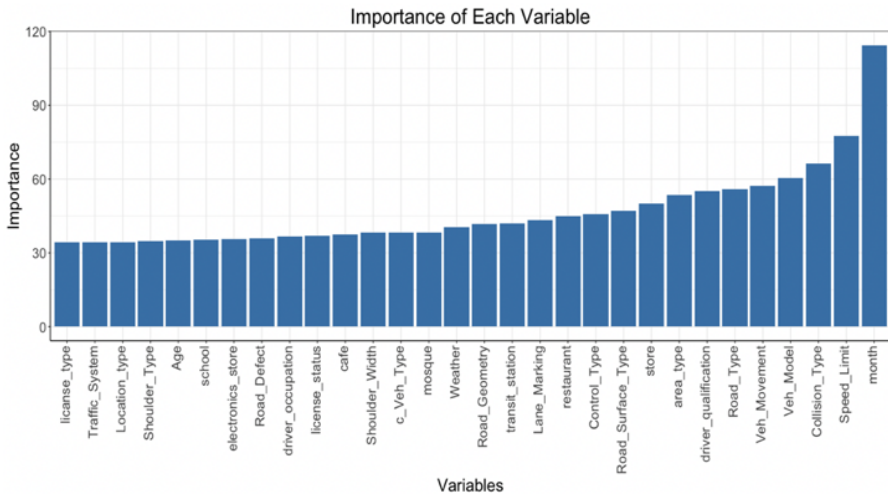


**Fig. 1.** The Performance of Top 30 Variables using RFE

Figure 1 depicts the top 30 important features selected by RFE that have strong contribution to accident severity. The findings suggested that *month* variable has the highest contribution towards accident severity while *speed\_limit*

ranked second and *collision\_type* ranked third. The figure has also indicated that *license\_type* ranked 30<sup>th</sup> in the feature list. The findings were shown to the domain experts for verification and both of them agreed with the findings. The next step was to construct and assess different predictive models for prediction of accident severity. In summary, the top 10 were *month*, *speed limit*, *collision type*, *vehicle model*, *vehicle movement*, *road type*, *driver qualification*, *area type*, *store* and *road surface type*.

## 5.2 Model Assessment

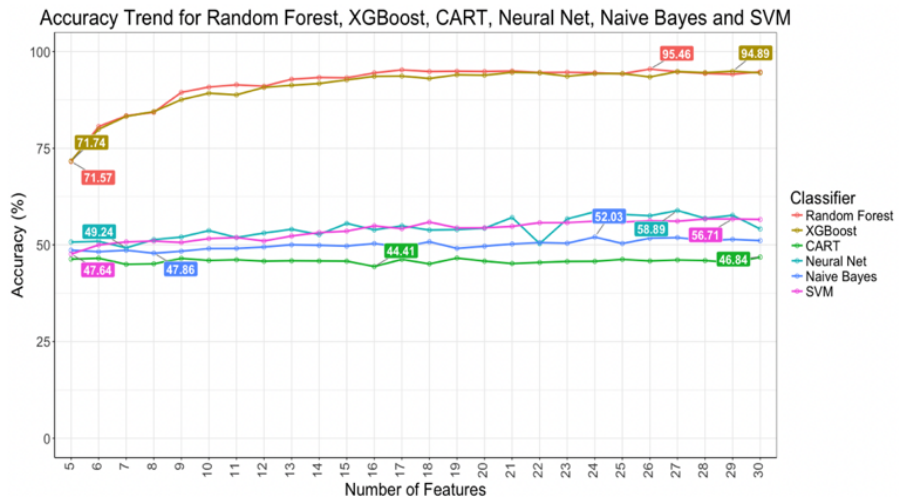


**Fig. 2.** Comparing the Accuracy of Six Different Classifiers

Figure 2 depicts the findings from experiments performed on different classifiers. The purpose of the experiments was to compare the accuracy of each classifier and to investigate the classifier that was optimal for the dataset. According to the figure, the highest accuracy was obtained through *Random Forest* was 95.46% with 26 variables, *XGBoost* performed slightly low with an accuracy of 94.84% with 29 variables, accuracy for *CART* was 46.84% with 30 variables, *Neural Net* was 58.89% with 27 variables, *Naive Bayes* was 52.03% with 24 variables and *SVM* was 56.71% with 29 variables.

Figure 2 has also shown that *Naive Bayes* required the least number of columns to reach the highest accuracy followed by *Random Forest*, *Neural Net*, *XGBoost*, *SVM* and *CART*. When comparing among the classifiers, *Random*

*Forest* and *XGBoost* depicted higher accuracy than *CART*, *Neral Net*, *Naive Bayes* and *SVM*. Between *Random Forest* and *XGBoost*, *Random Forest* performed slightly better than *XGBoost*. In summary, the highest accuracy obtained through the experiment was 95.46% through *Random Forest* using 26 variables.

Table 2 shows the distribution of the top 26 variables among the different components of the dataset. It was found that the *road* and *trade area* components contributed largely to accident severity. As shown in the table, the *road* component comprises 8 variables while trade area occupied 7 variables. The findings suggested that accident severity can be influenced by people movement and concentration. This is shown by the fact that school and transit station are important variables to determine the severity. Therefore, minimizing the risk asserted on these variables could decrease accident severity.

**Table 2.** Components of MIROS Accident Dataset

Dataset Component	Variables
Road	Speed_Limit, Road_Type, Area_Type, Road_Surface_Type, Control_Type, Lane_Marking, Road_Geometry, Shoulder_Width, Road_Defect
Demographic	Driver_Qualification, License_Status, Driver_Occupation, Age
Environment	Month, Weather
Vehicle	Veh_Model, Veh_Movement, c_Veh_Type
Accident	Collision_Type, Tempat_Kejadian
Trade Area	Store, Restaurant, Transit_Station, Mosque, Cafe, Electronics_Store, School

## 6 Conclusion

The work presented in this paper had aimed to firstly identify the important features contributed to severity of accident and subsequently use them to construct a predictive model. The uniqueness of this study is that the dataset was obtained from a Malaysian government agency named MIROS. The raw dataset was firstly preprocessed and transformed into analytical dataset before feature selection and model construction phases. The preprocessing steps had included missing value imputation and outlier removal. The feature selection phase had utilized Recursive Feature Elimination (RFE) algorithm to search for the optimal feature set. The feature set was then used for construction of several predictive models, from which *Random Forest* scored highest accuracy of 95.46%.

The study concluded with 26 features that were crucial for the prediction of a fatal road accident. Among the variables, the top 10 were *month*, *speed limit*, *collision type*, *vehicle model*, *vehicle movement*, *road type*, *driver qualification*, *area type*, *store* and *road surface type*. The finding of this study has also indicated

that tree-based classifier such as XGBoost and Random Forest outperformed other types of classifiers largely because for Random Forest, it constructs several decision trees independently at training time and return the mode of the class of individual trees without suffering from overfitting and overtraining. As for XGBoost, it will construct decision tree one at a time, where each tree will help to correct errors that is made by previous trained tree. As a conclusion, this study had achieved its objectives in looking for optimal feature set and construction of predictive model. However, further investigation can be extended from different aspects: (i) use dataset other than year 2015, (ii) apply different missing value imputation techniques, (iii) attempt other feature selection algorithms, (iv) perform optimization on the parameters of each predictive models.

## References

1. World Health Organization, <http://www.who.int/mediacentre/factsheets/fs358/en/>, last accessed 2017.
2. Jiang, C., Lu, L., Chen, S., & Lu, J. J.: Hit-and-run crashes in urban river-crossing road tunnels. *Accident Analysis & Prevention*, 95, 373–380 (2016).
3. Phillips, R. O., & Sagberg, F.: Road accidents caused by sleepy drivers: Update of a norwegian survey. *Accident Analysis & Prevention*, 50, 138–146 (2013).
4. Xie, W., Wang, J., & Ragland, D. R.: Utilizing the eigenvectors of freeway loop data spatiotemporal schematic for real time crash prediction. *Accident Analysis & Prevention*, 94, 59–64 (2016).
5. World Health Organization: Global status report on road safety 2015, (2015).
6. Institute for Health Metrics and Evaluation, <http://www.healthdata.org/Malaysia>, last accessed 2017.
7. Iranatalab, A., & Khattak, A.: Comparison of four statistical and machine learning methods for crash severity prediction. *Accident Analysis & Prevention*, 108, 27–36 (2017).
8. Jeong, H., Jang, Y., Bowman, P. J., & Masoud, N.: Classification of motor vehicle crash injury severity: a hybrid approach for imbalanced data. *Accident Analysis & Prevention*, 120, 250–261 (2018).
9. Ward, N., Linkenbach, J., Keller, S., & Otto, J.: Toward Zero Deaths: A National Strategy on Highway Safety. Western Transportation Institute, Bozeman (2010).
10. Garrido, R., Bastos, A., de Almeida, A., & Elvas, J. P.: Prediction of road accident severity using the ordered probit model. *Transportation Research Procedia*, 3, 214–223 (2014).
11. Xu, J., Kockelman, K. M., & Wang, Y.: Modeling crash and fatality counts along mainlanes and 1 frontage roads across Texas: 2 the roles of design, the built environment, and weather 3. In Presented at the 93rd Annual Meeting of the Transportation Research (p. 24). volume 22 (2014).
12. Fernandez-Delgado, M., Cernadas, E., Barro, S., & Amorim, D.: Do we need hundreds of classifiers to solve real world classification problems. *J. Mach. Learn. Res.*, 15, 3133–3181 (2014).
13. Goh, K., Currie, G., Sarvi, M., & Logan, D.: Factors affecting the probability of bus drivers being at-fault in bus-involved accidents. *Accident Analysis & Prevention*, 66, 20–26 (2014).
14. George, Y., Athanasios, T., & George, P.: Investigation of road accident severity per vehicle type. *Transportation research procedia*, 25, 2076–2083 (2017).

15. Azadeh, A., Zarrin, M., & Hamid, M.: A novel framework for improvement of road accidents considering decision-making styles of drivers in a large metropolitan area. *Accident Analysis & Prevention*, 87, 17–33 (2016).
16. Celik, A. K., & Oktay, E.: A multinomial logit analysis of risk factors influencing road traffic injury severities in the erzurum and kars provinces of turkey. *Accident Analysis & Prevention*, 72, 66–77 (2014).
17. Goel, G., & Sachdeva, S.: Analysis of road accidents on nh-1 between rd 98 km to 148 km. *Perspectives in Science*, 8, 392–394 (2016).
18. Fernandes, A., & Neves, J.: An approach to accidents modeling based on compounds road environments. *Accident Analysis & Prevention*, 53, 39–45 (2013).
19. Theofilatos, A., Yannis, G., Kopelias, P., & Papadimitriou, F.: Predicting road accidents: a rare-events modeling approach. *Transportation Research Procedia*, 14, 3399–3405 (2016).
20. Theofilatos, A.: Incorporating real-time traffic and weather data to explore road accident likelihood and severity in urban arterials. *Journal of safety research*, 61, 9–21 (2017).
21. Prieto, F., Gómez-Déniz, E., & Sarabia, J. M.: Modelling road accident black-spots data with the discrete generalized pareto distribution. *Accident Analysis & Prevention*, 71, 38–49 (2014).
22. Kumar, V., & Minz, S.: Feature selection. *SmartCR*, 4, 211–229 (2014).
23. Tang, J., Alelyani, S., & Liu, H.: Feature selection for classification: A review. *Data Classification: Algorithms and Applications*, (p. 37) (2014).
24. Lloyd, L. K., & Forster, J. J.: Modelling trends in road accident frequency bayesian inference for rates with uncertain exposure. *Computational Statistics & Data Analysis*, 73, 189–204 (2014).
25. Gitelman, V., Doveh, E., & Bekhor, S.: The relationship between free-flow travel speeds, infrastructure characteristics and accidents, on single-carriageway roads. *Transportation Research Procedia*, 25, 2026–2043 (2017).



# Location Analytics for Churn Service Type Prediction

Nicholas Yu-Zhe Tan, Choo-Yee Ting and Chuing Ching Ho

Faculty of Computing and Informatics, Multimedia University,  
Persiaran Multimedia, 63100 Cyberjaya, Selangor, Malaysia  
[nicholas.290696@gmail.com](mailto:nicholas.290696@gmail.com); [cyting@mmu.edu.my](mailto:cyting@mmu.edu.my); [ccho@mmu.edu.my](mailto:ccho@mmu.edu.my)

**Abstract.** Churn has always been a challenge for companies that trade products or services. Research work has been focusing on predicting customer churn, however, the relationship between churn and geospatial information have not been fully explored. In this work, it was hypothesized that geospatial information exhibits a correlation with churn pattern. Empirical study was conducted to employ five different similarity algorithms to investigate the similarity between one churn location to others. The findings suggested that location features do assert a positive effect on customer churn with the accuracy of 70.24% using *Hamming* algorithm based on top 31 rows of majority voting.

**Keywords:** Location Analytics · Churn · Prediction.

## 1 Introduction

Customer churn is also known as *customer attrition*, *customer turnover* or *customer defection*. It is a scenario describing the loss of a customer or client of a company. On average, a company could lose up to 25% of customers annually according to Don Peppers and Martha Rogers. Furthermore, the cost of obtaining new customers is five times more expensive than maintaining existing customers [1–3].

Location analytics can often be referred to as location intelligence or spatial intelligence. It is a process of deriving meaningful geospatial information into valuable information and provide insights to solve the problem. Location analytics have recently gained attention academically and commercially. This is largely due to the fact that location features can play an important role in a company's decision-making process [4, 5].

Nevertheless, the relationship between customer churn and geospatial information have not been fully explored to the best of my knowledge. In this light, the relationship between customer churn from existing service and the geospatial features surrounding the customer location.

## 2 Related Work

### 2.1 Customer Churn

Customer churn is a kind of action that customer shifts to the competitor of the customer current service provider [6]. Customer churn features include customer behavior information, demographic information and customer service package information [7]. There are several factors that will affect customer churn [8]: service price, quality, satisfaction and et cetera.

Several research work has been done on predicting customer churn pattern [6, 7, 9, 10]. To the best of my knowledge, there is no research work focus on the relationship between customer churn and the geospatial information surrounding the customer location.

### 2.2 Location Features

Location features include geography and trade area information given a particular point on a map. Location features have been applied to several industries to solve different challenges. For instance, predict business location [11–13], predict business sales [5], predict point of interest of the customer [14] and enhance electronic health record information [15].

### 2.3 Similarity Measures

The most commonly used similarity measures are as followed [5, 16]: *Euclidean distance*, *Manhattan distance*, *Hamming distance*, *Cosine distance*, *Minkowski distance*, *Gower distance* and many more. In this study, five similarity measure algorithms will be investigated, namely *Gower*, *Euclidean*, *Cosine*, *Hamming* and *Manhattan*.

**Gower Distance** *Gower* distance is a composite measure that can be used when the data has a mixture of categorical and numerical data. Before obtaining the weighted average of the distances for each variable, scaling each variable to [0,1] is required [17]. The formula is defined as

$$d(x, y) = 1 - S_{xy} \quad (1)$$

$$S_{xy} = \frac{\sum_{i=1}^n w_{xyi} S_{xyi}}{\sum_{i=1}^n w_{xyi}} \quad (2)$$

where  $S_{xyi}$  denotes the distance of variable  $i$  between observations of  $x$  and  $y$  and  $w_{xyi}$  represents the weight for variable  $i$  between  $x$  and  $y$  which will be within 0 to 1. For categorical variables,  $S_{xyi}$  is obtained as

$$S_{xyi} = \begin{cases} 0, & \text{if } X_{xi} = X_{yi} \\ 1, & \text{if } X_{xi} \neq X_{yi} \end{cases} \quad (3)$$

For numeric variables,  $S_{xyi}$  is the *manhattan* distance which can be computed as below

$$S_{xyi} = \frac{|X_{xi} - X_{yi}|}{\max(X_i) - \min(X_i)} \quad (4)$$

**Euclidean Distance** *Euclidean* distance which also known as ordinary distance [16] is the most well-known distance that is used for numerical data [18]. Euclidean is one of a special case of Minkowski distance [19, 20]. Euclidean distance determines the root of square differences between  $x$  and  $y$  [21]. Euclidean distance can be computed as below

$$d(x, y) = \sum_{i=1}^n \sqrt{(x_i - y_i)^2} \quad (5)$$

where  $x_i$  and  $y_i$  are vectors in n-dimensional space.

**Cosine Distance** *Cosine* distance is usually being applied to document related similarity [22]. Cosine distance will compute the angle between two vectors in n-dimensional space. The outcome of the algorithm will be  $[0,1]$  as  $\cos^{-1}$  of  $1^\circ$  is 0 and it is more than 0 and less than 1 for any other angle.

$$d(x, y) = 1 - \frac{\sum_{i=1}^n x_i y_i}{\sqrt{\sum_{i=1}^n x_i^2} \sqrt{\sum_{i=1}^n y_i^2}} \quad (6)$$

**Hamming Distance** *Hamming* distance is most widely used for channel coding for minimizing errors caused in code [23] and compute the distance between categorical variables [5]. A contingency table will be constructed in order to obtain the number of mismatches among the observations [5, 24]. The formula is shown below

$$d(x, y) = 1 - \frac{x \cap y}{x \cup y} \quad (7)$$

**Manhattan Distance** *Manhattan* distance is another special case of Minkowski distance [18]. Manhattan distance determines the sum of absolute values of differences between two observations [5]. The formula is as given below

$$d(x, y) = \sum_{i=1}^n |x_i - y_i| \quad (8)$$

### 3 Method

#### 3.1 Dataset

As shown in Table 1, there were six datasets used in this study, namely, Point of Interest( $D_{poi}$ ), YellowPages businesses( $D_{yp}$ ), economy and education data( $D_{ecoedu}$ ), population data( $D_{pop}$ ), property data( $D_{ppt}$ ) and churn data( $D_{churn}$ ).  $D_{pop}$  were obtained from Department of Statistics Malaysia (DOSM) while the rest were acquired from Telekom Malaysia (TM).

Table 1: Dataset Informations

Dataset	Rows	Columns
$D_{poi}$	417767	6
$D_{yp}$	293864	4
$D_{ecoedu}$	144	58
$D_{pop}$	2577	26
$D_{ppt}$	4982311	6
$D_{churn}$	10072	11

In this study, the location features are obtained from  $D_{poi}$ ,  $D_{yp}$ ,  $D_{ecoedu}$ ,  $D_{pop}$  and  $D_{ppt}$ .  $D_{poi}$  comprises of different point of interest that are categorized into 1248 categories (i.e., Chinese Food, Fashion, Saloon, Mosque and et cetera.).  $D_{yp}$ , however, focuses on company or business details.  $D_{poi}$  and  $D_{yp}$  will be merged into one because they served the same purpose in capturing relevant geographical information.  $D_{pop}$  contains population information about races at the district level, local authority area level and precinct level.

$D_{ecoedu}$  consists of two different information about economy and education. In terms of economy, there are in total of nine types of jobs, 21 type of industrial fields and four levels of employment status which are separated into different district. For education data, there are four levels of schooling status, eight levels of education status and 10 types of certificates which are also divided into different district.  $D_{ppt}$  consists of 28 different property types at street level for the entire Malaysia space.

The  $D_{churn}$  obtained from TM are churn data related to two telecommunication products, namely, *Unifi* and *Streamyx*. It contains information such as customer complaint information and customer churn information with location context from May 2015 to April 2019.

### 3.2 Data Preprocessing

In order to create an analytical dataset, all datasets were firstly transformed into a single dataset. The algorithm 1 shows steps for transformation.  $D_{pop}$  and  $D_{ecoedu}$  were supplemented with administrative division information (i.e., District, Local Authority Area or Precinct) while  $D_{poi}$ ,  $D_{yp}$  and  $D_{churn}$  were added with geographic coordinate system (i.e., Latitude and Longitude). Conversely,  $D_{ppt}$  were supplemented with both administrative division information and geographic coordinate system.

The first step is to map the  $D_{churn}$ 's churn\_code columns to two categories: *Service related* type or *Non-Service related* type (see Algo 1, line 1). The next step is to reverse geocode  $D_{churn}$ 's latitude and longitude to obtain the corresponding administrative division information using Malaysia shapefile data that was provided by TM (see Algo 1, line 2). The next step is to merge all the dataset based on their corresponding location information. For  $D_{pop}$  and  $D_{ecoedu}$ , they will be merged with  $D_{churn}$  using administrative division information to form  $D_{half}$  (see Algo 1, line 3).

**Algorithm 1** Data Preparation

---

**Input:**  $D_{poi}$ ,  $D_{yp}$ ,  $D_{ecoedu}$ ,  $D_{pop}$ ,  $D_{ppt}$ ,  $D_{churn}$

**Output:**  $D_{analytical}$

```

1:  $D_{churn} \leftarrow \text{map}(D_{churn})$ 
2:  $D_{churn} \leftarrow \text{reverseGeocode}(D_{churn})$ 
3:  $D_{half} \leftarrow \text{merge}(D_{pop}, D_{ecoedu}, D_{churn})$ 
4:  $D_{poiyip} \leftarrow \text{merge}(D_{poi}, D_{yp})$ 
5: for each latitude and longitude in  $D_{half}$  do
6:   for each latitude and longitude in  $D_{poiyip}$  do
7:      $D_{100m} \leftarrow \text{haversine}(Lat_{half}, Lng_{half}, Lat_{poiyip}, Lng_{poiyip}) \leq 100$ 
8:   end for
9:    $D_{loc} \leftarrow D_{poiyip} \cap D_{100m}$ 
10: end for
11:  $D_{analytical} \leftarrow \text{merge}(D_{half}, D_{loc})$ 

```

---

On the other hand,  $D_{poi}$  and  $D_{yp}$  will be merged first to obtain  $D_{poiyip}$  due to the fact that  $D_{poi}$  and  $D_{yp}$  are similar as they contain geographical information for a location in the whole Malaysia space (see Algo 1, line 4). The duplicated places name will be dropped from the  $D_{poiyip}$ . In order to merge  $D_{poiyip}$  with  $D_{half}$ , every single row from  $D_{half}$  will be compared with  $D_{poiyip}$  to calculate the great-circle distance of the two points using *haversine* formula. Great-circle distance is the shortest distance of two points on the surface of a sphere. The *haversine* formula is as follows:

$$d = 2r \arcsin\left(\sqrt{\sin^2\left(\frac{lat_2 - lat_1}{2}\right) + \cos(lat_1)\cos(lat_2)\sin^2\left(\frac{lng_2 - lng_1}{2}\right)}\right) \quad (9)$$

where:

- $lat_1, lat_2$  : latitude of point 1 and latitude of point 2
- $lng_1, lng_2$  : longitude of point 1 and longitude of point 2

After obtaining every distance from  $D_{half}$  with  $D_{poiyip}$ , location features will be subsetted only if the distance is smaller than 100 meters radius (see Algo 1, line 5-10). The subsetted location features will then be merged with  $D_{half}$  to produce an analytical dataset,  $D_{analytical}$  (see Algo 1, line 11).

### 3.3 Churn service type prediction for new location

Algorithm 2 shows the overall process for predicting churn service type based on their surrounding location features.  $D_{analytical}$  is the input for this algorithm whereas the output will be  $S_{gow}$ ,  $S_{euc}$ ,  $S_{cos}$ ,  $S_{ham}$  and  $S_{man}$  which are the top  $n$  numbers of most similar locations based on every row of  $D_{test}$ . The first step in the algorithm is to separate the  $D_{analytical}$  into  $D_{train}$  and  $D_{test}$  using 90:10 ratio (see Algo 2, line 1). The reason to separate into 90:10 ratio is because similarity algorithms do not actually need train and test dataset but the  $D_{test}$  are to simulate new data to compare with the  $D_{train}$ .

**Algorithm 2** Churn Service Type Prediction

---

**Input:**  $D_{analytical}$

**Output:**  $S_{gow}, S_{eucl}, S_{cos}, S_{ham}, S_{man}$

- 1:  $D_{train}, D_{test} \leftarrow \text{trainTestSplit}(D_{analytical}, 0.9)$
- 2: **for each row in**  $D_{test}$  **do**
- 3:    $F_{matched} \leftarrow \text{checkRadius}(\text{row}, D_{train})$
- 4:    $D_{newtrain} \leftarrow \text{select}(D_{train} \cap F_{matched})$
- 5:    $D_{newtrain} \leftarrow \text{removeCols}(D_{newtrain})$
- 6:    $S_{gow} \leftarrow \text{gower}(D_{newtrain}, \text{row})$
- 7:    $S_{eucl} \leftarrow \text{euclidean}(D_{newtrain}, \text{row})$
- 8:    $S_{cos} \leftarrow \text{cosine}(D_{newtrain}, \text{row})$
- 9:    $S_{ham} \leftarrow \text{hamming}(D_{newtrain}, \text{row})$
- 10:    $S_{man} \leftarrow \text{manhattan}(D_{newtrain}, \text{row})$
- 11:    $S_{gow}, S_{eucl}, S_{cos}, S_{ham}, S_{man} \leftarrow \text{rank}(S_{gow}, S_{eucl}, S_{cos}, S_{ham}, S_{man})$
- 12: **end for**

---

In order to get each similarity algorithms distance, several steps will be needed before able to run similarity algorithms. For each row of  $D_{test}$  will be checked with  $D_{train}$  to check their great-circle distance using *haversine* formula (see Algo 2, line 3) to subset the  $D_{train}$  that are within 100 meters to obtain  $D_{newtrain}$  (see Algo 2, line 4). Churn information will be removed from  $D_{newtrain}$  so that the similarity of each location will not be affected by the churn information (see Algo 2, line 5). The next step is to run *gower* distance algorithm, *euclidean* distance algorithm, *cosine* distance algorithm, *hamming* distance algorithm and *manhattan* distance algorithm with  $D_{newtrain}$  and each row of  $D_{test}$  (see Algo 2, line 6-10). After obtaining the distance from each algorithm, the distance obtained from each algorithm will be then be ranked and sort by the shortest distance to longest distance (see Algo 2, line 11). The distance will be mapped back with their corresponding churn service type to be able to compare with that particular row of  $D_{test}$ . By using majority voting system, churn service type will be obtained from the top  $n$  number of rows. The obtained churn service type will be compared with the churn service type of the particular row of  $D_{test}$ . If obtained churn service type matched with the churn service type of the test data, it will be labeled as **True**. The accuracy of each algorithm will be calculated using the number of **True** divided with the number of test data row and multiply with 100 with the formula given:

$$\text{Accuracy (\%)} = \left( \frac{\text{number of True}}{\text{number of row of } D_{test}} \right) * 100 \quad (10)$$

## 4 Results and Discussion

In this research work, five similarity algorithms were employed. Analytical dataset was obtained and churn service type prediction was performed as discussed in Section 3. Figure 1 and Table 2 depict the findings from experiments performed on different algorithms. The purpose of this experiments was to compare the accuracy of different similarity algorithms and to understand which algorithm

is the most suitable for this dataset. Based on Table 2, top  $n$  rows means the majority churn service type of the top one to  $n$  is obtained.

The top three similarity algorithms are as followed: *Hamming* algorithm, *Gower* algorithm and *Manhattan* algorithm. *Hamming* algorithm reached its highest accuracy earlier than the other four algorithms, with an accuracy of 70.24% based on top 31 rows of majority voting. *Gower* algorithm reached its highest accuracy of 70.24% based on top 39 rows of majority voting and *Manhattan* algorithm reached its highest accuracy of 70.24% based on top 45 rows of majority voting. Overall, the accuracy of *hamming* algorithm is higher than the other four algorithms most of the time except number of top nine rows, which *gower* algorithm is higher than *hamming* algorithm. The accuracy from all of the algorithms is rising if the number of top  $n$  rows to calculate the majority vote increases steadily.

The reason majority voting is used in this paper are due to similarity algorithms do not have a metric to evaluate the algorithms. In order to convert the similarity metric to accuracy metric, majority voting has been used. The accuracy result has been calculated from different top  $n$  rows of similar observations and calculates the number of correct and incorrect churn service type with the churn service type that is being compared with. The majority will be taken as predicted or not predicted according to the correct churn service type. Thus, 70.24% accuracy can be obtained by using *hamming* algorithm with number of top 31 rows can be explained as one new observation of churn service type will be 70.24% accurate if used top 31 similar observation to the new observation using *hamming* algorithm.

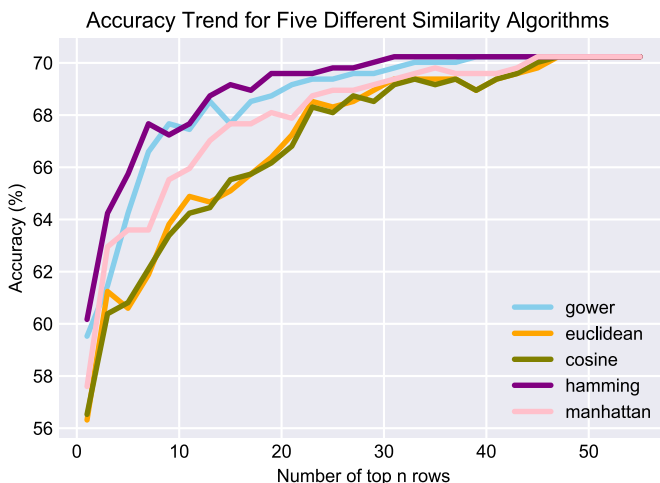


**Fig. 1.** Comparing the accuracy of five different algorithms based on different number of top  $n$  rows

Table 2: The accuracy results of different similarity algorithms

Top rows	n	Gower (%)	Euclidean (%)	Cosine (%)	Hamming (%)	Manhattan (%)
1	59.53	56.32	56.53	60.17	57.60	
3	61.46	61.24	60.39	64.24	62.96	
5	64.24	60.60	60.81	65.74	63.60	
7	66.60	61.88	62.10	67.67	63.60	
9	67.67	63.81	63.38	67.24	65.52	
11	67.45	64.88	64.24	67.67	65.95	
13	68.52	64.67	64.45	68.74	67.02	
15	67.67	65.10	65.52	69.16	67.67	
17	68.52	65.74	65.74	68.95	67.67	
19	68.74	66.38	66.17	69.59	68.09	
21	69.16	67.24	66.81	69.59	67.88	
23	69.38	68.52	68.31	69.59	68.74	
25	69.38	68.31	68.09	69.81	68.95	
27	69.59	68.52	68.74	69.81	68.95	
29	69.59	68.95	68.52	70.02	69.16	
31	69.81	69.38	69.16	<b>70.24</b>	69.38	
33	70.02	69.38	69.38	70.24	69.59	
35	70.02	69.38	69.16	70.24	69.81	
37	70.02	69.38	69.38	70.24	69.59	
39	<b>70.24</b>	68.95	68.95	70.24	69.59	
41	70.24	69.38	69.38	70.24	69.59	
43	70.24	69.59	69.59	70.24	69.81	
45	70.24	69.81	70.02	70.24	<b>70.24</b>	
47	70.24	<b>70.24</b>	<b>70.24</b>	70.24	70.24	
49	70.24	70.24	70.24	70.24	70.24	
51	70.24	70.24	70.24	70.24	70.24	
53	70.24	70.24	70.24	70.24	70.24	
55	70.24	70.24	70.24	70.24	70.24	

## 5 Conclusion

In conclusion, location feature is an important feature for predicting churn service type. In this study, 70.24% accuracy can be obtained just by using *hamming* algorithm with number of top 31 rows without any churn information provided as shown in Table 2. Thus, geospatial information does indeed exhibits a correlation with customer churn pattern as proven in this paper.

### 5.1 Future Work

For future work, more similarity algorithms can be considered for more comprehensive research. On top of that, machine learning techniques could be able to be applied to predict the churn service type.

## 6 Acknowledgement

This research work presented in this paper is supported by Telekom Malaysia.

## References

1. Zhao, Y., Li, B., Li, X., Liu, W., Ren, S.: Customer churn prediction using improved one-class support vector machine. In: International Conference on Advanced Data Mining and Applications. pp. 300–306. Springer (2005)
2. Grönroos, C.: A service quality model and its marketing implications. European Journal of marketing **18**(4), 36–44 (1984)
3. Amin, A., Al-Obeidat, F., Shah, B., Adnan, A., Loo, J., Anwar, S.: Customer churn prediction in telecommunication industry using data certainty. Journal of Business Research **94**, 290–301 (2019)
4. Yee, H.J., Ting, C.Y., Ho, C.C.: Human elicited features in retail site analytics. In: IOP Conference Series: Earth and Environmental Science. vol. 169, p. 012091. IOP Publishing (2018)
5. Ting, C.Y., Ho, C.C., Yee, H.J., Matsah, W.R.: Geospatial analytics in retail site selection and sales prediction. Big data **6**(1), 42–52 (2018)
6. Amin, A., Anwar, S., Adnan, A., Nawaz, M., Alawfi, K., Hussain, A., Huang, K.: Customer churn prediction in the telecommunication sector using a rough set approach. Neurocomputing **237**, 242–254 (2017)
7. Huang, Y., Zhu, F., Yuan, M., Deng, K., Li, Y., Ni, B., Dai, W., Yang, Q., Zeng, J.: Telco churn prediction with big data. In: Proceedings of the 2015 ACM SIGMOD international conference on management of data. pp. 607–618. ACM (2015)
8. Hejazinia, R., Kazemi, M.: Prioritizing factors influencing customer churn. Interdisciplinary Journal of Contemporary Research in Business **5**(12), 227–236 (2014)
9. Shirazi, F., Mohammadi, M.: A big data analytics model for customer churn prediction in the retiree segment. International Journal of Information Management (2018)
10. Strippling, E., vanden Broucke, S., Antonio, K., Baesens, B., Snoeck, M.: Profit maximizing logistic model for customer churn prediction using genetic algorithms. Swarm and Evolutionary Computation **40**, 116–130 (2018)
11. Yap, J.Y., Ho, C.C., Ting, C.Y.: Analytic hierarchy process (ahp) for business site selection. In: AIP Conference Proceedings. vol. 2016, p. 020151. AIP Publishing (2018)
12. Yee, H.J., Ting, C.Y., Ho, C.C.: Optimal geospatial features for sales analytics. In: AIP Conference Proceedings. vol. 2016, p. 020152. AIP Publishing (2018)
13. Bilen, T., Erel-Özçevik, M., Yaslan, Y., Oktug, S.F.: A smart city application: Business location estimator using machine learning techniques. In: 2018 IEEE 20th International Conference on High Performance Computing and Communications; IEEE 16th International Conference on Smart City; IEEE 4th International Conference on Data Science and Systems (HPCC/SmartCity/DSS). pp. 1314–1321. IEEE (2018)
14. Yi, X., Paulet, R., Bertino, E., Varadharajan, V.: Practical approximate k nearest neighbor queries with location and query privacy. IEEE Transactions on Knowledge and Data Engineering **28**(6), 1546–1559 (2016)
15. Xie, S., Greenblatt, R., Levy, M.Z., Himes, B.E.: Enhancing electronic health record data with geospatial information. AMIA Summits on Translational Science Proceedings **2017**, 123 (2017)

16. Irani, J., Pise, N., Phatak, M.: Clustering techniques and the similarity measures used in clustering: A survey. *International Journal of Computer Applications* **134**(7), 9–14 (2016)
17. Gower, J.C.: A general coefficient of similarity and some of its properties. *Biometrics* pp. 857–871 (1971)
18. Shirkhorshidi, A.S., Aghabozorgi, S., Wah, T.Y.: A comparison study on similarity and dissimilarity measures in clustering continuous data. *PloS one* **10**(12), e0144059 (2015)
19. Jain, A.K.: Mm (1999). data clustering: a review. *ACM Comput. Surv* **31**, 264–323
20. Mao, J., Jain, A.K.: A self-organizing network for hyperellipsoidal clustering (hec). *Ieee transactions on neural networks* **7**(1), 16–29 (1996)
21. Singh, A., Yadav, A., Rana, A.: K-means with three different distance metrics. *International Journal of Computer Applications* **67**(10) (2013)
22. Han, J., Pei, J., Kamber, M.: Data mining: concepts and techniques. Elsevier (2011)
23. McEliece, R., Mac Eliece, R.J.: The theory of information and coding. Cambridge University Press (2002)
24. Arif, M., Basalamah, S.: Similarity-dissimilarity plot for high dimensional data of different attribute types in biomedical datasets. *International Journal of Innovative Computing, Information and Control* **8**(2), 1275–1297 (2012)



# Development of Novel Gamified Online Electrocardiogram Learning Platform (GaMED ECG@™)

May Honey Ohn<sup>1</sup>, Khin Maung Ohn<sup>1</sup>, Shahril Yusof<sup>1</sup>, Urban D’Souza<sup>1</sup>, Zamhar Iswandono<sup>2</sup>, Issa Mchucha<sup>2</sup>

<sup>1</sup>Faculty of Medicine and Health Sciences, University Malaysia Sabah, Kota Kinabalu, Malaysia

<sup>2</sup> Faculty of Computing and Informatics, Universiti Malaysia Sabah, Kota Kinabalu, Malaysia  
mayhoney.ohn@ums.edu.my, drkmjohn@ums.edu.my,  
shahrily@ums.edu.my, dsouza@ums.edu.my, zamhar@ums.edu.my,  
issaramadhan87@gmail.com

**Abstract.** Following the advances of new technologies such as social networks, digital media, and the Internet, numerous learning materials nowadays incorporate multimedia technology to maximize the student learning experience. Greater student engagement, increased motivation and higher satisfaction of students using technology-enhanced learning can be achieved by gamification. Electrocardiogram (ECG) is a graphical image of cardiac electrical activity which needs to be interpreted timely and accurately in order to diagnose various types of life-threatening conditions in clinical practice. There is a call for innovative ECG instructional method that can actively engage learners and motivate them in order to interpret ECG correctly in a timely manner. In this case, we proposed and developed a gamified ECG learning platform in which ECG teaching materials were incorporated into gamification tool. A GaMED ECG@™ prototype was developed for ECG learning and then, GaMED ECG@™ software practicability was tested. An instructional design Analysis, design, development, implementation and Evaluation (ADDIE) model was followed in developing an online gamified learning platform GaMED ECG@™. The GaMED ECG@™ platform incorporates a game-based technique as a strategy to deliver positive learning outcomes to students. In view of the need for technological innovations in medical education, this gamified learning platform provides the interactive self-paced activities structured as gamified lessons to enlighten the students with ECG knowledge.

**Keywords:** Instructional Gamified Design; Gamified learning platform; online learning, Electrocardiogram learning

## 1 Introduction

Traditional teacher-centered learning is perceived as ineffective and boring by 21st-century students [1]. Following the advances of new technologies such as social networks, digital media, and the Internet, much learning material nowadays incorporates the multimedia technology to maximize the student learning experience both in synchronous and asynchronous learning environment [2]. However, many technology-enhanced student-centered learning systems do not attain the desired students’

engagement due to some users stopping usage after initial enrolment [3]. One of the major factors of poor satisfaction of students in electronic learning platform is due to the use of inappropriate motivational techniques [4]. Several studies found out that not only greater students' engagement but also increased motivation and higher satisfaction of students using technology-enhanced learning can be achieved by gamification [3,5]. Gamification does not imply creating a traditional game for entertainment per se but it, in fact, uses game-like features such as points and coins to educate [6].

Application of the game mechanics, dynamics and aesthetics allow technology-enhanced learning to move towards gamification design in order to reinforce learning[7]. Gamification enables students to gain inspiration towards studying, and due to the achievement, they become more absorbed and encouraged to learn. Gamification can represent an influential encouragement to govern them to read more. Therefore, in recent years, gamification has drawn the consideration of medical educators due to the possibility of making medical learning more motivating and engaging; this led to an increase of research in the medical education field [8].

Electrocardiogram (ECG) is a 3D graphical image of cardiac electrical activity which needs to interpret timely and accurately in order to diagnose various types of life-threatening conditions in clinical practice [9]. ECG learning is therefore very possible to assist learning with digital interactive multimedia teaching materials like ECG simulator. Little et.al., (2001) pointed out that despite the emphasis of ECG learning as a crucial learning outcome in undergraduate curriculum [10], the interpretation of ECG among graduating medical students has deteriorated to an unsatisfactory level [11-13]. One of the psychological factors is lack of confidence to interpret ECG that demotivates them to study ECG more [14].

To date, no teaching strategy is effective in delivering lessons on electrocardiogram interpretation [15]. Over the years, some of the methods that have been used in teaching electrocardiogram interpretation skills include lectures, tutorials, self-directed learning and teaching rounds. Recently, there has been rising interest in the use of web-based packages to deliver ECG lessons. However, there is a paucity of information about the most promising and engaging method that can be used to teach medical students electrocardiogram interpretation. Therefore, there is a call for innovative ECG instructional method that can actively engage learners and motivate them in order to interpret ECG correctly in a timely manner. In this case, we proposed a novel gamified ECG learning platform in which ECG teaching materials were incorporated into design idea of gamification. In this paper, we will discuss how a GaMED ECG@TM prototype was developed for ECG learning and then, GaMED ECG@TM software practicability was tested.

## 2 Literature Review

Gamification is the use of game design elements in non-game contexts [16]. These game elements refer to those usually found in most games, such as points, badges and leaderboards. The non-game contexts imply to health, education, and business settings [17]. As per Dominguez et al., (2013), gamification enhances user experience [18]

by providing opportunities for gamers to engage actively and reflectively during game-play [19]. According to Biro (2014), gamification has some common components with the behaviorist learning theory, similar to the predominance of uplifting reinforcements, little step-by-step assignments, instant feedback, and progressive challenges [20]. Educational gamification proposes the utilization of game-like rule systems and user experiences to shape learners' behavior [21]. Similarly, the incorporation of gamification in medical learning can increase satisfaction, engagement, effectiveness and efficiency of students [8]. Due to the use of game elements like time, accuracy, point systems integrated into all types of training programs encourage users to achieve their desired goals.

The prevalence of the use of gamification to enhance learning has been attributed to the following reasons: people do not feel as good in the classroom as they are in games and gamification resonates directly with the digital generation of today [22]. When individuals are confronted with obstacles, they may feel frustrated, cynical or overwhelmed. Such feelings are absent from the gaming environment. The gaming environment gives players instant gratification, which keeps them engaged and motivated all through the course of the game. The success of the application of gamification in the general marketplace has gradually redefined its applications in the spheres of learning. The current paradigm shift in the design of gamified elements has been attributed to the emerging technology trends in education [23].

As indicated by Grünberg (2014), game mechanics are the items and their relationships in the game [24]. They characterize the game as a rule-based system, indicating the means by which everything acts, and how players can interface with the game world. Well-known game mechanics components are [25]: points, levels, badges, achievements, and leaderboards. Game dynamics are the emergent behavior that emerges from gameplay when the mechanics are put into utilization and aesthetics are the emotional reaction from the players to the gameplay [24]. Some game dynamics components are rewards, status, and competition. All aimed at increasing inspiration and achieving higher levels of engagement in the learning process [26].

### **3 Game Elements involved in GaMED ECG@™ platform**

The GaMED ECG@™ platform incorporated a game-based technique as a strategy to deliver positive learning outcomes to students. Some of the features that were implemented to deliver these include the following:

#### **3.1 Competition**

Competition is an action to win that can be done by individuals competing against each other. GaMED ECG@™ evokes the competition instinct within users to be more productive and motivated. This aims to trigger students' engagement and performance.

### **3.2 Leaderboard**

It ranks learners based on their achievement and enables them to see the performance of each other. A leaderboard is the main reason for players to compete with each other.

### **3.3 Social Interaction**

It involves a real-time communication that gives students the opportunity to interact and invite other users to participate in the lesson.

### **3.4 Analytics**

This is an indicator tool that determines how satisfactory the platform engages the students.

### **3.5 Badge**

Registration badge, early bird badge, bronze, silver and gold medal badges are used in GaMED ECG@TM to represent users' accomplishment that has a meaningful result of an activity. Its main purpose is to engage in positive learning behavior, and to identify progress in learning and credential engagement, learning and achievement [27]. When it comes to engagement, a positive effect had shown more in online learning environments [28].

### **3.6 Level**

Students must show a certain level of understanding and pass the previous level to unlock the next level and proceed academically.

### **3.7 Timer and challenge**

Students can take challenge game with opponents in real time in GaMED ECG@TM; this gives rise to continuous improvement through peer learning. This, in turn, makes the GaMED ECG@TM platform very unique in its kind and this platform intends to train the students in enabling to interpret ECG accurately and as quick as possible to conquer the challenge game.

### **3.8 Failure to fail**

GaMED ECG@TM allows users to try again after game over, making failures recoverable. According to Lee and Hammer (2011), this freedom to fail allows students to experiment without fear of failure and increases student commitment [29].

## 4 Instructional Design Model (ADDIE model)

An instructional design ADDIE model was followed in developing an online gamified learning platform GaMED ECG@TM. The ADDIE model is the most common instructional systems design (ISD) model with vigorous and adaptable phases [30] which is appropriate for building online teaching courses [31]. Instructional theories such as behaviorism, constructivism, social learning and cognitivism, play an essential role in the designing and defining the outcome of instructional materials. It has five phases, which are Analysis, Design, Development, Implementation and Evaluation. The continual feedback system is the advantage of this model by revising problems while they are still easy to fix.

### 4.1 Analysis phase

At the beginning of the GaMED ECG project, the conceptualization of the platform was captured by the project team to determine the overall functionality and requirements of GaMED ECG. During this phase, the instructional problem was defined, and the instructional goals and objectives were established. The team also identified the learning environment and learner's existing knowledge and skills as part of the scope of the platform.

### 4.2 Design phase

As far as GaMED ECG@TM was concerned, the initial concept was transformed into computerized mockups. The design of the mockups, however, followed the requirements gathered by the researcher and also the knowledge acquired from the similar apps or platforms that make use of the gamification concepts. That being said, a wireframe and user interface (UI) prototyping tool (Moqups) was used during the development of the prototype. Therefore, when designing the UI for ECG platform, about fourteen mockups design have been created each portraying how the final layout of the activities involved in the platform would be. The homepage is comprised of either sign in or sign up as a student and a default teacher's login account. Figure 1 & 2 demonstrate the designs consisting of the GaMED ECG@TM platform from the teacher's and student's side respectively. The design of GaMed@TM flowchart is simple and log in page is used for security. This is to make sure only those who are eligible can login after being verified by admin.

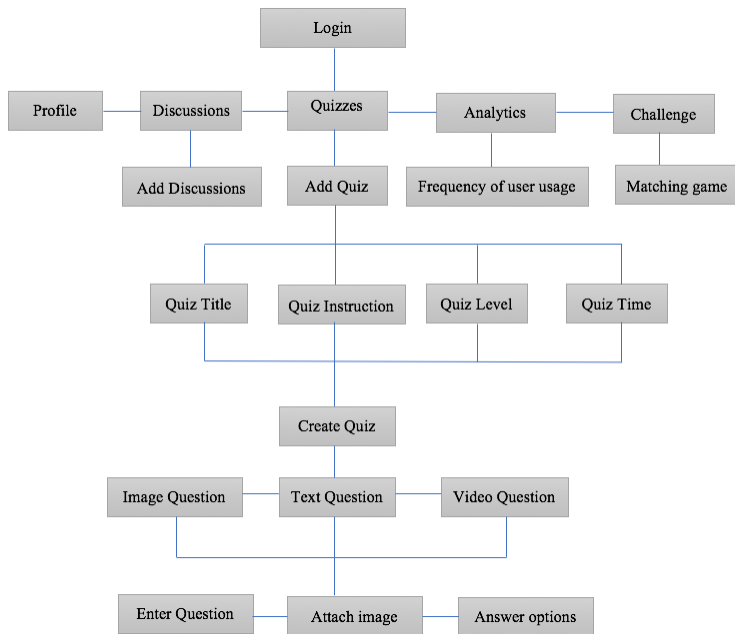


**Fig. 1.** Design flowchart of GaMED ECG@TM Teacher side

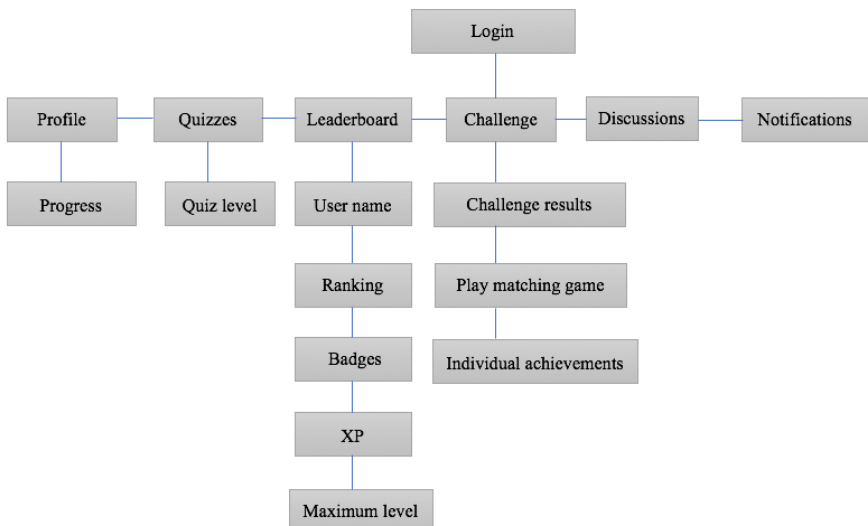


**Fig. 2.** Figure 2: Design flowchart of GaMED ECG@TM Student side

#### **4.3 Development Phase**

Development Phase. The development of GaMed ECG@TM platform involved the designing of front-end user interface as well as the backend development. The front-end development was mainly focusing on designing the graphical user interface (UI) for login, logout, admin, dashboard, footer, sidebar and toolbar. In order to deliver the desired effects, technologies such as CSS and Bootstrap frameworks were used to enhance the development. The backend process refers to designing and coding the database infrastructure for managing the users whereby both the users' and admin's pages were implemented. It involved designing MySQL databases to manage users and admin which gives a control on who has to log in and access the privileges such as creating or accessing lessons provided. Also, it involved working with user authentication, login, logout, and password reset.

#### **4.4 Implementation Phase**

The whole requirements and design flow were converted into a gamification environment. Throughout the implementation process, the main languages that were used are 'Slim' which is a PHP Framework, HTML-5, CSS and also JavaScript. MySQL was also used in managing the database.

#### **4.5 Evaluation Phase**

It is the last step of the GaMed ECG@TM platform development. This step is accompanied with modifying and/or refining some development processes so as to deliver a platform with fewer flaws and that meets the proposed requirements. Color and graphics correction, code debugging and initial testing were executed by the developer. Also, close collaboration between the researcher and the developer in the project team is essential to ensure that the final release would be able to achieve the intended outcome and objective of use. The system was then tested as a complete system initiated by the programmer to ensure the platform is free from errors and later on tested by the users. Similarly, the platform has to undergo the regular maintenance to ensure the instant fixing of the arising problem or any caught bugs during its use.

### **5 Design Principles for ECG Platform**

The instructional design of GaMED ECG@™ platform has undergone standard rules and principles of human-computer interaction (HCI). The HCI design rules offer the guidelines to be followed during the system development process. In general, there are about ten essential rules that govern the UI design process. These rules are also employed in the development of the GaMED ECG@™ platform. As far as GaMED ECG@™ platform is concerned, five design rules have been realized to be consistent in the development process.

### **5.1 Knowing the Users**

This means knowing what the users need, their behavior and expectations towards the system or application. This could easily be fulfilled by knowing the demographic data prior to conducting the design process. For this, background studies and literature have been conducted prior to GaMED ECG@TM development process.

### **5.2 Anticipate Mistakes**

During the design process, it is necessary to know that users always make mistakes. Therefore, a good design is that one which informs users about their mistakes and how they can avoid them. The saying “To err is human” is widely considered in this design rule. Likewise, the GaMED ECG@TM platform makes use of conventional design rules such as using pop-up messages for warning users or making buttons inactive if no appropriate data has been entered in the input field.

### **5.3 Instant Feedback**

Providing immediate feedback is one way to facilitate user behavior. In the real world, environment gives instant feedback towards our actions. Therefore, it is ideal to give feedback to users so that they will be aware of their actions and directions of use. Similarly, the GaMED ECG@TM platform provides users with instant messages on every action of interaction for better user experience.

### **5.4 Use of Standards**

A successful development is the one that abides by standard rules and guidelines of human-computer interaction (HCI). This is accompanied by using the conventional way of designing the interface (UI). While re-inventing the interfaces is not a bad idea, it is highly not recommended. The users are deemed as using the systems based on their past experiences. Therefore, any new design or complicated innovation will give users a hard time to use the platform. That being the case, GaMED ECG@TM platform is adapted to a simple and user-friendly interface design.

### **5.5 Familiarity**

Familiarity is one of the significant parts of interface design. A good system would require users to easily understand how they can use it without having someone to teach them. GaMED ECG@TM platform is, therefore, a self-explanatory in its use.

## 6 Challenges of GaMED ECG@TM

There were numerous challenges encountered when developing a GaMED ECG@TM platform which in one way or another limited its full potential to deliver the intended effects. Cross-browser incompatibility restricted the access and functionality of some features of the platform on other browsers. Also, contrary to other industrial-level platforms, the GaMED ECG@TM platform did not allow multiple accounts for teachers or admin as well as guest accounts for students. Regardless of that, the development of GaMED ECG@TM platform incorporated a number of richer features adapted to gamification concept that irrespective of the existing shortcomings made it an ideal learning platform.

## 7 GaMED ECG@TM mockup test

Developing the new instructional tool requires a number of modifications along the way. Therefore, gamified Mockup test was conducted during the evaluation phase to test the practicability of software and validation of the gamified tool. The study invited twenty medical students from the faculty of medicine and health sciences, University Malaysia Sabah to participate in the mockup test. User feedback and experiences are necessary to assess whether the objectives of fun learning meet their expectation, as well as the effectiveness of the GaMED ECG@TM learning tool. The preliminary results have been analyzed to ensure the improvement of the gamified learning platform. The interview session feedback suggested that being online web-based learning, it needs to have the strong internet connectivity during the gameplay. Students without internet assess couldn't be able to connect and play the game. Another shortcoming observed was that some error bug was unexpectedly encountered during the mockup gamified learning. Even though the preliminary mockup test findings with twenty students showed promising results in learning contexts as the students showed progress in performance over a short period of time, the sample size is not sufficient enough to generalize the finding. According to the researcher's observations, the preliminary findings reflected a primary concern of requirement to conduct the further experimental study after fixing all the technical flaws to examine the impact of the educational intervention.

## 8 Conclusions

It is undoubtedly that the prevalence of gamified learning platforms has diversified the way students perform their learning activities. This is due to the enticing nature that educational games provide in bringing about motivation and engagement to learners. Similarly, the present GaMED ECG@TM platform is developed to provide the interactive self-paced activities structured as gamified lessons to enlighten the students with ECG knowledge. Gamified learning (GaMED ECG@TM) aims to give a great inner motivation and self-satisfaction by seeing own achievements, badges, high leaderboard

rank and reaching the maximum level. Mastering an achievement while learning through failure, is the key game principles applied in GaMED ECG@TM platform.

## Acknowledgments

This project is partially supported by Universiti Malaysia Sabah Great Grant (GUG 144-01/2017).

## References

1. S. Kerr, "The decline of the Socratic method at Harvard." *Neb. L. Rev.* 78 (1999): 113.
2. S. Hrastinski, 2008, Asynchronous and synchronous e-learning. *Educ. Q.* 31, 4 (2008).
3. M. Urh, G. Vukovic, E. Jereb, R. Pintar, The Model for Introduction of Gamification into E-learning in Higher Education. *Procedia - Soc. Behav. Sci.* 197, (2015), 388–397.
4. M. Krajnc, E-Learning Usage During Chemical Engineering Courses. In *E-Learning - Engineering, On-Job Training and Interactive Teaching*. InTech. (2012)
5. D. Dicheva, C. Dichev, G. Agre, G. Angelova, Gamification in Education: A Systematic Mapping Study. *Journal of Educational Technology & Society* 18, 3 (2015), 75–88.
6. D. N. Karagiorgas, S. Niemann, Gamification and Game-Based Learning. *J. Educ. Technol. Syst.* 45, 4 (2017), 499–519.
7. S. Nazleen, A. Rabu, The Design and Implementation of Gamified Classroom through Schoology The 14 th International Scientific Conference eLearning and Software for Education Bucharest , April 19-20 , 2018. May (2018).
8. L. McCoy, J. H. Lewis, D. Dalton, Gamification and Multimedia for Medical Education: A Landscape Review. *J. Am. Osteopath. Assoc.* 116, 1 (2016), 22.
9. N. N. Chodankar, M. H. Ohn, U. J. A. D. Souza, Basics of Electrocardiogram (ECG) and Its Application in Diagnosis of Heart Ailments: An Educational Series. *Borneo J. Med. Sci.* 12, 1 (2018), 3–22.
10. B. Little, I. Mainie, K. J. Ho, L. Scott, I. Mainie, K. J. Ho, L. Scott, Electrocardiogram and rhythm strip interpretation by final year medical students. *Ulster Med. J.* 70, 2 (2001), 108–1.
11. R. S. Jablonover, E. Lundberg, Y. Zhang, A. S. Green, Competency in Electrocardiogram Interpretation Among Graduating Medical Students. *Teach. Learn. Med.* 26, 3 (2014), 279–284.
12. G. Kopeć, W. Magoń, M. Hołda, P. Podolec, Competency in ECG Interpretation Among Medical Students. *Med. Sci. Monit.* 21, (2015), 3386–94.
13. N.A. Lever, P.D. Larsen, M. Dawes, A. Wong, S. A. Harding, Are our medical graduates in New Zealand safe and accurate in ECG interpretation? *Journal of the New Zealand Medical Association NZMJ* 122 (2009), 9–15.
14. S. Gill, C. McAlloon, H. Leach, J. Trevelyan, Improving Undergraduate and Postgraduate Medical Trainees Confidence and Competence in Electrocardiogram Interpretation: Abstract 4 Table 1. *Heart* 100, Suppl 3 (2014), A2.1-A2.
15. G. Fent, J. Gosai, M. Purva, Teaching the interpretation of electrocardiograms: Which method is best'. *J. Electrocardiol.* 48, 2 (2015), 190–193.
16. S. Deterding, M. Sicart, L. Nacke, K. O. Hara, D. Dixon, Gamification. using game-design elements in non-gaming contexts. *Proc. Annu. Conf. Ext. Abstr. Hum. factors Comput. Syst. - CHI EA '11* (2011), 2425.

17. J. Hamari, J. Koivisto, H. Sarsa, Does Gamification Work? -- A Literature Review of Empirical Studies on Gamification. 47th Hawaii International Conference on System Sciences, (2014), 3025–3034.
18. A. Domínguez, J. S. D. Navarrete, L. D. Marcos, L. F. Sanz, C. Pagés, J. J. M. Herráiz, Gamifying learning experiences: Practical implications and outcomes. *Comput. Educ.* 63, (2013), 380–392.
19. J. P. Gee, What video games have to teach us about literacy and learning. Hampshire United Kingdom Palgrave Macmillan, 239 (2007).
20. G. I. Bíró, Didactics 2.0: A Pedagogical Analysis of Gamification Theory from a Comparative Perspective with a Special View to the Components of Learning. *Procedia - Soc. Behav. Sci.* 141, (2014), 148–151.
21. C. H. Su, C. H. Cheng, A Mobile Game-based Insect Learning System for Improving the Learning Achievements. *Procedia - Soc. Behav. Sci.* 103, (2013), 42–50.
22. W. H. Huang, D. Soman, A Practitioner's Guide to Gamification of Education. Research Reports Series, Behavioural Economics in Action. Toronto: Rotman School of Management, University of Toronto. (2013).
23. G. Surendeleg, V. Murwa, H. K. Yun, Y. S. Kim, The Role of Gamification in Education – A Literature Review. *Contemp. Eng. Sci.* 7, 29 (2014), 1609–1616.
24. T.K. Grüberg, Whats the difference between game mechanics and game dynamics. (2014).
25. I. Bunchball , Gamification 101: An introduction to the use of game dynamics to influence behavior. White paper, 9 (2010).
26. K. M. Kapp, The Gamification of Learning and Instruction. Pfeiffer Publishing. (2012).
27. D. Gibson, N. Ostashevski, K. Flintoff, S. Grant, E. Knight, Digital badges in education. *Educ. Inf. Technol.* 20, 2 (2015), 403–410.
28. J. Looyestyn, J. Kernot, K. Boshoff, J. Ryan, S. Edney, C. Maher, Does gamification increase engagement with online programs? A systematic review. *PLoS One* 12, 3 (2017), e0173403.
29. J.J. Lee, J. Hammer, Gamification in education: What, how, why bother?. *Academic exchange quarterly.* 15.2 (2011): 146.
30. K. Kruse, Introduction to Instructional Design and the ADDIE Model. (2002).
31. L. Tobase, H. H. Peres, D. M. D. Almeida, E. A. Tomazini, M. B. Ramos, T. F. Polastri, Instructional design in the development of an online course on Basic Life Support. *J. Sch. nusrsing. Univ. Sao Paulo* 51, e03288 (2017).

# Author Index

## A

- Abdennadher, Slim, 627  
Abdullah, Rosni, 199  
Abubacker, Nirase Fathima, 445  
Adon, Nazib, 373  
Ahmad, Tahir, 649  
Al-Ani, Ahmed K., 199  
Al-Ani, Ayman, 123  
Alashban, Monirah, 445  
Albakri, Ikmal Faiq, 65, 75  
Alfred, Rayner, 257, 269, 677  
Al-Ghaili, Abbas M., 43  
Alksher, Mostafa, 639  
Al-Mashhadi, Saif, 123  
Al-rimy, Bander Ali Saleh, 531  
Alshari, Eissa, 639  
Amin, Aamir, 179  
Amir, Nur ‘Aisyah, 373  
Anbar, Mohammed, 123  
Angeles, Maila R., 331  
Anuar, Nor Badrul, 543  
Apilado, Jose Ross Antonio R., 331  
Avinante, Rhommel S., 145  
Aziz, Noor Hafizah Abdul, 95  
Aziz, Norazreen Abd, 521  
Azlan, Abdul Azim, 669  
Azman, Azreen, 639  
Azmi, Nik Mohammad Wafiy, 75

## B

- Bakar, Normi Sham Awang Abu, 425  
Bari, Ahsanul, 105  
Barsoum, N. N., 659  
Basir, Mohammad Aizat, 585

Bdair, Adnan Hasan, 199

- Bolock, Alia El, 627  
Bolongkikit, Jetol, 257, 269  
Bono, A., 55  
Brenda Chandrawati, T., 23  
Buera, Daniel Joshua, 351  
Buyong, Muhamad Ramdan, 521

## C

- Carlos, Ma. Sharmaine L., 331  
Cheam, T. W., 227  
Chekima, Ali, 689  
Cheong, Soon-Nyeon, 247  
Chew, I. M., 55  
Chew, Yee Jian, 1  
Chiang, Liew Chean, 595  
Chin, Zi Hau, 575  
Connie, Tee, 105, 189

## D

- Dadiz, Bryan G., 145, 469  
Dahlan, Hadi A., 405  
Dargham, Jamal Ahmad, 689  
Dasril, Yosza, 311  
David, Francis John P., 331  
Dela Cruz, Myen D. C., 145  
Dizon, Jame Rald G., 501  
Doraisamy, Shyamala, 639  
D’Souza, Urban, 719

## E

- Esa, Mazlina, 373  
Escario, Hanna Joy R., 331

**F**

- Fathinul Syahir, A. S., 33  
 Fauzi, M. F. A., 227  
 Feng, Liying, 457  
 Foad Rohani, Mohd., 531  
 Foo, Yee-Loo, 247  
 Francisco, Harvey E., 501  
 Fun, Tan Soo, 595

**G**

- Gabda, Darmesah, 311  
 Gane, Christian Jason B., 501  
 Gao, Yuexian, 301  
 Garduque, Jasmine Anne, 351  
 Ghaleb, Fuad A., 531  
 Ghazali, Khadizah, 311  
 Goh, Michael, 105  
 Goh, Vik Tor, 169  
 Guillema, Johnry, 501

**H**

- Hamid, Siti Hafizah Ab, 543  
 Hamzah, Muzaffar, 605  
 Hamzah, Shipun Anuar, 373  
 Hancock, Edwin R., 405  
 Hashim, Hizal Hanis, 699  
 Herbert, Cornelia, 627  
 Hin, Lim Zee, 215  
 Ho, Chiung Ching, 291, 699, 709  
 Hossen, Md Ismail, 105  
 Husin, Wan Nur Hayati Wan, 521  
 Hussain, Nazabat, 179  
 Hussein, Burhan Rashid, 85, 321  
 Hussin, Mohamed Saifullah, 585

**I**

- Ibrahim, Awang Asri Awang, 605  
 Ibrahim, Zul-Azri, 43  
 Idris, Amidora, 649  
 Iida, Hiroyuki, 301  
 Inoue, Yuta C., 565  
 Iswandon, Zamhar, 719

**J**

- Jalal, Rana A., 123  
 Jalaludin, Azhar, 435  
 Jali, Mohd Zalisham, 543  
 Jen, Chen Chwen, 617  
 June, Tan Li, 257  
 Junn, Kuan Yik, 269

**K**

- Kady, Ahmed El, 627  
 Kamat, Maznah, 531

Kasim, Hairoladenan, 43

- Kee, Keh Kim, 393  
 Khairuddin, Muhammad Asyraf Bin, 617  
 Khalid, Mohd Nor Akmal, 301  
 Khalid, N. S., 33  
 Khoo, Michael Boon Chong, 113  
 Kitt, Wong Wei, 689  
 Kler, Balvinder Kaur, 383

**L**

- Lau, Siong Hoe, 105  
 Leau, Yu-Beng, 257, 269, 481  
 Lecciones, Isabel Nicole, 351  
 Lee, Nicholas, 11  
 Lee, Ren-Ting, 481  
 Lee, Ying Loong, 393  
 Lee, Youngsook, 341  
 Lim, Hooi Mei, 363  
 Lim, Ivana Koon Yee U., 565  
 Lim, Seong Liang Ooi, 363  
 Lim, Sok Li, 113  
 Lim, Wei Lun, 291  
 Ling, Lew Sook, 491  
 Liwanag, Jerome L., 145  
 Li, Wanxiang, 301  
 Lopez, Dennis C., 331

**M**

- Malik, Nik Noordini Nik Abd, 373  
 Malik, Owais Ahmed, 85, 321  
 Ma, Liyao, 457  
 Manickam, Selvakumar, 199  
 Marquez, Praxedis S., 415  
 Mbulwa, Abbas Ibrahim, 689  
 Mchucha, Issa, 719  
 Meon, Hasni, 543  
 Mohamad, Zarina, 669  
 Mokri, Siti Salasiah, 521  
 Mountstephens, James, 383  
 Muhiddin, Fatihah Anas, 511  
 Mustapa, Mohamad Sukri, 373

**N**

- Nandong, J., 55  
 Nematova, Gulshan, 179  
 Ng, Chin-Kit, 247  
 Ng, Giap Weng, 457  
 Ng, Hu, 169  
 Ng, Peh Sang, 113  
 Nik, Wan Nor Shuhadah Wan, 669  
 Nordin, Azlin, 135  
 Nor, Nor Fariza Mohd, 435

**O**

- Obit, Joe Henry, 257, 269, 481  
Ohn, Khin Maung, 719  
Ohn, May Honey, 719  
On, Chin Kim, 595  
Ongpeng, Jason, 351  
Ong, Wee-Hong, 85, 321  
Ooi, Shih Yin, 1, 11  
Othman, Zalinda, 215

**P**

- Pang, Ying Han, 1, 11  
Park, Yong Jin, 481  
Permatasari, Jessica, 189  
Phalip, Liyana Nadhirah, 95

**Q**

- Quintana, Kristian G., 501

**R**

- Raghavan, Subashini, 393  
Rahim, Mohd Shafry Mohd, 65, 75  
Rahman, Anis Nadiah Che Abdul, 435  
Rahman, Md Asifur, 491  
Rahman, Nurul Huda Abd, 95  
Ramli, Khairun Nidzam, 373  
Ramos, Anna Liza A., 469  
Ramos, Christine Diane L., 565  
Rañada, Jonrey V., 331, 501  
Ratna, Anak Agung Putri, 23  
Razak, Chempaka Seri Abdul, 543  
Razak, Shukor Abd, 531  
Regla, Alfio I., 415  
Rehman, Mobashar, 179  
Retumban, Joseph D., 501  
Rolloda, Andrea Isabel P., 331  
Rusli, Nordaliela Mohd, 595  
Ryu, Jihyeon, 341

**S**

- Sabino, Gerald Mel G., 501  
Salleh, Norsaremah, 135  
Santiago, John Andrew, 565  
Santos, Arman Bernard G., 145, 469  
Sari, Riri Fitri, 23  
Sazali, Mohd Ilyas Sobirin Bin Mohd, 281  
Seman, Fauziahanim Che, 373  
Shabadin, Akmalia, 699  
Shah, Mohd Arief, 531  
Shah, Shaharil Mohd, 373  
Shukor, S. A. A., 33  
Sia, Florence, 677

Sim, Doreen Ying Ying, 157

- Simon, Boung Yew Lau, 393  
Sing, Angeline Lee Ling, 605  
Slik, Johan Willem Frederik, 85, 321  
Smith, William A. P., 405  
Songkin, Myjessie, 659  
Song, Ong Thian, 189  
Soon, Gan Kim, 595  
Suaib, Norhaida Mohd, 65, 75  
Sulaiman, Jumat, 311, 511  
Sunarto, Andang, 511

**T**

- Tan, Eng Kee, 363  
Tan, Ian K. T., 575  
Tan, Nicholas Yu-Zhe, 699, 709  
Tan, Nigel Marcus, 565  
Tan, Tien-Ping, 363  
Tan, Wei Lun, 393  
Teh, Je Sen, 281  
Tham, K. Y., 227  
Ting, Choo-Yee, 291, 699, 709  
Tiun, Sabrina, 435  
Tolentino Jr., Efren Victor N., 501  
Tuah, Nooralisa Mohd, 553  
Tung, Yew Hoe, 689

**V**

- Valdez, Mari-Pearl M., 145  
Villanueva, Irish Claire L., 331

**W**

- Wafiy, Nik, 65  
Waishiang, Cheah, 617  
Weng, Ng Giap, 605  
Wi, Jason Teo Tze, 383  
Wills, Gary B., 553  
Witono, Timotius, 237  
Won, Dongho, 341  
Wong, Farrah, 55, 659  
Wong, H. L., 227  
Wong, K. I., 55  
Wong, Kok-Seng, 1  
Wong, Zi Jian, 169  
Wyai, Gary Loh Chee, 617

**Y**

- Yaakob, Razali, 639  
Yap, Timothy Tzen Vun, 169, 575  
Ya'u, Badamasu Imam, 135  
Yazid, Setiadi, 237  
Yeoh, Wei-Zhu, 281

Yeong, Wai Chung, 113  
Yin, Ooi Shih, 491  
Yin, Renee Chin Ka, 689  
Yu, Hongchuan, 65, 75  
Yung, Wong Chun, 605  
Yusof, Shahril, 719  
Yusof, Yuhanis, 585

**Z**

Zainal, Mohamad Shamian, 373  
Zakaria, Aznida Hayati, 669  
Zenian, Suzelawati, 649  
Zulkarnain, Muhammad Ameer, 543